IMAGING AND MECHANISM OF LEUKOCYTE RECRUITMENT AND FUNCTION IN INFLAMMATION AND INFECTIONS

EDITED BY: Zhichao Fan, Yuqing Huo, Hao Sun and Xunbin Wei

PUBLISHED IN: Frontiers in Cell and Developmental Biology

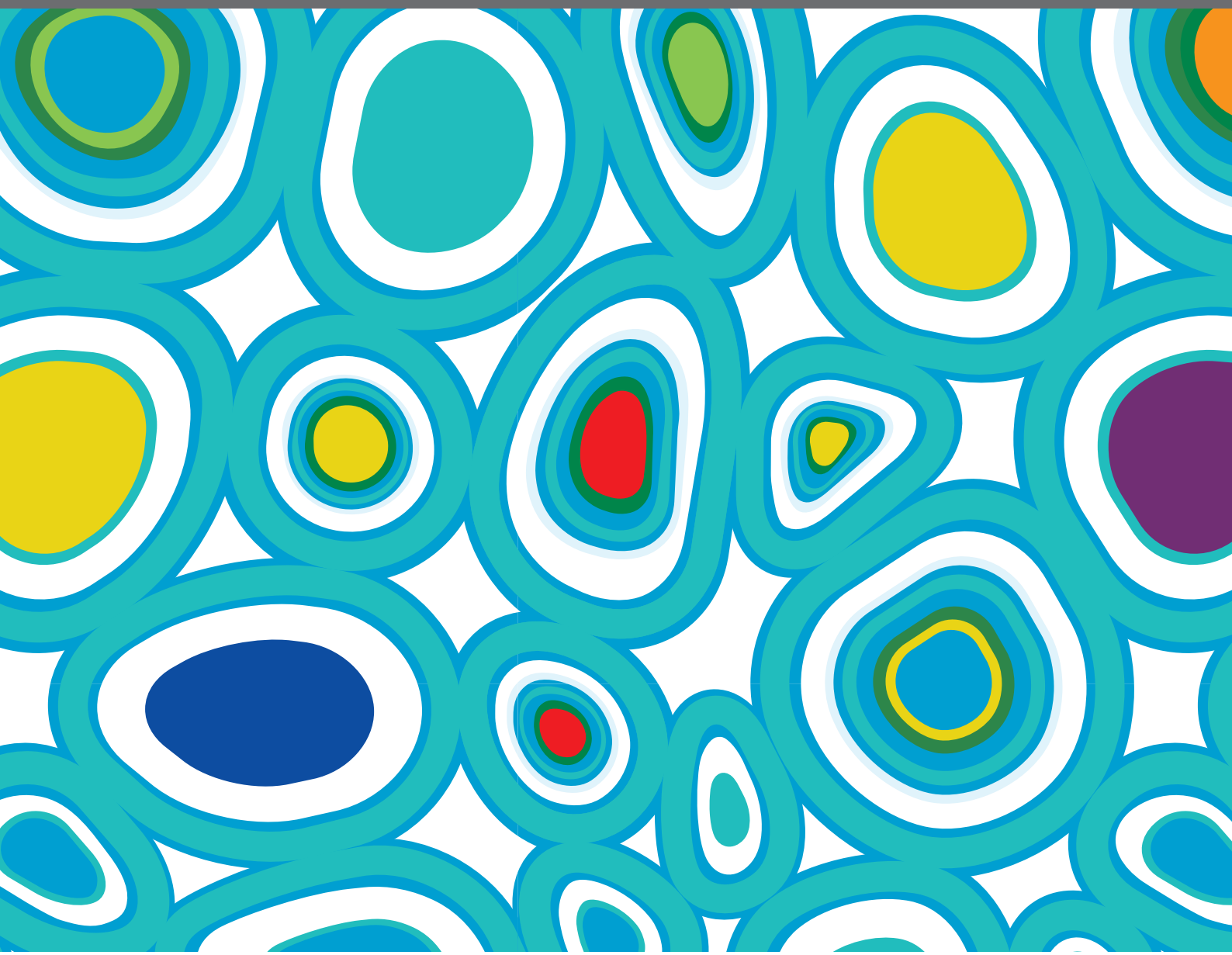

frontiers Research Topics

ISSN 1664-8714
ISBN 978-2-88966-975-2
DOI 10.3389/978-2-88966-975-2

About Frontiers

Frontiers is more than just an open-access publisher of scholarly articles: it is a pioneering approach to the world of academia, radically improving the way scholarly research is managed. The grand vision of Frontiers is a world where all people have an equal opportunity to seek, share and generate knowledge. Frontiers provides immediate and permanent online open access to all its publications, but this alone is not enough to realize our grand goals.

Frontiers Journal Series

The Frontiers Journal Series is a multi-tier and interdisciplinary set of open-access, online journals, promising a paradigm shift from the current review, selection and dissemination processes in academic publishing. All Frontiers journals are driven by researchers for researchers; therefore, they constitute a service to the scholarly community. At the same time, the Frontiers Journal Series operates on a revolutionary invention, the tiered publishing system, initially addressing specific communities of scholars, and gradually climbing up to broader public understanding, thus serving the interests of the lay society, too.

Dedication to Quality

Each Frontiers article is a landmark of the highest quality, thanks to genuinely collaborative interactions between authors and review editors, who include some of the world's best academicians. Research must be certified by peers before entering a stream of knowledge that may eventually reach the public - and shape society; therefore, Frontiers only applies the most rigorous and unbiased reviews.
Frontiers revolutionizes research publishing by freely delivering the most outstanding research, evaluated with no bias from both the academic and social point of view. By applying the most advanced information technologies, Frontiers is catapulting scholarly publishing into a new generation.

What are Frontiers Research Topics?

Frontiers Research Topics are very popular trademarks of the Frontiers Journals Series: they are collections of at least ten articles, all centered on a particular subject. With their unique mix of varied contributions from Original Research to Review Articles, Frontiers Research Topics unify the most influential researchers, the latest key findings and historical advances in a hot research area! Find out more on how to host your own Frontiers Research Topic or contribute to one as an author by contacting the Frontiers Editorial Office: frontiersin.org/about/contact

IMAGING AND MECHANISM OF LEUKOCYTE RECRUITMENT AND FUNCTION IN INFLAMMATION AND INFECTIONS

Topic Editors:
Zhichao Fan, UCONN Health, United States
Yuqing Huo, Augusta University, United States
Hao Sun, University of California, San Diego, United States
Xunbin Wei, Peking University, China

Citation: Fan, Z., Huo, Y., Sun, H., Wei, X., eds. (2021). Imaging and Mechanism of Leukocyte Recruitment and Function in Inflammation and Infections. Lausanne: Frontiers Media SA. doi: 10.3389/978-2-88966-975-2

Table of Contents

06 ***Editorial: Imaging and Mechanism of Leukocyte Recruitment and Function in Inflammation and Infections***
Hao Sun, Yuqing Huo and Zhichao Fan

11 ***TILRR Promotes Migration of Immune Cells Through Induction of Soluble Inflammatory Mediators***
Mohammad Abul Kashem, Xiaoou Ren, Hongzhao Li, Binhua Liang, Lin Li, Francis Lin, Francis A. Plummer and Ma Luo

24 ***Endothelial-Derived Interleukin-1a Activates Innate Immunity by Promoting the Bactericidal Activity of Transendothelial Neutrophils***
Xiaoye Liu, Hui Zhang, Shangwen He, Xiang Mu, Ge Hu and Hong Dong

33 ***MicroRNA-138-5p Suppresses Non-small Cell Lung Cancer Cells by Targeting PD-L1/PD-1 to Regulate Tumor Microenvironment***
Nannan Song, Peng Li, Pingping Song, Yintao Li, Shuping Zhou, Qinghong Su, Xiaofan Li, Yong Yu, Pengfei Li, Meng Feng, Min Zhang and Wei Lin

48 ***Corrigendum: MicroRNA-138-5p Suppresses Non-small Cell Lung Cancer Cells by Targeting PD-L1/PD-1 to Regulate Tumor Microenvironment***
Nannan Song, Peng Li, Pingping Song, Yintao Li, Shuping Zhou, Qinghong Su, Xiaofan Li, Yong Yu, Pengfei Li, Meng Feng, Min Zhang and Wei Lin

49 ***Let-7g* and miR-98 Reduce Stroke-Induced Production of Proinflammatory Cytokines in Mouse Brain***
David L. Bernstein and Slava Rom

59 ***Extracellular CIRP Induces Inflammation in Alveolar Type II Cells via TREM-1***
Chuyi Tan, Steven D. Gurien, William Royster, Monowar Aziz and Ping Wang

67 ***Integrin-Ligand Interactions in Inflammation, Cancer, and Metabolic Disease: Insights Into the Multifaceted Roles of an Emerging Ligand Irisins***
Eun Jeong Park, Phyoe Kyawe Myint, Atsushi Ito, Michael G. Appiah, Samuel Darkwah, Eiji Kawamoto and Motomu Shimaoka

84 ***Protein Palmitoylation in Leukocyte Signaling and Function***
Xiaoyuan Yang, Victor Chatterjee, Yonggang Ma, Ethan Zheng and Sarah Y. Yuan

103 ***The Secretive Life of Neutrophils Revealed by Intravital Microscopy***
Katia De Filippo and Sara M. Rankin

118 ***Membrane Dynamics and Organization of the Phagocyte NADPH Oxidase in PLB-985 Cells***
Jérémy Joly, Elodie Hudik, Sandrine Lecart, Dirk Roos, Paul Verkuijlen, Dominik Wrona, Ulrich Siler, Janine Reichenbach, Oliver Nüsse and Sophie Dupré-Crochet

128 ***Neutrophils Return to Bloodstream Through the Brain Blood Vessel After Crosstalk With Microglia During LPS-Induced Neuroinflammation***
Yu Rim Kim, Young Min Kim, Jaeho Lee, Joohyun Park, Jong Eun Lee and Young-Min Hyun

140 ***Molecular Basis for CCRL2 Regulation of Leukocyte Migration***
Tiziana Schioppa, Francesca Sozio, Ilaria Barbazza, Sara Scutera, Daniela Bosisio, Silvano Sozzani and Annalisa Del Prete

147 ***Mucin-Like Domain of Mucosal Addressin Cell Adhesion Molecule-1 Facilitates Integrin a4b7-Mediated Cell Adhesion Through Electrostatic Repulsion***
MengYa Yuan, YanRong Yang, Yue Li, ZhanJun Yan, ChangDong Lin and JianFeng Chen

157 ***Extracellular RNA as a Versatile DAMP and Alarm Signal That Influences Leukocyte Recruitment in Inflammation and Infection***
Klaus T. Preissner, Silvia Fischer and Elisabeth Deindl

181 ***Determinants of Phagosomal pH During Host-Pathogen Interactions***
Johannes Westman and Sergio Grinstein

190 ***Prkaa1 Metabolically Regulates Monocyte/Macrophage Recruitment and Viability in Diet-Induced Murine Metabolic Disorders***
Qiuhua Yang, Qian Ma, Jiean Xu, Zhiping Liu, Jianqiu Zou, Jian Shen, Yaqi Zhou, Qingen Da, Xiaoxiao Mao, Sarah Lu, David J. Fulton, Neal L. Weintraub, Zsolt Bagi, Mei Hong and Yuqing Huo

207 ***Intravital Imaging of Pulmonary Immune Response in Inflammation and Infection***
Nazli Alizadeh-Tabrizi, Stefan Hall and Christian Lehmann

219 ***Leukocyte Trafficking and Hemostasis in the Mouse Fetus* in vivo*: A Practical Guide***
Andreas Margraf and Markus Sperandio

234 ***Soluble CD83 Regulates Dendritic Cell–T Cell Immunological Synapse Formation by Disrupting Rab1a-Mediated F-Actin Rearrangement***
Wei Lin, Shuping Zhou, Meng Feng, Yong Yu, Qinghong Su and Xiaofan Li

248 ***Vedolizumab: Potential Mechanisms of Action for Reducing Pathological Inflammation in Inflammatory Bowel Diseases***
Matthew Luzentales-Simpson, Yvonne C. F. Pang, Ada Zhang, James A. Sousa and Laura M. Sly

258 ***Effect of Physical Training on Exercise-Induced Inflammation and Performance in Mice***
Luiz Alexandre Medrado de Barcellos, William Antonio Gonçalves, Marcos Paulo Esteves de Oliveira, Juliana Bohnen Guimarães, Celso Martins Queiroz-Junior, Carolina Braga de Resende, Remo Castro Russo, Cândido Celso Coimbra, Albená Nunes Silva, Mauro Martins Teixeira, Barbara Maximino Rezende and Vanessa Pinho

268 ***Glycans and Glycan-Binding Proteins as Regulators and Potential Targets in Leukocyte Recruitment***
Franziska Krautter and Asif J. Iqbal

283 ***Monitoring Phosphoinositide Fluxes and Effectors During Leukocyte Chemotaxis and Phagocytosis***
Fernando Montaño-Rendón, Sergio Grinstein and Glenn F. W. Walpole

308 ***Complement Receptors and Their Role in Leukocyte Recruitment and Phagocytosis***
Sofie Vandendriessche, Seppe Cambier, Paul Proost and Pedro E. Marques

333 ***Intravital Imaging Allows Organ-Specific Insights Into Immune Functions***
Selina K. Jorch and Carsten Deppermann

340 ***Inflammatory Cell Recruitment in Cardiovascular Disease***
Timoteo Marchini, Lucía Sol Mitre and Dennis Wolf

352 ***Use of Integrated Optical Clearing and 2-Photon Imaging to Investigate Sex Differences in Neuroimmune Interactions After Peripheral Nerve Injury***
Thomas A. Szabo-Pardi, Umar M. Syed, Zachary W. Castillo and Michael D. Burton

365 ***Regulation of the Migration of Distinct Dendritic Cell Subsets***
Meng Feng, Shuping Zhou, Yong Yu, Qinghong Su, Xiaofan Li and Wei Lin

378 ***Dysregulation of Leukocyte Trafficking in Type 2 Diabetes: Mechanisms and Potential Therapeutic Avenues***
Laleh Pezhman, Abd Tahrani and Myriam Chimen

397 ***Insights Into Leukocyte Trafficking in Inflammatory Arthritis – Imaging the Joint***
Julia E. Manning, Jonathan W. Lewis, Lucy-Jayne Marsh and Helen M. McGettrick

411 ***Elucidating the Biomechanics of Leukocyte Transendothelial Migration by Quantitative Imaging***
Amy B. Schwartz, Obed A. Campos, Ernesto Criado-Hidalgo, Shu Chien, Juan C. del Álamo, Juan C. Lasheras and Yi-Ting Yeh

426 ***The Role of PDE8 in T Cell Recruitment and Function in Inflammation***
Paul M. Epstein, Chaitali Basole and Stefan Brocke

frontiers in Cell and Developmental Biology

EDITORIAL
published: 07 May 2021
doi: 10.3389/fcell.2021.690003

Editorial: Imaging and Mechanism of Leukocyte Recruitment and Function in Inflammation and Infections

Hao Sun[1]*, *Yuqing Huo*[2] *and Zhichao Fan*[3]*

[1] Department of Medicine, University of California, San Diego, La Jolla, CA, United States, [2] Department of Cellular Biology and Anatomy, Vascular Biology Center, Medical College of Georgia, Augusta University, Augusta, GA, United States, [3] Department of Immunology, School of Medicine, UConn Health, Farmington, CT, United States

Keywords: leukocytes, leukocyte adhesion, leukocyte recruitment, leukocyte imaging, intravital imaging

Editorial on the Research Topic

Imaging and Mechanism of Leukocyte Recruitment and Function in Inflammation and Infections

The recruitment of leukocytes plays essential roles during protective and pathological immune responses of many diseases. Recruitment from circulation involves several processes such as rolling and adhesion to endothelial cells lining blood vessel inner walls, transmigration across vessel inner walls into surrounding tissue (diapedesis), and migration into other tissues. Leukocyte recruitment is precisely regulated by a complex network of adhesion molecules, including integrins, and their ligands to ensure the proper positioning of immune cells in local microenvironments. Many types of leukocytes help regulate immune defense and inflammation, including T cells, B cells, and natural killer cells, as well as myeloid cells, such as neutrophils, monocytes, macrophages, and dendritic cells (DCs). Microscopic imaging is a powerful visualization method to investigate leukocyte recruitment and functions.

The Frontiers Research Topic "Imaging and Mechanism of Leukocyte Recruitment and Function in Inflammation and Infections" highlights 31 recent studies that use imaging and other techniques to investigate leukocyte recruitment and functions in different infectious or non-infectious diseases.

GENERAL MECHANISMS OF LEUKOCYTE RECRUITMENT

Leukocytes can dynamically increase the affinity of integrins for their ligands (activation), an event central to many of their functions. Leukocyte integrins are critical for innate and adaptive immune responses and contribute to many immune-related conditions. It is not surprising then that integrins have emerged as promising treatment targets for autoimmune diseases and cancer. In a comprehensive overview, Park et al. detailed the role of integrin interactions in both health and disease. This review highlighted irisin, a novel exercise-dependent secretory integrin ligand, and its potential regulatory functions, proposing the αV integrin as a potential receptor for irisin, which is based on most of the recent publications about integrins and integrin-irisin interactions. Leukocytes homing from blood to gut-associated lymphoid tissue (GALT) are mediated by the interaction between integrin α4β7 with its ligand mucosal vascular addressin cell adhesion molecule 1 (MAdCAM-1). In an original research article, Yuan et al. demonstrated that heparan sulfate (HS), which is an acidic linear polysaccharide with a highly variable structure, could promote integrin α4β7-mediated cell adhesion on MAdCAM-1 under shear flow by imitating the negative charges of the extracellular microenvironment, suggesting the negative charges facilitate α4β7-MAdCAM-1

OPEN ACCESS

Edited and reviewed by:
Akihiko Ito,
Kindai University, Japan

***Correspondence:**
Zhichao Fan
zfan@uchc.edu
Hao Sun
has073@ucsd.edu

Specialty section:
This article was submitted to Cell Adhesion and Migration, a section of the journal Frontiers in Cell and Developmental Biology

Received: *01 April 2021*
Accepted: *09 April 2021*
Published: *07 May 2021*

Citation:
Sun H, Huo Y and Fan Z (2021) Editorial: Imaging and Mechanism of Leukocyte Recruitment and Function in Inflammation and Infections. Front. Cell Dev. Biol. 9:690003. doi: 10.3389/fcell.2021.690003

mediated leukocyte migration to GALT.

Chemokines guide leukocyte homing and trafficking through G protein-coupled receptor (GPCR) signaling pathways. C-C chemokine receptor-like 2 (CCRL2) shares structural and functional similarities with atypical chemokine receptors (ACKRs), which is a subset of chemokine receptors unable to activate signal transduction through G proteins. Schioppa et al. provided a valuable general overview of the current understanding of CCRL2 in terms of expression regulation, ligand binding, as well as its functions in leukocyte migration, which may provide novel therapeutic strategies for the control of inflammation and tumor immune surveillance. Along the same line, a recent study by Kashem et al. evaluated the effect of Toll-like interleukin-1 receptor regulator (TILRR)-induced pro-inflammatory cytokines/chemokines on the migration of immune cells. TILRR has been identified as an important modulator of inflammation responsive genes. This work demonstrated that culture supernatants from TILRR-overexpressed cervical epithelial cells can increase the migration of THP-1 monocytes and MOLT-4 T-lymphocytes, which may influence immune cell infiltration in tissues.

Leukocyte recruitment is regulated by the interaction between endothelium-expressed proteins and circulating leukocytes. The involvement of glycan and glycan-binding proteins in the leukocyte recruitment cascade has been well-studied. A review by Krautter and Iqbal focused on the role of glycan-glycan binding protein interactions in the regulation of leukocyte trafficking during inflammation. Given the prevalence and importance of glycan-mediated interactions for the regulation of leukocyte function, this review also highlighted the therapeutic targeting of glycans and glycan-binding proteins in the context of leukocyte recruitment during inflammation.

Palmitoylation is the covalent attachment of the fatty acid palmitic acid to cysteine. Recently, many studies have shown that leukocyte proteins undergo palmitoylation, including adhesion molecules, cytokine/chemokine receptors, T cell co-receptors, and signaling factors. In a review focusing on the function of palmitoylated proteins in leukocytes, Yang et al. illustrated the central role of palmitoylation in leukocyte migration and function. They proposed targeting palmitoylation may serve as a promising therapeutic strategy for aberrant immune responses.

Phosphoinositides are a family of minority acidic phospholipids in cell membranes with numerous functions, including attracting phospholipase C, protein kinase C, proteins involved in membrane budding and fusion, proteins regulating the actin cytoskeleton, and others. A review from Montaño-Rendón et al. summarized the most recent findings concerning the metabolic regulation of phosphoinositides during the leukocyte lifecycle. They mainly focused their attention on cellular processes, including diapedesis, migration, and phagocytosis, highlighting the importance of proper phosphoinositide interconversion to maintain cellular homeostatic functions.

The activation of complement receptors helps to regulate inflammation, leukocyte extravasation, and phagocytosis; activation also contributes to the adaptive immune response. This particular topic is illustrated in the review article by Vandendriessche et al., which focused on complement receptors and their roles in regulating phagocytosis and leukocyte recruitment during immunity and inflammation. Complement receptors participate in firm endothelial adhesion, diapedesis, and leukocyte chemotaxis toward the inflammatory trigger. Within tissues, they are involved in phagocytosis and cell type-specific immune regulatory roles. Chemotaxis and phagocytosis are fundamental processes that protect the body and maintain tissue homeostasis. Thus, the complement system is a promising therapeutic target for many diseases.

The phosphodiesterases (PDEs) that degrade cyclic adenosine monophosphate (cAMP) and cyclic guanosine monophosphate (cGMP) have been studied for over 40 years. Several drugs have been developed that target cGMP signaling, while drugs targeting cAMP have not been that successful; this is partly because cAMP is ubiquitous and critically required in virtually all tissues, while cGMP is more prominent and confined to cardiovascular tissues. cAMP-specific PDE4 and PDE8 are higher potential targets for inflammatory diseases. Epstein et al. provided a comprehensive overview of the potential unique roles of PDE8 (PDE8A) in T cell motility and T cell-mediated inflammation, with several details on the distinct signaling properties of PDE8 in a huge variety of *in vivo* and *ex vivo* models, and in different cell types. This provided evidence for the existence of a unique PDE8-dependent signaling complex disruptor.

Recently, much attention has been drawn to the leukocyte recruitment role of extracellular RNA (exRNA), which is released from cells under conditions of injury or vascular disease. Preissne et al. highlighted articles that investigated the role of the exRNA on various steps of leukocyte recruitment within the innate immune response. Based on their work in a variety of preclinical animal models, exRNA constituted a versatile damaging factor in several inflammatory cardiovascular diseases, whereby the natural endonuclease RNase1 provided an effective and safe antagonist by inhibiting or preventing the pathological effects of exRNA—suggesting it may serve as a new therapeutic target.

Neutrophils are a marker of innate immune activation against invading microorganisms, as they are the first leukocytes to migrate from the circulation to inflamed or infected sites. The research article by Liu et al. described the mechanisms of endothelium-neutrophil interactions on bactericidal activity. They disclosed that interleukin (IL)-1α promoted neutrophil adhesion by upregulating cell adhesion molecules (CAMs) during the early phase, while oxidative phosphorylation induced transmigration of neutrophils against bacteria. Understanding the role of neutrophils during neuroinflammation is of great importance, and the observations by Kim et al. on the migration of microglia and neutrophils in the inflamed brain are very intriguing. Using two-photon intravital microscopy, the authors found that neuroinflammation leads to both influx and transendothelial migration of neutrophils in the brain and promotes their interaction with microglia. These observations may indicate that neutrophils can prime microglia to initiate a neuroinflammatory response and deliver pro-inflammatory signals to the periphery through reverse trans-endothelial migration (rTEM).

Barcellos et al. discussed interesting reports that focused on how physical training regulates exercise-induced inflammation and performance. This study demonstrated that acute high-intensity exercise promoted inflammation, including an increase of IL-6 in blood, enhanced rolling and adhesion of leukocytes (primarily neutrophils) by intravital imaging, and promoted neutrophil chemotaxis *in vitro*. Aerobic training diminished exercise-induced inflammation in skeletal muscle tissue. They also proposed that reactive oxygen species (ROS) are potential factors affecting aerobic performance and inflammatory response.

In a review, Schwartz et al. focused on an aspect of the leukocyte trans-endothelial migration (or diapedesis), which is an important process that allows leukocytes to reach the sites of tissue damage or infection to elicit an adequate response linked to innate or acquired immunity and inflammation. This review presented the biomechanical mechanisms involved in trans-endothelial crossing of leukocytes and summarized the various imaging techniques currently used with their advantages and limitations.

DCs are powerful antigen-presenting cells, and their migration ability is the key to initiating protective pro-inflammatory and tolerant immune responses. Recent studies have emphasized the importance of DC migration in maintaining immune surveillance and tissue homeostasis, as well as the pathogenesis of a series of diseases. Feng et al. provided a comprehensive view of the migration of DCs, especially under various environments, which may help to develop new therapeutic and vaccination strategies for diseases. Along the same line, Lin et al. demonstrated that sCD83 could inhibit DC-T synapse formation by decreasing Rab1a activation to disrupt F-actin and MHC-II accumulation at sites of DC-T contact, providing a possible mechanism for the role of DCs in immunological synapse formation. In experimental autoimmune uveitis (EAU) mice, sCD83-treated DCs decreased the number of T cells in the eyes and lymph nodes, and alleviated symptoms of EAU.

Monocytes (Mo) and macrophages (Mφ) are key components of the innate immune system and actively participate in the development of many autoimmune diseases. The infiltration of Mo and Mφ in diseased tissues is a hallmark of several autoimmune diseases. In this topic, Yang et al. investigated the role played by adenosine monophosphate-activated protein kinase (AMPK) signaling-dependent metabolic reprogramming in Mo/Mφ migration and survival in metabolic diseases, such as high-fat diet (HFD)-induced diabetes and atherosclerosis. They observed enhanced protein kinase adenosine monophosphate-activated catalytic subunit alpha 1 (PRKAA1/2) expression in adipocyte-associated-leukocytes in mice on a HFD, and highlighted a critical role of PRKAA1 in Mo and Mφ metabolic modulation, migration, and survival.

An original article from Tan et al. showed the induction of inflammation in alveolar cells by the interaction of triggering receptor expressed on myeloid cells-1 (TREM-1) with extracellular cold-inducible RNA-binding protein (CIRP). The authors showed that adding recombinant eCIRP increases TREM-1 expression in alveolar epithelial cells and induces production of cytokines IL-6 and CXCL2. This study provides insights into molecular mechanisms of acute lung injury, which is a life-threatening condition involved in many diseases, with additional importance during the COVID-19 pandemic.

Phagocytosis is an essential response of innate immune cells that involes recognition, engulfment, and degradation of foreign or dead material. Westman and Grinstein provided a comprehensive view of how phagosomal pH is regulated during phagocytosis, including why it varies among different professional phagocytes, and how host defense and pathogen escape occur in phagocytosis. Indeed, metabolite transport and utilization are both exquisitely pH-sensitive events. Therefore, the establishment and regulation of luminal pH should be the core content of host-pathogen interactions in the future.

LEUKOCYTE IMAGING

With the advent of new imaging techniques, new ways of visualizing immune cells have emerged in recent years, enabling more detailed discoveries about cell properties, functions, and interactions. Jorch and Deppermann wrote a comprehensive review on novel imaging techniques that provide insights into neutrophil and macrophage functions under physiological and pathological conditions. This article introduced several optical imaging techniques, including epifluorescent microscopy, confocal microscopy, and multi-photon microscopy. They also discussed light-sheet microscopy used after optical tissue clearing, which is valuable to visualize the structure and distribution of neutrophils and macrophages in fixed tissue.

The use of intravital microscopy over recent decades significantly improved our understanding of neutrophil trafficking and functions in various microenvironmental niches under homeostasis and in response to infections. Such technological advances allow studies on the temporal and spatial regulation of neutrophil functions, as well as the emerging role of tissue-resident neutrophils in the lung, skin, spleen, and lymph nodes. Through the perspective of intravital microscopy, De Filippo and Rankin presented recent studies on the function, migratory behavior, and cell-cell interactions of neutrophils in various tissues, outlining the importance of neutrophil subsets, their functions under homeostasis, and their responses to infection. They also commented on how understanding these processes in greater detail at a molecular level can lead to new therapeutics.

The lung is one of the most difficult organs to assess using intravital optical imaging due to its enclosed position within the body, delicate nature, and vital role in sustaining proper physiology. Alizadeh-Tabrizi et al. reviewed studies of lung intravital imaging and lung disease mechanisms. They introduced the microscopy modalities used for intravital imaging and the procedure for lung intravital microscopy in mice. They also commented on infection and inflammation models of lung diseases in which lung intravital imaging was used, and listed a number of limitations of the technique.

Margraf and Sperandio provided a "practical guide" for intravital observation of leukocyte trafficking and homeostasis

in the developing mouse fetus to further understand immune defense and hemostatic capability. They provided a methodology for visualizing blood plasma and vessel walls, as well as cells in circulation. This model offers a potential technique to study *in vivo* processes in the developing mouse fetus.

By combining optical clearing and multi-photon microscopy, Szabo-Pardi et al. investigated the recruitment of peripheral leukocytes to key tissues of the pain system, the dorsal root ganglia (DRG) and sciatic nerve, after nerve injury. They observed robust sexual dimorphism in leukocyte recruitment to lumbar DRGs after nerve injury. As mentioned above, intravital imaging was also used to study leukocytes in the brain (Kim et al.) and muscles (Liu et al.).

Arthritis, an immune-mediated inflammatory disease, is induced by the inappropriate accumulation and activation of leukocytes. In a comprehensive review, Manning et al. provided an in-depth synopsis of rheumatic joint inflammatory imaging describing the evolving techniques to visualize migrating leukocytes. It elegantly described the inflammatory processes and the evolution of imaging methods along with the leukocyte profile of the joint and what is learned as the techniques advance. It showed the development and improvement of different techniques, which can improve our knowledge of this disease and allow observers to track treatment responses.

Super-resolution microscopy is a powerful tool for studying molecular details in leukocytes. An original article from Joly et al. explored whether endosomes contribute to NADPH oxidase 2 (NOX2) delivery to the phagosome in neutrophils and found that a fraction of the early and recycling endosomes contained NOX2. They used super-resolution microscopy for the first time to observe NOX2 organization in the membrane of PLB-985 cells. They observed a rise in the number of nanoclusters during phagocytosis that required the presence of the cytosolic oxidase subunit p47phox.

LEUKOCYTE RECRUITMENT AND FUNCTION IN DISEASES

Recent studies have highlighted the role of inflammation in obesity, diabetes, hypertension, autoimmune disease, and cardiovascular diseases, including stroke and atherosclerosis. Atherosclerosis is a chronic inflammatory disease that occurs within the arterial wall and is initiated mainly in response to endogenous ligands, particularly oxidized lipoproteins, which stimulate both innate and adaptive immune responses. The innate response starts with the activation of endothelial cells in vessel walls and Mo/Mϕ activation. It is rapidly followed by an adaptive immune response to an array of potential antigens presented to effector T lymphocytes by antigen-presenting cells, such as DCs. Thus, leukocyte adhesion and recruitment to the vascular intima is a key event in early atherosclerosis.

Marchini et al. provided a comprehensive overview of the mechanisms underlying leukocyte recruitment in the setting of cardiovascular disorders, including myocardial infarction and atherosclerosis. They described the inhibition of receptors and ligands involved in the generation, adhesion, and transmigration of leukocytes that revealed a great potential for anti-leukocyte therapies at the preclinical stage for cardiovascular diseases.

Type 2 diabetes is a metabolic disorder. However, recent research suggests that type 2 diabetes is also an autoimmune disease. Pezhman et al. provided a valuable general overview of the dysregulation of leukocyte trafficking in type 2 diabetes in recent decades, including the changes in expression of adhesion molecules, chemokines, and chemokine receptors, innate and adaptive immune cells, and the subsequent immune response. They also discussed the potential therapeutic avenues targeting leukocyte trafficking.

A key element in the pathogenesis of inflammatory bowel disease (IBD) is a massive influx of immune cells into the gastrointestinal mucosa. Aberrant infiltration of mononuclear phagocytes, neutrophils, and inflammatory lymphocytes is observed in the colonic lamina propria of IBD patients. Leukocyte trafficking is, therefore, a key determinant of the immune responses that take place in the gut. Thus, this rapid leukocyte recruitment from the circulation into GI during IBD provides a potential target for pharmaceutical inhibition of the inflammation. Luzentales-Simpson et al. reviewed multiple proposed mechanisms of action for the integrin α4β7 blocking antibody vedolizumab used to treat IBD. Understanding the mechanism of action of this drug will allow a determination of the primary mechanisms of disease treatment in people with IBD. They also described the potential effects of vedolizumab on innate immune cells (macrophages, monocytes, and DCs) in particular.

In the past few years, miR-138 has been identified as a putative tumor suppressor and is found down-regulated in most human cancer types. Multiple targets of miR-138 have been identified previously, including key molecules involved in proliferation, apoptosis, invasion, and migration. The review by Song et al. investigated the immune-regulatory mechanisms of miR-138-5p in the non-small-cell lung cancer (NSCLC) microenvironment and tumor proliferation. They revealed that miR-138 has two essential functions in NSCLC therapy by targeting PD-L1/PD-1: regulating the immune response in the tumor micro-environment; and inhibiting proliferation of NSCLC cells by decreasing expression of Cyclin D3, Ki67, and minichromosome maintenance. This comprehensive review provided depth in understanding the molecular mechanism of miR-138 as a tumor suppressor in NSCLC, which is critical in therapeutic applications.

Stroke is currently the third-leading cause of death in the United States. During ischemic stroke, the blood-brain barrier is significantly damaged, resulting in the infiltration of peripheral immune cells and dramatic changes in cytokine levels. Bernstein and Rom studied the impacts of let-7 microRNA families on cytokine release and neurovascular space following ischemic stroke in mice. Using *in vitro* luciferase reporter assays, they further identified C-X-C motif chemokine ligand 1 (human as IL-8) as a potential target of let-7 g, and interferon gamma-induced protein-10 as a target of miR-98, respectively. They proposed that let-7 microRNAs may inhibit the release of cytokines at the blood-brain barrier

and thus regulate endothelial-immune reactions following ischemic stroke.

In conclusion, this Research Topic provides detailed regulatory roles and molecular mechanisms for understanding leukocyte recruitment in health and disease. We would like to thank all the authors and referees for their valuable contributions. We believe that the collection of articles included in the topic will be of interest to all researchers studying molecular and cellular mechanisms of leukocyte migration and homing in development and diseases, enabling them to appreciate how a clearer understanding of these mechanisms can inspire therapeutics and diagnostics.

AUTHOR CONTRIBUTIONS

HS and ZF conceived the idea, designed, and edited the manuscript. YH corrected the manuscript. All authors listed have approved the work for publication.

ACKNOWLEDGMENTS

We would like to thank the authors, reviewers, and editors for their essential contribution to this exciting and unexplored research topic, as well as of the members of the Frontiers in Cell and Developmental Biology editorial office. We acknowledge Dr. Christopher Kit Bonin and Dr. Geneva Hargis from UConn Health School of Medicine for their help in the scientific writing and editing of this manuscript.

Conflict of Interest: The authors declare that the research was conducted in the absence of any commercial or financial relationships that could be construed as a potential conflict of interest.

frontiers in Cell and Developmental Biology

ORIGINAL RESEARCH
published: 03 July 2020
doi: 10.3389/fcell.2020.00563

TILRR Promotes Migration of Immune Cells Through Induction of Soluble Inflammatory Mediators

Mohammad Abul Kashem[1,2,3,4†], Xiaoou Ren[5,6†], Hongzhao Li[1,4], Binhua Liang[2,4,7], Lin Li[2,4], Francis Lin[5,6,8], Francis A. Plummer[1‡] and Ma Luo[1,2,4]*

[1] Department of Medical Microbiology and Infectious Diseases, University of Manitoba, Winnipeg, MB, Canada, [2] JC Wilt Infectious Diseases Research Centre, Winnipeg, MB, Canada, [3] Department of Microbiology and Veterinary Public Health, Chittagong Veterinary and Animal Sciences University, Chittagong, Bangladesh, [4] National Microbiology Laboratory, Public Health Agency of Canada, Winnipeg, MB, Canada, [5] Department of Biosystems Engineering, University of Manitoba, Winnipeg, MB, Canada, [6] Department of Physics and Astronomy, University of Manitoba, Winnipeg, MB, Canada, [7] Department of Biochemistry and Medical Genetics, University of Manitoba, Winnipeg, MB, Canada, [8] Department of Immunology, University of Manitoba, Winnipeg, MB, Canada

OPEN ACCESS

Edited by:
Zhichao Fan,
UCONN Health, United States

Reviewed by:
Kui Cui,
Harvard University, United States
Rongrong Liu,
Northwestern University, United States
Bo Liu,
University of California, Berkeley, United States

***Correspondence:**
Ma Luo
Ma.Luo@umanitoba.ca;
ma.luo@canada.ca

† These authors have contributed equally to this work

‡ In memoriam

Specialty section:
This article was submitted to Cell Adhesion and Migration, a section of the journal Frontiers in Cell and Developmental Biology

Received: *23 April 2020*
Accepted: *15 June 2020*
Published: *03 July 2020*

Citation:
Kashem MA, Ren X, Li H, Liang B, Li L, Lin F, Plummer FA and Luo M (2020) TILRR Promotes Migration of Immune Cells Through Induction of Soluble Inflammatory Mediators. Front. Cell Dev. Biol. 8:563. doi: 10.3389/fcell.2020.00563

TILRR has been identified as an important modulator of inflammatory responses. It is associated with NF-κB activation, and inflammation. Our previous study showed that TILRR significantly increased the expression of many innate immune responsive genes and increased the production of several pro-inflammatory cytokines/chemokines by cervical epithelial cells. In this study, we evaluated the effect of TILRR-induced pro-inflammatory cytokines/chemokines on the migration of immune cells. The effect of culture supernatants of TILRR-overexpressed cervical epithelial cells on the migration of THP-1 monocytes and MOLT-4 T-lymphocytes was evaluated using Transwell assay and a novel microfluidic device. We showed that the culture supernatants of TILRR-overexpressed HeLa cells attracted significantly more THP-1 cells (11–40%, $p = 0.0004$–0.0373) and MOLT-4 cells (14–17%, $p = 0.0010$–0.0225) than that of controls. The microfluidic device-recorded image analysis showed that significantly higher amount with longer mean cell migration distance of THP-1 ($p < 0.0001$–0.0180) and MOLT-4 ($p < 0.0001$–0.0025) cells was observed toward the supernatants of TILRR-overexpressed cervical epithelial cells compared to that of the controls. Thus, the cytokines/chemokines secreted by the TILRR-overexpressed cervical epithelial cells attracted immune cells, such as monocytes and T cells, and may potentially influence immune cell infiltration in tissues.

Keywords: TILRR, pro-inflammatory cytokines/chemokines, cervical epithelial cell culture supernatants, THP-1, MOLT-4, Transwell assay, microfluidic device

INTRODUCTION

Previous studies identified that TILRR (Toll-like/Interleukin-1 receptor regulator), a FREM1 isoform 2, is an important regulator of genes in the NF-κB signal transduction pathway and inflammatory responses (Zhang et al., 2010, 2012). TILRR is expressed in human peripheral blood mononuclear cells, including monocytes and macrophages, and a wide range of human and mouse

lymphocytic and mesenchymal cell lines (Zhang et al., 2010; Smith et al., 2017). It has been shown to cause aberrant inflammatory reactions and inflammation-driven pathological condition (Smith et al., 2017). Our previous study showed that the minor allele of FREM1 SNP (single nucleotide polymorphism) rs1552896 is associated with resistance to HIV-1 infection in the Pumwani sex worker cohort (PSWC) (Luo et al., 2012). Our group also showed that FREM1 is highly expressed in human epithelial tissues and immune cells, such as cervical tissues (Luo et al., 2012), CD4+ and CD8+ T cells, B cells, monocytes and natural killer (NK) cells (Omange et al., under revision). Recently, we have shown that TILRR modulates expression of many inflammation responsive genes and production of pro-inflammatory cytokines/chemokines such as IL-6, IL-8/CXCL8, IP-10/CXCL10, MCP-1/CCL2, MIP-1β/CCL4 and RANTES/CCL5 in cervico-vaginal epithelial cells (Kashem et al., 2019). The inflammatory cytokines/chemokines secreted by the TILRR-overexpressed cervical epithelial cells could influence immune cell migration to tissues. In fact, several studies have shown that chemo-attractants including IL-8/CXCL8, IP-10/CXCL10, MCP-1/CCL2, MIP-1α/CCL3, MIP-1β/CCL4, MIP-3α/CCL20, and RANTES/CCL5 produced by female genital epithelium induced rapid influx of circulating immune cells, resulting in increased risk of HIV acquisition (Mueller and Strange, 2004; Wira et al., 2005; Li et al., 2009; Masson et al., 2015; Arnold et al., 2016). Because cervical epithelial cells express FREM1 (Luo et al., 2012), and TILRR overexpression increases the production of pro-inflammatory mediators by cervical epithelial cell lines (Kashem et al., 2019), we hypothesized that the cytokines/chemokines produced by the cervical epithelial cell line may influence the migration and tissue infiltration of immune cells. In this study, we investigated the effect of supernatants of TILRR-overexpressed cervical epithelial cells (HeLa cells) on the migration of immune cells using two cell lines, THP-1 and MOLT-4, by Transwell assay and a novel microfluidic device that can record cell migration images. We report here that the supernatants of TILRR-overexpressed HeLa cells significantly attracted THP-1 (monocyte) and MOLT-4 (T-lymphocyte) cells than the controls.

MATERIALS AND METHODS

Cell Lines and Culture Conditions

THP-1 (ATCC) (NIH, Catalog# 9942), a human monocytic cell line, and MOLT-4 (NIH, Catalog# 175), a human T lymphoblastic cell line, were used for *in vitro* migration assay. MOLT-4 cells were maintained in complete RPMI 1640 growth medium (Sigma-Aldrich, Catalog# R0883) supplemented with 10% fetal bovine serum (FBS) (Giboco, Catalog# 12483-020), 2 mM GlutaMax-I (Gibco, Catalog# 35050-061), 10 mM HEPES (Gibco, Catalog# 15630-080), 1 mM sodium pyruvate (Gibco, Catalog# 11360070), and 1% Pen-Strep (Gibco, Catalog# 15140-122). THP-1 cells were also maintained in complete RPMI 1640 growth medium similar to the MOLT-4 cells with additional supplement of 0.05 mM 2-Mercaptoethanol (Sigma-Aldrich, Catalog# M3148). The medium was replaced every 2–3 days. Because THP-1 (monocytes) and MOLT-4 (lymphocytes) cells express HIV-1 receptor/co-receptors CD4, CCR5 and CXCR4 essential for R5- and X4- tropic HIV-1 strains to infect the host (Dejucq et al., 1999; Dejucq, 2000; Konopka and Duzgunes, 2002; Miyake et al., 2003; Melo et al., 2014; Huang et al., 2016), and these cells are widely used as *in vitro* model for HIV-1 infection (Ushijima et al., 1991; Dejucq et al., 1999; Konopka and Duzgunes, 2002; Blanco et al., 2004; Cassol et al., 2006; Guo et al., 2014; Lodge et al., 2017), we therefore utilized these cell lines as a model for *in vitro* cell migration assay. HeLa cells (NIH, Catalog# 153) were maintained as described in our earlier study (Kashem et al., 2019). Briefly, the cells were cultivated in Dulbecco's Modified Eagle's Medium (DMEM) (Sigma-Aldrich, Catalog# D5796) supplemented with 10% FBS (Gibco, Catalog# 12483-020) and 1% Antibiotic-Antimycotic (Gibco, Catalog# 15240062). HeLa cells were used to produce cell culture supernatants following overexpression of TILRR. As human cervical tissues highly express FREM1 mRNA and TILRR is a transcript variant of FREM1, we therefore used HeLa cells as a model system to study the effect of FREM1 variant TILRR in promoting migration of immune cells.

Overexpression of TILRR in HeLa Cells

We overexpressed the TILRR in HeLa cells as described previously (Kashem et al., 2019). In brief, approximately 2.5×10^5 cells/ml was plated into each well of a 12-well culture plate containing complete DMEM growth medium a day before transfection. Once the cells reached 80–90% confluency, the media was replaced with antibiotic free fresh growth media. Overexpression of TILRR was performed by using 1.0 μg/well of TILRR-plasmid (vector + TILRR) (GeneCopoeia, Catalog# EX-I2135-68) or empty vector-plasmid control (GeneCopoeia, catalog# EX-NEG-68) containing a CMV promoter, an ampicillin marker, and a puromycin marker. We co-transfected the cells with 0.2 μg/well of PmaxGFP (Lonza, Walkersville, MD, United States) as a standard enhanced GFP (Green fluorescence protein) control vector to monitor the transfection efficiency by Confocal microscopy and Flow Cytometry analysis. Cells were co-transfected by 2 μl/well of EndofectinMax transfection reagent (GeneCopoeia, Catalog# EFM1004-01).

Collection of Cervical Epithelial Cell Culture Supernatants

Secretion of inflammatory mediators from female genital epithelial cells demonstrated a critical role in rapid influx of immune cells at mucosal epithelia, resulting in heightened inflammation and vaginal microbial infection including HIV-1 (Fichorova et al., 2001; Kaul et al., 2008a,b; Li et al., 2009; Kaul et al., 2015). Thus, to mimic the physiological conditions of cervical epithelial microenvironment, TILRR-transfected HeLa cell culture supernatants were used as chemo-attractants in this study to investigate the effect on the migration of THP-1 monocytes and MOLT-4 lymphocytes. Culture supernatants from HeLa cells were produced as previously described (Kashem

et al., 2019). Briefly, co-transfected HeLa cells were selected with puromycin treatment after 24 h of transfection. Cells were then incubated with FBS- and antibiotic-antimycotic free DMEM medium (Sigma Aldrich, Catalog# D5796) for another 24 h and the supernatants were collected in sterile centrifuge tubes. The culture supernatants were centrifuged at 10,000 × *g* for 10 min at 4°C, aliquoted in protein low binding tubes (Thermofisher Scientific, Catalog# 90410), and stored at −80°C for downstream experiments.

Preparation of Cell Culture Supernatants

Immediately before the assay, cell culture supernatants were pulled from −80°C freezer and kept on ice to thaw. All samples were kept on ice until the assay plate was ready to use. The samples were vortexed for 15 s before being added to the plate. One freeze-thaw cycle was allowed for all culture supernatants to minimize sample degradation.

Bio-Plex Analysis of Culture Supernatants

We analyzed the cytokines/chemokines in HeLa cell culture supernatants using a custom 13-plex panel as previously described (Kashem et al., 2019). These cytokines/chemokines include granulocyte macrophage colony stimulating factor (GM-CSF), interferon gamma (IFNγ), interleukin (IL)-1β, IL-6, IL-8/CXCL8, IL-10, IL-17A, IFN-γ inducible protein (IP)-10/CXCL10, macrophage chemo-attractant protein (MCP)-1/CCL-2, monocyte inflammatory protein (MIP)-1α, MIP-1β, regulated upon activation, normal T cell expressed and secreted (RANTES)/CCL5, and tumor necrosis factor alpha (TNF-α) (**Supplementary Table 1**). Briefly, the assay was conducted according to the Bio-Plex Pro^{TM} assays protocol (Bio-Rad Laboratories Inc.). Antibody-coupled bead stocks were vortexed for 15 sec and combined at 1:600 dilutions in assay buffer (Bio-Plex Pro^{TM} reagent kit, Bio-Rad, Catalog# 171-304070M). Fifty microliter of diluted beads was added into each well of 96-well Bio-Plex Pro^{TM} Flat bottom plate (Bio-Rad, Catalog# 171025001). After 2x washes with Bio-Plex wash buffer (BioRad, Catalog# 171-304070M), 50 μl of HeLa cell culture supernatants was added to the plate, and incubated for 30 min on plate shaker (850 ± 50 rpm) at room temperature (RT). Following incubation, the plate was washed 3X with wash buffer and 25 μl of detection antibody (1 μg/ml) was added into each well. The plate was incubated again for 30 min on a plate shaker. Fifty microliter of streptavidin-PE (1x) conjugate (BioRad, Catalog# 171304501) was added per well after 3X washes, and incubated for 10 min at RT. Finally, the plate was washed three times, and 150 μl of assay buffer was added into each well, shaken for 10 s and then run by Bio-Plex^{TM} 200 System (Luminex xMAP technology) (Bio-Rad, Canada). Complete HeLa cell growth medium was used as a diluents for Bio-Plex Pro Human Cytokine Standards Group I 27-plex (Bio-Rad, Catalog# 171D50001) and as a blank control. To generate standard curve, 50 μl of fourfold standard dilutions was added in 8-wells in duplicates. Bio-Plex software version 6.1 was used to acquire data, which was optimized to calculate the upper limit of quantification (ULOQ) (pg/ml) and lower limit of quantification (LLOQ) (pg/ml) using logistic-5PL regression analysis with fitness probability ≥ 0.95.

Preparation of THP-1, and MOLT-4 -Cells for the Cell Migration Assays

The cell lines, following revival from the liquid nitrogen tank, were cultured for at least one passage before being used for the migration experiment. We used cells that were passaged for <10 times for this study. On the day of migration experiment, the cells were mixed gently and transferred to 50 ml BD Falcon tube, centrifuged for 10 min at 130 × *g* and the supernatants were discarded. Ten milliliters of RPMI 1640 complete medium without FBS and Pen-Strep was added to the pelleted cells, mixed gently, and the cell numbers were counted. For Transwell-based cell migration assay, a total of 5×10^5cells/100μl/assay was used, whereas 1×10^4 cells/10 μl/unit was used for microfluidic-based cell migration assay.

Preparation of Positive Control Chemo-Attractants

Since HeLa cells were incubated with DMEM medium during the production of culture supernatants, DMEM medium was used as a medium control and diluent in this study. MCP-1/CCL2 (Sigma-Aldrich, Catalog# SRP3109-20UG) and stromal cell-derived factor (SDF)-1α/CXCL12 (Sigma-Aldrich, Catalog# SRP3276-10UG) were used as positive chemo-attractant controls for the migration assays. Positive chemo-attractant controls were diluted to concentrations (5, 10, 50, 100, and 200 ng/ml) with DMEM medium (Sigma-Aldrich, Catalog# D5796) without FBS and antibiotic-antimycotic for the optimization assay.

Cell Migration Experiments in Transwell

Migration of cells was performed using 24-well polycarbonated membrane insert with 5 μm pore size (Corning, catalog# CLS3421) (**Supplementary Figure 1**). In the bottom chamber of Transwell plate, 600 μl of each chemo-attractant (DMEM control, diluted positive controls, culture supernatants of TILRR-overexpressed HeLa cells, culture supernatants of empty plasmid-transfected HeLa cells, or culture supernatants of non-transfected HeLa cells) was added. One hundred microliter of cells (5×10^5 cells) in RPMI 1640 migration media was added to the upper chamber (Transwell insert), and incubated for 24 h at 37°C with 5% CO_2. The number of input cells was calculated using three different counting methods, such as hemocytomer, automated cell counter (Invitrogen, Catalog# C10227), and flow cytometry (BD accuri C6, BD Biosciences, CA, United States). After 24 h of migration, Transwell insert was carefully removed from the well, and the medium containing the migrated cells in the bottom chamber was gently mixed and transferred to the 1.5 ml Eppendorf tube and migrated cells in the 50 μl medium were counted using hemocytometer and automated cell counter as described previously (Louis and Siegel, 2011; Cadena-Herrera et al., 2015; Pioli, 2019). For flow cytometry counting, the

remaining ∼550 μl volume of the medium containing the migrated cells was gently vortexed and analyzed with BD accuri C6 (BD Biosciences, CA, United States). The data obtained from flow cytometry were analyzed with FlowJo software (Treestar, United States).

Preparation of the Microfluidic Device

A previously designed radial microfluidic device was used in this study (**Figure 1**) (Wu et al., 2018). The device consisted of two layers with different thickness, the first layer (∼7 μm high) forms the cell docking structure to trap cells inside the cell loading channels; while the second layer (∼40 μm high) includes the cell loading ports and channels, and the gradient channels with chemical inlets and waste outlets. This device contains eight independent units, each one has its own two chemical inlets, one waste inlet, and one cell loading port, which allows eight independent experiments performed simultaneously. The device was fabricated by using previously described standard photolithography and soft lithography procedures (Wu et al., 2018; Ren et al., 2019, 2020). Briefly, the device pattern was designed by AUTOCAD and printed onto a transparent film at 24,000 dpi resolution (Fineline Imaging) served as the photomask for later photolithography. The pattern was then replicated by selected exposure of UV light through the photomask on top of a 3 inch silicon wafer (Silicon, Inc., ID, United States) with pre-coat of SU-8 negative photoresist (MicroChem). The wafer with patterns was used as the mold to reproduce polydimethylsiloxane (PDMS) (Sylgard 184, Dow Corning, Manufacturer SKU# 2065622) replicas, and then the replicas were cut off from the mold after 2 h of baking at 80°C. The chemical inlets (6 mm diameter), waste outlets (4 mm diameter), and cell loading ports (2 mm diameter) were punched out of the PDMS replica, and the replica was bonded onto a glass slide after air plasma treatment. The design of micropillar supports below the docking barrier increased the structural stability during bonding process. The device channels were coated with rat-tail collagen type I (20 μg/mL; Corning, Catalog# 354236) for 1 h, and then incubated with DMEM medium for another 30 min inside the incubator before the cell migration experiments.

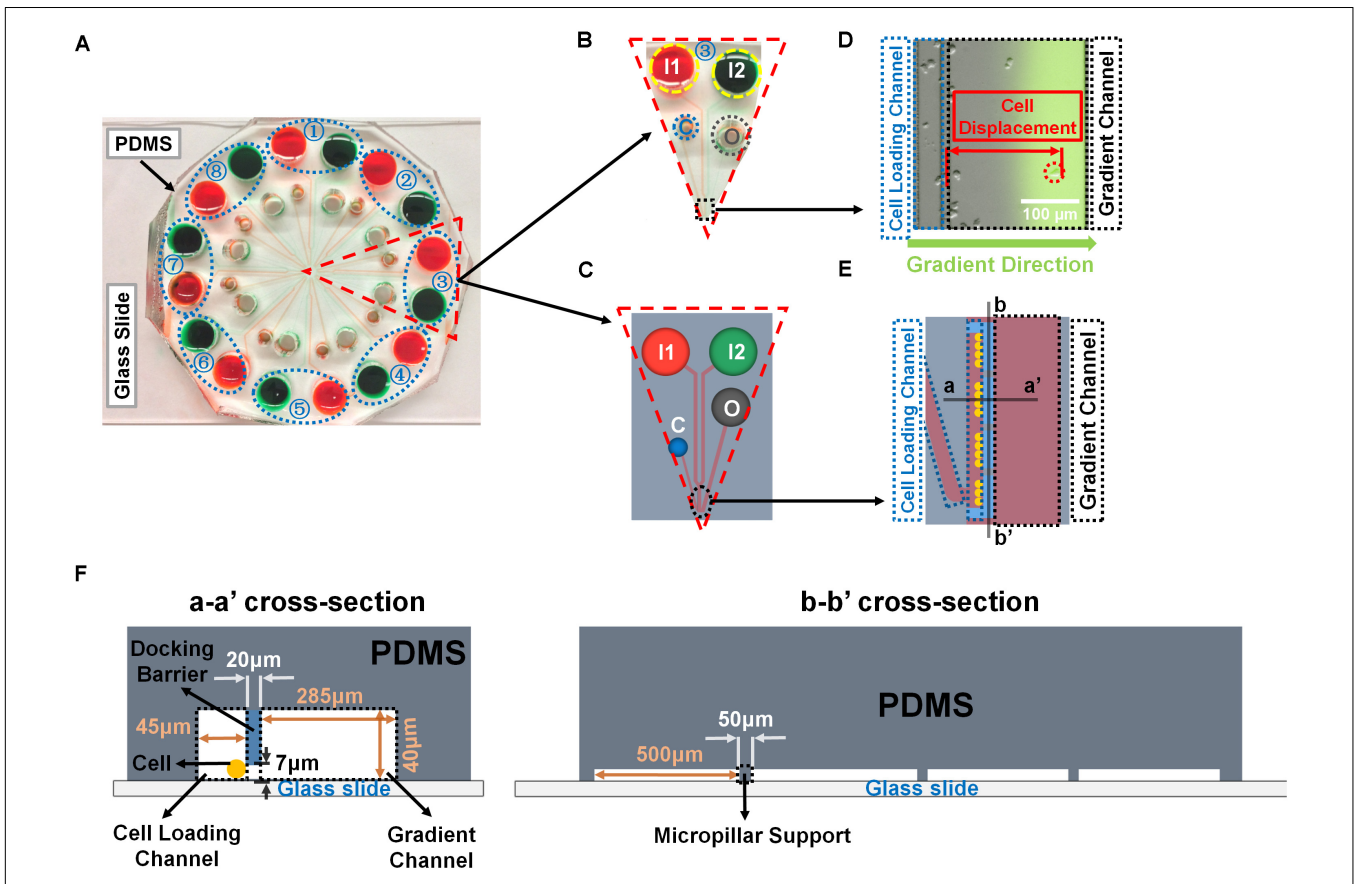

FIGURE 1 | Illustration of the radial microfluidic device and cell migration analysis. **(A)** A representative image of the real radial microfluidic device with colored dyes to show the major networks in each unit. The upper transparent part is PDMS replica, which is bonded onto the bottom part of the glass slide; the blue elliptical-dashed box and the number number (1–8) show the chemical inlets of each independent unit. **(B,C)** Magnified view of the selected unit 3 of A in real device B and in schematic diagram C. I1 and I2: chemical inlets; C: cell loading port; O: waste outlet. **(D)** A representative experimental image to illustrate the data analysis of cell migration displacement in the magnified view of selected black-dashed box in B. **(E)** Magnified view of the black elliptical-dashed box of schematic C. In D and E, the blue- and black-dashed boxes represent the cell loading and gradient channels, respectively; the green arrow indicates the gradient direction; red arrow shows the displacement of an individual migrated cell. **(F)** Cross sectional views to illustrate the detailed designs of the device as indicated in E.

Cell Migration Experiments With the Microfluidic Device

Cells and chemo-attractants were prepared as described above. Cells were loaded into the cell loading ports. Fluorescein isothiocyanate (FITC)-dextran (10 kDa, Sigma-Aldrich, Catalog# FD10S) was added into the chemo-attractant solutions to indicate the gradient profile. DMEM medium and chemo-attractants were injected into the chemical inlet I1 and I2, respectively, to generate the gradient (**Figures 1A–C**). In addition, the two chemical inlets of each unit were covered by silicone oil (Alfa Aesar, Tewksbury, United States, Catalog# A12728-22) in order to balance the pressure difference for better gradient generation as previously described (Wu et al., 2018). The device was then placed under an inverted fluorescence microscope (Nikon Ti-U) inside an environmental controlled chamber (*InVivo* Scientific) at 37°C. Differential interference contrast (DIC) images of cell migration were taken for all the units at 0 and 24 h, respectively. The microfluidic device was incubated inside the incubator when not taking images. The DIC images of cell migration were obtained using NIS Element Viewer (Nikon) and ImageJ software (NIH). Specifically, cells that migrated away from the boundary of docking barrier to the gradient direction inside the gradient channel within the microscope field were recorded, and the displacement of each targeted cell was measured in each group at the end of the experiment using ImageJ (**Figures 1D–F**).

Data Analysis

The data obtained with the Transwell assay was analyzed by GraphPad Prism software, version 8.3.0 (GraphPad Software, Inc., United States). The cell migration data obtained with the microfluidic device was processed by the OriginPro software. Each condition of experiment in this study was independently repeated at least three times. The statistical significant difference (p-value) between the treatment and control groups was determined by Student's t-test.

RESULTS

Optimization of Transwell Cell Migration Assay

To determine the optimal concentration of positive control chemo-attractants for inducing chemotaxis of the monocytes and lymphocytes in Transwell assay, a series of dilution experiments were conducted using MCP-1/CCL2 and SDF-1α/CXCL12. One hundred microliter of 5×10^5 cells diluted in RPMI 1640 medium was seeded into the apical chamber (insert) of Transwell plate, and allowed for migration at 37°C for 24 h. The results showed that THP-1 monocyte migration was gradually increased with increasing MCP-1/CCL2 concentration, and migration efficiency was gradually decreased to close to baseline level after 50 ng/ml MCP-1/CCL2 (**Figure 2A**). The highest percentage of THP-1 cell migration was observed at 50 ng/ml chemokine concentration, and the lowest percentage was with 5 ng/ml of MCP-1/CCL2 using three different cell counting methods. More specifically, the percentage of relative migration (PRM) was observed at 10 ng/ml (PRM: 51.53 ± 5.05%, p = 0.0077), 50 ng/ml (PRM: 78.57 ± 1.44%, p = 0.0007), 100 ng/ml (PRM: 70.41 ± 18.76%, p = 0.0424), and 200 ng/ml (PRM: 37.76 ± 1.45%, p = 0.0037) compared to the DMEM only control (PRM: 7.65 ± 2.16) by counting with hemocytometer. Similar migration behavior was also observed with automated cell counter, and flow cytometry analysis [10 ng/ml (PRM: 52.94 ± 4.16%, p = 0.0111; and PRM: 56.22 ± 6.18%, p = 0.0110), 50 ng/ml (PRM: 80.89 ± 18.72%, p = 0.0476; and PRM: 82.01 ± 9.92%, p = 0.0106), and 200 ng/ml (PRM: 33.82 ± 2.08%, p = 0.0299; and PRM: 43.02 ± 4.96%, p = 0.0153) of MCP-1/CCL2, respectively]. The highest PRM at 50 ng/ml of MCP-1/CCL2 was consistently determined with all three methods. MCP-1/CCL2 concentration higher than the 50 ng/ml diminished the effect of attracting THP-1 cells, and at 200 ng/ml the PRM was close to the baseline. Thus, 50 ng/ml of MCP-1/CCL2 is the best concentration to induce maximum percentage of THP-1 cells migration in conventional Transwell migration assay.

Similarly, the optimal concentration of SDF-1α/CXCL12 for MOLT-4 T-lymphocyte migration in Transwell assay was also determined (**Figure 2B**). The PRM of MOLT-4 T-lymphocyte significantly increased at 100 ng/ml (PRM: 49.64 ± 9.89%, p = 0.0184), and 200 ng/ml (PRM: 53.90 ± 9.19%, p = 0.0098) of SDF-1α/CXCL12 compared to that of DMEM control by counting with hemocytometer. MOLT-4 T-cell was also significantly migrated at 100 ng/ml (PRM: 46.92 ± 7.98%, p = 0.0359) and 200 ng/ml (PRM: 81.41 ± 14.70%, p = 0.0169) with automated cell counter and flow cytometry analysis, respectively. However, the PRM of MOLT-4 was reduced at 200 ng/ml of SDF-1α/CXCL12 by counting with automated cell counter. Because MOLT-4 T-cell significantly migrated at 100 ng/ml of SDF-1α/CXCL12, and the rate of migration was declined at 200 ng/ml by automated cell counter, we selected 100 ng/ml as the optimal concentration to induce maximum percentage of MOLT-4 cell migration in Transwell migration assay. This concentration was also found to be the best in inducing T-lymphocyte migration in earlier studies (Ottoson et al., 2001; Okabe et al., 2005; Tan et al., 2006). Taken together, the optimal concentration of both MCP-1/CCL2 and SDF-1α/CXCL12 were used as positive controls in Transwell and microfluidic device migration assays.

TILRR Overexpression in HeLa Cells Significantly Induced Cytokines/Chemokines Production in Cell Culture Supernatants

To assess whether TILRR overexpression induces the production of cytokines/chemokines in cervical epithelial cells, we transfected HeLa cells with TILRR plasmid DNA as described elsewhere (Kashem et al., 2019). Bio-Plex analysis of HeLa cell culture supernatants demonstrated that TILRR significantly induced the production of IL-6, IL-8/CXCL8, IP-10/CXCL10, RANTES/CCL5 and MCP-1/CCL2 following 24h of incubation in the absence or presence of IL-1β stimulation compared to that of controls (**Supplementary Figure 2**). Thus, overexpression

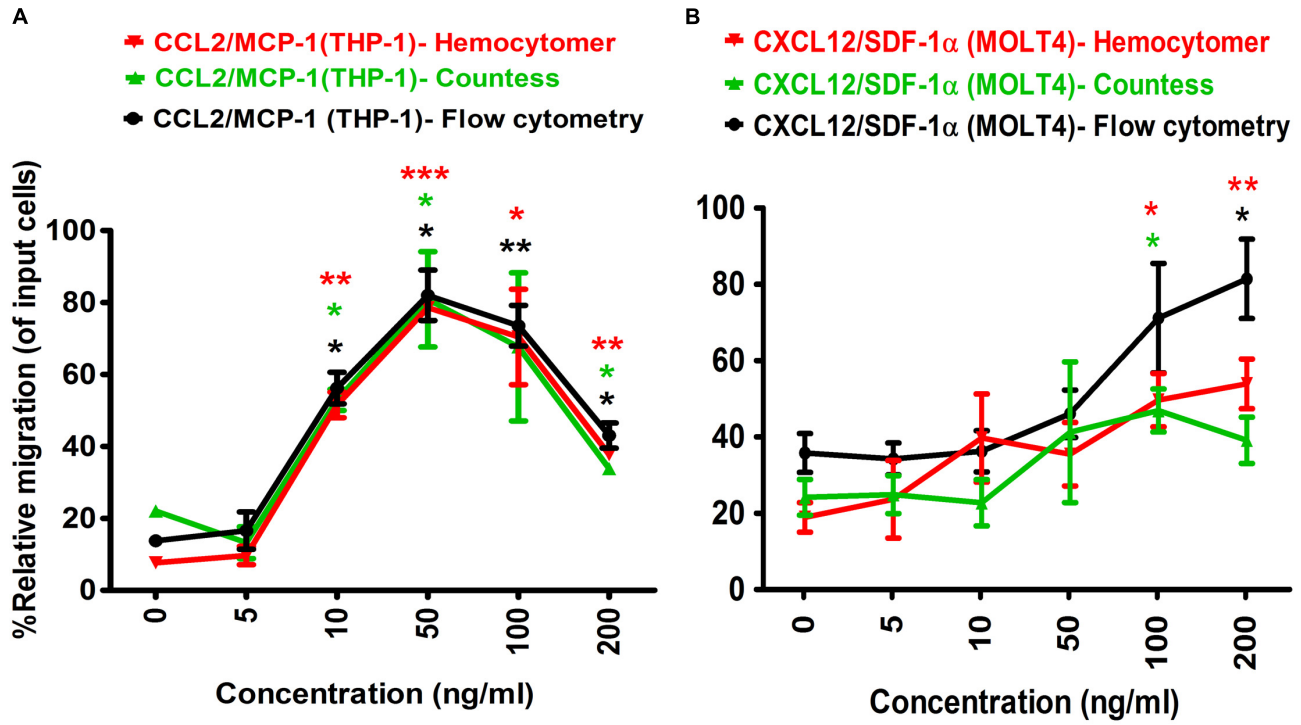

FIGURE 2 | Optimization of positive control chemo-attractants for monocytes and lymphocytes migration using Transwell assay. **(A)** THP-1 monocytes, and **(B)** MOLT-4 T-lymphocytes migration was optimized using known chemo-attractants of MCP-1/CCL2 and SDF-1α/CXCL12, respectively. Chemo-attractants were diluted in DMEM without FBS and antibiotic-antimycotic. Approximately 5.0 × 10^5 cells were used as input cells on upper chamber (insert) of Corning 24-well plate with 5.0 μm pore size polycarbonated membrane and incubated for 24 h. The line graph represents three independent experiments (mean ± SEM) compared to the DMEM base control (0 ng/ml chemo-attractants). Color-coded lines show the different counting methods. Red line and red asterisk' represents hemocytometer count, green line with green asterisk' for automated countess, and black line with black asterisk' indicates flow cytometry count. Statistical comparisons conducted using Student's *t*-test with 95% CI, all $p < 0.05$ were reported and indicated using an asterisks' $^*p < 0.05$, $^{**}p < 0.01$, and $^{***}p < 0.001$. Legend on the top of the figures represents the chemo-attractants, type of cell used and counting method. *X*-axis shows the different concentrations of MCP-1/CCL2 and SDF-1α/CXCL12.

of TILLR in HeLa cells potentiates the production of soluble inflammatory mediators.

The Culture Supernatants of TILRR-Transfected HeLa Cells Significantly Induced Migration of THP-1 Cells in Transwell Assay

To examine if the presence of TILRR-modulated soluble cytokines/chemokines influences the migration of monocytes, Transwell migration assay was conducted using THP-1 monocytes and HeLa cell culture supernatants. The results demonstrated that TILRR-transfected HeLa cell culture supernatants attracted significantly higher amount of THP-1 cells (11–40%) than the controls (**Figures 3A–D**). Data analysis showed that approximately 16-46% higher amount of THP-1 cells were migrated toward the culture supernatants of TILRR-overexpressed HeLa cells compared to the supernatants of empty vector-transfected (PRM: 52.26 ± 6.88% vs. 37.04 ± 3.09%, $p = 0.0250$), non-transfected (PRM: 52.26 ± 6.88% vs. 31.69 ± 9.35%, $p = 0.0373$) HeLa cell supernatants, or DMEM controls (PRM: 52.26 ± 6.88% vs. 6.58 ± 2.49%, $p = 0.0004$) (hemocytometer counts) (**Figure 3B**). Similarly, the migration of significantly higher amount of THP-1 cells (12–39%) was also observed toward TILRR-transfected culture medium than the empty vector-transfected (PRM: 49.39 ± 3.90% vs. 38.04 ± 4.22%, $p = 0.0267$), non-transfected (49.39 ± 3.90% vs. 36.32 ± 5.90%, $p = 0.0328$) HeLa cell supernatants, or DMEM controls (49.39 ± 3.90% vs. 10.96 ± 8.39%, $p = 0.0020$) (automated cell counter methods) (**Figure 3C**). Flow cytometry analysis also showed that the higher numbers of THP-1 cells migrated toward TILRR-transfected culture medium (11-35%) than the controls (**Figure 3D**). Thus, the supernatants of TILRR-overexpressed HeLa cells attracted the THP-1 monocytes.

The Culture Supernatants of TILRR-Transfected HeLa Cells Significantly Induced Migration of MOLT-4 T-lymphocytes in Transwell Assay

To assess whether the supernatants of TILRR-overexpressed HeLa cells attract T-lymphocytes, MOLT-4 cell migration was conducted using similar approach. MOLT-4 cells were also showed higher PRM (14-17%) toward TILRR-modulated

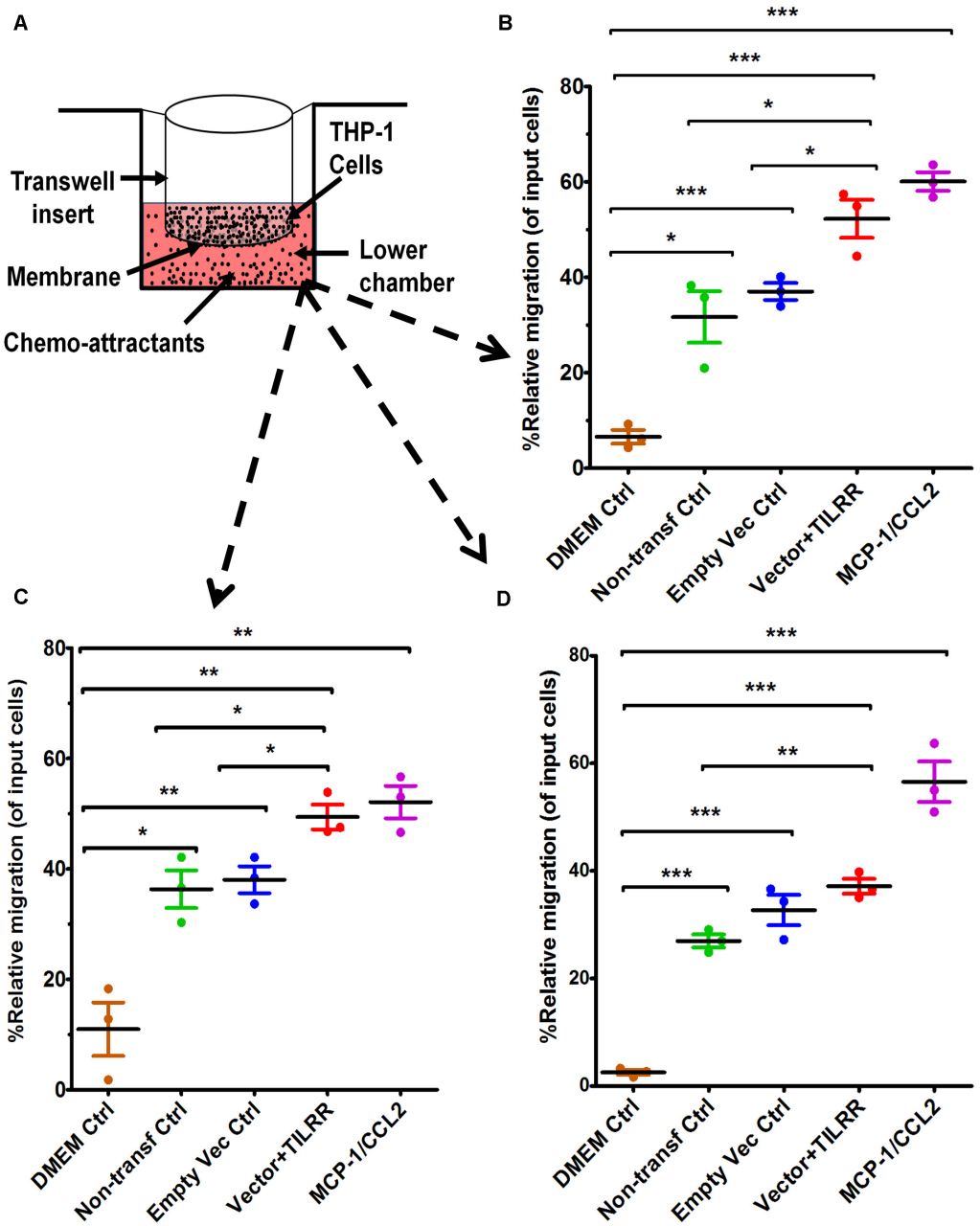

FIGURE 3 | THP-1 monocytes migration toward TILRR-modulated cervical cell culture supernatants in Transwell assay. **(A)** Representative image of polycarbonated membrane Transwell unit. Approximately 5.0 × 10^5 THP-1 cells were used as input cells on the upper chamber, and 600 μl of each chemo-attractant was dispensed in the bottom chamber of Transwell plate as described in materials and methods section. MCP-1/CCL2 (50 ng/ml) was used as a positive control chemo-attractant. Corning 24-well plate with 5.0 μm pore membrane used to conduct migration assay for 24 h. The migrated cells were counted with three independent counting methods, **(B)** hemocytometer, **(C)** automated countess, and **(D)** flow cytometry. Scatter dot plots represent the percent relative migration of cells in the presence of TILRR-transfected HeLa cell culture supernatants compared to the empty vector- and non-transfected control supernatants, and DMEM control. The data represent mean ± SEM of three independent experiments. Statistical comparisons conducted using Student's *t*-test with 95% CI, all $p < 0.05$ were reported and indicated using an asterisks' $^*p < 0.05$, $^{**}p < 0.01$, and $^{***}p < 0.001$. *X*-axis indicates the condition of chemo-attractants.

HeLa cell culture supernatants compared to that of controls (**Figures 4A–D**). Approximately 16–19% higher amount of MOLT-4 cells were significantly attracted to TILRR-overexpressed HeLa cell supernatants than the supernatants of empty vector-transfected (PRM: 27.63 ± 3.57% vs. 11.67 ± 1.17%, $p = 0.0018$), non-transfected (PRM: 27.63 ± 3.57% vs. 8.95 ± 2.94%, $p = 0.0022$) cells, or DMEM control (PRM: 27.63 ± 3.57% vs. 8.95 ± 1.78%, $p = 0.0013$) (hemocytometer counting method) (**Figure 4B**). Similar trend of MOLT-4 cell migration was observed

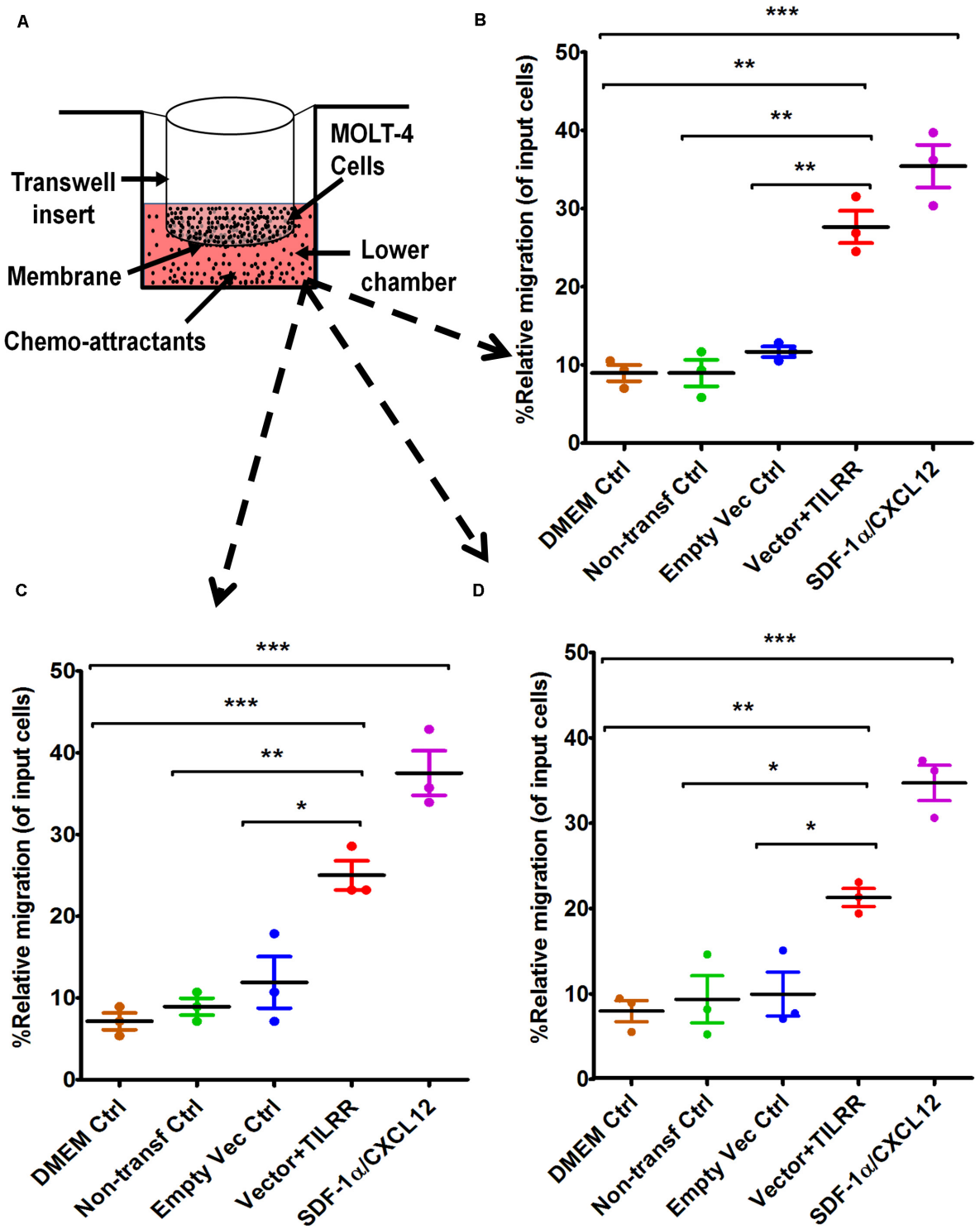

FIGURE 4 | MOLT-4 T-lymphocytes migration toward TILRR-modulated cell culture supernatants in Transwell assay. **(A)** Representative image of polycarbonated-membrane Transwell unit. Approximately 5.0 × 10^5 MOLT-4 lymphocytes cells were used, and 600 μl of culture media or positive control chemo-attractant slowly dispensed into the Transwell plate (bottom chamber) as described in materials and methods section. SDF-1α/CXCL12 (100 ng/ml) was used as a positive control. Similar Transwell plate (as THP-1) used to conduct migration of MOLT-4 cells for 24 h. The migrated cells were counted with three independent counting methods such as **(B)** hemocytometer, **(C)** automated countess, and **(D)** flow cytometry. Scatter dot plots represent the percent relative migration of cells in the presence of TILRR-transfected HeLa cell culture supernatants compared to the empty vector- and non-transfected control supernatants, and DMEM control. The data represent mean ± SEM of three independent experiments. Statistical comparisons conducted using Student's *t*-test with 95% CI, all $p < 0.05$ were reported and indicated using an asterisks' $^*p < 0.05$, $^{**}p < 0.01$, and $^{***}p < 0.001$. *X*-axis indicates the condition of chemo-attractants.

by automated cell counter and flow cytometry analysis where the PRM was observed approximately 14–18% and 12–14% higher in TILRR-overexpressed HeLa cell culture supernatants than that of controls, respectively (**Figures 4C,D**). Collectively, these data showed that the supernatants of TILRR-overexpressed HeLa cells also attract T-lymphocytes.

The Culture Supernatants of TILRR-Transfected HeLa Cells Significantly Induced Migration of THP-1 Monocytes by the Microfluidic Device Analysis

Because Transwell assay does not provide the data on how far (directional displacement) a cell can migrate toward the HeLa cell culture supernatants, we next sought to examine the displacement of THP-1 monocytes from their original location toward the gradient of culture supernatants by a novel microfluidic device. The microfluidic device offers better controlled chemical gradient with single cell analysis, which enables the data analysis of the displacement and distribution of individual migrated cell during the experiment. The results showed that TILRR-overexpressed HeLa cell culture supernatants attracted more THP-1 cells with significantly higher average cell displacement compared to the controls (**Figures 5A–E**). Furthermore, our data showed that THP-1 cells migrated further to the supernatants of TILRR-overexpressed HeLa cells in comparison to the supernatants of the empty vector-transfected HeLa cells (52.00 ± 52.00 vs. 34.00 ± 48.00 μm, $p = 0.0180$), non-transfected HeLa cells (52.00 ± 52.00 vs. 28.00 ± 29.00 μm, $p < 0.0001$), or DMEM control (52.00 ± 52.00 vs. 19.00 ± 23.00 μm, $p < 0.0001$) (**Figure 5E**). Thus, the TILRR-transfected HeLa cell supernatants promoted migration of THP-1 monocytes in microfluidic device assay.

The Culture Supernatants of TILRR-Transfected HeLa Cells Significantly Induced Migration of MOLT-4 T-lymphocytes by the Microfluidic Device Analysis

We also evaluated the effect of the culture supernatants of TILRR-transfected HeLa cells on the migration of MOLT-4 T-lymphocyte with the microfluidic device. The results showed that TILRR-overexpressed culture supernatants also attracted more MOLT-4 cells with significantly higher average cell displacement (**Figures 6A–E**). Similar to the THP-1 cells, MOLT-4 T-lymphocytes migrated further toward the supernatants of TILRR-overexpressed HeLa cells compared to the supernatants of empty vector-transfected HeLa cells (25.00 ± 10.00 vs. 19.00 ± 8.00 μm, $p < 0.0001$), non-transfected (25.00 ± 10.00 vs. 20.00 ± 13.00 μm, $p = 0.0025$) HeLa cells, or DMEM control (25.00 ± 10.00 vs. 14.00 ± 3.00 μm, $p < 0.0001$) (**Figure 6E**). Thus, TILRR-transfected HeLa cell supernatants also promoted MOLT-4 T-lymphocytes migration with microfluidic device assay.

DISCUSSION

Our previous study showed that TILRR regulates the expression of many inflammation-responsive genes in NF-κB signaling pathways, and influences the production of multiple pro-inflammatory mediators in cervical and vaginal mucosal epithelial cell lines (Kashem et al., 2019). Because TILRR expression promoted the production of several cytokines/chemokines in cervical epithelial cell lines, we investigated the effect of the supernatants of the TILRR-overexpressed HeLa cells on the migration of immune cells in this study using Transwell and microfluidic device assays. Our data showed that the supernatants of TILRR-overexpressed HeLa cells attracted migration of THP-1 and MOLT-4 cells in Transwell assay. In addition, with a novel microfluidic assay, we demonstrated that the THP-1 and MOLT-4 cells migrated further toward the supernatants of the TILRR-overexpressed HeLa cells. THP-1 cells (monocytes) and MOLT-4 cells (T cells) are CD4-expressing cells, the targets of HIV-1 (Berger et al., 1998; Verani et al., 1998; Borrajo et al., 2019). Thus, the supernatants of TILRR-overexpressed HeLa cells, containing multiple pro-inflammatory cytokines (Kashem et al., 2019), attracts HIV-1 target cells.

The purpose of using two different cell migration techniques in this study was to confirm the study findings in parallel. Traditional Transwell assay was used to analyze the ability of the cells to migrate through a porous membrane accompanied by the relative percentage of total cell migration toward the gradients of HeLa cell culture supernatants. Traditional Transwell assay is convenient, and compatible with all kinds of cell types, and most widely used sensitive quantification of *in vitro* cell migration technique (Boyden, 1962). However, Transwell assay does not provide how far a single cell can migrate toward the added chemo-attractants. Despite the popularity and advantages of Transwell for cell migration study, this assay only offers the endpoint readout of entire number of cells without providing other important migratory aspects on individual cell level. In order to fill the gap and exclude the possible effect on the gravity force of loaded cells during experiment, we applied a novel microfluidic device to further confirm the attraction effect of the same supernatants on the migration of THP-1 and MOLT-4 cells. Specifically, this microfluidic device enables eight independent experiment groups conducted simultaneously, which dramatically increased the experimental throughput. Unlike other microfluidic device that requires the external input such as pumps to generate and maintain a stable chemical gradient, this device offers stable chemical gradient generated by the pressure differences between the chemical inlets and waste outlets in a well-controlled manner (Wu et al., 2018). In addition, the advanced cell docking design provides the initial alignment of all the loaded cells in the cell-loading channel at the beginning, which increases the accuracy of displacement measurement on each individual migrated cell during the experiment. On the other hand, the presence of the docking barrier requires all loaded cells to transform the cell size to squeeze and horizontally migrate through the area when stimulated by the chemical gradient, which excludes the gravity issue that may exist in Transwell assay. Microfluidic devices have been widely applied

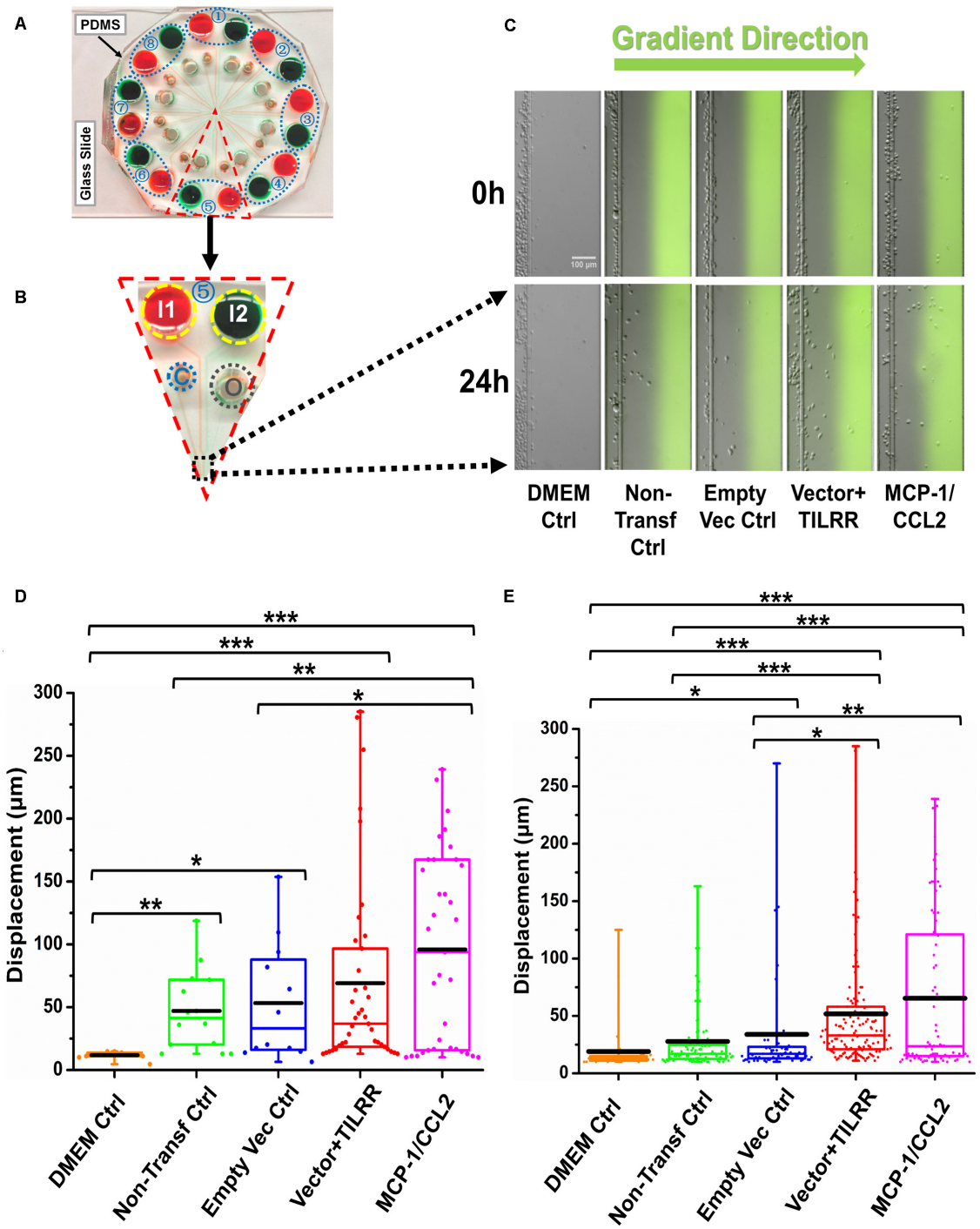

FIGURE 5 | THP-1 monocytes migration toward TILRR-modulated cell culture supernatants in microfluidic device. **(A)** A representative image of the real radial microfluidic device with colored dyes to show the major networks in each unit. The upper transparent part is PDMS replica, which is bonded onto the bottom part of the glass slide; the blue elliptical-dashed box and the number (1–8) show the chemical inlets of each independent unit. **(B)** One magnified triangular unit (randomly selected) from A showing the black-dashed square area from where migrated cells were analyzed. I1 and I2: chemical inlets; C: cell loading port; O: waste outlet. **(C)** Representative images of the migration of THP-1 cells in different conditions at 0 and 24 h analyzed from B. Green color in the image of all experimental conditions except DMEM control indicates the profile and most concentrated area of chemical gradient. **(D)** The colored box plots show the total displacement of each cell in the corresponding experimental groups in C. **(E)** The colored box plots show the total displacement of each cell in three independent experiments. The top and bottom of the whisker show the maximum and minimum value; the box shows the migrated cells within the range from 25% to 75% of total cells based on the ranked displacement value; the black bold line indicates the mean displacement. The data in different groups were compared using Student's *t*-test with 95% CI, all $p < 0.05$ were reported and indicated using asterisks' $^{*}p < 0.05$, $^{**}p < 0.01$, and $^{***}p < 0.001$.

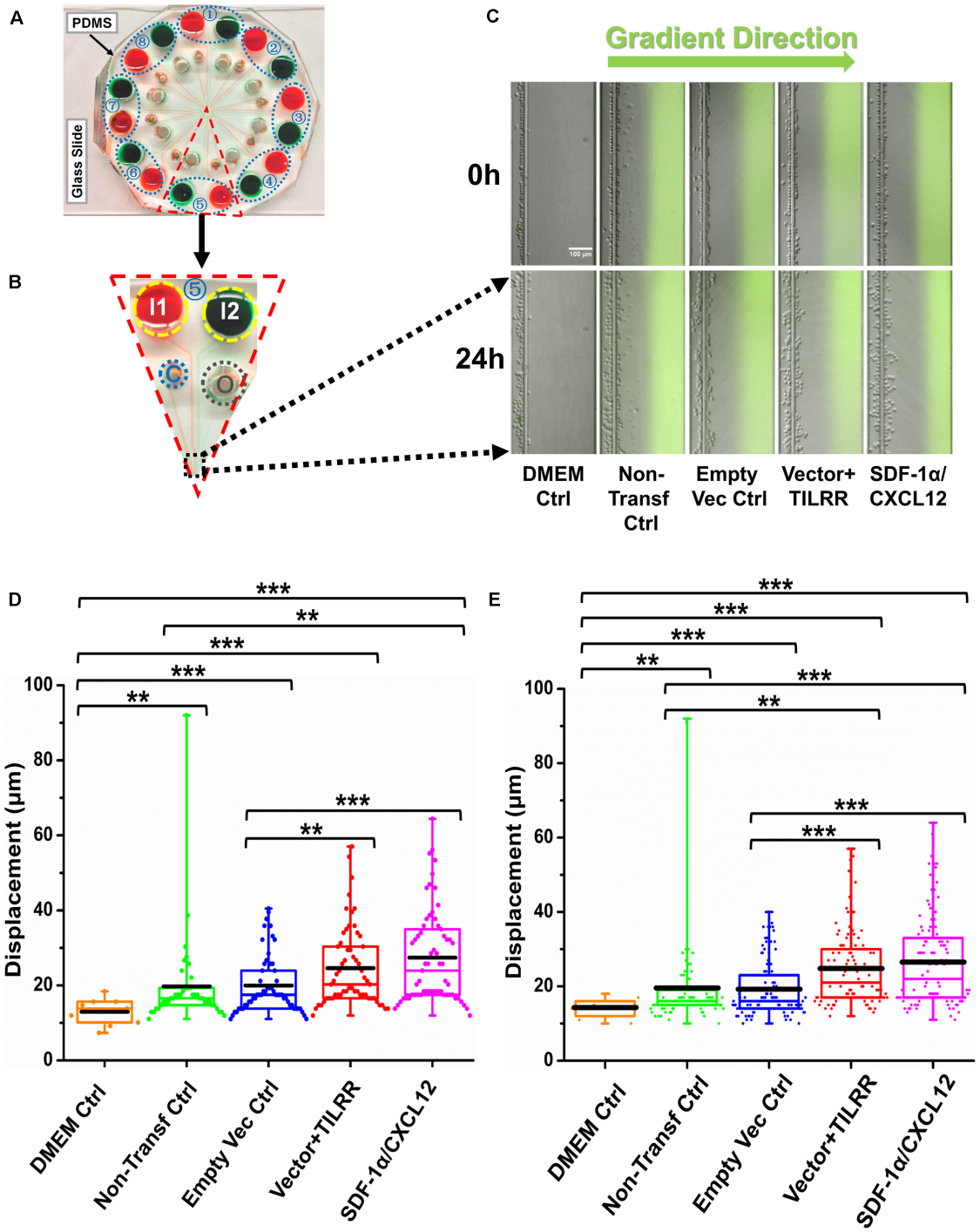

FIGURE 6 | MOLT-4 T cells migration toward TILRR-modulated cell culture supernatants in microfluidic device. **(A)** A representative image of the real radial microfluidic device with colored dyes to show the major networks in each unit. The upper transparent part is PDMS replica, which is bonded onto the bottom part of the glass slide; the blue elliptical-dashed box and the number (1–8) show the chemical inlets of each independent unit. **(B)** One magnified triangular unit (randomly selected) from A showing the black-dashed square area from where migrated cells were analyzed. I1 and I2: chemical inlets; C: cell loading port; O: waste outlet. **(C)** Representative images of the migration of THP-1 cells in different groups at 0 and 24 h analyzed from B. Green color image of all experimental conditions except DMEM control indicates the profile and most concentrated area of chemical gradient. **(D)** The colored box plots show the total displacement of each cell in the corresponding experiment conditions in C. **(E)** The colored box plots show the total displacement of each cell in three independent experiments. The top and bottom of the whisker show the maximum and minimum value; the box shows the migrated cells within the range from 25% to 75% of total cells based on the ranked displacement value; the black bold line indicates the mean displacement. The data in different groups were compared using Student's *t*-test with 95% CI, all $p < 0.05$ were reported and indicated using asterisks' $^{*}p < 0.05$, $^{**}p < 0.01$, and $^{***}p < 0.001$.

for cell migration studies because of several advantages, including extremely low cell and reagent consumption, stable chemical gradient generation, and live-cell tracking. Due to the versatile features of the microfluidic device, many important properties of individual migrated cell such as speed and displacement can be extracted from the migration experiment (Ren et al., 2017). Therefore, the combination of these two techniques in our experimental settings confirmed that immune cells, the HIV-1 target cells, were successfully migrated to the TILRR-overexpressed HeLa cell culture supernatants.

Studies have shown that pro-inflammatory cytokines/chemokines produced from female genital epithelial cells induce rapid influx of HIV-1 target cells leading to inflammation (Kaul et al., 2008a,b, 2015; Li et al., 2009; Haase, 2010). The elevated levels of cytokines/chemokines IL-8/CXCL8, MIP-1α/CCL3, and MIP-1β/CCL4 are strongly associated with the recruitment of monocytes/macrophages and neutrophils in female genital secretion (Fichorova et al., 2001). Our study showed that TILRR plays an important role in regulating this pro-inflammatory cytokine environment and immune cell infiltration in cervical epithelial tissue. TILRR could promote the migration of immune cells, especially the HIV-1 target cells, in the female genital epithelium through the modulation of pro-inflammatory cytokines/chemokines secretion, resulting in increased risk of vaginal HIV-1 infection and transmission. Thus, TILRR-promoted migration of immune cells warrants further studies.

While our *in vitro* study was the first to suggest the important role of TILRR in immune cell migration, the limitation of the current work is that it is the first insight based on *in vitro* systems and a follow up *in vivo* study will be an important future direction. Future studies using *in vivo* model, such as mouse model or macaque model (Rhesus macaque [*Macaca mulatta*]) will help to understand the novel role of TILRR in promoting migration of immune cells into genital epithelial tissues. The *in vivo* model(s) can further be combined with using human cervical biopsy samples. Collectively, these potential future studies as follow-up of the current work may identify new intervention technology to control TILRR-induced immune cell infiltration to the epithelial tissues, and inflammation-induced vaginal HIV-1 infection.

CONCLUSION

TILRR-modulated cytokines/chemokines from HeLa cells promote the migration of immune cells. We are the first to show that TILRR can regulate migration of HIV-1 target cells into cervical epithelial tissues. Targeting TILRR may lead to new interventions in reducing vaginal HIV-1 infection.

DATA AVAILABILITY STATEMENT

All datasets generated for this study are included in the article/**Supplementary Material**.

AUTHOR CONTRIBUTIONS

FP and ML acquired the funding. MK, ML, and FL conceived and designed the research. MK and XR performed the research, analyzed the data, and wrote the manuscript. ML and FL supervised the research. ML, FL, HL, BL, and LL edited the manuscript. MK revised, formatted and submitted to the journal. All the authors have approved this manuscript.

FUNDING

The study was funded by an operating grant from Canadian Institutes of Health Research (CIHR), operating grant - PA: CHVI Vaccine Discovery and Social Research (http://www.cihr-irsc.gc.ca/e/193.html) and by a discovery grant from the Natural Sciences and Engineering Research Council of Canada (NSERC) (RGPIN-2014-04789).

ACKNOWLEDGMENTS

We thank Dr. Matthew Gilmour, Director General, National Microbiology Laboratory, Manitoba, Canada, for his support for this study. We thank the NIH AIDS reagent program, United States, for providing the HeLa, THP-1 and MOLT-4 cells. We also acknowledge and thank National Microbiology Laboratory, and Children's Hospital Research Institute of Manitoba, Canada for their financial support. XR thanks the GETS Award at University of Manitoba for financial support.

SUPPLEMENTARY MATERIAL

The Supplementary Material for this article can be found online at: https://www.frontiersin.org/articles/10.3389/fcell.2020.00563/full#supplementary-material

REFERENCES

Arnold, K. B., Burgener, A., Birse, K., Romas, L., Dunphy, L. J., Shahabi, K., et al. (2016). Increased levels of inflammatory cytokines in the female reproductive tract are associated with altered expression of proteases, mucosal barrier proteins, and an influx of HIV-susceptible target cells. *Mucos. Immunol.* 9, 194–205. doi: 10.1038/mi.2015.51

Berger, E. A., Doms, R. W., Fenyo, E. M., Korber, B. T., Littman, D. R., Moore, J. P., et al. (1998). A new classification for HIV-1. *Nature* 391:240. doi: 10.1038/34571

Blanco, J., Bosch, B., Fernandez-Figueras, M. T., Barretina, J., Clotet, B., and Este, J. A. (2004). High level of coreceptor-independent HIV transfer induced by contacts between primary CD4 T cells. *J. Biol. Chem.* 279, 51305–51314. doi: 10.1074/jbc.M408547200

Borrajo, A., Ranazzi, A., Pollicita, M., Bellocchi, M. C., Salpini, R., Mauro, M. V., et al. (2019). Different patterns of HIV-1 replication in MACROPHAGES is led by co-receptor usage. *Medicina* 55:297. doi: 10.3390/medicina55060297

Boyden, S. (1962). The chemotactic effect of mixtures of antibody and antigen on polymorphonuclear leucocytes. *J. Exp. Med.* 115, 453–466. doi: 10.1084/jem.115.3.453

Cadena-Herrera, D., Esparza-De Lara, J. E., Ramirez-Ibanez, N. D., Lopez-Morales, C. A., Perez, N. O., Flores-Ortiz, L. F., et al. (2015). Validation of three viable-cell counting methods: manual, semi-automated, and automated. *Biotechnol. Rep.* 7, 9–16. doi: 10.1016/j.btre.2015.04.004

Cassol, E., Alfano, M., Biswas, P., and Poli, G. (2006). Monocyte-derived macrophages and myeloid cell lines as targets of HIV-1 replication and persistence. *J. Leukoc. Biol.* 80, 1018–1030. doi: 10.1189/jlb.0306150

Dejucq, N. (2000). HIV-1 replication in CD4+ T cell lines: the effects of adaptation on co-receptor use, tropism, and accessory gene function. *J. Leukoc. Biol.* 68, 331–337.

Dejucq, N., Simmons, G., and Clapham, P. R. (1999). Expanded tropism of primary human immunodeficiency virus type 1 R5 strains to CD4(+) T-cell lines determined by the capacity to exploit low concentrations of CCR5. *J. Virol.* 73, 7842–7847. doi: 10.1128/jvi.73.9.7842-7847.1999

Fichorova, R. N., Tucker, L. D., and Anderson, D. J. (2001). The molecular basis of nonoxynol-9-induced vaginal inflammation and its possible relevance to human immunodeficiency virus type 1 transmission. *J. Infect. Dis.* 184, 418–428. doi: 10.1086/322047

Guo, H., Gao, J., Taxman, D. J., Ting, J. P., and Su, L. (2014). HIV-1 infection induces interleukin-1beta production via TLR8 protein-dependent and NLRP3 inflammasome mechanisms in human monocytes. *J. Biol. Chem.* 289, 21716–21726. doi: 10.1074/jbc.M114.566620

Haase, A. T. (2010). Targeting early infection to prevent HIV-1 mucosal transmission. *Nature* 464, 217–223. doi: 10.1038/nature08757

Huang, X., Xiong, M., Jin, Y., Deng, C., Xu, H., An, C., et al. (2016). Evidence that high-migration drug-surviving MOLT4 leukemia cells exhibit cancer stem cell-like properties. *Intern. J. Oncol.* 49, 343–351. doi: 10.3892/ijo.2016.3526

Kashem, M. A., Li, H., Toledo, N. P., Omange, R. W., Liang, B., Liu, L. R., et al. (2019). Toll-like interleukin 1 receptor regulator is an important modulator of inflammation responsive genes. *Front. Immunol.* 10:272. doi: 10.3389/fimmu.2019.00272

Kaul, R., Pettengell, C., Sheth, P. M., Sunderji, S., Biringer, A., MacDonald, K., et al. (2008a). The genital tract immune milieu: an important determinant of HIV susceptibility and secondary transmission. *J. Reprod. Immunol.* 77, 32–40. doi: 10.1016/j.jri.2007.02.002

Kaul, R., Rebbapragada, A., Hirbod, T., Wachihi, C., Ball, T. B., Plummer, F. A., et al. (2008b). Genital levels of soluble immune factors with anti-HIV activity may correlate with increased HIV susceptibility. *AIDS* 22, 2049–2051. doi: 10.1097/QAD.0b013e328311ac65

Kaul, R., Prodger, J., Joag, V., Shannon, B., Yegorov, S., Galiwango, R., et al. (2015). Inflammation and HIV transmission in sub-saharan Africa. *Curr. HIV/AIDS Rep.* 12, 216–222. doi: 10.1007/s11904-015-0269-5

Konopka, K., and Duzgunes, N. (2002). Expression of CD4 controls the susceptibility of THP-1 cells to infection by R5 and X4 HIV type 1 isolates. *AIDS Res. Hum. Retrovirus.* 18, 123–131. doi: 10.1089/08892220252779665

Li, Q., Estes, J. D., Schlievert, P. M., Duan, L., Brosnahan, A. J., Southern, P. J., et al. (2009). Glycerol monolaurate prevents mucosal SIV transmission. *Nature* 458, 1034–1038. doi: 10.1038/nature07831

Lodge, R., Gilmore, J. C., Ferreira Barbosa, J. A., Lombard-Vadnais, F., and Cohen, E. A. (2017). Regulation of CD4 receptor and HIV-1 entry by microRNAs-221 and -222 during differentiation of THP-1 cells. *Viruses* 10:e010013. doi: 10.3390/v10010013

Louis, K. S., and Siegel, A. C. (2011). Cell viability analysis using trypan blue: manual and automated methods. *Methods Mol. Biol.* 740, 7–12. doi: 10.1007/978-1-61779-108-6_2

Luo, M., Sainsbury, J., Tuff, J., Lacap, P. A., Yuan, X. Y., Hirbod, T., et al. (2012). A genetic polymorphism of FREM1 is associated with resistance against HIV infection in the Pumwani sex worker cohort. *J. Virol.* 86, 11899–11905. doi: 10.1128/JVI.01499-12

Masson, L., Passmore, J. A., Liebenberg, L. J., Werner, L., Baxter, C., Arnold, K. B., et al. (2015). Genital inflammation and the risk of HIV acquisition in women. *Clin. Infect. Dis.* 61, 260–269. doi: 10.1093/cid/civ298

Melo, R. C. C., Longhini, A. L., Bigarella, C. L., Baratti, M. O., Traina, F., Favaro, P., et al. (2014). CXCR7 is highly expressed in acute lymphoblastic leukemia and potentiates CXCR4 response to CXCL12. *PLoS One* 9:e85926. doi: 10.1371/journal.pone.0085926

Miyake, H., Iizawa, Y., and Baba, M. (2003). Novel reporter T-cell line highly susceptible to both CCR5- and CXCR4-using human immunodeficiency virus type 1 and its application to drug susceptibility tests. *J. Clin. Microbiol.* 41, 2515–2521. doi: 10.1128/jcm.41.6.2515-2521.2003

Mueller, A., and Strange, P. G. (2004). The chemokine receptor, CCR5. *Intern. J. Biochem. Cell Biol.* 36, 35–38. doi: 10.1016/s1357-2725(03)00172-9

Okabe, S., Fukuda, S., Kim, Y. J., Niki, M., Pelus, L. M., Ohyashiki, K., et al. (2005). Stromal cell-derived factor-1alpha/CXCL12-induced chemotaxis of T cells involves activation of the RasGAP-associated docking protein p62Dok-1. *Blood* 105, 474–480. doi: 10.1182/blood-2004-03-0843

Ottoson, N. C., Pribila, J. T., Chan, A. S., and Shimizu, Y. (2001). Cutting edge: T cell migration regulated by CXCR4 chemokine receptor signaling to ZAP-70 tyrosine kinase. *J. Immunol.* 167, 1857–1861. doi: 10.4049/jimmunol.167.4.1857

Pioli, P. D. (2019). *Protocol: Hemocytometer Cell Counting*. Available online at: https://Med.Wmich.Edu/Sites/Default/Files/Hemacytometer_Cell_Counting.Pdf (accessed March 4, 2020).

Ren, X., Alamri, A., Hipolito, J., Lin, F., and Kung, S. K. P. (2020). Applications of microfluidic devices in advancing NK-cell migration studies. *Methods Enzymol.* 631, 357–370. doi: 10.1016/bs.mie.2019.05.052

Ren, X., Levin, D., and Lin, F. (2017). Cell migration research based on organ-on-chip-related approaches. *Micromachines* 8:324. doi: 10.3390/mi8110324

Ren, X., Wu, J., Levin, D., Santos, S., de Faria, R. L., Zhang, M., et al. (2019). Sputum from chronic obstructive pulmonary disease patients inhibits T cell migration in a microfluidic device. *Ann. N. Y. Acad. Sci.* 1445, 52–61. doi: 10.1111/nyas.14029

Smith, S. A., Samokhin, A. O., Alfadi, M., Murphy, E. C., Rhodes, D., Holcombe, W. M. L., et al. (2017). The IL-1RI co-receptor TILRR (FREM1 Isoform 2) Controls aberrant inflammatory responses and development of vascular Disease. *JACC Basic Transl. Sci.* 2, 398–414. doi: 10.1016/j.jacbts.2017.03.014

Tan, Y., Du, J., Cai, S., Li, X., Ma, W., Guo, Z., et al. (2006). Cloning and characterizing mutated human stromal cell-derived factor-1 (SDF-1): C-terminal alpha-helix of SDF-1alpha plays a critical role in CXCR4 activation and signaling, but not in CXCR4 binding affinity. *Exper. Hematol.* 34, 1553–1562. doi: 10.1016/j.exphem.2006.07.001

Ushijima, H., Dairaku, M., Honma, H., Yamaguchi, K., Shimizu, H., Tsuchie, H., et al. (1991). Human immunodeficiency virus infection in cells of myeloid-monocytic lineage. *Microbiol. Immunol.* 35, 487–492. doi: 10.1111/j.1348-0421.1991.tb01579.x

Verani, A., Pesenti, E., Polo, S., Tresoldi, E., Scarlatti, G., Lusso, P., et al. (1998). CXCR4 is a functional coreceptor for infection of human macrophages by CXCR4-dependent primary HIV-1 isolates. *J. Immunol.* 161, 2084–2088.

Wira, C. R., Fahey, J. V., Sentman, C. L., Pioli, P. A., and Shen, L. (2005). Innate and adaptive immunity in female genital tract: cellular responses and interactions. *Immunol. Rev.* 206, 306–335. doi: 10.1111/j.0105-2896.2005.00287.x

Wu, J., Kumar-Kanojia, A., Hombach-Klonisch, S., Klonisch, T., and Lin, F. (2018). A radial microfluidic platform for higher throughput chemotaxis studies with individual gradient control. *Lab Chip.* 18, 3855–3864. doi: 10.1039/C8LC00981C

Zhang, X., Pino, G. M., Shephard, F., Kiss-Toth, E., and Qwarnstrom, E. E. (2012). Distinct control of MyD88 adapter-dependent and Akt kinase-regulated responses by the interleukin (IL)-1RI co-receptor, TILRR. *J. Biol. Chem.* 287, 12348–12352. doi: 10.1074/jbc.C111.321711

Zhang, X., Shephard, F., Kim, H. B., Palmer, I. R., McHarg, S., Fowler, G. J., et al. (2010). TILRR, a novel IL-1RI co-receptor, potentiates MyD88 recruitment to control Ras-dependent amplification of NF-kappaB. *J. Biol. Chem.* 285, 7222–7232. doi: 10.1074/jbc.M109.073429

Conflict of Interest: The authors declare that the research was conducted in the absence of any commercial or financial relationships that could be construed as a potential conflict of interest.

frontiers in Cell and Developmental Biology

BRIEF RESEARCH REPORT
published: 07 July 2020
doi: 10.3389/fcell.2020.00590

Endothelial-Derived Interleukin-1α Activates Innate Immunity by Promoting the Bactericidal Activity of Transendothelial Neutrophils

Xiaoye Liu[1,2,3], Hui Zhang[1], Shangwen He[1], Xiang Mu[1], Ge Hu[1]* and Hong Dong[1]**

[1] Beijing Traditional Chinese Veterinary Engineering Center and Beijing Key Laboratory of Traditional Chinese Veterinary Medicine, Beijing University of Agriculture, Beijing, China, [2] Department of Mechanics and Engineering Science, College of Engineering, Academy for Advanced Interdisciplinary Studies, and Beijing Advanced Innovation Center for Engineering Science and Emerging Technology, College of Engineering, Peking University, Beijing, China, [3] Beijing Advanced Innovation Center for Food Nutrition and Human Health, College of Veterinary Medicine, China Agricultural University, Beijing, China

OPEN ACCESS

Edited by:
Hao Sun,
University of California, San Diego, United States

Reviewed by:
Lidija Radenovic,
University of Belgrade, Serbia
Takashi Kato,
Johns Hopkins University, United States

***Correspondence:**
Xiaoye Liu
xiaoyeliu@pku.edu.cn
Ge Hu
huge@bua.edu.cn
Hong Dong
donghongbua@163.com

Specialty section:
This article was submitted to Cell Adhesion and Migration, a section of the journal Frontiers in Cell and Developmental Biology

Received: *22 April 2020*
Accepted: *17 June 2020*
Published: *07 July 2020*

Citation:
Liu X, Zhang H, He S, Mu X, Hu G and Dong H (2020) Endothelial-Derived Interleukin-1α Activates Innate Immunity by Promoting the Bactericidal Activity of Transendothelial Neutrophils. Front. Cell Dev. Biol. 8:590. doi: 10.3389/fcell.2020.00590

Migration of neutrophils across endothelial barriers to capture and eliminate bacteria is served as the first line of innate immunity. Bacterial virulence factors damage endothelium to produce inflammatory cytokines interacts with neutrophils. However, the mechanisms that behind endothelial-neutrophil interaction impact on the bactericidal activity remain unclear. Therefore, we aimed to find the target proteins on endothelial cells that triggered the bactericidal activity of transendothelial neutrophils. Herein, we built the infected models on rats and endothelial-neutrophil co-cultural system (Transwell) and discovered that endothelial-derived IL-1α promoted the survival of rats under *Escherichia coli* infection and enhanced the bactericidal activity of transendothelial neutrophils *in vivo* and *in vitro*. Results further showed that IL-1α was inhibited by lipopolysaccharide (LPS) in the endothelial-neutrophil interaction. We found that LPS mainly damaged cell membrane and induced cell necrosis to interrupt neutrophil migration from endothelial barrier. Thus, we used the isobaric tags for relative and absolute quantification (iTRAQ) method to identify different proteins of endothelial cells. Results showed that IL-1α targeted cellular plasma membrane, endoplasmic reticulum and mitochondrial envelope and triggered eleven common proteins to persistently regulate. During the early phase, IL-1α triggered the upregulation of cell adhesion molecules (CAMs) to promote neutrophil adhesion, while oxidative phosphorylation was involved in long time regulation to induce transmigration of neutrophils against bacteria. Our results highlight the critical mechanism of endothelial-derived IL-1α on promoting bactericidal activity of transendothelial neutrophils and the findings of IL-1α triggered proteins provide the potentially important targets on the regulation of innate immunity.

Keywords: endothelial-derived interleukin-1α, transendothelial neutrophils, lipopolysaccharide, *Escherichia coli* infection, iTRAQ

Abbreviations: *E. coli*, *Escherichia coli*; IL-1α, Interleukin-1α; LPS, Lipopolysaccharide; RIMVECs, rat intestinal mucosa microvascular endothelial cells; iTRAQ, isobaric tags for relative and absolute quantification.

INTRODUCTION

Endothelial cells are the inner cell lines connected with immune cells and epithelium (Rohlenova et al., 2018). One kind of immune cells, neutrophils, must across endothelial cells to reach the infected sites against pathogenic infection (Papayannopoulos, 2018). In turn, bacteria employ their virulence factors to hijack endothelial cells and induce inflammatory cytokine release as the major strategy to break through epithelium barrier and inhibit innate immune system (Liu et al., 2017; Yuan et al., 2018). For instance, the lipopolysaccharide (LPS) secreted from *Escherichia coli* (*E. coli*) impacts the release of inflammatory mediators to regulate the progress of infection by leading immune cell damage (Li et al., 2016; Presicce et al., 2020). It worth to note that the inflammatory cytokine, interleukin-1α (IL-1α) can induce neutrophil extracellular traps (NETs) to activity endothelial cell (Folco et al., 2018). As similar as our previous research illustrated that endothelial IL-1α enhanced the bacterial killing of transendothelial neutrophils (Liu et al., 2016). In addition, IL-1α is primarily associated with inflammatory during the pathogenesis induced by bacterial infection (Dinarello, 2011; Menghini et al., 2019). However, the mechanisms of how endothelial-derived IL-1α regulate the killing ability of transendothelial neutrophils remain unknown. Thus, we hypothesized that endothelial IL-1α modulated endothelial cells to impact bacterial killing of transendothelial neutrophils.

In this work, we aimed to investigate how endothelial-derived IL-1α impacted the bactericidal activity of transendothelial neutrophils during endothelial-neutrophil interaction though two *E. coli* infected models of rats and endothelial-neutrophil co-cultural system (Transwell). Further, we intended to find the regulated difference proteins on endothelial cells that triggered by IL-1α via using iTRAQ-based quantitative proteomics.

MATERIALS AND METHODS

Animals

Rats (1-day rats and 1–2-month rats) were purchased from academy of military medical sciences, Beijing, China (Certificate Number: SCXK-PLA 2012-0004). One day rats were obtained to isolate primary RIMVECs and 1–2-months rats were used for the rat infection.

Ethics Statement

The experimental protocols involving rats were gained an approval by the Institutional Animal Care and Use Committee of the Academy of Military Medical Sciences (Beijing, China; approval no. SYXK2014-0002).

Rat Infection

Rats (1–2 month, about 500 g, 10 rats per group) were infected with 10^9 colony-forming units (CFUs) of *E. coli* (serotype O55:B5) orally. To simulate the situation of stress-induced LPS accumulation. We set up the group of additional LPS by adding 1 μg/g of LPS (from *E. coli* serotype O55:B5, Sigma-Aldrich) mixed with *E. coli* suspension. After 24 h infection, IL-1α, IL-1β, IL-6, intercellular adhesion molecule-1 (ICAM-1) and Tumor Necrosis Factor (TNF-α) from rat serums were detected by the ELISA kits (BD Biosciences) according to the instructions. For further investigating the survival of *E. coli* infected rats, simultaneous addition of IL-1α (rat recombinant, Sigma-Aldrich) with 10 ng/g for each infected group. Then the ratios of rat survival were recorded. Lastly the *E. coli* that survived in rat colons were detected by the colony count technique (colony-forming units, CFUs).

Primary Endothelial Cell Culture

Primary rat intestinal mucosal microvascular endothelial cells (RIMVECs) were separated from the colons of 1 day-rats and then cultured in complete Dulbecco's modified eagle medium (DMEM, Gibco) containing 2 mM L-glutamic acid, 50 mg/l gentamycin, 100 U/mL penicillin/streptomycin and 20% heat-inactivated fetal bovine serum (FBS, Gibco). The identification of RIMVECs was obtained as previous protocol (Liu et al., 2016).

Isolation of Blood Neutrophils

Rat fresh neutrophils were isolated from heparinized whole blood of healthy rats by gradient centrifugation assay using Percoll reagent (GE Healthcare) as previous published methods (Liu et al., 2016). Then neutrophils were washed with HBSS and preserved in RPMI-1640 medium (Gibco) for later use after counting and viability assessment.

Detecting the Damage of LPS on RIMVECs

RIMVECs (1×10^4 cells/well) were seeded in a 96-well plate and treated with a final concentrations of 1 μg/mL LPS for different time points (0.5, 1, 2, 4, 8, 12, and 24 h) at 37°C in a 5% CO_2 atmosphere. After treatment, the cytotoxicity of RIMVECs was detected by 10 μL of WST-1 reagents (Roche). After 1 h incubation at 37°C, the absorbance was detected by a fluorescence microplate reader (Life Science & Technology) at wavelength of 450 nm. The percentage of RIMVECs survival was calculated based on the ratio of absorbance compared to DMEM treated group. After RIMVECs treated with LPS, then cells were washed with PBS and incubated with PI (5 μg/mL, Sigma-Aldrich) for 30 min. The PI positive cells presented the membrane damaged cells and fluorescence intensity of PI was immediately detected with excitation wavelength at 535 nm and emission wavelength at 615 nm.

Flow Cytometry

To record the proportion of necrosis and apoptosis on RIMVECs leaded by LPS, we used an Annexin-V-FITC (Annexin-V-fluorescein isothiocyanate) and propidium iodide (PI) double staining kit (B&D system) to track the cytotoxicity of LPS. Annexin-V was employed to label membrane phosphatidylserine on the surface of early apoptotic cells, which displayed green fluorescence due to FITC. PI was used to sort the necrotic cells by further binding to cellular DNA and showing red fluorescence.

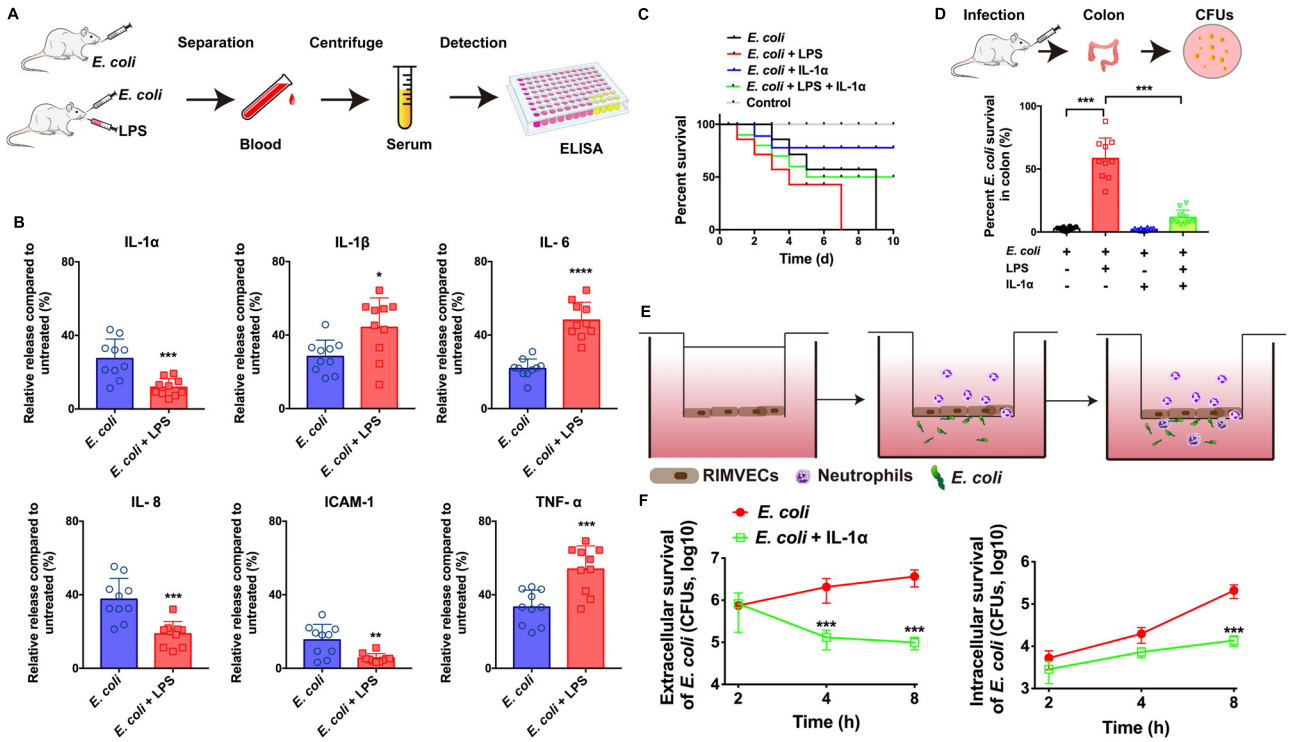

FIGURE 1 | IL-1α facilitated the bacterial killing on the *in vivo* and *in vitro* model of *E. coli* infection. **(A)** *E. coli* infection *in vivo* rat model workflow. **(B)** IL-1α, IL-1β, IL-6, IL-8, ICAM-1, and TNF-α were detected by ELISA. Rats were infected by *E. coli* (10^9 CFU/g) with or without LPS (1 μg/mL) treatment. After 24 h infection, the serum of every rats including both dead or live rats were collected to detect the inflammation-associated cytokines by ELISA. **(C)** IL-1α increase the survival of LPS-induced rat death. A total of 10^9 CFU/g *E. coli* were infected with rats for 24 h. LPS (1 μg/g) or IL-1α (10 ng/g) were treated with the infected rats. The ratios of rat survival were determined from 10 days' treatment. Gray line showed the percent survival of uninfected rats, red line represented the *E. coli* infection, blue line was the LPS treatment of *E. coli* infection, green line represented LPS plus IL-1α treated with *E. coli* infected rats. **(D)** IL-1α decreased the bacterial load in rat colon. The number of bacteria was counted by the colony count technique (CFU). Percentage of *E. coli* were compared to untreated group. Data are shown as means ± SD (*$P < 0.05$; **$P < 0.01$; ***$P < 0.001$, $n = 10$). **(E)** Scheme of co-culture system for RIMVECs-neutrophils interactions *in vitro*. RIMVECs were seeded on upper chambers for 24 h to form monolayer. Then neutrophils were added in the upper chambers. *E. coli* infected **(F)** IL-1α increased the transendothelial neutrophils killing. *E. coli* infected in bottom chambers treated for different time points (2, 4, and 8 h) and IL-1α (10 ng per well) was also treated in the upper chambers. Both the extracellular and intracellular bacteria in neutrophils (5×10^8 cells) were used to count the *E. coli* CFUs. The red lines represented *E. coli* infection and green lines showed the IL-1α treatment of *E. coli* infection. Values represent the mean ± SD (***$P < 0.001$, $n = 6$).

Detection and analysis of necrosis were used BD FACSAria™ flow cytometry and FACSDiva software (BD Biosciences) based as our previous publish method (Liu et al., 2017).

Infection of the Endothelial-Neutrophil Interaction

RIMVECs (1×10^4 cells/well) were seeded onto the 5.0 μm pore size polycarbonate resin transwell membranes to reach confluence and form a monolayer on the upper chamber of transwell system (Corning) and measured by TEER using the Millicell Electrical Resistance System (ERS)-2 (EMD Millipore, Billerica, United States). Then fresh neutrophils were added into the upper chambers and *E. coli* in the bottom chambers as illustrated in **Figure 1E**. All cells were cultured in a DMEM medium (Gibico) supplemented with 10% FBS at 37°C in a 5% CO_2 atmosphere. Images of RIMVECs and neutrophils were captured by a confocal microscopy (Leica, SP8). Then *E. coli* were infected with transendothelial neutrophils at the bottom chambers of transwell for 4 h. IL-1α or LPS were added in the co-culture medium at the final concentration of 1 μg/mL or 10 ng/mL, respectively. Lastly, both the extracellular and intracellular *E. coli* (neutrophils, 5×10^8 cells) were collected to calculate using the colony count technique (CFUs) according to previous study (Liu et al., 2016).

Western Blot

RIMVECs were collected from the transwell system. RIMVECs were lysed in 1 mL of RIPA lysis buffer with 10 μL phenylmethanesulfonyl fluoride (PMSF, 1 mmol/L, Beyotime) on the ice for 20 min. Then the cell lysates were used to gain the whole proteins by centrifugation at 15,000 rpm for 12 min and proteins were quantified by the BCA method (Pierce). Fifty microgram of proteins were used to detect the expression of IL-1α by Western Blot assay. Briefly, separation of proteins used SDS-PAGE with 15% polyacrylamide gels and transferred onto a PVDF membranes (Beyotime). The primary antibody of rabbit anti- IL-1α (a dilution of 1: 1000, Invitrogen) was incubated with membranes at 4°C overnight and secondary antibody of goat

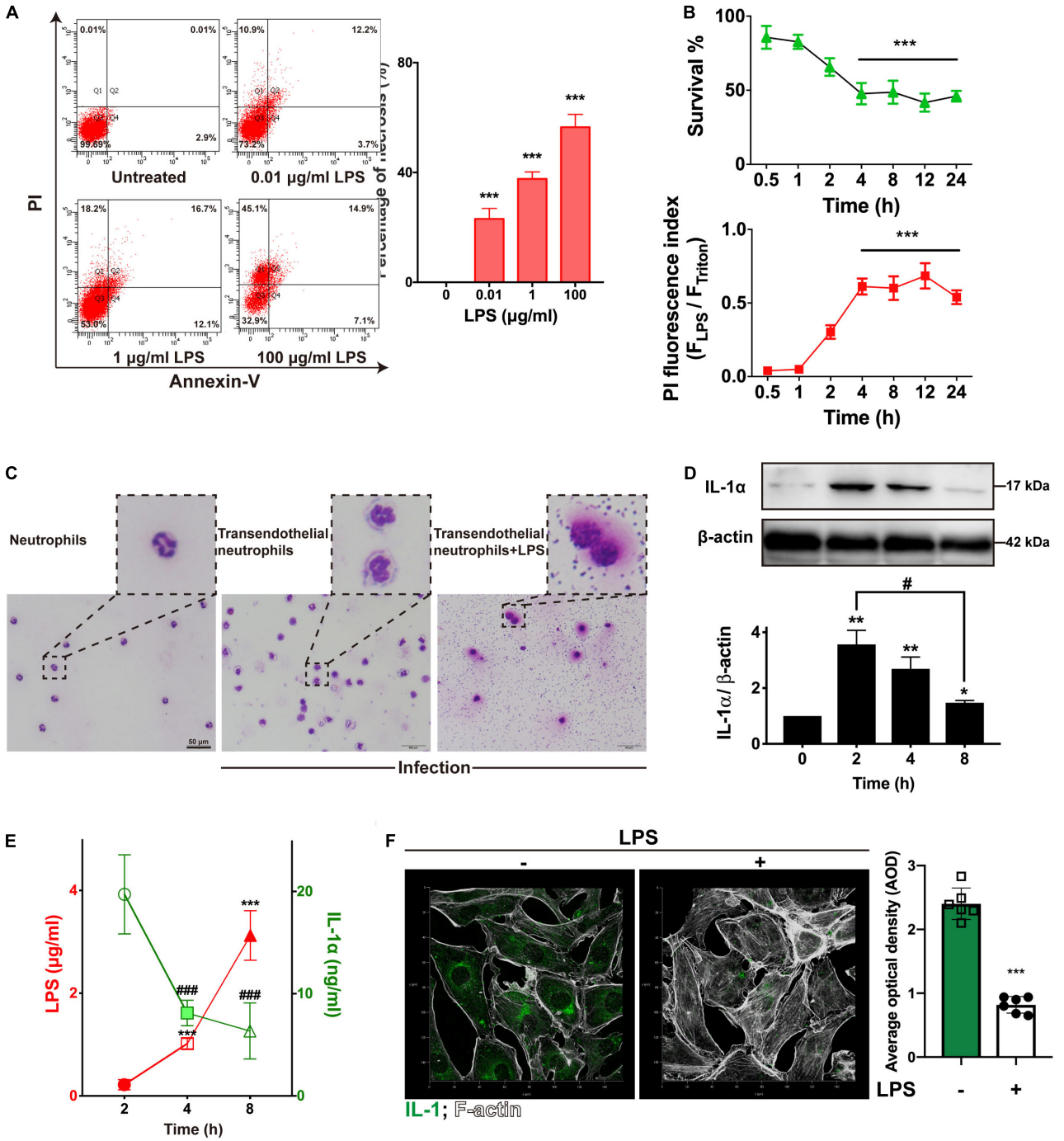

FIGURE 2 | LPS damaged endothelial cells and neutrophils to suppress IL-1α. **(A)** LPS induced RIMVECs necrosis. Different concentrations of LPS (0–100 μg/mL) were treated RIMVECs for 4 h. Then cells were labeled by PI and Annexin-V staining. Apoptosis and necrosis of RIMVECs (at least 10,000 cells) were distinguished by flow cytometry assay. The percentage of Q1 and Q2 area were counted from A presented the necrotic RIMVECs. **(B)** LPS induced cytotoxicity of RIMVECs in a time dependent manner. LPS (1 μg/mL) treated RIMVECs for different time points (0.5–24 h). Then the survival of RIMVECs were determined by WST-1 assay. PI positive RIMVECs were recorded by a plate reader (SpectraMax M5) at the excitation wavelength of 535 nm and emission wavelength of 615 nm. The detached RIMVECs were also counted. **(C)** Transwell system were treated with 1 μg/mL LPS for 4 h. Transendothelial neutrophils were dyed with Switzerland staining. Images were captured by an optical microscope (Olympus). **(D)** The expression of IL-1α in co-culture system was decreased in a time dependent manner. **(E)** LPS suppressed the release of IL-1α. IL-1α release and concentrations of LPS were detected by ELISA or LAL (Limulus Amebocyte Lysate) assay, respectively. **(F)** The immunofluorescence of IL-1α in RIMVECs with or without LPS treatment. Values represent the mean ± SD (*$P < 0.05$; **$P < 0.01$; ***$P < 0.001$; ###$P < 0.0001$, #$P < 0.05$, $n = 6$ or three independent biological repetition).

TABLE 1 | Functional analysis of common regulated proteins.

Protein name	Description	Function_GO	Location_GO	Pathway_KEGG
AATM	Aspartate aminotransferase, mitochondrial	Metabolic process	Plasma membrane	Alanine aspartate and glutamate metabolism
ACTN1	Alpha-actinin-1	Cell adhesion	Plasma membrane	Focal adhesion
AT2A2	Sarcoplasmic/endoplasmic reticulum calcium ATPase 2	Energy metabolic process	Endoplasmic reticulum	Calcium signaling pathway
ATPA	ATP synthase subunit alpha, mitochondrial	Energy metabolic process	Plasma membrane	Oxidative phosphorylation
CN37	2',3'-cyclic-nucleotide 3'-phosphodiesterase	Cell morphogenesis	Extracellular region	Unknown
DHI1	Corticosteroid 11-beta-dehydrogenase isozyme 1	Metabolic process	Endoplasmic reticulum	Steroid hormone biosynthesis
ENPL	Endoplasmin	Unknown	Unknown	Unknown
MUC18	Cell surface glycoprotein MUC18	Cell adhesion	Plasma membrane	Unknown
NDUS1	NADH-ubiquinone oxidoreductase 75 kDa subunit, mitochondrial	Oxidative phosphorylation	Mitochondrial envelope	Oxidative phosphorylation
SAC1	Phosphatidylinositide phosphatase SAC1	Metabolic process	Endoplasmic reticulum	Unknown %
TRAP1	Heat shock protein 75 kDa, mitochondrial	Protein folding	Mitochondrion	Unknown

The blue marked table frames represented the upregulated proteins, while unmarked were the downregulated proteins. Red marked the protein had both upregulation and downregulation.

anti-rabbit antibody (a dilution of 1: 3000, Beyotime) covered the membranes for 1 h at room temperature. Gray values of protein bands were quantified by ImageJ software.

LPS Detection

Concentrations of LPS were determined by a LAL (Limulus Amebocyte Lysate, LONZA) assay. Briefly, the samples including LPS were diluted in the free endotoxin water and detected by LAL reagent (sensitivity 0.125 EU/mL) as previous published protocols (Mitra et al., 2014). 2.5 EU of LPS approximated 1 ng.

Immunostaining and Confocal Microscopy

RIMVECs were seeded on glass coverslips (15 mm, NEST) in a 24-well plate and incubated with LPS for 4 h. Then cells were fixed by 4% paraformaldehyde and incubated with the primary antibodies, rabbit anti-IL-1α (a dilution of 1: 500, Invitrogen) at 4°C overnight. After PBS washed twice, cells were incubated with the FITC-labeled goat anti-rabbit IgG (H + L) (a dilution of 1: 1000, Beyotime) at 4°C for 2 h, which was used to visualize the IL-1α protein. Images were captured by the LAS AF Lite software (Leica).

Protein Preparation and iTRAQ Labeling

RIMVECs were treated with IL-1α (final concentration of 10 ng/mL) at 37°C incubated in a 5% CO_2 atmosphere for 0, 2, 4, and 8 h. The proteins of RIMVCEs were extracted by RIPA lysate buffer (Beyotime) and quantified by a BSA kit (Beyotime). The concentrations of sample proteins were detailed in **Supplementary Table S1**. Two hundred microgram proteins were incubated in iTRAQ-4-plex kit (AB Sciex, PN: 4352135) proteolysis. The iTRAQ labeled, LC-MS/MS analysis and MALDI-TOF-TOF identifications were conducted by BIOMS company. Labels of 114, 115, 116, and 117 are represented 2, 4, 6, and 0 h treatment, respectively (**Supplementary Table S1**).

LC-MS/MS Analysis Based on TripleTOF^{TM} 5600

The iTRAQ labeled samples were run though Durashell-C18 column (4.6 mm × 250 mm, 5 μm 100 AÅ, Agela, Catalog Number: DC952505-0) and dissolved in mobile phase A, which was 2% acetonitrile in water and phase B was 98% acetonitrile in water. The gradient elution program was: 0–5 min, 5% B; 5–35 min, 8% B; 35–62 min, 32% B; 62–64 min, 95% B; 64–68 min, 95% B; 68–72 min, 5% B. The injection volume was 3 μL and the flow rate was 0.7 mL/min. The parameters of mass spectrometry were: Ion spray voltage:2.3 kv; GS1:4; Curtain gas:35; DP:100; Top MS, m/z:350-1250; accumulation time: 0.25 s; product ion scan: IDA number:30; m/z:100-1500; accumulation time:0.1 s; Dynamic exclusion time: 25 s; Rolling CE: enabled; Adjust CE when using iTRAQ reagent: enabled; CES:5. Analysis of iTRAQ mass spectrometry by TripleTOF^{TM} 5600 system using the software of ProteinPilot 4.0 (AB Sciex) and the database come from http://www.uniprot.org.

Data Availability

iTRAQ-based quantitative mass spectrometry proteomics data had been deposited to the ProteomeXchange Consortium via the

PRIDE (Perez-Riverol et al., 2019) partner repository with the dataset identifier PXD019561.

Statistical Analysis

The significant differences between two groups were calculated using unpaired *t*-test with between two groups or one-way ANOVA among multiple groups and performed by GraphPad Prism 8.0 software. Results were expressed as means ± SD. Values are represented as column diagram ($^{*}P < 0.05$; $^{**}P < 0.01$; $^{***}P < 0.001$). All animals were used to analyze including both live and dead rats.

RESULTS

IL-1α Prevented *E. coli* Infection *in vivo* and *in vitro*

To investigate whether IL-1α can impact on the innate immunity against bacterial infection, we firstly built the *in vivo* model of *E. coli* infected rats (**Figure 1A**) and the infection on co-culture system of neutrophils and endothelial cells *in vitro* (**Figure 1E**). We found that LPS of *E. coli* promoted the release of TNF-α, IL-6, and IL-1β in the serums of infected rats, while LPS suppressed IL-1α, IL-8, and ICAM-1 (**Figure 1B**). It suggested that LPS might damage endothelial-neutrophil interaction due to interrupt the inflammation. Since IL-1α can secrete from endothelial cells as well as the IL-8 and ICAM-1 are crucial for neutrophils recruitment (Gunther et al., 2017). Therefore, based on our previous study as well (Liu et al., 2016), we hypothesized that IL-1α acted as the important role on endothelial cells to activate the innate immunity. Next, results also confirmed IL-1α could increase the survival of LPS induced the *E. coli* infected rats (**Figure 1C**) and decrease the bacterial loading in rat colon (**Figure 1D**), suggesting that IL-1α could prevent the LPS induced bacterial expansion *in vivo*. For more clearing illustrated the function of IL-1α on endothelial-neutrophil interaction, we employed a Transwell system to co-culture of rat intestinal microvascular endothelial cells (RIMVECs) and neutrophils to evaluate the bacterial killing ability of transendothelial neutrophils. As **Figure 1F** showed, IL-1α treatment decreased both the intracellular and extracellular *E. coli*, suggesting that the bacterial killing activity of transendothelial neutrophils was enhanced by IL-1α.

Endothelial-Derived IL-1α Was Inhibited by LPS Though Damaging Endothelial Cells and Neutrophils

LPS from *E. coli* are frequently reported that impairs endothelial cells (Yang et al., 2016; Zhou et al., 2018; Huang et al., 2019). To investigate how LPS impacted RIMVECs, we utilized a double staining of PI and Annexin-V to sort the LPS treated RIMVECs by flow cytometry. As showed in **Figure 2A**, LPS induced RIMVECs necrosis in a dose dependent manner (4 h treatment) and further led cell death and impaired cellular membranes in a time dependent way (**Figure 2B**). It was consisted with previous reports that LPS injury tissue and led cell necroptosis (Li et al., 2016; Huang et al., 2019). In fact, LPS action on endothelial cells is intend to occur an inflammation within endothelial-neutrophil interactions (Al-Banna et al., 2013; Shi et al., 2014), and IL-1 family is closely related with inflammation (Dinarello, 2011; Liu et al., 2016; Gunther et al., 2017). In addition, we found that LPS damaged the transendothelial neutrophils and led the bacterial escape from cells (**Figure 1C**). Take it together, IL-1α prevented *E. coli* infection by enhancing the killing ability of transendothelial neutrophils, while LPS destroyed it. Therefore, we next detected the amount of LPS and IL-1α in the co-culture system to reveal the function of each other. We found that the expression of endothelial-derive IL-1α was inhibited by LPS (**Figure 1D**). Results also indicated that the release of LPS and IL-1α in co-culture transwell system was competitive (**Figure 1E**) and the addition of LPS did weaken the expression of IL-1α (**Figure 1F**). Altogether, IL-1α might be the key factor that impact bacterial killing during endothelial-neutrophil interaction.

IL-1α Facilitated Neutrophil Killing via Sustaining Oxidative Phosphorylation Activity

For deeply exploring the modulatory function of IL-1α, iTRAQ labeling technology combined with mass spectrometry proteomic analysis were used for investigating the differentially expressed proteins of RIMVECs from Transwell system (**Figure 3A**). We first analyzed the location of different proteins and found that most of them were disturbed on plasma membrane compared to 0 h (2 h about 33%, 4 h was 35% and 8 h was 40%, **Figure 3B**). Venn diagram showed that there had 31 proteins of upregulation and 29 proteins of downregulation at 2 h, for 4 h treatment, 14 upregulations, 19 downregulations and 31 upregulations, 26 downregulations at 8 h (**Figure 3C**). As showed in the heat map (**Figure 2D**), compared to untreated group, there are 63, 37, or 63 proteins significant regulation in 2, 4, or 8 h treatment, respectively (**Supplementary Table S2**). These data showed that IL-1α is a complex regulation in protein levels. Combating with our previous results that IL-1α enhanced both extracellular and intracellular bacterial killing of transendothelial neutrophils mainly focused on the long-time treatment (4–8 h, **Figure 1F**). Thus, we believe that the common regulated proteins in all time points is playing the key role. Therefore, we analyzed that 11 proteins were sustained to regulate significantly, among them 5 proteins upregulation and 5 proteins downregulation (**Figure 3E**). Interesting, one protein named Endoplasmin (ENPL) was upregulated at 2 h while downregulated at 4 and 8 h. All the information and analysis of the common regulated proteins were detailed in **Table 1**. Nevertheless, the function and location of ENPL still remained unclear. But it was worth noting that there were two proteins including ATPA and NDUS1 upregulated responded to oxidative phosphorylation.

Next, we deduced that oxidative phosphorylation was required for IL-1α-dependent activation of endothelial cells. Therefore, in order to more detail the functional regulation, we analyzed that the pathway cascade in 2, 4, and 8 h. As showed in **Figure 3F**, cell adhesion molecules (CAMs) major responded to 2 h treatment of IL-1α. It was consisted with our previous results that LPS targeted ICAM-1 and IL-1α

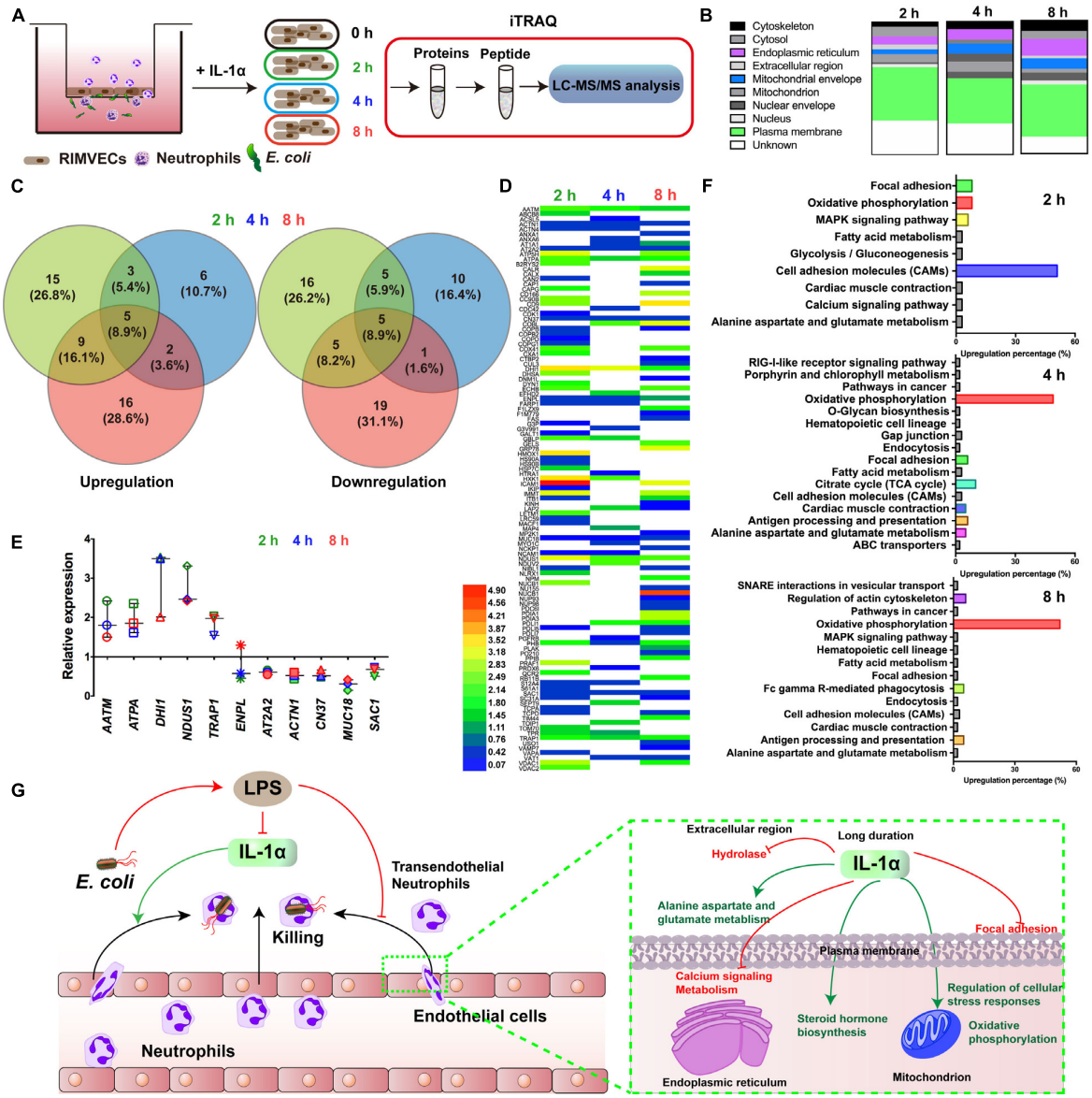

FIGURE 3 | Oxidative phosphorylation was required for IL-1α activated-endothelial cells. **(A)** Scheme of the iTRAQ experimental set-ups. **(B)** The regulated proteins were mostly distributed on plasma membrane. RIMVECs were treated with IL-1α (10 ng/mL) for 2, 4, or 8 h and the proteins regulation of RIMVECs were analyzed by iTRAQ. **(C)** Venn diagram showed the percentage of upregulated and downregulated proteins, which were drawn by Venny 2.1.0 software online. **(D)** Heat map of the differential protein analyzed by iTRAQ. RIMVECs were treated with IL-1α (10 ng/mL) for 2, 4, or 8 h. At every time points, the proteins of RIMVECs were collected for iTRAQ assay. The image of heat map was made by Heml software. **(E)** The common expressed proteins of RIMVECs induced by IL-1α at all the treated times (n = 3, down-up regulated difference >1.5-fold change). **(F)** IL-1α upregulated the cell adhesion molecules (CAMs) of RIMVECs at 2 h treatment, while mainly triggers oxidative phosphorylation at 4 and 8 h. **(G)** Scheme of endothelial IL-1α facilitated transendothelial neutrophil killing.

to affect the bacterial killing of transendothelial neutrophils. As we proposed that the accumulation of IL-1α is the importance factor that activates the transendothelial neutrophils, we found that in long time treatment of IL-1α, oxidative phosphorylation is mainly regulated pathways (4 h was 49% and 8 h was 52%). Oxidative phosphorylation is vital for physiological function regulations in most eukaryocyte, especially in endothelial cells (Papa et al., 2012; Montorfano et al., 2014; Nath and Villadsen, 2015). We further found that the oxidative phosphorylation induced by IL-1α occurred on mitochondrial envelope (**Table 1**). Take it together, it revealed that additional IL-1α treated in the *E. coli* infected co-culture system of endothelial cells and neutrophils was originally enhanced the adhesion of neutrophils and then promoted the migration of neutrophils by triggering oxidative phosphorylation to generates ROS. It consisted with the fact that neutrophil transmigration across endothelial cells was essential for ROS and sustaining the inflammatory response (Mittal et al., 2017).

Combining with these researches, our data further revealed a new function that IL-1α induced the oxidative phosphorylation of endothelial cells to assist transendothelial neutrophils killing.

DISCUSSION

Endothelial cells not only form the physical barrier against pathogenic invasion (Sturtzel, 2017; He et al., 2020), but also have the regulation of transendothelial neutrophils. Indeed, endothelial cells turn into the activated form during the migration of neutrophils (Mittal et al., 2017; Folco et al., 2018). The action of transendothelial migration is a series of complex physical and biological processes (Kolaczkowska and Kubes, 2013; Mooren et al., 2014). In general, bacterial infection is connected with endothelial cell activation and neutrophil migration. Many bacterial pathogens utilize their toxins to disrupt endothelial integrity and inhibited immune cells as confirmed as our results (**Figure 2**) and further trigger the inflammation (Kim et al., 2010; Amedei and Morbidelli, 2019; Le Guennec et al., 2020). However, we do not know the role of endothelial cells act on the transendothelial migration during innate immunity. In this study, we focused on endothelial-derived IL-1α, because accumulation of IL-1α release from endothelial cells is the signaling for transendothelial migration of neutrophils (Burzynski et al., 2015). Our previous results also showed that IL-1α activated endothelial cells to promote neutrophil killing by improving the lysozyme activation (Liu et al., 2016). In this paper, we also found that IL-1α promoted bacterial killing of transendothelial neutrophils (**Figure 1F**). More interesting, LPS inhibited the release of IL-1α *in vivo* and *in vitro* (**Figures 1**, **2**). It indicated that LPS damaged endothelial cells and interrupted the bacterial killing of transendothelial neutrophils was connected with IL-1α. Unlike other researches show that IL-1α has the ability to induce neutrophil-endothelial cell adhesion (Macmillan et al., 2010), these findings performed a novel link of IL-1α on the bacterial killing activity within transendothelial migration.

IL-1α modulates both endothelial cells and neutrophils, involving inflammation (Dinarello, 2011; Burzynski et al., 2015; Altmeier et al., 2016). Endothelial cells are the center role involved in neutrophils and inflammation (Sturtzel, 2017; Rohlenova et al., 2018). Therefore, we targeted on the different proteins of endothelial cells by IL-1α treatment. It worth to note that IL-1α have a specific time dependent function on protein regulations of endothelial cells. In the early state, IL-1α might promote neutrophil recruitment by upregulating ICAM, while oxidative phosphorylation was continuously required in the later stages (**Figure 3F**). These results had the important significance, it well explained that the generation of ROS was continuously required during endothelial-neutrophil interaction and inflammation (Papa et al., 2012; Montorfano et al., 2014; Mittal et al., 2017; Xu et al., 2019). More importantly, we also selected for specific functional proteins in detail (**Figure 3D** and **Table 1**), we believed these proteins would useful for further study of IL-1α on bactericidal activity of transendothelial neutrophils.

CONCLUSION

We demonstrated that endothelial-derived IL-1α was critical for neutrophil killing during endothelial-neutrophil interaction. As illustrated in **Figure 3G**, bacterial LPS inhibited the release of IL-1α from endothelial cells and further prevented the bacterial killing ability of transendothelial neutrophils. In turn, IL-1α was utilized as the signaling to trigger the transendothelial neutrophils killing. iTRAQ-based quantitative mass spectrometry proteomic analysis illustrated that IL-1α inhibited the hydrolase in the extracellular region, focal adhesion of plasma membrane and calcium signaling metabolism on endoplasmic reticulum. IL-1α promoted alanine aspartate and glutamate metabolism on plasma membrane, enhanced steroid hormone biosynthesis on endoplasmic reticulum and also increased the regulation of cellular stress responses and oxidative phosphorylation on mitochondrion.

DATA AVAILABILITY STATEMENT

The datasets presented in this study can be found in online repositories. The names of the repository/repositories and accession number(s) can be found in the article/ **Supplementary Material**.

ETHICS STATEMENT

The animal study was reviewed and approved by the experimental protocols involving rats were gained an approval (SCXK, 2016-006). All animals were approved by the Genentech Institutional Animal Care and Use Committee at the China Agricultural University (SYXK, 2016-0008).

AUTHOR CONTRIBUTIONS

HD and GH conceived the project. XL, XM, and HD did the research design. XL, HZ, and SH performed the experiments. XL, GH, and HD did the data analysis and wrote the manuscript. All authors contributed to the article and approved the submitted version.

FUNDING

This work was supported by the National Natural Science Foundation of China (Grant No. 3172558) and China's 13th Five-Year plan (2017YFD0501501).

SUPPLEMENTARY MATERIAL

The Supplementary Material for this article can be found online at: https://www.frontiersin.org/articles/10.3389/fcell.2020.00590/full#supplementary-material

REFERENCES

Al-Banna, N. A., Toguri, J. T., Kelly, M. E., and Lehmann, C. (2013). Leukocyte-endothelial interactions within the ocular microcirculation in inflammation and infection. *Clin. Hemorheol. Microcirc.* 55, 423–443. doi: 10.3233/ch-131780

Altmeier, S., Toska, A., Sparber, F., Teijeira, A., Halin, C., and Leibundgut-Landmann, S. (2016). IL-1 coordinates the neutrophil response to *C. albicans* in the oral mucosa. *PLoS Pathog.* 12:e1005882. doi: 10.1371/journal.ppat.1005882

Amedei, A., and Morbidelli, L. (2019). Circulating metabolites originating from gut microbiota control endothelial cell function. *Molecules* 24:3992. doi: 10.3390/molecules24213992

Burzynski, L. C., Humphry, M., Bennett, M. R., and Clarke, M. C. (2015). Interleukin-1alpha activity in necrotic endothelial cells is controlled by caspase-1 cleavage of interleukin-1 receptor-2: implications for allograft rejection. *J. Biol. Chem.* 290, 25188–25196. doi: 10.1074/jbc.m115.667915

Dinarello, C. A. (2011). Interleukin-1 in the pathogenesis and treatment of inflammatory diseases. *Blood* 117, 3720–3732. doi: 10.1182/blood-2010-07-273417

Folco, E. J., Mawson, T. L., Vromman, A., Bernardes-Souza, B., Franck, G., Persson, O., et al. (2018). Neutrophil extracellular traps induce endothelial cell activation and tissue factor production through interleukin-1alpha and cathepsin G. *Arterioscler. Thromb. Vasc. Biol.* 38, 1901–1912. doi: 10.1161/atvbaha.118.311150

Gunther, S., Deredge, D., Bowers, A. L., Luchini, A., Bonsor, D. A., Beadenkopf, R., et al. (2017). IL-1 Family cytokines use distinct molecular mechanisms to signal through their shared co-receptor. *Immunity* 47, 510–523.e514.

He, M., Martin, M., Marin, T., Chen, Z., and Gongol, B. (2020). Endothelial mechanobiology. *APL Bioeng.* 4:10904.

Huang, X., Zhu, J., Jiang, Y., Xu, C., Lv, Q., Yu, D., et al. (2019). SU5416 attenuated lipopolysaccharide-induced acute lung injury in mice by modulating properties of vascular endothelial cells. *Drug Des. Devel. Ther.* 13, 1763–1772. doi: 10.2147/dddt.s188858

Kim, M., Ashida, H., Ogawa, M., Yoshikawa, Y., Mimuro, H., and Sasakawa, C. (2010). Bacterial interactions with the host epithelium. *Cell Host. Microbe.* 8, 20–35. doi: 10.1016/j.chom.2010.06.006

Kolaczkowska, E., and Kubes, P. (2013). Neutrophil recruitment and function in health and inflammation. *Nat. Rev. Immunol.* 13, 159–175. doi: 10.1038/nri3399

Le Guennec, L., Coureuil, M., Nassif, X., and Bourdoulous, S. (2020). Strategies used by bacterial pathogens to cross the blood-brain barrier. *Cell Microbiol.* 22:e13132.

Li, Z., Scott, M. J., Fan, E. K., Li, Y., Liu, J., Xiao, G., et al. (2016). Tissue damage negatively regulates LPS-induced macrophage necroptosis. *Cell Death Differ.* 23, 1428–1447. doi: 10.1038/cdd.2016.21

Liu, X., Ding, S., Shi, P., Dietrich, R., Martlbauer, E., and Zhu, K. (2017). Non-hemolytic enterotoxin of *Bacillus cereus* induces apoptosis in Vero cells. *Cell Microbiol.* 19:e12684. doi: 10.1111/cmi.12684

Liu, X., Dong, H., Wang, M., Gao, Y., Zhang, T., Hu, G., et al. (2016). IL-1alpha-induced microvascular endothelial cells promote neutrophil killing by increasing MMP-9 concentration and lysozyme activity. *Immunol. Res.* 64, 133–142. doi: 10.1007/s12026-015-8731-4

Macmillan, H. F., Rowter, D., Lee, T., and Issekutz, A. C. (2010). Intravenous immunoglobulin G selectively inhibits IL-1α-induced neutrophil-endothelial cell adhesion. *Autoimmunity* 43, 619–627. doi: 10.3109/08916931003599062

Menghini, P., Corridoni, D., Butto, L. F., Osme, A., Shivaswamy, S., Lam, M., et al. (2019). Neutralization of IL-1alpha ameliorates Crohn's disease-like ileitis by functional alterations of the gut microbiome. *Proc. Natl. Acad. Sci. U.S.A.* 16, 26717–26726. doi: 10.1073/pnas.1915043116

Mitra, A., Joshi, S., Arjun, C., Kulkarni, S., and Rajan, R. (2014). Limulus amebocyte lysate testing: adapting it for determination of bacterial endotoxin in 99mTc-labeled radiopharmaceuticals at a hospital radiopharmacy. *J. Nucl. Med. Technol.* 42, 278–282. doi: 10.2967/jnmt.114.146779

Mittal, M., Nepal, S., Tsukasaki, Y., Hecquet, C. M., Soni, D., Rehman, J., et al. (2017). Neutrophil activation of endothelial cell-expressed TRPM2 mediates transendothelial neutrophil migration and vascular injury. *Circ. Res.* 121, 1081–1091. doi: 10.1161/circresaha.117.311747

Montorfano, I., Becerra, A., Cerro, R., Echeverria, C., Saez, E., Morales, M. G., et al. (2014). Oxidative stress mediates the conversion of endothelial cells into myofibroblasts via a TGF-beta1 and TGF-beta2-dependent pathway. *Lab. Invest.* 94, 1068–1082. doi: 10.1038/labinvest.2014.100

Mooren, O. L., Li, J., Nawas, J., and Cooper, J. A. (2014). Endothelial cells use dynamic actin to facilitate lymphocyte transendothelial migration and maintain the monolayer barrier. *Mol. Biol. Cell* 25, 4115–4129. doi: 10.1091/mbc.e14-05-0976

Nath, S., and Villadsen, J. (2015). Oxidative phosphorylation revisited. *Biotechnol. Bioeng.* 112, 429–437. doi: 10.1002/bit.25492

Papa, S., Martino, P. L., Capitanio, G., Gaballo, A., De Rasmo, D., Signorile, A., et al. (2012). The oxidative phosphorylation system in mammalian mitochondria. *Adv. Exp. Med. Biol.* 942, 3–37.

Papayannopoulos, V. (2018). Neutrophil extracellular traps in immunity and disease. *Nat. Rev. Immunol* 18, 134–147. doi: 10.1038/nri.2017.105

Perez-Riverol, Y., Csordas, A., Bai, J., Bernal-Llinares, M., Hewapathirana, S., Kundu, D. J., et al. (2019). The PRIDE database and related tools and resources in 2019: improving support for quantification data. *Nucleic Acids Res.* 47, D442–D450.

Presicce, P., Cappelletti, M., Senthamaraikannan, P., Ma, F., Morselli, M., Jackson, C. M., et al. (2020). TNF-signaling modulates neutrophil-mediated immunity at the feto-maternal interface during LPS-induced intrauterine inflammation. *Front. Immunol.* 11:558.

Rohlenova, K., Veys, K., Miranda-Santos, I., De Bock, K., and Carmeliet, P. (2018). Endothelial cell metabolism in health and disease. *Trends Cell Biol.* 28, 224–236. doi: 10.1016/j.tcb.2017.10.010

Shi, J., Zhao, Y., Wang, Y., Gao, W., Ding, J., Li, P., et al. (2014). Inflammatory caspases are innate immune receptors for intracellular LPS. *Nature* 514, 187–192. doi: 10.1038/nature13683

Sturtzel, C. (2017). Endothelial cells. *Adv. Exp. Med. Biol.* 1003, 71–91.

Xu, M., Wang, L., Wang, M., Wang, H., Zhang, H., Chen, Y., et al. (2019). Mitochondrial ROS and NLRP3 inflammasome in acute ozone-induced murine model of airway inflammation and bronchial hyperresponsiveness. *Free Radic Res.* 53, 780–790. doi: 10.1080/10715762.2019.1630735

Yang, X., Chang, Y., and Wei, W. (2016). Endothelial dysfunction and inflammation: immunity in rheumatoid arthritis. *Mediators. Inflamm.* 2016:6813016.

Yuan, H., Ma, J., Li, T., and Han, X. (2018). MiR-29b aggravates lipopolysaccharide-induced endothelial cells inflammatory damage by regulation of NF-kappaB and JNK signaling pathways. *Biomed. Pharmacother.* 99, 451–461. doi: 10.1016/j.biopha.2018.01.060

Zhou, H. S., Li, M., Sui, B. D., Wei, L., Hou, R., Chen, W. S., et al. (2018). Lipopolysaccharide impairs permeability of pulmonary microvascular endothelial cells via Connexin40. *Microvasc. Res.* 115, 58–67. doi: 10.1016/j.mvr.2017.08.008

Conflict of Interest: The authors declare that the research was conducted in the absence of any commercial or financial relationships that could be construed as a potential conflict of interest.

frontiers in Cell and Developmental Biology

ORIGINAL RESEARCH
published: 10 July 2020
doi: 10.3389/fcell.2020.00540

MicroRNA-138-5p Suppresses Non-small Cell Lung Cancer Cells by Targeting PD-L1/PD-1 to Regulate Tumor Microenvironment

Nannan Song[1,2†], Peng Li[1,2†], Pingping Song[3], Yintao Li[3], Shuping Zhou[1,2], Qinghong Su[1,2], Xiaofan Li[1,2], Yong Yu[1,2], Pengfei Li[4], Meng Feng[1,2,5], Min Zhang[4] and Wei Lin[1,2]*

[1] Institute of Basic Medicine, Shandong Provincial Hospital Affiliated to Shandong First Medical University, Jinan, China, [2] Institute of Basic Medicine, Shandong First Medical University & Shandong Academy of Medical Sciences, Jinan, China, [3] Department of Oncology, Shandong Cancer Hospital and Institute, Shandong First Medical University & Shandong Academy of Medical Sciences, Jinan, China, [4] Departments of Medicine, Tibet Nationalities University, Xianyang, China, [5] School of Medicine and Life Sciences, Shandong Academy of Medical Sciences, Jinan University, Jinan, China

OPEN ACCESS

Edited by:
Zhichao Fan,
UCONN Health, United States

Reviewed by:
Rongrong Liu,
Northwestern University, United States
Bo Liu,
University of California, Berkeley, United States

***Correspondence:**
Wei Lin
linw1978@163.com;
weilin11@fudan.edu.cn

[†]These authors share first authorship

Specialty section:
This article was submitted to Cell Adhesion and Migration, a section of the journal Frontiers in Cell and Developmental Biology

Received: 01 May 2020
Accepted: 09 June 2020
Published: 10 July 2020

Citation:
Song N, Li P, Song P, Li Y, Zhou S, Su Q, Li X, Yu Y, Li P, Feng M, Zhang M and Lin W (2020) MicroRNA-138-5p Suppresses Non-small Cell Lung Cancer Cells by Targeting PD-L1/PD-1 to Regulate Tumor Microenvironment. Front. Cell Dev. Biol. 8:540. doi: 10.3389/fcell.2020.00540

Non-small cell lung cancer (NSCLC) is still challenging for treatment owing to immune tolerance and evasion. MicroRNA-138 (miR-138) not only acts as a tumor suppressor to inhibit tumor cell proliferation and migration but also regulates immune response. The regulatory mechanism of miR-138 in NSCLC remains not very clear. Herein, we demonstrated that miR-138-5p treatment decreased the growth of tumor cells and increased the number of tumor-infiltrated DCs. miR-138-5p not only down-regulated the expression of cyclin D3 (CCND3), CCD20, Ki67, and MCM in A549/3LL cells, but also regulated the maturation of DCs in A549-bearing nude mice and the 3LL-bearing C57BL/6 mouse model, and DCs' capability to enhance T cells to kill tumor cells. Furthermore, miR-138-5p was found to target PD-L1 to down-regulate PD-L1 on tumor cells to reduce the expression of Ki67 and MCM in tumor cells and decrease the tolerance effect on DCs. miR-138-5p also directly down-regulates the expression of PD-L1 and PD-1 on DCs and T cells. Similar results were obtained from isolated human non-small cell lung cancer (NSCLC) cells and DCs. Thus, miR-138-5p inhibits tumor growth and activates the immune system by down-regulating PD-1/PD-L1 and it is a promising therapeutic target for NSCLC.

Keywords: non-small cell lung cancer, microRNA-138, dendritic cells, PD-1, PD-L1

INTRODUCTION

Lung cancer is the leading cause of cancer-related death in humans (Chen et al., 2011; Saika and Machii, 2012). Non-small cell lung cancer (NSCLC) accounts for approximately 85% of all lung cancer cases (Siegel et al., 2013). Although much progress has been made in the diagnosis and treatment of NSCLC, the mortality of lung cancer remains high (Yang et al., 2013; Smith et al., 2014). Thus, developing molecular targeted treatment approaches for NSCLC is urgently needed.

MicroRNAs (miRs) represent a class short non-coding RNAs. They cause the degradation and/or translation inhibition of respective target mRNAs by directly binding to the 3′-untranslated region (UTR) (Ambros, 2004; Calin and Croce, 2006). A large number of miRs have been associated with various biological processes, including cell survival, apoptosis, proliferation, differentiation, cell cycle progression and migration (Bartel, 2004; Croce and Calin, 2005), participating in the progression of diseases, e.g., cancer (Wen et al., 2015; Mannavola et al., 2016). The effect of miRs on anti-cancer was usually played by directly inhibiting tumor cells growth and/or regulating immune cells to kill tumor cells. MiR-138 has been reported to play a suppressive role in certain common types of human cancer, including brain cancer, osteosarcoma, cervical cancer, larynx carcinoma, and lung cancer, and so on (Sha et al., 2017; Yeh et al., 2019), and is considered to be a promising therapeutic target for cancer. The suppressive function of miR-138 was found to target enhancer of zeste homolog 2 (EZH2) (Zhang et al., 2013; Si et al., 2017), pyruvate dehydrogenase kinase 1 and G protein-coupled receptor 124 (GPR124) (Gao et al., 2014; Ye et al., 2015), SP1 (Liu et al., 2018), SOX9 (Hu et al., 2017), and cyclin D3 (Huang et al., 2015) to inhibit tumor cell growth and migration. Although some studies showed that over-expression of miR-138 in $CD4^+$ T cells from psoriasis patients decreased the amounts of Th1/Th2 cells (Fu et al., 2015), and miR-138 in T cells also targeted PD-1 and CTLA-4 to regulate T cell tolerance (Wei et al., 2016). The role and mechanism of miR-138 in the regulation of the tumor micro-environment remains not very clear.

The tumor microenvironment is well known to be immunosuppressive (Zou, 2005; Kim et al., 2006; Rabinovich et al., 2007). Tumor cells consistently release multiple immunosuppressive factors, including vascular endothelial growth factor (VEGF), TGF-β, IL-10, and PGE-2, to facilitate tumor growth and immune escape (Kusmartsev and Gabrilovich, 2006; Shurin et al., 2006; Lin and Karin, 2007). Immune cells in the tumor microenvironment usually are immunosuppressive or tolerant (Todryk et al., 1999; Liu et al., 2009). These immunosuppressive cells include myeloid-derived suppressor cells (MDSCs), Tregs, tumor-infiltrating DCs (TIDCs), and $CD11b^{high}$ Ia^{low} regulatory DCs (Bell et al., 1999; Li et al., 2008; Liu et al., 2009; Cai et al., 2010). The 3LL lung cancer microenvironment could drive DCs to differentiate into $CD11c^{low}CD11b^{high}Ia^{low}$ regulatory DCs to inhibit T cell response via TGF-β, PGE2, and NO, and so on (Tang et al., 2006; Li et al., 2008; Xia et al., 2008; Liu et al., 2009; Xue et al., 2017). Additionally, high expression of PD-L1 on tumor cells suppresses immune cells via cell-cell contact (Fife et al., 2009; Yokosuka et al., 2012; Chakrabarti et al., 2018; Pawelczyk et al., 2019; Schulz et al., 2019). Inhibiting PD-L1 expression on tumor cells could relieve immune tolerance induced by tumor cells, and blunts tumor cell proliferation (Fife et al., 2009; Topalian et al., 2015; Poggio et al., 2019). How to regulate immune balance in the tumor micro-environment remains a research hotspot.

Herein, the present study aimed to investigate the immune-regulatory mechanisms of miR-138-5p in the NSCLC micro-environment and tumor proliferation to reveal the multi-targeted immuno-modulatory effects of miR-138-5p in anti-cancer therapy.

MATERIALS AND METHODS

Lentivirus Production for miR-138-5p Overexpression

The sequences of human and murine miR-138 were obtained from the National Center for Biotechnology Information database using the Basic Local Alignment Search Tool[1]and miRBase[2]. The sequence of mature murine miR-138-5p is identical to that of humans. The primer pair of pri-miR-138-5p (sense: 5′ -AG CUGGUGUUGUGAAUCAGGCCGU-3′, antisense: 5′ -GGCCUGAUU CACAACACCAGCUGC-3′) was synthesized by Hanyin Co. (Shanghai, China). The pri-miR-138-5p sequence was cloned into the lentiviral vector PHY-502 carrying green fluorescent protein (GFP) and puromycin sequences by Hanyin Co. (Shanghai, China). Lentivirus which over-express recombinant miR-138-5p (lent-miR-138)and the negative control lentivirus (NC-lentivirus; Hanyin Co., Shanghai, China) were prepared to be 10^9 TU/ml (transfection unit/ml). To obtain cell lines stably over-expressing miR-138-5p, cells were infected with lent- miR-138, and selected with puromycin (1 μg/ml) for 48 h.

Animals and Animal Model

Specific pathogen-free C57BL/6 mice and nude mice (approximately 8–10 weeks old, with an average weight of 25 g) were obtained from Beijing Vital River Laboratory Animal Technology Co., Ltd. (Beijing, China). The mice were acclimatized in our animal facility and maintained under specific pathogen-free barrier conditions. All animal experiments were approved by the Animal Care and Use Committee of the Shandong Academy of Medical Sciences.

At day 0, nude mice were inoculated subcutaneously in the right flank with A549 cells labeled with RFP-fluorescent protein (1×10^7 viable cells per mouse in 0.2 ml of DMEM), and randomly divided into three groups, including the tumor (Tumor), lent-NC treatment (Tumor + lent-N), and lent-miR-138-5p-GFP treatment (Tumor + lent-M) groups. After 2 weeks, these mice were administered 1×10^8 PFU/ml NC or miR-138-5p at the tumor location every 4 days. The curative effect was determined by the tumor size, which was measured every 4 days. For the C57BL/6 mouse model, $4–5 \times 10^5$ 3LL viable cells/mouse in 0.2 ml of DMEM were subcutaneously injected into C57BL/6 mice. Primary tumor development was monitored by palpation. The largest perpendicular tumor diameters were measured with a caliper at 4-day intervals. Tumor volumes were calculated using the formula $\pi/6 \times \text{length} \times \text{width}^2$. Animals were sacrificed by cervical dislocation at day 30 or with subcutaneous tumor

[1]http://blast.ncbi.nlm.nih.gov/Blast.cgi

[2]http://www.mirbase.org/

volumes exceeding 3,000 mm^3. When the tumors became palpable with maximum diameter greater than 3 cm at days 10–12, the mice received subcutaneous injections of lent-miR-138-5p-GFP or lent-NC at 4-day intervals for 2 weeks. Control animals received the saline vehicle. *In vivo* live animal imaging was performed on an IVIS (®) Lumina III Imaging System (Caliper Life Sciences, Hopkinton, MA, United States). Freshly resected tumor tissue samples were fixed in 4.5% buffered formalin (Th. Geyer, Renningen, Germany) at room temperature for 12–24 h. The fixed tissue was paraffin-embedded, and slides were prepared as previously reported (Zhang et al., 2011; Yang et al., 2017). After dewaxing, the samples were blocked and permeabilized overnight at 4°C in PBS with triton-X100 (1% (w/v) and BSA (10% (w/v). Anti-CD11c or PD-L1 antibodies (Abcam, Cambridge, MA, United States) were diluted in blocking buffer at 4°C for 4 h with gentle shaking. Tissue samples were washed and incubated with secondary antibodies for 2 h before further washing with PBS and incubation with DAPI (10 μ M) for 2–3 h.

Cell Culture

The A549 human cell line was from the Cell Bank of the Chinese Academy of Sciences (Shanghai, China). 3LL Lewis lung carcinoma (clone D122) was a kind gift of professor Chu (Fudan University, Shanghai, China). Cells were cultured in Dulbecco's Modified Eagle Medium (DMEM) (Gibco BRL, Carlsbad, CA, United States) with 10% fetal bovine serum (Thermo Fisher Scientific Inc., Waltham, MA, United States) at 37°C in a humidified atmosphere containing 5% CO_2.

Human lung cancer cells were obtained from the tumor tissues of five NSCLC patients undergoing surgery in Cancer Hospital of Shandong Academy of Medical Sciences, after providing signed informed consent. The experiments were approved by the local ethics committee (Cancer Hospital of Shandong Academy of Medical Sciences, Jinan, China). The tumor tissue was homogenized and digested into a single cell suspension with DMEM containing 0.2% collagenase, 0.01% hyaluronidase, and 0.002% DNase at 37°C for 30 min. Then, the tumor cells were isolated with the tumor dissociation kit (Miltenyi Biotec GmbH, Bergisch Gladbach, Germany), according to the manufacturer's protocol. Human DCs, $CD4^+$T cells or $CD8^+$ T cells were isolated by Blood dendritic cells isolated Kit II, $CD4^+$ T cells or $CD8^+$ T cells isolated Kit II (Miltenyi Biotec GmbH, Bergisch Gladbach, Germany).

Cell Transfection and siRNA Interference

Cells were transfected with adenovirus loaded miR mimics (miR-NC), miR-138 (Genomeditech, Shanghai, China) according to the manufacturer's instructions.

The PD-L1-specific siRNA sequence (GenBank Accession No. NM_014143) (Zhao et al., 2016) was 5′-GATATTTGCTGTCTTTATA-3′. PD-L1 siRNA and scramble sequences were synthesized and purified by Shanghai Gene-Pharma Co. (Shanghai, China), and transfected into cells with Lipofectamine 2000 (Thermo Fisher Scientific, Inc., Waltham, MA, United States) according to the manufacturer's instructions.

Reverse Transcription-Quantitative Polymerase Chain Reaction (RT-qPCR)

Total RNA was extracted using TRIzol reagent (Thermo Fisher Scientific, Inc., Waltham, MA, United States), and reverse transcribed into complementary cDNA with a PrimeScript 1st Strand cDNA Synthesis kit (Takara, Otsu, Japan) according to the manufacturer's instructions. For mRNA quantitation, qPCR was performed with a SYBR-Green I Real-Time PCR kit (Biomics, Nantong, China) according to the manufacturer's instructions, with GAPDH as an internal control. The specific primer pairs were as follows: human CCND3 forward, 5′-GAGGTGCAATCCTCTCCTCG-3′ and reverse, 5′-GCTGCTCCTCACATACCTCC -3′; human CDC20 forward, 5′-TGTCAAGGCCGTAGCATGG-3′ and reverse, 5′-AGCACACATTCCAGATGCGA-3′; human MCM2 forward, 5′-ATCTACGCCAAGGAGAGGGT-3′ and reverse, 5′-GCTG CCTGTCGCCATAGATT-3′; human Ki67 forward, 5′-GTTC CAAAAGAAGAAGTGGTGCT-3′ and reverse, 5′-CACAGGCT TCTTTGGAGTAGCAG-3′; GAPDH forward, 5′-CTGGGCTA CACTGAGCACC-3′ and reverse, 5′-AAGTGGTCGTTGAGG GCAATG-3′. Mouse CCND3 forward, 5′- GTGCCCAGGAA ACGGAGTG-3′ and reverse, 5′-CAGCTCCATCCACTGCCAT CAT-3′; mouse CDC20 forward, 5′-CAAATGGAGCAGC CTGGAGA-3′ and reverse, 5′-GACCGTGAACCACTGGATA GG-3′; mouse MCM2 forward, 5′-GGATCTGATGGACAAG GCCAG-3′ and reverse, 5′-AGAGGGTCTGGCCAAGAAGA-3′; mouse Ki67 forward, 5′-AGAGCTAACTTGCGCTGACTG-3′ and reverse, 5′-TTCAATACTCCTTCCAAACAGGC-3′; iNOs forward, 5′-CAATGGCAACATCAGGTCGG-3′ and reverse, 5′-CGTACCGGATGAGCTGTGAA-3′; mVEGF forward, 5′-AGCTACTGCCGTCCAATT-3′ and reverse, 5′-TCTCCGCTCT GAACAAGG-3′; mTGF-β forward, 5′-AAATCAACGGG ATCAGC-3′ and reverse, 5′-TTGGTTGTAGAGGGCAAG-3′; GAPDH forward, 5′-CTGGGCTACACTGAGCACC-3′ and reverse, 5′-AAGTGGTCGTTGAGGGCAATG-3′. The reaction conditions were 95°C for 5 min, followed by 40 cycles of denudation at 95°C for 15 s and annealing/elongation at 60°C for 30 s. The data were analyzed by the $2^{-\Delta\Delta Cq}$ method.

Dual-Luciferase Reporter Assay

The human complementary DNA (cDNA) library was used for PD-L1 sequencing and amplification by PCR. The 3′-UTRs of wild-type PD-L1 (PD-$L1^{WT}$), and wild-type PD-1 (PD-1^{WT}), comprising the predicted has-miR-138 binding site, respectively, were cloned into the PHY-811-basic firefly luciferase plasmid (Promega, Madison, WI, United States). Mutant PD-L1 (PD-$L1^{mut}$), and PD-1 (PD-1^{mut}), 3′-UTRs, respectively, were generated with the QuickchangeXL mutagenesis kit (Stratagene, United States) to null the binding of has-miR-138 and cloned into the pGL3-basic plasmid. Then, HEK293T

cells were co-transfected with PD-L1^{WT} 3′-UTR or PD-L1^{mut} 3′-UTR, and Lent-NC or Lent-miR138-5p. Twenty-four hours after transfection, relative firefly luciferase activities were measured with the Dual-Luciferase Reporter Assay System (Promega, Madison, WI, United States) according to the manufacturer's protocol, normalized to the control with Lent-NC transfection. The interactions of miR138-5p with PD-1, PD-1^{mut} were assessed.

Western Blot

Cells were lysed with ice-cold lysis buffer (Thermo Fisher Scientific, Inc., Waltham, MA, United States), and protein amounts were determined with a Pierce BCA Protein Assay kit (Thermo Fisher Scientific, Inc., Waltham, MA, United States), according to the manufacturer's protocol. Proteins (50 μg per lane) were separated by 10% SDS-PAGE, followed by transfer onto a polyvinylidene difluoride membrane (Thermo Fisher Scientific, Inc., Waltham, MA, United States). The membrane was then incubated with PBS containing 5% milk at room temperature for 3 h, followed by incubation with rabbit anti-CCND3, CDC20, MCM2, Ki67, PD-1, and PD-L1 primary antibodies (Cell Signaling Technology Inc., Danvers, MA, United States) at room temperature for 3 h. After washing with PBS for 3 times, the membrane was incubated with goat anti-rabbit secondary antibodies (1:5,000, Abcam, Cambridge, MA, United States) at room temperature for 40 min. The samples were then washed three times with PBS, and a Super Signal West Pico Chemiluminescent Substrate kit (Thermo Fisher Scientific, Inc., Waltham, MA, United States) was used to detect signals on an X-ray film according to the manufacturer's instructions. The relative protein expression was presented as the density ratio vs. GAPDH.

MTT Assay

3LL or A549 cells (5×10^4 cells/well) were seeded in 96-well plates, and Lent-miR-138 or lent-NC was added for co-culture for 0, 24, 48, and 72 h, respectively. MTT (10 μl, 5 mg/ml, Thermo Fisher Scientific, Inc., Waltham, MA, United States) was added to each well, followed by incubation at 37°C for 4 h. The supernatant was removed, and 100 μl of dimethyl sulfoxide was added per well. Absorbance at 570 nm was determined on a Model 680 Microplate Reader (Bio-Rad Laboratories, Inc., Hercules, CA, United States).

Flow Cytometry and Antibodies

The tumors were weighed, minced into small fragments, and digested in medium containing 0.1 mg/ml DNase (Sigma-Aldrich) and 1 mg/ml collagenase IV (Sigma-Aldrich) at 37°C for 1 h (Zhang et al., 2011; Yang et al., 2017). The dissociated cells were then prepared for analysis by flow cytometry.

Antibodies targeting CD3ε, CD4, CD8, CD11b, CD80, CD86, CD54, I-a, CD11c conjugated to the corresponding fluorescent dyes were purchased from eBioscience (San Diego, CA, United States). Single-cell suspensions (1×10^6 cells) were stained with different monoclonal antibodies, according to the manufacturer's instructions. Then, samples were analyzed on a FACSuite using the CellQuest data acquisition and analysis software (BD Biosciences, CA, United States).

Phenotypic and Functional Identification of DCregs in the Tumor Tissue

Tumor-infiltrating mononuclear cells were isolated from the tumor tissue by Percoll density gradient centrifugation (Zhang et al., 2011; Yang et al., 2017). The obtained cells were labeled with anti-CD11b-PE-cy7, anti-CD11c-FITC, and anti-Ia-PE to analyze the percentage of DCs subsets. DCs was sorted by anti-mouse CD11c Kit (Miltenyi Biotec, Bergisch Gladbach, Germany), $CD4^+$ T cells or $CD8^+$ T cells was isolated by mouse CD4/CD8 (TIL) microBeads (Miltenyi Biotec, Bergisch Gladbach, Germany) The cells coculture of DC-$CD4^+$T cells (1:10), DC-$CD8^+$T cells (1:10), or $CD8^+$T cells-tumor cells (5:1,10:1, 50:1, or 100:1), DC-tumor cells (10:1) were performed for 72 h, respectively. The effect of DC cells on $CD4^+$T proliferation, CTL activation for tumor cell inhibition, and the inhibition on tumors cells were analyzed by flow cytometry with Ki67 and apoptosis detection kit (BD Biosciences, CA, United States).

Statistical Analysis

Data analysis was performed with GraphPad Prism 5 (GraphPad Software, San Diego, CA, United States). Values are mean ± standard deviation (SD) of three independent experiments. Two-tailed Student's *t*-test and one-way ANOVA were used as parametric tests. The Mann–Whitney *U*-test and Kruskal-Wallis test were used as non-parametric tests. $P < 0.05$ (*), 0.01 (**), and 0.001 (***) were considered statistically significant.

RESULTS

MiR-138 Treatment Inhibits Tumor Growth

To assess the anti-tumor effect of miR-138 in lung cancer, lent-miR-138-5p or lent-N was used to treat the nude mice bearing A549 cells. At 12 days after lent-miR-138-5p treatment, *in vivo* imaging showed lent-miR-138-5p-GFP was accumulated in the area of the tumor expressing red fluorescent proteins. However, lent-NC-GFP did not accumulate in tumor cells (**Figure 1A**, left upper panel). Similar results were found in mice bearing 3LL tumor cells (**Figure 1A**, left bottom panel). With lent-miR-138-5p treatment, the tumor volume was decreased (**Figure 1A**, right upper panel). However, NC treatment did not affect tumor volume (**Figure 1A**, right upper panel). Similar results were found in C57BL/6 mice bearing 3LL tumor cells (**Figure 1A**, right bottom panel). Furthermore, Ki67 expression in tumors from miR138-treated-mice was reduced compared with lent-NC-treated- and non-treated mice (**Figure 1B**). *In vitro* studies showed that Ki67 expression in lent-miR-138-5p-treated-A549 cells was lower compared with lent-NC-treated- and untreated A549 cells (**Figure 1C**). Meanwhile, the MTT assay confirmed

that A549 cell growth was inhibited by lent-miR-138-5p, but not by lent-NC (**Figure 1D**). Similar results were obtained in 3LL cells (**Supplementary Figure S1**).

In this study, we found that lent-miR-138-5p treatment increased the amounts of tumor-infiltrating DCs in A549 tumors (**Figure 1E**). Immunofluorescence showed that there were more CD11c + tumor-infiltrating DCs in the tumor tissue (**Figure 1F**). The amounts of tumor-infiltrating DCs, $CD4^+$ T cells, and $CD8^+$ T cells in lent-miR-138-5p-treated 3LL-bearing C57BL/6 mice were also increased compared with these in the other groups (**Supplementary Figure S2A**). Above all data indicated that miR-138-5p treatment inhibited the proliferation of tumor cells and could alter the immune microenvironment of tumors.

MiR-138 Treatment Direct Down-Regulates Cell Cycle Related Proteins in Tumor Cells

Furthermore, to analyze the direct effect of miR-138-5p on tumor cells, we detected the mRNA gene expression levels related to growth and immune regulation in tumor tissues by cancer pathway Finder PCR array (**Supplementary Table S1**). There were four down-regulated proliferation-related genes, which were further detected (**Supplementary Table S1**). The gene expression levels of Ki67, MCM2, CDC20, and CCND3 in tumor tissues from lent-miR-138-5p treated A549 lung adenocarcinoma tumor-bearing mice were lower than those of the other groups (**Figure 2A**). The expression levels of Ki67, MCM2, CDC20, and CCND3 were also lower in lent-miR-138-5p treated A549 cells compared with the other groups (**Figure 2B**). Western blot showed that the expression levels of all these molecules were lower in both lent-miR-138-5p treated A549 tumors and A549 cells compared with the other groups (**Figures 2C,D**). Lent-miR-138-5p also down-regulated the gene and protein levels of Ki67, MCM2, CDC20, and CCND3 in both lent-miR-138-5p treated 3LL tumors and 3LL cells (**Supplementary Figure S3**). These data indicated that miR-138-5p had a direct function in inhibiting the proliferation of tumor cells.

MiR-138-5p Treatment Promotes the Maturation of Tumor-Infiltrating DCs

Additionally, the immune micro-environment activated by microRNA-138-5p might be another factor for inhibiting the growth of tumors. The statuses of tumor-infiltrating DCs from lent-miR-138-5p treated A549-bearing mice, lent-NC-treated A549-bearing mice, and tumors without treatment were further analyzed. The percentage of I-a^{high}CD11b^{low} (mature DCs, DC_m) in tumor-infiltrating DCs in the microRNA-138 treatment group was higher than those of the other groups (**Figure 3A**). However, the percentage of I-a^{low}CD11b^{high} (regulatory DCs, DC_{reg}) in tumor-infiltrating DCs from microRNA-138-5p treatment mice was lower than those of other groups (**Figure 3A**). The ratio of I-a^{low}CD11b^{high}/I-a^{high}CD11b^{low} (regulatory DCs/mature DCs) was decreased in tumor-infiltrating DCs from microRNA-138-5p treatment mice, compared with other groups (**Figure 3A** and **Supplementary Figure S2B**). Furthermore, the expression levels of co-stimulatory molecules, including CD80, CD86, and I-ab, were higher on tumor-infiltrating DCs from lent-miR-138-5p treated mice compared with other groups (**Figure 3B** and **Supplementary Figure S2C**), indicating enhanced maturity of tumor-infiltrating DCs from lent-miR-138-5p treated A549 bearing mice. The effect of tumor-infiltrating DCs on tumor cells was measured to show that isolated tumor-infiltrating DCs from miR-138-5p-treated nude mice has a higher capability to kill A549 tumor cells/3LL cells (**Figure 3C** and **Supplementary Figure S2D**). DCs co-cultured with miR-138-5p-treated 3LL cells has a higher capability to kill miR-138-5p-treated 3LL cells (**Supplementary Figure S2E**) and promote the killing function of $CD8^+$ T cells and the proliferation of $CD4^+$ T cell (**Supplementary Figures S2F,G**).

However, lent-miR-138-5p could not influence the expression of CD80, CD86, and I-ab on isolated DCs in *in vitro* experiments (**Figure 3D** and **Supplementary Figure S4**) and could not influence the capability of DCs on A549 cells (**Figure 3E**), indicating that miR-138-5p could not influence the maturation of DC directly.

MiR-138-5p Treatment Down-Regulates the Expression of PD-L1 in Tumor Cells, and the Expression of PD-1 on DCs

The maturation of invasive DCs is influenced by many factors, including the secretion of VEGF, TGF-beta, PGE2, eNOS, and IL-10 by tumor cells (Todryk et al., 1999; Kim et al., 2006; Rabinovich et al., 2007; Li et al., 2008; Liu et al., 2009; Cai et al., 2010). The gene expression levels of VEGF, TGF-β, PGE2, and IL-10 in tumor cells from untreated, lent-miR-138-5p treated, and lent-NC treated A549 bearing mice were determined by RT-QPCR. As shown in **Supplementary Figure S5A**, the gene level of VEGF, TGF-β, PGE2, and IL-10 amounts in the tumors of lent-miR-138-5p-treated mice were similar to those of the lent-NC treated and untreated groups. Similar results were found in lent-miR-138-5p-treated, lent-NC-treated 3LL tumors (**Supplementary Figure S5B**). Although lent-miR-138-5p treated A549 and 3LL cells decreased the transcription levels of eNOS *in vitro*, the gene level of VEGF, TGF-β, PGE2, and IL-10 in lent-miR-138-5p-treated A549/3LL, lent-NC-treated A549/3LL, and A549 cells/3LL cells were not significantly different (**Supplementary Figures S5C,D**). This indicated that miR-138-5p may not affect the maturation of dendritic cells through these inhibitory cytokines.

PD-L1 is up-regulated in tumor cells and can regulate immune response (Fife et al., 2009; Topalian et al., 2015; Chakrabarti et al., 2018; Pawelczyk et al., 2019; Schulz et al., 2019). Thus, PD-L1 expression in tumor cells was detected. Upon miR-138-5p treatment, the gene and protein expression levels of PD-L1 in the lent-miR-138-5p-treated A549 or 3LL tumor tissue were decreased compared with the other groups (**Figures 4A,B** and **Supplementary Figures S6A,B**). Flow cytometry showed that PD-L1 expression decreased on lent-miR-138-5p-treated A549 cells compared with the other groups (**Figure 4C**). Immunofluorescence of the tumor tissue further proved that PD-L1 expression decreased on lent-miR-138-5p-treated A549

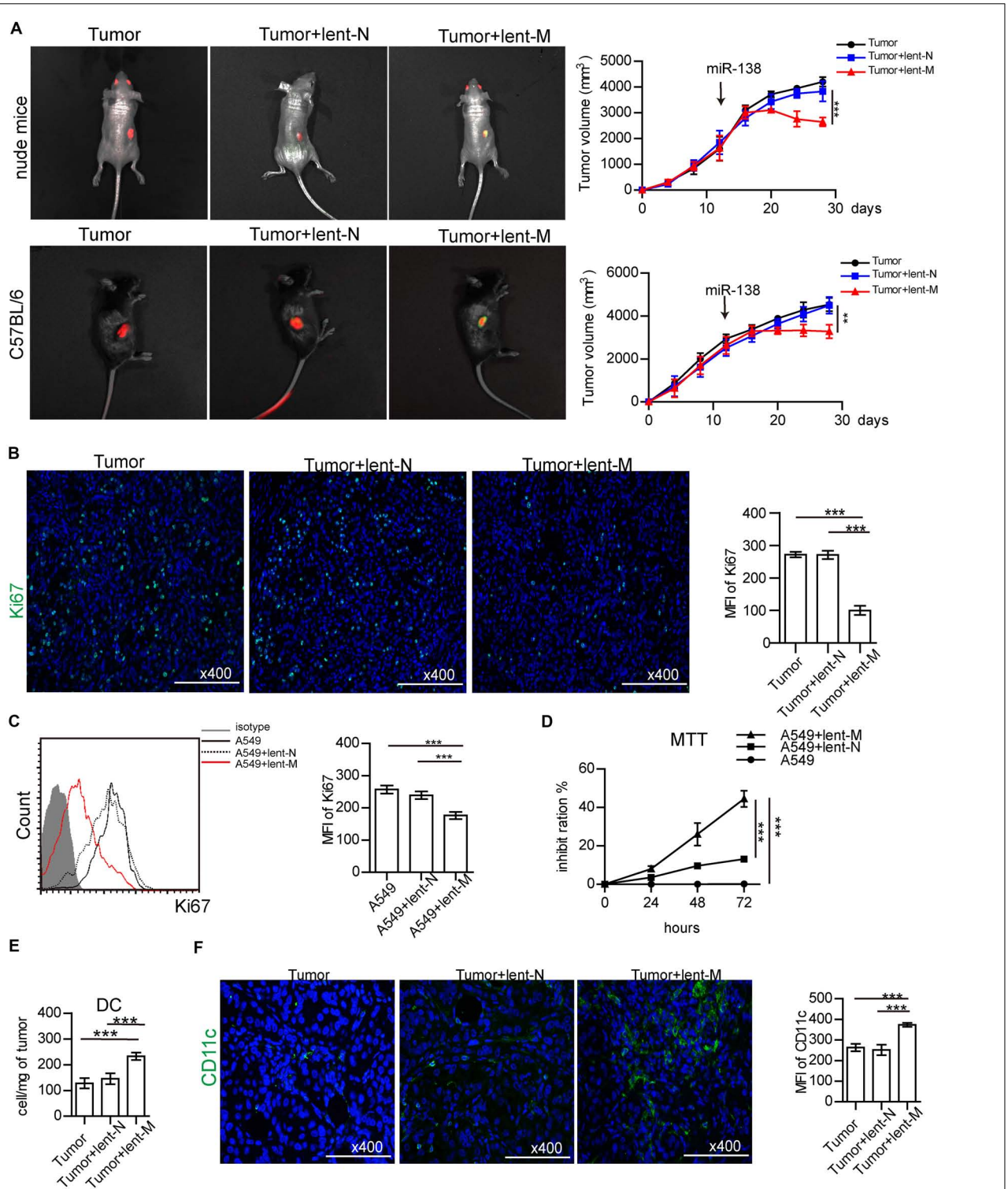

FIGURE 1 | MiR-138 treatment decreases the proliferation of lung tumor cells. **(A)** lent-NC (lent-N, green)/lent-miR-138 (lent-M, green) were administered to nude (left upper panel) or C57BL/6 mice (left bottom panel) bearing corresponding tumor cells (red). After Lent-M treatment, the mean of tumor volume was measured and analyzed (right panel). **(B)** The expression of Ki67 (green) in tumor tissues from lent-M/lent-N treated A549 tumor bearing mice or non-treated animals. (**A,B**, eight mice per group were assessed; $^{***}P < 0.001$). **(C)** Flow cytometry detection Ki67 expression on A549 cells, with or without lent-M/lent-N treatment. **(D)** With, lent-M or lent-N treatment or not, the inhibit ratio of the proliferation of A549 cells were measured by MTT. **(E)** The amounts of DCs were elevated in tumors from lent-M treated mice compared with the lent-N-treated and untreated groups. **(F)** Immunofluorescence was used to detect CD11c + cells (green) in tumor tissues from mice treated with lent-M and lent-N, respectively, as well as from untreated animals. The nucleus is blue, Bar = 100 μm. (**C–F**, three independent assays were performed; $^{***}P < 0.001$).

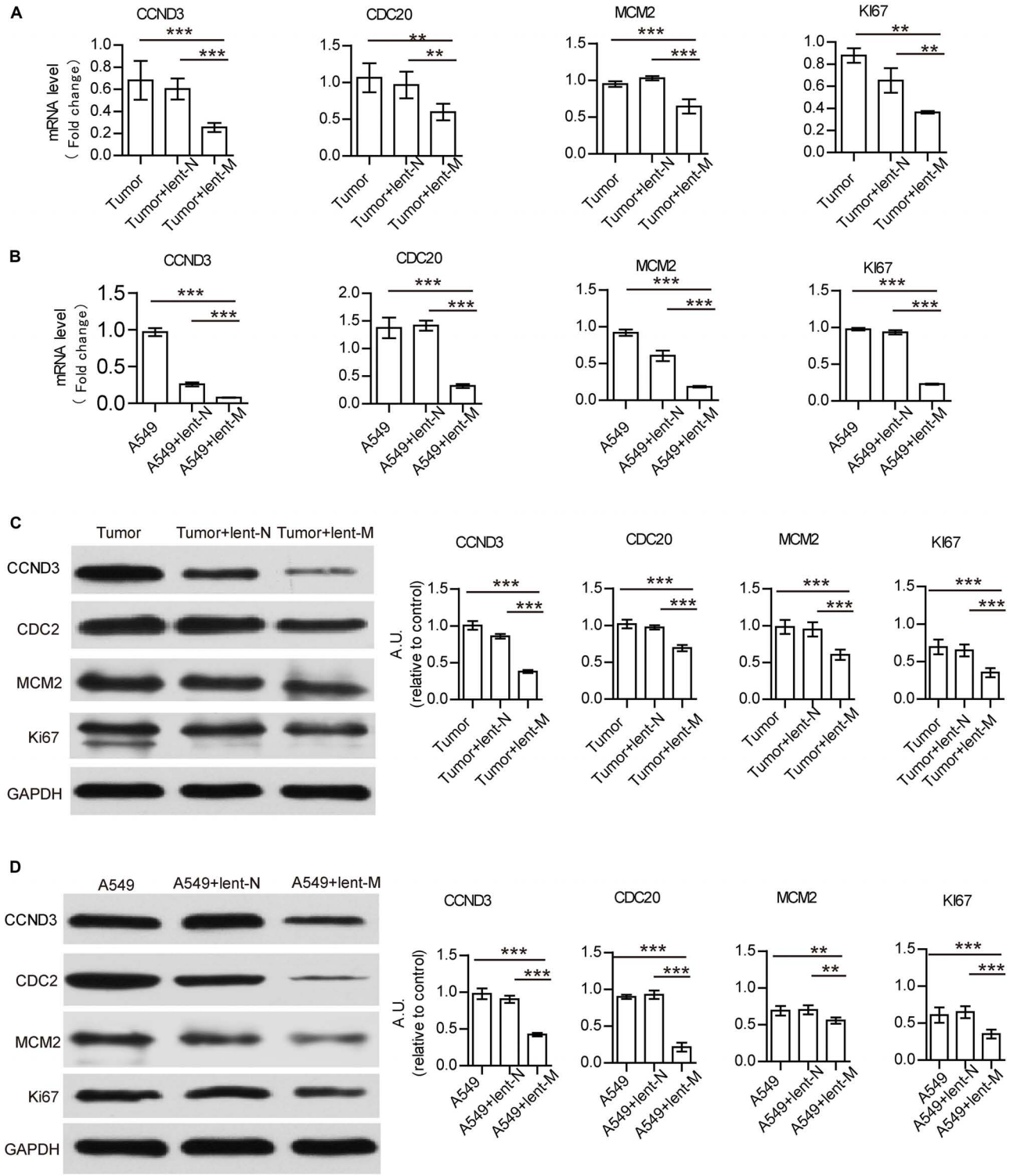

FIGURE 2 | MiR-138 treatment decreases the mRNA and protein expression levels of CCND3, CDC20, MCM2, and Ki67 in A549 tumors and A549 cells. **(A)** Lent-miR-138 treatment (lent-M) decreased the gene expression levels of CCND3, CDC20, MCM2, and Ki67 in tumors from A549 bearing mice, compared with the Lent-NC treated (lent-N) and non-treated tumors. **(B)** Decreased gene expression levels of CCND3, CDC20, MCM2, and Ki67 in lent-miR-138-5p treated A549 cells, lent-NC treated cells and untreated cells. **(C)** Lent-miR-138- treatment decreased the protein expression levels of CCND3, CDC20, MCM2, and Ki67 in A549 tumors or **(D)** A549 cells. (Three independent assays were performed; $^{**}P < 0.01$, $^{***}P < 0.001$).

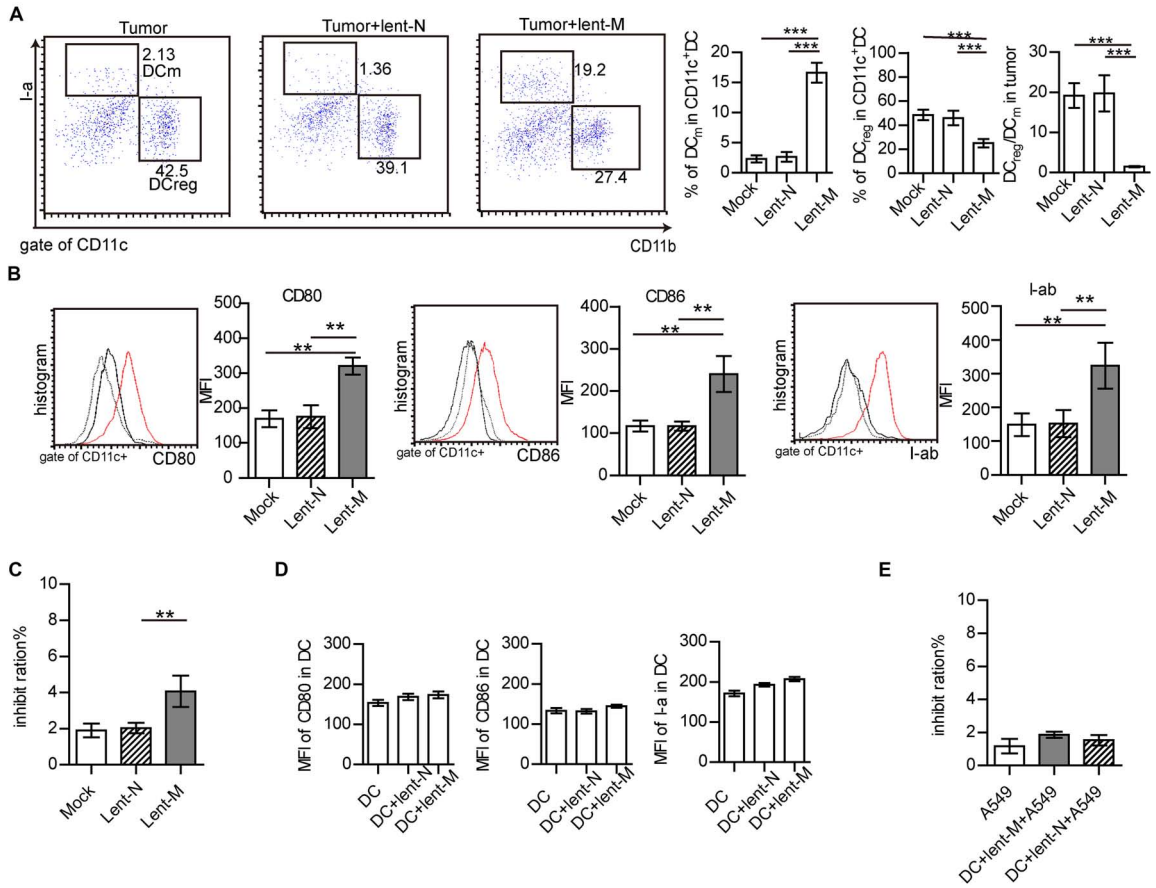

FIGURE 3 | MiR-138-5p treatment changed the statues of DCs in tumor. **(A)** The percentage of mature DCs (DC_m), regulatory DCs (DC_{reg}) and the ratios of regulator DCs to mature DCs (DC_{reg}/DC_m) in tumors from A549 bearing mice, which were treated with lent-miR-138 (Tumor + lent-M) or lent-NC (Tumor + lent-N) or not (Tumor). **(B)** The expression levels of CD80, CD86 and I-Ab on tumor infiltrating DCs from lent-M, lent-N treated A549 bearing mice or not. **(C)** The inhibit ration of tumor infiltrating DCs from lent-M, lent-N treated A549 bearing mice or not (mock). Tumor infiltrating DCs were isolated from every group and incubated with A549 cells for 24 h, and the apoptosis ratio of A549 cells was analyzed by flow cytometry. **(D)** With lent-M/lent-N treatment or not, the expression of CD80, CD86, and I-ab on isolated DCs cells. There are no significantly different between every group. **(E)** With lent-M, lent-N treatment, the inhibit ration of DCs on A549 cells were analyzed. There are no significantly different between every group. (**$P < 0.01$, ***$P < 0.001$).

tumor tissue compared with the other groups (**Figure 4D**). Furthermore, after lent-miR-138-5p treatment, the gene and protein expression levels of PD-L1 on A549 cells were also decreased (**Figures 4E–G**). Similar results were obtained in 3LL cells (**Supplementary Figures S6C,D**). Additionally, miR-138-5p treatment decreased the expression of PD-L1 and PD-1 on tumor-infiltrating DCs from lent-miR-138-5p treated mice (**Figure 4H**), and that on lent-miR-138-5p-treated DCs (**Supplementary Figure S7**).

MiR-138 Targets PD-L1/PD-1 to Down-Regulate PD-L1 in Tumor Cells and PD-1 in DCs

Further, the interactions of miR-138 and the *PD-L1, PD-1, eNOS, CDC20, CCND3, Ki67, and MCM2 genes* were analyzed by miRBase[3] and Targetscan[4]. Besides 3 binding sites were found between human/mouse *CCND3* and miR-138-5p as previous reports (Wang et al., 2012; Han et al., 2016), there are two binding sites between human/mouse *PD-L1* and miR-138-5p (**Figure 5A**), one binding site between human/mouse *PD-1* and miR-138-5p (**Figure 6A**). However, there were no direct interactions between miR-138 and *CDC20, Ki67,* or *MCM*. A dual-luciferase reporter assay confirmed that human/mouse *PD-L1* was targeted by miR-138-5p in 293T cells (**Figure 5B**). To this end, A549 cells were transfected with NC and mimic-miR138-5p, respectively, for 24 h. The gene expression levels of PD-L1 in A549 cells were not significantly different between those groups, but the protein expression levels of PD-L1 in A549 cells/3LL cells were lower than those of other groups (**Figures 5C,D**). These results demonstrated that miR-138-5p down-regulated the expression of PD-L1 in A549 cells and 3LL cells.

To assess whether PD-L1 affects the proliferation of A549 cells, the PD-L1 gene was suppressed by shRNA PD-L1. PD-L1 silencing did not alter the expression of CDC20 but decreased the gene expression levels of CCND3, MCM, and Ki67 in A549

[3]http://www.mirbase.org

[4]http://www.targetscan.org/

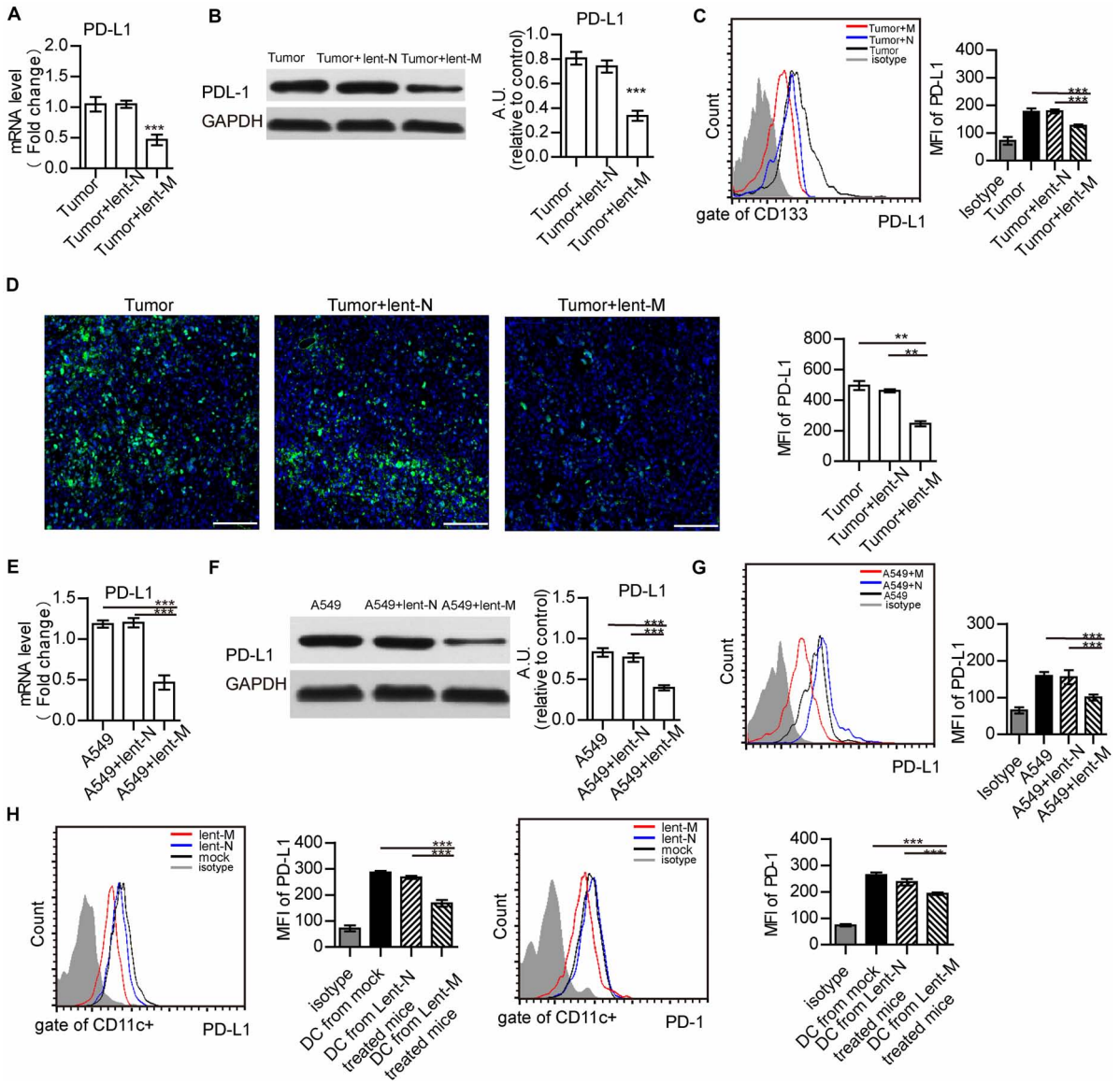

FIGURE 4 | MiR-138 treatment results in decreased expression of PD-L1 in tumor cells. **(A)** The gene expression levels of PD-L1 in tumors from lent-miR-138 (lent-M) treated mice were lower than those of the lent-NC (lent-N) treatment and untreated groups. **(B)** PD-L1 protein expression levels in tumors from microRNA-138 treated mice were lower than those of the NC treatment and untreated groups. **(C)** Flow cytometry analyzed showed that the level of PD-L1 expression on the CD133 + tumor cells from lent-M treated mice was lower than those of the lent-N treatment and untreated groups. **(D)** Immunofluorescence showed that the level of PD-L1 expression on tumors from lent-M treated mice was lower than those with lent-N treatment and untreated groups. Bar = 100 μm (**$P < 0.01$). **(E,F)** After miR-138 treatment, the gene and protein levels of PD-L1 were decreased in A549 cells. A549 cells were transfected with miR-138 mimic lentivirus (lent-M) or the corresponding negative control (lent-N). Twenty-four hours after lentiviral transfection, RT-qPCR **(E)** or Western-blot **(F)** was performed to examine the gene expression levels of miR-138 in A549 cells (***$P < 0.001$). **(G)** Flow cytometry analyzed showed that the expression of PD-L1 on the surface of untreated A549 cells, and A549 cells treated with lent-M and lent-N, respectively (***$P < 0.001$). **(H)** The expression of PD-L1 and PD-1 on the surface of tumor infiltrating DCs from lent-M, lent-N treated A549 bearing mice or not (mock), respectively (***$P < 0.001$).

cells (**Figure 5E**). This was similar to the effect of miR-138 on 3LL cells (**Supplementary Figure S8A**). Moreover, PD-L1 silencing resulted in reduced expression of Ki67 in A549 cells/3LL cells and decreased cell proliferation (**Figures 5F,G** and **Supplementary Figures S8B,C**). The killing capability of DC on shRNA PD-L1 treated-A549 cells/3LL was higher than those of the no-treatment and NC groups (**Figure 5H** and **Supplementary Figure S8D**).

Furthermore, a dual-luciferase reporter assay was performed to confirm that PD-1 was targeted by miR-138-5p in 293 T cells (**Figures 6A,B**). After lent-miR-138-5p treatment, PD-1 expression levels in human/mouse DCs were lower than those of other groups (**Figure 6C**). After lent-miR-138-5p treatment, PD-1 expression levels in human/mouse T cells were also lower compared with the other groups (**Figure 6D**).

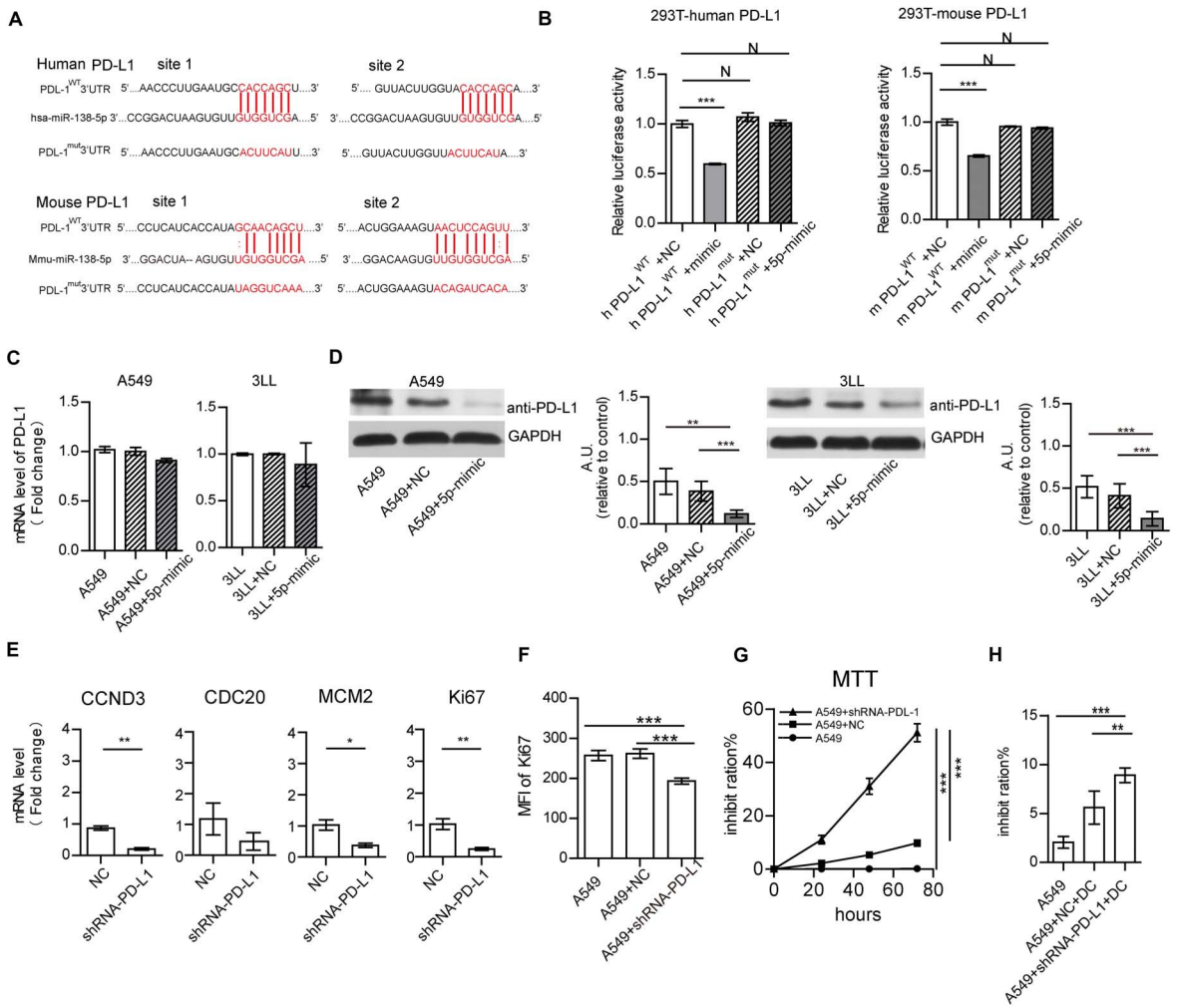

FIGURE 5 | MiR-138-5p targets PD-L1 to decrease proliferation A549 cells. **(A)** Diagram of the has-miR-138-5p binding site in wild-type (WT) human or mouse PD-L1 3′UTR. The mutation was generated at the binding site (Mut). **(B)** In a dual-luciferase reporter assay, a luciferase reporter gene containing the WT or Mut human or mouse PD-L1 3′UTR was co-transfected with NC or miR-138-5p mimic into HEK293T cells, and relative luciferase activities were assessed. The gene **(C)** and protein expression **(D)** of PD-L1 on A549 cells/3LL cells, which were transfected with NC or miR138 mimic or not. **(E)** Upon NC, shRNA PD-L1 treatment, the expression levels of CCND3, CDC20, MCM2, and Ki67 were assessed by RT-QPCR. After NC or shRNA PD-L1 silencing in A549 cells, cell proliferation was analyzed by flow cytometry detection of Ki67 **(F)** or the MTT assay **(G)**. **(H)** Percentages of apoptotic A549 tumor cells co-cultured with DCs, which were pretreated or not with shRNA PD-L1 or NC. (*$P < 0.05$, **$P < 0.01$, ***$P < 0.001$).

MiR-138-5p Downregulates the Expression of PD-L1 in Human Lung Cancer Cells

To further analyze the effects of microRNA-138 in human lung cancer cells, human lung cancer cells from NSCLC patients were isolated. After lent-miR-138-5p treatment, PD-L1 mRNA, and protein expression levels in human lung cancer cells were decreased (**Figures 7A,B**). Upon miR-138-5p treatment, the expression of Ki67 in human lung cancer cells was decreased as well as cell proliferation (**Figures 7C,D**). In addition, lent-miR-138-5p-treated-human lung cancer cells increased the killing capability of DC on tumor cells, compared with the non-treatment group (**Figure 7E**). Meanwhile, human DCs co-cultured with lent-miR-138-5p-treated-human lung cancer cells had a stronger ability to induce $CD8^+$ T cell killing of human lung cancer cells and promote $CD4^+$ T cells proliferation (**Figures 7F,G**).

DISCUSSION

The expression of miR-138 is reduced in various cancers, including anaplastic thyroid carcinoma (ATC), NSCLC, gallbladder carcinoma, and oral squamous cell carcinoma (OSCC) (Xu et al., 2015; Ye et al., 2015; Li et al., 2016; Hu et al., 2017; Si et al., 2017; Liu et al., 2018). In agreement, miR-138 overexpression can significantly inhibit tumor cell proliferation (Zhang et al., 2013; Li et al., 2015; Ye et al., 2015; Han et al., 2016). Moreover, miR-138 inhibits proliferation,

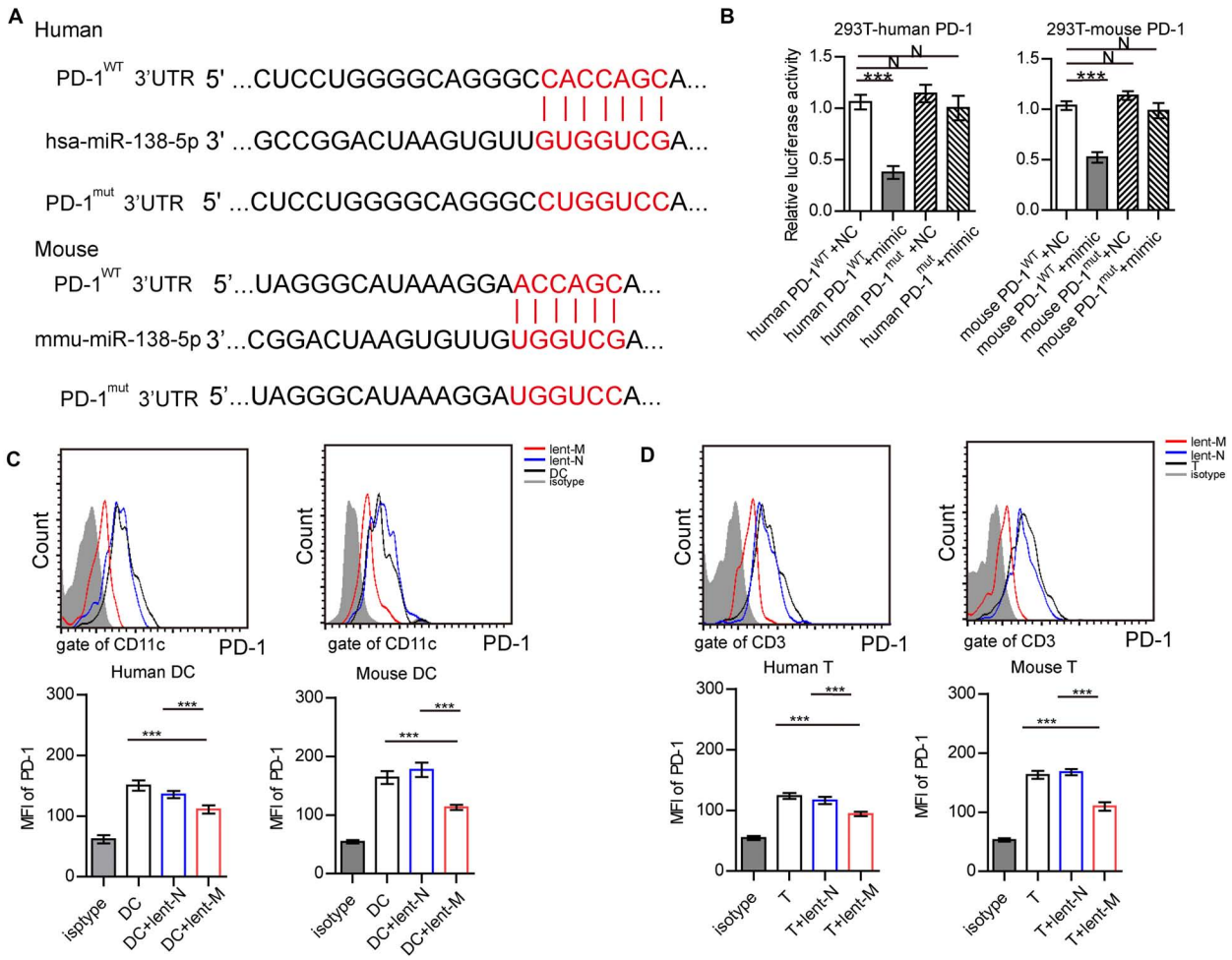

FIGURE 6 | MiR-138-5p targets PD-1 on DCs and T cells. **(A)** Diagram of the has-miR-138-5p binding site on wild-type (WT) human or mouse PD-1 3′UTR. A mutation was generated at the binding site (Mut). **(B)** In a dual-luciferase reporter assay, the firefly luciferase reporter containing the WT or Mut PD-1 3′UTR was co-transfected with NC or miR-138-5p mimic into HEK293T cells, and relative luciferase activities were assessed. After lent-miR-138-5p or lent-NC treatment, the expression levels of PD-1 on human or mouse DCs **(C)** and $CD4^+$ T cells **(D)** were determined. (Three independent assays were performed; $^{***}P < 0.001$).

induces apoptosis, restrains both metastasis and invasion, and enhances the chemosensitivity of tumor cells through the suppression of multiple targets (Zhang et al., 2013; Gao et al., 2014; Huang et al., 2015; Ye et al., 2015; Hu et al., 2017; Si et al., 2017; Liu et al., 2018). Thus, miR-138 can play various roles by targeting multiple genes in the biological processes of different cancers and is considered to be a promising molecular target for cancer treatment. MiR-138 also inhibits the proliferation and migration of NSCLC (Zhang et al., 2013; Gao et al., 2014; Ye et al., 2015; Han et al., 2016). However, the mechanism and the regulatory role of miR-138 in the tumor growth and tumor micro-environment remain undefined. Herein, we reported that miR-138-5p could decrease the expression levels of CDC20, CCND3, Ki67, and MCM in tumor cells. However, it only targets CCND3 to inhibit NSCLC, as previously reported (Wang et al., 2012; Han et al., 2016). In our studying, we found that miR-138-5p targets PD-L1 to down-regulate PD-L1 in NSCLC. Silencing PD-L1 reduced the mRNA levels of CCND3, Ki67, and MCM in A549 cells. Thus, miR-138-5p might influence the expression of CCND3, Ki67, and MCM in A549 cells by down-regulating PD-L1. Tumor-intrinsic PD-L1 signaling regulates the distinct tumor cell growth, pathogenesis and autophagy (Chakrabarti et al., 2018; Pawelczyk et al., 2019; Schulz et al., 2019). PD-L1 expression has a positive correlation with Ki-67 expression in glioma (Xue et al., 2017), and its suppression inhibits the proliferation of tumor cells (Topalian et al., 2015; Poggio et al., 2019). Although silencing PD-L1 can not reduce the gene expression of CCD2, lent-miR-138 treatment can decrease the gene expression of CCD2 directly. Thus, the effect of miR-138-5p on the growth of tumors may be through many pathways. Additionally, miR-138-5p treatment decreased the protein expression of PD-L1 in A549/3LL cells, but not the gene expression of PD-L1 in these cells *in vitro*. However, miR-138-5p treatment decreased the gene and protein expression of PD-L1 *in vivo* experiment. It suggested the

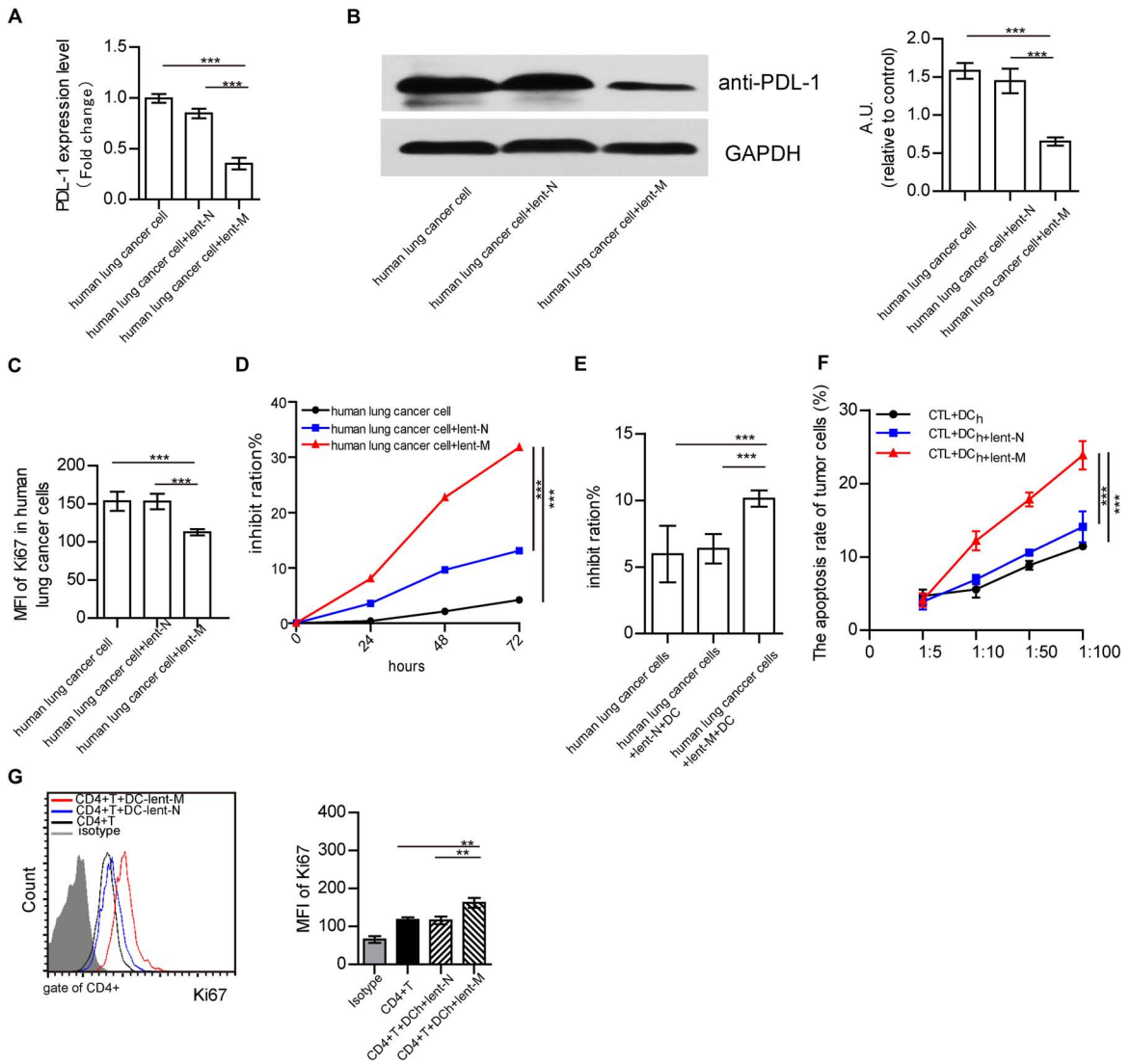

FIGURE 7 | Effects of lent-miR-138-5p on human NSCLC. After treatment with lent-miR-138-5p (Lent-M) or the corresponding negative control lentivirus (lent-N), PD-L1 expression on isolated human lung cancer cells was analyzed by qRT-PCR **(A)** or Western blot **(B)**. Upon lent-miR-138-5p (lent-M) or lent-N treatment, the proliferation of human NSCLC cells was analyzed by flow cytometry detection of Ki67 **(C)** and the inhibition rate of the proliferation of human NSCLC cells was analyzed by MTT assay **(D)**. **(E)** With lent-M, lent-N treatment, the inhibit ration of human DCs on isolated human lung cancer cells were analyzed. **(F)** Percentages of apoptotic tumor cells co-cultured with $CD3^+CD8^+$ human T cells (CTL) activated by human DCs pretreated or not with lent- miR138-5p or lent-N treated A549 cells. **(G)** The proliferation of human $CD4^+$ T cocultured with human DCs pretreated or not with lent- miR138 or lent-N treated A549 cells (Three independent assays were performed; $^{**}P < 0.01$, $^{***}P < 0.001$).

multiple mechanisms of miR-138-5p on NSCLC, which needs further studying.

Different from previous studies (Song et al., 2011; Wang et al., 2011, 2012; Zhang et al., 2013; Li et al., 2015, 2016; Ma et al., 2015; Xu et al., 2015; Ye et al., 2015; Han et al., 2016; Jiang et al., 2016), assessing the effects of microRNA-138 on tumor cells, our studying showed that miR-138-5p not only inhibits the proliferation of tumor cells but also regulates the tumor immune micro-environment. Lent-miR-138-5p treatment increased the number of tumor-infiltrated DCs and regulated the maturation of DCs in the A549/3LL-bearing mice model, and promoted DCs' capability to inhibit tumor cells and enhance T cells to kill tumor cells. But lent-miR-138-5p could not induce DC maturation and influence its function directly. Thus, the effect of lent-miR-138-5p on DCs might be through suppress the inhibition of tumor cells or regulate the tumor micro-environment.

The tumor micro-environment is well known to be immune-suppressive. Tumor cells consistently release many immuno-suppressive and pro-inflammatory factors such as vascular endothelial growth factor (VEGF), TGF-β, IL-10, PGE2, eNOS, which induce tumor-infiltrating immune cells to be tolerance

(Zhang et al., 2004; Zou, 2005; Kim et al., 2006; Tang et al., 2006; Rabinovich et al., 2007; Xia et al., 2008). Additionally, tumor cells can induce tumor-infiltrating immune cells to be tolerance by PD-L1. In this study, miR-138-5p did not affect the expression of VEGF, TGF-β, IL-10, eNOS and PGE2 in NSCLC cells, while targeting and down-regulating PD-L1, indicating that miR-138-5p could affect the function of DCs by decreasing the expression of PD-L1 on tumor cells. Moreover, down-regulating PD-L1 can reduce the inhibitory effects of tumor cells on DCs to promote CTL–mediated killing of tumor cells and increase the proliferation of T cells. Therefore, miR-138-5p regulates the function of DC by targeting PD-L1. Whether miR-138-5p can regulate the tumor immune micro-environment by targeting other inhibitors need to be further studied.

In cancer patients, miR-138 expression is negatively correlated with the expression of PD-L1 (Huang et al., 2019). PD-L1 is an essential inhibitory molecule in tumor cells that induces tolerance of the tumor micro-environment and immunosuppression. PD-L1 over-expression has been described in different cancers (Topalian et al., 2015; Clark et al., 2016; Chakrabarti et al., 2018; Pawelczyk et al., 2019; Schulz et al., 2019). It promotes immune tolerance in tumors by binding to PD-1 on T cells or DCs to trigger suppressive signaling pathways (Fife et al., 2009; Topalian et al., 2015; Xue et al., 2017; Poggio et al., 2019). Antibody blockade of PD-L1 activates an anti-tumor immune response leading to durable remission in a subset of cancer patients. Blocking PD-L1 expression on tumor cells could be better for tumor therapy and immune activation (Zhao et al., 2016; Poggio et al., 2019). Our studying showed that miR-138-5p targeted PD-L1 to down-regulate PD-L1 in NSCLC and reduce the inhibitory effects on DCs, promote CTL–mediated killing of tumor cells, and increase the proliferation of T cells. Additionally, miR-138-5p also targeted PD-L1 to down-regulate PD-L1 in DCs to relieve the inhibition of tumor-infiltrating DC on T cells. Thus, miR-138 functions not only in inhibiting tumor cell proliferation but also in regulating immune cells by down-regulating PD-L1 on tumor cells.

Similar to previous reports (Wei et al., 2016), miR-138-5p also significantly down-regulated PD-1 in T cells and DCs. PD-1, a receptor of PD-L1, is activated by PD-L1 to induce TCR stopping signals to suppress T cell activation (Parry et al., 2005; Hui et al., 2017). Down-regulating PD-1 can relieve the inhibition of tumor cells by immune cells. Thus, miR-138-5p could regulate immune tolerance by targeting multiple immune checkpoint molecules to inhibit the suppressive cell-cell contact for removing immune-suppression in NSCLC.

Based on these results, our studying showed that the immune-regulatory role of miR-138-5p in the NSCLC micro-environment. This effects of miR-138-5p in anti-cancer therapy were due to miR-138-5p targeting PD-L1/PD-1 to down-regulate the expression of PD-L1/PD-1 (**Supplementary Figures S9**, **S10**): (1) miR-138-5p regulated the immune response in the tumor micro-environment by reliving the inhibition of tumor cells on DCs; (2) miR-138-5p inhibited the proliferation of NSCLC cells by decreasing the expression levels of CCND3, Ki67, and MCM2 in tumor cells.

DATA AVAILABILITY STATEMENT

The datasets presented in this study can be found in online repositories. The names of the repository/repositories and accession number(s) can be found in the article/**Supplementary Material**.

ETHICS STATEMENT

The experiments were approved by the local ethics committee (Cancer Hospital of Shandong Academy of Medical Sciences, Jinan, China). The patients/participants provided their written informed consent to participate in this study. All animal experiments were approved by the Animal Care and Use Committee of Shandong Academy of medical Sciences.

AUTHOR CONTRIBUTIONS

WL designed this research and wrote the manuscript. WL, NS, and PL performed the animal experiments, RT-QPCR, and Western-blot. SZ, QS, YY, XL, PFL, and MF cultured cells and performed the flow cytometry experiment. PS and YL performed the human research experiments. WL and MZ analyzed the data. All authors contributed to the article and approved the submitted version.

FUNDING

This work was supported by grants from the Natural Science Foundation of China (Nos. 81500710 and 81860719), the Shandong Key Research and Development Project (2019GSF108189 and 2018GSF118115), the National Science and Technology Major Special Project of China (2017ZX09301058002), the General Program of Shandong Provincial Natural Science Foundation (ZR2019MH086), projects of medical and health technology development program in Shandong Province (Nos. 2015WS0194 and 2019WS186), the science and technology program from the Shandong Academy of Medical Sciences (No. 2015-25), and the Innovation Project of Shandong Academy of Medical Sciences.

ACKNOWLEDGMENTS

We acknowledge the experimental help from Dr. Yunbo Wei and Mrs. Tingting Han (Shandong Academy of Sciences, Jinan, China), and Prof. Yiwei Chu (Department of Immunology, Shanghai Medical School, Fudan University, Shanghai, China).

SUPPLEMENTARY MATERIAL

The Supplementary Material for this article can be found online at: https://www.frontiersin.org/articles/10.3389/fcell.2020.00540/full#supplementary-material

FIGURE S1 | MiR-138-5p treatment decreases the proliferation of 3LL tumor cells.

FIGURE S2 | MiR-138-5p treatment decreases the amounts of tumor infiltrating DCs and T cells from 3LL bearing mice.

FIGURE S3 | MiR-138-5p treatment decreases the mRNA and protein expression levels of CCND3, CDC20, MCM2 and Ki67 in 3LL cells bearing mice and 3LL cells.

FIGURE S4 | The transduction efficiency of lent-miR-138-5p-GFP in DCs and T cells.

FIGURE S5 | MiR-138-5p treatment decreases the mRNA expression levels of VEGF, TGF-β, eNOS, PGE2 and IL-10 in A549 tumor **(A)**, 3LL tumor **(B)**, A549 **(C)** and 3LL cells **(D)**.

FIGURE S6 | MiR-138-5p treatment decreases the mRNA and protein expression levels of PD-L1 in 3LL cells.

FIGURE S7 | With lent-miR-138-5p treatment, or lent-N treatment, or not, the level of PD-1 and PD-L1 expression on isolated DCs.

FIGURE S8 | shRNA PD-L1 influence proliferation of 3LL cell.

FIGURE S9 | The design map of our manuscript.

FIGURE S10 | The diagram of the effect of miR-138 on tumor cells and DCs.

TABLE S1 | With lent-miR138-5p treatment or not, the mRNA expression levels of molecules related to growth and immune regulation in A549 tumor cells by cancer pathway Finder PCR array and showed in table.

REFERENCES

Ambros, V. (2004). The functions of animal microRNAs. *Nature* 431, 350–355. doi: 10.1038/nature02871

Bartel, D. P. (2004). MicroRNAs: genomics, biogenesis, mechanism, and function. *Cell* 116, 281–297.

Bell, D., Chomarat, P., Broyles, D., Netto, G., Harb, G. M., Lebecque, S., et al. (1999). In breast carcinoma tissue, immature dendritic cells reside within the tumor, whereas mature dendritic cells are located in peritumoral areas. *J. Exp. Med.* 190, 1417–1426. doi: 10.1084/jem.190.10.1417

Cai, Z., Zhang, W., Li, M., Yue, Y., Yang, F., Yu, L., et al. (2010). TGF-beta1 gene-modified, immature dendritic cells delay the development of inflammatory bowel disease by inducing CD4(+)Foxp3(+) regulatory T cells. *Cell Mol. Immunol.* 7, 35–43. doi: 10.1038/cmi.2009.107

Calin, G. A., and Croce, C. M. (2006). MicroRNA signatures in human cancers. *Nat. Rev. Cancer* 6, 857–866. doi: 10.1038/nrc1997

Chakrabarti, J., Holokai, L., Syu, L., Steele, N. G., Chang, J., Wang, J., et al. (2018). Hedgehog signaling induces PD-L1 expression and tumor cell proliferation in gastric cancer. *Oncotarget* 9, 37439–37457. doi: 10.18632/oncotarget.26473

Chen, W., Zheng, R., Zeng, H., and Zhang, S. (2011). The updated incidences and mortalities of major cancers in China, 2011. *Chin. J. Cancer* 34, 502–507.

Clark, C. A., Gupta, H. B., Sareddy, G., Pandeswara, S., Lao, S., Yuan, B., et al. (2016). Tumor-intrinsic PD-L1 signals regulate cell growth, pathogenesis, and autophagy in ovarian cancer and melanoma. *Cancer Res.* 76, 6964–6974. doi: 10.1158/0008-5472.can-16-0258

Croce, C. M., and Calin, G. A. (2005). miRNAs, cancer, and stem cell division. *Cell* 122, 6–7. doi: 10.1016/j.cell.2005.06.036

Fife, B. T., Pauken, K. E., Eagar, T. N., Obu, T., Wu, J., Tang, Q., et al. (2009). Interactions between PD-1 and PD-L1 promote tolerance by blocking the TCR-induced stop signal. *Nat. Immunol.* 10, 1185–1192. doi: 10.1038/ni.1790

Fu, D., Yu, W., Li, M., Wang, H., Liu, D., Song, X., et al. (2015). MicroRNA-138 regulates the balance of Th1/Th2 via targeting RUNX3 in psoriasis. *Immunol. Lett.* 166, 55–62. doi: 10.1016/j.imlet.2015.05.014

Gao, Y., Fan, X., Li, W., Ping, W., Deng, Y., and Fu, X. (2014). miR-138-5p reverses gefitinib resistance in non-small cell lung cancer cells via negatively regulating G protein-coupled receptor 124. *Biochem. Biophys. Res. Commun.* 446, 179–186. doi: 10.1016/j.bbrc.2014.02.073

Han, L. P., Fu, T., Lin, Y., Miao, J. L., and Jiang, Q. F. (2016). MicroRNA-138 negatively regulates non-small cell lung cancer cells through the interaction with cyclin D3. *Tumour Biol.* 37, 291–298. doi: 10.1007/s13277-015-3757-8

Hu, B., Wang, J., and Jin, X. (2017). MicroRNA-138 suppresses cell proliferation and invasion of renal cell carcinoma by directly targeting SOX9. *Oncol. Lett.* 14, 7583–7588.

Huang, B., Li, H., Huang, L., Luo, C., and Zhang, Y. (2015). Clinical significance of microRNA 138 and cyclin D3 in hepatocellular carcinoma. *J. Surg. Res.* 193, 718–723. doi: 10.1016/j.jss.2014.03.076

Huang, C. Y., Zha, X. F., and Wen, W. R. (2019). [Expression and clinical significance of PD-L1 and MicroRNA-138-5p in patients with acute myeloid leukemia]. *Zhongguo Shi Yan Xue Ye Xue Za Zhi* 27, 373–378.

Hui, E., Cheung, J., Zhu, J., Su, X., Taylor, M. J., Wallweber, H. A., et al. (2017). T cell costimulatory receptor CD28 is a primary target for PD-1-mediated inhibition. *Science* 355, 1428–1433. doi: 10.1126/science.aaf1292

Jiang, B., Mu, W., Wang, J., Lu, J., Jiang, S., Li, L., et al. (2016). MicroRNA-138 functions as a tumor suppressor in osteosarcoma by targeting differentiated embryonic chondrocyte gene 2. *J. Exp. Clin. Cancer Res.* 35:69.

Kim, R., Emi, M., Tanabe, K., and Arihiro, K. (2006). Tumor-driven evolution of immunosuppressive networks during malignant progression. *Cancer Res.* 66, 5527–5536. doi: 10.1158/0008-5472.can-05-4128

Kusmartsev, S., and Gabrilovich, D. I. (2006). Effect of tumor-derived cytokines and growth factors on differentiation and immune suppressive features of myeloid cells in cancer. *Cancer Metastasis Rev.* 25, 323–331. doi: 10.1007/s10555-006-9002-6

Li, B., Yang, X. X., Wang, D., and Ji, H. K. (2016). MicroRNA-138 inhibits proliferation of cervical cancer cells by targeting c-Met. *Eur. Rev. Med. Pharmacol. Sci.* 20, 1109–1114.

Li, J., Wang, Q., Wen, R., Liang, J., Zhong, X., Yang, W., et al. (2015). MiR-138 inhibits cell proliferation and reverses epithelial-mesenchymal transition in non-small cell lung cancer cells by targeting GIT1 and SEMA4C. *J. Cell Mol. Med.* 19, 2793–2805. doi: 10.1111/jcmm.12666

Li, Q., Guo, Z., Xu, X., Xia, S., and Cao, X. (2008). Pulmonary stromal cells induce the generation of regulatory DC attenuating T-cell-mediated lung inflammation. *Eur. J. Immunol.* 38, 2751–2761. doi: 10.1002/eji.200838542

Lin, W. W., and Karin, M. (2007). A cytokine-mediated link between innate immunity, inflammation, and cancer. *J. Clin. Invest.* 117, 1175–1183. doi: 10.1172/jci31537

Liu, C., Zhu, J., Liu, F., Wang, Y., and Zhu, M. (2018). MicroRNA-138 targets SP1 to inhibit the proliferation, migration and invasion of hepatocellular carcinoma cells. *Oncol. Lett.* 15, 1279–1286.

Liu, Q., Zhang, C., Sun, A., Zheng, Y., Wang, L., and Cao, X. (2009). Tumor-educated CD11bhighIalow regulatory dendritic cells suppress T cell response through arginase I. *J. Immunol.* 182, 6207–6216. doi: 10.4049/jimmunol.0803926

Ma, F., Zhang, M., Gong, W., Weng, M., and Quan, Z. (2015). MiR-138 suppresses cell proliferation by targeting Bag-1 in gallbladder carcinoma. *PLoS One* 10:e0126499. doi: 10.1371/journal.pone.0126499

Mannavola, F., Tucci, M., Felici, C., Stucci, S., and Silvestris, F. (2016). miRNAs in melanoma: a defined role in tumor progression and metastasis. *Expert Rev. Clin. Immunol.* 12, 79–89. doi: 10.1586/1744666x.2016.1100965

Parry, R. V., Chemnitz, J. M., Frauwirth, K. A., Lanfranco, A. R., Braunstein, I., Kobayashi, S. V., et al. (2005). CTLA-4 and PD-1 receptors inhibit T-cell activation by distinct mechanisms. *Mol. Cell Biol.* 25, 9543–9553. doi: 10.1128/mcb.25.21.9543-9553.2005

Pawelczyk, K., Piotrowska, A., Ciesielska, U., Jablonska, K., Gletzel-Plucinska, N., Grzegrzolka, J., et al. (2019). Role of PD-L1 expression in non-small cell lung cancer and their prognostic significance according to clinicopathological factors and diagnostic markers. *Int. J. Mol. Sci.* 20:824. doi: 10.3390/ijms20040824

Poggio, M., Hu, T., Pai, C. C., Chu, B., Belair, C. D., Chang, A., et al. (2019). Suppression of Exosomal PD-L1 induces systemic anti-tumor immunity and memory. *Cell* 177, 414–427.e13. doi: 10.1016/j.cell.2019.02.016

Rabinovich, G. A., Gabrilovich, D., and Sotomayor, E. M. (2007). Immunosuppressive strategies that are mediated by tumor cells. *Annu. Rev. Immunol.* 25, 267–296. doi: 10.1146/annurev.immunol.25.022106.141609

Saika, K., and Machii, R. (2012). Cancer mortality attributable to tobacco in Asia based on the WHO global report. *Jpn. J. Clin. Oncol.* 42:985. doi: 10.1093/jjco/hys154

Schulz, D., Stancev, I., Sorrentino, A., Menevse, A. N., Beckhove, P., Brockhoff, G., et al. (2019). Increased PD-L1 expression in radioresistant HNSCC cell lines after irradiation affects cell proliferation due to inactivation of GSK-3beta. *Oncotarget* 10, 573–583. doi: 10.18632/oncotarget.26542

Sha, H. H., Wang, D. D., Chen, D., Liu, S. W., Wang, Z., Yan, D. L., et al. (2017). MiR-138: A promising therapeutic target for cancer. *Tumour Biol.* 39:1010428317697575.

Shurin, M. R., Shurin, G. V., Lokshin, A., Yurkovetsky, Z. R., Gutkin, D. W., Chatta, G., et al. (2006). Intratumoral cytokines/chemokines/growth factors and tumor infiltrating dendritic cells: friends or enemies? *Cancer Metastasis Rev.* 25, 333–356. doi: 10.1007/s10555-006-9010-6

Si, F., Sun, J., and Wang, C. (2017). MicroRNA-138 suppresses cell proliferation in laryngeal squamous cell carcinoma via inhibiting EZH2 and PI3K/AKT signaling. *Exp. Ther. Med.* 14, 1967–1974. doi: 10.3892/etm.2017.4733

Siegel, R., Naishadham, D., and Jemal, A. (2013). Cancer statistics, 2013. *CA Cancer J. Clin.* 63, 11–30. doi: 10.3322/caac.21166

Smith, R. A., Manassaram-Baptiste, D., Brooks, D., Cokkinides, V., Doroshenk, M., Saslow, D., et al. (2014). Cancer screening in the United States, 2014: a review of current American Cancer Society guidelines and current issues in cancer screening. *CA Cancer J. Clin.* 64, 30–51. doi: 10.3322/caac.21212

Song, T., Zhang, X., Wang, C., Wu, Y., Cai, W., Gao, J., et al. (2011). MiR-138 suppresses expression of hypoxia-inducible factor 1alpha (HIF-1alpha) in clear cell renal cell carcinoma 786-O cells. *Asian Pac. J. Cancer Prev.* 12, 1307–1311.

Tang, H., Guo, Z., Zhang, M., Wang, J., Chen, G., and Cao, X. (2006). Endothelial stroma programs hematopoietic stem cells to differentiate into regulatory dendritic cells through IL-10. *Blood* 108, 1189–1197. doi: 10.1182/blood-2006-01-007187

Todryk, S., Melcher, A. A., Hardwick, N., Linardakis, E., Bateman, A., Colombo, M. P., et al. (1999). Heat shock protein 70 induced during tumor cell killing induces Th1 cytokines and targets immature dendritic cell precursors to enhance antigen uptake. *J. Immunol.* 163, 1398–1408.

Topalian, S. L., Drake, C. G., and Pardoll, D. M. (2015). Immune checkpoint blockade: a common denominator approach to cancer therapy. *Cancer Cell* 27, 450–461. doi: 10.1016/j.ccell.2015.03.001

Wang, W., Zhao, L. J., Tan, Y. X., Ren, H., and Qi, Z. T. (2012). MiR-138 induces cell cycle arrest by targeting cyclin D3 in hepatocellular carcinoma. *Carcinogenesis* 33, 1113–1120. doi: 10.1093/carcin/bgs113

Wang, Y., Huang, J. W., Li, M., Cavenee, W. K., Mitchell, P. S., Zhou, X., et al. (2011). MicroRNA-138 modulates DNA damage response by repressing histone H2AX expression. *Mol. Cancer Res.* 9, 1100–1111. doi: 10.1158/1541-7786.mcr-11-0007

Wei, J., Nduom, E. K., Kong, L. Y., Hashimoto, Y., Xu, S., Gabrusiewicz, K., et al. (2016). MiR-138 exerts anti-glioma efficacy by targeting immune checkpoints. *Neuro Oncol.* 18, 639–648. doi: 10.1093/neuonc/nov292

Wen, Y., Han, J., Chen, J., Dong, J., Xia, Y., Liu, J., et al. (2015). Plasma miRNAs as early biomarkers for detecting hepatocellular carcinoma. *Int. J. Cancer* 137, 1679–1690. doi: 10.1002/ijc.29544

Xia, S., Guo, Z., Xu, X., Yi, H., Wang, Q., and Cao, X. (2008). Hepatic microenvironment programs hematopoietic progenitor differentiation into regulatory dendritic cells, maintaining liver tolerance. *Blood* 112, 3175–3185. doi: 10.1182/blood-2008-05-159921

Xu, R., Zeng, G., Gao, J., Ren, Y., Zhang, Z., Zhang, Q., et al. (2015). miR-138 suppresses the proliferation of oral squamous cell carcinoma cells by targeting Yes-associated protein 1. *Oncol. Rep.* 34, 2171–2178. doi: 10.3892/or.2015.4144

Xue, S., Hu, M., Li, P., Ma, J., Xie, L., Teng, F., et al. (2017). Relationship between expression of PD-L1 and tumor angiogenesis, proliferation, and invasion in glioma. *Oncotarget* 8, 49702–49712. doi: 10.18632/oncotarget.17922

Yang, J., Liu, H., Wang, H., and Sun, Y. (2013). Down-regulation of microRNA-181b is a potential prognostic marker of non-small cell lung cancer. *Pathol. Res. Pract.* 209, 490–494. doi: 10.1016/j.prp.2013.04.018

Yang, J., Liu, R., Deng, Y., Qian, J., Lu, Z., Wang, Y., et al. (2017). MiR-15a/16 deficiency enhances anti-tumor immunity of glioma-infiltrating CD8+ T cells through targeting mTOR. *Int. J. Cancer* 141, 2082–2092. doi: 10.1002/ijc.30912

Ye, X. W., Yu, H., Jin, Y. K., Jing, X. T., Xu, M., Wan, Z. F., et al. (2015). miR-138 inhibits proliferation by targeting 3-phosphoinositide-dependent protein kinase-1 in non-small cell lung cancer cells. *Clin. Respir. J.* 9, 27–33. doi: 10.1111/crj.12100

Yeh, M., Oh, C. S., Yoo, J. Y., Kaur, B., and Lee, T. J. (2019). Pivotal role of microRNA-138 in human cancers. *Am. J. Cancer Res.* 9, 1118–1126.

Yokosuka, T., Takamatsu, M., Kobayashi-Imanishi, W., Hashimoto-Tane, A., Azuma, M., and Saito, T. (2012). Programmed cell death 1 forms negative costimulatory microclusters that directly inhibit T cell receptor signaling by recruiting phosphatase SHP2. *J. Exp. Med.* 209, 1201–1217. doi: 10.1084/jem.20112741

Zhang, H., Zhang, H., Zhao, M., Lv, Z., Zhang, X., Qin, X., et al. (2013). MiR-138 inhibits tumor growth through repression of EZH2 in non-small cell lung cancer. *Cell Physiol. Biochem.* 31, 56–65. doi: 10.1159/000343349

Zhang, M., Luo, F., Zhang, Y., Wang, L., Lin, W., Yang, M., et al. (2011). *Pseudomonas aeruginosa* mannose-sensitive hemagglutinin promotes T-cell response via toll-like receptor 4-mediated dendritic cells to slow tumor progression in mice. *J. Pharmacol. Exp. Ther.* 349, 279–287. doi: 10.1124/jpet.113.212316

Zhang, M., Tang, H., Guo, Z., An, H., Zhu, X., Song, W., et al. (2004). Splenic stroma drives mature dendritic cells to differentiate into regulatory dendritic cells. *Nat. Immunol.* 5, 1124–1133. doi: 10.1038/ni1130

Zhao, L., Yu, H., Yi, S., Peng, X., Su, P., Xiao, Z., et al. (2016). The tumor suppressor miR-138-5p targets PD-L1 in colorectal cancer. *Oncotarget* 7, 45370–45384. doi: 10.18632/oncotarget.9659

Zou, W. (2005). Immunosuppressive networks in the tumour environment and their therapeutic relevance. *Nat. Rev. Cancer* 5, 263–274. doi: 10.1038/nrc1586

Conflict of Interest: The authors declare that the research was conducted in the absence of any commercial or financial relationships that could be construed as a potential conflict of interest.

frontiers in Cell and Developmental Biology

CORRECTION
published: 21 August 2020
doi: 10.3389/fcell.2020.00746

Corrigendum: MicroRNA-138-5p Suppresses Non-small Cell Lung Cancer Cells by Targeting PD-L1/PD-1 to Regulate Tumor Microenvironment

Nannan Song[1,2†], Peng Li[1,2†], Pingping Song[3], Yintao Li[3], Shuping Zhou[1,2], Qinghong Su[1,2], Xiaofan Li[1,2], Yong Yu[1,2], Pengfei Li[4], Meng Feng[1,2,5], Min Zhang[4] and Wei Lin[1,2]*

[1] Institute of Basic Medicine, Shandong Provincial Hospital Affiliated to Shandong First Medical University, Jinan, China, [2] Institute of Basic Medicine, Shandong First Medical University & Shandong Academy of Medical Sciences, Jinan, China, [3] Department of Oncology, Shandong Cancer Hospital and Institute, Shandong First Medical University & Shandong Academy of Medical Sciences, Jinan, China, [4] Departments of Medicine, Tibet Nationalities University, Xianyang, China, [5] School of Medicine and Life Sciences, Shandong Academy of Medical Sciences, Jinan University, Jinan, China

Keywords: non-small cell lung cancer, microRNA-138, dendritic cells, PD-1, PD-L1

OPEN ACCESS

Approved by:
Frontiers Editorial Office, Frontiers Media SA, Switzerland

***Correspondence:**
Wei Lin
linw1978@163.com;
weilin11@fudan.edu.cn

†*These authors share first authorship*

Specialty section:
This article was submitted to Cell Adhesion and Migration, a section of the journal Frontiers in Cell and Developmental Biology

Received: *15 July 2020*
Accepted: *16 July 2020*
Published: *21 August 2020*

Citation:
Song N, Li P, Song P, Li Y, Zhou S, Su Q, Li X, Yu Y, Li P, Feng M, Zhang M and Lin W (2020) Corrigendum: MicroRNA-138-5p Suppresses Non-small Cell Lung Cancer Cells by Targeting PD-L1/PD-1 to Regulate Tumor Microenvironment. Front. Cell Dev. Biol. 8:746. doi: 10.3389/fcell.2020.00746

A Corrigendum on

MicroRNA-138-5p Suppresses Non-small Cell Lung Cancer Cells by Targeting PD-L1/PD-1 to Regulate Tumor Microenvironment

by Song, N., Li, P., Song, P., Li, Y., Zhou, S., Su, Q., et al. (2020). Front. Cell Dev. Biol. 8:540. doi: 10.3389/fcell.2020.00540

In the published article, there were errors in affiliations 2 and 3. Instead of "Institute of Basic Medicine, Shandong First Medical University & Shandong Academy of Medical School, Jinan, China," affiliation 2 should be "Institute of Basic Medicine, Shandong First Medical University & Shandong Academy of Medical Sciences, Jinan, China." Instead of "Shandong Cancer Hospital and Institute, Shandong First Medical University & Shandong Academy of Medical School, Jinan, China," affiliation 3 should be "Department of Oncology, Shandong Cancer Hospital and Institute, Shandong First Medical University & Shandong Academy of Medical Sciences, Jinan, China."

The authors apologize for these errors and state that this does not change the scientific conclusions of the article in any way. The original article has been updated.

frontiers in Cell and Developmental Biology

BRIEF RESEARCH REPORT
published: 17 July 2020
doi: 10.3389/fcell.2020.00632

Let-7g* and miR-98 Reduce Stroke-Induced Production of Proinflammatory Cytokines in Mouse Brain

David L. Bernstein[1] *and Slava Rom*[1,2]*

[1] Department of Pathology and Laboratory Medicine, Lewis Katz School of Medicine, Temple University, Philadelphia, PA, United States, [2] Center for Substance Abuse Research, Lewis Katz School of Medicine, Temple University, Philadelphia, PA, United States

Stroke is a debilitating illness facing healthcare today, affecting over 800,000 people and causing over 140,000 deaths each year in the United States. Despite being the third-leading cause of death, very few treatments currently exist for stroke. Often, during an ischemic attack, the blood-brain barrier (BBB) is significantly damaged, which can lead to altered interactions with the immune system, and greatly worsen the damage from a stroke. The impaired, BBB promotes the infiltration of peripheral inflammatory cells into the brain, secreting deleterious mediators (cytokines/chemokines) and resulting in permanent barrier injury. let-7 microRNAs (miRs) are critical for regulating immune responses within the BBB, particularly after ischemic stroke. We have previously shown how transient stroke decreases expression of multiple let-7 miRs, and that restoration of expression confers significant neuroprotection, reduction in brain infiltration by neutrophils, monocytes and T cells. However, the specific mechanisms of action of let-7 miRs remain unexplored, though emerging evidence implicates a range of impacts on cytokines. In the current study, we evaluate the impacts of miR-98 and let-7g* on targeting of cytokine mRNAs, cytokine release following ischemic stroke, and cell-specific changes to the neurovascular space. We determined that miR-98 specifically targets IP-10, while let-7g* specifically aims IL-8, and attenuates their levels. Both produce strong impacts on CCL2 and CCL5. Further, let-7g* strongly improves neurovascular perfusion following ischemic stroke. Together, the results of the study indicate that let-7 miRs are critical for mediating endothelial-immune reactions and improving recovery following ischemic stroke.

Keywords: microRNA, let-7, cytokines, leukocyte-brain infiltration, blood brain barrier

OPEN ACCESS

Edited by:
Zhichao Fan,
UCONN Health, United States

Reviewed by:
Bo Liu,
University of California, Berkeley, United States
Rongrong Liu,
Northwestern University, United States

***Correspondence:**
Slava Rom
srom@temple.edu

Specialty section:
This article was submitted to Cell Adhesion and Migration, a section of the journal Frontiers in Cell and Developmental Biology

Received: *06 May 2020*
Accepted: *23 June 2020*
Published: *17 July 2020*

Citation:
Bernstein DL and Rom S (2020) Let-7g and miR-98 Reduce Stroke-Induced Production of Proinflammatory Cytokines in Mouse Brain. Front. Cell Dev. Biol. 8:632. doi: 10.3389/fcell.2020.00632*

INTRODUCTION

Stroke exerts a tremendous burden in lives, financial costs, and healthcare. Over 800,000 people have strokes each year in the United States and over 140,000 of them will die as a result, representing roughly one death out of every 20. Stroke is also a very expensive disease; the cost per hospitalization was ∼$20,000 in 2003–06 (Wang et al., 2014) and the total financial burden is estimated at 219 billion dollars each year (Yang et al., 2017). Despite such prevalence, very few treatments currently exist for stroke, and the ones that are available (namely tPA and mechanical thrombectomy),

contain significant side effects and contraindications. Further, neither offers protection from reperfusion injury, which arises from inflammation originating in the damaged blood vessels where the stroke occurred (Nour et al., 2013; Ahnstedt et al., 2016). This is a critical issue; inflammatory disease processes are a central element of the pathophysiology of stroke (Lambertsen et al., 2012). Inflammatory machinery is very important in the pathophysiologic processes following the onset of ischemic stroke, and cytokines are key players in the inflammatory mechanism and contribute to ischemia-reperfusion damage progression. As such, vascular-immune interactions represent a critical avenue for potential future stroke therapeutics. The let-7 family of microRNAs (miRs) is integral for vascular function, and considered strongly neuroprotective (Sen et al., 2009; Jolana and Kamil, 2017). let-7 miRs are critical for mediating the cellular response to inflammation. Low or impaired expression is associated with greater cellular damage (Rom et al., 2015; Li et al., 2019), while increased expression of let-7 miRs is associated with improved cellular function (Zhang et al., 2016), and resistance to oxidative stress (Hou et al., 2012). Within this family, two miRs appear to be particularly important for the vascular response to ischemic stroke: miR-98 and let-7g*. These are critical mediators of brain endothelial cells and are strongly downregulated during inflammatory events (Rom et al., 2015).

let-7 miRs may be particularly important in the progression of stroke. Following ischemic or hemorrhagic stroke, cytokine expression is significantly altered (Lambertsen et al., 2012), often lasting for many days (Tarkowski et al., 1997; Nayak et al., 2012). These changes to cytokine levels can profoundly alter the interactions between the endothelial cells comprising the vasculature and activated leukocytes and lymphocytes of the immune system (Pawluk et al., 2020), leading to changes in barrier permeability, and worsening the size of the stroke penumbra. Cytokines such as CCL2, CCL3, CCL5, and CXCL-1 have been particularly implicated in such processes (Dimitrijevic et al., 2006; Yang et al., 2019). let-7 miRs may be critical for regulating such processes, as they can strongly alter the expression of stroke-impacted cytokines (Rom et al., 2015; Jickling et al., 2016).

Restoration of endogenous expression of miR-98 (Bernstein et al., 2019) or let-7g*(Bernstein et al., 2020) can prevent a significant degree of damage following ischemia. However, the mechanisms through which this occurs may be widely different. Although both miRs can reduce the size of the ischemic penumbra, as well as the number of immune cells which extravasate into the infarcted region (Bernstein et al., 2019, 2020), there are important differences. miR-98 is associated with the integrity of tight junction proteins such as ZO-1 and claudin-5 (Zhuang et al., 2016), and protection against Cas-3-dependant apoptotic pathways (Li et al., 2015), while let-7g* modulates interactions with low density lipoproteins (Liu et al., 2017), and impedes apoptosis through Akt-dependent mechanisms (Joshi et al., 2016). The differences in gene targets is particularly important with regards to inflammation. miR-98 is associated with expression of IL-10 (Liu et al., 2011; Li et al., 2018, 2019), while let-7g is associated with the response to IGF-B signaling (Zhou et al., 2015; Huang et al., 2017), and with IL-6 (Huang et al., 2017). Such differences are critical for mediating the type of immune cells recruited following stroke, as well as the nature of their interactions with the endothelial cells of the BBB. However, such interactions do not fully explain the nature of the vascular changes.

In our previous investigations into the role of let-7 miRs in regulating post-stroke recovery, we determined that miR-98 overexpression reduces the infiltration of monocytes into the ischemic brain, and appears to attenuate the activation of microglia into a proinflammatory state (Bernstein et al., 2019). Conversely, let-7g* was more effective at limiting the infiltration of neutrophils, and other forms of T-cells (Bernstein et al., 2020). These results, combined with the diversity of other mRNA targets of the two let-7 miRs, indicate that let-7 miRs are capable of conferring neuroprotection from stroke through a wide range of cellular mechanisms. In addition, as let-7 miRs can produce pro- and anti-inflammatory effects, it is critical to better understand the specific actions of its constituent members, in order to guide future therapeutics for stroke. For this report, we characterized the specific mechanisms through which let-7g* and miR-98 promote recovery from ischemic stroke. We correlate sequence binding with the differing nature of cytokine release, as well as with structural changes to the neurovasculature. Both miRs are important for maintaining BBB integrity, and managing inflammation. With this study, we investigate the specific pathways through which this occurs.

MATERIALS AND METHODS

Animals

All animal experiments were approved by the Temple University Institutional Animal Care and Use Committee and were conducted in accordance with Temple University guidelines, which are based on the National Institutes of Health (NIH) guide for care and use of laboratory animals and in the ARRIVE (Animal Research: Reporting *in vivo* Experiments) guidelines (study design, experimental procedures, housing and husbandry, and statistical methods)[1]. 10-week old male C57BL/6 mice were purchased from the Jackson Laboratory (Bar Harbor, ME, United States) and given *ad libitum* access to food and water. Animals were kept in a 12 h light/12 h dark cycle for the duration of experiments. Animals were group-housed prior to surgery, and single-housed thereafter.

Transient Middle Cerebral Artery Occlusion (tMCAO) and miR Delivery

Mice were subjected to 60 min focal cerebral ischemia produced by transient intraluminal occlusion with a monofilament made of 6–0 nylon with a rounded tip (Doccol Corp., Sharon, MA, United States, cat# 602312PK10) into the middle cerebral artery (MCAO) as described previously (Jin et al., 2010a,b; Engel et al., 2011). Sham-operated mice were subjected to the same surgical procedure, but the filament was not advanced far enough to occlude the MCA. We then used a protocol recently developed

[1]www.nc3rs.org.uk/arrive-guidelines

in our laboratory (Rom et al., 2015; Bernstein et al., 2019) to mix 5 nmol synthetic miRNA with Lipofectamine 2000 (Life Technologies, Carlsbad, CA, United States) in RNase and DNase-free water (Life Technologies) prior to retroorbital injection in 100 uL sterile PBS (Bernstein et al., 2019, 2020).

Enzyme-Linked Immunosorbent Assay (ELISA)

Animals were sacrificed via intracardiac perfusion at 72 h following tMCAO, and brain hemispheres were extracted and dissolved in 400 uL lysis buffer (RayBiotech, Norcross, GA, United States). Following centrifuging at 10,000 × *g* for 10 min, supernatant was collected, and analyzed for cytokine level via multi-plex ELISA, in accordance with standard methods (Weng and Zhao, 2015). A sample titration curve was performed prior to all assays in order to determine the optimal dilution factor. Homogenate was measured for 29 common cytokines with MSD 29-plex ELISA kit (K15267G, Meso Scale Development, Rockville, MD, United States). Data were read on the MSD QuickPlex 120.

MicroCT

A harvest technique optimized for MicroCT was utilized in order to ensure maximal perfusion of the vascular space (Ghanavati et al., 2014). Animals were terminally anesthetized with 5% isoflurane, and transcardially perfused with 20 ml warm heparinized PBS, followed by 20 ml microfill solution MV-122 (MicroCT, San Francisco, CA, United States), mixed immediately before infusion. Fluids were infused at a rate of 2 ml/min. Brains were collected and fixed in 10% formalin solution for a minimum of 24 h, prior to scanning. Fixed brains were then scanned using the Skyscan 1172, 12-megapixel, high-resolution cone-beam microCT scanner (Bruker, Kontich, Belgium). Scan parameters involved using an isotropic voxel size of 3.0 μm, a source voltage of 100 kV, and a current of 100 μA. Following scanning, 3D reconstruction was performed using Skyscan N-recon software (Micro Photonics, Inc., Allentown, PA, United States). The vascular spaces were reconstructed at a resolution of 0.5 uM/pixel (Quintana et al., 2019) and analyzed for mean vessel thickness, overall perfusion, and number of vascular leakages (Quintana et al., 2019). All procedures were conducted in accordance with standardized methods for rodent tissue (Dyer et al., 2017; Karreman et al., 2017; Quintana et al., 2019).

miRNA Functional Analysis

The mature sequences of the miRNAs were retrieved using miRBase database: mu-mir-98 no. MIMAT0000096:UGAGGUAGUAAGUUGUAUUGUU and mu-let-7g* no. MIMAT0004584:CUGUACAGGCCACUGCCU-UGC and were synthetized by Integrated DNA Technologies, Inc. (IDT, Coralville, IA, United States). The IP-10 3′UTR and CXCL1 3′UTR sequences, cloned downstream to the firefly luciferase sequence in the pMirTarget reporter vector (further pMir), were purchased from OriGene (OriGene Technologies, Inc., Rockville, MD, United States). For the perfect match sequence, the mature sequence of mu-miR-98 or mu-let-7g* synthetic oligos was transfected together with pMir reporter plasmids, containing the corresponding 3′UTRs.

To confirm specificity of miR-mRNA binding to target 3′UTR, the miR's seed-binding sequence was mutated in each of the 3′ UTRs (marked in bold and underlined in **Figure 2**, the nucleotides were changed for complementary one). The IP-10 3′UTR mutated in the mir-98 or let-7g* seeding sequence was generated by site directed mutagenesis (Agilent Technologies, Santa Clara, CA, United States) using the pMir/IP-10 3′UTR as a template. The oligonucleotides for the mutagenesis were as follows: forward, 5′-GGACCACACAGAGGC**ACGG**TCT (mutated bases in the mir-98 seeding sequence are in bold and underlined) and 5′-CCCAAATTCTTTCAGT**CCGA**ACCTAC (mutated bases in the let-7g* seeding sequence are in bold and underlined). The CXCL1 3′UTR mutated in the mir-98 or let-7g* seeding sequence was generated by site directed mutagenesis (Agilent) using the pMir/CXCL1 3′UTR as a template. The oligonucleotides for the mutagenesis were as follows: forward, 5′-GATGGGTAGGCTTAAAATA**AAAG**AT (mutated bases in the mir-98 seeding sequence are in bold and underlined) and 5′-GGAGGCTGTGT**AACA**ATG (mutated bases in the let-7g* seeding sequence are in bold and underlined). The reverse primers were complementary to the forward for all mentioned above sequences. All primers were synthetized by IDT. *Caenorhabditis elegans* miR-39 (cel-39), MIMAT0020306:AGCUGAUUUCGUCUUGGUAAUA was synthetized by IDT and was used as a non-specific/non-targeting control (Rom et al., 2015; Bernstein et al., 2019, 2020).

Luciferase Assay

For miR target validation, HEK 293 cells were plated at a concentration of 8×10^4 cells/well in a 12-well plate in DMEM with 10% FBS medium. The following day, a total amount of 0.5 μg DNA/well was transfected utilizing Lipofectamine (Life Technologies) at a DNA:Lipofectamine ratio of 1:3. pcDNA3 was added to keep the total amount of DNA constant. Samples were harvested 48 h post-transfection and subjected to the luciferase assay system (Promega, Madison, WI, United States) following the manufacturer's instructions using a Infinity M200PRO chemiluminometer (Tecan Group Ltd., Mannedof, Switzerland). Relative units represent the ratio between luciferase values of the sample and the non-targeting control. The experiments were performed in duplicate and repeated at least three times (Rom et al., 2015), averaged and each mean shown in the graph as one point.

Statistical Analysis

Data are expressed as the mean ± SD of experiments conducted multiple times. Data were tested for normality using the Shapiro–Wilk test, and, if data were normally distributed, for multiple group comparisons. Multiple group comparisons were performed by one-way ANOVA with Tukey *post hoc* test with significance at $p < 0.05$. A paired two-tailed Student's test was used to compare before and after effects. Significant differences were considered to be at $p < 0.05$. Statistical analyses were performed utilizing Prism v8 software (GraphPad Software Inc.,

San Diego, CA, United States). To determine the number of samples used for quantitative assays, a power calculation was performed based on the expected variability between testing conditions using the following equation: $n = 1 + 2C\left(\frac{s}{d}\right)^2$, where C is a constant equal to 10.51 for a power of 90% and a confidence interval of 95%, s is the variance, and d is the difference between conditions. We determined optimal sample sizes by calculating the number of animals required to produce an N of sufficient size to perform one-way ANOVA analysis of a standard distribution, which we determined to be 4, and 3 animals analyzed in duplicates would provide at least six data points for each experiment. For ELISA and microCT, all samples were run in duplicate and combined to produce a weighted average value. Each calculation is represented by one data point. For reporter assays, experiments were repeated twice in triplicate with average value of both replicates used as a single data point.

RESULTS

Let-7g* and miR-98 Reduce Stroke-Induced Production of Proinflammatory Cytokines in Mouse Brain

In recent studies, we have shown that both let-7g* and miR-98 exert anti-inflammatory impacts on endothelial cells within the BBB (Rom et al., 2015; Bernstein et al., 2019, 2020) and reduce the damage caused by ischemic stroke. However, these miRs may produce differing effects on the specific nature of immune cell infiltration into the brain parenchyma following stroke. To determine which inflammatory signals were reduced by let-7 miRs, we measured the expression of 29 different cytokines from the homogenate of the stroke-infarcted hemisphere. We determined that tMCAO significantly increased the expression of IP-10 ($p < 0.01$), CXCL1 ($p < 0.005$), CXCL2 ($p < 0.01$), CCL2 ($p < 0.01$), CCL3 ($p < 0.05$), and CCL5 ($p < 0.05$) compared with baseline (**Figures 1A–F**). Both miRs significantly reduced the stroke-induced increase in CCL2 ($p < 0.05$) and CCL5 ($p < 0.01$; **Figures 1B,D**). However, only let-7g* was effective in reducing the stroke-driven increases in CCL3 ($p < 0.05$) and CXCL1 ($p < 0.005$; **Figures 1C,F**), while miR-98 attenuated the increase in IP-10 ($p < 0.05$) only (**Figure 1A**).

miR-98 Specifically Targets IP-10 mRNA, While Let-7g* Targets IL-8-Mouse Homolog KC/GRO (CXCL1)

Sequence complementarity is the most critical measure in the relative power of miRNAs to silence their mRNA targets. Despite the importance of strong seed binding, extensive downstream (toward the 3′ end) pairing can sometimes compensate for imperfect seed binding (Shin et al., 2010). To estimate binding affinity of the let-7 miRs of interest, we used the RNAhybrid sequence tool (Bibiserv, Bielefeld, Germany; Rehmsmeier et al., 2004) to predict the miRNA-mRNA hybridization of let-7g* and miR-98 with the 3′ UTR sequences of several cytokines, identified in our ELISA screen (**Figure 1**). We found substantial complementarity between let-7g* seed with IL-8-mouse homolog KC/GRO (CXCL1)′ 3′ UTR, yielding a minimum free energy of -23.5 kcal/mol. By contrast, miR-98 showed a lower binding affinity, resulting in a minimum free energy of 17.2 kcal/mol (**Figure 2D**). In addition, miR-98 was shown to have higher binding affinity with IP-10 3′ UTR, with a minimum free energy of −29.7 kcal/mol (**Figure 2A**). let-7g* also showed some degree of bonding affinity (mfe = −23.9 kcal/mol) with IP-10 3′ UTR sequence, but the complementarity was not significant (**Figure 2B**), due to imperfect binding in the seed region.

To confirm this binding affinity, we performed the dual-luciferase assay in 293 HEK cells following a standard transfection protocol[8]. Cells were transfected with plasmids containing wild-type (WT) or mutated 3′UTR of IP-10 or IL-8-mouse homolog CXCL1′ fused with luciferase reporter and co-transfected with miR-98 and let-7g* mimic miRNA sequences. Mutated 3′ UTRs contained four nucleotides switched within the miR-seed binding region (**Figures 2A,D**, in bold). miR-98 downregulated the activity of WT IP-10 3′UTR-reporter by nearly 3.1-fold ($p < 0.05$; **Figure 2B**), while in the mutated 3′UTR-reporter, miR-98 co-transfection induced almost no effect. By contrast, let-7g* produced a much more modest, statistically insignificant decline in WT IP-10 3′UTR-reporter activity, a luciferase levels of mutated IP-10 3′UTR-reporter activity was not much different from that produced in WT (**Figure 2C**). With WT IL-8 3′UTR, the impacts of the miRNAs were inverted. let-7g* reduced activity by 1.5-fold ($p < 0.05$) in WT IL-8 3′UTR, while in the mutated IL-8 3′UTR reporter, let-7g* did not alter activity significantly. Similar results were obtained when cells containing cloned IP-10 or IL-8-mouse homolog CXCL1′ 3′UTR fused with luciferase reporter were transfected with normal or mutated forms of miR-98 and let-7g* mimic miRNA sequences (**Supplementary Figure 1**). Mutated forms of miRs contained four nucleotides switched within the seed region (**Supplementary Figures 1A,B**, in bold). Normal miR-98 downregulated the activity of IP-10 3′UTR-reporter by nearly 77% ± 14% ($p < 0.05$; **Supplementary Figure 1C**), while the mutated form induced almost no effect. With IL-8 (CXCL1) 3′UTR, wild type let-7g* oligo reduced activity by 48% ± 7.5% ($p < 0.05$), while the mutated form did not alter activity significantly (**Supplementary Figure 1D**). This research expands significantly upon existing research regarding the regulation of cytokines by let-7 miRs. We have previously shown how let-7g* and miR-98 demonstrate strong seed binding to and inhibition of both CCL2 and CCL5 (Rom et al., 2015). In the same paper, we show that such impacts can strongly influence the degree of leukocyte adhesion to endothelial cells during inflammation. Together, our findings illustrate the importance of let-7 miRs in regulating the immune response to neurovascular insult.

Let-7g* Significantly Reduces Leakage and Improves Vascular Function After Stroke

Recent studies have denoted that restoration of let-7 miRNA levels may be strongly neuroprotective, particularly after

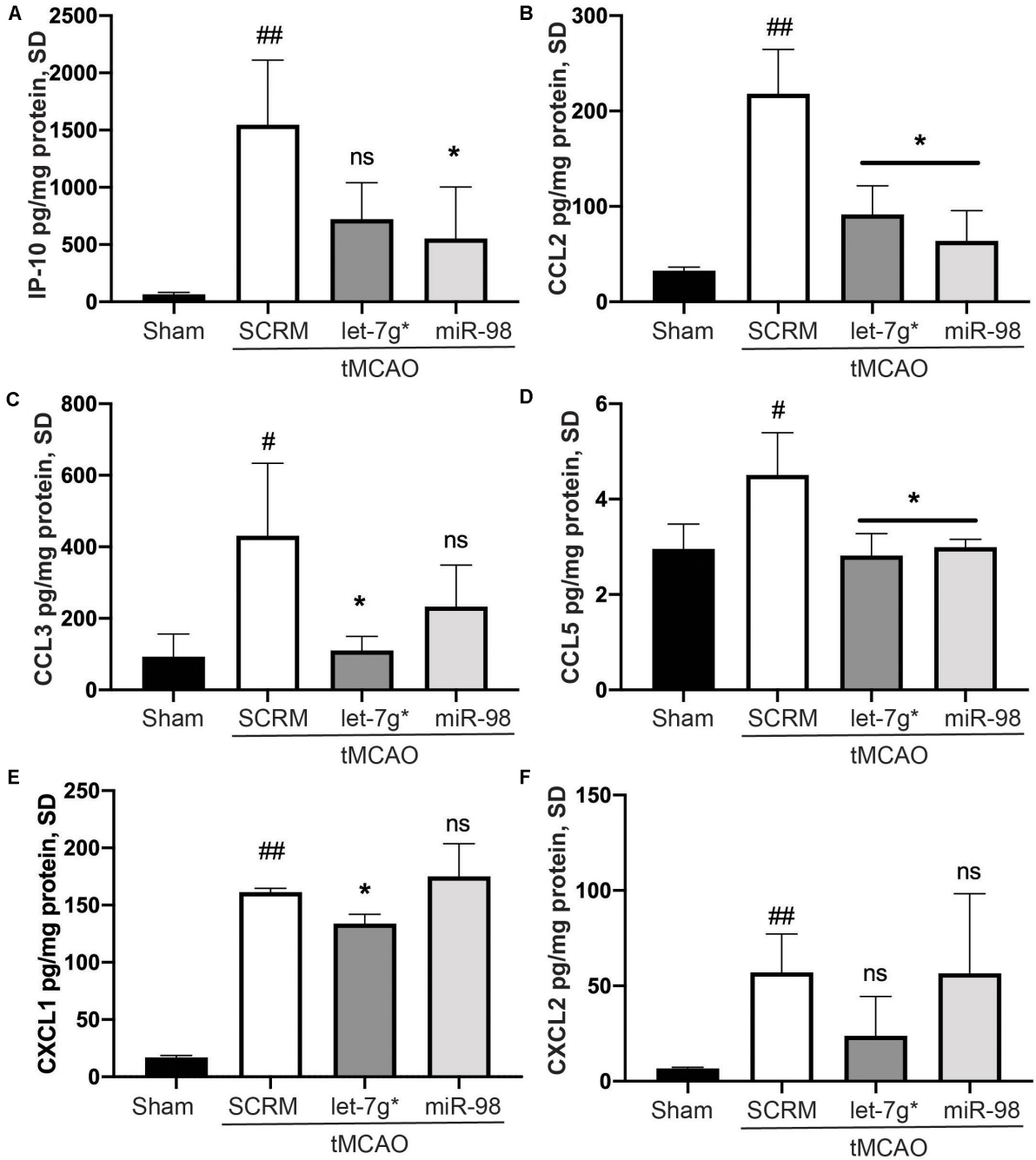

FIGURE 1 | Let-7 miRs differentially reduce cytokine release following stroke. ELISA analysis of IP-10 **(A)**, CCL2 **(B)**, CCL3 **(C)**, CCL5 **(D)**, CXCL2 **(E)**, and KC/GRO (CXCL-1 mouse analog) **(F)** expression. Mice were subjected to 60 min ischemia and 72 h reperfusion performed as described in section "Materials and Methods." Brains were harvested following anesthesia, homogenized, and were used to run all assays. Results are presented as mean ± SD from at least two independent experiments ($n = 4$). #$p < 0.05$ (SCRM); *$p < 0.05$ (let-7g*, miR-98). ##$p < 0.01$ (SCRM); ns is not significant.

significant inflammatory insults that occur following ischemic stroke (Li et al., 2019; Bernstein et al., 2020). We have previously shown that such treatments reduce the permeability toward both large (>10 kD) molecules, and multiple types of immune cells (Bernstein et al., 2019, 2020). To fully assess the impact upon the BBB, post-MCAO animals were perfused with Microfil, and the neurovasculature was mapped using X-ray tomography, with an enhanced focus on the MCA (**Figure 3A**). We determined that tMCAO reduced the average diameter of the MCA to ∼50% the size in control animals ($p < 0.01$), while treatment with let-7g* attenuated this decrease by nearly 60% (**Figures 3A,B**; $p < 0.05$). Further, injection of let-7g* prevented a significant

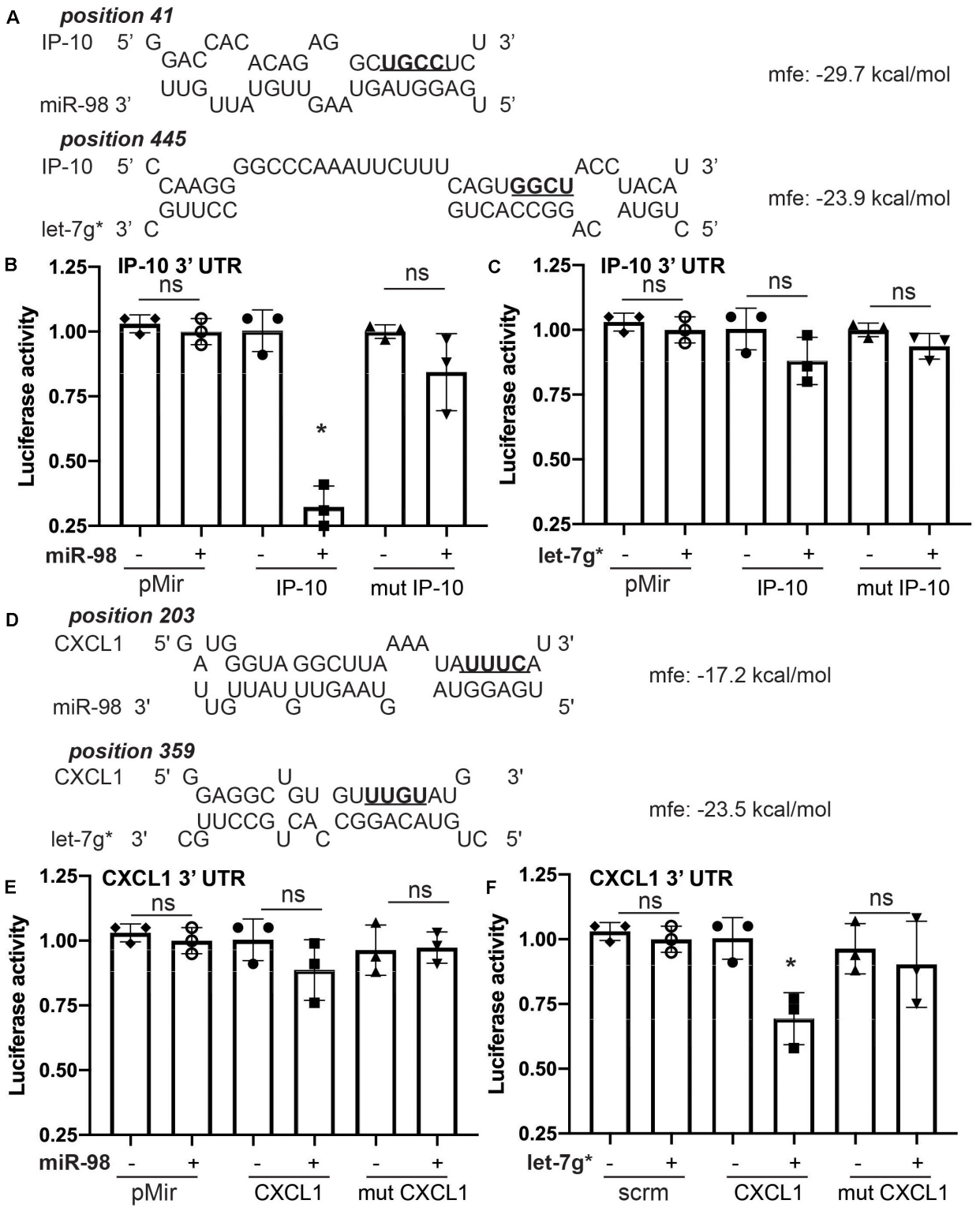

FIGURE 2 | Let-7g* and miR-98 selectively target different cytokine mRNAs. Prediction analysis for miR-98 and let-7g* for the ability to create miR-mRNA hybrid with IP-10 **(A)** and CXCL1 **(D)** 3′ UTRs, with minimum free energy recorded. Luciferase activity for IP-10's 3′ UTR reporter in HEK-293 cells transfected with mimic oligos of miR-98 **(B)** or let-7g* **(C)**. Luciferase activity for CXCL1's 3′ UTR reporter with mimic oligos of miR-98 **(E)** or let-7g* **(F)**. 3′ UTR sequences of IP-10 and CXCL1 were mutated in the seed-binding site (underlined and bolded). Data are shown as mean ± SD. *$p < 0.05$.

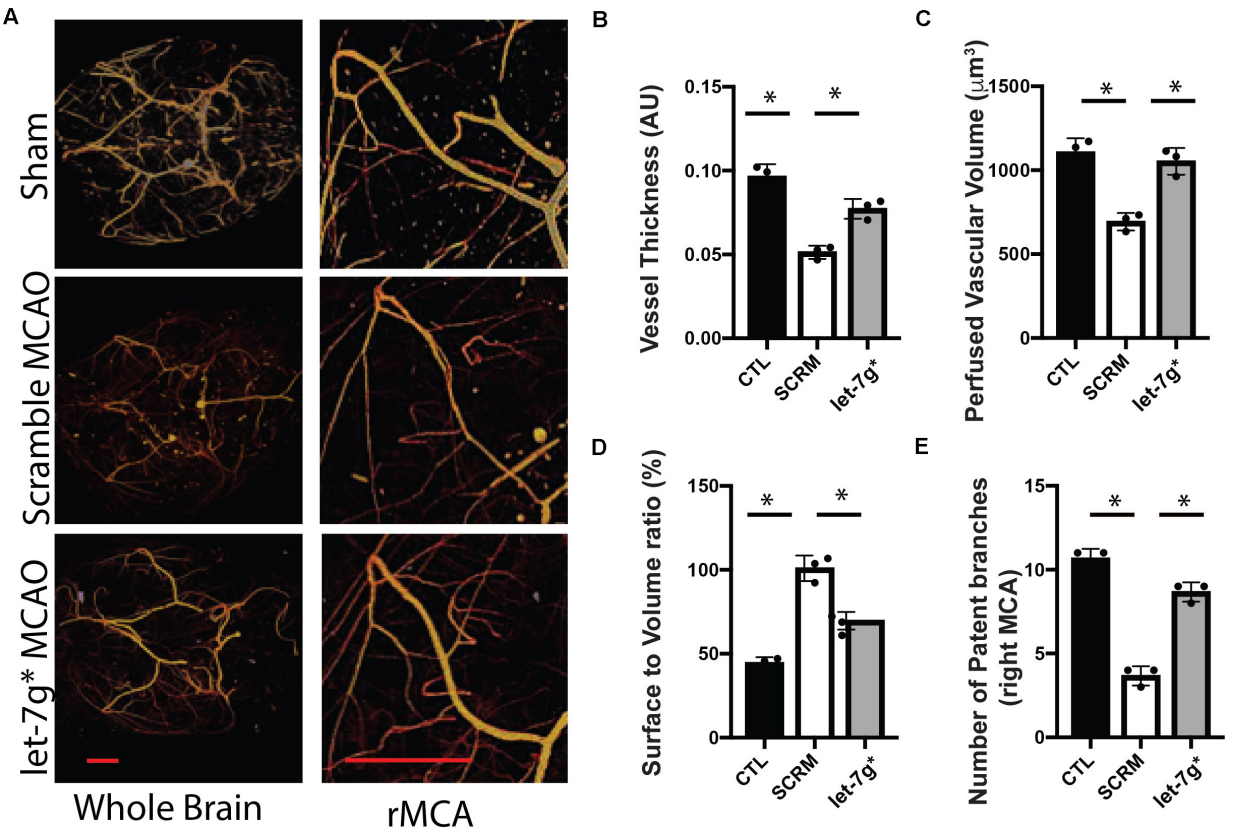

FIGURE 3 | let-7g* attenuates vascular damage after tMCAO. Cerebral neurovasculature following sham control or stroke was imaged with MicroCT, as detailed in section "Materials and Methods" **(A)**. In right (tMCAO) hemisphere, the mean perfused vessel thickness was measured relative to control hemisphere **(B)**, total volume of vascularized brain tissue **(C)**, vascular surface area relative to perfused volume **(D)**, and the number of patent branches originating from the right middle cerebral artery **(E)**. Data are shown as mean ± SD. *$p < 0.05$. Scale bar = 1 mm.

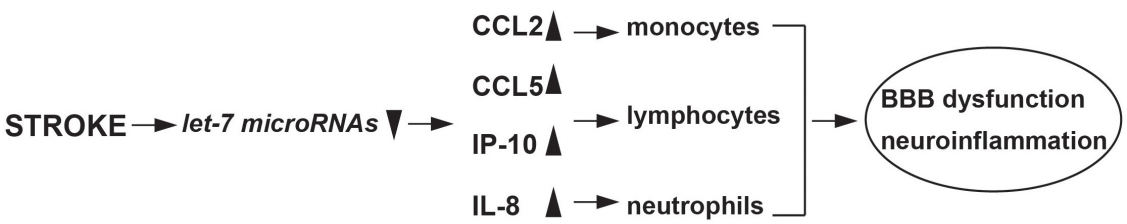

FIGURE 4 | Schematic of stroke induced let-7 miRNAs changes and immune response.

degree of the stroke-induced reduction of perfused vascular volume (**Figure 3C**), restored vessel volume-surface ratio to nearly baseline levels ($p = 0.69$) (**Figure 3D**), and prevented the loss of seven of nine major arterial branches on the MCA (**Figure 3E**).

Taken together with our previously published data, we conclude that let-7g* and miR-98 diminish stroke-induced increase in CXCL1 and IP-10 protein levels, respectively, by direct targeting their 3′ UTR sequence. Both miRs, let-7g* and miR-98 directly target CCL2 and CCL5 cytokines and regulate their expression (Rom et al., 2015). These effects on cytokine expression allow let-7 miRs to preserve the cerebral vasculature following tMCAO, exhibited by attenuating the stroke-induced reduction of vessel thickness, perfused brain volume, and number of patent arteries originating at the MCA, and by lessening the stroke-induced spike in vascular surface/volume ratio. These findings underscore the role of let-7g* overexpression in maintaining vascular homeostasis following inflammatory insult.

DISCUSSION

We have previously demonstrated how let-7 miRs preserve the integrity of the BBB, reduce cytokine release *in vitro*, and

inhibit recruitment of pro-inflammatory immune cells from both sides of the BBB, leading to better functional recovery. In this study, we show how miR-98 and let-7g* confer such neuroprotection through slightly different mechanisms. The current research denotes that let-7g* attenuates CXCL1 (IL-8-mouse homolog), which can lower CXCR2 activity, which is critical for recruiting neutrophils (Easton, 2013; Giles et al., 2018; Bernstein et al., 2020). This mechanism is likely responsible for a significant degree of let-7g*-induced neuroprotection; IL-8 is directly linked to endothelial activation and leukocyte recruitment (Wu et al., 2015), and silencing its activity in endothelial cells strongly decreases inflammation-induced permeability (Chen et al., 2018). Increased IL-8 binding to CXCR2 has been shown to reduce vascular wall thickness (Varney et al., 2006), which can worsen hypertension decrease in the area covered by the vasculature (Wang et al., 2016). As MicroCT scanning illustrated how let-7g* increases vascular thickness, vessel volume, and patent arterial branches, and previous work that indicated that let-7g* reduces the number of IL-8-recruited cells into the penumbra (Bernstein et al., 2020), we find it highly plausible that let-7g*-induced neuroprotection involves IL-8 mediated changes within the neurovasculature. The let-7g*-induced neuroprotection may stem from binding to the 3′ UTR of CXCR2 mRNA through targeting of its transcriptional regulators such as NF-kB and CREB (Amiri and Richmond, 2003), or a combination.

Conversely, the let-7 miR family member, miR-98, was shown to bind to and strongly reduce IP-10, which corresponds to the let-7-specific reduction of brain-infiltrating T-cells (Bernstein et al., 2019). These findings are in line with current research which indicates let-7s are critical for mediating endothelial-T cell interactions, and may exert a different effect on the neurovasculature, though some elements are common to both miRs. miRs from the let-7 family directly diminish the expression of MCP-1/CCL2 and RANTES/CCL5 cytokines (Rom et al., 2015), which are complicated in the progression of BBB inflammation that happens during traumatic brain injury (Lumpkins et al., 2008; Albert et al., 2017), various forms of encephalitis (Chowdhury and Khan, 2017) and diabetes (Zhang, 2008; Teler et al., 2017; Lee et al., 2019). Although there are numerous triggers for neuroinflammation, most of them include amplified levels of these particular cytokines, which can cause leukocyte adhesion (Schober, 2008) and rearrangement of tight junction proteins on endothelial cells (Stamatovic et al., 2005), leading to BBB compromise. BBB disruption, upregulation of cell adhesion molecules, and activation of resident microglia develop the post-stroke neuro-immune interactions. This report found that only let-7g* was effective in reducing the stroke-driven increases in CCL3, whereas miR-98 did not affect its expression. CCL3 cytokine has been implicated in the enhancement of BBB permeability and the reduction of TJ protein expression (Chai et al., 2014). Whether CCL3 reduction was due to direct or indirect let-7g* miR targeting should be investigated in future studies.

Previous research has shown how let-7g* and miR-98 can both activate the innate immune response, and this is corroborated by current findings, which indicate pronounced effects on CCL5 and CCL2 release (Rom et al., 2015), corresponding to reduced monocyte brain infiltration, macrophage, and microglial activation (Bernstein et al., 2019, 2020). This research adds to the growing pool of evidence on the diverse neurovascular impacts of the let-7 family (**Figure 4**). For instance, let-7a can inhibit the proinflammatory response in microglia, by lowering nitric oxide signaling and altering the pattern of cytokine release (Cho et al., 2015), and let-7 derived from exosomes can strongly inhibit atherosclerotic inflammation via the PTEN pathway (Li et al., 2019). However, not all miRs from the let-7 family produce beneficial effects to the vascular space. For instance, let-7f is capable of worsening the effects of stroke, by inhibiting insulin-like growth factor 1 (IGF-1) signaling (Selvamani et al., 2012). Further, let-7a, b, e, and f have been postulated to exacerbate neuronal damage following inflammation through actions on toll-like receptor 7 (Mueller et al., 2014). With such varied results, it is critical to understand the mechanisms through which let-7 miRs influence the vascular space and when their use might be contraindicated. The BBB can respond to inflammatory stimuli in multiple ways, and understanding the role of miRs in mediating such responses are critical for developing effective treatments for stroke. Combinatorial approaches have been suggested, which utilize multiple miRs from the same family (Khoshnam et al., 2017). This is an interesting approach, and one well-supported by current siRNA research, which suggests that multiple combinations of similar siRNAs can be more effective than a higher concentration of a single miRNA (Bahi et al., 2005). While further experiments are needed to fully elucidate the nature of let-7 impacts on ischemic stroke, studies such as this one are critical for understanding the role of miRs in mediating inflammatory damage, and will be critical for developing more effective treatments.

We found that changes in miRNA expression seen in primary human BMVEC *in vitro* occur *in vivo* in an animal model of neuroinflammation (Rom et al., 2015) and in a stroke tMCAO model (Bernstein et al., 2019, 2020). Overexpression of miR-98 and let-7g* in brain endothelium attenuated leukocyte adhesion/migration and diminished BBB permeability pointing to functional reproducibility of miRNA effects *in vitro* systems. We have previously established that let-7 miRs preserve the integrity of the BBB, diminish cytokine release *in vitro* (Rom et al., 2015), and reduce recruitment of pro-inflammatory immune cells from blood to CNS *in vivo*, leading to better functional recovery (Bernstein et al., 2019, 2020), corroborating that let-7 miRNAs have remedial potential in neuroinflammation. In the current study, we focused our analysis on the mechanisms by which miR-98 and let-7g* overexpression impacts cytokine expression following ischemic stroke and evaluated their impacts upon the neurovascular structure.

In summary, using a functional approach, we have identified a mechanism implicated in the negative regulation of inflammation in endothelium and brain after stroke. It involves the stroke-mediated decrease of miR-98 and let-7g*, which in turn, triggers expression of pro-inflammatory mediators, such as CCL2, CCL5, CXCL1, and IP-10. Our data support a role for let-7 miRNAs in modulation of inflammatory processes

in stroke-induced inflammation and preserve the cerebral vasculature following tMCAO.

DATA AVAILABILITY STATEMENT

The original contributions presented in the study are included in the article/**Supplementary Material**, further inquiries can be directed to the corresponding author.

ETHICS STATEMENT

The animal study was reviewed and approved by Temple University Institutional Animal Care and Use Committee.

AUTHOR CONTRIBUTIONS

DB: data acquisition and analysis, drafting and revising, and final approval. SR: conception and design, data acquisition, analysis and interpretation, drafting and revising the article, and final approval.

FUNDING

This work was supported in part by NIH research grants R01NS101135 to SR.

ACKNOWLEDGMENTS

The authors express their grateful acknowledgment for proofreading and editing to Nancy L. Reichenbach.

SUPPLEMENTARY MATERIAL

The Supplementary Material for this article can be found online at: https://www.frontiersin.org/articles/10.3389/fcell.2020.00632/full#supplementary-material

REFERENCES

Ahnstedt, H., Sweet, J., Cruden, P., Bishop, N., and Cipolla, M. J. (2016). Effects of early post-ischemic reperfusion and tPA on Cerebrovascular function and nitrosative stress in female rats. *Transl. Stroke Res.* 7, 228–238. doi: 10.1007/s12975-016-0468-4

Albert, V., Subramanian, A., Agrawal, D., Bhoi, S. K., Pallavi, P., and Mukhopadhayay, A. K. (2017). RANTES levels in peripheral blood, CSF and contused brain tissue as a marker for outcome in traumatic brain injury (TBI) patients. *BMC Res. Notes* 10:139. doi: 10.1186/s13104-017-2459-2

Amiri, K. I., and Richmond, A. (2003). Fine tuning the transcriptional regulation of the CXCL1 chemokine. *Prog. Nucleic Acid Res. Mol. Biol.* 74, 1–36. doi: 10.1016/s0079-6603(03)01009-2

Bahi, A., Boyer, F., Kolira, M., and Dreyer, J. L. (2005). In vivo gene silencing of CD81 by lentiviral expression of small interference RNAs suppresses cocaine-induced behaviour. *J. Neurochem.* 92, 1243–1255. doi: 10.1111/j.1471-4159.2004.02961.x

Bernstein, D. L., Gajghate, S., Reichenbach, N. L., Winfield, M., Persidsky, Y., Heldt, N. A., et al. (2020). let-7g counteracts endothelial dysfunction and ameliorating neurological functions in mouse ischemia/reperfusion stroke model. *Brain Behav. Immun.* 87, 543–555. doi: 10.1016/j.bbi.2020.01.026

Bernstein, D. L., Zuluaga-Ramirez, V., Gajghate, S., Reichenbach, N. L., Polyak, B., Persidsky, Y., et al. (2019). miR-98 reduces endothelial dysfunction by protecting blood-brain barrier (BBB) and improves neurological outcomes in mouse ischemia/reperfusion stroke model. *J. Cereb. Blood Flow Metab.* doi: 10.1177/0271678x19882264 [Epub ahead of print]

Chai, Q., He, W. Q., Zhou, M., Lu, H., and Fu, Z. F. (2014). Enhancement of blood-brain barrier permeability and reduction of tight junction protein expression are modulated by chemokines/cytokines induced by rabies virus infection. *J. Virol.* 88, 4698–4710. doi: 10.1128/jvi.03149-13

Chen, Q. F., Liu, Y. Y., Pan, C. S., Fan, J. Y., Yan, L., Hu, B. H., et al. (2018). Angioedema and Hemorrhage After 4.5-Hour tPA (Tissue-Type Plasminogen Activator) Thrombolysis Ameliorated by T541 via Restoring Brain Microvascular Integrity. *Stroke* 49, 2211–2219. doi: 10.1161/strokeaha.118.021754

Cho, K. J., Song, J., Oh, Y., and Lee, J. E. (2015). MicroRNA-Let-7a regulates the function of microglia in inflammation. *Mol. Cell Neurosci.* 68, 167–176. doi: 10.1016/j.mcn.2015.07.004

Chowdhury, P., and Khan, S. A. (2017). Significance of CCL2, CCL5 and CCR2 polymorphisms for adverse prognosis of Japanese encephalitis from an endemic population of India. *Sci. Rep.* 7:13716. doi: 10.1038/s41598-017-14091-8

Dimitrijevic, O. B., Stamatovic, S. M., Keep, R. F., and Andjelkovic, A. V. (2006). Effects of the chemokine CCL2 on blood-brain barrier permeability during ischemia-reperfusion injury. *J. Cereb. Blood Flow Metab.* 26, 797–810. doi: 10.1038/sj.jcbfm.9600229

Dyer, E. L., Gray Roncal, W., Prasad, J. A., Fernandes, H. L., Gursoy, D., De Andrade, V., et al. (2017). Quantifying Mesoscale Neuroanatomy Using X-Ray Microtomography. *eNeuro* 4:e0195-17. doi: 10.1523/eneuro.0195-17.2017

Easton, A. S. (2013). Neutrophils and stroke - can neutrophils mitigate disease in the central nervous system? *Int. Immunopharmacol.* 17, 1218–1225. doi: 10.1016/j.intimp.2013.06.015

Engel, O., Kolodziej, S., Dirnagl, U., and Prinz, V. (2011). Modeling stroke in mice - middle cerebral artery occlusion with the filament model. *J. Vis. Exp.* 47:2423. doi: 10.3791/2423

Ghanavati, S., Yu, L. X., Lerch, J. P., and Sled, J. G. (2014). A perfusion procedure for imaging of the mouse cerebral vasculature by X-ray micro-CT. *J. Neurosci. Methods* 221, 70–77. doi: 10.1016/j.jneumeth.2013.09.002

Giles, J. A., Greenhalgh, A. D., Denes, A., Nieswandt, B., Coutts, G., McColl, B. W., et al. (2018). Neutrophil infiltration to the brain is platelet-dependent, and is reversed by blockade of platelet GPIbalpha. *Immunology* 154, 322–328. doi: 10.1111/imm.12892

Hou, W., Tian, Q., Steuerwald, N. M., Schrum, L. W., and Bonkovsky, H. L. (2012). The let-7 microRNA enhances heme oxygenase-1 by suppressing Bach1 and attenuates oxidant injury in human hepatocytes. *Biochim. Biophys. Acta* 1819, 1113–1122. doi: 10.1016/j.bbagrm.2012.06.001

Huang, H. C., Yu, H. R., Hsu, T. Y., Chen, I. L., Huang, H. C., Chang, J. C., et al. (2017). MicroRNA-142-3p and let-7g Negatively Regulates Augmented IL-6 Production in Neonatal Polymorphonuclear Leukocytes. *Int. J. Biol. Sci.* 13, 690–700. doi: 10.7150/ijbs.17030

Jickling, G. C., Ander, B. P., Shroff, N., Orantia, M., Stamova, B., Dykstra-Aiello, C., et al. (2016). Leukocyte response is regulated by microRNA let7i in patients with acute ischemic stroke. *Neurology* 87, 2198–2205. doi: 10.1212/wnl.0000000000003354

Jin, R., Yang, G., and Li, G. (2010a). Inflammatory mechanisms in ischemic stroke: role of inflammatory cells. *J. Leukoc Biol.* 87, 779–789. doi: 10.1189/jlb.1109766

Jin, R., Yang, G., and Li, G. (2010b). Molecular insights and therapeutic targets for blood-brain barrier disruption in ischemic stroke: critical role of matrix metalloproteinases and tissue-type plasminogen activator. *Neurobiol. Dis.* 38, 376–385. doi: 10.1016/j.nbd.2010.03.008

Jolana, L., and Kamil, D. (2017). The role of microRNA in ischemic and hemorrhagic stroke. *Curr. Drug Deliv.* 14, 816–831. doi: 10.2174/1567201813666160919142212

Joshi, S., Wei, J., and Bishopric, N. H. (2016). A cardiac myocyte-restricted Lin28/let-7 regulatory axis promotes hypoxia-mediated apoptosis by inducing the AKT signaling suppressor PIK3IP1. *Biochim. Biophys. Acta* 1862, 240–251. doi: 10.1016/j.bbadis.2015.12.004

Karreman, M. A., Ruthensteiner, B., Mercier, L., Schieber, N. L., Solecki, G., Winkler, F., et al. (2017). Find your way with X-Ray: using microCT to correlate in vivo imaging with 3D electron microscopy. *Methods Cell Biol.* 140, 277–301. doi: 10.1016/bs.mcb.2017.03.006

Khoshnam, S. E., Winlow, W., Farbood, Y., Moghaddam, H. F., and Farzaneh, M. (2017). Emerging Roles of microRNAs in ischemic stroke: as possible therapeutic agents. *J. Stroke* 19, 166–187. doi: 10.5853/jos.2016.01368

Lambertsen, K. L., Biber, K., and Finsen, B. (2012). Inflammatory cytokines in experimental and human stroke. *J. Cereb. Blood Flow Metab.* 32, 1677–1698. doi: 10.1038/jcbfm.2012.88

Lee, C. P., Nithiyanantham, S., Hsu, H. T., Yeh, K. T., Kuo, T. M., and Ko, Y. C. (2019). ALPK1 regulates streptozotocin-induced nephropathy through CCL2 and CCL5 expressions. *J. Cell Mol. Med.* 23, 7699–7708. doi: 10.1111/jcmm.14643

Li, H. W., Meng, Y., Xie, Q., Yi, W. J., Lai, X. L., Bian, Q., et al. (2015). miR-98 protects endothelial cells against hypoxia/reoxygenation induced-apoptosis by targeting caspase-3. *Biochem. Biophys. Res. Commun.* 467, 595–601. doi: 10.1016/j.bbrc.2015.09.058

Li, S., Chen, L., Zhou, X., Li, J., and Liu, J. (2019). miRNA-223-3p and let-7b-3p as potential blood biomarkers associated with the ischemic penumbra in rats. *Acta Neurobiol. Exp.* 79, 205–216. doi: 10.21307/ane-2019-018

Li, W., Pan, R., Qi, Z., and Liu, K. J. (2018). Current progress in searching for clinically useful biomarkers of blood-brain barrier damage following cerebral ischemia. *Brain Circ.* 4, 145–152. doi: 10.4103/bc.bc_11_18

Liu, M., Tao, G., Liu, Q., Liu, K., and Yang, X. (2017). MicroRNA let-7g alleviates atherosclerosis via the targeting of LOX-1 in vitro and in vivo. *Int. J. Mol. Med.* 40, 57–64. doi: 10.3892/ijmm.2017.2995

Liu, Y., Chen, Q., Song, Y., Lai, L., Wang, J., Yu, H., et al. (2011). MicroRNA-98 negatively regulates IL-10 production and endotoxin tolerance in macrophages after LPS stimulation. *FEBS Lett.* 585, 1963–1968. doi: 10.1016/j.febslet.2011.05.029

Lumpkins, K., Bochicchio, G. V., Zagol, B., Ulloa, K., Simard, J. M., Schaub, S., et al. (2008). Plasma levels of the beta chemokine regulated upon activation, normal T cell expressed, and secreted (RANTES) correlate with severe brain injury. *J. Trauma* 64, 358–361. doi: 10.1097/TA.0b013e318160df9b

Mueller, M., Zhou, J., Yang, L., Gao, Y., Wu, F., Schoeberlein, A., et al. (2014). PreImplantation factor promotes neuroprotection by targeting microRNA let-7. *Proc. Natl. Acad. Sci. U.S.A.* 111, 13882–13887. doi: 10.1073/pnas.1411674111

Nayak, A. R., Kashyap, R. S., Kabra, D., Purohit, H. J., Taori, G. M., and Daginawala, H. F. (2012). Time course of inflammatory cytokines in acute ischemic stroke patients and their relation to inter-alfa trypsin inhibitor heavy chain 4 and outcome. *Ann. Indian Acad. Neurol.* 15, 181–185. doi: 10.4103/0972-2327.99707

Nour, M., Scalzo, F., and Liebeskind, D. S. (2013). Ischemia-reperfusion injury in stroke. *Interv. Neurol.* 1, 185–199. doi: 10.1159/000353125

Pawluk, H., Wozniak, A., Grzesk, G., Kolodziejska, R., Kozakiewicz, M., Kopkowska, E., et al. (2020). The role of selected pro-inflammatory cytokines in pathogenesis of ischemic stroke. *Clin. Interv. Aging* 15, 469–484. doi: 10.2147/cia.S233909

Quintana, D. D., Lewis, S. E., Anantula, Y., Garcia, J. A., Sarkar, S. N., Cavendish, J. Z., et al. (2019). The cerebral angiome: high resolution MicroCT imaging of the whole brain cerebrovasculature in female and male mice. *Neuroimage* 202, 116109. doi: 10.1016/j.neuroimage.2019.116109

Rehmsmeier, M., Steffen, P., Hochsmann, M., and Giegerich, R. (2004). Fast and effective prediction of microRNA/target duplexes. *RNA* 10, 1507–1517. doi: 10.1261/rna.5248604

Rom, S., Dykstra, H., Zuluaga-Ramirez, V., Reichenbach, N. L., and Persidsky, Y. (2015). miR-98 and let-7g* protect the blood-brain barrier under neuroinflammatory conditions. *J. Cereb. Blood Flow Metab.* 35, 1957–1965. doi: 10.1038/jcbfm.2015.154

Schober, A. (2008). Chemokines in vascular dysfunction and remodeling. *Arterioscler Thromb. Vasc. Biol.* 28, 1950–1959. doi: 10.1161/ATVBAHA.107.161224

Selvamani, A., Sathyan, P., Miranda, R. C., and Sohrabji, F. (2012). An antagomir to microRNA Let7f promotes neuroprotection in an ischemic stroke model. *PLoS One* 7:e32662. doi: 10.1371/journal.pone.0032662

Sen, C. K., Gordillo, G. M., Khanna, S., and Roy, S. (2009). Micromanaging vascular biology: tiny microRNAs play big band. *J. Vasc. Res.* 46, 527–540. doi: 10.1159/000226221

Shin, C., Nam, J. W., Farh, K. K., Chiang, H. R., Shkumatava, A., and Bartel, D. P. (2010). Expanding the microRNA targeting code: functional sites with centered pairing. *Mol. Cell* 38, 789–802. doi: 10.1016/j.molcel.2010.06.005

Stamatovic, S. M., Shakui, P., Keep, R. F., Moore, B. B., Kunkel, S. L., Van Rooijen, N., et al. (2005). Monocyte chemoattractant protein-1 regulation of blood-brain barrier permeability. *J. Cereb. Blood Flow Metab.* 25, 593–606. doi: 10.1038/sj.jcbfm.9600055

Tarkowski, E., Rosengren, L., Blomstrand, C., Wikkelso, C., Jensen, C., Ekholm, S., et al. (1997). Intrathecal release of pro- and anti-inflammatory cytokines during stroke. *Clin. Exp. Immunol.* 110, 492–499. doi: 10.1046/j.1365-2249.1997.4621483.x

Teler, J., Tarnowski, M., Safranow, K., Maciejewska, A., Sawczuk, M., Dziedziejko, V., et al. (2017). CCL2, CCL5, IL4 and IL15 gene polymorphisms in women with gestational diabetes mellitus. *Horm. Metab. Res.* 49, 10–15. doi: 10.1055/s-0042-111436

Varney, M. L., Johansson, S. L., and Singh, R. K. (2006). Distinct expression of CXCL8 and its receptors CXCR1 and CXCR2 and their association with vessel density and aggressiveness in malignant melanoma. *Am. J. Clin. Pathol.* 125, 209–216. doi: 10.1309/vpl5-r3jr-7f1d-6v03

Wang, G., Zhang, Z., Ayala, C., Dunet, D. O., Fang, J., and George, M. G. (2014). Costs of hospitalization for stroke patients aged 18-64 years in the United States. *J. Stroke Cerebrovasc. Dis.* 23, 861–868. doi: 10.1016/j.jstrokecerebrovasdis.2013.07.017

Wang, L., Zhao, X. C., Cui, W., Ma, Y. Q., Ren, H. L., Zhou, X., et al. (2016). Genetic and pharmacologic inhibition of the chemokine receptor CXCR2 prevents experimental hypertension and vascular dysfunction. *Circulation* 134, 1353–1368. doi: 10.1161/circulationaha.115.020754

Weng, Z., and Zhao, Q. (2015). Utilizing ELISA to monitor protein-protein interaction. *Methods Mol. Biol.* 1278, 341–352. doi: 10.1007/978-1-4939-2425-7_21

Wu, D., Cerutti, C., Lopez-Ramirez, M. A., Pryce, G., King-Robson, J., Simpson, J. E., et al. (2015). Brain endothelial miR-146a negatively modulates T-cell adhesion through repressing multiple targets to inhibit NF-kappaB activation. *J. Cereb. Blood Flow Metab.* 35, 412–423. doi: 10.1038/jcbfm.2014.207

Yang, C., Hawkins, K. E., Dore, S., and Candelario-Jalil, E. (2019). Neuroinflammatory mechanisms of blood-brain barrier damage in ischemic stroke. *Am. J. Physiol. Cell Physiol.* 316, C135–C153. doi: 10.1152/ajpcell.00136.2018

Yang, Q., Tong, X., Schieb, L., Vaughan, A., Gillespie, C., Wiltz, J. L., et al. (2017). Vital Signs: recent Trends in Stroke Death Rates - United States, 2000–2015. *MMWR Morb. Mortal Wkly Rep.* 66, 933–939. doi: 10.15585/mmwr.mm6635e1

Zhang, C. (2008). The role of inflammatory cytokines in endothelial dysfunction. *Basic Res. Cardiol.* 103, 398–406. doi: 10.1007/s00395-008-0733-0

Zhang, L., Yang, J., Xue, Q., Yang, D., Lu, Y., Guang, X., et al. (2016). An rs13293512 polymorphism in the promoter of let-7 is associated with a reduced risk of ischemic stroke. *J. Thromb. Thrombolysis* 42, 610–615. doi: 10.1007/s11239-016-1400-1

Zhou, J., Liu, J., Pan, Z., Du, X., Li, X., Ma, B., et al. (2015). The let-7g microRNA promotes follicular granulosa cell apoptosis by targeting transforming growth factor-beta type 1 receptor. *Mol. Cell Endocrinol.* 409, 103–112. doi: 10.1016/j.mce.2015.03.012

Zhuang, Y., Peng, H., Mastej, V., and Chen, W. (2016). MicroRNA regulation of endothelial junction proteins and clinical consequence. *Media. Inflamm.* 2016:5078627. doi: 10.1155/2016/5078627

Conflict of Interest: The authors declare that the research was conducted in the absence of any commercial or financial relationships that could be construed as a potential conflict of interest.

frontiers in Cell and Developmental Biology

ORIGINAL RESEARCH
published: 28 August 2020
doi: 10.3389/fcell.2020.579157

Extracellular CIRP Induces Inflammation in Alveolar Type II Cells via TREM-1

Chuyi Tan[1], Steven D. Gurien[1,2], William Royster[1,2], Monowar Aziz[1†] and Ping Wang[1,2*†]*

[1] Center for Immunology and Inflammation, The Feinstein Institutes for Medical Research, Manhasset, NY, United States,
[2] Department of Surgery, Donald and Barbara Zucker School of Medicine at Hofstra/Northwell, Manhasset, NY, United States

OPEN ACCESS

Edited by:
Hao Sun,
University of California, San Diego, United States

Reviewed by:
Patricia Zancan,
Federal University of Rio de Janeiro, Brazil
Elena P. Moiseeva,
Retired, Leicester, United Kingdom

***Correspondence:**
Monowar Aziz
maziz1@northwell.edu
Ping Wang
pwang@northwell.edu

† These authors have contributed equally to this work and share senior authorship

Specialty section:
This article was submitted to Cell Adhesion and Migration, a section of the journal Frontiers in Cell and Developmental Biology

Received: *01 July 2020*
Accepted: *12 August 2020*
Published: *28 August 2020*

Citation:
Tan C, Gurien SD, Royster W, Aziz M and Wang P (2020) Extracellular CIRP Induces Inflammation in Alveolar Type II Cells via TREM-1. Front. Cell Dev. Biol. 8:579157. doi: 10.3389/fcell.2020.579157

Extracellular cold-inducible RNA-binding protein (eCIRP) induces acute lung injury (ALI) in sepsis. Triggering receptor expressed on myeloid cells-1 (TREM-1) serves as a receptor for eCIRP to induce inflammation in macrophages and neutrophils. The effect of eCIRP on alveolar epithelial cells (AECs) remains unknown. We hypothesize that eCIRP induces inflammation in AECs through TREM-1. AECs were isolated from C57BL/6 mice and freshly isolated AECs were characterized as alveolar type II (ATII) cells by staining AECs with EpCAM, surfactant protein-C (SP-C), and T1 alpha (T1α) antibodies. AECs were stimulated with recombinant murine (rm) CIRP and assessed for TREM-1 by flow cytometry. ATII cells from WT and TREM-1$^{-/-}$ mice were stimulated with rmCIRP and assessed for interleukin-6 (IL-6) and chemokine (C-X-C motif) ligand 2 (CXCL2) in the culture supernatants. ATII cells from WT mice were pretreated with vehicle (PBS), M3 (TREM-1 antagonist), and LP17 (TREM-1 antagonist) and then after stimulating the cells with rmCIRP, IL-6 and CXCL2 levels in the culture supernatants were assessed. All of the freshly isolated AECs were ATII cells as they expressed EpCAM and SP-C, but not T1α (ATI cells marker). Treatment of ATII cells with rmCIRP significantly increased TREM-1 expression by 56% compared to PBS-treated ATII cells. Stimulation of WT ATII cells with rmCIRP increased IL-6 and CXCL2 expression, while the expression of IL-6 and CXCL2 in TREM-1$^{-/-}$ ATII cells were reduced by 14 and 23%, respectively. Pretreatment of ATII cells with M3 and LP17 significantly decreased the expression of IL-6 by 30 and 47%, respectively, and CXCL2 by 27 and 34%, respectively, compared to vehicle treated ATII cells after stimulation with rmCIRP. Thus, eCIRP induces inflammation in ATII cells via TREM-1 which implicates a novel pathophysiology of eCIRP-induced ALI and directs a possible therapeutic approach targeting eCIRP-TREM-1 interaction to attenuate ALI.

Keywords: eCIRP, TREM-1, type II pneumocyte, inflammation, cytokine, chemokine

Abbreviations: AECs, alveolar epithelial cells; ALI, acute lung injury; ATII, alveolar type II; CXCL2, chemokine (C-X-C motif) ligand 2; eCIRP, extracellular cold-inducible RNA-binding protein; EpCAM, epithelial cell adhesion molecule; IL-6, interleukin-6; NLRP3, NLR family pyrin domain containing 3; SP-C, surfactant protein-C; TLR4-MD2, Toll-like receptor 4-myeloid differentiation factor 2; TREM-1, triggering receptor expressed on myeloid cells-1.

INTRODUCTION

Acute lung injury (ALI) and acute respiratory distress syndrome (ARDS) are life-threatening complications of critically ill patients. They are characterized by severe inflammation, injury to the lungs, acute non-cardiogenic pulmonary edema, and hypoxemia (Ranieri et al., 2012). Pneumonia, sepsis, trauma, hemorrhage, and intestinal ischemia-reperfusion (I/R) often cause ALI (Matthay et al., 2019). The therapies of ALI are largely supportive and are often ineffective, leading to increased morbidity and mortality related to ALI (Bellani et al., 2016; Pham and Rubenfeld, 2017). Therefore, efforts focused on understanding the pathophysiology of ALI are important for finding new treatments.

Pathological specimens from patients with ALI and laboratory studies have demonstrated diffuse alveolar capillary barrier injury, increased permeability to liquids and proteins, and subsequent respiratory failure (Matthay et al., 2019). The alveolar capillary barrier is composed of squamous type I cells (ATI), cuboidal type II cells (ATII), interstitial space, and endothelium (Johnson and Matthay, 2010). The ATII cells secrete surfactant, a critical factor that reduces alveolar surface tension, allowing the alveoli to remain open, facilitating gas exchange (Ward and Nicholas, 1984). Injury to ATII cells results in decreased production of surfactant, which causes reduced lung compliance, leading to respiratory failure. The lung epithelium can be injured by pathogen-associated molecular patterns (PAMPs) such as bacterial products, viruses, and nucleic acids as well as damage-associated molecular patterns (DAMPs) which are endogenous danger molecules released by cells in states of stress such as hypoxia, mechanical force, sepsis, pancreatitis and other diseases (Saffarzadeh et al., 2012; Short et al., 2016; Matthay et al., 2019).

Cold-inducible RNA-binding protein (CIRP) is a glycine-rich RNA chaperone that facilitates RNA translation (Nishiyama et al., 1997). Upon release into the circulation, extracellular CIRP (eCIRP) serves as a DAMP which has a pro-inflammatory role in macrophages, neutrophils, lymphocytes, and endothelial cells (Aziz et al., 2019). In addition, increased expression of CIRP has been shown in the alveolar epithelium of lungs from chronic obstructive pulmonary disease (COPD) patients (Ran et al., 2016). The expression of CIRP in AECs was increased in mice treated with cold air (Chen et al., 2016). eCIRP's role in activating lung macrophages and neutrophils has been identified, but its effects on alveolar epithelial cells remains unknown.

Triggering receptor expressed on myeloid cells-1 (TREM-1), an amplifier of inflammatory responses, is expressed on myeloid cells, such as neutrophils and monocytes (Colonna, 2003). The mRNA expression of TREM-1 is elevated in lung tissue of mice with ALI. This increased expression is related to the severity of the inflammatory response in ALI (Liu et al., 2010). Blocking TREM-1 has been shown to exhibit protective effects in lipopolysaccharide (LPS)-induced ALI via inhibiting the activation of the NLR family pyrin domain containing 3 (NLRP3) inflammasome (Liu et al., 2016). Although the pro-inflammatory effect of TREM-1 and its implication in the pathogenesis of ALI are emerging, the mechanisms remain poorly understood.

We have recently discovered that eCIRP is a new endogenous ligand of TREM-1 and that the binding of eCIRP to TREM-1 induces the production of cytokines in macrophages (Denning et al., 2020). TREM-1 expression in AECs at base line and after exposure to eCIRP remains unknown. Similarly, the direct effect of eCIRP on AECs is also unknown. Here, we hypothesize that eCIRP induces TREM-1 expression on AECs, leading to increased cytokine and chemokine release. In this study, we report that eCIRP induced the production of interleukin-6 (IL-6), chemokine (C-X-C motif) ligand 2 (CXCL2), and the expression of TREM-1 in ATII cells. Genetic depletion or pharmacological inhibition of TREM-1 decreased the production of IL-6 and CXCL2 in ATII cells. Thus, eCIRP activates AECs in a TREM-1-dependent manner and is a potential target for anti-inflammatory therapies.

MATERIALS AND METHODS

Mice

C57BL/6 male mice were purchased from Charles River Laboratories (Wilmington, MA). TREM-$1^{-/-}$ mice [Trem1tm1(KOMP)Vlcg] were generated by the trans-National Institutes of Health Knock-Out Mouse Project (KOMP) and obtained from the KOMP Repository University of California, Davis, CA. Age (8–12 weeks) matched healthy mice were used in all experiments. All mice were housed and kept at room temperature with normal chow and drinking water and housed individually with free access to food and water throughout the experiment. The mice were kept on a 12 h light/dark cycle. All animal experimental protocols were performed according to the guidelines on the use of experimental animals by The National Institutes of Health (Bethesda, MD). The protocol was approved by our Institutional Animal Care and Use Committees.

Isolation of AECs

AECs were isolated from mice lungs as described previously (Chakraborty et al., 2017). In brief, mice were sacrificed by CO_2 asphyxiation. Exsanguinated mice were made aseptic with ethanol spray, and a long ventral incision was made to expose the abdomen and chest cavity. The inferior vena cava was severed and the right heart was then perfused with cold PBS in order to flush the pulmonary vasculature. We then exposed the trachea, inserted a 22G shielded catheter into the lumen, and injected 2 ml of Dispase II (Sigma-Aldrich, St Louis, MO) through the trachea into the lungs. We instilled 0.5 ml of 1% liquefied agarose (Sigma-Aldrich) into the lungs. We then removed the lungs and placed them into 2 ml Dispase for 20 min at 37°C with constant rotation. After removing the lungs from the Dispase solution, we dissected the lung parenchyma using forceps in petri-dishes containing 7 ml of DMEM media supplemented with 1% glutamine, 1% penicillin/streptomycin, and 0.01% DNase I (Sigma-Aldrich). We filtered the cell suspension through 100, 70, 40, and 30 μm strainers (Corning Biosciences, Corning, NY). The filtrate was centrifuged for 15 min at 160 × g and treated with erythrocyte lysis buffer to eliminate the erythrocytes. The cell pellet was resuspended in 500 μl DMEM and incubated with biotinylated

CD45 and CD16/32 antibodies (Biolegend, San Diego, CA) for 30 min. The cells were then incubated with streptavidin-coated magnetic beads for 30 min, and sorted by magnetic separation. The cells were then platted on petri-dishes for 4 h to remove adherent mesenchymal cells.

Cell Culture

Freshly isolated AECs were plated in fibronectin-coated 48 well plates at a density of 1×10^5 cells/well and cultured in airway epithelial cell growth medium along with the following supplements: bovine pituitary extract (0.004 ml/ml), epidermal growth factor (10 ng/ml), insulin (5 μg/ml), hydrocortisone (0.5 μg/ml), epinephrine (0.5 μg/ml), tri-iodo-l-thyronine (6.7 ng/ml), transferrin (10 μg/ml), and retinoic acid (0.1 ng/ml) all purchased from Promocell GmbH (Heidelberg, Germany). The cells were divided into two different treatment groups: AECs pre-treated with the TREM-1-eCIRP binding antagonist peptide M3 (RGFFRGG; GenScript USA Inc., Piscataway, NJ) (10 μg/ml) (Denning et al., 2020) or the TREM-1 decoy peptide LP17 (LQVTDSGLYRCVIYHPP; GenScript USA Inc.) (100 μg/ml) (Gibot et al., 2004). Both groups were pre-treated for 30 min, and then stimulated with recombinant mouse (rm) CIRP (1 μg/ml) for 24 h. The cells were not washed prior to the addition of rmCIRP. Then the supernatants were collected and stored at −20°C for cytokine and chemokine assays. rmCIRP was prepared in-house (Qiang et al., 2013). Briefly, rmCIRP was expressed in *E.coli*, and purified by using Ni^{2+}-NTA column (Novagen, Madison, Wisconsin). The quality of the purified protein was assessed by Western blotting. The level of LPS in the purified protein was measured by a limulus amebocyte lysate (LAL) assay (Cambrex, East Rutherford, New Jersey). Only the purified protein lots that were endotoxin free were considered for *in vitro* and *in vivo* experiments.

Assessment of TREM-1 Expression in AECs by Flow Cytometry

To detect TREM-1 expression in AECs, a total of 1×10^6 AECs were plated in 6-well plates and then stimulated with PBS or rmCIRP (1 μg/ml) for 24 h. After the stimulation, the cells were washed with FACS buffer and stained with PE anti-mouse EpCAM antibody (clone: G8.8, Biolegend, San Diego, CA) and BV421 anti-mouse TREM-1 antibody (clone: 174031, BD Biosciences, San Jose, CA) for 30 min at 4°C. BV421 rat IgG2 antibody (clone: RTK2758, Biolegend) was used as an isotype Ab. Unstained cells were used to control flow cytometry's voltage setting. Acquisition was performed on 30,000 events using a BD LSR Fortessa flow cytometer (BD Biosciences) and data were analyzed with FlowJo software (Tree Star, Ashland, OR).

Immunofluorescent Staining

Immunofluorescent staining of freshly isolated AECs to determine their types was performed according to a protocol previously described (Chakraborty et al., 2017). In brief, AECs were platted on fibronectin-coated 8-well LabTek chambers for 1 or 7 days. The cells were washed once with cold PBS and fixed with 4% paraformaldehyde for 10 min at room temperature. The fixed cells were washed three times with PBS, followed by permeabilization by 0.1% Triton X-100 for 10 min. After washing the cells with PBS, they were blocked with 1% BSA for 1 h. Immunofluorescent staining was performed using primary antibodies against surfactant protein-C (SP-C) (Abcam, Cambridge, MA) and T1 alpha (T1α) (R&D Systems, Minneapolis, MN) and fluorescently tagged secondary antibodies. Primary antibodies were diluted in 1% BSA and incubated with the cells overnight at 4°C. After washing with PBS, cells were incubated with the second antibodies in 1% BSA for 1 h at room temperature in the dark. After an additional washing, slides were mounted immediately on Vectashield mounting medium with DAPI. The cells were visualized using fluorescent microscopy (Nikon BR, Tokyo, Japan).

Enzyme-Linked Immunosorbent Assay

IL-6 and CXCL2 were measured in the culture supernatants of ATII cells following stimulation with rmCIRP by immunoreactivity in a double-sandwich enzyme-linked immunosorbent assay (ELISA) format using commercially available kits by following manufacturer's instructions. The IL-6 ELISA kit was purchased from BD Biosciences and the CXCL2 ELISA kit was purchased from R&D Systems.

Statistical Analysis

All statistical analyses were performed and the figures were prepared with GraphPad Prism version 7.0 software (GraphPad Software, La Jolla, CA). Comparisons between two groups were performed with a two-tailed Student's *t*-test (parametric). Comparisons between multiple groups were analyzed using a one-way analysis of variance (ANOVA), followed by Student–Newman–Keuls (SNK) or Tukey's multiple comparison test. The statistical significance was set at $p < 0.05$.

RESULTS

Identification of Isolated Murine Alveolar Epithelial Cells

A previously described protocol for isolation and culture of AECs was adopted to achieve the desired purification of AECs (Chakraborty et al., 2017). AECs were stained with antibodies against epithelial cell adhesion molecule (EpCAM), an epithelial cell-specific marker and analyzed by flow cytometry, which revealed the purity of sorted AECs to be 83% (**Figure 1A**). Our results were in agreement with the previous results of sorted AECs, which showed a purity of approximately 90% (Chakraborty et al., 2017). After isolation of primary murine AECs, all of the AECs were ATII cells, as characterized by their expression of SP-C, an ATII marker, but not T1α, an ATI marker (**Figure 1B**). To evaluate whether these cells were functionally active and capable of differentiation into ATI cells, the freshly isolated AECs (ATII) were cultured on fibronectin-coated culture plates for 7 days (Chakraborty et al., 2017). We found that after 7 days of culture of

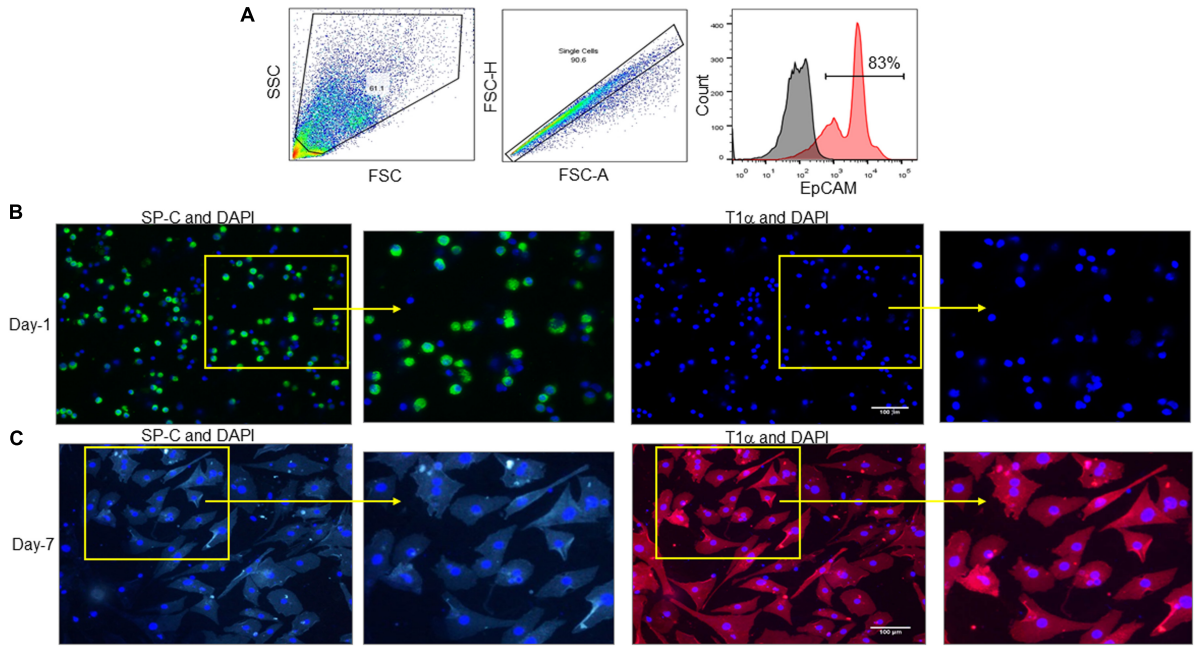

FIGURE 1 | Identification of isolated murine alveolar epithelial cells. **(A)** AECs were isolated from C57BL/6 mice and stained with PE-EpCAM Ab, followed by fixing the cells and assessment by flow cytometry. **(A)** Representative dot blots and the histogram of the frequencies of EpCAM expressing cells are shown. Black histogram depicts isotype control, red histogram depicts EpCAM stained population. EpCAM, epithelial cell adhesion molecule. **(B,C)** AECs were isolated from C57BL/6 mice and cultured on fibronectin-coated culture plates for **(B)** 1 or **(C)** 7 days, then the cells were washed with PBS and stained with ATII cell specific marker SP-C (green) and ATI cell specific marker T1α (red) Abs. Nuclei were stained with DAPI (blue). Imaging was performed by fluorescent microscopy. Scale bars are 100 μm. Experiments were repeated at least two times, which generated reproducible findings.

freshly isolated ATII cells, these cells differentiated into type I phenotype (ATI) as determined by their increased expression of T1α, but not SP-C (**Figure 1C**). Experiments were repeated at least two times, which generated reproducible findings. These data demonstrate that the freshly isolated AECs are mainly the ATII cells, which are viable and undergo differentiation into ATI cells.

Stimulation of AECs With rmCIRP Induces the Production of IL-6 and CXCL2

To determine the role of eCIRP on ATII cells, freshly isolated ATII cells were stimulated with increasing concentrations of rmCIRP. We found that ATII cells stimulated with rmCIRP significantly increased IL-6 production at doses of 1, 5, and 10 μg/ml, respectively, compared to PBS-treated cells (**Figure 2A**). Similarly, rmCIRP significantly increased the release of CXCL2 by AECII cells at doses of 1, 5, and 10 μg/ml, respectively, compared to PBS-treated cells (**Figure 2B**). The highest increase in the production of IL-6 and CXCL2 was found to occur at a dose of 10 μg/ml of rmCIRP. According to our previous studies (Denning et al., 2020; Murao et al., 2020), we chose 1 μg/ml of rmCIRP as an optimal stimulation concentration for the subsequent experiments. Therefore, eCIRP stimulation results in the release of pro-inflammatory cytokines and chemokines by alveolar epithelial type II cells in a dose-dependent manner.

eCIRP Stimulation Increases the Expression of TREM-1 in ATII Cells

We previously identified eCIRP as a new ligand of TREM-1 in macrophages and neutrophils (Denning et al., 2020;

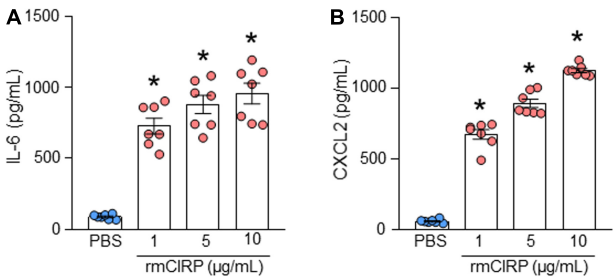

FIGURE 2 | rmCIRP induces the production of IL-6 and CXCL2 in ATII cells. A total of 2 × 10^6 AECs isolated from C57BL/6 mice were stimulated with PBS or rmCIRP (1, 5, 10 μg/ml) for 24 h. After stimulation, the supernatants of the cells were collected. The levels of **(A)** IL-6 and **(B)** CXCL2 in the supernatants were assessed by ELISA. Experiments were repeated at least three times using 3–4 samples/group each time. The figures represent the results of two experimental iterations combined together. We used 3–4 mice to isolate AECs, which usually gave rise to a total of 1.5–2 × 10^6 AECs. Data are expressed as means ± SE (n = 7 samples/group). The groups were compared by one-way ANOVA and Tukey's multiple comparison test (*$p < 0.05$ vs. PBS-treated group).

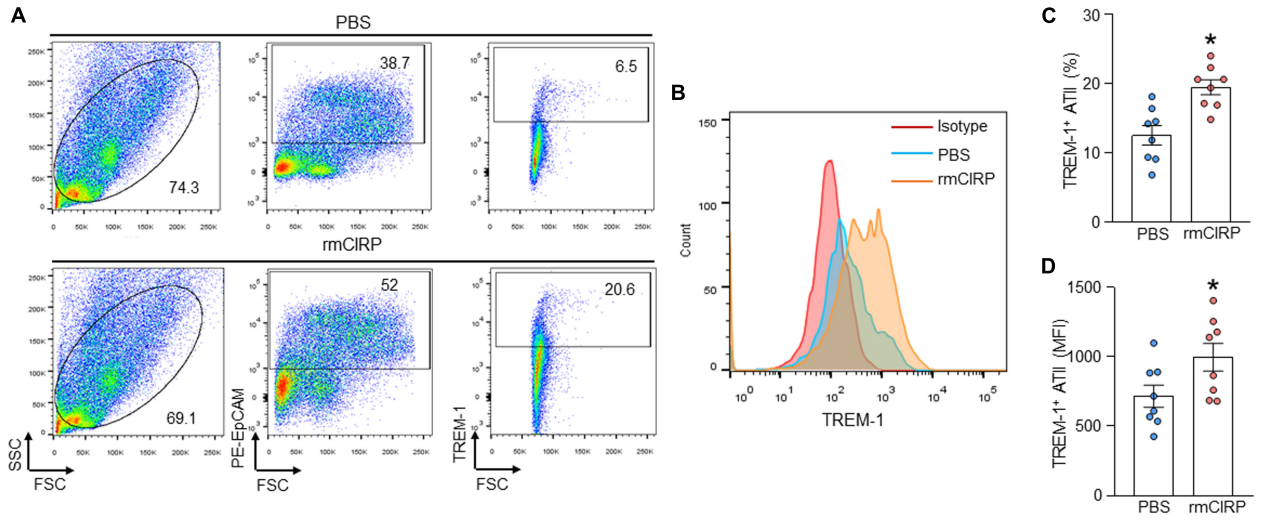

FIGURE 3 | rmCIRP increases the expression of TREM-1 in ATII cells. **(A–D)** AECs (5×10^5 cells) were isolated from C57BL/6 mice and were stimulated with PBS or rmCIRP (1 μg/ml) for 24 h. After stimulation, the cells were washed with PBS and stained with PE-EpCAM and BV421-TREM-1 Abs, followed by fixing the cells and assessment by flow cytometry. Representative **(A)** dot blots showing the gating strategy and **(C)** frequencies of TREM-1 expression and **(B)** histogram and **(D)** bar diagram showing mean immunofluorescence intensity (MFI) of TREM-1 expressing cells in EpCAM gated population are shown. Experiments were repeated at least three times, using 3–4 samples/group each time. The figures represent the results of two experimental iterations combined together. We used 3–4 mice to isolate AECs, which usually gave rise to a total of 1.5–2 $\times$ 10^6 AECs. Data are expressed as means ± SE (n = 8 samples/group). The groups were compared by a two-tailed Student's t-test (*$p < 0.05$ vs. PBS-treated group).

Murao et al., 2020). The expression of TREM-1 and its role in eCIRP-mediated inflammation in AECs remain unknown. We assessed the expression of TREM-1 at the surface of AECs by flow cytometry after stimulation with rmCIRP. We found that under normal conditions, the TREM-1 expressing AEC population was minimal. However, after stimulation of AEC cells with rmCIRP, the frequency of TREM-1 expressing AECs was significantly increased by a mean value of 56% compared to PBS-treated AECs (**Figures 3A,C**). Akin to this result, we also found that after stimulation with rmCIRP the expression of TREM-1, in terms of MFI, was significantly increased by 39% compared to PBS-treated AEC cells (**Figures 3B,D**). Since all the freshly isolated pneumocytes were ATII (**Figure 1**), it suggests that following rmCIRP stimulation, TREM-1 expression was upregulated in ATII cells.

TREM-1 Deficiency Results in Decreased Expression of IL-6 and CXCL2 in ATII Cells

We isolated AECs from WT and TREM-$1^{-/-}$ mice, stimulated them with rmCIRP, and then assessed IL-6 and CXCL2 in the culture supernatant. We found that in both WT and TREM-$1^{-/-}$ mice AECs, stimulation with rmCIRP significantly increased the expression of IL-6 and CXCL2 compared to PBS-treated cells isolated from WT and TREM-$1^{-/-}$ mice (**Figures 4A,B**). We noticed that the production of IL-6 and CXCL2 were significantly decreased in rmCIRP-treated AECs isolated from TREM-$1^{-/-}$ mice by 14 and 23%, respectively, compared to WT mice AECs (**Figures 4A,B**). Since TREM-1 acts as an amplifier of Toll-like receptor 4 (TLR4), we also focused on the effect of LPS induced expression of IL-6 and CXCL2 by AECs isolated from WT and TREM-$1^{-/-}$ mice. We found that LPS stimulation of AECs from both WT and TREM-$1^{-/-}$ mice significantly increased the expression of IL-6 and CXCL2. Nonetheless, we found significantly decreased expression of IL-6 and CXCL2 by 15 and 16% in AECs from TREM-$1^{-/-}$ mice, compared to WT mice in response to LPS stimulation (**Figures 4A,B**). These data indicate that TREM-1 contributes to rmCIRP- and LPS-induced inflammation in AECs.

Pharmacologic Inhibition of TREM-1 Attenuates IL-6 and CXCL2 Expression in ATII Cells

To explore the role of TREM-1 in the activation of ATII cells, ATII cells were isolated from WT mice and cultured for 1 day. AECs were pre-treated with M3, an eCIRP-derived TREM-1 antagonist (Denning et al., 2020), and LP17, a TREM-1 decoy peptide (Gibot et al., 2004), for 30 min before stimulation with rmCIRP for 24 h. The supernatants were subsequently analyzed for IL-6 and CXCL2 contents by ELISA. We found that stimulation of AECs with rmCIRP significantly increased the expression of IL-6 and CXCL2 compared to PBS-treated cells (**Figures 5A,B**). On the other hand, the cells pre-treated with M3, and LP17 significantly decreased IL-6 expression by 30 and 47%, respectively, and CXCL2 expression by 27 and 34%, respectively, compared to vehicle (PBS) treatment in response to rmCIRP stimulation (**Figures 5A,B**). These data suggest that the pharmacologic inhibition of TREM-1 by M3 or LP-17 attenuates eCIRP-induced IL-6 and CXCL2 release in AEC cells.

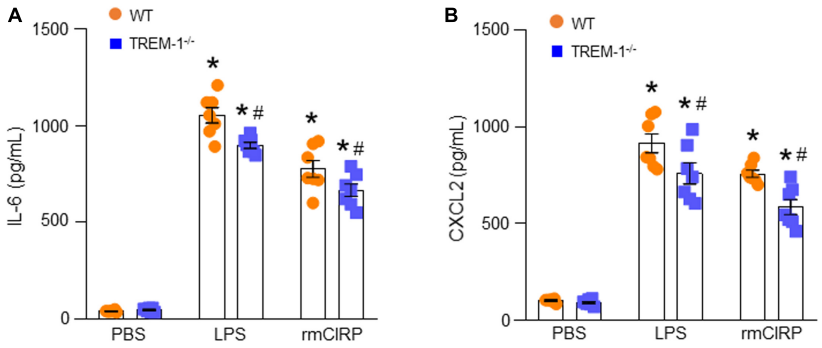

FIGURE 4 | TREM-1 deficiency results in decreased expression of IL-6 and CXCL2 in ATII cells. A total of 2 × 10^6 AECs isolated from WT or TREM-$1^{-/-}$ mice were stimulated with PBS or rmCIRP (1 μg/ml) or LPS (100 ng/ml) for 24 h. After stimulation, the supernatants of the cells were collected. The levels of **(A)** IL-6 and **(B)** CXCL2 in the supernatants were assessed by ELISA. Experiments were repeated at least three times, using 3–4 samples/group each time. The figures represent the results of two experimental iterations combined together. We used 3–4 mice to isolate AECs, which usually gave rise to a total of 1.5–2 × 10^6 AECs. Data are expressed as means ± SE (n = 7 samples/group). The groups were compared by one-way ANOVA and SNK method (*$p < 0.05$ vs. PBS-treated group, $^{\#}p < 0.05$ vs. WT group).

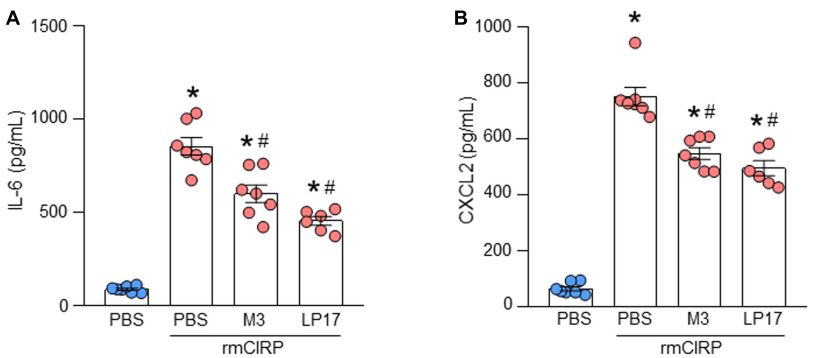

FIGURE 5 | Pharmacologic inhibition of TREM-1 attenuates IL-6 and CXCL2 expression in ATII cells. A total of 2 × 10^6 AECs isolated from C57BL/6 mice were treated with PBS, M3 (10 μg/ml), and LP17 (100 μg/ml). After 30 min of the pre-treatment the cells were then stimulated with rmCIRP at a dose of 1 μg/ml for 24 h. After stimulation, the culture supernatants were collected. The levels of **(A)** IL-6 and **(B)** CXCL2 in the cell culture supernatants were assessed by ELISA. Experiments were repeated at least three times, using 3–4 samples/group each time. The figures represent the results of two experimental iterations combined together. We used 3–4 mice to isolate AECs, which usually gave rise to a total of 1.5–2 × 10^6 AECs. Data are expressed as means ± SE (n = 7 samples/group). The groups were compared by one-way ANOVA and SNK method (*$p < 0.05$ vs. PBS-treated group, $^{\#}p < 0.05$ vs. rmCIRP-treated group).

DISCUSSION

eCIRP, a new DAMP, fuels inflammation by activating immune cells and parenchymal cells to produce pro-inflammatory cytokines, reactive oxygen species (ROS), and proteases. eCIRP subsequently promotes systemic inflammation and organ injury in various inflammatory diseases such as sepsis, hemorrhagic shock, ALI, and ischemia-reperfusion (I/R) injury (Qiang et al., 2013; Liu et al., 2016; Aziz et al., 2019). A recent study showed that eCIRP levels were up-regulated in the airway and alveolar epithelium of lungs from COPD patients (Ran et al., 2016). Intravenous injection of rmCIRP in healthy mice causes lung injury with evidence of increased leukocyte infiltration, enhanced production of pro-inflammatory cytokines, and vascular leakage and edema in the lung tissue (Yang et al., 2016). eCIRP induces lung injury by directly activating endothelial cells (ECs) and inducing EC pyroptosis (Yang et al., 2016). In addition, eCIRP causes sepsis-induced ALI by inducing endoplasmic reticulum (ER) stress and promoting downstream responses like apoptosis, NF-KB activation, and iNOS and pro-inflammatory cytokine production (Khan et al., 2017), while $CIRP^{-/-}$ mice are protected from sepsis-induced ALI (Khan et al., 2017). Thus, eCIRP plays a critical role in the development of ALI.

Under infectious conditions, PAMPs, like LPS, are released into the alveoli and activate alveolar macrophages to release cytokines/chemokines and DAMPs, like eCIRP (Meduri et al., 1995; Qiang et al., 2013). DAMPs further cause alveolar capillary barrier injury, finally resulting in uncontrolled neutrophil infiltration and lung injury. AECs are an important part of the alveolar capillary barrier, which helps with gas exchange and protects the lungs from pathogens (Johnson and Matthay, 2010). Along with alveolar macrophages, alveolar epithelial cells are also the first cells to respond to PAMPs and DAMPs. Regulation of AECs response to these PAMPs and DAMPs is crucial to preserving the normal physiologic function of the alveolar-capillary barrier.

To study the effects of eCIRP on AECs, we isolated primary AECs from murine lungs, and stimulated the cells with rmCIRP. The freshly isolated AECs were mostly AEC type II cells. This is consistent with the previous study (Chakraborty et al., 2017). We found eCIRP significantly induced cytokine IL-6 and chemokine CXCL2 production in a dose dependent manner in ATII cells. These data indicate that eCIRP induces a pro-inflammatory phenotype in ATII cells. Some of the hallmark features of ALI are the increased infiltration of neutrophils in the lung tissues and elevated production of pro-inflammatory cytokines (Matthay et al., 2019). The migration of neutrophils requires the binding of chemokines to chemokine receptors. Interaction between CXCL2 and CXCR2 plays an important role in the recruitment of neutrophils into infection sites (Alves-Filho et al., 2009). In the present study, we found that eCIRP significantly increased chemokine CXCL2 expression in ATII cells. Our previous study showed that CIRP$^{-/-}$ mice exhibited reduced lung injury with reduced infiltration of neutrophils in sepsis (Khan et al., 2017). This could be explained by the fact that sepsis induces eCIRP release into the lungs, which activates ATII cells to release cytokines and chemokines, such as IL-6 and CXCL2, resulting in a subsequent infiltration of neutrophils into the lung tissue causing ALI.

TREM-1 is predominantly expressed on myeloid cells such as macrophages and granulocytes (Bouchon et al., 2000). Prior studies have shown that during inflammation, TREM-1 is also detected on parenchymal cell types such as bronchial, gastric epithelial cells, and hepatic endothelial cells (Chen et al., 2008; Schmausser et al., 2008; Rigo et al., 2012; Tammaro et al., 2017). A previous study reported the mRNA and protein expression of TREM-1 in A549 cells, a human lung epithelial cell line (Liu et al., 2018). In the present study, our results show that murine resting alveolar epithelial cells have a low basal level of TREM-1 expression. TREM-1 is a potent amplifier of the inflammatory response and is associated with infectious diseases (Colonna, 2003). Recent evidence demonstrates that TREM-1 has a crucial role in the development of ALI and may be a potential therapeutic target for ALI and ARDS. The mRNA expression of TREM-1 was elevated in the lung tissue of mice with ALI. The elevated expression of TREM-1 was related to the severity of the inflammatory response in ALI (Liu et al., 2010). Blocking TREM-1 with LR12, a TREM-1 antagonist peptide, has shown a significant protective effect on LPS-induced acute lung injury via inhibiting the activation of the NLRP3 inflammasome (Liu et al., 2016).

We recently showed TREM-1 is a novel endogenous ligand of eCIRP and this interaction promotes an inflammatory response in sepsis (Denning et al., 2020). M3, a novel antagonist peptide of TREM-1, decreased eCIRP-induced systemic inflammation and tissue injury (Denning et al., 2020). This discovery led us to investigate the role of this receptor on the molecular mechanism underlying the activation of alveolar epithelial cells by eCIRP. In our current study, the results of flow cytometry showed that the expression of TREM-1 increased markedly in AECs after stimulation with eCIRP. M3 and LP17 are antagonists of TREM-1. M3 and LP17 suppressed the production of IL-6 and CXCL2 from eCIRP stimulated ATII cells, compared to PBS treated cells. In addition, IL-6 and CXCL2 release from LPS and eCIRP stimulated TREM-1$^{-/-}$ ATII cells were lower than the ATII cells isolated from WT mice. The effect of inhibitors and gene knockout of TREM-1 results in an approximately 20% decrease in pro-inflammatory cytokine production by AECs. This can be explained by the fact that there are other signaling pathways involved in this effect. Toll-like receptor 4-myeloid differentiation factor 2 (TLR4-MD2) was expressed in low amounts on the resting respiratory epithelial cells, and LPS-induced activation of respiratory epithelial cells is dependent on the TLR4 signaling pathway (Guillot et al., 2004). Our previous study proved that eCIRP activates macrophages via its direct binding to the TLR4-MD2 complex (Qiang et al., 2013). In line with this finding, a recent study has revealed that S100A8, an alarmin activates alveolar epithelial cells in the context of acute lung injury in a TLR4-dependent manner (Chakraborty et al., 2017).

CONCLUSION

In conclusion, our study revealed that resting respiratory epithelial cells express TREM-1 and that secretion of pro-inflammatory cytokine/chemokine upon exposure to eCIRP is a result of the TREM-1 signaling pathway. The discovery of the eCIRP/TREM-1 interaction involved in the activation of ATII cells will support the development of novel therapeutic targets for ALI or other lung diseases.

DATA AVAILABILITY STATEMENT

The raw data supporting the conclusions of this article will be made available by the authors, without undue reservation, to any qualified researcher.

ETHICS STATEMENT

The animal study was reviewed and approved by the Feinstein Institutes for Medical Research Animal Care and Use Committees.

AUTHOR CONTRIBUTIONS

CT, SG, and MA designed the experiments. CT, SG, and WR performed the experiments. CT, MA, SG, and PW analyzed the data. MA and CT prepared the figures and wrote the manuscript. WR, SG, and PW reviewed and edited the draft. PW conceived the idea and supervised the project. All authors contributed to the article and approved the submitted version.

FUNDING

This study was supported by the National Institutes of Health (NIH) grants R35GM118337 (PW) and R01GM129633 (MA).

REFERENCES

Alves-Filho, J. C., Freitas, A., Souto, F. O., Spiller, F., Paula-Neto, H., Silva, J. S., et al. (2009). Regulation of chemokine receptor by Toll-like receptor 2 is critical to neutrophil migration and resistance to polymicrobial sepsis. *Proc. Natl. Acad. Sci. U.S.A.* 106, 4018–4023. doi: 10.1073/pnas.0900196106

Aziz, M., Brenner, M., and Wang, P. (2019). Extracellular CIRP (eCIRP) and inflammation. *J. Leukoc. Biol.* 106, 133–146. doi: 10.1002/jlb.3mir1118-443r

Bellani, G., Laffey, J. G., Pham, T., Fan, E., Brochard, L., Esteban, A., et al. (2016). Epidemiology, patterns of care, and mortality for patients with acute respiratory distress syndrome in intensive care units in 50 Countries. *Jama* 315, 788–800. doi: 10.1001/jama.2016.0291

Bouchon, A., Dietrich, J., and Colonna, M. (2000). Cutting edge: inflammatory responses can be triggered by TREM-1, a novel receptor expressed on neutrophils and monocytes. *J. Immunol.* 164, 4991–4995. doi: 10.4049/jimmunol.164.10.4991

Chakraborty, D., Zenker, S., Rossaint, J., Holscher, A., Pohlen, M., Zarbock, A., et al. (2017). Alarmin S100A8 activates alveolar epithelial cells in the context of acute lung injury in a TLR4-dependent manner. *Front. Immunol.* 8:1493. doi: 10.3389/fimmu.2017.01493

Chen, L., Ran, D., Xie, W., Xu, Q., and Zhou, X. (2016). Cold-inducible RNA-binding protein mediates cold air inducible airway mucin production through TLR4/NF-kappaB signaling pathway. *Int. Immunopharmacol.* 39, 48–56. doi: 10.1016/j.intimp.2016.07.007

Chen, L. C., Laskin, J. D., Gordon, M. K., and Laskin, D. L. (2008). Regulation of TREM expression in hepatic macrophages and endothelial cells during acute endotoxemia. *Exp. Mol. Pathol.* 84, 145–155. doi: 10.1016/j.yexmp.2007.11.004

Colonna, M. (2003). TREMs in the immune system and beyond. *Nat. Rev. Immunol.* 3, 445–453. doi: 10.1038/nri1106

Denning, N. L., Aziz, M., Murao, A., Gurien, S. D., Ochani, M., Prince, J. M., et al. (2020). Extracellular CIRP as an endogenous TREM-1 ligand to fuel inflammation in sepsis. *JCI Insight* 5:e134172. doi: 10.1172/jci.insight.134172

Gibot, S., Kolopp-Sarda, M. N., Béné, M. C., Bollaert, P. E., Lozniewski, A., Mory, F., et al. (2004). A soluble form of the triggering receptor expressed on myeloid cells-1 modulates the inflammatory response in murine sepsis. *J. Exp. Med.* 200, 1419–1426. doi: 10.1084/jem.20040708

Guillot, L., Medjane, S., Le-Barillec, K., Balloy, V., Danel, C., Chignard, M., et al. (2004). Response of human pulmonary epithelial cells to lipopolysaccharide involves Toll-like receptor 4 (TLR4)-dependent signaling pathways: evidence for an intracellular compartmentalization of TLR4. *J. Biol. Chem.* 279, 2712–2718. doi: 10.1074/jbc.M305790200

Johnson, E. R., and Matthay, M. A. (2010). Acute lung injury: epidemiology, pathogenesis, and treatment. *J. Aerosol. Med. Pulm .Drug. Deliv.* 23, 243–252. doi: 10.1089/jamp.2009.0775

Khan, M. M., Yang, W. L., Brenner, M., Bolognese, A. C., and Wang, P. (2017). Cold-inducible RNA-binding protein (CIRP) causes sepsis-associated acute lung injury via induction of endoplasmic reticulum stress. *Sci. Rep.* 7:41363. doi: 10.1038/srep41363

Liu, F., Zhang, X., Zhang, B., Mao, W., Liu, T., Sun, M., et al. (2018). TREM1: a positive regulator for inflammatory response via NF-κB pathway in A549 cells infected with Mycoplasma pneumoniae. *Biomed. Pharmacother.* 107, 1466–1472. doi: 10.1016/j.biopha.2018.07.176

Liu, N., Gu, Q., and Zheng, Y. S. (2010). Expression of triggering receptor-1 in myeloid cells of mice with acute lung injury. *World J. Emerg. Med.* 1, 144–148.

Liu, T., Zhou, Y., Li, P., Duan, J. X., Liu, Y. P., Sun, G. Y., et al. (2016). Blocking triggering receptor expressed on myeloid cells-1 attenuates lipopolysaccharide-induced acute lung injury via inhibiting NLRP3 inflammasome activation. *Sci .Rep.* 6:39473. doi: 10.1038/srep39473

Matthay, M. A., Zemans, R. L., Zimmerman, G. A., Arabi, Y. M., Beitler, J. R., Mercat, A., et al. (2019). Acute respiratory distress syndrome. *Nat. Rev. Dis. Primers* 5:18. doi: 10.1038/s41572-019-0069-0

Meduri, G. U., Kohler, G., Headley, S., Tolley, E., Stentz, F., and Postlethwaite, A. (1995). Inflammatory cytokines in the BAL of patients with ARDS. Persistent elevation over time predicts poor outcome. *Chest* 108, 1303–1314. doi: 10.1378/chest.108.5.1303

Murao, A., Arif, A., Brenner, M., Denning, N. L., Jin, H., Takizawa, S., et al. (2020). Extracellular CIRP and TREM-1 axis promotes ICAM-1-Rho-mediated NETosis in sepsis. *Faseb J.* 34, 9771–9786. doi: 10.1096/fj.202000482R

Nishiyama, H., Itoh, K., Kaneko, Y., Kishishita, M., Yoshida, O., and Fujita, J. (1997). A glycine-rich RNA-binding protein mediating cold-inducible suppression of mammalian cell growth. *J. Cell Biol.* 137, 899–908. doi: 10.1083/jcb.137.4.899

Pham, T., and Rubenfeld, G. D. (2017). Fifty years of research in ARDS. the epidemiology of acute respiratory distress syndrome. a 50th birthday review. *Am. J. Respir. Crit. Care Med.* 195, 860–870. doi: 10.1164/rccm.201609-1773CP

Qiang, X., Yang, W. L., Wu, R., Zhou, M., Jacob, A., Dong, W., et al. (2013). Cold-inducible RNA-binding protein (CIRP) triggers inflammatory responses in hemorrhagic shock and sepsis. *Nat. Med.* 19, 1489–1495. doi: 10.1038/nm.3368

Ran, D., Chen, L., Xie, W., Xu, Q., Han, Z., Huang, H., et al. (2016). Cold-inducible RNA binding protein regulates mucin expression induced by cold temperatures in human airway epithelial cells. *Arch. Biochem. Biophys.* 603, 81–90. doi: 10.1016/j.abb.2016.05.009

Ranieri, V. M., Rubenfeld, G. D., Thompson, B. T., Ferguson, N. D., Caldwell, E., Fan, E., et al. (2012). Acute respiratory distress syndrome: the Berlin Definition. *Jama* 307, 2526–2533. doi: 10.1001/jama.2012.5669

Rigo, I., McMahon, L., Dhawan, P., Christakos, S., Yim, S., Ryan, L. K., et al. (2012). Induction of triggering receptor expressed on myeloid cells (TREM-1) in airway epithelial cells by 1,25(OH)2 vitamin D3. *Innate Immun.* 18, 250–257. doi: 10.1177/1753425911399796

Saffarzadeh, M., Juenemann, C., Queisser, M. A., Lochnit, G., Barreto, G., Galuska, S. P., et al. (2012). Neutrophil extracellular traps directly induce epithelial and endothelial cell death: a predominant role of histones. *PLoS One* 7:e32366. doi: 10.1371/journal.pone.0032366

Schmausser, B., Endrich, S., Beier, D., Moran, A. P., Burek, C. J., Rosenwald, A., et al. (2008). Triggering receptor expressed on myeloid cells-1 (TREM-1) expression on gastric epithelium: implication for a role of TREM-1 in *Helicobacter* pylori infection. *Clin. Exp. Immunol.* 152, 88–94. doi: 10.1111/j.1365-2249.2008.03608.x

Short, K. R., Kasper, J., van der Aa, S., Andeweg, A. C., Zaaraoui-Boutahar, F., Goeijenbier, M., et al. (2016). Influenza virus damages the alveolar barrier by disrupting epithelial cell tight junctions. *Eur. Respir. J.* 47, 954–966. doi: 10.1183/13993003.01282-2015

Tammaro, A., Derive, M., Gibot, S., Leemans, J. C., Florquin, S., and Dessing, M. C. (2017). TREM-1 and its potential ligands in non-infectious diseases: from biology to clinical perspectives. *Pharmacol. Ther.* 177, 81–95. doi: 10.1016/j.pharmthera.2017.02.043

Ward, H. E., and Nicholas, T. E. (1984). Alveolar type I and type II cells. *Aust. N. Z. J. Med.* 14(5 Suppl. 3), 731–734. doi: 10.1111/j.1445-5994.1984.tb04343.x

Yang, W. L., Sharma, A., Wang, Z., Li, Z., Fan, J., and Wang, P. (2016). Cold-inducible RNA-binding protein causes endothelial dysfunction via activation of Nlrp3 inflammasome. *Sci. Rep.* 6:26571. doi: 10.1038/srep26571

Conflict of Interest: The authors declare that the research was conducted in the absence of any commercial or financial relationships that could be construed as a potential conflict of interest.

frontiers in Cell and Developmental Biology

REVIEW
published: 26 October 2020
doi: 10.3389/fcell.2020.588066

Integrin-Ligand Interactions in Inflammation, Cancer, and Metabolic Disease: Insights Into the Multifaceted Roles of an Emerging Ligand Irisin

Eun Jeong Park[1], Phyoe Kyawe Myint[1], Atsushi Ito[1,2], Michael G. Appiah[1], Samuel Darkwah[1], Eiji Kawamoto[1,3] and Motomu Shimaoka[1]**

[1] *Department of Molecular Pathobiology and Cell Adhesion Biology, Mie University Graduate School of Medicine, Tsu, Japan,*
[2] *Department of Thoracic and Cardiovascular Surgery, Mie University Graduate School of Medicine, Tsu, Japan,*
[3] *Department of Emergency and Disaster Medicine, Mie University Graduate School of Medicine, Tsu, Japan*

OPEN ACCESS

Edited by:
Hao Sun,
University of California, San Diego, United States

Reviewed by:
Michael Sheetz,
University of Texas Medical Branch at Galveston, United States
Myeongwoo Lee,
Baylor University, United States
Tengqian Sun,
University of California, San Diego, United States
Monica Baiula,
University of Bologna, Italy

***Correspondence:**
Eun Jeong Park
epark@med.mie-u.ac.jp
Motomu Shimaoka
shimaoka@doc.medic.mie-u.ac.jp

Specialty section:
This article was submitted to Cell Adhesion and Migration, a section of the journal Frontiers in Cell and Developmental Biology

Received: *28 July 2020*
Accepted: *05 October 2020*
Published: *26 October 2020*

Citation:
Park EJ, Myint PK, Ito A, Appiah MG, Darkwah S, Kawamoto E and Shimaoka M (2020) Integrin-Ligand Interactions in Inflammation, Cancer, and Metabolic Disease: Insights Into the Multifaceted Roles of an Emerging Ligand Irisin. Front. Cell Dev. Biol. 8:588066. doi: 10.3389/fcell.2020.588066

Integrins are transmembrane proteins that mediate cellular adhesion and migration to neighboring cells or the extracellular matrix, which is essential for cells to undertake diverse physiological and pathological pathways. For integrin activation and ligand binding, bidirectional signaling across the cell membrane is needed. Integrins aberrantly activated under pathologic conditions facilitate cellular infiltration into tissues, thereby causing inflammatory or tumorigenic progressions. Thus, integrins have emerged to the forefront as promising targets for developing therapeutics to treat autoimmune and cancer diseases. In contrast, it remains a fact that integrin-ligand interactions are beneficial for improving the health status of different tissues. Among these ligands, irisin, a myokine produced mainly by skeletal muscles in an exercise-dependent manner, has been shown to bind to integrin αVβ5, alleviating symptoms under unfavorable conditions. These findings may provide insights into some of the underlying mechanisms by which exercise improves quality of life. This review will discuss the current understanding of integrin-ligand interactions in both health and disease. Likewise, we not only explain how diverse ligands play different roles in mediating cellular functions under both conditions via their interactions with integrins, but also specifically highlight the potential roles of the emerging ligand irisin in inflammation, cancer, and metabolic disease.

Keywords: integrin, ligand, irisin, inflammation, cancer, metabolic disease

INTRODUCTION (INTEGRIN BIOLOGY)

Integrins represent a large family of transmembrane cell-adhesion molecules that consist of non-covalently associated α/β heterodimers (Luo et al., 2007). Eighteen types of α chain and eight types of β chain associate with each other to form 24 different heterodimers (Takada et al., 2007). These can be classified into several groups including arginine-glycine-aspartate (RGD)-binding receptors, leukocyte-specific receptors, laminin receptors, and collagen receptors, depending on the traits of

their ligands (Barczyk et al., 2010). By forging a molecular link between cells and their milieu [e.g., the extracellular matrix (ECM) or other cells], integrins advance cellular dynamic processes such as adhesion, migration, and extravasation (Geiger et al., 2001; Kechagia et al., 2019). Integrin-triggered intracellular signaling leads to cell division, survival, differentiation, and/or death, which are pivotal for vital phenomena (Meredith et al., 1993; Leone et al., 2005; Livshits et al., 2012). The activation of integrins before their adherence to cognate ligands, constitutes a variety of global, reversible, and cooperative conformational changes involving multiple structural domains (Shimaoka et al., 2002; Calderwood, 2004). An integrin's ligand-binding affinity is enhanced in response to inside-out signals derived from activated G-protein or via coupling with other receptors (Takagi et al., 2002; Carman and Springer, 2003; Gahmberg et al., 2009; Springer and Dustin, 2012). Adhesion to ligands further stabilizes the high-affinity conformation of integrins for transmitting outside-in signaling, thereby achieving integrin clustering and strengthening adhesiveness (Takagi et al., 2002; Carman and Springer, 2003; Chen et al., 2006; Gahmberg et al., 2009). Specifically, their extracellular domains (e.g., the α-I domain for αLβ2 or the β-I domain for αVβ5) bind cognate ligands [e.g., intercellular adhesion molecule 1 (ICAM-1) for αLβ2 or fibronectin for αVβ5] to consequently signal bi-directionally across the cell membrane, which is called a hallmark of integrin activation (Takagi et al., 2002; Kim et al., 2003; Chen et al., 2006). **Figure 1** depicts the structures and domains of two kinds of integrins, α I domain-containing αLβ2 (A) and α I-domain-lacking αVβ (B).

Integrin-mediated cell adhesion and migration are the integrated and controlled events required for physiologic and pathologic pathways (Gumbiner, 1996; Cox and Huttenlocher, 1998; Collins and Nelson, 2015; McMillen and Holley, 2015). In the case of leukocytes, during their migration to the tissue from bloodstream they undergo dynamic and sequential processes including tethering, rolling, firm adhesion, trans-endothelial migration (TEM), and extravascular migration (Ley et al., 2007). Molecularly, the selectins and integrins of leukocytes play roles in tethering and rolling on contact with the vascular endothelium. Thus, integrins are involved in such processes as slow rolling, firm adhesion, vascular crawling, TEM, and interstitial locomotion depending upon their activation states (Alon et al., 1995; Lawrence et al., 1995; Li et al., 1996; Chesnutt et al., 2006; Shulman et al., 2009; Walling and Kim, 2018).

The interaction of leukocyte integrins (e.g., αLβ2) with their cognate ligands (e.g., ICAM-1) expressed on endothelial cells is crucial to the entire process of homing to tissues (Ley et al., 2007). Leukocytes are recruited from the bloodstream to inflamed sites under pathologic conditions, an event that is also initiated by the interaction between selectins and their ligands, which leads to the aberrant activation of integrins (Zarbock et al., 2011). Understanding the structural and molecular mechanisms underlying integrin-mediated adhesion and migration has advanced the basic science required to apply this knowledge in clinical settings (Horwitz, 2012). Integrin-targeted therapeutics have mostly been designed to modulate integrin functions and thereby either suppress or promote cellular infiltration to the tissues. This has led to the development of effective inhibitory or agonistic drugs to counter the effects of pro- or anti-inflammations, respectively, although in some instances there have been side effects and/or problems of inefficacy (Lu et al., 2008; Baiula et al., 2019).

The majority of integrin heterodimers containing αV chain are known to correlate with cancer (Brooks et al., 1994; Weis and Cheresh, 2011). Specifically, the binding of αV integrins to the RGD motif within ECM proteins is a critical event for angiogenesis in cancer (Koistinen and Heino, 2002; Kaido et al., 2004; Pedchenko et al., 2004; Weis and Cheresh, 2011). Thus, RGD-binding αV integrins have garnered considerable attention as a target of cancer therapeutics. Below, we discuss in detail the implication of integrins and their ligands in inflammation, cancer, and metabolic disease.

INTEGRIN LIGANDS ON THE CELL SURFACE AND IN THE ECM

Most integrins exhibit an ability to bind a wide range of ligands (Humphries et al., 2006). Located on the surfaces of cells are various sets of adhesion proteins involved in cell-cell interactions, as well as cell-ECM binding and interactions involving integrin receptors (Van Der Flier and Sonnenberg, 2001). These are collectively known as cell adhesion molecules (CAMs). CAMs function as ligands of integrins, facilitating the trafficking and homing of migratory cells such as leukocytes. Here, we briefly introduce several representative ligands for integrins.

ICAM-1 (CD54), the most biologically relevant member of the superfamily of immunoglobulin-like transmembrane glycoproteins, is a well-characterized molecule that has been implicated in pro-inflammatory immune responses (Muller, 2019). It is also known well as a receptor for rhinovirus in common colds, and as part of several receptors employed by *Plasmodium falciparum* in the infection of erythrocytes and vascular endothelium in Malaria (Berendt et al., 1989). ICAM-1 is natively expressed on endothelial cells, and its overexpression on endothelial, as well as antigen-presenting cells, is induced by surges of pro-inflammatory cytokines in several pathological states (Chirathaworn et al., 2002; Shaw et al., 2004). ICAM-1 on endothelial cells serves as a ligand for β2 integrins such as αLβ2 andαMβ2 expressed on leukocytes. **Figure 2A** illustrates the structure of ICAM-1. Interaction with ICAM-1 promotes the firm arrest and transmigration of leukocytes from the circulation into tissues (Muller, 2019; **Figure 3A**). The binding of αLβ2 on T cells to ICAM-1 on antigen-presenting cells, such as dendritic cells (DCs), forms the immune synapse that leads to full activation and polarization of T cells (**Figure 3B**; Wernimont et al., 2011; Morrison et al., 2015). Another member of β2 integrins, αDβ2, is expressed on macrophages, monocytes, neutrophils, eosinophils, basophils and a subset of lymphocytes. In addition, it is known to selectively bind to ICAM-3, though not to ICAM-1 (Van Der Vieren et al., 1995).

Vascular cell adhesion molecule 1 (VCAM-1; CD106) is expressed on activated endothelium and serves as a ligand for integrins, α4β1 (very late antigen-4; VLA-4) and α4β7.

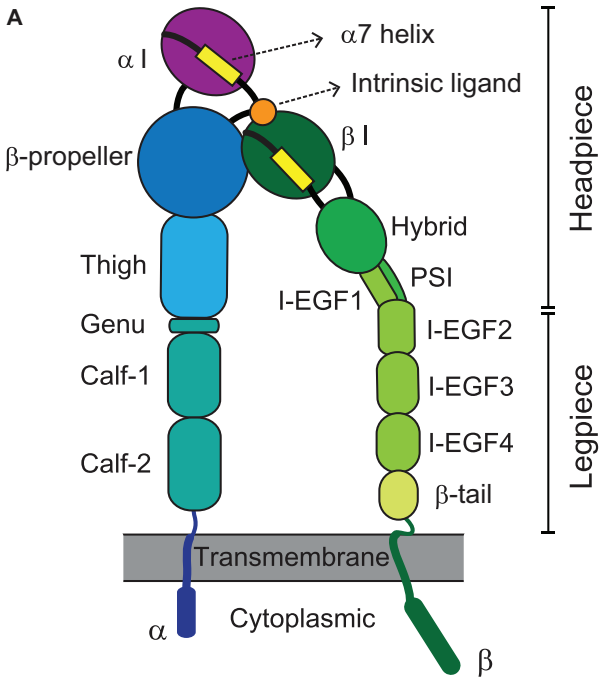

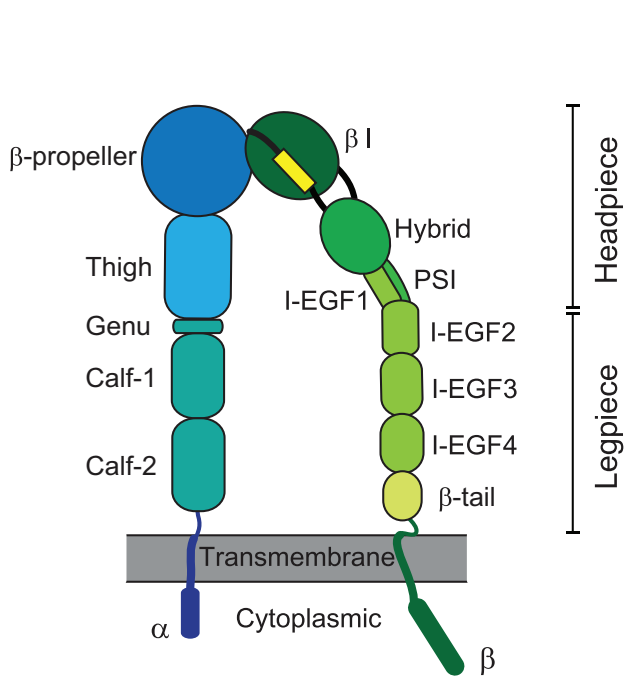

FIGURE 1 | Integrin domains and structures. Illustrations depict the extended conformation of integrins bearing the headpieces with high-affinity domains. Representative structures of α I domain-containing integrins (e.g., αLβ2) and -deficient integrins (e.g., αVβ5) are shown at left **(A)** and right **(B)**, respectively. The integrin α/β heterodimer is composed of multiple functional domains in extracellular (headpiece plus legpiece), transmembrane, and cytoplasmic portions. I-EGF, integrin-epidermal growth factor; and PSI, plexin/semaphorin/integrin.

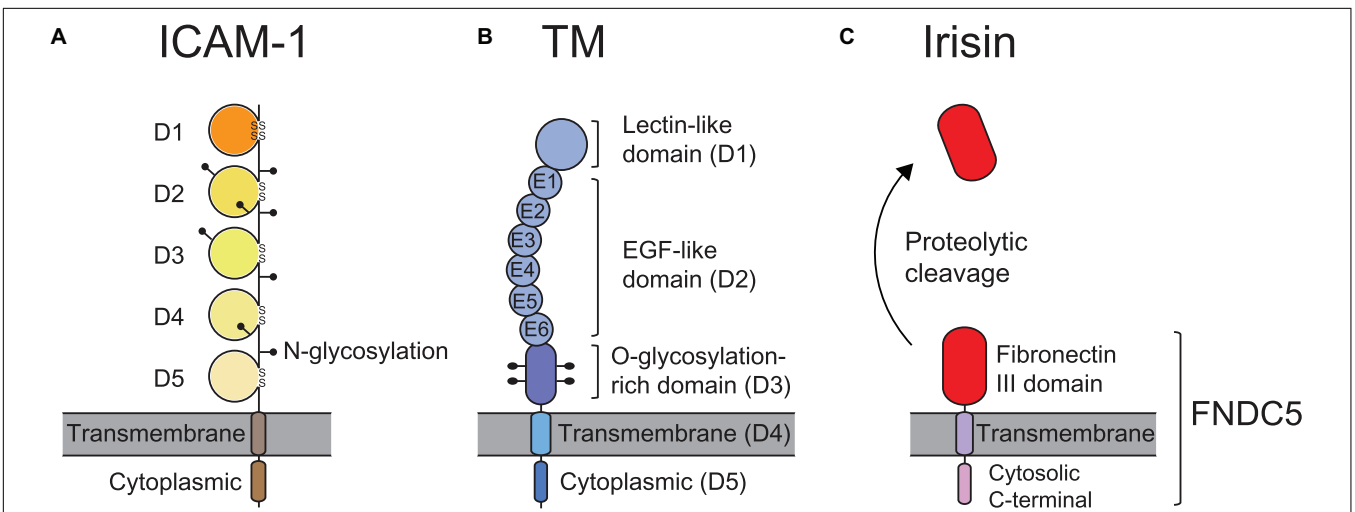

FIGURE 2 | ICAM-1, TM, and FNDC5 domains and structures. **(A)** ICAM-1 consists of 5 immunoglobulin (Ig)-like domains (D1∼D5), a transmembrane domain, and a cytoplasmic domain and contains 8 N-linked glycosylation sites. The disulfide bonds in the Ig-like domains are formed between cysteine residues that stabilize the structure. **(B)** Thrombomodulin (TM) contains a lectin-like domain (D1), 6 epidermal growth factor (EGF)-like domains (D2), an O-glycosylation-rich domain (D3), a transmembrane domain (D4), and a cytoplasmic domain (D5). **(C)** Fibronectin type III domain-containing protein 5 (FNDC5) is composed of a fibronectin III domain (irisin), a transmembrane domain, and a cytosolic C-terminal domain. Irisin is produced by the proteolytic cleavage of FNDC5.

The activation of VCAM-1 is induced by factors such as pro-inflammatory cytokines (e.g., tumor necrosis factor-α; TNF-α), shear stress, high glucose concentrations and reactive oxygen species (ROS) (Cook-Mills et al., 2011). Initial encounters between the post-capillary endothelium and circulating leukocytes in the vascular bed are partly mediated by the binding of α4 integrins to membrane-bound VCAM-1 expressed on endothelium (Berlin et al., 1995). Such interactions not only aid rolling adhesion, but also extend the contact duration between leukocytes and the endothelium before extravasation.

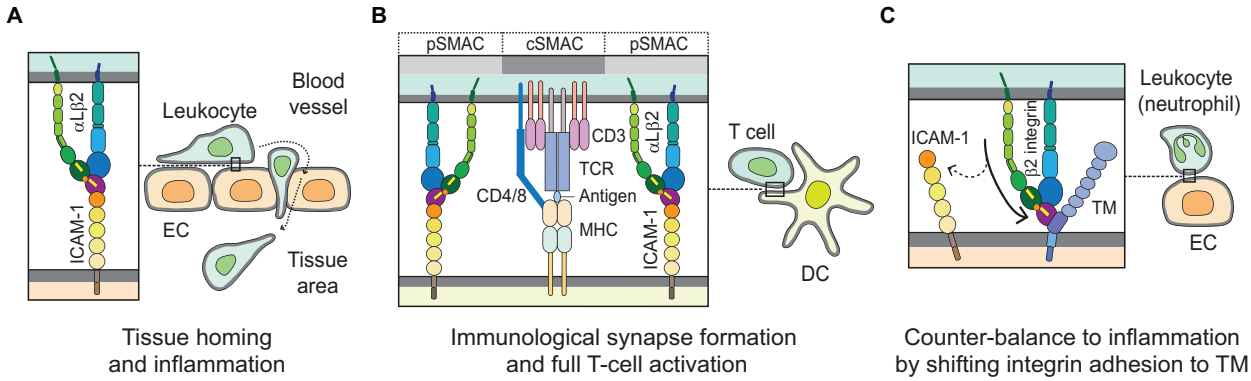

FIGURE 3 | Biological interactions mediated by integrins with ICAM-1 and TM. **(A)** During leukocyte homing to normal or inflamed tissues, integrin αLβ2 plays a key role by interacting with its cognate ligand ICAM-1 on EC, in mediating slow rolling, firm adhesion and trans-endothelial migration, or extravascular movement. **(B)** When T cells migrate to the extravascular space in tissue, they probe cognate antigen-presenting DCs and subsequently form stable and mature immunological synapses. In the immunological synapse, the interaction of αLβ2 with ICAM-1 builds up a distinct marginal region called the pSMAC; TCR and auxiliary molecules are enriched in cSMAC, which may empower T cells to become fully activated. **(C)** The β2 integrin on leukocytes (e.g., neutrophils) binds to the O-glycosylation-rich domain (D3) of TM on EC. This interaction may help counter-balancing inflammation by shifting adhesion from ICAM-1 to TM. EC, endothelial cell; DC, dendritic cell; TCR, T-cell receptor; pSMAC, peripheral supramolecular activation cluster; and cSMAC, central supramolecular activation cluster.

Integrin αDβ2 expressed on eosinophils has been shown to be a functional alternative binder to VCAM-1 involved in the static adhesion of eosinophils during chronic inflammation (Grayson et al., 1998). During leukocyte extravasation, the opening of tight junctions involves the signaling of VCAM-1 to VE-cadherin. Integrin α4β1 on the surface of leukocytes interacts with VCAM-1 and induces Rac-1 activation and the production of ROS, which subsequently leads to the phosphorylation of VE-cadherin by activated proline-rich tyrosine kinase (Pyk2). The result is a local loss of VE-cadherin function and the opening of junctions to facilitate TEM (Cain et al., 2010; Wessel et al., 2014). In relation to lymphocytes, the interaction of VCAM-1 on follicular dendritic cells and integrin α4β1 on B cells is necessary for their localization to lymphoid germinal centers and their subsequent differentiation (Freedman et al., 1990). Integrin α9β1 constitutively expressed in neutrophils binds to VCAM-1. The direct binding of α9β1 integrin to VCAM-1 has been implicated in the mechanism underlying survival and/or delayed neutrophil apoptosis and the maintenance of their physiologic function (Ross et al., 2006).

The recruitment of lymphocytes to the gut mucosa is mediated by the interaction between integrin α4β7 with mucosal addressin cell adhesion molecule 1 (MAdCAM-1) (Hamann et al., 1994). Expression of MAdCAM-1 is not only highly upregulated on inflamed venules in chronic inflammation such as colitis (McDonald et al., 1997), but also constitutively on the sinus-lining cells of the spleen, lactating mammary glands, post-capillary venules of the intestinal lamina propria, and the high endothelial venules of Peyer's patches and mesenteric lymph nodes (Nakache et al., 1989; Kraal et al., 1995). In addition, the interaction between α4β1 and MAdCAM-1 plays a role in an alternative response to the recruitment of inflammatory T cells to the gut during chronic intestinal inflammation (Rivera-Nieves et al., 2005).

E-cadherin is a type-1 homophilic transmembrane protein that functions as a cell adhesion molecule on epithelial cells, serving an important function in the maintenance of epithelial integrity (Vleminckx and Kemler, 1999). E-cadherin acts as a ligand for integrin αEβ7 expressed on mucosal T cells. The binding of αEβ7 integrin to E-cadherin is believed to be vital to the retention of lymphocytes in mucosal epithelial regions (Schon et al., 1999). Studies have also demonstrated the heterotypic binding of non-leukocytic integrin, α2β1 and E-cadherin (Whittard et al., 2002).

Platelet endothelial cell adhesion molecule 1 (PECAM-1; CD31) expressed on platelets, endothelial cells, monocytes and neutrophils has been shown to bind to integrin αVβ3 in order to mediate the interaction of leukocytes with endothelial cells, which might be involved in angiogenesis (Piali et al., 1995). Recombinant human activated protein C (APC) was the first Food and Drug Administration–approved drug for the treatment of hyper-coagulation and excessive inflammation in severe cases of sepsis (Marti-Carvajal et al., 2012). This drug and further studies related to it were discontinued due to the excessive bleeding it induced in sepsis patients. However, the fact that APC regulates leukocyte migration and adhesion was the first major finding suggesting that coagulation factors are involved in regulating inflammation in vascular endothelial cells.

Endothelial cell protein C receptor (EPCR) was the first identified protein C receptor expressed on vascular endothelial cells (Fukudome and Esmon, 1994). When bound to an EPCR, this protein C changes to an APC with the help of the thrombin-thrombomodulin complex. APC plays an important role in coagulation homeostasis by inactivating the pro-coagulation factors Va and VIIIa (Bretschneider et al., 2007). In addition, soluble EPCR released from vascular endothelial cells binds to neutrophils through leukocyte-specific β2 integrin, contributing to anti-inflammatory effects (Kurosawa et al., 2000; Fink et al., 2013). Therefore, EPCRs on endothelial cells may be an

important link between vascular inflammation and coagulation during sepsis. In fact, blood samples from patients with sepsis show elevated levels of soluble EPCR, indicating the pathological exacerbation of sepsis (Kurosawa et al., 1998). Increases in soluble EPCR may be involved in the homeostatic suppression of excessive inflammation during sepsis. Thus, soluble EPCR should be considered an option for sepsis treatment.

Thrombomodulin (TM), which is expressed largely on the luminal area of vascular endothelium, also possesses anti-coagulant and anti-inflammatory properties (Martin et al., 2013). It thus contributes to coagulation and inflammation crosstalk on vascular endothelial cells (Okamoto et al., 2012). **Figure 2B** shows TM domains and structures. The EGF-like domain (D2) in TM has an anticoagulant effect, while the lectin-like domain in TM has an anti-inflammatory effect. Leukocyte β2 integrins bind to the O-glycosylation-rich extracellular domain in TM (**Figure 3C**; Kawamoto et al., 2016); in fact, *in vivo* and *in vitro* experiments have shown that inhibiting adhesion between vascular endothelial cells and leukocytes produces an anti-inflammatory effect (Iba et al., 2013; Kawamoto et al., 2019). Because anticoagulant factors expressed on vascular endothelial cells function as integrin ligands, it is thought that they have a potential as novel drugs for the treatment of inflammation and hyper-coagulation in patients with sepsis.

Fibronectin (FN) is an abundant ECM protein containing three kinds of repeated modules and several binding sites that facilitate concurrent interactions with diverse extracellular components including integrins (Schwarzbauer and Desimone, 2011). Through the RGD motif, FN binds to integrins including α5β1 and αV-classes to participate in many biological functions (Johansson et al., 1997; Schwarzbauer and Desimone, 2011). αV-class integrins bound to FN mediate α5β1 binding to FN at different sites and α5β1 clustering, via eliciting intracellular signaling and mechano-sensing (Bharadwaj et al., 2017). Thus, while both integrins (αV and α5β1) compete for the binding of FN, ultimately they engage in cooperative crosstalk with each other to assemble cellular focal adhesion to ECM (Bharadwaj et al., 2017). Such integrin crosstalk is also mediated by an FN synergy site adjacent to the RGD motif (Benito-Jardon et al., 2017). In addition, lymphocyte interaction with FN via αV integrins (αVβ1/αVβ3) is pivotal for interstitial migration in dense tissues such as the skin, where they are upregulated under inflammatory conditions (Overstreet et al., 2013; Fernandes et al., 2020).

Collagen, another ample ECM component, functions as a coagulation factor. Collagen plays an important structural role in the extracellular matrix of many different tissues. It is also capable of interacting with the following integrins: α1β1, α2β1, α10β1, and α11β1 (Langholz et al., 1995; Zhang et al., 2003; Hamaia et al., 2017). Furthermore, collagen can efficiently attract platelets to damaged blood vessels to prevent extravascular bleeding. When blood vessels are damaged and the collagen fibers under vascular endothelial cells are exposed, α2β1 and αIIbβ3 integrins on the surfaces of platelets become activated. The α2β1 integrin binds to the collagen fibers and strengthens the adhesion of platelets to sites of damage (Morton et al., 1995). Additionally, αIIbβ3 integrin binds to fibrinogen, which contains an RGD sequence, in order to cross-link platelets. By this manner it promotes the formation of a platelet mass and modulates hemostatic functionality (Lefkovits et al., 1995).

Irisin, named after the Greek Goddess Iris, is an adipomyokine first discovered by Bostrom et al. (2012). It is an exercise-inducible peptide with 112 amino acids and a molecular weight of 12 kDa (Bostrom et al., 2012). It is a proteolytic-cleavage product of fibronectin type III domain-containing protein 5 (FNDC5), which is a glycosylated type I membrane protein containing a fibronectin III domain (**Figure 2C**; Ferrer-Martinez et al., 2002; Bostrom et al., 2012). The latter is regulated by the transcriptional regulator peroxisome proliferator-activated receptor-γ (PPAR-γ) co-activator 1α (PGC-1α) in skeletal muscles. In previous biochemical and X-ray crystallographic studies, irisin has been shown to be a homodimer structurally, with a beta sheet located between the monomers (Schumacher et al., 2013). Irisin, containing two sites for N-glycosylation at the Asn-7 and Asn-52 positions, can have a molecular weight of 22 or 25 kDa, depending on the addition of either one or two sugar chains (Zhang et al., 2014; Jedrychowski et al., 2015). Unlike other secreted molecules, both the structure and function of irisin are well preserved during the evolutionary process; for instance, mouse and human irisin are 100% identical (Bostrom et al., 2012; Aydin, 2014). Irisin is primarily secreted from skeletal muscles and adipose tissues. However, studies have shown that smaller quantities of irisin are produced from other organs such as the liver, pancreas, stomach, brain, heart, and spleen (Aydin et al., 2014; Martinez Munoz et al., 2018).

Many studies have suggested that serum irisin increases with physical activity, while the relationship between muscle FNDC5 (the precursor of irisin) mRNA and exercise remains debatable. The increment in serum irisin levels is accompanied by an increase in FNDC5 mRNA levels in skeletal muscles (Bostrom et al., 2012). A pilot study reported a 35% rise in plasma irisin levels in young healthy subjects, with the greatest increase following maximal workload (Daskalopoulou et al., 2014). Similarly, serum irisin levels rose after acute strenuous exercise (cycle ergometry) in both children and young adults (Loffler et al., 2015). In contrast, longer (6 weeks) or chronic (1 year) increases in physical activity did not affect irisin levels in school children (Loffler et al., 2015).

A randomized control trial revealed that a 3-times/week 26-week training program did not change pre-to-post training serum irisin levels (Hecksteden et al., 2013). Moreover, 8 weeks of endurance training by non-diabetic obese male subjects did not affect FNDC5 mRNA level in skeletal muscle (Besse-Patin et al., 2014). A cohort study demonstrated that only high-performance aerobic training caused an increase in FNDC5 mRNA in skeletal muscle (Lecker et al., 2012). These data heightened the speculation that serum irisin levels may be affected by the type of physical activity undertaken, the duration of training sessions, sample collection time and the time of sample analysis (Hecksteden et al., 2013; Tsuchiya et al., 2014; Loffler et al., 2015; Tsuchiya et al., 2015). A mass spectrometry analysis revealed that serum irisin levels averaged 3.6 ng/ml in sedentary young healthy adults, whereas they increased to 4.3 ng/ml in individuals who

partook in aerobic training (Jedrychowski et al., 2015), though it varied with age, gender, and/or body mass index (BMI) (Al-Daghri et al., 2014; Yan et al., 2014; Loffler et al., 2015; Fukushima et al., 2016).

A growing number of studies on the association of irisin with different subunits of integrin have drawn attention to the possibility that irisin may act as a new ligand for the integrin. Differential hydrogen-deuterium exchange linked to mass spectrometry (HDX/MS) data revealed that irisin has a putative integrin-binding region at amino acids 60–76 and 101–108 (Kim et al., 2018). The motif proximal to that region (amino acid 55–57) showed a close structural similarity to the RGD motif in fibronectin, an established ligand for integrin αV (Kim et al., 2018). Although irisin lacked a key amino acid sequence (RGD), except for aspartic acid (Schumacher et al., 2013), blockage of the RGD motif by commercially available RGD-containing peptides showed a significant reduction of irisin-induced signaling pathways in bone cells (Kim et al., 2018). In addition, irisin treatment promoted the invasion and induced the extravillous differentiation of trophoblast cells by switching integrin α6 to integrin α1 (Drewlo et al., 2020). Irisin treatment in rats was shown to improve endometrial receptivity by inducing integrin αVβ3 (Li et al., 2019). However, the molecular mechanisms that underlie these effects and benefits are not well understood, partly due to the lack of knowledge regarding the irisin receptor.

Bostrom et al. (2012) hypothesized that irisin binds to as yet unidentified receptors. The irisin receptors were postulated to exist in the membrane of cardiomyoblasts (Xie et al., 2015), preadipocytes (Zhang et al., 2014), gastrointestinal cancers (Aydin et al., 2016), and pancreatic cancer cell lines (Liu et al., 2018). However, these studies were unable to identify the receptor upon which irisin acts and exerts its pleiotropic effects. Kim et al. (2018) demonstrated that treating osteocytes with doses of irisin as low as 10 pM induced the phosphorylation of focal adhesion kinase (FAK), the major intracellular molecule responsible for integrin signaling. Irisin treatment also increased the phosphorylation of zyxin, another downstream molecule of the integrin-signaling pathway, confirming that irisin acts on the integrin-signaling pathway (Kim et al., 2018). In fact, irisin was revealed to bind to several integrins in adipocytes and osteocytes, with integrin αV classes, including αVβ5 and αVβ1, exhibiting the strongest binding affinity (Kim et al., 2018). Treatment with cyclo RGDyK, a specific αVβ5 antagonist, abolished all irisin-induced signaling responses (Kim et al., 2018). This is the very first finding in which the irisin receptor was identified, and the authors suggested that αV integrin family members are probably the functional irisin receptors in other tissues as well (Kim et al., 2018).

Several studies have identified both the co-receptors and the integrins engaged in irisin binding. The integrins αVβ5 and αVβ1 were found to be involved in irisin-mediated FAK signaling in $CD81^{+}$ adipocyte progenitor cells (Oguri et al., 2020). In this study, CD81 was found to form complexes with αVβ5 and αVβ1 and mediate irisin-induced FAK signaling (Oguri et al., 2020). Complete knockout or antibody-based blockage of either integrin β5 or β1 abolished the effect of irisin-induced FAK phosphorylation in adipocyte progenitor cells, suggesting that irisin plays a role as a ligand for αVβ5 and αVβ1 (Oguri et al., 2020). Moreover, irisin was proven to bind to the integrin αVβ5 receptor on gut epithelial cells both *in vitro* and *in vivo* (Bi et al., 2020a). Immunofluorescence analysis showed the co-localization of irisin and αVβ5, while the co-immunoprecipitation of both molecules revealed this integrin to be a receptor for irisin (Bi et al., 2020a). Treatment with cilengitide trifluoroacetate, an integrin αVβ5 inhibitor, reversed irisin's protective effects against intestinal ischemia reperfusion (IR) injury both *in vitro* and *in vivo* (Bi et al., 2020a). Irisin-dependent restoration of gut barrier function following IR injury was shown to occur via the integrin αVβ5-AMPK-UCP2 pathway (Bi et al., 2020a). The same group demonstrated that irisin binding of αVβ5 exerted ameliorating effects on endothelial and microvascular damage, which was dependent on integrin-triggered signaling to AMPK-Cdc/Rac1 (Bi et al., 2020b). Furthermore, irisin binding to αVβ5 was shown to directly promote osteoclast generation and bone resorption (Estell et al., 2020). Thus, it has been proven that irisin is an authentic ligand for integrin αVβ5 (and/or αVβ1) and exerts beneficial effects on various tissues, presumably by interacting with this integrin. However, the possibility that irisin acts on other membrane receptors cannot be ruled out, and further research is needed to validate these findings.

INTEGRINS IN HEALTH AND DISEASE I: INFLAMMATION

As mentioned earlier, upon being activated integrins interact with their ligands and mediate rolling, adhesion, crawling, and transendothelial migration of leukocytes in order to undergo tissue homing and inflammation. Proper regulation of integrin function is essential for controlling inflammatory responses (Herter and Zarbock, 2013). In order to home to a site of inflammation, leukocytes roll on the endothelium of blood vessels via interactions with selectins and chemokines on the endothelial surface. These interactions trigger inside-out and outside-in signaling cascades that result in the activation of integrins on the leukocytes into high-affinity conformations that facilitate the binding of integrins to their coordinate ligands (e.g., αLβ2/ICAM-1; α4β1/VCAM-1) and firm adhesion of leukocytes to the endothelial wall (Campbell et al., 1998; Herter and Zarbock, 2013). Thereafter, leukocytes move slowly along the surface of the endothelium in a process termed crawling, which ensures the location of an appropriate extravasation site for said leukocytes (Schenkel et al., 2004; Phillipson et al., 2006). Crawling is predominantly mediated by the integrin αLβ2 or αMβ2 depending on the leukocyte subtype (Sumagin et al., 2010). Subsequently, integrins αLβ2, αMβ2, and α3β1 interact with various ligands, including ICAM-1/2 and junctional adhesion molecules, to facilitate transendothelial migration and detachment of leukocytes (Williams et al., 2011; Subramanian et al., 2016). **Figure 3A** depicts the interaction of integrin (e.g., αLβ2) and ligand (e.g., ICAM-1) during leukocyte homing to normal or inflamed tissues.

Integrins play a significant role in adaptive immunity. As aforementioned, successful antigen presentation and T-cell activation by antigen-presenting cells at the specialized cell-cell interface known as the immunological synapse require firm adhesion of the cells (Makgoba et al., 1988), as well as co-stimulation in addition to the classical interactions between the T cell receptor (TCR) and the peptide-MHC complex (Van Seventer et al., 1990). The binding of integrin αLβ2 to ICAM-1 not only provides sustained contact between the T cells and antigen-presenting cells, but also induces the outside-in signaling cascade needed for full T-cell activation, proliferation, and differentiation (Makgoba et al., 1988; Van Seventer et al., 1990; Morgan et al., 2001). **Figure 3B** illustrates the immunological synapse formed by the αLβ2-ICAM-1 interaction required for full T-cell activation.

Resolution of an acute inflammatory response is pivotal to maintaining tissue homeostasis and serves to prevent the onset of an aberrant chronic inflammatory state. This is achieved largely through the removal of apoptotic cells (mainly neutrophils) by phagocytes in a process termed efferocytosis, in which integrins have been shown to be key player (Greenlee-Wacker, 2016). Additionally, the clearance of apoptotic immune cells re-programs phagocytic cells to a pro-resolving phenotype (Ortega-Gomez et al., 2013).

The expression of integrins αVβ3 and αVβ5 on myeloid cells (macrophages and dendritic cells, respectively) boosts the clearance of apoptotic cells, whereas αVβ8 induces the expansion of regulatory T (Treg) cells in a transforming growth factor β1 (TGF-β1)-dependent manner (Albert et al., 1998; Hanayama et al., 2002; Paidassi et al., 2011). This occurs in tandem with the loss of αV, thereby triggering the development of inflammatory bowel disease (IBD) and autoimmunity (Lacy-Hulbert et al., 2007; Travis et al., 2007). In a lipopolysaccharide (LPS)-induced lung inflammation model, intra-tracheal instillation of apoptotic cells was shown to elicit phagocytosis of these cells by $CD11c^{+}CD103^{+}$ DCs, which prime the expansion of Treg cells and mitigate lung inflammation (Zhang et al., 2020). Loss of integrin αV by these DCs results in impaired phagocytosis of apoptotic cells, suppression of TGF-β1 production and Treg-cell expansion, and consequently exacerbation of lung inflammation. Although αV integrin has been reported to be a major player in the onset of fibrosis in several organs (Conroy et al., 2016), it has emerged that fibroblast-specific loss of αV integrin may modulate localized inflammatory responses. In fact, it has been demonstrated that fibroblast-specific deletion of αV integrin decreases type 17-driven (but not type-2 driven) liver and lung fibroses. These fibrosis models further revealed not only a concurrent increase in type 2 inflammation markers such as interleukin-13 (IL-13), but also an accumulation of eosinophils in the lungs and livers of mice lacking αV on their fibroblasts. This suggests that blockade of αV integrin in the quest to ameliorate fibrosis may trigger pathologic type 2 inflammatory responses (Sciurba et al., 2019).

ECM stiffening and perpetual sedimentation are characteristics of fibrosis, which involves the stimulation of integrin signaling and dysregulation of matrix metalloprotease (MMP)-mediated ECM degradation (Bonnans et al., 2014). Under conditions of chronic inflammation, interstitial cytokines such as TGF-β1 and IL-13 induce fibroblasts to upregulate ECM production, resulting in fibrotic progression of the inflamed tissues (Biancheri et al., 2014; Bonnans et al., 2014). Thus, ECM remodeling and deposition are critical to building up the integrated process of fibrosis (Herrera et al., 2018).

Integrin β1 has also been shown to modulate lung inflammation, since deletion of β1 from type 2 alveolar epithelial cells (AECs) causes emphysema and a surge of macrophages in the lungs of adult mice. Furthermore, in younger mice, β1-loss results in defects in tight junctions and decreases in claudin-3 and claudin-4 in type 2 AECs. In addition to increased proliferation of type 2 AECs, a feature of lung injury, β1-deficient type 2 AECs showed an increased release of NF-κB-dependent cytokines and other inflammatory mediators, including those involved in macrophage chemotaxis both *in vivo* and in *ex vivo* cultures (Plosa et al., 2020). Blockade of integrin α4β7 has shown therapeutic benefits in IBD (Feagan et al., 2013; Sandborn et al., 2013). However, 36–54% of patients were refractory to this treatment (Peyrin-Biroulet et al., 2019). Sun et al. (2020) has reported that deficiency of integrin β7 in IL-10 null IBD mice exacerbates both spontaneous and induced colitis by inhibiting the homing of Treg cells to the gut and its associated lymphoid tissues. This suggests that although therapeutic blockade of β7 integrin limits the homing of conventional T cells to the gut, it may in turn abrogate the recruitment of Treg cells to the gut where they ameliorate inflammation.

Dysregulation of integrin αVβ3 and the integrin-associated glycoprotein CD47 have been shown to contribute to the development of osteoarthritis. Transcriptomic and proteomic analyses of osteoarthritic joint tissues from both humans and mice showed elevated levels of integrin αVβ3, as well as CD47 and multiple ligands of αVβ3 including cartilage oligomeric matrix protein, fibronectin, and vitronectin. Genetic deletion or pharmacological blockade of αVβ3 and CD47 and other downstream targets of integrin activation, such as FAK, protected mice against synovitis and cartilage degradation. For example, macrophages from integrin and CD47-deficient mice expressed lower levels of inflammatory and degradative mediators (Wang et al., 2019). Similarly, in a mouse sepsis model, deficiency in integrin β3 was shown to mitigate lung, kidney, and liver damage and enhance survival (Chen et al., 2016, 2020). *In vitro* treatment of β3-null, β3 neutralizing antibody or inhibitor pre-exposed peritoneal macrophages with LPS significantly reduced the secretion of TNF-α and IL-6, suggesting that integrin β3 may regulate the production of cytokines by these innate immune cells. Mechanistically, β3 was shown to upregulate CD14, a key factor that enhances toll-like receptor 4 (TLR4)-LPS interactions during the inflammatory response to sepsis. Thus, β3 may serve as a putative therapeutic target in ameliorating sepsis (Chen et al., 2020). In an ovalbumin-induced asthma murine model, administration of recombinant milk fat globule epidermal growth factor 8 (MFG-E8) suppressed both lung inflammation and airway remodeling by binding with its receptor integrin β3 (Zhi et al., 2018). It has been shown that integrin αMβ2 is essential for the adherence of neutrophils to endothelial cells as well as for transmigration (Hahm et al., 2013). In

models of sterile vascular and hepatic inflammations, neutrophil myeloperoxidase was shown to downregulate the expression of integrin αMβ2 on activated neutrophils and, moreover, negatively regulate the transmigration of neutrophils as well as their interaction with inflamed endothelium (Tseng et al., 2018).

INTEGRINS IN HEALTH AND DISEASE II: CANCERS

Integrins are involved in almost every step of cancer progression, including cancer initiation and proliferation, local invasion and intravasation into the vasculature, survival of circulating tumor cells, priming of the metastatic niche, extravasation into secondary sites and metastatic colonization of new tissues (Hamidi and Ivaska, 2018). Until now, a vast literature has documented altered integrin expression in different cancer types. Indeed, the expression of α3β1, α4β1, α5β1, α6β4, αVβ3, αVβ5, αVβ6, and αVβ8 are thought to correlate with metastasis and poor patient prognosis (Nieberler et al., 2017; Hamidi and Ivaska, 2018). Although the integrin regulation between cancer cells and the microenvironment is quite complicated, some key contributions to cancer progression, in particular to metastasis, have been established. Here, we will discuss selected known and emerging roles of integrins, and their relevance, to events critical for cancer progression and metastasis.

Epithelial-mesenchymal transition (EMT) is the first step of cancer invasion and metastasis. EMT involves the loss of epithelial characteristics via the down-regulation of proteins such as E-cadherin and a shift toward a fibroblast-like phenotype via the expression of mesenchymal proteins such as α-smooth muscle protein (α-SMA), MMPs, and enhanced motility (Brabletz et al., 2018). In this context, integrins play an important role in the induction of EMT and in mediating some of its effects. One of the major EMT inducers is TGF-β, which is a cytokine capable of exerting immunosuppressive, anti-inflammatory, and pro-fibrotic activities. TGF-β is produced and secreted to the extracellular space as an inactivate precursor in which mature TGF-β is caged in latency-associated protein (LAP), thereby confining its bioactivities (Travis and Sheppard, 2014). LAP contains an integrin-binding RGD motif, which allows αV integrins to bind and impose a mechanical force to open the LAP cage (Travis and Sheppard, 2014). Upon binding to the receptor, mature TGF-β induces the downregulation of epithelial proteins, such as E-cadherin, and the upregulation of mesenchymal proteins such as N-cadherin. In addition, integrin α3β1 expression is required for TGF-β-stimulated small mothers against decapentaplegic (SMAD) signaling, which leads to EMT (Kim et al., 2009; Alday-Parejo et al., 2019). On the other hand, epithelial cell stimulation with TGF-β leads to a down-regulation of β4 integrin, which is a typical epithelial integrin essential for epithelial integrity and stability, thus facilitating migration (Yang et al., 2009; Alday-Parejo et al., 2019). Cancer-cell invasion occurs preferentially along pre-existing ECM tracks followed by tissue remodeling.

Collagen crosslinks and ECM solidification strengthen β1-integrin clustering and signaling and focal adhesions, which comprise the dynamic and integrated processes that are prerequisite for breast cancer cell invasion (Levental et al., 2009). In addition, laminin chains increased by tumor-associated fibroblasts provide the altered ECM deposition favorable for α6β4-mediated migration of cervical cancer cells (Fullar et al., 2015). This study demonstrates the roles played by interstitial ECM remodeling and the cross-talk that occurs between tumor and stromal cells in invasive cancers. Therefore, ECM remodeling and degradation, in concert with integrin function, are critical for invasion. MMPs are the proteolytic enzyme of collagen, fibronectin, and laminin—the main components of ECM. In a cervical cancer-cell line, integrin α5β1-fibronectin interaction was found to induce the expression and activation of pro-MMP9 and moderate changes to pro-MMP2 activity involving the FAK, integrin-linked protein kinase, ERK, phosphoinositide 3-kinase (PI3K), and NF-κB signaling cascades (Ganguly et al., 2013). Interaction of integrin α5β1 with laminin also induced MMP-9 expression and activated the signaling cascade (Ganguly et al., 2013). This ligand-integrin interaction was also found to accelerate cell migration. In addition, not only integrin α5β1 but also integrin αVβ3 has been linked to MMP activity. For instance, integrin αVβ3 expression is a major determinant of breast cancer cell bone metastasis (Takayama et al., 2005; Ganguly et al., 2013). Moreover, integrin αVβ3 is found as a modulator of MMP-2 activation and lymph-node metastasis (Hosotani et al., 2002; Ganguly et al., 2013).

Angiogenesis is another important factor in cancer progression and metastasis. In general, tumors lacking blood circulation grow to 1–2 mm^3 in diameter and then stop; however, when placed in an area where angiogenesis has arisen they can grow > 2 mm^3 (Folkman, 1986). In the absence of vascular support, tumors may become necrotic or even apoptotic due to insufficient supplies of oxygen and nutrition. Furthermore, angiogenesis not only provides nutrients for the tumor to grow, but also supports an escape route for tumor cells to enter the circulation. The mechanism underlying angiogenesis is mostly modulated by chemical stimuli such as vascular endothelial growth factor (VEGF), fibroblast growth factor (FGF), angiopoietins, epidermal growth factor (EGF), etc., all of which are plentiful at tumor sites (Teleanu et al., 2019). In particular, VEGF and FGF and their receptors are the most potent activators of angiogenesis. In this context, three endothelial integrins play crucial roles: αVβ3, αVβ5, and α5β1. VEGF-mediated angiogenesis occurs via αVβ5, while FGF-mediated angiogenesis occurs via αVβ3 and α5β1 (Foubert and Varner, 2012; Bianconi et al., 2016). In preclinical studies, the inhibition of angiogenesis with αVβ3 antagonists suppressed tumor progression, raising high expectations that an αVβ3 blockade may represent a valuable anti-cancer strategy (Liu et al., 2008). However, while integrin αVβ3-deficient mice show normal developmental angiogenesis, there is an increase in pathological angiogenesis. One hypothesis to explain this disparity is that animals lacking integrin αV develop compensatory pathways for VEGF signaling to permit the onset of angiogenesis during embryogenesis (Foubert and Varner, 2012). In clinical settings,

administration of αVβ3 inhibitor "cilengitide" was unable to exert a potent therapeutic effect due to the induction of enhanced angiogenesis in the tumor environment (Bianconi et al., 2016; Wick et al., 2016). These reports demonstrate the functional complexity of integrins in regulating angiogenesis.

In addition to EMT and angiogenesis, a specialized microenvironment called the metastatic niche is important for disseminated cancer cells to adapt and survive in new tissues. Metastatic niches can be induced by primary tumors even before disseminated cancer cells reach the peripheral tissues to promote their survival and outgrowth. This implies some cross-talk between the primary tumor and peripheral tissues. In regards to the aforementioned mechanism, exosomes released by cancer cells play a vital role in cancer metastasis, contributing to the formation of metastatic niches, influencing cancer cells and the microenvironment, and determining specific organotropic metastasis (Hoshino et al., 2015). Breast cancer exosomes expressing high levels of αVβ5 were shown to disseminate to liver tissue containing a fibronectin-enriched ECM, whereas those expressing high levels of α6β4 disseminated to lung tissues containing laminin-enriched ECM (Hoshino et al., 2015; Shimaoka et al., 2019; Myint et al., 2020). The proposed mechanism underlying pre-metastatic niche formation involves the activation of the pro-inflammatory S100 genes found in lung and liver tissues (Hoshino et al., 2015). While exosomal transfer of the intact integrin-signaling complex has yet to be demonstrated, exosomally transferred integrin proteins could trigger the signals that lead to S100 activation by using Src Kinases derived from either exosomes or target cells (Hoshino et al., 2015). In this way, cancer-associated exosomes establish the organotropic pre-metastatic niche. These findings suggest that the interruption of integrin functions and ligand-dependent signaling could be a promising approach for developing therapeutics to combat various cancers.

IRISIN BIOGENESIS AND BIOLOGICAL ASPECTS

A collective number of molecules seems to co-operate in the synthesis and secretion of irisin, a cleaved fragment of FNDC5 protein, via the AMPK-PGC-1α-FNDC5 axis (Bostrom et al., 2012; Shan et al., 2013; Gamas et al., 2015). Skeletal muscle contractions due to exercise increase levels of cytoplasmic calcium, which in turn activates AMP-activated protein kinase (AMPK). Moreover, the rise in the AMP/ATP ratio also phosphorylates AMPK (Mu et al., 2001; Jessen and Goodyear, 2005), which subsequently upregulates PGC-1α. The latter is known to interact with and coactivate several transcription factors and nuclear receptors, among which FNDC5 is one of the downstream molecules (Lira et al., 2010; Bostrom et al., 2012; Gholamnezhad et al., 2020). Consequently, FNDC5 expression is upregulated (Bostrom et al., 2012). Moreover, muscle contractions initiate the cleavage of FNDC5 with the help of an unknown protease (**Figure 4**). Although the cleavage and release of irisin is believed to occur in a manner similar to those of transmembrane polypeptides, such as EGF and TGF-α (Bostrom et al., 2012), the molecular mechanism underlying proteolytic cleavage and the enzyme(s) involved remains unknown. After proteolytic cleavage, the C-terminal tail of FNDC5 is anchored in the cytoplasm, whereas the extracellular N-terminal part is released into the circulation as irisin (Ferrer-Martinez et al., 2002; Teufel et al., 2002; Bostrom et al., 2012; Wrann et al., 2013).

Irisin has been shown to exert its pleiotropic effects on different tissues and signaling pathways. Many studies have linked irisin's diverse effects with the AMPK pathway. In fact, via this pathway irisin has been shown to decrease inflammation and insulin resistance (Xiong et al., 2018), induce the browning of fat (Shan et al., 2013), lower blood pressure (Fu et al., 2016), promote differentiation and improve trophoblast functions in human placenta (Drewlo et al., 2020). Irisin treatment increased the expression of sclerostin in osteocytes to induce bone resorption (Kim et al., 2018). Irisin induces the browning of fat via the upregulation of UCP1 mRNA in subcutaneous adipose tissue (Kim et al., 2018). In addition, it reduces obesity and improves glucose tolerance in mice fed a high-fat diet (HFD) (Bostrom et al., 2012). Irisin's browning effect is exerted via p38 and ERK signaling (Zhang et al., 2014; **Figure 4**). Treatment with recombinant irisin significantly increases phosphorylated p38 and phosphorylated ERK in both primary rat and 3T3-L1 adipocytes, while cotreatment with an inhibitor of either p38 or ERK or both abolishes the irisin-induced upregulation of UCP1 expression (Zhang et al., 2014). Irisin has been shown to promote Nkx2.5-positive cardiac progenitor cell-induced cardiac regeneration, neovascularization and functional improvements in the ischemic heart (Zhao et al., 2019). Moreover, administration of irisin promotes the proliferation of human umbilical vein endothelial cells and cord formation via the ERK pathway (Wu et al., 2015), suggesting that irisin plays a role in guarding against cardiovascular diseases.

In the context of the brain, FNDC5/irisin is expressed in the hippocampus, cortex and cerebrospinal fluid of wild-type C57BL/6 mice (Lourenco et al., 2019). An Alzheimer's disease (AD) model of mice revealed a lower level of irisin in the brain, while conditional knockout of brain irisin resulted in impaired long-term potentiation and novel object recognition memory in mice. Boosting of brain irisin by intracerebroventricular infusion rescues memory impairment and provides protection against synaptic plasticity in AD mice (Lourenco et al., 2019). Another group showed that irisin binds with amyloid precursor protein at the N-terminal and that overexpression of FNDC5 in cells significantly decreased the secretion of amyloid-β protein into the media *in vitro* (Noda et al., 2018). In addition, pharmacological, but not physiological, concentrations of irisin (50–100 nM) increase the proliferation of a mouse hippocampal cell line, H19-7 HN, without influencing markers of neurite outgrowth or synaptogenesis *in vitro*. The proliferation of H19-7 HN cells occurs through the activation of the signal transducer and activator of transcription 3 (STAT3), but not the AMPK and/or ERK, signaling pathway (Moon et al., 2013).

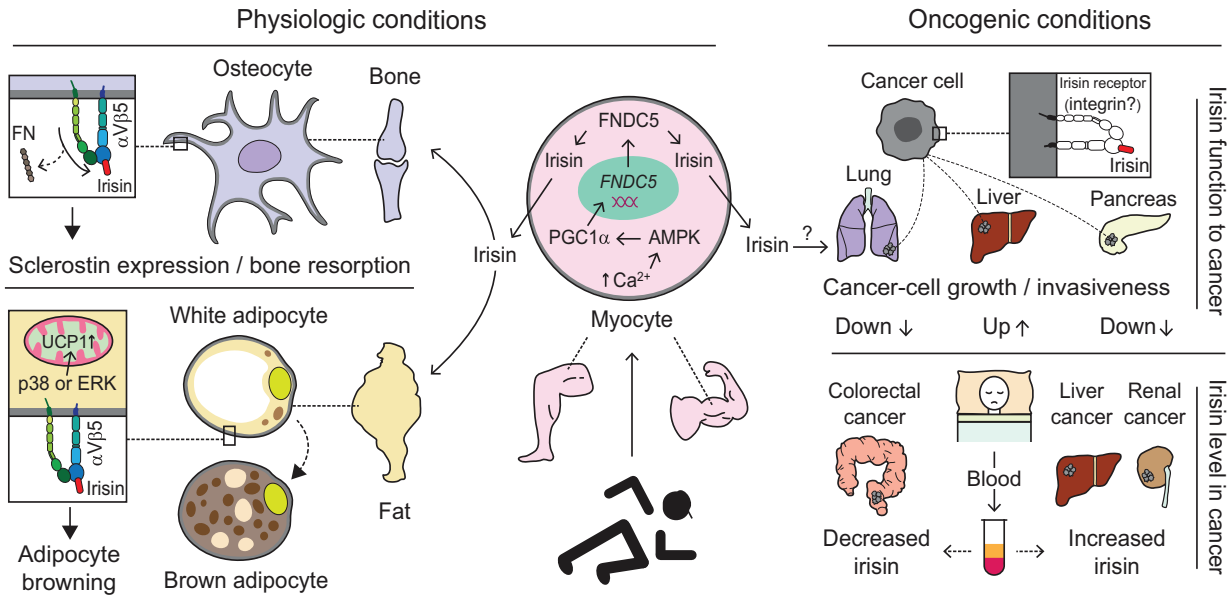

FIGURE 4 | Biological interactions mediated by integrins with irisin. Exercise-induced production and release of irisin from the myocytes of skeletal muscle through activation of the AMPK-PGC1α-FNDC5 axis alters biological pathways via interaction with integrin (Bostrom et al., 2012; Shan et al., 2013; Gamas et al., 2015). Under physiologic conditions, irisin migrated to the bone via blood circulation preferentially, compared to FN, interacts with integrin αVβ5 acting on osteocytes to induce sclerostin expression and bone resorption. Moreover, irisin binding to Vβ5 on adipocytes is believed to facilitate adipocyte browning through the activation of p38 or ERK followed by increases in UCP1 (Zhang et al., 2014; Kim et al., 2018). Under oncogenic conditions, irisin binding to cancer cells is thought to have different impacts, although irisin receptors specific to cancer cells exist remains an open question. Specifically, irisin plays a role in inhibiting the growth or invasiveness of lung- and pancreatic-cancer cells (Shao et al., 2017; Liu et al., 2018), whereas it stimulates liver-cancer cells to promote tumor progression (Shi et al., 2017). In addition, the levels of irisin in blood (serum or plasma) of cancer patients appear to vary depending on which organ is primarily cancerous. For example, increased levels of irisin were found in liver- and renal-cancer patients (Gaggini et al., 2017; Altay et al., 2018), while decreased levels were detected in colorectal-cancer patients (Zhu et al., 2018). This suggests irisin levels may serve as a diagnostic marker for different cancers. AMPK, adenosine monophosphate (AMP)-activated protein kinase; PGC1α, peroxisome proliferator-activated receptor coactivator 1α; FNDC5, fibronectin type III domain-containing protein 5; FN, fibronectin; ERK, extracellular signal-regulated kinase; and UCP1, uncoupling protein 1.

ROLES OF IRISIN IN INFLAMMATION, CANCER, AND METABOLIC DISEASE

Irisin has been shown to exhibit anti-inflammatory properties in adipocytes and in immune cells. A cohort study showed that irisin levels were negatively associated with TNF-α levels in adipocytes (Moreno-Navarrete et al., 2013). Irisin has been shown to stimulate the proliferation and phagocytic activity of macrophages, while decreasing ROS overproduction in macrophages. Irisin treatment inhibited LPS-induced M1 macrophage polarization and inflammatory cytokine production both in RAW264.7 cells and in peritoneal macrophages (Xiong et al., 2018). Overexpression of FNDC revealed the attenuation of inflammatory cytokines in HFD-induced obese mice (Xiong et al., 2018). Another study also illustrated how pre-treatment with irisin lowered LPS-induced cytokine production in RAW264.7 cells via the downregulation of TLR4 and myeloid differentiation primary response protein (MyD88) levels, which consequently lowered the phosphorylation and/or activation of molecules involved in downstream signaling pathways (Mazur-Bialy et al., 2017). These data suggest that irisin plays an important role in both physiological and pathological conditions.

Concerning cancers, many studies have suggested that exogenous irisin exerts anti-tumor and anti-metastatic effects (Kong et al., 2017; Shao et al., 2017; Liu et al., 2018), while others have reported its stimulatory effects on tumorigenesis (Shi et al., 2017). Irisin has been shown to suppress the progression and invasion of glioblastoma by inducing p21 and tissue factor pathway inhibitor-2 (Huang et al., 2020). In breast cancer subjects, serum irisin levels were significantly lower compared with healthy volunteers (Provatopoulou et al., 2015). The authors estimated that a 1 unit increase in irisin levels could reduce the probability of breast cancer by almost 90% (Provatopoulou et al., 2015). Moreover, serum irisin was shown to play a protective role against spinal metastasis in breast cancer patients after adjusting for age and BMI (Zhang et al., 2018). Those breast cancer patients without spinal metastasis had significantly higher serum irisin levels compared to those with spinal metastasis (Zhang et al., 2018). However the levels of irisin in the blood (serum or plasma) of cancer patients appear to vary depending on which organ is primarily cancerous. For example, increased levels of irisin were found in liver- and renal-cancer patients (Gaggini et al., 2017; Altay et al., 2018), while decreased levels were detected in colorectal- and breast-cancer patients (Provatopoulou et al., 2015; Zhang et al., 2018; Zhu et al., 2018; **Figure 4**).

This suggests irisin levels may serve as a diagnostic marker for different cancers.

It is well-known that the PI3K/AKT pathway is elevated in many cancers and is responsible for cancer cell growth, proliferation and survival (Vivanco and Sawyers, 2002). Irisin was found to inhibit the proliferation, migration and invasion of lung cancer cells by reversing the EMT via PI3K/AKT pathway activation (Shao et al., 2017). In line with that, the anti-metastatic effects of irisin was demonstrated on osteosarcoma cells. Irisin treatment reversed IL-6 induced EMT in U2OS and MG-63 osteosarcoma cells, and inhibited the migration and invasion of cancer cells through the STAT3/Snail-signaling pathway (Kong et al., 2017). Non-modified irisin decreased cancer cell counts, viability and migration through upregulated caspase-3/7 activity and NF-*K*B suppression in malignant breast cancer cell lines (Gannon et al., 2015). In this study, irisin was shown to enhance doxorubicin activity in malignant breast cancer cells, but not in non-malignant breast cancer cells (Gannon et al., 2015). In addition, irisin has been shown to suppress pancreatic cancer cell growth and proliferation (Liu et al., 2018), and to enhance doxorubicin-induced pancreatic cancer cell apoptosis through the upregulation of caspase-3 expression and the reduction of anti-apoptotic B-cell lymphoma 2 (Bcl-2) and Bcl-xL expression (Liu et al., 2019). Irisin potentiated the effects of chemo-therapeutic agents in pancreatic cancer cells via suppression of the PI3K/AKT/NF-*K*B signaling pathway (Liu et al., 2019; **Figure 4**).

In contrast, use of irisin in obesity-related cancer lines such as colon, esophageal, endometrial and thyroid cancer cells showed no effects in term of cell proliferation or invasion (Moon and Mantzoros, 2014). Irisin stimulated the proliferation and invasion of human hepatocellular carcinoma cells (Shi et al., 2017). There was an increase in irisin level in cancerous liver tissues obtained from hepatocellular carcinoma (HCC) patients, although there was no difference in serum irisin level between HCC patients and healthy volunteers (Shi et al., 2017). Moreover, irisin was found to not only increase proliferation and invasion of HepG2 cells, but also to decrease doxorubicin-induced HepG2 cell apoptosis, effects that occurred via the PI3K/AKT pathway (Shi et al., 2017; **Figure 4**). Although both the anti- and pro-tumor effects of irisin seem to involve the PI3K/AKT pathway, the underlying mechanism that might explain these discrepancies remains unknown (Moon and Mantzoros, 2014; Gannon et al., 2015; Shao et al., 2017; Shi et al., 2017; Liu et al., 2019). Further studies are required to validate the differential effects of irisin on different cancers.

Since the discovery that irisin might exert potentially beneficial effects on metabolic diseases (Bostrom et al., 2012), many researchers have tried to determine the nature of the association between serum irisin levels and these diseases. Obese subjects had significantly higher serum irisin levels compared to non-obese subjects (Sahin-Efe et al., 2018). Elevated levels of irisin in these subjects may be due to irisin resistance developed during the course of obesity (Sahin-Efe et al., 2018). Another study confirmed that obese subjects had significantly increased serum irisin levels compared to normal weight subjects (Pardo et al., 2014). In addition, a 1 kg increment in fat mass could result in a twofold increase in serum irisin levels (Pardo et al., 2014).

Serum irisin levels were positively associated with age, BMI and other metabolic parameters, whereas type 2 diabetic (T2DM) subjects showed significantly decreased serum irisin level irrespective of age or gender (Liu et al., 2013). Similarly, serum irisin levels were significantly decreased in T2DM and negatively associated with newly diagnosed T2DM (Choi et al., 2013). Interestingly, in both *in vivo* and *in vitro* experiments, disassociations resulted depending on the experimental setting (Kurdiova et al., 2014). Serum irisin levels were significantly lower in T2DM, while muscle FNDC5 mRNA expression showed no difference between healthy and diabetic subjects. Meanwhile, FNDC5 mRNA and irisin secretion in the culture supernatant of myotubes from T2DM subjects were significantly higher compared to healthy controls (Kurdiova et al., 2014). The authors assumed that endogenous signals regarding T2DM may play a role in regulating irisin secretion *in vivo* (Kurdiova et al., 2014). In a cross-sectional study including 1115 obese adults, serum irisin was significantly reduced in subjects with metabolic syndrome. Linear regression analysis data revealed that serum irisin levels were negatively associated with fasting insulin, hemoglobin A1c, and albumin/globulin ratios (Yan et al., 2014). Similarly, a study in rats showed that serum irisin was significantly lower in HFD- and streptozotocin-induced diabetic rats compared to healthy rats (Abdelhamid Fathy, 2017). Diabetic rats that underwent chronic exercise training, in this case swimming, exhibited not only increased serum irisin levels and improved blood glucose levels, but also a homeostatic model assessment of insulin resistance compared with sedentary diabetic rats (Abdelhamid Fathy, 2017).

A nested case-controlled study revealed that serum irisin levels were significantly lower in those elderly subjects with obesity, diabetes mellitus and/or hypertension (Guo et al., 2020). Serum irisin showed negative associations with BMI, blood pressure, fasting blood glucose, cholesterol, and triglyceride (Guo et al., 2020). The authors also found that higher levels of serum irisin were associated with reduced risks of hypertension, T2DM, overweight, and obesity (Guo et al., 2020). Animal studies revealed the differential regulatory effects of central and peripheral irisin on blood pressure (Zhang et al., 2015). Intraventricular injection of exogenous irisin increased blood pressure and cardiac contractility via the activation of neurons in the paraventricular nuclei of the hypothalamus, while intravenous injection lowered blood pressure through ATP-sensitive potassium channels in both normal and spontaneous hypertensive rats (Zhang et al., 2015). In congruence with these findings, intravenous injection of irisin lowered the blood pressure of spontaneously hypertensive rats (Fu et al., 2016). Irisin treatment increased nitric oxide production and phosphorylation of endothelial nitric oxide synthase (eNOS) in endothelial cells (Fu et al., 2016). The blood pressure-lowering effect of irisin was found to occur via the AMPK-AKT-eNOS-NO pathway (Fu et al., 2016). These data indicate that irisin plays a protective role in metabolic diseases.

In line with irisin's role in controlling metabolic diseases, Wagner and colleagues have previously reported the occurrence

of obesity phenotypes in mice genetically disrupted for ICAM-1 or αMβ2 (Dong et al., 1997). These findings indicate that some leukocyte integrins and ligands, or their adhesions, are involved in regulating metabolic diseases such as obesity. Thus, one cannot rule out the possibility that there is a functional connection to irisin and the other ligands that may contribute to the regulation of physiological imbalances.

CONCLUSION

Integrins on leukocytes and platelets have been validated in controlled clinical trials as therapeutic targets for inflammatory/autoimmune diseases and thrombotic diseases, respectively. In contrast, it has yet to be clinically established whether integrins on tumors and tumor vasculature could serve as therapeutic targets for cancer treatments. A better understanding of how integrins interact with, and signal through, novel ligands present on cancer and cancer stromal cells would help fill the critical knowledge gap currently hampering the development of clinically effective integrin-targeted cancer therapies.

AUTHOR CONTRIBUTIONS

EJP and MS contributed to the conceptualization, scope, and outline of this review. EJP, PKM, AI, MGA, SD, EK, and MS analyzed the referenced manuscripts in this manuscript and participated to preparing the manuscript. All authors read and approved the final version.

FUNDING

This work was supported by the JSPS KAKENHI Grants (EJP, 19K09392; AI, 19K18210; EK, 18K08917 and 19KK0224; and MS, 18H02622 and 19KK0196).

ACKNOWLEDGMENTS

We thank all of the other laboratory members for their technical assistance.

REFERENCES

Abdelhamid Fathy, M. (2017). Effect of chronic aerobic exercise training on serum irisin level in type 2 diabetic rats. *Al-Azhar Med. J.* 46, 919–938. doi: 10.12816/0045176

Albert, M. L., Pearce, S. F., Francisco, L. M., Sauter, B., Roy, P., Silverstein, R. L., et al. (1998). Immature dendritic cells phagocytose apoptotic cells via alphavbeta5 and CD36, and cross-present antigens to cytotoxic T lymphocytes. *J. Exp. Med.* 188, 1359–1368. doi: 10.1084/jem.188.7.1359

Al-Daghri, N. M., Alkharfy, K. M., Rahman, S., Amer, O. E., Vinodson, B., Sabico, S., et al. (2014). Irisin as a predictor of glucose metabolism in children: sexually dimorphic effects. *Eur. J. Clin. Invest.* 44, 119–124. doi: 10.1111/eci.12196

Alday-Parejo, B., Stupp, R., and Ruegg, C. (2019). Are integrins still practicable targets for anti-cancer therapy?. *Cancers* 11:978. doi: 10.3390/cancers11070978

Alon, R., Kassner, P. D., Carr, M. W., Finger, E. B., Hemler, M. E., and Springer, T. A. (1995). The integrin VLA-4 supports tethering and rolling in flow on VCAM-1. *J. Cell Biol.* 128, 1243–1253. doi: 10.1083/jcb.128.6.1243

Altay, D. U., Keha, E. E., Karaguzel, E., Mentese, A., Yaman, S. O., and Alver, A. (2018). The diagnostic value of FNDC5/irisin in renal cell cancer. *Int. Braz. J. Urol.* 44, 734–739. doi: 10.1590/s1677-5538.ibju.2017.0404

Aydin, S. (2014). Three new players in energy regulation: preptin, adropin and irisin. *Peptides* 56, 94–110. doi: 10.1016/j.peptides.2014.03.021

Aydin, S., Kuloglu, T., Aydin, S., Kalayci, M., Yilmaz, M., Cakmak, T., et al. (2014). A comprehensive immunohistochemical examination of the distribution of the fat-burning protein irisin in biological tissues. *Peptides* 61, 130–136. doi: 10.1016/j.peptides.2014.09.014

Aydin, S., Kuloglu, T., Ozercan, M. R., Albayrak, S., Aydin, S., Bakal, U., et al. (2016). Irisin immunohistochemistry in gastrointestinal system cancers. *Biotech. Histochem.* 91, 242–250. doi: 10.3109/10520295.2015.1136988

Baiula, M., Spampinato, S., Gentilucci, L., and Tolomelli, A. (2019). Novel ligands targeting alpha4beta1 integrin: therapeutic applications and perspectives. *Front. Chem.* 7:489. doi: 10.3389/fchem.2019.00489

Barczyk, M., Carracedo, S., and Gullberg, D. (2010). Integrins. *Cell Tissue Res.* 339, 269–280.

Benito-Jardon, M., Klapproth, S., Gimeno, L. I., Petzold, T., Bharadwaj, M., Muller, D. J., et al. (2017). The fibronectin synergy site re-enforces cell adhesion and mediates a crosstalk between integrin classes. *eLife* 6:e22264.

Berendt, A. R., Simmons, D. L., Tansey, J., Newbold, C. I., and Marsh, K. (1989). Intercellular adhesion molecule-1 is an endothelial cell adhesion receptor for Plasmodium falciparum. *Nature* 341, 57–59. doi: 10.1038/341057a0

Berlin, C., Bargatze, R. F., Von Andrian, U. H., Szabo, M. C., Hasslen, S. R., Nelson, R. D., et al. (1995). α4 integrins mediate lymphocyte attachment and rolling under physiologic flow. *Cell* 80, 413–422. doi: 10.1016/0092-8674(95)90491-3

Besse-Patin, A., Montastier, E., Vinel, C., Castan-Laurell, I., Louche, K., Dray, C., et al. (2014). Effect of endurance training on skeletal muscle myokine expression in obese men: identification of apelin as a novel myokine. *Int. J. Obes.* 38, 707–713. doi: 10.1038/ijo.2013.158

Bharadwaj, M., Strohmeyer, N., Colo, G. P., Helenius, J., Beerenwinkel, N., Schiller, H. B., et al. (2017). alphaV-class integrins exert dual roles on alpha5beta1 integrins to strengthen adhesion to fibronectin. *Nat. Commun.* 8:14348.

Bi, J., Zhang, J., Ren, Y., Du, Z., Li, T., Wang, T., et al. (2020a). Irisin reverses intestinal epithelial barrier dysfunction during intestinal injury via binding to the integrin alphaVbeta5 receptor. *J. Cell Mol. Med.* 24, 996–1009. doi: 10.1111/jcmm.14811

Bi, J., Zhang, J., Ren, Y., Du, Z., Zhang, Y., Liu, C., et al. (2020b). Exercise hormone irisin mitigates endothelial barrier dysfunction and microvascular leakage-related diseases. *JCI Insight* 5:e136277.

Biancheri, P., Giuffrida, P., Docena, G. H., Macdonald, T. T., Corazza, G. R., and Di Sabatino, A. (2014). The role of transforming growth factor (TGF)-beta in modulating the immune response and fibrogenesis in the gut. *Cytokine Growth. Factor. Rev.* 25, 45–55. doi: 10.1016/j.cytogfr.2013.11.001

Bianconi, D., Unseld, M., and Prager, G. W. (2016). Integrins in the spotlight of cancer. *Int. J. Mol. Sci.* 17:2037. doi: 10.3390/ijms17122037

Bonnans, C., Chou, J., and Werb, Z. (2014). Remodelling the extracellular matrix in development and disease. *Nat. Rev. Mol. Cell Biol.* 15, 786–801. doi: 10.1038/nrm3904

Bostrom, P., Wu, J., Jedrychowski, M. P., Korde, A., Ye, L., Lo, J. C., et al. (2012). A PGC1-alpha-dependent myokine that drives brown-fat-like development of white fat and thermogenesis. *Nature* 481, 463–468.

Brabletz, T., Kalluri, R., Nieto, M. A., and Weinberg, R. A. (2018). EMT in cancer. *Nat. Rev. Cancer* 18, 128–134.

Bretschneider, E., Uzonyi, B., Weber, A. A., Fischer, J. W., Pape, R., Lotzer, K., et al. (2007). Human vascular smooth muscle cells express functionally active endothelial cell protein C receptor. *Circ. Res.* 100, 255–262. doi: 10.1161/01.res.0000255685.06922.c7

Brooks, P. C., Clark, R. A., and Cheresh, D. A. (1994). Requirement of vascular integrin alpha v beta 3 for angiogenesis. *Science* 264, 569–571. doi: 10.1126/science.7512751

Cain, R. J., Vanhaesebroeck, B., and Ridley, A. J. (2010). The PI3K p110alpha isoform regulates endothelial adherens junctions via Pyk2 and Rac1. *J. Cell Biol.* 188, 863–876. doi: 10.1083/jcb.200907135

Calderwood, D. A. (2004). Integrin activation. *J. Cell Sci.* 117, 657–666.

Campbell, J. J., Hedrick, J., Zlotnik, A., Siani, M. A., Thompson, D. A., and Butcher, E. C. (1998). Chemokines and the arrest of lymphoyctes rolling under flow conditions. *Science* 279, 381–384. doi: 10.1126/science.279.5349.381

Carman, C. V., and Springer, T. A. (2003). Integrin avidity regulation: are changes in affinity and conformation underemphasized? *Curr. Opin. Cell Biol.* 15, 547–556. doi: 10.1016/j.ceb.2003.08.003

Chen, J., Yang, W., Kim, M., Carman, C. V., and Springer, T. A. (2006). Regulation of outside-in signaling and affinity by the beta2 I domain of integrin alphaLbeta2. *Proc. Natl. Acad. Sci. U.S.A.* 103, 13062–13067. doi: 10.1073/pnas.0605666103

Chen, Z., Ding, X., Jin, S., Pitt, B., Zhang, L., Billiar, T., et al. (2016). WISP1-alphavbeta3 integrin signaling positively regulates TLR-triggered inflammation response in sepsis induced lung injury. *Sci. Rep.* 6:28841.

Chen, Z., Wang, S., Chen, Y., Shao, Z., Yu, Z., Mei, S., et al. (2020). Integrin beta3 modulates TLR4-mediated inflammation by regulation of CD14 expression in macrophages in septic condition. *Shock* 53, 335–343. doi: 10.1097/shk.0000000000001383

Chesnutt, B. C., Smith, D. F., Raffler, N. A., Smith, M. L., White, E. J., and Ley, K. (2006). Induction of LFA-1-dependent neutrophil rolling on ICAM-1 by engagement of E-selectin. *Microcirculation* 13, 99–109. doi: 10.1080/10739680500466376

Chirathaworn, C., Kohlmeier, J. E., Tibbetts, S. A., Rumsey, L. M., Chan, M. A., and Benedict, S. H. (2002). Stimulation through intercellular adhesion molecule-1 provides a second signal for T cell activation. *J. Immunol.* 168, 5530–5537. doi: 10.4049/jimmunol.168.11.5530

Choi, Y. K., Kim, M. K., Bae, K. H., Seo, H. A., Jeong, J. Y., Lee, W. K., et al. (2013). Serum irisin levels in new-onset type 2 diabetes. *Diabetes Res. Clin. Pract.* 100, 96–101. doi: 10.1016/j.diabres.2013.01.007

Collins, C., and Nelson, W. J. (2015). Running with neighbors: coordinating cell migration and cell-cell adhesion. *Curr. Opin. Cell Biol.* 36, 62–70. doi: 10.1016/j.ceb.2015.07.004

Conroy, K. P., Kitto, L. J., and Henderson, N. C. (2016). alphav integrins: key regulators of tissue fibrosis. *Cell Tissue Res.* 365, 511–519. doi: 10.1007/s00441-016-2407-9

Cook-Mills, J. M., Marchese, M. E., and Abdala-Valencia, H. (2011). Vascular cell adhesion molecule-1 expression and signaling during disease: regulation by reactive oxygen species and antioxidants. *Antioxid. Redox. Signal.* 15, 1607–1638. doi: 10.1089/ars.2010.3522

Cox, E. A., and Huttenlocher, A. (1998). Regulation of integrin-mediated adhesion during cell migration. *Microsc. Res. Tech.* 43, 412–419. doi: 10.1002/(sici)1097-0029(19981201)43:5<412::aid-jemt7>3.0.co;2-f

Daskalopoulou, S. S., Cooke, A. B., Gomez, Y. H., Mutter, A. F., Filippaios, A., Mesfum, E. T., et al. (2014). Plasma irisin levels progressively increase in response to increasing exercise workloads in young, healthy, active subjects. *Eur. J. Endocrinol.* 171, 343–352. doi: 10.1530/eje-14-0204

Dong, Z. M., Gutierrez-Ramos, J. C., Coxon, A., Mayadas, T. N., and Wagner, D. D. (1997). A new class of obesity genes encodes leukocyte adhesion receptors. *Proc. Natl. Acad. Sci. U.S.A.* 94, 7526–7530. doi: 10.1073/pnas.94.14.7526

Drewlo, S., Johnson, E., Kilburn, B. A., Kadam, L., Armistead, B., and Kohan-Ghadr, H. R. (2020). Irisin induces trophoblast differentiation via AMPK activation in the human placenta. *J. Cell Physiol.* 235, 7146–7158. doi: 10.1002/jcp.29613

Estell, E. G., Le, P. T., Vegting, Y., Kim, H., Wrann, C., Bouxsein, M. L., et al. (2020). Irisin directly stimulates osteoclastogenesis and bone resorption in vitro and in vivo. *eLife* 9:e58172.

Feagan, B. G., Rutgeerts, P., Sands, B. E., Hanauer, S., Colombel, J. F., Sandborn, W. J., et al. (2013). Vedolizumab as induction and maintenance therapy for ulcerative colitis. *N. Engl. J. Med.* 369, 699–710.

Fernandes, N. R. J., Reilly, N. S., Schrock, D. C., Hocking, D. C., Oakes, P. W., and Fowell, D. J. (2020). CD4(+) T cell interstitial migration controlled by fibronectin in the inflamed skin. *Front. Immunol.* 11:1501. doi: 10.3389/fimmu.2020.01501

Ferrer-Martinez, A., Ruiz-Lozano, P., and Chien, K. R. (2002). Mouse PeP: a novel peroxisomal protein linked to myoblast differentiation and development. *Dev. Dyn.* 224, 154–167. doi: 10.1002/dvdy.10099

Fink, K., Busch, H. J., Bourgeois, N., Schwarz, M., Wolf, D., Zirlik, A., et al. (2013). Mac-1 directly binds to the endothelial protein C-receptor: a link between the protein C anticoagulant pathway and inflammation? *PLoS One* 8:e53103. doi: 10.1371/journal.pone.0053103

Folkman, J. (1986). How is blood vessel growth regulated in normal and neoplastic tissue? G.H.A. Clowes memorial Award lecture. *Cancer Res.* 46, 467–473.

Foubert, P., and Varner, J. A. (2012). Integrins in tumor angiogenesis and lymphangiogenesis. *Methods Mol. Biol.* 757, 471–486. doi: 10.1007/978-1-61779-166-6_27

Freedman, A. S., Munro, J. M., Rice, G. E., Bevilacqua, B. P., Morimoto, C., Mcintyre, B. W., et al. (1990). Adhesion of human B cells to germinal centers in vitro involves VLA-4 and INCAM-110. *Science* 249, 1030–1033. doi: 10.1126/science.1697696

Fu, J., Han, Y., Wang, J., Liu, Y., Zheng, S., Zhou, L., et al. (2016). Irisin lowers blood pressure by improvement of endothelial dysfunction via AMPK-Akt-eNOS-NO pathway in the spontaneously hypertensive rat. *J. Am. Heart Assoc.* 5:e003433.

Fukudome, K., and Esmon, C. T. (1994). Identification, cloning, and regulation of a novel endothelial cell protein C/activated protein C receptor. *J. Biol. Chem.* 269, 26486–26491.

Fukushima, Y., Kurose, S., Shinno, H., Cao Thi, Thu, H., Tamanoi, A., et al. (2016). Relationships between serum irisin levels and metabolic parameters in Japanese patients with obesity. *Obes. Sci. Pract.* 2, 203–209. doi: 10.1002/osp4.43

Fullar, A., Dudas, J., Olah, L., Hollosi, P., Papp, Z., Sobel, G., et al. (2015). Remodeling of extracellular matrix by normal and tumor-associated fibroblasts promotes cervical cancer progression. *BMC Cancer* 15:256. doi: 10.1186/s12885-015-1272-3

Gaggini, M., Cabiati, M., Del Turco, S., Navarra, T., De Simone, P., Filipponi, F., et al. (2017). Increased FNDC5/Irisin expression in human hepatocellular carcinoma. *Peptides* 88, 62–66. doi: 10.1016/j.peptides.2016.12.014

Gahmberg, C. G., Fagerholm, S. C., Nurmi, S. M., Chavakis, T., Marchesan, S., and Gronholm, M. (2009). Regulation of integrin activity and signalling. *Biochim. Biophys. Acta* 1790, 431–444.

Gamas, L., Matafome, P., and Seica, R. (2015). Irisin and myonectin regulation in the insulin resistant muscle: implications to adipose tissue: muscle crosstalk. *J. Diabetes Res.* 2015:359159.

Ganguly, K. K., Pal, S., Moulik, S., and Chatterjee, A. (2013). Integrins and metastasis. *Cell. Adh. Migr.* 7, 251–261.

Gannon, N. P., Vaughan, R. A., Garcia-Smith, R., Bisoffi, M., and Trujillo, K. A. (2015). Effects of the exercise-inducible myokine irisin on malignant and non-malignant breast epithelial cell behavior in vitro. *Int. J. Cancer* 136, E197–E202.

Geiger, B., Bershadsky, A., Pankov, R., and Yamada, K. M. (2001). Transmembrane crosstalk between the extracellular matrix–cytoskeleton crosstalk. *Nat. Rev. Mol. Cell Biol.* 2, 793–805. doi: 10.1038/35099066

Gholamnezhad, Z., Megarbane, B., and Rezaee, R. (2020). Molecular mechanisms mediating adaptation to exercise. *Adv. Exp. Med. Biol.* 1228, 45–61. doi: 10.1007/978-981-15-1792-1_3

Grayson, M. H., Van Der Vieren, M., Sterbinsky, S. A., Gallatin, W. M., Hoffman, P. A., Staunton, D. E., et al. (1998). αdβ2 integrin is expressed on human eosinophils and functions as an alternative ligand for vascular cell adhesion molecule 1 (VCAM-1). *J. Exp. Med.* 188, 2187–2191. doi: 10.1084/jem.188.11.2187

Greenlee-Wacker, M. C. (2016). Clearance of apoptotic neutrophils and resolution of inflammation. *Immunol. Rev.* 273, 357–370. doi: 10.1111/imr.12453

Gumbiner, B. M. (1996). Cell adhesion: the molecular basis of tissue architecture and morphogenesis. *Cell* 84, 345–357. doi: 10.1016/s0092-8674(00)81279-9

Guo, X., Xuan, X., Zhao, B., Wang, Y., Zhong, S., Su, Y., et al. (2020). Irisin in elderly people with hypertension, diabetes mellitus type 2, and overweight and obesity. *Int. J. Diabet. Dev. Countries* 40, 196–202. doi: 10.1007/s13410-019-00772-9

Hahm, E., Li, J., Kim, K., Huh, S., Rogelj, S., and Cho, J. (2013). Extracellular protein disulfide isomerase regulates ligand-binding activity of alphaMbeta2 integrin and neutrophil recruitment during vascular inflammation. *Blood* 121, 3789–3800. doi: 10.1182/blood-2012-11-467985

Hamaia, S. W., Luff, D., Hunter, E. J., Malcor, J. D., Bihan, D., Gullberg, D., et al. (2017). Unique charge-dependent constraint on collagen recognition by integrin alpha10beta1. *Matrix Biol.* 59, 80–94. doi: 10.1016/j.matbio.2016.08.010

Hamann, A., Andrew, D. P., Jablonski-Westrich, D., Holzmann, B., and Butcher, E. C. (1994). Role of alpha 4-integrins in lymphocyte homing to mucosal tissues in vivo. *J. Immunol.* 152, 3282–3293.

Hamidi, H., and Ivaska, J. (2018). Every step of the way: integrins in cancer progression and metastasis. *Nat. Rev. Cancer* 18, 533–548. doi: 10.1038/s41568-018-0038-z

Hanayama, R., Tanaka, M., Miwa, K., Shinohara, A., Iwamatsu, A., and Nagata, S. (2002). Identification of a factor that links apoptotic cells to phagocytes. *Nature* 417, 182–187. doi: 10.1038/417182a

Hecksteden, A., Wegmann, M., Steffen, A., Kraushaar, J., Morsch, A., Ruppenthal, S., et al. (2013). Irisin and exercise training in humans - results from a randomized controlled training trial. *BMC Med.* 11:235. doi: 10.1186/1741-7015-11-235

Herrera, J., Henke, C. A., and Bitterman, P. B. (2018). Extracellular matrix as a driver of progressive fibrosis. *J. Clin. Invest.* 128, 45–53. doi: 10.1172/jci93557

Herter, J., and Zarbock, A. (2013). Integrin regulation during leukocyte recruitment. *J. Immunol.* 190, 4451–4457. doi: 10.4049/jimmunol.1203179

Horwitz, A. R. (2012). The origins of the molecular era of adhesion research. *Nat. Rev. Mol. Cell Biol.* 13, 805–811. doi: 10.1038/nrm3473

Hoshino, A., Costa-Silva, B., Shen, T. L., Rodrigues, G., Hashimoto, A., Tesic Mark, M., et al. (2015). Tumour exosome integrins determine organotropic metastasis. *Nature* 527, 329–335. doi: 10.1038/nature15756

Hosotani, R., Kawaguchi, M., Masui, T., Koshiba, T., Ida, J., Fujimoto, K., et al. (2002). Expression of integrin alphaVbeta3 in pancreatic carcinoma: relation to MMP-2 activation and lymph node metastasis. *Pancreas* 25, e30–e35.

Huang, C. W., Chang, Y. H., Lee, H. H., Wu, J. Y., Huang, J. X., Chung, Y. H., et al. (2020). Irisin, an exercise myokine, potently suppresses tumor proliferation, invasion, and growth in glioma. *FASEB J.* 34, 9678–9693. doi: 10.1096/fj.202000573rr

Humphries, J. D., Byron, A., and Humphries, M. J. (2006). Integrin ligands at a glance. *J. Cell Sci.* 119, 3901–3903. doi: 10.1242/jcs.03098

Iba, T., Aihara, K., Watanabe, S., Yanagawa, Y., Takemoto, M., Yamada, A., et al. (2013). Recombinant thrombomodulin improves the visceral microcirculation by attenuating the leukocyte-endothelial interaction in a rat LPS model. *Thromb. Res.* 131, 295–299. doi: 10.1016/j.thromres.2012.11.025

Jedrychowski, M. P., Wrann, C. D., Paulo, J. A., Gerber, K. K., Szpyt, J., Robinson, M. M., et al. (2015). Detection and quantitation of circulating human irisin by tandem mass spectrometry. *Cell. Metab.* 22, 734–740. doi: 10.1016/j.cmet.2015.08.001

Jessen, N., and Goodyear, L. J. (2005). Contraction signaling to glucose transport in skeletal muscle. *J. Appl. Physiol.* 99, 330–337. doi: 10.1152/japplphysiol.00175.2005

Johansson, S., Svineng, G., Wennerberg, K., Armulik, A., and Lohikangas, L. (1997). Fibronectin-integrin interactions. *Front. Biosci.* 2, d126–d146. doi: 10.2741/a178

Kaido, T., Perez, B., Yebra, M., Hill, J., Cirulli, V., Hayek, A., et al. (2004). Alphav-integrin utilization in human beta-cell adhesion, spreading, and motility. *J. Biol. Chem.* 279, 17731–17737. doi: 10.1074/jbc.m308425200

Kawamoto, E., Nago, N., Okamoto, T., Gaowa, A., Masui-Ito, A., Sakakura, Y., et al. (2019). Anti-adhesive effects of human soluble thrombomodulin and its domains. *Biochem. Biophys. Res. Commun.* 511, 312–317. doi: 10.1016/j.bbrc.2019.02.041

Kawamoto, E., Okamoto, T., Takagi, Y., Honda, G., Suzuki, K., Imai, H., et al. (2016). LFA-1 and Mac-1 integrins bind to the serine/threonine-rich domain of thrombomodulin. *Biochem. Biophys. Res. Commun.* 473, 1005–1012. doi: 10.1016/j.bbrc.2016.04.007

Kechagia, J. Z., Ivaska, J., and Roca-Cusachs, P. (2019). Integrins as biomechanical sensors of the microenvironment. *Nat. Rev. Mol. Cell Biol.* 20, 457–473. doi: 10.1038/s41580-019-0134-2

Kim, H., Wrann, C. D., Jedrychowski, M., Vidoni, S., Kitase, Y., Nagano, K., et al. (2018). Irisin mediates effects on bone and fat via alphaV integrin receptors. *Cell* 175, 1756.e17–1768.e17.

Kim, M., Carman, C. V., and Springer, T. A. (2003). Bidirectional transmembrane signaling by cytoplasmic domain separation in integrins. *Science* 301, 1720–1725. doi: 10.1126/science.1084174

Kim, Y., Kugler, M. C., Wei, Y., Kim, K. K., Li, X., Brumwell, A. N., et al. (2009). Integrin alpha3beta1-dependent beta-catenin phosphorylation links epithelial Smad signaling to cell contacts. *J. Cell Biol.* 184, 309–322. doi: 10.1083/jcb.200806067

Koistinen, P., and Heino, J. (2002). The selective regulation of alpha Vbeta 1 integrin expression is based on the hierarchical formation of alpha V-containing heterodimers. *J. Biol. Chem.* 277, 24835–24841. doi: 10.1074/jbc.m203149200

Kong, G., Jiang, Y., Sun, X., Cao, Z., Zhang, G., Zhao, Z., et al. (2017). Irisin reverses the IL-6 induced epithelial-mesenchymal transition in osteosarcoma cell migration and invasion through the STAT3/Snail signaling pathway. *Oncol. Rep.* 38, 2647–2656. doi: 10.3892/or.2017.5973

Kraal, G., Schornagel, K., Streeter, P. R., Holzmann, B., and Butcher, E. C. (1995). Expression of the mucosal vascular addressin, MAdCAM-1, on sinus-lining cells in the spleen. *Am. J. Pathol.* 147, 763–771.

Kurdiova, T., Balaz, M., Vician, M., Maderova, D., Vlcek, M., Valkovic, L., et al. (2014). Effects of obesity, diabetes and exercise on Fndc5 gene expression and irisin release in human skeletal muscle and adipose tissue: in vivo and in vitro studies. *J. Physiol.* 592, 1091–1107. doi: 10.1113/jphysiol.2013.264655

Kurosawa, S., Esmon, C. T., and Stearns-Kurosawa, D. J. (2000). The soluble endothelial protein C receptor binds to activated neutrophils: involvement of proteinase-3 and CD11b/CD18. *J. Immunol.* 165, 4697–4703. doi: 10.4049/jimmunol.165.8.4697

Kurosawa, S., Stearns-Kurosawa, D. J., Carson, C. W., D'angelo, A., Della Valle, P., and Esmon, C. T. (1998). Plasma levels of endothelial cell protein C receptor are elevated in patients with sepsis and systemic lupus erythematosus: lack of correlation with thrombomodulin suggests involvement of different pathological processes. *Blood* 91, 725–727. doi: 10.1182/blood.v91.2.725

Lacy-Hulbert, A., Smith, A. M., Tissire, H., Barry, M., Crowley, D., Bronson, R. T., et al. (2007). Ulcerative colitis and autoimmunity induced by loss of myeloid alphav integrins. *Proc. Natl. Acad. Sci. U.S.A.* 104, 15823–15828. doi: 10.1073/pnas.0707421104

Langholz, O., Rockel, D., Mauch, C., Kozlowska, E., Bank, I., Krieg, T., et al. (1995). Collagen and collagenase gene expression in three-dimensional collagen lattices are differentially regulated by alpha 1 beta 1 and alpha 2 beta 1 integrins. *J. Cell Biol.* 131, 1903–1915. doi: 10.1083/jcb.131.6.1903

Lawrence, M. B., Berg, E. L., Butcher, E. C., and Springer, T. A. (1995). Rolling of lymphocytes and neutrophils on peripheral node addressin and subsequent arrest on ICAM-1 in shear flow. *Eur. J. Immunol.* 25, 1025–1031. doi: 10.1002/eji.1830250425

Lecker, S. H., Zavin, A., Cao, P., Arena, R., Allsup, K., Daniels, K. M., et al. (2012). Expression of the irisin precursor FNDC5 in skeletal muscle correlates with aerobic exercise performance in patients with heart failure. *Circ. Heart Fail.* 5, 812–818. doi: 10.1161/circheartfailure.112.969543

Lefkovits, J., Plow, E. F., and Topol, E. J. (1995). Platelet glycoprotein IIb/IIIa receptors in cardiovascular medicine. *N. Engl. J. Med.* 332, 1553–1559.

Leone, D. P., Relvas, J. B., Campos, L. S., Hemmi, S., Brakebusch, C., Fassler, R., et al. (2005). Regulation of neural progenitor proliferation and survival by beta1 integrins. *J. Cell Sci.* 118, 2589–2599. doi: 10.1242/jcs.02396

Levental, K. R., Yu, H., Kass, L., Lakins, J. N., Egeblad, M., Erler, J. T., et al. (2009). Matrix crosslinking forces tumor progression by enhancing integrin signaling. *Cell* 139, 891–906. doi: 10.1016/j.cell.2009.10.027

Ley, K., Laudanna, C., Cybulsky, M. I., and Nourshargh, S. (2007). Getting to the site of inflammation: the leukocyte adhesion cascade updated. *Nat. Rev. Immunol.* 7, 678–689. doi: 10.1038/nri2156

Li, C., Zhou, L., Xie, Y., Guan, C., and Gao, H. (2019). Effect of irisin on endometrial receptivity of rats with polycystic ovary syndrome. *Gynecol. Endocrinol.* 35, 395–400. doi: 10.1080/09513590.2018.1529158

Li, X., Abdi, K., Rawn, J., Mackay, C. R., and Mentzer, S. J. (1996). LFA-1 and L-selectin regulation of recirculating lymphocyte tethering and rolling on lung microvascular endothelium. *Am. J. Respir. Cell Mol. Biol.* 14, 398–406. doi: 10.1165/ajrcmb.14.4.8600945

Lira, V. A., Benton, C. R., Yan, Z., and Bonen, A. (2010). PGC-1alpha regulation by exercise training and its influences on muscle function and insulin sensitivity. *Am. J. Physiol. Endocrinol. Metab.* 299, E145–E161.

Liu, J., Huang, Y., Liu, Y., and Chen, Y. (2019). Irisin enhances doxorubicin-induced cell apoptosis in pancreatic cancer by inhibiting the PI3K/AKT/NF-kappaB pathway. *Med. Sci. Monit.* 25, 6085–6096. doi: 10.12659/msm.917625

Liu, J., Song, N., Huang, Y., and Chen, Y. (2018). Irisin inhibits pancreatic cancer cell growth via the AMPK-mTOR pathway. *Sci. Rep.* 8:15247.

Liu, J. J., Wong, M. D., Toy, W. C., Tan, C. S., Liu, S., Ng, X. W., et al. (2013). Lower circulating irisin is associated with type 2 diabetes mellitus. *J. Diabetes Complications* 27, 365–369. doi: 10.1016/j.jdiacomp.2013.03.002

Liu, Z., Wang, F., and Chen, X. (2008). Integrin alpha(v)beta(3)-targeted cancer therapy. *Drug Dev. Res.* 69, 329–339.

Livshits, G., Kobielak, A., and Fuchs, E. (2012). Governing epidermal homeostasis by coupling cell-cell adhesion to integrin and growth factor signaling, proliferation, and apoptosis. *Proc. Natl. Acad. Sci. U.S.A.* 109, 4886–4891. doi: 10.1073/pnas.1202120109

Loffler, D., Muller, U., Scheuermann, K., Friebe, D., Gesing, J., Bielitz, J., et al. (2015). Serum irisin levels are regulated by acute strenuous exercise. *J. Clin. Endocrinol. Metab.* 100, 1289–1299. doi: 10.1210/jc.2014-2932

Lourenco, M. V., Frozza, R. L., De Freitas, G. B., Zhang, H., Kincheski, G. C., Ribeiro, F. C., et al. (2019). Exercise-linked FNDC5/irisin rescues synaptic plasticity and memory defects in Alzheimer's models. *Nat. Med.* 25, 165–175. doi: 10.1038/s41591-018-0275-4

Lu, X., Lu, D., Scully, M. F., and Kakkar, V. V. (2008). The role of integrin-mediated cell adhesion in atherosclerosis: pathophysiology and clinical opportunities. *Curr. Pharm. Des.* 14, 2140–2158. doi: 10.2174/138161208785740199

Luo, B. H., Carman, C. V., and Springer, T. A. (2007). Structural basis of integrin regulation and signaling. *Annu. Rev. Immunol.* 25, 619–647. doi: 10.1146/annurev.immunol.25.022106.141618

Makgoba, M. W., Sanders, M. E., Luce, G. E. G., Dustin, M. L., Springer, T. A., Clark, E. A., et al. (1988). ICAM-1 a ligand for LFA-1 dependent adhesion of B, T and myeloid cell. *Nature* 331, 86–88. doi: 10.1038/331086a0

Marti-Carvajal, A. J., Sola, I., Gluud, C., Lathyris, D., and Cardona, A. F. (2012). Human recombinant protein C for severe sepsis and septic shock in adult and paediatric patients. *Cochrane Database. Syst. Rev.* 12:CD004388.

Martin, F. A., Murphy, R. P., and Cummins, P. M. (2013). Thrombomodulin and the vascular endothelium: insights into functional, regulatory, and therapeutic aspects. *Am. J. Physiol. Heart Circ. Physiol.* 304, H1585–H1597.

Martinez Munoz, I. Y., Camarillo Romero, E. D. S., and Garduno Garcia, J. J. (2018). Irisin a novel metabolic biomarker: present knowledge and future directions. *Int. J. Endocrinol.* 2018:7816806.

Mazur-Bialy, A. I., Pochec, E., and Zarawski, M. (2017). Anti-inflammatory properties of irisin, mediator of physical activity, are connected with TLR4/MyD88 signaling pathway activation. *Int. J. Mol. Sci.* 18:701. doi: 10.3390/ijms18040701

McDonald, S. A., Palmen, M. J., Van Rees, E. P., and Macdonald, T. T. (1997). Characterization of the mucosal cell-mediated immune response in IL-2 knockout mice before and after the onset of colitis. *Immunology* 91, 73–80. doi: 10.1046/j.1365-2567.1997.00217.x

McMillen, P., and Holley, S. A. (2015). Integration of cell-cell and cell-ECM adhesion in vertebrate morphogenesis. *Curr. Opin. Cell Biol.* 36, 48–53. doi: 10.1016/j.ceb.2015.07.002

Meredith, J. E. Jr., Fazeli, B., and Schwartz, M. A. (1993). The extracellular matrix as a cell survival factor. *Mol. Biol. Cell* 4, 953–961. doi: 10.1091/mbc.4.9.953

Moon, H. S., Dincer, F., and Mantzoros, C. S. (2013). Pharmacological concentrations of irisin increase cell proliferation without influencing markers of neurite outgrowth and synaptogenesis in mouse H19-7 hippocampal cell lines. *Metabolism* 62, 1131–1136. doi: 10.1016/j.metabol.2013.04.007

Moon, H. S., and Mantzoros, C. S. (2014). Regulation of cell proliferation and malignant potential by irisin in endometrial, colon, thyroid and esophageal cancer cell lines. *Metabolism* 63, 188–193. doi: 10.1016/j.metabol.2013.10.005

Moreno-Navarrete, J. M., Ortega, F., Serrano, M., Guerra, E., Pardo, G., Tinahones, F., et al. (2013). Irisin is expressed and produced by human muscle and adipose tissue in association with obesity and insulin resistance. *J. Clin. Endocrinol. Metab.* 98, E769–E778.

Morgan, M. M., Labno, C. M., Van Seventer, G. A., Denny, M. F., Straus, D. B., and Burkhardt, J. K. (2001). Superantigen-induced T cell:B cell conjugation is mediated by LFA-1 and requires signaling through Lck, but not ZAP-70. *J. Immunol.* 167, 5708–5718. doi: 10.4049/jimmunol.167.10.5708

Morrison, V. L., Uotila, L. M., Llort Asens, M., Savinko, T., and Fagerholm, S. C. (2015). Optimal T cell activation and B cell antibody responses in vivo require the interaction between leukocyte function-associated antigen-1 and Kindlin-3. *J. Immunol.* 195, 105–115. doi: 10.4049/jimmunol.1402741

Morton, L. F., Hargreaves, P. G., Farndale, R. W., Young, R. D., and Barnes, M. J. (1995). Integrin alpha 2 beta 1-independent activation of platelets by simple collagen-like peptides: collagen tertiary (triple-helical) and quaternary (polymeric) structures are sufficient alone for alpha 2 beta 1-independent platelet reactivity. *Biochem. J.* 306(Pt 2), 337–344. doi: 10.1042/bj3060337

Mu, J., Brozinick, J. T. Jr., Valladares, O., Bucan, M., and Birnbaum, M. J. (2001). A role for AMP-activated protein kinase in contraction- and hypoxia-regulated glucose transport in skeletal muscle. *Mol. Cell.* 7, 1085–1094. doi: 10.1016/s1097-2765(01)00251-9

Muller, N. (2019). The role of intercellular adhesion molecule-1 in the pathogenesis of psychiatric disorders. *Front. Pharmacol.* 10:1251. doi: 10.3389/fphar.2019.01251

Myint, P. K., Park, E. J., Gaowa, A., Kawamoto, E., and Shimaoka, M. (2020). Targeted remodeling of breast cancer and immune cell homing niches by exosomal integrins. *Diagn. Pathol.* 15:38.

Nakache, M., Berg, E. L., Streeter, P. R., and Butcher, E. C. (1989). The mucosal vascular addressin is a tissue-specific endothelial cell adhesion molecule for circulating lymphocytes. *Nature* 337, 179–181. doi: 10.1038/337179a0

Nieberler, M., Reuning, U., Reichart, F., Notni, J., Wester, H. J., Schwaiger, M., et al. (2017). Exploring the role of RGD-recognizing integrins in cancer. *Cancers* 9:116. doi: 10.3390/cancers9090116

Noda, Y., Kuzuya, A., Tanigawa, K., Araki, M., Kawai, R., Ma, B., et al. (2018). Fibronectin type III domain-containing protein 5 interacts with APP and decreases amyloid beta production in Alzheimer's disease. *Mol. Brain* 11:61.

Oguri, Y., Shinoda, K., Kim, H., Alba, D. L., Bolus, W. R., Wang, Q., et al. (2020). CD81 controls beige fat progenitor cell growth and energy balance via FAK signaling. *Cell* 182, 563.e20–577.e20.

Okamoto, T., Tanigami, H., Suzuki, K., and Shimaoka, M. (2012). Thrombomodulin: a bifunctional modulator of inflammation and coagulation in sepsis. *Crit. Care Res. Pract.* 2012:614545.

Ortega-Gomez, A., Perretti, M., and Soehnlein, O. (2013). Resolution of inflammation: an integrated view. *EMBO Mol. Med.* 5, 661–674. doi: 10.1002/emmm.201202382

Overstreet, M. G., Gaylo, A., Angermann, B. R., Hughson, A., Hyun, Y. M., Lambert, K., et al. (2013). Inflammation-induced interstitial migration of effector CD4(+) T cells is dependent on integrin alphaV. *Nat. Immunol.* 14, 949–958. doi: 10.1038/ni.2682

Paidassi, H., Acharya, M., Zhang, A., Mukhopadhyay, S., Kwon, M., Chow, C., et al. (2011). Preferential expression of integrin alphavbeta8 promotes generation of regulatory T cells by mouse CD103+ dendritic cells. *Gastroenterology* 141, 1813–1820. doi: 10.1053/j.gastro.2011.06.076

Pardo, M., Crujeiras, A. B., Amil, M., Aguera, Z., Jimenez-Murcia, S., Banos, R., et al. (2014). Association of irisin with fat mass, resting energy expenditure, and daily activity in conditions of extreme body mass index. *Int. J. Endocrinol.* 2014:857270.

Pedchenko, V., Zent, R., and Hudson, B. G. (2004). Alpha(v)beta3 and alpha(v)beta5 integrins bind both the proximal RGD site and non-RGD motifs within noncollagenous (NC1) domain of the alpha3 chain of type IV collagen: implication for the mechanism of endothelia cell adhesion. *J. Biol. Chem.* 279, 2772–2780. doi: 10.1074/jbc.m311901200

Peyrin-Biroulet, L., Danese, S., Argollo, M., Pouillon, L., Peppas, S., Gonzalez-Lorenzo, M., et al. (2019). Loss of response to vedolizumab and ability of dose intensification to restore response in patients with crohn's disease or ulcerative colitis: a systematic review and meta-analysis. *Clin. Gastroenterol. Hepatol.* 17, 838.e2–846.e2.

Phillipson, M., Heit, B., Colarusso, P., Liu, L., Ballantyne, C. M., and Kubes, P. (2006). Intraluminal crawling of neutrophils to emigration sites: a molecularly distinct process from adhesion in the recruitment cascade. *J. Exp. Med.* 203, 2569–2575. doi: 10.1084/jem.20060925

Piali, L., Hammel, P., Uherek, C., Bachmann, F., Gisler, R. H., Dunon, D., et al. (1995). CD31/PECAM-1 is a ligand for αvβ3 integrin involved in adhesion of leukocytes to endothelium. *J. Cell Biol.* 130, 451–460. doi: 10.1083/jcb.130.2.451

Plosa, E. J., Benjamin, J. T., Sucre, J. M., Gulleman, P. M., Gleaves, L. A., Han, W., et al. (2020). Beta1 Integrin regulates adult lung alveolar epithelial cell inflammation. *JCI Insight* 5:e129259.

Provatopoulou, X., Georgiou, G. P., Kalogera, E., Kalles, V., Matiatou, M. A., Papapanagiotou, I., et al. (2015). Serum irisin levels are lower in patients with breast cancer: association with disease diagnosis and tumor characteristics. *BMC Cancer* 15:898. doi: 10.1186/s12885-015-1898-1

Rivera-Nieves, J., Olson, T., Bamias, G., Bruce, A., Solga, M., Knight, R. F., et al. (2005). L-selectin, alpha 4 beta 1, and alpha 4 beta 7 integrins participate in CD4+ T cell recruitment to chronically inflamed small intestine. *J. Immunol.* 174, 2343–2352. doi: 10.4049/jimmunol.174.4.2343

Ross, E. A., Douglas, M. R., Wong, S. H., Ross, E. J., Curnow, S. J., Nash, G. B., et al. (2006). Interaction between integrin alpha9beta1 and vascular cell adhesion molecule-1 (VCAM-1) inhibits neutrophil apoptosis. *Blood* 107, 1178–1183. doi: 10.1182/blood-2005-07-2692

Sahin-Efe, A., Upadhyay, J., Ko, B. J., Dincer, F., Park, K. H., Migdal, A., et al. (2018). Irisin and leptin concentrations in relation to obesity, and developing type 2 diabetes: a cross sectional and a prospective case-control study nested in the normative aging study. *Metabolism* 79, 24–32. doi: 10.1016/j.metabol.2017.10.011

Sandborn, W. J., Feagan, B. G., Rutgeerts, P., Hanauer, S., Colombel, J. F., Sands, B. E., et al. (2013). Vedolizumab as induction and maintenance therapy for Crohn's disease. *N. Engl. J. Med.* 369, 711–721.

Schenkel, A. R., Mamdouh, Z., and Muller, W. A. (2004). Locomotion of monocytes on endothelium is a critical step during extravasation. *Nat. Immunol.* 5, 393–400. doi: 10.1038/ni1051

Schon, M. P., Arya, A., Murphy, E. A., Adams, C. M., Strauch, U. G., Agace, W. W., et al. (1999). Mucosal T lymphocyte numbers are selectively reduced in integrin αE (CD103)-deficient mice. *J. Immunol.* 162, 6641–6649.

Schumacher, M. A., Chinnam, N., Ohashi, T., Shah, R. S., and Erickson, H. P. (2013). The structure of irisin reveals a novel intersubunit beta-sheet fibronectin type III (FNIII) dimer: implications for receptor activation. *J. Biol. Chem.* 288, 33738–33744. doi: 10.1074/jbc.m113.516641

Schwarzbauer, J. E., and Desimone, D. W. (2011). Fibronectins, their fibrillogenesis, and in vivo functions. *Cold Spring Harb. Perspect. Biol.* 3:a005041. doi: 10.1101/cshperspect.a005041

Sciurba, J. C., Gieseck, R. L., Jiwrajka, N., White, S. D., Karmele, E. P., Redes, J., et al. (2019). Fibroblast-specific integrin-alpha V differentially regulates type 17 and type 2 driven inflammation and fibrosis. *J. Pathol.* 248, 16–29. doi: 10.1002/path.5215

Shan, T., Liang, X., Bi, P., and Kuang, S. (2013). Myostatin knockout drives browning of white adipose tissue through activating the AMPK-PGC1alpha-Fndc5 pathway in muscle. *FASEB J.* 27, 1981–1989. doi: 10.1096/fj.12-225755

Shao, L., Li, H., Chen, J., Song, H., Zhang, Y., Wu, F., et al. (2017). Irisin suppresses the migration, proliferation, and invasion of lung cancer cells via inhibition of epithelial-to-mesenchymal transition. *Biochem. Biophys. Res. Commun.* 485, 598–605. doi: 10.1016/j.bbrc.2016.12.084

Shaw, S. K., Ma, S., Kim, M. B., Rao, R. M., Hartman, C. U., Froio, R. M., et al. (2004). Coordinated redistribution of leukocyte LFA-1 and endothelial cell ICAM-1 accompany neutrophil transmigration. *J. Exp. Med.* 200, 1571–1580. doi: 10.1084/jem.20040965

Shi, G., Tang, N., Qiu, J., Zhang, D., Huang, F., Cheng, Y., et al. (2017). Irisin stimulates cell proliferation and invasion by targeting the PI3K/AKT pathway in human hepatocellular carcinoma. *Biochem. Biophys. Res. Commun.* 493, 585–591. doi: 10.1016/j.bbrc.2017.08.148

Shimaoka, M., Kawamoto, E., Gaowa, A., Okamoto, T., and Park, E. J. (2019). Connexins and integrins in exosomes. *Cancers* 11:106. doi: 10.3390/cancers11010106

Shimaoka, M., Takagi, J., and Springer, T. A. (2002). Conformational regulation of integrin structure and function. *Annu. Rev. Biophys. Biomol. Struct.* 31, 485–516. doi: 10.1146/annurev.biophys.31.101101.140922

Shulman, Z., Shinder, V., Klein, E., Grabovsky, V., Yeger, O., Geron, E., et al. (2009). Lymphocyte crawling and transendothelial migration require chemokine triggering of high-affinity LFA-1 integrin. *Immunity* 30, 384–396. doi: 10.1016/j.immuni.2008.12.020

Springer, T. A., and Dustin, M. L. (2012). Integrin inside-out signaling and the immunological synapse. *Curr. Opin. Cell Biol.* 24, 107–115. doi: 10.1016/j.ceb.2011.10.004

Subramanian, P., Mitroulis, I., Hajishengallis, G., and Chavakis, T. (2016). Regulation of tissue infiltration by neutrophils: role of integrin alpha3beta1 and other factors. *Curr. Opin. Hematol.* 23, 36–43. doi: 10.1097/moh.0000000000000198

Sumagin, R., Prizant, H., Lomakina, E., Waugh, R. E., and Sarelius, I. H. (2010). LFA-1 and Mac-1 define characteristically different intralumenal crawling and emigration patterns for monocytes and neutrophils in situ. *J. Immunol.* 185, 7057–7066. doi: 10.4049/jimmunol.1001638

Sun, H., Kuk, W., Rivera-Nieves, J., Lopez-Ramirez, M. A., Eckmann, L., and Ginsberg, M. H. (2020). beta7 integrin inhibition can increase intestinal inflammation by impairing homing of CD25(hi)FoxP3(+) regulatory T cells. *Cell. Mol. Gastroenterol. Hepatol.* 9, 369–385. doi: 10.1016/j.jcmgh.2019.10.012

Takada, Y., Ye, X., and Simon, S. (2007). The integrins. *Genome Biol.* 8:215.

Takagi, J., Petre, B. M., Walz, T., and Springer, T. A. (2002). Global conformational rearrangements in integrin extracellular domains in outside-in and inside-out signaling. *Cell* 110, 599–611. doi: 10.1016/s0092-8674(02)00935-2

Takayama, S., Ishii, S., Ikeda, T., Masamura, S., Doi, M., and Kitajima, M. (2005). The relationship between bone metastasis from human breast cancer and integrin alpha(v)beta3 expression. *Anticancer. Res.* 25, 79–83.

Teleanu, R. I., Chircov, C., Grumezescu, A. M., and Teleanu, D. M. (2019). Tumor angiogenesis and anti-angiogenic strategies for cancer treatment. *J. Clin. Med.* 9:84. doi: 10.3390/jcm9010084

Teufel, A., Malik, N., Mukhopadhyay, M., and Westphal, H. (2002). Frcp1 and Frcp2, two novel fibronectin type III repeat containing genes. *Gene* 297, 79–83. doi: 10.1016/s0378-1119(02)00828-4

Travis, M. A., Reizis, B., Melton, A. C., Masteller, E., Tang, Q., Proctor, J. M., et al. (2007). Loss of integrin alpha(v)beta8 on dendritic cells causes autoimmunity and colitis in mice. *Nature* 449, 361–365. doi: 10.1038/nature06110

Travis, M. A., and Sheppard, D. (2014). TGF-beta activation and function in immunity. *Annu. Rev. Immunol.* 32, 51–82. doi: 10.1146/annurev-immunol-032713-120257

Tseng, A., Kim, K., Li, J., and Cho, J. (2018). Myeloperoxidase negatively regulates neutrophil-endothelial cell interactions by impairing αMβ2 integrin function in sterile inflammation. *Front Med. (Lausanne)* 5:134. doi: 10.3389/fmed.2018.00134

Tsuchiya, Y., Ando, D., Goto, K., Kiuchi, M., Yamakita, M., and Koyama, K. (2014). High-intensity exercise causes greater irisin response compared with low-intensity exercise under similar energy consumption. *Tohoku J. Exp. Med.* 233, 135–140. doi: 10.1620/tjem.233.135

Tsuchiya, Y., Ando, D., Takamatsu, K., and Goto, K. (2015). Resistance exercise induces a greater irisin response than endurance exercise. *Metabolism* 64, 1042–1050. doi: 10.1016/j.metabol.2015.05.010

Van Der Flier, A., and Sonnenberg, A. (2001). Function and interactions of integrins. *Cell Tissue Res.* 305, 285–298.

Van Der Vieren, M., Trong, H. L., Wood, C. L., Moore, P. F., St. John, T., Staunton, D. E., et al. (1995). A novel leukointegrin, αdβ2, binds preferentially to ICAM-3. *Immunity* 3, 683–690. doi: 10.1016/1074-7613(95)90058-6

Van Seventer, G. A., Shimizu, Y., Horgan, K. J., and Shaw, S. (1990). The LFA-1 ligand ICAM-1 provides an important costimulatory signal for T cell receptor-mediated activation of resting T cells. *J. Immunol.* 144, 4579–4586.

Vivanco, I., and Sawyers, C. L. (2002). The phosphatidylinositol 3-Kinase AKT pathway in human cancer. *Nat. Rev. Cancer* 2, 489–501. doi: 10.1038/nrc839

Vleminckx, K., and Kemler, R. (1999). Cadherins and tissue formation: integrating adhesion and signaling. *Bioessays* 21, 211–220. doi: 10.1002/(sici)1521-1878(199903)21:3<211::aid-bies5>3.0.co;2-p

Walling, B. L., and Kim, M. (2018). LFA-1 in T cell migration and differentiation. *Front. Immunol.* 9:952. doi: 10.3389/fimmu.2018.00952

Wang, Q., Onuma, K., Liu, C., Wong, H., Bloom, M. S., Elliott, E. E., et al. (2019). Dysregulated integrin alphaVbeta3 and CD47 signaling promotes joint inflammation, cartilage breakdown, and progression of osteoarthritis. *JCI Insight* 4:e128616.

Weis, S. M., and Cheresh, D. A. (2011). alphaV integrins in angiogenesis and cancer. *Cold Spring Harb. Perspect. Med.* 1:a006478.

Wernimont, S. A., Wiemer, A. J., Bennin, D. A., Monkley, S. J., Ludwig, T., Critchley, D. R., et al. (2011). Contact-dependent T cell activation and T cell stopping require talin1. *J. Immunol.* 187, 6256–6267. doi: 10.4049/jimmunol.1102028

Wessel, F., Winderlich, M., Holm, M., Frye, M., Rivera-Galdos, R., Vockel, M., et al. (2014). Leukocyte extravasation and vascular permeability are each controlled in vivo by different tyrosine residues of VE-cadherin. *Nat. Immunol.* 15, 223–230. doi: 10.1038/ni.2824

Whittard, J. D., Craig, S. E., Mould, A. P., Koch, A., Pertz, O., Engel, J., et al. (2002). E-cadherin is a ligand for integrin α2β1. *Matrix Biol.* 21, 525–532. doi: 10.1016/s0945-053x(02)00037-9

Wick, W., Platten, M., Wick, A., Hertenstein, A., Radbruch, A., Bendszus, M., et al. (2016). Current status and future directions of anti-angiogenic therapy for gliomas. *Neuro Oncol.* 18, 315–328. doi: 10.1093/neuonc/nov180

Williams, M. R., Azcutia, V., Newton, G., Alcaide, P., and Luscinskas, F. W. (2011). Emerging mechanisms of neutrophil recruitment across endothelium. *Trends Immunol.* 32, 461–469. doi: 10.1016/j.it.2011.06.009

Wrann, C. D., White, J. P., Salogiannnis, J., Laznik-Bogoslavski, D., Wu, J., Ma, D., et al. (2013). Exercise induces hippocampal BDNF through a PGC-1alpha/FNDC5 pathway. *Cell Metab.* 18, 649–659. doi: 10.1016/j.cmet.2013.09.008

Wu, F., Song, H., Zhang, Y., Zhang, Y., Mu, Q., Jiang, M., et al. (2015). Irisin induces angiogenesis in human umbilical vein endothelial cells in vitro and in zebrafish embryos in vivo via activation of the ERK signaling pathway. *PLoS One* 10:e0134662. doi: 10.1371/journal.pone.0134662

Xie, C., Zhang, Y., Tran, T. D., Wang, H., Li, S., George, E. V., et al. (2015). Irisin controls growth, intracellular Ca2+ signals, and mitochondrial thermogenesis in cardiomyoblasts. *PLoS One* 10:e0136816. doi: 10.1371/journal.pone.0136816

Xiong, X. Q., Geng, Z., Zhou, B., Zhang, F., Han, Y., Zhou, Y. B., et al. (2018). FNDC5 attenuates adipose tissue inflammation and insulin resistance via AMPK-mediated macrophage polarization in obesity. *Metabolism* 83, 31–41. doi: 10.1016/j.metabol.2018.01.013

Yan, B., Shi, X., Zhang, H., Pan, L., Ma, Z., Liu, S., et al. (2014). Association of serum irisin with metabolic syndrome in obese Chinese adults. *PLoS One* 9:e94235. doi: 10.1371/journal.pone.0094235

Yang, X., Pursell, B., Lu, S., Chang, T. K., and Mercurio, A. M. (2009). Regulation of beta 4-integrin expression by epigenetic modifications in the mammary gland and during the epithelial-to-mesenchymal transition. *J. Cell Sci.* 122, 2473–2480. doi: 10.1242/jcs.049148

Zarbock, A., Ley, K., Mcever, R. P., and Hidalgo, A. (2011). Leukocyte ligands for endothelial selectins: specialized glycoconjugates that mediate rolling and signaling under flow. *Blood* 118, 6743–6751. doi: 10.1182/blood-2011-07-343566

Zhang, A., Lacy-Hulbert, A., Anderton, S., Haslett, C., and Savill, J. (2020). Apoptotic cell-directed resolution of lung inflammation requires myeloid alphav integrin-mediated induction of regulatory T lymphocytes. *Am. J. Pathol.* 190, 1224–1235. doi: 10.1016/j.ajpath.2020.02.010

Zhang, W., Chang, L., Zhang, C., Zhang, R., Li, Z., Chai, B., et al. (2015). Central and peripheral irisin differentially regulate blood pressure. *Cardiovasc. Drugs. Ther.* 29, 121–127. doi: 10.1007/s10557-015-6580-y

Zhang, W. M., Kapyla, J., Puranen, J. S., Knight, C. G., Tiger, C. F., Pentikainen, O. T., et al. (2003). alpha 11beta 1 integrin recognizes the GFOGER sequence in interstitial collagens. *J. Biol. Chem.* 278, 7270–7277. doi: 10.1074/jbc.m210313200

Zhang, Y., Li, R., Meng, Y., Li, S., Donelan, W., Zhao, Y., et al. (2014). Irisin stimulates browning of white adipocytes through mitogen-activated protein kinase p38 MAP kinase and ERK MAP kinase signaling. *Diabetes Metab. Res. Rev.* 63, 514–525. doi: 10.2337/db13-1106

Zhang, Z. P., Zhang, X. F., Li, H., Liu, T. J., Zhao, Q. P., Huang, L. H., et al. (2018). Serum irisin associates with breast cancer to spinal metastasis. *Medicine* 97:e0524. doi: 10.1097/md.0000000000010524

Zhao, Y. T., Wang, J., Yano, N., Zhang, L. X., Wang, H., Zhang, S., et al. (2019). Irisin promotes cardiac progenitor cell-induced myocardial repair and functional improvement in infarcted heart. *J. Cell. Physiol.* 234, 1671–1681. doi: 10.1002/jcp.27037

Zhi, Y., Huang, H., and Liang, L. (2018). MFG-E8/integrin beta3 signaling contributes to airway inflammation response and airway remodeling in an ovalbumin-induced murine model of asthma. *J. Cell. Biochem.* 119, 8887–8896. doi: 10.1002/jcb.27142

Zhu, H., Liu, M., Zhang, N., Pan, H., Lin, G., Li, N., et al. (2018). Serum and adipose tissue mRNA levels of ATF3 and FNDC5/irisin in colorectal cancer patients with or without obesity. *Front. Physiol.* 9:1125. doi: 10.3389/fphys.2018.01125

Conflict of Interest: The authors declare that the research was conducted in the absence of any commercial or financial relationships that could be construed as a potential conflict of interest.

frontiers in Cell and Developmental Biology

REVIEW
published: 28 October 2020
doi: 10.3389/fcell.2020.600368

Protein Palmitoylation in Leukocyte Signaling and Function

*Xiaoyuan Yang[1], Victor Chatterjee[1], Yonggang Ma[1], Ethan Zheng[1] and Sarah Y. Yuan[1,2]**

[1] Department of Molecular Pharmacology and Physiology, Morsani College of Medicine, University of South Florida, Tampa, FL, United States, [2] Department of Surgery, Morsani College of Medicine, University of South Florida, Tampa, FL, United States

Palmitoylation is a post-translational modification (PTM) based on thioester-linkage between palmitic acid and the cysteine residue of a protein. This covalent attachment of palmitate is reversibly and dynamically regulated by two opposing sets of enzymes: palmitoyl acyltransferases containing a zinc finger aspartate-histidine-histidine-cysteine motif (PAT-DHHCs) and thioesterases. The reversible nature of palmitoylation enables fine-tuned regulation of protein conformation, stability, and ability to interact with other proteins. More importantly, the proper function of many surface receptors and signaling proteins requires palmitoylation-meditated partitioning into lipid rafts. A growing number of leukocyte proteins have been reported to undergo palmitoylation, including cytokine/chemokine receptors, adhesion molecules, pattern recognition receptors, scavenger receptors, T cell co-receptors, transmembrane adaptor proteins, and signaling effectors including the Src family of protein kinases. This review provides the latest findings of palmitoylated proteins in leukocytes and focuses on the functional impact of palmitoylation in leukocyte function related to adhesion, transmigration, chemotaxis, phagocytosis, pathogen recognition, signaling activation, cytotoxicity, and cytokine production.

Keywords: palmitoylation, protein function, leukocyte function/activation, signal transduction, DHHC palmitoyl transferases, leukocyte behaviors

OPEN ACCESS

Edited by:
Zhichao Fan,
UCONN Health, United States

Reviewed by:
Rongrong Liu,
Northwestern University, United States
Bo Liu,
University of California, Berkeley, United States

***Correspondence:**
Sarah Y. Yuan
syuan@usf.edu

Specialty section:
This article was submitted to Cell Adhesion and Migration, a section of the journal Frontiers in Cell and Developmental Biology

Received: *29 August 2020*
Accepted: *30 September 2020*
Published: *28 October 2020*

Citation:
Yang X, Chatterjee V, Ma Y, Zheng E and Yuan SY (2020) Protein Palmitoylation in Leukocyte Signaling and Function. Front. Cell Dev. Biol. 8:600368. doi: 10.3389/fcell.2020.600368

INTRODUCTION

Leukocytes are critical components of innate and adaptive immunity by eradicating microbes and potentially harmful cells or substances. In addition to combating infection, leukocytes are also involved in the pathogenesis of many diseases, including cancer, neurological disorders, and cardiovascular diseases. In order to ensure effective leukocyte function without causing unwanted damages to normal tissues, the cascades of leukocyte responses are precisely controlled by many leukocyte proteins such as adhesion molecules, surface receptors, co-receptors, signaling effectors, adaptor proteins, cytokines, and chemokines (Yadav et al., 2003). Aberrant function of any of these proteins may lead to abnormal immune responses. Leukocyte proteins undergo a variety of post-translational modifications (PTMs) to ensure fine-tuned regulation and functional diversity. These modifications include acylation, phosphorylation, ubiquitination, glycosylation, nitrosylation, methylation, and proteolysis (Liu et al., 2016). Among these PTMs, protein palmitoylation is a prominent type of acylation that has gained increasing recognition for its roles in regulating leukocyte signaling and behaviors.

Palmitoylation belongs to a subtype of fatty acid modification called S-acylation, involving covalent attachment of 16-carbon palmitic acid to one or more cysteine residues of a protein through a thioester linkage (R-S-CO-R'). In 1979, palmitoylation was first identified by Schmidt and Schlesinger (1979). The source of palmitic acid is the cytosolic pool of palmitoyl-CoA (Resh, 2006a). The addition of palmitic acid is an enzyme-catalyzed reaction (Blaskovic et al., 2013). Palmitoylation differs from other types of lipid modifications (e.g., myristoylation and prenylation) in that palmitoylation is reversible and dynamically regulated. The attached palmitate is readily removed when the thioester linkage is cleaved. Cycles of palmitoylation and de-palmitoylation are precisely regulated in a fashion similar to phosphorylation and ubiquitination. The reversibility of palmitoylation allows for the dynamic regulation and fine-tuning of protein function and activities in leukocytes.

Although protein palmitoylation was discovered about 40 years ago, the field has substantially progressed only in recent years after the breakthrough of non-radioactive detection of palmitoylated proteins. Palmitoylation has since been extensively studied in cancer and neurological disorders (Kang et al., 2008; Ko and Dixon, 2018); however, research on palmitoylation regulation in leukocyte function is in its infancy, with many molecular mechanisms remaining largely unexplored. Recently, methodological advances have made it possible to perform sensitive and reliable large-scale palmitoyl proteome profiling in different subtypes of leukocytes, including monocyte/macrophages, dendritic cells, T cells and B cells, as well as in cells directly interacting with leukocytes, such as endothelial cells (ECs; Martin and Cravatt, 2009; Merrick et al., 2011; Ivaldi et al., 2012; Marin et al., 2012; Chesarino et al., 2014). These palmitoyl proteomic approaches have identified an array of palmitoylated proteins, including but not limited to cytokine/chemokine receptors CCR5, TNFR, and INFAR; adhesion molecules PECAM-1 and JAM-C; pattern recognition TLR/MYD88 complex; scavenger receptor CD36; T cell co-receptors CD4 and CD8; Src family kinases Lck and Fyn; transmembrane adaptor proteins linker of activated T cells (LAT) and PAG; signaling effectors Gα, Ras, and phospholipase C; and Ca^{2+} regulator IP3R. This growing list of palmitoylated proteins highlights the functional significance of palmitoylation in leukocytes. In this review, we discuss the latest advances in palmitoylation-mediated regulation of protein function and its impact on leukocyte signaling and behaviors.

PALMITOYLATION IN PROTEIN FUNCTION AND SIGNAL TRANSDUCTION

The regulatory mechanisms of palmitoylation in protein function and signal transduction are summarized in **Figure 1**.

Subcellular Effects

Covalent attachment of palmitic acid to proteins results in increased protein hydrophobicity and, therefore, affects protein function mainly through four mechanisms: altering conformation/structure, directing intracellular trafficking or compartmentalization, regulating stability/half-life, and influencing protein-protein interactions. Firstly, palmitoylation plays a critical role in regulating protein conformation. Many G-protein coupled receptors (GPCRs) in leukocytes require palmitoylation for their proper conformation. The insertion of the attached palmitate into plasma membrane creates the fourth loop of GPCRs between the cytoplasmic end of the seventh α-helix and palmitate insertion, which is essential for the propagation of GPCR signals (Chini and Parenti, 2009). Secondly, palmitoylation regulates protein trafficking and localization, as typically seen with small GTPase Ras, one of the most studied palmitoylated substrates. The palmitoylation and de-palmitoylation cycle dynamically regulates Ras shuttling between Golgi and plasma membrane (Hornemann, 2015). Likewise, many transmembrane or membrane-associated proteins rely on palmitoylation for their stable membrane anchor (Greaves and Chamberlain, 2007). Thirdly, emerging evidence has shown that palmitoylation can stabilize proteins and increase their half-life. Mutation of the palmitoylation site greatly shortens the life span of many proteins, as such proteins undergo misfolding during protein synthesis or become more susceptible to ubiquitination-mediated degradation (Resh, 2006a). Finally, palmitoylation modulates protein-protein interactions both directly and indirectly. The long hydrocarbon chain of the attached palmitic acid can interact directly with that of another protein. Palmitoylation also promotes the clustering of proteins in specialized membrane microdomains, which selectively brings specific proteins into proximity and facilitates their interactions indirectly (Blaskovic et al., 2013).

Impact in Signal Transduction

A growing list of receptors and signaling proteins in leukocytes have been recognized as palmitoylation substrates (Resh, 2006a). Their function can be modulated by palmitoylation in similar manners as stated above. Additionally, palmitoylation facilitates the sequestering of receptors, signaling proteins, and adaptor proteins into lipid rafts for effective signal transduction (Bijlmakers and Marsh, 2003). Lipid rafts are liquid-ordered microdomains in the external leaflet of plasma membrane enriched with cholesterol and glycosphingolipids; they are highly dynamic and serve as a platform for many signal transduction processes in leukocytes (Alonso and Millan, 2001). For example, the signaling proteins for T-cell activation, including the T cell receptor, its co-receptors (CD4 and CD8), Src-family kinases (Lyn and Fyn), and adaptor proteins are all clustered in lipid rafts of T cells (Kabouridis, 2006). As a saturated fatty acid, palmitate prefers to insert into liquid-ordered raft domains rather than the bulk plasma membrane (Resh, 2013). Palmitoylation-dependent segregation of proteins in lipid rafts is essential for the amplification of signal propagation in activated cells while preventing the signal activation in resting cells. Another unique function of palmitoylation in regulating signal transduction is mediating receptor desensitization and internalization (Resh, 2006a). Upon activation, many receptors become desensitized as a result of phosphorylation mediated by GPCR kinases (GRKs), the function of which is greatly

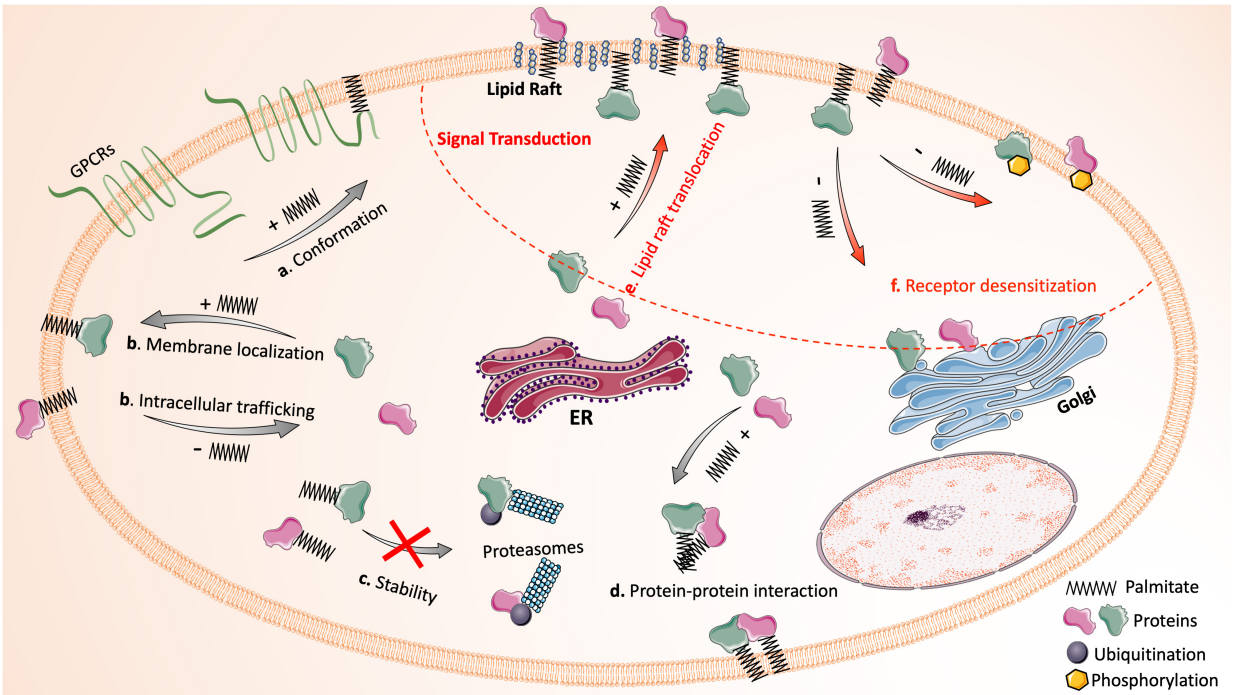

FIGURE 1 | Protein palmitoylation dynamically regulates protein function and signal transduction. The reversible attachment of palmitic acid affects protein function in many ways: **(a)** palmitoylation alters the conformation or structure of a protein (e.g., the fourth intracellular loop of GPCRs that is formed by inserting palmitate into the plasma membrane); **(b)** palmitoylation mediates protein intracellular trafficking and ensures stable membrane localization of proteins; **(c)** palmitoylation stabilizes proteins by preventing misfolding and ubiquitination-mediated degradation; **(d)** palmitoylation facilitates protein-protein interaction directly and indirectly. In addition, the palmitoylation and de-palmitoylation cycle has critical impact on signal transduction (upper right region circled by red dash line): **(e)** many signaling proteins require palmitoylation for their translocation into lipid rafts. **(f)** De-palmitoylation mediates receptor desensitization following activation by promoting the phosphorylation of receptors or the translocation of membrane signaling proteins to cytoplasm. Images of proteins and organelles were obtained from Smart Servier Medical Art (https://smart.servier.com).

enhanced by palmitoylation (Stoffel et al., 1998). Meanwhile, de-palmitoylation of receptors has been proved to increase the accessibility of their phosphorylation sites to kinases (Moffett et al., 1993; Qanbar and Bouvier, 2003). Thus, palmitoylation and de-palmitoylation precisely control signaling events in a spatial-temporal context, regulating many aspects of leukocyte function.

As the fundamental signaling events in many leukocytes, GPCR signal transduction is subjected to palmitoylation-dependent regulation at many levels. In addition to GPCRs themselves being affected by palmitoylation in the aforementioned manner, various GPCR downstream effectors are also substrates of palmitoylation. Upon GPCR activation, Gα subunit dissociates from Gβγ subunit, and their fragments subsequently activate three major signal transduction cascades: (1) *Adenylate cyclase cascade*, which catalyzes the conversion of ATP to cAMP and then activates PKA and its downstream effectors; (2) *Phospholipase c (PLC) cascade*, which promotes the conversion of phosphatidylinositol 4,5-bisphosphate [PI(4,5)P2] to diacylglycerol (DAG) and inositol 1,4,5-trisphospate (IP3). IP3 then binds to IP3 receptor (IP3R) localized on ER and induces the release of Ca^{2+} into cytoplasm. DAG and increased Ca^{2+} are both capable of activating PKC; (3) *Phosphatidylinositol 3 kinase (PI3K) cascade*, which hydrolyzes PI(4,5)P2 to produce phosphatidylinositol 3,4,5-triphosphate (PIP3), an effective activator of AKT (also known as PKB; Hilger et al., 2018; Lammermann and Kastenmuller, 2019; Wang X. et al., 2019). Many effector proteins of the GPCR signaling cascades, for example, Gα, PLC and IP3R, require palmitoylation for their proper localization and function. Gαq is palmitoylated at Cys9 and 10, while Gαs is palmitoylated at Cys3 (Wedegaertner et al., 1993). Gαq and Gαs with mutation at these cysteine sites exist in their soluble form in cytoplasm rather than their primary location in lipid rafts. Palmitoylation-defective Gαq and Gαs are incapable of coupling with GPCRs and fail to induce the activation of PLC or adenylate cyclase, respectively (Wedegaertner et al., 1993). A separate study shows that the palmitate turnover rate of Gα increases upon Gα activation and dissociation from Gβγ; de-palmitoylation mediates the internalization of Gα to cytoplasm, where it is repalmitoylated (Ross, 1995). This activation-dependent de-palmitoylation of Gα is essential to the desensitization process following GPCR activation (Vogler et al., 2008).

Ras, which belongs to the small GTPases, also functions as a signaling effector. Ras is one of the earliest identified palmitoylation substrates (Magee et al., 1987). All three Ras isoforms (H-, N-, and K-Ras) undergo farnesylation at the C-terminal CAAX motif, allowing Ras to loosely insert into endomembrane structures. N-Ras and H-Ras, but not K-Ras,

are further modified by attaching palmitates at one or two cysteines (Cys181 in N−Ras, Cys181 and 184 in H−Ras) adjacent to CAAX motif in Golgi (Hancock et al., 1990; Swarthout et al., 2005; Baumgart et al., 2010). The attached palmitate promotes the translocation of Ras to plasma membrane and facilities the stable membrane anchor of Ras. Reports show that palmitoylation-defective H-Ras is trapped in Golgi and unable to traffic to plasma membrane. Palmitoylation also influences the GTP-binding ability of Ras. Functional assay revealed that only palmitoylated N-Ras turns into the GTP-bound activated form in response to agonists (Song et al., 2013). The palmitate turnover rate of GTP-bound activated Ras is 25-fold higher than that of GDP-bound deactivated Ras (Baker et al., 2003). After de-palmitoylation, Ras traffics to Golgi, where it is palmitoylated again and redirected to plasma membrane for the next cycle.

PALMITOYLATION ENZYMES

The turnover of protein palmitoylation is generally much faster than the turnover of the particular protein being palmitoylated, indicating that the attachment of palmitate is dynamically regulated (Won et al., 2018). Protein palmitoylation is controlled by two opposing types of enzymes. Palmitoyl acyltransferases (PATs) catalyze the addition of palmitic acid, while the removal of palmitic acid is mediated by thioesterases, including palmitoyl protein thioesterases (PPTs), acyl-protein thioesterases (APTs) and α/β hydrolase domain-containing 17 proteins (ABHD17s; Won et al., 2018). Under the tight control of these enzymes, the palmitoylation and de-palmitoylation cycle normally occurs multiple times throughout the lifetime of a palmitoylated protein.

Palmitoyl Acyltransferases

Palmitoyl acyltransferases contain a highly conserved Asp-His-His-Cys (DHHC) tetrapeptide motif in its cysteine-rich domain; thus these enzymes are also known as DHHCs or PAT-DHHCs (Tabaczar et al., 2017). DHHCs were first identified by Deschenes and Davis labs in 2002 (Lobo et al., 2002; Roth et al., 2002). So far, 23 DHHCs have been identified in humans (Rana et al., 2019). DHHCs are transmembrane proteins that span the membrane four to six times and locate on the cytosolic face of the membrane (Blaskovic et al., 2013). The conserved cysteine-rich domain serves as the catalytic center for the enzyme, directly involved in the palmitoyl transfer reaction (Tabaczar et al., 2017; Rana et al., 2019). The majority of DHHCs are localized in endoplasmic reticulum (ER; DHHC1, 6, 14, 19, 23, 24) or Golgi apparatus (DHHC 3, 4, 7, 8, 15, 17, 18) or both (e.g., DHHC 2, 9, 12, 13, 22), while several others (e.g., DHHC 5, 20, 21) can be found on plasma membrane (Korycka et al., 2012; Hornemann, 2015; Ko and Dixon, 2018). DHHCs catalyze palmitoylation in a two-step manner: (1) auto-palmitoylation reaction where the cysteine residue in DHHC motif binds with palmitoyl-CoA; (2) acyl transfer reaction where the palmitoyl group is transferred from DHHCs to cysteine residues of a protein substrate (Tabaczar et al., 2017). To date, the substrate specificity of DHHCs is poorly understood. Although the palmitoylated cysteines share some common characteristics, there is no consensus palmitoylation sequence (Salaun et al., 2010). It is speculated that the protein-protein interaction domain of DHHCs (e.g., ankyrin repeats in DHHC13/17, Src-homology 3 domain in DHHC6) plays critical roles in recognizing specific substrates (Fredericks et al., 2014; Verardi et al., 2017; Matt et al., 2019).

Accumulating studies have revealed the functional impact of DHHCs in leukocytes. For example, mice with DHHC21 deficiency display a reduced number of slow-rolling and adherent leukocytes in post-capillary venules during systemic inflammation (Beard et al., 2016). There is evidence for DHHC6- catalyzed MyD88 palmitoylation in neutrophils, which is necessary for TLR-NF-κB signaling (Kim et al., 2019). In dendritic cells, surface expression and proper function of TLR2 depend on the palmitoylation of TLR2 by DHHC 2, 3, 6, 7, or 15 (Chesarino et al., 2014). DHHC7 is responsible for the palmitoylation of Fas, thus regulating T cell apoptosis and differentiation (Rossin et al., 2015). Although beyond the current focus, it is worth pointing out that palmitoylation can affect the infectivity of various viruses and bacteria, including coronavirus, HIV, influenza, and B anthrax (Sobocinska et al., 2017). It has been reported that DHHC-mediated palmitoylation of the SARS-CoV spike protein facilitates the virus entry into host cells (Petit et al., 2007). This may also hold true for the SARS-Cov2 virus, as a study has reported the interaction of SARS-Cov2 with DHHC5 (Gordon et al., 2020).

De-Palmitoylation Enzymes

Many signaling proteins in leukocytes, such as Ras and certain G protein subunits, undergo rapid de-palmitoylation upon activation, suggesting that de-palmitoylation enzymes participate in leukocyte responses (Won et al., 2018). So far, three classes of de-palmitoylation enzymes have been identified: PPTs, APTs and ABHD17s. ***PPTs*** (PPT1 and PPT2) mainly reside in lysosomes and mediate the removal of palmitate during the process of protein degradation (Resh, 2006a; Koster and Yoshii, 2019). PPT1 was the first identified enzyme that removes palmitate from a modified protein (Camp and Hofmann, 1993). Although PPT1 has been reported to show activities outside of lysosomes in certain neurons, it is unlikely that PPT1 contributes to the de-palmitoylation of cytoplasmic or plasma membrane proteins (Kim et al., 2008; Hornemann, 2015). PPT2 shares 18% of its amino acid sequence with PPT1 and shows a certain degree of cross-reactivity with PPT1 (Gupta et al., 2001; Kim et al., 2008; Cho and Park, 2016). However, PPT2 does not catalyze the de-palmitoylation of H-Ras as PPT1 does (Soyombo and Hofmann, 1997), suggesting a distinctive substrate specificity for PPT2. ***APTs*** (APT1 and APT2) are ubiquitously expressed serine hydrolases, localized predominantly in cytoplasm (Kong et al., 2013). APT1 (or LYPLA1) was first identified as a de-palmitoylation enzyme in 1998, based on its ability to remove [^{3}H] palmitate from palmitoylated Gα and H-Ras (Duncan and Gilman, 1998). Further studies show that APT1 catalyzes de-palmitoylation of numerous leukocyte proteins, including linker of activated T cells (LAT), endothelial nitric oxide synthase (eNOS), regulator of G protein signaling protein (RGS), and synaptosome associated protein 23 (SNAP-23; Ladygina et al., 2011). APT2 exhibits 68% of amino acid sequence similarity to

APT1 and has an almost identical 3D-structure to APT1 (Gadalla and Veit, 2020). APT2 seems to possess distinct substrate preference compared to APT1. Nevertheless, APT2 and APT1 are functionally redundant in de-palmitoylating certain proteins (e.g., Ras; Rusch et al., 2011). So far, little is known about the mechanism of APT substrate specificity. Several studies have investigated the regulatory mechanism and functional impact of APTs in leukocytes. The expression of APT1 in RAW264.7 macrophage-like cells decreases in response to LPS, while the expression of APT2 remains unaffected (Satou et al., 2010). A recent study of B cells shows that APTs are inhibited by miR-138 and -424, which exerts critical impacts on B cell apoptosis in a CD95-dependent mechanism (Berg et al., 2015). ***ABHD17s*** (ABHD17A, ABHD17B and ABHD17C) are mainly localized to plasma membrane of various cell types (Lin and Conibear, 2015; Won et al., 2018). The ABHD17s were first identified as the de-palmitoylase for N-Ras (Lin and Conibear, 2015). ABHD17s are palmitoylated at the N-terminal cysteine cluster, which is required for its plasma membrane localization and substrate interaction (Lin and Conibear, 2015). So far, there has been limited research to characterize the functional impacts and regulatory mechanisms of ABHD17s.

METHODS OF DETECTING PALMITOYLATION

Detection of palmitoylated protein has been technically challenging due to its reliance on time-consuming radioactive labeling. Recently, several methodological breakthroughs have been achieved for quantifying and imaging palmitoylated proteins, which greatly accelerate the research progress in this field. Currently, there are three major types of detection methods: radioactive metabolic incorporation, hydroxylamine-based acyl-exchange assay, and click chemistry-based metabolic labeling. All can be applied to detect palmitoylated proteins in leukocytes.

Radioactive Metabolic Incorporation

Palmitoylated proteins can be metabolically labeled with palmitic acid incorporated with a radioisotope. Tritiated palmitate (or [^{3}H] palmitate) is the most commonly used radioactive palmitate as it is commercially available and confirmed as reliable by many labs. This method consists of four steps: [^{3}H] palmitate labeling, immunoprecipitation proteins, SDS-PAGE, and photofluorographic exposure (Resh, 2006b). When coupling it with a pulse-chase approach, [^{3}H] palmitate labeling can be utilized to study the palmitate turnover of a specific protein substrate. For more than two decades, radioactive labeling has remained the gold standard for detecting palmitoylation (Yount et al., 2013). However, β particles emitted by [^{3}H] are weak, thus it often requires several weeks to develop a clear X-ray image through photofluorography. The time-consuming and cumbersome nature of this method limits its use in many research labs, not to mention the hazards associated with handling radioactive materials. Later, a more energetic radioactive palmitate analog [^{125}I]iodohexadecanoic acid (^{125}I-IC16) was adapted to this method. [^{125}I] generates gamma rays that are more penetrating, thus greatly shortening the exposure time to 24 h (Tsai et al., 2014). Other advances in radioactive labeling involve improving the sensitivity of X-ray films, which enables visualization of [^{3}H] palmitate-labeled proteins in 1–3 days (Tsai et al., 2014).

Hydroxylamine-Based Acyl-Exchange Assay

Hydroxylamine-based acyl-exchange assay is one of the two non-radioactive techniques invented to circumvent the drawbacks of radioactive labeling (Drisdel and Green, 2004). This method is comprised of four biochemical steps: (1) blocking the free thiols of extracted proteins; (2) cleaving the thioester linkage with hydroxylamine to liberate the previously palmitoylated cysteinyl thiols; (3) capturing the newly freed thiol groups with pyridyldithiol-biotin; (4) purifying the biotin-labeled proteins using streptavidin agarose beads (Wan et al., 2007; Brigidi and Bamji, 2013). More recently, acyl-biotin exchange assay (ABE) was modified to a simplified version called resin-assisted capture (RAC) in which proteins with hydroxylamine-liberated thiol groups are directly captured by pyridyldithiol-resin (Forrester et al., 2011). The acyl-exchange assays are more powerful when coupled with mass spectrometry-based proteomic studies. Unlike radioactive labeling that analyzes a single protein, acyl-exchange assays enable large-scale profiling of the proteome, leading to the discovery of numerous novel palmitoylation substrates in leukocytes (Ivaldi et al., 2012). Moreover, acyl-exchange assays are unique among all the palmitoylation detecting methods for their capability in providing a snapshot of the palmitoylated protein profile in cells. The major disadvantage of acyl-exchange assays lies within the fact that they are not compatible with pulse-chase experiments, as the entire acyl-exchange procedure is performed in protein lysates (Tsai et al., 2014).

"Click Chemistry"-Based Metabolic Labeling

"Click chemistry"-based metabolic labeling is the second type of non-radioactive techniques used to detect palmitoylation. The principle behind this method is the "click chemistry" reaction, also known as Cu^{1+}-catalyzed Huisgen cycloaddition reaction between azido- and alkynyl-groups (Hang et al., 2007; Charron et al., 2009; Hannoush and Arenas-Ramirez, 2009). The most commonly used alkynyl-palmitate analogs are ω-alkynyl-C16 (Alk-C16 or 15-hexadecynoic acid) and 17-octadecynoic acid (17-ODYA). "Click chemistry"-based metabolic labeling is most versatile in application compared to other methods due to the various types of azido-containing markers. First and foremost, palmitoylated proteins labeled with alkynyl groups can react with azido-fluorescent dye (e.g., Oregon Green 488 azide), which enables the robust imaging of global protein palmitoylation in cells (Hannoush and Arenas-Ramirez, 2009; Beard et al., 2016). Later, this imaging strategy was further improved by coupling with proximity ligation assay, which makes it possible to visualize a single palmitoylated protein and study its palmitoylation level and subcellular localization (Gao and Hannoush, 2014). Secondly, alkynyl-palmitoylated proteins

can also react with azido-biotin for streptavidin enrichment, followed by either single protein analysis or large-scale LC-MS/MS proteomic analysis in leukocytes (Ladygina et al., 2011). Thirdly, alkynyl-palmitoylated proteins can bind to azido-IRDye 800, omitting the streptavidin enrichment step and allowing the direct detection of leukocyte palmitoylated proteins using Li-COR infrared imaging (Akimzhanov and Boehning, 2015). However, alkynyl-palmitate analogs can only incorporate into accessible and reduced cysteine residues of a palmitoylated protein. Stalely palmitoylated proteins, which do not undergo dynamic palmitate turnover, cannot be labeled or purified by this method as their cysteines are not available to conjugate with alkynyl-palmitate analogs.

Method to Identify Palmitoylation Sites

The palmitoylation sites of the modified protein can be predicted by CSS-Palm 2.0 using a clustering and scoring strategy algorithm, or by other tools like GPS-lipid. To verify the predicted cysteine residues, mutagenesis of cysteine residue(s) is performed, often followed by studying the subsequent impacts on protein palmitoylation level, subcellular localization, stability, and activity. Cysteine residue of a palmitoylated protein is often substituted with alanine, though cysteine-to-serine mutagenesis is also employed by some research groups.

PROTEIN PALMITOYLATION REGULATION OF LEUKOCYTE FUNCTION

A growing number of palmitoylated proteins have been discovered in leukocytes, many of which play critical roles in regulating various leukocyte functions, including adhesion, transmigration, chemotaxis, phagocytosis, pathogen recognition, T cell receptor (TCR) and BCR signaling activation, cytotoxicity, cytokine production, and apoptosis. Below, we discuss the functional impact of palmitoylation in different types of leukocytes (**Figure 2**).

Neutrophils

Neutrophils are the most abundant type of leukocytes in human circulation that act as ongoing surveillance against potential invading pathogens and sterile inflammation. They are among the first responders to sites of infection and contribute to the initiation and propagation of inflammatory cascades (Ma et al., 2019). The neutrophil recruitment cascade is initiated with selectin-mediated slow rolling, followed by β2-integrin-mediated firm adhesion and PECAM-1-mediated transmigration across the endothelium (O'Brien et al., 2003; Mocsai et al., 2015).

Neutrophil Adhesion and Transendothelial Migration

Adhesion molecules, such as selectins and integrins, work cooperatively to regulate neutrophil recruitment. Although little is known about palmitoylation of adhesion molecules expressed on the neutrophil surface, it has been seen in many cells and cell fragments that directly interact with neutrophils. For instance, in ECs, PECAM-1 is palmitoylated by DHHC21, and knockdown of DHHC21 greatly reduces the protein level of PECAM-1 and decreases its surface expression (Marin et al., 2012). Another study reports that palmitoylation of PECAM-1 at Cys595 is required for its lipid raft localization (Sardjono et al., 2006). Additionally, P-selectin in platelets mediates the formation of the platelet-neutrophil complex via binding to its ligand PSGL-1 on neutrophils, a process that aids the firm adhesion of neutrophils to activated ECs and thereby promotes leukocyte transmigration (Lisman, 2018). Recent studies have shown that P-selectin undergoes palmitoylation in platelets and that de-palmitoylation of P-selectin by APT1 greatly inhibits the expression of P-selection in platelets (Sim et al., 2007). It is plausible that this palmitoylation-regulated P-selectin change in platelets may affect neutrophil recruitment.

Neutrophil adhesion molecules require partner protein tetraspanins for their stable membrane localization and proper function (Yeung et al., 2018). Tetraspanins are transmembrane proteins that contain a large extracellular loop to interact with adhesion molecules and other tetraspanins, forming a signal transducing complex called tetraspanin-enriched microdomains (TEMs) in cell membrane. Tetraspanins facilitate the recruitment of adhesion molecules to TEMs and amplify their intracellular signals, therefore playing important roles in regulating neutrophil function. For example, $CD37^{-/-}$ neutrophils exhibit an impaired ability to migrate toward chemotactic stimuli and to adhere to postcapillary venules (Wee et al., 2015); CD63 binds to Mac-1 and enhances Mac-1-mediated adhesion function (Skubitz et al., 1996). So far, a large body of tetraspanins, including CD9, CD37, CD53, CD63, CD81, CD82 and CD151, has been reported as palmitoylation substrates (Charrin et al., 2002; Yang et al., 2002; Termini et al., 2014). Investigating whether and how palmitoylation affects tetraspanin function in neutrophils is of great significance for the comprehensive understanding of the regulation of neutrophil functions.

Neutrophil Chemotaxis

Once migrated out of microvessels, neutrophils in tissues are capable of moving along chemoattractant gradients toward sites of infection or injury. Neutrophil chemotaxis starts with polarization, characterized by the formation of a leading-edge containing pseudopod and a highly contractile trailing edge (Hind et al., 2016). The migration of the neutrophil depends on dynamic polymerization and depolymerization of actin filament, which pushes the leading-edge forward and retracts the tail at the rear of the cell (Szczur et al., 2006; Mocsai et al., 2015). The key regulators of these coordinated processes are members of the small Rho GTPase family, including Rac, Cdc42, and Rho (Sun et al., 2004; Mocsai et al., 2015).

Rac is essential for neutrophil motility as well as directional sensing during migration. Similar to other members of small GTPase, Rac exists in two states: GTP-bound activated state or GDP-bound de-activated state. During neutrophil migration, GTP-bound Rac1 promotes the activation of p21-activated kinase (PAK) and the reorganization of actin, which subsequently aid membrane protrusion via lamellipodia formation (Filippi et al., 2007). Rac-1 is palmitoylated at Cys178, and the attachment of palmitate requires prior prenylation

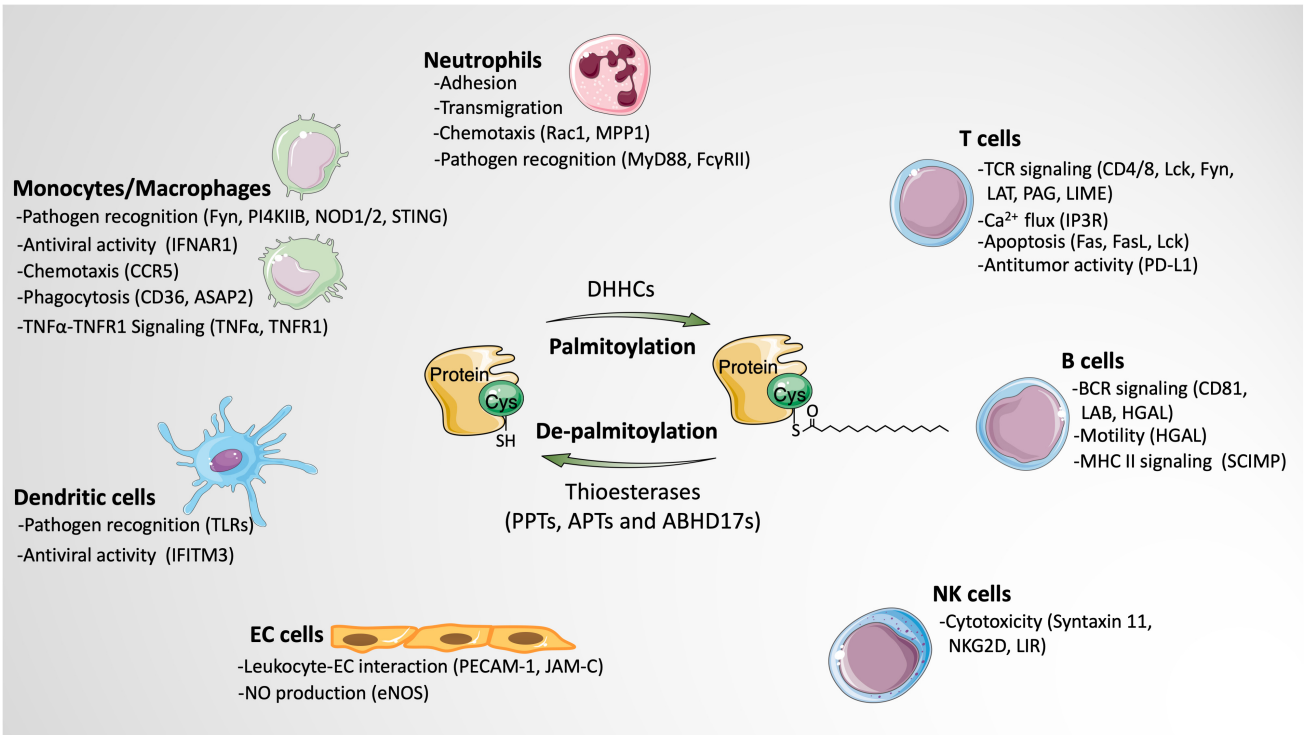

FIGURE 2 | The impact of protein palmitoylation on leukocyte signaling and function. Protein palmitoylation modulates various functions of leukocytes by altering the activities of palmitoylated proteins in different subtypes of leukocytes. Besides, palmitoylation also indirectly affects leukocyte behaviors through regulating the function of endothelial cells. Palmitoylated proteins involved in the particular function are listed in parentheses. Images of cells and proteins were obtained from Smart Servier Medical Art (https://smart.servier.com).

at Cys189 and a polybasic domain in C-terminal region. Palmitoylation-defective Rac1 (mutation at Cys178) shows reduced ability to load GTP and decreased lipid raft partitioning, which are accompanied by decreased PAK activity and F-actin recruitment at plasma membrane. Cells expressing Cys178 mutant Rac1 display defective spreading and migrate with less directionality, suggesting the essential roles of palmitoylation in regulating Rac1 function and neutrophil migration (Navarro-Lerida et al., 2012). In contrast to Rac, other members of the small GTPase family do not seem to be regulated by palmitoylation. For example, RhoA is a non-palmitoylated small GTPase (Navarro-Lerida et al., 2012), and Cdc42 only undergoes prenylation, with an exception of a brain-specific variant of Cdc42 which is palmitoylated by DHHC8 (Moutin et al., 2017).

In addition to small GTPases, other palmitoylated proteins are also involved in regulating neutrophil chemotactic migration. For example, membrane palmitoylated protein 1 (MPP1 or P55) is essential for the formation of a single pseudopod at the leading edge by confining small GTPase activation and actin polymerization to a localized region. MPP1 knockout neutrophils display multiple transient pseudopods in all directions upon stimulation and fail to perform chemotaxis efficiently (Quinn et al., 2009). However, the impacts of palmitoylation on MPP1 function remain to be addressed in neutrophils.

Pathogen Recognition

Neutrophils express several kinds of surface receptors for the recognition of invading pathogens such as Toll-like receptors (TLRs), Fcγ-receptors, and formyl-peptide receptors (Futosi et al., 2013). Growing evidence has shown that many of these receptors and their adaptor proteins are regulated by palmitoylation.

Toll-like receptors/MyD88 signaling

Toll-like receptors are responsible for recognizing pathogen-associated molecular patterns (PAMPs) and damage-associated molecular patterns (DAMPs). TLR signaling has previously been shown to be activated by saturated fatty acids even though fatty acids do not bind to TLR, suggesting a ligand-independent TLR activation meditated by fatty acids (Fessler et al., 2009; Lancaster et al., 2018). Further study reveals that MyD88, an adaptor molecule of TLR signaling, is palmitoylated by DHHC6 at Cys113 (Kim et al., 2019). The palmitoylation of MyD88 is required for its binding to IRAK4 and activation of downstream NF-κB. Reducing intracellular palmitate concentration by the inhibition of *de novo* fatty acid synthesis blocks LPS-induced neutrophil activation and MyD88-dependent cytokine production. The critical roles of palmitoylation in TLR/MyD88 signaling is further supported by the fact that the DHHC inhibitor 2-bromopalmitate (2-BP) inhibits NF-κB activation, whereas the APT inhibitor palmostatin B enhances the activation of NF-κB (Kim et al.,

2019). In fact, many isotypes of TLRs (TLR 2,5,6,10) are shown to be palmitoylated in other types of leukocytes, which will be discussed in detail later.

Fcγ receptors

Neutrophils constitutively express FcγRII (CD32) and FcγRIII (CD16) while transiently expressing FcγRI (CD64) upon activation. Neutrophil Fcγ receptors enable neutrophils to recognize antigens via immunoglobulins (Igs)-mediated interactions and regulate many neutrophil functions (Futosi et al., 2013; Kara et al., 2020). Thus, Fcγ receptors serve as a crucial link between innate immune effector cells and adaptive immune responses. The function of FcγR and its ability to bind to IgG complex requires FcγR partitioning into lipid rafts (Bournazos et al., 2009). It has been shown that the lipid raft targeting of FcγRII is regulated by palmitoylation at Cys208 in its juxtamembrane region; mutation of Cys208 results in diminished translocation of FcγRII to lipid rafts and impaired FcγRII downstream signaling (Barnes et al., 2006).

The palmitoylation of surface receptors like TNFRs, Fas, and CCRs, although not yet tested in neutrophils, have been established in other immune cells (Blanpain et al., 2001; Rossin et al., 2015; Zingler et al., 2019).

Monocytes/Macrophages

Monocytes and macrophages are critical components of innate immune systems. Monocytes patrol around the circulation and eliminate pathogens via phagocytosis. Once recruited to the sites of inflammation, monocytes differentiate into macrophages or dendritic cells. In addition to phagocytosis, monocytes and macrophages also produce inflammatory mediators and function as antigen presenting cells (APCs). An ABE-coupled proteomic study reveals 98 palmitoylated proteins in macrophages, 48% of which have been reported to be localized in lipid rafts (Merrick et al., 2011). Many of the previously reported palmitoylated proteins participate in various monocyte/macrophage functions, such as syntaxin-7 in phagocytosis, SNAP-23 in TNFα secretion and phospholipid scramblase 3 (PLSCR3) in apoptosis (Vogel and Roche, 1999; He and Linder, 2009; Merrick et al., 2011), suggesting critical roles of palmitoylation in modulating monocyte/macrophage functions.

Pathogen Recognition

TLR signaling pathway

Emerging evidence demonstrates that palmitoylation is involved in LPS-induced macrophage activation. A proteomics study using RAW264 macrophage-like cells reveals that LPS stimulates global changes in protein palmitoylation, affecting nearly 340 palmitoylated proteins (Kwiatkowska and Ciesielska, 2018). More importantly, TLR signaling in macrophages is regulated by many palmitoylated proteins. Src family kinase Fyn, an inhibitory regulator of TLR4, is palmitoylated at Cys3, a modification required for its lipid raft localization and catalytic function. LPS stimulation increases the level of palmitoylated Fyn in lipid rafts where Fyn mediates the suppression of both NF-κB and IRF3-dependent cytokine production (Borzecka-Solarz et al., 2017). Another LPS-upregulated palmitoylated protein is type II phosphatidylinositol 4-kinase (PI4KIIB). Palmitoylation of PI4KIIB triggers the activation of PI4KIIB and promotes the subsequent synthesis of PI(4,5)P2, a phospholipid compound that can activate TLR4 signaling on its own or through its hydrolytic products DAG, IP3, and PIP3 (Sobocinska et al., 2018).

Nucleotide oligomerization domain 1 (NOD1) and NOD2

Nucleotide oligomerization domain1/2 are cytosolic pattern recognition receptors that recognize bacterial peptidoglycans and promote subsequent immune responses such as NF-κB activation and cytokine production. The interaction of NOD1/2 with membrane structures (e.g., plasma membrane and bacterial-containing phagosomes) is essential for their function. NOD1/2 are palmitoylated at multiple cysteine residues: Cys558, 567, and 952 of NOD1 and Cys395 and 1033 of NOD2 (Lu et al., 2019). Administration of 2-BP greatly inhibits the recruitment of NOD1/2 to membrane structures and the production of cytokines in macrophages treated with bacterial peptidoglycans. DHHC5 is responsible for the palmitoylation of NOD1/2; silencing or knockout of DHHC5 abrogates NOD1/2-dependent NF-κB activation in bacterial peptidoglycans-stimulated macrophages (Lu et al., 2019).

Stimulator of interferon genes (STING)

STING recognizes cyclic dinucleotides of bacteria and DNA viruses, leading to potent cytokine production; it can also be activated by self-DNA that leaks from nucleus or mitochondria, which results in autoinflammatory diseases (Hansen et al., 2019). DHHC3, 7, and 15 mediated-palmitoylation of STING at Cys88 and 91 is required for STING activity and the subsequent promotion of type I interferon (IFN) responses (Mukai et al., 2016). Nitro-fatty acids, which directly target cysteine residues and therefore block STING palmitoylation, greatly reduce the production of type I IFN and IFN-induced CXCL10 and IL-6 in monocytes and macrophages upon virus infection (Hansen et al., 2018).

Antiviral Activity

Interferon-α/β receptor (IFNAR) is the receptor for antiviral cytokine type I IFNs that functions as a critical player in combating virus infection (Gonzalez-Navajas et al., 2012). It also possesses anti-bacterial and immunomodulatory properties by inducing the transcription of IFN-stimulated genes (Ivashkiv and Donlin, 2014). Upon binding to type I IFNs, IFNAR undergoes endocytosis and activates receptor-associated Jak kinases, which results in the phosphorylation of signal transducer and activator of transcription 1 (STAT1) and STAT2 and ultimately the transcription of the IFN-stimulated genes (Lee and Ashkar, 2018). Palmitoylation is required for the activation of IFNAR-Jak-Stat pathway. Palmitoylation inhibitor greatly diminishes the endocytosis of IFNAR1 and the phosphorylation of STAT1. Further study reveals that IFNAR1 is palmitoylated at Cys463, and mutation of Cys463 blocks the phosphorylation of STAT1 and 2 and their nuclear

translocation, without affecting IFNAR1 endocytosis and stability (Claudinon et al., 2009).

Chemotaxis

C-C chemokine receptor type 5 (CCR5) is a chemokine receptor that belongs to the GPCR superfamily. CCR5 regulates macrophage chemotaxis and also functions as a coreceptor for the macrophage-tropic human immunodeficiency (M-tropic HIV) virus entry into monocytes/macrophages and $CD4^+$ T lymphocytes (Tuttle et al., 1998). CCR5 is palmitoylated at Cys321, 323, and 324 located between the cytoplasmic end of the seventh transmembrane domain and the C-terminal tail (Percherancier et al., 2001). Mutation of these cysteine residues leads to the greatly reduced surface expression of CCR5. Moreover, palmitoylation prevents CCR5 from degradation, thus stabilizing CCR5; palmitoylation-defective CCR5 displays a 3-fold decease in its half-life compared to WT CCR5. Functional analysis shows that palmitoylation does not affect the binding ability of CCR5 with its agonist macrophage inflammatory protein-1β (MIP-1β). The reduced function of palmitoylation-defective CCR5 is attributed to its impaired surface expression (Blanpain et al., 2001; Percherancier et al., 2001).

Phagocytosis

CD36

CD36 is the primary scavenger receptor expressed on monocytes and macrophages that facilitates the phagocytosis of pathogens, dead cells, modified low-density lipoproteins, and long-chain fatty acids (Silverstein and Febbraio, 2009). Palmitoylation occurs at both N-terminal (Cys3 and Cys7) and C-terminal (Cys464 and Cys466) residues of CD36 (Meiler et al., 2013). Palmitoylation of CD36 requires ER protein Selk, the cofactor of DHHC6. $Selk^{-/-}$ macrophages exhibit reduced membrane expression of CD36 due to the decreased level of CD36 palmitoylation (Meiler et al., 2013). It is possible that Selk tethers DHHC6 to ER membrane via its SH3-binding domain, thus promoting DHHC6-mediated palmitoylation of CD36 in ER of macrophages. However, another study of adipocyte CD36 reveals that DHHC4 and DHHC5 are actually responsible for the palmitoylation of CD36 and its stable membrane localization (Wang J. et al., 2019). In adipocytes, DHHC4-mediated palmitoylation in Golgi targets CD36 to plasma membrane, while DHHC5-mediated palmitoylation in plasma membrane prevents CD36 disassociation with plasma membrane. Whether this modification mechanism also applies to macrophages needs to be further tested.

FcγR signaling

Fcγ receptors are also expressed on macrophages, mediating the phagocytosis of IgG-coated pathogens, the secretion of inflammatory mediators, and IgG-dependent elimination of infected cells (Fitzer-Attas et al., 2000). As mentioned in section "Neutrophils- Pathogen Recognition," palmitoylation is required for FcγR lipid raft partitioning and its binding ability with IgG complex (Barnes et al., 2006). In addition to the receptor itself being palmitoylated, effector protein downstream of FcγR is also palmitoylated in macrophages. Arf-GAP with SH3 domain, ANK repeat, and PH domain-containing protein 2 (ASAP2), is a scaffolding protein that regulates cytoskeletal rearrangement during FcγR-mediated phagocytotic cup formation (Norton et al., 2017). Once phagocytotic cups mature, ASAP2 is cleaved from the cups by calpain-2 to allow efficient phagocytosis to occur. ASAP2 is palmitoylated at Cys86 by DHHC6/Selk in ER, and palmitoylation is required for the cleavage of ASAP2 and the subsequent maturation of the phagocytic cups. Inhibition of ASAP2 palmitoylation by mutagenesis, palmitoylation inhibitor, or Selk mutation leads to prolonged retention of ASAP2 in phagocytic cups and impaired FcγR-mediated phagocytosis (Norton et al., 2017).

TNFα-TNFR1 Signaling

TNFα is a multifunctional pro-inflammatory cytokine primarily secreted by macrophages. Newly synthesized TNFα is a transmembrane protein (tmTNFα). Upon stimulation, the ectodomain of tmTNFα is cleaved by TNFα-converting enzyme ADAM17, producing biologically active soluble TNFα (sTNFα). The membrane-bound TNFα fragment is further cleaved by signal peptide peptidase-like 2b (SPPL2b) to generate the intracellular domain of TNFα (ICD-TNFα), which then activates IL-1β promoter. Palmitoylation of TNFα has been reported; the [^{3}H] labeled palmitate is detected in tmTNFα but not in sTNFα (Utsumi et al., 2001). Mutation of the palmitoylation site of tmTNFα does not affect ADAM17-dependent cleavage of its ectodomain. However, palmitoylation of tmTNFα regulates the sensitivity of TNFα receptor 1 (TNFR1). Palmitoylation facilitates tmTNFα partitioning to the lipid rafts, where it suppresses the activity of TNFR1 by competing with sTNFα. Whereas, palmitoylation-defective tmTNFα shows reduced ability to block the binding of sTNFα to TNFR1 and the transcription of TNFα target genes (Poggi et al., 2013). Palmitoylation is also required for the enzymatic cleavage of the membrane-bound TNFα fragment by SPPL2b. Mutagenesis of the palmitoylation site of TNFα results in a rapid degradation of the membrane-bound TNFα fragment prior to SPPL2b-mediated cleavage, thus reducing ICD-TNFα production and downstream IL-1β promoter activation (Poggi et al., 2013).

The majority of TNFα biological function is mediated by TNFR1, which belongs to a subgroup of death receptors. Upon binding to TNFα, TNFR1 induces two distinctive downstream signaling pathways depending on its subcellular localization. TNFR1 in plasma membrane signals for NF-κB activation, while internalized TNFR1 activates apoptosis signaling. TNFR1 is palmitoylated at Cys248, which is required for its plasma membrane localization in human monocytic U937 cells (Zingler et al., 2019). Mutagenesis of Cys248 results in decreased TNFR1 expression in plasma membrane, reducing both NF-κB and apoptosis signaling. Furthermore, activated TNFR1 undergoes APT2-mediated de-palmitoylation, which promotes TNFR1 translocation to designated signaling platforms to activate NF-κB. APT2 inhibitor blocks TNFR1 de-palmitoylation and its downstream NF-κB activation but enhances TNFR1-mediated apoptosis signaling (Zingler et al., 2019).

Dendritic Cells

Dendritic cells (DCs), functioning as the most potent APCs, are specialized to recognize, phagocytize, process, and present antigens to both memory and naïve T cells (Steinman and Banchereau, 2007). There is limited information regarding the roles of palmitoylation in DCs. Two Alk-C16 metabolic labeling-based palmitoyl proteomic studies reveal hundreds of palmitoylated proteins with diverse cellular function in DCs, such as TLR2 for pathogen recognition; IFITM3 for antiviral activity; G protein subunits, N-Ras and Lyn for signal transduction; CD81 for DC migration; and CD80 and 86 for immunomodulation (Yount et al., 2010; Quast et al., 2011; Chesarino et al., 2014; Yeung et al., 2018). Among these proteins, only TLR2 and IFITM3 palmitoylation have been investigated for their functional impact in DCs.

Pathogen Recognition

Toll-like receptors

In DCs, TLR2 is found to be palmitoylated on Cys609 at the cytoplasmic edge of the transmembrane domain (Chesarino et al., 2014). Multiple DHHCs (DHHC 2, 3, 6, 7, 15) are responsible for the palmitoylation of TLR2. Inhibition of TLR2 palmitoylation either by 2-BP or mutation of the palmitoylation site leads to the decreased surface expression of TLR2 in DCs, without affecting the overall protein level and stability of TLR2. Blocking TLR2 palmitoylation also inhibits microbial ligands-induced activation of NF-κB and production of IL-6 and TNFα, which is, at least partially, due to the insufficient surface expression of TLR2. Similar to TLR2, other TLRs (TLR5,6,10) have been shown to be palmitoylated in DCs (Chesarino et al., 2014). Whether and how palmitoylation regulates their function remain to be addressed.

Antiviral Activity

Interferon-induced transmembrane protein 3 (IFITM3), an INF-stimulated effector protein, plays important roles in restricting virus infection in host cells. Upon virus infection, IFITM3 interacts with the incoming virus particles and directs them to lysosomes for elimination. The essential roles of palmitoylation in the antiviral activity of IFITM3 have been well-recognized (Yount et al., 2010; Spence et al., 2019). In DCs, IFITM3 is palmitoylated on Cys71, Cys72 and Cys105 in the transmembrane proximal region (Yount et al., 2010). Mutation of IFITM3 palmitoylation sites does not affect the expression or subcellular localization of IFITM3 in DCs at steady state; however, palmitoylation-defective IFITM3 exhibits a greatly reduced ability to cluster with virus particles and impaired antivirus activity (Yount et al., 2010; Spence et al., 2019).

T Cells

T cells coordinate a variety of adaptive immune responses. The pivotal roles of protein palmitoylation in regulating T cell functions have been well recognized.

T Cell Receptor Signaling

T cells are activated by the binding of TCRs to the major histocompatibility complex (MHC):antigen peptide complex. Briefly, the TCR-pMHC engagement facilitated by co-receptors CD4/CD8 activates tyrosine kinase Lck and Fyn to phosphorylate the TCR/CD3 ζ-chain, recruiting tyrosine kinase ZAP-70 to phosphorylate transmembrane adaptor proteins (LAT, PAG, *etc.*). This initiates the propagation of several signaling pathways and eventually leads to the activation of the transcription factors NFAT, NF-κB, and AP-1. One study has shown that 2-BP disrupts signaling protein localization and blocks TCR signaling as evidenced by reduced tyrosine phosphorylation and impaired calcium influx (Webb et al., 2000). Moreover, several palmitoyl proteomic studies reveal that although T-cell receptor itself does not undergo palmitoylation, TCR co-receptors CD4, CD8, Src family kinases Lck and Fyn, and adaptor proteins LAT and PAG are all palmitoylated (Martin and Cravatt, 2009; Morrison et al., 2015). How palmitoylation regulates the function of TCR signaling proteins has been previously reviewed (Bijlmakers, 2009; Ladygina et al., 2011); therefore, it will only be briefly discussed in this section. Signaling effectors mentioned in previous sections like Ras and Rac will not be covered again in this section.

T cell receptor coreceptors CD4/CD8

The extracellular domain of CD4 and CD8 binds to the non-polymorphic regions of Class II and Class I MHC on APCs, respectively, facilitating the interaction of TCR with pMHC. Meanwhile, their intracellular cytoplasmic tails are closely associated with Lck (Artyomov et al., 2010; Courtney et al., 2018). Palmitoylation of CD4 occurs at Cys394 and Cys397 residues adjacent to the transmembrane domain (Crise and Rose, 1992). Palmitoylation functions as the lipid raft targeting signal of CD4, facilitating its partitioning in lipid raft and clustering with TCR and PKCθ there (Balamuth et al., 2004). CD4 also serves as a key coreceptor for HIV entry in T cells, and current research indicates that CD4 palmitoylation is not required for this function (Bijlmakers, 2009). CD8 is heterodimer consisting of CD8α and CD8β. Species-specific palmitoylation of CD8 has been reported. In mice, only CD8β, but not CD8α, undergoes palmitoylation on Cys179 in its cytoplasmic domain (Arcaro et al., 2001). In contrast, human CD8β contains two palmitoylated cysteine residues, and human CD8α is also palmitoylated. In mouse T cells, mutation of Cys179 abolishes CD8 lipid raft localization and impairs its association with Lck (Arcaro et al., 2001). Unexpectedly, palmitoylation of human CD8 does not seem to play a role in targeting CD8 to lipid raft (Pang et al., 2007). Instead, lipid raft targeting of CD8 solely relies on the positively charged amino acids in CD8β (Bijlmakers, 2009). The impact of palmitoylation on other functions of CD8 still remains unclear.

Src family kinases

Lck is actively involved in TCR signaling as well as T cell development (Molina et al., 1992; Palacios and Weiss, 2004). Lck is a dually acylated protein (Resh, 1994). Upon synthesis, Lck is myristoylated at Gly2, which is required for the subsequent palmitoylation at Cys3 and Cys5. Stable association between Lck and plasma membrane, which is critical for the activity of Lck, is mediated by palmitoylation at both Cys3 and Cys5 (Yurchak and Sefton, 1995). Multiple DHHCs (2, 3, 17, 18, 21)

are responsible for the palmitoylation of Lck (Aicart-Ramos et al., 2011; Zeidman et al., 2011; Akimzhanov and Boehning, 2015). Unexpectedly, Lck is mainly localized outside of lipid rafts in steady state T cells, yet T cell activation accelerates the palmitate turnover of Lck, which promotes the translocation of Lck into lipid rafts to phosphorylate Fyn and other substrates (Kosugi et al., 2001). Lck with mutation at both palmitoylation sites appears in a soluble form and is unable to interact with CD4 and promote downstream signaling events (Kabouridis et al., 1997). Fyn is another highly expressed Src family kinase in T cells. The absence of Fyn leads to reduced responses to TCR stimulation suggesting that Fyn is also involved in TCR signaling (Rodolfo et al., 1991; Tsygankov et al., 1996; Yasuda et al., 2002). Similar to Lck, Fyn also undergoes both myristoylation and palmitoylation. Attachment of palmitate can occur on both Cys3 and Cys6, although the majority of Fyn is only palmitoylated on Cys3 (Liang et al., 2001). The attached palmitate on Cys3 (with a half-life of 1.5–2 h) is important for membrane association and lipid raft sequestering of Fyn (Wolven et al., 1997). DHHC2,3,7,10,15,20 and 21 have all been shown to catalyze the palmitoylation of Fyn (Mill et al., 2009). In resting T cells, Fyn, unlike Lck, mainly resides in lipid rafts. Upon TCR ligation, Fyn is activated by Lck in lipid rafts which, in turn, catalyzes the phosphorylation of the TCR/CD3 ζ-chain and transduces the signals to downstream effectors (Filipp et al., 2003).

Transmembrane adaptor proteins (TRAPs)

TRAPs serve as the functional connection between TCR complex and intracellular signaling molecules. Following TCR ligation, TRAPs are phosphorylated by activated Src family kinases and ZAP-70, allowing the subsequent recruitment of cytoplasmic signaling effectors and the propagation of TCR-elicited signals into cytoplasm (Horejsi et al., 2004). Among all TRAPs, LAT is indispensable for peripheral T cell activation due to its ability to recruit and activate many key signaling molecules including PLCγ1, PI3K, Grb2, Grads, and SLP76 (Horejsi, 2004). LAT is palmitoylated at Cys26 and Cys29 in the juxtamembrane Cys-X-X-Cys motif. LAT palmitoylation is essential for the stability of LAT and its association with plasma membranes; mutation in two palmitoylation sites results in a remarkably reduced LAT expression and the retention of LAT in Golgi complex (Shogomori et al., 2005; Tanimura et al., 2006). Moreover, palmitoylation-defective LAT is not capable of interacting with TCR complex or recruiting PLCγ and Grb2 to propagate signals (Harder and Kuhn, 2000). T cells expressing palmitoylation-defective LAT display impaired Ca^{2+} influx, ERK activation, and transcription factor induction upon T cell activation (Zhang et al., 1999). Furthermore, LAT palmitoylation is closely related to T cell anergy. Compared to control T cells, anergic T cells display profoundly reduced LAT palmitoylation, which leads to reduced LAT recruitment to immunological synapses and lipid rafts (Hundt et al., 2006). Functionally, LAT in anergic T cells shows a reduced phosphorylation level upon TCR stimulation and an impaired ability to activate downstream PLCγ and PI3K (Hundt et al., 2006; Ladygina et al., 2011).

Other TRAPs like phosphoprotein associated with GEMs (PAG) and Lck-interacting membrane protein (LIME) are also palmitoylated at the same Cys-X-X-Cys motif in T cells, and both are concentrated in lipid rafts (Ladygina et al., 2011). PAG, also known as Csk-binding protein (Cbp), acts as negative regulator of T-cell signaling. PAG is capable of recruiting Csk to inhibit Src family kinases via phosphorylating tyrosine residues in their C-terminal regulatory domains. Upon TCR ligation, PAG rapidly releases Csk, resulting in the activation of Lck and Fyn (Davidson et al., 2003). PAG with a mutation in its palmitoylation motif displays normal expression level and plasma membrane localization, but it no longer resides in lipid rafts. Although it is able to recruit Csk, palmitoylation-defective PAG cannot inhibit proximal TCR signaling (Posevitz-Fejfar et al., 2008). Similar to PAG, LIME can also bind to Csk and Lck, yet the biological function of LIME in T cells remains unclear. One study has shown that LIME contributes to the activation of ERK and JNK and the production of IL-2 in Jurkat T cells (Hur et al., 2003). The attached palmitates at Cys28 and Cys31 in the Cys-X-X-Cys motif act as lipid raft targeting signals for LIME (Hur et al., 2003). However, the functional significance of palmitoylation on LIME has not yet been investigated.

Calcium Flux

Upon TCR activation, intracellular signaling effector PLCγ hydrolyzes PI(4,5)P2 to produce DAG and IP3; IP3, in turn, triggers Ca^{2+} release from ER stores via binding to IP3Rs on ER membrane (Nagaleekar et al., 2008). IP3Rs are palmitoylated by DHHC6/Selk complex in ER. The putative palmitoylation sites are reported to be at Cys56, 849, and 2214, which needs further confirmation (Fredericks et al., 2014). Knockdown of DHHC6 significantly reduces the expression of IP3R on ER membrane and attenuates IP3R-dependent Ca^{2+} flux in Jurkat T cells (Fredericks et al., 2014). The proper function of DHHC6 requires binding to its cofactor Selk via the SH3-binding domain in Selk. Selk deficiency also leads to decreased IP3R level, probably due to increased IP3R proteolysis. In fact, this DHHC/Selk-dependent regulation of Ca^{2+} release is shared by many immune cells. In Selk knockout mice, receptor-mediated Ca^{2+} flux is impaired in T cells, neutrophils, and macrophages, resulting in disrupted T cell proliferation, neutrophil migration, and macrophage oxidative burst (Verma et al., 2011).

Apoptosis

The ligation of Fas and FasL induces apoptosis of T cells that recognize self-antigens or are activated repeatedly, key for eliminating autoreactive T cells and preventing autoimmune diseases (Volpe et al., 2016). Palmitoylation plays critical roles in regulating the Fas-FasL signaling pathway in T cells as both Fas and FasL are palmitoylation substrates. Fas (also known as CD95, or APO1 or TNFRSF6) is a type I transmembrane protein that contains a death domain in its cytoplasmic region. Upon binding to FasL, Fas recruits death-inducing signaling complex (DISC), which, in turn, activates caspase-3 and induces programmed cell death. Promoting apoptosis signals requires Fas partition into actin cytoskeleton-linked lipid rafts and then internalization, both of which are regulated by Fas palmitoylation (Rossin et al., 2015). Mouse Fas is palmitoylated at Cys194 adjacent to the transmembrane domain, while human Fas is palmitoylated at

Cys199. One study shows that DHHC7 is responsible for the palmitoylation of Fas, and this modification stabilizes Fas by preventing its degradation by lysosomes (Rossin et al., 2015). Palmitoylation-defective Fas exerts severely reduced lipid raft localization, which impairs DISC assembly, Fas internalization, and T cell apoptosis (Chakrabandhu et al., 2007; Cruz et al., 2016). The impaired apoptosis-inducing ability of palmitoylation-defective Fas can also be observed in other Fas-expressing immune cells, like B cells and dendritic cells (Cruz et al., 2016).

Palmitoylation also participates in the signaling propagation downstream of Fas ligation, including Lck activation, PLC-γ1 phosphorylation, and proapoptotic Ca^{2+} release. 17-ODYA metabolic labeling reveals that Fas ligation leads to a rapid increase in Lck palmitoylation followed by quick de-palmitoylation, catalyzed by DHHC21 and APT1, respectively (Akimzhanov and Boehning, 2015). This rapid dynamic of Lck palmitoylation matches the activation kinetics of other signaling molecules subsequent to Fas stimulation. Re-expressing palmitoylation-defective Lck is unable to induce Fas-mediated Ca^{2+} release, caspase-3 activation, or cell death in Lck-deficient Jurkat T cells (Akimzhanov and Boehning, 2015). It is worth noting that, in abnormally or excessively activated T cells, the membrane FasL can be cleaved by metalloproteases (e.g., ADAM10 and AMDA17) to generate sFasL. sFasL binding to Fas is unable to activate Fas, thus sFasL serves as a competitor of FasL to suppress FasL-induced apoptosis (Suda et al., 1997). Shedding of FasL requires the colocalization of FasL, metalloproteinases, and Lck in lipid rafts. The lipid raft targeting of both FasL and Lck depends on palmitoylation, with FasL being palmitoylated on Cys82 and Lck at Cys3 and Cys5. Inhibition of palmitoylation with 2-BP remarkably blocks FasL shedding in T cells (Ebsen et al., 2015).

Antitumor Activity

Programmed cell death 1 (PD1), an inhibitory surface receptor of T cells, suppresses T cell activation through binding to its ligands programmed-death ligand 1 (PD-L1) and PD-L2, playing essential roles in self-tolerance. Many tumor cells often express high level of PD-L1, which inhibits the antitumor responses of T cells such as cytokine production and cytotoxicity (Juneja et al., 2017). PD-L1 is palmitoylated by DHHC3 in its cytoplasmic domain, and the attachment of palmitic acid stabilizes PD-L1 due to decreased ubiquitination. Inhibiting PD-L1 palmitoylation via 2-BP or silencing of DHHC3 greatly reduces the expression of PD-L1 in tumor cells and therefore promotes T cell-mediated antitumor immunity (Yao et al., 2019).

B Cells

B cells are specialized in producing highly specific antibodies in response to diverse foreign antigens, thus playing critical roles in adaptive immunity. They can also serve as APCs and produce a variety of cytokines (IL-6, IL-10, CXCL13, and CCL19, etc.), influencing the function of other immune cells (Fillatreau, 2018). Palmitoylation has been studied less in B cells compared to T cells. An ABE-based palmitoyl proteomic study in human B cells reveals over 100 palmitoylated proteins or candidates that are known to participate in diverse cellular events of B cells (e.g., signal transduction, vesicle fusion, molecular transport, metabolism and immune responses), highlighting the functional significance of palmitoylation in regulating B cell behaviors (Ivaldi et al., 2012).

B Cell Receptor Signaling

B cell receptor (BCR) coreceptors

B cell receptors binding to complement-tagged antigens requires the BCR coreceptor complex CD19/CD21/CD81 as they significantly lower the threshold of BCR activation to antigens. Upon BCR ligation, the BCR-CD19/CD21/CD81 complex translocates to lipid rafts for the efficient propagation of BCR-elicited signals. Similar to TCR, none of the BCR subunits are palmitoylated; yet, its co-receptor CD81 is a well-established palmitoylation substrate. CD81, which belongs to the tetraspanin superfamily, is palmitoylated at six cysteine residues in its juxtamembrane domain (Delandre et al., 2009; Yeung et al., 2018). The association of BCR and CD19/CD21/CD81 following BCR ligation rapidly promotes the palmitoylation of CD81, which regulates BCR signaling at many levels (Flaumenhaft and Sim, 2005). First, the prolonged residency of BCR-CD19/CD21/CD81 in lipid rafts depends on the palmitates attached to CD81 (Cherukuri et al., 2004). Moreover, the binding of CD81 to other co-receptors requires palmitoylation. Palmitoylation-defective CD81 exhibits impaired association with CD19 (Delandre et al., 2009). Finally, palmitoylation of CD81 affects the ability of CD81 to recruit the downstream signaling molecule 14-3-3, an adaptor protein regulating the activities of PKCs and PI3K (van Hemert et al., 2001). Inhibition of palmitoylation by 2-BP blocks BCR signaling activation, as evidenced by reduced PLCγ2 phosphorylation and Ca^{2+} mobilization (Cherukuri et al., 2004). Interestingly, CD81 palmitoylation is significantly decreased in the presence of the oxidative stress, indicating CD81 may be responsible for redox stress-induced B cell responses (Clark et al., 2004).

Adaptor proteins

Linker for activation of B cells (LAB), also known as non-T cell activation linker (NTAL), is a member of TRAPs that regulates BCR signaling. Similar to LAT, LAB is palmitoylated in a cytoplasmic juxtamembrane Cys-X-X-Cys motif and is therefore enriched in lipid rafts (Lupica et al., 1990; Brdicka et al., 2002). However, the functional impacts of LAB palmitoylation have not been explored.

Motility

Human germinal center-associated lymphoma (HGAL) is a newly identified adaptor protein regulating BCR signaling and B cell motility. HGAL is located in both plasma membrane and cytoplasm. Plasma membrane HGAL enhances BCR signaling by increasing Syk activity and its downstream Ca^{2+} mobilization (Romero-Camarero et al., 2013); cytosolic HGAL inhibits spontaneous and chemoattractant-induced B cell motility via suppressing the interaction between myosin and actin. The shuttling of HGAL between the cytoplasm to the plasma membrane requires the acylation modification as HGAL does not contain transmembrane domains. [^{3}H] palmitate labeling reveals that HGAL is palmitoylated at the Cys43-F-Cys45 motif

(Lu et al., 2015). Upon BCR ligation, palmitoylation, together with myristoylation at Gly2, facilitate the translocation of HGAL into lipid rafts where it binds to Syk and enhances Syk activity. HGAL with mutation at both palmitoylation sites fails to promote the phosphorylation of Syk and downstream Ca^{2+} influx in the presence of BCR stimulation. However, acylation site mutation of HGAL results in the accumulation of HGAL in cytoplasm and therefore induces a further reduction in B cell motility in response to chemoattractants (Lu et al., 2015).

MHC II Signaling

SLP65/SLP76, Csk-interacting membrane protein (SCIMP) belongs to the TRAP family and is involved in MHC II signaling in B cells during antigen presentation. SCIMP is mainly localized in lipid rafts and directly binds to Lyn. Upon MHC II stimulation, SCIMP is phosphorylated by Lyn, which, in turn, serves as a recruiting platform to interact with SLP65/SLP76, Csk, CD81, and Grb2 and regulates downstream MHC II signals. SCIMP is palmitoylated at its juxtamembrane palmitoylation motif (Cys-X-Cys; Draber et al., 2011. The roles of palmitoylation in SCIMP function, however, remain unclear.

Other palmitoylated proteins have been identified and confirmed in B cells (Ivaldi et al., 2012). For example, CD20, a four-transmembrane protein that participates in B cell development and differentiation, is palmitoylated on Cys111 and Cys220 in its intracellular domain; the low-affinity IgE receptor FcεRII (CD23) is a transmembrane glycoprotein involved in the regulation of IgE synthesis. Palmitoylation can occur at both Cys17 and Cys18 within the intracellular domain of CD23 (Ivaldi et al., 2012). The functional impacts of palmitoylation on these proteins have not yet been investigated. Since B cells share several common signaling pathways with other immune cells, many of the aforementioned palmitoylated proteins like Ras, Gα, Lck and Fyn, IP3R, and surface receptors will not be discussed again in this section.

Natural Killer Cells

Natural killer cells are potent cytotoxic lymphocytes that mediate the elimination of potentially harmful cells such as pathogen-infected cells, tumor cells, and cells from transplanted organs. The cytotoxicity is tightly controlled by activating receptors (e.g., NKG2D) that recognize cellular stress ligands and by inhibitory receptors (e.g., LIR and KIR) that recognize MHC class I proteins on target cells (Pegram et al., 2011). So far, there are only a few studies demonstrating that palmitoylation regulates NK cytotoxicity, by either modulating secretory lysosome exocytosis in NK cells or affecting NK receptor ligands in target cells.

Syntaxin 11

Upon ligation of activating receptors, NK cells, together with its target cells, form immunological synapses at contact points. NK cells undergo secretory lysosome exocytosis, during which the secretory lysosomes move toward immunological synapses and fuse with plasma membrane to release their cytotoxic contents (e.g., perforin and granzymes). Syntaxin 11, a soluble N-ethylmaleimide-sensitive factor attachment protein receptor (SNARE), catalyzes the membrane fusion reaction via its interaction with trans-SNARE in the opposing membrane. Syntaxin 11 is palmitoylated in its C-terminal cysteine-enriched domain in NK cells (Hellewell et al., 2014). The attached palmitate is required for the association of syntaxin 11 with cell membrane as syntaxin 11 does not contain a transmembrane domain. Mutation of cysteine residues in syntaxin 11 leads to the retention of syntaxin 11 in cytoplasm, causing impaired secretory lysosome exocytosis and reduced NK cytotoxicity (Hellewell et al., 2014).

Natural killer group 2 member D (NKG2D)

NKG2D is an activating receptor abundantly expressed on NK cells, mediating the cytotoxicity of NK cells (Wensveen et al., 2018). NKG2D itself has not been reported to be palmitoylated; however, its ligand MHC-class-I-related chain A (MICA) undergoes palmitoylation modification at Cys306 and Cys307 in its cytoplasmic tail (Aguera-Gonzalez et al., 2011). The majority of MICA is expressed on cell membranes of stressed target cells, yet MICA can also be clustered into lipid rafts to be cleaved by metalloproteases to produce soluble MICA, a negative regulator of NKG2D expression and activation. Palmitoylation is required for MICA translocation to lipid rafts and its subsequent shedding; mutation of palmitoylation sites greatly reduces the production of soluble MICA (Aguera-Gonzalez et al., 2011).

Leukocyte ig-like receptor (LIR)

LIR is an inhibitor receptor on NK cells that binds to MHC class I proteins on target cells, suppressing NK cell cytotoxicity and preventing NK cells from lysing normal "self" cells. MHC class I proteins are glycoproteins expressed on the plasma membrane of all nucleated cells in vertebrates (Hewitt, 2003). Some of the MHC class I proteins share the same unique cysteine residues in their cytoplasmic tails. Mutation of these cysteine residues abolishes the palmitoylation modification on these proteins. Concomitantly, their surface expression, extracellular confirmation, and interaction with LIR are all disrupted by cysteine residue mutation (Gruda et al., 2007). Whether palmitoylation plays a causative role in these impairments needs to be further elucidated.

INDIRECT REGULATION OF LEUKOCYTE FUNCTION BY EC PROTEIN PALMITOYLATION

Palmitoylation also regulates the function of non-immune cells that interact with leukocytes, thus indirectly affecting leukocyte functions and behaviors. A key initiation event of inflammation is the engagement of ECs with leukocytes. Our previous observations with ECs indicate that inflammatory mediators trigger a rapid increase in endothelial palmitoylated proteins (Beard et al., 2016). Palmitoylation is involved in many endothelial responses, such as the surface expression of adhesion molecules, secretion of vasoactive molecules (e.g., nitric oxide), and EC junction integrity. In our previous study, we show that the palmitoylation inhibitor 2-BP greatly attenuates the ICAM-1 surface expression of ECs in response to IL-1β

and blocks leukocyte-EC adhesion *in vitro*. In rats subjected to LPS stimulation, leukocyte slow-rolling and adhesion to postcapillary venules are remarkably inhibited by 2-BP. DHHC21 serves as one responsible PAT mediating leukocyte adhesion since DHHC21 loss-of-function greatly reduces the number of slow-rolling and adherent leukocytes in LPS-treated mice (Beard et al., 2016). In addition, junctional adhesion molecule c (JAM-C) is another palmitoylation-modified adhesion molecule that regulates leukocyte behaviors. JAM-C belongs to the immunoglobin superfamily and contains the PDZ-binding motif. Endothelial JAM-C is located at cell-cell contact, especially in tight junctions, interacting with other PDZ motif-containing molecules like JAM-B and ZO-1. JAM-C and JAM-B promote leukocyte adhesion and transmigration due to their ability to act as counterreceptors for Mac-1 and VLA-4, respectively (Bradfield et al., 2007; Scheiermann et al., 2009). JAM-C is palmitoylated at Cys264 and 265 by DHHC7, and the palmitoylation of JAM-C is required for its tight junction localization. Functionally, palmitoylation of JAM-C affects the transmigration of lung cancer cells (Aramsangtienchai et al., 2017). However, the functional impacts of JAM-C palmitoylation on leukocyte adhesion and transmigration need to be further investigated.

Endothelial nitric oxide synthase, which produces nitric oxide (NO), is a well-established palmitoylated substrate. Beyond its vasodilation function, eNOS-derived NO also exhibits important anti-inflammatory effects. Many studies have established that NO suppresses leukocyte adhesion, partly due to its ability to decrease the expression of adhesion molecules both on ECs and leukocytes, like VCAM-1, MCP-1 and CD11/CD18 (Shu et al., 2015). eNOS is primarily localized in Golgi and caveolae (Liu et al., 1996). It is dually acylated by both N-myristoylation at Gly2 and palmitoylation at Cys15 and Cys26 (Sessa et al., 1993; Liu et al., 1995). Palmitoylation of eNOS in ECs is highly dynamic with a turnover rate of 45 min. Multiple DHHCs (2,3,7,8,21) participate in the palmitoylation of eNOS. Inhibiting palmitoylation of eNOS via knockdown of DHHC21 leads to eNOS mislocalization and impaired production of NO in ECs (Liu et al., 1995; Fernandez-Hernando et al., 2006). It is plausible that this reduction in NO caused by DHHC21 knockdown then alters leukocyte function and behaviors.

CONCLUDING REMARKS AND PERSPECTIVE

The dynamic reaction of palmitoylation and de-palmitoylation rapidly and effectively regulates protein conformation, localization, lipid raft partitioning, intracellular trafficking, stability, and interactions with other proteins in leukocytes. Protein palmitoylation has great impact on many aspects of leukocyte function, including adhesion, transmigration, chemotaxis, phagocytosis, pathogen recognition, TCR and BCR signaling activation, cytotoxicity, cytokine production, and apoptosis. Despite the advancement in the field of palmitoylation, many critical issues remain. First, hundreds of putative palmitoylated proteins have been identified in leukocytes via large-scale palmitoyl proteomics, yet only a very small portion of them have been validated for functional impact. The large body of unexplored data contains extensive novel knowledge on palmitoylation in leukocytes that requires further investigation. Second, current understanding on how palmitoylation affects leukocyte proteins has been primarily concentrated on palmitoylation-mediated protein partitioning into membrane and/or lipid rafts; yet other regulatory mechanisms of palmitoylation have been studied to a much lesser extent. To acquire more comprehensive knowledge on palmitoylation, it will be essential to also understand its relationship with other PTMs (e.g., phosphorylation and ubiquitination), its impact on protein conformation, and its ability to mediate protein-protein interaction. Finally, our current knowledge on enzymes that catalyze palmitoylation and de-palmitoylation is still very limited, and the molecular basis of substrate recognition remains largely unknown. There is an urgent need for developing DHHC-selective inhibitors, as the most commonly used inhibitor 2-BP has been shown to exert off-target effects by interfering with fatty acid metabolism (Davda et al., 2013). Mechanisms regulating DHHC activity and substrate specificity will serve as a key in the development of DHHC specific inhibitors.

Taken together, palmitoylation influences many aspects of leukocyte function by altering protein localization and activity. Targeting palmitoylation may serve as a promising therapeutic strategy for aberrant immune responses during inflammatory injury, immune disorders, and infectious diseases.

AUTHOR CONTRIBUTIONS

XY performed literature search, drafted the manuscript, and prepared the figures. YM, VC, and SYY edited and revised the manuscript. EZ edited the manuscript and revised the figures. SYY initiated, directed, and sponsored the work throughout all levels of development. All authors approved it for publication.

FUNDING

This work was supported by NIH R35 HL150732 (to SYY) and R01 GM097270 (to SYY).

REFERENCES

Aguera-Gonzalez, S., Gross, C. C., Fernandez-Messina, L., Ashiru, O., Esteso, G., Hang, H. C., et al. (2011). Palmitoylation of MICA, a ligand for NKG2D, mediates its recruitment to membrane microdomains and promotes its shedding. *Eur. J. Immunol.* 41, 3667–3676. doi: 10.1002/eji.201141645

Aicart-Ramos, C., Valero, R. A., and Rodriguez-Crespo, I. (2011). Protein palmitoylation and subcellular trafficking. *Biochim. Biophys. Acta* 1808, 2981–2994. doi: 10.1016/j.bbamem.2011.07.009

Akimzhanov, A. M., and Boehning, D. (2015). Rapid and transient palmitoylation of the tyrosine kinase Lck mediates Fas signaling. *Proc. Natl. Acad. Sci. U S A* 112, 11876–11880. doi: 10.1073/pnas.1509929112

Alonso, M. A., and Millan, J. (2001). The role of lipid rafts in signalling and membrane trafficking in T lymphocytes. *J. Cell Sci.* 114(Pt 22), 3957–3965.

Aramsangtienchai, P., Spiegelman, N. A., Cao, J., and Lin, H. (2017). S-Palmitoylation of Junctional Adhesion Molecule C Regulates Its Tight Junction Localization and Cell Migration. *J. Biol. Chem.* 292, 5325–5334. doi: 10.1074/jbc.M116.730523

Arcaro, A., Gregoire, C., Bakker, T. R., Baldi, L., Jordan, M., Goffin, L., et al. (2001). CD8beta endows CD8 with efficient coreceptor function by coupling T cell receptor/CD3 to raft-associated CD8/p56(lck) complexes. *J. Exp. Med.* 194, 1485–1495. doi: 10.1084/jem.194.10.1485

Artyomov, M. N., Lis, M., Devadas, S., Davis, M. M., and Chakraborty, A. K. (2010). CD4 and CD8 binding to MHC molecules primarily acts to enhance Lck delivery. *Proc. Natl. Acad. Sci. U S A* 107, 16916–16921. doi: 10.1073/pnas.1010568107

Baker, T. L., Zheng, H., Walker, J., Coloff, J. L., and Buss, J. E. (2003). Distinct rates of palmitate turnover on membrane-bound cellular and oncogenic H-ras. *J. Biol. Chem.* 278, 19292–19300. doi: 10.1074/jbc.M206956200

Balamuth, F., Brogdon, J. L., and Bottomly, K. (2004). CD4 raft association and signaling regulate molecular clustering at the immunological synapse site. *J. Immunol.* 172, 5887–5892. doi: 10.4049/jimmunol.172.10.5887

Barnes, N. C., Powell, M. S., Trist, H. M., Gavin, A. L., Wines, B. D., and Hogarth, P. M. (2006). Raft localisation of FcgammaRIIa and efficient signaling are dependent on palmitoylation of cysteine 208. *Immunol. Lett.* 104, 118–123. doi: 10.1016/j.imlet.2005.11.007

Baumgart, F., Corral-Escariz, M., Perez-Gil, J., and Rodriguez-Crespo, I. (2010). Palmitoylation of R-Ras by human DHHC19, a palmitoyl transferase with a CaaX box. *Biochim. Biophys. Acta* 1798, 592–604. doi: 10.1016/j.bbamem.2010.01.002

Beard, R. S. Jr., Yang, X., Meegan, J. E., Overstreet, J. W., and Yang, C. G. (2016). Palmitoyl acyltransferase DHHC21 mediates endothelial dysfunction in systemic inflammatory response syndrome. *Nat. Commun.* 7:12823. doi: 10.1038/ncomms12823

Berg, V., Rusch, M., Vartak, N., Jungst, C., Schauss, A., Waldmann, H., et al. (2015). miRs-138 and -424 control palmitoylation-dependent CD95-mediated cell death by targeting acyl protein thioesterases 1 and 2 in CLL. *Blood* 125, 2948–2957. doi: 10.1182/blood-2014-07586511

Bijlmakers, M. J. (2009). Protein acylation and localization in T cell signaling (Review). *Mol. Membr. Biol.* 26, 93–103. doi: 10.1080/09687680802650481

Bijlmakers, M. J., and Marsh, M. (2003). The on-off story of protein palmitoylation. *Trends Cell Biol.* 13, 32–42. doi: 10.1016/s0962-8924(02)000089

Blanpain, C., Wittamer, V., Vanderwinden, J. M., Boom, A., Renneboog, B., Lee, B., et al. (2001). Palmitoylation of CCR5 is critical for receptor trafficking and efficient activation of intracellular signaling pathways. *J. Biol. Chem.* 276, 23795–23804. doi: 10.1074/jbc.M100583200

Blaskovic, S., Blanc, M., and van der Goot, F. G. (2013). What does S-palmitoylation do to membrane proteins? *FEBS J.* 280, 2766–2774. doi: 10.1111/febs.12263

Borzecka-Solarz, K., Dembinska, J., Hromada-Judycka, A., Traczyk, G., Ciesielska, A., Ziemlinska, E., et al. (2017). Association of Lyn kinase with membrane rafts determines its negative influence on LPS-induced signaling. *Mol. Biol. Cell* 28, 1147–1159. doi: 10.1091/mbc.E16-090632

Bournazos, S., Hart, S. P., Chamberlain, L. H., Glennie, M. J., and Dransfield, I. (2009). Association of FcgammaRIIa (CD32a) with lipid rafts regulates ligand binding activity. *J. Immunol.* 182, 8026–8036. doi: 10.4049/jimmunol.0900107

Bradfield, P. F., Scheiermann, C., Nourshargh, S., Ody, C., Luscinskas, F. W., Rainger, G. E., et al. (2007). JAM-C regulates unidirectional monocyte transendothelial migration in inflammation. *Blood* 110, 2545–2555. doi: 10.1182/blood-2007-03078733

Brdicka, T., Imrich, M., Angelisova, P., Brdickova, N., Horvath, O., Spicka, J., et al. (2002). Non-T cell activation linker (NTAL): a transmembrane adaptor protein involved in immunoreceptor signaling. *J. Exp. Med.* 196, 1617–1626. doi: 10.1084/jem.20021405

Brigidi, G. S., and Bamji, S. X. (2013). Detection of protein palmitoylation in cultured hippocampal neurons by immunoprecipitation and acyl-biotin exchange (ABE). *J. Vis. Exp.* 72:50031. doi: 10.3791/50031

Camp, L. A., and Hofmann, S. L. (1993). Purification and properties of a palmitoyl-protein thioesterase that cleaves palmitate from H-Ras. *J. Biol. Chem.* 268, 22566–22574.

Chakrabandhu, K., Herincs, Z., Huault, S., Dost, B., Peng, L., Conchonaud, F., et al. (2007). Palmitoylation is required for efficient Fas cell death signaling. *EMBO J.* 26, 209–220. doi: 10.1038/sj.emboj.7601456

Charrin, S., Manie, S., Oualid, M., Billard, M., Boucheix, C., and Rubinstein, E. (2002). Differential stability of tetraspanin/tetraspanin interactions: role of palmitoylation. *FEBS Lett.* 516, 139–144. doi: 10.1016/s0014-5793(02)02522-x

Charron, G., Zhang, M. M., Yount, J. S., Wilson, J., Raghavan, A. S., Shamir, E., et al. (2009). Robust fluorescent detection of protein fatty-acylation with chemical reporters. *J. Am. Chem. Soc.* 131, 4967–4975. doi: 10.1021/ja810122f

Cherukuri, A., Carter, R. H., Brooks, S., Bornmann, W., Finn, R., Dowd, C. S., et al. (2004). B cell signaling is regulated by induced palmitoylation of CD81. *J. Biol. Chem.* 279, 31973–31982. doi: 10.1074/jbc.M404410200

Chesarino, N. M., Hach, J. C., Chen, J. L., Zaro, B. W., Rajaram, M. V., Turner, J., et al. (2014). Chemoproteomics reveals Toll-like receptor fatty acylation. *BMC Biol.* 12:91. doi: 10.1186/s12915-014-009193

Chini, B., and Parenti, M. (2009). G-protein-coupled receptors, cholesterol and palmitoylation: facts about fats. *J. Mol. Endocrinol.* 42, 371–379. doi: 10.1677/JME-080114

Cho, E., and Park, M. (2016). Palmitoylation in Alzheimer's disease and other neurodegenerative diseases. *Pharmacol. Res.* 111, 133–151. doi: 10.1016/j.phrs.2016.06.008

Clark, K. L., Oelke, A., Johnson, M. E., Eilert, K. D., Simpson, P. C., and Todd, S. C. (2004). CD81 associates with 14-3-3 in a redox-regulated palmitoylation-dependent manner. *J. Biol. Chem.* 279, 19401–19406. doi: 10.1074/jbc.M312626200

Claudinon, J., Gonnord, P., Beslard, E., Marchetti, M., Mitchell, K., Boularan, C., et al. (2009). Palmitoylation of interferon-alpha (IFN-alpha) receptor subunit IFNAR1 is required for the activation of Stat1 and Stat2 by IFN-alpha. *J. Biol. Chem.* 284, 24328–24340. doi: 10.1074/jbc.M109.021915

Courtney, A. H., Lo, W. L., and Weiss, A. (2018). TCR Signaling: Mechanisms of Initiation and Propagation. *Trends Biochem. Sci.* 43, 108–123. doi: 10.1016/j.tibs.2017.11.008

Crise, B., and Rose, J. K. (1992). Identification of palmitoylation sites on CD4, the human immunodeficiency virus receptor. *J. Biol. Chem.* 267, 13593–13597.

Cruz, A. C., Ramaswamy, M., Ouyang, C., Klebanoff, C. A., Sengupta, P., Yamamoto, T. N., et al. (2016). Fas/CD95 prevents autoimmunity independently of lipid raft localization and efficient apoptosis induction. *Nat. Commun.* 7:13895. doi: 10.1038/ncomms13895

Davda, D., El Azzouny, M. A., Tom, C. T., Hernandez, J. L., Majmudar, J. D., Kennedy, R. T., et al. (2013). Profiling targets of the irreversible palmitoylation inhibitor 2-bromopalmitate. *ACS Chem. Biol.* 8, 1912–1917. doi: 10.1021/cb400380s

Davidson, D., Bakinowski, M., Thomas, M. L., Horejsi, V., and Veillette, A. (2003). Phosphorylation-dependent regulation of T-cell activation by PAG/Cbp, a lipid raft-associated transmembrane adaptor. *Mol. Cell Biol.* 23, 2017–2028. doi: 10.1128/mcb.23.6.2017-2028.2003

Delandre, C., Penabaz, T. R., Passarelli, A. L., Chapes, S. K., and Clem, R. J. (2009). Mutation of juxtamembrane cysteines in the tetraspanin CD81 affects palmitoylation and alters interaction with other proteins at the cell surface. *Exp. Cell Res.* 315, 1953–1963. doi: 10.1016/j.yexcr.2009.03.013

Draber, P., Vonkova, I., Stepanek, O., Hrdinka, M., Kucova, M., Skopcova, T., et al. (2011). SCIMP, a transmembrane adaptor protein involved in major histocompatibility complex class II signaling. *Mol. Cell Biol.* 31, 4550–4562. doi: 10.1128/MCB.058175811

Drisdel, R. C., and Green, W. N. (2004). Labeling and quantifying sites of protein palmitoylation. *Biotechniques* 36, 276–285. doi: 10.2144/04362RR02

Duncan, J. A., and Gilman, A. G. (1998). A cytoplasmic acyl-protein thioesterase that removes palmitate from G protein alpha subunits and p21(RAS). *J. Biol. Chem.* 273, 15830–15837. doi: 10.1074/jbc.273.25.15830

Ebsen, H., Lettau, M., Kabelitz, D., and Janssen, O. (2015). Subcellular localization and activation of ADAM proteases in the context of FasL shedding in T lymphocytes. *Mol. Immunol.* 65, 416–428. doi: 10.1016/j.molimm.2015.02.008

Fernandez-Hernando, C., Fukata, M., Bernatchez, P. N., Fukata, Y., Lin, M. I., Bredt, D. S., et al. (2006). Identification of Golgi-localized acyl transferases that palmitoylate and regulate endothelial nitric oxide synthase. *J. Cell Biol.* 174, 369–377. doi: 10.1083/jcb.200601051

Fessler, M. B., Rudel, L. L., and Brown, J. M. (2009). Toll-like receptor signaling links dietary fatty acids to the metabolic syndrome. *Curr. Opin. Lipidol.* 20, 379–385. doi: 10.1097/MOL.0b013e32832fa5c4

Filipp, D., Zhang, J., Leung, B. L., Shaw, A., Levin, S. D., Veillette, A., et al. (2003). Regulation of Fyn through translocation of activated Lck into lipid rafts. *J. Exp. Med.* 197, 1221–1227. doi: 10.1084/jem.20022112

Filippi, M. D., Szczur, K., Harris, C. E., and Berclaz, P. Y. (2007). Rho GTPase Rac1 is critical for neutrophil migration into the lung. *Blood* 109, 1257–1264. doi: 10.1182/blood-2006-04017731

Fillatreau, S. (2018). B cells and their cytokine activities implications in human diseases. *Clin. Immunol.* 186, 26–31. doi: 10.1016/j.clim.2017.07.020

Fitzer-Attas, C. J., Lowry, M., Crowley, M. T., Finn, A. J., Meng, F., DeFranco, A. L., et al. (2000). Fcgamma receptor-mediated phagocytosis in macrophages lacking the Src family tyrosine kinases Hck, Fgr, and Lyn. *J. Exp. Med.* 191, 669–682. doi: 10.1084/jem.191.4.669

Flaumenhaft, R., and Sim, D. S. (2005). Protein palmitoylation in signal transduction of hematopoietic cells. *Hematology* 10, 511–519. doi: 10.1080/10245330500141507

Forrester, M. T., Hess, D. T., Thompson, J. W., Hultman, R., Moseley, M. A., Stamler, J. S., et al. (2011). Site-specific analysis of protein S-acylation by resin-assisted capture. *J. Lipid. Res.* 52, 393–398. doi: 10.1194/jlr.D011106

Fredericks, G. J., Hoffmann, F. W., Rose, A. H., Osterheld, H. J., Hess, F. M., Mercier, F., et al. (2014). Stable expression and function of the inositol 1,4,5-triphosphate receptor requires palmitoylation by a DHHC6/selenoprotein K complex. *Proc. Natl. Acad. Sci. U S A* 111, 16478–16483. doi: 10.1073/pnas.1417176111

Futosi, K., Fodor, S., and Mocsai, A. (2013). Neutrophil cell surface receptors and their intracellular signal transduction pathways. *Int. Immunopharmacol.* 17, 638–650. doi: 10.1016/j.intimp.2013.06.034

Gadalla, M. R., and Veit, M. (2020). Toward the identification of ZDHHC enzymes required for palmitoylation of viral protein as potential drug targets. *Expert. Opin. Drug. Discov.* 15, 159–177. doi: 10.1080/17460441.2020.1696306

Gao, X., and Hannoush, R. N. (2014). Single-cell imaging of Wnt palmitoylation by the acyltransferase porcupine. *Nat. Chem. Biol.* 10, 61–68. doi: 10.1038/nchembio.1392

Gonzalez-Navajas, J. M., Lee, J., David, M., and Raz, E. (2012). Immunomodulatory functions of type I interferons. *Nat. Rev. Immunol.* 12, 125–135. doi: 10.1038/nri3133

Gordon, D. E., Jang, G. M., Bouhaddou, M., Xu, J., Obernier, K., White, K. M., et al. (2020). A SARS-CoV-2 protein interaction map reveals targets for drug repurposing. *Nature* 583, 459–468. doi: 10.1038/s41586-020-22862289

Greaves, J., and Chamberlain, L. H. (2007). Palmitoylation-dependent protein sorting. *J. Cell Biol.* 176, 249–254. doi: 10.1083/jcb.200610151

Gruda, R., Achdout, H., Stern-Ginossar, N., Gazit, R., Betser-Cohen, G., Manaster, I., et al. (2007). Intracellular cysteine residues in the tail of MHC class I proteins are crucial for extracellular recognition by leukocyte Ig-like receptor 1. *J. Immunol.* 179, 3655–3661. doi: 10.4049/jimmunol.179.6.3655

Gupta, P., Soyombo, A. A., Atashband, A., Wisniewski, K. E., Shelton, J. M., Richardson, J. A., et al. (2001). Disruption of PPT1 or PPT2 causes neuronal ceroid lipofuscinosis in knockout mice. *Proc. Natl. Acad. Sci. U S A* 98, 13566–13571. doi: 10.1073/pnas.251485198

Hancock, J. F., Paterson, H., and Marshall, C. J. (1990). A polybasic domain or palmitoylation is required in addition to the CAAX motif to localize p21ras to the plasma membrane. *Cell* 63, 133–139. doi: 10.1016/0092-8674(90)90294-o

Hang, H. C., Geutjes, E. J., Grotenbreg, G., Pollington, A. M., Bijlmakers, M. J., and Ploegh, H. L. (2007). Chemical probes for the rapid detection of Fatty-acylated proteins in Mammalian cells. *J. Am. Chem. Soc.* 129, 2744–2745. doi: 10.1021/ja0685001

Hannoush, R. N., and Arenas-Ramirez, N. (2009). Imaging the lipidome: omega-alkynyl fatty acids for detection and cellular visualization of lipid-modified proteins. *ACS Chem. Biol.* 4, 581–587. doi: 10.1021/cb900085z

Hansen, A. L., Buchan, G. J., Ruhl, M., Mukai, K., Salvatore, S. R., Ogawa, E., et al. (2018). Nitro-fatty acids are formed in response to virus infection and are potent inhibitors of STING palmitoylation and signaling. *Proc. Natl. Acad. Sci. U S A* 115, E7768–E7775. doi: 10.1073/pnas.1806239115

Hansen, A. L., Mukai, K., Schopfer, F. J., Taguchi, T., and Holm, C. K. (2019). STING palmitoylation as a therapeutic target. *Cell Mol. Immunol.* 16, 236–241. doi: 10.1038/s41423-019-0205205

Harder, T., and Kuhn, M. (2000). Selective accumulation of raft-associated membrane protein LAT in T cell receptor signaling assemblies. *J. Cell Biol.* 151, 199–208. doi: 10.1083/jcb.151.2.199

He, Y., and Linder, M. E. (2009). Differential palmitoylation of the endosomal SNAREs syntaxin 7 and syntaxin 8. *J. Lipid. Res.* 50, 398–404. doi: 10.1194/jlr.M800360-JLR200

Hellewell, A. L., Foresti, O., Gover, N., Porter, M. Y., and Hewitt, E. W. (2014). Analysis of familial hemophagocytic lymphohistiocytosis type 4 (FHL-4) mutant proteins reveals that S-acylation is required for the function of syntaxin 11 in natural killer cells. *PLoS One* 9:e98900. doi: 10.1371/journal.pone.0098900

Hewitt, E. W. (2003). The MHC class I antigen presentation pathway: strategies for viral immune evasion. *Immunology* 110, 163–169. doi: 10.1046/j.1365-2567.2003.01738.x

Hilger, D., Masureel, M., and Kobilka, B. K. (2018). Structure and dynamics of GPCR signaling complexes. *Nat. Struct. Mol. Biol.* 25, 4–12. doi: 10.1038/s41594-017-001117

Hind, L. E., Vincent, W. J., and Huttenlocher, A. (2016). Leading from the Back: The Role of the Uropod in Neutrophil Polarization and Migration. *Dev. Cell* 38, 161–169. doi: 10.1016/j.devcel.2016.06.031

Horejsi, V. (2004). Transmembrane adaptor proteins in membrane microdomains: important regulators of immunoreceptor signaling. *Immunol. Lett.* 92, 43–49. doi: 10.1016/j.imlet.2003.10.013

Horejsi, V., Zhang, W., and Schraven, B. (2004). Transmembrane adaptor proteins: organizers of immunoreceptor signalling. *Nat. Rev. Immunol.* 4, 603–616. doi: 10.1038/nri1414

Hornemann, T. (2015). Palmitoylation and depalmitoylation defects. *J. Inher. Metab. Dis.* 38, 179–186. doi: 10.1007/s10545-014-97539750

Hundt, M., Tabata, H., Jeon, M. S., Hayashi, K., Tanaka, Y., Krishna, R., et al. (2006). Impaired activation and localization of LAT in anergic T cells as a consequence of a selective palmitoylation defect. *Immunity* 24, 513–522. doi: 10.1016/j.immuni.2006.03.011

Hur, E. M., Son, M., Lee, O. H., Choi, Y. B., Park, C., Lee, H., et al. (2003). LIME, a novel transmembrane adaptor protein, associates with p56lck and mediates T cell activation. *J. Exp. Med.* 198, 1463–1473. doi: 10.1084/jem.20030232

Ivaldi, C., Martin, B. R., Kieffer-Jaquinod, S., Chapel, A., Levade, T., Garin, J., et al. (2012). Proteomic analysis of S-acylated proteins in human B cells reveals palmitoylation of the immune regulators CD20 and CD23. *PLoS One* 7:e37187. doi: 10.1371/journal.pone.0037187

Ivashkiv, L. B., and Donlin, L. T. (2014). Regulation of type I interferon responses. *Nat. Rev. Immunol.* 14, 36–49. doi: 10.1038/nri3581

Juneja, V. R., McGuire, K. A., Manguso, R. T., LaFleur, M. W., Collins, N., Haining, W. N., et al. (2017). PD-L1 on tumor cells is sufficient for immune evasion in immunogenic tumors and inhibits CD8 T cell cytotoxicity. *J. Exp. Med.* 214, 895–904. doi: 10.1084/jem.20160801

Kabouridis, P. S. (2006). Lipid rafts in T cell receptor signalling. *Mol. Membr. Biol.* 23, 49–57. doi: 10.1080/09687860500453673

Kabouridis, P. S., Magee, A. I., and Ley, S. C. (1997). S-acylation of LCK protein tyrosine kinase is essential for its signalling function in T lymphocytes. *EMBO J.* 16, 4983–4998. doi: 10.1093/emboj/16.16.4983

Kang, R., Wan, J., Arstikaitis, P., Takahashi, H., Huang, K., Bailey, A. O., et al. (2008). Neural palmitoyl-proteomics reveals dynamic synaptic palmitoylation. *Nature* 456, 904–909. doi: 10.1038/nature07605

Kara, S., Amon, L., Luhr, J. J., Nimmerjahn, F., Dudziak, D., and Lux, A. (2020). Impact of Plasma Membrane Domains on IgG Fc Receptor Function. *Front. Immunol.* 11:1320. doi: 10.3389/fimmu.2020.01320

Kim, S. J., Zhang, Z., Sarkar, C., Tsai, P. C., Lee, Y. C., Dye, L., et al. (2008). Palmitoyl protein thioesterase-1 deficiency impairs synaptic vesicle recycling at nerve terminals, contributing to neuropathology in humans and mice. *J. Clin. Invest.* 118, 3075–3086. doi: 10.1172/JCI33482

Kim, Y. C., Lee, S. E., Kim, S. K., Jang, H. D., Hwang, I., Jin, S., et al. (2019). Toll-like receptor mediated inflammation requires FASN-dependent MYD88 palmitoylation. *Nat. Chem. Biol.* 15, 907–916. doi: 10.1038/s41589-019-0344340

Ko, P. J., and Dixon, S. J. (2018). Protein palmitoylation and cancer. *EMBO Rep.* 19:e46666. doi: 10.15252/embr.201846666

Kong, E., Peng, S., Chandra, G., Sarkar, C., Zhang, Z., Bagh, M. B., et al. (2013). Dynamic palmitoylation links cytosol-membrane shuttling of acyl-protein

thioesterase-1 and acyl-protein thioesterase-2 with that of proto-oncogene H-ras product and growth-associated protein-43. *J. Biol. Chem.* 288, 9112–9125. doi: 10.1074/jbc.M112.421073

Korycka, J., Lach, A., Heger, E., Boguslawska, D. M., Wolny, M., Toporkiewicz, M., et al. (2012). Human DHHC proteins: a spotlight on the hidden player of palmitoylation. *Eur. J. Cell Biol.* 91, 107–117. doi: 10.1016/j.ejcb.2011.09.013

Koster, K. P., and Yoshii, A. (2019). Depalmitoylation by Palmitoyl-Protein Thioesterase 1 in Neuronal Health and Degeneration. *Front. Synap. Neurosci.* 11:25. doi: 10.3389/fnsyn.2019.00025

Kosugi, A., Hayashi, F., Liddicoat, D. R., Yasuda, K., Saitoh, S., and Hamaoka, T. (2001). A pivotal role of cysteine 3 of Lck tyrosine kinase for localization to glycolipid-enriched microdomains and T cell activation. *Immunol. Lett.* 76, 133–138. doi: 10.1016/s0165-2478(01)00174172

Kwiatkowska, K., and Ciesielska, A. (2018). Lipid-mediated regulation of pro-inflammatory responses induced by lipopolysaccharide. *Postepy Biochem.* 64, 175–182. doi: 10.18388/pb.2018_129

Ladygina, N., Martin, B. R., and Altman, A. (2011). Dynamic palmitoylation and the role of DHHC proteins in T cell activation and anergy. *Adv. Immunol.* 109, 1–44. doi: 10.1016/B978-0-12-387664-5.000017

Lammermann, T., and Kastenmuller, W. (2019). Concepts of GPCR-controlled navigation in the immune system. *Immunol. Rev.* 289, 205–231. doi: 10.1111/imr.12752

Lancaster, G. I., Langley, K. G., Berglund, N. A., Kammoun, H. L., Reibe, S., Estevez, E., et al. (2018). Evidence that TLR4 Is Not a Receptor for Saturated Fatty Acids but Mediates Lipid-Induced Inflammation by Reprogramming Macrophage Metabolism. *Cell. Metab.* 27(5):e1095. doi: 10.1016/j.cmet.2018.03.014

Lee, A. J., and Ashkar, A. A. (2018). The Dual Nature of Type I and Type II Interferons. *Front. Immunol.* 9:2061. doi: 10.3389/fimmu.2018.02061

Liang, X., Nazarian, A., Erdjument-Bromage, H., Bornmann, W., Tempst, P., and Resh, M. D. (2001). Heterogeneous fatty acylation of Src family kinases with polyunsaturated fatty acids regulates raft localization and signal transduction. *J. Biol. Chem.* 276, 30987–30994. doi: 10.1074/jbc.M104018200

Lin, D. T., and Conibear, E. (2015). ABHD17 proteins are novel protein depalmitoylases that regulate N-Ras palmitate turnover and subcellular localization. *Elife* 4:e11306. doi: 10.7554/eLife.11306

Lisman, T. (2018). Platelet-neutrophil interactions as drivers of inflammatory and thrombotic disease. *Cell Tissue Res.* 371, 567–576. doi: 10.1007/s00441-017-27272724

Liu, J., Garcia-Cardena, G., and Sessa, W. C. (1995). Biosynthesis and palmitoylation of endothelial nitric oxide synthase: mutagenesis of palmitoylation sites, cysteines-15 and/or -26, argues against depalmitoylation-induced translocation of the enzyme. *Biochemistry* 34, 12333–12340. doi: 10.1021/bi00038a029

Liu, J., Garcia-Cardena, G., and Sessa, W. C. (1996). Palmitoylation of endothelial nitric oxide synthase is necessary for optimal stimulated release of nitric oxide: implications for caveolae localization. *Biochemistry* 35, 13277–13281. doi: 10.1021/bi961720e

Liu, J., Qian, C., and Cao, X. (2016). Post-Translational Modification Control of Innate Immunity. *Immunity* 45, 15–30. doi: 10.1016/j.immuni.2016.06.020

Lobo, S., Greentree, W. K., Linder, M. E., and Deschenes, R. J. (2002). Identification of a Ras palmitoyltransferase in Saccharomyces cerevisiae. *J. Biol. Chem.* 277, 41268–41273. doi: 10.1074/jbc.M206573200

Lu, X., Sicard, R., Jiang, X., Stockus, J. N., McNamara, G., Abdulreda, M., et al. (2015). HGAL localization to cell membrane regulates B-cell receptor signaling. *Blood* 125, 649–657. doi: 10.1182/blood-2014-04571331

Lu, Y., Zheng, Y., Coyaud, E., Zhang, C., Selvabaskaran, A., Yu, Y., et al. (2019). Palmitoylation of NOD1 and NOD2 is required for bacterial sensing. *Science* 366, 460–467. doi: 10.1126/science.aau6391

Lupica, C. R., Cass, W. A., Zahniser, N. R., and Dunwiddie, T. V. (1990). Effects of the selective adenosine A2 receptor agonist CGS 21680 on in vitro electrophysiology, cAMP formation and dopamine release in rat hippocampus and striatum. *J. Pharmacol. Exp. Ther.* 252, 1134–1141.

Ma, Y., Yang, X., Chatterjee, V., Meegan, J. E., and Beard, R. S. Jr. (2019). Role of Neutrophil Extracellular Traps and Vesicles in Regulating Vascular Endothelial Permeability. *Front. Immunol.* 10:1037. doi: 10.3389/fimmu.2019.01037

Magee, A. I., Gutierrez, L., McKay, I. A., Marshall, C. J., and Hall, A. (1987). Dynamic fatty acylation of p21N-ras. *EMBO J.* 6, 3353–3357.

Marin, E. P., Derakhshan, B., Lam, T. T., Davalos, A., and Sessa, W. C. (2012). Endothelial cell palmitoylproteomic identifies novel lipid-modified targets and potential substrates for protein acyl transferases. *Circ. Res.* 110, 1336–1344. doi: 10.1161/CIRCRESAHA.112.269514

Martin, B. R., and Cravatt, B. F. (2009). Large-scale profiling of protein palmitoylation in mammalian cells. *Nat. Methods* 6, 135–138. doi: 10.1038/nmeth.1293

Matt, L., Kim, K., Chowdhury, D., and Hell, J. W. (2019). Role of Palmitoylation of Postsynaptic Proteins in Promoting Synaptic Plasticity. *Front. Mol. Neurosci.* 12:8. doi: 10.3389/fnmol.2019.00008

Meiler, S., Baumer, Y., Huang, Z., Hoffmann, F. W., Fredericks, G. J., Rose, A. H., et al. (2013). Selenoprotein K is required for palmitoylation of CD36 in macrophages: implications in foam cell formation and atherogenesis. *J. Leukoc. Biol.* 93, 771–780. doi: 10.1189/jlb.1212647

Merrick, B. A., Dhungana, S., Williams, J. G., Aloor, J. J., Peddada, S., Tomer, K. B., et al. (2011). Proteomic profiling of S-acylated macrophage proteins identifies a role for palmitoylation in mitochondrial targeting of phospholipid scramblase 3. *Mol. Cell Proteom.* 10:M110006007. doi: 10.1074/mcp.M110.006007

Mill, P., Lee, A. W., Fukata, Y., Tsutsumi, R., Fukata, M., Keighren, M., et al. (2009). Palmitoylation regulates epidermal homeostasis and hair follicle differentiation. *PLoS Gen.* 5:e1000748. doi: 10.1371/journal.pgen.1000748

Mocsai, A., Walzog, B., and Lowell, C. A. (2015). Intracellular signalling during neutrophil recruitment. *Cardiovasc. Res.* 107, 373–385. doi: 10.1093/cvr/cvv159

Moffett, S., Mouillac, B., Bonin, H., and Bouvier, M. (1993). Altered phosphorylation and desensitization patterns of a human beta 2-adrenergic receptor lacking the palmitoylated Cys341. *EMBO J.* 12, 349–356.

Molina, T. J., Kishihara, K., Siderovski, D. P., van Ewijk, W., Narendran, A., Timms, E., et al. (1992). Profound block in thymocyte development in mice lacking p56lck. *Nature* 357, 161–164. doi: 10.1038/357161a0

Morrison, E., Kuropka, B., Kliche, S., Brugger, B., Krause, E., and Freund, C. (2015). Quantitative analysis of the human T cell palmitome. *Sci. Rep.* 5:11598. doi: 10.1038/srep11598

Moutin, E., Nikonenko, I., Stefanelli, T., Wirth, A., Ponimaskin, E., De Roo, M., et al. (2017). Palmitoylation of cdc42 Promotes Spine Stabilization and Rescues Spine Density Deficit in a Mouse Model of 22q11.2 *Deletion Syndrome*. *Cereb. Cortex.* 27, 3618–3629. doi: 10.1093/cercor/bhw183

Mukai, K., Konno, H., Akiba, T., Uemura, T., Waguri, S., Kobayashi, T., et al. (2016). Activation of STING requires palmitoylation at the Golgi. *Nat. Commun.* 7:11932. doi: 10.1038/ncomms11932

Nagaleekar, V. K., Diehl, S. A., Juncadella, I., Charland, C., Muthusamy, N., Eaton, S., et al. (2008). IP3 receptor-mediated Ca2+ release in naive CD4 T cells dictates their cytokine program. *J. Immunol.* 181, 8315–8322. doi: 10.4049/jimmunol.181.12.8315

Navarro-Lerida, I., Sanchez-Perales, S., Calvo, M., Rentero, C., Zheng, Y., Enrich, C., et al. (2012). A palmitoylation switch mechanism regulates Rac1 function and membrane organization. *EMBO J.* 31, 534–551. doi: 10.1038/emboj.2011.446

Norton, R. L., Fredericks, G. J., Huang, Z., Fay, J. D., Hoffmann, F. W., and Hoffmann, P. R. (2017). Selenoprotein K regulation of palmitoylation and calpain cleavage of ASAP2 is required for efficient FcgammaR-mediated phagocytosis. *J. Leukoc. Biol.* 101, 439–448. doi: 10.1189/jlb.2A0316-156RR

O'Brien, C. D., Lim, P., Sun, J., and Albelda, S. M. (2003). PECAM-1-dependent neutrophil transmigration is independent of monolayer PECAM-1 signaling or localization. *Blood* 101, 2816–2825. doi: 10.1182/blood-2002-082396

Palacios, E. H., and Weiss, A. (2004). Function of the Src-family kinases, Lck and Fyn, in T-cell development and activation. *Oncogene* 23, 7990–8000. doi: 10.1038/sj.onc.1208074

Pang, D. J., Hayday, A. C., and Bijlmakers, M. J. (2007). CD8 Raft localization is induced by its assembly into CD8alpha beta heterodimers, Not CD8alpha alpha homodimers. *J. Biol. Chem.* 282, 13884–13894. doi: 10.1074/jbc.M701027200

Pegram, H. J., Andrews, D. M., Smyth, M. J., Darcy, P. K., and Kershaw, M. H. (2011). Activating and inhibitory receptors of natural killer cells. *Immunol. Cell Biol.* 89, 216–224. doi: 10.1038/icb.2010.78

Percherancier, Y., Planchenault, T., Valenzuela-Fernandez, A., Virelizier, J. L., Arenzana-Seisdedos, F., and Bachelerie, F. (2001). Palmitoylation-dependent control of degradation, life span, and membrane expression of the CCR5 receptor. *J. Biol. Chem.* 276, 31936–31944. doi: 10.1074/jbc.M104013200

Petit, C. M., Chouljenko, V. N., Iyer, A., Colgrove, R., Farzan, M., Knipe, D. M., et al. (2007). Palmitoylation of the cysteine-rich endodomain of the SARS-coronavirus spike glycoprotein is important for spike-mediated cell fusion. *Virology* 360, 264–274. doi: 10.1016/j.virol.2006.10.034

Poggi, M., Kara, I., Brunel, J. M., Landrier, J. F., Govers, R., Bonardo, B., et al. (2013). Palmitoylation of TNF alpha is involved in the regulation of TNF receptor 1 signalling. *Biochim. Biophys. Acta* 1833, 602–612. doi: 10.1016/j.bbamcr.2012.11.009

Posevitz-Fejfar, A., Smida, M., Kliche, S., Hartig, R., Schraven, B., and Lindquist, J. A. (2008). A displaced PAG enhances proximal signaling and SDF-1-induced T cell migration. *Eur. J. Immunol.* 38, 250–259. doi: 10.1002/eji.200636664

Qanbar, R., and Bouvier, M. (2003). Role of palmitoylation/depalmitoylation reactions in G-protein-coupled receptor function. *Pharmacol. Ther.* 97, 1–33. doi: 10.1016/s0163-7258(02)00300305

Quast, T., Eppler, F., Semmling, V., Schild, C., Homsi, Y., Levy, S., et al. (2011). CD81 is essential for the formation of membrane protrusions and regulates Rac1-activation in adhesion-dependent immune cell migration. *Blood* 118, 1818–1827. doi: 10.1182/blood-2010-12326595

Quinn, B. J., Welch, E. J., Kim, A. C., Lokuta, M. A., Huttenlocher, A., Khan, A. A., et al. (2009). Erythrocyte scaffolding protein p55/MPP1 functions as an essential regulator of neutrophil polarity. *Proc. Natl. Acad. Sci. U S A* 106, 19842–19847. doi: 10.1073/pnas.0906761106

Rana, M. S., Lee, C. J., and Banerjee, A. (2019). The molecular mechanism of DHHC protein acyltransferases. *Biochem. Soc. Trans.* 47, 157–167. doi: 10.1042/BST20180429

Resh, M. D. (1994). Myristylation and palmitylation of Src family members: the fats of the matter. *Cell* 76, 411–413. doi: 10.1016/0092-8674(94)90104-x

Resh, M. D. (2006a). Palmitoylation of ligands, receptors, and intracellular signaling molecules. *Sci. Stke* 2006:re14. doi: 10.1126/stke.3592006re14

Resh, M. D. (2006b). Use of analogs and inhibitors to study the functional significance of protein palmitoylation. *Methods* 40, 191–197. doi: 10.1016/j.ymeth.2006.04.013

Resh, M. D. (2013). Covalent lipid modifications of proteins. *Curr. Biol.* 23, R431–R435. doi: 10.1016/j.cub.2013.04.024

Rodolfo, M., Salvi, C., Bassi, C., Rovetta, G., Melani, C., Colombo, M. P., et al. (1991). Adjuvant adoptive immunotherapy with IL2 and lymphocytes from tumor-bearing mice: in vitro tumor-stimulated lymphocytes are more effective than LAK cells. *Nat. Immun. Cell Growth Regul.* 10, 308–319.

Romero-Camarero, I., Jiang, X., Natkunam, Y., Lu, X., Vicente-Duenas, C., Gonzalez-Herrero, I., et al. (2013). Germinal centre protein HGAL promotes lymphoid hyperplasia and amyloidosis via BCR-mediated Syk activation. *Nat. Commun.* 4:1338. doi: 10.1038/ncomms2334

Ross, E. M. (1995). Protein modification. *Palmitoylation in G-protein signaling pathways. Curr. Biol.* 5, 107–109. doi: 10.1016/s0960-9822(95)0002621

Rossin, A., Durivault, J., Chakhtoura-Feghali, T., Lounnas, N., Gagnoux-Palacios, L., and Hueber, A. O. (2015). Fas palmitoylation by the palmitoyl acyltransferase DHHC7 regulates Fas stability. *Cell Death Differ.* 22, 643–653. doi: 10.1038/cdd.2014.153

Roth, A. F., Feng, Y., Chen, L., and Davis, N. G. (2002). The yeast DHHC cysteine-rich domain protein Akr1p is a palmitoyl transferase. *J. Cell Biol.* 159, 23–28. doi: 10.1083/jcb.200206120

Rusch, M., Zimmermann, T. J., Burger, M., Dekker, F. J., Gormer, K., Triola, G., et al. (2011). Identification of acyl protein thioesterases 1 and 2 as the cellular targets of the Ras-signaling modulators palmostatin B and M. *Angew. Chem. Int. Ed. Engl.* 50, 9838–9842. doi: 10.1002/anie.201102967

Salaun, C., Greaves, J., and Chamberlain, L. H. (2010). The intracellular dynamic of protein palmitoylation. *J. Cell Biol.* 191, 1229–1238. doi: 10.1083/jcb.201008160

Sardjono, C. T., Harbour, S. N., Yip, J. C., Paddock, C., Tridandapani, S., Newman, P. J., et al. (2006). Palmitoylation at Cys595 is essential for PECAM-1 localisation into membrane microdomains and for efficient PECAM-1-mediated cytoprotection. *Thromb. Haem.* 96, 756–766.

Satou, M., Nishi, Y., Yoh, J., Hattori, Y., and Sugimoto, H. (2010). Identification and characterization of acyl-protein thioesterase 1/lysophospholipase I as a ghrelin deacylation/lysophospholipid hydrolyzing enzyme in fetal bovine serum and conditioned medium. *Endocrinology* 151, 4765–4775. doi: 10.1210/en.20102412

Scheiermann, C., Colom, B., Meda, P., Patel, N. S., Voisin, M. B., Marrelli, A., et al. (2009). Junctional adhesion molecule-C mediates leukocyte infiltration in response to ischemia reperfusion injury. *Arteriosc. Thromb. Vasc. Biol.* 29, 1509–1515. doi: 10.1161/ATVBAHA.109.187559

Schmidt, M. F., and Schlesinger, M. J. (1979). Fatty acid binding to vesicular stomatitis virus glycoprotein: a new type of post-translational modification of the viral glycoprotein. *Cell* 17, 813–819. doi: 10.1016/0092-8674(79)9032190320

Sessa, W. C., Barber, C. M., and Lynch, K. R. (1993). Mutation of N-myristoylation site converts endothelial cell nitric oxide synthase from a membrane to a cytosolic protein. *Circ. Res.* 72, 921–924. doi: 10.1161/01.res.72.4.921

Shogomori, H., Hammond, A. T., Ostermeyer-Fay, A. G., Barr, D. J., Feigenson, G. W., London, E., et al. (2005). Palmitoylation and intracellular domain interactions both contribute to raft targeting of linker for activation of T cells. *J. Biol. Chem.* 280, 18931–18942. doi: 10.1074/jbc.M500247200

Shu, X., Keller, T. C. T., Begandt, D., Butcher, J. T., Biwer, L., Keller, A. S., et al. (2015). Endothelial nitric oxide synthase in the microcirculation. *Cell Mol. Life Sci.* 72, 4561–4575. doi: 10.1007/s00018-015-20212020

Silverstein, R. L., and Febbraio, M. (2009). CD36, a scavenger receptor involved in immunity, metabolism, angiogenesis, and behavior. *Sci. Signal* 2:re3. doi: 10.1126/scisignal.272re3

Sim, D. S., Dilks, J. R., and Flaumenhaft, R. (2007). Platelets possess and require an active protein palmitoylation pathway for agonist-mediated activation and in vivo thrombus formation. *Arterios. Thromb. Vasc. Biol.* 27, 1478–1485. doi: 10.1161/ATVBAHA.106.139287

Skubitz, K. M., Campbell, K. D., Iida, J., and Skubitz, A. P. (1996). CD63 associates with tyrosine kinase activity and CD11/CD18, and transmits an activation signal in neutrophils. *J. Immunol.* 157, 3617–3626.

Sobocinska, J., Roszczenko-Jasinska, P., Ciesielska, A., and Kwiatkowska, K. (2017). Protein Palmitoylation and Its Role in Bacterial and Viral Infections. *Front. Immunol.* 8:2003. doi: 10.3389/fimmu.2017.02003

Sobocinska, J., Roszczenko-Jasinska, P., Zareba-Koziol, M., Hromada-Judycka, A., Matveichuk, O. V., Traczyk, G., et al. (2018). Lipopolysaccharide Upregulates Palmitoylated Enzymes of the Phosphatidylinositol Cycle: An Insight from Proteomic Studies. *Mol. Cell Proteom.* 17, 233–254. doi: 10.1074/mcp.RA117.000050

Song, S. P., Hennig, A., Schubert, K., Markwart, R., Schmidt, P., Prior, I. A., et al. (2013). Ras palmitoylation is necessary for N-Ras activation and signal propagation in growth factor signalling. *Biochem. J.* 454, 323–332. doi: 10.1042/BJ20121799

Soyombo, A. A., and Hofmann, S. L. (1997). Molecular cloning and expression of palmitoyl-protein thioesterase 2 (PPT2), a homolog of lysosomal palmitoyl-protein thioesterase with a distinct substrate specificity. *J. Biol. Chem.* 272, 27456–27463. doi: 10.1074/jbc.272.43.27456

Spence, J. S., He, R., Hoffmann, H. H., Das, T., Thinon, E., Rice, C. M., et al. (2019). IFITM3 directly engages and shuttles incoming virus particles to lysosomes. *Nat. Chem. Biol.* 15, 259–268. doi: 10.1038/s41589-018-0213212

Steinman, R. M., and Banchereau, J. (2007). Taking dendritic cells into medicine. *Nature* 449, 419–426. doi: 10.1038/nature06175

Stoffel, R. H., Inglese, J., Macrae, A. D., Lefkowitz, R. J., and Premont, R. T. (1998). Palmitoylation increases the kinase activity of the G protein-coupled receptor kinase. *GRK6. Biochemistry* 37, 16053–16059. doi: 10.1021/bi981432d

Suda, T., Hashimoto, H., Tanaka, M., Ochi, T., and Nagata, S. (1997). Membrane Fas ligand kills human peripheral blood T lymphocytes, and soluble Fas ligand blocks the killing. *J. Exp. Med.* 186, 2045–2050. doi: 10.1084/jem.186.12.2045

Sun, C. X., Downey, G. P., Zhu, F., Koh, A. L., Thang, H., and Glogauer, M. (2004). Rac1 is the small GTPase responsible for regulating the neutrophil chemotaxis compass. *Blood* 104, 3758–3765. doi: 10.1182/blood-2004-030781

Swarthout, J. T., Lobo, S., Farh, L., Croke, M. R., Greentree, W. K., Deschenes, R. J., et al. (2005). DHHC9 and GCP16 constitute a human protein fatty acyltransferase with specificity for H- and N-Ras. *J. Biol. Chem.* 280, 31141–31148. doi: 10.1074/jbc.M504113200

Szczur, K., Xu, H., Atkinson, S., Zheng, Y., and Filippi, M. D. (2006). Rho GTPase CDC42 regulates directionality and random movement via distinct MAPK pathways in neutrophils. *Blood* 108, 4205–4213. doi: 10.1182/blood-2006-03013789

Tabaczar, S., Czogalla, A., Podkalicka, J., Biernatowska, A., and Sikorski, A. F. (2017). Protein palmitoylation: Palmitoyltransferases and their specificity. *Exp. Biol. Med.* 242, 1150–1157. doi: 10.1177/1535370217707732

Tanimura, N., Saitoh, S., Kawano, S., Kosugi, A., and Miyake, K. (2006). Palmitoylation of LAT contributes to its subcellular localization and stability. *Biochem. Biophys. Res. Commun.* 341, 1177–1183. doi: 10.1016/j.bbrc.2006.01.076

Termini, C. M., Cotter, M. L., Marjon, K. D., Buranda, T., Lidke, K. A., and Gillette, J. M. (2014). The membrane scaffold CD82 regulates cell adhesion by altering alpha4 integrin stability and molecular density. *Mol. Biol. Cell* 25, 1560–1573. doi: 10.1091/mbc.E13-110660

Tsai, F. D., Wynne, J. P., Ahearn, I. M., and Philips, M. R. (2014). Metabolic labeling of Ras with tritiated palmitate to monitor palmitoylation and depalmitoylation. *Methods Mol. Biol.* 1120, 33–41. doi: 10.1007/978-1-62703-791-4_3

Tsygankov, A. Y., Mahajan, S., Fincke, J. E., and Bolen, J. B. (1996). Specific association of tyrosine-phosphorylated c-Cbl with Fyn tyrosine kinase in T cells. *J. Biol. Chem.* 271, 27130–27137. doi: 10.1074/jbc.271.43.27130

Tuttle, D. L., Harrison, J. K., Anders, C., Sleasman, J. W., and Goodenow, M. M. (1998). Expression of CCR5 increases during monocyte differentiation and directly mediates macrophage susceptibility to infection by human immunodeficiency virus type 1. *J. Virol.* 72, 4962–4969. doi: 10.1128/JVI.72.6.4962-4969.1998

Utsumi, T., Takeshige, T., Tanaka, K., Takami, K., Kira, Y., Klostergaard, J., et al. (2001). Transmembrane TNF (pro-TNF) is palmitoylated. *FEBS Lett.* 500, 1–6. doi: 10.1016/s0014-5793(01)02576-5

van Hemert, M. J., Steensma, H. Y., and van Heusden, G. P. (2001). 14-3-3 proteins: key regulators of cell division, signalling and apoptosis. *Bioessays* 23, 936–946. doi: 10.1002/bies.1134

Verardi, R., Kim, J. S., Ghirlando, R., and Banerjee, A. (2017). Structural Basis for Substrate Recognition by the Ankyrin Repeat Domain of Human DHHC17 Palmitoyltransferase. *Structure* 25(9):e1336. doi: 10.1016/j.str.2017.06.018

Verma, S., Hoffmann, F. W., Kumar, M., Huang, Z., Roe, K., Nguyen-Wu, E., et al. (2011). Selenoprotein K knockout mice exhibit deficient calcium flux in immune cells and impaired immune responses. *J. Immunol.* 186, 2127–2137. doi: 10.4049/jimmunol.1002878

Vogel, K., and Roche, P. A. (1999). SNAP-23 and SNAP-25 are palmitoylated in vivo. *Biochem. Biophys. Res. Commun.* 258, 407–410. doi: 10.1006/bbrc.1999.0652

Vogler, O., Barcelo, J. M., Ribas, C., and Escriba, P. V. (2008). Membrane interactions of G proteins and other related proteins. *Biochim. Biophys. Acta* 1778, 1640–1652. doi: 10.1016/j.bbamem.2008.03.008

Volpe, E., Sambucci, M., Battistini, L., and Borsellino, G. (2016). Fas-Fas Ligand: Checkpoint of T Cell Functions in Multiple Sclerosis. *Front. Immunol.* 7:382. doi: 10.3389/fimmu.2016.00382

Wan, J., Roth, A. F., Bailey, A. O., and Davis, N. G. (2007). Palmitoylated proteins: purification and identification. *Nat. Protoc.* 2, 1573–1584. doi: 10.1038/nprot.2007.225

Wang, J., Hao, J. W., Wang, X., Guo, H., Sun, H. H., Lai, X. Y., et al. (2019). DHHC4 and DHHC5 Facilitate Fatty Acid Uptake by Palmitoylating and Targeting CD36 to the Plasma Membrane. *Cell Rep.* 26(1):e205. doi: 10.1016/j.celrep.2018.12.022

Wang, X., Iyer, A., Lyons, A. B., Korner, H., and Wei, W. (2019). Emerging Roles for G-protein Coupled Receptors in Development and Activation of Macrophages. *Front. Immunol.* 10:2031. doi: 10.3389/fimmu.2019.02031

Webb, Y., Hermida-Matsumoto, L., and Resh, M. D. (2000). Inhibition of protein palmitoylation, raft localization, and T cell signaling by 2-bromopalmitate and polyunsaturated fatty acids. *J. Biol. Chem.* 275, 261–270. doi: 10.1074/jbc.275.1.261

Wedegaertner, P. B., Chu, D. H., Wilson, P. T., Levis, M. J., and Bourne, H. R. (1993). Palmitoylation is required for signaling functions and membrane attachment of Gq alpha and Gs alpha. *J. Biol. Chem.* 268, 25001–25008.

Wee, J. L., Schulze, K. E., Jones, E. L., Yeung, L., Cheng, Q., Pereira, C. F., et al. (2015). Tetraspanin CD37 Regulates beta2 Integrin-Mediated Adhesion and Migration in Neutrophils. *J. Immunol.* 195, 5770–5779. doi: 10.4049/jimmunol.1402414

Wensveen, F. M., Jelencic, V., and Polic, B. (2018). NKG2D: A Master Regulator of Immune Cell Responsiveness. *Front. Immunol.* 9:441. doi: 10.3389/fimmu.2018.00441

Wolven, A., Okamura, H., Rosenblatt, Y., and Resh, M. D. (1997). Palmitoylation of p59fyn is reversible and sufficient for plasma membrane association. *Mol. Biol. Cell* 8, 1159–1173. doi: 10.1091/mbc.8.6.1159

Won, S. J., Cheung See Kit, M., and Martin, B. R. (2018). Protein depalmitoylases. *Crit. Rev. Biochem. Mol. Biol.* 53, 83–98. doi: 10.1080/10409238.2017.1409191

Yadav, R., Larbi, K. Y., Young, R. E., and Nourshargh, S. (2003). Migration of leukocytes through the vessel wall and beyond. *Thromb. Haem.* 90, 598–606. doi: 10.1160/TH03-040220

Yang, X., Claas, C., Kraeft, S. K., Chen, L. B., Wang, Z., Kreidberg, J. A., et al. (2002). Palmitoylation of tetraspanin proteins: modulation of CD151 lateral interactions, subcellular distribution, and integrin-dependent cell morphology. *Mol. Biol. Cell* 13, 767–781. doi: 10.1091/mbc.01-050275

Yao, H., Lan, J., Li, C., Shi, H., Brosseau, J. P., Wang, H., et al. (2019). Inhibiting PD-L1 palmitoylation enhances T-cell immune responses against tumours. *Nat. Biomed. Eng.* 3, 306–317. doi: 10.1038/s41551-019-0375376

Yasuda, K., Nagafuku, M., Shima, T., Okada, M., Yagi, T., Yamada, T., et al. (2002). Cutting edge: Fyn is essential for tyrosine phosphorylation of Csk-binding protein/phosphoprotein associated with glycolipid-enriched microdomains in lipid rafts in resting T cells. *J. Immunol.* 169, 2813–2817. doi: 10.4049/jimmunol.169.6.2813

Yeung, L., Hickey, M. J., and Wright, M. D. (2018). The Many and Varied Roles of Tetraspanins in Immune Cell Recruitment and Migration. *Front. Immunol.* 9:1644. doi: 10.3389/fimmu.2018.01644

Yount, J. S., Moltedo, B., Yang, Y. Y., Charron, G., Moran, T. M., Lopez, C. B., et al. (2010). Palmitoylome profiling reveals S-palmitoylation-dependent antiviral activity of IFITM3. *Nat. Chem. Biol.* 6, 610–614. doi: 10.1038/nchembio.405

Yount, J. S., Zhang, M. M., and Hang, H. C. (2013). Emerging roles for protein S-palmitoylation in immunity from chemical proteomics. *Curr. Opin. Chem. Biol.* 17, 27–33. doi: 10.1016/j.cbpa.2012.11.008

Yurchak, L. K., and Sefton, B. M. (1995). Palmitoylation of either Cys-3 or Cys-5 is required for the biological activity of the Lck tyrosine protein kinase. *Mol. Cell Biol.* 15, 6914–6922. doi: 10.1128/mcb.15.12.6914

Zeidman, R., Buckland, G., Cebecauer, M., Eissmann, P., Davis, D. M., and Magee, A. I. (2011). DHHC2 is a protein S-acyltransferase for Lck. *Mol. Membr. Biol.* 28, 473–486. doi: 10.3109/09687688.2011.630682

Zhang, W., Irvin, B. J., Trible, R. P., Abraham, R. T., and Samelson, L. E. (1999). Functional analysis of LAT in TCR-mediated signaling pathways using a LAT-deficient Jurkat cell line. *Int. Immunol.* 11, 943–950. doi: 10.1093/intimm/11.6.943

Zingler, P., Sarchen, V., Glatter, T., Caning, L., Saggau, C., Kathayat, R. S., et al. (2019). Palmitoylation is required for TNF-R1 signaling. *Cell Commun. Sign.* 17:90. doi: 10.1186/s12964-019-0405408

Conflict of Interest: The authors declare that the research was conducted in the absence of any commercial or financial relationships that could be construed as a potential conflict of interest.

frontiers in Cell and Developmental Biology

REVIEW
published: 10 November 2020
doi: 10.3389/fcell.2020.603230

The Secretive Life of Neutrophils Revealed by Intravital Microscopy

Katia De Filippo and Sara M. Rankin*

Faculty of Medicine, National Heart and Lung Institute, Imperial College London, London, United Kingdom

Neutrophils are the most abundant circulating leukocyte within the blood stream and for many years the dogma has been that these cells migrate rapidly into tissues in response to injury or infection, forming the first line of host defense. While it has previously been documented that neutrophils marginate within the vascular beds of the lung and liver and are present in large numbers within the parenchyma of tissues, such as spleen, lymph nodes, and bone marrow (BM), the function of these tissue resident neutrophils under homeostasis, in response to pathogen invasion or injury has only recently been explored, revealing the unexpected role of these cells as immunoregulators or immune helpers and also unraveling their heterogeneity and plasticity. Neutrophils are highly motile cells and the use of intravital microscopy (IVM) to image cells within their environment with little manipulation has dramatically increased our understanding of the function, migratory behavior, and interaction of these short-lived cells with other innate and adaptive immune cells. Contrary to previous dogma, these studies have shown that marginated and tissue resident neutrophils are the first responders to pathogens and injury, critical in limiting the spread of infection and contributing to the orchestration of the subsequent immune response. The interplay of neutrophils, with other neutrophils, leukocytes, and stroma cells can also modulate and tune their early and late response in order to eradicate pathogens, minimize tissue damage, and, in certain circumstances, contribute to tissue repair. In this review, we will follow the extraordinary journey of neutrophils from their origin in the BM to their death, exploring their role as tissue resident cells in the lung, spleen, lymph nodes, and skin and outlining the importance of neutrophil subsets, their functions under homeostasis, and in response to infection. Finally, we will comment on how understanding these processes in greater detail at a molecular level can lead to development of new therapeutics.

Keywords: intravital microscopy, neutrophil subsets/heterogeneity, neutrophil mobilization, neutrophil migration, tissue resident neutrophils

OPEN ACCESS

Edited by:
Zhichao Fan,
UCONN Health, United States

Reviewed by:
Bo Liu,
University of California, Berkeley, United States
Rongrong Liu,
Northwestern University, United States

****Correspondence:***
Katia De Filippo
k.de-filippo@imperial.ac.uk

Specialty section:
This article was submitted to Cell Adhesion and Migration, a section of the journal Frontiers in Cell and Developmental Biology

Received: *05 September 2020*
Accepted: *09 October 2020*
Published: *10 November 2020*

Citation:
De Filippo K and Rankin SM (2020) The Secretive Life of Neutrophils Revealed by Intravital Microscopy. Front. Cell Dev. Biol. 8:603230. doi: 10.3389/fcell.2020.603230

INTRODUCTION

Neutrophils are the most abundant circulating leukocyte within the blood stream and play a critical role as part of the innate immune system as the first responders to infection. Clinically a blood neutrophilia is recognized as a sign of infection and the presence of large numbers of these cells in tissues observed in histology slides is a sign of infection or an ongoing chronic inflammatory disease, e.g., acute respiratory distress syndrome (ARDS), chronic obstructive pulmonary disease (COPD), and the most severe cases of asthma (Kamath et al., 2005;

Hughes et al., 2019; Potey et al., 2019). While neutrophils are essential for the resolution of infections their presence and activation in tissues in the context of inflammatory diseases, leads to tissue damage, thus identifying the molecular mechanisms regulating their trafficking and activation is central to the development of drugs that can limit their recruitment and activation, for the treatment of these inflammatory diseases.

The introduction of intravital microscopy (IVM) has changed our static view of approaching the study of the immune system, allowed the study of neutrophil trafficking in real time, and led to seminal work identifying the role of specific adhesion molecules, chemokines, cytokines, and signaling molecules in orchestrating neutrophil rolling, adhesion, and migration across postcapillary venules to accumulate in tissues.

The early IVM experiments were performed using fluorescent cellular dyes such as rhodamine 6G and acridine orange that labeled nuclei or intracellular organelles in all leukocytes (Mempel et al., 2004; Taqueti and Jaffer, 2013). The not selectivity of specific leukocyte subsets and the high excitation required to detect fluorescent signal caused photodamage and altered leukocyte adhesion and microvascular fluidity (Saetzler et al., 1997). Later studies used genetically modified mice that were generated as tools for *in vivo* imaging of neutrophil behavior (Stackowicz et al., 2019). In the Lys-EGFP^{+} mice, both neutrophils and monocyte are fluorescently labeled, neutrophils exhibiting high fluorescence, while monocytes are only dim green (Faust et al., 2000). However, *Listeria* inflammation has revealed a caveat of this mouse model because during infection, both neutrophils and monocyte upregulate expression level of EGFP becoming indistinguishable (Waite et al., 2011). The mouse model called Catchup overcomes this problem because only neutrophils are fluorescently labeled in red (Hasenberg et al., 2015). Fluorochrome-conjugated Ly6G mAbs are also highly used. It has been shown that low doses of i.v. injected Ly6G mAb labels neutrophils for several hours without affecting their migratory behavior and recruitment during inflammation (Yipp and Kubes, 2013).

Intravital microscopy allows imaging at microscopic resolution of ∼1 μm and temporal resolution of millisecond within the same animal allowing live cell tracking for several hours and longitudinal sessions are also possible (Masedunskas et al., 2012). The tissue penetration depth intrinsically depends on the optical properties of the tissue imaged, with transparent tissues highly penetrable, up to 300–500 μm, while highly vascularized tissue and tissue with air/liquid interface among the less penetrable (Choo et al., 2020). Limited penetration depth together with a small field of view (FOV) to image live cell behaviors are the limitations of IVM. Among the advantages, the real-time monitoring for several hours allows the design of the experiment to include homeostasis imaging followed by tissue insults or injection of pathogens in vessel or parenchyma allowing for internal controls, increasing reproducibility and importantly reducing the number of animals used. IVM allows for the long-term observation of neutrophils within different tissues of living animals giving the chance to study their behavior in the context of different physiological environments and also during different stages of diseases. Imaging of multiple channels allows for several features such as different cell types, tissue structures, or adhesion molecules to be achieved simultaneously through systemic injection of fluorescent dyes, specific mAbs, or making use of genetically modified mice in which fluorescent tags have been inserted in cell-type specific genes. Microscopes equipped to acquire several frames/s are essential to capture the single cell dynamics of highly migrating neutrophils, the interaction of neutrophils with other cells of the immune system and stromal cells and to generate quantitative data with respect to neutrophil numbers, velocity, and migratory behavior. The versatility of applying live imaging to almost all organs has also unraveled that neutrophils have tissue-specific functions and migratory behaviors increasing our knowledge on the first line of tissue protection. Further with current interest in neutrophil heterogeneity IVM allows characterization of the response of neutrophil subtypes and has provided much of the emerging evidence that indicates that the local milieu of a tissue constitutes a microenvironment capable of influencing and modulating immune cell functions. Finally, in addition to the tissue environment and neutrophil subtype being studied, there is now a convincing body of work that shows that neutrophil dynamics in health and disease are governed by circadian rhythms.

NEUTROPHILS ORIGIN AND MOBILIZATION FROM THE BM

Hematopoietic stem cells (HSCs) that exhibit a low proliferative activity but have a high self-renewal capacity are present in stem cell niches in the bone marrow (BM) and give rise to neutrophils by the process of haematopoiesis. Thus in the BM all the different stages of neutrophil differentiation are present; the multipotent high proliferative/lower self-renewal granulocyte-monocyte progenitors (GMP), granulocyte-committed progenitor myeloblasts, neutrophil-committed promyelocyte, myelocyte and metamyelocyte, finally differentiating from the immature so-called band-form neutrophils to the fully mature segmented neutrophils, these names referencing the shape of the nucleus (Borregaard, 2010; Tak et al., 2013). A recent study, making use of Fucci-(S-G2-M) reporter mouse, in which immune cells undergoing the S, G2, and M phase of the cell-cycle are fluorescent, has allowed identification, in the BM of the last three steps of neutrophil maturation process (after GMP stage), named preNeu, immature Neu, and mature Neu with unique surface marker signatures and proliferative capabilities (Evrard et al., 2018). PreNeu was identified as a proliferative committed neutrophil precursor, Fucci^{+}, expressed Ly6G^{low}/CXCR2^{-}/c-Kit^{+}/CXCR4^{+}. Among the non-proliferative neutrophils, Fucci^{-}, were immature Neu (Ly6G$^{low/+}$/CXCR2^{-}/CD101^{-}) and mature Neu (Ly6G^{+}/CXCR2^{+}/CD101^{+}), the latter genetically similar yet not identical to the circulating neutrophils (Evrard et al., 2018). These three stages of neutrophil maturation were also found in human BM. Xie et al. (2020) have profiled more than 25,000 mouse neutrophils using single-cell RNA sequencing and found four different clusters of neutrophils present in the BM, called G1-4, partially overlapping with the ones identified by Evrard et al. (2018). They constitute

four different sequential stages in the process of neutrophil maturation and up to 24 genes were differentially expressed in each subpopulation. G1 is the more proliferative and less differentiated cluster while G4 showed the higher maturation profile constituting the fully mature neutrophil subpopulation in the BM (Xie et al., 2020).

Not all mature neutrophils egress from the BM into the circulation immediately upon maturation. A significant number of mature neutrophils are retained within the BM, referred to as the BM reserve, indeed in mice the size of the reserve is such that the ratio of mature neutrophils between the BM and blood is 300 to 1 (Furze and Rankin, 2008a). CXCL12 is a chemokine generated constitutively in the BM and evidence suggests that expression of its receptor, CXCR4, by neutrophils is critical for their retention in the BM both in human and rodents (Lapidot and Kollet, 2002; Martin et al., 2003; Eash et al., 2009) reviewed in De Filippo and Rankin (2018). Thus genetic deletion of CXCR4 was shown to result in a shift of the pool of mature neutrophils from the BM to the circulation without affecting the life-span of neutrophils (Eash et al., 2009). Static visual imaging of calvarium (**Figure 1A**) or long bones (Evrard et al., 2018) revealed that BM neutrophils are organized in clusters around the BM vasculature (**Figure 1B**) (Evrard et al., 2018) and within CXCL12-rich niches pointing to the key function of this homeostatic chemokine in neutrophil retention (Lapidot and Kollet, 2002; De Filippo and Rankin, 2018). BM-mature neutrophils are retained in large reservoirs until their need in the periphery arise to either replace dying neutrophils or to increase mature neutrophil to support the fight during infection. Despite the daily production and release of $\sim 10^{11}$ neutrophils in human and $\sim 10^{7}$ neutrophils in mice (Furze and Rankin, 2008b) to support the turnover of these short-lived cells within the whole body, applying IVM to a FOV in the calvarium or longer bones has proven that neutrophil mobilization under homeostasis is a surprisingly rare event, difficult to capture (Kohler et al., 2011; Devi et al., 2013; Pillay et al., 2020). This could be explained by the vast extension of the BM tissue that covers the cavity of the host skeleton as compared with the small FOV imaged at any one time. Thus, for example, one femur represents only 7% of the entire BM in the mouse. A similar result was obtained when studying neutrophil mobilization by transmission electron microscopy, in that while neutrophil egress could be observed it was a rare event (Burdon et al., 2008). IVM applied to the tibia BM to study the migratory behavior of single neutrophils has shown that only 30% of the entire BM neutrophils within the FOV have a basal motility of 1.5 μm/min without directionality (Kohler et al., 2011) suggesting a high level of quiescence and a minimal level of motility of neutrophils within their BM niche. During inflammation, external cues, such as granulocyte-colony-stimulating factor (G-CSF) (Semerad et al., 2002) or neutrophil chemoattractants such as CXCL1-2 can cause a rapid release of neutrophils from the BM (Burdon et al., 2008; Wengner et al., 2008; Kohler et al., 2011). Kohler et al. (2011) applying IVM to long bones have visually showed for the first time that a single systemic dose of G-CSF was sufficient to induce an increase in the motility of 75% of BM neutrophils increasing their velocity of migration up to 5 μm/min and consequently causing the egress of neutrophils from the BM into the blood stream.

AMD3100 (Plerixafor) is a CXCR4 antagonist that successfully corrects circulating numbers of neutrophils in neutropenic patients with WHIM syndrome that has been approved for clinical use (McDermott et al., 2014, 2019). WHIM syndrome is caused by a genetic mutation of the CXCR4 gene causing a gain-of-function and consequently an impairment of neutrophil mobilization from the BM that ultimately results in blood neutropenia (Hernandez et al., 2003; Gulino et al., 2004). There is controversy in the literature on whether AMD3100 stimulates neutrophil mobilization directly from the BM or from other tissues, like the lung Martin et al. (2003) and Liu et al. (2015) support mobilization from the BM while Devi et al. (2013) support neutrophil de-margination from the lung microvasculature. Using IVM of the mouse calvarium and lung, we have recently directly shown that a single dose of AMD3100 causes an increase in BM neutrophil motility observed within 30 min and mobilization from the BM niche without causing neutrophil de-margination from the lung (Pillay et al., 2020).

The process of mature neutrophil release from the BM under homeostasis is not constant during the day but fluctuates according to the circadian rhythm with a maximum mobilization during the night in mice guaranteeing the maximum number of "fresh" circulating neutrophils when these nocturnal animals are active (Casanova-Acebes et al., 2018). This is also the case for humans, but with the clock inverted (Adrover et al., 2020). The impact of circadian rhythms on neutrophil mobilization, clearance, and inflammation has been more extensively reviewed here (Scheiermann et al., 2013; Hidalgo et al., 2019; Adrover et al., 2020; Aroca-Crevillen et al., 2020).

With respect to the BM and neutrophil mobilization one question that still remains is whether all the mature neutrophils mobilized are identical or whether there are neutrophil subsets within the BM that can be differentially mobilized.

The BM is also one of the major organs where some senescent neutrophils home back at the end of their life span to be cleared by stromal macrophages and this process feeds back on the maturation of neutrophils (Gordy et al., 2011). We will discuss this in more detail later in the senescent session of this review.

CIRCULATING AND MARGINATED POOLS OF NEUTROPHILS

Electron microscopy has shown that neutrophil extravasation from the BM occurs through specialized endothelial cells that exhibit diaphragmed fenestra. Neutrophils transmigrate across this BM sinusoidal endothelium through small pores in a transcellular manner (Burdon et al., 2008). This marks the "birth" of neutrophils passing from their niche in the BM into the blood stream where they are exposed to sheer forces. Mature neutrophils kept in the BM are only genetically similar yet not equal to circulating neutrophils (Evrard et al., 2018) suggesting that the environment may impact on neutrophils and induce their genetic changes. This concept is also indirectly supported by the change of surface markers expressed by neutrophils when they

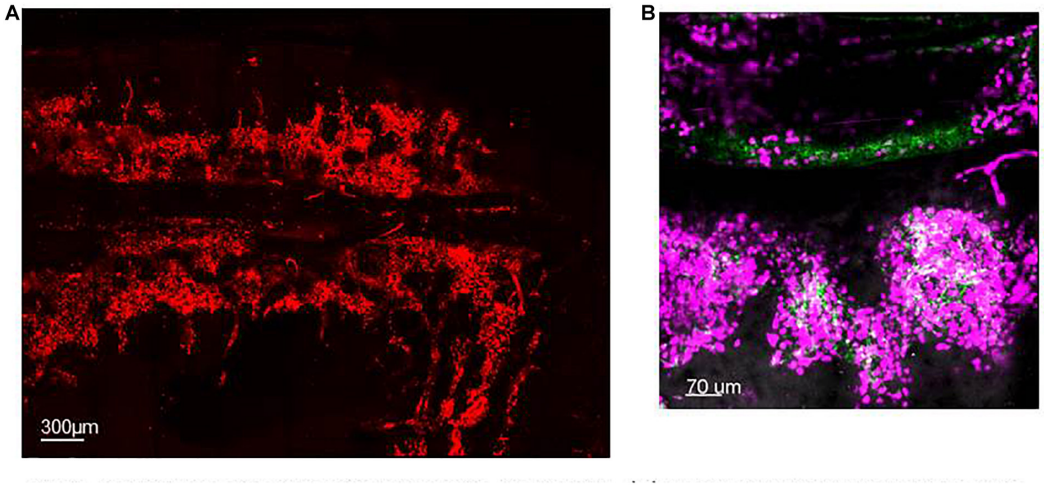

FIGURE 1 | Spatial organization of neutrophils in the BM. **(A)** Maximum projection of IVM tile scan image showing the spatial organization of neutrophils within the calvarium of mice (red). **(B)** Maximum projection of IVM tile scan image of the calvarium of mice showing clusters of neutrophils (magenta) tightly organized around BM blood vessels (green).

enter circulation (Evrard et al., 2018; He et al., 2018; Adrover et al., 2020). Based on the differential expression of more than 20 genes, in peripheral blood, three different subpopulations (G5a–c) have been identified. Xie et al. (2020) showed that blood G5a and G5b are two independent subsets of neutrophils that differentiate from G3 and G4 BM clusters, respectively.

Neutrophils are the most abundant leukocyte circulating within the blood. In this state, neutrophils do not interact with other cells and flow at a fast speed passively transported by the blood stream. The circulating number of neutrophils is the result of a fine balance between neutrophils that are mobilized from the BM (input) and neutrophils that emigrate into tissues or are cleared (output). This must be tightly regulated to avoid excessive numbers of circulating neutrophils or unregulated activation of neutrophils that could lead to vascular or tissue damage. Circadian release of neutrophils from the BM is reflected in the circadian oscillation of neutrophil number in the blood with a high number of aged neutrophils during the day and a high number of fresh neutrophils during the night in mice (Casanova-Acebes et al., 2013). These oscillations of neutrophil number are conserved among species and in human follow the opposite pattern to rodents (Adrover et al., 2020). Using an organism-wide circadian screening approach, it has been shown that circulating neutrophils in different stages of their life specifically upregulate or downregulate surface markers, including specific adhesion molecules and chemokine receptor CXCR4, that dictate their vasculature or tissue infiltration in a time-of-day-dependent manner during homeostasis and inflammation (He et al., 2018).

Within special vascular beds, under homeostasis, neutrophils can be found in direct contact with ECs, this population of neutrophils is referred to as the "marginated" or "intravascular retained" pool. The major organs where neutrophil localize within the microvessels of the blood are the lung (Gee and Albertine, 1993; Gebb et al., 1995) and the liver (Casanova-Acebes et al., 2018). It has been shown that circulating and intravascular retained neutrophils are at equilibrium and that adrenaline and physical exercise can increase the circulating pool of neutrophils, by releasing neutrophils from this intravascular compartment (Summers et al., 2010). Whether intravascular retention is an active process mediated by adhesion molecules or a passive process due to the mechanical constriction of these cells as they move through small microvessels is still under debate. However, several studies, making use of genetically modified mice, have shown that L-selectin is not essential for neutrophil margination (review Doerschuk, 2001; Kolaczkowska and Kubes, 2013). Likewise, direct imaging of lungs by IVM showed that CD11b expression on neutrophils and the β_2 integrin are not required for neutrophil margination in the microvessels of the lung but play an essential role during neutrophil locomotion toward systemic pathogens captured by lung ECs (Yipp et al., 2017).

ECs differ between tissues and have been shown to utilize different adhesion molecules to sustain neutrophil adhesion (Kolaczkowska and Kubes, 2013). Likewise, neutrophils themselves are plastic and highly adaptable cells equipped with different surface molecules so that they can adapt to interact with different types of ECs.

TISSUE NEUTROPHIL DYNAMICS UNDER HOMEOSTASIS

The dogma that under homeostasis tissues were virtually free of neutrophils was challenged by parabiotic experiments and IVM. Both these techniques directly showed that neutrophils infiltrate almost every naïve tissue apart from the reproductive organs and the brain (Casanova-Acebes et al., 2018). Moreover, the level of neutrophil infiltration is tissue-specific, with BM, spleen, lung, and liver among the highest neutrophil infiltrated organs, suggesting that these tissue resident neutrophils may

support tissue regulatory functions under homeostasis, and/or provide immune protection and surveillance under steady state (Casanova-Acebes et al., 2018). The spleen and intestine harbor neutrophils within the tissue parenchyma as an integral part of these organs elevating their surveillance functions and roles (Puga et al., 2011; Casanova-Acebes et al., 2013). As with the rhythmic fluctuation of circulating neutrophils, the absolute number of neutrophils retained in these tissues oscillates with a maximum retention within the tissues during the dark phase mirroring their maximum numbers in the blood (He et al., 2018). The circadian changes in neutrophil retention in tissues were shown to be under the control of adrenergic nerves, changing the expression of adhesion molecules, including ICAM-1, VCAM-1, P- and E-selectins, and MadCAM on the surface of ECs (Scheiermann et al., 2012) with a maximal expression at night in mice, promoting the release of neutrophils into the blood (He et al., 2018). Thus, in addition to fundamental differences in tissue microenvironments and the heterogeneity of ECs, changes in adhesion molecules driven by circadian rhythm all combine to determine neutrophil numbers in the blood and different tissue during homeostasis (Kolaczkowska and Kubes, 2013).

NEUTROPHIL DYNAMICS IN RESPONSE TO PATHOGENS

Neutrophils play a pivotal role as the first line of innate immune defense and constitute the first cells to be recruited within an infected tissue. In the absence of neutrophils, life will consist of recurrent and life frightening infections. Numbers of circulating and tissue-recruited neutrophils increase substantially during infection by several mechanisms: increased mobilization form the BM (Christopher and Link, 2007; Burdon et al., 2008), increased adhesion and transendothelial cell migration through ECs to tissues (Ley et al., 2007), and also by the extended neutrophil half-life (Tak et al., 2013; Silvestre-Roig et al., 2016). Neutrophil activation during infection has been proposed to happen via two sequential stages: priming and full activation (Summers et al., 2010; Kolaczkowska and Kubes, 2013). Neutrophils are primed by their exposure to mediators such as cytokines; increased surface expression of CD11b and decreased of L-selectin are features of activated neutrophils.

Intravital microscopy of the blood vessels in the cremaster muscle was one of the first models to be established and extensively used to study neutrophil interaction with the venular walls because of the accessibility and the transparency of the organ allowing imaging via transmitted light. This model has been used extensively to image and define the molecular mechanisms involved in the sequential phases of the leukocyte adhesion cascade, where selectins, chemokine receptors, and β_2 integrins as well as JAMs and PECAM are sequentially activated to guarantee neutrophil capture, rolling, firm adhesion, and transendothelial migration from the circulation into the infected tissue (Ley et al., 2007; Evans et al., 2009). Within activated vessels, neutrophils organize membrane protrusions at the back of the neutrophil termed the uropod that are rich in selectin ligand PSGL-1, and shown to transiently interact with activated platelets (Sreeramkumar et al., 2014). Using IVM, the PSGL-1 rich domains on neutrophils could be observed either protruding into the lumen of the blood vessels or laterally toward the endothelium to facilitate neutrophil interaction with platelets and ECs, respectively. It is the integrated signal from both activated vascular endothelium and platelets that triggers and supports neutrophil crawling within the activated blood vessels, an essential step that precedes neutrophil extravasation (Sreeramkumar et al., 2014).

Tracking neutrophil migratory behavior showed that their extravasation during challenge happens in the post capillary venules in the systemic circulation predominantly via a paracellular route and requires ∼6 min to complete (Woodfin et al., 2011). Infected tissues generate inflammatory molecules that on one hand instruct ECs to upregulate the expression of adhesion molecules to sustain vascular attachment of neutrophils, and on the other hand cause the direct activation of neutrophils and their increased diapedesis (Ley et al., 2007; Nourshargh and Alon, 2014). Moreover, IVM applied to this model has been essential to study the efficient and persistent neutrophil transmigration dissecting the sequential and unique role of the neutrophil selective chemokines, CXCL1 and CXCL2 during neutrophil diapedesis (Girbl et al., 2018). Girbl et al. (2018) showed that CXCL1, mainly produced by ECs, supported luminal and sub-EC crawling, whereas CXCL2, mainly produced by neutrophils, was essential for self-guiding neutrophils in breaching through EC junctions.

The process of neutrophil adhesion and transmigration has also been imaged in real time in an *in vitro* system of flowing human neutrophils across stimulated EC-cultured glass capillaries (Buckley et al., 2006). Using this system, neutrophils were observed to reverse the process of transendothelial migration, in a process referred to as reverse transmigration (R-TEM). IVM imaging of the cremaster muscle showed that this was not an *in vitro* artifact but occurred *in vivo* too.

Further, R-TEM was found to be a β_1-, β_2-, and β_3-integrin-independent mechanism. It was found that only neutrophils that phenotypically are ICAM-1^{high} CXCR1^{low} were able to reverse transmigrate. Tissue resident neutrophils are ICAM-1^{low} CXCR1^{low} while naïve circulating neutrophils are ICAM-1^{low} CXCR1^{high} therefore incapable of R-TEM (Buckley et al., 2006). As discussed above, high levels of the adhesion molecule JAM-C at the junctions between ECs constitute a physical barrier that regulates the polarized unidirectional transmigration of neutrophils from the lumen of vessels to the tissue (Ley et al., 2007). Loss of JAM-C by ECs at their junction was associated with a "hesitant" and R-TEM leading to the systemic dissemination of activated tissue-experienced neutrophils causing second organ injury specifically in the lung (Woodfin et al., 2011). Mechanistically it was found that LTB4 dependent release of neutrophil elastase (NE) lowered the levels of JAM-C on postcapillaries ECs, thus neutrophil activation was required to support their own R-TEM (Colom et al., 2015). Neutrophils that underwent R-TEM were uniquely characterized by a prolonged

lifespan and an inflammatory phenotype. They were found in distal organs like the lung causing tissue inflammation thereby disseminating the extent of organ injury (Woodfin et al., 2011; Hossain and Kubes, 2019).

In an infection model of *Candida albicans*, the time of day-night when the infection happens had a dramatic impact on the outcome of infection. Administration of infection during the night, when the number of aged neutrophils in the tissue was at its peak, conferred resistance to Candida (Adrover et al., 2019). The same was true in an intraperitoneal model of LPS, with the peak of recruited cells from the blood to the tissue during the dark phase (He et al., 2018). Collectively these circadian studies stress the fact that experimental variability in the number of recruited neutrophils to specific tissues could be related to the time of day when experiments are performed.

It is thought that resident populations of neutrophils in tissues can be rapidly deployed to mount a localized host response to pathogens, thus marginated neutrophils in the lung microvasculature constitute a critical part of the rapid lung immune response. Very little is currently known about the turnover of tissue resident neutrophils during homeostasis and the mechanisms required to keep these highly cytotoxic cells from causing tissue damage. During *Escherichia coli* challenge, it was shown that the different neutrophils subsets were still present but the transcriptional activity of several genes increased in each population (Xie et al., 2020).

Apart from this rapid deployment of neutrophils from the periphery to the site of infection, the function and role of tissue resident neutrophils need to be determined. One obvious function is that there is a population of neutrophils already within the local environment ready to respond to insults, thus increasing the speed of the immune response of the host in the tissues. In theory an even more effective level of tissue protection will result if these tissue resident neutrophils have been previously "instructed" by tissue resident stroma cells. How the tissue instructs neutrophils during homeostasis and how the neutrophils exist within the tissue without inflicting damage during homeostasis are still not fully understood.

Is it extensively documented that during systemic acute diseases, such as endotoxemia and chronic diseases, such as asthma and cystic fibrosis (CF), neutrophils showed plasticity with the appearance in both mouse and human of neutrophil subsets, identified by differential expression of surface molecules including, CD177, CD49d, VEGF-R1, CD11b, CD18, and CXCR4, and displaying different functional responses, review by Silvestre-Roig et al. (2016). Thus airway neutrophils from asthmatics and patients with CF exhibit metabolic reprogramming and a substantially prolonged lifespan, both of which have been shown to contribute to disease severity (Garlichs et al., 2004; Uddin et al., 2010; Laval et al., 2013). Moreover, transcriptional plasticity has been reported for neutrophils during inflammation and disease, suggesting that neutrophils adapt and respond to local environmental cues (Silvestre-Roig et al., 2016). Taken together these studies demonstrate that neutrophils exhibit plasticity and heterogeneity in the context of an inflammatory tissue environment. However, as yet it is not known whether the heterogeneity is intrinsic in neutrophils at birth or acquired during tissue persistence.

Many other factors can affect neutrophil trafficking including age, gender, diet, gut microbiota, metabolism, or genetics but these are outside the scope of this review.

One limitation of IVM is the number of cell types/surface adhesion molecules that can be directly and longitudinally tracked at any one time, due to the number of channels that can be imaged simultaneously. Currently usually three to four channels are imaged simultaneously by fluorescent IVM. To overcome this limitation, there is a move to use simultaneous label-free autofluorescent-multiharmonic microscopy (SLAM). This technique relies on the fact that different cells and ECM can be identified by their morphology, autofluorescence, and harmonic generation, thus there is no need to fluorescently label cells of interest. This technique can be used to visualize cell–stroma interactions, tissue remodeling, and metabolic activity (You et al., 2018). In one study using SLAM, it was shown that while the number of leukocytes increased and formed clusters in tissues in response to LPS, the density of collagen fibers and lipids decreased leaving space for the recruited leukocytes (You et al., 2018). Moreover, SLAM revealed that the local tissue environment was hypoxic and that the clustered leukocytes showed a reduced redox ratio indicating an increase in metabolic activity (You et al., 2018). Thus SLAM provides different information to IVM; however, it lacks the ability to unequivocally identify leukocyte subtypes or different subsets of neutrophils, thus SLAM could constitute a complementary approach to use alongside IVM.

NEUTROPHIL MARGINATION IN THE CAPILLARY OF THE SKIN AND MIGRATION WITHIN THE DERMA-SKIN AFTER CHALLENGE OR DAMAGE

The skin is a vast organ at the interface with the outside world and a robust level of defense must be provided to protect and quickly respond to potential harmful invading pathogens. Because vessels and tissue can be imaged directly through the skin, no surgery is required. Imaging of the mouse footpad has been extensively used as a model to unravel neutrophil migratory behavior in the derma (Zinselmeyer et al., 2008), while a more recent advanced method has been developed to study the epidermis and dermis of the mouse ear and dorsal skin (Li et al., 2012).

During homeostasis, visual imaging showed that neutrophils flow in the microvessels of the footpad at several hundred μm/s and rarely adhere to the endothelium of the skin (Zinselmeyer et al., 2008). Neutrophils reside transiently and in a small number within the connective tissue of the skin-derma and constantly exit via lymphatics during homeostasis (Ng et al., 2011) constituting a direct line of tissue protection.

The use of IVM to study the neutrophil dynamics during subcutaneous injection of parasites *Leishmaniasis* has shown

that neutrophils are involved in both protection of the host and disease progression (Peters et al., 2008). Thus 30 min post infection, IVM reveals a substantial accumulation of neutrophils inside the blood vessels near the infected area and subsequent diapedesis into the skin parenchyma (Peters et al., 2008; Zinselmeyer et al., 2008; Graham et al., 2009). Using IVM the interplay of neutrophils and macrophages in the clearance of parasites from the skin was observed, showing that apoptotic neutrophils decrease their velocity from 4–14 to 0–6 μm/min and release the parasites in the vicinity of the tissue macrophages for final clearance (Peters et al., 2008). However, surprisingly, in a neutrophil-depleted model, the dissemination and survival of parasites was reduced suggesting that neutrophils can also act like a "Trojan horse" supporting the spread of the live pathogens to distant organs (Peters et al., 2008). In a similar manner, Duffy et al. (2012) observed that during a dermal viral infection, neutrophils were able to migrate in a CCR1-dependent manner from the dermis to the BM carrying the virus, again functioning like a "Trojan horse," but in this context they interacted with antigen presenting cells (APCs) and primed BM CD8 T cells to mount an adaptive immune response. Moreover, in models of sterile dermal tissue damage caused by laser and during several cutaneous infections, single cell tracking of neutrophils by IVM revealed that they rapidly switched their probing migratory behavior during homeostasis into a highly directional mode of migration during tissue damage that reached mean velocity of 7.8 ± 2.5 μm/min (Graham et al., 2009; Ng et al., 2011), swarming around the damaged area of tissue or site of infection to clear the pathogens (Lammermann et al., 2013). By real-time investigation, Ng et al. (2011) showed that neutrophil locomotion occurs in three sequential phases with a few "scouting" neutrophils observed arriving within the first 15 min post damage, followed by an amplification phase with a synchronized attraction of a high number of neutrophils that traveled up to 150 μm and a stabilized phase in which neutrophils clustered around the damaged area. IVM allowed Lammermann et al. (2013) to show that in a radius of more than 300 μm, neutrophils sensed and directionally migrated toward the tissue lesion for up to 40 min.

In the model of *Staphylococcus aureus*, IVM was an essential tool to study the host–pathogen interaction, neutrophil migration, and abscess formation in the skin following infection (Liese et al., 2013). Moreover, IVM applied to a mouse skin flap with intact blood flow, allowed Liese et al. (2013) to dissect at the molecular level the temporal migratory dynamics of neutrophils during dermal infection showing that interstitial neutrophil migration during pathogen challenge is G-protein coupled receptor- and IL-1R-dependent process.

Intravital microscopy has also permitted the observation of neutrophil behavior within small capillaries, showing that neutrophils are dramatically elongated and are indecisively crawling back and forth over a distance of ∼100 μm closer to the subcutaneous nidus of *S. aureus* infection to prevent pathogen dissemination (Harding et al., 2014). This migratory behavior is LFA-1- and VLA-4-dependent but Mac-1-independent. Only a small number of those crawling neutrophils were observed exiting at the postcapillary venules and were recruited in the infected area (Harding et al., 2014).

NEUTROPHILS MARGINATE WITHIN THE MICROCAPILLARIES OF THE LUNG

In humans, the microvessels of the lung form an intricate network of approximately 2.8×10^{11} capillaries covering an estimated 10^8 alveoli (Hogg and Doerschuk, 1995), with diameters spanning from 2 to 15 μm they guaranty O_2–CO_2 exchange, thereby support gaseous exchange requirements for every single cell of the body. The entire output of the heart is distributed within this fine capillary network that has an extended surface area of ∼70 m^2. As such blood velocity is dramatically reduced facilitating neutrophil–EC interaction (Gee and Albertine, 1993). Indeed, there is a large pool of marginated mature neutrophils, anchored within these microvessels under homeostasis (**Figure 2A**). This is important because the lung is constantly exposed to potentially harmful pathogens and pollutants/particles due to direct contact with the external environment through the air we breathe, and this marginated pool of mature neutrophils serve as a first line of defense in the lung (Gee and Albertine, 1993). Intravascular retained neutrophils are uniquely positioned within the vascular space where they remain until they are required to migrate into inflamed alveoli or parenchyma of the lung depending whether the pathogen is located in the airspace or tissue, respectively (Hogg and Doerschuk, 1995). It was 1987 when Lien et al. first made use of fluorescent video microscopy to observe labeled neutrophil migrate and interact in the sub-pleural pulmonary microcirculation through a window inserted into the chest wall of dogs. In this pioneering study, the authors observed that under homeostasis neutrophils were making transient contacts with ECs and migrated within the pulmonary capillaries with a transit time ranging from 2 s to 20 min but in contrast had minimal engagement in arterioles or venules (Lien et al., 1987). For decades the precise nature, function, and size of the intravascular marginated pool, versus the circulating pool, has divided scientific opinion; moreover, the molecular mechanism behind this interaction has not been identified (Gee and Albertine, 1993; Peters, 1998). Early studies suggested that ∼36% of cells are in circulation and ∼64% are engaged with lung ECs forming the "physiological regional pool" (Peters, 1998). The increase in IVM image resolution and stabilization of imaging allowed Looney et al. (2011) to directly image up to 125 μm below the pleura and follow in the physiologically intact lung the migratory dynamic of neutrophils up to 3 h. In this study, neutrophils were reported to traverse the 10–15 μm capillaries with a track speed of ∼1.5 μm/s, while in the medium size vessels at ∼100 μm/s confirming that neutrophils were engaging with the endothelial cells of the lung capillaries. Confocal pulmonary IVM further showed that neutrophils under homeostasis possess an array of migratory behaviors; tethering, crawling, and firm arrest but not rolling (Looney et al., 2011). Under homeostasis, these marginated neutrophils crawled a distance of only few μm (Yipp et al., 2017), but this increased significantly after intratracheal

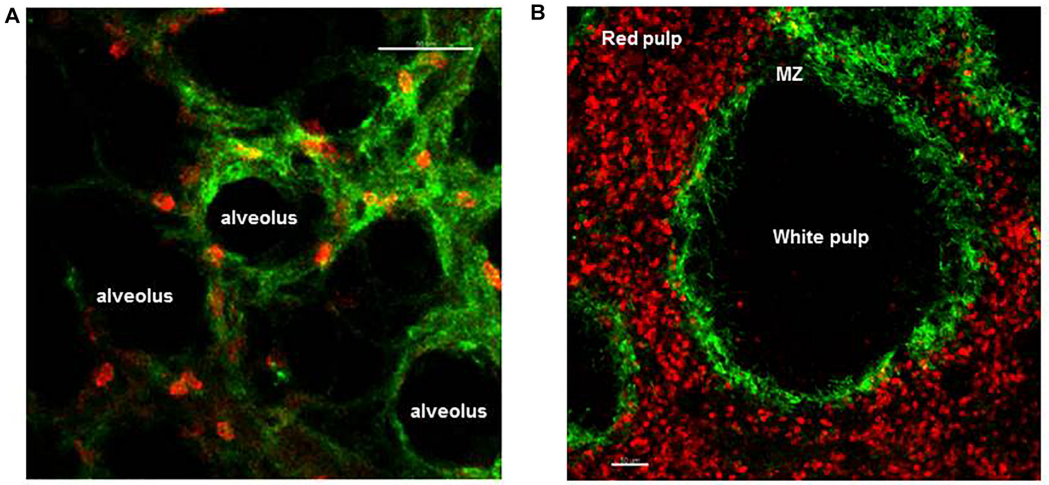

FIGURE 2 | Spatial organization of neutrophils in the lung and spleen during homeostasis. **(A)** Frame from lung IVM video showing marginated neutrophils (red) within the microvessels of the lung (green). **(B)** Precision cut spleen slice showing tissue resident neutrophils (red) and margiant zone macrophages (green) delimiting the MZ. Scale bar 50 μm.

administration of LPS or *E. coli* particles reaching a mean velocity of ∼9.68 μm/min (Kreisel et al., 2010). The role of adhesion molecules in sustaining firm and prolonged interaction of neutrophils with the lung ECs has been controversial with contradicting and inconclusive results (Gee and Albertine, 1993). L-selectin deficient mice were reported to have a normal pool of intravascular retained neutrophils in the lung (Doerschuk, 2001). Assuming that the pool of marginated neutrophils consists of "non-activated" neutrophils interacting with non-activated endothelium, it does not come as a surprise that the classical molecular mechanisms associated with adhesion in the context of inflammation do not apply to this pool of neutrophils interacting with the vasculature under homeostasis. The blood flow in the microcapillaries, as discussed above, is relatively low and due to the diameter of the capillaries it is clear that neutrophils change shape to squeeze through the microcapillaries and this results in their slow transit time. It has been argued that the mechanical mechanism of cell squeezing could stimulate their margination promoting interaction with the lung capillaries, an interesting hypothesis that requires further evidence (Kuebler and Goetz, 2002; Rossaint and Zarbock, 2013). We have recently directly shown, using IVM to image the pulmonary capillary network of mice that a single dose of the CXCR4 antagonist, AMD3100, did not compromise the lung intravascular retained pool of neutrophils under homeostatic conditions (Pillay et al., 2020). Further applying dynamic planar gamma scintigraphy, we have also shown that AMD3100 does not affect the retention of primed neutrophils in the capillary circulation of the lung in humans. Taken together these data suggest that the CXCR4-CXCL12 chemokine axis does not support neutrophil retention in the lung microvascular in either mouse or human (Pillay et al., 2020). Thus to date the precise molecular mechanisms underlying the retention of mature neutrophils in the pulmonary capillaries are unknown or still remain a mystery.

While neutrophils serve as a critical line of host defense in the lung, in the context of ARDS and a number of chronic lung diseases, e.g., COPD, IPF, and asthma, it is thought that the accumulation of excessive numbers of neutrophils supports disease progression (Kamath et al., 2005; Hughes et al., 2019; Potey et al., 2019). Thus, understanding the mechanisms underlying neutrophil influx is desirable to enable the development of targeted therapeutics that can reduce neutrophil numbers in these clinical scenarios. In contrast to the situation under homeostasis, there is consistent evidence from several studies showing the requirement of specific adhesion molecules to support increased neutrophil retention within the microvessels of the lung and their further migration within the infected parenchyma (Doerschuk, 2001). The nature of the adhesion molecules is stimulus dependent, thus neutrophil emigration utilizes β_2 integrins when elicited by *E. coli*, but not when elicited by *Streptococcus pneumoniae* (Doerschuk, 2001).

L-IVM showed that following systemic challenge, *E. coli* was sequestered within seconds by the lung ECs in the pulmonary capillary network and this was followed by the rapid migration of marginated neutrophil toward the immobilized pathogen (Yipp et al., 2017). This work indicates that the lung is an important host defense niche for the detection and capture of systemic pathogens, and requires cooperation between the vascular endothelium and marginated neutrophils (Yipp et al., 2017). In the search for new adhesion molecules that support neutrophil retention in the lung during inflammation, an *in vivo* functional screen surprisingly identified dipeptidase-1 (DEPEP1) (Rajotte and Ruoslahti, 1999; Choudhury et al., 2019). DEPEP1, a membrane enzyme expressed by activated pulmonary endothelium, was shown to support neutrophil adhesion, independent of its enzymatic activity. Moreover, genetic deletion studies and use of a blocking peptide showed that neutrophil adhesion and recruitment in the inflamed lung was

significantly attenuated in the absence of DEPEP1 during sepsis (Choudhury et al., 2019). Finally, when the DEPEP1 blocking peptide was used therapeutically in mice administered with a lethal dose of LPS, it showed a remarkable survival effect and an impressive reduction in neutrophil recruitment into the inflamed lung (Choudhury et al., 2019). With respect to the focus of this review, highlighting how IVM has been key to advancing our understanding and identifying the molecular pathways regulating neutrophil trafficking, this research is notable in that the initial screen involved using confocal IVM to identify a peptide that localized to both the lung and liver endothelium after LPS treatment and reduced neutrophil accumulation in these tissues. Importantly, while this research was carried out in mice, recombinant human DPEP1 supported the adhesion of human neutrophils *in vitro*, indicating its translational potential.

While neutrophils are important for host defense, as mentioned above, when they accumulate in large numbers in tissues, they also have the potential to cause considerable damage to the host tissue. This is due to the fact that their granule proteins and neutrophil extracellular traps (NETs), both important for their anti-microbial functions, are also cytotoxic. In this respect, a series of recent discoveries, also made using IVM, provide an explanation for why marginated neutrophils in the lung may not be as cytotoxic as those in the circulation. Following their release from the BM neutrophils only circulate for 6–10 h before they exit into tissues, including the spleen, BM, and lung (Casanova-Acebes et al., 2018). The migration into the lung is regulated by CXCL1 and the clock gene BMAM-1(Adrover et al., 2020), which in the mouse, means that the majority of circulating neutrophils infiltrate the lungs during the daylight (Adrover et al., 2019). At this time, as compared to neutrophils freshly mobilized from the BM, circulating neutrophils exhibited changes in their proteome, with a reduction in cytotoxic granule proteins, which in turn reduced their ability to form NETs. This process is termed neutrophil "disarming." Taken together, these findings explain how neutrophils can exist in large numbers as marginated cells in the microvasculature of the lungs without causing tissue damage. They also explain why acute lung injury caused by the influx of neutrophils in response to an inflammatory stimulus varies considerably dependent on the time of day. Thus in mice, LPS challenge of the lungs at night will result in greater host tissue damage, due to accumulation of neutrophils from the circulation that have a high content of cytotoxic proteins in their granules as compared to those that would accumulate during the day that have an aged phenotype with lower cytotoxic potential (Adrover et al., 2020). While these studies have been performed in mice, similar changes in neutrophil proteome have been reported human neutrophils with aging, suggesting that these findings are translatable (Adrover et al., 2020).

Another fascinating function of neutrophils has been identified by Wang et al. (2017) in their ability to promote tissue repair in a model of murine sterile thermal hepatic injury. IVM showed that following laser injury of the liver, tissue neutrophils were involved both in dismantling the injured vessels and then in directly contributing to the deposition of collagen in a honeycomb pattern to create a path to rebuild the new vasculature (Wang et al., 2017). In response to the hepatic injury, some neutrophils migrated away from the site of injury while a small number were observed to re-enter the circulation. These neutrophils were later found to "sojourn" in the lung where they upregulated CXCR4 before homing back to the BM in a final voyage to be cleared (Wang et al., 2017). While it is fascinating that a subset of neutrophils, having experienced tissue injury in one organ, makes a pit-stop in the lungs before being cleared in the BM, the reason for this process is still not fully understood. More models need to be tested in order to prove whether this is a specific mechanism that links the liver and the lung or broadly applies to any injured organ, and whether this is only linked to sterile damage or applies also to infection.

Recently, Fluorescent *influenza virus* (color-flu) has been developed as a means of studying influenza infection in the lungs of mice by IVM. Details of the model and a database of fluorescent dyes, antibodies, and reporter mouse lines that can be used in combination with Color-flu for multicolor analysis have also been reported (Xie et al., 2020). Using this model, pulmonary permeability (by dextran leakage from the lung vessels into the alveolar space) and blood flow speed (by i.v. injection of fluorescent microbeads) have been studied following infection, in addition to studying neutrophil dynamics (Ueki et al., 2018; Xie et al., 2020). Thus they reported a reduction in pulmonary permeability and blood perfusion speed during infection, highlighting the severe pulmonary damage created by the virus to the host (Ueki et al., 2018). Neutrophil dynamics exhibited a temporal change in speed, with a high migratory speed $\geq$ 50 μm/s during the early time points (30 min to 1 h) following virus infection and a slow migratory behavior characteristic of the later phase (Ueki et al., 2018).

NEUTROPHIL MARGINATION WITHIN THE PARENCHYMA OF THE SPLEEN AND LYMPH NODES

As a secondary lymphoid organ, an important function of the spleen is in mounting the adaptive immune response during pathogen challenge. In addition, three distinct subsets of macrophages (metallophilic, marginal, and red pulp) present in the spleen play a critical role in filtering the blood, removing senescent red blood cells and systemic pathogens. After the BM the spleen contains the largest number of neutrophils during homeostasis, but until recently the dynamics of these tissue neutrophils was unknown (Casanova-Acebes et al., 2013). IVM showed that two distinct splenic neutrophil populations, at distinct maturation stages, populate the red pulp of this organ under homeostasis (**Figure 2B**) and differentially respond to pathogen challenge (Deniset et al., 2017). Thus, Ly6G^{high} are mature neutrophils that scan the tissue at varied speeds from 0–2 μm/min and up to more than 10 μm/min under steady state. Their migratory speed declined 24 h after challenge increasing the dwelling time and number of firm interactions with local splenic macrophages. Ly6G^{intermediate} are immature and static neutrophils capable of undergoing emergency proliferation

during pathogen challenge contributing to the removal of pathogen and of plucking *S. pneumoniae* from the surface of red pulp macrophages (Deniset et al., 2017).

The very same preNeu, immature Neu, and mature Neu that populate the BM (described in detail above) were also found in the spleen under homeostasis even if in a reduced number compared with the population in the BM (Evrard et al., 2018). During sepsis, preNeu numbers in both the BM and spleen expanded with a greater fold of increase in the spleen indicating that both organs contribute to emergency granulopoiesis in response to infections (Evrard et al., 2018) and represent a store of immature cell reserves. The possibility that neutrophils can complete the last stages of their maturation outside of the BM in the spleen also give rise to the possibility that tissue specific education may prime neutrophils such that they are better tailored to the immune surveillance property of the spleen for a fast and more effective response to pathogens or tissue damage. Puga et al. (2011) identified another distinct subset of neutrophils in the spleen, the splenic neutrophil B-helper cells (N_{BH}), that can support marginal zone B cell maturation and induce their antibody secretion during pathogen challenge via the production of B cell-attracting chemokines such as CXCL12 and CXCL13. Confocal microscopy revealed that N_{BH} interact directly with MZ B cells via protrusion similar to DNA-containing-NET-like projections. Moreover, two genetically and phenotypically distinct subsets have been identified, called N_{BH1} and N_{BH2} (Puga et al., 2011). It is still unknown whether these two populations identified in humans are comparable to Ly6G^{high} and Ly6G^{intermediate} murine neutrophils identified by Deniset et al., as reviewed (Scapini and Cassatella, 2017).

The molecular mechanisms underlying the retention of splenic neutrophils are still under investigation. Applying IVM, Pillay et al. (2020) ruled out the CXCL12-CXCR4 chemokine axis-as molecular mechanism responsible of the splenic retention of neutrophil. In fact, treatment with the CXCR4 antagonist, AMD3100 caused an increase in the number of circulating and splenic neutrophils (Liu et al., 2015) as early as 30 min post challenge and while these splenic neutrophils showed an increase in their migratory speed, there was no evidence that they were activated (Pillay et al., 2020). These data suggest that the spleen can also functions as a sink, lowering the number of circulating neutrophils when they reach a specific threshold. It is possible that the pooling of neutrophils in the spleen protects other more fragile organs, such as the lung from neutrophil overload and potential damage.

Intravital microscopy also revealed that neutrophils patrol unstimulated draining lymph nodes of the skin, lung, and gastrointestinal track (Lok et al., 2019) and reside within the interstitium of the lymph nodes (Bogoslowski et al., 2020). They represent a phenotypically distinct subset of neutrophils when compared with circulating neutrophils with a high level of major histocompatibility complex II (MHCII)^{high} with the potential of influencing the adaptive immune system (Lok et al., 2019). IVM revealed that under homeostatic conditions a small population of neutrophils (∼1000 neutrophils per lymph node) continuously enter the lymph nodes via the high endothelial venules (HEV) in an L-selectin-dependent manner and leave the organ via efferent lymphatic in a sphingosine-1-phosphate (S1P)-dependent way (Bogoslowski et al., 2020). In contrast to other organs, neutrophil entry into the lymph nodes did not follow circadian rhythm. These temporarily resident neutrophils survey the tissue for pathogens and following bacterial infection, recruit additional neutrophils but not after sterile injury suggesting that lymph node neutrophils are able to discriminate the nature of the insult and respond accordingly (Bogoslowski et al., 2020).

Intravital microscopy has been pivotal in documenting the dynamic influx of neutrophil from inflamed tissues into the lymph nodes in response to infection (Hampton et al., 2015; Bogoslowski et al., 2020). Circulating and tissue-resident neutrophils have been shown to use both the afferent lymphatics of the infected tissue as well as HEV to enter the lymph nodes (Chtanova et al., 2008; Duffy et al., 2012; Gorlino et al., 2014; Hampton et al., 2015; Bogoslowski et al., 2020). The neutrophils that are able to migrate to lymph nodes and to modulate adaptive immune reactions express CD11b^{high}, CD62L^{low}, and CXCR2^{low}. They seem to use different molecular mechanism to enter the lymph nodes; CCR7 is essential for neutrophils to enter via afferent lymphatics (Beauvillain et al., 2011), while L-selectin is essential for neutrophil entry via HEV (Gorlino et al., 2014; Bogoslowski et al., 2020). The molecular mechanisms of neutrophil entry and their physiological and pathological implications have been reviewed by Voisin and Nourshargh (2019).

Intravital microscopy showed the entry of neutrophils into the popliteal lymph node (PLN) via multiple hotspots on HEV following influenza vaccination (Pizzagalli et al., 2019). Moreover, neutrophil positive for influenza virus were tracked entering into the PLN after vaccination and showed over a time of 2 h changes in their dynamic motility with a decrease in instantaneous and mean speed, directionality, displacement, and an increase in the arrest coefficient suggesting an increase in cell-to-cell interactions (Pizzagalli et al., 2019). Five distinct neutrophil migratory behaviors have been observed: flowing, arrested, patrolling, directed migration, and swarming (Pizzagalli et al., 2019). During swarming, neutrophils were observed forming clusters that enlarged over time in areas rich in tissue resident macrophages (Pizzagalli et al., 2019). In another study using a model of skin infection, neutrophils were observed migrating to the PLN recruited by tissue resident macrophages in an IL-1β-dependent manner to control the spread of pathogens (Kastenmuller et al., 2012).

In a model of *S. aureus* infection, imaging of the inguinal lymph nodes by IVM revealed a dynamic influx of neutrophils that occurred in two waves with the second one composed of neutrophils mobilized by the BM (Kamenyeva et al., 2015). Moreover, by imaging lymphocytes, neutrophils and fluorescently labeled pathogens at the same time, Kamenyeva et al. (2015) showed that neutrophils interact extensively and directly with lymph node resident B cells to dampen their IgG and IgM production.

Applying IVM has also revealed the remarkably coordinated movement of two consecutive neutrophils, called "two-neutrophil squads" within the small capillaries of lymph nodes and found that these innate immune cells use alternative branches at bifurcations in order to avoid the formation of "traffic jam" within the same branch (Wang et al., 2020). Moreover, when four consecutive neutrophils enter a capillary with branches, two alternative patterns were observed, left-right-left-right or vice versa. This pattern has been explained by the fact that when a neutrophil is traveling along a capillary of the lymph node, it reduces the chemoattractant gradient in the capillary segment where it has just traveled in and increases the hydraulic resistance of the capillary it is occupying, hence the following neutrophil uses the opposite branch to continue its journey where the chemokine gradient is higher and hydraulic resistance lower (Wang et al., 2020).

Two-photon scanning-laser microscopy has provided information on the coordinated migration pattern of neutrophils within the draining lymph nodes after tissue infection showing that neutrophils can swarm and form small, large, transient, or persistent clusters within the lymph nodes (Chtanova et al., 2008). Visual imaging over time revealed that neutrophils show a direct migration rather than random within the lymph node with a high average speed of 11.9 μm/min to form clusters even from a distance of more than 70 μm from the swarm center (Chtanova et al., 2008). Moreover, visual imaging helped in defining that neutrophil swarming is initiated by pioneering neutrophils that come together within the first minutes followed by a massive influx of neutrophils later on (Chtanova et al., 2008; Lammermann, 2016). Neutrophil persistence within the lymph nodes disrupted the continuous layer of $CD169^+$ macrophages present in the sub-capsular sinus suggesting tissue remodeling by infiltrated neutrophils (Chtanova et al., 2008). Making use of a photoconvertible system, Kikume reporter mouse, and two-photon microscopy, the fate of neutrophils first recruited to the inflamed skin and second into the lymph nodes have been imaged and showed a crawling speed of ∼13 μm/min via a CD11b and CXCR4-dependent mechanism (Hampton et al., 2015).

These data show that not all the neutrophils that infiltrate infected areas die *in situ*. At least some can re-enter either the blood vessels or the lymphatics and localize within the draining lymph nodes. These exciting studies show that neutrophils have many more functions beyond the direct killing of pathogens and tissue repair, including the recruitment and activation of other leukocytes, modulation of the adaptive immune system, antigen presentation, and blocking pathogen dissemination beyond the lymph nodes.

SENESCENCE AND NEUTROPHIL DEATH

In the aging process of a cell, senescence represents a step before apoptosis. Senescent neutrophils characterized by an increase in cell surface level of CXCR4 selectively return to the BM at the end of their life for clearance (Martin et al., 2003; Furze and Rankin, 2008b). Moreover, circulating senescent neutrophils are characterized by $Ly6G^+$ $CD62L^{low}$. Applying IVM to the calvarium to follow these aged neutrophils within the BM revealed these cells have a high migratory capability, supported by the upregulation of $CD11b^{high}$/$CD49d^{high}$. Moreover, 40% of $Ly6G^+$ $CD62L^{low}$ was found in direct contact with $CD169^+$ BM macrophages for their final clearance but far away from CAR cells (Evrard et al., 2018). This mechanism of clearance represents a homeostatic signal that modulates hematopoietic niches in the BM and that regulates appearance of progenitors into the circulation (Casanova-Acebes et al., 2013; Adrover et al., 2016). Moreover, the spatial difference in location of "fresh" and aged neutrophils supports the idea that the process of neutrophil maturation and clearance of senescent neutrophils happens in spatially separated areas of the BM, with special areas for maturation and retention of freshly produced neutrophils and others for phagocytosis of aged neutrophils.

Under homeostasis, spontaneous clearance of $CD62L^{low}$ neutrophils from the circulation follows a circadian rhythm with an accumulation during the light time between zeitgeber times (ZT) ZT5-ZT13 and clearance from the circulation during the night time ZT17-ZT5 in mice (Casanova-Acebes et al., 2013). While many studies have successfully imaged the BM via IVM, capturing the migration of neutrophils across the BM sinusoidal endothelium as they are mobilized into the blood, the uptake of senescent neutrophils by macrophages has proven extremely challenging, as well as quantitative analysis of these processes (Adrover et al., 2016).

Interestingly, the molecular profile of senescent neutrophils $CD62L^{low}$ and $CD11b^{high}$ resembles one of the activated neutrophils. As suggested by Casanova-Acebes et al. (2013), aged neutrophils could share a common program of activation signature to ensure the return of neutrophils to the BM for clearance. In fact, there are several studies showing that compromised clearance of cells leads to an unbalanced homeostasis and loss in vascular protection (Adrover et al., 2019). Thus in a model of zymosan-induced peritonitis, aged neutrophils showed an impaired ability to migrate within inflamed tissues, while retaining an ability to migrate toward tissues that support clearance suggesting a selective recruitment of "fresh" neutrophils for fighting infections (Adrover et al., 2019).

Neutrophil-specific deletion of CXCR2 or CXCR4 shows a disruption in the temporal changes of CD62L level on neutrophils. Circulating neutrophils of mice $CXCR2^{\Delta N}$ express constitutively high level of CD62L, while in $CXCR4^{\Delta N}$ constitutively low CD62L. Further CXCR2 has been shown to promote aging during the day while CXCR4 prevents it, suggesting that both chemokine receptors are responsible for controlling the process of neutrophil aging (Adrover et al., 2019).

Bone marrow is not the only organ where aged neutrophils can be cleared. This function is equally shared between the BM, spleen and liver (Suratt et al., 2001; Furze and Rankin, 2008b). However, the molecular mechanism of senescent neutrophil clearance in the spleen and liver is not fully understood (Furze and Rankin, 2008b). Aged neutrophils are cleared in the liver by tissue resident macrophages (Kupffer cells) in a G-α_i-independent manner,

while in the spleen half of senescent neutrophils are cleared in a G-α_i-independent manner and half in a G-α_i-dependent manner; however, the receptor involved is still not known (Furze and Rankin, 2008b). IVM imaging of the spleen treated with AMD3100 showed an increased number of splenic neutrophils but not activation or changes in CXCR4 expression suggesting that the process of senescent neutrophil clearance in the spleen is CXCR4 independent (Pillay et al., 2020).

DEVELOPMENT OF NEW THERAPEUTICS

The dynamics and molecular mechanisms underlying neutrophil trafficking in homeostasis and disease have been extensively studied by IVM over the last decades, with technological advances allowing researchers to continually uncover new functions and facets of these fascinating cells (**Figure 3**). Thus while the original seminal studies led to the generation of the adhesion cascade paradigm (tethering rolling, adhesion transmigration) increasingly more sophisticated IVM, together with availability of fluorescent reporter mice, and genetically modified mice has revealed increasing levels of complexity to this process (Girbl et al., 2018). Moreover, technological advances that have allowed imaging of tissues including the lung, spleen, and lymph nodes have led to an understanding that neutrophil responses are both tissue and pathogen specific, but moreover that there are distinct subsets of neutrophils in these tissues that have different responses and functions. Finally, the temporal nature of neutrophil responses has been revealed by IVM, whether that is early versus late response to a pathogen, or differential responses dependent on the time of day or night. This ever increasing level of complexity means that we are now in a stronger position to understand neutrophil related diseases and design targeted therapies. Going forward IVM is a technique that could help to test *in vivo* the mechanism of action of drugs and help design more potent or specific therapeutics, as has been shown recently with the identification of DEPEP1 the adhesion molecule for neutrophil retention in the lungs following LPS challenge, that could be a potential therapeutic target for ARDS (Choudhury et al., 2019). In addition to having more knowledge to specifically ameliorate inflammatory pathologies we can now start to understand in more detail, the function of tissue resident neutrophils, the different subsets of these cells,

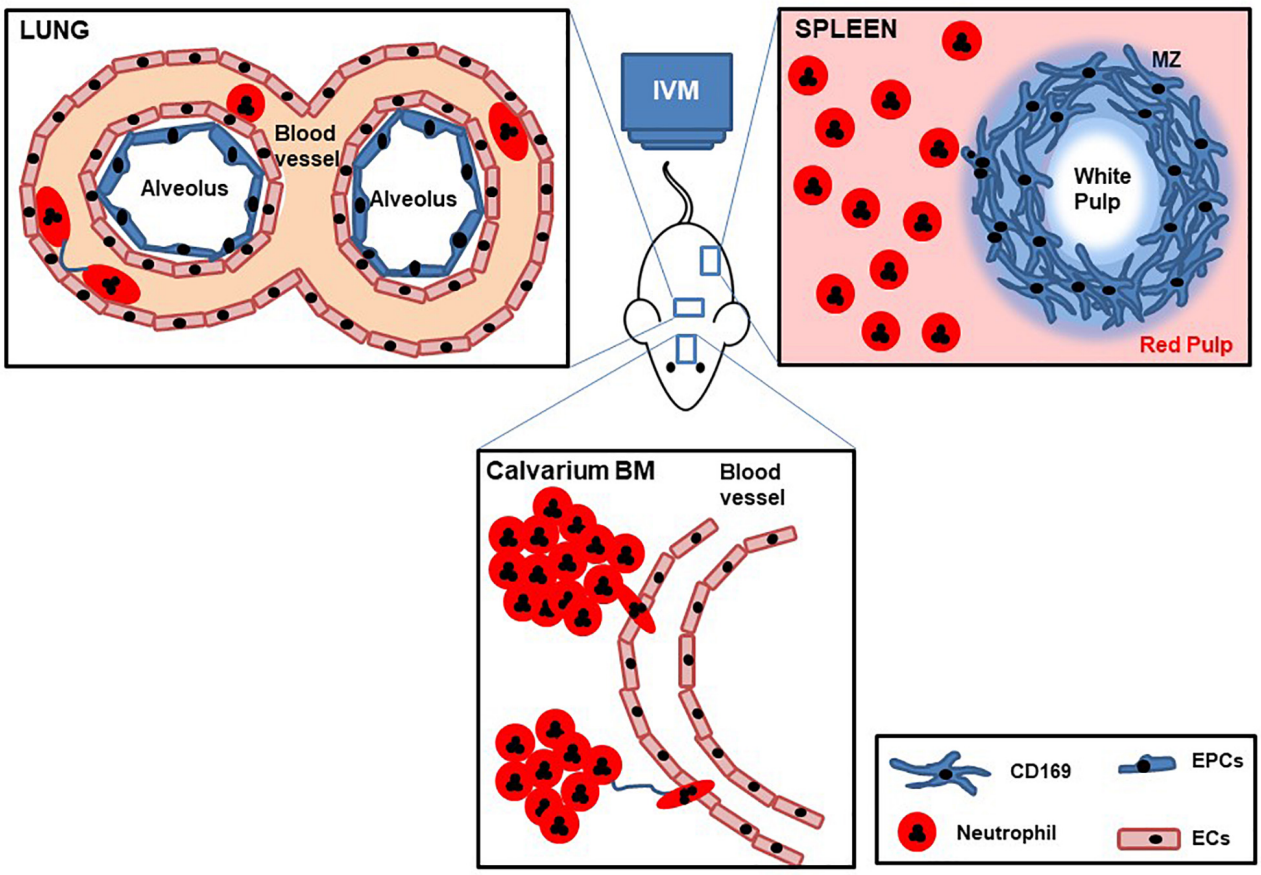

FIGURE 3 | Cartoon with schematic representation of lung, spleen, and calvarium BM IVM. Mice are deeply anesthetized, fluorescent Abs are intravenously injected, and internal organs are partially exposed to be imaged by IVM while maintaining blood flow. Dynamic behaviors of tissue neutrophil motility, cell–cell interactions, and temporal change in speed are recorded over time.

and the choreography of their recruitment, tissue retention, and maturation thanks to IVM.

AUTHOR CONTRIBUTIONS

KD performed the literature search and wrote the manuscript. SR contributed to the writing and revision of the manuscript. Both authors contributed to the article and approved the submitted version.

FUNDING

KD was supported by funding from the Wellcome Trust (201356/Z/16/Z).

REFERENCES

Adrover, J. M., Aroca-Crevillen, A., Crainiciuc, G., Ostos, F., Rojas-Vega, Y., Rubio-Ponce, A., et al. (2020). Programmed 'disarming' of the neutrophil proteome reduces the magnitude of inflammation. *Nat. Immunol.* 21, 135–144. doi: 10.1038/s41590-019-0571-2

Adrover, J. M., Del Fresno, C., Crainiciuc, G., Cuartero, M. I., Casanova-Acebes, M., Weiss, L. A., et al. (2019). A neutrophil timer coordinates immune defense and vascular protection. *Immunity* 51, 966–967. doi: 10.1016/j.immuni.2019.11.001

Adrover, J. M., Nicolas-Avila, J. A., and Hidalgo, A. (2016). Aging: a temporal dimension for neutrophils. *Trends Immunol.* 37, 334–345. doi: 10.1016/j.it.2016.03.005

Aroca-Crevillen, A., Adrover, J. M., and Hidalgo, A. (2020). Circadian features of neutrophil biology. *Front. Immunol.* 11:576. doi: 10.3389/fimmu.2020.00576

Beauvillain, C., Cunin, P., Doni, A., Scotet, M., Jaillon, S., Loiry, M. L., et al. (2011). CCR7 is involved in the migration of neutrophils to lymph nodes. *Blood* 117, 1196–1204. doi: 10.1182/blood-2009-11-254490

Bogoslowski, A., Wijeyesinghe, S., Lee, W. Y., Chen, C. S., Alanani, S., Jenne, C., et al. (2020). Neutrophils recirculate through lymph nodes to survey tissues for pathogens. *J. Immunol.* 204, 2552–2561.

Borregaard, N. (2010). Neutrophils, from marrow to microbes. *Immunity* 33, 657–670. doi: 10.1016/j.immuni.2010.11.011

Buckley, C. D., Ross, E. A., McGettrick, H. M., Osborne, C. E., Haworth, O., Schmutz, C., et al. (2006). Identification of a phenotypically and functionally distinct population of long-lived neutrophils in a model of reverse endothelial migration. *J. Leukocyte Biol.* 79, 303–311. doi: 10.1189/jlb.0905496

Burdon, P. C., Martin, C., and Rankin, S. M. (2008). Migration across the sinusoidal endothelium regulates neutrophil mobilization in response to ELR + CXC chemokines. *Br. J. Haematol.* 142, 100–108. doi: 10.1111/j.1365-2141.2008.07018.x

Casanova-Acebes, M., Nicolas-Avila, J. A., Li, J. L., Garcia-Silva, S., Balachander, A., Rubio-Ponce, A., et al. (2018). Neutrophils instruct homeostatic and pathological states in naive tissues. *J. Exp. Med.* 215, 2778–2795. doi: 10.1084/jem.20181468

Casanova-Acebes, M., Pitaval, C., Weiss, L. A., Nombela-Arrieta, C., Chevre, R., Alonso-Gonzalez, N., et al. (2013). Rhythmic modulation of the hematopoietic niche through neutrophil clearance. *Cell* 153, 1025–1035. doi: 10.1016/j.cell.2013.04.040

Choo, Y. W., Jeong, J., and Jung, K. (2020). Recent advances in intravital microscopy for investigation of dynamic cellular behavior in vivo. *BMB Rep.* 53, 357–366. doi: 10.5483/bmbrep.2020.53.7.069

Choudhury, S. R., Babes, L., Rahn, J. J., Ahn, B. Y., Goring, K. R., King, J. C., et al. (2019). Dipeptidase-1 is an adhesion receptor for neutrophil recruitment in Lungs and Liver. *Cell* 178 1205.e17-1221.e17.

Christopher, M. J., and Link, D. C. (2007). Regulation of neutrophil homeostasis. *Curr. Opin. Hematol.* 14, 3–8. doi: 10.1097/00062752-200701000-00003

Chtanova, T., Schaeffer, M., Han, S. J., van Dooren, G. G., Nollmann, M., Herzmark, P., et al. (2008). Dynamics of neutrophil migration in lymph nodes during infection. *Immunity* 29, 487–496. doi: 10.1016/j.immuni.2008.07.012

Colom, B., Bodkin, J. V., Beyrau, M., Woodfin, A., Ody, C., Rourke, C., et al. (2015). Leukotriene B4-neutrophil elastase axis drives neutrophil reverse transendothelial cell migration in vivo. *Immunity* 42, 1075–1086. doi: 10.1016/j.immuni.2015.05.010

De Filippo, K., and Rankin, S. M. (2018). CXCR4, the master regulator of neutrophil trafficking in homeostasis and disease. *Eur. J. Clin. Invest.* 48(Suppl. 2):e12949. doi: 10.1111/eci.12949

Deniset, J. F., Surewaard, B. G., Lee, W. Y., and Kubes, P. (2017). Splenic Ly6G(high) mature and Ly6G(int) immature neutrophils contribute to eradication of S. *pneumoniae*. *J. Exp. Med.* 214, 1333–1350. doi: 10.1084/jem.20161621

Devi, S., Wang, Y., Chew, W. K., Lima, R., Chew, S., Mattar, C. N., et al. (2013). Neutrophil mobilization via plerixafor-mediated CXCR4 inhibition arises from lung demargination and blockade of neutrophil homing to the bone marrow. *J. Exp. Med.* 210, 2321–2336. doi: 10.1084/jem.20130056

Doerschuk, C. M. (2001). Mechanisms of leukocyte sequestration in inflamed lungs. *Microcirculation* 8, 71–88. doi: 10.1111/j.1549-8719.2001.tb00159.x

Duffy, D., Perrin, H., Abadie, V., Benhabiles, N., Boissonnas, A., Liard, C., et al. (2012). Neutrophils transport antigen from the dermis to the bone marrow, initiating a source of memory CD8(+) T Cells. *Immunity* 37:1145. doi: 10.1016/j.immuni.2012.11.002

Eash, K. J., Means, J. M., White, D. W., and Link, D. C. (2009). CXCR4 is a key regulator of neutrophil release from the bone marrow under basal and stress granulopoiesis conditions. *Blood* 113, 4711–4719. doi: 10.1182/blood-2008-09-177287

Evans, R., Patzak, I., Svensson, L., De Filippo, K., Jones, K., McDowall, A., et al. (2009). Integrins in immunity. *J. Cell Sci.* 122(Pt. 2), 215–225.

Evrard, M., Kwok, I. W. H., Chong, S. Z., Teng, K. W. W., Becht, E., Chen, J., et al. (2018). Developmental analysis of bone marrow neutrophils reveals populations specialized in expansion, trafficking, and effector functions. *Immunity*. 48 364.e8-379.e8.

Faust, N., Varas, F., Kelly, L. M., Heck, S., and Graf, T. (2000). Insertion of enhanced green fluorescent protein into the lysozyme gene creates mice with green fluorescent granulocytes and macrophages. *Blood* 96, 719–726. doi: 10.1182/blood.v96.2.719.014k29_719_726

Furze, R. C., and Rankin, S. M. (2008a). Neutrophil mobilization and clearance in the bone marrow. *Immunology* 125, 281–288. doi: 10.1111/j.1365-2567.2008.02950.x

Furze, R. C., and Rankin, S. M. (2008b). The role of the bone marrow in neutrophil clearance under homeostatic conditions in the mouse. *FASEB J.* 22, 3111–3119. doi: 10.1096/fj.08-109876

Garlichs, C. D., Eskafi, S., Cicha, I., Schmeisser, A., Walzog, B., Raaz, D., et al. (2004). Delay of neutrophil apoptosis in acute coronary syndromes. *J. Leukocyte Biol.* 75, 828–835.

Gebb, S. A., Graham, J. A., Hanger, C. C., Godbey, P. S., Capen, R. L., Doerschuk, C. M., et al. (1995). Sites of leukocyte sequestration in the pulmonary microcirculation. *J. Appl. Physiol.* 79, 493–497. doi: 10.1152/jappl.1995.79.2.493

Gee, M. H., and Albertine, K. H. (1993). Neutrophil-endothelial cell interactions in the lung. *Annu. Rev. Physiol.* 55, 227–248. doi: 10.1146/annurev.ph.55.030193.001303

Girbl, T., Lenn, T., Perez, L., Rolas, L., Barkaway, A., Thiriot, A., et al. (2018). Distinct compartmentalization of the Chemokines CXCL1 and CXCL2 and the atypical receptor ACKR1 determine discrete stages of neutrophil diapedesis. *Immunity*. 49, 1062.e6-107.e6.

Gordy, C., Pua, H., Sempowski, G. D., and He, Y. W. (2011). Regulation of steady-state neutrophil homeostasis by macrophages. *Blood* 117, 618–629. doi: 10.1182/blood-2010-01-265959

Gorlino, C. V., Ranocchia, R. P., Harman, M. F., Garcia, I. A., Crespo, M. I., Moron, G., et al. (2014). Neutrophils exhibit differential requirements for homing molecules in their lymphatic and blood trafficking into draining lymph nodes. *J. Immunol.* 193, 1966–1974. doi: 10.4049/jimmunol.1301791

Graham, D. B., Zinselmeyer, B. H., Mascarenhas, F., Delgado, R., Miller, M. J., and Swat, W. (2009). ITAM signaling by vav family rho guanine nucleotide

exchange factors regulates interstitial transit rates of neutrophils in vivo. *PLoS One.* 4:e4652. doi: 10.1371/journal.pone.0004652

Gulino, A. V., Moratto, D., Sozzani, S., Cavadini, P., Otero, K., Tassone, L., et al. (2004). Altered leukocyte response to CXCL12 in patients with warts hypogammaglobulinemia, infections, myelokathexis (WHIM) syndrome. *Blood* 104, 444–452. doi: 10.1182/blood-2003-10-3532

Hampton, H. R., Bailey, J., Tomura, M., Brink, R., and Chtanova, T. (2015). Microbe-dependent lymphatic migration of neutrophils modulates lymphocyte proliferation in lymph nodes. *Nat. Commun.* 6:7139.

Harding, M. G., Zhang, K., Conly, J., and Kubes, P. (2014). Neutrophil crawling in capillaries; a novel immune response to *Staphylococcus aureus*. *PLoS Pathog.* 10:e1004379. doi: 10.1371/journal.ppat.1004379

Hasenberg, A., Hasenberg, M., Mann, L., Neumann, F., Borkenstein, L., Stecher, M., et al. (2015). Catchup: a mouse model for imaging-based tracking and modulation of neutrophil granulocytes. *Nat. Methods.* 12, 445–452. doi: 10.1038/nmeth.3322

He, W., Holtkamp, S., Hergenhan, S. M., Kraus, K., de Juan, A., Weber, J., et al. (2018). Circadian Expression of Migratory Factors Establishes Lineage-Specific Signatures that Guide the Homing of Leukocyte Subsets to Tissues. *Immunity* 49, 1175.e7-1190.e7.

Hernandez, P. A., Gorlin, R. J., Lukens, J. N., Taniuchi, S., Bohinjec, J., Francois, F., et al. (2003). Mutations in the chemokine receptor gene CXCR4 are associated with WHIM syndrome, a combined immunodeficiency disease. *Nat. Genet.* 34, 70–74. doi: 10.1038/ng1149

Hidalgo, A., Chilvers, E. R., Summers, C., and Koenderman, L. (2019). The neutrophil life cycle. *Trends Immunol.* 40, 584–597. doi: 10.1016/j.it.2019.04.013

Hogg, J. C., and Doerschuk, C. M. (1995). Leukocyte traffic in the lung. *Annu. Rev. Physiol.* 57, 97–114. doi: 10.1146/annurev.ph.57.030195.000525

Hossain, M., and Kubes, P. (2019). Innate immune cells orchestrate the repair of sterile injury in the liver and beyond. *Eur. J. Immunol.* 49, 831–841. doi: 10.1002/eji.201847485

Hughes, M. J., Sapey, E., and Stockley, R. (2019). Neutrophil phenotypes in chronic lung disease. *Exp. Rev. Respir. Med.* 13, 951–967. doi: 10.1080/17476348.2019.1654377

Kamath, A. V., Pavord, I. D., Ruparelia, P. R., and Chilvers, E. R. (2005). Is the neutrophil the key effector cell in severe asthma? *Thorax* 60, 529–530. doi: 10.1136/thx.2005.043182

Kamenyeva, O., Boularan, C., Kabat, J., Cheung, G. Y., Cicala, C., Yeh, A. J., et al. (2015). Neutrophil recruitment to lymph nodes limits local humoral response to Staphylococcus aureus. *PLoS Pathog.* 11:e1004827. doi: 10.1371/journal.ppat.1004827

Kastenmuller, W., Torabi-Parizi, P., Subramanian, N., Lammermann, T., and Germain, R. N. (2012). A spatially-organized multicellular innate immune response in lymph nodes limits systemic pathogen spread. *Cell* 150, 1235–1248. doi: 10.1016/j.cell.2012.07.021

Kohler, A., De Filippo, K., Hasenberg, M., van den Brandt, C., Nye, E., Hosking, M. P., et al. (2011). G-CSF-mediated thrombopoietin release triggers neutrophil motility and mobilization from bone marrow via induction of Cxcr2 ligands. *Blood* 117, 4349–4357. doi: 10.1182/blood-2010-09-308387

Kolaczkowska, E., and Kubes, P. (2013). Neutrophil recruitment and function in health and inflammation. *Nat. Rev. Immunol.* 13, 159–175. doi: 10.1038/nri3399

Kreisel, D., Nava, R. G., Li, W., Zinselmeyer, B. H., Wang, B., Lai, J., et al. (2010). In vivo two-photon imaging reveals monocyte-dependent neutrophil extravasation during pulmonary inflammation. *Proc. Natl. Acad. Sci. U.S.A.* 107, 18073–18078. doi: 10.1073/pnas.1008737107

Kuebler, W. M., and Goetz, A. E. (2002). The marginated pool. *Eur. Surg. Res.* 34, 92–100. doi: 10.1159/000048894

Lammermann, T. (2016). In the eye of the neutrophil swarm-navigation signals that bring neutrophils together in inflamed and infected tissues. *J. Leukocyte Biol.* 100, 55–63. doi: 10.1189/jlb.1mr0915-403

Lammermann, T., Afonso, P. V., Angermann, B. R., Wang, J. M., Kastenmuller, W., Parent, C. A., et al. (2013). Neutrophil swarms require LTB4 and integrins at sites of cell death in vivo. *Nature* 498, 371–375. doi: 10.1038/nature12175

Lapidot, T., and Kollet, O. (2002). The essential roles of the chemokine SDF-1 and its receptor CXCR4 in human stem cell homing and repopulation of transplanted immune-deficient NOD/SCID and NOD/SCID/B2m(null) mice. *Leukemia* 16, 1992–2003. doi: 10.1038/sj.leu.2402684

Laval, J., Touhami, J., Herzenberg, L. A., Conrad, C., Taylor, N., Battini, J. L., et al. (2013). Metabolic adaptation of neutrophils in cystic fibrosis airways involves distinct shifts in nutrient transporter expression. *J. Immunol.* 190, 6043–6050. doi: 10.4049/jimmunol.1201755

Ley, K., Laudanna, C., Cybulsky, M. I., and Nourshargh, S. (2007). Getting to the site of inflammation: the leukocyte adhesion cascade updated. *Nat. Rev. Immunol.* 7, 678–689. doi: 10.1038/nri2156

Li, J. L., Goh, C. C., Keeble, J. L., Qin, J. S., Roediger, B., Jain, R., et al. (2012). Intravital multiphoton imaging of immune responses in the mouse ear skin. *Nat. Prot.* 7, 221–234. doi: 10.1038/nprot.2011.438

Lien, D. C., Wagner, WW Jr, Capen, R. L., Haslett, C., Hanson, W. L., Hofmeister, S. E., et al. (1987). Physiological neutrophil sequestration in the lung: visual evidence for localization in capillaries. *J. Appl. Physiol.* 62, 1236–1243. doi: 10.1152/jappl.1987.62.3.1236

Liese, J., Rooijakkers, S. H., van Strijp, J. A., Novick, R. P., and Dustin, M. L. (2013). Intravital two-photon microscopy of host-pathogen interactions in a mouse model of *Staphylococcus aureus* skin abscess formation. *Cell. Microbiol.* 15, 891–909. doi: 10.1111/cmi.12085

Liu, Q., Li, Z., Gao, J. L., Wan, W., Ganesan, S., McDermott, D. H., et al. (2015). CXCR4 antagonist AMD3100 redistributes leukocytes from primary immune organs to secondary immune organs, lung, and blood in mice. *Eur. J. Immunol.* 45, 1855–1867. doi: 10.1002/eji.201445245

Lok, L. S. C., Dennison, T. W., Mahbubani, K. M., Saeb-Parsy, K., Chilvers, E. R., and Clatworthy, M. R. (2019). Phenotypically distinct neutrophils patrol uninfected human and mouse lymph nodes. *Proc. Natl. Acad.Sci.U.S.A.* 116, 19083–19089. doi: 10.1073/pnas.1905054116

Looney, M. R., Thornton, E. E., Sen, D., Lamm, W. J., Glenny, R. W., and Krummel, M. F. (2011). Stabilized imaging of immune surveillance in the mouse lung. *Nat. Methods* 8, 91–96. doi: 10.1038/nmeth.1543

Martin, C., Burdon, P. C., Bridger, G., Gutierrez-Ramos, J. C., Williams, T. J., and Rankin, S. M. (2003). Chemokines acting via CXCR2 and CXCR4 control the release of neutrophils from the bone marrow and their return following senescence. *Immunity* 19, 583–593. doi: 10.1016/s1074-7613(03)00263-2

Masedunskas, A., Milberg, O., Porat-Shliom, N., Sramkova, M., Wigand, T., Amornphimoltham, P., et al. (2012). Intravital microscopy: a practical guide on imaging intracellular structures in live animals. *Bioarchitecture* 2, 143–157. doi: 10.4161/bioa.21758

McDermott, D. H., Liu, Q., Velez, D., Lopez, L., Anaya-O'Brien, S., Ulrick, J., et al. (2014). A phase 1 clinical trial of long-term, low-dose treatment of WHIM syndrome with the CXCR4 antagonist plerixafor. *Blood* 123, 2308–2316. doi: 10.1182/blood-2013-09-527226

McDermott, D. H., Pastrana, D. V., Calvo, K. R., Pittaluga, S., Velez, D., Cho, E., et al. (2019). Plerixafor for the Treatment of WHIM Syndrome. *New Engl. J. Med.* 380, 163–170.

Mempel, T. R., Scimone, M. L., Mora, J. R., and von Andrian, U. H. (2004). In vivo imaging of leukocyte trafficking in blood vessels and tissues. *Curr. Opin. Immunol.* 16, 406–417. doi: 10.1016/j.coi.2004.05.018

Ng, L. G., Qin, J. S., Roediger, B., Wang, Y., Jain, R., Cavanagh, L. L., et al. (2011). Visualizing the neutrophil response to sterile tissue injury in mouse dermis reveals a three-phase cascade of events. *J. Invest. Dermatol.* 131, 2058–2068. doi: 10.1038/jid.2011.179

Nourshargh, S., and Alon, R. (2014). Leukocyte migration into inflamed tissues. *Immunity* 41, 694–707. doi: 10.1016/j.immuni.2014.10.008

Peters, A. M. (1998). Just how big is the pulmonary granulocyte pool? *Clin. Sci.* 94, 7–19. doi: 10.1042/cs0940007

Peters, N. C., Egen, J. G., Secundino, N., Debrabant, A., Kimblin, N., Kamhawi, S., et al. (2008). In vivo imaging reveals an essential role for neutrophils in leishmaniasis transmitted by sand flies. *Science* 321, 970–974. doi: 10.1126/science.1159194

Pillay, J., Tregay, N., Juzenaite, G., Carlin, L. M., Pirillo, C., Gaboriau, D. C. A., et al. (2020). Effect of the CXCR4 antagonist plerixafor on endogenous neutrophil dynamics in the bone marrow, lung and spleen. *J. Leukocyte Biol.* 107, 1175-1185.

Pizzagalli, D. U., Latino, I., Pulfer, A., Palomino-Segura, M., Virgilio, T., Farsakoglu, Y., et al. (2019). Characterization of the dynamic behavior of

neutrophils following influenza vaccination. *Front. Immunol.* 10:2621. doi: 10.3389/fimmu.2019.02621

Potey, P. M., Rossi, A. G., Lucas, C. D., and Dorward, D. A. (2019). Neutrophils in the initiation and resolution of acute pulmonary inflammation: understanding biological function and therapeutic potential. *J. Pathol.* 247, 672–685. doi: 10.1002/path.5221

Puga, I., Cols, M., Barra, C. M., He, B., Cassis, L., Gentile, M., et al. (2011). B cell-helper neutrophils stimulate the diversification and production of immunoglobulin in the marginal zone of the spleen. *Nat. Immunol.* 13, 170–180. doi: 10.1038/ni.2194

Rajotte, D., and Ruoslahti, E. (1999). Membrane dipeptidase is the receptor for a lung-targeting peptide identified by in vivo phage display. *J. Biol. Chem.* 274, 11593–11598. doi: 10.1074/jbc.274.17.11593

Rossaint, J., and Zarbock, A. (2013). Tissue-specific neutrophil recruitment into the lung, liver, and kidney. *J. Innate Immun.* 5, 348–357. doi: 10.1159/000345943

Saetzler, R. K., Jallo, J., Lehr, H. A., Philips, C. M., Vasthare, U., Arfors, K. E., et al. (1997). Intravital fluorescence microscopy: impact of light-induced phototoxicity on adhesion of fluorescently labeled leukocytes. *J. Histochem. Cytochem.* 45, 505–513. doi: 10.1177/002215549704500403

Scapini, P., and Cassatella, M. A. (2017). Location in the spleen dictates the function of murine neutrophils. *J. Exp. Med.* 214, 1207–1209. doi: 10.1084/jem.20170655

Scheiermann, C., Kunisaki, Y., and Frenette, P. S. (2013). Circadian control of the immune system. *Nat. Rev. Immunol.* 13, 190–198. doi: 10.1038/nri3386

Scheiermann, C., Kunisaki, Y., Lucas, D., Chow, A., Jang, J. E., Zhang, D., et al. (2012). Adrenergic nerves govern circadian leukocyte recruitment to tissues. *Immunity* 37, 290–301. doi: 10.1016/j.immuni.2012.05.021

Semerad, C. L., Liu, F., Gregory, A. D., Stumpf, K., and Link, D. C. (2002). G-CSF is an essential regulator of neutrophil trafficking from the bone marrow to the blood. *Immunity* 17, 413–423. doi: 10.1016/s1074-7613(02)00424-7

Silvestre-Roig, C., Hidalgo, A., and Soehnlein, O. (2016). Neutrophil heterogeneity: implications for homeostasis and pathogenesis. *Blood* 127, 2173–2181. doi: 10.1182/blood-2016-01-688887

Sreeramkumar, V., Adrover, J. M., Ballesteros, I., Cuartero, M. I., Rossaint, J., Bilbao, I., et al. (2014). Neutrophils scan for activated platelets to initiate inflammation. *Science* 346, 1234–1238. doi: 10.1126/science.1256478

Stackowicz, J., Jonsson, F., and Reber, L. L. (2019). Mouse Models and Tools for the in vivo Study of Neutrophils. *Front. Immunol.* 10:3130. doi: 10.3389/fimmu.2019.03130

Summers, C., Rankin, S. M., Condliffe, A. M., Singh, N., Peters, A. M., and Chilvers, E. R. (2010). Neutrophil kinetics in health and disease. *Trends Immunol.* 31, 318–324. doi: 10.1016/j.it.2010.05.006

Suratt, B. T., Young, S. K., Lieber, J., Nick, J. A., Henson, P. M., and Worthen, G. S. (2001). Neutrophil maturation and activation determine anatomic site of clearance from circulation. *Am. J. Physiol. Lung Cell. Mol. Physiol.* 281, L913–L921.

Tak, T., Tesselaar, K., Pillay, J., Borghans, J. A., and Koenderman, L. (2013). What's your age again? Determination of human neutrophil half-lives revisited. *J. Leukocyte Biol.* 94, 595–601. doi: 10.1189/jlb.1112571

Taqueti, V. R., and Jaffer, F. A. (2013). High-resolution molecular imaging via intravital microscopy: illuminating vascular biology in vivo. *Integr. Biol.* 5, 278–290. doi: 10.1039/c2ib20194a

Uddin, M., Nong, G., Ward, J., Seumois, G., Prince, L. R., Wilson, S. J., et al. (2010). Prosurvival activity for airway neutrophils in severe asthma. *Thorax* 65, 684–689. doi: 10.1136/thx.2009.120741

Ueki, H., Wang, I. H., Fukuyama, S., Katsura, H., da Silva Lopes, T. J., Neumann, G., et al. (2018). In vivo imaging of the pathophysiological changes and neutrophil dynamics in influenza virus-infected mouse lungs. *Proc. Natl. Acad. Sci.U.S.A.* 115, E6622–E6629.

Voisin, M. B., and Nourshargh, S. (2019). Neutrophil trafficking to lymphoid tissues: physiological and pathological implications. *J. Pathol.* 247, 662–671. doi: 10.1002/path.5227

Waite, J. C., Leiner, I., Lauer, P., Rae, C. S., Barbet, G., Zheng, H., et al. (2011). Dynamic imaging of the effector immune response to listeria infection in vivo. *PLoS Pathog.* 7:e1001326. doi: 10.1371/journal.ppat.1001326

Wang, J., Hossain, M., Thanabalasuriar, A., Gunzer, M., Meininger, C., and Kubes, P. (2017). Visualizing the function and fate of neutrophils in sterile injury and repair. *Science* 358, 111–116. doi: 10.1126/science.aam9690

Wang, X., Hossain, M., Bogoslowski, A., Kubes, P., and Irimia, D. (2020). Chemotaxing neutrophils enter alternate branches at capillary bifurcations. *Nat. commun.* 11:2385.

Wengner, A. M., Pitchford, S. C., Furze, R. C., and Rankin, S. M. (2008). The coordinated action of G-CSF and ELR + CXC chemokines in neutrophil mobilization during acute inflammation. *Blood* 111, 42–49. doi: 10.1182/blood-2007-07-099648

Woodfin, A., Voisin, M. B., Beyrau, M., Colom, B., Caille, D., Diapouli, F. M., et al. (2011). The junctional adhesion molecule JAM-C regulates polarized transendothelial migration of neutrophils in vivo. *Nat. Immunol.* 12, 761–769. doi: 10.1038/ni.2062

Xie, X., Shi, Q., Wu, P., Zhang, X., Kambara, H., Su, J., et al. (2020). Single-cell transcriptome profiling reveals neutrophil heterogeneity in homeostasis and infection. *Nat. Immunol.* 21, 1119–1133. doi: 10.1038/s41590-020-0736-z

Yipp, B. G., Kim, J. H., Lima, R., Zbytnuik, L. D., Petri, B., Swanlund, N., et al. (2017). The lung is a host defense niche for immediate neutrophil-mediated vascular protection. *Sci. Immunol.* 2:eaam8929. doi: 10.1126/sciimmunol.aam8929

Yipp, B. G., and Kubes, P. (2013). Antibodies against neutrophil LY6G do not inhibit leukocyte recruitment in mice in vivo. *Blood* 121, 241–242. doi: 10.1182/blood-2012-09-454348

You, S., Tu, H., Chaney, E. J., Sun, Y., Zhao, Y., Bower, A. J., et al. (2018). Intravital imaging by simultaneous label-free autofluorescence-multiharmonic microscopy. *Nat. Commun.* 9:2125.

Zinselmeyer, B. H., Lynch, J. N., Zhang, X., Aoshi, T., and Miller, M. J. (2008). Video-rate two-photon imaging of mouse footpad - a promising model for studying leukocyte recruitment dynamics during inflammation. *Inflamm. Res.* 57, 93–96. doi: 10.1007/s00011-007-7195-y

Conflict of Interest: The authors declare that the research was conducted in the absence of any commercial or financial relationships that could be construed as a potential conflict of interest.

frontiers in Cell and Developmental Biology

BRIEF RESEARCH REPORT
published: 12 November 2020
doi: 10.3389/fcell.2020.608600

Membrane Dynamics and Organization of the Phagocyte NADPH Oxidase in PLB-985 Cells

Jérémy Joly[1], Elodie Hudik[1], Sandrine Lecart[2], Dirk Roos[3], Paul Verkuijlen[3], Dominik Wrona[4], Ulrich Siler[4], Janine Reichenbach[4], Oliver Nüsse[1] and Sophie Dupré-Crochet[1]**

[1] Université Paris-Saclay, CNRS U8000, Institut de Chimie Physique, Orsay, France, [2] Light Microscopy Core Facility, Imagerie-Gif, Institut de Biologie Intégrative de la Cellule (I2BC), CEA, CNRS, Université Paris-Saclay, Gif-sur-Yvette, France, [3] Sanquin Research and Landsteiner Laboratory, Amsterdam University Medical Center, University of Amsterdam, Amsterdam, Netherlands, [4] Division of Gene and Cell Therapy, Institute for Regenerative Medecine, University of Zurich, Zurich, Switzerland

Neutrophils are the first cells recruited at the site of infections, where they phagocytose the pathogens. Inside the phagosome, pathogens are killed by proteolytic enzymes that are delivered to the phagosome following granule fusion, and by reactive oxygen species (ROS) produced by the NADPH oxidase. The NADPH oxidase complex comprises membrane proteins (NOX2 and $p22^{phox}$), cytoplasmic subunits ($p67^{phox}$, $p47^{phox}$, and $p40^{phox}$) and the small GTPase Rac. These subunits assemble at the phagosomal membrane upon phagocytosis. In resting neutrophils the catalytic subunit NOX2 is mainly present at the plasma membrane and in the specific granules. We show here that NOX2 is also present in early and recycling endosomes in human neutrophils and in the neutrophil-like cell line PLB-985 expressing GFP-NOX2. In the latter cells, an increase in NOX2 at the phagosomal membrane was detected by live-imaging after phagosome closure, probably due to fusion of endosomes with the phagosome. Using super-resolution microscopy in PLB-985 WT cells, we observed that NOX2 forms discrete clusters in the plasma membrane. The number of clusters increased during frustrated phagocytosis. In PLB-985*NCF1*ΔGT cells that lack $p47^{phox}$ and do not assemble a functional NADPH oxidase, the number of clusters remained stable during phagocytosis. Our data suggest a role for $p47^{phox}$ and possibly ROS production in NOX2 recruitment at the phagosome.

Keywords: phagocytosis, NOX2, super-resolution imaging, dSTORM, nanoclusters

OPEN ACCESS

Edited by:
Zhichao Fan,
UCONN Health, United States

Reviewed by:
Rongrong Liu,
Northwestern University, United States
Christine Winterbourn,
University of Otago, New Zealand

****Correspondence:***
Oliver Nüsse
oliver.nusse@universite-paris-saclay.fr
Sophie Dupré-Crochet
sophie.dupre@universite-paris-saclay.fr

Specialty section:
This article was submitted to Cell Adhesion and Migration, a section of the journal Frontiers in Cell and Developmental Biology

Received: *21 September 2020*
Accepted: *20 October 2020*
Published: *12 November 2020*

Citation:
Joly J, Hudik E, Lecart S, Roos D, Verkuijlen P, Wrona D, Siler U, Reichenbach J, Nüsse O and Dupré-Crochet S (2020) Membrane Dynamics and Organization of the Phagocyte NADPH Oxidase in PLB-985 Cells. Front. Cell Dev. Biol. 8:608600. doi: 10.3389/fcell.2020.608600

INTRODUCTION

The phagocytic NADPH oxidase produces reactive oxygen species (ROS) that are crucial for killing pathogens during phagocytosis. NADPH oxidase is a multi-subunit enzyme comprising several membrane and cytosolic components, the flavocytochrome b_{558} (NOX2) and $p22^{phox}$ in membranes, and the cytosolic subunits ($p47^{phox}$, $p67^{phox}$, and $p40^{phox}$) and the small GTPase

Abbreviations: dSTORM, direct stochastic optical resolution microscopy; DBSCAN, density based spatial clustering of applications with noise; EEA1, early endosome antigen1; IgG, Immunoglobulin G; PC, Pearson coefficient; ROS, reactive oxygen species; TIRFM, total internal reflection fluorescence microscopy.

Rac. Upon phagocytosis, the cytosolic subunits and Rac assemble with the membrane subunits. This translocation allows electron flow from NADPH in the cytosol to oxygen in the phagosome, through the catalytic subunit NOX2, leading to superoxide anion production, which is the precursor of other types of ROS (Nunes et al., 2013; Valenta et al., 2020). A lack of a functional NADPH oxidase such as in chronic granulomatous disease results in life-threatening infections with bacteria and fungi (O'Neill et al., 2015). Thus, ROS production is necessary for the immune response against many pathogens. NOX2 forms a heterodimer with $p22^{phox}$ in the endoplasmic reticulum. The heterodimer formation is necessary for its trafficking in the Golgi, where NOX2 is further glycosylated (DeLeo et al., 2000). In neutrophils, the heterodimer has been localized in the plasma membrane, in specific and gelatinase granules, and in secretory vesicles (Borregaard et al., 1983; Lominadze et al., 2005). In macrophages, the heterodimer is present in the plasma membrane and in Rab5 and Rab11-positive endosomes (Casbon et al., 2009). Since the early and recycling endosomes fuse with the phagosome during phagocytosis (Niedergang et al., 2003; Pauwels et al., 2017), they may add new heterodimers within the phagosomal membrane.

In order to explore whether the endosomal pathway contributes to the enrichment in phagosomal NOX2 in neutrophils, as in macrophages, we used the neutrophil-like PLB-985 cells that express neither specific and gelatinase granules nor secretory vesicles (Pivot-Pajot et al., 2010; Rincón et al., 2018). First, using live imaging and the X^0-CGD PLB-985 cell line expressing GFP-NOX2 (van Manen et al., 2008), we observed an increase in phagosomal NOX2 after phagosomal closure. Immunofluorescence studies indicated that PLB-985 cells, as well as primary human neutrophils, contained early and recycling endosomes positive for NOX2. During phagocytosis, these endosomes were in close contact with the phagosome suggesting that they could contribute to the phagosomal gain in NOX2. Moreover, using direct stochastic optical resolution microscopy (dSTORM) in a total internal reflection fluorescence microscopy (TIRFM) configuration, we observed that NOX2 formed discrete clusters during frustrated phagocytosis. The number of clusters increased during phagocytosis in PLB-985 WT cells but not in PLB-985 NCF1ΔGT cells that lack a functional oxidase due to the absence of $p47^{phox}$ (Wrona et al., 2017). These data suggest that the presence of $p47^{phox}$ and/or NADPH oxidase activity triggers a positive feedback with the recruitment of NOX2 positive vesicles.

MATERIALS AND METHODS

Cell Culture

Several PLB-985 cell lines were used in this study. The human myeloid leukemia cell lines PLB-985 WT was a generous gift from Dr. Marie-José Stasia (Faculty of Medecine, Université de Grenoble Alpes, France). The X^0-CGD PLB-985 GFP-NOX2 cell line corresponds to PLB-985 WT cells deleted for endogenous NOX2 (Zhen et al., 1993) but expressing GFP-NOX2 (van Manen et al., 2008). PLB-985 NCF1ΔGT cells lack a functional oxidase due to deletion of a dinucleotide in the *NCF1* gene, encoding $p47^{phox}$, by CRISPR/Cas9 manipulation (Wrona et al., 2017). PLB-985 cells were cultured and differentiated for 5 or 6 days with 1.25% DMSO as previously described (Song et al., 2020). IFN-γ (2000 U/ml, 11343536, Immunotools) was added to the culture 24 h before the experiments.

Neutrophil Preparation

Human blood samples were taken with the understanding and written consent of each volunteer by the "Etablissement Français du Sang, Cabanel, Paris" (the French blood transfusion service and National Blood Bank: https://www.ints.fr/). An agreement (N°11/Necker/103) allowing us to use blood samples from the volunteers for research purposes was signed between this organization and our laboratory. Neutrophils were isolated from healthy donor whole blood as previously described (El Benna et al., 1997). For all the experiments, the cells were resuspended in Hank's Balanced Salt Solution (H8624, Sigma-Aldrich).

Opsonization of Zymosan and Phagocytosis

Zymosan (Z2849, Invitrogen™) and Texas-Red-zymosan (Z2843, Invitrogen™) from *S. cerevisiae* were opsonized with human serum (diluted 50%, H4522, Sigma-Aldrich) as described previously (Tlili et al., 2011).

For live-imaging, zymosan particles were added directly to 5×10^5 cells (5 particles per cell). For short-term live-imaging, a Z-stack with an increment of 0.5 μm was taken, from the start of phagocytosis, every 30 s. For longer term live-imaging (>3 min), the contact between zymosan and cells was obtained by centrifugation at 13°C at 400 *g* during 3 min. The end of the centrifugation was defined as Time Zero for the phagocytosis. A Z-stack with an increment of 1 μm was made every 5 min.

Frustrated Phagocytosis

For super-resolution microscopy, coverslips were washed for 30 min with 0.1% (w/v) Decon 90 and 100 mM sodium hydroxide under sonication. The coverslips were then kept in 2 N sodium hydroxide for 2 h before washing with pure water followed by 70% ethanol. Finally, they were soaked for 1 h in absolute ethanol followed by an acetone wash and then dried in an oven for 30 min at 70°C. For frustrated phagocytosis, coverslips were coated with BSA (10 mg/ml, B1529, Sigma-Aldrich) overnight. After a washing step, a rabbit anti-BSA antibody was added (1:500, B1520, Sigma-Aldrich) at room temperature for 1 h. Cell adhesion on poly-lysine (P4707, Sigma-Aldrich) coated coverslip was carried out as described previously (Mularski et al., 2018).

Immunofluorescence

The immunofluorescence experiments were performed as described previously (Tlili et al., 2012) except that, after paraformaldehyde fixation, the coverslips were incubated 5 min twice with 10% (w/v) glycine in PBS. The cells were immunostained with a rabbit anti-EEA1 antibody (1:100, PA5-17228, Invitrogen) or a rabbit anti-Rab11 (1-5μg, 71-5300, Thermofisher) and a mouse anti-NOX2 antibody (1:1000, Abcam, ab80897), followed by Alexa-488 goat anti-mouse

antibody (1:1000, A11029, Life Technologies) or Dylight 405 goat anti-rabbit (1:200, 35550, Thermofisher).

The same protocol was used for dSTORM experiments, the only difference concerned the secondary antibody. After the mouse anti-NOX2 antibody, a mix with Alexa-647 $F(ab')_2$ goat anti-mouse Immunoglobulin G (IgG; 1:3000, A21237, Thermo Fisher Scientific) and a blocking antibody against free rabbit anti-BSA antibody (1:1000, ab6831, Abcam) were used during 1 h at room temperature.

Microscopy

Imaging was carried out with a Spinning-Disk Confocal System (Yokogawa CSU-X1-A1, Yokogawa Electric, Yokogawa, Japan), mounted on a Nikon Eclipse Ti E inverted microscope, equipped with a 100x APO 1.4 oil immersion objective and an EM-CCD eVolve 512 camera (Photometrics), driven by MetaMorph 7 software (Molecular Devices). GFP-NOX2 protein was excited at 491 nm (Cobolt Calypso, 100 mW) with an exposure time of 200 ms. Fluorescence was detected with a double-band beam splitter (491–561 nm) and a 525/45-nm emission filter. For immunofluorescence, 561 nm (Coherent, 100 mW) and 405 nm (Vortran, 100 mW) lasers were also used with a quad-band beam splitter and a quad band emission filter (440/40 nm, 521/20 nm, 607/34 nm, 700/45 nm, Semrock).

DSTORM super-resolution microscopy is based on stochastic blinking of individual fluorophores. Each detection sequence detects a small number of fluorophores in the microscope field. A large number of images (20000) was recorded in order to detect each individual blinking fluorophore and to reconstruct images with high spatial precision. To achieve the blinking process for dSTORM, the coverslips (thickness 0.17 mm) were incubated in a specific imaging buffer composed of 0.63 mg/ml glucose oxidase (G2133, Sigma-Aldrich) and its substrate (0.1 g/ml glucose), 40 μg/ml catalase (C100, Sigma-Aldrich) and 110 mM mercaptoethylamine. Depletion in oxygen by the glucose oxidase, and the thiols stabilize the fluorophores in a dark state thereby reducing the number of fluorophores that are blinking at the same time (Endesfelder and Heilemann, 2015). Imaging was carried out with a Nikon Eclipse Ti E inverted microscope, equipped with a motorized *x,y,z* perfect focus system and a 100x APO TIRF SR (N.A. 1.49) oil immersion objective and an Andor iXon Ultra 897 EM-CCD camera driven by NIS-Elements Advanced Research software (Nikon). A 647 nm laser (MPB Communication, 300 mW) and a 405 nm diode (Cube, Coherent, 100 mW) were used. The fluorescence was detected with a quad band emission filter (450/60-525/50-605/50-730/120, Chroma). 20,000 images, each with an exposure of 16 ms were taken per acquisition.

Image Processing and Analysis

Image J software was used to analyze immunofluorescence images, to quantify fluorescence in real-time microscopy and to determine the cell surface after frustrated phagocytosis. A line over plasma and phagosomal membrane was drawn and the ratio between fluorescence at the phagosomal membrane (minus background) and fluorescence at the plasma membrane (minus background) was calculated for each time point. Co-localization was analyzed using the JACoP ImageJ plugin (Bolte and Cordelières, 2006). A negative control was made by recalculating the Pearson coefficient using the NOX2 image rotated by 180° (Dunn et al., 2011).

Direct stochastic optical resolution microscopy analysis was performed using thunderSTORM software (Ovesný et al., 2014). First, images were filtered using the "difference of averaging" filter. Blinking events were detected using the local maximum method and then sub-pixel localization was estimated using a point spread function model (PSF integrated Gaussian). The detection process thus provided a list of every fluorophore with an estimation of the number of emitted photons and their precise localization. Artifactual detections were avoided by removing all molecules whose localization lacked precision, having a variability greater than 20 nm. We estimated the maximal radius of a sphere containing the NOX2 plus antibody-complex to be 20 nm since the radius of NOX2 can be estimated as 3 nm (Erickson, 2009), the length of the primary antibody is 10-15 nm and the $F(ab')_2$ fragment of the IgG is 5 nm (Hainfeld and Powell, 2000).

Using SR-Tesseler software (Levet et al., 2015) the molecule list was then analyzed with the density based spatial clustering of applications with noise algorithms (DBSCAN, Ester et al., 1996) used to detect cluster organization. The algorithms gather points that are close together taking into account a minimum number of fluorophores within a minimum distance. We considered as the minimal distance the estimated diameter of NOX2 plus the antibody complex (40 nm). The minimum number of fluorophores in clusters was 15 in order to get at least two molecules of NOX2 in one cluster. Indeed one Alexa-647 $F(ab')_2$ goat anti-mouse IgG can carry up to 7 Alexa-647 molecules, and we assumed that 2 Alexa 647 $F(ab')_2$ fragment can bind one primary anti-NOX2 antibody. The algorithm thus gave a list of clusters indicating their position, size and the number of fluorophores in each cluster, making it possible to compare different experimental conditions.

Data Analysis

Graphpad prism8 software (GraphPad Software, United States) was used for statistical analyses. Since the values were not normally distributed, Mann–Whitney tests were performed to compare 2 groups, and Kruskal Wallis tests were used to compare multiple groups. For the live-imaging experiments, ratio-paired *t*-tests were used to compare fluorescence ratios at the different times. Differences were considered significant when $p < 0.05$. Statistical test results are indicated in the figure legends.

RESULTS

Phagosomal NOX2 Level Increases After Phagosome Closure

We first investigated whether the level of NOX2 in the phagosomal membrane increases during phagocytosis in PLB-985 cells. The NOX2 increase could be due to lateral diffusion of NOX2 protein in the plasma membrane, which might then

accumulate in the phagosomal cup, or to fusion of NOX2-containing organelles with the phagosomes. X^0-CGD PLB-985 GFP-NOX2 were used to follow GFP-NOX2 accumulation in the phagosomal membrane. X^0-CGD PLB-985 cells do not express NOX2, thus we checked that expression of GFP-NOX2 in these cells was able to restore ROS production upon phagocytosis of serum opsonized zymosan in our luminometry assay using L-012 although the production was a bit reduced as compared to PLB-WT cells (unpublished data). GFP fluorescence was located at the plasma membrane and also in discrete dots inside the cells (**Figure 1A**). The phagocytosis of opsonized zymosan was followed using 4D live imaging during the first 180 s after the phagosome closure (**Figure 1A**). At the onset of phagocytosis, the fluorescence ratio of GFP-NOX2 between the phagosomal membrane and the plasma membrane was about 1, indicating that the phagosomal level of NOX2 did not increase before phagosome sealing. However, 1 min after phagosomal closure a gain in phagosomal membrane NOX2 was measured. To observe GFP-NOX2 over a longer period of time after phagosomal closure, we synchronized the phagocytosis by centrifugation and followed the phagosome maturation using 4D live imaging (**Figure 1B**). At 5 min after the centrifugation, the fluorescence ratio was 1.4 (±0.18), close to that obtained in the previous experiment 3 min after phagosome closure. This ratio further increased to 1.7 (±0.19) after 20 min of phagocytosis, indicating that the phagosomal membrane had gained new NOX2 molecules. Our data thus indicate that in PLB-985 cells part of GFP-NOX2 was recruited within the phagosomal membrane after phagosome sealing, suggesting that some organelles can deliver new NOX2 molecules to the phagosome.

NOX2 Is Localized in Some EEA1 and Rab11-Positive Endosomes

The endosomal compartment is a potential source for NOX2 delivery. Indeed, upon endotoxin stimulation, NADPH oxidase has been described to assemble at the early endosome (Lamb et al., 2012). We used immunofluorescence to detect NOX2 in early and recycling endosomes in resting PLB-985 cells

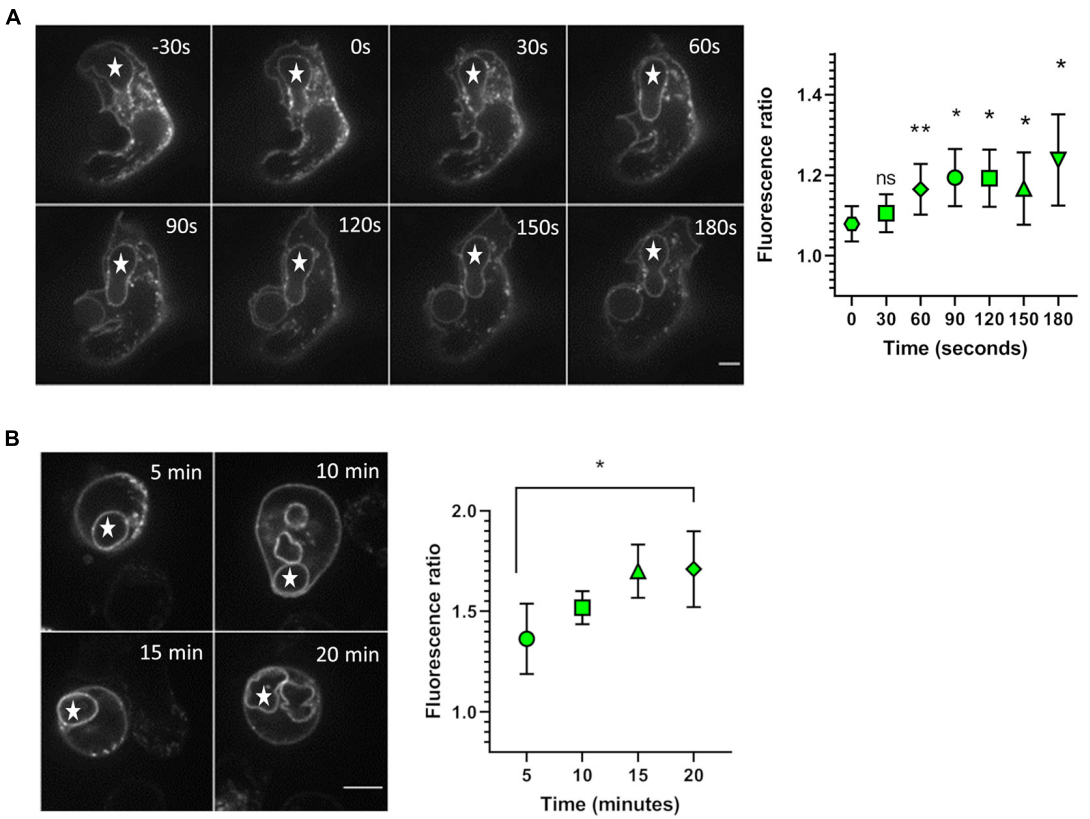

FIGURE 1 | Accumulation of NOX2 in the phagosomal membrane. **(A)** X^0-CGD PLB-985 GFP-NOX2 cells were incubated with opsonized zymosan and the phagocytosis was observed by spinning disk confocal video-microscopy. Left: representative images of zymosan (*) phagocytosis at the indicated times. Time 0 represents the closure of the phagosome. The images shown are single planes from a Z-stack. Scale bar = 5 μm. Right: kinetics of NOX2 accumulation at the phagosome. The fluorescence ratio represents the ratio of NOX2 fluorescence intensity at the phagosome to that at the plasma membrane. Data are means ± SEM. Nineteen videos were analyzed from three independent experiments, $^*p < 0.05$, $^{**}p < 0.01$ (ratio paired *t*-test comparing value at the indicated time with that at time 0). **(B)** X^0-CGD PLB-985 GFP-NOX2 cells were incubated with opsonized zymosan and immediately centrifuged at 13°C. The end of centrifugation corresponds to time 0. Phagocytosis was then observed, at 37°C, using spinning disk confocal microscopy, a Z-stack was taken every 5 min. Left: representative images of zymosan (*) phagocytosis. The images shown are single planes from a Z-stack. Scale bar = 5 μm. Right: kinetics of NOX2 accumulation at the phagosome between 5 and 20 min. Data are means ± SEM. Sixteen cells were analyzed from four independent experiments, $^*p < 0.05$ (ratio paired *t*-test).

and neutrophils. We observed NOX2 and early endosome antigen1 (EEA1) co-localization. EEA1 is a marker of early endosomes (Mu et al., 1995). NOX2 was present in some EEA1-positive endosomes in PLB-985 WT cells and neutrophils (**Figures 2Ai,ii** and **Supplementary Figures 1Ai,ii**). Using the JACoP plugin in Image J, we determined that (1) the Pearson coefficient was 0.35 (±0.05), indicating partial co-localization, and (2) that 27.3% of the EEA1-positive endosomes contained NOX2 (n = 67 cells). Similar results were obtained for the neutrophils (**Supplementary Figure 1A**) and the X^0-CGD PLB-985 GFP-NOX2 cells (data not shown). We then examined the localization of NOX2 in Rab11-positive endosomes. Rab11 and its effectors define the endosomal recycling compartment. Rab11 is also involved in transport of cargo from the Golgi to the plasma membrane (Vale-Costa and Amorim, 2016). Rab11-positive structures were localized close to the plasma membrane in PLB-985 WT cells. NOX2 was detected in 21.7% (n = 63 cells) of Rab11-positive endosomes. The Pearson coefficient was 0.45 (±0.05) indicating partial co-localization (**Figure 3A**). Similar results were obtained for neutrophils (**Supplementary Figures 1A, 2A**) and X^0-CGD PLB-985 GFP-NOX2 cells (data not shown). Thus, part of NOX2 is localized in a fraction of early and recycling endosomes.

Some EEA1 and Rab11-Positive Endosomes Are Found Close to the Phagosome

To ascertain whether endosomes are able to deliver NOX2 to the phagosome, we examined the localization of endosomes after 10 min of opsonized zymosan phagocytosis in PLB-985 WT cells and in neutrophils. We observed both EEA1- and Rab11-positive endosomes close to the phagosomes (**Figures 2B**, **3B** and **Supplementary Figures 1B, 2B**). Some of these endosomes were also positive for NOX2. Indeed, the fluorescence profiles of NOX2 and EEA1 or Rab11 around the phagosome show overlapping peaks, indicating co-localization, in some spots (**Figures 2B**, **3B** and **Supplementary Figures 1B, 2B**). The same results were obtained for the X^0-CGD PLB-985 GFP-NOX2 cells (data not shown). Our data suggest that a proportion of the total NOX2 is localized in certain EEA1- and Rab11-positive endosomes and that these endosomes may fuse with the phagosome to convey new NOX2 molecules to the phagosomal membrane.

NOX2 Forms Clusters and Their Number Increases During Phagocytosis

The phagocytic cup has a spatial and temporal arrangement of receptors and signaling molecules (Goodridge et al., 2011; Freeman et al., 2016) that is similar to the immunologic synapse (Yokosuka et al., 2005). This specific arrangement of molecules at the phagocytic cup is known as "phagocytic synapse" (Niedergang et al., 2016). The spatial arrangement of NOX2 at the phagocytic cup is as yet unknown. To gain insight into NOX2 spatial organization and dynamics in the membrane during phagocytosis, we used a frustrated phagocytosis paradigm in which the cells are allowed to spread on IgG-coated coverslips (Marion et al., 2012). The PLB-985 WT cells were activated in this manner for 1 and 10 min. For the control condition (non-activated), poly-L-lysine-coated coverslips were used. The cells were then stained for NOX2 by immunofluorescence and imaged using a dSTORM approach with a TIRFM configuration. TIRFM allows the imaging of the fluorophores in the membrane in proximal contact with the coverslip while avoiding potentially confusing contribution from cytoplasmic fluorophores. A density-based representation of dSTORM images revealed that NOX2 distribution was similar in the 3 conditions: non-activated, frustrated phagocytosis for 1 or 10 min (**Figure 4A** and data not shown). The spatial distribution of NOX2 analyzed using the DBSCAN cluster detection analysis implemented in SR-Tesseler software (materials and methods) indicated that NOX2 organized in nanoclusters. These clusters had a similar size distribution in the cell membrane in each condition (**Figure 4B**). The mean diameter of the nanoclusters was about 60 nm in each condition (60.5 ± 7.1 nm in the non-activated condition; 66.2 ± 10.5 nm after 1 min of frustrated phagocytosis, 63.6 ± 17.25 nm after 10 min of frustrated phagocytosis). In each condition, almost all the fluorophores detected following the analyses of dSTORM images (materials and methods) were found inside clusters, and the number of fluorophores per cluster was similar (**Supplementary Figure 3**). However, a significant rise in the number of clusters was observed in the PLB-985 WT cells after 10 min of phagocytosis as compared to that after 1 min of phagocytosis or in non-activated cells (**Figure 4C**). This increase was correlated with a larger frustrated phagosomal surface after 10 min as compared to the surface observed in the 2 othet conditions (**Supplementary Figure 5A**). It has been shown that this spreading of the phagosomal surface during frustrated phagocytosis is not only due to a passive membrane extension, but that it also involved the delivery of new membranes (Zak, 2019, manuscript in preparation). Thus, this increase in the number of clusters indicated that new NOX2 molecules were delivered to the membrane between 1 and 10 min after the start of frustrated phagocytosis.

The Increase in the Number of NOX2 Clusters During Phagocytosis Requires $p47^{phox}$

In order to know whether the increase in NOX2 clusters requires a functional oxidase, we performed the same experiments as before using PLB-985 NCF1ΔGT cells, which lack a functional oxidase since they are deficient for $p47^{phox}$ (Wrona et al., 2017). The distribution of NOX2 nanocluster sizes in these cells was the same as for the WT cells in the 3 conditions (**Supplementary Figure 4**), as was the number of fluorophores per clusters (data not shown). However, in contrast to the results obtained using WT cells, in the cells lacking a functional oxidase no difference was detected either in the number of clusters or in the frustrated phagosomal surface after 10 min of phagocytosis compared to that after 1 min of phagocytosis or in non-activated cells (**Figure 4D** and **Supplementary Figure 5B**). The number of clusters was significantly different,

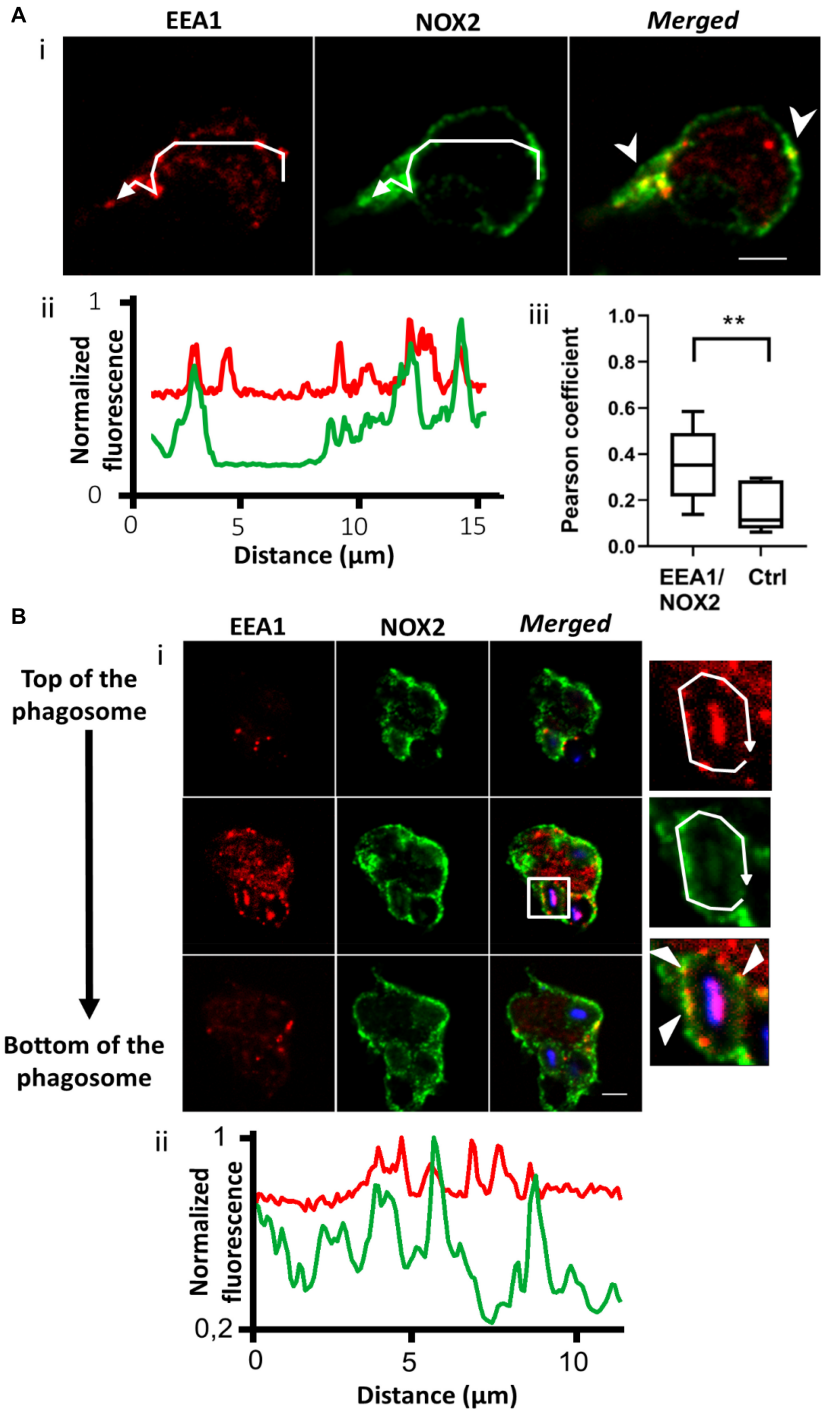

FIGURE 2 | NOX2 is present in some EEA1-positive endosomes that localize close to the phagosome during phagocytosis. **(A)** EEA1 (red) and NOX2 (green) were detected by immunofluorescence in resting PLB-985 WT cells using spinning disk confocal microscopy. **(Ai)** Representative images of single planes from a Z-stack. Scale bar = 3 µm. Three independent experiments. **(Aii)** Normalized fluorescence of EEA1 and NOX2 along the white arrow shown in **Ai**. Overlapping peaks of fluorescence indicate localization of NOX2 and EEA1 in the same structures. **(Aiii)** Co-localization of EEA1 and NOX2 estimated using the Pearson coefficient (PC) calculated with the JACoP plug-in in Image J. PCs correlating EEA1 and NOX2 images (EEA1/NOX2) were controlled by comparison with the PCs correlating the EEA1 image and the image of NOX2 rotated by 180° (Control, Ctrl). Eight images from three independent experiments were analyzed. Each boxplot represents the inter-quartile range with the median, ** represents $p < 0.01$ (Mann Whitney test). **(B)** EEA1 (red) and NOX2 (green) were detected by immunofluorescence after 10 min of phagocytosis with opsonized Texas Red-zymosan. **(Bi)** Three planes from a series of Z-stack planes (0.5 µm). Some EEA1 endosomes were observed close to or at the phagosomes. Scale bar = 3 µm. Three independent experiments. **(Bii)** Normalized fluorescence of EEA1 and NOX2 along the white arrow showing some overlapping peaks of NOX2 and EEA1 fluorescence at the phagosome.

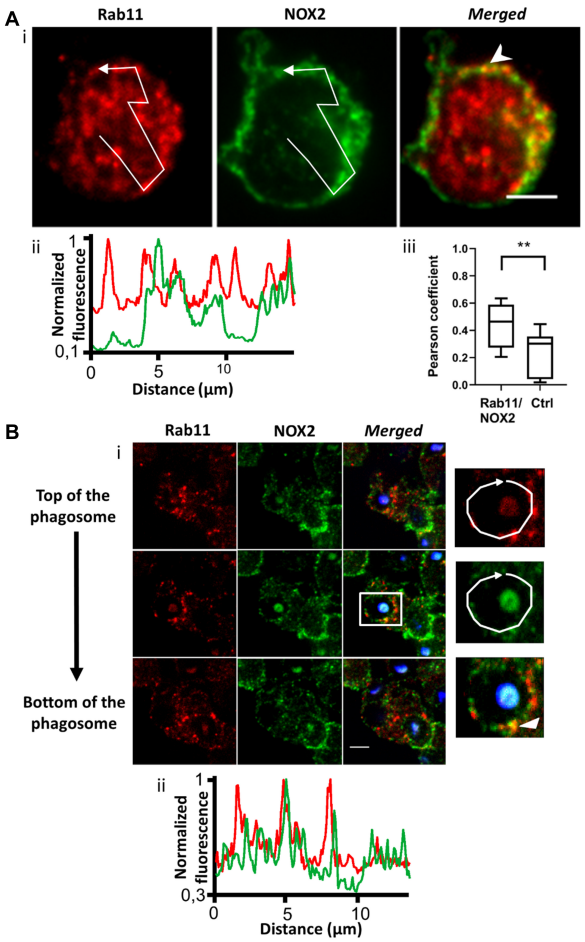

FIGURE 3 | NOX2 is present in some Rab11-positive endosomes that are localized close to the phagosome during phagocytosis. **(A)** Rab11 (red) and NOX2 (green) were detected by immunofluorescence in resting PLB-985 WT cells using spinning disk confocal microscopy. **(Ai)** Representative images of single planes from a Z-stack. Scale bar = 3 µm. Three independent experiments. **(Aii)** Normalized fluorescence of Rab11 and NOX2 along the white arrow shown in **Ai**. Overlapping peaks of fluorescence indicate co-localization of NOX2 and Rab11 in the same structures. **(Aiii)** Co-localization between Rab11 and NOX2 was estimated using the Pearson coefficient (PC) calculated with the JACoP plug-in in Image J. PCs correlating Rab11 and NOX2 images (Rab11/NOX2) were controlled by comparison with the PCs correlating the Rab11 image and the image of NOX2 rotated by 180° (Control, Ctrl). Eight images were analyzed from three independent experiments. Each boxplot represents the inter-quartile range with the median, ** represents $p < 0.01$ (Mann Whitney test). **(B)** Rab11 (red) and NOX2 (green) were detected by immunofluorescence after 10 min of phagocytosis with opsonized Texas Red-zymosan. **(Bi)** Three planes from a Z-stack series (0.5 µm). Some Rab11 structures were observed close to or at the phagosomes. Scale bar = 3 µm. Three independent experiments. **(Bii)** Normalized fluorescence of Rab11 and NOX2 along the white arrow showing some overlapping peaks at the phagosome.

after 10 min of phagocytosis, between PLB-985 NCF1ΔGT cells and PLB-985 WT cells (**Figure 4E**). Thus, taken together, our data indicate that the presence of $p47^{phox}$ and/or ROS production are required for the delivery of NOX2 clusters during frustrated phagocytosis.

DISCUSSION

In this study, we have examined for the first time the spatial arrangement of NOX2 in the phagosome membrane using super-resolution microscopy. This has revealed that NOX2 molecules are organized in nanoclusters. These clusters increased during frustrated phagocytosis, indicating the delivery of NOX2 to the phagosomal membrane. This delivery required the presence of $p47^{phox}$.

We used X^0-CGD PLB-985 GFP-NOX2 cells to follow the modifications of NOX2 in the phagosomal membrane during phagocytosis. We observed an accumulation of NOX2 compared to the plasma membrane just after phagosome closure. Using immunofluorescence, we detected that NOX2 was localized in a fraction of the EEA1- and Rab11-positive organelles in PLB-985 cells and also in neutrophils. It is of interest to note that no co-localization with the lysosome marker LAMP1 could be detected (data not shown). Some of these organelles were positioned close to the phagosomes after 10 min of phagocytosis, suggesting their involvement in the delivery of new NOX2 molecules to the phagosome in the PLB-985 cells as well as in neutrophils.

These results are also coherent with the super-resolution data in which we observed an increase in the frustrated phagosomal surface and in the number of NOX2 nanoclusters during phagocytosis. These nanoclusters have a random distribution in the membrane, unlike receptors such as Dectin, FcRs and the phosphatase CD45 at the beginning of phagocytosis (Goodridge et al., 2011; Freeman et al., 2016). This cluster organization of NOX2 was previously observed by Wientjes et al. (1997) using immuno-electronmicroscopy. These investigators observed nanodomains with a diameter of 200–360 nm. This size is larger than the one we detected (**Figure 4B**), although the discrepancy can be explained by the different techniques used. In the future, double labeling experiments should reveal, which proportion of these clusters contains cytosolic subunits and produces ROS.

A nanocluster organization has been observed for many membrane proteins. Garcia-Parajo et al. (2014) proposed several hypotheses to explain this organization, one being that it may facilitate ligand binding. In our case, it could facilitate the binding of the cytosolic subunits and Rac to the heterodimer NOX2-$p22^{phox}$ when the neutrophils are activated. The average diameter of NOX2 clusters was 60 nm. Similar cluster size has been reporter for other proteins such as the z chain of CD3, which is the co-receptor of the T-cell receptor (Garcia-Parajo et al., 2014; Pageon et al., 2016). However, upon activation of the T-cell receptor, CD3 formed clusters of 185 nm in diameter (Pageon et al., 2016). In the case of NOX2, neither the cluster size nor the number of fluorophores per cluster (about 100) changed during phagocytosis. If we assume that we have around 5 fluorophores attached to each secondary antibody, and two secondary antibodies per primary antibody against NOX2, then we would have an average of 10 NOX2 molecules per cluster. A similar result has been found for the dendritic cell receptor DC-SIGN (Garcia-Parajo et al., 2014).

In PLB-985 WT cells an increase in the number of clusters occurred between 1 min and 10 min after the start of phagocytosis, indicating that new NOX2 molecules were delivered to the membrane. The increase may be explained by the fusion of endosomes containing NOX2 with the phagosomal membrane. The NOX2 clusters might already be formed in the endosomal membrane. We don't know whether NOX2 is already assembled with the cytosolic subunits and active inside the endosomes. Such an endosomal ROS production has been described upon endotoxin priming in neutrophils (Lamb et al., 2012). Moreover, the specific granules have also described to be site of ROS production (Karlsson and Dahlgren, 2002). Anderson et al. observed ROS production in extra-phagosomal sites upon phagocytosis and in reponse to Fcg receptor stimulation (Anderson et al., 2010). It would be of interest to examine whether ROS production is detectable at endosomal sites and what could be the functions of this ROS production.

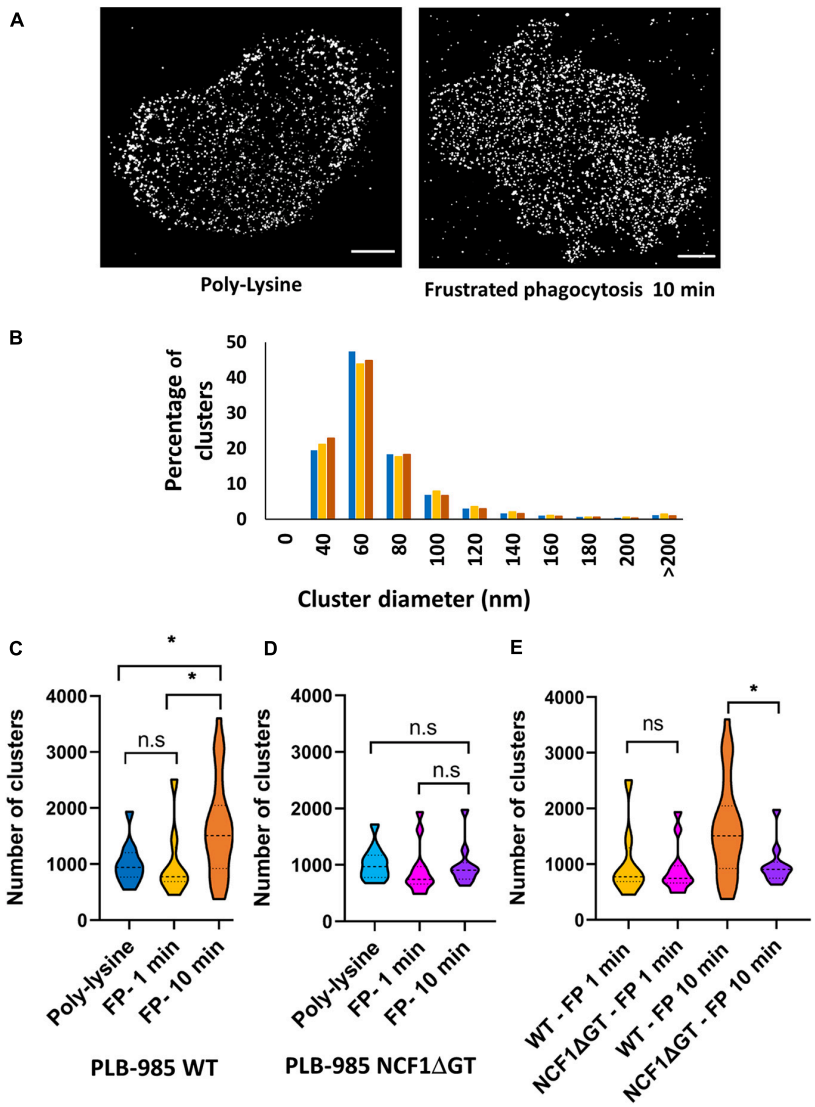

FIGURE 4 | The number of NOX2 nanoclusters increases during frustrated phagocytosis in PLB-985 WT cells but not in PLB-985 NCF1ΔGT cells. Cells were incubated on poly-lysine or for 1 or 10 min on IgG-coated coverslips. The latter conditions promoted frustrated phagocytosis. Following fixation and permeabilization, NOX2 labeling was observed using dSTORM in a TIRFM configuration. **(A)** Representative images of NOX2 in PLB-985 WT cells coated on poly-lysine or following 10 min on IgG-coated coverslips. **(B)** Clusters of NOX2 were detected using SR-Tesseler software. The graph illustrates the distribution of NOX2 nanoclusters according to size on the PLB-985 WT cell surface in the different conditions: non-activated (poly-L-lysine, blue, 11 cells) or after 1 min (yellow, 8 cells) and 10 min (red, 28 cells) of frustrated phagocytosis. Three independent experiments. **(C,D)** Numbers of NOX2 nanoclusters on the cell surface in the different conditions described above for PLB-985 WT cells **(C)** and PLB-985 NCF1ΔGT cells **(D)**. For D, the conditions are the same as C: non-activated cells (cyan, 10 cells), 1 min (pink, 12 cells) or 10 min (purple, 10 cells) of frustrated phagocytosis, three independent experiments. FP: frustrated phagocytosis. **(E)** Comparison between the number of clusters in PLB-985 WT and PLB-985 NCF1ΔGT cells during frustrated phagocytosis for 1 or 10 min. Each violin plot represents the spread of the values. The interquartile range and medians are represented as dotted line. *$p < 0.05$; ns: non-significant (Mann Whitney tests).

Neither the number of clusters nor the degree of cell spreading were modified between 1 and 10 min of phagocytosis in the PLB-985 NCF1ΔGT cells lacking $p47^{phox}$. Thus, $p47^{phox}$ may have a structural role in the recruitment of NOX2 to the phagosome. Alternatively, as these cells lack a functional NADPH oxidase, ROS may be necessary for the delivery of new NOX2 clusters at the phagosome. In order to check this hypothesis, PLB-985 cells expressing inactive mutants of NOX2 (Picciocchi et al., 2011) would be appropriate.

Thus, NADPH oxidase activity may trigger a positive feedback with the recruitment of additional NOX2 positive vesicles. One hypothesis to explain this phenomenon would be that ROS allow the sustained activation of kinases like Erk (Ray et al., 2012) by inactivating protein tyrosine phosphatases such as PTP1B. The Erk kinase favors exocytosis from the Rab11-recycling compartment (Robertson et al., 2006). Thus, a sustained activation of Erk would allow the fusion of Rab-11 vesicles with the phagosome. Further work will be necessary to investigate this hypothesis i.e., the involvement of ROS in membrane fusion in PLB_985 cells but also in neutrophils, which have specific granules containing NOX2.

DATA AVAILABILITY STATEMENT

The original contributions presented in the study are included in the article/**Supplementary Material**, further inquiries can be directed to the corresponding author/s.

AUTHOR CONTRIBUTIONS

JJ, SD-C, and ON designed the research. SD-C supervised the research project. JJ and EH performed the experiments. JJ set up the experiments with the help of SL for the dSTORM and JJ analyzed the experiments. PV and DR constructed the X^0-CGD PLB-985 GFP-NOX2 cells. DW, US, and JR constructed the PLB-985 NCF1ΔGT cells. SD-C wrote the manuscript with the help of JJ. ON and DR commented on the manuscript. All authors contributed to the article and approved the submitted version.

FUNDING

This work was supported by the CNRS and the Université Paris-Saclay. The present work has benefited from the Imagerie-Gif core facility supported by l'Agence Nationale de la Recherche (ANR-11-EQPX-0029/Morphoscope, ANR-10-INBS-04/FranceBioImaging; ANR-11-IDEX-0003-02/Saclay Plant Sciences) and the platform SpICy at Institut de Chimie Physique.

ACKNOWLEDGMENTS

We thank Dr. A. Zak, Dr. A. Mularski, and Dr. F. Niedergang for their help with setting up the frustrated phagocytosis experimental protocols and R. Le Bars for his help at the Imagerie-Gif core facility. We also thank Dr. K. Grant for reading and correcting the manuscript.

SUPPLEMENTARY MATERIAL

The Supplementary Material for this article can be found online at: https://www.frontiersin.org/articles/10.3389/fcell.2020.608600/full#supplementary-material

REFERENCES

Anderson, K. E., Chessa, T. A. M., Davidson, K., Henderson, R. B., Walker, S., Tolmachova, T., et al. (2010). PtdIns3P and Rac direct the assembly of the NADPH oxidase on a novel, pre-phagosomal compartment during FcR-mediated phagocytosis in primary mouse neutrophils. *Blood* 116, 4978–4989. doi: 10.1182/blood-2010-03-275602

Bolte, S., and Cordelières, F. P. (2006). A guided tour into subcellular colocalization analysis in light microscopy. *J. Microsc.* 224, 213–232. doi: 10.1111/j.1365-2818.2006.01706.x

Borregaard, N., Heiple, J. M., Simons, E. R., and Clark, R. A. (1983). Subcellular localization of the b-cytochrome component of the human neutrophil microbicidal oxidase: translocation during activation. *J. Cell Biol.* 97, 52–61. doi: 10.1083/jcb.97.1.52

Casbon, A.-J., Allen, L.-A. H., Dunn, K. W., and Dinauer, M. C. (2009). Macrophage NADPH oxidase flavocytochrome b localizes to the plasma membrane and Rab11-positive recycling endosomes. *J. Immunol.* 182, 2325–2339. doi: 10.4049/jimmunol.0803476

DeLeo, F. R., Burritt, J. B., Yu, L., Jesaitis, A. J., Dinauer, M. C., and Nauseef, W. M. (2000). Processing and maturation of flavocytochrome b558 include incorporation of heme as a prerequisite for heterodimer assembly. *J. Biol. Chem.* 275, 13986–13993. doi: 10.1074/jbc.275.18.13986

Dunn, K. W., Kamocka, M. M., and McDonald, J. H. (2011). A practical guide to evaluating colocalization in biological microscopy. *Am. J. Physiol. Cell Physiol.* 300, C723–C742. doi: 10.1152/ajpcell.00462.2010

El Benna, J., Dang, P. M. C., Gaudry, M., Fay, M., Morel, F., Hakim, J., et al. (1997). Phosphorylation of the respiratory burst oxidase subunit p67(phox) during human neutrophil activation: regulation by protein kinase C-dependent and independent pathways. *J. Biol. Chem.* 272, 17204–17208. doi: 10.1074/jbc.272.27.17204

Endesfelder, U., and Heilemann, M. (2015). "Direct stochastic optical reconstruction microscopy (dSTORM)," in *Methods in Molecular Biology*, ed. J. M. Walker (Totowa, NJ: Humana Press), 263–276. doi: 10.1007/978-1-4939-2080-8_14

Erickson, H. P. (2009). Size and shape of protein molecules at the nanometer level determined by sedimentation, gel filtration, and electron microscopy. *Biol. Proced. Online* 11, 32–51. doi: 10.1007/s12575-009-9008-x

Ester, M., Kriegel, H.-P., Sander, J., and Xu, X. (1996). "A density-based algorithm for discovering clusters in large spatial databases with noise," in *Proceedings of the 2nd International Conference on Knowledge Discovery and Data Mining*, Portland, OR, 226–231.

Freeman, S. A., Goyette, J., Furuya, W., Woods, E. C., Bertozzi, C. R., Bergmeier, W., et al. (2016). Integrins form an expanding diffusional barrier that coordinates phagocytosis. *Cell* 164, 128–140. doi: 10.1016/j.cell.2015.11.048

Garcia-Parajo, M. F., Cambi, A., Torreno-Pina, J. A., Thompson, N., and Jacobson, K. (2014). Nanoclustering as a dominant feature of plasma membrane organization. *J. Cell Sci.* 127, 4995–5005. doi: 10.1242/jcs.146340

Goodridge, H. S., Reyes, C. N., Becker, C. A., Katsumoto, T. R., Ma, J., Wolf, A. J., et al. (2011). Activation of the innate immune receptor Dectin-1 upon formation of a "phagocytic synapse". *Nature* 472, 471–475. doi: 10.1038/nature10071

Hainfeld, J. F., and Powell, R. D. (2000). New frontiers in gold labeling. *J. Histochem. Cytochem.* 48, 471–480. doi: 10.1177/002215540004800404

Karlsson, A., and Dahlgren, C. (2002). Assembly and activation of the neutrophil NADPH oxidase in granule membranes. *Antioxid. Redox Signal.* 4, 49–60. doi: 10.1089/152308602753625852

Lamb, F. S., Hook, J. S., Hilkin, B. M., Huber, J. N., Volk, A. P. D., and Moreland, J. G. (2012). Endotoxin priming of neutrophils requires endocytosis and NADPH oxidase-dependent endosomal reactive oxygen species. *J. Biol. Chem.* 287, 12395–12404. doi: 10.1074/jbc.M111.306530

Levet, F., Hosy, E., Kechkar, A., Butler, C., Beghin, A., Choquet, D., et al. (2015). SR-Tesseler: a method to segment and quantify localization-based super-resolution microscopy data. *Nat. Methods* 12, 1065–1071. doi: 10.1038/nmeth.3579

Lominadze, G., Powell, D. W., Luerman, G. C., Link, A. J., Ward, R. A., and McLeish, K. R. (2005). Proteomic analysis of human neutrophil granules. *Mol. Cell. Proteomics* 4, 1503–1521. doi: 10.1074/mcp.M500143-MCP200

Marion, S., Mazzolini, J., Herit, F., Bourdoncle, P., Kambou-Pene, N., Hailfinger, S., et al. (2012). The NF-κB signaling protein Bcl10 regulates actin dynamics by controlling AP1 and OCRL-bearing vesicles. *Dev. Cell* 23, 954–967. doi: 10.1016/j.devcel.2012.09.021

Mu, F.-T., Callaghan, J. M., Steele-Mortimer, O., Stenmark, H., Parton, R. G., Campbell, P. L., et al. (1995). EEA1, an early endosome-associated protein. *J. Biol. Chem.* 270, 13503–13511. doi: 10.1074/jbc.270.22.13503

Mularski, A., Marie-Anaïs, F., Mazzolini, J., and Niedergang, F. (2018). "Observing frustrated phagocytosis and phagosome formation and closure using total internal reflection fluorescence microscopy (TIRFM)," in *Methods in Molecular Biology*, ed. J. M. Walker (Totowa, NJ: Humana Press), 165–175. doi: 10.1007/978-1-4939-7837-3_16

Niedergang, F., Colucci-Guyon, E., Dubois, T., Raposo, G., and Chavrier, P. (2003). ADP ribosylation factor 6 is activated and controls membrane delivery during phagocytosis in macrophages. *J. Cell Biol.* 161, 1143–1150. doi: 10.1083/jcb.200210069

Niedergang, F., Di Bartolo, V., and Alcover, A. (2016). Comparative anatomy of phagocytic and immunological synapses. *Front. Immunol.* 7:18. doi: 10.3389/fimmu.2016.00018

Nunes, P., Demaurex, N., and Dinauer, M. C. (2013). Regulation of the NADPH oxidase and associated ion fluxes during phagocytosis. *Traffic* 14, 1118–1131. doi: 10.1111/tra.12115

O'Neill, S., Brault, J., Stasia, M.-J., and Knaus, U. G. (2015). Genetic disorders coupled to ROS deficiency. *Redox Biol.* 6, 135–156. doi: 10.1016/j.redox.2015.07.009

Ovesný, M., Křížek, P., Borkovec, J., Švindrych, Z., and Hagen, G. M. (2014). ThunderSTORM: a comprehensive ImageJ plug-in for PALM and STORM data analysis and super-resolution imaging. *Bioinformatics* 30, 2389–2390. doi: 10.1093/bioinformatics/btu202

Pageon, S. V., Tabarin, T., Yamamoto, Y., Ma, Y., Nicovich, P. R., Bridgeman, J. S., et al. (2016). Functional role of T-cell receptor nanoclusters in signal initiation and antigen discrimination. *Proc. Natl. Acad. Sci. U.S.A.* 113, E5454–E5463. doi: 10.1073/pnas.1607436113

Pauwels, A.-M., Trost, M., Beyaert, R., and Hoffmann, E. (2017). Patterns, receptors, and signals: regulation of phagosome maturation. *Trends Immunol.* 38, 407–422. doi: 10.1016/j.it.2017.03.006

Picciocchi, A., Debeurme, F., Beaumel, S., Dagher, M.-C., Grunwald, D., Jesaitis, A. J., et al. (2011). Role of putative second transmembrane region of Nox2 protein in the structural stability and electron transfer of the phagocytic NADPH oxidase. *J. Biol. Chem.* 286, 28357–28369. doi: 10.1074/jbc.M111.220418

Pivot-Pajot, C., Chouinard, F. C., Amine El Azreq, M., Harbour, D., and Bourgoin, S. G. (2010). Characterisation of degranulation and phagocytic capacity of a human neutrophilic cellular model, PLB-985 cells? *Immunobiology* 215, 38–52. doi: 10.1016/j.imbio.2009.01.007

Ray, P. D., Huang, B.-W., and Tsuji, Y. (2012). Reactive oxygen species (ROS) homeostasis and redox regulation in cellular signaling. *Cell. Signal.* 24, 981–990. doi: 10.1016/j.cellsig.2012.01.008

Rincón, E., Rocha-Gregg, B. L., and Collins, S. R. (2018). A map of gene expression in neutrophil-like cell lines. *BMC Genomics* 19:573. doi: 10.1186/s12864-018-4957-6

Robertson, S. E., Setty, S. R. G., Sitaram, A., Marks, M. S., Lewis, R. E., and Chou, M. M. (2006). Extracellular signal-regulated kinase regulates clathrin-independent endosomal trafficking. *Mol. Biol. Cell* 17, 645–657. doi: 10.1091/mbc.e05-07-0662

Song, Z., Hudik, E., Le Bars, R., Roux, B., Dang, P. M. C., El Benna, J., et al. (2020). Class I phosphoinositide 3-kinases control sustained NADPH oxidase activation in adherent neutrophils. *Biochem. Pharmacol.* 178:114088. doi: 10.1016/j.bcp.2020.114088

Tlili, A., Dupre-Crochet, S., Erard, M., and Nusse, O. (2011). Kinetic analysis of phagosomal production of reactive oxygen species. *Free Radic. Biol. Med.* 50, 438–447. doi: 10.1016/j.freeradbiomed.2010.11.024

Tlili, A., Erard, M., Faure, M. C., Baudin, X., Piolot, T., Dupre-Crochet, S., et al. (2012). Stable accumulation of p67(phox) at the phagosomal membrane and ROS production within the phagosome. *J. Leukoc. Biol.* 91, 83–95. doi: 10.1189/jlb.1210701

Vale-Costa, S., and Amorim, M. (2016). Recycling endosomes and viral infection. *Viruses* 8:64. doi: 10.3390/v8030064

Valenta, H., Erard, M., Dupré-Crochet, S., and Nüβe, O. (2020). The NADPH Oxidase and the Phagosome. *Adv. Exp. Med. Biol.* 1246, 153–177. doi: 10.1007/978-3-030-40406-2_9

van Manen, H.-J., Verkuijlen, P., Wittendorp, P., Subramaniam, V., van den Berg, T. K., Roos, D., et al. (2008). Refractive index sensing of green fluorescent proteins in living cells using fluorescence lifetime imaging microscopy. *Biophys. J.* 94, L67–L69. doi: 10.1529/biophysj.107.127837

Wientjes, F. B., Segal, A. W., and Hartwig, J. H. (1997). Immunoelectron microscopy shows a clustered distribution of NADPH oxidase components in the human neutrophil plasma membrane. *J. Leukoc. Biol.* 61, 303–312. doi: 10.1002/jlb.61.3.303

Wrona, D., Siler, U., and Reichenbach, J. (2017). CRISPR/Cas9-generated p47phox-deficient cell line for chronic granulomatous disease gene therapy vector development. *Sci. Rep.* 7:44187. doi: 10.1038/srep44187

Yokosuka, T., Sakata-Sogawa, K., Kobayashi, W., Hiroshima, M., Hashimoto-Tane, A., Tokunaga, M., et al. (2005). Newly generated T cell receptor microclusters initiate and sustain T cell activation by recruitment of Zap70 and SLP-76. *Nat. Immunol.* 6, 1253–1262. doi: 10.1038/ni1272

Zak, A. (2019). *Mécanique de la Phagocytose et Comparaison Avec D'autres Processus Immunitaires*. master's thesis, Ecole Polytechnique-Université, Paris.

Zhen, L., King, A. A. J., Xiao, Y., Chanock, S. J., Orkin, S. H., and Dinauer, M. C. (1993). Gene targeting of X chromosome-linked chronic granulomatous disease locus in a human myeloid leukemia cell line and rescue by expression of recombinant gp91phox. *Proc. Natl. Acad. Sci. U.S.A.* 90, 9832–9836. doi: 10.1073/pnas.90.21.9832

Conflict of Interest: The authors declare that the research was conducted in the absence of any commercial or financial relationships that could be construed as a potential conflict of interest.

frontiers in Cell and Developmental Biology

BRIEF RESEARCH REPORT
published: 08 December 2020
doi: 10.3389/fcell.2020.613733

Neutrophils Return to Bloodstream Through the Brain Blood Vessel After Crosstalk With Microglia During LPS-Induced Neuroinflammation

Yu Rim Kim[1,2†], Young Min Kim[3†], Jaeho Lee[1,2], Joohyun Park[1,2], Jong Eun Lee[1,2] and Young-Min Hyun[1,2]*

[1] Department of Anatomy, Yonsei University College of Medicine, Seoul, South Korea, [2] BK21 PLUS Project for Medical Science, Yonsei University College of Medicine, Seoul, South Korea, [3] Department of Medicine, Yonsei University College of Medicine, Seoul, South Korea

OPEN ACCESS

Edited by:
Zhichao Fan,
UCONN Health, United States

Reviewed by:
Rongrong Liu,
Northwestern University, United States
Bo Liu,
University of California, Berkeley, United States
Souvarish Sarkar,
Brigham and Women's Hospital and Harvard Medical School, United States

***Correspondence:**
Young-Min Hyun
ymhyun@yuhs.ac

[†] *These authors have contributed equally to this work*

Specialty section:
This article was submitted to Cell Adhesion and Migration, a section of the journal Frontiers in Cell and Developmental Biology

Received: *03 October 2020*
Accepted: *20 November 2020*
Published: *08 December 2020*

Citation:
Kim YR, Kim YM, Lee J, Park J, Lee JE and Hyun Y-M (2020) Neutrophils Return to Bloodstream Through the Brain Blood Vessel After Crosstalk With Microglia During LPS-Induced Neuroinflammation. Front. Cell Dev. Biol. 8:613733. doi: 10.3389/fcell.2020.613733

The circulatory neutrophil and brain tissue-resident microglia are two important immune cells involved in neuroinflammation. Since neutrophils that infiltrate through the brain vascular vessel may affect the immune function of microglia in the brain, close investigation of the interaction between these cells is important in understanding neuroinflammatory phenomena and immunological aftermaths that follow. This study aimed to observe how morphology and function of both neutrophils and microglia are converted in the inflamed brain. To directly investigate cellular responses of neutrophils and microglia, $LysM^{GFP/+}$ and $CX_3CR1^{GFP/+}$ mice were used for the observation of neutrophils and microglia, respectively. In addition, low-dose lipopolysaccharide (LPS) was utilized to induce acute inflammation in the central nervous system (CNS) of mice. Real-time observation on mice brain undergoing neuroinflammation via two-photon intravital microscopy revealed various changes in neutrophils and microglia; namely, neutrophil infiltration and movement within the brain tissue increased, while microglia displayed morphological changes suggesting an activated state. Furthermore, neutrophils seemed to not only actively interact with microglial processes but also exhibit reverse transendothelial migration (rTEM) back to the bloodstream. Thus, it may be postulated that, through crosstalk with neutrophils, macrophages are primed to initiate a neuroinflammatory immune response; also, during pathogenic events in the brain, neutrophils that engage in rTEM may deliver proinflammatory signals to peripheral organs outside the brain. Taken together, these results both show that neuroinflammation results in significant alterations in neutrophils and microglia and lay the pavement for further studies on the molecular mechanisms behind such changes.

Keywords: neuroinflammation, neutrophil, microglia, reverse transendothelial migration, two-photon intravital imaging

Abbreviations: BBB, Blood-brain barrier; CNS, Central nervous system; GFP, Green fluorescent protein; LPS, Lipopolysaccharide; rTEM, reverse Transendothelial migration; SPF, Specific pathogen-free; TEM, Transendothelial migration; WGA, Wheat-germ agglutinin.

INTRODUCTION

Neuroinflammation is generally defined as the response of brain cells to infection and other sources of cell death, involving infiltration of circulating immune cells to the brain. Such infiltration of immune cells occur due to microglial and glial cell activation and blood-brain barrier (BBB) dysfunction during the pathogenesis of various illnesses, such as Alzheimer's disease, Parkinson's disease, and Amyotrophic lateral sclerosis (Shastri et al., 2013; Mammana et al., 2018).

Neutrophils are commonly known as the earliest responders to acute inflammation, aiding the initiation and continuation of immune reactions throughout the human body (Nathan, 2006). Neutrophils are highly versatile cells with various immune functions, such as inflammation mediation, microbial capture via granular proteins, and repair of sterile wounds (Kruger et al., 2015). In particular, during neuroinflammation, neutrophils participate in the general immune response by signaling to diverse cell types, including endothelial cells, mesenchymal stem cells, lymphocytes, and microglia (Ahn et al., 2020). Recent reports have emphasized the variety of roles neutrophils can play in neuroinflammation, where brain resident cells participate in a coordinated fashion (Liu et al., 2018).

Microglia, the resident macrophages of the central nervous system (CNS), are distinguished from other glial cells, such as astrocytes and oligodendrocytes by their gene expression, morphology, and function (Ransohoff and Perry, 2009; Kettenmann et al., 2011; Zhao et al., 2019). In contrast to other glial cells, microglia function as the primary reacting cells for regulating neuroinflammatory response by phagocytizing and removing myelin inhibitors, debris and dead cells in the CNS (Li et al., 2005; Zhao et al., 2019). Microglia also take part in innate and adaptive immunity by regulating immune tolerance (Saijo and Glass, 2011). Microglia are functionally and morphologically divided into three forms: the ramified, activated and ameboid morphologies. Ramified microglia, with a small cell body and long branches, have no functional capability of phagocytosis and antigen presentation but maintain an immunologically stable environment. When ramified microglia are stimulated by neurodegeneration, endotoxin, interferon, or endothelial activation, activation pathways cause them to transform into activated microglia. Activated microglia exhibit thicker and more retracted branches and possess the ability exhibit antigen presentation and phagocytosis. Additionally, activated microglia, when changed to the ameboid shape, display free movement during phagocytosis but do not engage in antigen presentation and inflammation (Cai et al., 2014). In addition, excessive or long-term activation of microglia induces neuronal death and an increase in pro-inflammatory cytokines.

In this study, we aimed to observe the effects of lipopolysaccharide (LPS)-induced neuroinflammation on neutrophils and microglia within brain tissue of live mice. To this end, we attempted to obtain visual evidence of the effects of neuroinflammation on neutrophils and microglia using two-photon intravital imaging, which may then serve as a basis for further research on the molecular and mechanistic bases of such modifications.

MATERIALS AND METHODS

Mice

$LysM^{GFP/+}$ (Faust et al., 2000) and $CX_3CR1^{GFP/+}$ (Jung et al., 2000) mice, in which the lysozyme and the CX_3CR1 gene are replaced by green fluorescent protein (GFP), respectively, were obtained and used for the visualization of neutrophil and microglia. All mice were kept in a specific pathogen-free (SPF) room, a light cycle from 7:00 AM to 7:00 PM at 23 ± 2°C, and 55 ± 10% humidity. All procedures were conducted in accordance with the guidelines of the Institutional Animal Care and Use Committee of Yonsei University College of Medicine, South Korea (IACUC, 2019-0097).

Identification of Mouse Genotype

Genotyping for each strain ($LysM^{GFP/+}$ and $CX_3CR1^{GFP/+}$ mice) was performed using a Genomic DNA Prep Kit (BioFACT, South Korea). A toe of 7–10 day-old mice was severed, and then DNA extraction from the acquired toe was conducted using the Genomic DNA Prep Kit. Template DNA (50 ng/μl), primers and 2×Taq PCR master mix2 10 μl (BioFACT, South Korea) were mixed in a PCR tube, in which distilled water was added up to 20 μl reaction volume.

Cranial Window Surgery

The cranial window was implanted on the calvaria for intravital brain imaging as previously described (Baik et al., 2014). Mice were deeply anesthetized using intraperitoneal injection of zoletil (Virbac, France) at a dose of 30 mg/kg and rompun (Bayer, Germany) at a dose of 10 mg/kg. Body temperature in each mouse was maintained at 37 ± 0.5°C using heating pads during cranial window surgery (**Supplementary Figure 1**). Mice were fixed in a stereotaxic instrument (Live Cell Instrument, South Korea) during all procedures. A cranial window of 5 mm in diameter was made in the right hemisphere. The head skin and the periosteum on the calvaria were removed from between the eyes to the caudal region of the ears. Between the lambda and bregma regions on the right hemisphere, a circular opening was carved with a micro drill, frequently washed with cool phosphate-buffered saline (PBS), and sealed with a round coverslip (diameter = 5 mm) using tissue glue on the skull using the optical microscope. A metal frame was glued and fixed using dental cement (B.J.M laboratory, Israel) on the borders of the cranial window and skull area for filling imaging area with distilled water. The metal frame was assembled with a stereotactic head fixation device attached to the heating plate.

Two-Photon Intravital Microscopy

Mice were anesthetized using intraperitoneal injection of Zoletil at a dose of 30 mg/kg and rompun at a dose of 10 mg/kg during imaging. The imaging stage was composed of a XY micro stage and a stereotactic head fixation device connected to a DC temperature controller (**Supplementary Figure 1A**). Both two-photon microscopies with W Plan-Apochromat 20×/1.0 water immersion lens from Carl-Zeiss, Germany (LSM7MP) and from IVIM Technology, South Korea (IVM-M) were used for imaging

data generation. LysM$^{GFP/+}$ mice were intravenously injected with 70-kDa Texas red dextran (2.5 mg/kg, Sigma-Aldrich, Germany) for visualizing blood vessels. $CX_3CR1^{GFP/+}$ mice were intravenously injected with CF405M-conjugated Wheat germ agglutinin (WGA) (2.5 mg/kg, Biotium, CA, United States) for visualizing blood vessels and PE-conjugated anti-Ly6G antibody (0.1 mg/kg, BioLegend, CA, United States) for observing neutrophils. For two-photon excitation, each mouse brain was excited with light of 800 nm and 880 nm wavelength for imaging of green, red, and blue. All images were acquired at a resolution of 512 × 512 pixels using steps of size 1 μm to a depth of 40–50 μm for 1 min (Park et al., 2018; Lee et al., 2019).

LPS-Induced Neuroinflammatory Mouse Model

Previous studies established that LPS-induced inflammation in the periphery can prompt immune responses in the central nervous system (Ebersoldt et al., 2007; Zhao et al., 2019). To investigate the migratory patterns of neutrophil and microglia during neuroinflammation, mice were treated with daily intraperitoneal injections of lipopolysaccharide (1.0 mg/kg, Sigma-Aldrich, Germany) for 2 consecutive days. Control mice were intraperitoneally injected with daily PBS injections for 2 consecutive days. Intravital imaging was performed at 6 h after LPS injections for 2 consecutive days.

Imaging Data Analysis

Volocity (PerkinElmer, MA, United States), Imaris (Bitplane, Switzerland), and Fiji/Image J (NIH, United States) were used for 3D and 4D imaging data analysis.

Chemokine Microarray

Following LPS stimulation, brains of mice were lysed by adding protease inhibitor cocktail (Roche, Germany) containing PRO-PREP (Intron biotechnology, South Korea) and 1% Triton X-100. Cytokine and chemokine levels were detected using Proteome Profiler Mouse Cytokine Array Panel A (R&D systems, MN, United States) according to the manufacturer's instruction. The Array kit detected C5/C5a, G-CSF, M-CSF, GM-CSF, sICAM-1, IFN-γ, IL-1α, IL-1β, IL-1ra, IL-2, IL-3, IL-4, IL-5, IL-6, IL-7, IL-10, IL-13, IL-12p70, IL-16, IL-17, IL-23, IL-27, CXCL1, CXCL2, CXCL9, CXCL10, CXCL11, CXCL12, CXCL13, CCL1, CCL2, CCL3, CCL4, CCL5, CCL11, CCL12, CCL17, TIMP-1, TNF-α, and TREM-1. The blots were analyzed using the quick spots tool in HLImage++ (Western Vision Software, UT, United States).

Statistical Analysis

All experiments were repeated at least three times. Statistical analyses were expressed as mean ± standard error of the mean (S.E.M). Statistical analysis was performed using Prism (GraphPad software, CA, United States). For comparison of two groups, unpaired two-sided Student *t*-tests were applied. *p*-values less than 0.05 were considered statistically significant.

RESULTS

LPS-Induced Systemic Inflammation Triggers Intravascular Adhesion and Infiltration of Neutrophils Through Brain Blood Vessels

To investigate the effect of inflammatory status via LPS injection, the weight of mice injected with LPS was compared to that of the control group, as weight loss is a hallmark of systemic inflammation. The LPS group showed an 11.75% loss in body weight compared to the control group, confirming that inflammation had indeed been induced in the LPS-injected mice (**Figure 1A**). Previous studies have demonstrated that neutrophils are recruited in the brain during LPS-induced systemic inflammation to fulfill their roles in the immune response (Zhou et al., 2009; He et al., 2016). Our results confirmed this result, as neutrophil extravasation to the brain parenchyma was observed more frequently in response to LPS injection. In addition, an increased number of neutrophils were observed, which resulted from intravascular adhesion and infiltration (**Figures 1B,C** and **Supplementary Video 1**). Consistent with such findings, transendothelial migration (TEM) of neutrophils was also facilitated in the LPS group, where neutrophils actively emerged out to the brain parenchyma (**Figure 1D** and **Supplementary Video 2**). Altogether, these data demonstrate that LPS injection and the subsequent inflammatory consequences that follow yield a considerable increase in neutrophil influx to the brain parenchyma.

Neutrophils Exhibit Active Motility in the Brain Parenchyma During Neuroinflammation

Along with an increment in cell number, neutrophils displayed an increase in motility, as exhibited in various motion-related criteria. The motility of neutrophils was determined and assessed using various factors, including track length, track velocity, displacement, and meandering index. The track length and track velocity of migrating neutrophils in the brain parenchyma were significantly higher in the LPS group compared to the control group, indicating more active locomotion in response to LPS injection. Furthermore, these results revealed that infiltrated neutrophils showed constant migration within a 20 μm radius for 30 min, suggesting significant motility of neutrophils during neuroinflammatory response; in addition, a lower meandering index compared to the control group may signify more directionality in neutrophil movement in LPS-injected mice (**Figures 1E–I**). Thus, these results indicate that during neuroinflammation, the motility of neutrophils in the brain parenchyma is notably increased, suggesting a change in the molecular and biochemical profile of the neutrophils.

Inflammation in the Brain Triggers Numerical Reduction and Morphological Shortening of Microglia

As the predominant innate immune cell population that is resident to the brain, microglia play a role in the process of

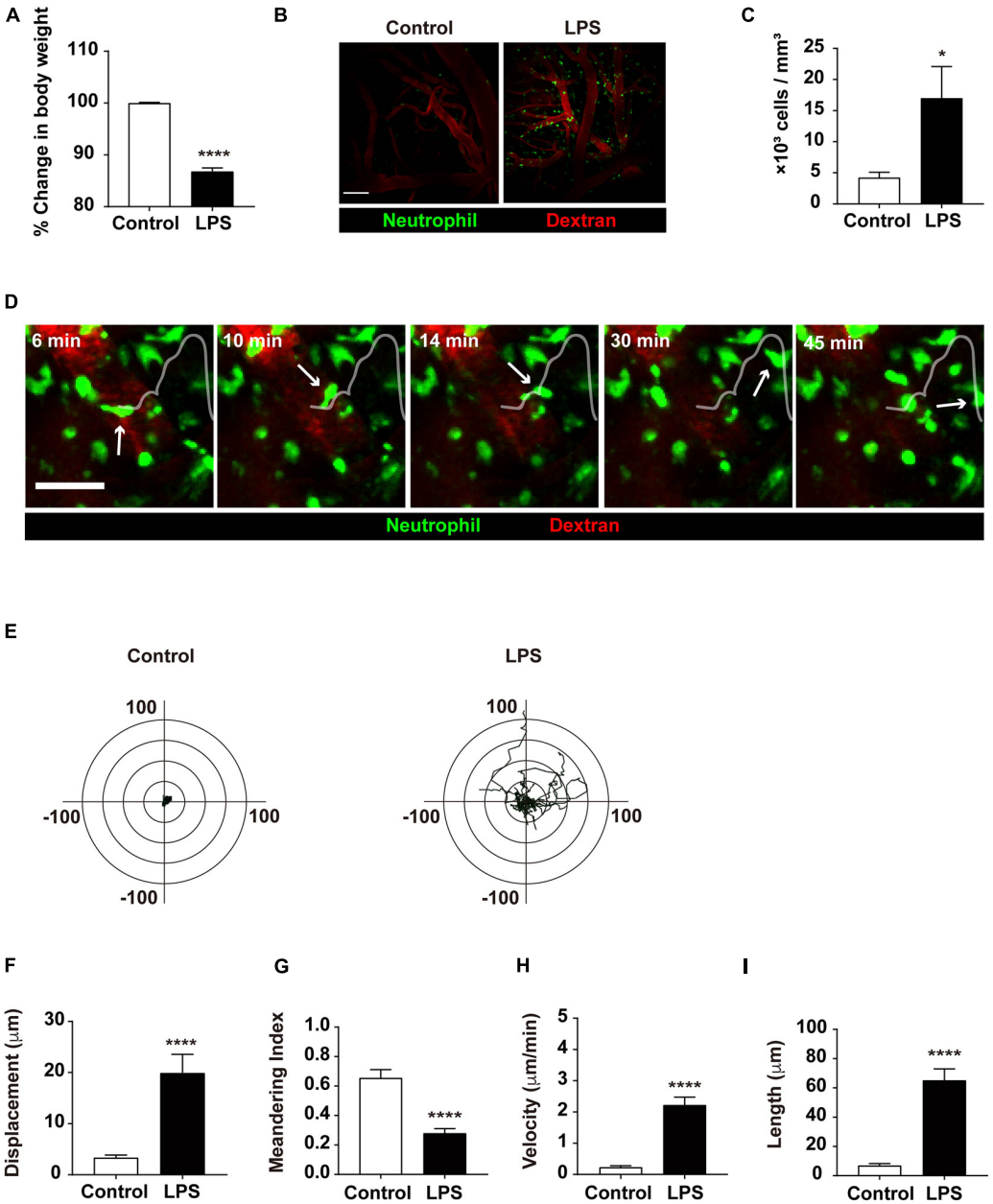

FIGURE 1 | Quantitative analysis of neutrophil infiltration from the blood vessel to brain parenchyma. **(A)** Representative graph of weight loss in the LPS-treated group compared to the control group. The % change in body weight was calculated as (body weight before LPS treatment/body weight after LPS treatment) × 100. Data indicate mean ± SEM using Student's *t*-test (****$p < 0.0001$, $n = 7$ mice per group). **(B)** LysM$^{GFP/+}$ mice were used to visualize neutrophils (green) via TPIM. Texas red dextran was i.v. injected to stain blood vessels (red). Representative images are shown from the brain of mice injected with PBS (control) or LPS, respectively. Scale bar, 100 μm (see **Supplementary Video 1**). **(C)** Measurement of infiltrated neutrophils in the control and LPS groups. Data indicate mean ± SEM using Student's *t*-test (*$p < 0.05$, $n = 3$ mice per group of three independent experiments). **(D)** A series of representative time-lapse images show neutrophil infiltration into inflamed brain parenchyma of LysM$^{GFP/+}$ mice. Scale bar, 50 μm (see **Supplementary Video 2**). **(E)** Overlay of the representative migration tracks of neutrophils in brain parenchyma for 30 min. *x*-, *y*-axis (length), -100 to 100 μm. $n = 30$ cells per group, PBS or LPS-treated mice for three independent experiments. Migration was quantitatively assessed with tracking analyses: **(F)** displacement (μm), **(G)** meandering index (displacement/length), **(H)** velocity (μm/min), and **(I)** length (μm) in two different conditions for 30 min. Data indicate mean ± SEM using Student's *t*-test (****$p < 0.0001$, $n = 30$ cells per group of three independent experiments).

neuroinflammation. Therefore, it was important that the effects of LPS injection and the ensuing inflammatory aftermaths on microglia were investigated. Specifically, it had previously been suggested that neutrophils may interact with microglia; as our aforementioned results indicate various changes in neutrophils during neuroinflammation, it is crucial to unravel any microglial

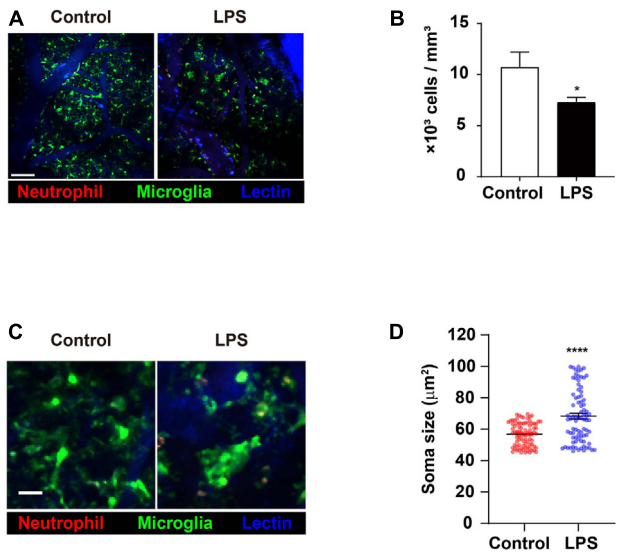

FIGURE 2 | Numerical reduction and morphological shortening of microglia in LPS-treated mice. $CX_3CR1^{GFP/+}$ mice were used to visualize microglia (green) in brain parenchyma using TPIM. CF405M-conjugated lectin was i.v. injected to stain blood vessels (blue). PE-conjugated anti-Ly6G antibody was i.v. injected to label neutrophils (red). **(A)** Representative images from brains of mice injected with PBS (control) and LPS, respectively (see **Supplementary Video 3**). Scale bar, 100 μm. **(B)** Measurement of microglia numbers. Data indicate mean ± SEM using Student's *t*-test (*$p < 0.05$, $n = 3$ mice per group of three independent experiments). **(C)** Representative image showing difference in microglial morphologies between control and LPS groups. Scale bar, 30 μm (see **Supplementary Video 4**). **(D)** Quantification of microglia soma size. Data indicate mean ± SEM using Student's *t*-test (****$p < 0.0001$, more than 70 cells were analyzed per group from three independent experiments).

changes during similar situations in order to pinpoint any biomolecular interactions between the two innate immune cell populations (Sevenich, 2018). Imaging data in the brain showed that the number of microglia in LPS-injected mice had decreased compared to the control group, a phenomenon that may have been caused by a variety of apoptosis-inducing agents (**Figures 2A,B** and **Supplementary Video 3**; Steff et al., 2001; Fortin et al., 2005). Also, while microglia in the control group predominantly displayed the morphology of ramified microglia, those in the LPS group showed the morphology of activated microglia, with short and thick processes and enlarged cell bodies (**Figure 2C** and **Supplementary Video 4**). To focus on a more detailed analysis, such as the microglia cell soma, we quantified the change in microglia soma size between control and LPS group. Compared to control mice, the average of soma size increased (56.85 vs. 68.32 μm^2) (**Figure 2D**). The result demonstrated the LPS exposure leads to activated microglia that features bigger soma size than ramified microglia called "resting" cells (Kozlowski and Weimer, 2012; Davis et al., 2017). Taken together, these results demonstrate that LPS-induced neuroinflammation may activate microglia, leading to morphological alterations that suggest an activated state (Liu and Hong, 2003).

Neutrophil-Microglia Crosstalk in Inflamed Brain Parenchyma Leads to Engulfment of Neutrophils by Microglia

During the neuroinflammatory response, neutrophils have been thought to actively interact with cells in the vicinity, such as astrocytes, microglia, and adaptive immune cells (He et al., 2016; Girbl et al., 2018). Imaging data from the present study supports this idea, as contact between infiltrated neutrophils and brain tissue-resident microglia was observed (**Figures 3A,B** and **Supplementary Video 5**). After neutrophils made contact with microglial processes, microglia seemed to engulf the neutrophils, indicating the possibility of molecular crosstalk between the two cell groups. On the other hand, during neutrophil-microglial contact, nearby microglial processes were observed to stretch toward the point of contact (**Figures 3C,D** and **Supplementary Video 6**). Such phenomena further reinforces the idea that contact between neutrophil and microglia accompanies intercellular crosstalk, affecting not only the cells making contact but also the surrounding environment. Overall, while the underlying mechanisms are yet to be revealed, these results strongly suggest that inflammatory states not only prompt crosstalk and contact between neutrophils and microglia, but also attract other microglia toward sites of neutrophil-microglia contact.

Reverse Transendothelial Migration of Neutrophils Is Observed in Inflamed Brain Parenchyma

An interesting event regarding neutrophils that have been reported in previous literature is reverse transendothelial migration (rTEM), where neutrophils that had extravasated out of the blood vessel re-enters the bloodstream (Colom et al., 2015; Wu et al., 2016; Burn and Alvarez, 2017). While rTEM had been observed in various parts of the body, imaging results from the present study are the first to suggest that the process also takes place in brain blood vessels (**Figures 4A,B** and **Supplementary Videos 7, 8**). Neutrophils engaging in rTEM first approach the blood vessel, and after a period of movement along the perivascular region, re-enters and eventually gets swept away by the bloodstream. Albeit a rare phenomenon, rTEM of neutrophils that had been exposed to inflammatory environments may lead to significant repercussions, as it is possible that the molecular profile of re-entering neutrophils is altered; nevertheless, the present results suggest that rTEM is a readily observable phenomenon during neuroinflammation.

To investigate the molecular aftereffects of LPS injection that may have stimulated neutrophil rTEM, brain chemokine arrays were conducted to detect changes in chemokine expression levels following LPS injection (**Figure 4C**). As a result, levels of the chemokines CXCL1, CXCL10, CXCL13, CCL2, and CCL5 were found to be increased, a consequence which may affect the function and motility of microglia and neutrophils. As such, it may be postulated that increased levels of the aforementioned chemokines had stimulated neutrophil migration and rTEM as presented above.

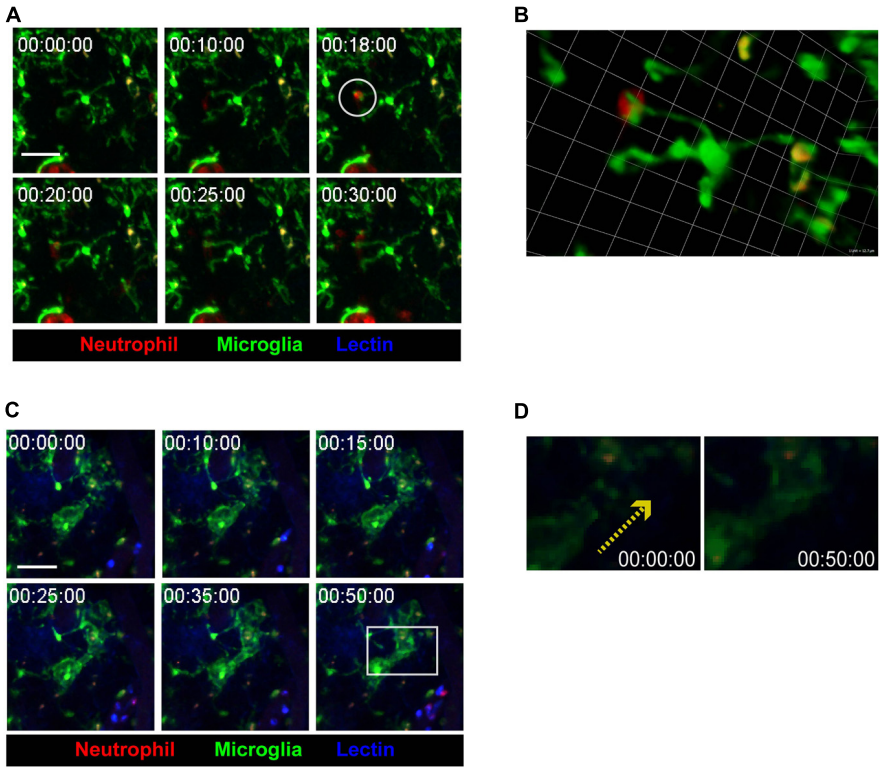

FIGURE 3 | Crosstalk between microglia and neutrophils in inflamed brain parenchyma. $CX_3CR1^{GFP/+}$ mice were used to visualize microglia (green) in brain parenchyma using TPIM. CF405M-conjugated lectin was i.v. injected to stain blood vessels (blue). PE-conjugated anti-Ly6G antibody was i.v. injected to label neutrophils (red). **(A)** A series of representative time-lapse images showing contact between microglia and neutrophils (white circle). Scale bar, 40 μm (see **Supplementary Video 5**). **(B)** Magnification of a region of interest, indicated by a white circle in **(A)**, in 3D. Scale bar per 1 unit. Scale bar, 12.7 μm. **(C)** A series of representative time-lapse images showing elongation of microglial processes toward site neutrophil-microglial contact (white square). Scale bar, 40 μm (see **Supplementary Video 6**). **(D)** Direction of microglial process elongation from 0 to 50 min (yellow-dotted arrow).

DISCUSSION

The CNS had been known to be an "immune privileged site," most likely due to the presence of the highly impenetrable BBB; yet recent studies have demonstrated flexibility in the BBB in response to inflammation-related needs and stimuli (Kanashiro et al., 2020). Indeed, in neuroinflammatory situations, neutrophils and CNS-resident microglia are suggested to participate in the inflammatory response, as supported by the imaging results of this study. With such visual evidence at hand, investigation of the molecular bases behind the observed phenomena is of significant importance, especially in clinical settings. In previous literature, the molecules responsible for the recruitment of neutrophils to neuroinflammatory sites have been given substantial attention. For instance, in the case of autoimmune diseases, such as multiple sclerosis or experimental autoimmune encephalomyelitis, neutrophils are known to be attracted by the release of CXCL1, CXCL2, and CXCL5, which are in turn stimulated by different molecules, such as IL-17 or IFN-γ (Christy et al., 2013; Simmons et al., 2014). The behavior of neutrophils in neurodegenerative diseases including Alzheimer's has also been a target of scrutiny, as neutrophil infiltration is known to contribute to the exacerbation of such diseases. In particular, it has been suggested that neutrophils accumulate in regions rich in amyloid-β deposits via the integrin LFA-1; in addition, CXCL12 and CCL2 levels in the CNS were shown to be principal factors resulting in neutrophil infiltration (Zenaro et al., 2015; Echeverria et al., 2016; Jiang et al., 2016). In line with results from previous literature, expression levels of certain chemokines were increased after LPS injection in this study; in specific, among the aforementioned chemokines, CXCL1 and CCL2 demonstrated a surge in expression, along with CXCL13, CXCL10, and CCL5. CXCL1 and CCL2 are well-known for their roles in stimulating neutrophil migration, while CXCL10, CCL2, and CCL5 have been reported to be released by neutrophils in inflammatory situations, mostly in order to recruit other innate or adaptive immune cells (Kobayashi, 2008; Sawant et al., 2016; Capucetti et al., 2020). Therefore, chemokines that are chemotactic for neutrophils, such as CXCL1 or CCL2 may be the principal factor driving the various migratory phenomena observed in this paper: neutrophil extravasation and rTEM. In addition, it may be postulated that LPS-induced neuroinflammation had caused phenotypical modifications in neutrophils, prompting them to release chemokines that yield further steps down the inflammatory cascade, including further recruitment of neutrophils or chemoattraction of adaptive

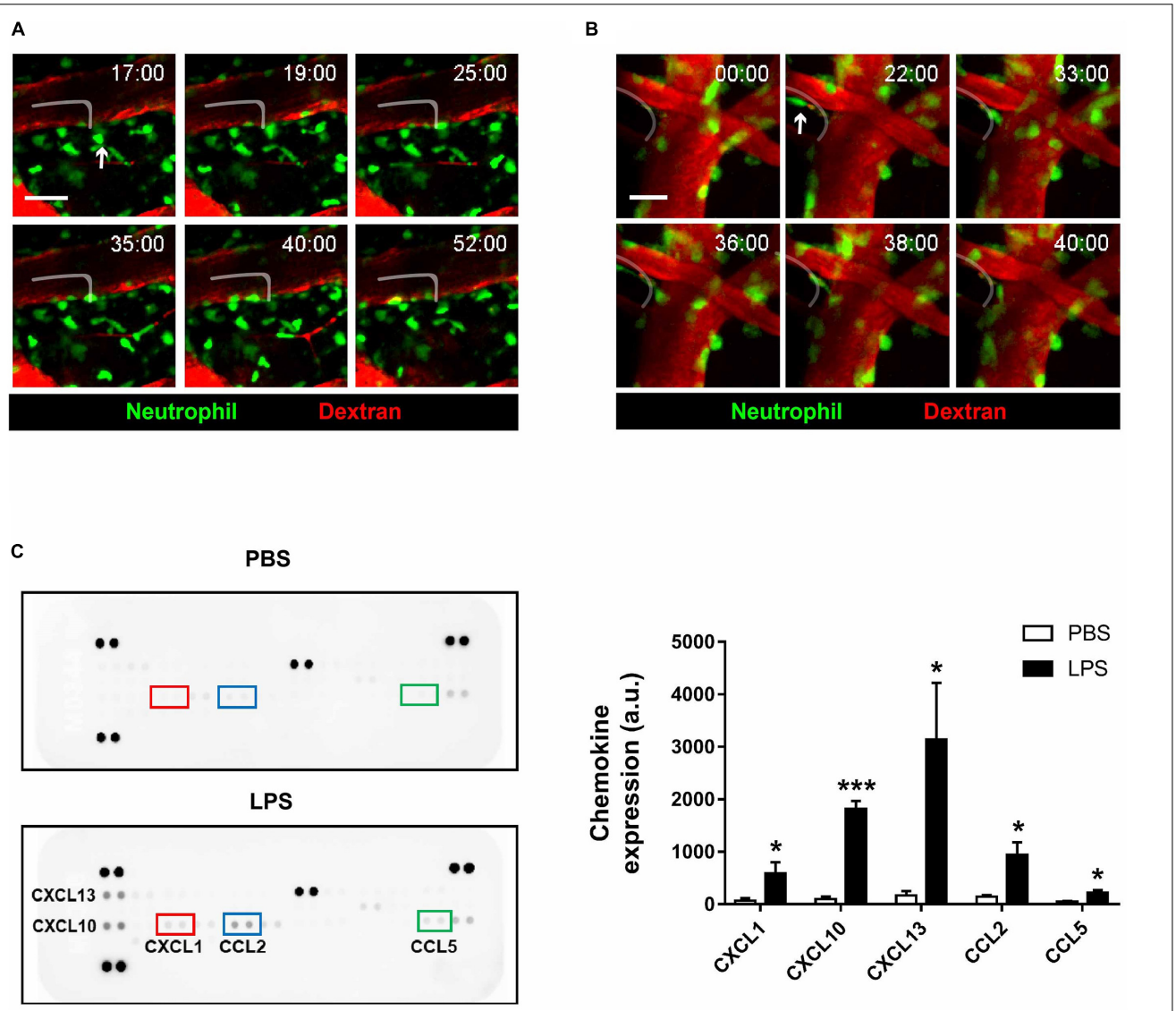

FIGURE 4 | Reverse-transendothelial migration of neutrophils in inflamed brain parenchyma. LysM$^{GFP/+}$ mice were used to visualize neutrophils (green) during neuroinflammation. Texas red dextran was i.v. injected to stain blood vessels (red). **(A)** A series of representative time-lapse images showing neutrophil crawling along the perivascular region in inflamed brain parenchyma. Tracking of neutrophil (white line). Scale bar, 50 μm (see **Supplementary Video 7**). **(B)** A series of representative time-lapse images showing reverse-transendothelial migration of neutrophils from brain parenchyma into blood vessels. Tracking of neutrophil (white line). Scale bar, 20 μm. **(C)** Brain chemokine array results demonstrating altered expression levels of chemokines following LPS injection. Data indicate mean ± SEM using Student's *t*-test (*$p < 0.005$, ***$p < 0.001$). Three independent experiments were performed.

immune cells. On the other hand, CXCL13 plays a role in adaptive immune cell organization, being especially chemotactic for B cells; yet, it is not known to be expressed in neutrophils (Havenar-Daughton et al., 2016).

One of the most interesting phenomena that deserve attention in the present study is rTEM, the reverse migration of neutrophils from the brain parenchyma back to the bloodstream. Although its exact purpose and mechanism are yet to be clearly defined, rTEM has been observed in numerous previous studies, and accumulation of relevant data is continuing to provide new insight into the topic (Burn and Alvarez, 2017). For instance, several studies have attempted to pinpoint the molecular signals that seem to induce or influence rTEM; in one study, cold-inducible RNA-binding protein (CIRP) has been suggested to stimulate neutrophil rTEM in septic conditions via an increase in neutrophil elastase and a decrease in junctional adhesion molecule-C (JAM-C) (Jin et al., 2019). In addition, the chemoattractant leukotriene B_4 (LTB4) has been proposed to be a potential factor which causes proteolytic cleavage of JAM-C via neutrophil elastase, further reinforcing the possible roles of neutrophil elastase and JAM-C in rTEM (Colom et al., 2015). Along with JAM-C, netrin-1, a protein highly expressed in endothelial cells and is known to disrupt leukocyte transendothelial migration, has also been proposed as a factor

that may hinder rTEM (Ly et al., 2005; Podjaski et al., 2015). In particular, it has been shown that netrin-1 activation is dependent on hypoxia inducible factor 1 alpha (Hif-1α), which in turn seems to promote continuation of inflammation and prevent neutrophil clearance from perivascular regions (Rosenberger et al., 2009; Elks et al., 2011). Furthermore, Tanshinone IIA, a compound originated from an Asian medicinal herb, has been shown to promote inflammation resolution via the induction of neutrophil apoptosis and rTEM (Robertson et al., 2014). Yet, as Tanshinones have also been suggested to play an inhibitory role on NFkB, AP-1, and STAT1 activation and thus possess anti-inflammatory functions, additional research on the matter is necessary to confirm the role of Tanshinones in the context of rTEM and neutrophil clearance (Xu et al., 2008; Tang et al., 2011).

Yet while the molecular mechanisms underlying rTEM is crucial, another important issue is perhaps the consequences of neutrophil rTEM, especially the effects of the neutrophils returning to the bloodstream on other organs. Post-rTEM neutrophils were suggested to play diverse roles, including inhibition of T cell proliferation, neutrophil clearance from tissues, enhancement of reactive oxygen species (ROS) and neutrophil extracellular trap (NET) formation, and exacerbation of systemic inflammation (Buckley et al., 2006; Mathias et al., 2006; Woodfin et al., 2011; Yoo and Huttenlocher, 2011; Brinkmann and Zychlinsky, 2012; Pillay et al., 2012; Cheng and Palaniyar, 2013). Notably, the molecular profile of neutrophils that had underwent rTEM exhibited high levels of CD11b, CD54, and ICAM-1, while showing low levels of CD62L, CXCR1, and CXCR2 markers (Walcheck et al., 1996; Buckley et al., 2006; Woodfin et al., 2011). The distinguishable molecular expression pattern in neutrophils that had returned to the bloodstream presents various inquiries, including what effects such patterns may have on the function of neutrophils after rTEM. Another important question that arises would be how those neutrophils acquired such a state; one likely hypothesis is that the neutrophils experienced molecular modification via active interaction with other cells. For example, it had been postulated that the high expression of ICAM-1 on the surface of post-rTEM neutrophils may have resulted from a mechanism that resembles trogocytosis, by which neutrophils acquired ICAM-1 high membranes from endothelial cells (Joly and Hudrisier, 2003; Burn and Alvarez, 2017).

In this context, it is natural to speculate whether neutrophils that had been chemically stimulated or modified by interactions with microglia engage in rTEM, thereby spreading inflammatory signals from the brain to other peripheral organs of the body. Although the accumulation of neutrophils in inflammatory conditions is a well-established concept, the interaction between neutrophils and microglia during neuroinflammation has yet to be extensively studied. Our study presents compelling evidence of neutrophil-microglial contact, which also led to further mobilization of nearby microglia toward the site of contact. Previously, the same phenomenon had been observed via two-photon imaging in a stroke model, where neutrophils infiltrated the brain parenchyma following cortical ischemia and microglia engulfed the neutrophils, in line with the results of the present study (Neumann et al., 2018). The fact that identical observations were made in neuroinflammatory situations via different inducers (systemic inflammation via LPS injection vs. ischemic stroke) demonstrates that neutrophil-microglia contact might be a general phenomenon in neuroinflammation, raising questions regarding the molecular mechanisms or cell signaling underlying such interactions. Despite the fact that studies on such topics are scarce, previous research has suggested that molecules, such as RGD peptides of GlcNAC may hinder microglia-neutrophil interactions *in vitro*, possibly laying the pavement for further mechanistic studies (Neumann et al., 2008). Furthermore, previous research on neutrophil rTEM indicate that the majority of neutrophils that engage in rTEM had prior interaction with macrophages, strongly suggesting a role of macrophages promoting neutrophil rTEM not only in the brain but also in other organs in general (Burn and Alvarez, 2017). In particular, the redox-SRC family kinase (SFK) signaling pathway was shown to be relevant to the rTEM-inducing capabilities of macrophages, with p22phox and Yes-related kinases being key players (Tauzin et al., 2014). While contact with macrophages was not necessary for neutrophil rTEM, the number of neutrophils that undergo rTEM significantly diminished in a setting that lacked macrophages; such previous data, combined with the results of the present study, presents the need to delve further into the impact of neutrophil-macrophage interactions on neutrophil rTEM. Meanwhile, combining the present results with observations from previous literature, we may even speculate that the neutrophils that had interacted with microglia in the brain parenchyma had underwent molecular modifications that predispose them to engage in rTEM; in this sense, neutrophil-microglia crosstalk may be crucial in the resolution of inflammation in the brain.

One key discrepancy between previous studies on neutrophil rTEM and the present study is the rate in which rTEM was observed; although it had been proposed that up to 80% of the neutrophils that accumulated in inflammatory sites may engage in rTEM, the phenomenon was not seen as frequently in the brain (Mathias et al., 2006; Yoo and Huttenlocher, 2011). This may be possibly due to the complexity and relative impenetrability of the BBB, which often results in various complications regarding leukocyte migration (Ransohoff et al., 2003). In this context, further research is necessary to investigate why rTEM is observed in a much lower frequency in the brain. At the same time, the occurrence of rTEM, however rare as it may be, also presents a need to decipher the brain-specific mechanisms behind rTEM through the BBB. The aforementioned netrin-1 may be a reasonable starting point, as the molecule is known to be involved in BBB function (Podjaski et al., 2015).

In the present study, we have demonstrated that neuroinflammation induced by LPS injection yields increased recruitment and mobility of neutrophils in the brain parenchyma, while activating microglia, as observed from their morphological changes. In addition, neutrophils that had infiltrated brain tissue were seen to engage in neutrophil-microglia interaction, where microglia engulfed the neutrophils in contact. Such a phenomenon also attracted nearby microglia, inducing dendritic movement toward the site of contact. Furthermore, infiltrated neutrophils also exhibited rTEM, returning to the bloodstream

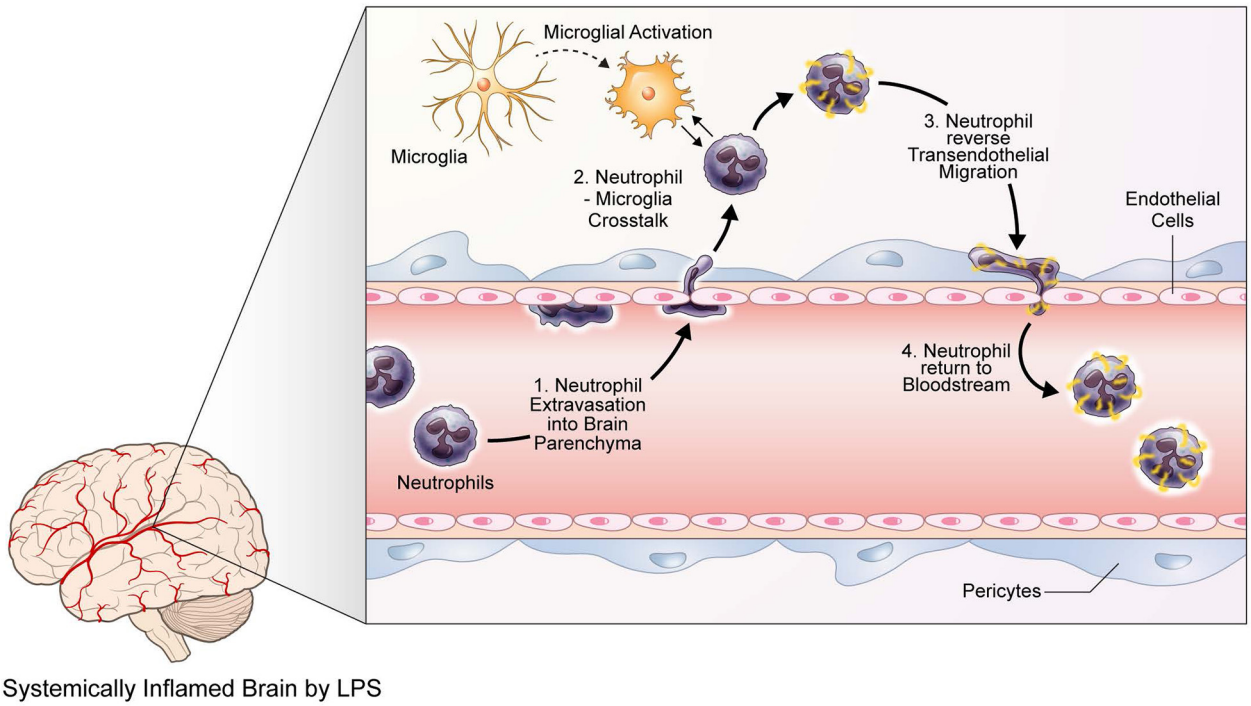

FIGURE 5 | Neutrophils and microglia exhibit various behavioral and phenotypical responses to LPS-induced neuroinflammation. A graphic illustration describing the responses of neutrophils and microglia to LPS-induced neuroinflammation, as identified via two-photon microscopy. Upon LPS injection and the following neuroinflammatory situations, neutrophils first respond by extravasating into the brain parenchyma. Meanwhile, microglia are activated and thus undergo morphological changes, such as enlargement of cell bodies and shortening of processes. Such activated microglia interact with infiltrated neutrophils, possibly causing molecular modifications on the neutrophils; thereafter, neutrophils engage in reverse transendothelial migration, returning to the bloodstream.

after entering the brain parenchyma (**Figure 5**). Despite such compelling evidence, this paper possesses several limitations. First and foremost, it would benefit greatly from further research that is able to observe rTEM at a higher frequency, as one of the biggest gaps between data in this paper and data on rTEM studies was that between the rate of rTEM observation. Another limitation is that in this study, we were not able to quantify meaningful ratios and proportions of cells exhibiting desired behavior. For instance, the ratio of neutrophils that engaged in extravasation to those that circulated within the blood vessel, the ratio of neutrophils that infiltrated to the brain parenchyma to those that interacted with microglia, and the ratio of neutrophils that interacted with microglia to those that exhibited rTEM are all of much importance but were unattainable due to technological issues. Also, as most of the results of this paper are of an observational nature, future studies utilizing *in vivo* or *in vitro* methods may assist in underpinning the biomolecular mechanisms behind the observations of this paper, specifically in relation to neutrophil-microglial interactions. Finally, while the current study utilized LPS injection to induce neuroinflammation, the variety of neuroinflammatory models existing today will be of tremendous usefulness in verifying the present results, in perhaps a more clinical setting. For example, in our previous data, we had demonstrated neutrophil infiltration into the brain parenchyma and accumulation around amyloid beta plaques in 5XFAD mice, an AD mouse model, using two-photon microscopy; Zenaro et al., later confirmed similar results in 3×Tg-AD mice, another murine model of AD. As such, further studies that corroborate the results of the present study using disease-specific models of neuroinflammation may help investigating the clinical implications of neutrophil infiltration, neutrophil-microglia interaction, and neutrophil rTEM in neuroinflammation. Taking such future research suggestions into consideration, this paper presents strong visual data on the behavior of neutrophils in response to neuroinflammatory situations and may establish the groundwork for future research on the molecular mechanisms underlying innate immune cell responses to neuroinflammation and systemic inflammation alike.

DATA AVAILABILITY STATEMENT

The original contributions presented in the study are included in the article/**Supplementary Material**, further inquiries can be directed to the corresponding author/s.

ETHICS STATEMENT

The animal study was reviewed and approved by the Institutional Animal Care and Use Committee of Yonsei University College of Medicine, South Korea.

AUTHOR CONTRIBUTIONS

YRK performed the experiments, wrote the manuscript, and analyzed the data. YMK wrote the manuscript and analyzed the data. JL and JP performed the experiments. JEL helped design the study. Y-MH directed the study design and wrote the manuscript. All authors contributed to the article and approved the submitted version.

FUNDING

This research was supported by the National Research Foundation of Korea (NRF) grant funded by the Korea government (MSIT) (2016M3C7A1905098 to JEL and 2020R1A4A1019009 to Y-MH).

ACKNOWLEDGMENTS

We thank Medical Illustration & Design, part of the Medical Research Support Services of Yonsei University College of Medicine, for all artistic support related to this work.

SUPPLEMENTARY MATERIAL

The Supplementary Material for this article can be found online at: https://www.frontiersin.org/articles/10.3389/fcell.2020.613733/full#supplementary-material

Supplementary Figure 1 | Cranial window surgery setup for brain intravital imaging. **(A)** Brain chambers with heating plates for maintaining body temperature at 37 ± 0.5°C. **a.** Metal and rubber heating plates, **b.** DC temperature controller, **c.** Stereotactic instrument for cranial window surgery, **d.** Head fixation device for imaging. **(B)** Subsidiary tools for surgery **a.** cotton swab, **b.** air blower, **c.** tissue glue, **d.** cover glass (diameter = 5 μm), **e.** metal frame, **f.** pen, **g.** dental cement, **h.** resin tip, **i.** forceps, **j.** a pair of scissors, **k.** forceps, **l.** micro forceps, **m.** micro drill. **(C)** Surgical procedure of cranial window surgery for intravital brain imaging. **i.** Fix the mouse in a stereotactic heating plate, **ii.** Remove head skin and the periosteum, **iii.** Coordinate predestinate location carved on right hemisphere, **iv.** Moisturize a circular opening with a drop of isotonic saline solution and seal a circular opening with a 5 μm coverslip, **v.** Glue and fix the metal frame on the borders of the cranial window and skull area using dental cement, **vi.** Place the mouse on a head fixation device for intravital imaging.

Supplementary Video 1 | TPIM of brain parenchyma in $LysM^{GFP/+}$ mice injected with PBS (control) and LPS, respectively. Green, neutrophil (GFP); Red, blood vessels (Texas Red dextran). Scale bar, 100 μm.

Supplementary Video 2 | TPIM of neutrophil infiltration during neuroinflammation. Green, neutrophil (GFP); Red, blood vessels (Texas Red dextran); White, track line of neutrophil. Scale bar, 50 μm.

Supplementary Video 3 | TPIM of brain parenchyma in $CX_3CR1^{GFP/+}$ mice injected with PBS (control) and LPS, respectively. Green, microglia (GFP); Red, neutrophils (Ab Ly6G); Blue, blood vessels (Lectin). Scale bar, 100 μm.

Supplementary Video 4 | TPIM of morphological changes in microglia in brain parenchyma. Green, microglia (GFP); Red, neutrophils (Ab Ly6G); Blue, blood vessels (Lectin). Scale bar, 30 μm.

Supplementary Video 5 | TPIM showing contact between microglial processes and neutrophils in inflamed brain parenchyma. Green, microglia (GFP); Red, neutrophils (Ab Ly6G); Blue, blood vessels (Lectin). Scale bar, 40 μm.

Supplementary Video 6 | TPIM showing elongation of microglial processes toward point of microglia-neutrophil contact (white arrow). Green, microglia (GFP); Red, neutrophils (Ab Ly6G); Blue, blood vessels (Lectin).

Supplementary Video 7 | TPIM showing neutrophil crawling along the perivascular region in inflamed brain parenchyma. Green, neutrophil (GFP); Red, blood vessels (Texas Red dextran); White, tracking of neutrophil. Scale bar, 50 μm.

Supplementary Video 8 | TPIM showing neutrophil reverse-transendothelial migration from brain parenchyma into blood vessel. Green, neutrophil (GFP); Red, blood vessels (Texas Red dextran); White, tracking of neutrophil; Blue, the replacement of reverse-migrated neutrophil. Scale bar, 20 μm.

REFERENCES

Ahn, S. Y., Maeng, Y. S., Kim, Y. R., Choe, Y. H., Hwang, H. S., and Hyun, Y. M. (2020). In vivo monitoring of dynamic interaction between neutrophil and human umbilical cord blood-derived mesenchymal stem cell in mouse liver during sepsis. *Stem. Cell Res. Ther.* 11:44.

Baik, S. H., Cha, M. Y., Hyun, Y. M., Cho, H., Hamza, B., and Kim, D. K. (2014). Migration of neutrophils targeting amyloid plaques in Alzheimer's disease mouse model. *Neurobiol. Aging* 35, 1286–1292. doi: 10.1016/j.neurobiolaging.2014.01.003

Brinkmann, V., and Zychlinsky, A. (2012). Neutrophil extracellular traps: is immunity the second function of chromatin? *J. Cell Biol.* 198, 773–783. doi: 10.1083/jcb.201203170

Buckley, C. D., Ross, E. A., McGettrick, H. M., Osborne, C. E., Haworth, O., and Schmutz, C. (2006). Identification of a phenotypically and functionally distinct population of long-lived neutrophils in a model of reverse endothelial migration. *J. Leukoc. Biol.* 79, 303–311. doi: 10.1189/jlb.0905496

Burn, T., and Alvarez, J. I. (2017). Reverse transendothelial cell migration in inflammation: to help or to hinder? *Cell Mol. Life Sci.* 74, 1871–1881. doi: 10.1007/s00018-016-2444-2

Cai, Z., Hussain, M. D., and Yan, L. J. (2014). Microglia, neuroinflammation, and beta-amyloid protein in Alzheimer's disease. *Int. J. Neurosci.* 124, 307–321. doi: 10.3109/00207454.2013.833510

Capucetti, A., Albano, F., and Bonecchi, R. (2020). Multiple roles for chemokines in neutrophil biology. *Front. Immunol.* 11:1259.

Cheng, O. Z., and Palaniyar, N. (2013). NET balancing: a problem in inflammatory lung diseases. *Front. Immunol.* 4:1.

Christy, A. L., Walker, M. E., Hessner, M. J., and Brown, M. A. (2013). Mast cell activation and neutrophil recruitment promotes early and robust inflammation in the meninges in EAE. *J. Autoimmun.* 42, 50–61. doi: 10.1016/j.jaut.2012.11.003

Colom, B., Bodkin, J. V., Beyrau, M., Woodfin, A., Ody, C., and Rourke, C. (2015). Leukotriene B4-neutrophil elastase axis drives neutrophil reverse transendothelial cell migration In Vivo. *Immunity* 42, 1075–1086. doi: 10.1016/j.immuni.2015.05.010

Davis, B. M., Salinas-Navarro, M., Cordeiro, M. F., Moons, L., and De Groef, L. (2017). Characterizing microglia activation: a spatial statistics approach to maximize information extraction. *Sci. Rep.* 7:1576.

Ebersoldt, M., Sharshar, T., and Annane, D. (2007). Sepsis-associated delirium. *Intensive Care Med.* 33, 941–950. doi: 10.1007/s00134-007-0622-2

Echeverria, V., Yarkov, A., and Aliev, G. (2016). Positive modulators of the alpha7 nicotinic receptor against neuroinflammation and cognitive impairment in Alzheimer's disease. *Prog. Neurobiol.* 144, 142–157. doi: 10.1016/j.pneurobio.2016.01.002

Elks, P. M., van Eeden, F. J., Dixon, G., Wang, X., and Reyes-Aldasoro, C. C. (2011). Activation of hypoxia-inducible factor-1alpha (Hif-1alpha) delays inflammation resolution by reducing neutrophil apoptosis and reverse migration in a zebrafish inflammation model. *Blood* 118, 712–722. doi: 10.1182/blood-2010-12-324186

Faust, N., Varas, F., Kelly, L. M., Heck, S., and Graf, T. (2000). Insertion of enhanced green fluorescent protein into the lysozyme gene creates mice with green fluorescent granulocytes and macrophages. *Blood* 96, 719–726. doi: 10.1182/blood.v96.2.719

Fortin, M., Steff, A. M., and Hugo, P. (2005). High-throughput technology: green fluorescent protein to monitor cell death. *Methods Mol. Med.* 110, 121–137. doi: 10.1385/1-59259-869-2:121

Girbl, T., Lenn, T., Perez, L., Rolas, L., Barkaway, A., and Thiriot, A. (2018). Distinct compartmentalization of the chemokines CXCL1 and CXCL2 and the atypical receptor ACKR1 determine discrete stages of neutrophil diapedesis. *Immunity* 49, 1062–1076.e6.

Havenar-Daughton, C., Lindqvist, M., Heit, A., Wu, J. E., Reiss, S. M., and Kendric, K. (2016). CXCL13 is a plasma biomarker of germinal center activity. *Proc. Natl. Acad. Sci. U.S.A.* 113, 2702–2707. doi: 10.1073/pnas.1520112113

He, H., Geng, T., Chen, P., Wang, M., Hu, J., Kang, L., et al. (2016). NK cells promote neutrophil recruitment in the brain during sepsis-induced neuroinflammation. *Sci. Rep.* 6:27711.

Jiang, W., St-Pierre, S., Roy, P., Morley, B. J., Hao, J., and Simard, A. R. (2016). Infiltration of CCR2+Ly6Chigh proinflammatory monocytes and neutrophils into the central nervous system is modulated by nicotinic acetylcholine receptors in a model of multiple sclerosis. *J. Immunol.* 196, 2095–2108. doi: 10.4049/jimmunol.1501613

Jin, H., Aziz, M., Ode, Y., and Wang, P. (2019). CIRP Induces neutrophil reverse transendothelial migration in sepsis. *Shock* 51, 548–556. doi: 10.1097/shk.0000000000001257

Joly, E., and Hudrisier, D. (2003). What is trogocytosis and what is its purpose? *Nat. Immunol.* 4:815. doi: 10.1038/ni0903-815

Jung, S., Aliberti, J., Graemmel, P., Sunshine, M. J., Kreutzberg, G. W., Sher, A., et al. (2000). Analysis of fractalkine receptor CX(3)CR1 function by targeted deletion and green fluorescent protein reporter gene insertion. *Mol. Cell Biol.* 20, 4106–4114. doi: 10.1128/mcb.20.11.4106-4114.2000

Kanashiro, A., Hiroki, C. H., da Fonseca, D. M., Birbrair, A., Ferreira, R. G., and Bassi, G. S. (2020). The role of neutrophils in neuro-immune modulation. *Pharmacol. Res.* 151:104580. doi: 10.1016/j.phrs.2019.104580

Kettenmann, H., Hanisch, U. K., Noda, M., and Verkhratsky, A. (2011). Physiology of microglia. *Physiol. Rev.* 91, 461–553.

Kobayashi, Y. (2008). The role of chemokines in neutrophil biology. *Front. Biosci.* 13:2400–2407. doi: 10.2741/2853

Kozlowski, C., and Weimer, R. M. (2012). An automated method to quantify microglia morphology and application to monitor activation state longitudinally in vivo. *PLoS One* 7:e31814. doi: 10.1371/journal.pone.0031814

Kruger, P., Saffarzadeh, M., Weber, A. N., Rieber, N., Radsak, M., and von Bernuth, H. (2015). Neutrophils: between host defence, immune modulation, and tissue injury. *PLoS Pathog.* 11:e1004651. doi: 10.1371/journal.ppat.1004651

Lee, S. H., Choe, Y. H., Kang, R. H., Kim, Y. R., Kim, N. H., and Kang, S. (2019). A bright blue fluorescent dextran for two-photon in vivo imaging of blood vessels. *Bioorg. Chem.* 89:103019. doi: 10.1016/j.bioorg.2019.103019

Li, W. W., Setzu, A., Zhao, C., and Franklin, R. J. (2005). Minocycline-mediated inhibition of microglia activation impairs oligodendrocyte progenitor cell responses and remyelination in a non-immune model of demyelination. *J. Neuroimmunol.* 158, 58–66. doi: 10.1016/j.jneuroim.2004.08.011

Liu, B., and Hong, J. S. (2003). Role of microglia in inflammation-mediated neurodegenerative diseases: mechanisms and strategies for therapeutic intervention. *J. Pharmacol. Exp. Ther.* 304, 1–7. doi: 10.1124/jpet.102.035048

Liu, Y. W., Li, S., and Dai, S. S. (2018). Neutrophils in traumatic brain injury (TBI): friend or foe? *J. Neuroinflam.* 15:146.

Ly, N. P., Komatsuzaki, K., Fraser, I. P., Tseng, A. A., Prodhan, P., Moore, K. J., et al. (2005). Netrin-1 inhibits leukocyte migration in vitro and in vivo. *Proc. Natl. Acad. Sci. U.S.A.* 102, 14729–14734. doi: 10.1073/pnas.0506233102

Mammana, S., Fagone, P., Cavalli, E., Basile, M. S., Petralia, M. C., Nicoletti, F., et al. (2018). The role of macrophages in neuroinflammatory and neurodegenerative pathways of Alzheimer's disease, amyotrophic lateral sclerosis, and multiple sclerosis: pathogenetic cellular effectors and potential therapeutic targets. *Int. J. Mol. Sci.* 19:831. doi: 10.3390/ijms19030831

Mathias, J. R., Perrin, B. J., Liu, T. X., Kanki, J., Look, A. T., and Huttenlocher, A. (2006). Resolution of inflammation by retrograde chemotaxis of neutrophils in transgenic zebrafish. *J. Leukoc. Biol.* 80, 1281–1288. doi: 10.1189/jlb.0506346

Nathan, C. (2006). Neutrophils and immunity: challenges and opportunities. *Nat. Rev. Immunol.* 6, 173–182. doi: 10.1038/nri1785

Neumann, J., Henneberg, S., von Kenne, S., Nolte, N., Muller, A. J., and Schraven, B. (2018). Beware the intruder: real time observation of infiltrated neutrophils and neutrophil-Microglia interaction during stroke in vivo. *PLoS One* 13:e0193970. doi: 10.1371/journal.pone.0193970

Neumann, J., Sauerzweig, S., Ronicke, R., Gunzer, F., Dinkel, K., Ullrich, O., et al. (2008). Microglia cells protect neurons by direct engulfment of invading neutrophil granulocytes: a new mechanism of CNS immune privilege. *J. Neurosci.* 28, 5965–5975. doi: 10.1523/jneurosci.0060-08.2008

Park, S. A., Choe, Y. H., Park, E., and Hyun, Y. M. (2018). Real-time dynamics of neutrophil clustering in response to phototoxicity-induced cell death and tissue damage in mouse ear dermis. *Cell Adh. Migr.* 12, 424–431.

Pillay, J., Kamp, V. M., van Hoffen, E., Visser, T., Tak, T., and Lammers, J. W. (2012). A subset of neutrophils in human systemic inflammation inhibits T cell responses through Mac-1. *J. Clin. Invest.* 122, 327–336. doi: 10.1172/jci57990

Podjaski, C., Alvarez, J. I., Bourbonniere, L., Larouche, S., Terouz, S., and Bin, J. M. (2015). Netrin 1 regulates blood-brain barrier function and neuroinflammation. *Brain* 138, 1598–1612. doi: 10.1093/brain/awv092

Ransohoff, R. M., Kivisakk, P., and Kidd, G. (2003). Three or more routes for leukocyte migration into the central nervous system. *Nat. Rev. Immunol.* 3, 569–581. doi: 10.1038/nri1130

Ransohoff, R. M., and Perry, V. H. (2009). Microglial physiology: unique stimuli, specialized responses. *Annu. Rev. Immunol.* 27, 119–145. doi: 10.1146/annurev.immunol.021908.132528

Robertson, A. L., Holmes, G. R., Bojarczuk, A. N., Burgon, J., Loynes, C. A., and Chimen, M. (2014). A zebrafish compound screen reveals modulation of neutrophil reverse migration as an anti-inflammatory mechanism. *Sci. Transl Med.* 6:225ra29. doi: 10.1126/scitranslmed.3007672

Rosenberger, P., Schwab, J. M., Mirakaj, V., Masekowsky, E., Mager, A., Morote-Garcia, J. C., et al. (2009). Hypoxia-inducible factor-dependent induction of netrin-1 dampens inflammation caused by hypoxia. *Nat. Immunol.* 10, 195–202. doi: 10.1038/ni.1683

Saijo, K., and Glass, C. K. (2011). Microglial cell origin and phenotypes in health and disease. *Nat. Rev. Immunol.* 11, 775–787. doi: 10.1038/nri3086

Sawant, K. V., Poluri, K. M., Dutta, A. K., Sepuru, K. M., Troshkina, A., Garofalo, R. P., et al. (2016). Chemokine CXCL1 mediated neutrophil recruitment: Role of glycosaminoglycan interactions. *Sci. Rep.* 6:33123.

Sevenich, L. (2018). Brain-resident microglia and blood-borne macrophages orchestrate central nervous system inflammation in neurodegenerative disorders and brain cancer. *Front. Immunol.* 9:697.

Shastri, A., Bonifati, D. M., and Kishore, U. (2013). Innate immunity and neuroinflammation. *Med. Inflamm.* 2013:342931.

Simmons, S. B., Liggitt, D., and Goverman, J. M. (2014). Cytokine-regulated neutrophil recruitment is required for brain but not spinal cord inflammation during experimental autoimmune encephalomyelitis. *J. Immunol.* 193, 555–563. doi: 10.4049/jimmunol.1400807

Steff, A. M., Fortin, M., Arguin, C., and Hugo, P. (2001). Detection of a decrease in green fluorescent protein fluorescence for the monitoring of cell death: an assay amenable to high-throughput screening technologies. *Cytometry* 45, 237–243. doi: 10.1002/1097-0320(20011201)45:4<237::aid-cyto10024>3.0.co;2-j

Tang, C., Xue, H. L., Bai, C. L., and Fu, R. (2011). Regulation of adhesion molecules expression in TNF-alpha-stimulated brain microvascular endothelial cells by tanshinone IIA: involvement of NF-kappaB and ROS generation. *Phytother. Res.* 25, 376–380.

Tauzin, S., Starnes, T. W., Becker, F. B., Lam, P. Y., and Huttenlocher, A. (2014). Redox and Src family kinase signaling control leukocyte wound attraction and neutrophil reverse migration. *J. Cell Biol.* 207, 589–598. doi: 10.1083/jcb.201408090

Walcheck, B., Kahn, J., Fisher, J. M., Wang, B. B., Fisk, R. S., and Payan, D. G. (1996). Neutrophil rolling altered by inhibition of L-selectin shedding in vitro. *Nature* 380, 720–723. doi: 10.1038/380720a0

Woodfin, A., Voisin, M. B., Beyrau, M., Colom, B., Caille, D., and Diapouli, F. M. (2011). The junctional adhesion molecule JAM-C regulates polarized transendothelial migration of neutrophils in vivo. *Nat. Immunol.* 12, 761–769. doi: 10.1038/ni.2062

Wu, D., Zeng, Y., Fan, Y., Wu, J., Mulatibieke, T., Ni, J., et al. (2016). Reverse-migrated neutrophils regulated by JAM-C are

involved in acute pancreatitis-associated lung injury. *Sci. Rep.* 6: 20545.

Xu, Y., Feng, D., Wang, Y., Lin, S., and Xu, L. (2008). Sodium tanshinone IIA sulfonate protects mice from ConA-induced hepatitis via inhibiting NF-kappaB and IFN-gamma/STAT1 pathways. *J. Clin. Immunol.* 28, 512–519. doi: 10.1007/s10875-008-9206-3

Yoo, S. K., and Huttenlocher, A. (2011). Spatiotemporal photolabeling of neutrophil trafficking during inflammation in live zebrafish. *J. Leukoc. Biol.* 89, 661–667. doi: 10.1189/jlb.1010567

Zenaro, E., Pietronigro, E., Della Bianca, V., Piacentino, G., Marongiu, L., and Budui, S. (2015). Neutrophils promote Alzheimer's disease-like pathology and cognitive decline via LFA-1 integrin. *Nat. Med.* 21, 880–886. doi: 10.1038/nm.3913

Zhao, J., Bi, W., Xiao, S., Lan, X., Cheng, X., and Zhang, J. (2019). Neuroinflammation induced by lipopolysaccharide causes cognitive impairment in mice. *Sci. Rep.* 9:5790.

Zhou, H., Andonegui, G., Wong, C. H., and Kubes, P. (2009). Role of endothelial TLR4 for neutrophil recruitment into central nervous system microvessels in systemic inflammation. *J. Immunol.* 183, 5244–5250. doi: 10.4049/jimmunol.0901309

Conflict of Interest: The authors declare that the research was conducted in the absence of any commercial or financial relationships that could be construed as a potential conflict of interest.

frontiers in Cell and Developmental Biology

MINI REVIEW
published: 10 December 2020
doi: 10.3389/fcell.2020.615031

Molecular Basis for CCRL2 Regulation of Leukocyte Migration

Tiziana Schioppa[1,2†], Francesca Sozio[1,2†], Ilaria Barbazza[1], Sara Scutera[3], Daniela Bosisio[1], Silvano Sozzani[4‡] and Annalisa Del Prete[1,2‡]*

[1] Department of Molecular and Translational Medicine, University of Brescia, Brescia, Italy, [2] Humanitas Clinical and Research Center Rozzano-Milano, Rozzano, Italy, [3] Microbiology Section, Department of Public Health and Pediatric Sciences, University of Torino, Turin, Italy, [4] Laboratory Affiliated to Istituto Pasteur Italia-Fondazione Cenci Bolognetti, Department of Molecular Medicine, Sapienza University of Rome, Rome, Italy

CCRL2 is a seven-transmembrane domain receptor that belongs to the chemokine receptor family. At difference from other members of this family, CCRL2 does not promote chemotaxis and shares structural features with atypical chemokine receptors (ACKRs). However, CCRL2 also differs from ACKRs since it does not bind chemokines and is devoid of scavenging functions. The only commonly recognized CCRL2 ligand is chemerin, a non-chemokine chemotactic protein. CCRL2 is expressed both by leukocytes and non-hematopoietic cells. The genetic ablation of CCRL2 has been instrumental to elucidate the role of this receptor as positive or negative regulator of inflammation. CCRL2 modulates leukocyte migration by two main mechanisms. First, when CCRL2 is expressed by barrier cells, such endothelial, and epithelial cells, it acts as a presenting molecule, contributing to the formation of a non-soluble chemotactic gradient for leukocytes expressing CMKLR1, the functional chemerin receptor. This mechanism was shown to be crucial in the induction of NK cell-dependent immune surveillance in lung cancer progression and metastasis. Second, by forming heterocomplexes with other chemokine receptors. For instance, CCRL2/CXCR2 heterodimers were shown to regulate the activation of β2-integrins in mouse neutrophils. This mini-review summarizes the current understanding of CCRL2 biology, based on experimental evidence obtained by the genetic deletion of this receptor in *in vivo* experimental models. Further studies are required to highlight the complex functional role of CCRL2 in different organs and pathological conditions.

Keywords: leukocyte recruitment, chemerin, inflammatory diseases, tumor microenvironment, atypical chemokine receptors

OPEN ACCESS

Edited by:
Zhichao Fan,
UCONN Health, United States

Reviewed by:
Qing Deng,
Purdue University, United States
Bo Liu,
University of California, Berkeley, United States

****Correspondence:***
Silvano Sozzani
silvano.sozzani@uniroma1.it
orcid.org/0000-0002-3144-8743

†These authors share first authorship
‡These authors share last authorship

Specialty section:
This article was submitted to Cell Adhesion and Migration, a section of the journal Frontiers in Cell and Developmental Biology

Received: *07 October 2020*
Accepted: *23 November 2020*
Published: *10 December 2020*

Citation:
Schioppa T, Sozio F, Barbazza I, Scutera S, Bosisio D, Sozzani S and Del Prete A (2020) Molecular Basis for CCRL2 Regulation of Leukocyte Migration. Front. Cell Dev. Biol. 8:615031. doi: 10.3389/fcell.2020.615031

INTRODUCTION

Leukocyte migration is a tightly regulated process that takes place under both homeostatic and pathological conditions (David and Kubes, 2019). Chemokines control leukocyte trafficking through the interaction with their cognate receptors, belonging to the family of G protein-coupled membrane proteins (GPCRs) (Bachelerie et al., 2014; Sozzani et al., 2015; Hughes and Nibbs, 2018). A subset of proteins highly homologous to conventional chemokine receptors but unable to activate signal transduction through G proteins was identified and named Atypical Chemokine Receptors

(ACKRs) (Bachelerie et al., 2014). ACKRs bind to chemokines in a rather promiscuous manner and are generally characterized by the ability to scavenge their ligands. *In vivo* evidence obtained using gene-targeted animals have highlighted the crucial role of these molecules in the negative control of inflammation (Bonecchi and Graham, 2016).

Chemokine (C–C motif) receptor-like 2 (CCRL2, also called HCR or CRAM in humans and L-CCR in mice) is a seven transmembrane receptor closely related to the chemokine receptors CCR1, CCR2, CCR3, and CCR5 (Fan et al., 1998; An et al., 2011; Del Prete et al., 2013; De Henau et al., 2016). Nevertheless, CCRL2 is unable to activate conventional G-protein dependent signaling and to induce cell directional migration, since it lacks the canonical high conserved DRYLAIV motif. Therefore, CCRL2 was originally considered a member of ACKRs family (Bondue et al., 2011). In the past few years, several ligand were proposed for CCRL2, such as CCL2, CCL5, CCL7, CCL8 (Biber et al., 2003), or CCL19 (Leick et al., 2010), but these findings were not subsequently confirmed (Zabel et al., 2008; Del Prete et al., 2013; De Henau et al., 2016). So far, the only commonly accepted CCRL2 ligand is the non-chemokine chemotactic protein chemerin (Zabel et al., 2008), a ligand shared with two other signaling receptors, namely Chemokine-Like Receptor 1 (CMKLR1) and G protein-coupled receptor 1 (GPR1) (Bondue et al., 2011; De Henau et al., 2016). Chemerin binding to CCRL2 does not induce calcium fluxes or ligand scavenging (Zabel et al., 2008; De Henau et al., 2016; Mazzotti et al., 2017) and this atypical behavior makes CCRL2 a unique member of the non-signaling GPCR chemotactic receptor family. Here we summarize the current knowledge on the expression and functions of the atypical receptor CCRL2 mostly based on the results obtained in gene targeting experiments.

REGULATION OF CCRL2 EXPRESSION

In humans, two different CCRL2 splice variants are present, namely CCRL2A (or CRAM-A) coding for a 357 amino acid protein and CCRL2B (or CRAM-B) coding for a shorter receptor, lacking the first 12 amino acids in the amino-terminal domain (Yoshimura and Oppenheim, 2011; Del Prete et al., 2013). By contrast, mouse CCRL2 consists only of one single variant corresponding to CCRL2B. These orthologs are quite divergent in sequence, with only 51% identity, as compared to 80% of most of the other mouse-to-man GPCR receptor pairs (Fan et al., 1998; DeVries et al., 2006). The identity raises to 81% when considering only the first 16 amino-terminal amino acids, a short-conserved sequence that may represent the critical binding domain for chemerin (Zabel et al., 2008). However, the impact on ligand binding, if any, of the longer amino-terminal domain of CCRL2A has never been assessed. In general, only a few studies clearly indicate which variant is being investigated, or address possible differences in their expression and regulation; this is partly due to the paucity of specific reliable reagents. Nevertheless, it is becoming increasingly clear that the two isoforms may be differentially expressed and regulated: for example, CCRL2A expression is restricted to pre-B cells while other B cell-maturation stages express mainly CCRL2B (Hartmann et al., 2008). Furthermore, CCRL2A can be specifically upregulated in certain pathological conditions, such as in breast cancer by IFN-γ (Sarmadi et al., 2015). Thus, the two splice variants may possess so far unknown different biological roles and significance.

CCRL2 is expressed by cells in the hematopoietic and non-hematopoietic compartments. Among the hematopoietic cells, both CCRL2 mRNA and protein were detected in monocytes, macrophages, neutrophils, CD4 and CD8 positive T lymphocytes, B cells, monocyte-derived dendritic cells, and CD34 positive cells (Patel et al., 2001; Migeotte et al., 2002; Galligan et al., 2004; Auer et al., 2007; Hartmann et al., 2008; Catusse et al., 2010; Del Prete et al., 2013). In agreement with the first description of CCRL2 as an early LPS-inducible gene in the mouse macrophage cell line RAW264 (Shimada et al., 1998), in most of the cases, CCRL2 expression is upregulated by proinflammatory stimuli. In human monocytes, LPS alone or in combination with IFN-γ induced CCRL2 expression (Patel et al., 2001; Migeotte et al., 2002). CCRL2 mRNA was rapidly upregulated in mouse bone marrow-derived dendritic cells activated with LPS, Poly (I:C) or CD40L, reaching peak levels after 2–4 h, and decreased afterward, while CCRL2 protein levels peaked later at around 12 h and declined at the basal levels after 40 h of stimulation (Otero et al., 2010). In human neutrophils, the expression of CCRL2 was increased by proinflammatory stimuli, such as LPS or TNF-α alone or in combination with IFN-γ or GM-CSF (Galligan et al., 2004) and in neutrophils isolated from inflamed joints of arthritis patients (Auer et al., 2007). Similar CCRL2 expression kinetics was shown in mouse neutrophils (Del Prete et al., 2017). Furthermore, in mouse mast cells, CCRL2 was found to be constitutively expressed and to be further upregulated *in vitro* in BM-derived cells (Zabel et al., 2008). Also microglia and astrocytes were shown to express CCRL2 both *in vitro* and *in vivo* under inflammatory conditions (Zuurman et al., 2003; Brouwer et al., 2004). Within the non-hematopoietic compartment, CCRL2 mRNA was detected in inflamed bronchial epithelium (Oostendorp et al., 2004). Other reports described CCRL2 expression in hepatic stellate cells (Zimny et al., 2017), in adipocytes (Muruganandan et al., 2010), in skin (Banas et al., 2015) and in different cancer tissues including breast (Sarmadi et al., 2015) and prostate cancers (Reyes et al., 2017). In primary human endothelial cells, either derived from umbilical veins, dermal microvascular or brain vasculature, CCRL2 was significantly upregulated by proinflammatory stimuli (e.g., the combination of LPS, IFN-γ, and TNF-α) (Monnier et al., 2012). In endothelial cells freshly isolated from mouse lung, CCRL2 was found constitutively expressed, while in mouse liver the expression was strongly increased by inflammatory stimuli (Monnier et al., 2012). CCRL2 regulation was detected also *in vitro* in lymphatic endothelial cells stimulated with retinoid acid (Gonzalvo-Feo et al., 2014). Organ specific regulation may

underscore specific functional properties of CCRL2 in different anatomical districts.

ROLE OF CCRL2 IN THE REGULATION OF LEUKOCYTE MIGRATION

A detailed analysis of CCRL2 membrane trafficking confirmed that CCRL2 efficiently binds the chemotactic protein chemerin without triggering receptor internalization, ligand scavenging, or calcium mobilization (Mazzotti et al., 2017). These results depict a unique functional profile of CCRL2 among members of non-signaling seven-transmembrane domain receptor family.

Two main functions have been described for CCRL2, both having a role in leukocyte trafficking (**Figure 1**). First, CCRL2, when expressed on the surface of barrier cells, such as endothelial and epithelial cells, can increase the local concentration of chemerin to form a membrane-bound chemotactic gradient for leukocytes expressing the functional chemerin receptor CMKLR1 (Zabel et al., 2008; Bondue et al., 2011; Monnier et al., 2012; Gonzalvo-Feo et al., 2014). CCRL2 binds chemerin at the N-terminus leaving the C-terminal peptide sequence accessible for the interaction with CMKLR1 (Zabel et al., 2008). By this mean, CCRL2 may promote the recruitment of CMKLR1-expressing cells, such monocytes/macrophages, dendritic cells, plasmacytoid dendritic cells, and NK cells (Del Prete et al., 2006; Sozzani et al., 2010; Tiberio et al., 2018). This CCRL2/CMKLR1 axis was shown to be active *in vivo* in the regulation of dendritic cells, mast cells, and NK cells trafficking (Parolini et al., 2007; Zabel et al., 2008; Otero et al., 2010; Monnier et al., 2012; Gonzalvo-Feo et al., 2014; Del Prete et al., 2019; **Figure 1A**).

A second proposed function is unrelated to the interaction with its ligand and consists in the formation of heterodimers with chemokine receptors. CCRL2/CXCR2 heterodimers were shown to represent a mechanism of fine-tuning of neutrophil migration in pathological contextures, such as inflammatory arthritis (Del Prete et al., 2017). The feature of G-protein coupled receptors to form oligomers has emerged as a physiological phenomenon that can affect several aspects of receptor functions, such as ligand targeting, signaling, and internalization properties (Mellado et al., 2001; de Poorter et al., 2013). Heterodimerization of chemokine receptors is a potential crucial step for the proper function of immune cells and represents an additional level of complexity in the promiscuous chemokine system (Mellado et al., 2001; Thelen et al., 2010; Martínez-Muñoz et al., 2018). FRET analysis revealed that CCRL2/CXCR2 heterodimers were detectable both at the cell membrane and in the cytoplasm, suggesting that the CCRL2 is involved in the intracellular retention of the CCRL2/CXCR2 heterocomplexes. Indeed, modulation of CXCR2 membrane expression by CCRL2 was shown both in transfected cells and in primary bone marrow-derived neutrophils where Ccrl2 deficiency was related with increased CXCR2 membrane expression (Del Prete et al., 2017). CCRL2 expression was also associated with increased CXCR2 signaling through ERK1/2 and small GTPases phosphorylation, and activation of β2-integrin, as detected both *in vitro* and *in vivo* by underflow and intravital microscopy (see below; **Figure 1B**; Del Prete et al., 2017). Collectively, these findings identify CXCR2 as a target of CCRL2 regulation. The involvement of CCRL2 in the regulation of other chemotactic receptors needs to be further explored.

ROLE OF CCRL2 IN INFLAMMATORY DISEASES

The role of CCRL2 has emerged by the use of Ccrl2-deficient mice tested in several experimental models of inflammatory diseases (Otero et al., 2010; Gonzalvo-Feo et al., 2014; Mazzon et al., 2016; Del Prete et al., 2017). In a model of OVA-induced airways hypersensitivity, the genetic ablation of CCRL2 caused defective trafficking of antigen-loaded dendritic cells from the lung to mediastinal lymph nodes (Otero et al., 2010). In these experimental conditions, Ccrl2-deficient mice showed a protected phenotype, characterized by reduced recruitment of eosinophils and mononuclear cells to the bronchoalveolar compartment and decreased production of lung Th2 cytokines and chemokines. The defect in Th2-skewed response was directly ascribed to impaired dendritic cells migration, since it was abrogated by the intratracheal instillation of wild type dendritic cells (Otero et al., 2010). Considering the ability of CCRL2 to form heterodimers as a way to regulate chemotactic receptor function (Del Prete et al., 2017), it is possible that CCRL2 might play an unpredicted ligand-independent role in the control of pulmonary dendritic cell trafficking by the molecular interaction with CCR7, the main lymph node homing dendritic cell receptor. Similarly, CCRL2 increased tissue swelling and leukocyte infiltration in an IgE-mediated experimental model of passive cutaneous anaphylaxis (Otero et al., 2010; Gonzalvo-Feo et al., 2014; Mazzon et al., 2016; Del Prete et al., 2017). Ccrl2-deficient mice were also protected in experimental models of inflammatory arthritis. The mechanism of protection was mostly due to a defective neutrophils recruitment in the inflamed joints (Del Prete et al., 2017). The process of tissue neutrophils infiltration is implicated in the pathophysiology of rheumatoid arthritis and is controlled by a well-defined temporally and spatially cascade of chemoattractants and their cognate receptors, being the CXCL8/CXCR2 axis a major player (Chou et al., 2010; Wright et al., 2014). CCRL2 expression was described in neutrophils purified from the synovial fluid of rheumatoid arthritis patients (Galligan et al., 2004). In Ccrl2-deficient mice, CXCL8-induced neutrophils recruitment to the peritoneal cavity was found to be impaired. Similarly, neutrophils infiltration to inflamed joints was impaired in Ccrl2-deficient mice tested in collagen induced-and serum transfer induced-arthritis, two experimental models of inflammatory arthritis. In both experimental conditions, Ccrl2-deficient mice showed decreased severity of disease, lower incidence and delayed clinical onset, with reduced histopathological score. Disease protection was reversed by the adoptive transfer of CCRL2 competent neutrophils. Intravital microscopy clearly revealed that Ccrl2-deficient neutrophils displayed a strong reduction in their ability to adhere to the surface of endothelial cells in the vessels present in inflamed knee, with an increased number of rolling neutrophils on the endothelial surface.

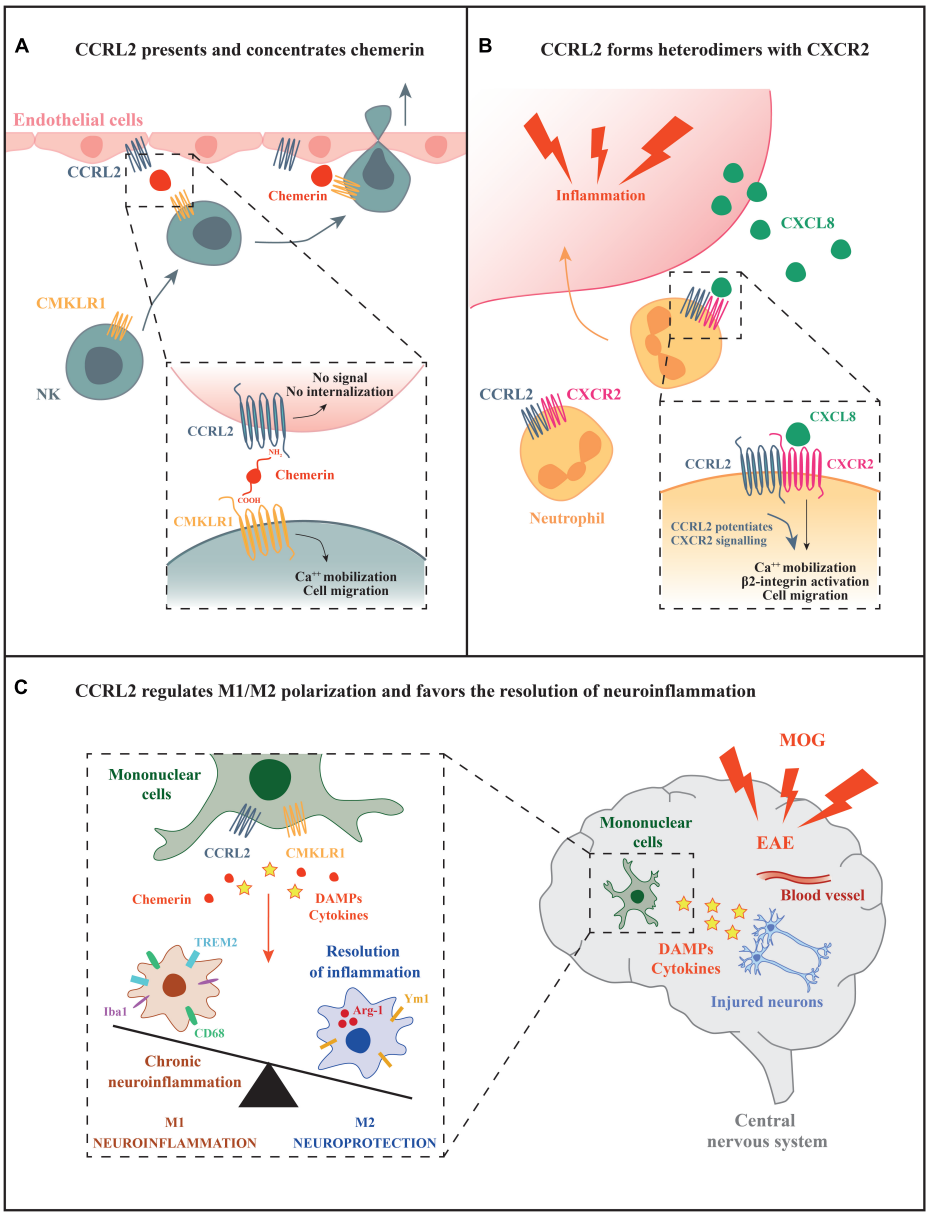

FIGURE 1 | Potential mechanisms of CCRL2 regulation of leukocyte migration. **(A)** CCRL2, expressed on barrier cells, such as epithelial or endothelial cells, can act as a chemerin presenting molecule. CCRL2 binding to the N-terminus leaves chemerin C-terminus available for the interaction with CMKLR1, the functional chemerin receptor expressed by different leukocyte subsets, such as NK cells. **(B)** CCRL2 regulates CXCR2 membrane expression and integrin-mediated arrest of neutrophils on endothelial cells forming CCRL2/CXCR2 heterodimers. **(C)** CCRL2 can favor the resolution of inflammation through the regulation of M1/M2 polarization balance.

Similar results were obtained in experiments performed under flow conditions showing defective capacity of Ccrl2-deficient neutrophils to undergo rapid β2 integrin-mediated arrest in response to CXCL8. Taken together, these results support a role for CCRL2 in the regulation of CXCR2-mediated inside-out β2-integrin activation (Del Prete et al., 2017). Using different models of acute inflammation induced by zymosan and thioglycolate, Regan-Komito et al. (2017) reported that Ccrl2-deficient mice expressed an exacerbated phenotype characterized by increased neutrophils infiltration associated to increased local and systemic levels of chemerin and CXCL1. It is possible that different experimental conditions might be responsible for this apparently contrasting phenotype. Of note, the role of CCRL2 in mast cell activation *in vivo* was previously reported to be influenced by the strength of the response (Zabel et al., 2008).

A possible role for CCRL2 in the resolution phase of inflammation emerged in the chronic phase of MOG-induced experimental autoimmune encephalitis (EAE), a model that resembles the inflammatory process that characterizes multiple sclerosis (Mazzon et al., 2016; **Figure 1C**). In the central nervous

system, CCRL2 was expressed by infiltrating mononuclear cells at the peak of clinical development of the disease. Ccrl2-deficient mice displayed increased mortality and severity of clinical score compared to control animals. In addition, the histopathological examination revealed enlarged demyelination areas and hyperactivation of microglia with unbalanced M1/M2 rate of polarization, especially during the recovery phase of the disease (Mazzon et al., 2016). Furthermore, in a model of DSS-induced colitis, chemerin has been associated with mononuclear cell polarization (Lin et al., 2014). These findings highlight a potential involvement of the chemerin/CCRL2 axis in the dynamic process of macrophage polarization, a fundamental step in the resolution of inflammation and tissue repair. Taken together, the use of mice with genetic deletion of CCRL2 has provided important insights in deciphering the molecular mechanisms of CCRL2-mediated regulation of leukocyte trafficking and pathological conditions.

ROLE OF CCRL2 IN TUMORS

CCRL2 expression was described in different cancer cells, including prostate and breast carcinoma, colorectal cancer liver metastasis and glioblastoma (Yin et al., 2012; Wang et al., 2015; Akram et al., 2016; Reyes et al., 2017). However, the functional role of CCRL2 in cancer is still unknown and needs further investigations. In NSCLC patients, elevated expression of CCRL2 was found to have a beneficial effect on overall survival and correlated with better clinical outcome, particularly at the early phase of lung tumor progression (Del Prete et al., 2019; Treeck et al., 2019).

During lung carcinogenesis CCRL2 exerts a protective role in different experimental models. Indeed, CCRL2 deficiency was associated with increased tumor burden in urethane-induced lung carcinogenesis and in a genetic model of Kras/Tp53-driven ($Kras^{G12D/+}/p53^{LoxP}$) lung tumor. Similarly, Ccrl2-deficient mice were more permissive for tumor growth following orthotopic injection of a tumor cell line obtained from $Kras^{G12D/+}/p53^{LoxP}$ mice. In all these experimental conditions, lung tumor microenvironment revealed the decrease of some myeloid cell subsets, such as monocytes, macrophages and neutrophils, and a consistent reduction of lung NK cell frequency, with the more mature NK cell subset ($CD27^{-}$ $CD11b^{+}$) being the most affected one. Since CCRL2 is not expressed by mouse NK cells, but was found expressed by $CD31^{+}$ cells in the lung of tumor-bearing mice, these results further support the role of CCRL2 expression by endothelial cells in the regulation of NK cell recruitment to the lung. CCRL2 present on the surface of lung endothelial cells may act as a chemerin-presenting molecule regulating the recruitment of $CMKLR1^{+}$ NK cells. By this mechanism, CCRL2 may shape the immune tumor microenvironment in lung cancer (Del Prete et al., 2019). This mechanism may have a more general relevance for lung tumor and metastasis (Pachynski et al., 2012). Whether the CCRL2/CMKLR1 axis is a selective pathway for the recruitment of NK cells to the lung microenvironment or rather is a pathway shared by different organs is still under investigation.

CONCLUSION AND FUTURE PERSPECTIVES

Chemokines and chemotactic agonists play a crucial role in the control of leukocyte trafficking acting at different levels of regulation. Over the last few years ACKRs, a small subset of GPCRs, attracted the attention for their ability to regulate inflammatory responses. CCRL2 is closely related to ACKRs but differs from them since it does not bind chemokines or possess ligand scavenging functions (De Henau et al., 2016; Mazzotti et al., 2017). CCRL2 regulates leukocyte migration and is involved in the control of both innate and adaptive immune responses in different inflammatory diseases and cancer. Depending on the cellular context and pathological condition, CCRL2 may act as a chemerin presenting molecule or modulate the function of chemokine receptors in a ligand-independent manner. Many aspects of the biology and activity of CCRL2 remain still unexplored and need to be further elucidated. A better understanding of the precise role of this atypical receptor may pave the way toward novel and improved therapeutic strategies for the control of inflammation and tumor immune surveillance.

AUTHOR CONTRIBUTIONS

TS and FS conceptualized the contents. TS, FS, IB, SS, IB, DB, AD, and SS contributed to writing the manuscript. IB prepared the figure. AD and SS supervised the final version of the review manuscript. All authors contributed to the article and approved the submitted version.

FUNDING

This work was supported by the Italian Association for Cancer Research (AIRC, IG 2017-20776 to SS), Ministero dell'Istruzione, dell'Università e della Ricerca (MIUR) (PRIN 2017 to SS), and Ministero della Salute (ID 2020010161 to SS). TS was a recipient of a fellowship from Fondazione Veronesi.

REFERENCES

Akram, I. G., Georges, R., Hielscher, T., Adwan, H., and Berger, M. R. (2016). The chemokines CCR1 and CCRL2 have a role in colorectal cancer liver metastasis. *Tumour Biol.* 37, 2461–2471. doi: 10.1007/s13277-015-4089-4

An, P., Li, R., Wang, J. M., Yoshimura, T., Takahashi, M., Samudralal, R., et al. (2011). Role of exonic variation in chemokine receptor genes on AIDS: CCRL2 F167Y association with pneumocystis pneumonia. *PLoS Genet.* 7:e1002328. doi: 10.1371/journal.pgen.1002328

Auer, J., Bläss, M., Schulze-Koops, H., Russwurm, S., Nagel, T., Kalden, J. R., et al. (2007). Expression and regulation of CCL18 in synovial fluid neutrophils

of patients with rheumatoid arthritis. *Arthritis Res. Ther.* 9:R94. doi: 10.1186/ar2294

Bachelerie, F., Ben-Baruch, A., Burkhardt, A. M., Combadiere, C., Farber, J. M., Graham, G. J., et al. (2014). International Union of Basic and Clinical Pharmacology. [corrected]. LXXXIX. Update on the extended family of chemokine receptors and introducing a new nomenclature for atypical chemokine receptors. *Pharmacol. Rev.* 66, 1–79. doi: 10.1124/pr.113.007724

Banas, M., Zegar, A., Kwitniewski, M., Zabieglo, K., Marczynska, J., Kapinska-Mrowiecka, M., et al. (2015). The expression and regulation of chemerin in the epidermis. *PLoS One* 10:e0117830. doi: 10.1371/journal.pone.0117830

Biber, K., Zuurman, M. W., Homan, H., and Boddeke, H. W. (2003). Expression of L-CCR in HEK 293 cells reveals functional responses to CCL2, CCL5, CCL7, and CCL8. *J. Leukoc. Biol.* 74, 243–251. doi: 10.1189/jlb.0802415

Bondue, B., Wittamer, V., and Parmentier, M. (2011). Chemerin and its receptors in leukocyte trafficking, inflammation and metabolism. *Cytokine Growth Factor Rev.* 22, 331–338. doi: 10.1016/j.cytogfr.2011.11.004

Bonecchi, R., and Graham, G. J. (2016). Atypical chemokine receptors and their roles in the resolution of the inflammatory response. *Front. Immunol.* 7:224. doi: 10.3389/fimmu.2016.00224

Brouwer, N., Zuurman, M. W., Wei, T., Ransohoff, R. M., Boddeke, H. W., and Biber, K. (2004). Induction of glial L-CCR mRNA expression in spinal cord and brain in experimental autoimmune encephalomyelitis. *Glia* 46, 84–94. doi: 10.1002/glia.10352

Catusse, J., Leick, M., Groch, M., Clark, D. J., Buchner, M. V., Zirlik, K., et al. (2010). Role of the atypical chemoattractant receptor CRAM in regulating CCL19 induced CCR7 responses in B-cell chronic lymphocytic leukemia. *Mol. Cancer* 9:297. doi: 10.1186/1476-4598-9-297

Chou, R. C., Kim, N. D., Sadik, C. D., Seung, E., Lan, Y., Byrne, M. H., et al. (2010). Lipid-cytokine-chemokine cascade drives neutrophil recruitment in a murine model of inflammatory arthritis. *Immunity* 33, 266–278. doi: 10.1016/j.immuni.2010.07.018

David, B. A., and Kubes, P. (2019). Exploring the complex role of chemokines and chemoattractants *in vivo* on leukocyte dynamics. *Immunol. Rev.* 289, 9–30. doi: 10.1111/imr.12757

De Henau, O., Degroot, G. N., Imbault, V., Robert, V., De Poorter, C., Mcheik, S., et al. (2016). Signaling properties of chemerin receptors CMKLR1, GPR1 and CCRL2. *PLoS One* 11:e0164179. doi: 10.1371/journal.pone.0164179

de Poorter, C., Baertsoen, K., Lannoy, V., Parmentier, M., and Springael, J. Y. (2013). Consequences of ChemR23 heteromerization with the chemokine receptors CXCR4 and CCR7. *PLoS One* 8:e58075. doi: 10.1371/journal.pone.0058075

Del Prete, A., Bonecchi, R., Vecchi, A., Mantovani, A., and Sozzani, S. (2013). CCRL2, a fringe member of the atypical chemoattractant receptor family. *Eur. J. Immunol.* 43, 1418–1422. doi: 10.1002/eji.201243179

Del Prete, A., Locati, M., Otero, K., Riboldi, E., Mantovani, A., Vecchi, A., et al. (2006). Migration of dendritic cells across blood and lymphatic endothelial barriers. *Thromb. Haemost.* 95, 22–28.

Del Prete, A., Martínez-Muñoz, L., Mazzon, C., Toffali, L., Sozio, F., Za, L., et al. (2017). The atypical receptor CCRL2 is required for CXCR2-dependent neutrophil recruitment and tissue damage. *Blood* 130, 1223–1234. doi: 10.1182/blood-2017-04-777680

Del Prete, A., Sozio, F., Schioppa, T., Ponzetta, A., Vermi, W., Calza, S., et al. (2019). The atypical receptor CCRL2 is essential for lung cancer immune surveillance. *Cancer Immunol. Res.* 7, 1775–1788. doi: 10.1158/2326-6066.CIR-19-0168

DeVries, M. E., Kelvin, A. A., Xu, L., Ran, L., Robinson, J., and Kelvin, D. J. (2006). Defining the origins and evolution of the chemokine/chemokine receptor system. *J. Immunol.* 176, 401–415. doi: 10.4049/jimmunol.176.1.401

Fan, P., Kyaw, H., Su, K., Zeng, Z., Augustus, M., Carter, K. C., et al. (1998). Cloning and characterization of a novel human chemokine receptor. *Biochem. Biophys. Res. Commun.* 243, 264–268. doi: 10.1006/bbrc.1997.7981

Galligan, C. L., Matsuyama, W., Matsukawa, A., Mizuta, H., Hodge, D. R., Howard, O. M., et al. (2004). Up-regulated expression and activation of the orphan chemokine receptor, CCRL2, in rheumatoid arthritis. *Arthritis Rheum.* 50, 1806–1814. doi: 10.1002/art.20275

Gonzalvo-Feo, S., Del Prete, A., Pruenster, M., Salvi, V., Wang, L., Sironi, M., et al. (2014). Endothelial cell-derived chemerin promotes dendritic cell transmigration. *J. Immunol.* 192, 2366–2373. doi: 10.4049/jimmunol.1302028

Hartmann, T. N., Leick, M., Ewers, S., Diefenbacher, A., Schraufstatter, I., Honczarenko, M., et al. (2008). Human B cells express the orphan chemokine receptor CRAM-A/B in a maturation-stage-dependent and CCL5-modulated manner. *Immunology* 125, 252–262. doi: 10.1111/j.1365-2567.2008.02836.x

Hughes, C. E., and Nibbs, R. J. B. (2018). A guide to chemokines and their receptors. *FEBS J.* 285, 2944–2971. doi: 10.1111/febs.14466

Leick, M., Catusse, J., Follo, M., Nibbs, R. J., Hartmann, T. N., Veelken, H., et al. (2010). CCL19 is a specific ligand of the constitutively recycling atypical human chemokine receptor CRAM-B. *Immunology* 129, 536–546. doi: 10.1111/j.1365-2567.2009.03209.x

Lin, Y., Yang, X., Yue, W., Xu, X., Li, B., Zou, L., et al. (2014). Chemerin aggravates DSS-induced colitis by suppressing M2 macrophage polarization. *Cell. Mol. Immunol.* 11, 355–366. doi: 10.1038/cmi.2014.15

Martínez-Muñoz, L., Villares, R., Rodríguez-Fernández, J. L., Rodríguez-Frade, J. M., and Mellado, M. (2018). Remodeling our concept of chemokine receptor function: from monomers to oligomers. *J. Leukoc. Biol.* 104, 323–331. doi: 10.1002/JLB.2MR1217-503R

Mazzon, C., Zanotti, L., Wang, L., Del Prete, A., Fontana, E., Salvi, V., et al. (2016). CCRL2 regulates M1/M2 polarization during EAE recovery phase. *J. Leukoc. Biol.* 99, 1027–1033. doi: 10.1189/jlb.3MA0915-444RR

Mazzotti, C., Gagliostro, V., Bosisio, D., Del Prete, A., Tiberio, L., Thelen, M., et al. (2017). The atypical receptor CCRL2 (C-C chemokine receptor-like 2) does not act as a decoy receptor in endothelial cells. *Front. Immunol.* 8:1233. doi: 10.3389/fimmu.2017.01233

Mellado, M., Rodríguez-Frade, J. M., Vila-Coro, A. J., Fernández, S., Martín de Ana, A., Jones, D. R., et al. (2001). Chemokine receptor homo- or heterodimerization activates distinct signaling pathways. *EMBO J.* 20, 2497–2507. doi: 10.1093/emboj/20.10.2497

Migeotte, I., Franssen, J. D., Goriely, S., Willems, F., and Parmentier, M. (2002). Distribution and regulation of expression of the putative human chemokine receptor HCR in leukocyte populations. *Eur. J. Immunol.* 32, 494–501.

Monnier, J., Lewén, S., O'Hara, E., Huang, K., Tu, H., Butcher, E. C., et al. (2012). Expression, regulation, and function of atypical chemerin receptor CCRL2 on endothelial cells. *J. Immunol.* 189, 956–967. doi: 10.4049/jimmunol.1102871

Muruganandan, S., Roman, A. A., and Sinal, C. J. (2010). Role of chemerin/CMKLR1 signaling in adipogenesis and osteoblastogenesis of bone marrow stem cells. *J. Bone Miner. Res.* 25, 222–234. doi: 10.1359/jbmr.091106

Oostendorp, J., Hylkema, M. N., Luinge, M., Geerlings, M., Meurs, H., Timens, W., et al. (2004). Localization and enhanced mRNA expression of the orphan chemokine receptor L-CCR in the lung in a murine model of ovalbumin-induced airway inflammation. *J. Histochem. Cytochem.* 52, 401–410. doi: 10.1177/002215540405200311

Otero, K., Vecchi, A., Hirsch, E., Kearley, J., Vermi, W., Del Prete, A., et al. (2010). Nonredundant role of CCRL2 in lung dendritic cell trafficking. *Blood* 116, 2942–2949. doi: 10.1182/blood-2009-12-259903

Pachynski, R. K., Zabel, B. A., Kohrt, H. E., Tejeda, N. M., Monnier, J., Swanson, C. D., et al. (2012). The chemoattractant chemerin suppresses melanoma by recruiting natural killer cell antitumor defenses. *J. Exp. Med.* 209, 1427–1435. doi: 10.1084/jem.20112124

Parolini, S., Santoro, A., Marcenaro, E., Luini, W., Massardi, L., Facchetti, F., et al. (2007). The role of chemerin in the colocalization of NK and dendritic cell subsets into inflamed tissues. *Blood* 109, 3625–3632. doi: 10.1182/blood-2006-08-038844

Patel, L., Charlton, S. J., Chambers, J. K., and Macphee, C. H. (2001). Expression and functional analysis of chemokine receptors in human peripheral blood leukocyte populations. *Cytokine* 14, 27–36. doi: 10.1006/cyto.2000.0851

Regan-Komito, D., Valaris, S., Kapellos, T. S., Recio, C., Taylor, L., Greaves, D. R., et al. (2017). Absence of the non-signalling chemerin receptor CCRL2 exacerbates acute inflammatory responses. *Front. Immunol.* 8:1621. doi: 10.3389/fimmu.2017.01621

Reyes, N., Benedetti, I., Rebollo, J., Correa, O., and Geliebter, J. (2017). Atypical chemokine receptor CCRL2 is overexpressed in prostate cancer cells. *J. Biomed. Res.* 33, 17–23. doi: 10.7555/JBR.32.20170057

Sarmadi, P., Tunali, G., Esendagli-Yilmaz, G., Yilmaz, K. B., and Esendagli, G. (2015). CRAM-A indicates IFN-γ-associated inflammatory response in breast cancer. *Mol. Immunol.* 68(2 Pt C), 692–698. doi: 10.1016/j.molimm.2015.10.019

Shimada, T., Matsumoto, M., Tatsumi, Y., Kanamaru, A., and Akira, S. (1998). A novel lipopolysaccharide inducible C-C chemokine receptor related gene in murine macrophages. *FEBS Lett.* 425, 490–494. doi: 10.1016/s0014-5793(98)00299-3

Sozzani, S., Del Prete, A., Bonecchi, R., and Locati, M. (2015). Chemokines as effector and target molecules in vascular biology. *Cardiovasc. Res.* 107, 364–372. doi: 10.1093/cvr/cvv150

Sozzani, S., Vermi, W., Del Prete, A., and Facchetti, F. (2010). Trafficking properties of plasmacytoid dendritic cells in health and disease. *Trends Immunol.* 31, 270–277. doi: 10.1016/j.it.2010.05.004

Thelen, M., Muñoz, L. M., Rodríguez-Frade, J. M., and Mellado, M. (2010). Chemokine receptor oligomerization: functional considerations. *Curr. Opin. Pharmacol.* 10, 38–43. doi: 10.1016/j.coph.2009.09.004

Tiberio, L., Del Prete, A., Schioppa, T., Sozio, F., Bosisio, D., and Sozzani, S. (2018). Chemokine and chemotactic signals in dendritic cell migration. *Cell. Mol. Immunol.* 15, 346–352. doi: 10.1038/s41423-018-0005-3

Treeck, O., Buechler, C., and Ortmann, O. (2019). Chemerin and cancer. *Int. J. Mol. Sci.* 20:3750. doi: 10.3390/ijms20153750

Wang, L. P., Cao, J., Zhang, J., Wang, B. Y., Hu, X. C., Shao, Z. M., et al. (2015). The human chemokine receptor CCRL2 suppresses chemotaxis and invasion by blocking CCL2-induced phosphorylation of p38 MAPK in human breast cancer cells. *Med. Oncol.* 32:254. doi: 10.1007/s12032-015-0696-6

Wright, H. L., Moots, R. J., and Edwards, S. W. (2014). The multifactorial role of neutrophils in rheumatoid arthritis. *Nat. Rev. Rheumatol.* 10, 593–601. doi: 10.1038/nrrheum.2014.80

Yin, F., Xu, Z., Wang, Z., Yao, H., Shen, Z., Yu, F., et al. (2012). Elevated chemokine CC-motif receptor-like 2 (CCRL2) promotes cell migration and invasion in glioblastoma. *Biochem. Biophys. Res. Commun.* 429, 168–172. doi: 10.1016/j.bbrc.2012.10.120

Yoshimura, T., and Oppenheim, J. J. (2011). Chemokine-like receptor 1 (CMKLR1) and chemokine (C-C motif) receptor-like 2 (CCRL2); two multifunctional receptors with unusual properties. *Exp. Cell Res.* 317, 674–684. doi: 10.1016/j.yexcr.2010.10.023

Zabel, B. A., Nakae, S., Zúñiga, L., Kim, J. Y., Ohyama, T., Alt, C., et al. (2008). Mast cell-expressed orphan receptor CCRL2 binds chemerin and is required for optimal induction of IgE-mediated passive cutaneous anaphylaxis. *J. Exp. Med.* 205, 2207–2220. doi: 10.1084/jem.20080300

Zimny, S., Pohl, R., Rein-Fischboeck, L., Haberl, E. M., Krautbauer, S., Weiss, T. S., et al. (2017). Chemokine (CC-motif) receptor-like 2 mRNA is expressed in hepatic stellate cells and is positively associated with characteristics of non-alcoholic steatohepatitis in mice and men. *Exp. Mol. Pathol.* 103, 1–8. doi: 10.1016/j.yexmp.2017.06.001

Zuurman, M. W., Heeroma, J., Brouwer, N., Boddeke, H. W., and Biber, K. (2003). LPS-induced expression of a novel chemokine receptor (L-CCR) in mouse glial cells *in vitro* and *in vivo*. *Glia* 41, 327–336. doi: 10.1002/glia.10156

Conflict of Interest: The authors declare that the research was conducted in the absence of any commercial or financial relationships that could be construed as a potential conflict of interest.

frontiers in Cell and Developmental Biology

ORIGINAL RESEARCH
published: 14 December 2020
doi: 10.3389/fcell.2020.603148

Mucin-Like Domain of Mucosal Addressin Cell Adhesion Molecule-1 Facilitates Integrin α4β7-Mediated Cell Adhesion Through Electrostatic Repulsion

MengYa Yuan[1†], YanRong Yang[1†], Yue Li[1,2], ZhanJun Yan[3], ChangDong Lin[1] and JianFeng Chen[1,2]**

[1] State Key Laboratory of Cell Biology, Shanghai Institute of Biochemistry and Cell Biology, Center for Excellence in Molecular Cell Science, Chinese Academy of Sciences, University of Chinese Academy of Sciences, Shanghai, China, [2] School of Life Science, Hangzhou Institute for Advanced Study, University of Chinese Academy of Sciences, Hangzhou, China, [3] Suzhou Ninth People's Hospital, Soochow University, Suzhou, China

OPEN ACCESS

Edited by:
Yuqing Huo,
Augusta University, United States

Reviewed by:
Simone Diestel,
University of Bonn, Germany
Maja Vulovic,
University of Kragujevac, Serbia

***Correspondence:**
ChangDong Lin
linchangdong@sibcb.ac.cn
JianFeng Chen
jfchen@sibcb.ac.cn

[†] These authors have contributed equally to this work

Specialty section:
This article was submitted to Cell Adhesion and Migration, a section of the journal Frontiers in Cell and Developmental Biology

Received: 05 September 2020
Accepted: 24 November 2020
Published: 14 December 2020

Citation:
Yuan M, Yang Y, Li Y, Yan Z, Lin C and Chen J (2020) Mucin-Like Domain of Mucosal Addressin Cell Adhesion Molecule-1 Facilitates Integrin α4β7-Mediated Cell Adhesion Through Electrostatic Repulsion. Front. Cell Dev. Biol. 8:603148. doi: 10.3389/fcell.2020.603148

The homing of lymphocytes from blood to gut-associated lymphoid tissue is regulated by interaction between integrin α4β7 with mucosal vascular addressin cell adhesion molecule 1 (MAdCAM-1) expressed on the endothelium of high endothelial venules (HEVs). However, the molecular basis of mucin-like domain, a specific structure of MAdCAM-1 regulating integrin α4β7-mediated cell adhesion remains obscure. In this study, we used heparan sulfate (HS), which is a highly acidic linear polysaccharide with a highly variable structure, to mimic the negative charges of the extracellular microenvironment and detected the adhesive behaviors of integrin α4β7 expressing 293T cells to immobilized MAdCAM-1 *in vitro*. The results showed that HS on the surface significantly promoted integrin α4β7-mediated cell adhesion, decreased the percentage of cells firmly bound and increased the rolling velocities at high wall shear stresses, which was dependent on the mucin-like domain of MAdCAM-1. Moreover, breaking the negative charges of the extracellular microenvironment of CHO-K1 cells expressing MAdCAM-1 with sialidase inhibited cell adhesion and rolling velocity of 293T cells. Mechanistically, electrostatic repulsion between mucin-like domain and negative charges of the extracellular microenvironment led to a more upright conformation of MAdCAM-1, which facilitates integrin α4β7-mediated cell adhesion. Our findings elucidated the important role of the mucin-like domain in regulating integrin α4β7-mediated cell adhesion, which could be applied to modulate lymphocyte homing to lymphoid tissues or inflammatory sites.

Keywords: MAdCAM-1, integrin α4β7, mucin-like domain, electrostatic repulsion, cell adhesion

INTRODUCTION

Integrins are important cell surface adhesion molecules, which are widely expressed on the cell membrane. They are heterodimers formed by non-covalent bonds between α and β subunits. In vertebrates, 18 α subunits and 8 β subunits combine to form 24 different integrins, specifically or cross-recognizing multiple extracellular matrix ligands (Hynes, 2002; Takada et al., 2007). Based on EM and atomic structures of integrins, the extracellular domain of integrin exists in at least three distinct global conformational states: (i) bent with a closed headpiece, (ii) extended with a closed headpiece, (iii) extended with an open headpiece. The closed and open headpieces of integrin have a low and high affinity for the ligand, respectively (Wang et al., 2018).

The homing of lymphocytes from blood to secondary lymphoid nodes or inflammatory sites is regulated by interaction with specific capillary venules, especially high endothelial venules (HEVs) (Ager, 2017). A highly ordered adhesion cascade mediates the recruitment process, including tethering and rolling of lymphocytes along vessel walls of HEVs, chemokine-induced integrin activation, firm arrest and transendothelial migration (von Andrian and Mempel, 2003; Lin et al., 2019). During this process, α4 integrins (α4β1 and α4β7) and β2 integrins (e.g., αLβ2 and αMβ2) on lymphocytes bind to their distinct ligands on vascular endothelial cells to mediate cell adhesion and migration. Among these integrins, α4 integrins, especially integrin α4β7 mediates both rolling and firm adhesion to mucosal vascular addressin cell adhesion molecule 1 (MAdCAM-1) (Berlin et al., 1993; Sun et al., 2014; Wang et al., 2018), which plays an important role to support efficient lymphocyte homing.

MAdCAM-1 is the primary ligand of integrin α4β7, specifically expressed on the endothelium of HEVs in the gut and gut-associated lymphoid tissues such as Peyer's patches (PPs) and mesenteric lymph nodes (MLNs) (Springer, 1994; Cox et al., 2010). Integrin α4β7-MAdCAM-1 binding-mediated pathological lymphocyte recruitment to the gut initiates and accelerates inflammatory bowel disease (IBD), consisting of ulcerative colitis (UC) and Crohn's disease (CD) (Hoshino et al., 2011). Thus, the regulation of lymphocyte adhesion mediated by the interaction between integrin α4β7 and MAdCAM-1 need to be further illustrated. MAdCAM-1 is a type I transmembrane glycoprotein molecule and belongs to a subclass of the immunoglobulin superfamily (IgSF), containing two Ig-like domains and a mucin-like domain (Tan et al., 1998). Mucin-like domain is a serine/threonine-rich region which serves as a backbone to support the interaction with lymphocytes (Briskin et al., 1993). Although the crystal structure of MAdCAM-1 has revealed that MAdCAM-1 binds directly to integrin α4β7 via Asp42 in the CD loop of Ig-like domain 1 (D1), and an unusual long D strand in Ig-like domain 2 (Ig-like domain 2) is also necessary for α4β7 binding (Tan et al., 1998), the function and molecular basis of mucin-like domain on the regulation of integrin α4β7-mediated cell adhesion is poorly understood. Considering the extracellular parts of plasma membrane proteins are generally glycosylated, which gives the microenvironment of plasma membrane negative charges, whether mucin-like domain forms electrostatic repulsion with the extracellular microenvironment, so as to affect integrin α4β7-mediated cell adhesion remains obscure.

In this study, we used heparan sulfate (HS) to mimic the negative charges of the extracellular microenvironment and detected the adhesive behaviors of integrin α4β7 expressing 293T cells to immobilized MAdCAM-1 *in vitro*. The results showed that HS on the surface promoted integrin α4β7-mediated cell adhesion to immobilized MAdCAM-1, which was dependent on the mucin-like domain of MAdCAM-1. Moreover, breaking the negative charges of the extracellular microenvironment of CHO-K1 cells expressing MAdCAM-1 with sialidase inhibited cell adhesion and rolling velocity of 293T cells. Mechanistically, electrostatic repulsion between mucin-like domain and negative charges of the extracellular microenvironment led to a more upright conformation of MAdCAM-1, which facilitates integrin α4β7-mediated cell adhesion. Our findings elucidated the important role of the mucin-like domain in regulating integrin α4β7-mediated cell adhesion, which could be applied to modulate lymphocyte homing to lymphoid tissues or inflammatory sites.

RESULTS

Negative Charges on the Surface Facilitates Integrin α4β7-Mediated Cell Adhesion to Immobilized MAdCAM-1

To study whether negative charges of the extracellular microenvironment affect integrin α4β7-mediated cell adhesion to MAdCAM-1 *in vitro*, we firstly purified Fc/His tagged extracellular domain of MAdCAM-1 (including Ig-like-1, Ig-like-2 and mucin-like domains, Met1-Gln317) in 293T cells (**Figure 1A**). Then we examined the effect of negative charges on cell adhesion to immobilized MAdCAM-1 in the presence of physiological cations (1 mM Ca^{2+} + Mg^{2+}). Heparan sulfate (HS) was used to mimic the extracellular microenvironment, which is a highly acidic linear polysaccharide with a very variable structure (Simon Davis and Parish, 2013). It is widely expressed on cell surfaces and the presence of sulfate groups at specific positions in HS chains imparts an overall high negative charge (Esko and Lindahl, 2001; Weiss et al., 2017). Firstly, we studied the adhesive behavior of 293T cells stably expressing integrin α4β7 (293T-α4β7) on MAdCAM-1 with HS or not in shear flow using flow chamber system. The shear stress was increased incrementally and the velocity of rolling cells at each increment was determined. At the wall shear stress of 1 dyn/cm^2, HS coated on the surface significantly increased the numbers of both firmly adherent cells (7.25 ± 0.75 vs. 10.5 ± 1.04) and rolling cells (15.25 ± 2.18 vs. 34.75 ± 4.03) (**Figure 1B** and **Supplementary Movies S1–S5**). Meanwhile, cells did not directly adhere to HS at all and cells pre-treated with α4β7 blocking antibody Act-1 did not adhere to MAdCAM-1 (**Figure 1B**), indicating that the adhesion is specifically integrin α4β7 dependent. The percentage of cells firmly bound to ligand decreased from 35.86 to 23.70% by the addition of HS (**Figure 1C**), which means HS might prefer to promote rolling adhesion. Consistent to the hypothesis, the average rolling velocity of cells was upregulated at the wall shear

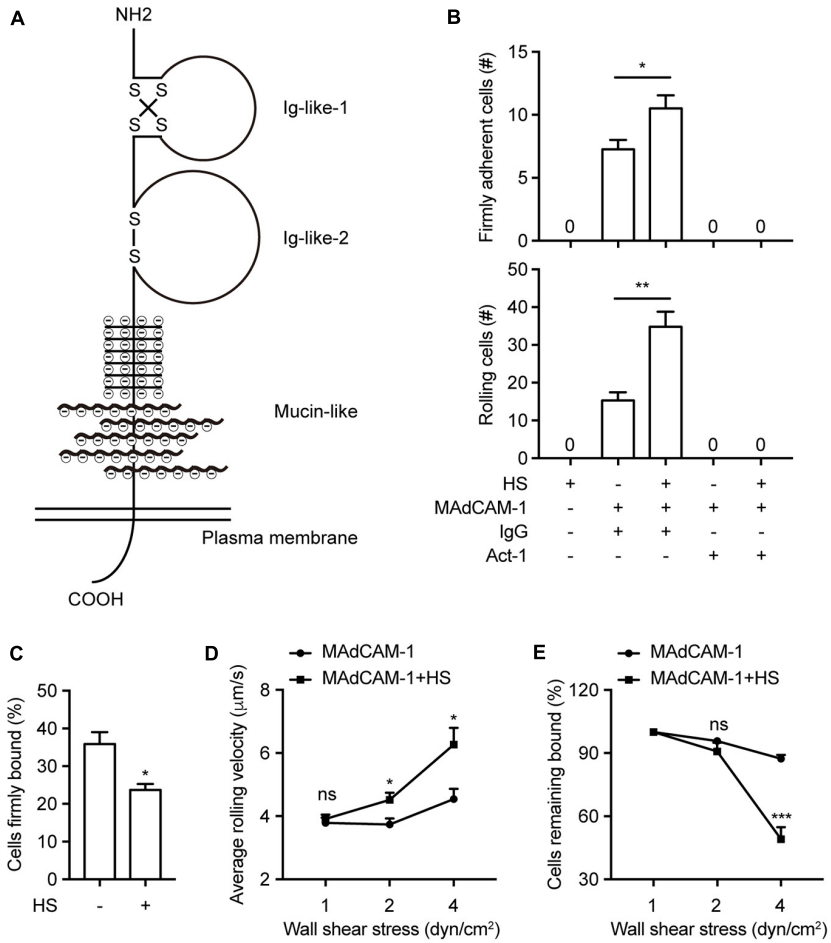

FIGURE 1 | HS on the surface promotes integrin α4β7-mediated cell adhesion to immobilized MAdCAM-1. **(A)** Schematic diagram of the structure of MAdCAM-1, the extracellular domain of MAdCAM-1 includes Ig-like-1, Ig-like-2 and mucin-like (serine/threonine-rich) three domains. **(B–E)** Adhesive behaviors of 293T-α4β7 cells on immobilized HS (100 μg/ml) or MAdCAM-1 (25 μg/ml) substrates in 1 mM Ca^{2+}/Mg^{2+}. The number of rolling and firmly adherent 293T-α4β7 cells was measured at a wall shear stress of 1 dyn/cm^2. Cells were pre-treated with murine IgG (10 μg/ml) or α4β7 blocking antibody Act-1 (10 μg/ml) for 10 min at 37°C **(B)**. Percentage of cells firmly bound to ligand at a wall shear stress of 1 dyn/cm^2 **(C)**. Average rolling velocity of 293T-α4β7 cells that adhered to MAdCAM-1 substrates at indicated wall shear stresses **(D)**. Resistance of 293T-α4β7 cells to detachment at increasing wall shear stresses. The total number of cells remaining bound at each indicated wall shear stress was determined as a percent of adherent cells at 1 dyn/cm^2 **(E)**. One representative result of three independent experiments is shown in **(B–E)**. Data represent the mean ± SEM ($n \geq 3$) in **(B–E)**. *$p < 0.05$, **$p < 0.01$, ***$p < 0.001$, ns: not significant (Student's *t*-test).

stress of 2 dyn/cm^2 and 4 dyn/cm^2 (**Figure 1D**). Furthermore, we tested the effect of HS on the strength of α4β7-mediated adhesion to MAdCAM-1 by calculating the cell resistance to detachment by increasing wall shear stresses. Cells adhered to the surface with HS detached much more rapidly from MAdCAM-1 (**Figure 1E**). These data demonstrate that HS on the surface promotes integrin α4β7-mediated cell adhesion to immobilized MAdCAM-1, which might be due to the negative charges of sulfate groups in HS chains.

Mucin-Like Domain of MAdCAM-1 Is Responsible for HS-Enhanced Integrin α4β7-Mediated Cell Adhesion

Mucin-like domain contains a serine/threonine-rich region, which may form an electrostatic repulsion with negative charges of the extracellular microenvironment. To investigate whether this specific domain play a role in supporting the interaction with lymphocytes, we deleted the mucin-like domain from the full length MAdCAM-1 (MAdCAM-1-Δmucin). Fc/His tagged extracellular domain of MAdCAM-1-Δmucin (including only Ig-like-1 and Ig-like-2, Met1-His225) (**Figure 2A**) was also purified in 293T cells. Then we examined the adhesive behavior of 293T-α4β7 cells to immobilized MAdCAM-1-Δmucin with HS or not. As expected, HS coated on the surface could not influence the number and the percentage of either firmly adherent cells (17.00 ± 2.05 vs. 17.33 ± 1.93) or rolling cells (22.50 ± 1.80 vs. 23.17 ± 0.98) at the wall shear stress of 1 dyn/cm^2 (**Figures 2B,C**). Similarly, the average rolling velocities of cells adhered to MAdCAM-1-Δmucin with HS or not showed to be comparable at all indicated wall shear stresses (**Figure 2D**) and the cell resistance to detachment from

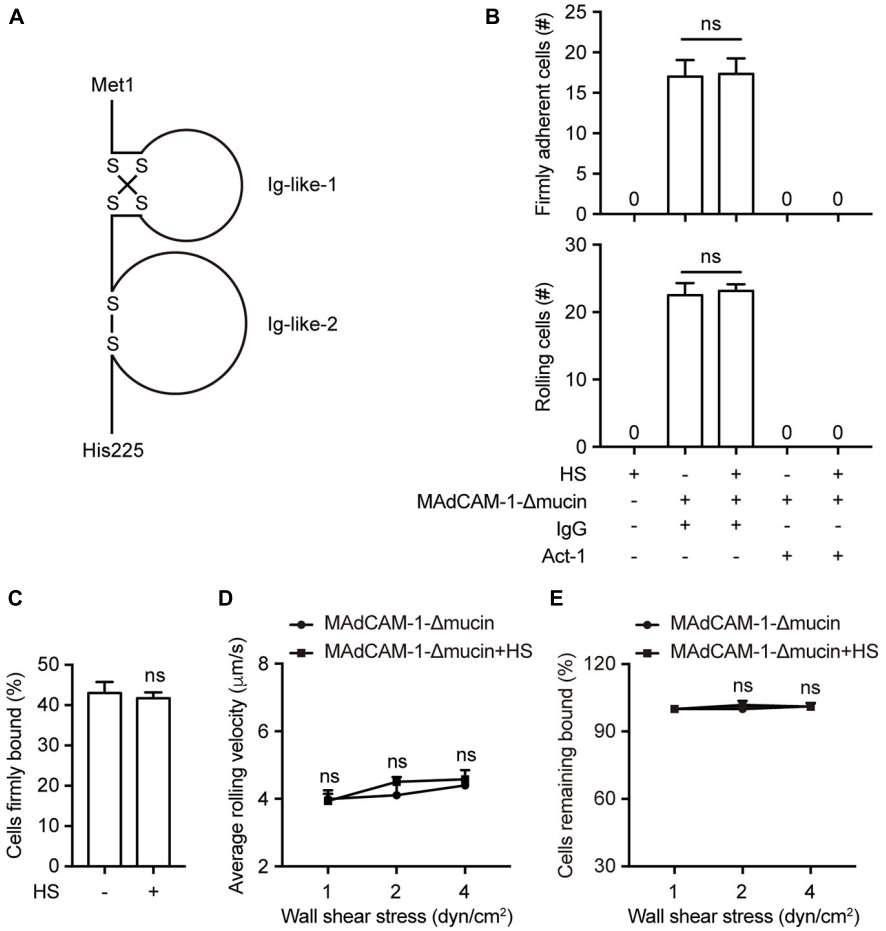

FIGURE 2 | HS-enhanced integrin α4β7-mediated cell adhesion is dependent on mucin-like domain of MAdCAM-1. **(A)** Schematic diagram of the structure of the extracellular domain of MAdCAM-1 with a deletion of mucin-like domain. **(B–E)** Adhesive behaviors of 293T-α4β7 cells on immobilized HS (100 μg/ml) or MAdCAM-1-Δmucin (100 μg/ml) substrates in 1 mM Ca^{2+}/Mg^{2+}. The number of rolling and firmly adherent 293T-α4β7 cells was measured at a wall shear stress of 1 dyn/cm^2. Cells were pre-treated with murine IgG (10 μg/ml) or α4β7 blocking antibody Act-1 (10 μg/ml) for 10 min at 37°C **(B)**. Percentage of cells firmly bound to ligand at a wall shear stress of 1 dyn/cm^2 **(C)**. Average rolling velocity of 293T-α4β7 cells that adhered to MAdCAM-1-Δmucin substrates at indicated wall shear stresses **(D)**. Resistance of 293T-α4β7 cells to detachment at increasing wall shear stresses **(E)**. One representative result of three independent experiments is shown in **(B–E)**. Data represent the mean ± SEM ($n \geq 3$) in **(B–E)**. ns: not significant (Student's *t*-test).

MAdCAM-1-Δmucin was also not changed by the addition of HS on the surface (**Figure 2E**). Taken together, HS-enhanced integrin α4β7-mediated cell adhesion is dependent on mucin-like domain of MAdCAM-1.

Breaking the Negative Charges of the Extracellular Microenvironment Suppresses Integrin α4β7-Mediated Cell Adhesion

To assess the requirement of negative charges of the extracellular microenvironment for integrin α4β7-mediated cell adhesion, CHO-K1 cells stably expressing full length MAdCAM-1 (CHO-K1/MAdCAM-1) were established (**Supplementary Figure S1**). Sialidase (also known as neuraminidase) was used to remove cell surface anionic sialic acid of glycoconjugate, so as to break the negative charges of the extracellular microenvironment (Thaysen-Andersen et al., 2013; Ashdown et al., 2020). CHO-K1/MAdCAM-1 cells were pre-treated with sialidase or not and then used in flow chamber assay to study the adhesive behavior of 293T-α4β7 cells in shear flow. At the wall shear stress of 1 dyn/cm^2, the numbers of both firmly adherent cells (59.33 ± 2.85 vs. 39.50 ± 5.32) and rolling cells (33.67 ± 2.67 vs. 20.25 ± 1.60) decreased significantly when CHO-K1/MAdCAM-1 cells were pre-treated with sialidase (**Figure 3A**). Of note, although 293T-α4β7 cells were pre-treated with α4β7 blocking antibody Act-1, there existed some cells adhered to the surface of CHO-K1/MAdCAM-1 cells (**Figure 3A**), suggesting that the remaining cell adhesion is integrin α4β7 independent. Meanwhile, pre-treatment with sialidase upregulated the percentage of cells firmly bound to CHO-K1/MAdCAM-1 cells from 64.00 to 70.52% (**Figure 3B**) and decreased the average rolling velocity of 293T-α4β7 cells at the wall shear stress of 2 and 4 dyn/cm^2 (**Figure 3C**). Furthermore, 293T-α4β7 cells showed to be more

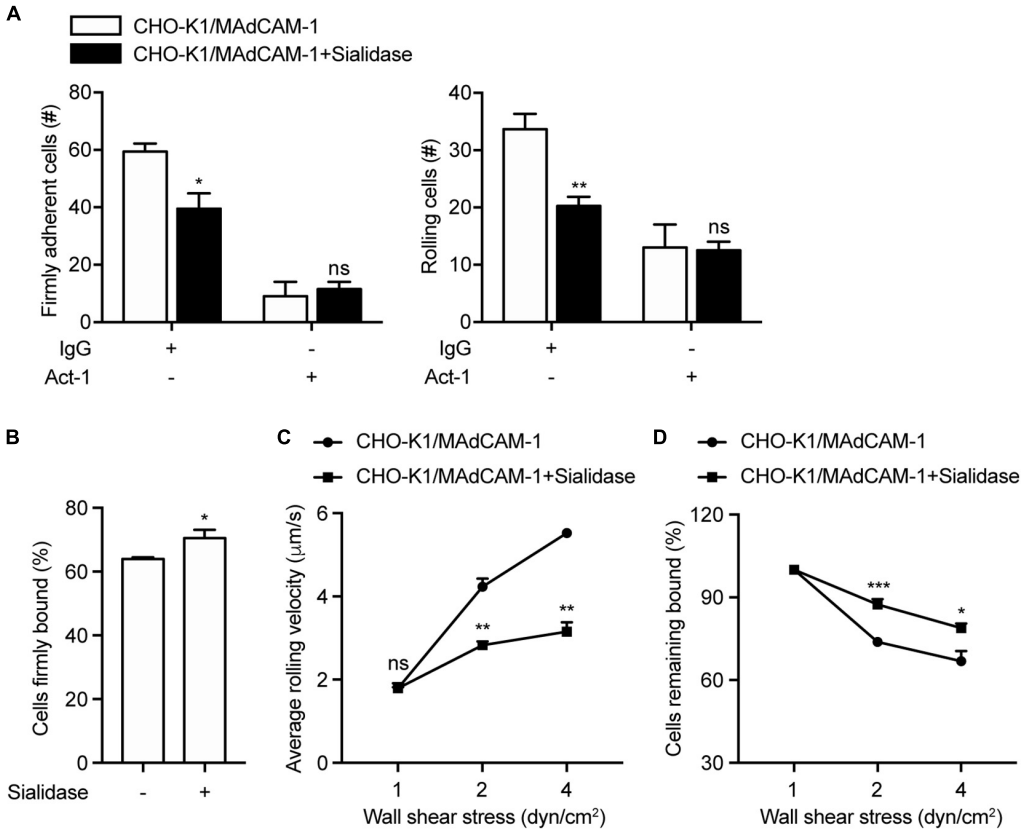

FIGURE 3 | Breaking the negative charges of the extracellular microenvironment suppresses integrin α4β7-mediated cell adhesion. Adhesive behaviors of 293T-α4β7 cells on CHO-K1/MAdCAM-1 cells. **(A)** The number of rolling and firmly adherent 293T-α4β7 cells was measured at a wall shear stress of 1 dyn/cm^2. Cells were pre-treated with murine IgG (10 μg/ml) or α4β7 blocking antibody Act-1 (10 μg/ml) for 10 min at 37°C. **(B)** Percentage of cells firmly bound to CHO-K1/MAdCAM-1 cells at a wall shear stress of 1 dyn/cm^2. **(C)** Average rolling velocity of 293T-α4β7 cells that adhered to CHO-K1/MAdCAM-1 cells at indicated wall shear stresses. **(D)** Resistance of 293T-α4β7 cells to detachment at increasing wall shear stresses. One representative result of three independent experiments is shown. Data represent the mean ± SEM ($n \geq 3$). *$p < 0.05$, **$p < 0.01$, ***$p < 0.001$, ns: not significant (Student's *t*-test).

resistant to detachment by increasing wall shear stresses when adhered to the surface of CHO-K1/MAdCAM-1 cells pre-treated with sialidase (**Figure 3D**). These data indicate that breaking the negative charges of the extracellular microenvironment by sialidase suppresses integrin α4β7-mediated cell adhesion to MAdCAM-1 expressed on CHO-K1 cells.

Deletion of Mucin-Like Domain of MAdCAM-1 Abolishes the Influence of Sialidase on Integrin α4β7-Mediated Cell Adhesion to CHO-K1 Cells

Above data have demonstrated that mucin-like domain of MAdCAM-1 is responsible for negative charges-enhanced integrin α4β7-mediated cell adhesion. To further confirm the results, CHO-K1 cells stably expressing MAdCAM-1-Δmucin (CHO-K1/MAdCAM-1-Δmucin) were established, which showed a similar level to that of CHO-K1/MAdCAM-1 cells (**Supplementary Figure S1**). Then we examined the adhesive behavior of 293T-α4β7 cells on CHO-K1/MAdCAM-1-Δmucin cells. Pre-treatment of sialidase did not influence the number and the percentage of either firmly adherent cells (51.67 ± 1.20 vs. 51.00 ± 2.08) or rolling cells (30.67 ± 0.88 vs. 30.67 ± 4.10) and the average rolling velocity at all wall shear stresses (**Figures 4A–C**). Furthermore, the cell resistance to detachment from CHO-K1/MAdCAM-1-Δmucin cells was also not changed by the treatment of sialidase (**Figure 4D**). Thus, mucin-like domain of MAdCAM-1 is responsible for the interaction with negative charges of the extracellular microenvironment, which is derived from cell surface anionic sialic acid of CHO-K1 cells.

Electrostatic Repulsion Between Mucin-Like Domain and Negative Charges of the Extracellular Microenvironment Affects the Conformation of MAdCAM-1

Next, we examined the conformational change of MAdCAM-1 ectodomain using fluorescence resonance energy transfer (FRET). To assess the orientation of MAdCAM-1 ectodomain relative to the plasma membrane, Ig-like-1 domain was labeled

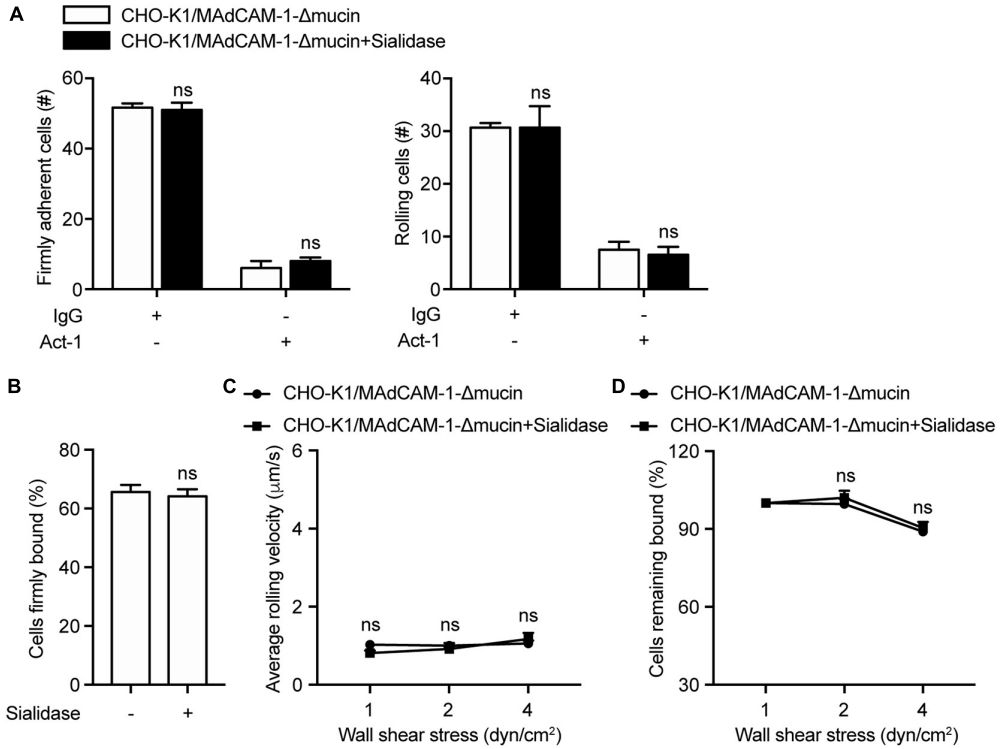

FIGURE 4 | Deletion of mucin-like domain of MAdCAM-1 abolishes the influence of sialidase on integrin α4β7-mediated cell adhesion to CHO-K1 cells. Adhesive behaviors of 293T-α4β7 cells on CHO-K1/MAdCAM-1-Δmucin cells. **(A)** The number of rolling and firmly adherent 293T-α4β7 cells was measured at a wall shear stress of 1 dyn/cm^2. Cells were pre-treated with murine IgG (10 μg/ml) or α4β7 blocking antibody Act-1 (10 μg/ml) for 10 min at 37°C. **(B)** Percentage of cells firmly bound to CHO-K1/MAdCAM-1-Δmucin cells at a wall shear stress of 1 dyn/cm^2. **(C)** Average rolling velocity of 293T-α4β7 cells that adhered to CHO-K1/MAdCAM-1-Δmucin cells at indicated wall shear stresses. **(D)** Resistance of 293T-α4β7 cells to detachment at increasing wall shear stresses. One representative result of three independent experiments is shown. Data represent the mean ± SEM ($n \geq 3$). ns: not significant (Student's *t*-test).

with Alexa Fluor 488-conjugated 8C1 Fab fragment as the FRET donor. The plasma membrane was labeled with FM 4-64FX as the FRET acceptor (**Figure 5A**). Pre-treatment with sialidase significantly increased FRET efficiency in CHO-K1/MAdCAM-1 cells (3.33 ± 0.29 vs. 6.05 ± 0.42) but not in CHO-K1/MAdCAM-1-Δmucin cells (10.31 ± 0.28 vs. 10.01 ± 0.33) (**Figure 5B**), indicating that sialidase-induced bent conformation of MAdCAM-1 ectodomain was dependent on mucin-like domain. Furthermore, the results showed that the FRET efficiency in CHO-K1/MAdCAM-1 cells was much lower than that in CHO-K1/MAdCAM-1-Δmucin cells in the absent of sialidase, which could be due to the fact that deletion of mucin-like domain lowers the height of MAdCAM-1 molecule and Ig-like-1 domain closes to the plasma membrane (**Figure 5B**). Thus, electrostatic repulsion between mucin-like domain and negative charges of the extracellular microenvironment leads to a more upright conformation of MAdCAM-1, which facilitates integrin α4β7-mediated cell adhesion.

DISCUSSION

Gut-associated lymphoid tissue (GALT), including isolated and aggregated lymphoid follicles (PPs, MLNs et al.), is one of the largest lymphoid organs in the body (Corr et al., 2008). It contains 70% of the body's lymphocytes and plays vital roles in gastrointestinal mucosal immunity (Hoshino et al., 2011). The homing of lymphocytes to GALT is dependent of the interaction between integrin α4β7 and MAdCAM-1. The disfunction of integrin α4β7-mediated cell adhesion to MAdCAM-1 could result in pathological lymphocyte recruitment to the gut and the initiation and progression of IBD (Hoshino et al., 2011). In the previous studies, most work focused on the regulation of integrin conformational changes. Chemokine stimulations, inside-out signaling and metal ions all could influence global conformational change of the integrin extracellular domain and the subsequent the adhesin to the distinct ligand (Montresor et al., 2012; Springer and Dustin, 2012; Zhang and Chen, 2012). For example, in Ca^{2+}, α4β7 mediates rolling adhesion, whereas in Mg^{2+} alone and in Mn^{2+}, α4β7 mediates firm adhesion on MAdCAM-1, mimicking the two steps in lymphocyte accumulation in HEVs or the vasculature at inflammatory sites (de Chateau et al., 2001; Chen et al., 2003). However, little is known whether the conformation of MAdCAM-1 is affected by the extracellular microenvironment.

The crystal structure of MAdCAM-1 exhibits two protruding loops from the two Ig-like domains, the CC' loop in D1 and DE loop in D2. These two loops are responsible for the interaction

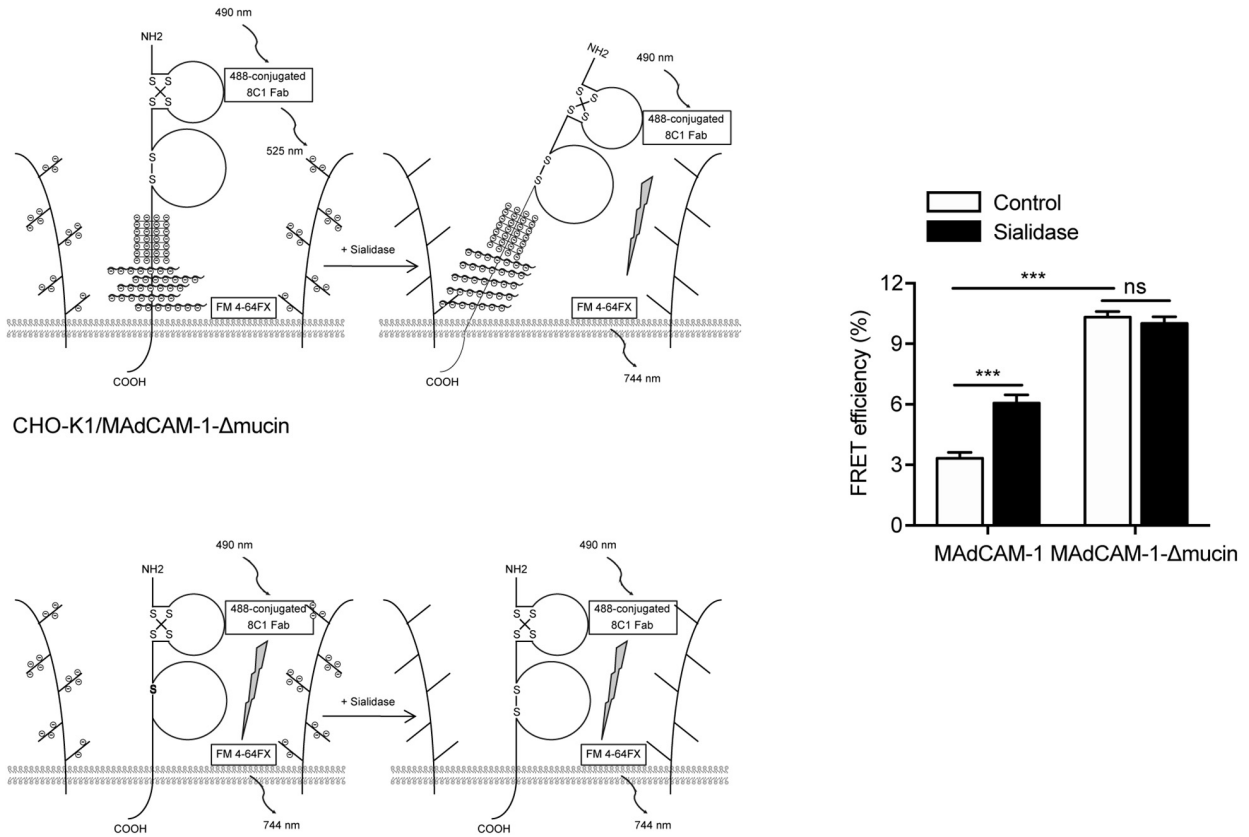

FIGURE 5 | Electrostatic repulsion between mucin-like domain and negative charges of the extracellular microenvironment affects the conformation of MAdCAM-1. **(A)** Experiment setup for measuring FRET efficiency between Ig-like-1 domain and the plasma membrane. A composite of all molecules used is depicted. **(B)** FRET efficiency of CHO-K1/MAdCAM-1 and CHO-K1/MAdCAM-1-Δmucin cells before and after treatment with sialidase. Data represent the mean ± SEM ($n \geq 3$). ***$p < 0.001$, ns: not significant (Student's *t*-test).

between MAdCAM-1 and α4β7 (Sun et al., 2011). Furthermore, a shift in D1 topology from the I2-set to I1-set was demonstrated by new crystals of MAdCAM-1 and two different Fabs, inducing a switch of integrin-binding loop from CC' to CD (Yu et al., 2013). The different conformations seen in crystal structures suggest that the integrin-binding loop of MAdCAM-1 is inherently flexible, which may explain why MAdCAM-1 could mediate both rolling and firm adhesion by binding to integrin α4β7 in different conformational states.

A mucin-like domain of MAdCAM-1 is unique among integrin ligands, which connects the two Ig-like domains to the plasma membrane. In this respect, MAdCAM-1 resembles selectin ligands (Berg et al., 1993). Selectins selectively mediate rolling adhesion but not firm adhesion on blood vessels and recognize carbohydrate residues displayed on proteins consisting mucin-like regions (Springer, 1994). Furthermore, mucin-like domain is a serine/threonine-rich region. It is proposed that MAdCAM-1 molecule is repelled by the electrostatic repulsion between the highly negatively charged mucin-like region and the extracellular microenvironment, which could help orient the integrin-binding Ig-like domains on cell surface for recognition.

In this study, we found that HS on the surface significantly promoted integrin α4β7-mediated cell rolling adhesion and firm adhesion, decreased the percentage of cells firmly bound and increased the rolling velocities at high wall shear stresses, implying the negative charges of the extracellular microenvironment actually facilitates integrin α4β7-MAdCAM-1 function. Conversely, reducing the negative charges of CHO-K1/MAdCAM-1 extracellular microenvironment by sialidase inhibited cell adhesion and rolling velocity of α4β7 expressing 293T cells. The results of FRET assay gave the direct evidence that electrostatic repulsion between mucin-like domain and negative charges of the extracellular microenvironment leads to a more upright conformation of MAdCAM-1. It is speculated that this electrostatic repulsion-induced extended conformation could further affect the topology of integrin-binding loop in D1 and D2, thereby promoting the binding to integrin α4β7. The detailed conformational change needs to be further clarified with the crystal structures of MAdCAM-1

stabilized by the electrostatic repulsion. Moreover, the deletion of the mucin-like domain significantly increased the FRET efficiency between Ig-like-1 domain and the plasma membrane, indicating a lower height of MAdCAM-1 molecule. Thus, the distance between the binding sites of MAdCAM-1 and integrin α4β7 is also thought to influence the binding efficiency of these two molecules.

In conclusion, mucin-like domain of MAdCAM-1 facilitates integrin α4β7-mediated cell adhesion through electrostatic repulsion with negatively charged extracellular microenvironment (**Figure 6**), which could be applied to modulate lymphocyte homing to lymphoid tissues or inflammatory sites.

MATERIALS AND METHODS

Protein Expression and Purification

Recombinant human extracellular domain of MAdCAM-1 (Met1-Gln317) or MAdCAM-1-Δmucin (Met1-His225) was constructed in vector pHLsec-Fc/His using restriction enzymes *Age*I and *Kpn*I. 293T cells were transiently transfected with plasmids expressing MAdCAM-1 or MAdCAM-1-Δmucin by the method of $Ca_3(PO_4)_2$ transfection as described (Chen et al., 2003). Recombinant proteins were purified with Protein A Agarose (Thermo Fisher Scientific).

Cell Lines

Human embryonic kidney HEK293T cells were cultured at 37°C with 5% CO_2 in Dulbecco's modified Eagle medium (DMEM) (Gibco) containing 2 mM L-glutamine, 100 U/mL penicillin, 100 μg/mL streptomycin, and 10% (vol/vol) fetal bovine serum (Gibco). CHO-K1 cells were cultured at 37°C with 5% CO_2 in Ham's F12 Medium (Corning) containing 2 mM L-glutamine, 100 U/mL penicillin, 100 μg/mL streptomycin, and 10% (vol/vol) fetal bovine serum (Gibco). CHO-K1 cells stably expressing full length MAdCAM-1 or MAdCAM-1-Δmucin by electroporation and selection by 0.2 mg/ml hygromycin (Amresco) as described (Yue et al., 2013).

Flow Chamber Assay

Flow chamber assay was performed as described (Chen et al., 2003; Lu et al., 2016). To study integrin α4β7-mediated cell adhesion to recombinant proteins, a polystyrene Petri dish was coated with a 5 mm diameter, 20 μl spot of HS (100 μg/ml), MAdCAM-1 (25 μg/ml) or MAdCAM-1-Δmucin (100 μg/ml) in coating buffer (PBS, 10 mM $NaHCO_3$, pH 9.0) for 1 h at 37°C, and then treated by 2% BSA in coating buffer for 1 h at 37°C to block non-specific binding sites. Otherwise, CHO-K1/MAdCAM-1 or CHO-K1/MAdCAM-1-Δmucin cells were seeded to a polystyrene Petri dish the day before the experiment, and washed by HBS (20 mM Hepes, pH 7.4) twice to clean up the culture medium. Then CHO-K1 cells were treated with HBS or 0.01 U/ml sialidase in HBS for 20 min at 37°C to remove cell surface anionic sialic acid of glycoconjugate. Integrin α4β7 expressing 293T cells were washed twice with HBS containing 5 mM EDTA and 0.5% BSA and diluted to 1×10^6/ml in buffer A (HBS, 0.5% BSA) containing 1 mM Ca^{2+} + Mg^{2+}. Then cells were infused in the chamber using a Harvard apparatus programmable syringe pump immediately. Cells were allowed to accumulate for 30 s at 0.3 dyn/cm^2 and for 10 s at 0.4 dyn/cm^2. Afterward, shear stress was increased every 10 s

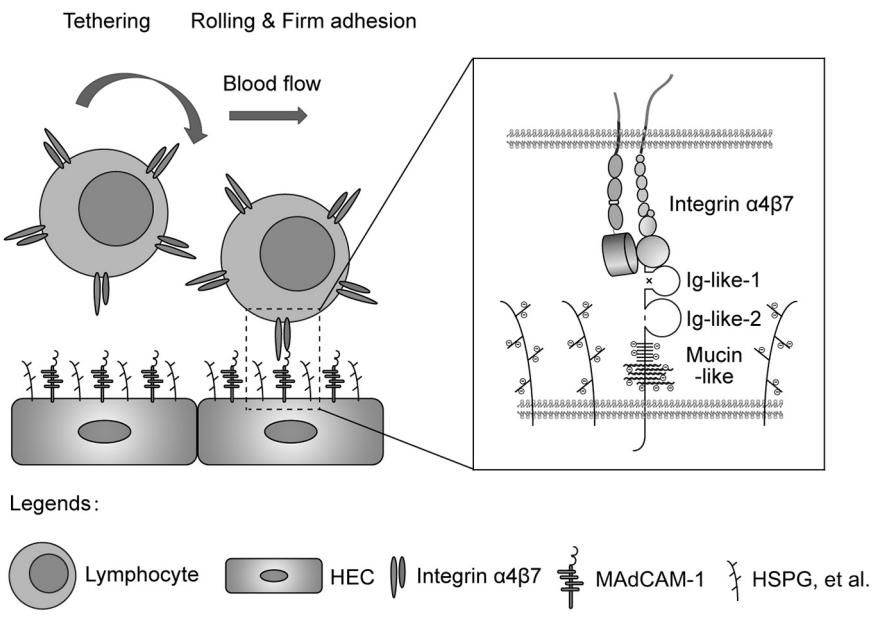

FIGURE 6 | Electrostatic repulsion between mucin-like domain and negative charges of the extracellular microenvironment facilitates integrin α4β7-mediated cell adhesion. Schematic diagram of the adhesion of lymphocytes from blood to the endothelium of HEVs in gut-associated lymphoid tissues. HEC, high endothelial cell; HSPG, heparan sulfate proteoglycan.

from 1 dyn/cm^2 up to 32 dyn/cm^2 in 2-fold increments. The rolling velocity at each shear stress was calculated from the average distance traveled by rolling cells in 3 s. A velocity of 1 μm/s corresponded to a movement of 1/2 cell diameter during the 3 s measurement interval. It was the minimum velocity required to define a cell adhesion behavior as rolling or firmly adherent. The number of cells remaining bound at the end of each 10 s interval was determined. Cells were pre-treated with murine IgG (10 μg/ml) or α4β7 blocking antibody Act-1 (10 μg/ml) for 10 min at 37°C before they were infused into the flow chamber.

Flow Cytometry

Flow cytometry was performed as described (Lu et al., 2016). CHO-K1/MAdCAM-1 or CHO-K1/MAdCAM-1-Δmucin cells were stained with monoclonal antibody 8C1 against human MAdCAM-1 and then measured using FACSCelesta^{TM} (BD Biosciences). Data were analyzed using FlowJo 7.6.1 software.

Fluorescence Resonance Energy Transfer (FRET)

For detecting the orientation of MAdCAM-1 ectodomain relative to cell membrane, CHO-K1/MAdCAM-1 or CHO-K1/MAdCAM-1-Δmucin cells were seeded on poly-L-Lysine (100 μg/ml) coated surface in HBS and incubated for 30 min at 37°C. Adherent cells were treated with HBS or 0.01 U/ml sialidase in HBS for 20 min at 37°C to remove cell surface anionic sialic acid of glycoconjugate. Then cells were fixed with 3.7% paraformaldehyde for 10 min at room temperature. Non-specific sites were blocked by incubation with 10% serum in HBS for 10 min at room temperature. 20 μg/ml Alexa Fluor 488-conjugated 8C1 Fab fragment was used to stain cells for 30 min at 37°C. Then cells were washed twice with HBS and labeled with 10 μM FM^{TM} 4-64FX (Invitrogen) for 1 min on ice. After one wash, cells were immediately mounted with Mowiol® 4-88 (Polysciences) mounting solution under a coverslip. The slides were kept in dark and subjected to photobleach FRET acquisition by a confocal microscope (TCS SP8, Leica). FRET efficiency (E) was calculated as $E = 1 - (F_{donor}(d)_{Pre}/F_{donor}(d)_{Post})$, where $F_{donor}(d)_{Pre}$ and $F_{donor}(d)_{Post}$ are the mean donor emission intensity of pre- and post-photobleaching.

Quantification and Statistical Analysis

Statistical significance was determined by Student's t test using Prism software (GraphPad, version 5.01). The resulting p values are indicated as follows: ns, not significant; $^{*}p < 0.05$; $^{**}p < 0.01$; $^{***}p < 0.001$. Data represent the mean ± SEM of at least three independent experiments.

DATA AVAILABILITY STATEMENT

The original contributions presented in the study are included in the article/**Supplementary Material**, further inquiries can be directed to the corresponding author/s.

AUTHOR CONTRIBUTIONS

CL and JC conceptualized the project and designed the experiments. MY, YY, and YL performed the experiments. ZY, CL, and JC interpreted the results. CL drafted the manuscript. JC edited the manuscript. All authors contributed to the article and approved the submitted version.

FUNDING

This work was supported by grants from the National Natural Science Foundation of China (31525016, 31830112, 32030024 to JC, 31701219, 31970702 to CL), National Key Research and Development Program of China (2020YFA0509100), Program of Shanghai Academic Research Leader (19XD1404200), Personalized Medicines-Molecular Signature-based Drug Discovery and Development, the Strategic Priority Research Program of the Chinese Academy of Sciences (XDA12010101), the Youth Innovation Promotion Association of the Chinese Academy of Sciences, the Young Elite Scientist Sponsorship Program by CAST (2019QNRC001), and National Ten Thousand Talents Program.

ACKNOWLEDGMENTS

We gratefully acknowledge the support of SA-SIBS scholarship program.

SUPPLEMENTARY MATERIAL

The Supplementary Material for this article can be found online at: https://www.frontiersin.org/articles/10.3389/fcell.2020.603148/full#supplementary-material

Supplementary Figure 1 | MAdCAM-1 expression on CHO-K1/MAdCAM-1 and CHO-K1/MAdCAM-1-Δmucin cells. MAdCAM-1 expression on CHO-K1/MAdCAM-1 and CHO-K1/MAdCAM-1-Δmucin cells was determined by flow cytometry. Numbers within the panel showed the specific mean fluorescence intensities. Opened histogram: mock control.

Supplementary Movie 1 | Adhesive behaviors of 293T-α4β7 cells on immobilized HS (100 μg/ml).

Supplementary Movie 2 | Adhesive behaviors of 293T-α4β7 cells on immobilized MAdCAM-1 (25 μg/ml) substrates. Cells were pre-treated with murine IgG (10 μg/ml) for 10 min at 37°C.

Supplementary Movie 3 | Adhesive behaviors of 293T-α4β7 cells on immobilized HS (100 μg/ml) and MAdCAM-1 (25 μg/ml) substrates. Cells were pre-treated with murine IgG (10 μg/ml) for 10 min at 37°C.

Supplementary Movie 4 | Adhesive behaviors of 293T-α4β7 cells on immobilized MAdCAM-1 (25 μg/ml) substrates. Cells were pre-treated with α4β7 blocking antibody Act-1 (10 μg/ml) for 10 min at 37°C.

Supplementary Movie 5 | Adhesive behaviors of 293T-α4β7 cells on immobilized HS (100 μg/ml) and MAdCAM-1 (25 μg/ml) substrates. Cells were pre-treated with α4β7 blocking antibody Act-1 (10 μg/ml) for 10 min at 37°C.

REFERENCES

Ager, A. (2017). High endothelial venules and other blood vessels: critical regulators of lymphoid organ development and function. *Front. Immunol.* 8:45. doi: 10.3389/fimmu.2017.00045

Ashdown, C. P., Johns, S. C., Aminov, E., Unanian, M., Connacher, W., Friend, J., et al. (2020). Pulsed low-frequency magnetic fields induce tumor membrane disruption and altered cell viability. *Biophys. J.* 118, 1552–1563. doi: 10.1016/j.bpj.2020.02.013

Berg, E. L., McEvoy, L. M., Berlin, C., Bargatze, R. F., and Butcher, E. C. (1993). L-selectin-mediated lymphocyte rolling on MAdCAM-1. *Nature* 366, 695–698. doi: 10.1038/366695a0

Berlin, C., Berg, E. L., Briskin, M. J., Andrew, D. P., Kilshaw, P. J., Holzmann, B., et al. (1993). Alpha 4 beta 7 integrin mediates lymphocyte binding to the mucosal vascular addressin MAdCAM-1. *Cell* 74, 185–195. doi: 10.1016/0092-8674(93)90305-a

Briskin, M. J., Mcevoy, L. M., and Butcher, E. C. (1993). Madcam-1 has homology to immunoglobulin and mucin-like adhesion receptors and to Iga1. *Nature* 363, 461–464. doi: 10.1038/363461a0

Chen, J., Salas, A., and Springer, T. A. (2003). Bistable regulation of integrin adhesiveness by a bipolar metal ion cluster. *Nat. Struct. Biol.* 10, 995–1001. doi: 10.1038/nsb1011

Corr, S. C., Gahan, C. C., and Hill, C. (2008). M-cells: origin, morphology and role in mucosal immunity and microbial pathogenesis. *FEMS Immunol. Med. Microbiol.* 52, 2–12. doi: 10.1111/j.1574-695x.2007.00359.x

Cox, D., Brennan, M., and Moran, N. (2010). Integrins as therapeutic targets: lessons and opportunities. *Nat. Rev. Drug Discov.* 9, 804–820. doi: 10.1038/nrd3266

de Chateau, M., Chen, S., Salas, A., and Springer, T. A. (2001). Kinetic and mechanical basis of rolling through an integrin and novel Ca2+-dependent rolling and Mg2+-dependent firm adhesion modalities for the alpha 4 beta 7-MAdCAM-1 interaction. *Biochemistry* 40, 13972–13979. doi: 10.1021/bi011582f

Esko, J. D., and Lindahl, U. (2001). Molecular diversity of heparan sulfate. *J. Clin. Invest.* 108, 169–173. doi: 10.1172/jci200113530

Hoshino, H., Kobayashi, M., Mitoma, J., Sato, Y., Fukuda, M., and Nakayama, J. (2011). An integrin alpha4beta7*IgG heterodimeric chimera binds to MAdCAM-1 on high endothelial venules in gut-associated lymphoid tissue. *J. Histochem. Cytochem.* 59, 572–583. doi: 10.1369/0022155411404416

Hynes, R. O. (2002). Integrins: bidirectional, allosteric signaling machines. *Cell* 110, 673–687.

Lin, C., Zhang, Y., Zhang, K., Zheng, Y., Lu, L., Chang, H., et al. (2019). Fever promotes T lymphocyte trafficking via a thermal sensory pathway involving heat shock protein 90 and alpha4 integrins. *Immunity* 50:e136.

Lu, L., Lin, C., Yan, Z., Wang, S., Zhang, Y., Wang, J., et al. (2016). Kindlin-3 is essential for the resting alpha4beta1 integrin-mediated firm cell adhesion under shear flow conditions. *J. Biol. Chem.* 291, 10363–10371. doi: 10.1074/jbc.m116.717694

Montresor, A., Toffali, L., Constantin, G., and Laudanna, C. (2012). Chemokines and the signaling modules regulating integrin affinity. *Front. Immunol.* 3:127. doi: 10.3389/fimmu.2012.00127

Simon Davis, D. A., and Parish, C. R. (2013). Heparan sulfate: a ubiquitous glycosaminoglycan with multiple roles in immunity. *Front. Immunol.* 4:470. doi: 10.3389/fimmu.2013.00470

Springer, T. A. (1994). Traffic signals for lymphocyte recirculation and leukocyte emigration: the multistep paradigm. *Cell* 76, 301–314. doi: 10.1016/0092-8674(94)90337-9

Springer, T. A., and Dustin, M. L. (2012). Integrin inside-out signaling and the immunological synapse. *Curr. Opin. Cell. Biol.* 24, 107–115. doi: 10.1016/j.ceb.2011.10.004

Sun, H., Liu, J., Zheng, Y., Pan, Y., Zhang, K., and Chen, J. (2014). Distinct chemokine signaling regulates integrin ligand specificity to dictate tissue-specific lymphocyte homing. *Dev. Cell* 30, 61–70. doi: 10.1016/j.devcel.2014.05.002

Sun, H., Wu, Y., Qi, J., Pan, Y., Ge, G., and Chen, J. (2011). The CC' and DE loops in Ig domains 1 and 2 of MAdCAM-1 play different roles in MAdCAM-1 binding to low- and high-affinity integrin alpha4beta7. *J. Biol. Chem.* 286, 12086–12092. doi: 10.1074/jbc.m110.208900

Takada, Y., Ye, X., and Simon, S. (2007). The integrins. *Genome Biol.* 8:215.

Tan, K., Casasnovas, J. M., Liu, J. H., Briskin, M. J., Springer, T. A., and Wang, J. H. (1998). The structure of immunoglobulin superfamily domains 1 and 2 of MAdCAM-1 reveals novel features important for integrin recognition. *Structure* 6, 793–801. doi: 10.1016/s0969-2126(98)00080-x

Thaysen-Andersen, M., Larsen, M. R., Packer, N. H., and Palmisano, G. (2013). Structural analysis of glycoprotein sialylation - Part I: pre-LC-MS analytical strategies. *RSC Adv.* 3, 22683–22705. doi: 10.1039/c3ra42960a

von Andrian, U. H., and Mempel, T. R. (2003). Homing and cellular traffic in lymph nodes. *Nat. Rev. Immunol.* 3, 867–878. doi: 10.1038/nri1222

Wang, S., Wu, C., Zhang, Y., Zhong, Q., Sun, H., Cao, W., et al. (2018). Integrin alpha4beta7 switches its ligand specificity via distinct conformer-specific activation. *J. Cell Biol.* 217, 2799–2812. doi: 10.1083/jcb.201710022

Weiss, R. J., Esko, J. D., and Tor, Y. (2017). Targeting heparin and heparan sulfate protein interactions. *Org. Biomol. Chem.* 15, 5656–5668. doi: 10.1039/c7ob01058c

Yu, Y., Zhu, J., Huang, P. S., Wang, J. H., Pullen, N., and Springer, T. A. (2013). Domain 1 of mucosal addressin cell adhesion molecule has an I1-set fold and a flexible integrin-binding loop. *J. Biol. Chem.* 288, 6284–6294. doi: 10.1074/jbc.m112.413153

Yue, J., Pan, Y. D., Sun, L. F., Zhang, K., Liu, J., Lu, L., et al. (2013). The unique disulfide bond-stabilized W1 beta 4-beta 1 loop in the alpha(4)beta-Propeller domain regulates integrin alpha(4)beta(7) affinity and signaling. *J. Biol. Chem.* 288, 14228–14237. doi: 10.1074/jbc.m113.462630

Zhang, K., and Chen, J. (2012). The regulation of integrin function by divalent cations. *Cell Adh. Migr.* 6, 20–29. doi: 10.4161/cam.18702

Conflict of Interest: The authors declare that the research was conducted in the absence of any commercial or financial relationships that could be construed as a potential conflict of interest.

frontiers in Cell and Developmental Biology

REVIEW
published: 18 December 2020
doi: 10.3389/fcell.2020.619221

Extracellular RNA as a Versatile DAMP and Alarm Signal That Influences Leukocyte Recruitment in Inflammation and Infection

Klaus T. Preissner[1,2], Silvia Fischer[1] and Elisabeth Deindl[3,4]*

[1] *Department of Biochemistry, Medical School, Justus Liebig University Giessen, Giessen, Germany,*
[2] *Kerckhoff-Heart-Research-Institute, Department of Cardiology, Medical School, Justus Liebig University Giessen, Giessen, Germany,* [3] *Walter-Brendel-Centre of Experimental Medicine, University Hospital, LMU Munich, Munich, Germany,*
[4] *Biomedical Center, Institute of Cardiovascular Physiology and Pathophysiology, LMU Munich, Munich, Germany*

OPEN ACCESS

Edited by:
Zhichao Fan,
UConn Health, United States

Reviewed by:
Rongrong Liu,
Northwestern University, United States
Lothar C. Dieterich,
ETH Zürich, Switzerland

***Correspondence:**
Klaus T. Preissner
klaus.t.preissner@biochemie.med.uni-giessen.de

Specialty section:
This article was submitted to Cell Adhesion and Migration, a section of the journal Frontiers in Cell and Developmental Biology

Received: *19 October 2020*
Accepted: *30 November 2020*
Published: *18 December 2020*

Citation:
Preissner KT, Fischer S and Deindl E (2020) Extracellular RNA as a Versatile DAMP and Alarm Signal That Influences Leukocyte Recruitment in Inflammation and Infection. Front. Cell Dev. Biol. 8:619221. doi: 10.3389/fcell.2020.619221

Upon vascular injury, tissue damage, ischemia, or microbial infection, intracellular material such as nucleic acids and histones is liberated and comes into contact with the vessel wall and circulating blood cells. Such "Danger-associated molecular patterns" (DAMPs) may thus have an enduring influence on the inflammatory defense process that involves leukocyte recruitment and wound healing reactions. While different species of extracellular RNA (exRNA), including microRNAs and long non-coding RNAs, have been implicated to influence inflammatory processes at different levels, recent *in vitro* and *in vivo* work has demonstrated a major impact of ribosomal exRNA as a prominent DAMP on various steps of leukocyte recruitment within the innate immune response. This includes the induction of vascular hyper-permeability and vasogenic edema by exRNA via the activation of the "vascular endothelial growth factor" (VEGF) receptor-2 system, as well as the recruitment of leukocytes to the inflamed endothelium, the M1-type polarization of inflammatory macrophages, or the role of exRNA as a pro-thrombotic cofactor to promote thrombosis. Beyond sterile inflammation, exRNA also augments the docking of bacteria to host cells and the subsequent microbial invasion. Moreover, upon vessel occlusion and ischemia, the shear stress-induced release of exRNA initiates arteriogenesis (i.e., formation of natural vessel bypasses) in a multistep process that resembles leukocyte recruitment. Although exRNA can be counteracted for by natural circulating RNase1, under the conditions mentioned, only the administration of exogenous, thermostable, non-toxic RNase1 provides an effective and safe therapeutic regimen for treating the damaging activities of exRNA. It remains to be investigated whether exRNA may also influence viral infections (including COVID-19), e.g., by supporting the interaction of host cells with viral particles and their subsequent invasion. In fact, as a consequence of the viral infection cycle, massive amounts of exRNA are liberated, which can provoke further tissue damage and enhance

virus dissemination. Whether the application of RNase1 in this scenario may help to limit the extent of viral infections like COVID-19 and impact on leukocyte recruitment and emigration steps in immune defense in order to limit the extent of associated cardiovascular diseases remains to be studied.

Keywords: extracellular nucleic acids, danger-associated molecular patterns, inflammatory vascular diseases, arteriogenesis, endothelial cells, virus infection, RNase1

BACKGROUND

DAMPs/Alarmins, PAMPs, and the Innate Immunity Response in Sterile Inflammation and Infection

Following cell stress, trauma, or exposure of the body to infectious or damaging factors, an immediate host response is mobilized by virtue of the innate immune system to recognize the external (pathogen-associated molecular patterns, PAMPs) or the body's own (danger-associated molecular patterns, DAMPs) agonists and to provoke the release of alarm molecules, which is followed by a spatiotemporal and localized inflammatory response, including the release of cytokines (Tisoncik et al., 2012). The subsequent recruitment and accumulation of circulating leukocytes (neutrophils and monocytes/macrophages in a sequential order) to the site of inflammation culminates in their phagocytic action to remove cell debris and microbes with the help of the complement system. Both, intracellular killing (following phagocytosis of pathogens) and extracellular killing, which is carried out by neutrophils and involves "neutrophil extracellular traps" (NETs, de-condensed extracellular chromatin, a DNA-histone network on which neutrophil-derived components are concentrated), are vital parts of the innate host defense (Castanheira and Kubes, 2019). This is followed by the resolution of inflammation, including the recruitment of stem and endothelial cells, in order to restore tissue homeostasis. When DAMPs are cleared, the pro-inflammatory status of recruited leukocytes is changed to a reparative program, also directed by natural killer T cells (Van Kaer et al., 2013). As a consequence, neutrophils exit the site of inflammation by reverse transmigration back into the bloodstream (Zindel and Kubes, 2020). The concomitant tissue repair and regeneration process is achieved by platelet-dependent hemostasis and the blood coagulation machinery, resulting in temporary wound sealing by aggregated platelets and the formation of a stable fibrin network, which also prevents further entry of microorganisms (Kolaczkowska and Kubes, 2013).

Within the initial phase of innate immunity related to sterile inflammation, mediated by, e.g., hypoxia, hyperthermia, or oxygen radicals, the disturbed tissue homeostasis and cell damage is accompanied by the liberation of DAMPs or alarmins from necrotic cells or from activated immune cells (**Figure 1**). The structurally diverse and unrelated multifunctional alarmins include cytosolic, mitochondrial, or nuclear proteins (such as heat-shock proteins, histones, amphoterin/"high mobility group B1," HMGB1 or neutrophilic calprotectin) as well as diverse self-nucleic acids (including nuclear DNA, ribosomal RNA, microRNAs) or heme and ATP. These DAMPs not only play an essential role inside cells prior to tissue injury but also serve multi-tasking functions (as "moonlighting factors") outside cells by the activation of innate immune and vascular cells, including the recruitment of leukocytes and the sensing of antigen-presenting cells engaged in host defense and tissue repair (Bianchi, 2007). Upon uncontrolled release or overexpression, alarmins also play a pathophysiological role in a wide range of sterile or infection-induced immune and inflammatory disorders (Ehrchen et al., 2009; Andersson and Tracey, 2011). Alarmins may also induce the adaptive arm of the immune response via direct or indirect activation of antigen-presenting cells, including dendritic cells, thereby providing a relevant link between the innate and adaptive parts of the immune response (Bianchi and Manfredi, 2007). Hence, the diverse functional repertoire of alarmins renders them intriguing therapeutic targets, both, to reduce unwanted hyper-inflammation as well as to uncouple the innate and adaptive immune responses in chronic pathologies, including autoimmune disorders (Chan et al., 2012). Finally, alarmins may serve as useful diagnostic and prognostic biomarkers in inflammatory disorders.

Pattern Recognition Receptors for PAMPs and DAMPs, Including Self-ExRNA

In situations arising from bacterial or viral infections, the host's primary line of microbial recognition and pathogen sensing is made up of pattern recognition receptors such as cell membrane or endosomal Toll-like receptors (TLRs), many of which have also a key role in the detection of endogenous alarmins through signaling events associated with the induction of anti-inflammatory genes (Gong et al., 2020). More than 10 different TLRs exist, which are able to bind diverse exogenous infectious ligands classified as PAMPs (including bacterial DNA, lipopolysaccharide, flagellin, peptidoglycans, or viral double-stranded RNA). Other TLRs like TLR13 (only expressed in mice) recognize a conserved 10-nucleotide sequence from bacterial 23S ribosomal RNA that trigger immune responses, whereas TLR8 senses specific motifs in bacterial and mitochondrial RNAs (Kruger et al., 2015; Wang et al., 2016).

The body's own alarmins, including nucleic acids originating from stressed or dying host cells, were found to induce pathological inflammatory responses by direct activation of specific TLRs to promote cellular signaling pathways: These involve either myeloid differentiation factor 88 (MyD88) or Toll- interleukin-1 receptor domain-containing adaptor-inducing interferon β (TRIF), both leading to the activation of

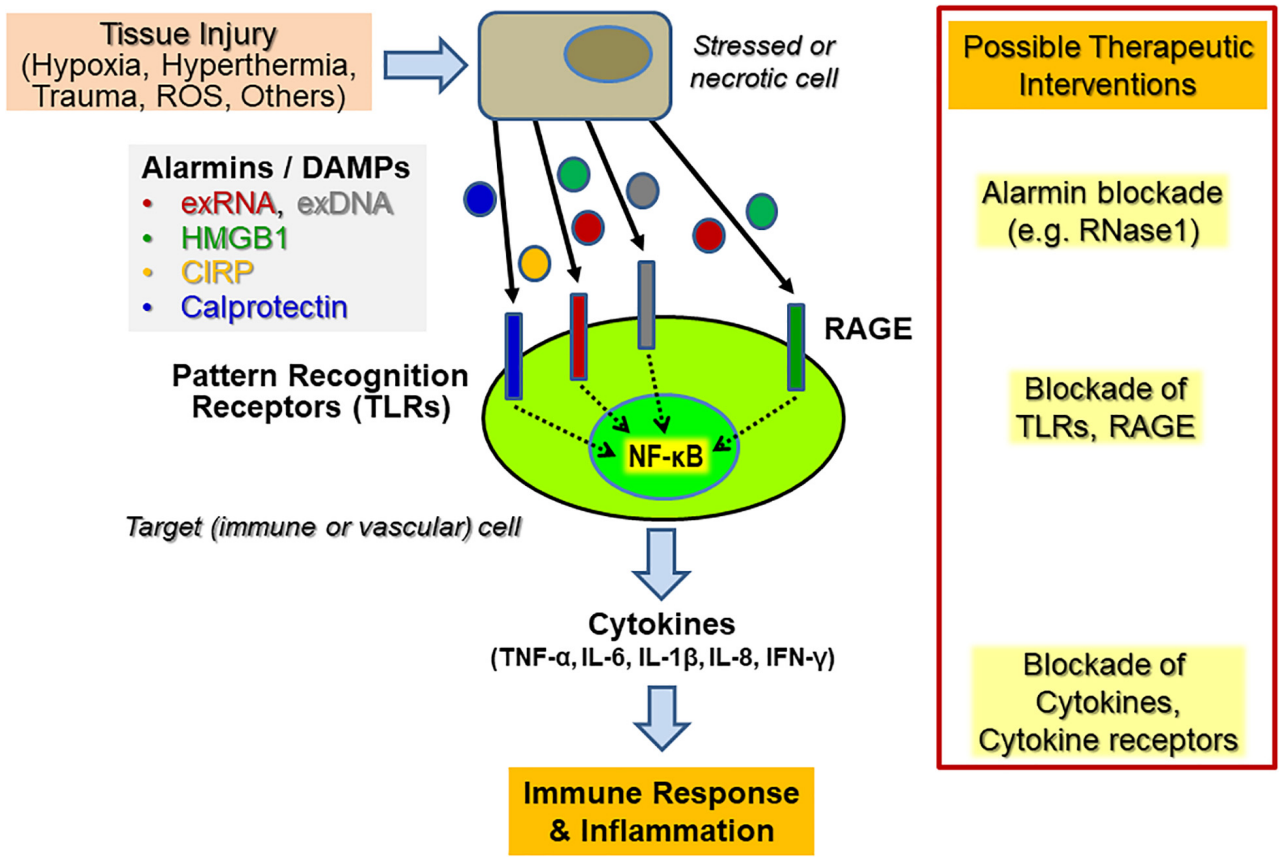

FIGURE 1 | Endogenous cytokine release induced by alarmins upon sterile inflammation and potential targets for therapeutic interventions. Upon diverse types of cellular stress and activation of tissue and immune cells, a variety of alarmins or DAMPs ("Danger-associated molecular patterns") such as HMGB1, extracellular RNA and DNA (exRNA, exDNA), CIRP ("Cold-inducible RNA-binding protein") or calprotectin, are liberated and become recognized by various "Pattern recognition receptors" (PRRs), including Toll-like receptors (TLRs) and the "Receptor of advanced glycation end-products" (RAGE). Their subsequent signal transduction culminates in the promotion of, e.g., NF-κB activation in vascular cells and leukocytes (predominantly neutrophils and monocytes/macrophages) to trigger an enhanced cytokine release within the innate immune response, resulting in subsequent inflammatory reactions. Potential therapeutic targets for immunomodulation in both acute and chronic inflammatory diseases are alarmins, PRRs, and the induced downstream cytokines or cytokine receptors. Direct targeting can be achieved by inhibitory antibodies, by competitive inhibitors, by targeting the PRRs with antibodies or soluble decoy receptors. In the case of exRNA, RNase1 has been successfully used in preclinical animal models to prevent or inhibit the respective adverse outcome of inflammatory reactions.

transcription factors such as c-Jun N-terminal kinase or nuclear factor (NF)-κB. As a consequence, cytokines including tumor necrosis factor (TNF)-α, interleukin (IL)-1β or IL-6 will be released (Barrat et al., 2005; Yu et al., 2010; Leifer and Medvedev, 2016). The adaptor molecule MyD88 is involved in all signaling pathways activated by TLRs except for endosomal TLR3, which recognizes (viral) double-stranded RNA, single-stranded RNA, and also self-RNA fragments that mediate cellular activation through TRIF (Yamamoto et al., 2003). TLR10 was shown to play a role as an RNA-sensing receptor by binding to double-stranded RNA and regulating interferon-dependent responses (Lee et al., 2018). In another example, myocardial infarction was found to be attenuated in TLR3-deficient mice as a result of the activation of the TLR3-TRIF pathway by extracellular RNA (exRNA) released from damaged tissue, although the authors did not define the source and identity of the RNA (Chen et al., 2014). Alternatively, self-exRNA (mainly consisting of ribosomal RNAs) can induce pro-inflammatory activities to a large extent by TLR-independent mechanisms, which are poorly defined thus far (Preissner and Herwald, 2017) (see below). Finally, while microRNAs (miRNAs) can also serve as ligands of TLRs, the therapeutic administration of structurally similar short-interfering RNAs (siRNAs) may lead to undesirable activation of particular TLRs, such as the induction of inflammatory responses via TLR3 (Li and Shi, 2013; Pirher et al., 2017).

Moreover, the same TLR-dependent recognition machinery, either on the cell surface or on intracellular endosomes of host immune cells, appears to be responsible for recognizing endogenous alarmins together with exogenous factors in order to foster and maintain inflammatory reactions and to initiate their eventual resolution. However, it is not surprising that DAMPs and PAMPs may exhibit functional overlaps, influence each other, or even synergize in their functional activities, eventually provoking severe inflammatory disorders or chronic

inflammation. In any event, the recognition of PAMPs by the host's immune system is followed by the recruitment of leukocytes to the site of inflammation or infection with the release of diverse cytokines and the engagement of their phagocytic activities, culminating in the catching and killing of microbial invaders by neutrophilic granulocytes and macrophages. At this stage, NETs provide a functional scaffold in immune defense that drives (micro-)thrombosis as a principal mechanism of inflammation-hemostasis crosstalk (also designated "immuno-thrombosis") that ultimately prevents the dissemination of microbes (Engelmann and Massberg, 2013). Following neutrophil apoptosis and the subsequent clearance of dying cells by macrophages (known as "efferocytosis"), the final resolution stage of these cells under physiological conditions is characterized by an anti-inflammatory cytokine signature (Kourtzelis et al., 2020).

Scope

The aim of this review article is to provide an overview of the current state of the (patho-) physiological functions, particularly of ribosomal exRNAs as DAMP and alarmin, with special emphasis on their role in leukocyte recruitment as a central process in the innate immune response. Despite the fact that other extracellular RNA-species such as microRNAs and long non-coding RNAs do play an important role in inflammation and cardiovascular diseases as well (Weber et al., 2010; Heward and Lindsay, 2014), they would not be considered as DAMPs in the narrow sense and will not be dealt with here. Thus, ribosomal exRNAs with their multi-faceted roles as damaging factors in inflammation-driven diseases appear to be potential and challenging targets for therapeutic interventions using various approaches to antagonize exRNA-mediated pathophysiological actions (Sullenger and Nair, 2016; Bedenbender and Schmeck, 2020).

THE MULTI-STEP PROCESS OF LEUKOCYTE RECRUITMENT TO THE SITE OF INFLAMMATION

As part of the innate immune response, leukocyte recruitment is crucial in the pathways mediating sterile inflammation, infection, inflammatory disorders such as atherosclerosis, and autoimmune diseases like psoriasis, rheumatoid arthritis, vasculitis, or chronic lung diseases that involve a number of balanced cell-adhesive interactions between mobile blood cells and the activated endothelium (Muller, 2013; Kourtzelis et al., 2017). All of these pathophysiological situations are characterized by multiple forms of acute or chronic stress of cells and tissues, resulting in the appearance of a variety of DAMPs. A substantial increase in the levels of ribosomal exRNAs was observed in the circulation of patients (and preclinical animal models), and exRNAs were found concentrated at exposed sites in the vessel wall such as in atherosclerotic plaques (Simsekyilmaz et al., 2014; Zernecke and Preissner, 2016; Stieger et al., 2017). In any event, under the regimen of the innate immune system, leukocyte extravasation directs neutrophils within hours and macrophages within a few days to the extravascular site of inflammation or infection, comprising several cell-adhesive steps. A prerequisite for the leukocyte transmigration cascade, prior to the described cell–cell interactions, is the breakdown of the vessel wall permeability barrier by vasoactive mediators such as histamine that are generated via activation of perivascular mast cells and the complement system (Petri and Sanz, 2018). This allows the extravasation of blood solute and proteins near the site of inflammation before leukocytes initiate their rolling and extravasation process (**Figure 2**).

Initial Selectin-Dependent Rolling of Leukocytes at the "Inflamed" Apical Side of the Vascular Endothelium

The motility of leukocytes in the bloodstream is slowed down near a locus of inflammation by their selectin-mediated rolling along the vessel wall in order to prepare these mobile cells for their transmigration toward the site of inflammation. Rolling interactions last seconds and are transient and reversible under conditions of blood flow due to the weak binding of P- and E-selectin to their common ligand, S-Lewis-x antigen. This is an oligosaccharide present in glycolipids and various glycoproteins on the surface of all mobile and stationary vascular cells. The expression of P- and E-selectins on the apical side of activated endothelial cells is a tightly regulated process that depends on the inflammatory conditions: Upon activation of the endothelium by various stimuli, including exRNA, P-selectin is immediately translocated from its storage site, the Weibel–Palade granules that serve as a vascular "emergency kit" (which also harbor IL-8, von Willebrand factor, tissue plasminogen activator, and RNase1), to the luminal endothelial cell surface (Fischer et al., 2011; Schillemans et al., 2019). This process allows the normally non-sticky and non-thrombogenic vessel wall surface to capture the patrolling leukocytes out of the bloodstream, providing a cell-to-cell approximation that is necessary for the subsequent leukocyte activation step mediated by chemokines. If the inflammatory stimulation of the endothelium continues for a longer period of time, E-selectin is expressed *de novo* on the apical side of the endothelium as well to augment leukocyte rolling.

Chemokine-Induced Leukocyte Activation and Integrin-Mediated Firm Adhesion of Immune Cells

In addition to functioning as a kind of brake, rolling interactions along the vessel wall allow neutrophils to sense chemokines (such as IL-8, which is released during the initial exocytosis from endothelial Weibel–Palade granules) that are tightly associated with the apical endothelial glycocalyx by ionic interactions via heparan sulfate proteoglycans. Other chemo-attractants (including complement anaphylatoxin C5a, leukotriene LTB4, platelet activating factor, or bacteria-derived formylated peptides) derived from activated mast cells and tissue macrophages, and vasoactive agents such as histamine, released in the very early phase of the innate immune response, help to induce rapid neutrophil adhesion. This is achieved by converting the low-affinity, selectin-mediated interaction into a high-affinity,

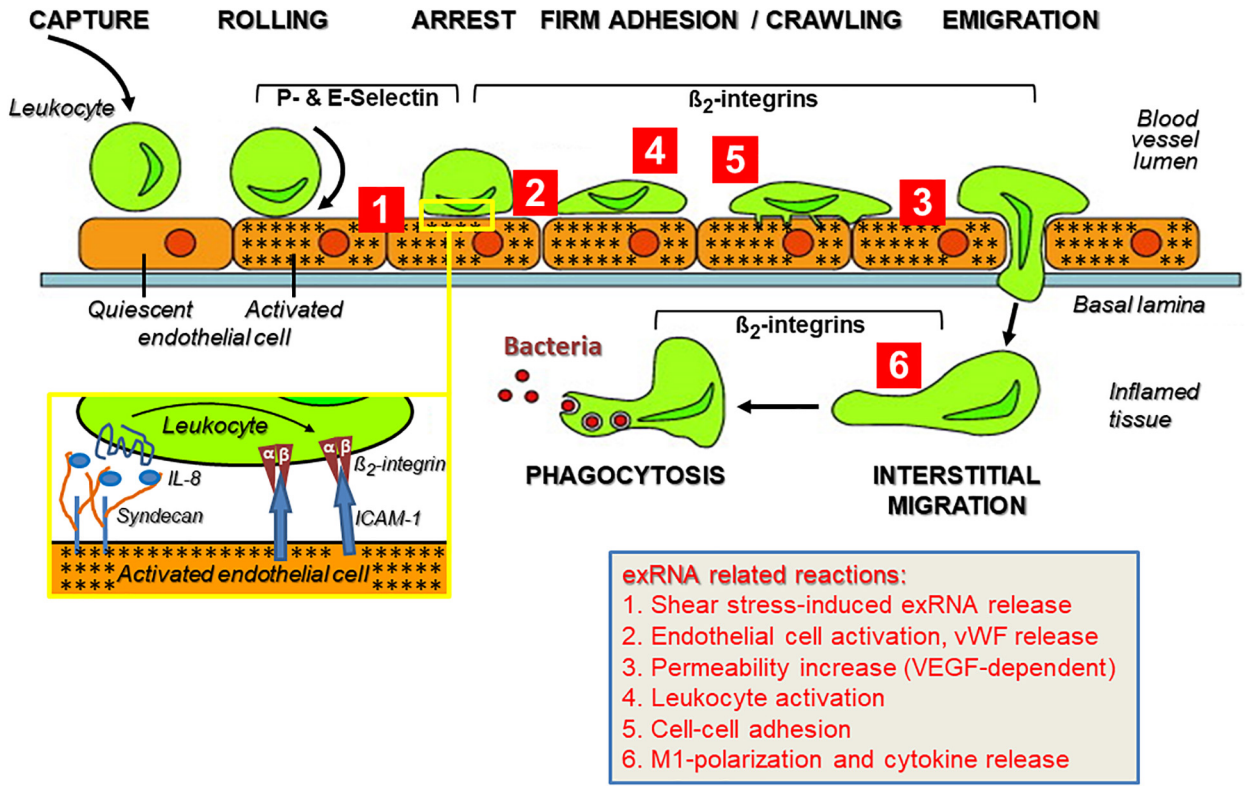

FIGURE 2 | The multi-step recruitment of leukocytes to the source of inflammation and the influence of exRNA at multiple sites during this process. In an inflammatory situation, either initiated by microbial agonists or in their absence (sterile inflammation), leukocytes in the blood stream approach the inflamed vessel wall to find the shortest way toward the source of inflammation/infection in the tissue. Following their capture on the vessel wall, leukocytes start rolling on the inflamed endothelium (indicated by stars) due to blood stream-mediated mechanical forces together with weak adhesive interactions between leukocytes and endothelial P- and E-selectins. Based on the close approximation of both cell types, heparan sulfate proteoglycan (syndecan)-fixed chemokines (such as Interleukin-8) can reach and activate their leukocytic receptors (inset) as well as induce "inside-out" activation of β2-integrins with the result that the tethered leukocytes become firmly attached to the vessel wall via ICAM-1 and start crawling toward the nearest point of emigration. The transmigration phase along a chemotactic gradient is also supported by β2-integrins, as is the subsequent recognition of complement-activated bacteria by leukocytes for the ultimate phagocytosis reaction within the inflamed tissue. This route of consecutive steps of immune cell recruitment is taken by neutrophils (within hours) and monocytes/macrophages (within a few days) to execute a proper immune response. Modified from Schymeinsky et al. (2011). Ribosomal extracellular RNA (exRNA) is capable of influencing cellular interactions at multiple sites during leukocyte recruitment (indicated by red numbers): (Tisoncik et al., 2012; Castanheira and Kubes, 2019). Fluid shear stress in the circulation can mediate liberation of exRNA from endothelial cells, and exRNA induces vascular permeability in a VEGF-receptor-2/neuropilin-1-dependent fashion as well as the release of components stored in Weibel–Palade granules. (Van Kaer et al., 2013) exRNA induces activation of leukocytes to acquire an adhesive phenotype and to release cytokines that further promote immune cell activation (Kolaczkowska and Kubes, 2013; Zindel and Kubes, 2020). As a consequence, exRNA-primed leukocytes are further promoted to firmly attach to the inflamed endothelium as a prerequisite for their transmigration. (Bianchi, 2007) exRNA can induce M1-polarization of monocytes/macrophages and thereby provoke a significant pro-inflammatory cytokine release by these cells. The details on exRNA-cell interactions in this context are outlined in the text.

integrin-dependent firm arrest (Ley et al., 2007). The firm adherence of leukocytes to endothelial cells adjacent to the locus of inflammation is mediated by leukocyte integrins such as VLA-4 (α4β1), α4β7-integrin, Mac-1 (αMβ2), and LFA-1 (αLβ2) and their endothelial counter-receptors of the immunoglobulin superfamily, including intercellular adhesion molecules (ICAMs) as well as vascular cell adhesion molecule-1 (VCAM-1), all of which had been upregulated on the inflamed endothelium prior to leukocyte adherence (Yonekawa and Harlan, 2005). In this regard, exRNA serves as one of the endothelial cell-activating agonists to promote integrin- rather than selectin-dependent leukocyte adhesion, as observed in the cremaster vascular inflammation model (Fischer et al., 2012). While VCAM-1 interacts with leukocytic VLA-4, both ICAM-1 and ICAM-2 predominantly bind to β2-integrins (including LFA-1 and Mac-1) on leukocytes.

Chemokine-induced leukocyte adherence is primarily regulated via conformational changes and clustering of the indicated integrins through "inside-out" signaling, particularly involving several GTPase-dependent pathways (Rot and von Andrian, 2004; Wittchen et al., 2005). Integrin-mediated adhesion is relevant for neutrophil extravasation and the immune response as demonstrated by studies that utilized either mice that were deficient in one or more leukocyte integrin or patients with "Leukocyte Adhesion Deficiency" (LAD I) syndrome who lack functional β2-integrins (Springer et al., 1984; Ding et al.,

1999; Yonekawa and Harlan, 2005). Neutrophil adhesion to the inflamed endothelium is reinforced by integrin-mediated "outside-in" signaling as a result of receptor clustering and conformational changes due to integrin ligation by multivalent adhesive protein ligands such as fibronectin or collagens. In addition to ICAMs on the activated endothelium, the DAMP binding protein "Receptor for advanced glycation end-products" (RAGE) has been identified as a receptor particularly for leukocytic Mac-1 under strong inflammatory conditions as in diabetes. Thus, in a preclinical model of inflammation, only the inhibition of both ICAM-1 and RAGE resulted in the total blockade of leukocyte arrest and transmigration (Chavakis et al., 2003). Finally, alternative integrin activation signals appear to be operative as well in the fine-tuning during the early arrest phase of neutrophils (but not monocytes), since both zinc ions as well as the glycolipid-anchored urokinase receptor were shown to provide an essential contribution to integrin activation, as demonstrated in preclinical animal models (May et al., 1998; Chavakis et al., 1999).

Trans-Endothelial Migration of Leukocytes

After their firm adhesion, leukocytes crawl over the endothelial cell surface, involving their integrins Mac-1 and LFA-1 until they reach the nearest junction appropriate for transmigration (Schenkel et al., 2004). Trans-endothelial migration (also designated "diapedesis") primarily takes place at the intercellular junctions in a para-cellular manner, whereby tricellular junctions as well as endothelial junctions positioned above thin-layer basement membranes have been proposed as preferential sites for transmigrating neutrophils *in vivo* (Burns et al., 1997; Wang et al., 2006). Alternatively, a minority of neutrophils and other leukocytes (about 5–10%) may enter the extravascular tissue via a transcellular route, i.e., through the endothelial cells, particularly when intravascular locomotion is disabled *in vivo* (Shaw et al., 2004; Nourshargh and Marelli-Berg, 2005; Phillipson et al., 2006). In essence, the preferred routing of emigrating leukocytes may depend on the level of the pro-inflammatory stimuli as well as the type of blood vessel (wall). In addition to their importance in leukocyte-endothelial adherence, ICAM-1 and ICAM-2 also participate in leukocyte trans-endothelial migration (Shang and Issekutz, 1998).

The subsequent sub-endothelial interstitial migration of leukocytes into the inflamed tissue is predominantly mediated by β1-integrin family members as well as by the β2-integrin Mac-1 that also binds to fibrin(ogen) in the wound matrix. This process is facilitated by leukocyte-associated or secreted proteases as well as by glycosaminoglycan-degrading enzymes, which help the neutrophils and macrophages to invade the extracellular matrix (Stamenkovic, 2003). After leukocytes have terminated their emigration, leaks in the vessel wall are prevented by contractile actin filaments surrounding the diapedesis pore, keeping this opening tightly closed around the transmigrating neutrophils, and platelets interacting with endothelial von Willebrand factor activate endothelial Tie-2 receptors to secrete angiopoietin-1, thereby preventing diapedesis-induced leakiness (Duong and Vestweber, 2020). Finally, leukocytes migrate along the sub-endothelial side, traverse the basement membrane, and invade the inflamed tissue toward the gradient of chemotactic activity (e.g., activated mast cells, complement-related anaphylatoxins), where they start their program of defensive actions as phagocytic cells to remove invading microbes and cell debris (Underhill et al., 2016; Voisin and Nourshargh, 2019). Although exRNAs bind to heparin-binding growth factors such as "Vascular endothelial growth factor" VEGF (Fischer et al., 2007), it remains to be demonstrated whether the extracellular matrix-bound ribonucleic acids could serve as a guidance cue for migrating phagocytes toward their destiny.

Contribution of Cell Adhesion Receptors to Leukocyte Diapedesis

Along the para-cellular diapedesis pathway, endothelial junctions are the major barriers for transmigrating leukocytes, whereby several types of junctions are involved (Bazzoni and Dejana, 2001): (i) Adherence junctions (*zonula adherens*) that mediate cell–cell contacts via homophilic, calcium-dependent binding between adjacent VE-cadherin molecules; (ii) the most apical tight junctions (*zonula occludens*), which form a close intercellular adhesive web that consists of three types of transmembrane proteins; and (iii) junctional adhesion molecules (JAMs), which are linked intracellularly to cytoskeletal signaling proteins such as zonula occludens-1 and which can form cell–cell contacts by homophilic interactions and can act as receptors for leukocyte integrins (Weber et al., 2007). As demonstrated *in vitro* by cell culture experiments as well as *in vivo* (brain edema), exRNA can disturb the integrity of the vessel wall by disconnecting cell–cell junctions in an irreversible fashion, as compared to thrombin which acts in a temporary manner as a permeability-increasing factor (Fischer et al., 2007, 2014).

A well-known adhesive component in leukocyte transmigration is platelet endothelial cell adhesion molecule-1 (PECAM-1), which is expressed both on platelets and leukocytes as well as at the inter-endothelial cell junctions. Like JAMs, it can interact in a homophilic as well as a heterophilic fashion to regulate leukocyte trans-endothelial migration (Sullivan and Muller, 2014). Here, PECAM-1 may recycle in vesicular structures between the junctions and the sub-junctional plasma-lemma and is thereby targeted to the sites of the vessel wall where leukocyte transmigration takes place. Altogether, the variable interactions of these transmembrane adhesion molecules, whose expression pattern differs at the leading and the trailing edges of each emigrating leukocyte as well as within the endothelial cell clefts, guide the transmigrating cells within minutes from the luminal to the basolateral side; however, their precise molecular coordination still remains a mystery (Vestweber, 2015; Duong and Vestweber, 2020).

ExRNAs AS UBIQUITOUS DAMPs AND PRO-INFLAMMATORY FACTORS

More than 50 years ago, extracellular nucleic acids were identified in blood plasma and in extracellular body fluids as well as

in cell supernatants, and their appearance was found to be associated with some disease states (Mandel and Metais, 1948). For example, RNA-proteolipid complexes and also free exRNA were initially identified in cancer patients and were proposed to mediate host-tumor interactions (Wieczorek et al., 1985; Kopreski et al., 1999, 2001). Basic research as well as clinical studies have provided experimental evidences that the body's own extracellular nucleic acids are important players in the crosstalk between immunity and cardiovascular pathologies or other diseases. Following stress- or injury-induced liberation, these endogenous polyanionic macromolecules not only serve as alarmins/DAMPs or biomarkers of, e.g., cell necrosis, rather, their functional repertoire reaches far beyond their activities in innate immunity. In fact, (patho-) physiological functions of exRNAs and of extracellular DNA (exDNA) as well are associated with and in many cases causally related to, e.g., arterial and venous thrombosis, atherosclerosis, ischemia/reperfusion injury, or tumor progression, especially in association with the elevated inflammatory status of these diseases (Fischer et al., 2007, 2012, 2013; Kannemeier et al., 2007; Simsekyilmaz et al., 2014; Cabrera-Fuentes et al., 2015b). However, many of the underlying molecular mechanisms are far from being completely understood. Interestingly enough, novel *in vitro* and *in vivo* approaches, including natural endonucleases or synthetic nucleic acid binding/neutralizing polymers as antagonists, seem to be promising and safe therapeutic options for future investigations to combat the damaging nature of exRNA or exDNA (Preissner and Herwald, 2017; Naqvi et al., 2018; Thålin et al., 2019).

In the context of innate immunity, both in sterile inflammation as well as with regard to infectious conditions, exRNAs constitute typical DAMPs, which are released during tissue damage by either active or passive processes (Vénéreau et al., 2015) or following bacterial and viral infections (Chen et al., 2017; Kawasaki and Kawai, 2019). Depending on their size, composition, and complexity, exRNAs are involved in the typical recognition by membrane-bound PRRs as outlined above, including TLRs or RAGE (Bertheloot et al., 2016), as well as cytosolic receptors including retinoic acid-inducible gene I, melanoma differentiation-associated protein 5, or cyclic GMP-AMP synthase (Roers et al., 2016). Binding of exRNAs by such PRRs leads to the induction of different signaling pathways that result in the activation of transcription factors like c-Jun-N-terminal kinase or NF-κB and the subsequent release of cytokines including TNF-α, IL-1β, or IL-6 (Yu et al., 2010; Leifer and Medvedev, 2016). Ribosomal-type exRNAs (which constitute the majority of exRNAs in plasma) (Cabrera-Fuentes et al., 2015b) are different from other nucleic acid DAMPs, in that they fulfill a number of additional extracellular functions independent of recognition by PRRs, particularly related to the onset and progression of different cardiovascular diseases as will be outlined below.

Types of ExRNAs and Their Characteristics

Extracellular RNAs are a heterogenous group of ribonucleic acids, including small RNAs (e.g., miRNAs), mRNAs, tRNAs, ribosomal RNAs, and long non-coding as well as circular RNAs, each of which has different (extracellular) functions and a different impact on the respective cells and tissues in their microenvironment, either alone or together with other molecules. ExRNAs can be liberated from cells in a free form or bound to proteins or phospholipids as well as in association with extracellular vesicles (EVs) or apoptotic bodies (Valadi et al., 2007; Zernecke et al., 2009; Arroyo et al., 2011; Vickers et al., 2011; Creemers et al., 2012). Some mechanisms of exRNA biogenesis and its vesicular loading have been described elsewhere (Patton et al., 2015; Abels and Breakefield, 2016; Pérez-Boza et al., 2018). Analyses of EV-associated exRNAs indicated that miRNAs together with ribosomal RNAs form the majority of this fraction; yet, on a weight basis, ribosomal RNAs are the far most abundant type of exRNA in human blood plasma (Crescitelli et al., 2013; Danielson et al., 2017). The association of exRNA with various proteins or with ribonucleoprotein complexes as well as the binding to high-density lipoproteins not only provides protection of exRNAs from degradation by extracellular RNases, but these interactions may modulate the reactivity and immunogenicity of the respective binding partners (Wieczorek et al., 1985; Fischer and Preissner, 2013; Jaax et al., 2013). While only low levels of circulating exRNA can be detected in extracellular fluids under quiescent conditions *in vivo* and *in vitro* (<100 ng/ml), under conditions of cell activation or tissue injury such as hypoxia, infection, inflammation, or tumor growth the concentration of self-exRNAs can increase dramatically (Rykova et al., 2012; Zhou et al., 2019).

The majority of self-exRNAs (including microRNAs and ribosomal RNAs) is released in association with EVs by a wide range of cells under shear stress or following different types of stimulation by endogenous or exogenous inflammatory and other agonists (Lasch et al., 2019; O'Brien et al., 2020). EVs are divided into three subclasses depending on their site of origin inside the cells they are derived from: apoptotic bodies (large EVs: 800–5000 nm) are released from cells undergoing apoptosis; micro-vesicles (medium-sized EVs: 100–1000 nm) are released by budding from the plasma membrane; exosomes (small EVs: 30–150 nm) originate from the internal surface of multi-vesicular bodies in the endosomal compartment of cells (Kim et al., 2017). In particular, these nano-sized bodies provide intercellular communication functions by delivering intracellular material (such as miRNAs and mRNAs) to target cells and fulfilling regulatory functions by altering cell activities (Dinger et al., 2008; Ekström et al., 2012). These aspects are of particular relevance for exosome-delivered miRNAs, whose main intracellular functions are to regulate gene expression and translational processes in target cells, including those related to pathological processes in cancer, cardiovascular diseases, or autoimmune disorders (Kim et al., 2017). In contrast, ribosomal exRNAs, which constitute the majority of exRNA, are believed to fulfill a variety of functions outside of cells that will be discussed in more detail.

Upon microbial infection, with the appearance of viral or bacterial nucleic acids, several mechanisms exist to prevent a (counterproductive) activation of PRRs by self-nucleic acids. Generally, endosomal TLRs respond to double- or single-stranded viral or bacterial RNAs and DNAs, whereas cell-surface

TLRs recognize a variety of other accessible microbial patterns. Viruses and bacteria typically enter the cells via endocytosis or phagocytosis, whereby their DNAs or RNAs are protected from degradation, e.g., by capsid proteins, until they are released within the endo-lysosomal compartment of host cells to trigger TLR-dependent signaling pathways. In contrast, self-extracellular nucleic acids are degraded by extracellular nucleases unless they are protected in association with nucleoprotein complexes or cell membranes (Marek and Kagan, 2011). Thus, under physiological conditions, self-nucleic acid-related signaling may be limited by nuclease activities, thus preventing their detection by nucleic acid sensors.

Analysis of Self-ExRNAs

Since exRNA-containing EVs are found in most body fluids, their potential use as biomarkers for particular disease conditions has been explored, and the "National Institutes of Health" and other institutions[1] are evaluating the use of exRNAs, in particular miRNAs, as biomarkers for various human pathologies (Quinn et al., 2015; Das et al., 2019). The easy access and stability of EV-miRNAs in biological fluids makes them potentially suitable for use as diagnostic biomarkers, and in patients, different miRNA profiles implicate their participation in disease pathogenesis (Bellingham et al., 2012; Gui et al., 2015; Lugli et al., 2015). For example, the nature of a particular exRNA species contained in EVs can be assessed by RTqPCR (Bellingham et al., 2012; Gui et al., 2015; Lugli et al., 2015). The composition of exRNA is further analyzed by capillary electrophoresis and RNA sequencing (Tanriverdi et al., 2016; Yuan et al., 2016; Saugstad et al., 2017). Other methods, either qualitative/semi-quantitative or quantitative, depending on the respective reagent, utilize the specific reaction of fluorescent dyes with exRNA (Jones et al., 1998; Wu et al., 2020). Furthermore, methods currently available to isolate exRNA in biofluids have been compared and described previously, including the characteristics of exRNA-loaded EVs. They can be monitored by intra-vital microscopy and immunohistochemistry, provided EVs are fluorescently labeled via expression of palmitoylated green-fluorescent protein in donor cells (van der Vos et al., 2016; Small et al., 2018). Yet, the heterogeneity of exRNAs together with their presence in different cellular fractions require further modes of analyses and interpretations. In particular, the association of exRNA with multiple subtypes of EVs as well as with ribonucleoproteins and lipoprotein complexes or the formation of soluble vesicle-free supramolecular complexes with proteins, which are RNase-resistant, may complicate the analysis of exRNA (Tosar and Cayota, 2018; Das et al., 2019).

ExRNA AND LEUKOCYTE RECRUITMENT IN THE CONTEXT OF INNATE IMMUNITY

Although several subtypes of exRNA, including miRNA, long non-coding RNA, and ribosomal exRNA, have been described in the context of inflammatory cell signaling, the following paragraphs will focus on exRNAs, mostly consisting of ribosomal RNA, as a direct/indirect DAMP in inflammatory situations that influences the different steps of leukocyte recruitment. This includes the role of exRNA as (i) an ubiquitous alarmin, (ii) a cofactor for bacteria-host cell interaction and microbial invasion, (iii) a hyper-permeability factor that induces vasogenic edema, (iv) a promoter of leukocyte interaction with the inflamed endothelium, (v) an inducer of cytokine release from macrophages, (vi) an important mediator of arteriogenesis, and (vii) a potent pro-thrombotic cofactor.

ExRNA as an Alarmin and DAMP and Recognition of Self- and Non-self-ExRNAs

To minimize the recognition of self-nucleic acids, the binding of non-self nucleic acid ligands to the signaling receptors (particularly belonging to the TLR family) will induce their sequestration away from the cell surface in the cytoplasm or in endosomes. Thus, isolated ribosomal exRNA appears not to be recognized by TLRs expressed on the cell surface in a classical way, unless prior modification or complexation of the ligand takes place. When self-nucleic acids are highly abundant, e.g., as a result of cell damage, defects in the degradation or processing machinery of nucleic acids, or in the binding and cellular uptake into endosomes, self-nucleic acids may activate endosomal PRRs (Bertheloot et al., 2016; Roers et al., 2016; Miyake et al., 2017). Self-exRNA may also reach endo-lysosomes and PRRs if bound to proteins or manipulated by transfection agents (**Figure 3**).

Autoimmune diseases like psoriasis serve as an example of how self-exRNA may play a role in immune responses. Complexes of self-exRNA and the antimicrobial peptide LL37 were shown to be recognized mainly by TLR7 and TLR8 to promote an autoimmune response (Zakrzewicz et al., 2016). LL37 constitutes the C-terminal portion of human cathelicidin from which LL37 is proteolytically released during immune cell activation. It serves as basic immune-modulatory peptide, and by forming complexes with polyanionic exRNA and exDNA it prevents their degradation. Together with exRNA derived from necrotic cells, LL37 activates "mitochondrial antiviral-signaling protein" and induces production of, e.g., interferon (IFN)-β to provoke maturation of dendritic cells (Zhang et al., 2016). Moreover, the exRNA-LL37 complex is capable of activating TLR7-expressing dendritic cells, thereby triggering the secretion of IFN-α, but not IL-6 or TNF-α. Also, exRNA-LL37 complex-mediated activation of TLR8 can lead to differentiation of myeloid dendritic cells and the release of IL-6 and TNF-α. Thus, the cationic antimicrobial peptide LL37 may convert self-exRNA into a trigger of TLR7/TLR8 in human dendritic cells in psoriatic lesions, allowing the initiation and progression of this autoimmune response (Ganguly et al., 2009). Interestingly enough, this complex was also found to trigger the TLR8/TLR13-mediated release of cytokines and NETs together with exRNA in neutrophils, thereby establishing a self-propagating vicious cycle that contributes to chronic inflammation in psoriasis (Herster et al., 2020).

[1] http:/exRNA.org/

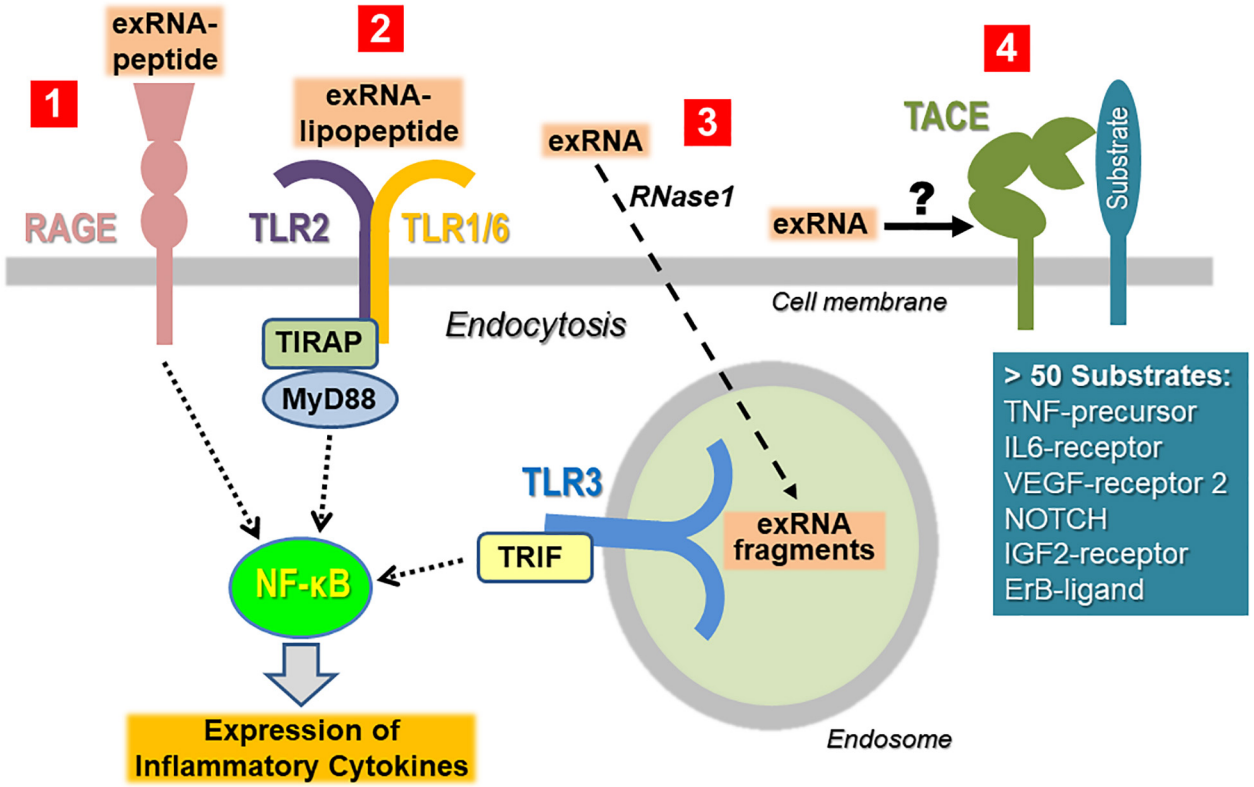

FIGURE 3 | Cellular recognition of exRNA by various unrelated cell surface proteins/receptors. Once the concentration of exRNA has reached a certain level upon cell necrosis or other stress situations, the ribonucleic acid can induce activation of immune and tissue cells either in isolated, in complexed form as indicated, or in association with extracellular vesicles. To simplify the illustration, the latter case has not been depicted (Tisoncik et al., 2012). ExRNA-polypeptide complexes are recognized by RAGE, which also serves as receptor site for other DAMPs and PAMPs (Castanheira and Kubes, 2019). Likewise, in complex with certain PAMPs such as lipopeptides, exRNA can be recognized in a synergistic way in a TLR2-dependent fashion and thereby augments the immune cell activation of the PAMP (Van Kaer et al., 2013). Macromolecular exRNA, which can be degraded by extracellular RNase1, can be taken up by cells and promotes cellular activation via endosomal TLR3 under certain conditions. All of these pathways culminate in activation of NF-κB-dependent signaling, ultimately leading to the expression and liberation of cytokines, often in excess to provoke hyper-inflammation (Zindel and Kubes, 2020). ExRNA can potentially trigger the activation of the sheddase "TNF-α converting enzyme" (TACE) to induce the proteolytic cleavage of cell surface-bound protein substrates such as the precursor form of TNF-α in order to release the active cytokine. Since TACE can act as a sheddase for a number of cell-bound substrates, it is proposed that exRNA can trigger this protease to generate a variety of (inflammatory) products at multiple sites in the body.

There are other examples of the participation of self-and non-self-exRNA in immune responses. TLR7 (or TLR3), the classical receptors for small non-self-viral RNAs, appear not to be activated by exRNA alone in macrophage cell cultures, whereas a synergistic effect of exRNA together with the lipopeptide Pam2CSK4 on TLR2 activation was found, resulting in the synergistically elevated expression of cytokines in macrophages (Noll et al., 2017). Thus, certain isolated PAMPs are unable to mount a robust inflammatory response on their own unless self-exRNA (derived from trauma or necrosis) acts as a potent adjuvant. Moreover, in myocardial ischemia, cell-free exRNA has been proposed to promote apoptosis of cardiac muscle cells by activation of TLR3-TRIF signaling pathways (Chen et al., 2014). In this study, however, the nature of self-exRNA was not further defined, making it difficult to relate these results to our knowledge about self-exRNA-mediated pathways and their role in disease.

For endosomal TLRs in immune cells to be available for binding to non-self exRNAs upon infection and immune signaling, the access of self-nucleic acids from the extracellular environment to these TLRs needs to be limited. Here, cell-membrane expressed RAGE as a primary recognition site for glycated proteins fulfills functions as DAMP-receptor, for e.g., HMGB1, but has also been identified to promote the uptake of both exDNA and exRNA into endosomes. This may lower the immune recognition threshold for the activation of TLR9, the principal DNA-recognizing signaling receptor. Moreover, RAGE is important for the detection of nucleic acids *in vivo*, since mice deficient in RAGE were unable to mount an inflammatory response to exDNA in the lung (Sirois et al., 2013). In addition, RAGE was shown to bind self-exRNA in a sequence-independent manner to enhance cellular uptake of exRNA into endosomes. Gain- and loss-of-function studies demonstrated that RAGE increased the sensitivity of all single-stranded RNA-sensing TLRs (TLR7, TLR8, TLR13), indicating that RAGE appears to be an integral part of the endosomal nucleic acid-sensing system (Sirois et al., 2013).

ExRNA Interactions With Microbes During the Process of Infection

The adherence to and invasion of eukaryotic cells and tissues by pathogenic bacteria are the main mechanisms for microbial colonization, evasion of immune defenses, survival and propagation, and the cause for infectious diseases in their mammalian hosts. Several structurally and functionally distinct "adhesins" of bacteria facilitate their specific recognition and their interactions with host cell surfaces (e.g., by integrins) and the extracellular matrix (e.g., by fibronectin or vitronectin) (Hammerschmidt et al., 2019). In tissue fluids, the binding of microbial components to (adhesive) host proteins may alter their structure or can influence cellular mechanisms that determine cell and tissue invasion of pathogens (Hammerschmidt, 2009; Hammerschmidt et al., 2019). In addition to host plasma proteins such as plasminogen or vitronectin which serve as essential virulence factors for the invasion of several Gram-positive bacteria, self-exRNA in a dose-dependent manner was found to increase the binding and uptake of *Streptococcus pneumoniae* in alveolar epithelial cells (Bergmann et al., 2009; Zakrzewicz et al., 2016). Extracellular enolase, a plasminogen receptor, was identified as an exRNA-binding protein on the *S. pneumoniae* surface, with several basic amino acid residues serving as exRNA-binding sites. Moreover, additional exRNA-binding proteins were identified in the pneumococcal cell wall using mass spectrometry. Due to the high number of such RNA-interacting proteins on pneumococci, treatment with RNase1 successfully inhibited exRNA-mediated pneumococcal alveolar epithelial cell infection (Zakrzewicz et al., 2016). These data support further efforts to employ RNase1 as an antimicrobial agent to combat pneumococcal infectious diseases.

ExRNA and Vascular Permeability

The endothelium constitutes the inner lining of all blood and lymphatic vessels and functions as a natural barrier between the flowing blood or lymph and the underlying tissues. The balance in the exchange of molecules and mobile leukocytes across the vascular endothelium is maintained by several systemic as well as site-specific homeostatic transport mechanisms involving the dynamic contribution of junctional proteins and adhesion receptors, as indicated above. In response to a variety of (patho-)physiological stimuli, including histamine, thrombin, VEGF or activated neutrophils, endothelial cells immediately start to reorganize intercellular junctions to facilitate trans-endothelial flux resulting in an increased para-cellular leakage (Kumar et al., 2009). Likewise, edemagenic agonists as well as lipid mediators induce intracellular signaling pathways, involving different protein kinases as well as the cytoskletal machinery to disrupt cell–cell adhesion, resulting in hyper-permeability (Sukriti et al., 2014; Karki and Birukov, 2018). In fact, this scenario is a significant problem in vascular inflammation observed in a variety of pathologies, including, ischemia-reperfusion injury, sepsis, acute respiratory distress syndrome (ARDS) and others.

While the regulation and fine-tuning of endothelial barrier functions also involve the contribution of intracellular microRNAs (Cichon et al., 2014), platelet-derived EV-associated non-coding exRNAs (predominantly microRNAs) can functionally influence the integrity and other features of the endothelium, thereby providing a molecular communication between blood cellular components and the vessel wall (Randriamboavonjy and Fleming, 2018). In this regard, various exRNA species were shown to directly or indirectly disturb the permeability barrier of the endothelium by changing the expression profile of vasoactive molecules or altering the quality of cell-to-cell junctions (Fischer et al., 2007, 2014). Following the initial phase of DAMP- or PAMP-sensing mechanisms by host pattern recognition receptors (such as TLRs or RAGE) on immune and tissue cells, an immediate consequence is the release of a variety of cytokines, chemokines, and other factors (including exRNA) from mast cells, tissue macrophages, and endothelial cells. Thus, blood vessels in close proximity to the site of inflammation or the inflammatory agonists subsequently adopt an appreciable level of cellular activation to participate in the immune response. Here, endothelial cells are particularly prone to various stimuli and switch their phenotype from non-adhesive, non-thrombogenic to inflammatory, reflected by elevated cellular permeability, the expression of adhesion receptors (such as selectins, ICAMs), and the coating of their apical glycocalyx surface by chemokines to indicate this pro-inflammatory status. Together, these aspects are crucial in the primary phase of leukocyte attraction to the inflamed vessel wall, as previously outlined (Pober and Sessa, 2007; Petri et al., 2008).

In fact, ribosomal exRNA elicits an immediate and largely irreversible permeability-increasing activity in vascular endothelial cells *in vitro* that is associated with a robust rise in intracellular calcium ions; *in vivo* this is reflected by edema formation due to *Sinus sagittalis* thrombosis or stroke in animal models (Fischer et al., 2007; Walberer et al., 2009; Bálint et al., 2013). In particular, the exRNA-provoked increase in vessel permeability correlates with the disorganization of the tight and adherence junctional proteins zonula occludens-1, occludin, and VE-cadherin. Mechanistically, the permeability-enhancing function of exRNA is mediated by its direct high-affinity interaction with extracellularly bound VEGF, resulting in the activation of the VEGF-receptor-2/neuropilin-1 signaling complex that is reminiscent of the function of cell-surface heparan sulfate proteoglycans which act as co-receptors for VEGF (Fischer et al., 2009, 2014). This is followed by activation of phospholipase C and intracellular release of calcium ions, which together promote hyper-permeability of the endothelium. Also, fluid shear stress in blood vessels may lead to the release of endothelial cell-derived exRNA, which subsequently interacts (like heparin) with VEGF to promote vascular hyper-permeability in a VEGF-receptor-2/neuropilin-1-dependent fashion. In addition, locally enhanced VEGF-dependent signaling results in the exocytosis of Weibel–Palade granules (Lasch et al., 2019) to provide additional alarming molecules such as the chemokine IL-8, as will be detailed below for the process of arteriogenesis.

Due to its ability to induce cytokine release in monocytes/macrophages, exRNA also indirectly contributes to cytokine-mediated destabilization of the endothelium.

Although direct activation of endothelial TLR3 (an endosomal receptor for non-self, double-stranded RNA) by ribosomal self-exRNA does not play a dominant role in vascular permeability changes (Fischer et al., 2009), synthetic virus-mimicking double-stranded RNA or the TLR3-agonists poly (I:C) caused a permeability increase of the blood-brain-barrier or provoked lung endothelial barrier dysfunction, respectively (Huang et al., 2016; Noda et al., 2018). It remains to be clarified, however, whether exRNA released *in situ* may also promote the activity of other vasodilators such as bradykinin, since exRNA was found to be a potent auto-activating cofactor for the precursor protein of this peptide, high-molecular-weight kininogen (HMWK), as well as of other proteins of the contact phase system of blood coagulation, including factors XI and XII (Kannemeier et al., 2007).

ExRNA, Leukocyte Transmigration, and Inflammation-Based Pathologies

Besides the established inflammatory agonists mentioned above, the exposure of quiescent endothelial cells (*in vitro* as well as *in vivo*) toward ribosomal exRNA not only induces vascular permeability to allow the enhanced trans-endothelial trafficking of molecules, but also triggers the recruitment of inflammatory cells to the vessel wall. This was demonstrated *in vivo* using a murine cremaster muscle vasculature model (Fischer et al., 2012). The observed exRNA-induced expression of ICAM-1 on the endothelium, which was comparable in its extent to the agonistic action of TNF-α, reduced the selectin-dependent rolling of leukocytes and promoted their firm adhesion and extravasation by utilizing activated β2-integrins. Moreover, exRNA-induced leukocyte adhesion and transmigration was shown to depend on the activation of the VEGF-receptor 2 system and to be reinforced by exRNA-mediated release of cytokines such as monocytic TNF-α, which by itself already aggravates the inflammatory process. Furthermore, exRNA facilitated the acute hypoxia-induced leukocyte adhesion and infiltration in murine lungs through TLR-interferon-γ-STAT1 signaling pathways (Biswas et al., 2015). Since RNase1 was shown to significantly prevent the exRNA-provoked inflammatory outcome in the indicated preclinical animal models, the endonuclease might constitute a new type of therapeutic intervention for patients with inflammation-based diseases (see below).

The indicated functional relationships between exRNA and inflammatory responses has been corroborated in patients (presented with elevated plasma levels of exRNA) and especially in authentic animal models of atherosclerosis and rheumatoid arthritis, two established pathological scenarios of chronic inflammation. Under disease conditions, significantly increased levels of exRNA were found to be deposited at the typical sites of injury in atherosclerotic lesions as well as in affected joints in patients with rheumatoid arthritis (Simsekyilmaz et al., 2014; Zimmermann-Geller et al., 2016). Moreover, under conditions of ischemia-reperfusion injury, following intervention in occluded carotid arteries *in vivo*, exRNA was found to be a potent damaging factor, leading to cytokine (particularly TNF-α) release and cardiomyocyte death as well as to the accumulation of macrophages (Cabrera-Fuentes et al., 2014). The fatal situations in all of the *in vivo* models cited were prevented or dampened by degrading exRNA with the help of RNase1 administration, which thereby acts as an efficient anti-inflammatory and tissue-protective factor for improving the overall outcome (see below).

ExRNA-Induced Release Reactions in Immune Cells (Macrophages, Mast Cells)

The levels of both exRNA and TNF-α were found to be concomitantly increased under the inflammatory conditions in the animal models discussed above as well as in human blood plasma in the transient perioperative ischemic situation associated with cardiac surgery (Cabrera-Fuentes et al., 2015b). The same elevation of these parameters was found in an ischemia-reperfusion injury model in mice and in isolated rat hearts, whereby cardiomyocytes could be identified as a major source of ribosomal exRNA. Functionally, exRNA and TNF-α appear to act in a feed-forward loop to promote cardiac ischemia-reperfusion injury: the increase in exRNA leads to an accumulation of TNF-α, and in turn, TNF-α activation of adjacent cells via TNF-receptor-1 provokes an increase in exRNA as well, resulting in a hyper-inflammatory situation (Cabrera-Fuentes et al., 2014). As an example, exRNA and TNF-α together induce the expression of reactive oxygen species (ROS) and inducible NO synthase or monocyte chemo-attracting protein (MCP)-1 to amplify the extent of inflammation (Cabrera-Fuentes et al., 2014).

In vitro studies using different tissue and immune cell cultures revealed the prominent exRNA-induced expression (via the intracellular NF-κB signaling machinery) and the release of TNF-α, supported by data from *in vivo* tumor models (Fischer et al., 2013; Cabrera-Fuentes et al., 2014; Han et al., 2019; Tielking et al., 2019). This reaction requires specific intracellular proteolytic processing as well as cleavage of the premature transmembrane form of TNF-α by TNF-α-converting enzyme (TACE, also denoted as ADAM17) (**Figure 3**). Here, exRNA was found to promote this shedding process to liberate the functionally active trimeric TNF-α from macrophages or other cells (Scheller et al., 2011). Since TACE recognizes and cleaves more than 50 cell membrane-anchored substrates other than pro-TNF (such as IL-6 receptor, VEGF-receptor 2, ICAM-1, E-selectin, NOTCH), the majority of which are directly or indirectly related to inflammation, it was proposed that exRNA could serve as a universal DAMP or alarmin, triggering such events at an early time point and at any site in the body (Zunke and Rose-John, 2017; Lambrecht et al., 2018). Yet, further experimental proof for such molecular mechanisms that would govern the exRNA-TNF-α axis or other TACE-related inflammatory reactions is still needed.

When exposed to external stimuli, monocytes/macrophages respond with rapid changes in the expression of various inflammation-related genes while undergoing polarization toward the M1-like (pro-inflammatory) or the M2-like (anti-inflammatory) phenotype. While both, extracellular microRNAs and long-non-coding RNAs could influence

macrophage polarization, associated with "meta-inflammation" (Li et al., 2018), the exposure of murine bone marrow-derived macrophages (which were differentiated with mouse macrophage colony-stimulating factor) toward ribosomal exRNA resulted in their robust polarization toward the M1-like phenotype. A variety of typical M1 markers, including TNF-α, iNOS, IL-1β, or IL-6, were highly expressed, whereas anti-inflammatory genes, such as macrophage mannose receptor-2 (CD206) and other M2-markers, were significantly downregulated (Cabrera-Fuentes et al., 2015a). Likewise, treatment of human peripheral blood monocytes with exRNA followed by microarray analyses of the whole human genome revealed an appreciable upregulation of more than 70 genes, many of which are coupled to inflammation and the related signal transduction. Since the described macrophage responses to exRNA are independent of TLR3- or TLR7/TLR8-related signaling pathways (Cabrera-Fuentes et al., 2015a), it is fair to assume that ribosomal exRNA-mediated cytokine mobilization is largely independent of TLR-induced signaling, as was already noted for the transmigration of leukocytes (Zernecke and Preissner, 2016; Fischer, 2018). However, the typical TLR3-agonist poly (I:C) was capable of inducing M1-like polarization of tumor-associated macrophages, thereby inhibiting the tumor growth in a subcutaneous transplantation tumor model (Liu et al., 2016).

Together, these relationships are consistent with a still hypothetical but possibly general type of exRNA-dependent endogenous inflammatory cascade that begins with the liberation of exRNA (as a universal alarmin or DAMP) at a damage or infection site in any tissue of the body. Based on the ubiquitous expression of TACE, exRNA may induce the production of inflammatory products derived from proteolytic cleavage of the corresponding substrate(s) by TACE in a cell type-specific manner (as described for macrophage TNF-α). Thus, the "non-specific" alarmin exRNA could be capable of promoting "site-specific" cellular responses, some of which are of profound relevance for inflammation. Based on these considerations, not only is RNase1 an anti-inflammatory antagonist for exRNA-induced reactions, but TACE, the sheddase responsible for the release of TNF-α and other products (Preissner and Herwald, 2017), appears to be a considerable target as well. In fact, the TACE inhibitor TAPI has been demonstrated to inhibit exRNA-mediated shedding of TNF-α in peripheral blood mononuclear cells as well as in different preclinical *in vivo* models of cardiovascular disease, such as cardiac ischemia-reperfusion injury (Fischer et al., 2012; Cabrera-Fuentes et al., 2014). The increased adhesion of leukocytes to endothelial cells induced by exRNA *in vivo* was also attenuated by TAPI (Fischer et al., 2012).

Tissue-resident, perivascular mast cells are well known for their role as primary DAMP- or PAMP-sensing immune cells in inflammatory responses as well as for their immediate response in allergic and anaphylactic reactions. Their contribution to the process of arterial remodeling will be discussed below. In mature mast cells, secretory granules are located in close proximity to ribosomes and cytosolic ribosomal RNAs, and following cell activation and degranulation, these are released together with the content of granules (such as cytokines, lipid mediators, vasoactive substances) (Dvorak et al., 2003). *In vitro*, various agonists were found to induce the degranulation of mast cells and the concomitant release of appreciable amounts of EV-associated exRNA (Elsemuller et al., 2019). Although exRNA is not located in granules, the liberation of exRNA can be prevented by mast cell stabilizers or by abolishing the increase of intracellular Ca^{2+} levels in these cells. Mast cell-derived and EV-associated exRNA was further shown to promote the increased expression and release of cytokines (such as MCP-1 or IL-6) in vascular endothelial cells in a dose-dependent manner. These data indicate that exRNA-containing EVs from mast cells are likely to be involved in inflammatory responses and support earlier observations on the pivotal role of EVs in inflammation (Chen et al., 2019). However, which mechanistic route such EV-associated exRNA may take to activate and even enter target cells, possibly by using connexin-43 hemi-channels (Willebrords et al., 2016), needs to be further investigated.

ExRNA and Arteriogenesis: A Blueprint for the Creation of Natural Vessel Bypasses Through Innate Immunity Reactions

Collateral artery growth, defined as arteriogenesis, is the only natural way for the body to spontaneously create blood vessel bypasses to counteract and circumvent the disastrous consequences of arterial occlusion, as in association with myocardial infarction (Faber et al., 2014). The initial trigger for this multistep intricate process is an increased fluid shear stress in pre-existing arterioles; this mediates endothelial cell activation, leukocyte recruitment, cytokine release, and subsequent endothelial and smooth muscle cell proliferation to finally induce controlled blood vessel expansion (Pipp et al., 2004; Lasch et al., 2019). Yet, how these different steps all work together for blood vessel regeneration remained unanswered for a long time (Deindl and Schaper, 2005). Based on the recent findings that exRNA is liberated from shear stress-exposed endothelium, we hypothesized that exRNA may serve as a trigger and promoter of collateral vessel growth, including endothelial activation, leukocyte recruitment and cytokine release as well as stimulation of the VEGF signaling axis (Kluever et al., 2019; Lasch et al., 2019; **Figure 4**).

As investigated in appropriate animal models, elevated fluid shear stress proximal to the occluded vessel(s) leads to the release of exRNA from endothelial cells and to platelet activation. Together, these reactions promote the exocytosis of Weibel–Palade granules with the release of von Willebrand factor from endothelial cells in a VEGF-receptor 2-dependent manner (Chandraratne et al., 2015; Lasch et al., 2019). In turn, von Willebrand factor initiates further activation of platelets and the formation of platelet-neutrophil aggregates, which release several pro-inflammatory agonists, including ROS, in the perivascular zone. Subsequent activation and degranulation of perivascular mast cells, which appear to orchestrate the extravascular reactions, result in the local increase and bioavailability of pro-inflammatory cytokines such as TNF-α and MCP-1, feeding a

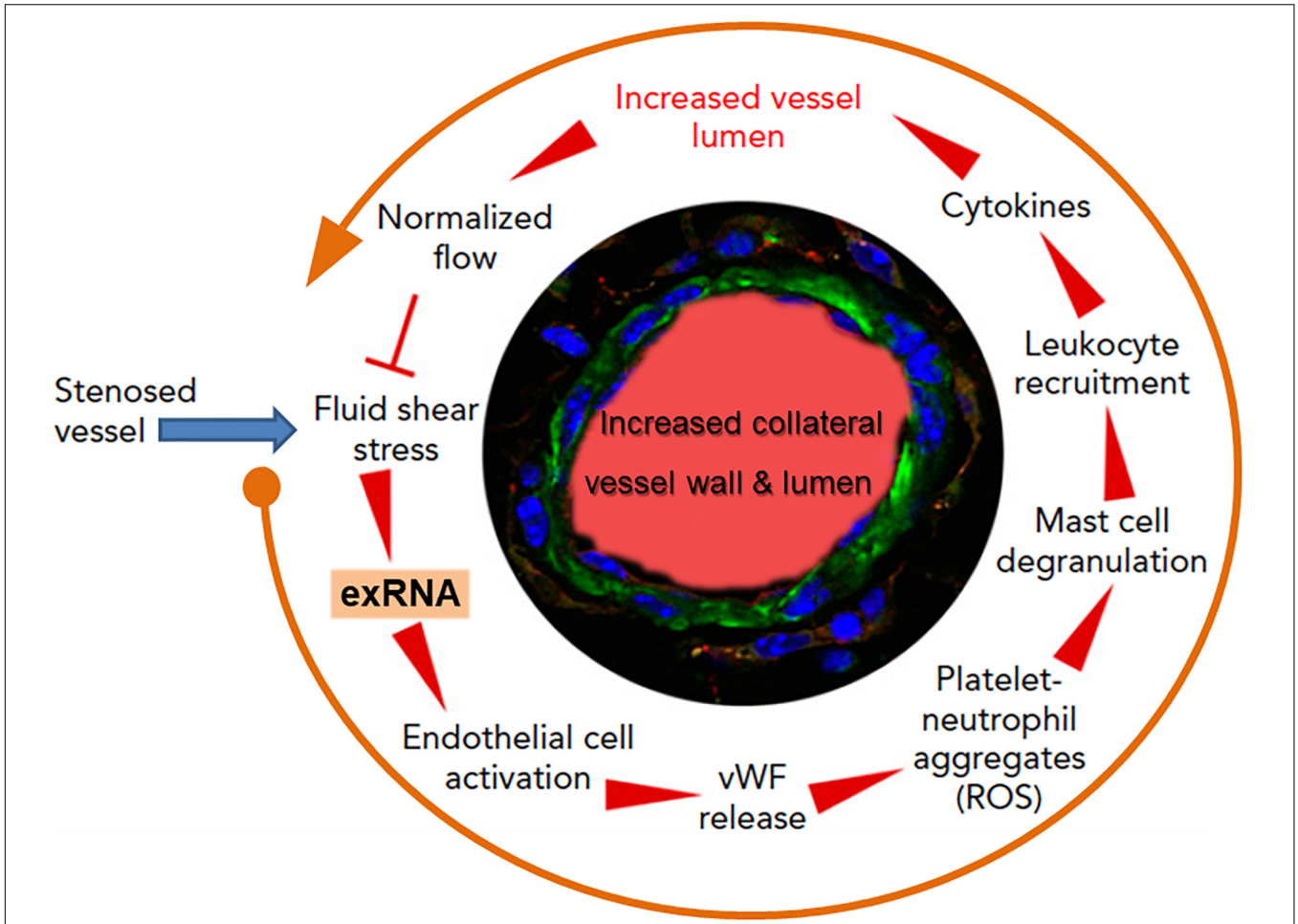

FIGURE 4 | The multi-step cycle of exRNA-initiated arteriogenesis: a blueprint for blood vessel regeneration based on leukocyte recruitment. Upon occlusion of a feeding artery (e.g., in the heart), blood flow is redirected into collateral blood vessels that are formed by arteriogenesis from pre-existing arterioles within several days, thereby circumventing the stenosed artery. Due to the initially disturbed blood flow causing increased fluid shear stress, exRNA is released from endothelial cells and serves as a mechano-transducer, provoking further activation of vascular cells (in a VEGF-dependent manner). Thus, activated endothelial cells liberate von Willebrand factor (vWF) and other components from their Weibel–Palade granules, leading to platelet activation and formation of platelet-neutrophil aggregates with the production of reactive oxygen species (ROS). These, in turn, are essential for the activation of perivascular mast cells with the release of vasoactive factors (such as histamine) and chemo-attractive cytokines, a prerequisite for the recruitment of leukocytes that boost vascular cell proliferation by supplying growth factors and cytokines to promote collateral vessel growth. When collaterals reach a critical size of their lumen and vessel wall, allowing them to substitute for the function of the occluded artery, blood flow is normalized, and the collaterals cease to grow. Modified from Lasch et al. (2019).

positive-feedback loop for the recruitment of more neutrophils, additional monocytes, and T cells (Chillo et al., 2016). Together, these factors all promote vascular cell proliferation and positive outward remodeling of the vessel wall, finally resulting in an arterial bypass that compensates the dysfunction of an occluded artery. The different steps of leukocyte recruitment appear to be a blueprint for arteriogenesis taken from the respective steps in innate immunity, whereby exRNA is considered in this context not to be a damaging component but rather a vessel and tissue regenerating factor. Although the aforementioned process of collateral artery growth also entails reactions of vasculogenesis and angiogenesis at distant sites, a definitive role of exRNA here is still speculative (Lasch et al., 2020). Nevertheless, in an *ex vivo* cellular spheroid model of vasculogenesis, exRNA was found to stimulate the formation of new vessels and leukocyte differentiation in embryonic bodies via increased VEGF-dependent signaling and ROS production (Sharifpanah et al., 2015). The underlying mechanisms remain to be described.

ExRNA AND VASCULAR DEFENSE SYSTEMS (CONTACT PHASE/COAGULATION, BLOOD PRESSURE REGULATION)

Based on the recent characterization of new humoral and cellular factors, hemostasis as part of the wound healing process has gained considerable interest as contributor to the body's life-saving defense mechanism that is embedded in the functional

context of innate immunity. Here, self-exRNA and -exDNA were found to be potent cofactors in the initiation of blood coagulation, whereby the neutrophil-derived exDNA/histone scaffolds (designated as NETs) not only serve as potent anti-inflammatory gate-keepers that catch and kill microbes but also work as promoters of thrombotic situations in a variety of diseases (Fuchs et al., 2010; Massberg et al., 2010; von Brühl et al., 2012; Döring et al., 2017; Sorvillo et al., 2019; Thålin et al., 2019; Thiam et al., 2020). Since the identification of exRNA as a cofactor for several coagulation and platelet-derived proteins, the exRNA-mediated link between the discussed processes of innate immunity/leukocyte recruitment and the hemostasis system has become apparent.

The four plasma proteins factor XII, factor XI, prekallikrein, and HMWK are designated as "contact phase proteins" because they bind with high affinity to negatively charged surfaces on which they eventually become (auto-) activated and/or they reciprocally activate each other in a zinc ion-dependent manner (Kannemeier et al., 2007; Schmaier, 2016). Under *in vitro* settings or conditions of severe trauma *in vivo* this self-amplifying system promotes the intrinsic pathway of blood coagulation, culminating in thrombin generation and fibrin clot formation (Schmaier, 2016; Amiral and Seghatchian, 2019). Bioactive surfaces that promote contact phase activation include the activated endothelium and platelets, leukocytes, bacteria, and denatured proteins. Although factor XII appears to be dispensable for physiological hemostasis, under pathological situations associated with thrombotic complications the contact phase system contributes to enhanced clot formation, particularly in arterial thrombosis (Maas et al., 2011). This appears to be due to exposed collagens, sulfatides, platelet-derived polyphosphates, and misfolded proteins as well as exRNA and exDNA, which become accessible under conditions of severe trauma or inflammation or upon vascular pathologies and thereby serve as major natural activators or cofactors of contact phase activation (Kannemeier et al., 2007; Björkqvist et al., 2014; Naudin et al., 2017). These poly-anionic molecules induce auto-activation of factor XII and factor XI with major consequences for enhanced thrombin formation and thrombosis; they also promote selective generation of kallikrein, which in turn induces bradykinin formation from HMWK, relevant for vasodilation in the context of inflammation and edema (Schmaier, 2018). In order to prevent uncontrolled clotting, histidine-rich glycoprotein in plasma has been identified and characterized as exRNA- and factor XIIa-binding protein to attenuate their capacity to trigger coagulation (Vu et al., 2015). In fact, carotid artery occlusion was accelerated in histidine-rich glycoprotein-deficient mice which could be counteracted for by RNase administration as indicated above, supporting the pro-thrombotic role of exRNA in hemostasis. Independent of its function in coagulation, factor XII/XIIa exerts mitogenic activity in vascular cells, upregulates neutrophil functions, contributes to macrophage polarization, and induces T-cell differentiation (Schmaier and Stavrou, 2019). Thus, the exRNA-factor XII axis not only influences hemostasis and wound repair but may also contribute to other reactions in innate immunity (Bender et al., 2017; Renné and Stavrou, 2019).

In this context it is worthwhile mentioning that complex formation of exRNA (or exDNA) with basic platelet proteins such as platelet factor 4 (exposed during trauma, surgery, or infection) induces neo-epitopes in this basic protein that provoke the formation of autoantibodies, designated as HIT ("Heparin-induced thrombocytopenia") antibodies (Jaax et al., 2013). Once the titer of these HIT antibodies increases, e.g., by administration of heparin in the same patient several years later, a thrombo-embolic scenario is generated due to the autoimmune character of HIT with the formation of micro-thrombi and the reduction of circulating platelets (Greinacher et al., 2017). These data indicate that exRNA (and other poly-anions) can induce autoimmunity in connection with the adaptive part of the immune system. Moreover, additional pathological situations have been recognized in neurological disorders in association with cellular damage, where autoantibodies against intracellular RNA-binding proteins have been recognized in plasma, possibly contributing to the onset or progress of autoimmune diseases such as Opsoclonus-Myoclonus syndrome (Blaes et al., 2007).

THE EXTRACELLULAR RNA/RNASE SYSTEM

The lifespan as well as the reactivity of exRNA species in the vasculature or in other extracellular body fluids depends to a large degree on the type of complexes formed with proteins, EVs, or cell surfaces. Despite these constraints, exRNA is continuously degraded in the vascular system by circulating RNases, of which the thermo-stable RNase1 is the by far most powerful natural antagonist of exRNA. RNase1 belongs to the RNaseA family, which consists of eight members that have endonuclease activities and which are secreted by a large variety of different tissues and cells (Koczera et al., 2016). Eosinophil (RNase 2, RNase3) or epithelial cell-derived RNase7 serves as an anti-microbial protein, whereas RNase5 (also designated angiogenin) has potent angiogenic functions without having an appreciable ribonucleolytic activity (Cho et al., 2005; Sorrentino, 2010). Extracellular RNases can also be internalized by cells via endosomal pathways (Haigis and Raines, 2003), but due to the action of RNase inhibitor, which binds mammalian RNaseA family members with an extremely high affinity, these endonucleases are immediately inactivated and do not express any intracellular cytotoxic activity (Dickson et al., 2005; Rutkoski and Raines, 2008).

Pancreatic RNase1 is produced in the exocrine pancreas and constitutes the major ribonuclease of the gastrointestinal tract, whereas vascular RNase1 is predominantly expressed and released by endothelial cells from medium and large vessels as well as in the umbilical vein (Landré et al., 2002; Barrabés et al., 2007; Fischer et al., 2011; Eller et al., 2014; Ohashi et al., 2017). Interestingly, the counteracting function of RNase1 that, as we reported in various preclinical cardiovascular models, combats the damaging functions of exRNA is robust and safe due to the fact that RNase inhibitor with its extremely high affinity for RNases is present in all cell types of the body (Arnold, 2011). Thus, RNase1 bears considerable potential as new therapeutic

agent based on its tissue- and vessel-protective functions that all may translate into anti-inflammatory properties in different pathological situations (Cabrera-Fuentes et al., 2015b; Kleinert et al., 2016; Zernecke and Preissner, 2016; Ma et al., 2017; Stieger et al., 2017; **Table 1**).

Different stimulatory agonists or conditions such as pro-inflammatory or pro-thrombotic agents, exRNA itself, vasopressin as well as ischemic conditioning may induce the short-term release of RNase1 from its endothelial storage sites, the Weibel–Palade granules. Consequently, the exRNA/RNase1 system can be considered as an integral regulatory part of vascular homeostasis, vessel wall integrity, and the innate immune response, including the recruitment of leukocytes (Fischer et al., 2011; Zernecke and Preissner, 2016; Lomax et al., 2017). Under inflammatory conditions, however, such as long-term stimulation by thrombin or TNF-α, the expression and protein synthesis of the protective RNase1 in endothelial cells was found to be repressed as a result of epigenetic mechanisms (Gansler et al., 2014; Bedenbender et al., 2019). The inhibitory and protective effects of RNase1 are most likely due to the degradation and the elimination of damaging exRNA species; whether the hydrolysis products of exRNA, such as (oligo-) nucleotides or nucleosides (as vaso- or neuro-active compounds) that are generated, may contribute to the overall protective function of RNase1 in the body remains to be investigated. Studies of plasma from RNase1-deficient mice demonstrated that its pro-coagulant status was much higher than the plasma of wild-type mice, which confirmed that one of the physiological functions of RNase1 is to degrade exRNA in blood plasma and to serve potent anticoagulant functions (Kannemeier et al., 2007; Garnett et al., 2019). RNase1 is furthermore involved in immune responses by inducing phenotypic and functional maturation of dendritic cells and viral defense mechanisms, e.g., in the inactivation of HIV (Lee-Huang et al., 1999; Yang et al., 2004).

Based on the different exRNA/inflammation-driven preclinical pathological situations discussed above, in a rat model of cerebral stroke initiated by *Sinus sagittalis* thrombosis, the edema formation and infarct size were significantly reduced after pretreating the animals with RNase1 but not with DNase, confirming the permeability-increasing activity of exRNA *in vivo* (Fischer et al., 2007). Likewise, in a preclinical mouse model of myocardial infarction (ligation of the left anterior descending coronary artery), increased levels of exRNA were found to provoke myocardial edema formation 24 h after ligation as compared with controls. Consequently, the systemic application of RNase1 (but not DNase) markedly increased the area of vital myocardium (Stieger et al., 2017). Thus, RNase1 efficiently counteracts exRNA-induced edema formation and preserves perfusion of the infarction border zone, resulting in a reduction of infarct size and the protection of cardiac function after myocardial infarction. Finally, successful translational approaches are underway to target the adverse functions of extracellular nucleic acids in patients by using nucleic-acid binding polymers such as poly-amidoamine dendrimers as novel anti-inflammatory and anti-thrombotic drugs (Lee et al., 2011; Holl et al., 2013; Naqvi et al., 2018). Together, these approaches underline the utmost importance of further defining and understanding the (patho-) physiological role of exRNA in immune defense.

PERSPECTIVES AND HYPOTHESES: POSSIBLE CONTRIBUTIONS OF EXRNA IN SPREADING CARDIOPULMONARY AND VASCULAR DISEASES IN ASSOCIATION WITH COVID-19

At present, a detailed characterization of the interactions of exRNA with viruses in general and with severe acute respiratory syndrome-related coronavirus 2 (SARS-CoV-2) in particular is pending; however, as alluded to in the topics discussed here, self-exRNA may serve a prominent role in promoting and disseminating a viral infection and its subsequent adverse side effects in the human host (**Figure 5**). This hypothesis is based on the fact that virus infections in particular are known to damage and destroy host cells with the liberation of a number of DAMPs and that cardiovascular diseases appear to be serious adverse effects of coronavirus infections. In fact, HMGB1 or NETs could serve as potential targets for therapies in coronavirus disease (COVID-19) (Andersson et al., 2020; Cicco et al., 2020).

Severe acute respiratory syndrome-related coronavirus 2 is a positive-sense, single-stranded enveloped RNA virus responsible for the ongoing COVID-19 that initially appeared in China in 2019 (Perlman and Netland, 2009; Huang et al., 2020; Ren et al., 2020; Zhu et al., 2020). Several types of coronaviruses with a zoonotic potential have been described to infect humans and animals. While those viruses mainly infecting the upper respiratory tract cause only minor symptoms, the coronaviruses infecting the lower respiratory tract (with SARS-CoV-2 and MERS-CoV among them) can also provoke fatal pathological side effects associated with cardiovascular diseases, with an estimated mortality rate between 3 (SARS-CoV-2) and 35% (MERS) (Labò et al., 2020; Tay et al., 2020). The case fatality for COVID-19 caused by SARS-CoV2 has been variably estimated between <1 and 15% (Rajgor et al., 2020). ARDS, sepsis, and multi-organ failure involving the kidney and heart were described as causes of mortality in the majority of severe SARS-CoV-2 infections (Chen et al., 2020; Goh et al., 2020; Wu and McGoogan, 2020). Accordingly, it is of major interest to understand the fundamental molecular and immunological mechanisms of SARS-CoV-2-caused pathologies, and identifying effective drugs for treating patients and combating viral infection will be critical.

To initiate a viral infection with SARS-CoV-2, the protein spike subunit S12 is recognized by several host cell-surface receptors, the prominent one being angiotensin-converting enzyme 2 (ACE2), which triggers the endocytosis of the virus (Tay et al., 2020). To facilitate host cell entry, the virus engages the cellular transmembrane protease serine 2 (TMPRSS2), which processes the viral spike protein, a prerequisite for coronavirus entry (Hoffmann et al., 2020). TMPRSS2 is also able to cleave ACE2 and thereby competes with the sheddase TACE: While TACE-induced proteolysis is associated with the release of TNF-α, only TMPRSS2-mediated shedding appears to augment the

TABLE 1 | ExRNA-counteracting properties of RNase1 as studied *in vitro* and in preclinical disease models.

Biological system, pathological process	Influence/activity of RNase1	References
Blood coagulation, thrombosis	Destruction of exRNA as cofactor for coagulation proteases; anti-thrombotic	Kannemeier et al., 2007
Vascular hyperpermeability, vasogenic edema formation, stroke	Destruction of exRNA as cofactor for VEGF; vessel-protective	Fischer et al., 2007; Walberer et al., 2009
Inflammation	Destruction of exRNA as cytokine cofactor; anti-inflammatory	Bedenbender and Schmeck, 2020
Tumor growth in xenograft, immuno-compromised model	Destruction of exRNA as triggering factor for promoting tumor cell trafficking; anti-tumorigenic	Fischer et al., 2013
Atherosclerosis, arterial vessel degeneration	Destruction of exRNA as multifunctional cell-damaging factor; anti-atherogenic	Simsekyilmaz et al., 2014
Cardiac ischemia-reperfusion injury, heart failure	Destruction of exRNA as cardiomyocyte-damaging and cytokine-mobilizing factor; anti-cytotoxic, cardio-protective	Cabrera-Fuentes et al., 2014
Experimental heart transplantation	Prolongation of graft survival; tissue-protective	Kleinert et al., 2016
Microbial infection	Prevention of exRNA-mediated bacterial adherence and invasion; anti-microbial	Zakrzewicz et al., 2016
Myocardial infarction	Reduction of cardiac edema and infarct size; cardio-protective	Stieger et al., 2017
Shear stress-mediated induction of arteriogenesis	Reduction of collateral vessel formation; anti-inflammatory	Lasch et al., 2019

amplification of viral entry upon SARS-CoV-2 infection (Haga et al., 2008; Heurich et al., 2014). Here, it would be relevant to analyze the influence of exRNA on these proteolytic processing events, since we have proposed that there is a direct effect of exRNA on triggering TACE to augment substrate cleavage (Fischer et al., 2013). Moreover, exRNA was shown to directly affect the (auto-)activation of proteases in blood plasma such as contact phase enzymogens or factor VII-activating protease (Nakazawa et al., 2005; Fischer et al., 2013).

Recent data indicated that neuropilin-1 significantly potentiates SARS-Cov-2 infectivity, implying a particular role in viral pathogenicity for this co-receptor of VEGF-receptor-2 (Cantuti-Castelvetri et al., 2020; Moutal et al., 2020). Based on the expression of neuropilin-1 in endothelial and epithelial cells of the olfactory and respiratory system, its upregulation in SARS-CoV-2-infected blood vessels of COVID-19 patients was associated with vascular endothelialitis, angiogenesis, and thrombosis (Ackermann et al., 2020). Considering the previously described relations of exRNA to these components in provoking vascular permeability, angiogenesis, and inflammatory reactions, it is fair to propose an influence of exRNA on the VEGF-receptor-2/neuropilin-1 system in the context of virus infection, thereby enhancing the leakiness of blood vessels and promoting dissemination of virus and its penetration into tissues (**Figure 5**).

Cellular infections by cytopathic viruses such as SARS-Cov-2 cause cell damage and pyroptosis, a highly inflammatory form of cell death, which results in release of DAMPs such as cellular nucleic acids, including self-exRNA (Tay et al., 2020). These inflammatory agonists are recognized by neighboring tissue and immune cells to trigger the release of pro-inflammatory cytokines and chemokines, including IL-6, IFN-γ, and MCP-1 as described (Tay et al., 2020). In this context, exRNA as well could amplify this response, also by attracting leukocytes and other immune cells in a VEGF-receptor-2-dependent manner, as demonstrated in several preclinical studies (Fischer et al., 2012; Kluever et al., 2019; Lasch et al., 2019). In the ultimate phase of inflammation under physiological conditions, the attracted neutrophils and macrophages need to clear the site of infection/inflammation by phagocytosis and induce the final inflammatory step of resolution and recovery. In patients with severe COVID-19, however, a dysfunctional immune response results in further mobilization of immune cells causing an amplification of the cytokine storm with fatal consequences not only for the lung but also for other organs (Huang et al., 2020; Sariol and Perlman, 2020). Based on the observed cell damage under these pathological conditions, it might be speculated whether exRNA is involved in this self-amplifying cytokine storm and whether administration of RNase1 might help to suppress this fatal scenario (**Figure 5**).

There might be another, yet undefined connection between exRNA and the systemic cytokine storm, hemorrhage, and sepsis that are the major causes of death in COVID-19 patients. This potential connection is based on the role of "cold-inducible-RNA binding protein" (CIRP) and its relevance for community-acquired pneumonia, whose severity is related to microbial pathogenicity and virus load (Guo et al., 2020). As a typical DAMP, nuclear CIRP is liberated by macrophages and other cells upon stress and promotes inflammatory responses (cytokine release) via the TLR4-myeloid differentiation factor 2 complex, also causing endothelial dysfunction (Qiang et al., 2013; **Figure 1**). The blockade of CIRP using antisera to CIRP has been shown to attenuate inflammatory cytokine release and mortality after hemorrhage and sepsis. CIRP was also documented to

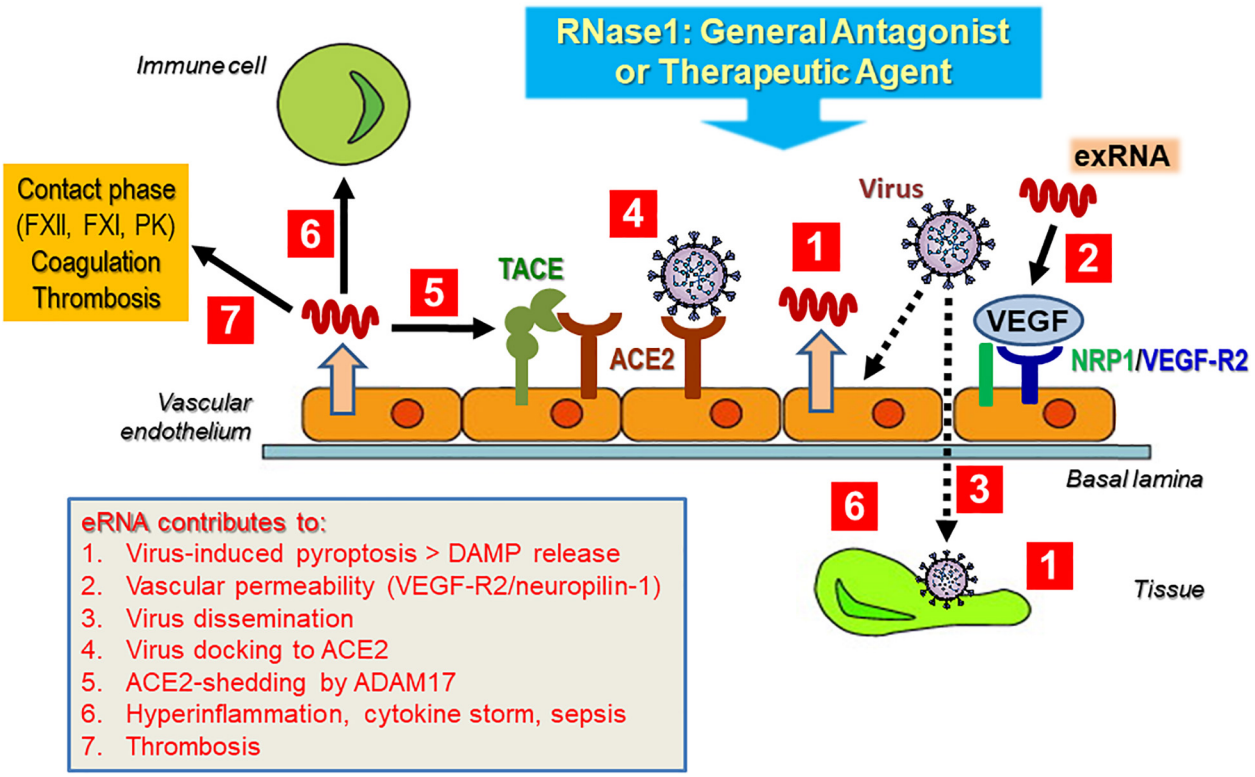

FIGURE 5 | Hypothetical contribution of exRNA to virus infection and subsequent cardiovascular disease. Upon infection of the tissue (vascular endothelium) by (SARS-CoV-2) virus, DAMPS including exRNA are released from tissue cells (Tisoncik et al., 2012; Castanheira and Kubes, 2019). Virus particles activate tissue and immune cells of the host to release inflammatory mediators, including exRNA, which in turn can induce vascular hyper-permeability in a VEGF-receptor-2-neuropilin-1 (NRP1)-dependent manner (Van Kaer et al., 2013). This allows virus particles to further invade particular tissue sites to disseminate their infection potential, including the liberation of cytokines (Kolaczkowska and Kubes, 2013; Zindel and Kubes, 2020). A major docking site for SARS-Cov-2 is the endothelial cell-associated metalloproteinase ACE2, whose processing, carried out by ADAM17, could be triggered by exRNA to allow virus entry (Bianchi, 2007; Andersson and Tracey, 2011). Together, these mostly hypothetical exRNA-mediated processes not only could provoke a robust cytokine release, associated with hyper-inflammation and cardiovascular disease. In addition, exRNA as a pro-thrombotic cofactor can further induce the intrinsic pathway of blood coagulation, resulting in the thrombotic phenotype of COVID-19 patients. As a general antagonist or potential therapeutic agent, RNase1 may inhibit or prevent the multiple actions of the damaging exRNA, associated with viral infections and their adverse side effects. For details please see text.

induce NET formation, which causes tissue damage in lungs during sepsis, whereas for COVID-19 patients it was noted that organ dysfunction was due to vascular occlusion by NETs (Ode et al., 2019; Leppkes et al., 2020). Interestingly, injection of CIRP into mice caused vascular leakage, edema formation, and leukocyte infiltration with cytokine production in the lungs that was accompanied by endothelial cell activation and pyroptosis (Yang et al., 2016). Altogether, these observations are reminiscent of the multiple functions of exRNA as a DAMP and damaging factor, as summarized in this review, suggesting that CIRP and exRNA might work together and amplify each other as potent inflammatory companions, as was demonstrated for TLR2-ligands and exRNA (Noll et al., 2017). In fact, complexes of DAMPs such as HMGB1 or CIRP with exRNA could drastically enhance the stimulatory function of each factor, e.g., to induce TNF-α expression and release in macrophages (Andersson et al., 2020). Moreover, treatment of mice suffering from septic cardiomyopathy with RNase1 resulted in a reduction of cardiac apoptosis, TNF-α expression, cardiac injury, and dysfunction (Zechendorf et al., 2020). Together, these data demonstrate that exRNA could play a crucial role in the patho-physiology of organ dysfunction in sepsis, a very critical situation in COVID-19 patients.

The observed vascular damage in SARS-CoV-2 infections is related to virus-mediated endothelial cell injury that exacerbates endothelial dysfunction, as it is known from aging, hypertension, and obesity, and which is likely to be associated with the complications and mortality observed in COVID-19 patients (Amraei and Rahimi, 2020). Endothelial dysfunction in COVID-19 is linked to hypercoagulability as indicated by increased fibrinogen and von Willebrand factor levels as well as elevated numbers of activated platelets and their complexes with leukocytes together with abnormal coagulation parameters (Spiezia et al., 2020; Tang et al., 2020b). Whether exRNA and other procoagulant DAMPs such as NETs might directly or indirectly worsen this thrombogenic situation in COVID-19 patients remains to be confirmed (Thierry and Roch, 2020). In order to tackle a given thrombotic risk situation, anticoagulants

such as heparin have been successfully administered as versatile drugs to treat COVID-19 patients to reduce their mortality rate (Tang et al., 2020a; Thachil, 2020). The high affinity of different types of heparin for the SARS-CoV-2 spike protein appears to be relevant for these poly-anions to interfere with the mechanism of virus entry into host cells (Kwon et al., 2020). Although heparin and exRNA are known to compete in binding to several cytokines and growth factors that contain basic heparin binding sites, data showing competition between exRNA and virus proteins are not available (Fischer et al., 2007). Taking these findings together, one can speculate that elimination of exRNA as an endogenous prothrombotic cofactor by RNase1 might help to reduce the adverse thrombotic complications in COVID-19 patients.

Finally, the involvement of vascular components like ACE2 as the SARS-CoV-2 entry site of host cells has a profound influence on the homeostasis of blood pressure regulation via the renin-angiotensin-aldosterone system. Not only does virus docking to ACE2 cause its masking and downregulation, but there is also a concurrent loss of protease activity to generate angiotensin (Bianchi, 2007; Andersson and Tracey, 2011; Tisoncik et al., 2012; Kolaczkowska and Kubes, 2013; Van Kaer et al., 2013; Castanheira and Kubes, 2019; Zindel and Kubes, 2020) from angiotensin II (Amraei and Rahimi, 2020). This leads to a substantial drop in the intrinsic control of the hypertensive arm of the system, resulting in cardiovascular complications in COVID-19 patients. Moreover, ACE2 is expressed in endothelial cells of capillaries, arterioles, arteries, and veins in many organs of the body, and ACE2 knockdown in mice was found to be associated with increased expression of inflammatory cytokines, metalloproteinases, and endothelial adhesion receptors, all molecules that are relevant for leukocyte recruitment (Hamming et al., 2004; Thomas et al., 2010). This would indicate that a reduction or loss of ACE2 under conditions of SARS-CoV-2 infection might lead to an accentuation of vascular inflammation and even atherosclerosis. However, in retrospective studies no higher risk of infection in patients with ACE inhibitors was found (Chung et al., 2020). Whether these critical situations can be counteracted in COVID-19 patients by intervention with RNase1 as described above remains to be investigated. Nevertheless, at different steps and the respective host responses during a SARS-CoV-2 infection, there are several scenarios where exRNA appears to be involved or serves as a virulence factor, and the antagonistic role of RNase1 may provide general anti-viral and tissue-protective functions. Further research activities are needed to prove this hypothesis.

AUTHOR CONTRIBUTIONS

All authors contributed to the design and the production of the review article.

FUNDING

The work by the authors cited in this article was supported by the Deutsche Forschungsgemeinschaft (Bonn, Germany), including the Excellence Cluster Cardio-Pulmonary System (ECCPS) (Giessen, Germany), the von-Behring-Röntgen Foundation (Marburg, Germany), and the Lehre@LMU program of the Ludwig-Maximilians-Universität (Munich, Germany).

REFERENCES

Abels, E. R., and Breakefield, X. O. (2016). Introduction to Extracellular Vesicles: Biogenesis, RNA Cargo Selection, Content, Release, and Uptake. *Cell Mol. Neurobiol.* 36, 301–12. doi: 10.1007/s10571-016-0366-z

Ackermann, M., Verleden, S. E., Kuehnel, M., Haverich, A., Welte, T., Laenger, F., et al. (2020). Pulmonary Vascular Endothelialitis, Thrombosis, and Angiogenesis in Covid-19. *N Engl. J. Med.* 383, 120–8. doi: 10.1056/nejmoa2015432

Amiral, J., and Seghatchian, J. (2019). The contact system at the crossroads of various key patho- physiological functions: Update on present understanding, laboratory exploration and future perspectives. *Transf. Apher. Sci.* 58, 216–22. doi: 10.1016/j.transci.2019.03.013

Amraei, R., and Rahimi, N. (2020). COVID-19, Renin-Angiotensin System and Endothelial Dysfunction. *Cells* 9:1652. doi: 10.3390/cells9071652

Andersson, U., and Tracey, K. J. (2011). HMGB1 is a therapeutic target for sterile inflammation and infection. *Annu. Rev. Immunol.* 29, 139–62. doi: 10.1146/annurev-immunol-030409-101323

Andersson, U., Ottestad, W., and Tracey, K. J. (2020). Extracellular HMGB1: a therapeutic target in severe pulmonary inflammation including COVID-19? *Mole. Med.* 26(1):42.

Arnold, U. (2011). Stability and stabilization of proteins: the ribonuclease A example. *Prot. Fold.* 2, 83–118.

Arroyo, J. D., Chevillet, J. R., Kroh, E. M., Ruf, I. K., Pritchard, C. C., Gibson, D. F., et al. (2011). Argonaute2 complexes carry a population of circulating microRNAs independent of vesicles in human plasma. *Proc. Natl. Acad. Sci. U S A.* 108, 5003–8. doi: 10.1073/pnas.1019055108

Bálint, Z., Zabini, D., Konya, V., Nagaraj, C., Végh, A. G., Váró G, et al. (2013). Double-stranded RNA attenuates the barrier function of human pulmonary artery endothelial cells. *PLoS One.* 8:e63776. doi: 10.1371/journal.pone.0063776

Barrabés S, Pagès-Pons, L., Radcliffe, C. M., Tabarés G, Fort, E., Royle, L., Harvey, D. J., Moenner, M., et al. (2007). Glycosylation of serum ribonuclease 1 indicates a major endothelial origin and reveals an increase in core fucosylation in pancreatic cancer. *Glycobiology* 17, 388–400. doi: 10.1093/glycob/cwm002

Barrat, F. J., Meeker, T., Gregorio, J., Chan, J. H., Uematsu, S., Akira, S., et al. (2005). Nucleic acids of mammalian origin can act as endogenous ligands for Toll-like receptors and may promote systemic lupus erythematosus. *J. Exp. Med.* 202, 1131–9. doi: 10.1084/jem.20050914

Bazzoni, G., and Dejana, E. (2001). Pores in the sieve and channels in the wall: Control of paracellular permeability by junctional proteins in endothelial cells. *Microcirculation* 8, 143–52. doi: 10.1111/j.1549-8719.2001.tb00165.x

Bedenbender, K., and Schmeck, B. T. (2020). Endothelial Ribonuclease 1 in Cardiovascular and Systemic Inflammation. *Front. Cell Devel. Biol.* 8:576491. doi: 10.3389/fcell.2020.576491

Bedenbender, K., Scheller, N., Fischer, S., Leiting, S., Preissner, K. T., Schmeck, B. T., et al. (2019). Inflammation-mediated deacetylation of the ribonuclease 1 promoter via histone deacetylase 2 in endothelial cells. *FASEB J.* 33, 9017–9029. doi: 10.1096/fj.201900451r

Bellingham, S. A., Coleman, B. M., and Hill, A. F. (2012). Small RNA deep sequencing reveals a distinct miRNA signature released in exosomes from prion-infected neuronal cells. *Nucleic Acids Res.* 40, 10937–49. doi: 10.1093/nar/gks832

Bender, L., Weidmann, H., Rose-John, S., Renné T, and Long, A. T. (2017). Factor XII-Driven Inflammatory Reactions with Implications for Anaphylaxis. *Front. Immunol.* 8:1115. doi: 10.3389/fimmu.2017.01115

Bergmann, S., Lang, A., Rohde, M., Agarwal, V., Rennemeier, C., Grashoff, C., et al. (2009). Integrin-linked kinase is required for vitronectin-mediated internalization of Streptococcus pneumoniae by host cells. *J. Cell Sci.* 122, 256–67. doi: 10.1242/jcs.035600

Bertheloot, D., Naumovski, A. L., Langhoff, P., Horvath, G. L., Tengchuan, J., Xiao, T. S., et al. (2016). RAGE enhances TLR responses through binding and internalization of RNA. *J. Immunol.* 197, 4118–26. doi: 10.4049/jimmunol.1502169

Bianchi, M. E. (2007). DAMPs, PAMPs and alarmins: all we need to know about danger. *J. Leukoc. Biol.* 81, 1–5. doi: 10.1189/jlb.0306164

Bianchi, M. E., and Manfredi, A. A. (2007). High-mobility group box 1 (HMGB1) protein at the crossroads between innate and adaptive immunity. *Immunol. Rev.* 220, 35–46.

Biswas, I., Singh, B., Sharma, M., Agrawala, P. K., and Khan, G. A. (2015). Extracellular RNA facilitates hypoxia-induced leukocyte adhesion and infiltration in the lung through TLR3-IFN-γ-STAT1 signaling pathway. *Eur. J. Immunol.* 45, 3158–73. doi: 10.1002/eji.201545597

Björkqvist, J., Nickel, K. F., Stavrou, E., and Renné, T. (2014). In vivo activation and functions of the protease factor XII. *Thromb. Haemos.* 112, 868–75. doi: 10.1160/th14-04-0311

Blaes, F., Fühlhuber, V., and Preissner, K. T. (2007). Identification of autoantigens in pediatric opsoclonus-myoclonus syndrome. *Exp. Rev. Clin. Immunol.* 3, 975–82. doi: 10.1586/1744666x.3.6.975

Burns, A. R., Walker, D. C., Brown, E. S., Thurmon, L. T., Bowden, R. A., Keese, C. R., et al. (1997). Neutrophil transendothelial migration is independent of tight junctions and occurs preferentially at tricellular corners. *J. Immunol.* 159, 2893–903.

Cabrera-Fuentes, H. A., Lopez, M. L., McCurdy, S., Fischer, S., Meiler, S., Baumer, Y., et al. (2015a). Regulation of monocyte/macrophage polarisation by extracellular RNA. *Thromb. Haemost.* 113, 473–81. doi: 10.1160/th14-06-0507

Cabrera-Fuentes, H. A., Niemann, B., Grieshaber, P., Wollbrueck, M., Gehron, J., Preissner, K. T., et al. (2015b). RNase1 as a potential mediator of remote ischaemic preconditioning for cardioprotection. *Eur. J. Cardiothorac. Surg.* 48, 732–7. doi: 10.1093/ejcts/ezu519

Cabrera-Fuentes, H. A., Ruiz-Meana, M., Simsekyilmaz, S., Kostin, S., Inserte, J., Saffarzadeh, M., et al. (2014). RNase1 prevents the damaging interplay between extracellular RNA and tumour necrosis factor-alpha in cardiac ischaemia/reperfusion injury. *Thromb. Haemos.* 112, 1110–9. doi: 10.1160/th14-08-0703

Cantuti-Castelvetri, L., Ojha, R., Pedro, L. D., Djannatian, M., Franz, J., Kuivanen, S., et al. (2020). Neuropilin-1 facilitates SARS-CoV-2 cell entry and infectivity. *Science* 370, 856–60.

Castanheira, F. V. S, and Kubes, P. (2019). Neutrophils and NETs in modulating acute and chronic inflammation. *Blood* 133, 2178–85. doi: 10.1182/blood-2018-11-844530

Chan, J. K., Roth, J., Oppenheim, J. J., Tracey, K. J., Vogl, T., Feldmann, M., et al. (2012). Alarmins: awaiting a clinical response. *J. Clin. Invest.* 122, 2711–9. doi: 10.1172/jci62423

Chandraratne, S., von Bruehl, M. L., Pagel, J. I., Stark, K., Kleinert, E., Konrad, I., et al. (2015). Critical role of platelet glycoprotein ibα in arterial remodeling. *Arterioscl. Throm. Vascul. Biol.* 35, 589–97.

Chavakis, T., Bierhaus, A., Al-Fakhri, N., Schneider, D., Witte, S., Linn, T., et al. (2003). The pattern recognition receptor (RAGE) is a counterreceptor for leukocyte integrins: a novel pathway for inflammatory cell recruitment. *J. Exp. Med.* 198, 1507–15.

Chavakis, T., May, A. E., Preissner, K. T., and Kanse, S. M. (1999). Molecular mechanisms of zinc-dependent leukocyte adhesion involving the urokinase receptor and beta2-integrins. *Blood* 93, 2976–83. doi: 10.1182/blood.v93.9.2976

Chen, C., Feng, Y., Zou, L., Wang, L., Chen, H. H., Cai, J. Y. (2014). Role of extracellular RNA and TLR3-Trif signaling in myocardial ischemia-reperfusion injury. *J. Am. Heart Assoc.* 3:e000683.

Chen, N., Xia, P., Li, S., Zhang, T., Wang, T. T., and Zhu, J. (2017). RNA sensors of the innate immune system and their detection of pathogens. *IUBMB Life* 69, 297–304. doi: 10.1002/iub.1625

Chen, N., Zhou, M., Dong, X., Qu, J., Gong, F., Han, Y., et al. (2020). Epidemiological and clinical characteristics of 99 cases of 2019 novel coronavirus pneumonia in Wuhan, China: a descriptive study. *Lancet* 395, 507–13. doi: 10.1016/s0140-6736(20)30211-7

Chen, Z., Larregina, A. T., and Morelli, A. E. (2019). Impact of extracellular vesicles on innate immunity. *Curr. Opin. Organ Transpl.* 24, 670–8. doi: 10.1097/mot.0000000000000701

Chillo, O., Kleinert, E. C., Lautz, T., Lasch, M., Pagel, J. I., Heun, Y., et al. (2016). Perivascular Mast Cells Govern Shear Stress-Induced Arteriogenesis by Orchestrating Leukocyte Function. *Cell Rep.* 16, 2197–207. doi: 10.1016/j.celrep.2016.07.040

Cho, S., Beintema, J. J., and Zhang, J. (2005). The Ribonuclease A superfamily of mammals and birds: identifying new members and tracing evolutionary histories. *Genomics* 85, 208–20. doi: 10.1016/j.ygeno.2004.10.008

Chung, M. K., Karnik, S., Saef, J., Bergmann, C., Barnard, J., Lederman, M. M., et al. (2020). SARS-CoV-2 and ACE2: The biology and clinical data settling the ARB and ACEI controversy. *EBioMedicine* 58:102907. doi: 10.1016/j.ebiom.2020.102907

Cicco, S., Cicco, G., Racanelli, V., and Vacca, A. (2020). Neutrophil Extracellular Traps (NETs) and Damage-Associated Molecular Patterns (DAMPs): Two Potential Targets for COVID-19 Treatment. *Mediat. Infl.* 2020:75 27953.

Cichon, C., Sabharwal, H., Rüter, C., and Schmidt, M. A. (2014). MicroRNAs regulate tight junction proteins and modulate epithelial/endothelial barrier functions. *Tissue Barr.* 2:e944446. doi: 10.4161/21688362.2014.944446

Creemers, E. E., Tijsen, A. J., and Pinto, Y. M. (2012). Circulating miroRNAs: novel biomarkers and extracellular communicators in cardiovascular disease? *Circ. Res.* 110, 483–95. doi: 10.1161/circresaha.111.247452

Crescitelli, R., Lässer, C., Szabó TG, Kittel, A., Eldh, M., Dianzani, I., et al. (2013). Distinct RNA profiles in subpopulations of extracellular vesicles: apoptotic bodies, microvesicles and exosomes. *J. Extr. Vesicl.* 12:2.

Danielson, K. M., Rubio, R., Abderazzaq, F., Das, S., and Wang, Y. E. (2017). High Throughput Sequencing of Extracellular RNA from Human Plasma. *PLoS One.* 12:e0164644. doi: 10.1371/journal.pone.0164644

Das, S., Ansel, K. M., Bitzer, M., Breakefield, X. O., Charest, A., Galas, D. J., et al. (2019). The Extracellular RNA Communication Consortium: Establishing Foundational Knowledge and Technologies for Extracellular RNA Research. *Cell* 177, 231–42.

Deindl, E., and Schaper, W. (2005). The art of arteriogenesis. *Cell Biochem. Biophys.* 43, 1–15.

Dickson, K. A., Haigis, M. C., and Raines, R. T. (2005). Ribonuclease inhibitor: structure and function. *Progr. Nucl. Acid Res. Mole. Biol.* 80, 349–74.

Ding, Z. M., Babensee, J. E., Simon, S. I., Lu, H., Perrard, J. L., Bullard, D. C., et al. (1999). Relative contribution of LFA-1 and Mac-1 to neutrophil adhesion and migration. *J. Immunol.* 163, 5029–38.

Dinger, M. E., Mercer, T. R., and Mattick, J. S. (2008). RNAs as extracellular signaling molecules. *J. Mol. Endocrinol.* 40, 151–9. doi: 10.1677/jme-07-0160

Döring, Y., Soehnlein, O., and Weber, C. (2017). Neutrophil Extracellular Traps in Atherosclerosis and Atherothrombosis. *Circul. Res.* 120, 736–43. doi: 10.1161/circresaha.116.309692

Duong, C. N., and Vestweber, D. (2020). Mechanisms Ensuring Endothelial Junction Integrity Beyond VE-Cadherin. *Front. Physiol.* 11:519. doi: 10.3389/fphys.2020.00519

Dvorak, A. M., Morgan, E. S., and Weller, P. F. (2003). RNA is closely associated with human mast cell lipid bodies. *Histol. Histopathol.* 18, 943–68.

Ehrchen, J. M., Sunderkötter, C., Foell, D., Vogl, T., and Roth, J. (2009). The endogenous Toll-like receptor 4 agonist S100A8/S100A9 (calprotectin) as innate amplifier of infection, autoimmunity, and cancer. *J. Leukocyte Biol.* 86, 557–66. doi: 10.1189/jlb.1008647

Ekström, K, Valadi, H., Sjöstrand, M., Malmhäll, C., Bossios, A., Eldh, M., et al. (2012). Characterization of mRNA and microRNA in human mast cell-derived exosomes and their transfer to other mast cells and blood CD34 progenitor cells. *J. Extr. Vesicl.* 1:18389 doi: 10.3402/jev.v1i0.18389

Eller, C. H., Lomax, J. E., and Raines, R. T. (2014). Bovine brain ribonuclease is the functional homolog of human ribonuclease 1. *J. Biol. Chem.* 289, 25996–6006. doi: 10.1074/jbc.m114.566166

Elsemuller, A. K., Tomalla, V., Gartner, U., Troidl, K., Jeratsch, S., Graumann, J., et al. (2019). Characterization of mast cell-derived rRNA-containing microvesicles and their inflammatory impact on endothelial cells. *FASEB J.* 33, 5457–67. doi: 10.1096/fj.201801853rr

Engelmann, B., and Massberg, S. (2013). Thrombosis as an intravascular effector of innate immunity. *Nat. Rev. Immunol.* 13, 34–45. doi: 10.1038/nri3345

Faber, J. E., Chilian, W. M., Deindl, E., von Royen, N., and Simons, M. (2014). A brief etymology of the collateral circulation. *Arterioscl. Thromb. Vasc. Biol.* 34, 1854–9.

Fischer, S. (2018). Pattern Recognition Receptors and Control of Innate Immunity: Role of Nucleic Acids. *Curr. Pharm. Biotechnol.* 19, 1203–9. doi: 10.2174/1389201012804583087

Fischer, S., and Preissner, K. T. (2013). Extracellular nucleic acids as novel alarm signals in the vascular system: Mediators of defence and disease. *Hämostaseologie* 33, 37–42. doi: 10.5482/hamo-13-01-0001

Fischer, S., Cabrera-Fuentes, H. A., Noll, T., and Preissner, K. T. (2014). Impact of extracellular RNA on endothelial barrier function. *Cell Tissue Res.* 355, 635–45. doi: 10.1007/s00441-014-1850-8

Fischer, S., Gerriets, T., Wessels, C., Walberer, M., Kostin, S., Stolz, E., et al. (2007). Extracellular RNA mediates endothelial-cell permeability via vascular endothelial growth factor. *Blood* 110, 2457–65. doi: 10.1182/blood-2006-08-040691

Fischer, S., Gesierich, S., Griemert, B., Schänzer, A., Acker, T., Augustin, H. G., et al. (2013). Extracellular RNA liberates Tumor-Necrosis-Factor-α to promote tumor cell trafficking and progression. *Cancer Res.* 73, 5080–9. doi: 10.1158/0008-5472.can-12-4657

Fischer, S., Grantzow, T., Pagel J-I, Tschernatsch, M., Sperandio, M., Preissner, K. T., et al. (2012). Extracellular RNA promotes leukocyte recruitment in the vascular system by mobilizing proinflammatory cytokines. *Thromb. Haemost.* 108, 730–41. doi: 10.1160/th12-03-0186

Fischer, S., Nishio, M., Dadkhahi, S., Gansler, J., Saffarzadeh, M., Shibamiyama, A., et al. (2011). Expression and localisation of vascular ribonucleases in endothelial cells. *Thromb. Haemost.* 105, 345–55. doi: 10.1160/th10-06-0345

Fischer, S., Nishio, M., Peters, S. C., Tschernatsch, M., Walberer, M., Weidemann, S., et al. (2009). Signaling mechanism of extracellular RNA in endothelial cells. *FASEB, J.* 23, 2100–9. doi: 10.1096/fj.08-121608

Fuchs, T. A., Brill, A., Duerschmied, D. (2010). Extracellular DNA traps promote thrombosis. *Proc. Natl. Acad. Sci.* 107, 15880–5. doi: 10.1073/pnas.1005743107

Ganguly, D., Chamilos, G., Lande, R., Gregorio, J., Meller, S., Facchinetti, V., et al. (2009). Self-RNA-antimicrobial peptide complexes activate human dendritic cells through TLR7 and TLR8. *J. Exp. Med.* 206, 1983–94. doi: 10.1084/jem.20090480

Gansler, J., Preissner, K. T., and Fischer, S. (2014). Influence of proinflammatory stimuli on the expression of vascular ribonuclease1 i endothelial cells. *FASEB J.* 28, 252–60.

Garnett, E. R., Lomax, J. E., Mohammed, B. M., Gailani, D., Sheehan, J. P., and Raines, R. T. (2019). Phenotype of ribonuclease 1 deficiency in mice. *RNA* 25, 921–34. doi: 10.1261/rna.070433.119

Goh, K. J., Choong, M. C., Cheong, E. H., Kalimuddin, S., Duu Wen, S., Phua, G. C., et al. (2020). Rapid Progression to Acute Respiratory Distress Syndrome: Review of Current Understanding of Critical Illness from COVID-19 Infection. *Anna. Acad. Med. Singap.* 49, 108–18. doi: 10.47102/annals-acadmedsg.202057

Gong, T., Liu, L., Jiang, W., and Zhou, R. (2020). DAMP-sensing receptors in sterile inflammation and inflammatory diseases. *Nat. Rev. Immunol.* 20, 95–112. doi: 10.1038/s41577-019-0215-7

Greinacher, A., Selleng, K., and Warkentin, T. E. (2017). Autoimmune heparin-induced thrombocytopenia. *J. Thromb. Haemos.* 15, 2099–114.

Gui, Y., Liu, H., Zhang, L., Lv, W., and Hu, X. (2015). Altered microRNA profiles in cerebrospinal fluid exosome in Parkinson disease and Alzheimer disease. *Oncotarget* 6, 37043–53. doi: 10.18632/oncotarget.6158

Guo, Q., Song, W. D., Li, H. Y., Li, M., Chen, X. K., Liu, H., et al. (2020). Cold-inducible RNA-binding protein might determine the severity and the presences of major/minor criteria for severe community-acquired pneumonia and best predicted mortality. *Respir. Res.* 21(1):192.

Haga, S., Yamamoto, N., Nakai-Murakami, C., Osawa, Y., Tokunaga, K., Sata, T., et al. (2008). Modulation of TNF-alpha-converting enzyme by the spike protein of SARS-CoV and ACE2 induces TNF-alpha production and facilitates viral entry. *Proc. Natl. Acad. Sci. U S A.* 105, 7809–14. doi: 10.1073/pnas.0711241105

Haigis, M. C., and Raines, R. T. (2003). Secretory ribonucleases are internalized by a dynamin-independent endocytic pathway. *J. Cell Sci.* 116, 313–24. doi: 10.1242/jcs.00214

Hammerschmidt, S. (2009). Surface-exposed adherence molecules of Streptococcus pneumoniae. *Methods Mole. Biol.* 470, 29–45. doi: 10.1007/978-1-59745-204-5_3

Hammerschmidt, S., Rohde, M., and Preissner, K. T. (2019). "Medicine, Nursing & Dentistry,"in *Gram-positive pathogens*. eds V. A. Fischetti, R. P. Novick,, J. J. Ferretti, D. A. Portnoy, M. Braunstein, and, J. I. Rood, (New Jersey: Wiley Online Library), 108–24.

Hamming, I., Timens, W., Bulthuis, M. L., Lely, A. T., Navis, G., and van Goor, H. (2004). Tissue distribution of ACE2 protein, the functional receptor for SARS coronavirus. A first step in understanding SARS pathogenesis. *J. Pathol.* 203, 631–7. doi: 10.1002/path.1570

Han, E. C., Choi, S. Y., Lee, Y., Park, J. W., Hong, S. H., and Lee, H. J. (2019). Extracellular RNAs in periodontopathogenic outer membrane vesicles promote TNF-α production in human macrophages and cross the blood-brain barrier in mice. *FASEB J.* 33, 13412–22. doi: 10.1096/fj.201901575r

Herster, F., Bittner, Z., Archer, N. K., Dickhöfer, S., Eisel, D., Eigenbrod, T., et al. (2020). Neutrophil extracellular trap-associated RNA and LL37 enable self-amplifying inflammation in psoriasis. *Nat. Commun.* 11(1):105.

Heurich, A., Hofmann-Winkler, H., Gierer, S., Liepold, T., Jahn, O., and Pöhlmann, S. (2014). TMPRSS2 and ADAM17 cleave ACE2 differentially and only proteolysis by TMPRSS2 augments entry driven by the severe acute respiratory syndrome coronavirus spike protein. *J. Virol.* 88, 1293–307. doi: 10.1128/jvi.02202-13

Heward, J. A., and Lindsay, M. A. (2014). Long non-coding RNAs in the regulation of the immune response. *Trends Immunol.* 35, 408–19. doi: 10.1016/j.it.2014.07.005

Hoffmann, M., Kleine-Weber, H., Schroeder, S., Krüger, N., Herrler, T., Erichsen, S., et al. (2020). SARS-CoV-2 Cell Entry Depends on ACE2 and TMPRSS2 and Is Blocked by a Clinically Proven Protease Inhibitor. *Cell* 181, 271–80.e8.

Holl, E. K., Shumansky, K. L., Pitoc, G., Ramsburg, E., and Sullenger, B. A. (2013). Nucleic acid scavenging polymers inhibit extracellular DNA-mediated innate immune activation without inhibiting anti-viral responses. *PLoS One.* 8(7):e69413. doi: 10.1371/journal.pone.0069413

Huang, C., Wang, Y., Li, X., Ren, L., Zhao, J., Hu, Y., et al. (2020). Clinical features of patients infected with 2019 novel coronavirus in Wuhan, China. *Lancet* 395, 497–506.

Huang, L. Y., Stuart, C., Takeda, K., D'Agnillo, F., and Golding, B. (2016). Poly(I:C) Induces Human Lung Endothelial Barrier Dysfunction by Disrupting Tight Junction Expression of Claudin-5. *PLoS One.* 11(8):e0160875. doi: 10.1371/journal.pone.0160875

Jaax, M. E., Krauel, K., Marschall, T., Brandt, S., Gansler, J., Fürll, B., et al. (2013). Complex formation with nucleic acids and aptamers alters the antigenic properties of platelet factor 4. *Blood* 122, 272–81. doi: 10.1182/blood-2013-01-478966

Jones, L. J., Yue, S. T., Cheung, C. Y., and Singer, V. L. (1998). RNA quantitation by fluorescence-based solution assay: RiboGreen reagent characterization. *Analyt. Biochem.* 265, 368–74. doi: 10.1006/abio.1998.2914

Kannemeier, C., Shibamiya, A., Nakazawa, F., Trusheim, H., Ruppert, C., Markart, P., et al. (2007). Extracellular RNA constitutes a natural procoagulant cofactor in blood coagulation. *Proc. Natl. Acad. Sci. U S A.* 104, 6388–93. doi: 10.1073/pnas.0608647104

Karki, P., and Birukov, K. G. (2018). Lipid mediators in the regulation of endothelial barriers. *Tissue Barr.* 6(1):e1385573. doi: 10.1080/21688370.2017.1385573

Kawasaki, T., and Kawai, T. (2019). Discrimination Between Self and Non-Self-Nucleic Acids by the Innate Immune System. *Int. Rev. Cell Mole. Biol.* 344, 1–30. doi: 10.1016/bs.ircmb.2018.08.004

Kim, K. M., Abdelmohsen, K., Mustapic, M., Kapogiannis, D., and Gorospe, M. (2017). RNA in extracellular vesicles. *Wiley Interdisc. Rev.* 8:1413

Kleinert, E., Langenmayer, M. C., Reichart, B., Kindermann, J., Griemert, B., Blutke, A., et al. (2016). Ribonuclease (RNase) prolongs survival of grafts in experimental heart transplantation. *J. Am. Heart Assoc.* 5:e003429.

Kluever, A. K., Braumandl, A., Fischer, S., Preissner, K. T., and Deindl, E. (2019). The Extraordinary Role of Extracellular RNA in Arteriogenesis, the Growth of Collateral Arteries. *Int. J. Mole. Sci.* 20:6177. doi: 10.3390/ijms20246177

Koczera, P., Martin, L., Marx, G., and Schuerholz, T. (2016). The ribonuclease A superfamily in humans: canonical RNases as the buttress of innate immunity. *Int. J. Mol. Sci.* 17, 1–16.

Kolaczkowska, E., and Kubes, P. (2013). Neutrophil recruitment and function in health and inflammation. *Nat. Rev. Immunol.* 13, 159–75. doi: 10.1038/nri3399

Kopreski, M. S., Benko, F. A., and Gocke, C. D. (2001). Circulating RNA as a tumor marker: detection of 5T4 mRNA in breast and lung cancer patient serum. *Ann. N Y Acad. Sci.* 945, 172–8. doi: 10.1111/j.1749-6632.2001.tb03882.x

Kopreski, M. S., Benko, F. A., Kwak, L. W., and Gocke, C. D. (1999). Detection of tumor messenger RNA in the serum of patients with malignant melanoma. *Clin. Cancer Res.* 5, 1961–5.

Kourtzelis, I., Hajishengallis, G., and Chavakis, T. (2020). Phagocytosis of Apoptotic Cells in Resolution of Inflammation. *Front. Immunol.* 11:553. doi: 10.3389/fimmu.2020.00553

Kourtzelis, I., Mitroulis, I., von Renesse, J., Hajishengallis, G., and Chavakis, T. (2017). From leukocyte recruitment to resolution of inflammation: the cardinal role of integrins. *J. Leukoc. Biol.* 102, 677–83. doi: 10.1189/jlb.3mr0117-024r

Kruger, A., Oldenburg, M., Chebrolu, C., Beisser, D., Kolter, J., Sigmund, A. M., et al. (2015). Human TLR8 senses UR/URR motifs in bacterial and mitochondrial RNA. *EMBO Rep.* 16, 1656–63. doi: 10.15252/embr.201540861

Kumar, P., Shen, Q., Pivetti, C. D., Lee, E. S., Wu, M. H., and Yuan, S. Y. (2009). Molecular mechanisms of endothelial hyperpermeability: implications in inflammation. *Exp. Rev. Mole. Med.* 11:e19.

Kwon, P. S., Oh, H., Kwon, S. J., Jin, W., Zhang, F., Fraser, K., et al. (2020). Sulfated polysaccharides effectively inhibit SARS-CoV-2 in vitro. *Cell Discov.* 6:50.

Labò N, Ohnuki, H., and Tosato, G. (2020). Vasculopathy and Coagulopathy Associated with SARS-CoV-2 Infection. *Cells* 9:1583. doi: 10.3390/cells9071583

Lambrecht, B. N., Vanderkerken, M., and Hammad, H. (2018). The emerging role of ADAM metalloproteinases in immunity. *Nat. Rev. Immunol.* 18, 745–58. doi: 10.1038/s41577-018-0068-5

Landré JB, Hewett, P. W., Olivot, J. M., Friedl, P., Ko, Y., Sachinidis, A., Moenner, M. et al. (2002). Human endothelial cells selectively express large amounts of pancreatic-type ribonuclease (RNase 1). *J. Cell Biochem.* 86, 540–52.

Lasch, M., Kleinert, E. C., Meister, S., Kumaraswami, K., Buchheim, J. I., Grantzow, T., et al. (2019). Extracellular RNA released due to shear stress controls natural bypass growth by mediating mechanotransduction in mice. *Blood* 134, 1469–79. doi: 10.1182/blood.2019001392

Lasch, M., Kumaraswami, K., Nasiscionyte, S., Kircher, S., van den Heuvel, D., Meister, S., et al. (2020). RNase A treatment interferes with leukocyte recruitment, neutrophil extracellular trap formation, and angiogenesis in ischemic muscle tissue. *Front. Physiol.* 11:576736. doi: 10.3389/fphys.2020.576736

Lee, J., Sohn, J. W., Zhang, Y., Leong, K. W., Pisetsky, D., and Sullenger, B. A. (2011). Nucleic acid-binding polymers as anti-inflammatory agents. *Proc. Natl. Acad. Sci. U S A.* 108, 14055–60. doi: 10.1073/pnas.1105777108

Lee, S. M., Yip, T. F., Yan, S., Jin, D. Y., Wei, H. L., Guo, R. T., et al. (2018). Recognition of Double-Stranded RNA and Regulation of Interferon Pathway by Toll-Like Receptor 10. *Front. Immunol.* 9:516. doi: 10.3389/fimmu.2018.00516

Lee-Huang, S., Huang, P. L., Sun, Y., Huang, P. L., Kung, H. F., Blithe, D. L., et al. (1999). Lysozyme and RNases as anti-HIV components in beta-core preparations of human chorionic gonadotropin. *Proc. Natl. Acad. Sci. U S A.* 96, 2678–81. doi: 10.1073/pnas.96.6.2678

Leifer, C. A., and Medvedev, A. E. (2016). Molecular mechanisms of regulation of Toll-like receptor signaling. *J. Leukoc. Biol.* 100, 927–41. doi: 10.1189/jlb.2mr0316-117rr

Leppkes, M., Knopf, J., Naschberger, E., Lindemann, A., Singh, J., Herrmann, I., et al. (2020). Vascular occlusion by neutrophil extracellular traps in COVID-19. *EBioMedicine* 58:102925.

Ley, K., Laudanna, C., Cybulsky, M. I., and Nourshargh, S. (2007). Getting to the site of inflammation: the leukocyte adhesion cascade updated. *Nat. Rev. Immunol.* 7, 678–89. doi: 10.1038/nri2156

Li, C., Xu, M. M., Wang, K., Adler, A. J., Vella, A. T., and Zhou, B. (2018). Macrophage polarization and meta-inflammation. *Transl. Res.* 191, 29–44.

Li, Y., and Shi, X. (2013). MicroRNAs in the regulation of TLR and RIG-I pathways. *Cell. Mole. Immunol.* 10, 65–71. doi: 10.1038/cmi.2012.55

Liu, B., Wang, X., Chen, T. Z., Li, G. L., Tan, C. C., Chen, Y., et al. (2016). Polarization of M1 tumor associated macrophage promoted by the activation of TLR3 signal pathway. *Asian Pacific J. Tropical Med.* 9, 484–8. doi: 10.1016/j.apjtm.2016.03.019

Lomax, J. E., Eller, C. H., and Raines, R. T. (2017). Comparative functional analysis of ribonuclease 1 homolog: molecular insights into evolving vertebrate physiology. *Biochem. J.* 474, 2219–33. doi: 10.1042/bcj20170173

Lugli, G., Cohen, A. M., Bennett, D. A., Shah, R. C., Fields, C. J., Hernandez, A. G., et al. (2015). Plasma Exosomal miRNAs in Persons with and without Alzheimer Disease: Altered Expression and Prospects for Biomarkers. *PLoS One.* 10:e0139233. doi: 10.1371/journal.pone.0139233

Ma, G., Chen, C., Jiang, H., Qiu, Y., Li, Y., Li, X., et al. (2017). Ribonuclease attenuates hepatic ischemia reperfusion induced cognitive impairment through the inhibition of inflammatory cytokines in aged mice. *Biomed. Pharmacother.* 90, 62–8. doi: 10.1016/j.biopha.2017.02.094

Maas, C., Oschatz, C., and Renné T. (2011). The plasma contact system 2.0. *Semin. Thromb. Hemos.* 37, 375–81.

Mandel, P., and Metais, P. (1948). Les acides nucleíques du plasma sangiun chez l'homme. *C R Acad. Sci.* 142, 241–3.

Marek, L. R., and Kagan, J. C. (2011). Deciphering the function of nucleic acid sensing TLRs one regulatory step at a time. *Front. Biosci.* 1, 2060–8. doi: 10.2741/3839

Massberg, S., Grahl, L., von Bruehl, M. L., Manukyan, D., Pfeiler, S., Goosmann, C., et al. (2010). Reciprocal coupling of coagulation and innate immunity via neutrophil serine proteases. *Nat. Med.* 16, 887–96. doi: 10.1038/nm.2184

May, A. E., Kanse, S. M., Lund, L. R., Gisler, R. H., Imhof, B. A., and Preissner, K. T. (1998). Urokinase receptor (CD87) regulates leukocyte recruitment via beta 2 integrins in vivo. *J. Exp. Med.* 188, 1029–37.

Miyake, K., Shibata, T., Ohto, U., and Shimizu, T. (2017). Emerging roles of the processing of nucleic acids and Toll-like receptors in innate immune responses to nucleic acids. *J. Leukoc. Biol.* 101, 135–42. doi: 10.1189/jlb.4mr0316-108r

Moutal, A., Martin, L. F., Boinon, L., Gomez, K., Ran, D., Zhou, Y., et al. (2020). SARS-CoV-2 Spike protein co-opts VEGF-A/Neuropilin-1 receptor signaling to induce analgesia. *bioRxiv : the preprint server for biology*. doi: 10.1101/2020.07.17.209288

Muller, W. A. (2013). Getting leukocytes to the site of inflammation. *Veter. Pathol.* 50, 7–22. doi: 10.1177/0300985812469883

Nakazawa, F., Kannemeier, C., Shibamiya, A., Song, Y., Tzima, E., Schubert, U., et al. (2005). Extracellular RNA is a natural cofacotr for the (auto-)activation of Factor VII-activating protease (FSAP). *Biochem. J.* 385, 831–8.

Naqvi, I., Gunaratne, R., McDade, J. E., Moreno, A., Rempel, R. E., Rouse, D. C., et al. (2018). Polymer-Mediated Inhibition of Pro-invasive Nucleic Acid DAMPs and Microvesicles Limits Pancreatic Cancer Metastasis. *Mole. Ther* 26, 1020–31. doi: 10.1016/j.ymthe.2018.02.018

Naudin, C., Burillo, E., Blankenberg, S., Butler, L., and Renné, T. (2017). Factor XII Contact Activation. *Semin. Thromb. Hemos.* 43, 814–26.

Noda, M., Ifuku, M., Hossain, M. S., and Katafuchi, T. (2018). Glial Activation and Expression of the Serotonin Transporter in Chronic Fatigue Syndrome. *Front. Psych.* 9:589. doi: 10.3389/fpsyt.2018.00589

Noll, F., Behnke, J., Leiting, S., Troidl, K., Alves, G. T., Muller-Redetzky, H., et al. (2017). Self-extracellular RNA acts in synergy with exogenous danger signals to promote inflammation. *PLoS One.* 12(12):e0190002. doi: 10.1371/journal.pone.0190002

Nourshargh, S., and Marelli-Berg, F. M. (2005). Transmigration through venular walls: a key regulator of leukocyte phenotype and function. *Trends Immunol.* 26, 157–65. doi: 10.1016/j.it.2005.01.006

O'Brien, K., Breyne, K., Ughetto, S., Laurent, L. C., and Breakefield, X. O. (2020). RNA delivery by extracellular vesicles in mammalian cells and its applications. *Nat. Rev. Mole. Cell Biol.* 21, 585–606. doi: 10.1038/s41580-020-0251-y

Ode, Y., Aziz, M., Jin, H., Arif, A., Nicastro, J. G., and Wang, P. (2019). Cold-inducible RNA-binding Protein Induces Neutrophil Extracellular Traps in the Lungs during Sepsis. *Scient. Rep.* 9(1):6252.

Ohashi, A., Murata, A., Cho, Y., Ichinose, S., Sakamaki, Y., Nishio, M., et al. (2017). The expression and localization of RNase and RNase inhibitor in blood cells and vascular endothelial cells in homeostasis of the vascular system. *PLoS One.* 12:e0174237. doi: 10.1371/journal.pone.0174237

Patton, J. G., Franklin, J. L., Weaver, A. M., Vickers, K., Zhang, B., Coffey, R. J., et al. (2015). Biogenesis, delivery, and function of extracellular RNA. *J. Extr. Vesicl.* 4:27494. doi: 10.3402/jev.v4.27494

Pérez-Boza, J., Lion, M., and Struman, I. (2018). Exploring the RNA landscape of endothelial exosomes. *RNA* 24, 423–35. doi: 10.1261/rna.064352.117

Perlman, S., and Netland, J. (2009). Coronaviruses post-SARS: update on replication and pathogenesis. *Nat. Rev. Microbiol.* 7, 439–50. doi: 10.1038/nrmicro2147

Petri, B., and Sanz, M. J. (2018). Neutrophil chemotaxis. *Cell Tissue Res.* 371, 425–36.

Petri, B., Phillipson, M., and Kubes, P. (2008). The physiology of leukocyte recruitment: an in vivo perspective. *J. Immunol.* 180, 6439–46. doi: 10.4049/jimmunol.180.10.6439

Phillipson, M., Heit, B., Colarusso, P., Liu, L., Ballantyne, C. M., and Kubes, P. (2006). Intraluminal crawling of neutrophils to emigration sites: a molecularly distinct process from adhesion in the recruitment cascade. *J. Exp. Med.* 203, 2569–75. doi: 10.1084/jem.20060925

Pipp, F., Boehm, K., Cai, W., Adili, W. J., Ziegler, B., Karanovic, G., et al. (2004). elevated fluid shear stress enhances postocclusive collateral growth and gene expression in the pig hind limb. *Arterioscl. Thromb. Vasc. Biol.* 24, 1664–8. doi: 10.1161/01.atv.0000138028.14390.e4

Pirher, N., Pohar, J., Mancek-Keber, M., Bencina, M., and Jerala, R. (2017). Activation of cell membrane-localized Toll-like receptor 3 by siRNA. *Immunol. Lett.* 189, 55–63. doi: 10.1016/j.imlet.2017.03.019

Pober, J. S., and Sessa, W. C. (2007). Evolving functions of endothelial cells in inflammation. *Nat. Rev. Immunol.* 7, 803–15. doi: 10.1038/nri2171

Preissner, K. T., and Herwald, H. (2017). Extracellular nucleic acids in immunity and cardiovascular responses: between alert and disease. *Thrombosis Haemostasis* 117, 1272–82. doi: 10.1160/th-16-11-0858

Qiang, X., Yang, W. L., Wu, R., Zhou, M., Jacob, A., Dong, W., et al. (2013). Cold-inducible RNA-binding protein (CIRP) triggers inflammatory responses in hemorrhagic shock and sepsis. *Nat. Med.* 19, 1489–95.

Quinn, J. F., Patel, T., Wong, D., Das, S., Freedman, J. E., Laurent, L. C., et al. (2015). Extracellular RNAs: development as biomarkers of human disease. *J. Extr. Vesicl.* 4:27495. doi: 10.3402/jev.v4.27495

Rajgor, D. D., Lee, M. H., Archuleta, S., Bagdasarian, N., and Quek, S. C. (2020). The many estimates of the COVID-19 case fatality rate. *Lancet Infect. Dis.* 20, 776–7. doi: 10.1016/s1473-3099(20)30244-9

Randriamboavonjy, V., and Fleming, I. (2018). Platelet communication with the vascular wall: role of platelet-derived microparticles and non-coding RNAs. *Clin. Sci.* 132, 1875–88. doi: 10.1042/cs20180580

Ren, L. L., Wang, Y. M., Wu, Z. Q., Xiang, Z. C., Guo, L., Xu, T., et al. (2020). Identification of a novel coronavirus causing severe pneumonia in human: a descriptive study. *Chin. Med. J.* 133, 1015–24.

Renné T, and Stavrou, E. X. (2019). Roles of Factor XII in Innate Immunity. *Front. Immunol.* 10:2011. doi: 10.3389/fimmu.2019.02011

Roers, A., Hiller, B., and Hornung, V. (2016). Recognition of endogenous nucleic acids by the innate immune system. *Immunity* 44, 739–54. doi: 10.1016/j.immuni.2016.04.002

Rot, A., and von Andrian, U. H. (2004). Chemokines in innate and adaptive host defense: basic chemokinese grammar for immune cells. *Annu. Rev. Immunol.* 22, 891–928. doi: 10.1146/annurev.immunol.22.012703.104543

Rutkoski, T. J., and Raines, R. T. (2008). Evasion of ribonuclease inhibitor as a determinant of ribonuclease cytotoxicity. *Curr. Pharm. Biotechnol.* 9, 185–9. doi: 10.2174/138920108784567344

Rykova, E. Y., Morozkin, E. S., Ponomaryova, A. A., Loseva, E. M., Zaporozhchenko, I. A., Dherdyntseva, N. V., et al. (2012). Cell-free and cell-bound circulating nucleic acid complexes: mechanism of generation, concentration and content. *Expert. Opin. Biol. Ther.* 12, 141–53.

Sariol, A., and Perlman, S. (2020). Lessons for COVID-19 Immunity from Other Coronavirus Infections. *Immunity* 53, 248–63. doi: 10.1016/j.immuni.2020.07.005

Saugstad, J. A., Lusardi, T. A., Van Keuren-Jensen, K. R., Phillips, J. I., Lind, B., Harrington, C. A., et al. (2017). Analysis of extracellular RNA in cerebrospinal fluid. *J. Extra. Vesicl.* 6:1317577.

Scheller, J., Chalaris, A., Garbers, C., and Rose-John, S. (2011). ADAM17: a molecular switch to control inflammation and tissue regeneration. *Trends Immunol.* 32, 380–7. doi: 10.1016/j.it.2011.05.005

Schenkel, A. R., Mamdouh, Z., and Muller, W. A. (2004). Locomotion of monocytes on endothelium is a critical step during extravasation. *Nat. Immunol.* 5, 393–400. doi: 10.1038/ni1051

Schillemans, M., Karampini, E., Kat, M., and Bierings, R. (2019). Exocytosis of Weibel-Palade bodies: how to unpack a vascular emergency kit. *J. Thromb. Haemos.* 17, 6–18. doi: 10.1111/jth.14322

Schmaier, A. H. (2016). The contact activation and kallikrein/kinin systems: pathophysiologic and physiologic activities. *J. Thromb. Haemos.* 14, 28–39. doi: 10.1111/jth.13194

Schmaier, A. H. (2018). Plasma Prekallikrein: Its Role in Hereditary Angioedema and Health and Disease. *Front. Med.* 5:3. doi: 10.3389/fmed.2018.00003

Schmaier, A. H., and Stavrou, E. X. (2019). Factor XII - What's important but not commonly thought about. *Res. Pract. Thromb. Haemos.* 3, 599–606. doi: 10.1002/rth2.12235

Schymeinsky, J., Sperandio, M., and Walzog, B. (2011). The mammalian actin-binding protein 1 (mAbp1): a novel molecular player in leukocyte biology. *Trends Cell Biol.* 21, 247–55. doi: 10.1016/j.tcb.2010.12.001

Shang, X. Z., and Issekutz, A. C. (1998). Contribution of CD11a/CD18, CD11b/CD18, ICAM-1 (CD54) and -2 (CD102) to human monocyte migration through endothelium and connective tissue fibroblast barriers. *Eur. J. Immunol.* 28, 1970–9. doi: 10.1002/(sici)1521-4141(199806)28:06<1970::aid-immu1970>3.0.co;2-h

Sharifpanah, F., De Silva, S., Bekhite, M. M., Hurtado-Oliveros, J., Preissner, K. T., Wartenberg, M., et al. (2015). Stimulation of vasculogenesis and leukopoiesis of embryonic stem cells by extracellular transfer RNA and ribosomal RNA. *Free Radic. Biol. Med.* 89, 1203–17. doi: 10.1016/j.freeradbiomed.2015.10.423

Shaw, S. K., Ma, S., Kim, M. B., Rao, R. M., Hartman, C. U., Froio, R. M., et al. (2004). Coordinated redistribution of leukocyte LFA-1 and endothelial cell ICAM-1 accompany neutrophil transmigration. *J. Exp. Med.* 200, 1571–80. doi: 10.1084/jem.20040965

Simsekyilmaz, S., Cabrera-Fuentes, H. A., Meiler, S., Kostin, S., Baumer, Y., Liehn, E. A., et al. (2014). The Role of Extracellular RNA in Atherosclerotic Plaque Formation in Mice. *Circulation* 129, 598–606. doi: 10.1161/circulationaha.113.002562

Sirois, C. M., Jin, T., Miller, A. L., Bertheloot, D., Nakamura, H., Horvath, G. L., et al. (2013). RAGE is a nucleic acid receptor that promotes inflammatory responses to DNA. *J. Exp. Med.* 210, 2447–63. doi: 10.1084/jem.20120201

Small, J., Roy, S., Alexander, R., and Balaj, L. (2018). Overview of Protocols for Studying Extracellular RNA and Extracellular Vesicles. *Methods Mole. Biol.* 1740, 17–21. doi: 10.1007/978-1-4939-7652-2_2

Sorrentino, S. (2010). The eight human canonical ribonucleases: molecular diversity, catalytic properties, and special biological actions of the enzyme proteins. *FEBS Lett.* 584, 2194–200. doi: 10.1016/j.febslet.2010.04.018

Sorvillo, N., Cherpokova, D., Martinod, K., and Wagner, D. D. (2019). Extracellular DNA NET-Works With Dire Consequences for Health. *Circul. Res.* 125, 470–88. doi: 10.1161/circresaha.119.314581

Spiezia, L., Boscolo, A., Poletto, F., Cerruti, L., Tiberio, I., Campello, E., et al. (2020). COVID-19-Related Severe Hypercoagulability in Patients Admitted to Intensive Care Unit for Acute Respiratory Failure. *Thromb. Haemos.* 120, 998–1000. doi: 10.1055/s-0040-1710018

Springer, T. A., Thompson, W. S., Miller, L. J., Schmalstieg, F. C., and Anderson, D. C. (1984). Inherited deficiency of the Mac-1, LFA-1, p150,95 glycoprotein family and its molecular basis. *J. Exp. Med.* 160, 1901–18. doi: 10.1084/jem.160.6.1901

Stamenkovic, I. (2003). Extracellular matrix remodelling: the role of matrix metalloproteinases. *J. Pathol.* 200, 448–64. doi: 10.1002/path.1400

Stieger, P., Daniel, J. M., Thölen, C., Dutzmann, J., Knöpp, K., Gündüz, D, et al. (2017). Targeting of extracellular RNA reduces edema formation and infarct size and improves survival after myocardial infarction in mice. *J. Am. Heart Assoc.* 21:e004541.

Sukriti, S., Tauseef, M., Yazbeck, P., and Mehta, D. (2014). Mechanisms regulating endothelial permeability. *Pulmon. Circul.* 4, 535–51. doi: 10.1086/677356

Sullenger, B. A., and Nair, S. (2016). From the RNA world to the clinic. *Science* 352, 1417–20. doi: 10.1126/science.aad8709

Sullivan, D. P., and Muller, W. A. (2014). Neutrophil and monocyte recruitment by PECAM, CD99, and other molecules via the LBRC. *Semin. Immunopathol.* 36, 193–209. doi: 10.1007/s00281-013-0412-6

Tang, N., Bai, H., Chen, X., Gong, J., Li, D., and Sun, Z. (2020a). Anticoagulant treatment is associated with decreased mortality in severe coronavirus disease 2019 patients with coagulopathy. *J. Thromb. Haemos.* 18, 1094–9. doi: 10.1111/jth.14817

Tang, N., Li, D., Wang, X., and Sun, Z. (2020b). Abnormal coagulation parameters are associated with poor prognosis in patients with novel coronavirus pneumonia. *J. Thromb. Haemos.* 18, 844–7. doi: 10.1111/jth.14768

Tanriverdi, K., Kucukural, A., Mikhalev, E., Tanriverdi, S. E., Lee, R., Ambros, V. R., et al. (2016). Comparison of RNA isolation and associated methods for extracellular RNA detection by high-throughput quantitative polymerase chain reaction. *Analyt. Biochem.* 501, 66–74. doi: 10.1016/j.ab.2016.02.019

Tay, M. Z., Poh, C. M., Rénia, L., MacAry, P. A., and Ng, L. F. P. (2020). The trinity of COVID-19: immunity, inflammation and intervention. *Nat. Rev. Immunol.* 20, 363–74. doi: 10.1038/s41577-020-0311-8

Thachil, J. (2020). The versatile heparin in COVID-19. *J. Thromb. Haemos.* 18, 1020–2. doi: 10.1111/jth.14821

Thålin, C., Hisada, Y., Lundström, S, Mackman, N., and Wallén, H. (2019). Neutrophil Extracellular Traps: Villains and Targets in Arterial, Venous, and Cancer-Associated Thrombosis. *Arterioscl. Thromb. Vascul. Biol.* 39, 1724–38. doi: 10.1161/atvbaha.119.312463

Thiam, H. R., Wong, S. L., Wagner, D. D., and Waterman, C. M. (2020). Cellular Mechanisms of NETosis. *Annu. Rev. Cell Devel. Biol.* 36, 191–218. doi: 10.1146/annurev-cellbio-020520-111016

Thierry, A. R., and Roch, B. (2020). Neutrophil Extracellular Traps and By-Products Play a Key Role in COVID-19: Pathogenesis, Risk Factors, and Therapy. *J. Clin. Med.* 9:2942. doi: 10.3390/jcm9092942

Thomas, M. C., Pickering, R. J., Tsorotes, D., Koitka, A., Sheehy, K., Bernardi, S., et al. (2010). Genetic Ace2 deficiency accentuates vascular inflammation and atherosclerosis in the ApoE knockout mouse. *Circul. Res.* 107, 888–97. doi: 10.1161/circresaha.110.219279

Tielking, K., Fischer, S., Preissner, K. T., Vajkoczy, P., and Xu, R. (2019). Extracellular RNA in Central Nervous System Pathologies. *Front. Mole. Neurosci.* 12:254. doi: 10.3389/fnmol.2019.00254

Tisoncik, J. R., Korth, M. J., Simmons, C. P., Farrar, J., Martin, T. R., and Katze, M. G. (2012). Into the eye of the cytokine storm. *Microbiol. Mol. Biol. Rev.* 76, 16–32.

Tosar, J. P., and Cayota, A. (2018). Detection and Analysis of Non-vesicular Extracellular RNA. *Methods Mole. Biol.* 1740, 125–37. doi: 10.1007/978-1-4939-7652-2_10

Underhill, D. M., Gordon, S., Imhof, B. A., Núñez, G., and Bousso, P. (2016). Élie Metchnikoff (1845-1916): celebrating 100 years of cellular immunology and beyond. *Nat. Rev. Immunol.* 16, 651–6.

Valadi, H., Ekström, K, Bossios, A., Sjöstrand, M., Lee, J. J., and Lötvall, J. O. (2007). Exosome-mediated transfer of mRNAs and microRNAs is a novel mechanism of genetic exchange between cells. *Nat. Cell Biol.* 9, 654–9. doi: 10.1038/ncb1596

van der Vos, K. E., Abels, E. R., Zhang, X., Lai, C., Carrizosa, E., Oakley, D., et al. (2016). Directly visualized glioblastoma-derived extracellular vesicles transfer RNA to microglia/macrophages in the brain. *Neuro. Oncol.* 18, 58–69. doi: 10.1093/neuonc/nov244

Van Kaer, L., Parekh, V. V., and Wu, L. (2013). Invariant natural killer T cells as sensors and managers of inflammation. *Trends Immunol.* 34, 50–8. doi: 10.1016/j.it.2012.08.009

Vénéreau, E., Ceriotti, C., and Bianchi, M. E. (2015). DAMPs from cell death to new life. *Front. Immunol.* 6, 1–11. doi: 10.3389/fimmu.2015.00422

Vestweber, D. (2015). How leukocytes cross the vascular endothelium. *Nat. Rev. Immunol.* 15, 692–704. doi: 10.1038/nri3908

Vickers, K. C., Palmisano, B. T., Shoucri, B. M., Shamburek, R. D., and Remaley, A. T. (2011). MicroRNAs are transported in plasma and delivered to recipient cells by high-density lipoproteins. *Nat. Cell Biol.* 13, 423–33. doi: 10.1038/ncb2210

Voisin, M. B., and Nourshargh, S. (2019). Neutrophil trafficking to lymphoid tissues: physiological and pathological implications. *J. Pathol.* 247, 662–71. doi: 10.1002/path.5227

von Brühl, M. L., Stark, K., Steinhart, A., Chandraratne, S., Konrad, I., Lorenz, M., et al. (2012). Monocytes, neutrophils, and platelets cooperate to initiate and propagate venous thrombosis in mice in vivo. *J. Exp. Med.* 209, 819–35. doi: 10.1084/jem.20112322

Vu, T. T., Zhou, J., Leslie, B. A., Stafford, A. R., Fredenburgh, J. C., Ni, R., et al. (2015). Arterial thrombosis is accelerated in mice deficient in histidine-rich glycoprotein. *Blood* 125, 2712–9. doi: 10.1182/blood-2014-11-611319

Walberer, M., Tschernatsch, M., Fischer, S., Ritschel, N., Volk, K., Friedrich, C., et al. (2009). RNase therapy assessed by magnetic resonance imaging reduces cerebral edema and infarction size in acute stroke. *Curr. Neurovasc. Res.* 6, 12–9. doi: 10.2174/156720209787466037

Wang, J., Chai, J., and Wang, H. (2016). Structure of the mouse Toll-like receptor 13 ectodomain in complex with a conserved sequence from bacterial 23S ribosomal RNA. *FEBS J.* 283, 1631–5. doi: 10.1111/febs.13628

Wang, S., Voisin, M. B., Larbi, K. Y., Dangerfield, J., Scheiermann, C., Tran, M., et al. (2006). Venular basement membranes contain specific matrix protein low expression regions that act as exit points for emigrating neutrophils. *J. Exp. Med.* 203, 1519–32. doi: 10.1084/jem.20051210

Weber, C., Fraemohs, L., and Dejana, E. (2007). The role of junctional adhesion molecules in vascular inflammation. *Nat. Rev. Immunol.* 7, 467–77. doi: 10.1038/nri2096

Weber, C., Schober, A., and Zernecke, A. (2010). MicroRNAs in arterial remodelling, inflammation and atherosclerosis. *Curr. Drug Target* 11, 950–6. doi: 10.2174/138945010791591377

Wieczorek, A. J., Rhyner, C., and Block, L. H. (1985). Isolation and characterization of an RNA-proteolipid complex assiciated with the malignant state in humans. *Proc. Natl. Acad. Sci. U S A.* 82, 3455–9. doi:10.1073/pnas.82.10.3455

Willebrords, J., Crespo Yanguas, S., Maes, M., Decrock, E., Wang, N., Leybaert, L., et al. (2016). Connexins and their channels in inflammation. *Crit. Rev. Biochem. Mole. Biol.* 51, 413–39.

Wittchen, E. S., van Buul, J. D., Burridge, K., and Worthylake, R. A. (2005). Trading spaces: Rap, Rac, and Rho as architects of transendothelial migration. *Curr. Opin. Hematol.* 12, 14–21. doi: 10.1097/01.moh.0000147892.83713.a7

Wu, Y., Liu, Y., Lu, C., Lei, S., Li, J., and Du, G. (2020). Quantitation of RNA by a fluorometric method using the SYTO RNASelect stain. *Analyt. Biochem.* 606:113857. doi: 10.1016/j.ab.2020.113857

Wu, Z., and McGoogan, J. M. (2020). Characteristics of and Important Lessons From the Coronavirus Disease 2019 (COVID-19) Outbreak in China: Summary of a Report of 72 314 Cases From the Chinese Center for Disease Control and Prevention. *JAMA* 323, 1239–42. doi: 10.1001/jama.2020.2648

Yamamoto, M., Sato, S., Hemmi, H., Hoshino, K., Kaisho, T., Sanjo, H., et al. (2003). Role of Adaptor TRIF in the MyD88-independent toll-like receptor signaling pathway. *Science* 301, 640–2. doi: 10.1126/science.1087262

Yang, D., Chen, Q., Rosenberg, H. F., Rybak, S. M., Newton, D. L., Wang, Z. Y., et al. (2004). Human ribonuclease A superfamily members, eosinophil-derived neurotoxin and pancreatic ribonuclease, induce dendritic cell maturation and activation. *J. Immunol.* 173, 6134–42. doi: 10.4049/jimmunol.173.10.6134

Yang, W. L., Sharma, A., Wang, Z., Li, Z., Fan, J., and Wang, P. (2016). Cold-inducible RNA-binding protein causes endothelial dysfunction via activation of Nlrp3 inflammasome. *Scient. Rep.* 6:26571.

Yonekawa, K., and Harlan, J. M. (2005). Targeting leukocyte integrins in human diseases. *J. Leukoc. Biol.* 77, 129–40. doi: 10.1189/jlb.0804460

Yu, L., Wang, L., and Chen, S. (2010). Endogenous toll-like receptor ligands and their biological significance. *J. Cell Mol. Med.* 14, 2592–603. doi: 10.1111/j.1582-4934.2010.01127.x

Yuan, T., Huang, X., Woodcock, M., Du, M., Dittmar, R., Wang, Y., et al. (2016). Plasma extracellular RNA profiles in healthy and cancer patients. *Sci. Rep.* 6:19413.

Zakrzewicz, D., Bergmann, S., Didiasova, M., Giaimo, B. D., Borggrefe, T., Mieth, M., et al. (2016). Host-derived extracellular RNA promotes adhesion of Streptococcus pneumoniae to endothelial and epithelial cells. *Sci. Rep.* 6, 1–13.

Zechendorf, E., O'Riordan, C. E., Stiehler, L., Wischmeyer, N., Chiazza, F., Collotta, D., et al. (2020). Ribonuclease 1 attenuates septic cardiomyopathy and cardiac apoptosis in a murine model of polymicrobial sepsis. *JCI Insight.* 5:e131571.

Zernecke, A., and Preissner, K. T. (2016). Extracellular ribonucleic acids (RNA) enter the stage in cardiovascular disease. *Circ. Res.* 118, 469–79. doi: 10.1161/circresaha.115.307961

Zernecke, A., Bidzhekov, K., Noels, H., Shagdarsuren, E., Gan, L., Denecke, B., et al. (2009). Delivery of microRNA-126 by apoptotic bodies induces CXCL12-dependent vascular protection. *Sci. Signal.* 2:ra81. doi: 10.1126/scisignal.2000610

Zhang, L. J., Sen, G. L., Ward, N. L., Johnston, A., Chun, K., Chen, Y., et al. (2016). Antimicrobial Peptide LL37 and MAVS Signaling Drive Interferon-β Production by Epidermal Keratinocytes during Skin Injury. *Immunity* 45, 119–30. doi: 10.1016/j.immuni.2016.06.021

Zhou, Z., Wu, Q., Yan, Z., Zheng, H., Chen, C. J., Liu, Y., et al. (2019). Extracellular RNA in a single droplet of human serum reflects physiologic and disease states. *Proc. Natl. Acad. Sci. U S A.* 116, 19200–8. doi: 10.1073/pnas.1908252116

Zhu, N., Zhang, D., Wang, W., Li, X., Yang, B., Song, J., et al. (2020). A Novel Coronavirus from Patients with Pneumonia in China, 2019. *N Engl. J. Med.* 382, 727–33.

Zimmermann-Geller, B., Köppert, S., Fischer, S., Cabrera-Fuentes, H. A., Lefévre, S., Rickert, M., et al. (2016). Influence of extracellular RNAs, released by rheumatoid arthritis synovial fibroblasts, on their adhesive and invasive properties. *J. Immunol.* 197, 2589–97. doi: 10.4049/jimmunol.1501580

Zindel, J., and Kubes, P. (2020). DAMPs, PAMPs, and LAMPs in Immunity and sterile inflammation. *Annu. Rev. Pathol. Mech. Dis.* 15, 493–518. doi:10.1146/annurev-pathmechdis-012419-032847

Zunke, F., and Rose-John, S. (2017). The shedding protease ADAM17: Physiology and pathophysiology. *Biochim. Biophys. Acta Mole. Cell Res.* 1864, 2059–70. doi:10.1016/j.bbamcr.2017.07.001

Conflict of Interest: The authors declare that the research was conducted in the absence of any commercial or financial relationships that could be construed as a potential conflict of interest.

frontiers in Cell and Developmental Biology

MINI REVIEW
published: 11 January 2021
doi: 10.3389/fcell.2020.624958

Determinants of Phagosomal pH During Host-Pathogen Interactions

Johannes Westman[1] *and Sergio Grinstein*[1,2]*

[1] Program in Cell Biology, The Hospital for Sick Children, Toronto, ON, Canada, [2] Department of Biochemistry, University of Toronto, Toronto, ON, Canada

The ability of phagosomes to halt microbial growth is intimately linked to their ability to acidify their luminal pH. Establishment and maintenance of an acidic lumen requires precise co-ordination of H^+ pumping and counter-ion permeation to offset the countervailing H^+ leakage. Despite the best efforts of professional phagocytes, however, a number of specialized pathogens survive and even replicate inside phagosomes. In such instances, pathogens target the pH-regulatory machinery of the host cell in an effort to survive inside or escape from phagosomes. This review aims to describe how phagosomal pH is regulated during phagocytosis, why it varies in different types of professional phagocytes and the strategies developed by prototypical intracellular pathogens to manipulate phagosomal pH to survive, replicate, and eventually escape from the phagocyte.

Keywords: pH, phagocytosis, macrophage, pathogen, V-ATPase, proton, phagosome acidification, ion transport

OPEN ACCESS

Edited by:
Xunbin Wei,
Peking University, China

Reviewed by:
Thierry Soldati,
Université de Genève, Switzerland
Rongrong Liu,
Northwestern University, United States
Lai Wen,
La Jolla Institute for Immunology (LJI), United States

***Correspondence:**
Sergio Grinstein
sergio.grinstein@sickkids.ca

Specialty section:
This article was submitted to Cell Adhesion and Migration, a section of the journal Frontiers in Cell and Developmental Biology

Received: *01 November 2020*
Accepted: *15 December 2020*
Published: *11 January 2021*

Citation:
Westman J and Grinstein S (2021) Determinants of Phagosomal pH During Host-Pathogen Interactions. Front. Cell Dev. Biol. 8:624958. doi: 10.3389/fcell.2020.624958

INTRODUCTION TO PHAGOCYTOSIS

Innate immune cells such as macrophages, neutrophils and dendritic cells (DC) carry out an astounding variety of functions, ranging from killing invading pathogens to cytokine production, antigen presentation, and tissue homeostasis. Phagocytosis, an essential response of these cells – collectively termed professional phagocytes– is an elegant and complex process involving the recognition, engulfment, and degradation of foreign or dead material, which has unquestionable importance in innate immunity. Phagocytes are endowed with an assortment of receptors that initiate the internalization of diverse target particles. Some phagocytic receptors recognize endogenous patterns on the surface of the foreign target, while others identify their prey indirectly by interacting with opsonins (serum components) bound to the target's surface (Flannagan et al., 2012). Independently of the receptors and ligands involved, their interaction spawns an intricate intracellular signaling system culminating in the protrusion of the plasma membrane around the target, leading to its complete envelopment and internalization (Niedergang and Grinstein, 2018). After internalization, phagosomes acquire microbicidal and degradative capacity by a graded process called phagosome maturation. The nascent phagosome sequentially fuses with early endosomes, late endosomes, and ultimately, lysosomes, leading to the accrual of vacuolar proton (H^+)-pumping ATPases (V-ATPases), NADPH oxidase, and a variety of microbicidal peptides and degradative enzymes (Flannagan et al., 2012). Regulation of the phagosomal pH is of importance for most phagosomal functions. V-ATPases –that are normally enriched in late endosomes and lysosomes– are gradually acquired by phagosomes during the course of their maturation and are the source of their luminal acidification; they utilize energy derived from ATP hydrolysis to pump cytosolic H^+ into the phagosome lumen. Regulation of the phagosomal pH is, however, an intricate

process, also depending on the permeability to counter-ions and the "leak" of H^+ equivalents. Why these events are of high importance, how they are strictly regulated, and how pathogens share strategies to subvert phagosomal pH are further discussed in this review.

WHY IS THERE A NEED FOR PHAGOSOMAL PH REGULATION?

Phagosomal acidification is a hallmark of phagosome maturation, and the progressive luminal acidification results from the gradual increase of active V-ATPases. Various key functions of professional phagocytes require phagosomal acidification. For example, phagocytic receptors, including Fcγ receptors, integrins, and C-type lectin receptors such as dectin-1, are initially internalized along with the prey but need to be recycled to the cell surface. pH alters the affinity of the interaction between the phagocytic receptors and their ligands. The intraphagosomal acidification enables the dissociation and recycling of phagocytic receptors back to the plasmalemma (Buckley et al., 2016).

Perhaps more apparent is the role of phagosomal acidification in facilitating the microbicidal response. Low pH is critical for the converting of zymogens, such as nucleases, lipases, and proteases, to their active, degradative form. For example, cathepsin B is delivered to immature phagosomes as pro-cathepsin B. Progression to the more acidic mature phagosome (or phagolysosome) is accompanied by a conformational change of the pro-cathepsin B followed by its autoactivation and cleavage, yielding the mature enzyme (Pungercar et al., 2009). Additionally, the NADPH oxidase requires H^+ to generate hydrogen peroxide (H_2O_2), an important microbicidal reactive oxygen species (ROS), inside the phagosome (**Figure 1**). Superoxide anions (O_2^-), the primary product of the NADPH oxidase, are spontaneously dismutated into H_2O_2 in an acidic environment, consuming luminal H^+ (Nauseef, 2019; **Figure 1**). Along with chloride (Cl^-), H^+ are also required for the generation of hypochlorous acid (HOCl) from H_2O_2 by phagosomal myeloperoxidase (MPO) (**Figure 1**). HOCl is yet another powerful antimicrobial agent, and similar to H^+, a deficient supply of this anion in phagosomes is linked to defects in innate immunity (Wang, 2016).

Phagocytes can also exert microbiostatic or microbicidal effects by limiting the macro- and micro-nutrients available to the ingested pathogen while inside the phagosome. To limit intraphagosomal microbial replication, the membrane-associated transporter of divalent metal cations natural resistance-associated macrophage protein 1 (NRAMP1, also known as SLC11A1) depletes the phagosome of Fe^{2+}, Mn^{2+}, and Mg^{2+} (**Figure 1**). The force driving the efflux of these essential metal ions is the transmembrane H^+ gradient generated by the V-ATPase. Attesting to its importance, mutations in NRAMP1 impair the resistance of mice to infections with intracellular pathogens such as *Salmonella, Leishmania*, and *Mycobacterium* (Govoni and Gros, 1998), and susceptibility to leprosy is linked to the human NRAMP1 gene (Abel et al., 1998). Luminal H^+ are likewise crucial for nutrient absorption after microbial killing. For example, amino acids derived from the degradation of dead microbial or apoptotic cells are transported out of the phagolysosome into the cytosol via H^+-coupled solute carrier (SLC) transporters (**Figure 1**).

Protonation of microbial components in the acidic phagosomal lumen will, in some cases, stimulate acid stress responses of the microorganism, which can either facilitate or impair their ability to survive intracellularly (Guan and Liu, 2020).

Lastly, precise regulation of the phagosomal pH is also required for optimal antigen presentation, an essential reaction linking the innate and acquired immune systems. DCs, the quintessential antigen-presenting cells, must degrade incoming proteins to generate peptides suitable for presentation to lymphoid cells. Unrestrained degradation, however, will yield inappropriately small peptides; thus, an intermediate phagosomal pH is required to prevent excessive proteolysis of antigens prior to loading onto MHC class II glycoproteins.

HOW IS PHAGOSOMAL PH REGULATED?

Phagocytosis can be conceptually divided into two events: phagosome formation and phagosome maturation. Phagosome formation refers to the binding of the target particle followed by the actin-dependent extension of pseudopodia and lamellipodia that are often circular that encircle and ultimately trap the prey in a sealed vacuole, the nascent phagosome (see review (Niedergang and Grinstein, 2018) for how to build a phagosome). Immediately after closure and scission, the nascent phagosome's luminal pH reflects the extracellular pH, as the bulk fluid inside the lumen originates from the surrounding milieu. As stated earlier, a gradual maturation process ensues, whereby early endosomes, late endosomes, and lysosomes fuse with phagosomes. Phosphoinositides, Rab GTPases, soluble N-ethylmaleimide-sensitive-factor attachment protein receptors (SNAREs) and coat/tubulating proteins dictate maturation by signaling and mediating fusion and fission events at the phagosomal membrane (Fairn and Grinstein, 2012). These events ensure that the phagosomal membrane and luminal contents transition into a degradative and microbicidal structure, while maintaining its size approximately constant. Fusion of the late phagosome with lysosomes is a fundamental event. This is the stage where most of the V-ATPases are acquired, an event accompanied by the profound luminal acidification that reaches pH $\leq$ 5 (Levin et al., 2016). V-ATPases, are large, multi-subunit complexes that convert chemical energy stored in ATP into mechanically driven H^+ translocation (Forgac, 2007). Clearly, the number of V-ATPases inserted into the phagolysosomal membrane will be an important determinant of the rate and extent luminal acidification. However, not all the V-ATPases will be equally active at all times and the factors controlling the rate of pumping need to be considered (Maxson and Grinstein, 2014). Remarkably, little is known about the regulation of mammalian V-ATPases. Their activity is affected by the lipid composition of the lysosomal membrane:

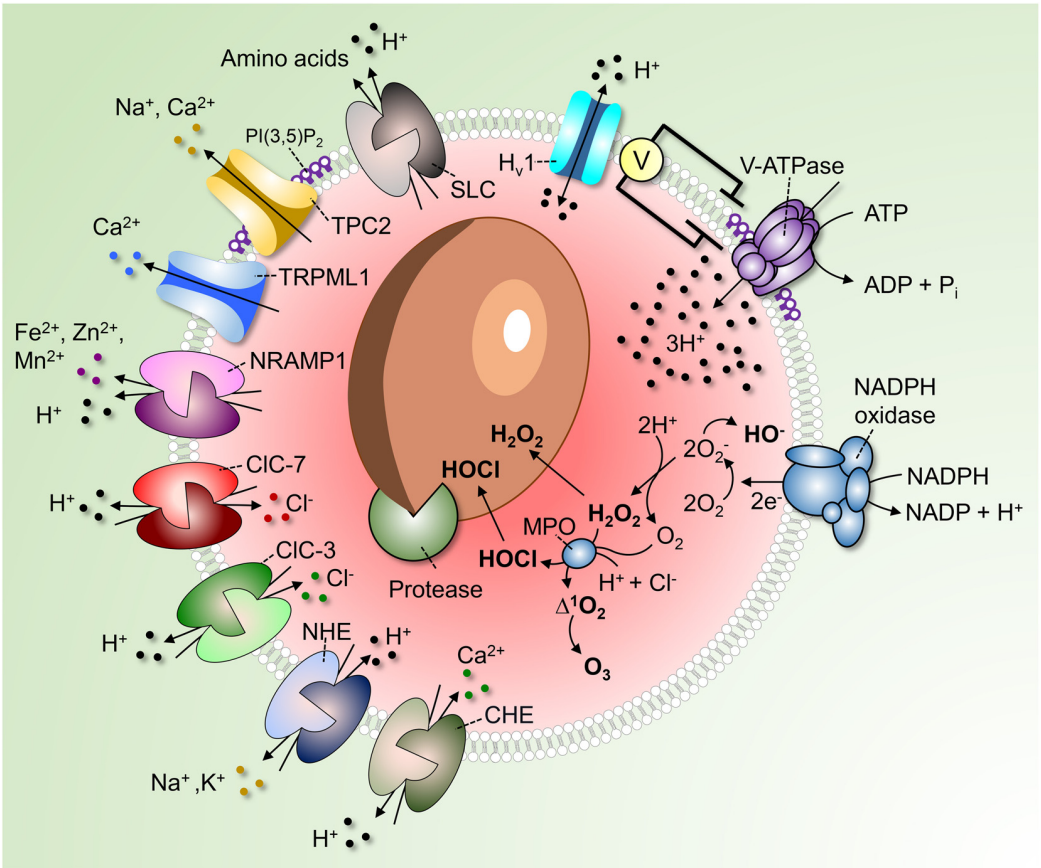

FIGURE 1 | Regulation of phagosomal pH in phagocytes. V-ATPases hydrolyze ATP to pump $3H^+$ into the phagosome. As the V-ATPase is electrogenic, its continued operation is dependent on parallel counter-ion influxes. These can be provided by rheogenic anion antiporters like ClC-7 and ClC-3 and/or through cation efflux via channels such as TPC2 and TRPML1. Conversion of PI(3)P into $PI(3,5)P_2$ by PIKfyve regulates TRPML1, TCP-2 and possibly also the V-ATPase itself. A number of pathways promote the "leakage" of H^+ out of phagosomes. These include monovalent and divalent cation/H^+ antiporters (NHE and CHE) or symporters (NRAMP1), Hv1 H^+-selective channels and amino acid-H^+ cotransporters of the SLC family. In addition, H^+ is consumed during antimicrobial activities by products of the NADPH oxidase to produce hydroxyl radicals, HOCl, and H_2O_2. Low luminal pH is required for the autoactivation of various phagosomal proteases and for protonation of microbicidal effectors.

sphingolipids are required for optimal ATP hydrolysis, and lack of these sphingolipids results in impaired acidification (Chung et al., 2003). Moreover, the phosphoinositide $PtdIns(3,5)P_2$, which has gotten much attention lately as a regulator of phagosomal ion channels, is suggested to be required for acidification. At least in some systems, absence of $PtdIns(3,5)P_2$ is associated with decreased V-ATPase activity and H^+ pumping rate (Li et al., 2014).

Active V-ATPases transport $3H^+$ per ATP hydrolyzed; the V-ATPases deliver H^+ across the membrane unaccompanied by other ions and, as such, are electrogenic. It follows that counter-ion fluxes must occur in parallel to enable measurable changes in pH; in their absence, an electrical potential would be generated that would oppose significant H^+ flux. The source of counter-ion fluxes that neutralize the electrogenic H^+ flux is uncertain; one promising candidate is the influx of Cl^- via channels or rheogenic antiporters (Kornak et al., 2001; Di et al., 2006; Graves et al., 2008). To our knowledge, counter-ion fluxes have not been directly analyzed in phagolysosomes. However, as the phagolysosomal membrane resembles that of lysosomes, it is reasonable to assume that H^+ fluxes are similarly regulated. Therefore, extrapolation of the knowledge obtained from lysosomes seems warranted. Some Cl^- conductive pathways function as *bona fide* channels: these include Cl^- intracellular channels, cystic fibrosis transmembrane conductance regulator (CFTR), and the volume-regulated anion channel (VRAC or LRRC8) plasmalemmal regulated channels, the presence and operation of which in lysosomes is still debated. Others, originally thought to be conductive channels, were subsequently found to operate as antiporters: members of the Cl^- channel (ClC) family mediate the uptake of 2 Cl^- ions in exchange for a luminal H^+. The resulting charge imbalance renders these antiporters rheogenic, effectuating the net uptake of one negative charge when operating in their "normal" forward direction. Some members of the ClC family, namely, ClC-4, ClC-5, and ClC-6 are found in early compartments of the endosomal pathway, whereas ClC-3 is found in early/late endosomes, and ClC-7 predominantly localizes to lysosomes (Kornak et al., 2001;

Wang, 2016), and therefore most likely also to phagolysosomes. At first glance, operation of ClC-7 as a $2Cl^-/H^+$ antiport would appear counterproductive, as it tends to decrease the accumulation of luminal H^+ that is the objective of the V-ATPases. However, it should be borne in mind that exchange of 2 cytosolic Cl^- for one luminal H^+ results in the net intraphagosomal gain of 3 negative charge equivalents, and that V-ATPases translocate $3H^+$ per functional cycle. Thus, sacrificing the loss of one H^+ to enable the neutralization of the two net H^+ gained appears justified.

The role of ClC-7 in establishing the acidification of lysosomes (and presumably, by extension, of phagolysosomes) can best be established by knocking out the antiporters. This seemingly definitive and straightforward approach, however, has yielded contradictory results, with some authors reporting impairment of lysosomal acidification (Graves et al., 2008), while others found no significant effect (Steinberg et al., 2010; Weinert et al., 2010). It is clear, nevertheless, that the antiporter is required for the function of lysosomes in at least some specialized settings since mice deficient in ClC-7 display severe osteopetrosis and retinal degeneration presumably associated with improper endolysosomal acidification (Kornak et al., 2001). It is nevertheless puzzling that ClC-7 knockout mice show neurodegeneration and severe lysosomal storage disease without elevated lysosomal pH (Kasper et al., 2005).

Redundancy with other anion transporters could explain the apparent discrepancies reported in ClC-7-deficient animals. ClC-3 also functions as a late endo(lyso)somal $2Cl^-/H^+$ exchanger. However, due to the strong voltage-dependence of ClC-3, luminal positive voltage or acidic phagosomal pH could shift the exchange mode to a conductive Cl^- channel (Matsuda et al., 2010; Stauber et al., 2012). On the other hand, an alternative –but not mutually exclusive– mechanism could counteract the V-ATPase's electrogenic nature. Specifically, it has been suggested that an efflux of luminal cations (as opposed to the influx of anions) may serve to neutralize the electrogenicity of H^+ pumping via the V-ATPase. Steinberg et al. (2010) investigated the role of both anion influx and cation efflux from lysosomes, assessing their individual contribution to luminal acidification. In their study, replacement of cytosolic Cl^- with impermeant anions did not significantly alter the rate of V-ATPase pumping. These authors found that lysosomes acidified similarly in CFTR- and ClC-7-deficient cells. Instead, they demonstrated that lysosomes required Na^+ and K^+ efflux for proper luminal acidification (Steinberg et al., 2010). A similar efflux of Na^+ and K^+ could support (phago)lysosomal acidification.

Besides Na^+ and K^+, (phago)lysosomes also store Ca^{2+} (Westman et al., 2019). Lysosomes are thought to accumulate Ca^{2+}, at least in part, via Ca^{2+}/H^+ exchange; accordingly, V-ATPase inhibition using well-established pharmacological agents impairs Ca^{2+} loading. The Ca^{2+} accumulated by this ostensibly electroneutral exchange (two H^+ are thought to exchange for each Ca^{2+}) could in principle be released via conductive pathways, serving as a counter-ion. Lysosomal Ca^{2+} is predominantly released via TRPML1 and, to some extent, via two-pore channels (TPC) (Jin et al., 2020). Though not widely acknowledged in the literature, TPCs are considerably more permeable to Na^+ than Ca^{2+} (Morgan and Galione, 2014; Guo et al., 2017). As such, these channels could provide the route for the efflux of monovalent cationic counter-ions needed to neutralize the electrogenic H^+ pumping. Consistent with this notion, studies of lysosomal pH in macrophages from mice lacking TPC-1 and TPC-2 show that lysosomes exhibited elevated lysosomal pH under starvation (Cang et al., 2013).

Other divalent cations, including Zn^{2+}, Cu^{2+} and Fe^{2+} are also transported across endosomes and lysosomes by carriers coupled to the H^+ gradient, including the above mentioned NRAMP1 and also NRAMP2. While there has been some discrepancy regarding the mode of NRAMP coupling (i.e., co- vs. counter-transport), it is nevertheless clear that these transporters are essential for heavy metal homeostasis and for proper host responsiveness to pathogens (Forbes and Gros, 2001). In contrast, it is clear that the endomembrane Zn^{2+} transporters (ZnT) of the SLC30 family function as H^+ antiporters (Baltaci and Yuce, 2018).

The concomitant efflux ("leak") of H^+ from (phago)lysosomes is another important determinant of their steady state pH. Multiple pathways contribute to the leak and some are probably unsuspected at present. Known pathways include the ClC-7 ($2Cl^-/H^+$), ClC-3 ($2Cl^-/H^+$), and CHE ($Ca^{2+}/2H^+$) antiporters mentioned above, as well as monovalent cation NHE (Na^+ and or K^+/H^+) antiporters, H^+-conductive channels such as the voltage-gated Hv1 (El Chemaly et al., 2014), and H^+-coupled amino acid symporters. How active each of these systems is and how much they contribute to the regulation of pH is not at all clear, although they are collectively active at steady state. This is readily demonstrated by the alkalinization initiated immediately after inhibition of the V-ATPases by specific blockers like concanamycin or bafilomycin.

The acidifying effects of the V-ATPase are offset by H^+ leakage, but also by H^+ (equivalent) consumption by metabolic reactions occurring in the organellar lumen. Especially in neutrophils, which produce large amounts of ROS, H^+ are consumed inside phagosomes in the course of O_2^- dismutation and during the generation of H_2O_2 and HOCl. Hydrolytic reactions involved in cargo degradation are similarly likely to involve H^+ consumption (**Figure 1**).

Lastly, it is worth mentioning that the lysosomal pH will inevitably be affected by changes in the pH of the surrounding cytosol. In this regard, it was recently reported that phagosomal acidification is dependent on the activity of the plasma membrane bicarbonate transporter SLC4A7, which determines the cytosolic pH. Knockout of SLC4A7 leads to cytosolic acidification and an associated impairment in phagosomal maturation, v-ATPase function, and acquisition of the NADPH oxidase (Sedlyarov et al., 2018).

HOW DO PROFESSIONAL PHAGOCYTES AND THEIR PHAGOSOMES DIFFER IN PH REGULATION?

Macrophages, DCs and neutrophils all internalize pathogens, apoptotic and necrotic debris with varying efficiency and for

different purposes (Flannagan et al., 2012; Westman et al., 2020a). Depending on their localization and on environmental stimuli, phagocytes respond by undergoing cell polarization into distinct functional phenotypes. For macrophages these phenotypes can be divided into classically activated (M1-like) macrophages and alternatively activated (M2-like) macrophages. Naturally, macrophage polarization affects the properties of their phagosomes. M1-like macrophages (classically activated by LPS + IFNγ) are associated with engulfment and killing of pathogens, while M2-like macrophages (alternatively activated by IL-4) prioritize efferocytosis. The buffering capacity and H^+ leakage permeability remain relatively unaltered between the two subtypes, which, however, show drastic changes in V-ATPase-dependent H^+ pumping (Canton et al., 2014). In M1-like macrophages, the elimination of pathogens via NADPH oxidase activity is given priority at the expense of delayed acidification. Accordingly, M1-like macrophages show alkaline oscillations caused by H^+ consumption upon O_2^- dismutation, and the ROS generated delay the acquisition of V-ATPases. In contrast, M2-like macrophages, have reduced NADPH oxidase activity, rapidly acidify to clear apoptotic and necrotic debris.

Phagosomes formed by neutrophils are less acidic than those of macrophages and DCs (Nordenfelt and Tapper, 2011). Similar to phagosomes of M1-like polarized macrophages, neutrophil phagosomes are more alkaline for various reasons, all related to phagosomal ROS generation. Firstly, ROS production increases the permeability of the phagosomes, leading to increased H^+ leak. Secondly, as in M1-like macrophages, O_2^- dismutation associated with the robust NADPH oxidase activity consumes the majority of phagosomal H^+. As the lumen remains neutral or even slightly alkaline, H^+ enter the phagosome via voltage-gated Hv1 channels to facilitate the continuous production of high amounts of ROS. Lastly, H_2O_2 has been shown to impair V-ATPase recruitment to the neutrophil phagosome, further excluding it from the phagosome, which consequently decreases H^+ influx (Jankowski et al., 2002; El Chemaly et al., 2014).

Phagocytosis plays a significantly different role in DCs compared to macrophages and neutrophils. Their primary role as professional antigen-presenting cells is to alert the immune system of the ongoing infection, rather than clearing the invading microorganisms. How DCs process antigenic epitopes directly affects the efficiency of their presentation to T cells (Delamarre et al., 2005). DCs sample the extracellular environment, engulf protein- and lipid-containing material, and process and present antigens to lymphocytes, which is essential for their differentiation, clonal expansion, and antibody production. In comparison to macrophages, the phagosomes of DCs acidify to a lower extent. Accordingly, phagosomes of DCs acquire lower amounts of the V-ATPase, and luminal H^+ are continuously consumed by products of the NADPH oxidase. Moreover, the oxidase tightly regulates the level of proteolysis in the phagosomes of DCs. The consequence of the intermediate phagosomal pH and decreased protease activity is a more moderate digestion of epitopes, required for processing and presentation of microbial antigens (Mantegazza et al., 2008).

Monocytes circulating in the bloodstream supply peripheral tissues with monocyte-derived macrophages and DCs. Besides participating in the clearance of circulating platelets, monocytes can also internalize pathogens, a phenomenon that might play a protective role during disseminated bacterial infection and sepsis. Accordingly, certain monocytic populations increase their phagocytic activity during early stages of sepsis (Döring et al., 2015). Yet, remarkably little is known about how monocytes establish and regulate their phagosomal pH (Döring et al., 2015).

Cells other than mammalian innate immune cells can also ingest foreign particles. A well-studied example is *Dictyostelium discoideum*, a soil-dwelling ameba which feeds on bacteria (Dunn et al., 2018). Indeed, several important findings of phagocyte behavior have been unveiled studying *D. discoideum*, which has been used as a model system because many of its genes are homologous to human genes. As in mammalian phagocytes, the *D. discoideum* phagosome creates an antimicrobial environment via V-ATPase-dependent acidification, delivery of hydrolytic enzymes, generation of ROS, and regulation of metal ions fluxes (Dunn et al., 2018). The *D. discoideum* phagosome acidifies within 10–30 min by fusing with endo-lysosomes, that deliver V-ATPases (Clarke et al., 2002). Lysosomes of *D. discoideum* have been reported to acidify to ≤pH 3.5 (Marchetti et al., 2009) and it has therefore been suggested that their phagosomes could reach a comparable level of acidity. However, others report that *D. discoideum* phagosomes reach pH ≈5.0 (Rupper et al., 2001a,b; Sattler et al., 2013), similar to that of mammalian phagosomes. Following processing of their contents, *D. discoideum* phagosomes give rise to a post-lysosomal structure containing non-digestible bacterial remnants. Of note, this post-lysosome has a neutral pH as the V-ATPases, together with lysosomal enzymes, are removed for reuse by a mechanism involving the WASH complex (Carnell et al., 2011). The luminal contents of such post-lysosomes are expelled from the cells by exocytosis.

HOW DO PATHOGENS HIJACK PHAGOSOMAL PH?

Even though phagocytes are efficient in killing most pathogens (**Figure 2A**), several species can survive and adapt after phagocytic uptake. Mechanisms for survival differ, but many unrelated pathogens focus their efforts on preventing phagosomal acidification. Some pathogens prevent the V-ATPase-dependent H^+ accumulation by interfering with the endolysosomal fusion machinery (**Figure 2B**); others escape the phagosome. Inhibition of lysosomal fusion is a strategy shared by several distantly related bacteria including *Mycobacterium* spp. and *Salmonella* spp. (Buchmeier and Heffron, 1991; Russell, 2001). *M. tuberculosis* (Mtb) can arrest lysosomal insertion into phagosomes (at least partially) by producing the phosphatases SapM and MptpB. These target different phosphatidylinositol derivates that signal and direct phagosomal maturation (Walpole et al., 2018). Moreover, Mtb secretes the glycolipids phosphatidylinositol mannosides (PIM) and lipoarabinomannan (ManLAM), which redirect lipid-mediated trafficking by acting as decoys of mammalian lipids (Chua et al., 2004; Mishra et al., 2011). Mtb was also

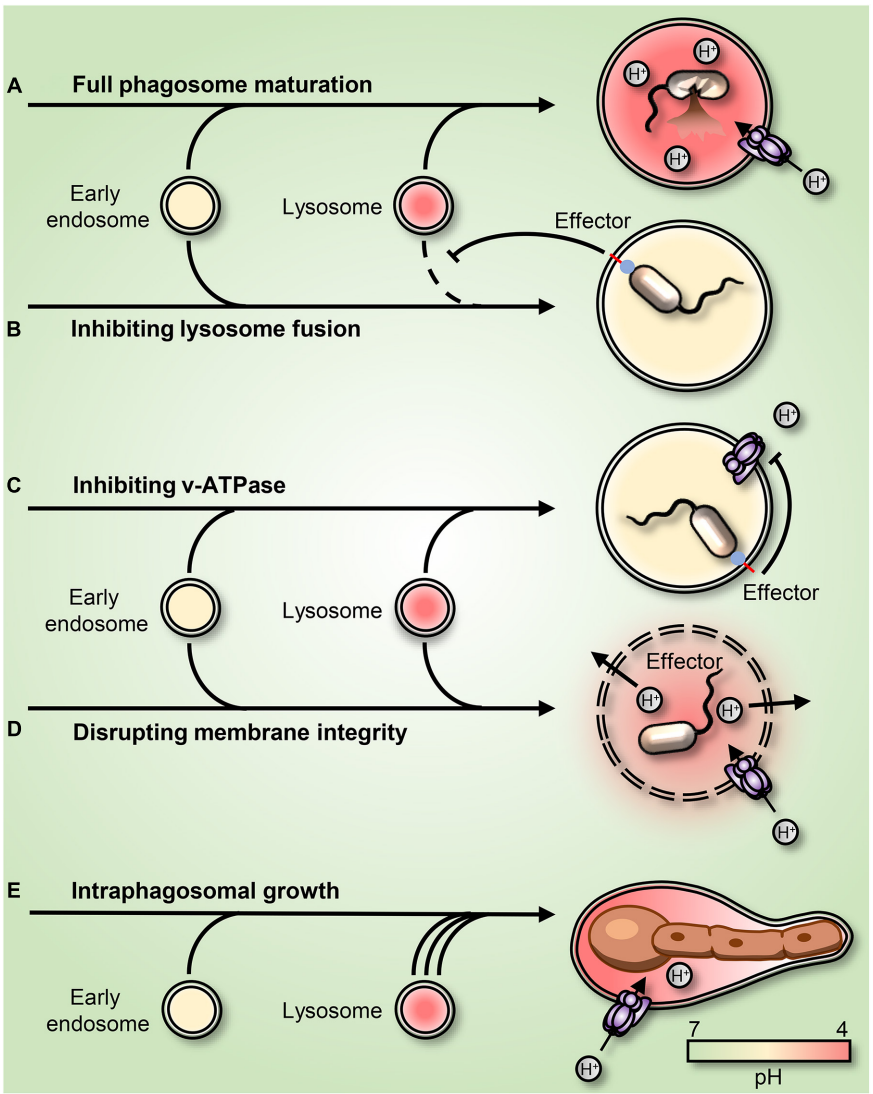

FIGURE 2 | Strategies employed by pathogens to subvert or adapt to the acidic phagosomal pH. **(A)** Phagosome maturation leads to luminal acidification and subsequent killing of the internalized prey. **(B)** Mycobacteria and *Salmonella enterica* arrest phagosome maturation by impairing endo-lysosome insertion into the maturing phagosome. **(C)** *Legionella pneumophila* secretes into the host cytosol the effector sidK that binds and inhibits H^+ pumping by the V-ATPase, leading to impaired acidification. **(D)** *Listeria monocytogenes* secretes the pore-forming toxin listeriolysin O and phospholipases, leading to a rupture of the phagosomal membrane. **(E)** *Candida albicans* survives and grows as filaments inside the acidic phagosome. The *C. albicans*-containing phagosome expands and remains acidic for hours before permanent rupture causes H^+ leakage.

reported to regulate phagosomal acidification by interfering with the retention of the V-ATPases at the phagosomal surface (Wong et al., 2011). *S. enterica* employs a type III secretion system (TTSS) to inject bacterial effectors, including SopB, into the cytosol. Although the enzymatic activity of SopB is still under debate, it is clearly involved in the impairment of the maturation of the *Salmonell*a-containing phagosome (Norris et al., 1998; Hernandez et al., 2004; Mallo et al., 2008). *Shigella flexneri* similarly inserts effectors into its host cells using a TTSS. One of its main effectors, IpgD, is a homolog of *S. enterica* SopB and similarly dephosphorylates plasmalemmal and phagosomal phosphoinositides (Niebuhr et al., 2002).

Some pathogens survive in phagosomes by directly targeting the V-ATPase. *Legionella pneumophilia*, the causative agent of Legionnaires' Disease, allows phagosomes to mature but not acidify. The bacterium produces several effectors to create a niche supportive of its replication. Amongst these is sidK, which *Legionella* secretes into the cytosol where it directly binds to the V-ATPase, inhibiting its function (Zhao et al., 2017; **Figure 2C**). *Listeria monocytogenes* escape phagosomes by secreting listeriolysin O and phospholipases (Smith et al., 1995; Nguyen et al., 2019; **Figure 2D**). Other intraphagosomal pathogens, such as *H. pylori*, Mtb, and *Candida albicans* have been reported to produce and secrete NH_3, which in principle can

bind to and buffer phagolysosomal H^+, leading to phagosomal alkalinization (Schwartz and Allen, 2006; Song et al., 2011; Vylkova and Lorenz, 2014). Similarly, Mtb was proposed to release an antacid compound in an attempt to neutralize acidic phagosomes (Buter et al., 2019). However, the *C. albicans*-containing phagosome was recently shown to be permeable to NH_3. Instead, it was demonstrated that *C. albicans* yeast convert into filaments that grow inside acidic phagosomes and that phagosomal alkalinization resulted from phagosomal H^+ leakage caused by the associated mechanical strain (Westman et al., 2018). Whether the NH_3-mediated buffering hypothesis applies in the cases of *H. pylori* and Mtb remains to be confirmed.

Other pathogens transcriptionally adapt to survive and grow within the microbicidal and nutrient-deprived environment of the phagosome. *C. albicans*, *Staphylococcus aureus*, and *Coxiella burnetti* all adapt to the microbicidal phagosome. Instead of interfering with phagosomal pH, these unrelated microorganisms use a convergent strategy, adapting metabolically to the nutrient-deprived environment inside acidic phagolysosomes (Lorenz et al., 2004; Voth and Heinzen, 2007; Flannagan et al., 2016). Like innate immune cells, engulfed microbes depend on amino acid/H^+ symporters for nutrient acquisition and therefore require an inward H^+ gradient. Most bacteria can pump excess H^+ out of their cytoplasm to maintain pH homeostasis (Guan and Liu, 2020), and many manage to grow and even replicate within phagosomes. However, their intraphagosomal growth does not necessarily lead to phagosomal escape. In this regard, it was recently demonstrated that when subjected to the mechanical stress imposed by growing microorganisms, phagosomes have means to expand their surface area. This remarkable response is mediated by a secondary wave of lysosome insertion that maintains phagosome integrity and preserves the microbiostatic environment (Westman et al., 2020b; **Figure 2E**).

CONCLUDING REMARKS AND FUTURE DIRECTIONS

While the ability of phagosomes to acidify has been appreciated for more than a century, since Metchnikoff made his pioneering observations, the underlying determinants and its biological significance remain incompletely understood. The importance of the luminal acidification is highlighted by the convergent strategies developed by diverse pathogens to neutralize or bypass it. They appreciated these subtleties long before researchers did and developed means to manipulate the luminal pH to secure their survival and proliferation.

As should be apparent from this review, our understanding of phagosomal pH regulation and its role in immune function are woefully incomplete. While we have made major progress in understanding some aspects of pH regulation during phagosome maturation, we are just beginning to appreciate the existence and importance of phagosome resolution and know little about pH regulation at this stage. Also, as pathways connecting phagocytosis, microbial survival within phagosomes, and metabolic reprogramming in both host and pathogen are progressively revealed, the role of pH in these processes needs to be evaluated in detail. Indeed, metabolite transport and utilization are both exquisitely pH sensitive events. As such, the establishment and regulation of the luminal pH should remain a central component of future studies of host-pathogen interactions.

Lastly, it is worth emphasizing that past studies on pH regulation have been essentially limited to *in vitro* and *ex vivo* studies using isolated cells. We anticipate that advances in intravital imaging will extend these analyses to more complex, physiological settings.

AUTHOR CONTRIBUTIONS

JW and SG wrote and critically reviewed the manuscript. Both authors contributed to the article and approved the submitted version.

FUNDING

JW is supported by the Swedish Society of Medicine and Restracomp. SG is supported by Canadian Institutes of Health Research grant FDN-143202.

REFERENCES

Abel, L., Sánchez, F. O., Oberti, J., Thuc, N. V., Hoa, L. V., Lap, V. D., et al. (1998). Susceptibility to leprosy is linked to the human NRAMP1 gene. *J. Infect. Dis.* 177, 133–145. doi: 10.1086/513830

Baltaci, A. K., and Yuce, K. (2018). Zinc transporter proteins. *Neurochem. Res.* 43, 517–530. doi: 10.1007/s11064-017-2454-y

Buchmeier, N. A., and Heffron, F. (1991). Inhibition of macrophage phagosome-lysosome fusion by *Salmonella* typhimurium. *Infect. Immun.* 59, 2232–2238. doi: 10.1128/IAI.59.7.2232-2238.1991

Buckley, C. M., Gopaldass, N., Bosmani, C., Johnston, S. A., Soldati, T., Insall, R. H., et al. (2016). WASH drives early recycling from macropinosomes and phagosomes to maintain surface phagocytic receptors. *Proc. Natl. Acad. Sci. U S A.* 113, E5906–E5915. doi: 10.1073/pnas.1524532113

Buter, J., Cheng, T. Y., Ghanem, M., Grootemaat, A. E., Raman, S., Feng, X., et al. (2019). Mycobacterium tuberculosis releases an antacid that remodels phagosomes. *Nat. Chem. Biol.* 15, 889–899. doi: 10.1038/s41589-019-0336-0

Cang, C., Zhou, Y., Navarro, B., Seo, Y.-J., Aranda, K., Shi, L., et al. (2013). mTOR regulates lysosomal ATP-sensitive two-pore Na(+) channels to adapt to metabolic state. *Cell* 152, 778–790. doi: 10.1016/j.cell.2013.01.023

Canton, J., Khezri, R., Glogauer, M., and Grinstein, S. (2014). Contrasting phagosome pH regulation and maturation in human M1 and M2 macrophages. *Mol. Biol. Cell* 25, 3330–3341. doi: 10.1091/mbc.E14-05-0967

Carnell, M., Zech, T., Calaminus, S. D., Ura, S., Hagedorn, M., Johnston, S. A., et al. (2011). Actin polymerization driven by WASH causes V-ATPase retrieval and vesicle neutralization before exocytosis. *J. Cell Biol.* 193, 831–839. doi: 10.1083/jcb.201009119

Chua, J., Vergne, I., Master, S., and Deretic, V. (2004). A tale of two lipids: Mycobacterium tuberculosis phagosome maturation arrest. *Curr. Opin. Microbiol.* 7, 71–77. doi: 10.1016/j.mib.2003.12.011

Chung, J.-H., Lester, R. L., and Dickson, R. C. (2003). Sphingolipid requirement for generation of a functional v1 component of the vacuolar ATPase. *J. Biol. Chem.* 278, 28872–28881. doi: 10.1074/jbc.M300943200

Clarke, M., Köhler, J., Arana, Q., Liu, T., Heuser, J., and Gerish, G. (2002). Dynamics of the vacuolar H^+-ATPase in the contractile vacuole complex and the endosomal pathway of *Dictyostelium* cells. *J. Cell Sci.* 115, 2893–2905.

Delamarre, L., Pack, M., Chang, H., Mellman, I., and Trombetta, E. S. (2005). Differential lysosomal proteolysis in antigen-presenting cells determines antigen fate. *Science* 307, 1630–1634. doi: 10.1126/science.1108003

Di, A., Brown, M. E., Deriy, L. V., Li, C., Szeto, F. L., Chen, Y., et al. (2006). CFTR regulates phagosome acidification in macrophages and alters bactericidal activity. *Nat. Cell Biol.* 8, 933–944. doi: 10.1038/ncb1456

Döring, M., Stanchi, K. M. C., Erbacher, A., Haufe, S., Schwarze, C. P., Handgretinger, R., et al. (2015). Phagocytic activity of monocytes, their subpopulations and granulocytes during post-transplant adverse events after hematopoietic stem cell transplantation. *Immunobiology* 220, 605–613. doi: 10.1016/j.imbio.2014.12.002

Dunn, J. D., Bosmani, C., Barisch, C., Raykov, L., Lefrançois, L. H., Cardenal-Muñoz, E., et al. (2018). Eat prey, live: Dictyostelium discoideum as a model for cell-autonomous defenses. *Front. Immunol.* 8:1906. doi: 10.3389/fimmu.2017.01906

El Chemaly, A., Nunes, P., Jimaja, W., Castelbou, C., and Demaurex, N. (2014). Hv1 proton channels differentially regulate the pH of neutrophil and macrophage phagosomes by sustaining the production of phagosomal ROS that inhibit the delivery of vacuolar ATPases. *J. Leukoc. Biol.* 95, 827–839. doi: 10.1189/jlb.0513251

Fairn, G. D., and Grinstein, S. (2012). How nascent phagosomes mature to become phagolysosomes. *Trends Immunol.* 33, 397–405. doi: 10.1016/j.it.2012.03.003

Flannagan, R. S., Heit, B., and Heinrichs, D. E. (2016). Intracellular replication of Staphylococcus aureus in mature phagolysosomes in macrophages precedes host cell death, and bacterial escape and dissemination. *Cell. Microbiol.* 18, 514–535. doi: 10.1111/cmi.12527

Flannagan, R. S., Jaumouillé, V., and Grinstein, S. (2012). The Cell Biology of Phagocytosis. *Annu. Rev. Pathol. Mech. Dis.* 7, 61–98. doi: 10.1146/annurev-pathol-011811-132445

Forbes, J. R., and Gros, P. (2001). Divalent metal transport by NRAMP proteins at the interface of host-pathogen interactions. *Trends Microbiol.* 9, 397–403. doi: 10.1016/s0966-842x(01)02098-4

Forgac, M. (2007). Vacuolar ATPases: rotary proton pumps in physiology and pathophysiology. *Nat. Rev. Mol. Cell Biol.* 8, 917–929. doi: 10.1038/nrm2272

Govoni, G., and Gros, P. (1998). Macrophage NRAMP1 and its role in resistance to microbial infections. *Inflamm. Res.* 47, 277–284. doi: 10.1007/s000110050330

Graves, A. R., Curran, P. K., Smith, C. L., and Mindell, J. A. (2008). The Cl-/H+ antiporter ClC-7 is the primary chloride permeation pathway in lysosomes. *Nature* 453, 788–792. doi: 10.1038/nature06907

Guan, N., and Liu, L. (2020). Microbial response to acid stress: mechanisms and applications. *Appl. Microbiol. Biotechnol.* 104, 51–65. doi: 10.1007/s00253-019-10226-1

Guo, J., Zeng, W., and Jiang, Y. (2017). Tuning the ion selectivity of two-pore channels. *Proc. Natl. Acad. Sci. U S A.* 114, 1009–1014. doi: 10.1073/pnas.1616191114

Hernandez, L. D., Hueffer, K., Wenk, M. R., and Galán, J. E. (2004). *Salmonella* modulates vesicular traffic by altering phosphoinositide metabolism. *Science* 304, 1805–1807. doi: 10.1126/science.1098188

Jankowski, A., Scott, C. C., and Grinstein, S. (2002). Determinants of the phagosomal pH in neutrophils. *J. Biol. Chem.* 277, 6059–6066. doi: 10.1074/jbc.M110059200

Jin, X., Zhang, Y., Alharbi, A., Hanbashi, A., Alhoshani, A., and Parrington, J. (2020). Targeting Two-Pore Channels: Current Progress and Future Challenges. *Trends Pharmacol. Sci.* 41, 582–594. doi: 10.1016/j.tips.2020.06.002

Kasper, D., Planells-Cases, R., Fuhrmann, J. C., Scheel, O., Zeitz, O., Ruether, K., et al. (2005). Loss of the chloride channel ClC-7 leads to lysosomal storage disease and neurodegeneration. *EMBO J.* 24, 1079–1091. doi: 10.1038/sj.emboj.7600576

Kornak, U., Kasper, D., Bösl, M. R., Kaiser, E., Schweizer, M., Schulz, A., et al. (2001). Loss of the ClC-7 chloride channel leads to osteopetrosis in mice and man. *Cell* 104, 205–215. doi: 10.1016/s0092-8674(01)00206-9

Levin, R., Grinstein, S., and Canton, J. (2016). The life cycle of phagosomes: formation, maturation, and resolution. *Immunol. Rev.* 273, 156–179. doi: 10.1111/imr.12439

Li, S. C., Diakov, T. T., Xu, T., Tarsio, M., Zhu, W., Couoh-Cardel, S., et al. (2014). The signaling lipid PI(3,5)P2 stabilizes V1-V(o) sector interactions and activates the V-ATPase. *Mol. Biol. Cell* 25, 1251–1262. doi: 10.1091/mbc.E13-10-0563

Lorenz, M. C., Bender, J. A., and Fink, G. R. (2004). Transcriptional response of Candida albicans upon internalization by macrophages. *Eukaryot. Cell* 3, 1076–1087. doi: 10.1128/EC.3.5.1076-1087.2004

Mallo, G. V., Espina, M., Smith, A. C., Terebiznik, M. R., Alemán, A., Finlay, B. B., et al. (2008). SopB promotes phosphatidylinositol 3-phosphate formation on *Salmonella* vacuoles by recruiting Rab5 and Vps34. *J. Cell Biol.* 182, 741–752. doi: 10.1083/jcb.200804131

Mantegazza, A. R., Savina, A., Vermeulen, M., Pérez, L., Geffner, J., Hermine, O., et al. (2008). NADPH oxidase controls phagosomal pH and antigen cross-presentation in human dendritic cells. *Blood* 112, 4712–4722. doi: 10.1182/blood-2008-01-134791

Marchetti, A., Lelong, E., and Cosson, P. (2009). A measure of endosomal pH by flow cytometry in Dictyostelium. *BMC Res. Notes* 2:7. doi: 10.1186/1756-0500-2-7

Matsuda, J. J., Filali, M. S., Collins, M. M., Volk, K. A., and Lamb, F. S. (2010). The ClC-3 Cl-/H+ antiporter becomes uncoupled at low extracellular pH. *J. Biol. Chem.* 285, 2569–2579. doi: 10.1074/jbc.M109.018002

Maxson, M. E., and Grinstein, S. (2014). The vacuolar-type H^+-ATPase at a glance - more than a proton pump. *J. Cell Sci.* 127, 4987–4993. doi: 10.1242/jcs.158550

Mishra, A. K., Driessen, N. N., Appelmelk, B. J., and Besra, G. S. (2011). Lipoarabinomannan and related glycoconjugates: structure, biogenesis and role in Mycobacterium tuberculosis physiology and host-pathogen interaction. *FEMS Microbiol. Rev.* 35, 1126–1157. doi: 10.1111/j.1574-6976.2011.00276.x

Morgan, A. J., and Galione, A. (2014). Two-pore channels (TPCs): current controversies. *Bioessays* 36, 173–183. doi: 10.1002/bies.201300118

Nauseef, W. M. (2019). The phagocyte NOX2 NADPH oxidase in microbial killing and cell signaling. *Curr. Opin. Immunol.* 60, 130–140. doi: 10.1016/j.coi.2019.05.006

Nguyen, B. N., Peterson, B. N., and Portnoy, D. A. (2019). Listeriolysin O: A phagosome-specific cytolysin revisited. *Cell. Microbiol.* 21:e12988. doi: 10.1111/cmi.12988

Niebuhr, K., Giuriato, S., Pedron, T., Philpott, D. J., Gaits, F., Sable, J., et al. (2002). Conversion of PtdIns(4,5)P(2) into PtdIns(5)P by the S.flexneri effector IpgD reorganizes host cell morphology. *EMBO J.* 21, 5069–5078. doi: 10.1093/emboj/cdf522

Niedergang, F., and Grinstein, S. (2018). How to build a phagosome: new concepts for an old process. *Curr. Opin. Cell Biol.* 50, 57–63. doi: 10.1016/j.ceb.2018.01.009

Nordenfelt, P., and Tapper, H. (2011). Phagosome dynamics during phagocytosis by neutrophils. *J. Leukoc. Biol.* 90, 271–284. doi: 10.1189/jlb.0810457

Norris, F. A., Wilson, M. P., Wallis, T. S., Galyov, E. E., and Majerus, P. W. (1998). SopB, a protein required for virulence of *Salmonella* dublin, is an inositol phosphate phosphatase. *Proc. Natl. Acad. Sci. U S A.* 95, 14057–14059. doi: 10.1073/pnas.95.24.14057

Pungercar, J. R., Caglic, D., Sajid, M., Dolinar, M., Vasiljeva, O., Pozgan, U., et al. (2009). Autocatalytic processing of procathepsin B is triggered by proenzyme activity. *FEBS J.* 276, 660–668. doi: 10.1111/j.1742-4658.2008.06815.x

Rupper, A. C., Rodriguez-Paris, J. M., Grove, B. D., and Cardelli, J. A. (2001a). p110-Related PI 3-kinases regulate phagosome-phagosome fusion and phagosomal pH through a PKB/Akt dependent pathway in Dictyostelium. *J. Cell Sci.* 114, 1283–1295.

Rupper, A., Grove, B., and Cardelli, J. (2001b). Rab7 regulates phagosome maturation in Dictyostelium. *J. Cell Sci.* 114, 2449–2460.

Russell, D. G. (2001). Mycobacterium tuberculosis: here today, and here tomorrow. *Nat. Rev. Mol. Cell Biol.* 2, 569–577. doi: 10.1038/35085034

Sattler, N., Monroy, R., and Soldati, T. (2013). Quantitative Analysis of Phagocytosis and Phagosome Maturation. *Methods Mol. Biol.* 983, 383–402. doi: 10.1007/978-1-62703-302-2_21

Schwartz, J. T., and Allen, L.-A. H. (2006). Role of urease in megasome formation and *Helicobacter* pylori survival in macrophages. *J. Leukoc. Biol.* 79, 1214–1225. doi: 10.1189/jlb.0106030

Sedlyarov, V., Eichner, R., Girardi, E., Essletzbichler, P., Goldmann, U., Nunes-Hasler, P., et al. (2018). The Bicarbonate Transporter SLC4A7 Plays a Key Role in Macrophage Phagosome Acidification. *Cell Host Microbe* 23, 766.e–774.e. doi: 10.1016/j.chom.2018.04.013

Smith, G. A., Marquis, H., Jones, S., Johnston, N. C., Portnoy, D. A., and Goldfine, H. (1995). The two distinct phospholipases C of Listeria monocytogenes have overlapping roles in escape from a vacuole and cell-to-cell spread. *Infect. Immun.* 63, 4231–4237. doi: 10.1128/IAI.63.11.4231-4237.1995

Song, H., Huff, J., Janik, K., Walter, K., Keller, C., Ehlers, S., et al. (2011). Expression of the ompATb operon accelerates ammonia secretion and adaptation of Mycobacterium tuberculosis to acidic environments. *Mol. Microbiol.* 80, 900–918. doi: 10.1111/j.1365-2958.2011.07619.x

Stauber, T., Weinert, S., and Jentsch, T. J. (2012). Cell biology and physiology of CLC chloride channels and transporters. *Compr. Physiol.* 2, 1701–1744. doi: 10.1002/cphy.c110038

Steinberg, B. E., Huynh, K. K., Brodovitch, A., Jabs, S., Stauber, T., Jentsch, T. J., et al. (2010). A cation counterflux supports lysosomal acidification. *J. Cell Biol.* 189, 1171–1186. doi: 10.1083/jcb.200911083

Voth, D. E., and Heinzen, R. A. (2007). Lounging in a lysosome: the intracellular lifestyle of *Coxiella burnetii*. *Cell. Microbiol.* 9, 829–840. doi: 10.1111/j.1462-5822.2007.00901.x

Vylkova, S., and Lorenz, M. C. (2014). Modulation of phagosomal pH by Candida albicans promotes hyphal morphogenesis and requires Stp2p, a regulator of amino acid transport. *PLoS Pathog.* 10:e1003995. doi: 10.1371/journal.ppat.1003995

Walpole, G. F. W., Grinstein, S., and Westman, J. (2018). The role of lipids in host-pathogen interactions. *IUBMB Life* 70, 384–392. doi: 10.1002/iub.1737

Wang, G. (2016). Chloride flux in phagocytes. *Immunol. Rev.* 273, 219–231. doi: 10.1111/imr.12438

Weinert, S., Jabs, S., Supanchart, C., Schweizer, M., Gimber, N., Richter, M., et al. (2010). Lysosomal pathology and osteopetrosis upon loss of H+-driven lysosomal Cl- accumulation. *Science* 328, 1401–1403. doi: 10.1126/science.1188072

Westman, J., Grinstein, S., and Marques, P. E. (2020a). Phagocytosis of Necrotic Debris at Sites of Injury and Inflammation. *Front. Immunol.* 10:3030. doi: 10.3389/fimmu.2019.03030

Westman, J., Grinstein, S., and Maxson, M. E. (2019). Revisiting the role of calcium in phagosome formation and maturation. *J. Leukoc. Biol.* 106, 837–851. doi: 10.1002/JLB.MR1118-444R

Westman, J., Moran, G., Mogavero, S., Hube, B., and Grinstein, S. (2018). Candida albicans Hyphal Expansion Causes Phagosomal Membrane Damage and Luminal Alkalinization. *MBio* 9:18. doi: 10.1128/mBio.01226-18

Westman, J., Walpole, G. F. W., Kasper, L., Xue, B. Y., Elshafee, O., Hube, B., et al. (2020b). Lysosome Fusion Maintains Phagosome Integrity during Fungal Infection. *Cell Host Microbe* 28, 798.e–812.e. doi: 10.1016/j.chom.2020.09.004

Wong, D., Bach, H., Sun, J., Hmama, Z., and Av-Gay, Y. (2011). Mycobacterium tuberculosis protein tyrosine phosphatase (PtpA) excludes host vacuolar-H+-ATPase to inhibit phagosome acidification. *Proc. Natl. Acad. Sci. U S A.* 108, 19371–19376. doi: 10.1073/pnas.1109201108

Zhao, J., Beyrakhova, K., Liu, Y., Alvarez, C. P., Bueler, S. A., Xu, L., et al. (2017). Molecular basis for the binding and modulation of V-ATPase by a bacterial effector protein. *PLoS Pathog.* 13:e1006394. doi: 10.1371/journal.ppat.1006394

Conflict of Interest: The authors declare that the research was conducted in the absence of any commercial or financial relationships that could be construed as a potential conflict of interest.

frontiers in Cell and Developmental Biology

ORIGINAL RESEARCH
published: 12 January 2021
doi: 10.3389/fcell.2020.611354

Prkaa1 Metabolically Regulates Monocyte/Macrophage Recruitment and Viability in Diet-Induced Murine Metabolic Disorders

*Qiuhua Yang[1†], Qian Ma[1,2†], Jiean Xu[1,2], Zhiping Liu[1,2], Jianqiu Zou[1], Jian Shen[3], Yaqi Zhou[2], Qingen Da[4], Xiaoxiao Mao[1,2], Sarah Lu[5], David J. Fulton[1], Neal L. Weintraub[1], Zsolt Bagi[6], Mei Hong[2] and Yuqing Huo[1]**

[1] Vascular Biology Center, Department of Cellular Biology and Anatomy, Medical College of Georgia, Augusta University, Augusta, GA, United States, [2] State Key Laboratory of Chemical Oncogenomics, Key Laboratory of Chemical Genomics, School of Chemical Biology and Biotechnology, Peking University Shenzhen Graduate School, Shenzhen, China, [3] Department of Cardiology, Second Affiliated Hospital of Zhejiang University School of Medicine, Hangzhou, China, [4] Department of Cardiovascular Surgery, Peking University Shenzhen Hospital, Shenzhen, China, [5] Trinity College of Arts & Sciences, Duke University, Durham, NC, United States, [6] Department of Physiology, Medical College of Georgia, Augusta University, Augusta, GA, United States

OPEN ACCESS

Edited by:
Mitsugu Fujita,
Kindai University, Japan

Reviewed by:
Patricia Zancan,
Federal University of Rio de Janeiro, Brazil
Srikala Raghavan,
Institute for Stem Cell Science and Regenerative Medicine (inStem), India

***Correspondence:**
Yuqing Huo
yhuo@augusta.edu

[†] These authors have contributed equally to this work

Specialty section:
This article was submitted to Cell Adhesion and Migration, a section of the journal Frontiers in Cell and Developmental Biology

Received: 28 September 2020
Accepted: 14 December 2020
Published: 12 January 2021

Citation:
Yang Q, Ma Q, Xu J, Liu Z, Zou J, Shen J, Zhou Y, Da Q, Mao X, Lu S, Fulton DJ, Weintraub NL, Bagi Z, Hong M and Huo Y (2021) Prkaa1 Metabolically Regulates Monocyte/Macrophage Recruitment and Viability in Diet-Induced Murine Metabolic Disorders. Front. Cell Dev. Biol. 8:611354. doi: 10.3389/fcell.2020.611354

Myeloid cells, including monocytes/macrophages, primarily rely on glucose and lipid metabolism to provide the energy and metabolites needed for their functions and survival. AMP-activated protein kinase (AMPK, its gene is *PRKA* for human, *Prka* for rodent) is a key metabolic sensor that regulates many metabolic pathways. We studied recruitment and viability of *Prkaa1*-deficient myeloid cells in mice and the phenotype of these mice in the context of cardio-metabolic diseases. We found that the deficiency of Prkaa1 in myeloid cells downregulated genes for glucose and lipid metabolism, compromised glucose and lipid metabolism of macrophages, and suppressed their recruitment to adipose, liver and arterial vessel walls. The viability of macrophages in the above tissues/organs was also decreased. These cellular alterations resulted in decreases in body weight, insulin resistance, and lipid accumulation in liver of mice fed with a high fat diet, and reduced the size of atherosclerotic lesions of mice fed with a Western diet. Our results indicate that AMPKα1/PRKAA1-regulated metabolism supports monocyte recruitment and macrophage viability, contributing to the development of diet-induced metabolic disorders including diabetes and atherosclerosis.

Keywords: AMPKα1/PRKAA1, glycolysis, monocyte recruitment, macrophage viability, metabolic disorders

INTRODUCTION

Metabolic syndrome, including obesity and diabetes as well as their vascular complications such as atherosclerosis, are chronic inflammatory diseases (Ross, 1999; Libby, 2002; Weisberg et al., 2003; Xu et al., 2003; Lumeng and Saltiel, 2011). These diseases are initiated by recruitment of circulating leukocytes, including monocytes, T cells, neutrophils, and NK cells, to the metabolic organs/tissues

and vascular walls (Ley et al., 2007; Shi and Pamer, 2011). The infiltrated leukocytes survive in the affected organs/tissues, modulate their activation status and subsequently conquer the progression of these metabolic disorders and their complications. The importance of leukocyte recruitment and activation in the development and progression of these diseases has been demonstrated in various studies in which disease development is suppressed by genetic or pharmacologic blockade of leukocyte recruitment molecules such as selectins, selectin ligands, integrins, ligands for integrins, chemokines and chemokine receptors (Ley et al., 2007; Wu and Ballantyne, 2020). Furthermore, reduction of survival and activation of these infiltrated leukocytes are also able to inhibit these metabolic disorders and their complications (Murray and Wynn, 2011).

The role of cellular metabolism in redirecting the fate of leukocytes and their activities has attracted interest in the field. A large number of studies focused on the metabolic status of leukocytes and its dynamic changes during homeostasis and inflammation and highlighted that the metabolic status of leukocytes can undergo reprogramming in response to environmental stimuli (Webb et al., 2017; Marelli-Berg and Jangani, 2018). Aerobic glycolysis appears to be the most important metabolic pathway in leukocytes to produce ATP rapidly and sufficiently to support leukocyte recruitment and migration. It has been reported that macrophage HIF1α deficiency significantly suppressed migration under hypoxia conditions, and the results suggest that glycolysis sustains macrophage migration into inflamed tissues (Semba et al., 2016). In addition to macrophage migration, it has been demonstrated that macrophages largely depend on glucose supply through glycolysis-induced ATP production in cell spreading and protrusion formation (Venter et al., 2014). However, less is known about the impact of metabolic alterations on leukocyte recruitment and survival in diet-induced metabolic syndrome.

AMPK/PRKA acts as a major cellular energy sensor and a master regulator of metabolic homeostasis, including regulating the signals involved in glucose, lipid and cholesterol metabolism (Hardie and Hawley, 2001; Hardie, 2004). In mammals, AMPK/PRKA exists as a conserved serine/threonine kinase comprised of a catalytic subunit (α) and two regulatory subunits (β and γ). AMPKα1/PRKAA1 is the predominant isoform found in vascular cells and monocytes/macrophages, while AMPKα2/PRKAA2 is the catalytic isoform expressed in the liver, muscle and hypothalamus (Kahn et al., 2005; Fisslthaler and Fleming, 2009; Hardie, 2011). A few groups have extensively studied the role of AMPKα1/PRKAA1 in regulating cardiovascular functions and the development of cardiovascular diseases (Cai et al., 2016; Ding et al., 2017; Wu and Zou, 2020). In most of these studies, the kinase function of AMPKa1/PRKAA1 has been emphasized. AMPKa1/PRKAA1 is a well-characterized molecule for modulating cellular metabolism, including metabolism of glucose and fatty acid oxidation, in metabolic tissue/organs (Garcia and Shaw, 2017; Boudaba et al., 2018; Wu et al., 2018). For cardiovascular cells, we recently examined the role of AMPKa1/PRKAA1/Prkaa1 in glucose metabolism of cultured human endothelial cells and mouse endothelial cells *in vivo* (Yang et al., 2018); the role of AMPKa1/PRKAA1/Prkaa1 in macrophage metabolism, such as glucose metabolism, has not been studied. Here, we examined glycolysis in *Prkaa1*-deficient myeloid cells and the effects of this changed metabolism to myeloid cell recruitment and survival, as well as to the development of chronic inflammatory diseases, including diet-induced diabetes and atherosclerosis.

MATERIALS AND METHODS

Mouse Generation and Breeding

Prkaa1-floxed (*Prkaa1*$^{Lox/Lox}$, *Prkaa1*^{WT}) mice were kindly provided by Dr. Benoit Viollet (Institut Cochin, Paris, France). These mice were first crossed with myeloid-specific Cre recombinase-expressing mice (*Lysm*$^{Cre/Cre}$ mice, Cat. No. 004718, the Jackson Laboratory, Bar Harbor, ME, United States) to generate *Prkaa1*$^{Lox/Lox}$; Lysm$^{Cre/+}$ (*Prkaa1*$^{\Delta M\varphi}$) mice, and then these mice were further bred with apolipoprotein E-deficient mice (*Apoe*$^{-/-}$ mice, Cat. No. 002052, the Jackson Laboratory, Bar Harbor, ME, United States) to generate *Apoe*$^{-/-}$/*Prkaa1*$^{\Delta M\varphi}$ and *Apoe*$^{-/-}$/*Prkaa1*^{WT} mice. All mice were bred on the C57BL/6J background. In this study, both male and female deficient mice and their littermate controls were used for experiments. Mice were generally maintained on a 12:12-h of light: dark cycle in temperature-controlled cages and had free access to water and diet. All animal experiments were performed in accordance with the National Institutes of Health guidelines and approved by the IACUC (Institutional Animal Care & Use Committee) of Augusta University.

Glucose and Insulin Tolerance Tests

Six-week-old *Prkaa1*$^{\Delta M\varphi}$ and *Prkaa1*^{WT} mice were fed a high-fat diet (HFD) (Cat. No. D12492, Research Diet, New Brunswick, NJ, United States) for 12 weeks. For glucose tolerance test (GTT), mice fed with HFD for 10 weeks were fasted for 6 h and administered D-glucose (1 g/kg; Cat. No. G8270, Sigma-Aldrich, St. Louis, MO, United States) by intraperitoneal (IP) injection. Insulin tolerance was assessed after 4 h fast by IP injection of insulin (1 U/kg; Cat. No. HI0219, Lilly, Indianapolis, IN, United States). Blood samples were collected from the tail vein and the blood glucose was measured with a glucometer (OneTouch UltraEasy, Johnson & Johnson, New Brunswick, NJ, United States) at the indicated time after injection.

Evaluation of Energy Homeostasis

The volume of carbon dioxide production (VCO_2), volume of oxygen consumption (VO_2), energy expenditure, and food and drink intake were monitored individually in *Prkaa1*$^{\Delta M\varphi}$ and *Prkaa1*^{WT} mice fed the HFD for 12 weeks with Comprehensive Lab Animal Monitoring System (CLAMS) (Columbus Instruments, Columbus, OH, United States). The ratio of VCO_2 to VO_2 was calculated for the respiratory exchange ratio (RER). Body composition of fat and lean mass was determined by a nuclear magnetic resonance (NMR) system (MiniSpec LF90II TD-NMR Analyzer, Bruker, Billerica, MA, United States).

Leukocyte Sorting From Adipose Tissue

Epididymal adipose tissue was excised from *Prkaa1*$^{\Delta M\varphi}$ and *Prkaa1*^{WT} mice and minced into small pieces, digested with collagenase type I (5 mg/ml, Cat. No. 4194, Worthington, Lakewood, NJ, United States) in DMEM (Cat. No. 11054020, Gibco, Waltham, MA, United States) for 30 min at 37°C with shaking. After centrifugation at 500 *g* for 5 min, the stromal vascular fraction (SVF) was resuspended in FACS buffer (0.5% FBS in PBS) and passed through a 70-μm cell strainer. The cells were incubated with FcR blocking reagent (Cat. No. 553142, BD Biosciences, San Jose, CA, United States) for 10 min at 4°C, then incubated with 7-AAD (Cat. No. 559925, BD Biosciences, San Jose, CA, United States), PE anti-mouse CD31 (4 μg/ml; Cat. No. 553373, BD Biosciences, San Jose, CA, United States) and APC anti-mouse CD45 (3 μg/ml; Cat. No. 558702, BD Biosciences, San Jose, CA, United States) for 30 min at 4°C. After washing, the cells were sorted using a FACS Caliber. The $CD45^+CD31^-7\text{-}AAD^-$ population was collected for RT-PCR analysis.

Atherosclerotic Lesion Analysis

Apoe$^{-/-}$/*Prkaa1*$^{\Delta M\varphi}$ and *Apoe*$^{-/-}$/*Prkaa1*^{WT} male and female mice at 7 weeks of age were fed a Western diet (Cat. No. TD88137, ENVIGO, Indianapolis, IN, United States) for 16 weeks. Mice were anesthetized and the blood samples were collected. After that, mouse hearts and aorta were dissected after perfusion with phosphate buffered saline (PBS) (Cat. No. BP665-1, Fisher Scientific, Pittsburgh, PA, United States) and 4% paraformaldehyde (PFA) (Cat. No. sc281692, Santa Cruz Biotechnology, Dallas, TX, United States), respectively. Tissues were then fixed with 4% PFA overnight. For the preparation of aortas, the periadventitial fat and connective tissue were removed, and atherosclerotic lesions on the aortas were stained with 2% Oil Red O (Cat. No. O0625, Sigma-Aldrich, Louis, MO, United States). The size of atherosclerotic lesions was evaluated by a quantification of *en face* Oil Red O staining with Image-Pro Plus software (Media Cybernetics, Bethesda, MD, United States) in a blinded manner.

For the preparation of aortic sinus, one-third of the heart with aortic root was cut transversally and embedded in optimum cutting temperature (OCT) compound (Cat. No. 23-730-571, Fisher Scientific, Waltham, MA, United States) and further processed to 5-μm-thick frozen sections of aortic sinus for Hematoxylin and Eosin (HE) and Oil Red O staining. The size of necrotic cores and lipid deposition in the aortic sinus were quantified with Image-Pro Plus software in a blinded manner. Nine sections were quantified for each mouse in each group.

Histology

To characterize the necrotic areas in atherosclerotic lesions, HE staining was performed on 5 μm-thick sections of aortic sinus with Hematoxylin (Cat. No. 22050111, Thermo Scientific, Waltham, MA, United States) and Eosin (Cat. No. 22050110, Thermo Scientific, Waltham, MA, United States). For analysis of collagen and fibrosis, Masson trichrome staining was performed on 5 μm-thick sections of aortic sinus with Masson's Trichrome Stain Kit (Cat. No. KTMTR, American MasterTech, Lodi, CA, United States) according to the manufacturer's instruction. For Mac-2 immunohistochemistry staining on mouse adipose, sections of adipose were quenched with 3% hydrogen peroxide and blocked with 10% goat serum. Sections were then incubated with anti-Mac-2 (3 μg/ml, Cat. No. ACL8942F, Accurate Chemical & Scientific, Westbury, NY, United States) at 4°C overnight. Biotinylated secondary antibodies were incubated and VECTASTAIN® ABC kit (Cat. No. PK-6100, Vector Labs, Burlingame, CA, United States) were applied according to the manufacturer's instructions. Necrotic area and collagen content and Mac-2 staining area were quantified with Image-Pro Plus software.

Immunofluorescence Analysis

Frozen sections were fixed with 4% PFA and permeabilized with PBS containing 0.5% Triton X-100. Paraffin sections were heated in citric acid buffer (10 mM, PH6.0) at 98°C for 10 min for antigen retrieval. Tissues were blocked with 10% normal goat serum (Cat. No. 50062Z, Thermo Fisher Scientific, Waltham, MA, United States) at room temperature for 1 h and incubated with primary antibodies, anti-Mac2 (Cat. No. ACL8942F, Accurate Chemical & Scientific, Westbury, NY, United States), anti-Prkaa1 (Cat. No. GTX112998, GeneTex, Irvine, CA, United States), anti-P-Prka (Cat. No. GTX52341, GeneTex, Irvine, CA, United States), anti-CD36 (Cat. No. Ab80080, Abcam, Cambridge, United Kingdom), anti-Pfkfb3 (Cat. No. 13763-1-AP, Proteintech, Rosemont, IL, United States), anti-Slc2a1 (Cat. No. Ab115730, Abcam, Cambridge, United Kingdom), anti-F4/80 (Cat. No. Ab6640, Abcam, Cambridge, United Kingdom), anti-CD68 (Cat. No. MA5-13324, Thermo Scientific, Waltham, MA, United States) at 4°C overnight. Sections were then incubated with AlexaFluor conjugated secondary antibodies (1:250, Invitrogen, Grand Island, NY, United States) or TUNEL mixture for 1 h according to the manufacturer's instructions. Sections were stained with DAPI (1 μg/mL, Thermo Fisher Scientific) for 5 min at room temperature and mounted. Images were obtained using an upright confocal microscope (Zeiss 780; Carl Zeiss).

Leukocyte Recruitment in the Mouse Cremaster Microcirculation

To perform the leukocyte recruitment analysis, the cremaster muscle model of TNF-α-induced inflammation was used. Each group included four *Prkaa1*$^{\Delta M\varphi}$ and *Prkaa1*^{WT} male mice at 8–12 weeks old. Briefly, mice were injected IP with 10 μg/kg recombinant murine TNF-α (Cat. No. 410-MT-010, R&D Systems, Minneapolis, MN, United States). 4 h later, mice were anesthetized with ketamine (125 mg/kg) and xylazine (12.5 mg/kg). Cremaster muscle was exteriorized from the scrotum and spread on the cover glass and superfused with warmed (35–37°C) saline to keep it wet. Movies were obtained with intravital microscopy (Axioskop; Carl Zeiss, Goettingen, Germany) with a digital camera (AxioCam MRm, Carl Zeiss) and analyzed using digital video software (ZEN 2012, Carl Zeiss). For each cremaster, 3–4 different postcapillary venules were examined and 3 different segments were recorded for

each venule. In total, 36–48 video clips were obtained and analyzed for each group. The number of cells rolling through a perpendicular line to the vessel axis per minute was measured as rolling flux. Leukocyte adhesion was defined as leukocyte adhesion to endothelium more than 30 s and measured as cell numbers per surface area. Surface area was calculated for each vessel as S = π*d*lV where d is the diameter and lV is the length of the vessel.

Plasma Cholesterol, Triglyceride, Glucose, and Blood Leukocyte Analysis

Blood was drawn from *Apoe*$^{-/-}$/*Prkaa1*^{WT} and *Apoe*$^{-/-}$/*Prkaa1*$^{\Delta M\varphi}$ mice that were fasted for 12–14 h following 16 weeks of being fed a Western diet. The subsequent plasma samples were assayed enzymatically with the respective reagents (Cat. No. TR15421, TR13421, TR22421, Thermo Scientific) for measurement of glucose, cholesterol, and triglycerides. Leukocyte numbers in blood were counted with an automated blood cell counter (Hemavet 850FS, CDC Technologies, Oxford, CT, United States).

Bone Marrow Derived Macrophage (BMDM) Culture and Treatments

Prkaa1^{WT} and *Prkaa1*$^{\Delta M\varphi}$ mice at 8 weeks of age were euthanized. Femurs and tibias were isolated and transected. Bone marrow cells were obtained by flushing femurs and tibias with RPMI 1640 medium (Cat. No. SH30809.01B, HyClone, Logan, UT, United States). The cell suspension was pipetted repeatedly to obtain a single cell suspension, which was then filtered with a 70-μm cell strainer and centrifuged at 2000 rpm for 5 min. The acquired cells were plated at a density of 2×10^6/mL and cultured in RPMI 1640 medium supplemented with 10% FBS, 20% L929-conditioned medium, and 1% penicillin-streptomycin. Cells were incubated at 37°C, 5% CO_2 with medium changes at days 3, 5, and 7. After 7 days, the bone marrow cells were differentiated into adherent macrophages, which were used to perform experiments.

Extracellular Acidification Rate (ECAR) Measurement

Extracellular acidification rate (ECAR) of BMDMs was analyzed with an XF96 Extracellular Flux Analyzer (Seahorse Bioscience, North Billerica, MA, United States). Wild-type (WT) and *Prkaa1*-deficient BMDMs were first plated onto Seahorse XF96 cell culture plates at a concentration of 2.0×10^4 per well, and incubated with RPMI 1640 medium at 37°C overnight. The next day, the culture medium was changed to XF base Medium (Seahorse Bioscience) supplemented with 2 mM glutamine, and the cells were incubated in a non-CO_2 incubator at 37°C for 1 h. Cells were then assayed with XFe96 extracellular flux analyzer. Chemicals were used in the test at the following concentration: glucose (10 mM), oligomycin (1 μM), and 2-DG (50 mM).

Fatty Acid Oxidation Rate Measurement

Fatty acid oxidation was measured by XFe24 Seahorse metabolic flux analyzer (Seahorse Bioscience, North Billerica, MA, United States). WT and *Prkaa1*-deficient BMDMs were first seeded onto Seahorse XF24 culture cell plates at a concentration of 1.0×10^5 per well, and incubated with RPMI 1640 medium at 37°C overnight. The next day, the medium was replaced with substrate-limited medium (DMEM supplemented with 0.5 mM Glucose, 1 mM GlutaMAX, 0.5 mM carnitine and 1% FBS) for 24 h. Then cells were incubated with FAO assay medium (KHB supplemented with 2.5 mM glucose, 0.5 mM carnitine, and 5 mM HEPES, pH 7.0) for 45 min in a non-CO_2 incubator at 37°C. XF Palmitate-BSA FAO Substrate or BSA (Cat. No. 102720-100, Agilent, Santa Clara, CA, United States) was added to the appropriate wells prior to starting the assay. Plates were then loaded onto an XFe24 extracellular flux analyzer for XF Cell Mito Stress Test. Compounds were used in the test at the following concentrations: oligomycin (2 μM), FCCP (2 μM), rotenone (1 μM), and antimycin A (1 μM). Fatty acid oxidation was calculated by subtracting oxygen consumption rate (OCR) with palmitate-BSA by OCR with BSA. Spare respiratory capacity was calculated by subtracting baseline OCR from maximum OCR after FCCP injection.

Lactate Measurement

The lactate levels of WT and *Prkaa1*-deficient BMDMs were determined with the Lactate Assay Kit (Cat. No. MAK064, Sigma, Louis, MO, United States) according to the manufacturer's instructions. Briefly, cells were homogenized with lactate assay buffer and centrifuged at 13,000 *g* for 10 min. Samples were deproteinized with 10 kDa MWCO spin filter, and the soluble fraction was used directly to measure the intracellular lactate. The cell culture medium was used for measurement of the extracellular lactate level.

F-2,6-P2 Level Assay

The intracellular F-2, 6-P2 level was measured with the previously described method (Van Schaftingen et al., 1982). WT and *Prkaa1*-deficient BMDMs were homogenized with 0.05M NaOH and inactivated at 80°C for 5 min. The samples were then centrifuged and neutralized with acetic acid. The mixture was centrifuged and the supernatants were collected for measurement. The levels of F-2,6-P2 were measured by a PPi-PFK-based kinetic reaction assay as shown in the table below (**Table 1**). The kinetic reaction was monitored at 340 nm for 30 min with Synergy H1 Hybrid

TABLE 1 | Assay reaction for F2,6-P2 level.

Substrate	Initial concentration	Work concentration
Tris-HCl (pH7.5)	50 mM	50 mM
NADH	20 mM	0.2 mM
DTT	1 M	5 mM
F6P	200 mM	1 mM
MgCl2	1 M	2 mM
Aldolase	700 U/ml	0.7 U/ml
GDH	450 U/ml	0.45 U/ml
TIM	1200 U/ml	0.6 U/ml
PPi-Na	25 mM	0.5 mM
PPi-PFK		10 μg/assay

Reader (BioTek, Winooski, VT, United States). The relative F2,6-P2 levels were normalized by protein concentration.

Apoptosis Analysis

Apoptosis analysis were performed with fluorescein isothiocyanate (FITC) Annexin V Apoptosis Detection Kit I (Cat. No. 556547, BD Biosciences) according to the manufacturer's protocol. Briefly, WT and *Prkaa1*-deficient BMDMs were seeded into 6-well plates at a density of 2×10^6 cells/ml. After incubation for 24 h, cells were detached with 0.25% trypsin and incubated with 5 μl propidium iodide (PI) and 5 μl FITC Annexin V in 100 μl of 1 × binding buffer at room temperature for 15 min in the dark. The samples were analyzed by FACSCalibur flow cytometer (FACSCantor II, BD Biosciences) within 1 h. Apoptotic-positive cells were quantified with FlowJo.

For terminal transferase deoxytidyl uridine end labeling (TUNEL) staining, WT and *Prkaa1*-deficient BMDMs were seeded on glass coverslips at a density of 2×10^6 cells/ml. After incubation for 24 h, cells were stained with *In Situ* Cell Death Detection Kit (Cat. No. 12156792910, Roche) according to the manufacturer's protocol. Briefly, cells were washed with PBS twice, fixed with 4% PFA for 15 min and permeabilized with PBS containing 0.5% Triton X-100 for 20 min at room temperature. Cells were then incubated with the TUNEL mixture containing TMR-dUTP and terminal deoxynucleotidyl transferase for 1 h at 37°C in the dark. Nuclei were stained with DAPI before mounting. Images were obtained using an upright confocal microscope (Zeiss 780, Carl Zeiss). The number of TUNEL-positive cells was counted in seven fields per slide.

Chemotaxis Assays

Chemotaxis assay of WT and *Prkaa1*-deficient BMDMs was performed in a transwell chamber equipped with a 6.5-mm-diameter polycarbonate filter with 8-μm pore inserts (Cat. No.353097, Corning, NY, United States). Briefly, RPMI 1640 medium containing 0.5% FBS with or without MCP-1 (50 ng/ml, Cat. No.479-JE, R&D Systems Inc., Minneapolis, MN, United States) was placed in the lower wells. 2×10^5 BMDMs suspended in RPMI 1640 containing 0.5% FBS were placed in the inserts. The chambers were incubated at 37°C for 8 h. Non-migrated cells on the upper side of inserts were removed with a cotton tip, and migrated cells on the lower side were fixed and stained with crystal violet. BMDMs in 5–7 random fields were counted for each transwell.

Western-Blot Analysis

Wild-type and *Prkaa1*-deficient BMDMs were lysed with RIPA lysis buffer (Sigma) supplemented with 1% phosphatase inhibitors and 1% protease (Roche) for 10 min on ice. After centrifugation of cell lysates at 4°C for 5 min, samples were assayed for protein concentrations by the BCA assay and then separated with SDS-PAGE gel with 10–20 μg protein per lane. Western-blot analysis was performed with primary antibodies against Prkaa1 (1:1000, Cat. No. ab110036, Abcam), Slc2a1 (1:5000, Cat. No. ab115730, Abcam), Pfkfb3 (1:1000, Cat. No. ab181681, Abcam), and β-actin (1:2000, Cat. No. sc47778, Santa Cruz Biotechnology). Images were obtained with the CheminDoc MP System (Bio-Rad) and quantified with Image J software. All protein levels were normalized with β -actin level.

Real-Time PCR Analysis

Total RNA of WT and *Prkaa1*-deficient BMDMs were extracted using Trizol Reagent (Cat. No. 15596018, Invitrogen, Grand Island, NY, United States). 0.5–1 μg total RNA was used for reverse transcription reaction with iScript cDNA synthesis kit (Cat. No. 170-8891, Bio Rad, Hercules, CA, United States). Real-Time PCR was performed in a StepOne Plus system (Applied Biosystems) with Power SYBR Green PCR Master Mix (Cat. No. 4367659, Life Technologies) according to the manufacturer's protocol. Gene-specific primers used in this study are listed in **Table 2**. Relative gene expression was calculated with the efficiency-corrected $2^{-\Delta\Delta CT}$ method by using mouse Rplp0 RNA as the internal control.

Statistical Analysis

Statistical analysis was conducted with GraphPad Prism (La Jolla, CA, United States). The significance of the data was analyzed using unpaired Student's *t*-test between two groups. Multiple comparisons were performed with one-way ANOVA analysis followed by Bonferroni's *post hoc* tests. Statistical significance was defined as follows: $^*p < 0.05$, $^{**}p < 0.01$, $^{***}p < 0.001$. Data are represented as mean ± SEM. All biological experiments were repeated at least three times with independent cell cultures or individual animals (biological replications).

RESULTS

Prkaa1 Expression Is Increased in Adipose Leukocytes of HFD-Fed Mice

Obesity is a chronic, low-grade inflammation with progressive immune cell infiltration into adipose tissue (Bai and Sun, 2015). Many circulating leukocytes, especially monocytes, recruit to adipose tissue to enhance the inflammatory response, accelerating adipocyte necrosis and insulin resistance

TABLE 2 | Sequences of primers used in real-time PCR analysis.

Gene name	Forward primer (5′-3′)	Reverse primer (5'-3')
Rplp0	GGCCCTGCACTCTCGCTTTC	TGCCAGGACGCGCTTGT
Scl2a1	GCAGTTCGGCTATAACACTGG	GCGGTGGTTCCATGTTTGATTG
Pfkfb3	GATCTGGGTGCCCGTCGATC ACCG	CAGTTGAGGTAGCGAGTCAGCTTC
Hk1	AACGGCCTCCGTCAAGATG	GCCGAGATCCAGTGCAATG
Pkm2	AGGATGCCGTGCTGAATG	TAGAAGAGGGGCTCCAGAGG
Idha	CCAAAGACTACTGTGTAACT GCGA	TGGACTGTACTTGACAATGTTGG
Eno1	TGCGTCCACTGGCATCTAC	CAGAGCAGGCGCAATAGTTTTA
Gpi	CTCAAGCTGCGCGAACTTTTT	GGTTCTTGGAGTAGTCCACCAG
Cd36	TGCTGGAGCTGTTATTGGTG	TCTTTGATGTGCAAAACCCA
Cpt1a	GTCGCTTCTTCAAGGTCTGG	AAGAAAGCAGCACGTTCGAT
Fabp4	AAGAAGTGGGAGTGGGCTTT	TCGACTTTCCATCCCACTTC

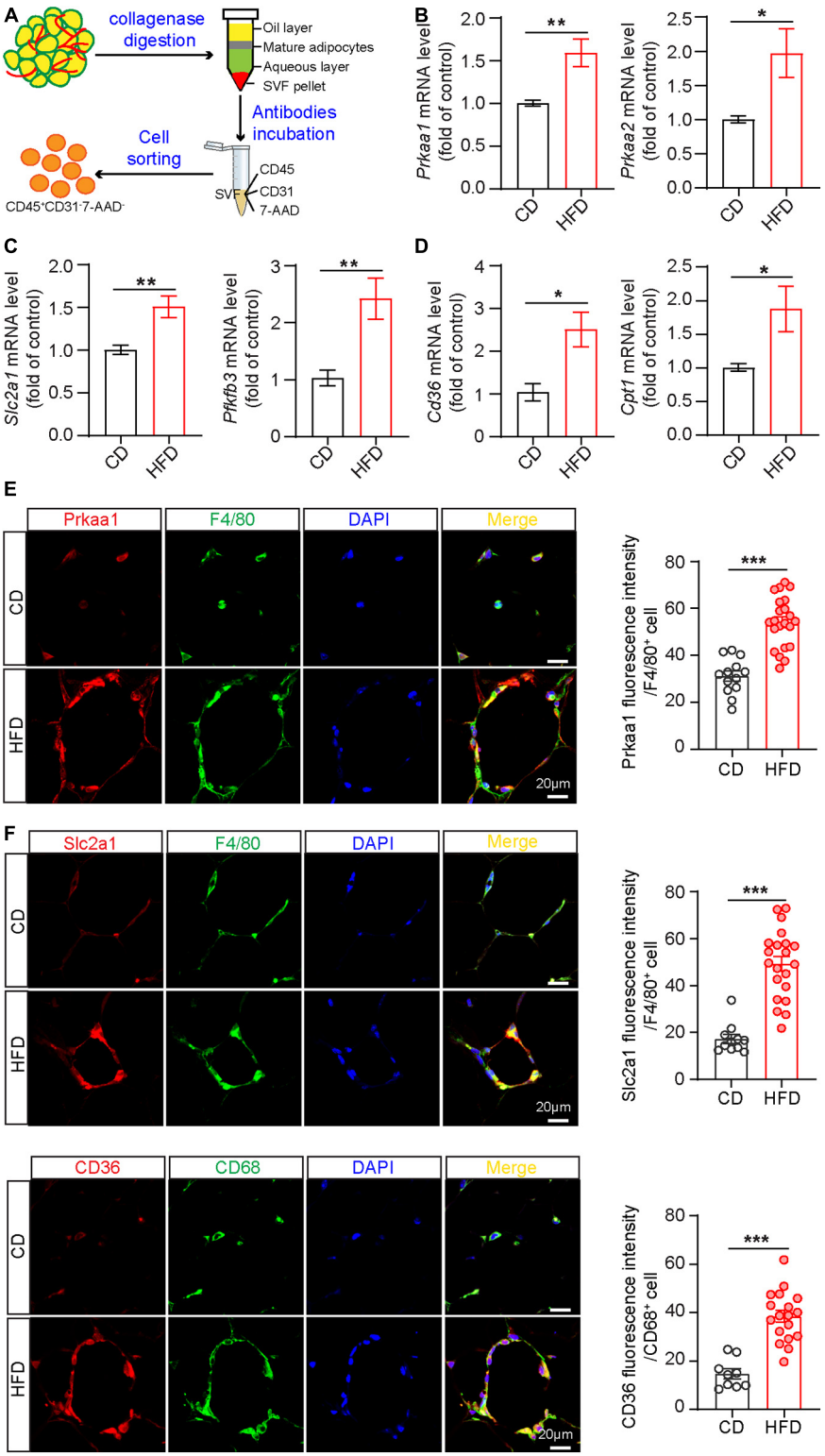

FIGURE 1 | Prkaa1 upregulation is associated with macrophage metabolism in mice fed a high-fat diet. **(A)** Schema illustrating leukocyte sorting from adipose tissues by CD45-positive staining. **(B)** Real-time PCR analysis and quantification of mRNA levels of *Prkaa1* and *Prkaa2* in leukocytes sorted from stromal vascular cells in HFD- and CD-fed mice. $n = 8$. **(C,D)** Real-time PCR analysis and quantification of mRNA levels of *Slc2a1*, *Pfkfb3*, *Cd36,* and *Cpt1* in leukocytes sorted from stromal vascular cells in HFD- and CD-fed mice. $n = 8$. **(E,F)** Representative images and quantification data of Prkaa1, Slc2a1, and CD36 co-staining with F4/80 or CD68 (macrophage markers) in adipose tissues from HFD- and CD-fed mice. $n = 4$, Scale bars, 20 μm. All data were expressed as mean ± SEM. Statistical significance was determined by unpaired Student's *t*-test. $^{*}p < 0.05$ was considered significant, $^{**}p < 0.01$, $^{***}p < 0.001$.

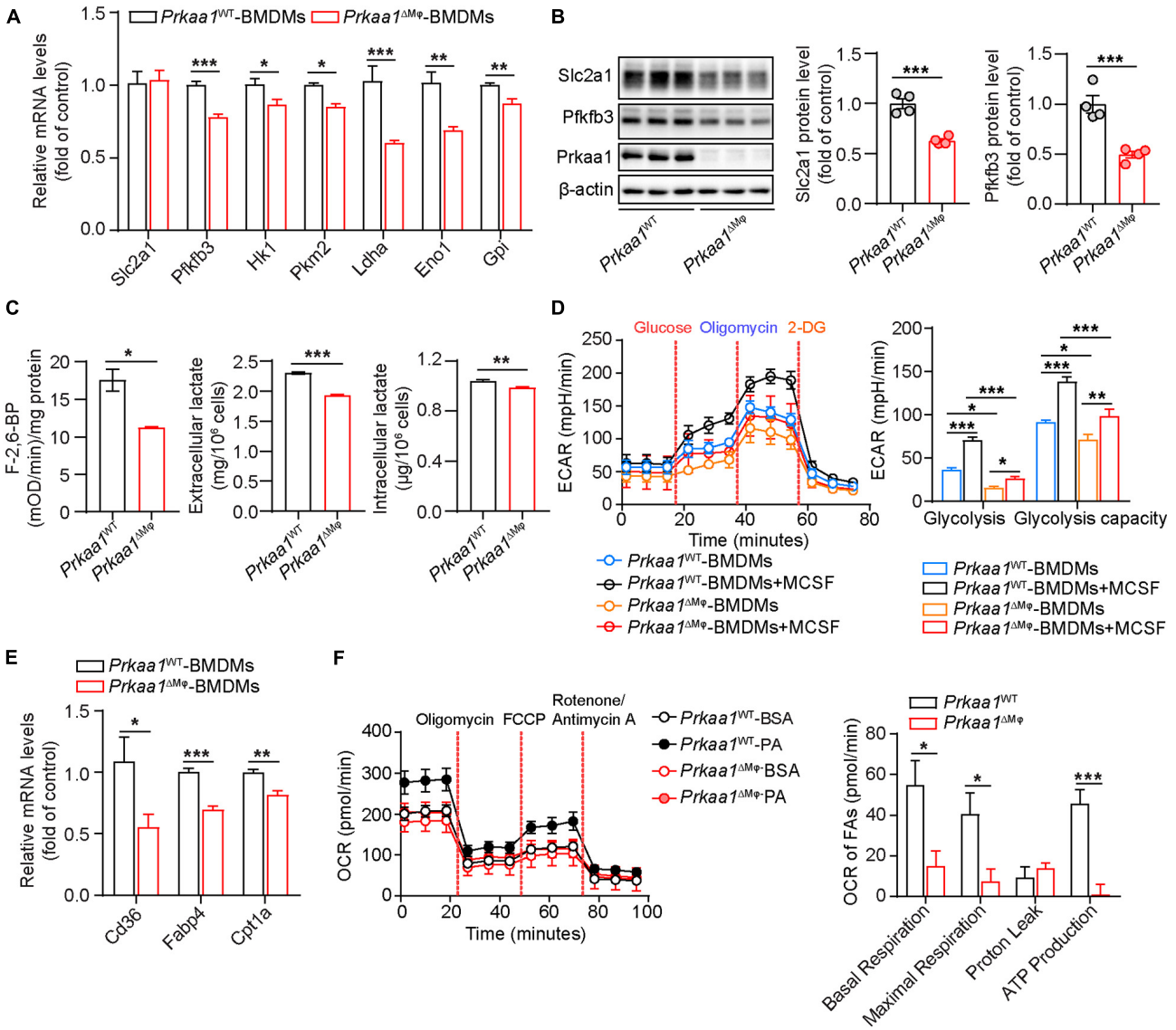

FIGURE 2 | Prkaa1 regulates macrophage glycolysis and fatty acid oxidation. **(A)** Real time-PCR analysis and quantification of mRNA levels of *Slc2a1*, *Pfkfb3*, *Hk1*, *Pkm2*, *Ldha*, *Eno1,* and *Gpi* in BMDMs cultured from *Prkaa1*^{WT} and *Prkaa1*$^{\Delta M\varphi}$ mice. $n = 4$. **(B)** Western-blot analysis and quantification of protein levels of Slc2a1, Pfkfb3, and Prkaa1 in BMDMs cultured from *Prkaa1*^{WT} and *Prkaa1*$^{\Delta M\varphi}$ mice. $n = 4$. **(C)** Measurement of F-2,6-BP, intracellular and extracellular lactate in BMDMs cultured from *Prkaa1*^{WT} and *Prkaa1*$^{\Delta M\varphi}$ mice. $n = 6$. **(D)** ECAR profile showing glycolytic function and quantification of glycolytic function parameters in BMDMs cultured from *Prkaa1*^{WT} and *Prkaa1*$^{\Delta M\varphi}$ mice under control and MCSF (20 ng/mL, 12 h) treatment. Dash lines indicate the time of addition of glucose (10 mM), oligomycin (1 μM), and 2-DG (50 mM). $n = 12$ for each treatment group, repeated four times. **(E)** Real time-PCR analysis and quantification of mRNA levels of *Cd36*, *Fabp4*, and *Cpt1a* in BMDMs cultured from *Prkaa1*^{WT} and *Prkaa1*$^{\Delta M\varphi}$ mice. $n = 4$. **(F)** OCR profile showing fatty acid oxidation and quantification of function parameters in BMDMs cultured from *Prkaa1*^{WT} and *Prkaa1*$^{\Delta M\varphi}$ mice under BSA-palmitate treatment. Etomoxir (Eto, 40 μM) was added to some wells 15 min prior to the assay. $n = 12$ for each treatment group, repeated four times. All data are expressed as mean ± SEM. Statistical significance was determined by unpaired Student's *t*-test and one-way ANOVA followed by Bonferroni test. $^*p < 0.05$ was considered significant, $^{**}p < 0.01$, and $^{***}p < 0.001$.

(Catalan et al., 2013). To explore Prka expression in infiltrating leukocytes in the context of metabolic diseases, we performed fluorescence-activated cell sorting (FACS) to isolate leukocytes from adipose tissues. Briefly, we digested adipose tissue with collagenase I to obtain SVFs, followed by incubation of SVFs with antibodies against CD31 (endothelial cell marker), CD45 (leukocyte marker) and 7-AAD (dead cell marker), and eventually harvested cells labeled as $CD31^{-}CD45^{+}$ 7-AAD^{-} from the cell suspension (**Figure 1A** and **Supplementary Figure 1**). Next, the sorted leukocytes were subjected to Real-time PCR analysis for the mRNA expression of *Prkaa1* and *Prkaa2*. The results showed that the mRNA levels of *Prkaa1* and *Prkaa2* were much higher in leukocytes from adipose tissues of mice fed HFD for 8 weeks than mice fed chow diet (CD) (**Figure 1B**). Prkaa1 is the major isoform of Prkaa in leukocytes (Zhang et al., 2017), and our recent study shows

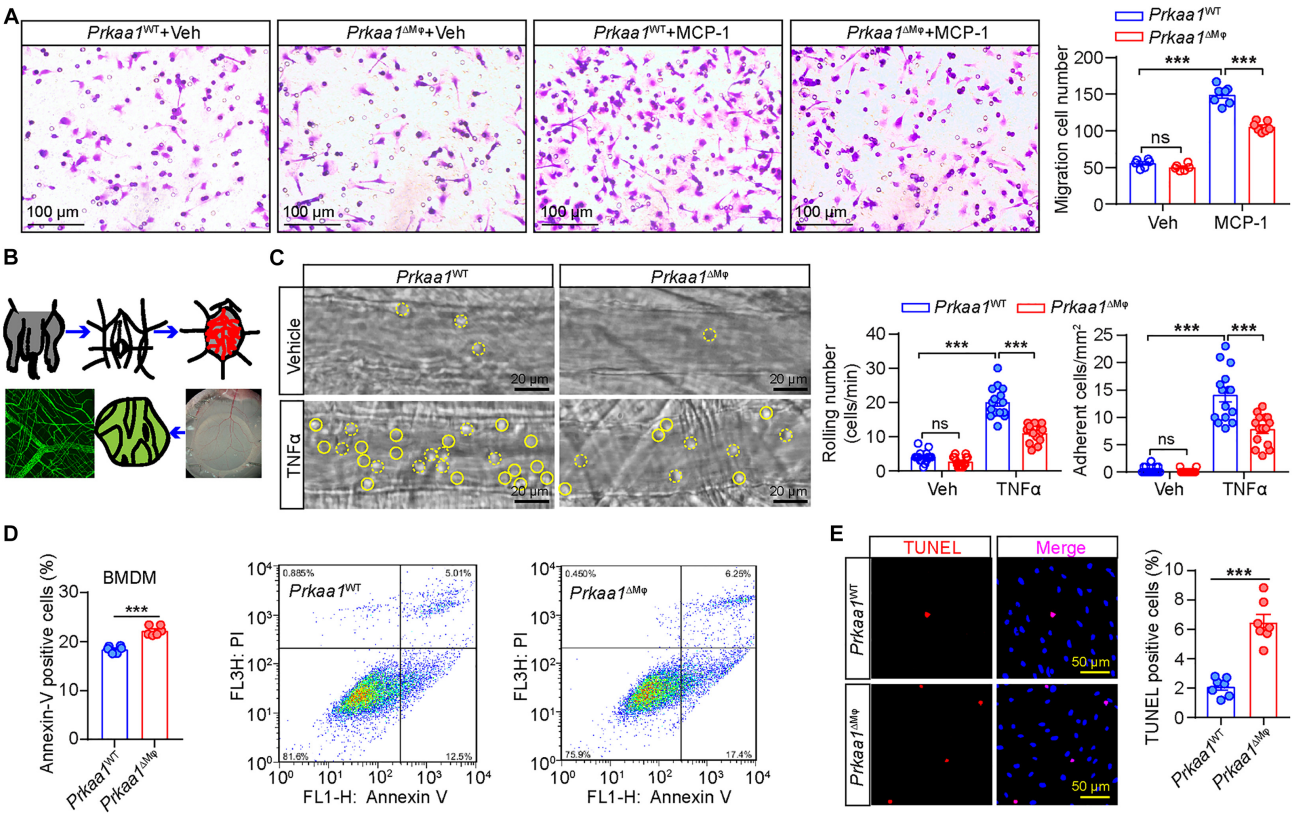

FIGURE 3 | Prkaa1-mediated metabolism is required for leukocyte recruitment and macrophage viability. **(A)** Representative images and quantification of MCP-1-induced migration between BMDMs cultured from *Prkaa1*^{WT} and *Prkaa1*$^{\Delta M\varphi}$ mice. $n = 7$. Scale bars, 100 μm. **(B)** Schematic illustration of *en face* staining of postcapillary venules of mouse cremaster muscle. **(C)** Representative images of leukocyte rolling and adhesion on the endothelium of postcapillary venules in the cremaster muscles of *Prkaa1*$^{\Delta M\varphi}$ and *Prkaa1*^{WT} mice with TNFα or vehicle treatment for 4 h. Rolling and adherent cells are quantified and indicated with dotted and solid circle line, respectively (scale bar, 20 μm). **(D)** Quantification data and representative images of flow cytometry analysis of Annexin V staining in BMDMs cultured from *Prkaa1*^{WT} and *Prkaa1*$^{\Delta M\varphi}$ mice. $n = 6$. **(E)** Representative images and quantification data of TUNEL staining in BMDMs cultured from *Prkaa1*^{WT} and *Prkaa1*$^{\Delta M\varphi}$ mice. $n = 10$, Scale bars, 50 μm. All data are expressed as mean ± SEM. Statistical significance was determined by unpaired Student's *t*-test. ***$p < 0.001$.

a critical role of Prkaa1 in metabolic regulation in vascular cells (Yang et al., 2018). We analyzed expression of metabolic genes in sorted cells with qPCR. The mRNA levels of *Slc2a1*, a glucose transporter, and 6-phosphofructo-2-kinase/fructose-2, 6-bisphosphatase isoform 3 (*Pfkfb3*), a critical glycolytic regulatory enzyme (activator), were much higher in adipose leukocytes of HFD-fed mice than those of CD-fed mice (**Figure 1C**). Additionally, the mRNA levels of *Cd36*, a transporter for free fatty acids and *Cpt1*, a mitochondrial enzyme important for fatty acid oxygenation, were also increased in adipose leukocytes of HFD-fed mice compared with those of chow diet-fed mice (**Figure 1D**). Since macrophages are the predominate leukocytes infiltrating in adipose, we examined the expression of Prkaa1 and some of the above metabolic molecules in F4/80-positive cells by immunostaining adipose sections with the relevant antibodies. The levels of Prkaa1, pPrkaa1, Slc2a1, Pfkfb3 and CD36 were much higher in HFD-fed mice than CD-fed mice (**Figures 1E,F** and **Supplementary Figure 2**). Taken together, the data suggest that leukocytes infiltrated into adipose tissue, especially monocytes/macrophages, exhibit increased levels of Prkaa1, and the latter is associated with increased expression of molecules important for glucose and lipid metabolism.

Prkaa1 Regulates Macrophage Glycolysis

Since macrophages are the major population of infiltrated leukocytes in adipose, we used cultured BMDMs to examine the causal effect of *Prkaa1* on macrophage metabolism. BMDMs were cultured with bone marrow cells from *Prkaa1*^{WT} and *Prkaa1*$^{\Delta M\varphi}$ mice (**Supplementary Figures 3A,B**). BMDMs cultured with bone marrow cells of *Prkaa1*$^{\Delta M\varphi}$ mice barely expressed Prkaa1 at the protein level compared to BMDMs of control *Prkaa1*^{WT} mice (**Supplementary Figure 3C**), indicating that *Prkaa1* was successfully knocked out in myeloid cells. With qPCR, the major genes important for glycolysis were examined, and the mRNA levels of glycolytic genes, including *Pfkfb3, Hk1, Pkm2, Ldha, Eno1,* and *Gpi,* were significantly reduced in *Prkaa1*-deficient BMDMs compared with those of *Prkaa1* WT BMDMs (**Figure 2A**). Expression of Slc2a1 and Pfkfb3 were examined with Western blotting. The protein

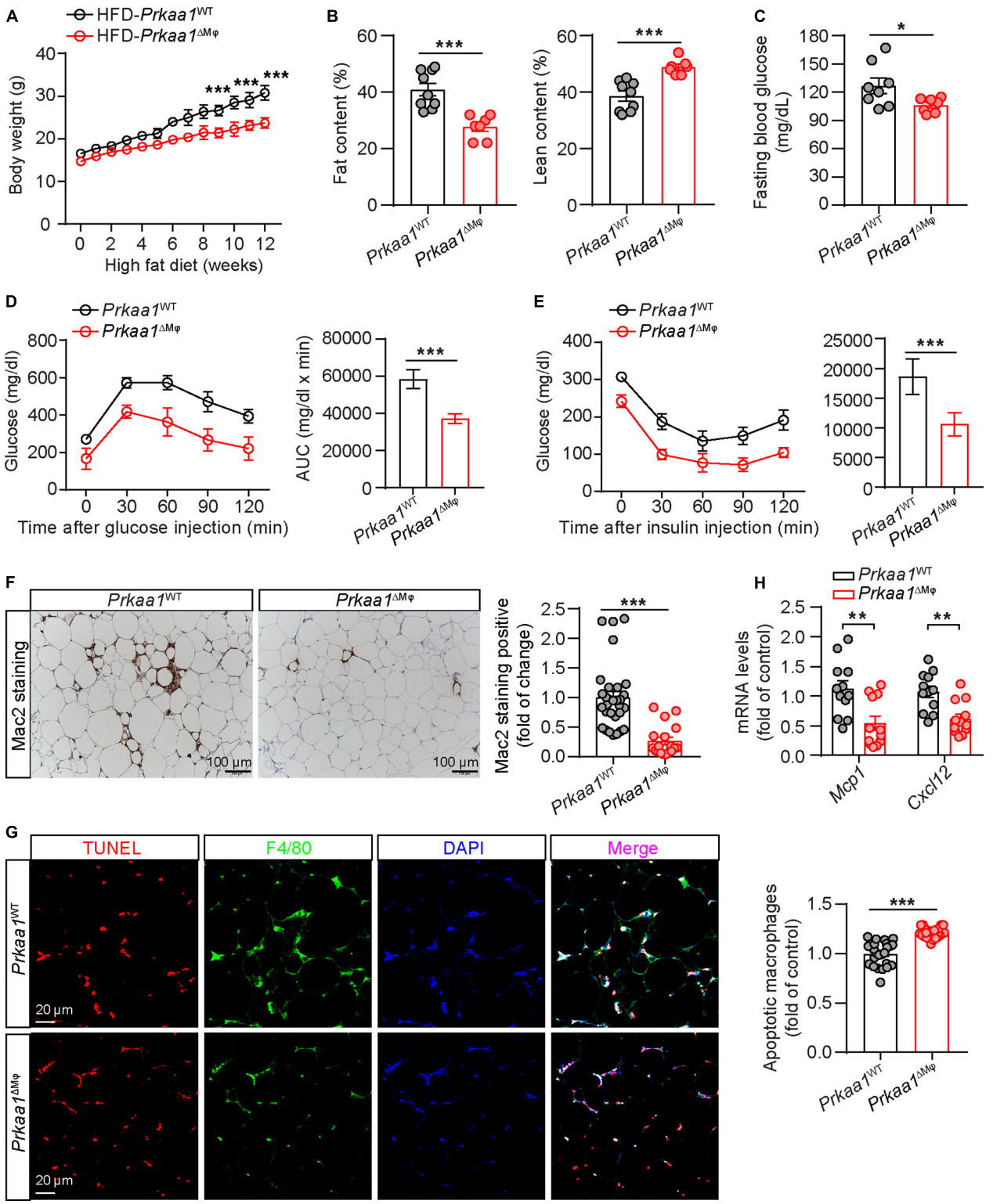

FIGURE 4 | Myeloid *Prkaa1* deficiency protects mice from HFD-induced insulin resistance. **(A)** Body weight of *Prkaa1*^{WT} and *Prkaa1*$^{\Delta M\varphi}$ male mice during 12 weeks of HFD feeding. $n = 9$. **(B)** Fat and lean content of *Prkaa1*^{WT} and *Prkaa1*$^{\Delta M\varphi}$ male mice after being fed HFD for 12 weeks. $n = 9$. **(C)** Fasting blood glucose levels of *Prkaa1*^{WT} and *Prkaa1*$^{\Delta M\varphi}$ male mice after being fed HFD for 12 weeks. $n = 8$. **(D)** Blood glucose levels (left) and AUC (area under the curve, right) during GTT (glucose tolerance test) in *Prkaa1*^{WT} and *Prkaa1*$^{\Delta M\varphi}$ male mice after being fed HFD for 10 weeks. $n = 6$. Mice were fasted for 16 h and injected with glucose (2 g/kg IP). **(E)** Blood glucose levels (left) and AUC (right) during ITT (insulin tolerance test) in *Prkaa1*^{WT} and *Prkaa1*$^{\Delta M\varphi}$ male mice after being fed HFD for 11 weeks. $n = 6$.

(Continued)

FIGURE 4 | Continued
Mice were fasted for 4 h and injected with insulin (0.75 unit/kg body weight through IP injection). **(F)** Representative images and quantification of Mac2 (macrophage marker) staining in adipose tissues from *Prkaa1*^{WT} and *Prkaa1*$^{\Delta M\varphi}$ male mice after being fed HFD for 12 weeks. $n = 5$ mice/group, 5 areas/mice quantified. Scale bar, 100 μm. **(G)** Representative images and quantification of apoptotic macrophages (TUNEL and F4/80 double-positive cells) in adipose tissues from *Prkaa1*^{WT} and *Prkaa1*$^{\Delta M\varphi}$ male mice after being fed HFD for 12 weeks. $n = 5$ mice/group, 5 areas/mice quantified. Scale bar, 20 μm. **(H)** Quantitative RT-PCR analysis of the mRNA level of *Mcp1* and *Cxcl12* in adipose tissue from *Prkaa1*^{WT} and *Prkaa1*$^{\Delta M\varphi}$ male mice after being fed HFD for 12 weeks. $n = 12$ mice per group. All data are expressed as mean ± SEM. Statistical significance was determined by unpaired Student's *t*-test. $^{**}p < 0.01$, $^{***}p < 0.001$.

levels of these molecules were much lower in *Prkaa1*-deficient BMDMs than WT BMDMs (**Figure 2B**). Posttranscriptional regulation of Slc2a1 by Prkaa1 may occur since the decreased expression of Prkaa1 at the protein, but not mRNA, level was observed in *Prkaa1*-deficient BMDMs. Consistent with the decreased expression of Pfkfb3, the level of fructose-2,6-biphosphate [(the product of Pfkfb3, and the most potent allosteric activator of 6-phosphofructo-1-kinase (PFK1)] was also decreased in *Prkaa1*-deficient BMDMs (**Figure 2C**). The level of lactate, the end product of glycolysis, was also reduced in *Prkaa1*-deficient BMDMs compared with that in control cells (**Figure 2C**). Importantly, we assessed glycolytic metabolism in *Prkaa1*-deficient BMDMs using Seahorse Extracellular Flux analysis via measurement of the ECAR. As shown in **Figure 2D**, the glycolytic metabolism was increased in BMDMs stimulated with MCSF. In contrast, *Prkaa1*-deficient BMDMs exhibited significantly reduced basic glycolysis and glycolytic capacity compared with control cells either in the presence or absence of MCSF. Altogether, these results indicate that PRKAA1/*Prkaa1* is an endogenous regulator of glycolysis in macrophages.

We also evaluated fatty acid oxidation (FAO) in these BMDMs. The mRNA levels of FAO-associated genes, including *Cd36, Fabp4,* and *Cpt1a,* were significantly decreased in *Prkaa1*-deficient BMDMs compared with those in control BMDMs (**Figure 2E**). We next performed the Seahorse assay to determine the OCR in the presence of palmitate. As shown in **Figure 2F**, FAO was dramatically decreased in *Prkaa1*-deficient BMDMs compared with control cells. These results collectively suggest that Prkaa1 regulates FAO in macrophages.

Prkaa1 Deficiency Reduces Leukocyte Recruitment and Macrophage Viability

Glycolysis and FAO are important for leukocyte recruitment and survival. Therefore, we examined whether the decreased metabolism in PRKAA1/*Prkaa1*-deficient leukocytes affects leukocyte recruitment and viability. We first compared the migration capability of WT and *Prkaa1*-deficient BMDMs. In a transwell migration assay, WT macrophages exhibited robust migration to medium supplemented with MCP-1. This ability was markedly decreased for *Prkaa1*-deficient BMDMs (**Figure 3A**). To determine the functional consequences of Prkaa1 deficiency in leukocyte recruitment *in vivo*, *Prkaa1*$^{\Delta M\varphi}$ and control *Prkaa1*^{WT} mice were injected with TNF-α (10 μg/ml) IP to induce vascular inflammation *in vivo*. Four hours after TNF-α treatment, leukocyte rolling and adhesion in the endothelium of postcapillary venules of mouse cremaster muscle were observed with intravital microscopy (**Figure 3B**). Mild trauma caused by the exteriorization of the cremaster muscle led to fast leukocyte rolling. In *Prkaa1*$^{\Delta M\varphi}$ mice, the number of fast rolling leukocytes were comparable to that in *Prkaa1*^{WT} mice (**Figure 3C**). TNF-α treatment stimulated the expression of adhesion molecules on the endothelium and induced slow rolling and adhesion of leukocytes in mice. The numbers of slow rolling and adhesion of leukocyte were reduced by 40–50% in *Prkaa1*$^{\Delta M\varphi}$ mice compared with those in control mice (**Figure 3C**). These results indicate compromised recruitment ability of *Prkaa1*-deficient leukocytes in mice. Taken together, these *in vitro* and *in vivo* findings support that Prkaa1-mediated metabolism is required for leukocyte recruitment and macrophage viability.

We also tested whether Prkaa1-mediated metabolism is important for viability of BMDMs. Flow cytometry analysis showed the percentage of Annexin V-positive BMDMs was much higher in *Prkaa1*-deficient BMDMs than WT cells (**Figure 3D**). Consistent results were obtained in BMDMs stained with TUNEL (**Figure 3E**). In mimicking the *in vivo* diabetic condition, we performed the above assays using BMDMs treated with high glucose (25 mM). The percentage of Annexin V-positive BMDMs was also increased for *Prkaa1*-deficient cells compared with that for WT cells (**Supplementary Figure 4**). These results reveal increased rates of apoptosis in the *Prkaa1*-deficient myeloid cells.

Myeloid *Prkaa1* Deficiency Protects Mice From HFD-Induced Insulin Resistance

Leukocytes, including myeloid cells, participate in the development of HFD-induced metabolic syndrome (Weinstock et al., 2020). We examined whether *Prkaa1* deficiency-mediated decreased leukocyte recruitment affects diet-induced metabolic syndrome. After being fed of HFD for 12 weeks, *Prkaa1*$^{\Delta M\varphi}$ mice displayed resistance to HFD-induced body-weight gain compared with that of *Prkaa1*^{WT} mice (**Figure 4A**). Meanwhile, body composition analysis after feeding of HFD showed that *Prkaa1*$^{\Delta M\varphi}$ mice had a lower body fat content and correspondingly a higher percentage of lean mass than *Prkaa1*^{WT} mice (**Figure 4B**). Of note, the fasting blood glucose level was significantly reduced in *Prkaa1*$^{\Delta M\varphi}$ mice compared with that in *Prkaa1*^{WT} mice under the HFD condition (**Figure 4C**). Consistent with these results, *Prkaa1*$^{\Delta M\varphi}$ mice exhibited improved glucose clearance in GTTs, as well as improved insulin sensitivity in insulin tolerance tests (ITTs) compared with *Prkaa1*^{WT} mice (**Figures 4D,E**). Furthermore, Mac2 staining on adipose sections showed a significant reduction in macrophage infiltration into adipose of *Prkaa1*$^{\Delta M\varphi}$ mice compared with that of *Prkaa1*^{WT} mice (**Figure 4F**). Accordingly, lower levels of chemokines including Mcp-1 and Cxcl12 was also observed in adipose of *Prkaa1*$^{\Delta M\varphi}$ mice compared to *Prkaa1*^{WT} mice under

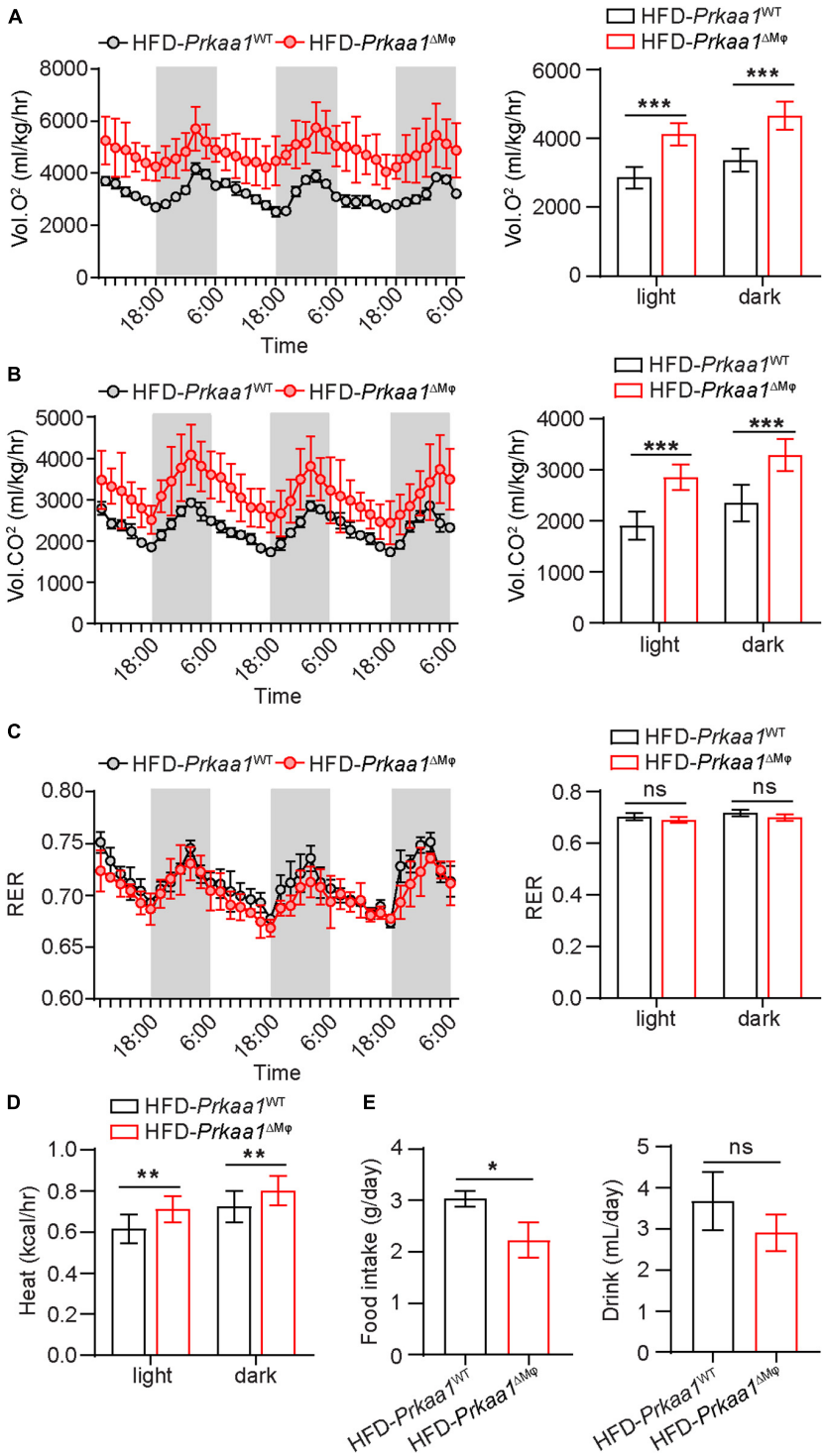

FIGURE 5 | Myeloid *Prkaa1* deficiency increases energy expenditure in response to HFD. **(A)** Oxygen consumption (VO_2) of *Prkaa1*^{WT} and *Prkaa1*$^{\Delta M\varphi}$ male mice during 12-h light and dark cycles recorded on the second day after acclimatization. **(B)** Carbon dioxide consumption (VCO_2) of *Prkaa1*^{WT} and *Prkaa1*$^{\Delta M\varphi}$ male mice during 12-h light and dark cycles recorded on the second day after acclimatization. **(C)** Respiratory exchange ratio (RER) of *Prkaa1*^{WT} and *Prkaa1*$^{\Delta M\varphi}$ male mice during 12-h light and dark cycles recorded on the second day after acclimatization. **(D)** Heat production of *Prkaa1*^{WT} and *Prkaa1*$^{\Delta M\varphi}$ male mice during 12-h light and dark cycles. **(E)** Daily food and drink intake of *Prkaa1*^{WT} and *Prkaa1*$^{\Delta M\varphi}$ male mice during light and dark cycles of animals fed HFD at room temperature (22°C). Area under the curve was calculated during light and dark cycles for each individual animal. RER is calculated by the ratio of VO_2 and VCO_2. Black horizontal bars denote the dark period of the day (12 h). AUC, area under the curve. All data are expressed as mean ± SEM. Statistical significance was determined by unpaired Student's *t*-test. $^*p < 0.05$ was considered significant, $^{**}p < 0.01$, $^{***}p < 0.001$.

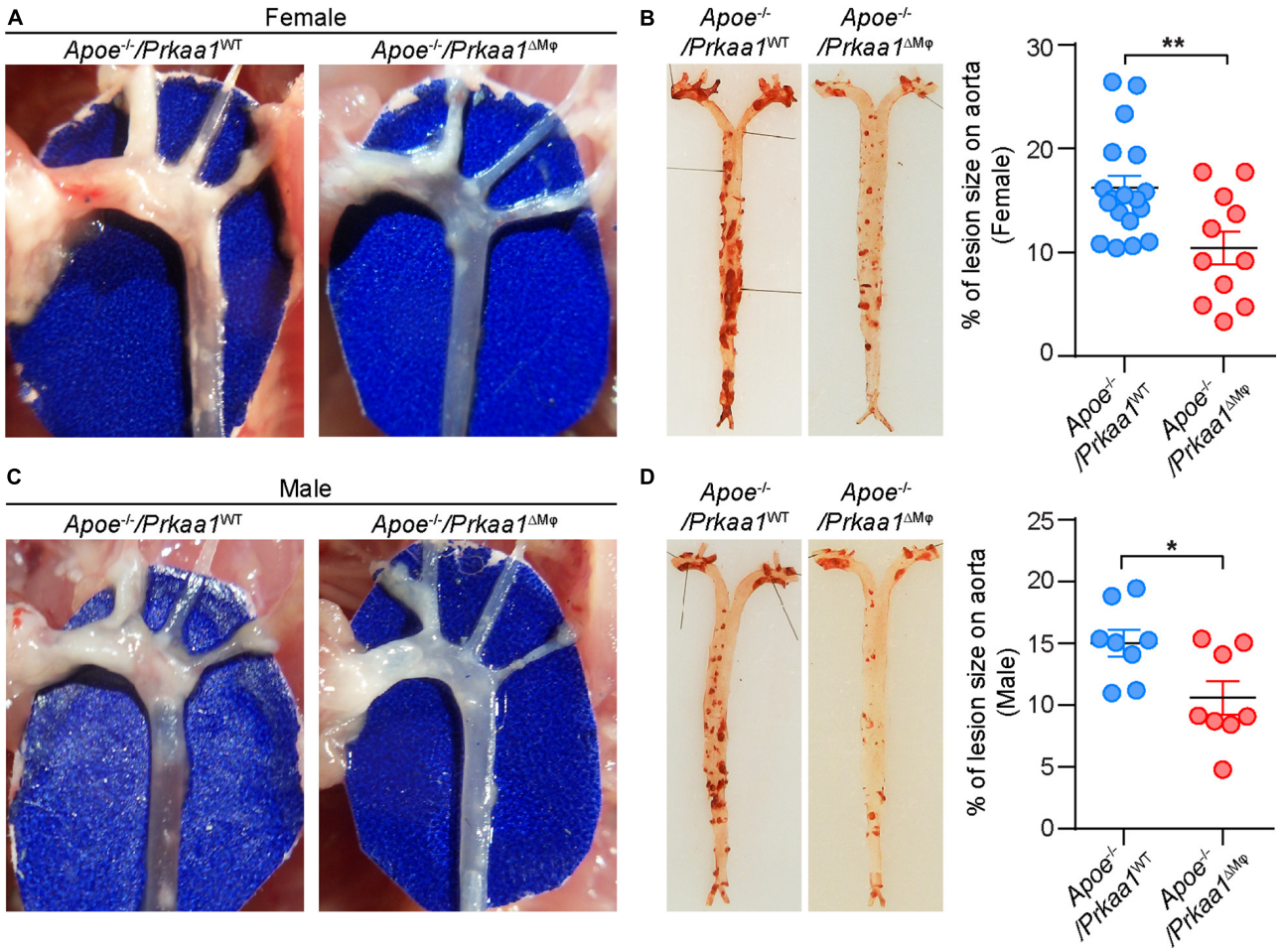

FIGURE 6 | Myeloid *Prkaa1* deficiency decreases Western diet-induced atherosclerotic lesion size. **(A,C)** Aortic arches were dissected and photographed from *Apoe*$^{-/-}$*/Prkaa1*^{WT} and *Apoe*$^{-/-}$*/Prkaa1*$^{\Delta M\varphi}$ female and male mice fed with Western diet for 16 weeks. **(B,D)** Representative images and lesion area quantification of Oil Red O-stained-aortas (*en face*) from *Apoe*$^{-/-}$*/Prkaa1*^{WT} (female $n = 18$, male $n = 8$), *Apoe*$^{-/-}$*/Prkaa1*$^{\Delta M\varphi}$ (female $n = 11$, male $n = 8$) mice after being fed Western diet for 16 weeks. All data are expressed as mean ± SEM. Statistical significance was determined by unpaired Student's *t*-test. $^{*}p < 0.05$ was considered significant, $^{**}p < 0.01$.

the HFD condition (**Figure 4H**). Additionally, TUNEL-staining showed that the percentage of apoptotic cells among F4/80-positive macrophages was much higher in adipose of *Prkaa1*$^{\Delta M\varphi}$ mice than *Prkaa1*^{WT} mice (**Figure 4G**). These results suggest that the low number of myeloid cells due to decreased recruitment and increased apoptosis in adipose of *Prkaa1*$^{\Delta M\varphi}$ mice reduces HFD-induced metabolic syndrome.

We next examined the metabolic rate and RER of these mice via assessments of oxygen consumption and carbon dioxide production using the Comprehensive Lab Animal Monitoring System (CLAMS). *Prkaa1*$^{\Delta M\varphi}$ mice showed higher oxygen consumption and carbon dioxide production than *Prkaa1*^{WT} mice, indicating a higher metabolic rate in the knockout mice (**Figures 5A,B**). However, there was no difference in RER (calculated by the ratio of CO_2 production to O_2 consumption), suggesting that myeloid *Prkaa1* deficiency may not affect energy substrate selection (**Figure 5C**). The heat production of *Prkaa1*$^{\Delta M\varphi}$ mice also trailed higher than those of *Prkaa1*^{WT} mice at both light and dark cycles (**Figure 5D**). In addition to higher energy expenditure, myeloid *Prkaa1* deficiency also exhibited lower energy intake as indicated by lower daily food and drink intake. As shown in **Figure 5E**, *Prkaa1*$^{\Delta M\varphi}$ mice showed decreased daily food intake compared to *Prkaa1*^{WT} mice. Although average daily drink has no significant difference between these two groups, the *Prkaa1*$^{\Delta M\varphi}$ mice still exhibited the trend of slightly lower drink intake than that of *Prkaa1*^{WT} mice. As such, these results indicate that myeloid *Prkaa1* increases energy expenditure and reduces energy intake in response to HFD-induced excessive nutrition.

Myeloid *Prkaa1* Deficiency Decreases Western-Diet Induced Atherosclerosis

We also examined whether *Prkaa1* deficiency-mediated decreased leukocyte recruitment reduces diet-induced atherosclerosis. We bred *Prkaa1*$^{\Delta M\varphi}$ mice with *Apoe*$^{-/-}$

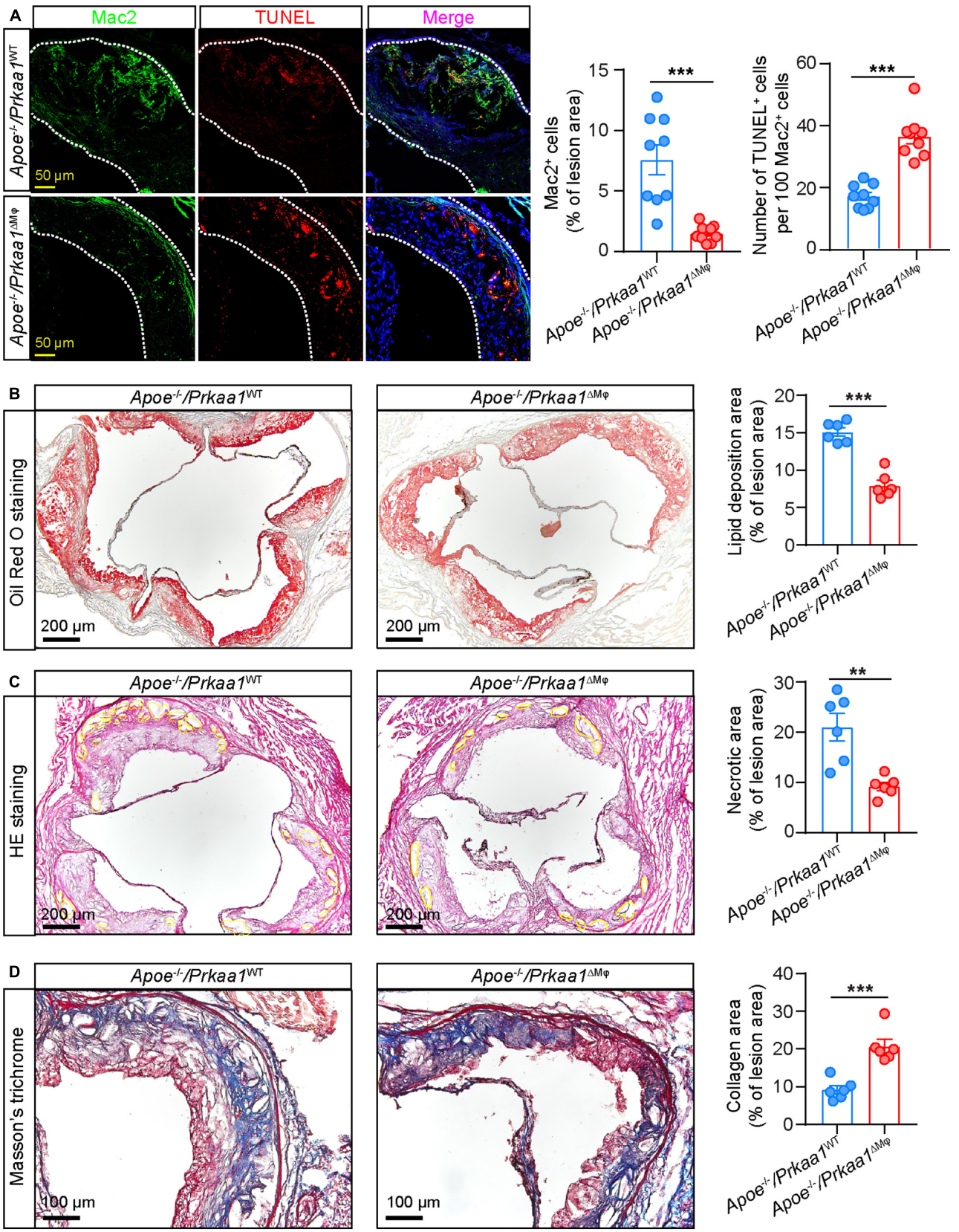

FIGURE 7 | Continued

FIGURE 7 | Myeloid *Prkaa1* deficiency improves features of plaque instability and decreases macrophage viability. **(A)** Representative images and quantification data of Mac2 and TUNEL staining of aortic sinuses from *Apoe*$^{-/-}$/*Prkaa1*^{WT}, *Apoe*$^{-/-}$/*Prkaa1*$^{\Delta M\varphi}$ mice fed Western diet for 16 weeks. Apoptotic cells were labeled by TUNEL (Alexa Fluor-594, Red), macrophages were labeled by Mac2 staining (Alexa Fluor-488, green), and nuclei were counterstained with DAPI (blue). Scale bar: 50 μm; $n = 9$ mice per group. **(B)** Oil Red O staining of aortic sinuses of *Apoe*$^{-/-}$/*Prkaa1*^{WT} and *Apoe*$^{-/-}$/*Prkaa1*$^{\Delta M\varphi}$ male mice fed Western diet for 16 weeks, and quantification of lipid deposition. $n = 6$, Scale bar: 200 μm. **(C)** HE staining of necrotic core area in aortic sinuses of *Apoe*$^{-/-}$/*Prkaa1*^{WT} and *Apoe*$^{-/-}$/*Prkaa1*$^{\Delta M\varphi}$ male mice fed Western diet for 16 weeks, and percentages of necrotic core area. $n = 6$, Scale bar: 200 μm. **(D)** Masson trichrome staining of collagen in aortic sinuses of *Apoe*$^{-/-}$/*Prkaa1*^{WT} and *Apoe*$^{-/-}$/*Prkaa1*$^{\Delta M\varphi}$ male mice fed Western diet for 16 weeks, and percentages of collagen area. $n = 6$. Scale bar: 100 μm. All data are expressed as mean ± SEM. Statistical significance was determined by unpaired Student's *t*-test. * $p < 0.05$ was considered significant, ** $p < 0.01$, *** $p < 0.001$.

mice and generated *Apoe*$^{-/-}$/*Prkaa1*$^{\Delta M\varphi}$ atherosclerotic mice and their littermate *Apoe*$^{-/-}$/*Prkaa1*^{WT} mice. Starting from 7 weeks of age, these age- and gender-matched mice were fed a Western diet containing 42% calories from fat and 0.2% (wt/wt) cholesterol for 16 weeks. *Apoe*$^{-/-}$/*Prkaa1*$^{\Delta M\varphi}$ mice showed significantly fewer and smaller lesions at the aortic arches both in male and female mice than littermate control mice (**Figures 6A,C**). This observation was confirmed with quantitative measurement of atherosclerotic lesions following Oil Red O (ORO) staining of aortas (**Figures 6B,D**). Decreased levels of cholesterol, triglyceride, and glucose in blood of both male and female *Apoe*$^{-/-}$/*Prkaa1*$^{\Delta M\varphi}$ mice were found (**Supplementary Figure 5**), likely contributing to the alleviated atherosclerosis in *Apoe*$^{-/-}$/*Prkaa1*$^{\Delta M\varphi}$ mice. Additionally, *Apoe*$^{-/-}$/*Prkaa1*$^{\Delta M\varphi}$ mice exhibited no significant difference in the number of circulating white blood cells, including neutrophils, leukocytes and monocytes, compared with *Apoe*$^{-/-}$/*Prkaa1*^{WT} mice (**Supplementary Figure 5**).

Aortic sinuses from these mice were further examined to evaluate the effect of *Prkaa1*-deficient myeloid cells in determining the size and stability of atherosclerotic lesions. Immunostaining of aortic sinus sections with antibody of the macrophage marker Mac2 showed that the number of macrophages was much less in *Apoe*$^{-/-}$/*Prkaa1*$^{\Delta M\varphi}$ mice than control mice (**Figure 7A**). Additionally, macrophage viability in aortic sinuses of these mice was analyzed by TUNEL staining. The number of TUNEL-positive cells was markedly increased in the aortic sinuses of *Apoe*$^{-/-}$/*Prkaa1*$^{\Delta M\varphi}$ mice compared with those of control mice (**Figure 7A**). These observations indicate that the decreased number of macrophages in lesions of *Apoe*$^{-/-}$/*Prkaa1*$^{\Delta M\varphi}$ mice is due to both decreased recruitment of monocytes to arterial vessels and increased apoptosis of macrophages in atherosclerotic lesions. As a result, the size of atherosclerotic lesions (**Figure 7B**), indicated with ORO staining, was decreased while the stability of atherosclerotic lesions, evident with necrotic cores with HE staining and collagen content by Masson's trichrome staining (**Figures 7C,D**), was increased in *Apoe*$^{-/-}$/*Prkaa1*$^{\Delta M\varphi}$ mice compared to those of control mice. Thus, mice with myeloid deletion of *Prkaa1* exhibit less severe and more stable atherosclerosis.

DISCUSSION

In the present study, we found that *Prkaa1* expression is upregulated in leukocytes sorted from adipose tissue of HFD-fed mice, and this was accompanied with upregulated genes associated with glycolysis and FAO. Accordingly, compromised glycolysis and FAO was observed in *Prkaa1*-deficient macrophages. Leukocyte recruitment, evidenced with macrophage migration *in vitro* and leukocyte rolling and adhesion *in vivo,* was compromised in the absence of *Prkaa1*. Consequently, chronic inflammatory disorders, including diet-induced diabetes and atherosclerosis, were reduced in *Prkaa1*$^{\Delta M\varphi}$ mice.

AMPKα1/PRKAA1 mediates glycolysis and FAO in macrophages. AMPK/PRKA serves as a master regulator of energy metabolism to control key factors involved in the many pathways to maintain energy balance. In addition to hypoxia, other stresses such as chronic inflammation and aberrant glucose and lipid levels enhance and/or activate AMPK/PRKA. *Apoe* deficiency dysregulates the levels of glucose and lipids and causes chronic inflammation in mice. This may also result in increased function of AMPK. AMPK/PRKA maintains energy homeostasis by activating catabolic processes to increase ATP production and inhibiting anabolic processes to suppress ATP consumption. In order to replenish ATP stores, AMPK/PRKA actively stimulates glucose utilization by inducing glucose transporter expression and further increases glucose uptake into cells (Kim et al., 2010). AMPK/PRKA also has been reported to regulate glycolytic flux through the pathway by phosphorylating phosphofructo-2-kinase/fructose 2,6-bisphosphatase 3 (PFKFB3), which affects the activity of PFK1, a rate-limiting enzyme in glycolysis (Bando et al., 2005). Our previous study has demonstrated that AMPK/PRKA regulates glycolysis in part via the HIF1α pathway (Yang et al., 2018), and increased HIF1A expression promotes glycolysis, resulting in a rapid supply of ATP (Semenza, 2012). In addition to stimulating glycolysis, AMPK/PRKA also increases FAO by a reduction of the activity of ACC, decreased the level of malonyl-CoA, and resulted in increased fatty acid import into mitochondria for β-oxidation (Saggerson, 2008). The studies indicated that the AMPK–ACC–malonyl CoA–carnitine palmitoyl transferase 1 mechanism plays a key role in the physiological regulation of FAO (Dagher et al., 2001). Although these studies have indicated an interaction between AMPK/PRKA and cellular metabolism in cells of other types, our study has demonstrated that Prkaa1 is also critical in regulation of glycolysis and FAO in leukocytes in mice. Compromised production of ATP, especially on the actin compartment in *Prkaa1*-deficient leukocytes, may dramatically affect many steps of leukocyte recruitment, including rolling, adhesion and migration. Additionally, decreased energy production plus decreased metabolites of glycolysis and FAO may also result in compromised repair, leading to apoptosis of infiltrated macrophages.

The physiological effect of *Prkaa1* in leukocytes revealed in this study may not explain the pharmacological effect of AMPK/PRKA activation. Over the past decades, much work has emerged to support the beneficial role of AMPK in chronic inflammatory disorders such as metabolic syndrome and inflammatory diseases (Cheang et al., 2014; Guma et al., 2015; Kjøbsted et al., 2015). It has been reported that metformin or AICAR attenuates Ang II-induced atheromatous plaque formation and protects against hyperglycemia-induced atherosclerosis (Li et al., 2010; Vasamsetti et al., 2015; Wang et al., 2017) and also reduces insulin resistance (Yang et al., 2012). These beneficial effects may operate mainly through the effect on cells other than myeloid cells, such as vascular cells or metabolic cells. Also, some beneficial effect from the use of metformin, AICAR or A769662 may be through an AMPK-independent pathway (Guigas et al., 2006; Kirchner et al., 2018). Additionally, pharmacological activation of AMPKa1 in leukocytes may also reduce inflammation through many other pathways than the metabolism induced by pharmacologically activated AMPKa1. All of these possibilities will be explored in our future studies.

Phenotypic variance is noted in myeloid *Prkaa1*-deficient mice. Mice that were deficient in myeloid *Prkaa1*, when bred to $Ldlr^{-/-}$ mice, displayed enhanced macrophage inflammation, increased plasma cholesterol and triglyceride levels, and a phenotype of enhanced diet-induced obesity and insulin resistance as well as accelerated atherosclerosis (Cao et al., 2016). In contrast, $Apoe^{-/-}$ mice with *Prkaa1* deletion or myeloid *Prkaa1* deletion showed reduced monocyte differentiation and survival, thus attenuating the initiation and progression of atherosclerosis (Zhang et al., 2017). $Apoe^{-/-}$ mice with myeloid *Prkaa2* deficiency developed smaller atherosclerotic plaques that contained fewer macrophages and less MMP9 than plaques from control mice through regulating myeloid DNA methylation (Fisslthaler et al., 2019). A very recent study did not find any difference in the size of atherosclerotic lesions between control $Apoe^{-/-}$ mice and $Apoe^{-/-}$ mice deficient in both *Prkaa1* and *Prkaa2* in myeloid cells (LeBlond et al., 2020). These inconsistent results from different studies indicate the disease phenotype is affected by many important experimental factors, such as background strain, littermate control, diet and the stages of disease when mice were evaluated. In our study, we have followed a recently published protocol for rodent atherosclerosis (Daugherty et al., 2017). With our expertise in cell metabolism and leukocyte recruitment, we are confident of our conclusion in which AMPK/PRKAA1/Prkaa1-mediated metabolism is critical for myeloid cell recruitment and survival.

CONCLUSION

In conclusion, these findings clarify that AMPKα1 plays a key role in regulating macrophage glucose and lipid metabolism, further controls monocyte recruitment and macrophage viability, and eventually promotes the development of diet-induced insulin resistance and atherosclerosis. Targeting AMPKα1-driven macrophage metabolism could be a therapeutic intervention in cardiovascular diseases.

DATA AVAILABILITY STATEMENT

The raw data supporting the conclusions of this article will be made available by the authors, without undue reservation.

ETHICS STATEMENT

The animal study was reviewed and approved by IACUC (Institutional Animal Care & Use Committee) of Augusta University.

AUTHOR CONTRIBUTIONS

QY, QM, and YH designed the experiments and co-wrote the manuscript. QY, QM, JX, JZ, SL, and ZL performed the experiments and prepared the figures and manuscript. QY, YZ, QD, ZL, and JS provided input on experimental design, methods, and research strategy. JZ, DF, and NW critically reviewed and revised the manuscript. ZB and MH provided the reagents or materials and participated in designing the experiments. All authors contributed to the article and approved the submitted version.

FUNDING

This work was supported by the National Science Foundation of China (Grant 81870324); Shenzhen Science and Technology Innovation Committee (Grants JCYJ20190808155605447, JCYJ20170810163238384, JCYJ20190808155801648, and JCYJ20170412150405310); Guangdong Natural Science Foundation (Grants 2020A1515010010 and 2014A030312004); Shenzhen-Hong Kong Institute of Brain Science–Shenzhen Fundamental Research Institutions (2019SHIBS0004); China Postdoctoral Science Foundation (8206300346); American Heart Association (Grants 19POST34430119 and 19TPA34910043); National Institutes of Health (Grants R01HL134934, R01EY030500, R01HL142097, and R01HL138410); and VA Merit Review (Grant BX002035).

SUPPLEMENTARY MATERIAL

The Supplementary Material for this article can be found online at: https://www.frontiersin.org/articles/10.3389/fcell.2020.611354/full#supplementary-material

Supplementary Figure 1 | Schematic diagram of leukocyte sorting from adipose tissues. Stromal vascular cells (SVFs) were isolated from adipose tissues and stained with antibodies against CD45, CD31, and 7AAD. The cell subtypes identified using flow cytometry defined the leukocytes as $CD45^{+}$ $CD31^{-}7AAD^{-}$.

Supplementary Figure 2 | Representative images and quantification data of p-Prka and Pfkfb3 co-staining with F4/80 (macrophage markers) in adipose

tissues from HFD- and CD-fed mice. $n = 4$, Scale bars, 20 μm. All data were expressed as mean ± SEM. Statistical significance was determined by unpaired Student's *t*-test. $^{*}p < 0.05$ was considered significant, $^{**}p < 0.01$, $^{***}p < 0.001$.

Supplementary Figure 3 | (A) Schematic diagram of myeloid-specific Prkaa1-deficient mouse generation by crossing *Prkaa1*$^{f/f}$ with *Lysm*^{cre} mice. **(B)** Representative genotyping gel demonstrating the generation of *Prkaa1* myeloid knockout mice. **(C)** Western blot analysis and densitometric quantification of Prkaa1 protein levels in BMDMs cultured from *Prkaa1*^{WT} and *Prkaa1*$^{\Delta M\varphi}$ mice. $n = 6$. All data are expressed as mean ± SEM. Statistical significance was determined by unpaired Student's *t*-test. $^{*}p < 0.05$ was considered significant, $^{**}p < 0.01$, $^{***}p < 0.001$.

Supplementary Figure 4 | (A) Representative images and quantification of MCP-1-induced migration in BMDMs cultured from *Prkaa1*^{WT} and *Prkaa1*$^{\Delta M\varphi}$ mice in normal and high glucose conditions (NG: 5.5 mM, HG: 30 mM). $n = 8$, Scale bars, 100 μm. **(B)** Quantification data and representative images of flow cytometry analysis of Annexin V staining in BMDMs cultured from bone marrow of Prkaa1WT and Prkaa1 ΔMφ mice in NG and HG conditions. $n = 6$. All data are expressed as mean ± SEM. Statistical significance was determined by one-way ANOVA followed by Bonferroni test. $^{*}p < 0.05$ was considered significant, $^{**}p < 0.01$, $^{***}p < 0.001$.

Supplementary Figure 5 | (A) Levels of total cholesterol in plasma of *Apoe*$^{-/-}$/*Prkaa1*^{WT} (female, $n = 8$; male, $n = 8$), *Apoe*$^{-/-}$/*Prkaa1*$^{\Delta M\varphi}$ (female, $n = 7$; male, $n = 7$) mice fed Western diet for 16 weeks. **(B)** Levels of triglyceride in plasma of *Apoe*$^{-/-}$/*Prkaa1*^{WT} (female, $n = 7$; male, $n = 8$), *Apoe*$^{-/-}$/*Prkaa1*$^{\Delta M\varphi}$ (female, $n = 5$; male, $n = 7$) mice fed Western diet for 16 weeks. **(C)** Levels of glucose in plasma of *Apoe*$^{-/-}$/*Prkaa1*^{WT} (*Prkaa1*$^{\Delta M\varphi}$, female, $n = 7$; male, $n = 9$) mice fed Western diet for 16 weeks. All data are expressed as mean ± SEM. Statistical significance was determined by unpaired Student's *t*-test. $^{*}p < 0.05$ was considered significant, $^{**}p < 0.01$, $^{***}p < 0.001$.

Supplementary Figure 6 | Hemavet data analysis of white blood cells (WBC), neutrophils (NE), leukocytes (LY) and monocytes (MO) from *Apoe*$^{-/-}$/*Prkaa1*^{WT} (female, $n = 13$; male, $n = 15$), *Apoe*$^{-/-}$/*Prkaa1*$^{\Delta M\varphi}$ (female, $n = 14$; male, $n = 11$) mice fed Western diet for 16 weeks. All data are expressed as mean ± SEM. Statistical significance was determined by unpaired Student's *t*-test. $^{*}p < 0.05$ was considered significant, $^{**}p < 0.01$, $^{***}p < 0.001$. (PLT, primed lymphocyte typing).

REFERENCES

Bai, Y., and Sun, Q. (2015). Macrophage recruitment in obese adipose tissue. *Obes. Rev.* 16, 127–136. doi: 10.1111/obr.12242

Bando, H., Atsumi, T., Nishio, T., Niwa, H., Mishima, S., Shimizu, C., et al. (2005). Phosphorylation of the 6-phosphofructo-2-kinase/fructose 2,6-bisphosphatase/PFKFB3 family of glycolytic regulators in human cancer. *Clin. Cancer Res.* 11, 5784–5792. doi: 10.1158/1078-0432.ccr-05-0149

Boudaba, N., Marion, A., Huet, C., Pierre, R., Viollet, B., and Foretz, M. (2018). AMPK re-activation suppresses hepatic steatosis but its downregulation does not promote fatty liver development. *EBioMedicine* 28, 194–209. doi: 10.1016/j.ebiom.2018.01.008

Cai, Z., Ding, Y., Zhang, M., Lu, Q., Wu, S., Zhu, H., et al. (2016). Ablation of adenosine monophosphate-activated protein kinase alpha1 in vascular smooth muscle cells promotes diet-induced atherosclerotic calcification in vivo. *Circ. Res.* 119, 422–433. doi: 10.1161/CIRCRESAHA.116.308301

Cao, Q., Cui, X., Wu, R., Zha, L., Wang, X., Parks, J. S., et al. (2016). Myeloid deletion of alpha1AMPK exacerbates *Atherosclerosis* in LDL receptor knockout (LDLRKO) mice. *Diabetes* 65, 1565–1576. doi: 10.2337/db15-0917

Catalan, V., Gomez-Ambrosi, J., Rodríguez, A., and Frühbeck, G. (2013). Adipose tissue immunity and cancer. *Front. Physiol.* 4:275. doi: 10.3389/fphys.2013.00275

Cheang, W. S., Tian, X. Y., Wong, W. T., Lau, C. W., Lee, S. S., Chen, Z. Y., et al. (2014). Metformin protects endothelial function in diet-induced obese mice by inhibition of endoplasmic reticulum stress through 5' adenosine monophosphate–activated protein kinase–peroxisome proliferator–activated receptor δ pathway. *Arterioscleros. Thromb. Vasc. Biol.* 34, 830–836. doi: 10.1161/ATVBAHA.113.301938

Dagher, Z., Ruderman, N., Tornheim, K., and Ido, Y. (2001). Acute regulation of fatty acid oxidation and AMP-activated protein kinase in human umbilical vein endothelial cells. *Circ. Res.* 88, 1276–1282. doi: 10.1161/hh1201.092998

Daugherty, A., Tall, A. R., Daemen, M. J. A. P., Falk, E., Fisher, E. A., García-Cardeña, G., et al. (2017). Recommendation on design, execution, and reporting of animal atherosclerosis studies: a scientific statement from the american heart association. *Arterioscleros. Thromb. Vasc. Biol.* 37, e131–e157. doi: 10.1161/ATV.0000000000000062

Ding, Y., Zhang, M., Song, P., and Zou, M.-H. (2017). Deficiency of AMP-activated protein kinase alpha 1 promotes the vulnerability of atherosclerotic plaques at brachiocephalic arteries. *FASEB J.* 31, 183–186. doi: 10.1096/fasebj.31.1_supplement.183.6

Fisslthaler, B., and Fleming, I. (2009). Activation and signaling by the AMP-activated protein kinase in endothelial cells. *Circ. Res.* 105, 114–127. doi: 10.1161/circresaha.109.201590

Fisslthaler, B., Zippel, N., Abdel Malik, R., Delgado Lagos, F., Zukunft, S., Thoele, J., et al. (2019). Myeloid-specific deletion of the AMPKα2 subunit alters monocyte protein expression and atherogenesis. *Int. J. Mol. Sci.* 20:3005. doi: 10.3390/ijms20123005

Garcia, D., and Shaw, R. J. (2017). AMPK: mechanisms of cellular energy sensing and restoration of metabolic balance. *Mol. Cell.* 66, 789–800. doi: 10.1016/j.molcel.2017.05.032

Guigas, B., Bertrand, L., Taleux, N., Foretz, M., Wiernsperger, N., Vertommen, D., et al. (2006). 5-Aminoimidazole-4-carboxamide-1-beta-D-ribofuranoside and metformin inhibit hepatic glucose phosphorylation by an AMP-activated protein kinase-independent effect on glucokinase translocation. *Diabetes* 55, 865–874. doi: 10.2337/diabetes.55.04.06.db05-1178

Guma, M., Wang, Y., Viollet, B., and Liu-Bryan, R. (2015). AMPK activation by A-769662 controls IL-6 expression in inflammatory arthritis. *PLoS One* 10:e0140452. doi: 10.1371/journal.pone.0140452

Hardie, D. G. (2004). The AMP-activated protein kinase pathway–new players upstream and downstream. *J. Cell. Sci.* 117(Pt 23), 5479–5487. doi: 10.1242/jcs.01540

Hardie, D. G. (2011). AMP-activated protein kinase: an energy sensor that regulates all aspects of cell function. *Genes Dev.* 25, 1895–1908. doi: 10.1101/gad.17420111

Hardie, D. G., and Hawley, S. A. (2001). AMP-activated protein kinase: the energy charge hypothesis revisited. *Bioessays* 23, 1112–1119. doi: 10.1002/bies.10009

Kahn, B. B., Alquier, T., Carling, D., and Hardie, D. G. (2005). AMP-activated protein kinase: ancient energy gauge provides clues to modern understanding of metabolism. *Cell Metab.* 1, 15–25. doi: 10.1016/j.cmet.2004.12.003

Kim, J. H., Park, J. M., Yea, K., Kim, H. W., Suh, P. G., and Ryu, S. H. (2010). Phospholipase D1 mediates AMP-activated protein kinase signaling for glucose uptake. *PLoS One* 5:e9600. doi: 10.1371/journal.pone.0009600

Kirchner, J., Brüne, B., and Namgaladze, D. (2018). AICAR inhibits NFκB DNA binding independently of AMPK to attenuate LPS-triggered inflammatory responses in human macrophages. *Sci. Rep.* 8:7801. doi: 10.1038/s41598-018-26102-3

Kjøbsted, R., Treebak, J. T., Fentz, J., Lantier, L., Viollet, B., Birk, J. B., et al. (2015). Prior AICAR stimulation increases insulin sensitivity in mouse skeletal muscle in an AMPK-dependent manner. *Diabetes* 64, 2042–2055. doi: 10.2337/db14-1402

LeBlond, N. D., Ghorbani, P., O'Dwyer, C., Ambursley, N., Nunes, J. R. C., Smith, T. K. T., et al. (2020). Myeloid deletion and therapeutic activation of AMP-activated protein kinase (AMPK) do not alter atherosclerosis in male or female mice. *BioRxiv* [Preprint]. doi: 10.1101/2020.07.15.204487

Ley, K., Laudanna, C., Cybulsky, M. I., and Nourshargh, S. (2007). Getting to the site of inflammation: the leukocyte adhesion cascade updated. *Nat. Rev. Immunol.* 7, 678–689. doi: 10.1038/nri2156

Li, D., Wang, D., Wang, Y., Ling, W., Feng, X., and Xia, M. (2010). Adenosine monophosphate-activated protein kinase induces cholesterol efflux from macrophage-derived foam cells and alleviates atherosclerosis in apolipoprotein E-deficient mice. *J. Biol. Chem.* 285, 33499–33509. doi: 10.1074/jbc.M110.159772

Libby, P. (2002). Inflammation in atherosclerosis. *Nature* 420, 868–874. doi: 10.1038/nature01323

Lumeng, C. N., and Saltiel, A. R. (2011). Inflammatory links between obesity and metabolic disease. *J. Clin. Investig.* 121, 2111–2117. doi: 10.1172/jci57132

Marelli-Berg, F. M., and Jangani, M. (2018). Metabolic regulation of leukocyte motility and migration. *J. Leukoc. Biol.* 104, 285–293. doi: 10.1002/jlb.1mr1117-472r

Murray, P. J., and Wynn, T. A. (2011). Protective and pathogenic functions of macrophage subsets. *Nat. Rev. Immunol.* 11, 723–737. doi: 10.1038/nri3073

Ross, R. (1999). Atherosclerosis–an inflammatory disease. *N. Engl. J. Med.* 340, 115–126. doi: 10.1056/NEJM199901143400207

Saggerson, D. (2008). Malonyl-CoA, a key signaling molecule in mammalian cells. *Annu. Rev. Nutr.* 28, 253–272. doi: 10.1146/annurev.nutr.28.061807.155434

Semba, H., Takeda, N., Isagawa, T., Sugiura, Y., Honda, K., Wake, M., et al. (2016). HIF-1α-PDK1 axis-induced active glycolysis plays an essential role in macrophage migratory capacity. *Nat. Commun.* 7:11635. doi: 10.1038/ncomms11635

Semenza, G. L. (2012). Hypoxia-inducible factors in physiology and medicine. *Cell* 148, 399–408. doi: 10.1016/j.cell.2012.01.021

Shi, C., and Pamer, E. G. (2011). Monocyte recruitment during infection and inflammation. *Nat. Rev. Immunol.* 11, 762–774. doi: 10.1038/nri3070

Van Schaftingen, E., Lederer, B., Bartrons, R., and Hers, H. G. (1982). A kinetic study of pyrophosphate: fructose-6-phosphate phosphotransferase from potato tubers. Application to a microassay of fructose 2,6-bisphosphate. *Eur. J. Biochem.* 129, 191–195. doi: 10.1111/j.1432-1033.1982.tb07039.x

Vasamsetti, S. B., Karnewar, S., Kanugula, A. K., Thatipalli, A. R., Kumar, J. M., and Kotamraju, S. (2015). Metformin inhibits monocyte-to-macrophage differentiation via AMPK-mediated inhibition of STAT3 activation: potential role in atherosclerosis. *Diabetes* 64, 2028–2041. doi: 10.2337/db14-1225

Venter, G., Oerlemans, F. T. J. J., Wijers, M., Willemse, M., Fransen, J. A. M., and Wieringa, B. (2014). Glucose controls morphodynamics of LPS-stimulated macrophages. *PLoS One* 9:e96786. doi: 10.1371/journal.pone.0096786

Wang, Q., Zhang, M., Torres, G., Wu, S., Ouyang, C., Xie, Z., et al. (2017). Metformin suppresses diabetes-accelerated atherosclerosis via the inhibition of Drp1-mediated mitochondrial fission. *Diabetes* 66, 193–205. doi: 10.2337/db16-0915

Webb, B. A., Dosey, A. M., Wittmann, T., Kollman, J. M., and Barber, D. L. (2017). The glycolytic enzyme phosphofructokinase-1 assembles into filaments. *J. Cell Biol.* 216, 2305–2313. doi: 10.1083/jcb.201701084

Weinstock, A., Silva, H. M., Moore, K. J., Schmidt, A. M., and Fisher, E. A. (2020). Leukocyte heterogeneity in adipose tissue, including in obesity. *Circ. Res.* 126, 1590–1612. doi: 10.1161/CIRCRESAHA.120.316203

Weisberg, S. P., McCann, D., Desai, M., Rosenbaum, M., Leibel, R. L., and Ferrante, A. W. Jr. (2003). Obesity is associated with macrophage accumulation in adipose tissue. *J. Clin. Invest.* 112, 1796–1808. doi: 10.1172/jci19246

Wu, H., and Ballantyne, C. M. (2020). Metabolic inflammation and insulin resistance in obesity. *Circ. Res.* 126, 1549–1564. doi: 10.1161/circresaha.119.315896

Wu, L., Zhang, L., Li, B., Jiang, H., Duan, Y., Xie, Z., et al. (2018). AMP-activated protein kinase (AMPK) regulates energy metabolism through modulating thermogenesis in adipose tissue. *Front. Physiol.* 9:122. doi: 10.3389/fphys.2018.00122

Wu, S., and Zou, M.-H. (2020). AMPK, mitochondrial function, and cardiovascular disease. *Int. J. Mol. Sci.* 21:4987. doi: 10.3390/ijms21144987

Xu, H., Barnes, G. T., Yang, Q., Tan, G., Yang, D., Chou, C. J., et al. (2003). Chronic inflammation in fat plays a crucial role in the development of obesity-related insulin resistance. *J. Clin. Invest.* 112, 1821–1830. doi: 10.1172/jci19451

Yang, Q., Xu, J., Ma, Q., Liu, Z., Sudhahar, V., Cao, Y., et al. (2018). PRKAA1/AMPKalpha1-driven glycolysis in endothelial cells exposed to disturbed flow protects against atherosclerosis. *Nat. Commun.* 9:4667. doi: 10.1038/s41467-018-07132-x

Yang, Z., Wang, X., He, Y., Qi, L., Yu, L., Xue, B., et al. (2012). The full capacity of AICAR to reduce obesity-induced inflammation and insulin resistance requires myeloid SIRT1. *PLoS One* 7:e49935. doi: 10.1371/journal.pone.0049935

Zhang, M., Zhu, H., Ding, Y., Liu, Z., Cai, Z., and Zou, M. H. (2017). AMP-activated protein kinase alpha1 promotes atherogenesis by increasing monocyte-to-macrophage differentiation. *J. Biol. Chem.* 292, 7888–7903. doi: 10.1074/jbc.M117.779447

Conflict of Interest: The authors declare that the research was conducted in the absence of any commercial or financial relationships that could be construed as a potential conflict of interest.

frontiers in Cell and Developmental Biology

REVIEW
published: 15 January 2021
doi: 10.3389/fcell.2020.620471

Intravital Imaging of Pulmonary Immune Response in Inflammation and Infection

Nazli Alizadeh-Tabrizi[1]*, *Stefan Hall*[1] and *Christian Lehmann*[1,2]

[1] Department of Physiology & Biophysics, Dalhousie University, Halifax, NS, Canada, [2] Department of Anesthesia, Pain Management and Perioperative Medicine, Dalhousie University, Halifax, NS, Canada

Intravital microscopy (IVM) is a unique imaging method providing insights in cellular functions and interactions in real-time, without the need for tissue extraction from the body. IVM of the lungs has specific challenges such as restricted organ accessibility, respiratory movements, and limited penetration depth. Various surgical approaches and microscopic setups have been adapted in order to overcome these challenges. Among others, these include the development of suction stabilized lung windows and the use of more advanced optical techniques. Consequently, lung IVM has uncovered mechanisms of leukocyte recruitment and function in several models of pulmonary inflammation and infection. This review focuses on bacterial pneumonia, aspiration pneumonia, sepsis-induced acute lung Injury, and cystic fibrosis, as examples of lung inflammation and infection. In addition, critical details of intravital imaging techniques of the lungs are discussed.

Keywords: inflammation, infection, lung, intravital microscopy, leukocytes

OPEN ACCESS

Edited by:
Xunbin Wei,
Peking University, China

Reviewed by:
Pedro Elias Marques,
KU Leuven, Belgium
Heather Hickman,
National Institutes of Health (NIH),
United States

***Correspondence:**
Nazli Alizadeh-Tabrizi
nazli.tabrizi@dal.ca

Specialty section:
This article was submitted to Cell Adhesion and Migration, a section of the journal Frontiers in Cell and Developmental Biology

Received: *23 October 2020*
Accepted: *18 December 2020*
Published: *15 January 2021*

Citation:
Alizadeh-Tabrizi N, Hall S and Lehmann C (2021) Intravital Imaging of Pulmonary Immune Response in Inflammation and Infection. Front. Cell Dev. Biol. 8:620471. doi: 10.3389/fcell.2020.620471

INTRODUCTION

The application of microscopy to live tissues (syn.: intravital microscopy, IVM), allows imaging of cellular processes at high resolution in real-time. This technology provides unique information in addition to *ex vivo/in vitro* methods without the need for removing the tissue from the physiological environment, processing sections, fixation, or staining (Wells et al., 2018). Various experimental IVM models have been successfully established to demonstrate time-sequential cellular changes in several organs under different physiological and pathophysiological conditions, e.g., in liver, brain, or skeletal muscle (Kuhnle et al., 1993; Kramer et al., 2000; McCormack et al., 2000; Mempel et al., 2003; Khandoga et al., 2005; Kuebler et al., 2007; Lindert et al., 2007; Tabuchi et al., 2008; Ochi et al., 2019). Yet, one of the most difficult organs for intravital imaging is the lung due to limited accessibility based on its enclosed position within the body, its respiratory movements, and the physical impact of the heart beat (Tabuchi et al., 2008). Although there are different imaging strategies to study cell populations—both, *in vitro* such as histology, immunohistochemistry, and *in vivo* such as MRI, and CT–any of these methods is not able to visualize dynamic cellular behavior and mechanisms during physiological and pathophysiological condition. For instance, clinical modalities such as positron emission tomography (PET), magnetic resonance imaging (MRI), and computed tomography (CT)

can provide non-invasive images of the lungs. However, they lack the resolution necessary to study cellular mechanisms. Classical fluorescence techniques using ultraviolet (UV) light marked the beginning of lung IVM and are still used by the scientific community (Entenberg et al., 2015; Fiole and Tournier, 2016). Confocal microscopy and modern fluorescence-based technologies, such as multiphoton excitation microscopy have revealed more complex as well as deeper pulmonary structures (Krahl, 1963; Looney et al., 2011; Presson et al., 2011; Entenberg et al., 2015). Ultimately, all these achievements largely contributed to the establishment of intravital imaging as a gold standard in cellular lung research (Fiole and Tournier, 2016; Rodriguez-Tirado et al., 2016). In this review, we first describe the technical aspects of lung IVM. In the second part, we review experimental lung inflammation and infection models utilizing lung IVM.

SETUP

Lung IVM can be performed by using different microscopic techniques. Historically, fluorescence microscopy was used first to study pulmonary inflammation and infection. Newer technologies include laser scanning confocal microscopy, single-photon microscopy, and two/multiphoton microscopy (Fiole and Tournier, 2016; Wang, 2016).

Fluorescence Microscopy

Fluorescence microscopy is a technique in which a sample stained with fluorescent dye is visualized using a halogen lamp such as xenon, mercury, or tungsten as a light source (Lindon et al., 2016). The objective lens focuses the excitation light, allowing maximal collection of emitted fluorescence and magnification for the observation of fine details (Herman, 1998). The fluorescent dye in the sample is excited with a relatively short wavelength, usually blue or ultraviolet light, that matches the fluorophore excitation wavelength. The emitted fluorescence has longer wavelength and less energy in comparison to the absorbed excitation light, which is blocked by the emission filter. A beam splitter is required to separate the excitation light from emission fluorescence and prevent overlap in their light paths. The dichroic mirror reflects the shorter wavelength excitation light and transmits the longer wavelength of emitted fluorescence through the barrier filter (Lichtman and Conchello, 2005). Emitted fluorescence from the specimen that is collected by the objective passes through the dichroic mirror and the barrier filter to the eyepieces or detector (Sanderson et al., 2014). The selectivity for specific wavelengths facilitates the visualization of different fluorescent objects as a bright structure against a dark background (Lichtman and Conchello, 2005; Lindon et al., 2016). Although fluorescence microscopy has been widely used to study tissues *in vivo* (Lindon et al., 2016), its application in lung IVM is limited to superficial layers and low resolution (Witte, 1992; Presson et al., 2011; Lefrançais et al., 2017).

Confocal Microscopy

Confocal microscopes differ from conventional fluorescence microscopes in that they use a laser light source and improve image resolution due to reduced detection of out of focus light (Norman, 2005). According to the principle of confocal microscopy, light is collected through narrow apertures (pinholes) that exclude out of focus light. The elimination of out of focus light results in an improvement in lateral and axial resolution. Both laser scanning and spinning disk confocal microscopes pass a single beam of laser light through the pinhole. It should be noted that while confocal laser scanning microscopy focuses the light through one small pinhole in order to sequentially scan the sample point by point, confocal spinning disk microscopy exploits multiple pinholes for simultaneous confocal illumination (Masedunskas et al., 2012; Sanderson et al., 2014; Lefrançais et al., 2017). Therefore, either X–Y-deflection of the laser or a spinning disk with a spatial array of pinholes and automated-focus (z-axis) control enables the visualization of sequential optical sections of the specimen and three-dimensional images. Several factors determine the resolution of confocal microscopy, including the diameter of the pinhole, the light wavelength and the numerical aperture of the objective (Tauer, 2002; Norman, 2005). Confocal microscopy has been used to visualize capillary and alveolar networks in the lung. Although confocal microscopy provides superior spatial resolution, live imaging with this microscope results in a large proportion of emitted light being blocked due to the small size of the pinhole. In addition, penetration depth in confocal laser scanning microscopy is limited to about 50–100 μm which precludes imaging of deeper tissues. Moreover, imaging with confocal microscopy requires a bright sample in order to negate the need for a strong excitation signal which may otherwise cause photodamage and photobleaching. In this regard, spinning disk confocal microscopy is superior as its high acquisition speed helps to restrict photobleaching (Croix et al., 2006; Masedunskas et al., 2012; Lefrançais et al., 2017).

Multiphoton Microscopy

Multiphoton microscopy involves application of an infrared laser light source and subsequent absorption of lower energy photons by a fluorophore inside the tissue (Tauer, 2002; Norman, 2005; Presson et al., 2011; Lefrançais et al., 2017). This method uses long-wavelength photons to penetrate farther into tissues and allow for imaging of thicker sections (Lefrançais et al., 2017). Using multiphoton microscopy, lungs have been imaged to a depth of $\sim$500 μm (Croix et al., 2006). Hence, application of multiphoton microscopy is superior in intravital studies (Norman, 2005). However, multiphoton microscopy also has some drawbacks. Although the likelihood of phototoxicity is decreased in comparison to conventional fluorescence and confocal microscopy, photodamage is still considered as a disadvantage for multiphoton microscopy when compared to single-photon microscopy, at least in the focal plane (Tauer, 2002; Croix et al., 2006; Presson et al., 2011). Additionally, increased penetration depth leads to significant decrease in spatial resolution (Niesner et al., 2007). Since excitation only occurs at the focal point and multiphoton excitation efficiency of fluorophores are very low in comparison to single photon, longer acquisition times are required. This has the effect of restricting observation of dynamic processes which possess high

temporal resolution (Niesner et al., 2007; Presson et al., 2011). Despite these drawbacks, multiphoton microscopy is nonetheless advantageous for IVM studies because the infrared excitation light is less prone to scatter, which allows for deeper penetration into the tissue (Croix et al., 2006; Lefrançais et al., 2017).

Surgery

The surgical preparation needed for intravital lung imaging requires that the animals are anesthetized, usually by intraperitoneal injection or inhalation of an anesthetic drug. Animals will be intubated or tracheotomized to facilitate mechanical ventilation (Fiole and Tournier, 2016). The following steps include techniques to create a thoracic window and mechanically stabilize the lung in order to perform IVM. Several techniques have been developed in recent decades. In 1926, Wearn et al. (1926) described for the first time a surgical procedure in dogs, where the thoracic wall was resected to the pleural layer. A second opening was made through the diaphragm down to the pleura for illumination (Rodriguez-Tirado et al., 2016). Other authors studied the physiological movement of the canine lung via an implanted lung window over a relatively stationary region (Wagner, 1965), or utilized a vacuum during the surgical window preparation to stabilize the tissue (Wagner, 1969). In general, two alternative lung stabilization methods for imaging in mice are used today, namely gluing of the parenchyma onto a glass coverslip (Kreisel et al., 2010) or the utilization of a suction system to stabilize the lung under a glass window (Looney et al., 2011). Other techniques have their own merits and pitfalls, and no one has excelled in comparison to another (Fiole and Tournier, 2016). For example, bronchus clamping, and sequential apnea impact the normal gas exchange in the lung and may cause atelectasis, which refers to impaired gas exchange resulting from reversible collapse of small airways (Grott and Dunlap, 2020). Gated imaging and oversampled acquisition do not have these disadvantages but require high-speed or specialized imaging equipment, which is not widely accessible. Neither gluing of the lung or utilization of the suction window cause the above-mentioned drawbacks, but either may result in shear force induced injury. In recent years, the suction window has been miniaturized and adapted for use in mice (Rodriguez-Tirado et al., 2016). Confocal and multiphoton microscopy have been used (Funakoshi et al., 2000; Looney et al., 2011; Presson et al., 2011) to obtain excellent high-resolution imaging (Entenberg et al., 2015). At the end of the experiment, mice are always euthanized in accordance with international animal care guidelines (Fiole and Tournier, 2016).

Cell Labeling

With recent advances of fluorescent probes, fluorescent proteins and exogenous fluorophores, IVM allows the detection of molecular events with subcellular resolution in real time in the intact animal (Presson et al., 2011). Tracking the movement, morphology and behavior of leukocytes and blood vessels in the lung requires labeling methods such as the use of fluorescent dyes, transgenic mice, or fluorescently stained antibodies (Kim et al., 2019). Moreover, knockout mice can be used to study the cellular mechanisms involved in pulmonary pathophysiological conditions (Aird, 2003; Gill et al., 2015) (**Table 1**).

Fluorescent dyes such as Alexa Fluor 488, FITC, phycoerythrin, and Rhodamine 6G allow for visualization of separate cells (Chiang et al., 2007). In addition, genetically different mouse strains have been utilized to visualize a specific cell subset. For instance, Lysozyme M-green fluorescent protein (LysM-GFP) mice are used for visualization of neutrophils because Lysozyme M, encoded by the *Lyz2* gene, is expressed mainly in neutrophils and partly in macrophages (Faust et al., 2000; Orthgiess et al., 2016). Kreisel et al. (2010) examined leukocyte trafficking in LysM-GFP mice (Faust et al., 2000) in which endogenous neutrophils are brightly labeled and monocytes and macrophages are labeled to a lesser extent (Chtanova et al., 2008). Another transgenic mouse line, CX3Cr1-GFP, is used for fluorescent imaging of monocytes and macrophages (CX3C chemokine receptor 1 (CX3Cr1) is a marker for macrophages and monocytes) (Medina-Contreras et al., 2011; Garcia et al., 2013).

Another method for imaging of leukocyte subsets, besides the use of fluorescent dyes or transgenic mouse lines, is the application of fluorescently stained antibodies capable of binding to specific antigens. For instance, one of the cell surface proteins that is highly expressed in murine neutrophils is Ly6G (Lee et al., 2013), whereas Ly6C and F4/80 are highly expressed in macrophages or monocytes (Wynn et al., 2013). Kuebler et al. fluorescently labeled leukocytes *in vivo* with Rhodamine 6G and imaged the subpleural microcirculation in rabbits (Kuebler et al., 1994). Lien et al. labeled neutrophils *in vitro* and used fluorescence videomicroscopy in dogs to image neutrophil in pulmonary arteries (Lien et al., 1987). These two studies demonstrated that although rolling leukocytes were observed in arteries, venules, and capillaries, the anatomical site of neutrophil margination is in the pulmonary capillaries (Lien et al., 1987; Kuebler et al., 1994). This differs from murine systemic circulation, where rolling leukocytes are predominately observed in postcapillary venules and rarely in arterioles (Broide et al., 1998). To visualize the pulmonary vasculature and determine whether neutrophils were extravascular, Kreisel et al. injected quantum-dots, and reported that neutrophils were sequestered in the pulmonary microcirculation (Lien et al., 1987; Kreisel et al., 2010). Additionally, to study cellular mechanisms for neutrophil recruitments in lung after induction of experimental sepsis, $CD11b^{-/-}$,$TLR4^{-/-}$, $Myd88^{-/-}$mice (Yipp et al., 2017) and $iNOS^{-/-}$ mice were used (Razavi et al., 2004).

Changes in microvessel diameter and blood flow under various physiological and pathophysiological conditions is widely visualized via intravenous administration of fluorophore-conjugated dextran or albumin (Kim et al., 2019). Higher molecular weight dextran (70 kDa) is particularly useful for visualization of microvessels because extravasation through the intact endothelium is minimal. Tabuchi et al. demonstrated changes in pulmonary vessel diameters by injection of FITC-dextran into the jugular vein of mice (Tabuchi et al., 2008). Another study involved administration of intravenous FITC-albumin to enable measurement of microvascular leakage in rat mesentery through visualization of blood vessels (Alves et al.,

TABLE 1 | Cell labeling strategies that have been used for lung IVM.

Florescent probes/dye	Florescent antibodies	Florescent reporter mice	Knockout Mice
Leukocytes • Rhodamine 6G (Razavi et al., 2004; Kreisel et al., 2010; Roller et al., 2013; Brown et al., 2014; Gill et al., 2014, 2015) **Microvessels** • Fluorescein isothiocyanate (FITC)-dextran (Tabuchi et al., 2008; Brown et al., 2014) • FITC-albumin (Noda et al., 2014) • Texas Red dextran (Alves et al., 2018) **Cell death** • Propidium iodide (PI) (Gill et al., 2014, 2015)	**Neutrophil** • Ly6G (Lien et al., 1987; Kuebler et al., 1994; Lee et al., 2013) • Anti-CD45 (Naumenko et al., 2018) **Monocyte/macrophages** • Ly6C/F4/80 (Wynn et al., 2013) **Neutrophil Elastase (NE)** • Anti-neutrophil elastase (NE)-AF647 (Carestia et al., 2019) **Vascular endothelium** • Anti-CD31 (Yipp et al., 2017)	**Neutrophils** • Lysozyme M-green fluorescent protein (LysM-GFP) mice (Faust et al., 2000; Orthgiess et al., 2016) • LysM-GFP mice (Kreisel et al., 2010) **Monocyte/macrophages** • CX3CR1-GFP mice (Medina-Contreras et al., 2011; Garcia et al., 2013)	iNOS$^{-/-}$ mice (Razavi et al., 2004) CD11b$^{-/-}$ mice (Yipp et al., 2017) TLR4$^{-/-}$ mice (Yipp et al., 2017) Myd88$^{-/-}$ mice (Yipp et al., 2017)

2018)In mice with GFP-labeled immune cell populations, blood vessels have been marked with Texas Red dextran for better contrast (Noda et al., 2014). Visualization of blood vessels and immune cells can be improved through application of novel labeling materials, proper combination of inflammation models, superior surgical methods, and advances in microscopic imaging.

INFECTION AND INFLAMMATION MODELS

Bacterial Pneumonia

Two common nosocomial pathogens that lead to bacterial infection of the respiratory tract are *Pseudomonas aeruginosa* and *Staphylococcus aureus*. *Pseudomonas aeruginosa* is a Gram-negative opportunistic bacterium that can cause lung infection in patients with impaired immunity and is the main cause of morbidity and mortality in cystic fibrosis (CF) patients (Moradali et al., 2017). Wild type (PAO1) and human-derived (PA14, LESB58) strains are often used in animal infection models. It should be noted that while PAO1 and PA14 are localized in alveolar regions 7 days post infection, LESB58 has been shown to persist in the bronchial lumen (Kukavica-Ibrulj et al., 2008). *Staphylococcus aureus* spp. are Gram-positive bacteria and their most studied pathogenicity factors recognized by immune cells are lipoteichoic acid and peptidoglycan (Fournier and Philpott, 2005). In this context, antibiotic-resistant strains (e.g., methicillin-resistant *S. aureus*, MRSA), are commonly used for animal infection studies (Kim et al., 2014). Lung IVM can be utilized to visualize pathogen recognition and bacterial clearance by immune cells (Fournier and Philpott, 2005; Lavoie et al., 2011). In addition, dynamic immune cell responses such as formation of neutrophil clusters and neutrophil extracellular traps (NETs) are often observed in the lungs in response to bacterial infection (Lien et al., 1987; Looney and Bhattacharya, 2014; Lefrançais et al., 2018).

Lefrançais et al. utilized multiphoton microscopy for visualization of neutrophil recruitment and NET formation in experimental MRSA-induced pneumonia (Lefrançais et al., 2018). The left lung of the mice was exposed surgically and stabilized via a flanged thoracic window with a coverslip and vacuum suction. Infection with MRSA rapidly induced neutrophil recruitment and sequestration in the lung beginning 2 h post infection. In addition, after PAO1 challenge, neutrophil swarming and formation of neutrophils clusters around the bacteria were observed (**Figure 1**).

Kreisel et al. exposed the left rodent lung by thoracotomy and attach it to the cover glass using tissue glue. Non-targeted Q-dots were injected intravenously to image blood vessels, and LysM-GFP mice were used for visualization of neutrophils by means of multiphoton microscopy. Diluted *Escherichia coli* (K-12 strain) Bioparticles conjugated with tetramethylrhodamine or *L. monocytogenes* in PBS were administered intratracheally prior to imaging. Ten minutes following administration, a dramatic influx of cells from the circulation and a significant increase in resident neutrophil motility was observed in lung tissue. However, neutrophil recruitment to the lung, specifically at the transendothelial migration step, was inhibited after the depletion of blood monocytes, which suggests interaction of monocytes and neutrophils in lung inflammation (Kreisel et al., 2010).

In another study, Fiole et al. performed lung IVM via multiphoton microscopy to examine early steps of pulmonary infection by *Bacillus anthracis*, the causative agent of anthrax that impacts livestock and humans. The authors observed interactions among macrophages, DCs and spores which was considered to result in an exchange of information including exchange of pathogen-derived particles or exosomes containing pathogen-derived antigens released by macrophages directed to DCs. Results from this study indicates that infection induced by *B. anthracis* spores significantly increases long-duration (> 30 min) contact between macrophages and CX3CR1-DCs (Fiole et al., 2014). Alveolar macrophages, the most efficient phagocytes in the lung, capture spores within minutes in a first step. After 30 min, spores are transported to lymph nodes following capture by DCs (Cleret et al., 2007). However, mean cell velocity in both macrophages and CX3CR1 cells did not significantly increase correlated to increased contact ratio at 5 h post-infection (Fiole et al., 2014). Fiole et al. observed the last phase of spore transfer from macrophage to CX3CR1 cell *in situ* and

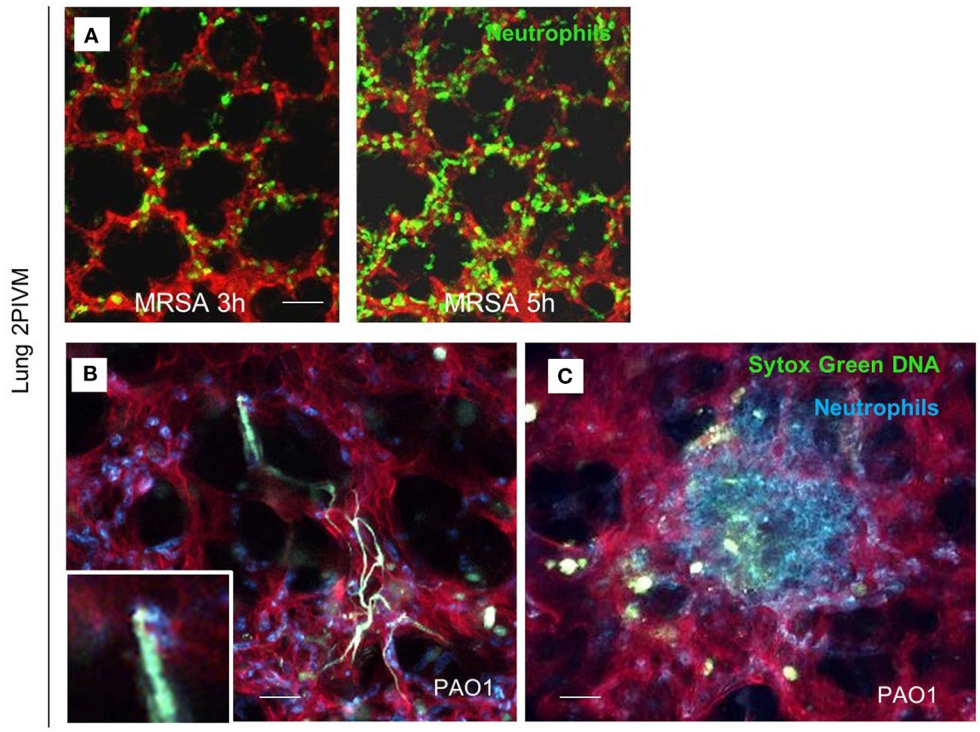

FIGURE 1 | Lung 2-photon intravital microscopy. **(A)** LysM-GFP mice (green neutrophils) were challenged with MRSA (2×10^7 CFU, i.t.), injected with Texas Red–dextran i.v. to stain the vasculature, and observed from 3 to 5 h after infection. **(B,C)** MRP8-mTmG mice (red vasculature, blue neutrophils) were challenged with PAO1 (5×10^6 CFU, i.t.) and observed from 3 to 5 h after the infection. Extracellular DNA was stained with SYTOX Green (Lefrançais et al., 2018).

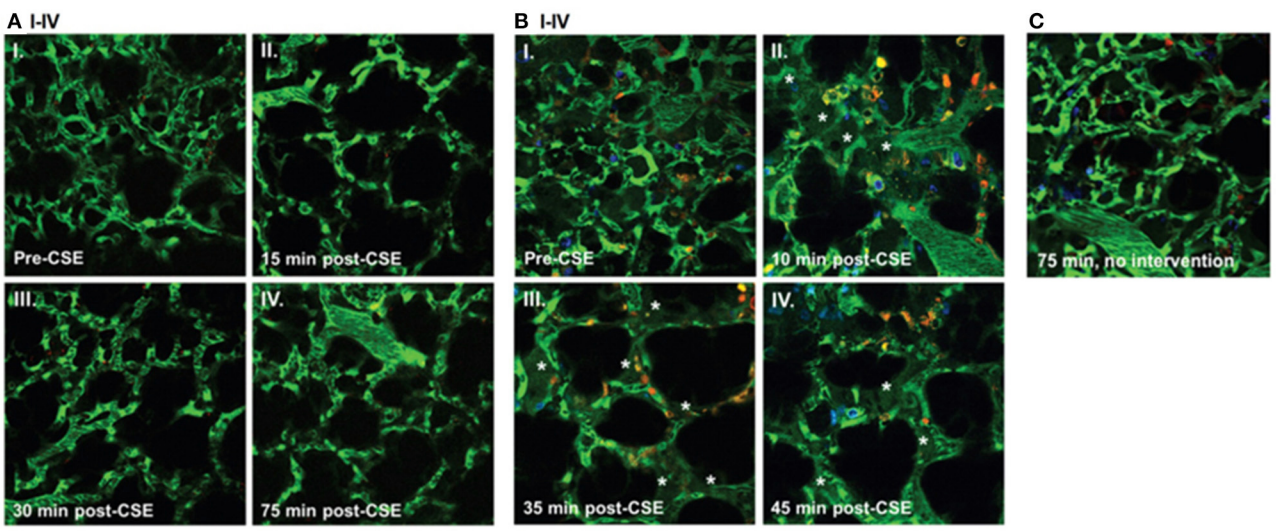

FIGURE 2 | Effect of cigarette smoke extract (CSE) on the lung microcirculation captured in real time in the pulmonary microvasculature of a living wild-type (WT) **(A)**; and cystic fibrosis transmembrane conductance regulator (CFTR)–deficient **(B)** mouse. Three-dimensional reconstruction of fluorescein isothiocyanate– labeled vessels (green) surrounding alveoli (dark regions) and Rho-G6-labeled neutrophils (orange) imaged via intravital 2-photon microscopy before (**A**I and **B**I) and after (**A** and **B**II–IV) intravenous administration of CSE (100 μL of 20% CSE). Nuclei were stained with intravenous Hoechst (blue). Note increasing neutrophil trafficking and plasma extravasation (asterisks) into airspaces after CSE administration in the CFTR-deficient **(B)** but not WT **(A)** mouse and compared to a CFTR-deficient mouse not receiving CSE **(C)** (Brown et al., 2014).

in vivo, a mechanism previously only demonstrated *in vitro* (Blank et al., 2011).

Administration of lipopolysaccharide (LPS), a cell wall component of Gram-negative bacteria, induces an inflammatory response by activation of immune cells through Toll-like receptor (TLR)-4 (Aderem and Ulevitch, 2000; Opal, 2010; Kim et al., 2019). Following LPS administration as well as bacterial infection, neutrophils are the first group of leukocytes that respond to inflammation. This response involves adhesion and migration across the endothelium from bloodstream into inflammatory tissues. Carestia et al. studied in LPS induced inflammation the establishment of intravascular neutrophil extracellular traps (NETs) and immunothrombi by intravital microscopy. In this study, the left side of the chest was opened to access the lung in tracheotomized mice. The lung was gently immobilized with a thoracic suction attached to the manipulator on the microscope stage. The authors studied platelet aggregates, neutrophil numbers, bacterial capture by each cell type, and the number of stationary ($\geq$30s in the same location) bacteria in contact with platelet aggregates. They visualized neutrophils through labeling with anti-Ly6G-BV42. Anti-neutrophil elastase (NE)-AF647 antibodies, which bind to extracellular neutrophil elastase were injected via tail vein, prior to IVM imaging. The authors found that platelet aggregation, neutrophil recruitment, and NET release were induced 4 h following intraperitoneal injection of LPS (Carestia et al., 2019). Pulmonary inflammation induced by inhalation of LPS from *Salmonella enteritis* (Reutershan et al., 2005) was confirmed by lung IVM with application of a mild vacuum to hold the lung under the window of a custom-built fixation device. Fluorescein isothiocyanate (FITC)- dextran (150 kDa) was used to assess the glycocalyx. The results from this study indicated that glycocalyx thickness in the lung was significantly reduced after 8 and 24 h following LPS inhalation, thus resulting in increased vascular permeability (Margraf et al., 2018).

Viral Infections

In addition to bacterial infections, also viral infection can be studied by IVM. In particular, influenza has been studied widely in lungs using IVM. In a study from Paul Kubes group in Calgary, anesthetised, thoracotomized mice were given anti-Ly6G/GR1 and anti-CD31 to identify neutrophils and vasculature, respectively, and studied using confocal intravital microscopy. The IVM images demonstrated that after 30 min and even 2 h post infection AMs actively detected and crawled toward inhaled *P. aeruginosa* via chemotaxis. AMs crawling behavior was defected during infection with Influenza A compared to control and after infection with *P. aeruginosa* or *S. aureus*, fewer AMs from flu-infected mice captured the inhaled *P. aeruginosa* and *S. aureus*. These findings suggest that Influenza A impairs the ability of AMs to crawl and capture the inhaled bacteria and increase neutrophil infiltration (Neupane et al., 2020). In another study with similar microscopic and surgical preparation, confocal microscopy of the lung demonstrated interactions between leukocytes which were visualized using anti-CD45 and oncolytic vesicular stomatitis virus (VSV) which was identified by Alexa Fluor 647 staining. Occasional capture of virions by leukocytes within the lung vasculature was observed 10 min after i.v. injection of VSV-AF647 (Naumenko et al., 2018).

Cystic Fibrosis

Cystic Fibrosis (CF), an autosomal-recessive genetic disorder, causes chronic changes including inflammation of the lungs and other organs due to the defect in the cystic fibrosis transmembrane conductance regulator (CFTR). CF patients have a high incidence of lung infections limiting their quality of life. In this regard, there is only one study using intravital microscopy in CFTR mice thus far. Brown et al. studied the role of CFTR in preserving the lung endothelial barrier through the use of multiphoton microscopy. Thoracotomy was performed on the left chest wall to create a window for lung IVM. FITC-dextran (for labeling the circulating plasma), Hoechst 33258 (for labeling the nuclei), and Rhodamine-6G (for labeling of leukocyte mitochondria) were injected intravenously. Lung imaging in CFTR-deficient mice demonstrated a significant increase in neutrophil trafficking and plasma extravasation into airspaces following administration of cigarette smoke (CS) extracts compared to wild type mice exposed to similar level of CS extracts (see **Figure 2**). These results suggested that CFTR function might be required for lung endothelial barrier, including adherence junction stability. Loss of CFTR function, especially concomitant to CS exposure, might promote lung inflammation by increasing endothelial cell permeability. The results from *in vitro* experiments in this study also indicated that dose-dependent treatment with CFTR inhibitors such as GlyH-101 or CFTRinh172 was associated primarily with the redistribution of the junctional protein ß-catenin and its internalization from cell periphery. CS had inhibitory effects on CFTR function. It caused sphingosine-1 phosphate (S1P)/ceremide imbalance in which the enhanced level of ceremide leads to lung inflammation and increased susceptibility to *P. aeruginosa* infection. This imbalance and subsequent susceptibility to infection are also typical in clinical CF. S1P supplementation was able to reverse endothelial cell barrier dysfunction induced by CFTR inhibition or CS exposure (Brown et al., 2014). Furthermore, in *ex vivo* lung preparations, Lindert et al. studied alveoli from the pleural aspect down to a depth of up to 40 µm, using multiphoton microscopy to examine alveolar wall liquid (AWL). They found that AWL was absent in CFTR $^{-/-}$ mice, and it was blocked when chloride was depleted from the perfusate of WT mice, suggesting that CFTR-dependent chloride secretion causes AWL formation (Lindert et al., 2007).

Sepsis Induced Acute Lung Injury

According to the third international consensus definitions for sepsis and septic shock (Sepsis-3), sepsis is a dysregulated host systemic responses to infection, that can cause life-threatening organ dysfunction (Singer et al., 2016). Sepsis affects more than 30 million people every year worldwide, and is one of the major causes of death (Vincent, 2012; Fleischmann et al., 2016). Therefore, understanding the pathogenesis of sepsis is a critical step in early diagnosis and treatment of sepsis which can limit onset of organ dysfunction and reduce mortality (Kim and Choi, 2020). The various aspects of sepsis pathogenesis include

immune dysfunction, endothelial activation, cardiopulmonary pathology, increased microvascular permeability, edema formation, and disseminated intravascular coagulation (DIC) (Aird, 2003; Gotts and Matthay, 2016). Infection sites in septic patients include the abdomen, bloodstream, lung, central nervous system, and renal or genitourinary tract (Gotts and Matthay, 2016). Alternatively, sepsis also has the potential to induce acute lung injury (ALI) without primary lung infection. Lung IVM represents a useful method for studying pulmonary microcirculation changes in sepsis-induced ALI. The following paragraphs summarize various studies on sepsis-induced ALI and describe application of lung IVM in septic mice models.

Yipp et al. assessed the roles of CD11b, TLR4, and Myd88 in pulmonary neutrophil host defense during sepsis through the use of knockout mice. Researchers applied a vacuum chamber on the exposed left lung to facilitate pulmonary imaging by means of either spinning disk or resonant scanning confocal microscopy. Ten minutes prior to imaging, fluorescence-conjugated anti-Ly6G antibody and anti-CD31 antibody were administered intravenously in order to visualize neutrophils and the vascular endothelium. Three behavioral phenotypes of neutrophils were directly visualized within the pulmonary microvasculature during sepsis: tethering, crawling, and adhering. Results indicated no significant changes in the number of crawling neutrophils within pulmonary capillaries following administration of intravenous LPS in CD11b-, TLR4-, and Myd88-knockout mice, thereby confirming the role of these molecules in pulmonary neutrophil host defense (Yipp et al., 2017).

To demonstrate apoptosis of pulmonary microvascular endothelial cells (PMVEC) in sepsis-induced ALI, Gill et al. conducted lung IVM (Gill et al., 2014, 2015) in anesthetized, tracheotomized, mechanically ventilated mice. A transparent window on the right thoracic wall allowed visualization of the pulmonary microcirculation with an epi-fluorescence microscope (Razavi et al., 2004). A bolus of Rhodamine 6G was injected into the penile vein 3.5 h after sham or CLP surgery to label pulmonary microvascular PMN sequestration (Gill et al., 2014). Propidium iodide (PI), a fluorescent marker of cell death used to label non-viable PMVEC (Gill et al., 2014, 2015), was intravenously injected into septic mice immediately before IVM. Quantification of the number of PI positive cells and Rhodamine 6G labeled PMN sequestrated in recorded images indicated a significant increase in PMN sequestrated in pulmonary microvasculature. However, it is unclear whether the authors employed PI and Rhodamine 6G in separate experiments or in the same animals, which would raise the issue of separating fluorophores with such close emission wavelengths. Nonetheless, the authors' findings are consistent with results from other studies (Razavi et al., 2004; Roller et al., 2013) and with increased PMVEC death following CLP-induced sepsis at 2 and 4 h after CLP-sepsis compared to sham (Gill et al., 2014, 2015).

Razavi et al. quantified pulmonary microvascular neutrophil sequestration by IVM with intravenous injection of dihydro-rhodamine-6G. Results indicated that pulmonary microvascular leukocyte sequestration was significantly increased in iNOS+/+ (wild-type) mice and in iNOS$^{-/-}$ mice from 1 to 18 h after CLP, although significantly fewer sequestered leukocytes were observed in iNOS$^{-/-}$ vs. iNOS$^{+/+}$ mice at all time points (Razavi et al., 2004). Therefore, neutrophil iNOS appears to be an important contributor to pulmonary neutrophil infiltration.

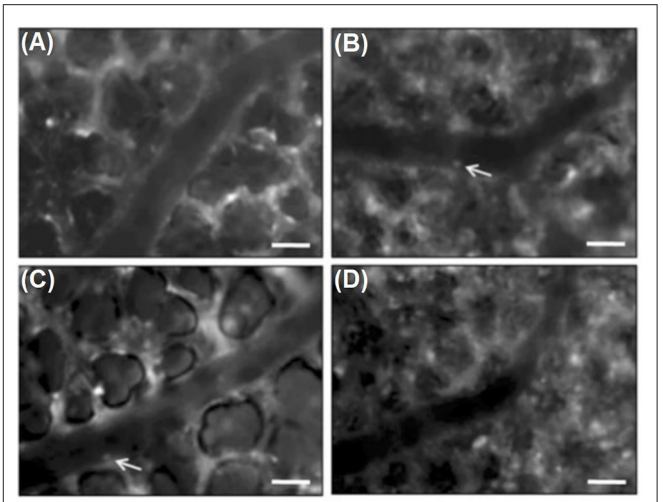

FIGURE 3 | Intravital fluorescence microscopy of adherent leukocytes (arrows) in pulmonary arterioles. Note, that CLP enhanced the number of firmly adherent leukocytes in arterioles by two-fold (**B**, arrows) compared to sham-treated animals (**A**, arrows). Immunoneutralization of PSGL-1 reduced CLP-induced leukocyte adhesion in pulmonary arterioles by almost 50 % **(C,D)**. Green-light epi-illumination with direct staining of leukocytes by rhodamine 6 G. Scale bars 35 lm (Roller et al., 2013).

Rahman et al. used a micromanipulator to fix the coverslip to the right lung surface during surgical preparation. After retrobulbar injection of rhodamine 6G and FITC dextran, fluorescence microscopy was performed. Results indicated that the matrix metalloproteinase (MMP) inhibitor, GM6001, administered prior to CLP induction reduced CLP-induced leukocyte adhesion in pulmonary venules, which suggests the role of metalloproteinases in infiltration of neutrophils in septic lung injury (Rahman et al., 2012). Another study from this group (Roller et al., 2013) with the equal intravital microscopic setup demonstrated significant increases in the number of rolling and adhering leukocytes in arterioles and venules, as well as in leukocytes trapped in capillaries, 4 h after CLP induction (see **Figure 3**). IVM indicated that CLP induction markedly decreased flow velocity and shear rate in pulmonary venules and arterioles and also decreased functional capillary density in lung microcirculation (Roller et al., 2013).

Lung IVM was also used to show that immunoneutralization of PSGL-1 significantly reduces not only the number of rolling leukocytes in arterioles and venules but also the number of adherent leukocytes in arterioles and trapped leukocytes in capillaries. In one particular study, PSGL-1 antibody was shown not to affect the number of firm leukocytes in pulmonary venules, thus suggesting that leukocyte rolling is not a prerequisite for pulmonary venular leukocytes adhesion in sepsis. In addition, capillary trapping of leukocytes and enhanced sticky leukocytes in arterioles is dependent on PSGL-1 function (Roller et al., 2013).

Moreover, several studies have shown that targeting CD11a/CD18 or CD11b/CD18 reduces infiltration of leukocytes in the lung in models of endotoxemia (Basit et al., 2006) and sepsis (Asaduzzaman et al., 2008). To confirm this theory with *in vivo* imaging, Wang et al. performed lung IVM 4 h after CLP induction. Results indicated that intravenous pretreatment with CD11a or CD11b antibodies immediately prior to CLP abolished CLP-induced arteriolar and venular leukocyte adhesion in lung tissue and reduced leukocyte sequestration in pulmonary capillaries. It also restored diameter, flow velocity, and shear rate in lung arterioles and venules in CLP mice. Their findings showed that CD11a and CD11b mediate leukocyte adhesion in both arterioles and venules as well as trapping in capillaries in the lung. In addition, the data demonstrates that CD11a, but not CD11b, supports leukocyte rolling in pulmonary arterioles (Wang et al., 2013).

Aspiration Pneumonia

Intratracheal instillation of hydrochloric acid is an experimental mouse model that mimics human aspiration of gastric contents, which can cause acute ALI (Kobayashi et al., 2016). Aspiration is classified under the non-infectious group of ALI etiology (Zarbock and Ley, 2009). Acid aspiration causes direct injury to lung epithelial and endothelial cells, leading to tissue edema and neutrophil accumulation in the lung (Kobayashi et al., 2016).

Grommes et al. performed lung IVM in mice after acid aspiration. Microspheres coupled to polyclonal antibodies to CXCL4 or CCL5 were injected intravenously 15 min prior to intravital imaging using a multiphoton system in single-beam mode. The authors showed the deposition of CCL5 and CXCL4 on microvascular lung endothelium and reported that platelets in LPS-, acid-, and sepsis-induced ALI release the CCL5-CXCL4 heterodimer. This heterodimer is involved in neutrophil recruitment, and its disruption prevents acid- and sepsis induced ALI (Grommes et al., 2012). Additionally, it has been shown that thromboxane A2 (TXA_2), which is actively involved in the inflammatory response, is produced by lung epithelial cells in aggregation with platelets and neutrophils (Zarbock and Ley, 2009) and is detectable in bronchoalveolar fluids (BALF) in acid aspiration-induced ALI (Kobayashi et al., 2016). TXA_2 binding to its receptor on the epithelial cells promotes upregulation of intracellular adhesion molecule-1 (ICAM-1) and may be indirectly involved in neutrophil recruitment (Rossaint and Zarbock, 2013).

Mertens et al. implemented Tabuchi et al. method (Tabuchi et al., 2008) for thoracic window implantation to analyze dynamics of alveolar clusters at different time points and applied pressures after HCl aspiration. Mice were ventilated at 60 breaths/ min and images were captured at 0 cm H2O ventilation pressure in end-expiration and at 6, 12, 18, 24 cm H2O in end-inspiration. Subpleural alveoli were visualized using an upright microscope and darkfield illumination, 30 min after lung stabilization. Delimited aerated structures discernible on the lung surface were defined as individual alveolar clusters. For each pressure step, in each area of interest (AOI), the number of alveolar clusters was counted and the boundaries of the subpleural projection of each cluster were traced, and the respective area was measured. Alveolar compliance was calculated as the fold increase in alveolar area between images taken at 0 and 24 cm H2O ventilation pressure. The total number of visualized alveolar cluster per AOI, after acid aspiration, did not change between 0 and 24 cm H2O. Dark-field illumination also demonstrated that density of light-refracting structures in the acid aspiration group increased. In the NaCl instillation (control) group, these structures disappeared with increasing ventilatory pressure, while in the HCl instillation group, they no longer disappeared with alveolar expansion. Additionally, alveolar distensibility was primarily reduced in small alveoli in acid-induced ALI. Optical Coherence Tomography (OCT) imaging also showed increased heterogeneous density in acid-injured lungs to confirm the IVM results (Mertens et al., 2009). In healthy lungs, cyclic changes in alveolar size are in synchrony with the ventilatory cycle, whereas asynchronous alveolar dynamics occurs in 10 min after ALI induced by acid instillation (Tabuchi et al., 2016). Altered alveolar dynamics in ALI cause impaired respiratory mechanics and alveolar gas exchange. Hence, requiring high distending pressures between and within alveoli results in the progression and aggravation of lung disease (Mertens et al., 2009; Tabuchi et al., 2016; Mandler et al., 2018).

LIMITATIONS

Although lung IVM provides unique insights into pulmonary microvascular responses, cell-cell-interactions as well as alveolar mechanics in real time, it also carries some limitations due to the enclosed position of the lung in the body and restricted accessibility of the organ, thus necessitating the implementation of a surgical window for imaging. In some studies, part of the thoracic wall was removed to provide access for lung *in vivo* imaging without providing any protection for the parenchyma. However, this area of observation is prone to drying and is exposed to environmental pathogens and/or artificial surfaces (including cover slips) in these approaches. Moreover, cyclic lung movement during respiration and the heartbeat's effect on the lung both impact lung imaging due to motion artifacts. Some lung windows, for example, employ a thoracic suction window fitted with a vacuum chamber, and are implanted to stabilize the lung surface for improved imaging with reduced motion artifacts (Looney et al., 2011). While this technique has proven highly efficient for immunology studies, it does disrupt certain physiological phenomena such as ventilation-dependent effects on lung perfusion and alveolar dynamics. Some lung windows employ glued coverslips (Kreisel et al., 2010) or transparent polyvinylidene membranes (Tabuchi et al., 2008) instead of suction and allow physiological movement of the lung, but do not provide high resolution imaging.

Another factor that should be taken into consideration is the physiologically negative pressure in the thoracic cavity. This necessitates the use of great caution during the surgery as well as application of ventilatory support to keep the animal alive. Therefore, imaging must be performed under positive pressure ventilation instead of spontaneous breathing (Looney

et al., 2011). However, the effects of artificial ventilation on lung physiology must be acknowledged (Poobalasingam et al., 2017). Manipulations in mechanics of the thoracic wall and the interplay between intrapleural and transpulmonary pressures impact both alveolar dynamics and microvascular perfusion (Tabuchi et al., 2020). Therefore, although mechanical ventilation is essential for survival of the animal, it can cause permanent damage to the lung as ventilator induced lung injury (VILI) or ventilator-associated lung injury (VALI) (Amato et al., 1998).

Furthermore, application of IVM in longitudinal studies has been faced with limitations as most implanted lung windows are too invasive to allow long term imaging. Since lung IVM is a terminal method used for short term imaging, multiple animals are needed for longer studies (Masterson et al., 2019). However, it has been reported that certain lung windows may allow for long-term observations in dogs, rabbits (De Alva and Rainer, 1963), rats (Fingar et al., 1994) or mice (Kimura et al., 2010), without stabilization and at low spatial resolution. Entenberg et al. recently developed a permanent lung window which may present a promising method for long-term imaging (Entenberg et al., 2018; Tabuchi et al., 2020).

There are some limitations that apply to all models and methods of lung IVM in mice regardless of different adaptions based on the subject of study. First, the small size of mice means that miniature equipment is required for IVM, thus making intubation or tracheotomy challenging. A typical mouse lung window is ∼10 mm in diameter and provides a very small observational area during imaging (Masterson et al., 2019). Stabilizing the lung via thoracic chamber implantation is also a challenge in mice as a result of their smaller size and higher respiratory rate in comparison to larger animals (Frevert et al., 2014). Second, although classical fluorescence IVM provides adequate spatial resolution, its two-dimensional imaging provides little information about three-dimensional alveolar dynamics such as alveolar walls and alveolar diameter during different physiological and pathophysiological conditions (Tabuchi et al., 2020). Third, limited penetration depth of current microscopes allows only for superficial imaging of the lung. Penetration depth in lung tissue for conventional fluorescence microscopy is ∼30–50 μm, compared to 100–150 μm for confocal microscopy, and 500 μm for multiphoton microscopy. This restricted penetration depth is caused by the lung's complex structure and the light-scattering properties of the abundant air-liquid interfaces in the alveolo-capillary units. Therefore, lung IVM is currently restricted to superficial layers of the lung including subpleural alveoli and surface-level microvascular networks, neither of which are representative of internal alveoli and vessels. In contrast to deeper lung regions in which all sides of a given alveolus are surrounded by other alveoli, subpleural alveoli are attached to the visceral pleura on one side. Consequently, alveolar dynamics differ between subpleural alveoli and deeper lung regions. In addition, subpleural pulmonary microvasculature is less dense and consists of larger capillaries compared to the interior pulmonary microvascular network (Tabuchi et al., 2008, 2020; Kuebler, 2011; Looney et al., 2011; Looney and Bhattacharya, 2014; Masterson et al., 2019). Fourth, creating a window to access the lung involves a surgical procedure which can cause baseline leukocyte activation. However, these alterations in leukocyte behavior are not comparable to inflammatory situations such as response to bacterial infection. Hence, exercising extreme care during surgery and comparing *in vivo* images with histological figures could lessen this issue (Hickey and Westhorpe, 2013). Fifth, lung observation by means of IVM is limited to a specific location that is not typically representative of the whole lung, usually the anterior part of the murine lung and a specific number of alveoli and microvessels within this area. It should be noted that ventilation and perfusion vary between different regions of the lung. Furthermore, any IVM–not only of the lungs–has to be performed at physiological body temperature, which in the case of mice is 37°C, by use of a homeothermic system (Park et al., 2018), warmed lung window chambers (Kreisel et al., 2010), or water immersion microscopy and continuous superfusion of the window with a pre-warmed solution (Kuhnle et al., 1993; Kuebler et al., 1994). IVM cannot be applied in clinical studies as it is an invasive and terminal method. Although some labels used in intravital imaging are non-toxic, do not alter cell morphology or phenotype, and have a sensitivity at micron range, they likely compromise either the administered cell's function or the host itself.

CONCLUSION

Despite the aforementioned limitations, lung IVM is the gold standard for studying lung immune cell interactions in real time in living animals. This technique can be applied in different inflammatory models, including bacterial and viral infections, sepsis-induced ALI, aspiration, and cystic fibrosis in order to reveal dynamic alterations in physiological parameters and cellular behavior in comparison to non-inflammatory conditions.

AUTHOR CONTRIBUTIONS

All authors listed have made a substantial, direct and intellectual contribution to the work, and approved it for publication.

REFERENCES

Aderem, A., and Ulevitch, R. J. (2000). Toll-like receptors in the induction of the innate immune response. *Nature* 406:782. doi: 10.1038/35021228

Aird, W. C. (2003). The role of the endothelium in severe sepsis and multiple organ dysfunction syndrome. *Blood J. Am. Soc. Hematol.* 101, 3765–3777. doi: 10.1182/blood-2002-06-1887

Alves, N. G., Motawe, Z. Y., Yuan, S. Y., and Breslin, J. W. (2018). Endothelial protrusions in junctional integrity and barrier function. *Curr. Top. Membr.* 82, 93–140. doi: 10.1016/bs.ctm.2018.08.006

Amato, M. B. P., Barbas, C. S. V., Medeiros, D. M., Magaldi, R. B., Schettino, G. P., Lorenzi-Filho, G., et al. (1998). Effect of a protective-ventilation strategy on mortality in the acute respiratory distress syndrome. *N. Engl. J. Med.* 338, 347–354. doi: 10.1056/NEJM199802053380602

Asaduzzaman, M., Zhang, S., Lavasani, S., Wang, Y., and Thorlacius, H. (2008). LFA-1 and MAC-1 mediate pulmonary recruitment of neutrophils and tissue damage in abdominal sepsis. *Shock* 30, 254–259. doi: 10.1097/shk.0b013e318162c567

Basit, A., Reutershan, J., Morris, M. A., Solga, M., Rose, C. E. Jr., and Ley, K. (2006). ICAM-1 and LFA-1 play critical roles in LPS-induced neutrophil recruitment into the alveolar space. *Am. J. Physiol. Cell Mol. Physiol.* 291, L200–L207. doi: 10.1152/ajplung.00346.2005

Blank, F., Wehrli, M., Lehmann, A., Baum, O., Gehr, P., von Garnier, C., et al. (2011). Macrophages and dendritic cells express tight junction proteins and exchange particles in an *in vitro* model of the human airway wall. *Immunobiology* 216, 86–95. doi: 10.1016/j.imbio.2010.02.006

Broide, D. H., Humber, D., and Sriramarao, P. (1998). Inhibition of eosinophil rolling and recruitment in P-selectin–and intracellular adhesion molecule-1–deficient mice. *Blood* 91, 2847–2856. doi: 10.1182/blood.V91.8.2847.2847_2847_2856

Brown, M. B., Hunt, W. R., Noe, J. E., Rush, N. I., Schweitzer, K. S., Leece, T. C., et al. (2014). Loss of cystic fibrosis transmembrane conductance regulator impairs lung endothelial cell barrier function and increases susceptibility to microvascular damage from cigarette smoke. *Pulm Circ.* 4, 260–268. doi: 10.1086/675989

Carestia, A., Davis, R. P., Davis, L., and Jenne, C. N. (2019). Inhibition of immunothrombosis does not affect pathogen capture and does not promote bacterial dissemination in a mouse model of sepsis. *Platelets*. 31, 925–931. doi: 10.1080/09537104.2019.1704711

Chiang, E. Y., Hidalgo, A., Chang, J., and Frenette, P. S. (2007). Imaging receptor microdomains on leukocyte subsets in live mice. *Nat. Methods* 4:219. doi: 10.1038/nmeth1018

Chtanova, T., Schaeffer, M., Han, S.-J., van Dooren, G. G., Nollmann, M., Herzmark, P., et al. (2008). Dynamics of neutrophil migration in lymph nodes during infection. *Immunity* 29, 487–496. doi: 10.1016/j.immuni.2008.07.012

Cleret, A., Quesnel-Hellmann, A., Vallon-Eberhard, A., Verrier, B., Jung, S., Vidal, D., et al. (2007). Lung dendritic cells rapidly mediate anthrax spore entry through the pulmonary route. *J. Immunol.* 178, 7994–8001. doi: 10.4049/jimmunol.178.12.7994

Croix, C. M. S., Leelavanichkul, K., and Watkins, S. C. (2006). Intravital fluorescence microscopy in pulmonary research. *Adv. Drug Deliv. Rev.* 58, 834–840. doi: 10.1016/j.addr.2006.07.007

De Alva, W. E., and Rainer, W. G. (1963). A method of high speed *in vivo* pulmonary microcinematography under physiologic conditions. *Angiology* 14, 160–164. doi: 10.1177/000331976301400402

Entenberg, D., Rodriguez-Tirado, C., Kato, Y., Kitamura, T., Pollard, J. W., and Condeelis, J. (2015). *In vivo* subcellular resolution optical imaging in the lung reveals early metastatic proliferation and motility. *Intravital* 4, 1–11. doi: 10.1080/21659087.2015.1086613

Entenberg, D., Voiculescu, S., Guo, P., Borriello, L., Wang, Y., Karagiannis, G. S., et al. (2018). A permanent window for the murine lung enables high-resolution imaging of cancer metastasis. *Nat. Methods* 15:73. doi: 10.1038/nmeth.4511

Faust, N., Varas, F., Kelly, L. M., Heck, S., and Graf, T. (2000). Insertion of enhanced green fluorescent protein into the lysozyme gene creates mice with green fluorescent granulocytes and macrophages. *Blood* 96, 719–726. doi: 10.1182/blood.V96.2.719

Fingar, V. H., Taber, S. W., and Wieman, T. J. (1994). A new model for the study of pulmonary microcirculation: determination of pulmonary edema in rats. *J. Surg. Res.* 57, 385–393. doi: 10.1006/jsre.1994.1159

Fiole, D., Deman, P., Trescos, Y., Mayol, J.-F., Mathieu, J., Vial, J.-C., et al. (2014). Two-photon intravital imaging of lungs during anthrax infection reveals long-lasting macrophage-dendritic cell contacts. *Infect. Immun.* 82, 864–872. doi: 10.1128/IAI.01184-13

Fiole, D., and Tournier, J. (2016). Intravital microscopy of the lung: minimizing invasiveness. *J. Biophotonics* 9, 868–878. doi: 10.1002/jbio.201500246

Fleischmann, C., Scherag, A., Adhikari, N. K. J., Hartog, C. S., Tsaganos, T., Schlattmann, P., et al. (2016). Assessment of global incidence and mortality of hospital-treated sepsis. Current estimates and limitations. *Am. J. Respir. Crit. Care Med.* 193, 259–272. doi: 10.1164/rccm.201504-0781OC

Fournier, B., and Philpott, D. J. (2005). Recognition of *Staphylococcus aureus* by the innate immune system. *Clin. Microbiol. Rev.* 18, 521–540. doi: 10.1128/CMR.18.3.521-540.2005

Frevert, U., Nacer, A., Cabrera, M., Movila, A., and Leberl, M. (2014). Imaging Plasmodium immunobiology in the liver, brain, and lung. *Parasitol. Int.* 63, 171–186. doi: 10.1016/j.parint.2013.09.013

Funakoshi, N., Onizuka, M., Yanagi, K., Ohshima, N., Tomoyasu, M., Sato, Y., et al. (2000). A new model of lung metastasis for intravital studies. *Microvasc. Res.* 59, 361–367. doi: 10.1006/mvre.2000.2238

Garcia, J. A., Cardona, S. M., and Cardona, A. E. (2013). "Analyses of microglia effector function using CX3CR1-GFP knock-in mice," in *Microglia. Methods in Molecular Biology (Methods and Protocols),* Vol. 1041, eds B. Joseph and J. Venero (Totowa, NJ: Humana Press), 307–317.

Gill, S. E., Rohan, M., and Mehta, S. (2015). Role of pulmonary microvascular endothelial cell apoptosis in murine sepsis-induced lung injury *in vivo*. *Respir. Res.* 16:109. doi: 10.1186/s12931-015-0266-7

Gill, S. E., Taneja, R., Rohan, M., Wang, L., and Mehta, S. (2014). Pulmonary microvascular albumin leak is associated with endothelial cell death in murine sepsis-induced lung injury *in vivo*. *PLoS ONE* 9:e88501. doi: 10.1371/journal.pone.0088501

Grommes, J., Alard, J.-E., Drechsler, M., Wantha, S., Mörgelin, M., Kuebler, W. M., et al. (2012). Disruption of platelet-derived chemokine heteromers prevents neutrophil extravasation in acute lung injury. *Am. J. Respir. Cri.t Care Med.* 185, 628–636. doi: 10.1164/rccm.201108-1533OC

Grott, K., and Dunlap, J. D. (2016). "Atelectasis," in *StatPearls* (Treasure Island, FL: StatPearls Publishing).

Grott, K., and Dunlap, J. D. (2020). *Atelectasis*. StatPearls.

Herman, B. (1998). "Fluorescence microscopy," in *Fluorescence Microscopy* (New York, NY: Springer-Verlag), 15–38.

Hickey, M. J., and Westhorpe, C. L. V. (2013). Imaging inflammatory leukocyte recruitment in kidney, lung and liver—challenges to the multi-step paradigm. *Immunol. Cell Biol.* 91, 281–289. doi: 10.1038/icb.2012.83

Khandoga, A., Kessler, J. S., Meissner, H., Hanschen, M., Corada, M., Motoike, T., et al. (2005). Junctional adhesion molecule-A deficiency increases hepatic ischemia-reperfusion injury despite reduction of neutrophil transendothelial migration. *Blood* 106, 725–733. doi: 10.1182/blood-2004-11-4416

Kim, H. K., Missiakas, D., and Schneewind, O. (2014). Mouse models for infectious diseases caused by *Staphylococcus aureus*. *J. Immunol. Methods* 410, 88–99. doi: 10.1016/j.jim.2014.04.007

Kim, M.-H., and Choi, J.-H. (2020). An update on sepsis biomarkers. *Infect. Chemother.* 52, 1–18. doi: 10.3947/ic.2020.52.1.1

Kim, Y. M., Jeong, S., Choe, Y. H., and Hyun, Y.-M. (2019). Two-photon intravital imaging of leukocyte migration during inflammation in the respiratory system. *Acute Crit Care* 34, 101–107. doi: 10.4266/acc.2019.00542

Kimura, H., Hayashi, K., Yamauchi, K., Yamamoto, N., Tsuchiya, H., Tomita, K., et al. (2010). Real-time imaging of single cancer-cell dynamics of lung metastasis. *J. Cell Biochem.* 109, 58–64. doi: 10.1002/jcb.22379

Kobayashi, K., Horikami, D., Omori, K., Nakamura, T., Yamazaki, A., Maeda, S., et al. (2016). Thromboxane A 2 exacerbates acute lung injury via promoting edema formation. *Sci. Rep.* 6:32109. doi: 10.1038/srep32109

Krahl, V. E. (1963). A method of studying the living lung in the closed thorax, and some preliminary observations. *Angiology* 14, 149–159. doi: 10.1177/000331976301400401

Kramer, K., Voss, H.-P., Grimbergen, J. A., Mills, P. A., Huetteman, D., Zwiers, L., et al. (2000). Telemetric monitoring of blood pressure in freely moving mice: a preliminary study. *Lab. Anim.* 34, 272–280. doi: 10.1258/002367700780384663

Kreisel, D., Nava, R. G., Li, W., Zinselmeyer, B. H., Wang, B., Lai, J., et al. (2010). In vivo two-photon imaging reveals monocyte-dependent neutrophil extravasation during pulmonary inflammation. *Proc. Natl. Acad. Sci.U.S.A.* 107, 18073–18078. doi: 10.1073/pnas.1008737107

Kuebler, W. M. (2011). Real-time imaging assessment of pulmonary vascular responses. *Proc. Am. Thorac. Soc.* 8, 458–465. doi: 10.1513/pats.201101-005MW

Kuebler, W. M., Kuhnle, G. E., Groh, J., and Goetz, A. E. (1994). Leukocyte kinetics in pulmonary microcirculation: intravital fluorescence microscopic study. *J. Appl. Physiol.* 76, 65–71. doi: 10.1152/jappl.1994.76.1.65

Kuebler, W. M., Parthasarathi, K., Lindert, J., and Bhattacharya, J. (2007). Real-time lung microscopy. *J. Appl. Physiol.* 102, 1255–1264. doi: 10.1152/japplphysiol.00786.2006

Kuhnle, G. E., Leipfinger, F. H., and Goetz, A. E. (1993). Measurement of microhemodynamics in the ventilated rabbit lung by intravital fluorescence

microscopy. *J. Appl. Physiol.* 74, 1462–1471. doi: 10.1152/jappl.1993.74.3.1462

Kukavica-Ibrulj, I., Bragonzi, A., Paroni, M., Winstanley, C., Sanschagrin, F., O'Toole, G. A., et al. (2008). In vivo growth of *Pseudomonas aeruginosa* strains PAO1 and PA14 and the hypervirulent strain LESB58 in a rat model of chronic lung infection. *J. Bacteriol.* 190, 2804–2813. doi: 10.1128/JB.01572-07

Lavoie, E. G., Wangdi, T., and Kazmierczak, B. I. (2011). Innate immune responses to *Pseudomonas aeruginosa* infection. *Microbes Infect.* 13, 1133–1145. doi: 10.1016/j.micinf.2011.07.011

Lee, P. Y., Wang, J., Parisini, E., Dascher, C. C., and Nigrovic, P. A. (2013). Ly6 family proteins in neutrophil biology. *J. Leukoc Biol.* 94, 585–594. doi: 10.1189/jlb.0113014

Lefrançais, E., Mallavia, B., and Looney, M. R. (2017). "Lung imaging in animal models," in *Acute Lung Injury and Repair*. (Springer), 107–32. doi: 10.1007/978-3-319-46527-2_8

Lefrançais, E., Mallavia, B., Zhuo, H., Calfee, C. S., and Looney, M. R. (2018). Maladaptive role of neutrophil extracellular traps in pathogen-induced lung injury. *JCI Insight* 3:e98178. doi: 10.1172/jci.insight.98178

Lichtman, J. W., and Conchello, J.-A. (2005). Fluorescence microscopy. *Nat. Methods* 2, 910–919. doi: 10.1038/nmeth817

Lien, D. C., Wagner, W. W. Jr., Capen, R. L., Haslett, C., Hanson, W. L., Hofmeister, S. E., et al. (1987). Physiological neutrophil sequestration in the lung: visual evidence for localization in capillaries. *J. Appl. Physiol.* 62, 1236–1243. doi: 10.1152/jappl.1987.62.3.1236

Lindert, J., Perlman, C. E., Parthasarathi, K., and Bhattacharya, J. (2007). Chloride-dependent secretion of alveolar wall liquid determined by optical-sectioning microscopy. *Am. J. Respir. Cell Mol. Biol.* 36, 688–696. doi: 10.1165/rcmb.2006-0347OC

Lindon, J. C., Tranter, G. E., and Koppenaal, D. (2016). *Encyclopedia of Spectroscopy and Spectrometry*. Oxford, UK: Academic Press.

Looney, M. R., and Bhattacharya, J. (2014). Live imaging of the lung. *Annu. Rev. Physiol.* 76, 431–445. doi: 10.1146/annurev-physiol-021113-170331

Looney, M. R., Thornton, E. E., Sen, D., Lamm, W. J., Glenny, R. W., and Krummel, M. F. (2011). Stabilized imaging of immune surveillance in the mouse lung. *Nat. Methods.* 8:91. doi: 10.1038/nmeth.1543

Mandler, W. K., Nurkiewicz, T. R., Porter, D. W., Kelley, E. E., and Olfert, I. M. (2018). Microvascular dysfunction following multiwalled carbon nanotube exposure is mediated by Thrombospondin-1 receptor CD47. *Toxicol. Sci.* 165, 90–99. doi: 10.1093/toxsci/kfy120

Margraf, A., Herter, J. M., Kühne, K., Stadtmann, A., Ermert, T., Wenk, M., et al. (2018). 6% Hydroxyethyl starch (HES 130/0.4) diminishes glycocalyx degradation and decreases vascular permeability during systemic and pulmonary inflammation in mice. *Crit. Care* 22:111. doi: 10.1186/s13054-017-1846-3

Masedunskas, A., Milberg, O., Porat-Shliom, N., Sramkova, M., Wigand, T., Amornphimoltham, P., et al. (2012). Intravital microscopy: a practical guide on imaging intracellular structures in live animals. *Bioarchitecture* 2, 143–157. doi: 10.4161/bioa.21758

Masterson, C. H., Curley, G. F., and Laffey, J. G. (2019). Modulating the distribution and fate of exogenously delivered MSCs to enhance therapeutic potential: knowns and unknowns. *Intensive Care Med. Exp.* 7:41. doi: 10.1186/s40635-019-0235-4

McCormack, D. G., Mehta, S., Tyml, K., Scott, J. A., Potter, R., and Rohan, M. (2000). Pulmonary microvascular changes during sepsis: evaluation using intravital videomicroscopy. *Microvasc. Res.* 60, 131–140. doi: 10.1006/mvre.2000.2261

Medina-Contreras, O., Geem, D., Laur, O., Williams, I. R., Lira, S. A., Nusrat, A., et al. (2011). CX3CR1 regulates intestinal macrophage homeostasis, bacterial translocation, and colitogenic Th17 responses in mice. *J. Clin. Invest.* 121, 4787–4795. doi: 10.1172/JCI59150

Mempel, T. R., Moser, C., Hutter, J., Kuebler, W. M., and Krombach, F. (2003). Visualization of leukocyte transendothelial and interstitial migration using reflected light oblique transillumination in intravital video microscopy. *J. Vasc. Res.* 40, 435–441. doi: 10.1159/000073902

Mertens, M., Tabuchi, A., Meissner, S., Krueger, A., Schirrmann, K., Kertzscher, U., et al. (2009). Alveolar dynamics in acute lung injury: heterogeneous distension rather than cyclic opening and collapse. *Crit. Care Med.* 37, 2604–2611. doi: 10.1097/CCM.0b013e3181a5544d

Moradali, M. F., Ghods, S., and Rehm, B. H. A. (2017). *Pseudomonas aeruginosa* lifestyle: a paradigm for adaptation, survival, and persistence. *Front. Cell Infect. Microbiol.* 7:39. doi: 10.3389/fcimb.2017.00039

Naumenko, V., Van S, Dastidar, H., Kim, D.-S., Kim, S.-J., Zeng, Z., et al. (2018). Visualizing oncolytic virus-host interactions in live mice using intravital microscopy. *Mol. Ther.* 10, 14–27. doi: 10.1016/j.omto.2018.06.001

Neupane, A. S., Willson, M., Chojnacki, A. K., Castanheira, F. V. E. S., Morehouse, C., Carestia, A., et al. (2020). Patrolling alveolar macrophages conceal bacteria from the immune system to maintain homeostasis. *Cell* 183, 110–125. doi: 10.1016/j.cell.2020.08.020

Niesner, R., Andresen, V., Neumann, J., Spiecker, H., and Gunzer, M. (2007). The power of single and multibeam two-photon microscopy for high-resolution and high-speed deep tissue and intravital imaging. *Biophys. J.* 93, 2519–2529. doi: 10.1529/biophysj.106.102459

Noda, S., Asano, Y., Nishimura, S., Taniguchi, T., Fujiu, K., Manabe, I., et al. (2014). Simultaneous downregulation of KLF5 and Fli1 is a key feature underlying systemic sclerosis. *Nat. Commun.* 5:5797. doi: 10.1038/ncomms6797

Norman, K. (2005). Techniques: Intravital microscopy–a method for investigating disseminated intravascular coagulation? *Trends Pharmacol. Sci.* 26, 327–332. doi: 10.1016/j.tips.2005.04.002

Ochi, H., Iijima, T., and Ushiyama, A. (2019). Intra-vital observation of lung water retention following intravenous injection of anti-MHC-class I (H-2K) monoclonal antibody in mice. *In Vivo (Brooklyn)* 33, 1477–1484. doi: 10.21873/invivo.11627

Opal, S. M. (2010). "Endotoxins and other sepsis triggers," in *Endotoxemia and Endotoxin Shock*. (Karger Publishers), 14–24. doi: 10.1159/000315915

Orthgiess, J., Gericke, M., Immig, K., Schulz, A., Hirrlinger, J., Bechmann, I., et al. (2016). Neurons exhibit Lyz2 promoter activity *in vivo*: implications for using LysM-Cre mice in myeloid cell research. *Eur. J. Immunol.* 46, 1529–1532. doi: 10.1002/eji.201546108

Park, I., Choe, K., Seo, H., Hwang, Y., Song, E., Ahn, J., et al. (2018). Intravital imaging of a pulmonary endothelial surface layer in a murine sepsis model. *Biomed. Opt. Express* 9, 2383–2393. doi: 10.1364/BOE.9.002383

Poobalasingam, T., Salman, D., Li, H., Alçada, J., and Dean, C.H. (2017) Imaging the lung: the old ways and the new. *Histol. Histopathol.* 32, 325–337. doi: 10.14670/HH-11-827

Presson, R. G. Jr., Brown, M. B., Fisher, A. J., Sandoval, R. M., Dunn, K. W., Lorenz, K. S., et al. (2011). Two-photon imaging within the murine thorax without respiratory and cardiac motion artifact. *Am. J. Pathol.* 179, 75–82. doi: 10.1016/j.ajpath.2011.03.048

Rahman, M., Roller, J., Zhang, S., Syk, I., Menger, M. D., Jeppsson, B., et al. (2012). Metalloproteinases regulate CD40L shedding from platelets and pulmonary recruitment of neutrophils in abdominal sepsis. *Inflamm. Res.* 61, 571–579. doi: 10.1007/s00011-012-0446-6

Razavi, H. M., Wang, L. F., Weicker, S., Rohan, M., Law, C., McCormack, D. G., et al. (2004). Pulmonary neutrophil infiltration in murine sepsis: role of inducible nitric oxide synthase. *Am. J. Respir. Crit. Care Med.* 170, 227–233. doi: 10.1164/rccm.200306-846OC

Reutershan, J., Basit, A., Galkina, E. V., and Ley, K. (2005). Sequential recruitment of neutrophils into lung and bronchoalveolar lavage fluid in LPS-induced acute lung injury. *Am. J. Physiol. Cell Mol. Physiol.* 289, L807–L815. doi: 10.1152/ajplung.00477.2004

Rodriguez-Tirado, C., Kitamura, T., Kato, Y., Pollard, J. W., Condeelis, J. S., and Entenberg, D. (2016). Long-term high-resolution intravital microscopy in the lung with a vacuum stabilized imaging window. *JoVE J. Vis. Exp.* 116:e54603. doi: 10.3791/54603

Roller, J., Wang, Y., Rahman, M., Schramm, R., Laschke, M. W., Menger, M. D., et al. (2013). Direct *in vivo* observations of P-selectin glycoprotein ligand-1-mediated leukocyte–endothelial cell interactions in the pulmonary microvasculature in abdominal sepsis in mice. *Inflamm. Res.* 62, 275–282. doi: 10.1007/s00011-012-0575-y

Rossaint, J., and Zarbock, A. (2013). Tissue-specific neutrophil recruitment into the lung, liver, and kidney. *J. Innate Immun.* 5, 348–357. doi: 10.1159/000345943

Sanderson, M. J., Smith, I., Parker, I., and Bootman, M. D. (2014). Fluorescence microscopy. *Cold Spring Harb. Protoc.* 2014:pdb-top071795. doi: 10.1101/pdb.top071795

Singer, M., Deutschman, C. S., Seymour, C. W., Shankar-Hari, M., Annane, D., Bauer, M., et al. (2016). The third international consensus definitions for sepsis and septic shock (Sepsis-3). *JAMA* 315, 801–810. doi: 10.1001/jama.2016.0287

Tabuchi, A., Matuszak, J., and Kuebler, W. M. (2020). Ventilation and perfusion at the alveolar level: insights from lung intravital microscopy. *Front. Physiol.* 11:291. doi: 10.3389/fphys.2020.00291

Tabuchi, A., Mertens, M., Kuppe, H., Pries, A. R., and Kuebler, W. M. (2008). Intravital microscopy of the murine pulmonary microcirculation. *J. Appl. Physiol.* 104, 338–346. doi: 10.1152/japplphysiol.00348.2007

Tabuchi, A., Nickles, H. T., Kim, M., Semple, J. W., Koch, E., Brochard, L., et al. (2016). Acute lung injury causes asynchronous alveolar ventilation that can be corrected by individual sighs. *Am. J. Respir. Crit. Care Med.* 193, 396–406. doi: 10.1164/rccm.201505-0901OC

Tauer, U. (2002). Advantages and risks of multiphoton microscopy in physiology. *Exp. Physiol.* 87, 709–714. doi: 10.1113/eph8702464

Vincent, J.-L. (2012). Increasing awareness of sepsis: World Sepsis Day. *Crit Care* 16:152. doi: 10.1186/cc11511

Wagner, W. W. (1965). Microscopic observation of the lung *in vivo*. *Vasc. Dis.* 2, 229–241.

Wagner, W. W. Jr. (1969). Pulmonary microcirculatory observations *in vivo* under physiological conditions. *J. Appl. Physiol.* 26, 375–377. doi: 10.1152/jappl.1969.26.3.375

Wang, Y., Roller, J., Menger, M. D., and Thorlacius, H. (2013). Sepsis-induced leukocyte adhesion in the pulmonary microvasculature *in vivo* is mediated by CD11a and CD11b. *Eur. J. Pharmacol.* 702, 135–141. doi: 10.1016/j.ejphar.2013.01.024

Wang, Z. (2016). Imaging nanotherapeutics in inflamed vasculature by intravital microscopy. *Theranostics* 6:2431. doi: 10.7150/thno.16307

Wearn, J. T., Barr, J. S., and German, W. J. (1926). The Behavior of the Arterioles and Capillaries of the Lung. *Proc. Soc. Exp. Biol. Med.* 24, 114–115. doi: 10.3181/00379727-24-3250

Wells, W. A., Thrall, M., Sorokina, A., Fine, J., Krishnamurthy, S., Haroon, A., et al. (2018). *In vivo and ex vivo* microscopy: moving toward the integration of optical imaging technologies into pathology practice. *Arch. Pathol. Lab. Med.* 143, 288–298. doi: 10.5858/arpa.2018-0298-RA

Witte, S. (1992). Fluorescence microscopic techniques in intravital microvascular studies: plasma proteins and cells. *Behring Inst. Mitt.* 91, 210–229.

Wynn, T. A., Chawla, A., and Pollard, J. W. (2013). Macrophage biology in development, homeostasis and disease. *Nature* 496:445. doi: 10.1038/nature12034

Yipp, B. G., Kim, J. H., Lima, R., Zbytnuik, L. D., Petri, B., Swanlund, N., et al. (2017). The lung is a host defense niche for immediate neutrophil-mediated vascular protection. *Sci. Immunol.* 2:eaam8929. doi: 10.1126/sciimmunol.aam8929

Zarbock, A., and Ley, K. (2009). The role of platelets in acute lung injury (ALI). *Front. Biosci. J. Virtual Libr.* 14:150. doi: 10.2741/3236

Conflict of Interest: The authors declare that the research was conducted in the absence of any commercial or financial relationships that could be construed as a potential conflict of interest.

frontiers in Cell and Developmental Biology

METHODS
published: 21 January 2021
doi: 10.3389/fcell.2020.632297

Leukocyte Trafficking and Hemostasis in the Mouse Fetus *in vivo*: A Practical Guide

Andreas Margraf[1,2]* *and Markus Sperandio*[1]*

[1] *Institute of Cardiovascular Physiology and Pathophysiology, Walter Brendel Center of Experimental Medicine, Ludwig-Maximilians-University Munich, Munich, Germany,* [2] *Department of Anesthesiology, Intensive Care Medicine and Pain Therapy, University Hospital Muenster, Muenster, Germany*

In vivo observations of blood cells and organ compartments within the fetal mammalian organism are difficult to obtain. This practical guide describes a mouse model for *in vivo* observation of the fetal yolk-sac and corporal microvasculature throughout murine gestation, including imaging of various organ compartments, microvascular injection procedures, different methods for staining of blood plasma, vessel wall and circulating cell subsets. Following anesthesia of pregnant mice, the maternal abdominal cavity is opened, the uterus horn exteriorized, and the fetus prepared for imaging while still connected to the placenta. Microinjection methods allow delivery of substances directly into the fetal circulation, while substances crossing the placenta can be easily administered via the maternal circulation. Small volume blood sample collection allows for further *in vitro* workup of obtained results. The model permits observation of leukocyte-endothelial interactions, hematopoietic niche localization, platelet function, endothelial permeability studies, and hemodynamic changes in the mouse fetus, using appropriate strains of fluorescent protein expressing reporter mice and various sophisticated intravital microscopy techniques. Our practical guide is of interest to basic physiologists, developmental biologists, cardiologists, and translational neonatologists and reaches out to scientists focusing on the origin and regulation of hematopoietic niches, thrombopoiesis and macrophage heterogeneity.

Keywords: fetal development, intravital microscopy, leukocytes, neutrophils, platelets, neonatology, physiology

OPEN ACCESS

Edited by:
Yuqing Huo,
Augusta University, United States

Reviewed by:
Jianshe Yan,
Shanghai University, China
Takaki Miyata,
Nagoya University, Japan

***Correspondence:**
Andreas Margraf
andreas.margraf@anit.uni-muenster.de
Markus Sperandio
markus.sperandio@lmu.de

Specialty section:
This article was submitted to Cell Adhesion and Migration, a section of the journal Frontiers in Cell and Developmental Biology

Received: *22 November 2020*
Accepted: *31 December 2020*
Published: *21 January 2021*

Citation:
Margraf A and Sperandio M (2021) Leukocyte Trafficking and Hemostasis in the Mouse Fetus in vivo: A Practical Guide. Front. Cell Dev. Biol. 8:632297. doi: 10.3389/fcell.2020.632297

INTRODUCTION

Background

Developmental processes including formation and function of blood cells and organs in mammalian fetuses are still incompletely understood. Mortality in very low and ultra-low birth weight premature infants shows only modest improvements, remains very high (mortality in 23 week old premature infants 73 vs 67% 2009 vs. 2012, respectively), and is the leading cause of death for children under 5 years of age according to the World Health Organization (WHO), showcasing the lack of adequate research and translational endeavors (Callaghan et al., 2006; Stoll et al., 2015). Human preterm infants are at high risk for infections and bleeding complications. Coping with increasingly younger gestational ages at birth challenges the clinical field, demanding further experimental workup of developmental processes. Cord blood samples of premature infants or *in vitro/ex vivo*

analyses of animal fetuses are the sources used so far to obtain information about developmental processes of the blood system and its consequences for bleeding, inflammation and development. So far, for organ development, radiologic imaging techniques, such as CT-scans, MRIs, or pathologists' and anatomists' workup of deceased fetuses are our most suitable source of information. In this practical overview, we describe an intravital microscopy (IVM) approach to observe the growing mouse fetus including yolk sac, focusing on the fetal vasculature and blood cells with a particular interest on leukocyte trafficking during inflammation and fetal platelet function.

In vivo Imaging of Fetal Yolk-Sac Vessels and Organ Compartments

The fetal IVM model was developed to investigate functional maturation and development of blood cell populations and progenitors in the living mouse fetus and elucidate underlying mechanisms of the regulation of homing processes and cell-cell interactions in the fetus.

Due to lack of knowledge about *in vivo* fetal responses to inflammatory stimuli together with clinical findings regarding postnatal complications in preterm infants, we set out to study leukocyte recruitment and leukocyte-endothelial cell interactions in the developing mouse fetus demonstrating an ontogenetic regulation of fetal leukocyte function with diminished leukocyte recruitment in the yolk-sac and fetal skull during fetal development (Sperandio et al., 2013). Subsequently, we focused on platelet function and platelet-leukocyte interactions *in vivo*. We wanted to understand to what extent thrombus formation could occur in the fetal vasculature (Margraf et al., 2017). This is an important question, as premature infants exhibit a high incidence of severe bleeding complications. In addition, adverse outcomes of premature infants have been reported in those infants receiving transfusions of adult platelets (Margraf et al., 2019). Our results herein showed that young fetuses have difficulties to form thrombi, with platelet hyporeactivity due to diminished expression levels of integrin adaptor molecules and decreased platelet counts (Margraf et al., 2017). More recently, we could use our fetal model in additional applications related to developmental processes of different cell populations and organ compartments, including the development of monocytes/macrophages in the fetus (Stremmel et al., 2018a,b) and the impact of blood flow properties on the development of the fetal thymus (Moretti et al., 2018). Here, we provide a concise approach for the preparation and subsequent IVM observation of fetal blood vessels and microinjection into the fetal vasculature in the mouse, including techniques to image platelets and leukocytes as well as different organ compartments.

Applications of the Fetal Intravital Microscopy Model

While examination of blood cell function is one of the major benefits of the fetal IVM model, it features a large variety of possible applications. These include vascular function and development, vessel distribution and reactivity, yolk-sac stability, as well as healing and regeneration processes. As IVM is well established in adult models of the mouse [e.g., cremaster muscle preparation (Sperandio et al., 2006), dorsal skinfold chamber (Lehr et al., 1993), vessel injury (Pircher et al., 2012)], experimental protocols, such as trauma-induced inflammation, endothelial damage and/or stimulation with pro-inflammatory agents (using LPS, fMLP, TNF-α etc.) can be transferred to the fetal *in vivo* model. Also, barrier-crossing of maternally administered substances can be traced, and intrauterine exposure to inflammatory stimuli can be mimicked.

Comparison With Other Methods and Advantages of the System

In past decades, different approaches to examine the fetal blood system or organ compartments have been applied. Christiansen and Bacon used trans-illumination microscopy on completely exteriorized fetuses to analyze vessel patterns in the developing posterior limb of mouse fetuses (Christiansen and Bacon, 1961). Echtler et al. (2010) applied a model of prematurity, where fetuses were born through cesarean section, intubated and used for experiments. This model allowed simulation and studying of clinically relevant problems, such as ductus arteriosus closure, while the preterm infant was challenged through outside influences, representing a disease-state setting, yet not allowing analysis of a developmentally regular surrounding, such as the yolk-sac. Another approach used a partial incision of the uterus musculature and yolk sac in combination with a suture-glue-fixation to prevent fluctuation of amniotic fluid, while displaying the fetal cranium in a fixed position for further analysis of the developing brain (Ang et al., 2003).

Additional methods featured MRI-trans-sections, where any movement could cause artifacts and no detailed analysis of blood cell subpopulations can be acquired at this moment due to limitations in traceable probes as well as low sensitivity (Dhenain et al., 2001; Speier et al., 2008). Garcia et al. (2011) chose an *ex vivo* embryo culture method to gain insight into morphogenetic events in the developing fetus, while Laufer et al. (2012) used photoacustic imaging techniques for CD-1 mice to examine embryos *ex vivo* and *in vivo*. Boisset et al. (2011) developed an approach where *ex vivo* confocal image acquisition of the embryo aorta was performed in order to monitor hematopoietic and endothelial cells during development. Yanagida et al. (2012) used a model for the visualization of migrating cortical interneurons in which an exteriorized E16.5 fetus, attached to the umbilical vessels is positioned in agarose gel with or without gallamine triethiodide application and scalp removal. Other techniques equally rely on incision of the yolk-sac and placement of the fetus into a heating chamber for example filled with artificial cerebrospinal fluid (Yuryev et al., 2015). Another technique used a fully mobilized uterine horn in which the mesometrium was cut and ovarian vessels had been ligated. The preparation was then mechanically immobilized, fixed in low-melting agarose and the embryo accessed by pressing it against the uterine wall and imaging it through the wall using two photon microscopy (Hattori et al., 2020).

Experimental models for murine fetal *in vivo* imaging are surprisingly rare and existing models have limitations regarding optical resolution, imaging techniques, or surgical preparation procedures with unintentional harming of the fetus itself. Thus, a model to study physiologically relevant developmental aspects has been lacking so far. Our *in vivo* model allows rather long observation times and a less artificial surrounding for the fetus itself, which remains vital throughout the experiments. Our preparatory techniques also allow removal of minute amounts of blood for further analysis from fetuses as young as age E13.5 (out of 21 days of gestation), e.g., for FACS analysis.

MATERIALS

Experimental Design and Level of Expertise Needed

Animals and Timed Matings

One major logistic effort lies within the requirement of pregnant animals. Thus, timed matings are needed to ensure adequate estimates of developmental age, which further needs to be specified through correlation of anatomical properties. In our setting, timed matings were conducted through two females and one male animal in the cage put together for one night. Depending on the specific need of pregnant mice we calculated with three to four cages per successful pregnancy. Influence of pheromones is minimized through spatial separation and hygiene precautions. For this purpose, female animals are placed in a separate room, while mating takes place in the room where the male mating animals are housed. After mating, animals are checked for plug-presentation, separated into plug positive and negative and placed back into the female room and a separate plug-positive room, respectively. Behavior, weight and change of abdominal configuration are checked daily. Prior to experiments weight, agility, and abdominal curvature are re-evaluated to prevent false positive pregnancies.

Choice of Anesthetics

For *in vivo* experiments involving muscular preparations and requiring stable images, a combination of ketamine and xylazine (both known to cross the placental barrier) is used, to reduce movement of the uterine musculature, while ensuring sufficient anesthesia, and analgesia for the animal.

Choice of Fluorophores and Antibodies

It is crucial for *in vivo* imaging to ensure sufficient image contrast, stability, and penetration depth. While the last two points are mainly influenced by preparational skills and technical setup, the image contrast relies on the appropriate choice of fluorophores and plasma markers. Equally, choice of antibodies is important when only a limited amount of colors can be imaged at once. **Table 1** gives a list of fluorophores and antibodies we and others have used in fetal blood cell imaging.

Fetal Ages

The choice of different developmental stages for IVM analysis is important for the experiments and depends on goal, site of expected observational events, preparational skills, and experimental duration (also compare "Limitations"). The maturation state of the fetus can be assessed by classical anatomical features and size of the mouse fetus, as described by Kaufmann (2005).

In vivo Imaging and Duration of Experiment

As any artificial manipulation can lead to serious consequences for the fetus, careful preparation and observation are necessary. Inflammatory stimulation or thrombus induction are harmful events occurring within the fetal vasculature, therefore limiting any subsequent experiments within the same fetus. Intravital imaging experiments were carried out for a maximum duration of 1 h per fetus (**Figure 1**).

Microinjection Volume Considerations

The developing murine fetus itself possesses only a small blood volume depending on the weight of the fetus (estimated 7–10% of the body weight). Thus, any injected substance will crucially influence circulatory mechanisms, cardiac output and vascular tone within the fetus (Russel et al., 1968). We observed that injection of volumes exceeding 5–10 μL strongly compromised the fetus and should therefore be avoided.

Animals

Mice

Adult female (C57/Bl6; minimal age 12 weeks) and male mice are used for timed matings. Pregnant female mice are used for *in vivo* experiments. Through mating strategies and use of appropriate genetically modified reporter mice (**Table 1**), it is possible to generate different phenotypes in the fetus and mother. This might help to distinguish fetal from maternal structures (cells).

Reagents

Anesthetic

Use a ketamine/xylazine mix (125 mg/kg bodyweight of ketamine; 12,5 mg/kg bodyweight of xylazine) in a volume of 0.1 ml per 8g bodyweight for anesthesia of the mother animal.

FITC-Dextran-Solution

Used to stain microvasculature and for phototoxicity-induced thrombus formation. Dissolve FITC-dextran in sterile injectable distilled water or sterile phosphate-buffered saline at a final concentration of 10%.

Acridine-Orange-Solution

Injectable *in vivo* dye capable of crossing the placental barrier. Dissolve at a concentration of 2 mg/ml in sterile phosphate-buffered saline. Prepare an injection volume of about max. 150 μl in a syringe for later administration (usually as needed, approx. 50 – 100 μl).

Microbeads

Used for *in vivo* blood flow velocity measurements. Ultrasonicate beads prior to usage. Dilute stock concentration of 1×10^{10} beads/ml per factor 10 to 100 according to wished study purpose. For injection into yolk sac vessels, dilute 1 μl of bead-solution in a total of 5 μl of sterile NaCl or PBS injection solution.

TABLE 1 | Antibodies, fluorophores, and markers used for *in vivo* imaging in the mouse fetus.

Fluorophore, antibody or genetic marker	Category	Used for	Advantage	Disadvantage	Expected consequences	Considerations	Citations
FITC (high MW)	Fluorophore	Thrombus induction; Plasma marker	Bright, good contrast	Photoreactivity limits application as regular plasma-marker	Phototoxicity leads to vessel-wall injury and thrombus formation	Phototoxic	Margraf et al., 2017
TRITC (high MW)	Fluorophore	Plasma marker	Almost no leakage		Labeling of plasma and passive visualization of fluorescence-negative blood cells		Honkura et al., 2018
Low MW dextrans (for example 70 kDa Texas-red dextran and 40 kDa FITC dextran)	Fluorophore	Endothelial permeability assessment	Leakage		Observation of plasma staining and time-dependent increase in perivascular fluorescence intensity		Lee et al., 2018
Acridine orange	Fluorophore	Leukocyte and vessel wall labeling	Crosses placental barrier	Vessel constriction, thrombus induction	Labeling of leukocytes and endothelial cells	Phototoxic	Sperandio et al., 2013
GpIbβ-X488 antibody	Antibody	Platelet labeling	Non-blocking	Expensive	Labeling of platelets and megakaryocytes		Margraf et al., 2017
PeCam (CD31)-antibody	Antibody	Endothelial cell labeling		Expensive	Labeling of platelets and endothelial cells		Cappenberg et al., 2019
Gr-1 antibody	Antibody	Neutrophil labeling		Expensive, not specific; depletion (?)	Labeling of neutrophils and other leukocyte populations	Transient expression in monocytes	Volmering et al., 2016
Ly6G antibody	Antibody	Neutrophil labeling	Specific	Expensive, depletion (?), blocking (?)	Labeling of neutrophils		Wang et al., 2012; Yipp and Kubes, 2013; Cunin et al., 2019
Lyz2-EGFP	Genetic	Neutrophil analysis	Good signal intensity	Unspecific	Observation of leukocytes		Sperandio et al., 2013
CX3CR1 GFP	Genetic	Monocyte/macrophage analysis		Unspecific	Labeling of multiple monocytic/macrophage populations and progenitors		Stremmel et al., 2018a,b
IVM Catchup	Genetic	Neutrophil analysis	Good signal	Specific for neutrophils	Labeling of neutrophils	Homozygous animals have been described as Ly6G-deficient	Hasenberg et al., 2015
*Cdh5*Cre	Genetic	Crossing with floxed stop reporter mouse (f.e. Rosa26-floxed stop fluorescent protein) line to create endothelial cell labeling within fetus and/or mother	Allows differentiating maternal and fetal vessels	Complex breeding schemes for fetal vs. maternal labeling; depending on mouse line unspecific HC-expression	Labeling of endothelial cells in either maternal vessels, fetal vessels or both, depending on breeding scheme.		Payne et al., 2018

TABLE 1 | Antibodies, fluorophores, and markers used for *in vivo* imaging in the mouse fetus.

Fluorophore, antibody or genetic marker	Category	Used for	Advantage	Disadvantage	Expected consequences	Considerations	Citations
Sca-1 GFP	Genetic	Hematopoietic stem and progenitor cell labeling	Good visualization of fetal circulation and organs	Unspecific	Labeling of progenitor cells and endothelial cells.		Ma et al., 2002a,b
CD41	Genetic or antibody	Platelet labeling		Unspecific	Labeling of platelets, megakaryocytes and various progenitor cells		Ferkowicz et al., 2003; Mikkola et al., 2003; Li et al., 2005; Zhang et al., 2007
Pf4tdRFP	Genetic	Platelet and megakaryocyte labeling	Allows visualization of platelets	Unspecific	Labeling of platelets, megakaryocytes and progenitor cells		Calaminus et al., 2012

In vivo Superfusion Buffer

Classical superfusion solution for IVM experiments as reported earlier (Klitzman and Duling, 1979). Prepare solution I, containing 292.9 g of NaCl, 13.3 g of KCl, 11.2 g of CaCl2, and 7.7 g of MgCl2 in a total of 3.8 liters of deionized water. Prepare solution II, containing 57.5 g of NaHCO3 in 3.8 liters of deionized water. The *in vivo* superfusion buffer is then obtained by adding 200 ml of solution I into a two liter cylinder. Fill the cylinder then up to 1,800 ml with deionized water. Then add 200 ml of solution II to the cylinder. Mix the solution and add a gas-combination of 95% N2/5% CO2 using a foam-disperser. If needed, inflammatory stimuli (for example fMLP) can be added to the superfusion buffer.

Equipment

Intravital Microscope

The intravital microscopic setup consists of an upright microscope, together with a motorized *xyz*-stage, which allows to save *xy*-positions and to move to a previously determined exact position again later throughout an experiment. Usage of inverted microscopes are not recommended as they can result in excessive pressure application onto the fetus and thus deterioration of blood flow in the field of observation. Equally, inverted microscopes do not allow for adequate superfusion of a fetus. For illumination different light sources (halogen lamp, Hg-lamp, stroboscopic flash lamp system, laser) are used together with a CCD-camera or photomultiplier tubes as appropriate for the type of microscopic technique (f.e., conventional fluorescence microscopy, multiphoton laser scanning microscopy, spinning disk microscopy and others, compare **Table 3**). The choice for usage of a specific microscope should depend on the research question in which either a fast image acquisition, long-term image stability or high resolution or tissue penetration are needed (see **Table 3**). To ensure optimal conditions for the animals during the IVM observation period, a heating pad and superfusion solution are used. The heating pad is placed below the mother animal to ensure adequate temperature of the maternal blood circulation which nurtures the placenta. Heating pad performance must be regularly controlled to guarantee appropriate environmental temperature. The superfusion solution is administered constantly with the use of a turning-pump/roller-pump. A polyethylene-tubing system is used to connect the superfusion system to the microscope objective. Temperature of the superfusion system must be adjusted to reach adequate temperature at the point of administration, thus measurements have to be performed directly at the objective. The temperature-controlled superfusion buffer in which the fetus is constantly immersed thus prevents cooling of the fetus itself. To guarantee a stable temperature of the superfusion buffer on the preparation, the superfusion buffer is continuously removed from the microscope stage through a small hole, connected to a vacuum pump reservoir (compare **Supplementary Figure 1**).

To keep the preparation in a fixed position, the mother animal is placed on a custom-made plexiglass animal stage, with the fetus positioned inside a petri dish (construction plan see **Supplementary Figures 1–3**), from which on one side, one part

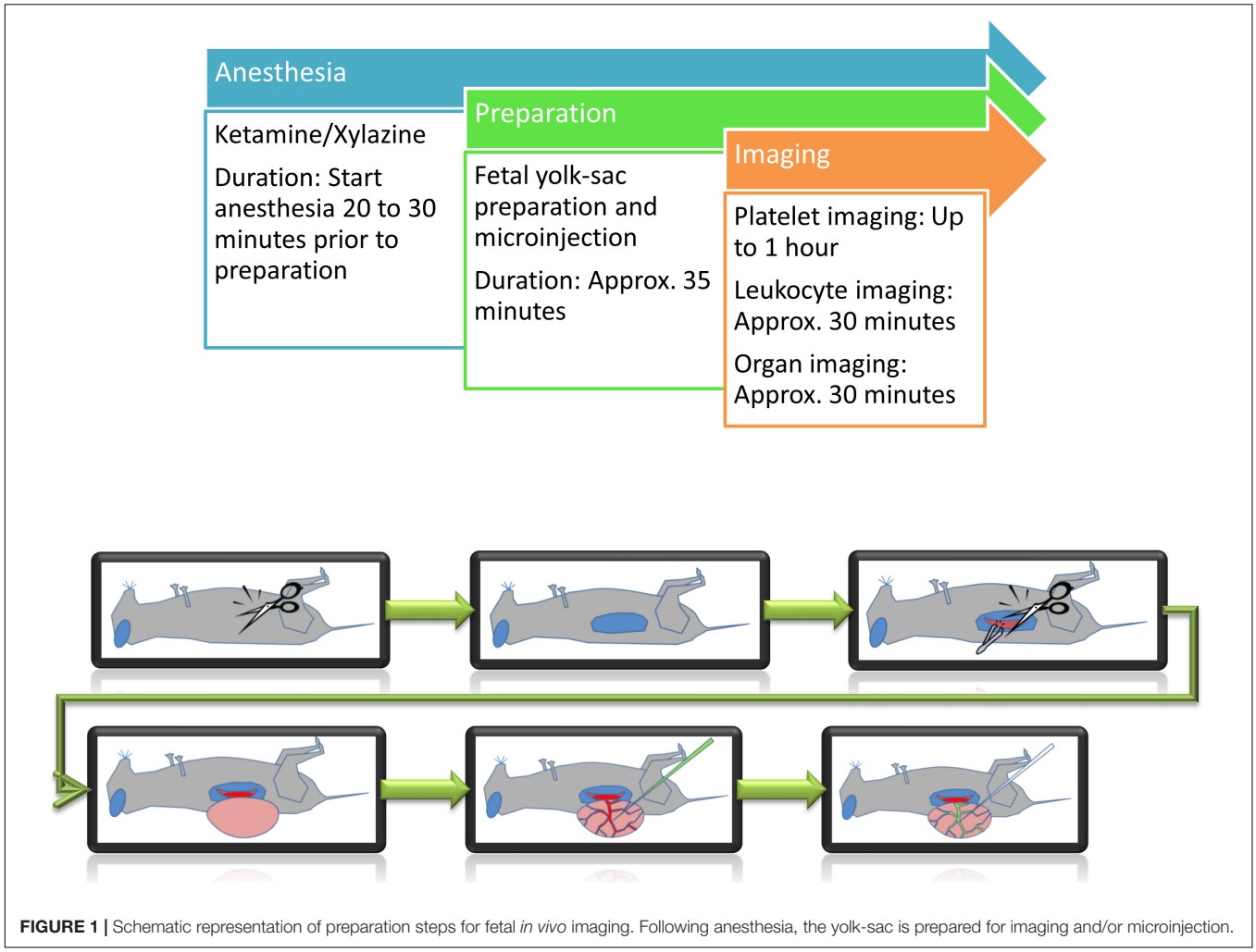

FIGURE 1 | Schematic representation of preparation steps for fetal *in vivo* imaging. Following anesthesia, the yolk-sac is prepared for imaging and/or microinjection.

of the wall is removed to allow the fetus to lay inside the petri dish without the application of pressure or force onto it. The fetus is kept in place within the petri dish containing medical silicone-gel and the use of a custom made magnetic space-holder, which reduces the influence of the breathing movement of the mother-animal on the observation field. The space-holder contains a hole for microscopic access. A coverslip is placed on top of the fetus and used for observation. Care must be taken that the blood flow is not restricted by pressure application. Imaging techniques such as multiphoton-laser scanning-microscopy (MPLSM) are more sensitive to motion artifacts and thus require a higher degree of stabilization compared to conventional epifluorescence recordings. If the setup described herein is insufficient to achieve acceptable imaging conditions, users should consider the following options (also compare **Tables 2**, **3**):

1. If insufficient perfusion of the yolk-sac is observed, try to reduce pressure exerted by the stabilization device. If necessary (especially in very old fetuses), try to only use a cover slip without fixation device and keep the cover slip in position by application of additional medical silicone-gel outside of the field of observation.
2. If the image is unstable, increase pressure while directly observing the microcirculation through the microscope, without affecting blood circulation within the yolk-sac or fetus. Generally, ensure the mother animal is not in contact with the cover slip or holding device otherwise breathing artifacts are transferred to the preparation. Also, it is helpful to model the silicone-gel against the fetus to ensure it remains within its position for the duration of the recording. Additional care must be taken to ensure adequate anesthesia, which might require re-injection of anesthetics depending on the duration of recording.

Recording of the *in vivo* observations is conducted via a digital recording system.

Generation of Micropipettes for Fetal Microinjection

For microinjection purposes, glass capillaries are being heat-pulled utilizing a vertical heat-puller. Employing a stereoscope, pulled glass capillaries (micropipettes) are placed in a grinding device and grinded to create a syringe-like tip (open tip diameter 1-2 μm), which allows easier penetration of blood vessels.

TABLE 2 | Troubleshooting.

Step	Problem	Possible reason	Solution
Searching for the right microscopic image	The vessels are not satisfactory/too small/too big/none in the field of view.	Placement of animal, constricted blood circulation.	Place the mother animal on the abdomen and thus turn the whole preparation upside down, gaining access to other vessels within the yolk sac.
Microinjection	The vessel gets ruptured/it is difficult to get into the tissue.	Diameter of glass capillary is too big, not well grinded.	Try to choose a smaller diameter and make sure you check the grinded tip again before injection.
Microinjection	It is impossible to get the substance out of the glass capillary.	Diameter too small, blood clotting at the tip.	Grind the capillary to a larger diameter, try to apply pressure before the injection onto paper tissue to see if you can successfully inject, do not re-use used glass capillaries, as smallest amounts of blood can lead to closure of the tip.
Microinjection	I have a backflow into the glass capillary.	Pressure too low.	Adjust pressure to a higher level, making sure you keep a baseline level throughout puncturing and injection.
Microinjection	After injection and occlusion, tissue gets pulled out and the yolk-sac ruptures.	The cauterization device is sticking to the site of heat-occlusion.	Try to use only the tip of the cauterization device to occlude the vessel. Make sure you do it quick and precise. The bigger the area of heat-application, the more likely the yolk-sac will rupture.
Imaging	Using multiphoton microscopy, the resulting stacks are not showing the complete vessel in time lapse recordings.	The z-shift moves the vessel out of the focus. Shadow-effects by large amounts of erythrocytes contribute to poor penetration depth inside the vessel.	Increasing the z-stack size to levels sufficiently above and below the vessel of observation will prevent it from shifting out of the field of observation.
Thrombus induction	Mechanical vessel occlusion is not successful using local pressure application.	The stimulus is insufficient for studying thrombus formation.	Try to use a 8–0 suture in order to ligate the vessel locally. Keep the ligation for a longer time to increase flow restriction and vessel damage.
Imaging	Image quality is not satisfactory in the liver region.	Penetration depth is not sufficient.	Remove the surrounding tissue and liver capsule. Try to either ligate one of the ribs and pull it with a suture to the cranial direction, gaining access to the liver, or to carefully dissect part of the forming rib.

RESULTS/PROCEDURES

A single experiment from the beginning of anesthesia until the end of image acquisition takes between one to one and a half hours for leukocyte imaging and two and a half hours for platelet function studies (**Figure 1**).

Mouse Anesthesia and Surgical Procedure

Anesthetize the pregnant mother animal, using 100 µl narcotic cocktail per 8 g bodyweight. Administration of anesthesia should be i.m., rather than i.p., as effectiveness of i.p. injection might be influenced by the surgical procedure of the model, which requires opening of the abdominal cavity with potential leakage of the applied anesthetic drugs. In addition, i.p. injection might also harm the fetuses by misplaced injection. After administration wait for about 20 min, until the mouse is securely unconscious. Check anesthesia through a pain stimulus (e.g., compression of the foot-limb). Place the mother animal with its back on the heating pad. Disinfect the abdominal site of preparation with 70% ethanol. Shaving can be performed as needed. Make a lateral horizontal incision in the expected size of the fetus (approx. 1 cm) to open the abdominal cavity. Cauterize blood vessels from which bleeding might occur either before or during incision of the peritoneum.

Preparation of Fetal Yolk-Sac Vessels

Localize the uterus horn and carefully grab it with blunt tweezers (**Supplementary Movie 1**). Try to hold on to muscle tissue of the uterine wall only, without grabbing the fetal body in order to prevent injury. This is most conveniently done in a region between two fetuses. Exteriorize the uterus. Make sure you prevent cooling and drying through administration of heated superfusion buffer (37°C) prior, during and after exteriorization. Incise the uterine musculature in a horizontal manner to reach to one vital fetus within its yolk sac. Place another incision in a vertical manner (90° to prior incision) to reduce pressure of the uterine musculature onto the placenta. Ensure to start the incision at the opposite site of the placenta, between two fetuses, where you can easily hold the uterus muscle tissue with blunt forceps, without harming the yolk sac. From there, extend the incision, using manually blunted microsurgery scissors. The uterus muscle fibers will start to contract and retract, giving access to the yolk-sac. It is very easy to puncture and/or rupture the yolk-sac while trying to cut through the uterine wall. Also, a high amount of pressure resulting from the contraction of uterine muscle fibers of the incised uterine horn, especially in older fetuses, can lead to the rupture of the yolk-sac and worsening perfusion. At this step, patience is necessary. Very often, the fetus within the yolk-sac finds its way out through the surgical opening of the placenta without external support.

After the fetus is exteriorized (**Figure 2A**) and still inside the yolk-sac, the fetus is gently placed into a modified petri dish (5 ml) (**Figure 2B**), filled with silicone and warmed superfusion

TABLE 3 | Microscope applications.

Microscopic technique	Light source and detection method	Advantage	Disadvantage	Possible application	Fetal tissue
Conventional epifluorescence microscopy	Mercury bulb; digital camera.	Fast	Limited penetration depth, bleaching, and light scattering.	Assessment of leukocyte rolling, adhesion, and migration.	Yolk-sac, brain.
Spinning disc confocal microscopy	Laser; photomultiplier tubes and/or digital camera.	Fast with higher spatial resolution.	Does not reach penetration depth of MPSLM imaging.	Assessment of slow leukocyte rolling, adhesion, and migration.	Yolk-sac, brain, liver, and skin.
Conventional confocal microscopy	Laser; photomultiplier tubes.	High spatial resolution.	Slow	Analysis of expression patterns, assessment of stable structures or slow cell movement (migration).	Yolk-sac, brain, and liver.
Multi-Photon-Laser-Scanning-Microscopy (MPLSM)	Laser; photomultiplier tubes.	Label-free cell and tissue detection (second- and/or third-harmonic generation signals); high penetration depth; good spatial resolution.	Relatively slow, risk of laser damage depending on settings; motion sensitivity leads to artifacts and/or shifting of images.	Assessment of anatomical features; analysis of deeper organ compartments; migration; and laser-injury.	Yolk-sac, brain, liver, skin, bone marrow, and heart.

buffer solution. Lifting cannot be done by directly pulling on the yolk-sac, as it will easily rupture. Therefore, try to pull on surrounding uterine musculature, located next to the preparation site. It is also possible to load the fetus onto a pre-wetted cotton-stick and carefully mobilize it. It is important not to damage the placenta to decrease the risk of bleeding. After having secured the fetus within the yolk sac, the animal stage can be transferred to the IVM for imaging.

We have performed extensive imaging studies on yolk sac vessels (a) to elucidate the maturation of neutrophil recruitment during inflammation throughout mouse fetal development and (b) to investigate platelet function during fetal ontogeny. The following sections will describe how we approached these two processes by intravital imaging:

Studying *in vivo* Neutrophil Recruitment During Fetal Development

Depending on the purpose of the project, the preparation of the fetus/yolk-sac can be performed in unstimulated pregnant mice or pregnant mice in which the uterus has been pre-stimulated with proinflammatory agents (f.e., intrauterine LPS, fMLP, or TNF-α, **Figure 2C**) prior to imaging. If no proinflammatory stimulus is applied, the surgical procedure itself will cause a mild inflammatory response with some rolling and adherent leukocytes, which can be compared to trauma-induced injury as described in the mouse cremaster muscle (Sperandio et al., 2001).

Using reporter mice such as *Lyz2* EGFP mice (Faust et al., 2000) or Catchup IVM mice (Hasenberg et al., 2015), neutrophils can be visualized by their fluorescent signal. The yolk sac microcirculation does not need to be stained as the auto-fluorescence signal is bright enough for conventional fluorescence microscopy. Observation of rolling, adhesion and crawling of fluorescently labeled blood cells as neutrophils is then possible. In case no external stimuli are used, we see some rolling and adherent neutrophils, which increase in number with gestational age. For application of additional dyes or other agents into the maternal organism, a carotid artery catheter can be placed into the pregnant mouse before imaging. Injection of acridine-orange solution into the carotid artery will stain maternal and fetal leukocytes (placental passage!) and can be used as alternative approach in case reporter mice are not available.

Measuring of blood flow velocity:

Three different techniques can be applied to study blood flow characteristics during fetal ontogeny. The most precise and reproducible technique is the microbead based method. Overall, velocity is calculated as the displacement of a bead or cell from point a to point b during a pre-determined time interval, resulting in:

$$\text{Velocity} = \frac{\left(\text{Distance point } a \text{ to point } b\right)\,[\mu\text{m}]}{(\text{Time})\,[s]}.$$

1. Leukocyte based method: Using a flowing leukocyte in the center of the vessel, the movement of the cell is followed frame by frame. This gives you information on traveled distance over time.
2. Microbead based method: Microbeads are microinjected into the fetus and allowed to circulate prior to imaging.

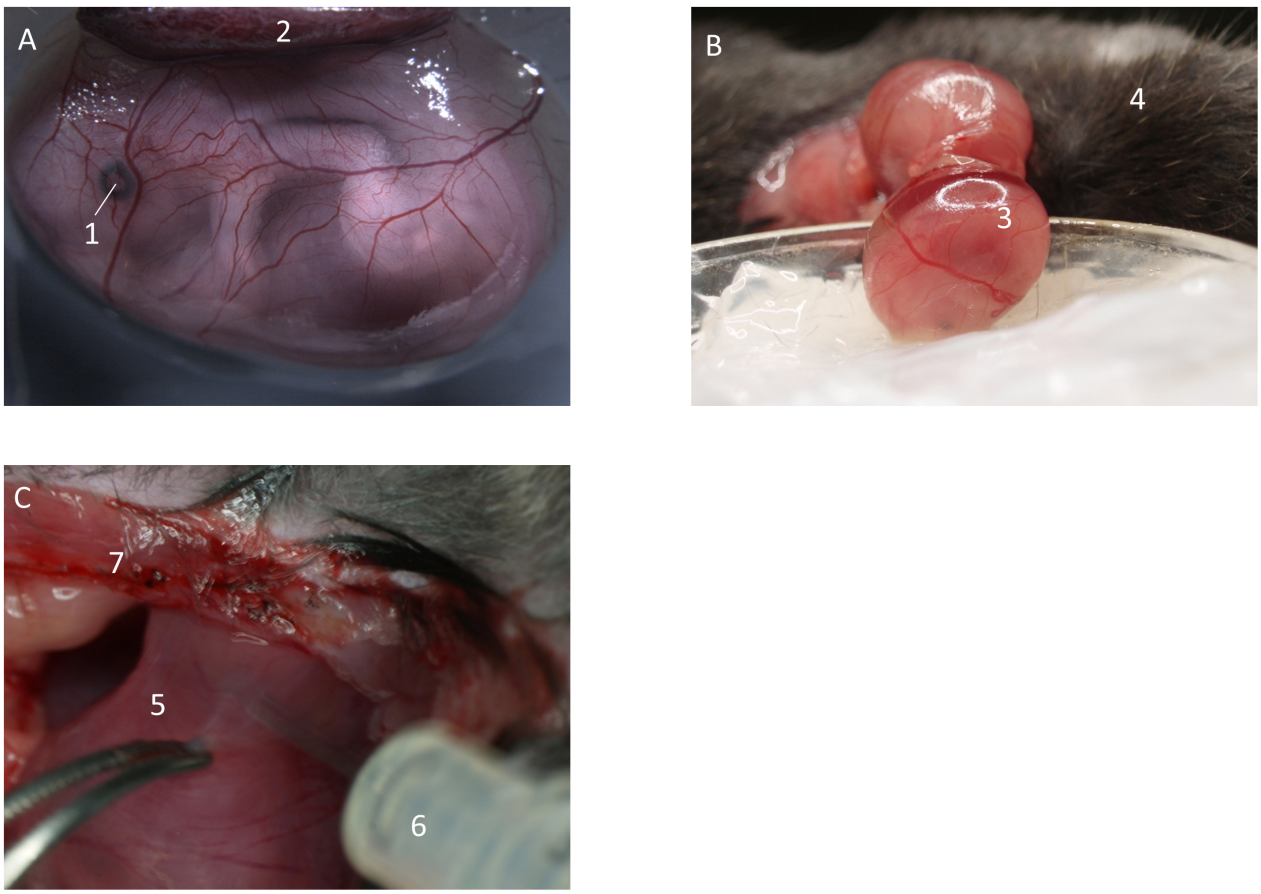

FIGURE 2 | Preparation of fetal yolk-sac. **(A)** Preparation allows access to the yolk-sac microvasculature. Image from Margraf (2018). **(B)** Following incision of the uterus, the fetus inside the yolk-sac is carefully mobilized and placed in a modified petri dish filled with medical silicone gel and superfusion buffer. **(C)** If needed, inflammatory stimuli can be injected into the uterus by puncturing in-between two separate fetuses. (1) Eye of the fetus. (2) Placenta. (3) Fetus inside yolk-sac. (4) Mother animal. (5) Uterus horn in-between two fetuses. (6) Syringe. (7) Abdominal opening of the mother animal.

As described under (1) two consecutive frames can then be used and microbead displacement assessed over time.

3. Multiphoton-laser scanning microscopy-based line-shift determination of blood flow velocity can be performed as previously described (Dietzel et al., 2014).

Studying Thrombus Formation and Platelet-Leukocyte Interaction in the Growing Mouse Fetus

Microinjection: Fill one grinded and prepared glass microcapillary with FITC-dextran, to a volume of approximately 5 μl (/beads/antibody-solution, respectively). Depending on the desired injection site, volume and opening diameter of the glass capillary, either manual pressure infusion, or a transjector-based approach can be chosen; equally, either manual puncturing or micromanipulator-based puncturing of the yolk-sac vessel can be performed.

Connect the microcapillary to the pressure-application tube. Hold the glass-capillary like a pencil, with the tip of your fingers, while using the other hand to stabilize. Make sure, to put the cauterization device close to the other hand (**Supplementary Movie 1**). Optional, you can hold it with your other hand (e.g., left, if right-handed), while puncturing the yolk-sac, to immediately occlude the injection-vessel in order to prevent bleeding out of the injected substance from the penetration point. Puncture a sidebranch vessel. Before doing so, observe blood flow characteristics, as it is crucial to choose a vessel which ensures distribution and flow into a bigger blood vessel. Rupturing and/or penetration of the yolk-sac is very easy during this step. Practice is necessary, while it can be helpful to know that due to the size of the glass capillary (depending on purpose of injection), tissue can be folded and pushed away during pressure application by the tip of the glass capillary (the bigger the tip diameter, the more difficult it will be to penetrate a vessel; yet the smaller the tip diameter, the more likely it will break or demolish the grinded tip). Once the applied puncturing-pressure is high enough, the tissue will allow access and the glass-capillary will slide into the blood vessel.

Applying constant injection pressure, administer the dye and/or antibody-solution into the vessel. Observe it through the stereo-microscope. Make sure to observe the level of the injection

solution to prevent injection of air into the fetal vasculature. Thus, stop the injection right before air application and proceed to the next step, while maintaining a constant slightly positive pressure equivalent to the current intravascular blood pressure. It is easiest to manually adapt this pressure.

Remove the glass capillary from the vessel and immediately occlude the injection point with the electric-cauterization device. Be quick. If too slow, the injected solution will flow out of the vessel again. Additionally, it is important to minimize the applied heat/trauma using the cauterization device, to ensure sufficient blood flow in the surrounding vessels.

Leave the fetus for approximately 5–10 min in the dark room in warm superfusion buffer to guarantee circulation and thus distribution of the phototoxic dye and/or antibody-solution.

Imaging of the yolk-sac: Place the fetus onto the imaging-stage. Make sure not to rupture the connection between fetus and mother animal while positioning or moving the preparation. Transfer the preparation to the *in vivo* microscope setup. Choose appropriate light/filter/detector settings. For imaging choose a vessel away from the point of microinjection. Apply superfusion buffer throughout the experiment.

Thrombus induction: For thrombus induction, we recommend the phototoxic or laser-induced approach, yet depending on availability of techniques, also the mentioned other approaches can be used. Nonetheless, variation in results is greater in subsequently mentioned techniques.

Phototoxic Injury

For thrombus induction use phototoxic FITC-dextran as microinjection-solution. Perform imaging using a high intensity light source (e.g., mercury lamp). For FITC-Dextran, use a filter for excitation maximum: 490 nm, emission maximum: 520 nm. Observe one vessel (20–50 μm) for up to 1 h or until stop of flow occurs. Determine fluorescence intensity using histogram values. For our experiments we chose a camera exposure time of 10 ms. Of note, the field of view will be constantly illuminated by the light source throughout the experiment. Examine platelet adherence and vessel occlusion. Examine reflow-phenomena as an inverse correlate of thrombus stability for 10 min after complete occlusion of a vessel occurred. Once reflow appears, continue observation again for up to 1 h or until stop of flow occurs.

Laser-Induced Injury

For thrombus induction use 2-photon-imaging (Nishimura et al., 2006; Kamocka et al., 2010; Koike et al., 2011). Depending on laser-settings, use a small point laser scan in the level of the vessel wall. Create a vessel-wall injury using beam intensity slightly below apparent heat damage. Observe thrombus formation using time-laps stack acquisition. Movements in z-direction are difficult to outbalance. Thus, appropriate stack settings need to be chosen, allowing for a range of motion.

Chemical Injury

Prepare a 1 mm × 2 mm filter paper patch. Place the filter paper patch into FeCl3-Solution of desired concentration (e.g., 1%). Microinject GpIbβ-X488-antibody into the fetal vasculature and occlude the vessel (see above). A concentration of 0,1 μg/g body weight is recommended. Now apply the FeCl3-saturated paper patch onto the desired vessel under the stereomicroscope. Observe the surrounding area (borderline) of the patch-applied vessel for blood flow cessation. Remove the FeCl3-paper patch after a minimum time of 30 s and proceed quickly to the next step in order to observe the different steps of platelet-vessel-wall interaction. Perform imaging under the *in vivo* microscope using the appropriate filter sets for platelet observation. The forming clot can be noted as fluorescence enhancement at the site of adhering platelets. The antibody recommendation for imaging are to use FITC-fluorescence filter sets and exposure times between 200 and 400 ms depending on camera setup and excitation light source.

Platelet-Leukocyte Interactions

Utilizing antibody or genetic knock-in strategies to fluorescently label platelets and leukocytes (for example using a GFP-knock in for leukocytes and an Alexa649 antibody staining for platelets), platelet-leukocyte interaction can be quantified by counting double-positive (GFP+ and Alexa649+) cellular events and assessing rolling of leukocytes on adherent platelets. Both thrombotic (interaction of leukocytes with injury-related adherent platelets) and free circulating platelet-leukocyte aggregates can be enumerated. At early gestational ages no platelet-leukocyte aggregates can be observed as P-selectin and PSGL-1 expression levels are low. Transfusion of isolated, labeled adult platelets and/or leukocytes into older fetuses can help in dissecting cell- and maturation-specific phenotypes.

Fetus Exteriorization and Organ Imaging

Carefully open the yolk-sac and exteriorize the fetus (**Figure 3A**). Ensure the umbilical vessels are still intact and not damaged. Remove disturbing tissue and liquid. Place the fetus inside a modified petri dish filled with superfusion buffer. Proceed with preparation and imaging as described below:

Skin

Place a cover slip onto the skin pattern you wish to image. Apply the fixation device. Perform *in vivo* imaging with constant superfusion. MPLSM can be used for deep tissue penetration.

Liver

Make a small incision within the posterio-lateral area of the fetus (**Figures 3B,C**), in an area where the liver is clearly visible through the thin skin (**Figure 3D**). From there, gently open the lateral side of the abdominal cavity of the fetus to display the fetal liver. If needed, carefully remove one of the forming ribs. It might be necessary to remove the liver capsule (Glisson's capsule). The liver is a well perfused organ. Thus, preparation and manipulation within this area features high bleeding risk. Place a cover slip and the fixation device on top and transfer it to the imaging setup. MPLSM might hold best results due to its penetration depth.

Cranial Imaging

Carefully incise the skin in the head region (temporal region) and place a small silicon ring (approx. 0,5 to 1 cm diameter,

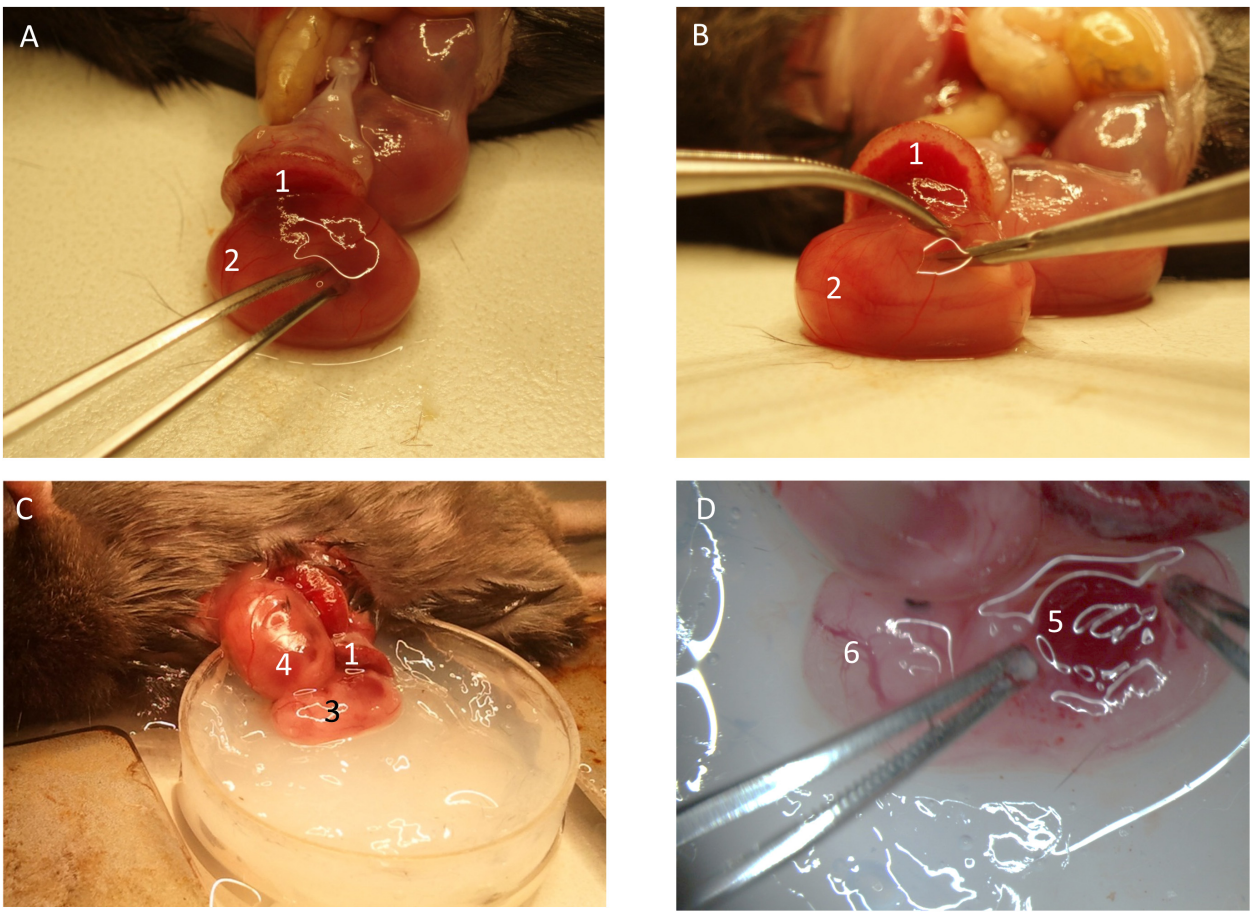

FIGURE 3 | Preparation of fetal liver. **(A)** The yolk-sac is carefully opened. **(B)** The fetus is removed from the yolk-sac and **(C)** placed into the imaging-dish. **(D)** The liver region is prepared for imaging. (1) Placenta. (2) Fetus inside yolk-sac being mobilized. (3) Fetus without yolk-sac. (4) Fetus within yolk-sac. (5) Fetal liver. (6) Cranial region of fetus.

depending on objective used for imaging) onto the top. Fill the ring with superfusion buffer for imaging of the cranial-window. Proceed to imaging.

Blood Sampling for Flow Cytometry and Systemic Blood Cell Counts

Acquisition for systemic fetal blood cell counts requires exact volumes as the cell amount can be fairly low.

To collect fetal blood the following procedure can be applied: Completely exteriorize the fetus from the yolk-sac, dry the fetus and remove any amniotic fluid with soft cotton sticks, perform a lateral neck incision, and discard the first small droplet of blood. Then place a 5 μl collecting glass capillary onto the incision site, where the blood vessels are clearly visible. Observe blood collection through a stereomicroscope to ensure no surrounding tissue leakage is collected into the capillary. Transfer the collected sample into citrate solution (45 μl 0.11 M sodium citrate solution, pH 6.5). Prepare the sample by adding appropriate antibodies directed against the required cell subpopulation. Add microbeads of known quantity and volume for later volume determination. Transfer samples to the flow cytometer for analysis.

If functional assays with fetal blood cells are planned and higher blood volumes are necessary, the following procedure can be used: Remove the yolk-sac and completely exteriorize the fetus and wash fetus and placenta quickly once in PBS. Dry the fetus and place it into a large petri dish filled with modified Tyrodes-HEPES-heparin-buffer. Make sure to leave the placenta outside of the petri dish. Dissect the umbilical cord and cut the fetal head with sharp scissors. Leave fetuses to bleed for approx. 10 min. Remove the fetus from the petri dish and collect the suspended blood. Washing, adding of antibodies and flow cytometry analysis can then be performed.

DISCUSSION/LIMITATIONS

The described preparation and imaging techniques allow several different applications. Yolk-sac analysis and microinjection of fluorescent substances enable examination of vessel- and blood cell properties. 3D-image reconstruction will show fluorescently

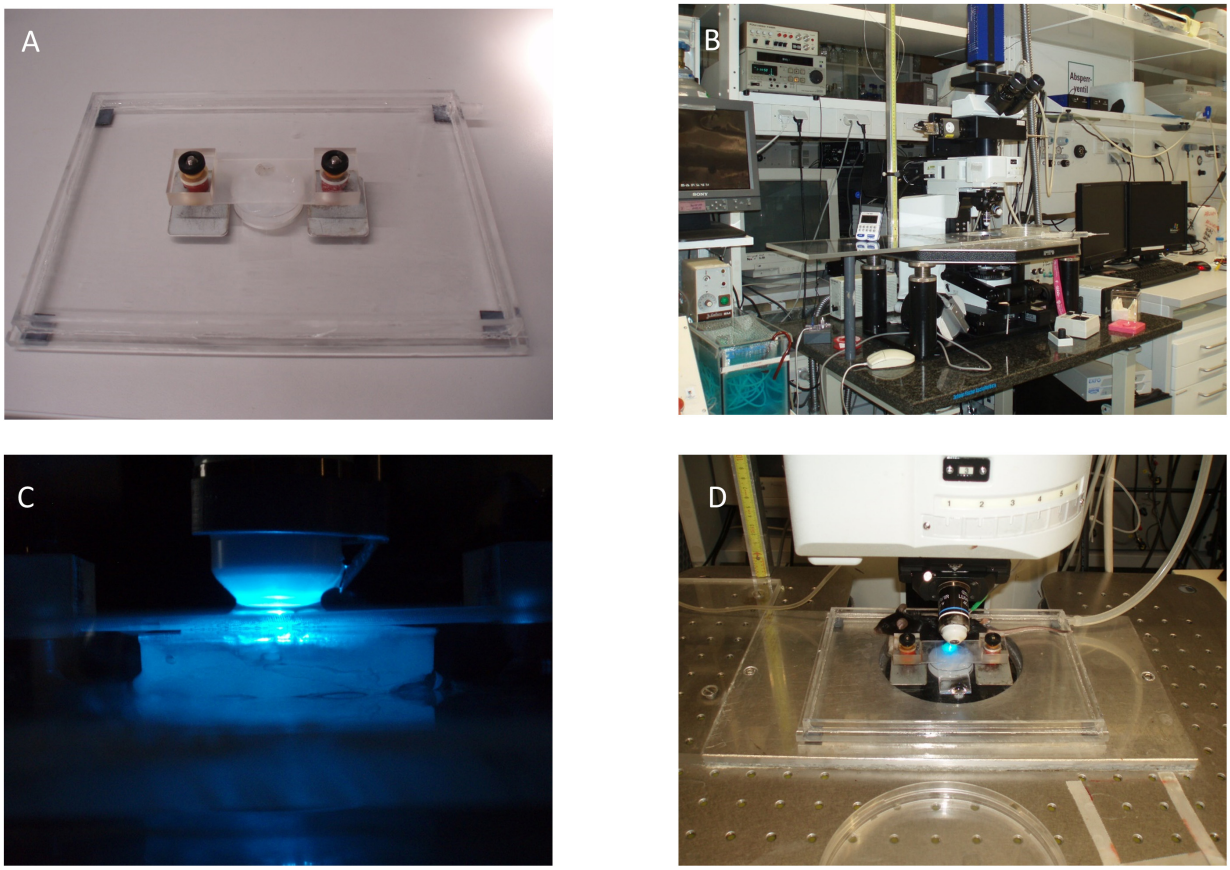

FIGURE 4 | Exemplary fixation and microscope setup. **(A)** Microscope stage with magnetic spring-counter-weighed holding device. **(B)** *In vivo* microscopy setup including water bath and roller pump (lower left of the image). **(C)** Epifluorescence setup with superfusion-buffer needle attached to the objective. **(D)** Placement of the fetus and mother animal for imaging.

labeled vessels following microinjection of plasma markers in both the yolk-sac layer and the deeper layers of the fetal body. Thrombus induction with phototoxic dyes results in a negative contrast image, in which the forming thrombus can be noted as a reduction in fluorescence intensity compared to the plasma marker FITC dextran. A stable image with only slight movement at young gestational ages and more intense motion at older gestational stages, is expected. In the setting of thrombus formation, platelet adherence followed by complete vessel occlusion can be observed within 30 min to 1 h in only a reduced number of animals, depending on fluorescent dye concentration, excitation light source and gestational age of the fetus. Leukocyte observation will show slight fluorescence of the surrounding vessel wall with strong fluorescent leukocytes within the blood which show a reduced recruitment phenotype in young gestational ages. Additionally, multiphoton-microscopy can be used, to generate SHG and THG (second- and third-harmonic-generation)-signals. Most commonly, a simple 2-D fluorescence image acquisition can be used, to display blood cells circulating in the microvasculature of the fetal yolk-sac.

Our model holds great potential for *in vivo* imaging of developmentally regulated processes. Nonetheless, only a restricted range of developmental stages can be selected for yolk-sac experiments, as insufficient size and the onset of circulation at young stages and yolk-sac involution processes at older stages of fetal development limit the practicability of such preparations. In accordance with this, our model is most suitable for *in vivo* experiments between developmental stages E13 and E18. Yet, with further manual skills and practice, also younger animals can be used (E9.5 onward). For older fetuses (E18 and E19), opening of the yolk-sac in the required region will facilitate vessel imaging also at this stage of development. In particular, a small incision in the cranial temporal region will allow access to the fetus for cerebral imaging purposes. Fetuses below the age of E13 are difficult to prepare due to the watery structure and lacking stability of the organism. Therefore, exteriorization of the fetus at this stage is accompanied by high fetal mortality.

As the yolk-sac is exteriorized and a counter-weighed fixation-device is used to stabilize the imaging setup, the experimenter must be aware of the possible influence of these manipulations on basic physiologic processes (**Figure 4**). Additional pitfalls include usage of large beads at high concentrations to study blood flow velocity. This could result in blockage of circulatory routes. Modulations in the cardiovascular and hemodynamic parameters

of the mother animal will impact placenta perfusion and thus affect the fetus. Consequently, strict control of vital parameters and physiologic conditions not only for the fetus itself but also of the mother animal is needed throughout the experiment.

Using antibodies, labeling substances or fluorescent protein-expressing genetically modified animals (compare **Table 1**), this model has a wide range of applications. In this context, one must be aware of the difficulties of genetically engineered reporter mice as well as antibody labeling, as classical cell markers might be developmentally regulated and only appear late during fetal life or are temporally expressed in other cell types during fetal ontogeny. Examples include CD41 for platelets (Mikkola et al., 2003).

Ongoing research focusses on developmental aspects of leukocytes, platelets, megakaryocytes, macrophages, endothelial, and progenitor cells. Whereas general developmental aspects (platelet-hyporeactivity and leukocyte hyporeactivity) are of great interest for neonatologists and physiologists, more specific research questions will have to address the precise underlying mechanisms for each uncovered phenotype. Not only therapeutic options in the neonatal period depend on this, but knowledge with regard to aging and maturation could potentially be obtained and translated to the understanding of adult malignancies or modification of therapies. Even though this model holds great advancements for the scientific community, the performing researcher must be aware of inherent ethical conflicts. Ethical considerations with regard to the mentioned techniques must include not only general animal welfare regulations but should place special focus on the protection of unborn life, hindering unnecessary application of such invasive methodology without justifiable scientific and translatable purpose.

Summarizing, this model offers a powerful technique to study *in vivo* processes in the developing mouse fetus and advance our understanding of basic physiologic and disease-related processes during ontogeny.

DATA AVAILABILITY STATEMENT

The original contributions presented in the study are included in the article/**Supplementary Material**, further inquiries can be directed to the corresponding author/s.

ETHICS STATEMENT

The animal study was reviewed and approved by the responsible authorities at the Regierung von Oberbayern.

AUTHOR CONTRIBUTIONS

AM and MS developed the protocol, composed the manuscript, and performed experiments including image acquisition. Both authors contributed to the article and approved the submitted version.

FUNDING

This study was supported by the FöFoLe-scholarship-program of the Ludwig-Maximilians-University, Munich (AM and MS), the Lehre@LMU-student-research-grant (AM), the Collaborative Research Grant CRC914, projects B01, Z3 (MS), and CRC914 IRTG (AM and MS).

ACKNOWLEDGMENTS

We thank all scientists who have greatly supported us to develop this exciting intravital microscopy fetal mouse model including Elizabeth Quackenbush, Ulrich von Andrian, David Frommhold, and Friedemann Kiefer.

SUPPLEMENTARY MATERIAL

The Supplementary Material for this article can be found online at: https://www.frontiersin.org/articles/10.3389/fcell.2020.632297/full#supplementary-material

Supplementary Figure 1 | Measurements of imaging stage.

Supplementary Figure 2 | Measurements of holding device.

Supplementary Figure 3 | Measurements of incised petri dish.

Supplementary Figure 4 | Exemplary imaging setup.

Supplementary Movie 1 | Preparation and microinjection of fetal yolk-sac vessels.

Supplementary Movie 2 | Conventional epifluorescence recording of leukocyte rolling (green) and recruitment in the yolk-sac of a *Lyz2*-GFP positive fetus. Autofluorescence of tissue allows for identification of blood vessel lumen.

Supplementary Movie 3 | MPLSM recording of a *Lyz2*-GFP positive fetus (green) injected with TRITC-dextrane (red-gray) and an Alexa649-coupled non-blocking Gplb antibody (blue).

REFERENCES

Ang, E. S. Jr., Haydar, T. F., Gluncic, V., and Rakic, P. (2003). Four-dimensional migratory coordinates of GABAergic interneurons in the developing mouse cortex. *J. Neurosci.* 23, 5805–5815. doi: 10.1523/jneurosci.23-13-05805.2003

Boisset, J. C., Andrieu-Soler, C., van Cappellen, W. A., Clapes, T., and Robin, C. (2011). Ex vivo time-lapse confocal imaging of the mouse embryo aorta. *Nat. Protoc.* 6, 1792–1805. doi: 10.1038/nprot.2011.401

Calaminus, S. D., Guitart, A. V., Sinclair, A., Schachtner, H., Watson, S. P., Holyoake, T. L., et al. (2012). Lineage tracing of Pf4-Cre marks hematopoietic stem cells and their progeny. *PLoS One* 7:e51361. doi: 10.1371/journal.pone.0051361

Callaghan, W. M., MacDorman, M. F., Rasmussen, S. A., Qin, C., and Lackritz, E. M. (2006). The contribution of preterm birth to infant mortality rates in the United States. *Pediatrics* 118, 1566–1573. doi: 10.1542/peds.2006-0860

Cappenberg, A., Margraf, A., Thomas, K., Bardel, B., McCreedy, D. A., Van Marck, V., et al. (2019). L-selectin shedding affects bacterial clearance in the lung: a new

regulatory pathway for integrin outside-in signaling. *Blood* 134, 1445–1457. doi: 10.1182/blood.2019000685

Christiansen, G. E., and Bacon, R. L. (1961). Direct observations of developing microcirculatory patterns in the posterior limb buds of fetal mice. *Angiology* 12, 517–524. doi: 10.1177/000331976101201014

Cunin, P., Lee, P. Y., Kim, E., Schmider, A. B., Cloutier, N., Pare, A., et al. (2019). Differential attenuation of beta2 integrin-dependent and -independent neutrophil migration by Ly6G ligation. *Blood Adv.* 3, 256–267. doi: 10.1182/bloodadvances.2018026732

Dhenain, M., Ruffins, S. W., and Jacobs, R. E. (2001). Three-dimensional digital mouse atlas using high-resolution MRI. *Dev. Biol.* 232, 458–470. doi: 10.1006/dbio.2001.0189

Dietzel, S., Pircher, J., Nekolla, A. K., Gull, M., Brandli, A. W., Pohl, U., et al. (2014). Label-free determination of hemodynamic parameters in the microcirculaton with third harmonic generation microscopy. *PLoS One* 9:e99615. doi: 10.1371/journal.pone.0099615

Echtler, K., Stark, K., Lorenz, M., Kerstan, S., Walch, A., Jennen, L., et al. (2010). Platelets contribute to postnatal occlusion of the ductus arteriosus. *Nat. Med.* 16, 75–82. doi: 10.1038/nm.2060

Faust, N., Varas, F., Kelly, L. M., Heck, S., and Graf, T. (2000). Insertion of enhanced green fluorescent protein into the lysozyme gene creates mice with green fluorescent granulocytes and macrophages. *Blood* 96, 719–726. doi: 10.1182/blood.v96.2.719.014k29_719_726

Ferkowicz, M. J., Starr, M., Xie, X., Li, W., Johnson, S. A., Shelley, W. C., et al. (2003). CD41 expression defines the onset of primitive and definitive hematopoiesis in the murine embryo. *Development* 130, 4393–4403. doi: 10.1242/dev.00632

Garcia, M. D., Udan, R. S., Hadjantonakis, A. K., and Dickinson, M. E. (2011). Live imaging of mouse embryos. *Cold Spring Harb. Protoc.* 2011:pdb.top104. doi: 10.1101/pdb.top104

Hasenberg, A., Hasenberg, M., Mann, L., Neumann, F., Borkenstein, L., Stecher, M., et al. (2015). Catchup: a mouse model for imaging-based tracking and modulation of neutrophil granulocytes. *Nat. Methods* 12, 445–452. doi: 10.1038/nmeth.3322

Hattori, Y., Naito, Y., Tsugawa, Y., Nonaka, S., Wake, H., Nagasawa, T., et al. (2020). Transient microglial absence assists postmigratory cortical neurons in proper differentiation. *Nat. Commun.* 11:1631.

Honkura, N., Richards, M., Lavina, B., Sainz-Jaspeado, M., Betsholtz, C., and Claesson-Welsh, L. (2018). Intravital imaging-based analysis tools for vessel identification and assessment of concurrent dynamic vascular events. *Nat. Commun.* 9:2746.

Kamocka, M. M., Mu, J., Liu, X., Chen, N., Zollman, A., Sturonas-Brown, B., et al. (2010). Two-photon intravital imaging of thrombus development. *J. Biomed. Opt.* 15:016020. doi: 10.1117/1.3322676

Kaufmann, M. H. (2005). *The Atlas of Mouse Development*. Cambridge, MA: Academic Press.

Klitzman, B., and Duling, B. R. (1979). Microvascular hematocrit and red cell flow in resting and contracting striated muscle. *Am. J. Physiol.* 237, H481–H490.

Koike, Y., Tanaka, K., Okugawa, Y., Morimoto, Y., Toiyama, Y., Uchida, K., et al. (2011). In vivo real-time two-photon microscopic imaging of platelet aggregation induced by selective laser irradiation to the endothelium created in the beta-actin-green fluorescent protein transgenic mice. *J. Thromb. Thrombolysis* 32, 138–145. doi: 10.1007/s11239-011-0600-y

Laufer, J., Norris, F., Cleary, J., Zhang, E., Treeby, B., Cox, B., et al. (2012). In vivo photoacoustic imaging of mouse embryos. *J. Biomed. Opt.* 17:061220.

Lee, S., Kang, B. M., Kim, J. H., Min, J., Kim, H. S., Ryu, H., et al. (2018). Real-time in vivo two-photon imaging study reveals decreased cerebro-vascular volume and increased blood-brain barrier permeability in chronically stressed mice. *Sci. Rep.* 8:13064.

Lehr, H. A., Leunig, M., Menger, M. D., Nolte, D., and Messmer, K. (1993). Dorsal skinfold chamber technique for intravital microscopy in nude mice. *Am. J. Pathol.* 143, 1055–1062.

Li, W., Ferkowicz, M. J., Johnson, S. A., Shelley, W. C., and Yoder, M. C. (2005). Endothelial cells in the early murine yolk sac give rise to CD41-expressing hematopoietic cells. *Stem Cells Dev.* 14, 44–54. doi: 10.1089/scd.2005.14.44

Ma, X., de Bruijn, M., Robin, C., Peeters, M., Kong, A. S. J., de Wit, T., et al. (2002a). Expression of the Ly-6A (Sca-1) lacZ transgene in mouse haematopoietic stem cells and embryos. *Br. J. Haematol.* 116, 401–408. doi: 10.1046/j.1365-2141.2002.03250.x

Ma, X., Robin, C., Ottersbach, K., and Dzierzak, E. (2002b). The Ly-6A (Sca-1) GFP transgene is expressed in all adult mouse hematopoietic stem cells. *Stem Cells* 20, 514–521. doi: 10.1634/stemcells.20-6-514

Margraf, A., Nussbaum, C., Rohwedder, I., Klapproth, S., Kurz, A. R. M., Florian, A., et al. (2017). Maturation of platelet function during murine fetal development in vivo. *Arterioscler Thromb Vasc. Biol.* 37, 1076–1086. doi: 10.1161/atvbaha.116.308464

Margraf, Andreas (2018). Untersuchung der ontogenetischen Regulation der Thrombozytenfunktion im Mausfetus in-vivo und in-vitro. Dissertation, LMU München: Medizinische Fakultät. doi: 10.5282/edoc.23178

Margraf, A., Nussbaum, C., and Sperandio, M. (2019). Ontogeny of platelet function. *Blood Adv.* 3, 692–703. doi: 10.1182/bloodadvances.2018024372

Mikkola, H. K., Fujiwara, Y., Schlaeger, T. M., Traver, D., and Orkin, S. H. (2003). Expression of CD41 marks the initiation of definitive hematopoiesis in the mouse embryo. *Blood* 101, 508–516. doi: 10.1182/blood-2002-06-1699

Moretti, F. A., Klapproth, S., Ruppert, R., Margraf, A., Weber, J., Pick, R., et al. (2018). Differential requirement of kindlin-3 for T cell progenitor homing to the non-vascularized and vascularized thymus. *eLife* 6:7.

Nishimura, N., Schaffer, C. B., Friedman, B., Tsai, P. S., Lyden, P. D., and Kleinfeld, D. (2006). Targeted insult to subsurface cortical blood vessels using ultrashort laser pulses: three models of stroke. *Nat. Methods* 3, 99–108. doi: 10.1038/nmeth844

Payne, S., De Val, S., and Neal, A. (2018). Endothelial-Specific Cre Mouse Models. *Arterioscler Thromb Vasc. Biol.* 38, 2550–2561. doi: 10.1161/atvbaha.118.309669

Pircher, J., Merkle, M., Wornle, M., Ribeiro, A., Czermak, T., Stampnik, Y., et al. (2012). Prothrombotic effects of tumor necrosis factor alpha in vivo are amplified by the absence of TNF-alpha receptor subtype 1 and require TNF-alpha receptor subtype 2. *Arthritis Res. Ther.* 14:R225.

Russel, E. S., Thompson, M. W., and McFarland, E. (1968). Analysis of effects of W and f genic substitutions on fetal mouse hematology. *Genetics* 58, 259–270.

Speier, S., Nyqvist, D., Kohler, M., Caicedo, A., Leibiger, I. B., and Berggren, P. O. (2008). Noninvasive high-resolution in vivo imaging of cell biology in the anterior chamber of the mouse eye. *Nat. Protoc.* 3, 1278–1286. doi: 10.1038/nprot.2008.118

Sperandio, M., Frommhold, D., Babushkina, I., Ellies, L. G., Olson, T. S., Smith, M. L., et al. (2006). Alpha 2,3-sialyltransferase-IV is essential for L-selectin ligand function in inflammation. *Eur. J. Immunol.* 36, 3207–3215. doi: 10.1002/eji.200636157

Sperandio, M., Quackenbush, E. J., Sushkova, N., Altstatter, J., Nussbaum, C., Schmid, S., et al. (2013). Ontogenetic regulation of leukocyte recruitment in mouse yolk sac vessels. *Blood* 121, e118–e128.

Sperandio, M., Thatte, A., Foy, D., Ellies, L. G., Marth, J. D., and Ley, K. (2001). Severe impairment of leukocyte rolling in venules of core 2 glucosaminyltransferase-deficient mice. *Blood* 97, 3812–3819. doi: 10.1182/blood.v97.12.3812

Stoll, B. J., Hansen, N. I., Bell, E. F., Walsh, M. C., Carlo, W. A., Shankaran, S., et al. (2015). Trends in Care practices. morbidity, and mortality of extremely preterm neonates, 1993-2012. *JAMA* 314, 1039–1051.

Stremmel, C., Schuchert, R., Wagner, F., Thaler, R., Weinberger, T., Pick, R., et al. (2018a). Author correction: yolk sac macrophage progenitors traffic to the embryo during defined stages of development. *Nat. Commun.* 9:3699.

Stremmel, C., Schuchert, R., Wagner, F., Thaler, R., Weinberger, T., Pick, R., et al. (2018b). Yolk sac macrophage progenitors traffic to the embryo during defined stages of development. *Nat. Commun.* 9:75.

Volmering, S., Block, H., Boras, M., Lowell, C. A., and Zarbock, A. (2016). The neutrophil btk signalosome regulates integrin activation during sterile inflammation. *Immunity* 44, 73–87. doi: 10.1016/j.immuni.2015.11.011

Wang, J. X., Bair, A. M., King, S. L., Shnayder, R., Huang, Y. F., Shieh, C. C., et al. (2012). Ly6G ligation blocks recruitment of neutrophils via a beta2-integrin-dependent mechanism. *Blood* 120, 1489–1498. doi: 10.1182/blood-2012-01-404046

Yanagida, M., Miyoshi, R., Toyokuni, R., Zhu, Y., and Murakami, F. (2012). Dynamics of the leading process, nucleus, and Golgi apparatus of migrating cortical interneurons in living mouse embryos. *Proc. Natl. Acad. Sci. U S A.* 109, 16737–16742. doi: 10.1073/pnas.1209166109

Yipp, B. G., and Kubes, P. (2013). Antibodies against neutrophil LY6G do not inhibit leukocyte recruitment in mice in vivo. *Blood* 121, 241–242. doi: 10.1182/blood-2012-09-454348

Yuryev, M., Pellegrino, C., Jokinen, V., Andriichuk, L., Khirug, S., Khiroug, L., et al. (2015). In vivo calcium imaging of evoked calcium waves in the embryonic cortex. *Front. Cell Neurosci.* 9:500. doi: 10.3389/fncel.2015.00500

Zhang, J., Varas, F., Stadtfeld, M., Heck, S., Faust, N., and Graf, T. (2007). CD41-YFP mice allow in vivo labeling of megakaryocytic cells and reveal a subset of platelets hyperreactive to thrombin stimulation. *Exp. Hematol.* 35, 490–499. doi: 10.1016/j.exphem.2006.11.011

Conflict of Interest: The authors declare that the research was conducted in the absence of any commercial or financial relationships that could be construed as a potential conflict of interest.

frontiers in Cell and Developmental Biology

ORIGINAL RESEARCH
published: 22 January 2021
doi: 10.3389/fcell.2020.605713

Soluble CD83 Regulates Dendritic Cell–T Cell Immunological Synapse Formation by Disrupting Rab1a-Mediated F-Actin Rearrangement

Wei Lin, Shuping Zhou, Meng Feng, Yong Yu, Qinghong Su and Xiaofan Li*

Institute of Basic Medicine, Shandong Provincial Hospital Affiliated to Shandong First Medical University, Shandong First Medical University & Shandong Academy of Medical Science, Jinan, China

OPEN ACCESS

Edited by:
Zhichao Fan,
UCONN Health, United States

Reviewed by:
Rongrong Liu,
Northwestern University, United States
Michael Loran Dustin,
University of Oxford, United Kingdom
Shuhong Qi,
Huazhong University of Science and Technology (HUST), China

***Correspondence:**
Wei Lin
linw1978@163.com;
weilin11@fudan.edu.cn

Specialty section:
This article was submitted to Cell Adhesion and Migration, a section of the journal Frontiers in Cell and Developmental Biology

Received: *13 September 2020*
Accepted: *11 December 2020*
Published: *22 January 2021*

Citation:
Lin W, Zhou S, Feng M, Yu Y, Su Q and Li X (2021) Soluble CD83 Regulates Dendritic Cell–T Cell Immunological Synapse Formation by Disrupting Rab1a-Mediated F-Actin Rearrangement. Front. Cell Dev. Biol. 8:605713. doi: 10.3389/fcell.2020.605713

Dendritic cell–T cell (DC-T) contacts play an important role in T cell activation, clone generation, and development. Regulating the cytoskeletal protein rearrangement of DCs can modulate DC-T contact and affect T cell activation. However, inhibitory factors on cytoskeletal regulation in DCs remain poorly known. We showed that a soluble form of CD83 (sCD83) inhibited T cell activation by decreasing DC-T contact and synapse formation between DC and T cells. This negative effect of sCD83 on DCs was mediated by disruption of F-actin rearrangements, leading to alter expression and localization of major histocompatibility complex class II (MHC-II) and immunological synapse formation between DC and T cells. Furthermore, sCD83 was found to decrease GTP-binding activity of Rab1a, which further decreased colocalization and expression of LRRK2 and F-actin rearrangements in DCs, leading to the loss of MHC-II at DC-T synapses and reduced DC-T synapse formation. Further, sCD83-treated DCs alleviated symptoms of experimental autoimmune uveitis in mice and decreased the number of T cells in the eyes and lymph nodes of these animals. Our findings demonstrate a novel signaling pathway of sCD83 on regulating DC-T contact, which may be harnessed to develop new immunosuppressive therapeutics for autoimmune disease.

Keywords: sCD83, DC-T contact, Rab1A, immunological synapse, autoimmune uveitis

INTRODUCTION

Dendritic cells (DCs) play a crucial regulatory role in autoimmune disease and regulate the immune response by governing T cell activation or development. Immunological synapses (ISs) formed between DCs and T cells (DC-T) support direct communication between cells and are a key factor for T cell clone generation and development (Dustin and Shaw, 1999; Grakoui et al., 1999; Davis and Dustin, 2004). IS of DC-T contacts is a multimolecular assembly of receptors and adhesion molecules that act as a platform for cell activation and cell–cell communication (Dustin and Shaw, 1999; Grakoui et al., 1999; Davis and Dustin, 2004), and it is formed by cytoskeletal proteins around one or more major histocompatibility complex class II–peptide–T cell receptor (MHC-II–peptide–TCR) cluster. Regulating the IS of DC-T would influence T cell activation directly. Cytoskeletal

rearrangement is one of the most important factors in altering DC-T contacts (Al-Alwan et al., 2001; Comrie et al., 2015). F-actin provides essential support for the platform on the DC side of the synapse (Al-Alwan et al., 2001) and could regulate DC-T contact and T cell activation (Lin et al., 2015; Chen et al., 2017). Furthermore, F-actin acts as a scaffold to sustain signaling pathway molecules and controls the spatial and temporal distribution of Ca^{2+} sources and sinks to influence the activation and maturation of DCs toward DC-T contact and T cell activation (Nolz et al., 2006; Quintana et al., 2006, 2007). Therefore, inhibition of the cytoskeleton of DCs would influence DC-T synapse formation and the aggregation of immune-stimulating molecules between DC–T cells, which as a result would further decrease DC-T contact and T cell activation. Superfamily small GTPases (e.g., Rho and Ras) are believed to control cytoskeletal function through the regulation of effector kinases. Recently, Rab1a is found to control the actin cytoskeleton by regulating Roco2 kinase activity (Kicka et al., 2011), although its major function is related to vesicle trafficking and autophagy (Ali et al., 2004; Webster et al., 2016). It indicates that Rab1a may participate to the DC-T IS formation. However, the regulatory mechanism of DC-T contact formation is still not very clear.

Soluble CD83 (sCD83) is an immunosuppressive mediator involved in the pathogenesis of immune-related diseases in humans such as multiple sclerosis and animal models of experimental autoimmune encephalomyelitis (Pashine et al., 2008), experimental autoimmune uveitis (EAU) (Lin et al., 2018), systemic lupus erythematosus (Starke et al., 2013), and transplant rejection (Xu et al., 2007; Lan et al., 2010). These studies investigated the effects of sCD83 inhibition on DC regulation by activation of interleukin 10 (IL-10) and indoleamine 2,3-dioxygenase, which further suppresses T cell activation (Lan et al., 2010; Lin et al., 2018). In the same study, we also showed that sCD83 inhibits calcium release in DCs to suppress T cell activation (Lin et al., 2018). A different study reported that sCD83 completely changes the cytoskeleton of mature DCs, altering cells to become rounded and having either short or truncated cytoplasmic veils or no veils at all (Kotzor et al., 2004). They also found that sCD83-treated cells were completely inhibited in their ability to stimulate T cells (Kotzor et al., 2004). Nevertheless, the mechanism underlying the effect of sCD83 on DCs remains unclear, and how sCD83-mediated regulation of the DC cytoskeleton inhibits DC-T contact and T cell activation is still unknown.

Autoimmune uveitis is a group of organ-specific immune disorders characterized by an inflammatory process, which includes increased $CD4^+$ T cells infiltration in the eyes (Caspi et al., 1986; Muhaya et al., 1999; Ilhan et al., 2008), and is usually activated by DCs. Abnormal DC activation is a major cause of the pathogenesis of uveitis (Xu et al., 2007; Heuss et al., 2012; Constantino-Jonapa et al., 2020). Thus, regulating DC activation may reverse the inflammatory state of this disease by influencing either DC-T contact or T cell activation. Exploring the regulatory factors on DC function and DC-T contact will help identify new therapeutic targets for this disease.

In the current study, we identify a regulatory pathway of sCD83 on DC-T contact formation. We demonstrate that sCD83 inhibits IS formation of DC-Ts by disrupting the distribution of F-actin and MHC-II at DC-T contacts, and we find that this inhibitory effect of sCD83 on DCs is via suppression of Rab1a, which controls the LRRK2 and F-actin colocalization. Furthermore, sCD83-treated DCs alleviates the symptoms of EAU and decreases the number of T cells in the eyes and lymph nodes of mice with EAU. Our findings provide a possible mechanism of sCD83 on DC-T contact by Rab1a-mediated F-actin and MHC-II localization and may provide a new therapeutic approach for the treatment of EAU.

MATERIALS AND METHODS

Animals and EAU Model

Pathogen-free female C57BL/6 (6–8-week-old) mice were purchased from Beijing Vital River Laboratory Animal Technology Co., Ltd. (Beijing, China). These mice were maintained in specific pathogen-free conditions according to the guide for the care and use of laboratory animals of Shandong First Medical University & Shandong Academy of Medical Sciences (Jinan, China). The experiments were approved by the ethics committee of Shandong First Medical University & Shandong Academy of Medical Sciences (Jinan, China). The induction of EAU in C57BL/6 mice has been described in previous reports (Thurau et al., 1997; Beibei Wang et al., 2017; Lin et al., 2017). Briefly, C57BL/6 mice were subcutaneously immunized with 350 μg of human interphotoreceptor retinoid-binding protein $peptide_{1-20}$ ($IRBP_{1-20,}$ China Peptides Co., Ltd., Suzhou, Jiangsu, China) that was emulsified in the complete Freund's adjuvant (Sigma–Aldrich Company, MA, USA). Concurrently, a single dose of 500 ng of pertussis toxin (PTX, Enzo Life Sciences, Farmingdale, NY, USA) was injected intraperitoneally. After immunization for 21 days, the mice were examined by histopathological examination or immunofluorescence examination, and the degree of disease was evaluated by a scoring system according to previously described (Thurau et al., 1997; Harimoto et al., 2014).

sCD83 Construction and Usage

Mouse sCD83 protein consists of the extracellular domain of the membrane-bound CD83 (mCD83) molecule (22–133 aa), which was purified from the supernatant of transiently transfected eukaryotic cells (Roman-Sosa et al., 2016). Purified sCD83 was detected by sodium dodecyl sulfate–polyacrylamide gel electrophoresis (SDS-PAGE) and Western blot (**Supplementary Figure 1**). For animal treatment, sCD83 (10 μg/mouse) was used on day 8 after EAU immunization and was administered intravenously every other day. The eyes were harvested on 21 days for immunofluorescence staining or hematoxylin-eosin stain. The eyes and lymph nodes were harvested and prepared for flow cytometry. For cell stimulation, sCD83 (100 ng/mL) was added to the culture of isolated wild-type (WT) DC or DC2.4 cell line for pretreatment 24 h, and then

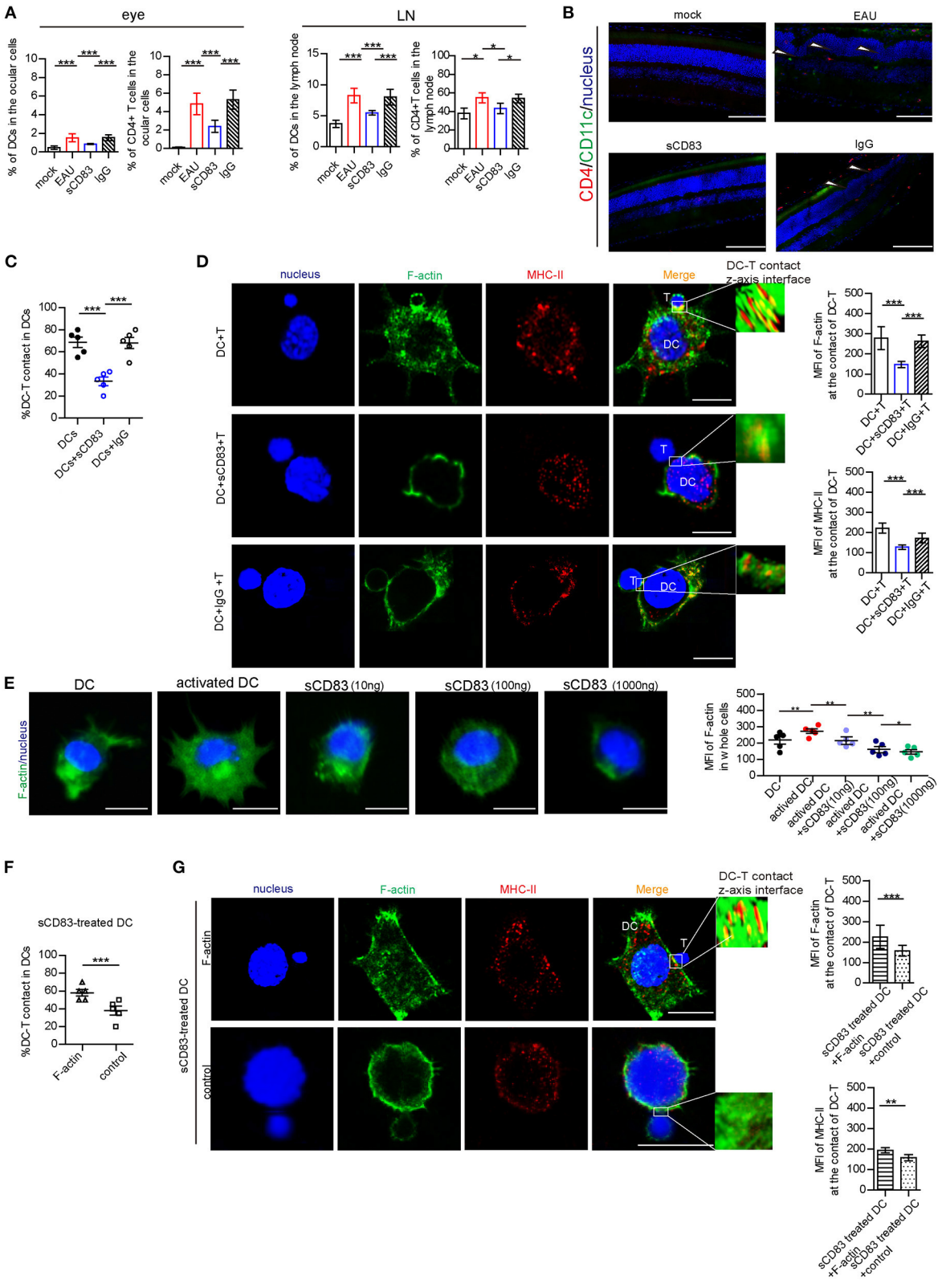

FIGURE 1 | The effect of sCD83 on T cells and DCs *in vivo* and in *in vitro* experiment. **(A)** sCD83 treatment decreased the increased percentage of $CD11c^+$ $MHC\text{-}II^+$ DCs and $CD4^+$ T cells in eyes and lymph nodes of EAU mice. These data are from three separate experiments; five mice were used for every group and shown as mean ± SEM. $^*p < 0.05$, $^{***}p < 0.001$. **(B)** The retinal lesions (white arrow showed multiple protrusions were found in the outer nuclear layer), $CD4^+$ T cells (red). and

(Continued)

FIGURE 1 | $CD11c^+$DC lymphocyte subpopulation (green) in the eyes of mock, EAU, and sCD83-treated EAU mice were detected by immunofluorescence. Nucleus is blue. Bar = 100 μm. **(C)** sCD83 treatment decreases the percentage of DC2.4-T contacts. **(D)** sCD83 treatment also decreases the IS formation of DC2.4-T contacts that require both F-actin and MHC-II (left panel). Mean fluorescence value of F-actin and MHC-II at DC-T contacts (right panel). Five cell–cell contacts/group were analyzed by confocal and Imaris Software. DC-T contact was reconstructed and analyzed by Imaris Software. The middle section or the largest section of the *z*-axis was selected and displayed in the right panel. Total fluorescence value of MHC class II or F-actin was quantified after 3D image reconstructed. **(E)** The distribution (left panel) and the mean value of F-actin (right panel) in DC2.4, which was under different concentrations of sCD83 stimulation. Five cell–cell contacts/group were analyzed. **(F)** Overexpression of F-actin into sCD83-treated DCs increased the percentage of DC2.4-T contact in DCs. **(G)** The distribution (left panel) and the mean value of F-actin and MHC-II (right panel) in F-actin overexpressed sCD83-treated DCs compared to empty plasmid overexpressed sCD83-treated DCs (control). Five cell–cell contacts/group were analyzed. Data of **(C–F)** are shown as mean ± SEM. $^*p < 0.05$, $^{**}p < 0.01$, $^{***}p < 0.001$. Bar = 5 μm.

the cells were collected for detection. Human immunoglobulin G (IgG) protein was used as a negative control.

Plasmid Construction

$Rab1a^{Q70L}$ (a GTP-restricted mutant, activated form) was generated by polymerase chain reaction site-directed mutagenesis and confirmed by sequencing. The pCAG-LifeAct-RFP plasmid was used for F-actin visualization in DCs according to the manufacturer's instructions (ibidi, Martinsried, Germany).

Non-targeting control shRNA and targeting shRNA were constructed by JiMan Sigma (Shanghai, China). The sequence of effective Rab1a shRNA is 5′-GCACAATTGGTGTGGATTT-3′, and the sequence of MD-2 shRNA is 5′-AGTTATTGTGAT CACTTGA-3′, respectively. They were constructed into PGMLV-SC5, separately. The cells were then transfected with 5–20 nM PGMLV-SC5-Rab1a shRNA or non-targeting control shRNA (NC) as per the protocol provided by the manufacturer. The pCAG-LifeAct-RFP plasmid was used for F-actin visualization in DCs according to the manufacturer's instructions (ibidi, Martinsried, Germany). pCAG-RFP empty plasmid was used as control.

Cells Culture and Isolation

DC2.4 cell line (a kind gift from Professor Yiwei Chu, Fudan University, Shanghai, China) was cultured in RPMI-1640 containing 10% fetal bovine serum and double antibodies. These cells were stimulated with $IRBP_{1-20}$ (10 ng/mL) and PTX (10 ng/mL) overnight.

WT DCs or $CD4^+$ T cells were obtained from the spleen and selected using a CD4-negative and CD11c-positive selection kit (Miltenyi Biotec, Bergisch Gladbach, Germany), respectively. Splenocytes were obtained, and red blood cell lysis buffer (Solarbio Science & Technology Co., Ltd., Beijing, China) was used to obtain the single-cell suspension as previously reported (Shao et al., 2003; Lin et al., 2017). And then, $CD4^+$ T cells and DCs were isolated by kits according to manuscript protocol.

DC-T Contact Detected by Immunofluorescence

Wild-type DCs or DC2.4 cell lines were incubated with $IRBP_{1-20}$ (10 ng/mL) and PTX (5 ng/mL) overnight to be activated (Lin et al., 2018). sCD83 (10 ng/mL) were added to stimulate overnight. $CD4^+$ T cells were purified from the spleen of $IRBP_{1-20}$-immunized B6 mice and were stimulated with $IRBP_{1-20}$ (10 μg/mL) in the presence of 1×10^7 irradiated syngeneic spleen cells as antigen presenting cells (APCs) in the presence of IL-2 (10 ng/mL), and then antigen-specific $CD4^+$ T cells were obtained by $CD4^+$ magnetic beads (Miltenyi Biotec, Bergisch Gladbach, Germany). $CD4^+$ T cells were cocultured with antigen-pulsed mature DCs (T cell:DC ratio = 10:1) overnight. And then, the cells were fixed in phosphate-buffered saline (PBS)/4% paraformaldehyde for 10 min, followed by incubation with PBS/0.1 M of glycine for 3 min. Cells were permeabilized with 0.1% Triton X-100 for 20 min and then blocked with 2% bovine serum albumin buffer for 20 min. Next, the cells were stained with a 1:500 dilution of TRITC phalloidin (Molecular Probes, Carlsbad, CA, USA) as previously reported (Quintana et al., 2009; Lin et al., 2015), or cells were stained with anti-Rab1a (Abcam, Cambridge, MA, USA), anti-MHC-II (R&D Systems, Inc., Minneapolis, MN, Canada), and anti-LRRK2 (Abcam, Cambridge, MA, USA) antibody (1:1,000 dilution) for 60 min. After washing three times, corresponding fluorescent antibodies were added and detected by a confocal microscope.

Confocal Imaging

Images of the cells were taken with a confocal microscope (LMS 780, Zeiss, Germany) equipped with an APO oil immersion objective lens (63 ×, NA = 1.40) (Lin et al., 2015). The images were analyzed with the Imaris Software (Bitplane AG, Zurich, Switzerland) and ImageJ (National Institutes of Health, Bethesda, MD, USA). DC-T contact was observed by *z*-axis scanning. Three-dimensional (3D) intercellular contacts were reconstructed and analyzed by Imaris Software and ImageJ. Total fluorescence value of MHC class II or F-actin was quantified after 3D image reconstructed. Colocalization of Rab1a and LRRK2, or Rab1a and MHC-II, in DCs were analyzed by ImageJ with colocalization index (Pearson correlation coefficient, Pearson's *r*).

Rab1a Activation Assay

Cells were lysed with ice-cold lysis buffer [50 mM Tris-HCl (pH 7.5), 2% Nonidet P-40, 10 mM $MgCl_2$, 300 mM NaCl, and protease inhibitor]. Collected lysates were incubated with GTP-agarose beads (Novus Biologicals, Co, USA) at 4°C for 2 h. And then, the beads were collected by centrifugation, and the binding of Rab1a was analyzed by Western blot with anti–Rab1a mAb.

Flow Cytometry

Aliquots of 1×10^6 cells were stained with different monoclonal antibodies according to standard protocols. The cells were analyzed on a FACSVerse cytometer (BD Biosciences, San Diego, CA, USA). Fluorescent antibodies of CD45 (clone 30-F-11), CD3ε (clone 145-2C11), CD4 (clone GK1.5), CD83 (clone Michel-19), CD11b (clone M1/70), ly6c(clone HK1.4), F4/80

(clone BM8), B220 (clone RA3-6B2), NK1.1 (clone PK136), MHC-II (clone M5/114.15.2), CD11c (clone N418), CD69 (clone H1.2F3), and Ki67 (clone B56) conjugated with the corresponding fluorescent dyes (eBioscience, San Diego, CA, USA) were used in the experiments.

Western Blot

DC2.4 cells or sCD83-treated DC2.4 cells were lysed with RIPA buffer (Beyotime Biotechnology, Shanghai, China). Identical quantities of protein were separated by 10% SDS-PAGE and transferred to polyvinylidene difluoride membranes. Subsequently, 5% non-fat dry milk in Tris-buffered saline 0.1% Tween 20 (TBS-T) was used to block non-specific binding sites for 1 h. After washing with TBS-T, membranes were incubated with primary antibodies against mouse Rab1a (Abcam, Cambridge, MA, USA), LRRK2 (Abcam, Cambridge, MA, USA), F-actin, MHC-II (R&D Systems, Inc., Minneapolis, MN, USA), and GAPDH (Cell Signaling Technology, Beverly, MA, USA) at 4°C for overnight. Membranes were then washed and incubated with secondary antibodies (goat-anti-rabbit IgG antibodies) conjugated to horseradish peroxidase (Beyotime Biotechnology, Shanghai, China) for 1 h. Finally, the membranes were developed using the Super Signal West Pico Chemiluminescent Substrate (Thermo Scientific, Rockford, IL, USA). Densitometric analyses were performed using the ImageJ software (National Institutes of Health, Bethesda, MD, USA).

Statistical Analysis

Data analysis was performed using GraphPad Prism 5 (GraphPad Software, San Diego, CA, USA). Two-tailed Student *t*-test or one-way analysis of variance was used as parametric tests. Mann–Whitney *U*-test or Kruskal-Wallis test were used as nonparametric tests. Data were represented as mean ± SEM. $p < 0.05$ (*), 0.01 (**), and 0.001 (***) were considered to be significant.

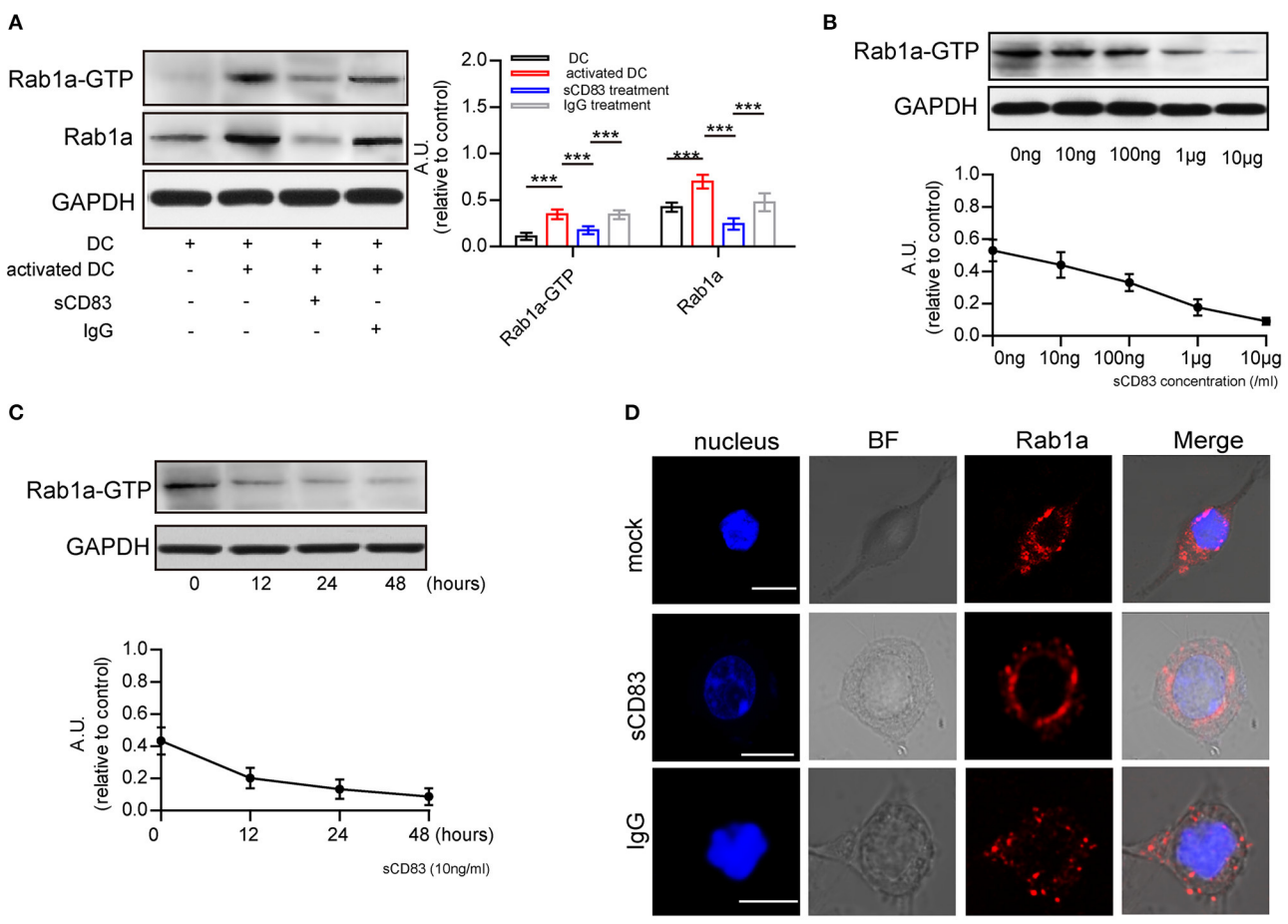

FIGURE 2 | sCD83 inhibits the expression of Rab1a-GTP and the distribution of Rab1a. **(A)** The expression of Rab1a and Rab1a-GTP in DC2.4, activated DC2.4 and sCD83-treated activated DC2.4. **(B)** With different concentrations of sCD83 treatment for 24 h, the expression of Rab1a-GTP in activated DC2.4 was analyzed by Western blot. **(C)** With 10 ng/mL sCD83 treatment for 6, 12, or 24 h, the expression of Rab1a-GTP in activated DCs was analyzed by Western blot. Data of **(A–C)** are from three separate experiments and shown as mean ± SEM. ***$p < 0.001$. **(D)** The distribution of Rab1a (red) in activated DC2.4 cells, sCD83-treated activated DC2.4 cells, and IgG-treated activated DC2.4 cells. Nucleus is blue. Bar = 5 μm.

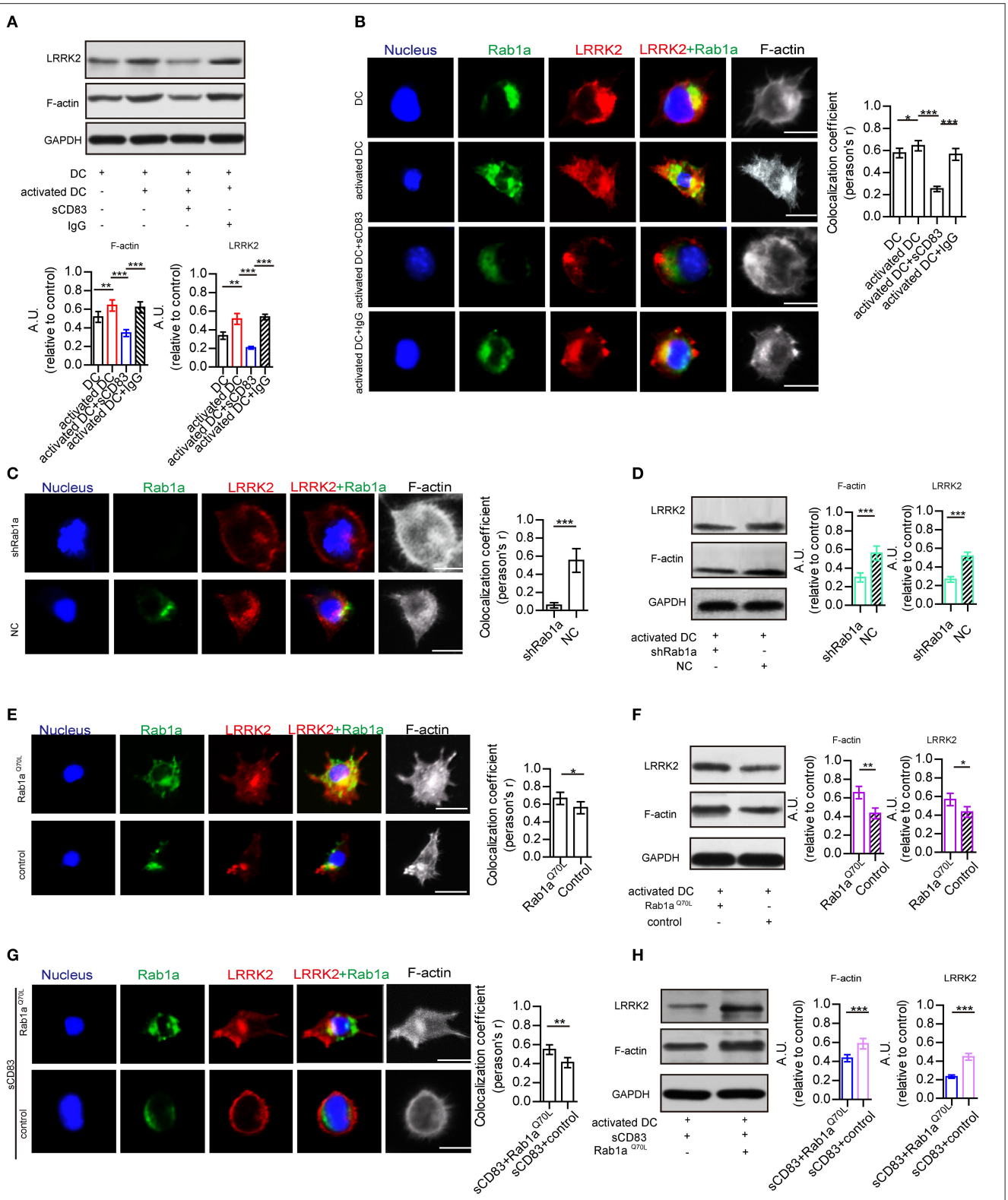

FIGURE 3 | Rab1a plays an important role in regulating the effect of sCD83 on the F-actin in DCs. **(A)** The expression of F-actin and LRRK2 in the DC2.4, activated DC2.4 cells, activated DCs with sCD83 treatment, or activated DCs with IgG treatment. **(B)** The localization of Rab1a (green), LRRK2 (red), and F-actin (white) in DC2.4 cells or activated DC2.4 cells, sCD83 treated-activated DCs, and IgG-treated activated DCs. Colocalization index (Pearson'*r*) was graphically represented (right panel). **(C)** With shRab1a or NC treatment, the localization of Rab1a (green), LRRK2 (red), and F-actin (white) in DC2.4 cells. Colocalization index (Pearson'*r*) was graphically represented (right panel). **(D)** The expression of F-actin and LRRK2 in activated DC2.4 cells with shRNA Rab1a (shRab1a) treatment, or activated DCs with

(Continued)

FIGURE 3 | NC treatment. **(E)** The localization of Rab1a (green), LRRK2 (red), and F-actin (white) in $Rab1a^{Q70L}$-treated DC2.4 cells, or empty plasmid-treated DC2.4 cells (control). Colocalization index (Pearson'*r*) was graphically represented (right panel). **(F)** The expression of F-actin and LRRK2 in activated DC2.4 cells with $Rab1a^{Q70L}$ treatment or empty plasmid treatment (control). **(G)** Overexpressed $Rab1a^{Q70L}$ (green) or empty plasmid (control) influence the distribution of F-actin (white) and LRRK2 (red) in DC2.4 cells. Colocalization index (Pearson'*r*) was graphically represented (right panel). **(H)** Overexpressed $Rab1a^{Q70L}$ promotes the expression of F-actin and LRRK2 in sCD83-treated DCs, but empty plasmid (control) could not. Nucleus is blue. Bar = 5 μm. Data of **(A,D,F,H)** were from three separate experiments, and data of **(B,C,E,G)** were form six cells/group and shown as mean ± SEM. $^{*}p < 0.05$, $^{**}p < 0.01$, $^{***}p < 0.001$.

RESULTS

sCD83 Decreases DC-T Synapse Formation by Reducing Assembly of F-Actin at Sites of DC-T Contact

As previously reported (Lin et al., 2018), sCD83 treatment decreases the symptoms in EAU. In our study, we found that sCD83 treatment decreased the increased percentage of $CD11c^{+}$ $MHC\text{-}II^{+}$ DCs and $CD4^{+}$ T cells in the eyes and lymph nodes of infected mice (**Figure 1A**). The retinal lesions of each group and T and DC lymphocyte subpopulation imaging are shown in **Figure 1B**. In the eyes of EAU, multifocal retinal fold (white arrows) and $CD4^{+}$ T cells (red) and DCs (green) infiltration were found (**Figure 1B**), and DC-T contacts were found in lymph nodes of EAU (**Supplementary Figure 2**). However, almost no retina damage and the less lymphocytes infiltration were found in the eyes of sCD83-treated EAU mice (**Figures 1A,B**). Based on *in vitro* experiments, sCD83-treated DCs formed fewer DC-T contacts than those without treatment (**Figure 1C**). With sCD83 treatment, the mean fluorescence value of F-actin and MHC-II at DC-T contacts decreased (**Figure 1D**), and F-actin lost to accumulate and around with MHC-II to form DC-T synapse (**Figure 1D**). F-actin and MHC-II were essentially diffused at the sCD83-treated DC-T contact (**Figure 1D**). As a result, sCD83 treatment disrupts IS formation that requires both F-actin and MHC-II. However, sCD83 treatment did not influence the activation of T cells and did not influence sCD83-treated T cell contact with DCs (**Supplementary Figure 3**).

Further, the mean fluorescence value of F-actin increased in activated DCs (**Figure 1E**). However, under different concentrations of sCD83 stimulation, we found that F-actin fluorescence in DCs gradually reduced with increased sCD83 concentration (**Figure 1E**). In addition, disrupting F-actin with cytochalasin D reduced DC-T contact and MHC-II accumulation at DC-T contacts (**Supplementary Figure 4**), whereas overexpression of F-actin in DCs promoted DC-T contact and MHC-II accumulation at DC-T contacts (**Supplementary Figure 4**). Overexpression of F-actin rescued the negative effect of sCD83 on DCs, causing increased DC-T contact, and F-actin and MHC-II accumulation at DC-T contacts (**Figures 1F,G**). Thus, sCD83 regulates DC-T synapse formation and MHC-II accumulation at DC-T contacts by controlling F-actin in DCs.

sCD83 Decreases Rab1a Expression in DCs

Next, we investigated the possible mechanism underlying sCD83-mediated regulation of F-actin at DC-T contacts. F-actin assembly is controlled by activated Rab1a (Kicka et al., 2011). As a small G protein, Rab1a is activated by binding with GTP. Using DCs incubated with Rab-GTP-agarose beads and an anti-Rab1a antibody to detect Rab1a binding, we found following PTX and IRBP stimulation a significant increase in the GTP-binding activity of Rab1a, as well as Rab1a in DCs (**Figure 2A**), Both of Rab1a and Rab1a-GTP decreased in response to sCD83 stimulation (**Figure 2A**). Moreover, we found that GTP-binding activity of Rab1a decreased following sCD83 administration at high concentrations (**Figure 2B**), as well as in response to the time of sCD83 action (**Figure 2C**). Thus, these findings indicate that sCD83 affects the amount of GTP-binding activity of Rab1a. Moreover, following sCD83 treatment, we found that the average fluorescence of Rab1a decreased and that localization was mainly around the nucleus (**Figure 2D**). Based on these findings, we conclude that sCD83 influences the expression and cellular localization of Rab1a in DCs.

sCD83 Disrupts LRRK2/F-Actin Distribution in DCs Through Rab1a

As Rab1a regulates localization of members of the LRRK2-related kinase family (Kicka et al., 2011), which controls the actin cytoskeleton of DCs, we hypothesized that sCD83 regulates DC morphology by affecting the expression and localization of F-actin and LRRK2 in DCs through Rab1a. First, we evaluated the expression and localization of Rab1a, F-actin, and LRRK2 in DCs with and without sCD83 treatment. Using PTX and IRBP stimulation, we found increased expression of F-actin and LRRK2 in activated DCs (**Figure 3A**). We also found that activated DCs were morphologically elongated in multiple directions, with F-actin distributed and supporting multiple directions, and Rab1a and LRRK2 were colocalized in these DCs (**Figure 3B**). Following sCD83 treatment, the expression of F-actin and LRRK2 decreased (**Figure 3A**), and Rab1a and LRRK2 were no longer colocalized so well (**Figure 3B**), and the distribution of F-actin was disrupted.

To further investigate the role of Rab1a in regulating the distribution of LRRK2 and F-actin in DCs, shRNA-Rab1a was used to interfere with Rab1a expression (**Supplementary Figure 5**). Following shRNA-Rab1a treatment, we found that DCs became morphologically round with short spikes (**Figure 3C**). The expression of F-actin and LRRK2 decreased in shRNA Rab1a-treated DCs (**Figure 3D**). In contrast, overexpression of an activated form of Rab1a ($Rab1a^{Q70L}$) resulted in morphological changes of DCs, which became elongated with multiple extensions (**Figure 3E**). Rab1a colocalized with LRRK2 in $Rab1a^{Q70L}$-treated DCs (**Figure 3E**), and LRRK2 and F-actin were

uniformly distributed in cells and supported extended spike formation (**Figure 3E**). Further, Rab1a^{Q70L} overexpression increased expression of F-actin and LRRK2 (**Figure 3F**). These findings indicate that activation of Rab1a correlates with the expression and localization of LRRK2 and F-actin in DCs.

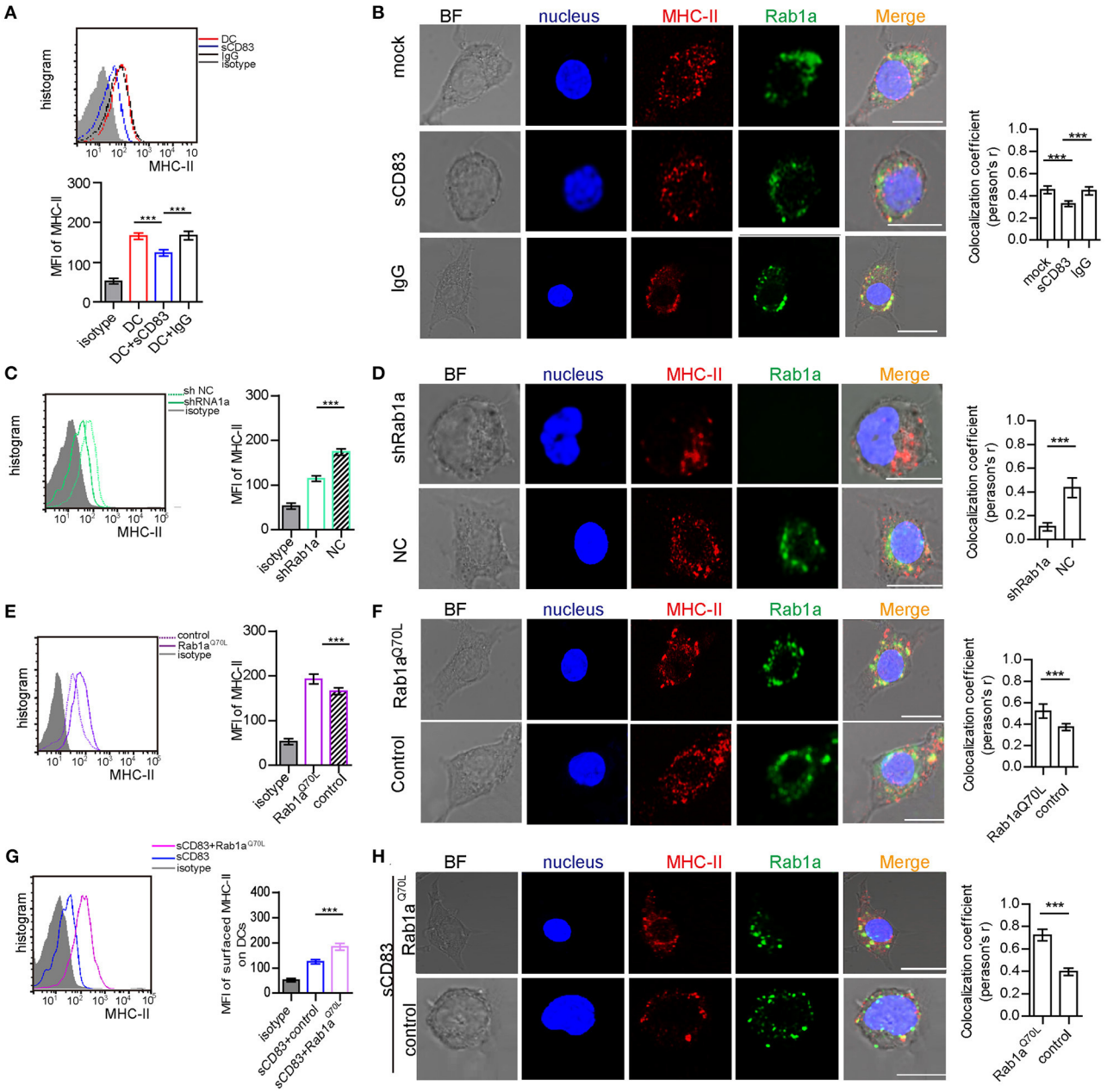

FIGURE 4 | Rab1a controls expression and localization of MHC-II on the surface of DCs. **(A)** The expression of MHC-II on the surface of activated DC2.4, sCD83-treated activated DC2.4, or IgG-treated activated DC2.4 cells. **(B)** The localization of MHC-II (red) and Rab1a (green) in activated DC2.4, sCD83-treated activated DC2.4, and IgG-treated activated DC2.4. Colocalization index (Pearson'*r*) was graphically represented (right panel). **(C)** The expression of MHC-II on the surface of shRNA Rab1a-treated activated DC2.4, compared to NC-treated activated DC2.4. **(D)** The localization of MHC-II (red) and Rab1a (green) in shRNA Rab1a-treated or NC-treated activated DC2.4. Colocalization index (Pearson'*r*) was graphically represented (right panel). **(E)** The expression of MHC-II on the surface of Rab1a^{Q70L} overexpressed activated DC2.4, compared to empty plasmid transfected activated DC2.4 (control). **(F)** The localization of MHC-II (red) and Rab1a (green) in Rab1a^{Q70L} overexpressed activated DC2.4 or empty plasmid transfected activated DC2.4. Colocalization index (Pearson'*r*) was graphically represented (right panel). **(G)** The expression of MHC-II on the surface of Rab1a^{Q70L} overexpressed sCD83-treated activated DC2.4, compared to empty plasmid transfected sCD83-treated activated DC2.4 (control). **(H)** The localization of MHC-II (red) and Rab1a (green) in Rab1a^{Q70L} overexpressed sCD83-treated DC2.4 or empty plasmid transfected sCD83-treated activated DC2.4 (control). Colocalization index (Pearson'*r*) was graphically represented (right panel). Bar = 5 μm. Data are from three separate experiments; six cells/group were used and shown as mean ± SEM. ***$p < 0.001$.

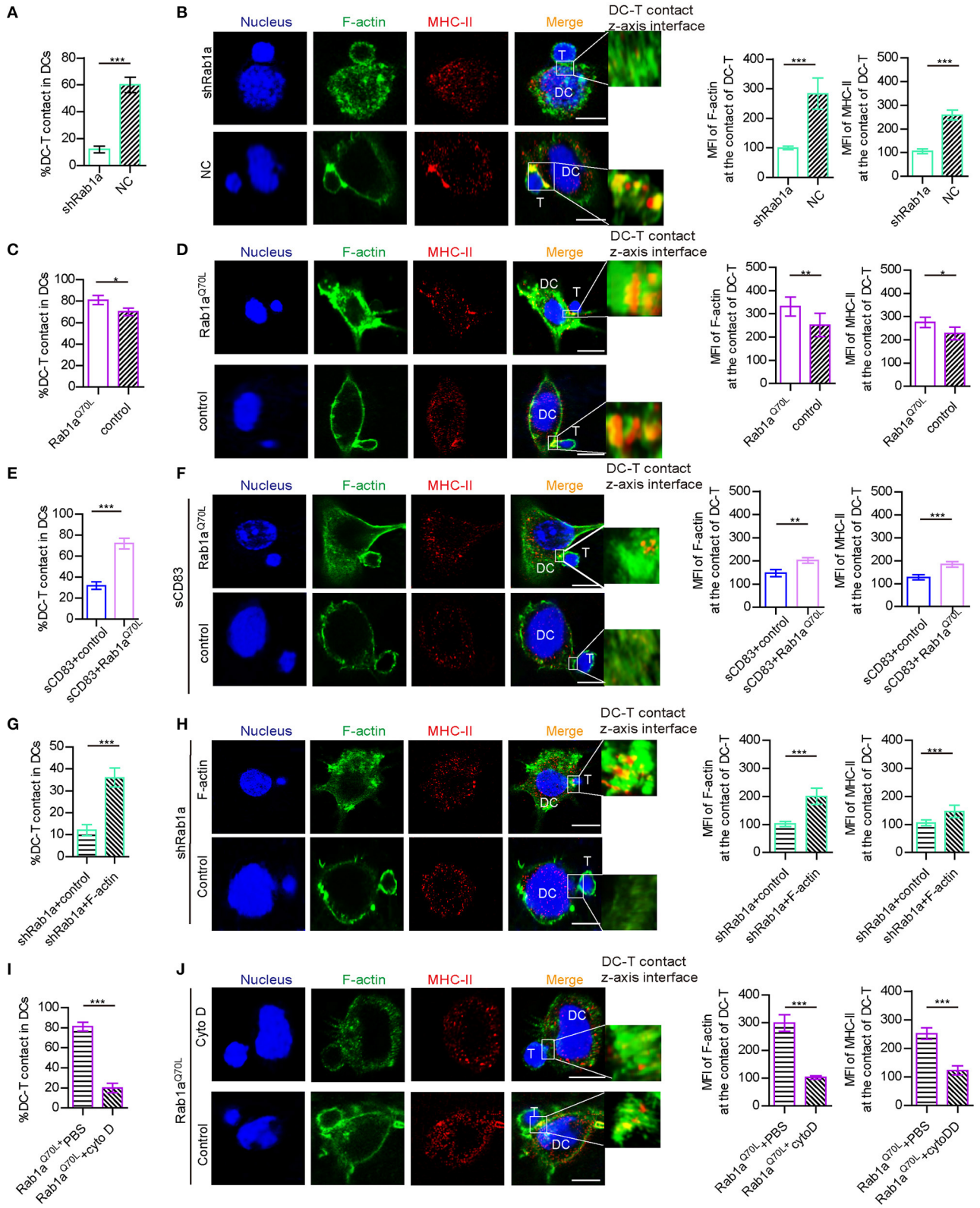

FIGURE 5 | Rab1a-mediated F-actin regulated IS formation between DC and T cells. **(A)** With shRNA Rab1a or NC treatment, the percentage of DC-T contact in DCs. **(B)** With shRNA Rab1a, or NC treatment, the distribution (left panel) and mean fluorescence value (right panel) of F-actin and MHC-II at the contact between DC 2.4 and T cells. **(C)** Overexpression of Rab1a^{Q70L} in DC promotes the percentage of DC-T contacts and **(D)** promotes the accumulation (left panel) and mean

(Continued)

FIGURE 5 | fluorescence value (right panel) of F-actin and MHC-II at the contacts of DC-T, compared to the empty plasmid transfected DC. **(E)** Overexpression of Rab1a^{Q70L} in sCD83-treated DC promotes the percentage of DC-T contacts and **(F)** promotes the accumulation (left panel) and mean fluorescence value (right panel) of F-actin and MHC-II at the contacts of DC-T, compared to the empty plasmid transfected sCD83-treated DC. **(G)** Overexpression of F-actin in shRab1a-treated DC promotes the percentage of DC-T contacts and **(H)** promotes the accumulation (left panel) and mean fluorescence value (right panel) of F-actin and MHC-II at the contacts of DC-T, compared to the empty plasmid transfected shRab1a-treated DC (control). **(I)** Cytochalasin D treatment decreased the percentage of DC-T contact (left panel) in Rab1a^{Q70L} overexpressed DCs, compared to PBS-treated Rab1a^{Q70L} overexpressed DCs. **(J)** Cytochalasin D treatment distributed the accumulation (left panel) and mean fluorescence value (right panel) of F-actin and MHC-II in Rab1a^{Q70L} overexpressed DCs, compared to PBS (control)–treated Rab1a^{Q70L} overexpressed DCs. Bar = 5 μm. Data of **(A,C,E,G,I)** are from three separate experiments, and data of **(B,D,F,H,J)** were from five cells/group and were shown as mean ± SEM. $^{*}p < 0.05$, $^{**}p < 0.01$, $^{***}p < 0.001$.

Next, to determine whether the effect of sCD83 on DCs was regulated by Rab1a, Rab1a^{Q70L} was overexpressed in sCD83-treated DCs for 72 h. We found that Rab1a^{Q70L} overexpression promoted F-actin and LRRK2 expression and colocalization of Rab1a and LRRK2 in sCD83-treated DCs (**Figures 3G,H**). Based on these findings, we concluded that Rab1a participated in the regulation of sCD83 on F-actin in DCs by controlling colocalization of Rab1a and LRRK2.

Rab1a Controls Expression and Localization of MHC-II on the Surface of DCs

As a central molecule of IS, MHC-II expression in sCD83-treated DC-T contacts decreased and no longer accumulated in synapses (**Figure 1D**). In addition, sCD83 treatment decreased the surface expression of MHC-II on DCs (**Figure 4A**). And MHC-II in sCD83-treated DCs prefers to accumulate around the nucleus (**Figure 4B**). In activated DCs, MHC-II can colocalize with Rab1a (**Figure 4B**). However, sCD83 treatment disrupted the colocalization of MHC-II and Rab1a (**Figure 4B**). Based on these findings, sCD83 influences the expression and localization of MHC-II in DCs. We next investigated to determine whether the regulatory effect of sCD83 on MHC-II expression and localization in DCs was controlled by Rab1a, which is involved in vesicle transport, a process that transports proteins to the cell membrane. Following shRNA-Rab1a treatment, we found that MHC-II expression decreased (**Figure 4C**), and MHC-II accumulated around the nucleus of DCs (**Figure 4D**). In contrast, overexpression of Rab1a^{Q70L} increased MHC-II expression (**Figure 4E**), and MHC-II preferred to colocalize with Rab1a in these DCs (**Figure 4F**). Moreover, overexpression of Rab1a^{Q70L} in sCD83-treated DCs also increased MHC-II expression on the surface of DCs and promoted MHC-II colocalized with Rab1a (**Figures 4G,H**). Thus, these findings indicate that sCD83 influences the localization of MHC-II in DCs by Rab1a.

Inhibitory Effect of sCD83 on DC-T IS Formation Is Regulated by Rab1a-Mediated F-Actin

Because Rab1a affects the expression and localization of F-actin and MHC-II, which are essential for DC-T IS formation, we explored whether Rab1a may be a regulator of DC-T synapse formation. Following shRNA-Rab1a treatment, we found that DC-T contact decreased, and IS formation between DC-T was disrupted (**Figures 5A,B**). However, overexpression of Rab1a^{Q70L} increased the percentage of DC-T contact and promoted IS formation to accumulate F-actin and MHC-II at DC-T contact (**Figures 5C,D**). Based on these findings, we conclude that Rab1a regulates DC-T synapse formation.

In addition, overexpression of Rab1a^{Q70L} rescued the expression and altered localization of MHC-II in sCD83-treated DCs (**Figures 3G,H**). Overexpression of Rab1a^{Q70L} also increased the percentage of DC-T contacts and promoted MHC-II relocation to contacts of sCD83-treated DC-T (**Figures 5E,F**). Based on these findings, we conclude that sCD83 influences localization of MHC-II by Rab1a and that the inhibitory effect of sCD83 on IS formation between DC-Ts is regulated by Rab1a.

Furthermore, we found that overexpression of F-actin in shRNA Rab1a-treated DCs partially increased the percentage of DC-T contact and promoted IS formation between DC-T (**Figures 5G,H**). Following overexpression of Rab1a^{Q70L} in DCs for 72 h and then disruption of F-actin arrangement by cytochalasin D, DC-T contact formation decreased, and cells lost the ability to form IS (**Figures 5I,J**). Therefore, Rab1a regulates DC-T contact and DC-T IS by F-actin.

sCD83-Treated DCs Decrease T Cell Number in EAU Mice

We then prepared and transferred sCD83-treated DCs to a mouse model of EAU and found that the retinal damage of EAU was alleviated (**Figure 6A**), and there was a decreased number of T cells in the eyes and lymph nodes of these mice with sCD83-treated DCs transferring (**Figure 6B**). However, transferring activated DCs into EAU aggravated the retinal damage of EAU and increased the percentage of T cells in the eyes and lymph nodes of these mice (**Figures 6A,B**). Moreover, the expression of Rab1a-GTP in DCs from sCD83-treated DCs transferred to animals with EAU was lower than that found in controls and activated DCs transferred mice (**Figure 6C**). In addition, we found that sCD83 decreased the percentage of WT DC-T contacts as well as reduced the expression and localization of MHC-II and F-actin at the site of DC-T contacts *in vitro* experiments (**Figure 6D**). Thus, these findings demonstrate that sCD83-treated DCs alleviate symptoms in a mouse model of EAU by inhibiting DC-T contact.

DISCUSSION

The findings from our study show that sCD83 disrupts the accumulation of F-actin in DCs, resulting in decreased IS

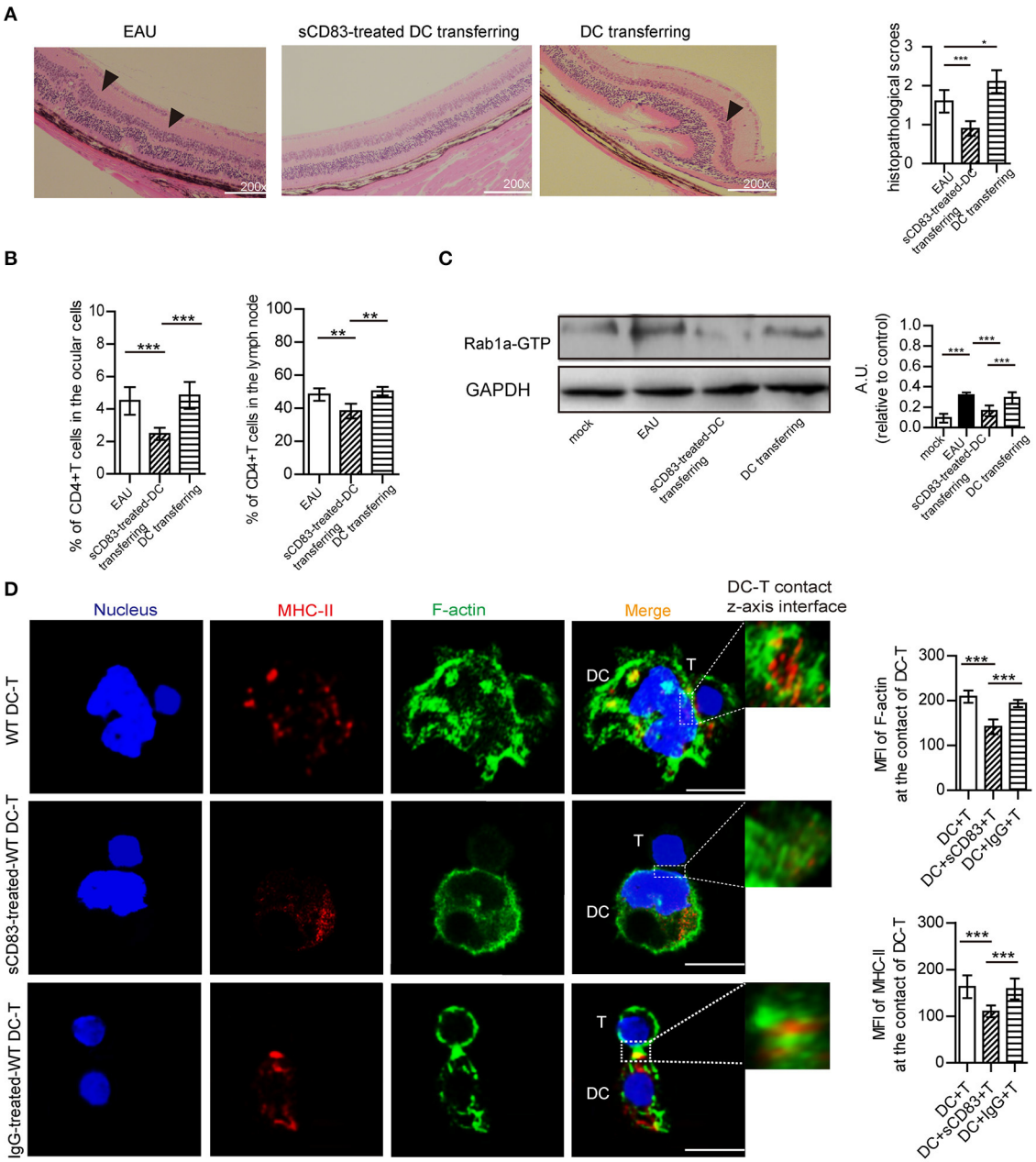

FIGURE 6 | The effect of sCD83-treated DCs on EAU and the synapse formation between sCD83-treated DCs and T cells *in vitro* experiment. **(A)** Representative images of the retina from an EAU, EAU with sCD83-treated DCs transferring, and EAU with activated DCs transferring as assessed by histology. Hematoxylin-eosin staining of the retina at 200× magnification. Black arrows mark retinal disorganization. Scale bar = 100 μm. The histopathological scores were evaluated in three mice every group (right panel). **(B)** The percentage of T cells in the eyes and lymph nodes of these mice with sCD83-treated DCs transferring or activated DCs transferring or not. **(C)** The expression of Rab1a-GTP in DCs from mock, EAU, and EAU with sCD83-treated DCs transferring. **(D)** sCD83 treatment reduces the expression and localization of MHC-II and F-actin at the site of DC-T contacts *in vitro* experiments. Bar = 5 μm. Data of **(A–C)** were from three separate experiments, and three mice/group were used. Data of **(D)** are from three separate experiments and shown as mean ± SEM. $^{*}p < 0.05$, $^{**}p < 0.01$, $^{***}p < 0.001$.

formation between DC-T, and that effect of sCD83 on DCs is mediated by decreased the expression of Rab1a to suppress the LRRK2/F-actin pathway and disrupt MHC-II localization on sites of DC-T contact (**Supplementary Figure 6**). In addition, our findings identify a new regulatory mechanism of DC-T contact formation. The activation and clonal expansion of naive T cells by antigen-loaded DCs are key events during immune response, and this activation involves the formation of a specialized IS between a mature DC and a $CD4^{+}$ T cell (Dustin, 2009). Most prior studies on IS have focused on the T cell aspect of the synapse,

with little information on the DC side (Rodriguez-Fernandez and Corbi, 2005; Rodriguez-Fernandez et al., 2009). The activation status of an encountered T cell controls the length of DC–T cell contact and drives cytoskeletal polarization in DC. In turn, disruption of DC IS formation blocks T cell activation (Al-Alwan et al., 2001). F-actin is an important cytoskeletal protein that clusters at DC-T contacts to maintain the structure and probably the signaling from this region (Al-Alwan et al., 2001). It also regulates DC synapse formation and function by promoting cell polarization and intracellular redistribution of proteins and organelles (Lin et al., 2015; Schulz et al., 2015). Disruption of the F-actin cytoskeleton in DCs severely diminishes T cell activation (Al-Alwan et al., 2001). In the current study, we found that sCD83 regulates F-actin by decreasing Rab1a activation. As a small G protein, activation of Rab1a may result in binding to Roco2 and further regulation of the activity of members of the Roco2 kinase family, including LRRK2, which controls F-actin rearrangement. In contrast to previous reports that found inhibitor cytokines such as IL-10–regulated F-actin in DCs (Xu et al., 2017), we showed an sCD83-based mechanism on regulating F-actin in DCs, a finding that contributes to a better understanding of the underlying regulatory mechanism of the DC cytoskeleton and DC-T contact.

Additionally, sCD83 regulated DC-T contact by decreasing Rab1a expression, which mediated endoplasmic reticulum (ER)–Golgi transport, and could result in the decrease of cell surface protein expression to influence DC-T contact. sCD83 may decrease the surface protein expression in DCs by Rab1a to inhibit DC-T contact and T cell activation. In this article, DCs were activated by PTX stimulation, which may increase cAMP (Burch et al., 1988) and up-regulate class II transcription in DCs. sCD83 may inhibit these activated DCs by down-regulating the expression of Rab1a to disrupt cAMP-mediated F-actin polymerization (Kicka et al., 2011).

As the extracellular domain of immunoglobulin CD83, sCD83 is absorbed by DCs (Yang et al., 2015) and may be degraded by Rab1a-mediated autophagy. sCD83 is secreted by activated $CD83^+$ DC or other $CD83^+$ cells, which may result in a large amount of sCD83 consumption or inhibition of Rab1a activity, leading to inhibition of the cytoskeleton and disruption of surface molecules in DCs, thereby preventing cell activation and function. This process would inherently act as a self-regulatory mechanism of sCD83 on DCs. Furthermore, sCD83 binds with MD-2 to inhibit the MD-2/TLR4 signaling pathway (Horvatinovich et al., 2017). However, MD-2 knockdown in DCs had no effect on the F-actin arrangement in DCs (**Supplementary Figure 7**). Thus, we propose that the effect of sCD83 on F-actin is independent of the MD-2/TLR4 pathway and that determination of the specific mechanism of sCD83 in DCs warrants further study.

Rab1a mediates ER–Golgi transport and some membrane molecules transport (Ali et al., 2004), and it also plays a role in autophagy (Webster et al., 2016). In addition, Rab1a regulates localization of members of the LRRK2-related kinase family to influence F-actin accumulation (Kicka et al., 2011), which further affects the accumulation of MHC-II at the site of DC-T contacts in our studying. Further, Rab1a regulates sorting of early endocytic vesicles involving Rab5, Rab7, Rab9, and Rab11, all of which would be required for MHC-II expression on DCs (Mukhopadhyay et al., 2014; Perez-Montesinos et al., 2017). Therefore, Rab1a may participate in antigen presentation processing by MHC-II. Further, Rab1a has a role in COPII vesicle traffic (Constantino-Jonapa et al., 2020; Westrate et al., 2020), which is important for MHC and antigen processing in the ER. Although Rab1a may have an important role in regulating antigen presentation processing by different means, a detailed understanding of the regulatory process of Rab1a in DCs warrants additional study.

Uveitis, an inflammatory disease involving the uvea, retina, retinal vessels, and/or vitreous body, can result in visual impairment and blindness (Rothova et al., 1996). The treatment of uveitis remains a challenging undertaking and an area of active research (Rothova et al., 1996; You et al., 2017; Zhao and Zhang, 2017). We demonstrated that increased sCD83 acts as a suppressive molecule in EAU alleviating symptoms of the disease by disrupting DC-T contact through IS inhibition in DCs, but not T cells (**Supplementary Figure 3**). This potential mechanism may underlie the decreased number of T cells and DCs following sCD83 treatment in mice with EAU and the amelioration of symptoms in affected animals. Furthermore, increased sCD83 in animals with EAU may be a result of self-regulation in the immune response, which warrants further investigation to better understand immune regulation in EAU. In addition, we found that administration of sCD83-treated DCs decreased the number of T cells and DCs in mice with EAU and reduced the symptoms of EAU. The mechanism of sCD83-treated DCs on EAU might be that these sCD83-treated DCs inhibit T cell activation by losing to interact with T cells well, or these sCD83-treated DCs would secrete IL-10 or IDO to inhibit T cell activation (Lin et al., 2018) or suppress the endogenous DCs by IL-10 to further inhibit T cell activation (Lin et al., 2018). The mechanism of sCD83-treated DC on EAU needs further study. Our findings may provide a new direction for the treatment of autoimmune uveitis using DCs.

To conclude, we demonstrate that sCD83 inhibits DC-T synapse formation by decreasing Rab1a activation to disrupt F-actin and MHC-II accumulation at sites of DC-T contact. Furthermore, our findings provide a possible mechanism of sCD83 on the role of DCs in IS and show that Rab1a may be a potential regulator of DC function. Finally, sCD83-treated DCs alleviate symptoms of EAU in mice, providing a potentially new avenue for EAU treatment.

DATA AVAILABILITY STATEMENT

The original contributions presented in the study are included in the article/**Supplementary Materials**, further inquiries can be directed to the corresponding author/s.

ETHICS STATEMENT

The animal study was reviewed and approved by Shandong First Medical University & Shandong Academy of Medical Sciences.

AUTHOR CONTRIBUTIONS

WL designed this research, wrote the paper, and analyzed data. WL, SZ, and MF performed animal experiments, western blot, and flow cytometry experiment. QS, XL, and YY cultured cells and performed animal experiments. All authors agreed to the published version of the manuscript.

FUNDING

This work was supported by grants from the Natural Science Foundation of China (81500710); Shandong Key Research and Development Project (2019GSF108189); projects of medical and health technology development program in Shandong province (2019WS186); the science and technology program from Shandong Academy of Medical Sciences (2015-25); and the Innovation Project of Shandong Academy of Medical Sciences.

ACKNOWLEDGMENTS

We acknowledgment for a kind experimental help from professor Yiwei Chu (Department of immunology, Shanghai medical school, Fudan university, Shanghai, China).

SUPPLEMENTARY MATERIAL

The Supplementary Material for this article can be found online at: https://www.frontiersin.org/articles/10.3389/fcell.2020.605713/full#supplementary-material

REFERENCES

Al-Alwan, M. M., Rowden, G., Lee, T. D., and West, K. A. (2001). The dendritic cell cytoskeleton is critical for the formation of the immunological synapse. *J. Immunol.* 166, 1452–1456. doi: 10.4049/jimmunol.166.3.1452

Ali, B. R., Wasmeier, C., Lamoreux, L., Strom, M., and Seabra, M. C. (2004). Multiple regions contribute to membrane targeting of rab GTPases. *J. Cell. Sci.* 117, 6401–6412. doi: 10.1242/jcs.01542

Beibei Wang, W. L., Jike, S., Xiaofeng, X., and Hongsheng, B. (2017). The interaction of dendritic cells and γδ T cells promotes the activation of γδ T cells in experimental autoimmune uveitis. *J. Innov. Opt. Health Sci.* 10:1650042. doi: 10.1142/S1793545816500425

Burch, R. M., Jelsema, C., and Axelrod, J. (1988). Cholera toxin and pertussis toxin stimulate prostaglandin E2 synthesis in a murine macrophage cell line. *J. Pharmacol. Exp. Ther.* 244, 765–773.

Caspi, R. R., Roberge, F. G., McAllister, C. G., el-Saied, M., Kuwabara, T., Gery, I., et al. (1986). T cell lines mediating experimental autoimmune uveoretinitis (EAU) in the rat. *J. Immunol.* 136, 928–933.

Chen, J., Ganguly, A., Mucsi, A. D., Meng, J., Yan, J., Detampel, P., et al. (2017). Strong adhesion by regulatory T cells induces dendritic cell cytoskeletal polarization and contact-dependent lethargy. *J. Exp. Med.* 214, 327–338. doi: 10.1084/jem.20160620

Comrie, W. A., Li, S., Boyle, S., and Burkhardt, J. K. (2015). The dendritic cell cytoskeleton promotes T cell adhesion and activation by constraining ICAM-1 mobility. *J. Cell. Biol.* 208, 457–473. doi: 10.1083/jcb.201406120

Constantino-Jonapa, L. A., Hernandez-Ramirez, V. I., Osorio-Trujillo, C., and Talamas-Rohana, P. (2020). EhRab21 associates with the golgi apparatus in entamoeba histolytica. *Parasitol. Res.* 119, 1629–1640. doi: 10.1007/s00436-020-06667-7

Davis, D. M., and Dustin, M. L. (2004). What is the importance of the immunological synapse? *Trends Immunol.* 25, 323–327. doi: 10.1016/j.it.2004.03.007

Dustin, M. L. (2009). The cellular context of T cell signaling. *Immunity* 30, 482–492. doi: 10.1016/j.immuni.2009.03.010

Dustin, M. L., and Shaw, A. S. (1999). Costimulation: building an immunological synapse. *Science* 283, 649–650. doi: 10.1126/science.283.5402.649

Grakoui, A., Bromley, S. K., Sumen, C., Davis, M. M., Shaw, A. S., Allen, P. M., et al. (1999). The immunological synapse: a molecular machine controlling T cell activation. *Science* 285, 221–227. doi: 10.1126/science.285.5425.221

Harimoto, K., Ito, M., Karasawa, Y., Sakurai, Y., and Takeuchi, M. (2014). Evaluation of mouse experimental autoimmune uveoretinitis by spectral domain optical coherence tomography. *Br. J. Ophthalmol.* 98, 808–812. doi: 10.1136/bjophthalmol-2013-304421

Heuss, N. D., Lehmann, U., Norbury, C. C., McPherson, S. W., and Gregerson, D. S. (2012). Local activation of dendritic cells alters the pathogenesis of autoimmune disease in the retina. *J. Immunol.* 188, 1191–1200. doi: 10.4049/jimmunol.1101621

Horvatinovich, J. M., Grogan, E. W., Norris, M., Steinkasserer, A., Lemos, H., Mellor, A. L., et al. (2017). Soluble CD83 inhibits T cell activation by binding to the TLR4/MD-2 complex on CD14(+) monocytes. *J. Immunol.* 198, 2286–2301. doi: 10.4049/jimmunol.1600802

Ilhan, F., Demir, T., Turkcuoglu, P., Turgut, B., Demir, N., and Godekmerdan, A. (2008). Th1 polarization of the immune response in uveitis in behcet's disease. *Can. J. Ophthalmol.* 43, 105–108. doi: 10.3129/i07-179

Kicka, S., Shen, Z., Annesley, S. J., Fisher, P. R., Lee, S., Briggs, S., et al. (2011). The LRRK2-related Roco kinase Roco2 is regulated by Rab1A and controls the actin cytoskeleton. *Mol. Biol. Cell.* 22, 2198–2211. doi: 10.1091/mbc.e10-12-0937

Kotzor, N., Lechmann, M., Zinser, E., and Steinkasserer, A. (2004). The soluble form of CD83 dramatically changes the cytoskeleton of dendritic cells. *Immunobiology* 209, 129–140. doi: 10.1016/j.imbio.2004.04.003

Lan, Z., Ge, W., Arp, J., Jiang, J., Liu, W., Gordon, D., et al. (2010). Induction of kidney allograft tolerance by soluble CD83 associated with prevalence of tolerogenic dendritic cells and indoleamine 2,3-dioxygenase. *Transplantation* 90, 1286–1293. doi: 10.1097/TP.0b013e3182007bbf

Lin, W., Buscher, K., Wang, B., Fan, Z., Song, N., Li, P., et al. (2018). Soluble CD83 alleviates experimental autoimmune uveitis by inhibiting filamentous actin-dependent calcium release in dendritic cells. *Front. Immunol.* 9:1567. doi: 10.3389/fimmu.2018.01567

Lin, W., Man, X., Li, P., Song, N., Yue, Y., Li, B., et al. (2017). NK cells are negatively regulated by sCD83 in experimental autoimmune uveitis. *Sci. Rep.* 7:12895. doi: 10.1038/s41598-017-13412-1

Lin, W., Suo, Y., Deng, Y., Fan, Z., Zheng, Y., Wei, X., et al. (2015). Morphological change of CD4(+) T cell during contact with DC modulates T-cell activation by accumulation of F-actin in the immunology synapse. *BMC Immunol.* 16:49. doi: 10.1186/s12865-015-0108-x

Muhaya, M., Calder, V. L., Towler, H. M., Jolly, G., McLauchlan, M., and Lightman, S. (1999). Characterization of phenotype and cytokine profiles of T cell lines derived from vitreous humour in ocular inflammation in man. *Clin. Exp. Immunol.* 116, 410–414. doi: 10.1046/j.1365-2249.1999.00921.x

Mukhopadhyay, A., Quiroz, J. A., and Wolkoff, A. W. (2014). Rab1a regulates sorting of early endocytic vesicles. *Am. J. Physiol. Gastrointest. Liver Physiol.* 306, G412–424. doi: 10.1152/ajpgi.00118.2013

Nolz, J. C., Gomez, T. S., Zhu, P., Li, S., Medeiros, R. B., Shimizu, Y., et al. (2006). The WAVE2 complex regulates actin cytoskeletal reorganization and CRAC-mediated calcium entry during T cell activation. *Curr. Biol.* 16, 24–34. doi: 10.1016/j.cub.2005.11.036

Pashine, A., Göpfert, U., Chen, J., Hoffmann, E., Dietrich, P. S., Peng, S. L. (2008). Failed efficacy of soluble human CD83-Ig in allogeneic mixed lymphocyte reactions and experimental autoimmune encephalomyelitis: implications for a lack of therapeutic potential. *Immunol Lett.* 115, 9–15. doi: 10.1016/j.imlet.2007.10.015

Perez-Montesinos, G., Lopez-Ortega, O., Piedra-Reyes, J., Bonifaz, L. C., and Moreno, J. (2017). Dynamic changes in the intracellular association of selected

rab small GTPases with MHC class II and DM during dendritic cell maturation. *Front. Immunol.* 8:340. doi: 10.3389/fimmu.2017.00340

Quintana, A., Kummerow, C., Junker, C., Becherer, U., and Hoth, M. (2009). Morphological changes of T cells following formation of the immunological synapse modulate intracellular calcium signals. *Cell Calcium* 45, 109–122. doi: 10.1016/j.ceca.2008.07.003

Quintana, A., Schwarz, E. C., Schwindling, C., Lipp, P., Kaestner, L., and Hoth, M. (2006). Sustained activity of calcium release-activated calcium channels requires translocation of mitochondria to the plasma membrane. *J. Biol. Chem.* 281, 40302–40309. doi: 10.1074/jbc.M607896200

Quintana, A., Schwindling, C., Wenning, A. S., Becherer, U., Rettig, J., Schwarz, E. C., et al. (2007). T cell activation requires mitochondrial translocation to the immunological synapse. *Proc. Natl. Acad. Sci. U.S.A.* 104, 14418–14423. doi: 10.1073/pnas.0703126104

Rodriguez-Fernandez, J. L., and Corbi, A. L. (2005). Adhesion molecules in human dendritic cells. *Curr. Opin. Investig. Drugs* 6, 1103–1111.

Rodriguez-Fernandez, J. L., Riol-Blanco, L., Delgado-Martin, C., and Escribano-Diaz, C. (2009). The dendritic cell side of the immunological synapse: exploring terra incognita. *Discov. Med.* 8, 108–112.

Roman-Sosa, G., Brocchi, E., Schirrmeier, H., Wernike, K., Schelp, C., and Beer, M. (2016). Analysis of the humoral immune response against the envelope glycoprotein Gc of schmallenberg virus reveals a domain located at the amino terminus targeted by mAbs with neutralizing activity. *J. Gen. Virol.* 97, 571–580. doi: 10.1099/jgv.0.000377

Rothova, A., Suttorp-van Schulten, M. S., Frits Treffers, W., and Kijlstra, A. (1996). Causes and frequency of blindness in patients with intraocular inflammatory disease. *Br. J. Ophthalmol.* 80, 332–336. doi: 10.1136/bjo.80.4.332

Schulz, A. M., Stutte, S., Hogl, S., Luckashenak, N., Dudziak, D., Leroy, C., et al. (2015). Cdc42-dependent actin dynamics controls maturation and secretory activity of dendritic cells. *J. Cell. Biol.* 211, 553–567. doi: 10.1083/jcb.201503128

Shao, H., Van Kaer, L., Sun, S. L., Kaplan, H. J., and Sun, D. (2003). Infiltration of the inflamed eye by NKT cells in a rat model of experimental autoimmune uveitis. *J. Autoimmun.* 21, 37–45. doi: 10.1016/S0896-8411(03)00049-0

Starke, C., Steinkasserer, A., Voll, R. E., and Zinser, E. (2013). Soluble human CD83 ameliorates lupus in NZB/W F1 mice. *Immunobiology* 218, 1411–1415. doi: 10.1016/j.imbio.2013.06.002

Thurau, S. R., Chan, C. C., Nussenblatt, R. B., and Caspi, R. R. (1997). Oral tolerance in a murine model of relapsing experimental autoimmune uveoretinitis (EAU): induction of protective tolerance in primed animals. *Clin. Exp. Immunol.* 109, 370–376. doi: 10.1046/j.1365-2249.1997.4571356.x

Webster, C. P., Smith, E. F., Bauer, C. S., Moller, A., Hautbergue, G. M., Ferraiuolo, L., et al. (2016). The C9orf72 protein interacts with Rab1a and the ULK1 complex to regulate initiation of autophagy. *EMBO J.* 35, 1656–1676. doi: 10.15252/embj.201694401

Westrate, L. M., Hoyer, M. J., Nash, M. J., and Voeltz, G. K. (2020). Vesicular and uncoated Rab1-dependent cargo carriers facilitate ER to golgi transport. *J. Cell. Sci.* 133:jcs239814. doi: 10.1242/jcs.239814

Xu, J. F., Huang, B. J., Yin, H., Xiong, P., Feng, W., Xu, Y., et al. (2007). A limited course of soluble CD83 delays acute cellular rejection of MHC-mismatched mouse skin allografts. *Transpl. Int.* 20, 266–276. doi: 10.1111/j.1432-2277.2006.00426.x

Xu, X., Liu, X., Long, J., Hu, Z., Zheng, Q., Zhang, C., et al. (2017). Interleukin-10 reorganizes the cytoskeleton of mature dendritic cells leading to their impaired biophysical properties and motilities. *PLoS ONE* 12:e0172523. doi: 10.1371/journal.pone.0172523

Yang, Y., Xin, Z., Chu, J., Li, N., and Sun, T. (2015). Involvement of caveolin-1 in CD83 internalization in mouse dendritic cells. *Cell. Transplant.* 24, 1395–1404. doi: 10.3727/096368914X682116

You, C., Sahawneh, H. F., Ma, L., Kubaisi, B., Schmidt, A., and Foster, C. S. (2017). A review and update on orphan drugs for the treatment of noninfectious uveitis. *Clin. Ophthalmol.* 11, 257–265. doi: 10.2147/OPTH.S121734

Zhao, C., and Zhang, M. (2017). Immunosuppressive treatment of non-infectious uveitis: history and current choices. *Chin. Med. Sci. J.* 32, 48–61. doi: 10.24920/J1001-9242.2007.007

Conflict of Interest: The authors declare that the research was conducted in the absence of any commercial or financial relationships that could be construed as a potential conflict of interest.

frontiers in Cell and Developmental Biology

REVIEW
published: 03 February 2021
doi: 10.3389/fcell.2021.612830

Vedolizumab: Potential Mechanisms of Action for Reducing Pathological Inflammation in Inflammatory Bowel Diseases

*Matthew Luzentales-Simpson, Yvonne C. F. Pang, Ada Zhang, James A. Sousa and Laura M. Sly**

Division of Gastroenterology, Department of Pediatrics, BC Children's Hospital and the University of British Columbia, Vancouver, BC, Canada

OPEN ACCESS

Edited by:
Zhichao Fan,
UCONN Health, United States

Reviewed by:
Rongrong Liu,
Northwestern University, United States
Dror S. Shouval,
Edmond and Lily Safra Children's Hospital, Israel
Vito Annese,
Fakeeh University Hospital, United Arab Emirates

***Correspondence:**
Laura M. Sly
laurasly@mail.ubc.ca

Specialty section:
This article was submitted to Cell Adhesion and Migration, a section of the journal Frontiers in Cell and Developmental Biology

Received: *30 September 2020*
Accepted: *12 January 2021*
Published: *03 February 2021*

Citation:
Luzentales-Simpson M, Pang YCF, Zhang A, Sousa JA and Sly LM (2021) Vedolizumab: Potential Mechanisms of Action for Reducing Pathological Inflammation in Inflammatory Bowel Diseases. Front. Cell Dev. Biol. 9:612830. doi: 10.3389/fcell.2021.612830

Inflammatory bowel diseases (IBD), encompassing ulcerative colitis (UC), and Crohn's disease (CD), are a group of disorders characterized by chronic, relapsing, and remitting, or progressive inflammation along the gastrointestinal tract. IBD is accompanied by massive infiltration of circulating leukocytes into the intestinal mucosa. Leukocytes such as neutrophils, monocytes, and T-cells are recruited to the affected site, exacerbating inflammation and causing tissue damage. Current treatments used to block inflammation in IBD include aminosalicylates, corticosteroids, immunosuppressants, and biologics. The first successful biologic, which revolutionized IBD treatment, targeted the pro-inflammatory cytokine, tumor necrosis factor alpha (TNFα). Infliximab, adalimumab, and other anti-TNF antibodies neutralize TNFα, preventing interactions with its receptors and reducing the inflammatory response. However, up to 40% of people with IBD become unresponsive to anti-TNFα therapy. Thus, more recent biologics have been designed to block leukocyte trafficking to the inflamed intestine by targeting integrins and adhesins. For example, natalizumab targets the α4 chain of integrin heterodimers, α4β1 and α4β7, on leukocytes. However, binding of α4β1 is associated with increased risk for developing progressive multifocal leukoencephalopathy, an often-fatal disease, and thus, it is not used to treat IBD. To target leukocyte infiltration without this life-threatening complication, vedolizumab was developed. Vedolizumab specifically targets the α4β7 integrin and was approved to treat IBD based on the presumption that it would block T-cell recruitment to the intestine. Though vedolizumab is an effective treatment for IBD, some studies suggest that it may not block T-cell recruitment to the intestine and its mechanism(s) of action remain unclear. Vedolizumab may reduce inflammation by blocking recruitment of T-cells, or pro-inflammatory monocytes and dendritic cells to the intestine, and/or vedolizumab may lead to changes in the programming of innate and acquired immune cells dampening down inflammation.

Keywords: vedolizumab, inflammatory bowel disease, cell trafficking, macrophages, innate immunity

INTRODUCTION

Inflammatory bowel disease (IBD), encompassing ulcerative colitis (UC), and Crohn's disease (CD) are a group of disorders that are characterized by chronic, relapsing, and remitting, or progressive inflammation along the gastrointestinal tract. UC involves continuous inflammation of the colon and the rectum (Fakhoury et al., 2014). It is limited to the mucosal layer of the intestinal wall. In contrast, CD causes discontinuous, transmural inflammation that can occur anywhere along the digestive tract, though it most commonly affects the distal ileum (Fakhoury et al., 2014). Canada has among the highest prevalence of IBD with 1 in 140 people affected (Kaplan et al., 2019). IBD has traditionally been regarded as a disease of developed and high-income nations, though incidence rates appear to have stabilized with high burden and prevalence. Incidence of IBD is now rapidly rising in newly industrialized countries (GBD 2017 Inflammatory Bowel Disease Collaborators, 2020). There were 6.8 million cases of IBD globally in 2017, with approximately 1.5 million in North America and 2 million in Europe (GBD 2017 Inflammatory Bowel Disease Collaborators, 2020; Jairath and Feagan, 2020). Individuals with IBD suffer from intestinal inflammation that can lead to debilitating symptoms including pain, nausea, and diarrhea (Rosen et al., 2015). In addition to disease burden, the chronic nature of IBD and its requirement for lifelong treatment causes significant economic burden for the individual and society. As analyzed by Park et al. (2020), the annual mean health care cost for people with IBD is over 3-fold higher than for people without IBD (selected from the general population using a health plan member database). Mehta (2016) estimated that extrapolated direct costs of IBD are between $11 to 28 billion in the United States. Including direct and indirect costs associated with loss of productivity and earnings, the total cost of IBD is between $14.6 and 31.6 billion annually (Mehta, 2016).

The etiology of IBD is multifactorial and includes genetic susceptibility, inappropriate immune activity, and environmental triggers. For example, a loss of function gene variant in the NOD2 gene is associated with increased susceptibility to CD due to increased production of pro-inflammatory cytokines (Ogura et al., 2001). Environmental factors affecting incidence of disease include geography, smoking, and pollution (Ananthakrishnan et al., 2018). Genetics, immune responses, and environmental variables also impact the host intestinal microbiota, which is often included as a fourth important factor in the development of IBD (Ananthakrishnan et al., 2018). While the exact cause is unknown, it is widely accepted that IBD occurs in genetically susceptible individuals with environmental influences that result in a dysregulated immune response to commensal intestinal microbiota (Rosen et al., 2015). The wide variation in disease presentation and treatment efficacy reflects the complexity of IBD pathogenesis (Chichlowski and Hale, 2008).

In this review, we will focus on the role of specific immune cells in IBD pathogenesis and how their trafficking and activity may be affected be vedolizumab. IBD is characterized by massive infiltration of circulating leukocytes into the inflamed intestinal mucosa. Diseased sections of the intestines have cytokine profiles that differ from healthy sections, indicating that cytokines play a pivotal role in the incidence and progression of disease (Murch et al., 1993; McAlindon et al., 1998). In particular, immune cells that are isolated from people with IBD display increased expression of pro-inflammatory cytokines and chemokines (Singh et al., 2016). Chemokine production leads to inappropriate recruitment and retention of cells such as T-cells, dendritic cells, and macrophages, which cause inflammation and establish the chronic inflammation that is characteristic of IBD (Singh et al., 2016). Chronic activation and proliferation of these immune cells leads to disruption of healthy tissues and thus further exacerbation of disease (Schippers et al., 2016). Macrophages in particular have a unique role in IBD due to their ability to exhibit pro-inflammatory activity that contributes to disease and Interleukin-10 (IL-10)-mediated anti-inflammatory activity (Kozicky et al., 2015). Anti-inflammatory macrophage activity has recently been described in the resolution of IBD during anti-TNFα therapies in mice and humans (Koelink et al., 2020). Specifically, macrophage IL-10 signaling was described to be the driving force behind the therapeutic effect of these therapies (Koelink et al., 2020). With respect to these studies, IBD therapies can reduce inflammation by targeting leukocyte trafficking to the intestine and pro-inflammatory activity.

There is no standard treatment for IBD. Therapeutic options are non-specific anti-inflammatories that include aminosalicylates, corticosteroids, and other immunosuppressants, and some biologics. New biological therapies have been designed to be specific to the gut to minimize side effects and increase responsiveness (Hazel and O'Connor, 2020). In particular, anti-integrin antibodies target key players in leukocyte trafficking to the gut to reduce immune cell infiltration and the resulting inflammation (Hazel and O'Connor, 2020). Vedolizumab is a therapy that was designed to reduce pathological inflammation in IBD by blocking T-cell recruitment to the intestine (Zeissig et al., 2019). However, some evidence suggests that it does not affect T-cell migration to the intestine (Zeissig et al., 2019). Herein, we describe the potential mechanisms of action by which vedolizumab may reduce pathological inflammation in IBD.

LEUKOCYTE TRAFFICKING AND ACTIVATION IN IBD PATHOGENESIS

Leukocyte Trafficking

Inflammatory bowel diseases is characterized by immune infiltration from the circulation into the inflamed intestinal mucosa. This migration is facilitated by complex interactions between circulating leukocytes and intestinal endothelial cells. Sialyl LewisX-modified glycoproteins on leukocytes bind selectins on the endothelial cells with low affinity, allowing leukocytes to roll along the endothelium (Wright and Cooper, 2014). Chemokines act as chemoattractants for the rolling leukocytes to promote their infiltration into the mucosa (Wright and Cooper, 2014). Integrins on leukocytes mediate adhesion by binding cellular adhesion molecules (CAMs) that are expressed

on the endothelial cells during inflammation (Wright and Cooper, 2014). Integrins are heterodimeric receptors composed of an α and a β subunit, which exist in several forms that can combine to allow tissue-specific adhesion (Arseneau and Cominelli, 2015). For example, the α4β7 receptor is a marker for leukocyte trafficking to the intestine (Clahsen et al., 2015).

Three CAMs have been reported to mediate leukocyte trafficking to the inflamed intestine, contributing to IBD: intracellular adhesion molecule (ICAM)-1, mucosal addressin cellular adhesion molecule (MAdCAM)-1, and vascular cell adhesion molecule (VCAM)-1 (Arseneau and Cominelli, 2015). Pro-inflammatory cytokines that are expressed during inflammation increase ICAM-1 expression, which binds the αLβ2 receptor on leukocytes (Bendjelloul et al., 2000; Arseneau and Cominelli, 2015). MAdCAM-1, which is expressed within Peyer's patches and intestinal lymphoid tissues, binds the α4β7 receptor on memory/effector T-cells to regulate their homing to the intestine (DeNucci et al., 2010; Arseneau and Cominelli, 2015). It is upregulated at sites of inflammation in people with IBD (Briskin et al., 1997). VCAM-1 binds the α4β1 and α4β7 receptors, which mediate leukocyte trafficking to the central nervous system and intestine, respectively, (Arseneau and Cominelli, 2015; Schippers et al., 2016). Blocking the integrin-CAM interactions in the intestine is used as a strategy for IBD therapy aimed at reducing immune cell infiltration into the inflamed intestine.

T-Cells

T-cells play a prominent role in the regulation of the inflammatory response associated with IBD. In the past, CD was thought to be a Th1-mediated disease characterized by elevated levels of the pro-inflammatory mediators interleukin-2 (IL-2), interferon gamma (IFNγ), and tumor necrosis factor alpha (TNFα; Fais et al., 1991; Breese et al., 1993; Fuss et al., 1996). Since then, additional cytokines have been implicated in the pathogenesis of CD. Neurath et al. (1995) reported that antibodies against the p40 subunit of IL-12, a cytokine which induces Th1 cell differentiation, were able to attenuate 2,4,6-trinitrobenzene sulfonic acid (TNBS)-induced colitis (Jacobson et al., 1995; Neurath et al., 1995). Th17 cells were implicated in intestinal inflammation when IL-23, which maintains and expands Th17 populations, was found to share the p40 subunit with IL-12 (Oppmann et al., 2000; Stritesky et al., 2008). Furthermore, IL-23 was also shown to be a key driver of intestinal inflammation in the *Helicobacter hepaticus* infection and T-cell transfer models of colitis (Hue et al., 2006). UC is characterized by higher expression of IL-5 and IL-13, but not IL-4 (Karttunnen et al., 1994; Fuss et al., 1996). IL-13 is a key effector, synergizing with TNFα to modulate the proteins in tight junction formation, thereby disrupting the epithelial barrier (Heller et al., 2005; Chen and Sundrud, 2016). Recently, Rosen et al. (2017) showed that *IL-17A* and *IL-23* mRNA in pediatric rectal mucosal samples were increased in UC in addition to higher *IL-5* and *IL-13* mRNA. Thus, targeting T-cell trafficking may reduce the relative concentration of proinflammatory cytokines described to be involved in IBD. Finally, T-regulatory (Treg) cells regulate self-reactive lymphocytes by secreting inhibitory cytokines such as IL-10 and transforming growth factor-β (TGFβ; Taylor et al., 2006). By suppressing immune responses and maintaining tolerance to commensal microbes, Tregs are involved in intestinal homeostasis (Himmel et al., 2012).

Recent developments show multiple IBD susceptibility loci associated with T-cell activation and memory formation (Liu et al., 2015). Genes such as CD28 (T-cell co-stimulation), CCL20 and CCR6 (T-cell migration), NFATC1 (lymphocyte proliferation), NFKBIZ (Th17 development) associated with T-cell function demonstrate the potential for therapeutic strategies, which target different stages of T-cell involvement in IBD, such as recruitment, activation, proliferation, and retention. Genome-Wide Association Studies (GWAS) are crucial to explore potential genes associated with disease susceptibility and are further supported by literature that shows protein-level discrepancies between people with IBD and healthy control study participants. The presence of T-cells in the gut of people with IBD may be mediated *via* CCR6, CCL20, or the α4β7 integrin (Perez-Jeldres et al., 2019). Thus, blocking the interaction of these molecules with their respective ligands or receptors has not been accepted as the sole mechanism of T-cell trafficking. Drugs such as natalizumab, which binds α4 integrin, and vedolizumab, which targets the α4β7 heterodimer, have been developed specifically to target T-cell trafficking (Hazel and O'Connor, 2020). Therefore, it is crucial that we continue to explore the potential mechanisms of these, and other, therapies in order to improve existing therapies and to develop new ones.

Dendritic Cells

Dendritic cells (DCs) are professional antigen-presenting cells that control the innate and adaptive immune responses. In the intestine, there are two described subsets: conventional (cDCs) and plasmacytoid DCs (pDCs). Depending on their location within the epithelium, cDCs either secrete IL-10 and induce Th2 cells or secrete IL-12 and induce Th1 cells (Guan, 2019). They can be further distinguished by their expression of cell surface receptors, such as the integrin subunit CD103 (αE), which binds β7 to form the αEβ7 complex (Johansson-Lindbom et al., 2005; Clahsen et al., 2015). CD103 facilitates the retention of lymphocytes in the epithelium by binding E-cadherin (Johansson-Lindbom et al., 2005). CD103+ cDCs make up the majority of the DC population in the small intestine (Johansson-Lindbom et al., 2005; Clahsen et al., 2015). They are located in the lamina propria and intraepithelial compartment, but they can migrate to the mesenteric lymph node (MLN) to induce expression of the gut homing receptors CCR9 and α4β7 integrin on B and T-cells (Annacker et al., 2005; Schulz et al., 2009). Additionally, CD103+ cDCs can promote the development of Treg cells (Annacker et al., 2005; Clahsen et al., 2015). In contrast, CD103- (CX3CRI+) cDCs do not migrate (Schulz et al., 2009). Instead, they penetrate the epithelium to sample antigens in the lumen and present antigen to CD4+ T-cells, which differentiate into effector T-cells that secrete pro-inflammatory cytokines (Guan, 2019). Finally, pDCs are rare cells that secrete large quantities of type I interferons (Guan, 2019).

During IBD, DCs are attracted to sites of inflammation in the intestine by chemokines, such as CCL20 and MAdCAM-1 (Guan, 2019). Large numbers of activated DCs are found in the lamina propria and MLN and promote inflammation in murine models of IBD (Berndt et al., 2007; Guan, 2019). Conversely, ablation of DCs can also exacerbate disease (Muzaki et al., 2016). By regulating immune responses and tolerance to the microbiota, DCs play a critical role in IBD pathogenesis.

Macrophages

Macrophages play a role in all stages of inflammation: recognition, response, and resolution. They are highly heterogeneous, demonstrating a wide range of activation states (Kozicky et al., 2015). Cues from the microenvironment polarize macrophages to specific activation states (Kozicky et al., 2015). The three main phenotypes are grouped by function: inflammatory, wound-healing, and regulatory/anti-inflammatory, as reviewed in Steinbach and Plevy (2014). Inflammatory macrophages are promoted by IFNγ from NK and T-helper 1 (Th1) cells and TNFα from antigen presenting cells (Steinbach and Plevy, 2014). TNFα can also result from innate immune stimuli signaling that activates suppressor of cytokine signaling 3 (Steinbach and Plevy, 2014). Inflammatory macrophages produce high levels of the pro-inflammatory cytokines TNFα, IL-12, IL-6, and reactive oxygen and nitrogen species, which promote Th1 and Th17 cell activity and low levels of the anti-inflammatory cytokine, IL-10 (Hausmann et al., 2001; Heinsbroek and Gordon, 2009). Inflammatory macrophages are essential in the response to intracellular infections but can aggravate IBD due to their production of pro-inflammatory cytokines (Heinsbroek and Gordon, 2009). Wound-healing macrophages are induced by IL-4 from granulocytes or Th2 cells in response to tissue injury (Kozicky et al., 2015). They produce relatively lower levels of pro-inflammatory cytokines and higher levels of IL-10, protecting against parasites and promoting wound healing through the suppression of NLRP3 inflammasome activation, angiogenesis, tissue remodeling, and debris scavenging (Steinbach and Plevy, 2014; Yao et al., 2015). Wound-healing macrophages are protective in murine models of intestinal inflammation but may contribute to fibrosis in CD (Steinbach and Plevy, 2014). Regulatory or anti-inflammatory macrophages are a recently described phenotype that require two stimuli, one of which is pro-inflammatory (Mosser and Edwards, 2008; Kozicky et al., 2015). They can be activated by macrophage-derived TGFβ, IL-10, or immune complexes and a pro-inflammatory stimulus (Anderson et al., 2002; Mosser and Edwards, 2008; Kozicky et al., 2015). They produce high levels of IL-10 (Kozicky et al., 2015). In addition, regulatory macrophages express costimulatory molecules that activate T-cells (Steinbach and Plevy, 2014). They further differ from wound-healing macrophages in their lack of extracellular matrix production (Steinbach and Plevy, 2014). Regulatory macrophages play a key role in turning off the inflammatory response by reducing IL-12 synthesis (Kozicky et al., 2019) and are not predicted to promote fibrosis (Steinbach and Plevy, 2014).

In the lamina propria, macrophages control homeostasis by responding to infectious challenges with phagocytic and microbicidal activity while maintaining immune tolerance to commensal microbes. Differentiation into a tolerant phenotype is promoted by the presence of IL-10 and TFGβ in the microenvironment (Smythies et al., 2005). In contrast to the resident macrophages that do not mount an oxidative burst or inflammatory response, circulating blood monocytes are recruited to the sites of inflammation in the intestinal epithelium *via* chemokines and aggravate disease (Guan, 2019). Infiltration of these blood monocytes to local tissues is facilitated through tight α4β7-MAdCAM-1 interactions among other adhesion molecule and cadherin interactions (Berlin et al., 1993; Gorfu et al., 2009). Acute intestinal inflammation and chronic inflammation cause an influx of pro-inflammatory blood monocytes, which differentiate into inflammatory macrophages and exacerbate disease (Schippers et al., 2016). Macrophages isolated from people with IBD have increased oxidative burst activity and pro-inflammatory cytokine production (Guan, 2019). However, invading monocytes have been shown to dampen the inflammatory response through the release of IL-10 (Koelink et al., 2020). There is growing evidence that intestinal macrophages may play a critical role in the resolution of IBD, especially when activated towards regulatory or wound-healing phenotypes (Koelink et al., 2020). For this reason, macrophages, and subcellular molecules that modulate macrophages like chemokines and cytokines are potential therapeutic targets to ameliorate intestinal inflammation in IBD.

CURRENT TREATMENTS

The increasing disease burden of IBD reflects a need for a greater understanding of the mechanisms of IBD pathogenesis to improve existing therapies and develop new and effective therapies. IBD typically causes significant morbidity and requires lifelong medication in addition to possible dietary and lifestyle changes (Seyedian et al., 2019). There is no standard treatment regimen for individuals with IBD. Therapy relies on non-specific immune suppression to reduce symptoms, maintain remission, and prevent relapse (Hazel and O'Connor, 2020). Therapies include aminosalicylates, non-specific immunosuppressants, steroids, and biologics that target pro-inflammatory cytokines or leukocyte trafficking to the gut (Shi and Ng, 2018; Seyedian et al., 2019; Hazel and O'Connor, 2020). Surgery, which involves removal of the affected region, is an option for some people with acute, severe, refractory UC (Sica and Biancone, 2013), but not CD (Seyedian et al., 2019). Efficacy of therapy can be limited by a lack of primary response, secondary loss of response, and adverse side effects (Shi and Ng, 2018).

Anti-TNFα Biologics

Tumor necrosis factor alpha is an inflammatory cytokine that plays a prominent role in active inflammation associated with IBD (Fakhoury et al., 2014). An increase in TNFα has been shown to induce cell proliferation, differentiation, and upregulation of adhesion molecules on the endothelium to increase cell trafficking to the site of inflammation (Nawroth and Stern, 1986; Fakhoury et al., 2014). Considering its role in IBD, neutralizing TNFα has been used effectively to treat

IBD (mechanisms of action reviewed by Park and Jeen (2015) and Adegbola et al. (2018)).

Anti-TNFα biologics, including golimumab, certolizumab, infliximab, and adalimumab, have revolutionized IBD treatment. However, many people with IBD are unresponsive or experience significant adverse effects; up to 40% of people with IBD are predicted to become unresponsive to anti-TNFα antibodies (Shi and Ng, 2018). More specifically, a recent meta-analysis showed secondary loss of response occurs in approximately 33% of people taking infliximab and 41% of people taking adalimumab with a median follow up of 1 year (Qiu et al., 2017). These studies highlight the need for developing new therapeutics to treat IBD.

Anti-interleukin Biologics

Ustekinumab is a monoclonal antibody which binds the p40 subunit of IL-12 and IL-23 and acts as an antagonist (Feagan et al., 2016; Sands et al., 2019). People with CD who received ustekinumab had significantly higher clinical response rates in the UNITI-1 and UNITI-2 clinical trials compared to placebo (Feagan et al., 2016). People with UC who were treated with ustekinumab had significantly higher rates of achieving and maintaining clinical remission compared to placebo (Sands et al., 2019). The FDA approved ustekinumab for treatment of moderate to severe CD in September 2016, and for treatment of moderate to severe UC in October 2019.

Anti-integrin Biologics

Natalizumab

Natalizumab is a humanized monoclonal antibody that targets the α4 chain of the α4β1 and α4β7 integrins expressed on the surface of leukocytes (Leger et al., 1997; Stuve et al., 2006; Haanstra et al., 2013). α4β1 binds VCAM-1 expressed by endothelial cells, which allows leukocytes to firmly adhere to the surface (Alon et al., 1995; Cerutti and Ridley, 2017; Chae et al., 2018). Natalizumab blocks the interaction between α4β1 and VCAM-1, which is required for leukocytes to cross the blood-brain barrier into the central nervous system (CNS; Kumar et al., 1975; Burkly et al., 1991).

Natalizumab was first used successfully for the treatment of relapsing and remitting multiple sclerosis (MS; Polman et al., 2006; Rudick et al., 2006). In January 2008, natalizumab was also approved by the United States Food and Drug Administration (FDA) for treatment of CD (Guagnozzi and Caprilli, 2008). It was the first anti-adhesion biologic used to treat IBD and established evidence for the potential efficacy of blocking leukocyte trafficking to treat IBD. However, clinical trials and market distribution of natalizumab were discontinued due to reports that two people had developed progressive multifocal leukoencephalopathy (PML; Kleinschmidt-DeMasters and Tyler, 2005; Langer-Gould et al., 2005; Van Assche et al., 2005). PML is an aggressive demyelinating disease of the central nervous system (CNS) caused by the opportunistic John Cunningham (JC) virus, for which the majority of the population (75–80%) is seropositive. The recall of natalizumab prompted the retrospective analysis of samples from a deceased person with CD who had been treated with natalizumab in a separate clinical trial (Van Assche et al., 2005). The individual's serum and brain lesion samples were positive for JC virus, and there was a temporal relationship between natalizumab treatment and increase in viral load (Van Assche et al., 2005). Natalizumab was reapproved by the FDA and European Medicine Agencies (EMA) for the treatment of relapsing-remitting MS but it is not used for CD, due to risk of serious infections (European Medicines Agency, 2007; Ransohoff, 2007; Planas et al., 2014; Avasarala, 2015).

Vedolizumab

Vedolizumab is a humanized monoclonal antibody that was developed to reduce lymphocyte trafficking to the intestine by specifically targeting the α4β7 heterodimer, which is expressed on the surface of gut-specific lymphocytes (Soler et al., 2009; Feagan et al., 2013). In contrast to natalizumab, vedolizumab does not interfere with lymphocyte trafficking to the brain (Feagan et al., 2013).

Three Phase 3 clinical trials evaluated the efficacy and safety of vedolizumab for the induction and maintenance of clinical response and remission in people with moderate to severe UC (GEMINI 1) and CD (GEMINI 2 and GEMINI 3; Feagan et al., 2013; Sandborn et al., 2013; Sands et al., 2014). In the GEMINI 1 trial, 47.1% of people with UC had clinical responses by week 6 compared to 25.5% on placebo (Feagan et al., 2013). For the maintenance arm, 41.8% of people with UC who were treated with vedolizumab every 8 weeks and 44.8% of people with UC who were treated every 4 weeks maintained clinical remission at week 52 of the trial compared to only 15.9% of people with UC on placebo (Feagan et al., 2013). In the GEMINI 2 trial, 14.5% of people with CD who were treated with vedolizumab achieved clinical remission by week 6 compared to 6.8% on placebo (Sandborn et al., 2013). For the maintenance arm, 39.0% of people with CD who received vedolizumab every 8 weeks and 36.4% who received vedolizumab every 4 weeks were in clinical remission at 52 weeks, compared to 21.6% on placebo (Sandborn et al., 2013). In the GEMINI 3 trial, vedolizumab was subsequently shown to be effective for people who have moderate to severe CD and are refractory to TNF antagonists, but induction of remission required 10 weeks of treatment (Sands et al., 2014). Based on this, in May 2014, the FDA and European Medicines Agency (EMA) approved vedolizumab for the treatment of UC and CD (Raine, 2014).

VEDOLIZUMAB: POTENTIAL MECHANISMS OF ACTION

Vedolizumab was designed to reduce intestinal inflammation by interfering with the T-cell trafficking to the intestines (Picarella et al., 1997; Feagan et al., 2013). As mentioned earlier, α4β7 integrin is a receptor expressed on lymphocytes that recognizes MAdCAM-1 (Berlin et al., 1993). MAdCAM-1 is constitutively expressed on venular endothelium and upregulated during inflammation (Briskin et al., 1997). Though already approved by the FDA for treatment of UC and CD,

the molecular mechanisms of vedolizumab in humans have not been elucidated and still require further study.

In a study by Zeissig et al. (2019), T-cell trafficking to the intestinal lamina propria in people with CD and UC, who were treated with vedolizumab, was not reduced. Vedolizumab treatment did not affect the intestinal T-cell receptor repertoire or the relative abundance of lamina propria CD4+ T-cells, CD8+ T-cells, central memory T-cells, or effector memory T-cells. However, *in vitro* and *in vivo* models of intestinal inflammation have been used to investigate the potential effects of vedolizumab on T-cell migration to the intestine (Fischer et al., 2016; Binder et al., 2018). An inventive *in vitro* model of blood flow using glass tubes and a peristaltic pump to mimic blood flow through capillaries was highlighted by Binder et al. (2018). The model allowed for researchers to study the effects of vedolizumab treatment on integrin adhesion properties and expression in various T-cell subsets in a distinct, controlled environment (Binder et al., 2018). The group reported that vedolizumab treatment reduced the adhesion of CD4+ and CD8+ T-cells to MAdCAM-1 (Binder et al., 2018). Fischer et al. (2016) injected human T-cells or PBMCs into the ileocolic artery of mice lacking murine lymphocytes and NK cells. They demonstrated that vedolizumab specifically restricts the migration of Tregs from people with UC in this model but does not affect the migration of effector T-cells (Fischer et al., 2016). In contrast, Lord et al. (2018) reported differences in α4β7 expression on circulating lymphocytes, postulating that vedolizumab may preferentially block the recruitment of pro-inflammatory cells to the intestine. Moreover, because Tregs express less α4β7 than effector cells, they may be less affected by vedolizumab and successfully recruited to inflammatory sites where they suppress local inflammation (Lord et al., 2018). *Ex vivo* work with blood and colonic biopsies from people with IBD, published by Rath et al. (2018), suggests that vedolizumab treatment reduces α4β7 integrin expression on B cells, NK cells, Th1, Th2, and Th17 CD4+ T-cell subsets. In addition, vedolizumab therapy-induced clinical remission was associated with a reduction of α4β7 expression on Th2 and Th17 mucosal CD4+ T-cells, which together could reduce recruitment of pro-inflammatory cells to the gut mucosa. Moreover, Rath et al. (2018) suggested that higher α4β7 expression on T-cells before vedolizumab treatment was associated with clinical remission. Together these studies suggest that vedolizumab may act *via* selective inhibition of specific T-cell subtypes migrating to the gut.

Clahsen et al. (2015) reported the CD103+ (a subunit of the αEβ7 integrin) subpopulation of cDCs is reduced in MAdCAM-1 deficient mice. CD103+ cDCs play a role in inducing the expression of α4β7 integrin on T-cells and promoting Treg cell development. This may explain the observation made by Fischer et al. (2016) that Treg cell migration was reduced by vedolizumab. If vedolizumab treatment similarly results in fewer CD103+ cDCs, α4β7 expression would be reduced, limiting T-cell recruitment. Fuchs et al. (2017) found an association of αEβ7 expression on effector T-cells with worsened clinical parameters. They propose that αEβ7 upregulation may be an alternative pathway for lymphocytes beyond the α4β7-MAdCAM-1 axis (Fuchs et al., 2017). Furthermore, Zundler et al. (2017) reported that αEβ7 expression was increased on CD8+ T-cells following vedolizumab treatment in people with IBD, suggesting that lymphocytes may use an alternative integrin to ensure their localization in the intestine despite vedolizumab-mediated inhibition of α4β7. Together, this suggests that vedolizumab may indeed cause changes in T-cell recruitment. Though results of these studies suggest that vedolizumab restricts T-cell recruitment *via* integrin binding, there are limitations in the applicability of *in vitro* and *in vivo* animal models when studying vedolizumab, and additional work is required to translate these findings for people with IBD.

Alternative mechanisms of action in blocking monocyte and dendritic cell recruitment have been proposed (**Figure 1**). Zeissig et al. (2019) investigated the migration of leukocytes to the intestines by staining and labeling peripheral blood leukocytes with Indium-111 and fluorescein for scintigraphy and endomicroscopy. Imaging showed the accumulation of leukocytes in the intestines was not affected by vedolizumab. However, there was a strong association between vedolizumab treatment and the downregulation of genes involved in the innate immune system in the sigmoid colon. Genes that regulate innate effectors, innate immune receptors, chemokines, and chemokine receptors were downregulated in people with UC and CD who achieved clinical remission with vedolizumab. Interestingly, the relative abundance of inflammatory and wound-healing macrophages was also affected by vedolizumab treatment, skewing macrophages toward a healing phenotype (**Figure 1A**).

Conversely, vedolizumab treatment has also been reported to interfere with homing of non-classical monocytes, which skew toward wound-healing macrophages (Olingy et al., 2017; Schleier et al., 2020). Approximately 5% of non-classical monocytes express α4β7 integrin, so it has been suggested that vedolizumab may actually disrupt intestinal wound healing and lead to complications (Schleier et al., 2020). Despite that, Danese et al. (2019) found that people with moderate to severe CD who were treated with vedolizumab presented with endoscopic and histological healing at both 26 and 52 weeks. Furthermore, Shen et al. (2019) analyzed data from the GEMINI 1, GEMINI 2, GEMINI Long Term Safety studies, and Vedolizumab Global Safety Database, reporting only a minor difference in the frequency of postoperative complications after intestinal surgery in people treated with vedolizumab compared to placebo. Together, this suggests that the beneficial anti-inflammatory effects of vedolizumab may override concerns about a lack of recruitment of non-classical monocytes, compromised wound healing, and downstream complications.

Schippers et al. (2016) suggested that the therapeutic efficacy of vedolizumab is linked to changes in the innate immune system rather than the adaptive immune system. They reported that the β7-integrin chain leads to recruitment of more inflammatory monocytes to the colon in the dextran sodium sulfate (DSS) model of IBD. In this model, DSS is administered in the drinking water of mice to disrupt the intestinal epithelial layer. The compromised intestinal barrier allows the luminal microbes to interact with underlying immune cells, leading to colitis that models human UC. β7-integrin deficient mice had

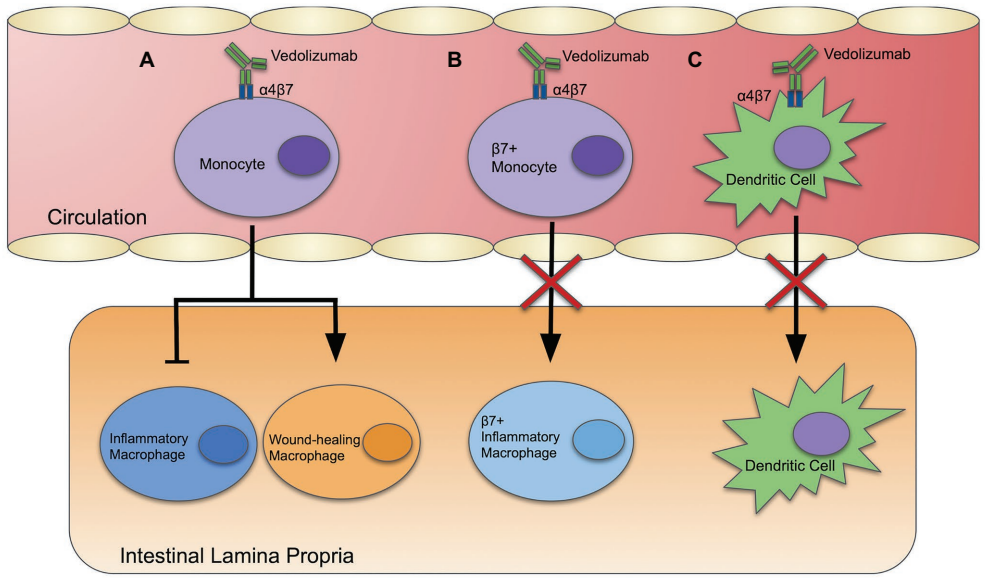

FIGURE 1 | Vedolizumab: three potential mechanisms of action. **(A)** Vedolizumab binds α4β7 integrin, which alters gene expression of blood monocytes, skewing the population toward a wound-healing phenotype, and away from an inflammatory phenotype. **(B)** Vedolizumab binds to α4β7 integrin on blood monocytes, thereby inhibiting their ability to enter the intestinal epithelium. **(C)** Vedolizumab blocks localization of cDC and pDCs in the intestinal epithelium by binding α4β7.

a lower disease activity index (DAI; an additive score based on weight loss, stool consistency, and fecal blood). Colonic mRNA expression of inducible nitric oxide synthase (iNOS), proinflammatory cytokines, such as IL-6 and TNFα, and the chemokine CCL2 was lower in β7-integrin deficient mice than wild-type mice. RAG2 deficient mice, which lack mature T and B cells (Shinkai et al., 1992), were more susceptible to DSS-induced colitis than their wild-type counterparts. β7-integrin deficiency protected DSS-treated RAG2 deficient mice and mice double deficient in β7 and RAG2 in DAI and histopathology (Schippers et al., 2016). This suggests that an anti-integrin therapy, like vedolizumab, may block the recruitment of proinflammatory monocytes to the site of inflammation (**Figure 1B**).

Mucosal addressin cellular adhesion molecule primarily interacts with the α4β7 integrin to mediate lymphocyte homing, including effector and memory T-cells. Clahsen et al. (2015) propose a novel role for MAdCAM-1 in mediating intestinal localization of DCs to the intestinal epithelium. They found that MAdCAM-1 deficient mice and β7-integrin deficient mice had lower numbers of cDCs and pDCs in the intestinal epithelium compared to wild-type mice. They propose that MAdCAM-1 may mediate localization of cDCs and pDCs into the gut *via* the α4β7 integrin. Thus, vedolizumab may work, in part, by blocking recruitment of DCs that promote inflammation (**Figure 1C**).

FUTURE DIRECTIONS

A long-term goal including a system wide analysis of the effect of vedolizumab on α4β7- and αEβ7-mediated trafficking, myeloid and T-cell populations in the intestine, and clinical outcomes would be of tremendous value in this field. Additionally, the possibility that selective T-cell trafficking is blocked by vedolizumab should continue to elucidate the effect of less abundant T-cell populations, like Tregs, and the important ratio of Tregs/effector T-cells in the gut after vedolizumab treatment. Vedolizumab may also work in part by blocking pro-inflammatory monocyte and dendritic cell recruitment. Further studies on the properties of leukocyte populations in relation to vedolizumab treatment for people with IBD should be conducted. Additional studies using data derived from people with IBD being treated with vedolizumab are essential to translate potential mechanisms elucidated *in vitro* and in murine models to people with IBD.

CONCLUSION

In this paper, we reviewed multiple proposed mechanisms of action for vedolizumab, a relatively new biologic used to treat IBD. It was specifically developed to block T-cell trafficking to the gut, but recent evidence suggests that this may not be its sole mechanism of action. Three alternative mechanisms of action have been reported. Zeissig et al. (2019) examined a mechanism where vedolizumab intervention led to the downregulation of inflammatory gene expression in innate immune cells like monocytes. Clahsen et al. (2015) described a mechanism in which the MAdCAM-1 interaction with α4β7 integrin of pDCs and cDCs is necessary for migration into the intestinal epithelium, where these dendritic cells have been known to exhibit pro-inflammatory phenotypes. Lastly, Schippers et al. (2016) demonstrated a mechanism whereby vedolizumab restricts the recruitment of β7+ effector monocytes to the intestinal epithelium, thereby limiting the inflammatory response. Understanding the mechanism(s) of action of vedolizumab may

enable us to improve the efficacy of current treatment and the develop new therapeutic strategies to treat IBD.

AUTHOR CONTRIBUTIONS

This concept for this work was created by LMS with contributions from ML-S, YP, and AZ. ML-S, YP, and AZ contributed equally to manuscript preparation. Figures were prepared by JS with contributions from ML-S, YP, AZ, and LMS. All authors contributed to the article and approved the submitted version.

FUNDING

This work was funded by an operating grant from the Canadian Institutes of Health Research (PJT-166100) awarded to LMS.

ACKNOWLEDGMENTS

LMS is a Biomedical Scholar of the Michael Smith Foundation for Health Research. AZ is supported by a Canada Graduate Scholarship – Master's program.

REFERENCES

Adegbola, S. O., Sahnan, K., Warusavitarne, J., Hart, A., and Tozer, P. (2018). Anti-TNF therapy in Crohn's disease. *Int. J. Mol. Sci.* 19:2244. doi: 10.3390/ijms19082244

Alon, R., Kassner, P. D., Carr, M. W., Finger, E. B., Hemler, M. E., and Springer, T. A. (1995). The integrin VLA-4 supports tethering and rolling in flow on VCAM-1. *J. Cell Biol.* 128, 1243–1253. doi: 10.1083/jcb.128.6.1243

Ananthakrishnan, A. N., Bernstein, C. N., Iliopoulos, D., Macpherson, A., Neurath, M. F., Ali, R. A. R., et al. (2018). Environmental triggers in IBD: a review of progress and evidence. *Nat. Rev. Gastroenterol. Hepatol.* 15, 39–49. doi: 10.1038/nrgastro.2017.136

Anderson, C. F., Gerber, J. S., and Mosser, D. M. (2002). Modulating macrophage function with IgG immune complexes. *J. Endotoxin Res.* 8, 477–481. doi: 10.1179/096805102125001118

Annacker, O., Coombes, J. L., Malmstrom, V., Uhlig, H. H., Bourne, T., Johansson-Lindbom, B., et al. (2005). Essential role for CD103 in the T cell-mediated regulation of experimental colitis. *J. Exp. Med.* 202, 1051–1061. doi: 10.1084/jem.20040662

Arseneau, K. O., and Cominelli, F. (2015). Targeting leukocyte trafficking for the treatment of inflammatory bowel disease. *Clin. Pharmacol. Ther.* 97, 22–28. doi: 10.1002/cpt.6

Avasarala, J. (2015). The TOUCH program and natalizumab: fundamental flaw in patient protection. *F1000Res.* 4:1450. doi: 10.12688/f1000research.7513.3

Bendjelloul, F., Maly, P., Mandys, V., Jirkovska, M., Prokesova, L., Tuckova, L., et al. (2000). Intercellular adhesion molecule-1 (ICAM-1) deficiency protects mice against severe forms of experimentally induced colitis. *Clin. Exp. Immunol.* 119, 57–63. doi: 10.1046/j.1365-2249.2000.01090.x

Berlin, C., Berg, E. L., Briskin, M. J., Andrew, D. P., Kilshaw, P. J., Holzmann, B., et al. (1993). Alpha 4 beta 7 integrin mediates lymphocyte binding to the mucosal vascular addressin MAdCAM-1. *Cell* 74, 185–195. doi: 10.1016/0092-8674(93)90305-a

Berndt, B. E., Zhang, M., Chen, G. H., Huffnagle, G. B., and Kao, J. Y. (2007). The role of dendritic cells in the development of acute dextran sulfate sodium colitis. *J. Immunol.* 179, 6255–6262. doi: 10.4049/jimmunol.179.9.6255

Binder, M. T., Becker, E., Wiendl, M., Schleier, L., Fuchs, F., Leppkes, M., et al. (2018). Similar inhibition of dynamic adhesion of lymphocytes from IBD patients to MAdCAM-1 by vedolizumab and etrolizumab-s. *Inflamm. Bowel Dis.* 24, 1237–1250. doi: 10.1093/ibd/izy077

Breese, E., Braegger, C. P., Corrigan, C. J., Walker-Smith, J. A., and MacDonald, T. T. (1993). Interleukin-2- and interferon-gamma-secreting T cells in normal and diseased human intestinal mucosa. *Immunology* 78, 127–131.

Briskin, M., Winsor-Hines, D., Shyjan, A., Cochran, N., Bloom, S., Wilson, J., et al. (1997). Human mucosal addressin cell adhesion molecule-1 is preferentially expressed in intestinal tract and associated lymphoid tissue. *Am. J. Pathol.* 151, 97–110.

Burkly, L. C., Jakubowski, A., Newman, B. M., Rosa, M. D., Chi-Rosso, G., and Lobb, R. R. (1991). Signaling by vascular cell adhesion molecule-1 (VCAM-1) through VLA-4 promotes CD3-dependent T cell proliferation. *Eur. J. Immunol.* 21, 2871–2875. doi: 10.1002/eji.1830211132

Cerutti, C., and Ridley, A. J. (2017). Endothelial cell-cell adhesion and signaling. *Exp. Cell Res.* 358, 31–38. doi: 10.1016/j.yexcr.2017.06.003

Chae, Y. K., Choi, W. M., Bae, W. H., Anker, J., Davis, A. A., Agte, S., et al. (2018). Overexpression of adhesion molecules and barrier molecules is associated with differential infiltration of immune cells in non-small cell lung cancer. *Sci. Rep.* 8:1023. doi: 10.1038/s41598-018-19454-3

Chen, M. L., and Sundrud, M. S. (2016). Cytokine networks and T-Cell subsets in inflammatory bowel diseases. *Inflamm Bowel Dis.* 22, 1157–1167. doi: 10.1097/MIB.0000000000000714

Chichlowski, M., and Hale, L. P. (2008). Bacterial-mucosal interactions in inflammatory bowel disease: an alliance gone bad. *Am. J. Physiol. Gastrointest. Liver Physiol.* 295, G1139–G1149. doi: 10.1152/ajpgi.90516.2008

Clahsen, T., Pabst, O., Tenbrock, K., Schippers, A., and Wagner, N. (2015). Localization of dendritic cells in the gut epithelium requires MAdCAM-1. *Clin. Immunol.* 156, 74–84. doi: 10.1016/j.clim.2014.11.005

Danese, S., Sandborn, W. J., Colombel, J. F., Vermeire, S., Glover, S. C., Rimola, J., et al. (2019). Endoscopic, radiologic, and histologic healing with vedolizumab in patients with active Crohn's disease. *Gastroenterology* 157, 1007.e1007–1018.e1007. doi: 10.1053/j.gastro.2019.06.038

DeNucci, C. C., Pagan, A. J., Mitchell, J. S., and Shimizu, Y. (2010). Control of alpha4beta7 integrin expression and CD4 T cell homing by the beta1 integrin subunit. *J. Immunol.* 184, 2458–2467. doi: 10.4049/jimmunol.0902407

European Medicines Agency. (2007). Questions and answers on the recommendation for the refusal of the marketing authorization for Natalizumab Elan Pharma. Available at: https://www.ema.europa.eu/en/documents/smop-initial/questions-answers-recommendation-refusal-marketing-authorization-natalizumab-elan-pharma_en.pdf (Accessed August 15, 2020).

Fais, S., Capobianchi, M. R., Pallone, F., Di Marco, P., Boirivant, M., Dianzani, F., et al. (1991). Spontaneous release of interferon gamma by intestinal lamina propria lymphocytes in Crohn's disease. Kinetics of in vitro response to interferon gamma inducers. *Gut* 32, 403–407. doi: 10.1136/gut.32.4.403

Fakhoury, M., Negrulj, R., Mooranian, A., and Al-Salami, H. (2014). Inflammatory bowel disease: clinical aspects and treatments. *J. Inflamm. Res.* 7, 113–120. doi: 10.2147/JIR.S65979

Feagan, B. G., Rutgeerts, P., Sands, B. E., Hanauer, S., Colombel, J. F., Sandborn, W. J., et al. (2013). Vedolizumab as induction and maintenance therapy for ulcerative colitis. *N. Engl. J. Med.* 369, 699–710. doi: 10.1056/NEJMoa1215734

Feagan, B. G., Sandborn, W. J., Gasink, C., Jacobstein, D., Lang, Y., Friedman, J. R., et al. (2016). Ustekinumab as induction and maintenance therapy for Crohn's disease. *N. Engl. J. Med.* 375, 1946–1960. doi: 10.1056/NEJMoa1602773

Fischer, A., Zundler, S., Atreya, R., Rath, T., Voskens, C., Hirschmann, S., et al. (2016). Differential effects of alpha4beta7 and GPR15 on homing of effector and regulatory T cells from patients with UC to the inflamed gut in vivo. *Gut* 65, 1642–1664. doi: 10.1136/gutjnl-2015-310022

Fuchs, F., Schillinger, D., Atreya, R., Hirschmann, S., Fischer, S., Neufert, C., et al. (2017). Clinical response to vedolizumab in ulcerative colitis patients is associated with changes in integrin expression profiles. *Front. Immunol.* 8:764. doi: 10.3389/fimmu.2017.00764

Fuss, I. J., Neurath, M., Boirivant, M., Klein, J. S., de la Motte, C., Strong, S. A., et al. (1996). Disparate CD4+ lamina propria (LP) lymphokine secretion profiles in inflammatory bowel disease. Crohn's disease LP cells manifest increased secretion of IFN-gamma, whereas ulcerative colitis LP cells manifest increased secretion of IL-5. *J. Immunol.* 157, 1261–1270.

GBD 2017 Inflammatory Bowel Disease Collaborators (2020). The global, regional, and national burden of inflammatory bowel disease in 195 countries and territories, 1990-2017: a systematic analysis for the global burden of disease study 2017. *Lancet Gastroenterol. Hepatol.* 5, 17–30. doi: 10.1016/S2468-1253(19)30333-4

Gorfu, G., Rivera-Nieves, J., and Ley, K. (2009). Role of beta7 integrins in intestinal lymphocyte homing and retention. *Curr. Mol. Med.* 9, 836–850. doi: 10.2174/156652409789105525

Guagnozzi, D., and Caprilli, R. (2008). Natalizumab in the treatment of Crohn's disease. *Biologics* 2, 275–284.

Guan, Q. (2019). A comprehensive review and update on the pathogenesis of inflammatory bowel disease. *J. Immunol. Res.* 2019:7247238. doi: 10.1155/2019/7247238

Haanstra, K. G., Hofman, S. O., Lopes Estevao, D. M., Blezer, E. L., Bauer, J., Yang, L. L., et al. (2013). Antagonizing the alpha4beta1 integrin, but not alpha4beta7, inhibits leukocytic infiltration of the central nervous system in rhesus monkey experimental autoimmune encephalomyelitis. *J. Immunol.* 190, 1961–1973. doi: 10.4049/jimmunol.1202490

Hausmann, M., Spottl, T., Andus, T., Rothe, G., Falk, W., Scholmerich, J., et al. (2001). Subtractive screening reveals up-regulation of NADPH oxidase expression in Crohn's disease intestinal macrophages. *Clin. Exp. Immunol.* 125, 48–55. doi: 10.1046/j.1365-2249.2001.01567.x

Hazel, K., and O'Connor, A. (2020). Emerging treatments for inflammatory bowel disease. *Ther. Adv. Chronic Dis.* 11:2040622319899297. doi: 10.1177/2040622319899297

Heinsbroek, S. E., and Gordon, S. (2009). The role of macrophages in inflammatory bowel diseases. *Expert Rev. Mol. Med.* 11:e14. doi: 10.1017/S1462399409001069

Heller, F., Florian, P., Bojarski, C., Richter, J., Christ, M., Hillenbrand, B., et al. (2005). Interleukin-13 is the key effector Th2 cytokine in ulcerative colitis that affects epithelial tight junctions, apoptosis, and cell restitution. *Gastroenterology* 129, 550–564. doi: 10.1016/j.gastro.2005.05.002

Himmel, M. E., Yao, Y., Orban, P. C., Steiner, T. S., and Levings, M. K. (2012). Regulatory T-cell therapy for inflammatory bowel disease: more questions than answers. *Immunology* 136, 115–122. doi: 10.1111/j.1365-2567.2012.03572.x

Hue, S., Ahern, P., Buonocore, S., Kullberg, M. C., Cua, D. J., McKenzie, B. S., et al. (2006). Interleukin-23 drives innate and T cell-mediated intestinal inflammation. *J. Exp. Med.* 203, 2473–2483. doi: 10.1084/jem.20061099

Jacobson, N. G., Szabo, S. J., Weber-Nordt, R. M., Zhong, Z., Schreiber, R. D., Darnell, J. E. Jr., et al. (1995). Interleukin 12 signaling in T helper type 1 (Th1) cells involves tyrosine phosphorylation of signal transducer and activator of transcription (stat)3 and Stat4. *J. Exp. Med.* 181, 1755–1762. doi: 10.1084/jem.181.5.1755

Jairath, V., and Feagan, B. G. (2020). Global burden of inflammatory bowel disease. *Lancet Gastroenterol. Hepatol.* 5, 2–3. doi: 10.1016/S2468-1253(19)30358-9

Johansson-Lindbom, B., Svensson, M., Pabst, O., Palmqvist, C., Marquez, G., Forster, R., et al. (2005). Functional specialization of gut CD103+ dendritic cells in the regulation of tissue-selective T cell homing. *J. Exp. Med.* 202, 1063–1073. doi: 10.1084/jem.20051100

Kaplan, G. G., Bernstein, C. N., Coward, S., Bitton, A., Murthy, S. K., Nguyen, G. C., et al. (2019). The impact of inflammatory bowel disease in Canada 2018: epidemiology. *J. Can. Assoc. Gastroenterol.* 2(Suppl. 1), S6–S16. doi: 10.1093/jcag/gwy054

Karttunnen, R., Breese, E. J., Walker-Smith, J. A., and MacDonald, T. T. (1994). Decreased mucosal interleukin-4 (IL-4) production in gut inflammation. *J. Clin. Pathol.* 47, 1015–1018. doi: 10.1136/jcp.47.11.1015

Kleinschmidt-DeMasters, B. K., and Tyler, K. L. (2005). Progressive multifocal leukoencephalopathy complicating treatment with natalizumab and interferon beta-1a for multiple sclerosis. *N. Engl. J. Med.* 353, 369–374. doi: 10.1056/NEJMoa051782

Koelink, P. J., Bloemendaal, F. M., Li, B., Westera, L., Vogels, E. W. M., van Roest, M., et al. (2020). Anti-TNF therapy in IBD exerts its therapeutic effect through macrophage IL-10 signalling. *Gut* 69, 1053–1063. doi: 10.1136/gutjnl-2019-318264

Kozicky, L. K., Menzies, S. C., Hotte, N., Madsen, K. L., and Sly, L. M. (2019). Intravenous immunoglobulin (IVIg) or IVIg-treated macrophages reduce DSS-induced colitis by inducing macrophage IL-10 production. *Eur. J. Immunol.* 49, 1251–1268. doi: 10.1002/eji.201848014

Kozicky, L. K., Zhao, Z. Y., Menzies, S. C., Fidanza, M., Reid, G. S., Wilhelmsen, K., et al. (2015). Intravenous immunoglobulin skews macrophages to an anti-inflammatory, IL-10-producing activation state. *J. Leukoc. Biol.* 98, 983–994. doi: 10.1189/jlb.3VMA0315-078R

Kumar, A. P., Wrenn, E. L. Jr., Fleming, I. D., Hustu, H. O., Pratt, C. B., and Pinkel, D. (1975). Preoperative therapy for unresectable malignant tumors in children. *J. Pediatr. Surg.* 10, 657–670. doi: 10.1016/0022-3468(75)90369-3

Langer-Gould, A., Atlas, S. W., Green, A. J., Bollen, A. W., and Pelletier, D. (2005). Progressive multifocal leukoencephalopathy in a patient treated with natalizumab. *N. Engl. J. Med.* 353, 375–381. doi: 10.1056/NEJMoa051847

Leger, O. J., Yednock, T. A., Tanner, L., Horner, H. C., Hines, D. K., Keen, S., et al. (1997). Humanization of a mouse antibody against human alpha-4 integrin: a potential therapeutic for the treatment of multiple sclerosis. *Hum. Antibodies* 8, 3–16.

Liu, J. Z., van Sommeren, S., Huang, H., Ng, S. C., Alberts, R., Takahashi, A., et al. (2015). Association analyses identify 38 susceptibility loci for inflammatory bowel disease and highlight shared genetic risk across populations. *Nat. Genet.* 47, 979–986. doi: 10.1038/ng.3359

Lord, J. D., Long, S. A., Shows, D. M., Thorpe, J., Schwedhelm, K., Chen, J., et al. (2018). Circulating integrin alpha4/beta7+ lymphocytes targeted by vedolizumab have a pro-inflammatory phenotype. *Clin. Immunol.* 193, 24–32. doi: 10.1016/j.clim.2018.05.006

McAlindon, M. E., Hawkey, C. J., and Mahida, Y. R. (1998). Expression of interleukin 1 beta and interleukin 1 beta converting enzyme by intestinal macrophages in health and inflammatory bowel disease. *Gut* 42, 214–219. doi: 10.1136/gut.42.2.214

Mehta, F. (2016). Report: economic implications of inflammatory bowel disease and its management. *Am. J. Manag. Care* 22(Suppl. 3), s51–s60.

Mosser, D. M., and Edwards, J. P. (2008). Exploring the full spectrum of macrophage activation. *Nat. Rev. Immunol.* 8, 958–969. doi: 10.1038/nri2448

Murch, S. H., Braegger, C. P., Walker-Smith, J. A., and MacDonald, T. T. (1993). Location of tumour necrosis factor alpha by immunohistochemistry in chronic inflammatory bowel disease. *Gut* 34, 1705–1709. doi: 10.1136/gut.34.12.1705

Muzaki, A. R., Tetlak, P., Sheng, J., Loh, S. C., Setiagani, Y. A., Poidinger, M., et al. (2016). Intestinal CD103(+)CD11b(−) dendritic cells restrain colitis via IFN-gamma-induced anti-inflammatory response in epithelial cells. *Mucosal Immunol.* 9, 336–351. doi: 10.1038/mi.2015.64

Nawroth, P. P., and Stern, D. M. (1986). Modulation of endothelial cell hemostatic properties by tumor necrosis factor. *J. Exp. Med.* 163, 740–745. doi: 10.1084/jem.163.3.740

Neurath, M. F., Fuss, I., Kelsall, B. L., Stuber, E., and Strober, W. (1995). Antibodies to interleukin 12 abrogate established experimental colitis in mice. *J. Exp. Med.* 182, 1281–1290. doi: 10.1084/jem.182.5.1281

Ogura, Y., Bonen, D. K., Inohara, N., Nicolae, D. L., Chen, F. F., Ramos, R., et al. (2001). A frameshift mutation in NOD2 associated with susceptibility to Crohn's disease. *Nature* 411, 603–606. doi: 10.1038/35079114

Olingy, C. E., San Emeterio, C. L., Ogle, M. E., Krieger, J. R., Bruce, A. C., Pfau, D. D., et al. (2017). Non-classical monocytes are biased progenitors of wound healing macrophages during soft tissue injury. *Sci. Rep.* 7:447. doi: 10.1038/s41598-017-00477-1

Oppmann, B., Lesley, R., Blom, B., Timans, J. C., Xu, Y., Hunte, B., et al. (2000). Novel p19 protein engages IL-12p40 to form a cytokine, IL-23, with biological activities similar as well as distinct from IL-12. *Immunity* 13, 715–725. doi: 10.1016/s1074-7613(00)00070-4

Park, K. T., Ehrlich, O. G., Allen, J. I., Meadows, P., Szigethy, E. M., Henrichsen, K., et al. (2020). The cost of inflammatory bowel disease: an initiative from the Crohn's & colitis foundation. *Inflamm. Bowel Dis.* 26, 1–10. doi: 10.1093/ibd/izz104

Park, S. C., and Jeen, Y. T. (2015). Current and emerging biologics for ulcerative colitis. *Gut Liver* 9, 18–27. doi: 10.5009/gnl14226

Perez-Jeldres, T., Tyler, C. J., Boyer, J. D., Karuppuchamy, T., Yarur, A., Giles, D. A., et al. (2019). Targeting cytokine signaling and lymphocyte traffic via small molecules in inflammatory bowel disease: JAK inhibitors and S1PR agonists. *Front. Pharmacol.* 10:212. doi: 10.3389/fphar.2019.00212

Picarella, D., Hurlbut, P., Rottman, J., Shi, X., Butcher, E., and Ringler, D. J. (1997). Monoclonal antibodies specific for beta 7 integrin and mucosal addressin cell adhesion molecule-1 (MAdCAM-1) reduce inflammation in

the colon of scid mice reconstituted with CD45RBhigh CD4+ T cells. *J. Immunol.* 158, 2099–2106.

Planas, R., Martin, R., and Sospedra, M. (2014). Long-term safety and efficacy of natalizumab in relapsing-remitting multiple sclerosis: impact on quality of life. *Patient Relat. Outcome Meas.* 5, 25–33. doi: 10.2147/PROM.S41768

Polman, C. H., O'Connor, P. W., Havrdova, E., Hutchinson, M., Kappos, L., Miller, D. H., et al. (2006). A randomized, placebo-controlled trial of natalizumab for relapsing multiple sclerosis. *N. Engl. J. Med.* 354, 899–910. doi: 10.1056/NEJMoa044397

Qiu, Y., Chen, B. L., Mao, R., Zhang, S. H., He, Y., Zeng, Z. R., et al. (2017). Systematic review with meta-analysis: loss of response and requirement of anti-TNFalpha dose intensification in Crohn's disease. *J. Gastroenterol.* 52, 535–554. doi: 10.1007/s00535-017-1324-3

Raine, T. (2014). Vedolizumab for inflammatory bowel disease: changing the game, or more of the same? *United European Gastroenterol J* 2, 333–344. doi: 10.1177/2050640614550672

Ransohoff, R. M. (2007). Natalizumab for multiple sclerosis. *N. Engl. J. Med.* 356, 2622–2629. doi: 10.1056/NEJMct071462

Rath, T., Billmeier, U., Ferrazzi, F., Vieth, M., Ekici, A., Neurath, M. F., et al. (2018). Effects of anti-integrin treatment with vedolizumab on immune pathways and cytokines in inflammatory bowel diseases. *Front. Immunol.* 9:1700. doi: 10.3389/fimmu.2018.01700

Rosen, M. J., Dhawan, A., and Saeed, S. A. (2015). Inflammatory bowel disease in children and adolescents. *JAMA Pediatr.* 169, 1053–1060. doi: 10.1001/jamapediatrics.2015.1982

Rosen, M. J., Karns, R., Vallance, J. E., Bezold, R., Waddell, A., Collins, M. H., et al. (2017). Mucosal expression of type 2 and type 17 immune response genes distinguishes ulcerative colitis from colon-only Crohn's disease in treatment-naive pediatric patients. *Gastroenterology* 152, 1345.e1347–1357.e1347. doi: 10.1053/j.gastro.2017.01.016

Rudick, R. A., Stuart, W. H., Calabresi, P. A., Confavreux, C., Galetta, S. L., Radue, E. W., et al. (2006). Natalizumab plus interferon beta-1a for relapsing multiple sclerosis. *N. Engl. J. Med.* 354, 911–923. doi: 10.1056/NEJMoa044396

Sandborn, W. J., Feagan, B. G., Rutgeerts, P., Hanauer, S., Colombel, J. F., Sands, B. E., et al. (2013). Vedolizumab as induction and maintenance therapy for Crohn's disease. *N. Engl. J. Med.* 369, 711–721. doi: 10.1056/NEJMoa1215739

Sands, B. E., Feagan, B. G., Rutgeerts, P., Colombel, J. F., Sandborn, W. J., Sy, R., et al. (2014). Effects of vedolizumab induction therapy for patients with Crohn's disease in whom tumor necrosis factor antagonist treatment failed. *Gastroenterology* 147, 618.e613–627.e613. doi: 10.1053/j.gastro.2014.05.008

Sands, B. E., Sandborn, W. J., Panaccione, R., O'Brien, C. D., Zhang, H., Johanns, J., et al. (2019). Ustekinumab as induction and maintenance therapy for ulcerative colitis. *N. Engl. J. Med.* 381, 1201–1214. doi: 10.1056/NEJMoa1900750

Schippers, A., Muschaweck, M., Clahsen, T., Tautorat, S., Grieb, L., Tenbrock, K., et al. (2016). Beta7-integrin exacerbates experimental DSS-induced colitis in mice by directing inflammatory monocytes into the colon. *Mucosal Immunol.* 9, 527–538. doi: 10.1038/mi.2015.82

Schleier, L., Wiendl, M., Heidbreder, K., Binder, M. T., Atreya, R., Rath, T., et al. (2020). Non-classical monocyte homing to the gut via alpha4beta7 integrin mediates macrophage-dependent intestinal wound healing. *Gut* 69, 252–263. doi: 10.1136/gutjnl-2018-316772

Schulz, O., Jaensson, E., Persson, E. K., Liu, X., Worbs, T., Agace, W. W., et al. (2009). Intestinal CD103+, but not CX3CR1+, antigen sampling cells migrate in lymph and serve classical dendritic cell functions. *J. Exp. Med.* 206, 3101–3114. doi: 10.1084/jem.20091925

Seyedian, S. S., Nokhostin, F., and Malamir, M. D. (2019). A review of the diagnosis, prevention, and treatment methods of inflammatory bowel disease. *J. Med. Life* 12, 113–122. doi: 10.25122/jml-2018-0075

Shen, B., Blake, A., Lasch, K., Smyth, M., and Bhayat, F. (2019). Vedolizumab use in patients with inflammatory bowel diseases undergoing surgery: clinical trials and post-marketing experience. *Gastroenterol. Rep.* 7, 322–330. doi: 10.1093/gastro/goz034

Shi, H. Y., and Ng, S. C. (2018). The state of the art on treatment of Crohn's disease. *J. Gastroenterol.* 53, 989–998. doi: 10.1007/s00535-018-1479-6

Shinkai, Y., Rathbun, G., Lam, K. P., Oltz, E. M., Stewart, V., Mendelsohn, M., et al. (1992). RAG-2-deficient mice lack mature lymphocytes owing to inability to initiate V(D)J rearrangement. *Cell* 68, 855–867. doi: 10.1016/0092-8674(92)90029-c

Sica, G. S., and Biancone, L. (2013). Surgery for inflammatory bowel disease in the era of laparoscopy. *World J. Gastroenterol.* 19, 2445–2448. doi: 10.3748/wjg.v19.i16.2445

Singh, U. P., Singh, N. P., Murphy, E. A., Price, R. L., Fayad, R., Nagarkatti, M., et al. (2016). Chemokine and cytokine levels in inflammatory bowel disease patients. *Cytokine* 77, 44–49. doi: 10.1016/j.cyto.2015.10.008

Soler, D., Chapman, T., Yang, L.-L., Wyant, T., Egan, R., and Fedyk, E. R. (2015). The binding specificity and selective antagonism of vedolizumab, an anti-a4ß7 integrin therapeutic antibody in development for inflammatory bowel diseases. *J. Pharmacol. Exp. Ther.* 330, 864–875. doi: 10.1124/jpet.109.153973

Smythies, L. E., Sellers, M., Clements, R. H., Mosteller-Barnum, M., Meng, G., Benjamin, W. H., et al. (2005). Human intestinal macrophages display profound inflammatory anergy despite avid phagocytic and bacteriocidal activity. *J. Clin. Invest.* 115, 66–75. doi: 10.1172/JCI19229

Steinbach, E. C., and Plevy, S. E. (2014). The role of macrophages and dendritic cells in the initiation of inflammation in IBD. *Inflamm. Bowel Dis.* 20, 166–175. doi: 10.1097/MIB.0b013e3182a69dca

Stritesky, G. L., Yeh, N., and Kaplan, M. H. (2008). IL-23 promotes maintenance but not commitment to the Th17 lineage. *J. Immunol.* 181, 5948–5955. doi: 10.4049/jimmunol.181.9.5948

Stuve, O., Marra, C. M., Jerome, K. R., Cook, L., Cravens, P. D., Cepok, S., et al. (2006). Immune surveillance in multiple sclerosis patients treated with natalizumab. *Ann. Neurol.* 59, 743–747. doi: 10.1002/ana.20858

Taylor, A., Verhagen, J., Blaser, K., Akdis, M., and Akdis, C. A. (2006). Mechanisms of immune suppression by interleukin-10 and transforming growth factor-beta: the role of T regulatory cells. *Immunology* 117, 433–442. doi: 10.1111/j.1365-2567.2006.02321.x

Van Assche, G., Van Ranst, M., Sciot, R., Dubois, B., Vermeire, S., Noman, M., et al. (2005). Progressive multifocal leukoencephalopathy after natalizumab therapy for Crohn's disease. *N. Engl. J. Med.* 353, 362–368. doi: 10.1056/NEJMoa051586

Wright, R. D., and Cooper, D. (2014). Glycobiology of leukocyte trafficking in inflammation. *Glycobiology* 24, 1242–1251. doi: 10.1093/glycob/cwu101

Yao, Y., Vent-Schmidt, J., McGeough, M. D., Wong, M., Hoffman, H. M., Steiner, T. S., et al. (2015). Tr1 cells, but not Foxp3+ regulatory T cells, suppress NLRP3 inflammasome activation via an IL-10-dependent mechanism. *J. Immunol.* 195, 488–497. doi: 10.4049/jimmunol.1403225

Zeissig, S., Rosati, E., Dowds, C. M., Aden, K., Bethge, J., Schulte, B., et al. (2019). Vedolizumab is associated with changes in innate rather than adaptive immunity in patients with inflammatory bowel disease. *Gut* 68, 25–39. doi: 10.1136/gutjnl-2018-316023

Zundler, S., Schillinger, D., Fischer, A., Atreya, R., Lopez-Posadas, R., Watson, A., et al. (2017). Blockade of alphaEbeta7 integrin suppresses accumulation of CD8(+) and Th9 lymphocytes from patients with IBD in the inflamed gut in vivo. *Gut* 66, 1936–1948. doi: 10.1136/gutjnl-2016-312439

Conflict of Interest: The authors declare that the research was conducted in the absence of any commercial or financial relationships that could be construed as a potential conflict of interest.

frontiers in Cell and Developmental Biology

BRIEF RESEARCH REPORT
published: 04 February 2021
doi: 10.3389/fcell.2021.625680

Effect of Physical Training on Exercise-Induced Inflammation and Performance in Mice

Luiz Alexandre Medrado de Barcellos[1†], William Antonio Gonçalves[2†], Marcos Paulo Esteves de Oliveira[2], Juliana Bohnen Guimarães[1], Celso Martins Queiroz-Junior[2], Carolina Braga de Resende[3], Remo Castro Russo[4], Cândido Celso Coimbra[4], Albená Nunes Silva[5], Mauro Martins Teixeira[6], Barbara Maximino Rezende[7†] and Vanessa Pinho[2*†]*

[1] Departamento de Ciências do Movimento Humano, Universidade do Estado de Minas Gerais (UEMG) – Unidade Ibirité, Ibirité, Brazil, [2] Departamento de Morfologia, Instituto de Ciências Biológicas (ICB), Universidade Federal de Minas Gerais (UFMG), Belo Horizonte, Brazil, [3] Hospital das Clínicas, Universidade Federal de Minas Gerais (UFMG), Belo Horizonte, Brazil, [4] Departamento de Fisiologia e Biofísica, Instituto de Ciências Biológicas (ICB), Universidade Federal de Minas Gerais (UFMG), Belo Horizonte, Brazil, [5] Laboratório de Inflamação e Imunologia do Exercício, Departamento de Educação Física, Escola de Educação Física da Universidade Federal de Ouro Preto, Ouro Preto, Brazil, [6] Departamento de Bioquímica e Imunologia, Instituto de Ciências Biológicas (ICB), Universidade Federal de Minas Gerais (UFMG), Belo Horizonte, Brazil, [7] Departamento de Enfermagem Básica, Escola de Enfermagem, Universidade Federal de Minas Gerais (UFMG), Belo Horizonte, Brazil

OPEN ACCESS

Edited by:
Zhichao Fan,
UCONN Health, United States

Reviewed by:
Katsuhiko Suzuki,
Waseda University, Japan
Nan Zhang,
Washington University in St. Louis, United States
Yuanzhen Suo,
Peking University, China

***Correspondence:**
Barbara Maximino Rezende
barbaramaximino@ufmg.br;
barbaramaximinorez@gmail.com
Vanessa Pinho
vpinhos@gmail.com

† These authors have contributed equally to this work

Specialty section:
This article was submitted to Cell Adhesion and Migration, a section of the journal Frontiers in Cell and Developmental Biology

Received: *03 November 2020*
Accepted: *18 January 2021*
Published: *04 February 2021*

Citation:
Barcellos LAM, Gonçalves WA, Esteves de Oliveira MP, Guimarães JB, Queiroz-Junior CM, Resende CB, Russo RC, Coimbra CC, Silva AN, Teixeira MM, Rezende BM and Pinho V (2021) Effect of Physical Training on Exercise-Induced Inflammation and Performance in Mice. Front. Cell Dev. Biol. 9:625680. doi: 10.3389/fcell.2021.625680

Acute exercise increases the amount of circulating inflammatory cells and cytokines to maintain physiological homeostasis. However, it remains unclear how physical training regulates exercise-induced inflammation and performance. Here, we demonstrate that acute high intensity exercise promotes an inflammatory profile characterized by increased blood IL-6 levels, neutrophil migratory capacity, and leukocyte recruitment to skeletal muscle vessels. Moreover, we found that physical training amplified leukocyte–endothelial cell interaction induced by acute exercise in skeletal muscle vessels and diminished exercise-induced inflammation in skeletal muscle tissue. Furthermore, we verified that disruption of the gp-91 subunit of NADPH-oxidase inhibited exercise-induced leukocyte recruitment on skeletal muscle after training with enhanced exercise time until fatigue. In conclusion, the training was related to physical improvement and immune adaptations. Moreover, reactive oxygen species (ROS) could be related to mechanisms to limit aerobic performance and its absence decreases the inflammatory response elicited by exercise after training.

Keywords: physical training, muscular inflammation, neutrophil, exercise, oxidative stress

INTRODUCTION

Inflammation is a natural process of mammalian immune responses to tissue damage, triggered by invading pathogens or sterile tissue injury. This response comprises temporally and spatially orchestrated events in which inflammatory cells and mediators act to interrupt harmful stimuli and induce tissue repair, promoting a return to homeostasis (Medzhitov, 2010; Alessandri et al., 2013). Exercise-induced inflammation has been shown to be an essential for restoring homeostasis and improving physical capacity (Deyhle et al., 2015). During exercise, muscle resident cells and vascular endothelium release inflammatory mediators that generate chemotactic signals, which drive leukocyte trafficking to muscular tissue (Kolaczkowska and Kubes, 2013). The presence of these cells is associates with loss of muscular architecture after exercise (Ogilvie et al., 1988;

Hortobagyi et al., 1998). This effect could be induced by metabolic processes characterized by events involving oxidative stress (Barbieri and Sestili, 2012).

Oxidative stress induced by reactive oxygen species (ROS) is increased by muscular contraction (Jackson et al., 2007) and is able to prolong muscular inflammation induced by acute exercise. Several studies have indicated that ROS produced during the exercise are required to activate signal transduction pathways in inflammation mechanisms and have an essential role in the physiological adaptive process in muscle cells (Barbieri and Sestili, 2012). An increase in antioxidant capacity through the intake of nutritional supplements appears to reduce exercise-induced muscle damage and may improve performance and recovery (Child et al., 1999; Taherkhani et al., 2020). However, whether training is able to provoke an adaptation in the inflammatory response induced by exercise and whether ROS are important to this process remain unclear. Thus, the present study aimed to assess the influence of physical training on inflammation and physical performance and the role of ROS in this process.

MATERIALS AND METHODS

Ethics Statement

The animal care and handling procedures were in accordance with the guidelines of the Institutional Animal Care and Use Committee, and the study received prior approval from Animal Ethics Committee of Universidade Federal de Minas Gerais (UFMG; protocol 7412/2012).

Mice

Eight to twelve weeks-old wild-type C57BL/6 male mice were obtained from the Centro de Bioterismo (UFMG) and gp91^{phox} knockout C57BL/6 male mice were provided from Jackson Farms (Glensville, NJ, United States) and maintained at our laboratory. All mice were housed under standard conditions in a temperature-controlled room (23 ± 1°C) on an automatic 12 h/12 h light/dark cycle and had free access to commercial rodent food and water.

Running Treadmill Familiarization

Running treadmill familiarization was performed on different treadmills (LE400, Panlab, Harvard Apparatus, Cornella, Spain or Gaustec Magnetismo, Nova Lima, MG, Brazil) according to each design as previous protocols (Lacerda et al., 2005; Primola-Gomes et al., 2007).

Incremental-Speed Running Test Until Fatigue

An incremental-speed running test until fatigue on a treadmill (LE400, Panlab, Harvard Apparatus, Cornella, Spain) was performed to assess the peak speed (S_{peak}). All these incremental running tests were performed at least 24 h after the last familiarization session. During this test, the mice began running at 6 m min^{-1} and the speed was increased by 3 m min^{-1} every 3 min at 5° slope until fatigue (Ferreira et al., 2007). Fatigue was defined as the moment at which the animals were unable to maintain their pace with the treadmill speed for at least 10 s, even when exposed to slight electrical stimulation.

Rest and Low or High Intensity Exercise

Wild-type C57BL/6 male mice were allocated into three groups, rest, low intensity (40% of S_{peak}), or high intensity (80% of S_{peak}) of exercise on the treadmill to analyze oxygen consumption (VO_2) (LE400, Panlab, Harvard Apparatus, Cornella, Spain). The exercise intensity was calculated from S_{peak} achieved in the incremental speed-running test until fatigue. Each exercise or rest lasted 30 min. The slope of the treadmill was maintained at 5°. All these procedures were performed at least 48 h after the incremental-speed running test until fatigue.

Fixed-Speed Running Test Until Fatigue

The workload and the VO_2 of the mice at fixed-speed running test until fatigue on treadmill was evaluated (LE400, Panlab, Harvard Apparatus, Cornella, Spain) pre (at least 48 h after incremental-speed running test until fatigue) and post 4 weeks aerobic training (at least 48 h after the last training session). The intensity of this test corresponded to 80% of the S_{peak} achieved at incremental-speed running test until fatigue and the treadmill slope adopted was also 5°. The workload attained in the fixed-speed running test was used as a reference for the load prescription in the exercise sessions throughout the aerobic training.

Physical Training Protocol

In all procedures involving training the mice were randomized allocated into sedentary or trained experimental groups. The trained group was submitted to exercise on a treadmill (Gaustec Magnetismo, Nova Lima, MG, Brazil) across 4 weeks, with 5 weekly sessions always performed at the same time of the day (8:00 a.m. to 10:00 a.m.). The slope of the treadmill was maintained at 5° throughout the training protocol. To ensure similar handling and exposure for each treadmill setup, the sedentary group mice performed an exercise at a speed of 6 m min^{-1} with maximal duration of 5 min, which was adjusted daily according to the body mass of the mice. The aerobic training load from the first to the last week was equivalent to 60, 70, 80, and 90% of the workload (%W) performed in the fixed-speed running test until fatigue prior to the 4 weeks aerobic training.

VO_2 Measurement

VO_2 was measured via open-flow indirect calorimeter (LE400, Panlab, Harvard Apparatus, Cornella, Spain) calibrated with a certified gas mixture (high O_2 = 50.05%, high CO_2 = 1.51%, low O_2 = 20.02% and low CO_2 = 0.00%). The air flow rate established was equivalent to 0.6 L min^{-1} throughout the procedures. VO_2 data were analyzed using a computerized system (Metabolism software version 2.2.01 Panlab, Harvard Apparatus), transformed to milliliters per minute and relativized by the mice body mass (mLO_2 kg$^{-0.75}$ min^{-1}).

Body Mass

The percentage of the body mass variation was calculated by the difference between the weight of the mouse before the second test (post training) and the weight before the first test (pre training) divided by the pre training weight, multiplied by 100.

Assessment of Pulmonary Mechanics

Pulmonary dysfunction was measured as we previously described (Campa et al., 2018; Russo et al., 2018). For invasive *in vivo* assessment, mice were anesthetized and tracheostomized, then were placed in a whole-body plethysmograph to maintain spontaneous breathing connected to a computer-controlled ventilator (Forced Pulmonary Maneuver System®, Buxco Research Systems©, Wilmington, North Carolina, United States). Under mechanical respiration the Dynamic Compliance (Cdyn) and Lung Resistance (Rl) were determined by Resistance and Chord Compliance RC test. To measure the Inspiratory Capacity (IC) a Pressure-Volume maneuver was performed, which inflates the lungs to a standard pressure of +30 cm H_2O and then slowly exhales until a negative pressure of −30 cm H_2O is reached. To evaluate airway hyperresponsiveness (AHR), the same mice used in previous maneuvers (basal condition) received Methacholine, 1 mg Kg^{-1} (Acetyl-β-methylcholine chloride, A-2251, Sigma-Aldrich St. Louis, MO, United States) i.v. and after 10 s, a new set of maneuvers were conducted to assess Rl changes. Suboptimal maneuvers were rejected and for each test at least three acceptable maneuvers were conducted in every single mouse to obtain a reliable mean for all numeric parameters.

Intravital Microscopy

The mice were anesthetized, and the femoral straight muscle venules were exposed by a resection in the anterior part of the thigh for exhibition of the femoral straight muscle. The animals received an i.v. injection from Rodamin 6G (0.3 mg kg^{-1}, Sigma-Aldrich, Germany) to fluorescent labeling of leukocytes. An intravital microscope (ECLIPSE 50i; Nikon) with a 20 objective lens was used to examine the muscle microcirculation. A digital camera (DS-Qi1MC; Nikon) was used to acquire the images that were recorded for playback analysis with Nikon imaging software. The counting of rolling and adherent leukocytes was realized according to our previously published method (Rezende et al., 2017). Rolling leukocytes was defined as those cells moving thought the observed field at a velocity less than that of erythrocytes within a given vessel during 1 min. Leukocyte was considered to be adherent if it remained stationary for at least 30 s, and total leukocyte adhesion is quantified as the number of adherent cells within a 100 μm length of venule in 1 min.

Quantification of Cytokines

Hundred milligrams of the quadriceps muscle (wet) were separated and homogenized with PBS containing antiproteases (0.1 mM PMSF, 0.1 nM hydrochloric benzethonium, 10 mM EDTA and 20 Ki aprotinin A) and 0.05% Tween 20. The samples were centrifuged for 10 min, at 10,000 rpm and at 4°C. The supernatant was used for the ELISA assay with a 1: 4 dilution. The ELISA assay was performed according to the manufacturer's instructions (R&D System) and quantified from the 492 nm wavelength acquired in a plate reader (Spectramax plus 384, Molecular Devices, United States).

Histology

Left femoral quadriceps was sectioned transversely in half, with the proximal half placed in O.C.T (Tissue-Tek®; Sakura, Netherlands) at −25°C. The tissues were sliced at 10 μm thickness using a cryostat (Leica CM1850, Leica Biosystems, Germany), immediately placed on silanized slide and fixed for 1 h in acetone at −80°C. The tissue sections were stained with HE according to standard histological technique and evaluated histologically in a blinded manner. The following parameters were evaluated and classified as absent, mild, moderate, or intense: fiber atrophy (morphological alteration), muscle necrosis/degeneration, inflammatory infiltrate in the endomysium/perimysium, endomysium/perimysium distension. These criteria were first described by Rizo-Roca et al. (2015).

Neutrophil Chemotaxis Assays

Neutrophil chemotaxis assay was performed using a modified Boyden chamber (Neuroprobe, Pleasanton, United States) and polycarbonate filters (4 μm; Neuroprobe, Pleasanton, United States) as previously described by Tavares-Murta et al. (2002). Bone marrow neutrophils were isolated and submitted to chemotactic stimulus with 28 μL of N-formyl-methionyl-leucyl-phenylalanine (fMLP). On one side of the membrane, the fMLP was placed, and on the other, a suspension of 1.0×10^6 neutrophils/mL. After 60 min of incubation at 37°C, the filter was removed, washed and fixed in methanol. Then, the membranes were stained in panotic for microscopic counting. Five random fields per sample were selected on the membrane to count cell migration.

Statistical Analysis

Data are expressed as mean ± SEM. The normal distribution was verified by the Shapiro-Wilk test. Comparisons among the groups were performed by unpaired Student's *t*-test, one-way ANOVA or two-way ANOVA followed by the Tukey or Sidak *post hoc* analysis, whenever applicable. Statistical significance was set as $p < 0.05$. The statistical package used was GraphPad Software's Prism 6®.

RESULTS

The magnitude and amount of stress induced by movement are important factors for morphological and functional changes in the body. We first determined the exercise intensity required to induce an efficient acute response during a single exercise session consisting of running on a treadmill. We observed that high intensity exercise (80% of the S_{peak}) triggered an aerobic demand that increased in a time dependent manner. This was observed as a gradual increase in oxygen consumption (VO_2) during the course of exercise (**Figure 1A**). Low exercise intensity (40% of the S_{peak}) was unable to induce significant changes in VO_2 (**Figure 1A**). Moreover, we found increased muscular levels

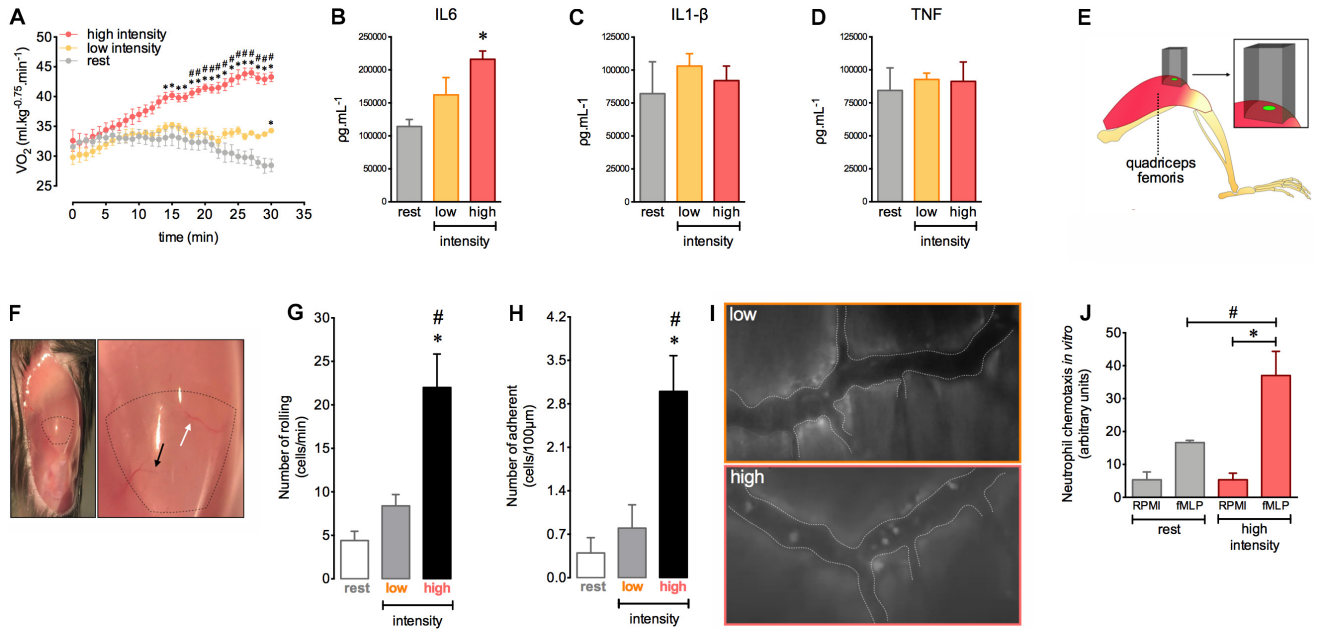

FIGURE 1 | Homeostasis disruption by exercise induces leukocyte recruitment and late alteration of IL-6 balance in quadriceps muscles. VO_2 immediately before and during 30 min at rest (n = 5) or at low (n = 5) and at high (n = 6) intensity exercises **(A)**. IL-6 **(B)**, IL-1β **(C)**, and TNF **(D)** levels in the quadriceps femoris 12 h after rest (n = 4) or low (n = 4) and high intensity (n = 4) exercises. Neutrophil chemotaxis by Boyden chamber assay. Bone marrow isolated-neutrophils (1×10^6 cells/ml) from rest (n = 3) or high intensity (n = 3) groups stimulated by fMLP (28 μl) **(E)**. The light beam from intravital microscopy targeting the distal region of the quadriceps femoris for intravital analysis **(F)**. Exposed quadriceps for intravital experiment **(G)**. The most (black arrows) and least (white arrows) frequently accessed vessels in the delimited region of the quadriceps. Leukocyte rolling **(H)** and adhesion **(I)** on microvasculature 12 h after rest (n = 5), low (n = 5) or high intensity (n = 6). Representative figure showing the vessel (dotted white line) and leukocytes (luminous bodies) quantified in **(H–J)**. Data are expressed as mean ± SEM; $^*p < 0.05$ compared to: rest **(A,B,H,I)** and RPMI high intensity group **(E)** and $^\#p < 0.05$ compared to: low intensity group **(A,H,I)** and fMLP rest group **(E)** using two-way ANOVA **(A)** or one-way ANOVA **(B–E,H,I)** followed by Tukey *post hoc* analysis.

of IL-6 after 12 h in mice subjected to high intensity exercise (**Figure 1B**). The levels of IL1-β and TNF-α were similar in all groups (**Figures 1C,D**).

Given the importance of the immune response during physical training, we next evaluated the interactions between leukocytes and muscle microvasculature after a single exercise session at different intensities. We assessed a specific distal region of the quadriceps femoris, localized near the rectus femoris tendon (**Figure 1E**). To ensure reproducibility and to reduce variability during measurements, we chose two vessels in this muscle region to better track the vessels during intravital microscopy analysis (**Figure 1F**). We observed an increase in leukocyte rolling and adhesion in the muscular vessels after 12 h in the group subjected to high intensity exercise (**Figures 1G–I**). We also found increased neutrophil chemotaxis toward chemotactic factor fMLP *ex vivo* using cells purified from the bone marrow of exercised mice (**Figure 1J**). Together, these results indicate that high intensity exercise applied by running on a treadmill offers the optimal conditions to provoke an important inflammatory response in muscular tissue.

Our experimental design (**Figure 2A**) was able to induce several adaptations in mice. Of note, the proposed aerobic training protocol offered a gradual increase in the load based on a targeted workload for each training session (**Figure 2B**, for more details see section "Materials and Methods"). Here, this experimental approach was efficient to elicit consistent change in mice aerobic status. We observed that mice increased the workload and total running distances in aerobic tests after the training period (**Figures 2C,D**, respectively). Moreover, the body mass variation in trained mice was less pronounced compared to the sedentary group (**Figure 2E**). These consistent alterations in aerobic status and control of the increase in body mass were accompanied by enhanced lung function in response to stressful exercise. We observed that 72 h after a single exercise session under fatigue conditions, the sedentary mice group displayed reduced inspiratory capacity and compliance (Cchord) in response to stressful exercise and an increased sensitivity to bronchoconstriction evoked by methacholine injection. However, the trained mice did not present this impact of stressful exercise, showing preserved inspiratory capacity and compliance accompanied by reduced airway hyper reactivity induced by methacholine (**Figures 2F–H**, respectively). No changes in the basal resistance were observed (**Figure 2I**).

The aerobic training protocol was able to induce inflammatory response adaptations in muscular tissue. After 12 h of the fixed-speed running test there was an increase in both rolling and adhesion of leukocytes in muscle vessels of trained mice (**Figures 3A–C**). Nevertheless, 72 h after this test the loss in muscular architecture and the increase of inflammatory

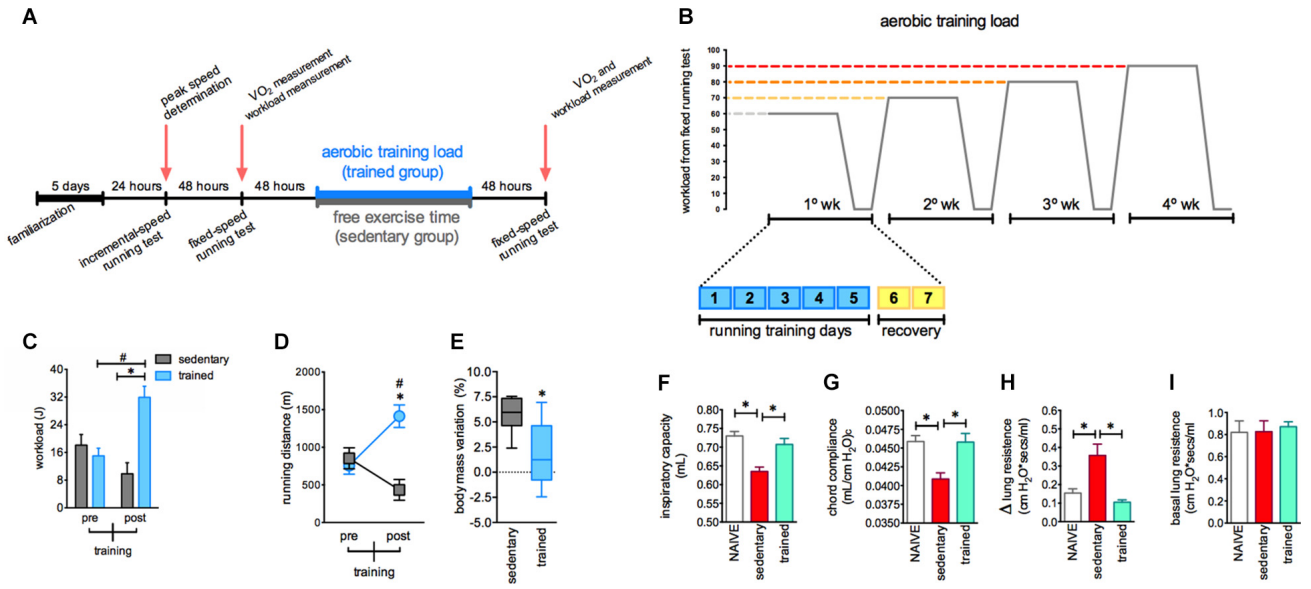

FIGURE 2 | The aerobic training changes body mass gain dynamics, aerobic performance and respiratory mechanics in mice. Schematic diagram for experimental approach visualization **(A)**. Aerobic training load characteristics **(B)**. Workload **(C)** and running distance **(D)** evaluated pre and post aerobic training in both sedentary (n = 7) and trained (n = 8) groups. Body mass variation in sedentary and trained groups **(C)**. Inspiratory capacity **(F)**, chord compliance **(G)**, lung resistance **(H)**, and basal lung resistance **(I)** in the naive (n = 8), sedentary (n = 6) and trained groups (n = 8) evaluated 72 h after the fixed-speed running test until fatigue post training. Data are expressed as mean **(C,D,F–I)** or min to max in the box plot graph **(E)** ± SEM. $^{*}p < 0.05$ compared to: sedentary post **(C)**; trained pre **(D)**; sedentary **(E–I)** and $^{\#}p < 0.05$ compared to: trained pre **(C)**; sedentary post **(D)** using two-way ANOVA following by Sidak *post hoc* analysis **(C,D)**, two-tailed *t*-test **(E)** or one-way ANOVA followed by Tukey's *post hoc* analysis **(F–I)**.

cells were more pronounced in sedentary than trained mice (**Figures 3D,E**). These results indicated that the profile of inflammatory response induced by exercise exhibited by trained mice could be important to the subsequent recovery of muscular tissue. Moreover, we demonstrated that trained mice presented a slight alteration in cellular profile with an increase in the blood CD8 + lymphocytes and a decrease in the bone marrow macrophages F4/80 + (**Supplementary Figures 1D,G**, respectively). We not observed any alterations in other leukocytes recovered in either blood (**Supplementary Figures 1A–C**) or bone marrow (**Supplementary Figure 1F,H,I**).

To verify the influence of ROS production on aerobic status after training and in leucocyte interactions with the muscular vasculature after exercise, we used gp91$^{phox-/-}$ mice, which are animals with non-functional NADPH-oxidase. Trained mice showed a higher VO_2 at the moment of fatigue than sedentary mice. Furthermore, it was observed that physical training improved the time to fatigue in both WT and gp91$^{phox-/-}$ as demonstrated by the higher workload achieved in the fixed-running test compared to the respective sedentary mice. However, exercise interruption post training was delayed for gp91$^{phox-/-}$ trained mice compared to WT trained mice (**Figure 4A**). In addition, the lack in ROS production potentializes the improvement in the running performance induced by aerobic training, which could be evidenced by the superior increase of workload realized by gp91$^{phox-/-}$ trained mice compared to workload of WT trained mice (**Figure 4B**). In contrast, the increase of rolling and adhesion expected 12 h after a single exercise session was inhibited in trained mice with a deficiency of ROS production (**Figures 4C–E**).

DISCUSSION

Although it has been established that a single session of intense exercise is able to induce a considerable local and systemic inflammatory response, which could be reduced by short period of exercise repetition (Suzuki et al., 1996, 1999), little is known about the chronic effects of the training process on exercise-induced inflammation. The results found in this study can be summarized by the following points: acute high intensity exercise induced an important inflammatory response in the muscular tissue as demonstrated by (1) increases in the level of IL-6 in muscle, the amplified number of rolling and adhesion cells in the quadriceps vessels, and the stimulation of neutrophil chemotactic activity isolated from bone marrow in exercised mice. Moreover, we developed an effective running training for mice that was able to induce several adaptations, including (2) elevated workload and running distances reached in aerobic tests after the training period accompanied by reduced gains in body mass; (3) enhanced lung function; (4) high number of rolling and adherent cells on muscle vessels, but preserved quadriceps muscular architecture with a predominance of mononuclear cells. Finally, the deficiency in ROS production by NADPH oxidase enzyme (5) potentialized the improvement in the running performance induced by

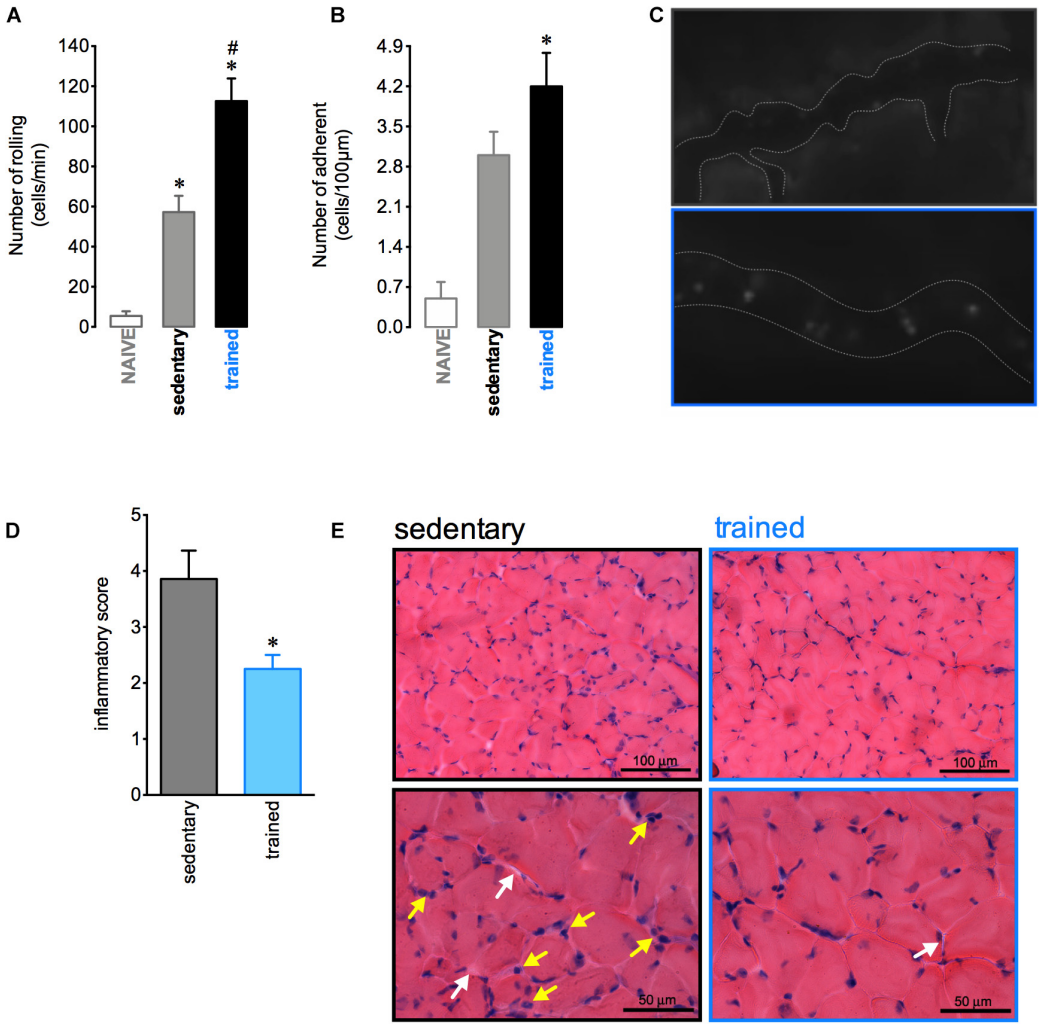

FIGURE 3 | Aerobic training changes the inflammatory response in the muscle. Quantification of leukocyte rolling **(A)** and adhesion **(B)** on microvasculature of the naive (n = 6), sedentary (n = 5), and trained (n = 6) mice 12 h after the fixed-speed running test until fatigue post training. Representative figure showing the vessel (dotted white line) and leukocytes (luminous bodies) quantified in **(A–C)**. Histopathological quantification **(D)** and representative histological slide from H&E staining **(E)** of muscular tissue samples from sedentary (n = 7) or trained (n = 5) mice 72 h after the fixed-speed running test until fatigue post training. The yellow and white rows represent the inflammatory cells and endomysium distension, respectively. Data are expressed as mean ± SEM; $^{*}p < 0.05$ compared to: naive **(A,B)** or sedentary group **(D)** and $^{\#}p < 0.05$ compared to: sedentary group **(A)** using one-way ANOVA followed by Tukey's *post hoc* analysis **(A,B)** or two-tailed t-test **(C,D)**.

physical training, and (6) diminished the rolling and adhesion cells related to exercise.

In this work, the intensity of exercise was decisive in stimulating the muscle IL-6 synthesis assessed 12 h post exercise. Muscle production of IL-6 is related to the exercise mode, intensity, and duration (Nieman et al., 1998; Ostrowski et al., 2001). Muscle-produced IL-6 may act on skeletal muscle, in a paracrine manner, by regulating myogenesis, glucose uptake and use of glycogen by the contracting muscle and also exert systemic effects such as increased hepatic glucose production and lipolysis, when released into the circulation (Fischer, 2006; Serrano et al., 2008). Circulating IL-6 normally increases immediately in response to contracting muscle and declines in the post-exercise period (Suzuki et al., 2002). Raised plasma IL-6 after exercise may a play role in neutrophil mobilization into the circulation (Yamada et al., 2002). In fact, the kinetics of IL-6 may be different depending on whether there was muscle damage induced by exercise (Febbraio and Pedersen, 2002; Petersen and Pedersen, 2006). Thus, it is suggested that the highest level of IL-6 in the muscle 12 h after the exercise event could originate from immune cells present in the damaged muscle during high-intensity exercise. We also observed that acute high intensity exercise induced elevation of the number of rolling and adherent cells in the muscle vasculature. It is well established that prolonged exercise is associated with high levels of oxidative stress that stimulate the inflammatory response. This inflammation may result from muscle damage triggered by mechanical and metabolic exercise loads (Barbieri and Sestili, 2012). Previous notable results from our group also showed the interaction of neutrophils with endothelial cells in

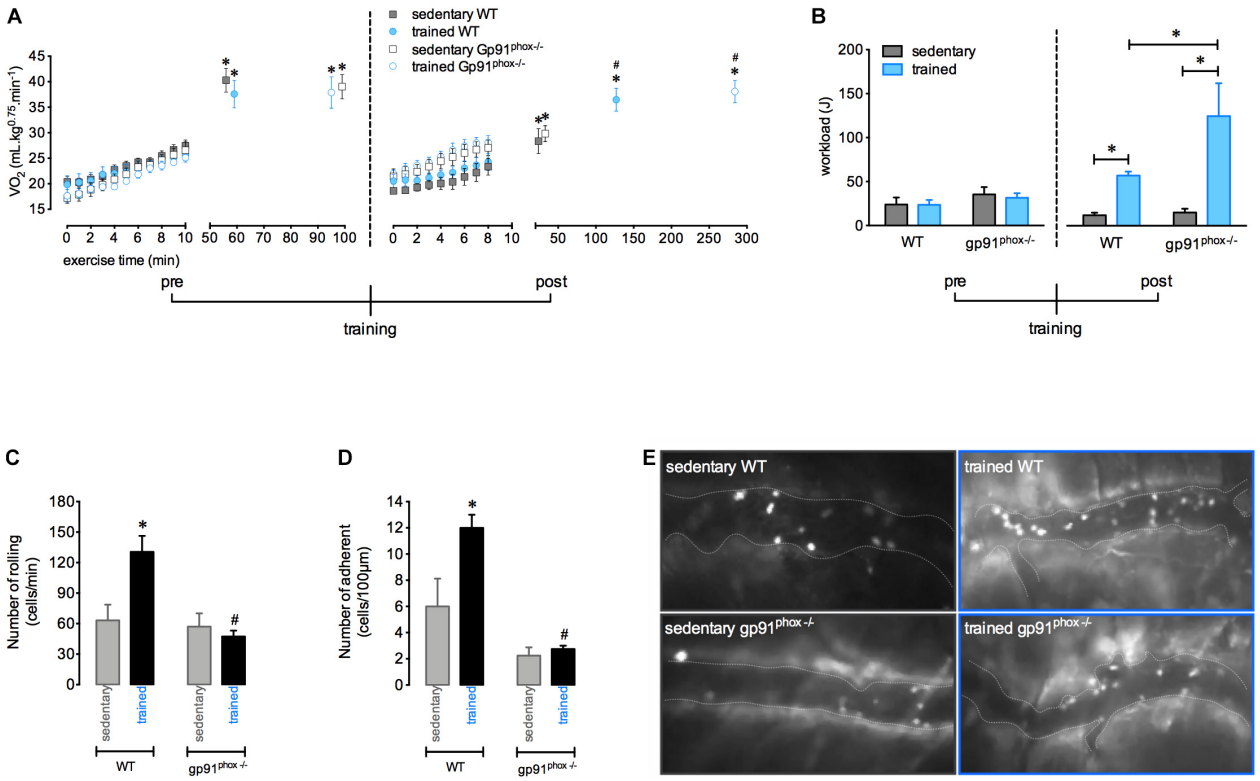

FIGURE 4 | The absence of ROS from NADPH-oxidase increases running capacity and abrogates the greater exercise-induced leukocyte interaction on vasculature after aerobic training. VO_2 immediately before and during the fixed-running test until fatigue in the wild-type (sedentary, $n = 7$ and trained, $n = 6$) and gp91$^{phox-/-}$ (sedentary, $n = 5$ and trained, $n = 4$) groups, pre and post aerobic training **(A)**. Workload pre- and post-aerobic training in all groups **(B)**. Leukocytes rolling **(C)** and adhesion **(D)** on microvasculature 12 h after the fixed-speed running test until fatigue in all groups. Representative figure showing the vessel (dotted white line) and leukocytes (luminous bodies) quantified in **(C–E)**. Data are expressed as mean ± SEM; $^{*}p < 0.05$ compared to: 0 min **(A)** and respective sedentary groups **(B–D)** and $^{\#}p < 0.05$ compared to: respective sedentary **(A)** and respective trained groups **(C,D)** using two-way ANOVA followed by Tukey's *post hoc* analysis.

quadriceps muscles after exercise until fatigue by using intravital microscopy, corroborating our findings. We found that high intensity exercise stimulated the *ex vivo* migratory capacity of neutrophils isolated from bone marrow 12 h post-exercise. The migration of neutrophils from bone marrow to the circulation is influenced by stress hormones, G-CSF and cytokines released during exercise (Suzuki et al., 2000; Yamada et al., 2002; Summers et al., 2010). Additionally, it has been showed that aerobic exercise mobilizes hematopoietic stem cells in an intensity-dependent manner (Baker et al., 2017). However, the precise mechanisms by which exercise inflammation leads to hematopoiesis and consequently neutrophilia still need to be better elucidated.

We demonstrated an effective protocol of running training for mice that was able to improvement of physical capacity and pulmonary function, including inspiratory capacity, chord compliance, and lung resistance. It has been previously shown that pulmonary capability is correlated with exercise tolerance (Kerti et al., 2018) and it may be associated with our results from the elevated workload and running distances reached in the aerobic tests after the training period.

Interestingly, although we observed a greater number of rolling and adherent cells in trained mice compared to sedentary mice, this result was accompanied by a lower inflammatory score in the quadriceps of the trained group, with a predominance of mononuclear cells. Usually, neutrophils infiltrate the extracellular space around the damage, peaking between 6 and 24 h after exercise. Subsequently, there is an increase of pro-inflammatory macrophages within 72 h followed by an influx of macrophages with anti-inflammatory and pro-myogenic phenotypes, which may remain for more than 6 days after damage (Saini et al., 2016). In the present study, reduced muscular inflammation infiltration and endomysium distension indicate less tissue damage, which may be related to mononuclear cells with anti-inflammatory properties, but the profile and role of these cells in muscle repair were not investigated here. Exercise is accepted as an anti-inflammatory therapy in inflammatory diseases such as cardiovascular disease, diabetes, and Alzheimer's (Pedersen and Saltin, 2015). The mechanisms by which exercise training induces these anti-inflammatory effects remains unclear, but there are several intriguing possibilities, including release of endogenous products, such as heat shock proteins, selective reduction of visceral adipose tissue mass or reduction of infiltration of adipocytes by macrophages, shifts in immune cell phenotype, cross-tolerizing effects, or exercise-induced shifts in accessory proteins of toll-like receptor signaling (Petersen and Pedersen, 2006; Flynn et al., 2007). It is also important to assess whether

the arrival dynamics of cell subtypes is modified by physical training, as monocytes, which could orchestrate inflammation resolution, repair, and increase muscle performance. This possibility deserves further investigation in the future.

In a previous study published by our group pharmacological blockade (apocynin) or genetic deletion of NADPH-oxidase ($gp91^{phox-/-}$ mice) inhibited leukocytes recruitment after a single fatiguing exercise. Furthermore, the reduction of ROS production by apocycnin prevented the exercise-induced adhesion molecules (E-selectin, L-selectin and PECAM) expression, which may explain the increasing in the numbers of rolling, adherent, and transmigrating neutrophil, showing the role of ROS from NADPH-oxidase in the skeletal muscle inflammation process (Nunes-Silva et al., 2014). Thus, ROS may regulate cell adhesiveness to the vessel wall of the exercised muscle. ROS- mediated leukocytes recruitment after exercise may also contribute to the muscle remodeling signaling, including angiogenesis, hypertrophic response and mitochondrial biogenesis (Gomes et al., 2012). Similarly, using the genetically modified animals $gp91^{phox-/-}$, we demonstrated that deficiency of ROS is related to a lower number of rolling and adherent leukocytes in the muscle vessels after training. Moreover, the $gp91^{phox-/-}$ mice presented an exacerbation in the increase of the workload induced by training. This result suggests that the chronic absence of ROS could impair a probable role of exercise-induced inflammation in controlling fatigue mechanisms and perhaps expose the organism to risks related to excessive exercise. Thus, the importance of investigations on the use of antioxidant strategies for exercise performance is highlighted. In fact, several studies have explored the effectiveness of antioxidant supplementation to enhance performance and adaptation to training, but its benefits and risks remain unknown (Bjornsen et al., 2016; Rothschild and Bishop, 2020).

In conclusion, acute high intensity exercise induced an evident inflammatory response. Additionally, the training was related to physical improvement and immune adaptations. Finally, our data suggest that ROS could be related to maintaining signaling for the limits of aerobic physical performance adaptation to training through the increased inflammatory response elicited by exercise. Nevertheless, the role of oxidative balance on aerobic performance and exercise-induced inflammation after training still needs to be elucidated.

DATA AVAILABILITY STATEMENT

The original contributions presented in the study are included in the article/**Supplementary Material**, further inquiries can be directed to the corresponding author/s.

ETHICS STATEMENT

The animal study was reviewed and approved by Animal Ethics Committee of Universidade Federal de Minas Gerais (UFMG; protocol 7412/2012).

AUTHOR CONTRIBUTIONS

LB: data collection, analysis of the results, and writing of the manuscript. WG: data collection, writing of the manuscript, and built the figures. ME and CR: data collection. JG: assisted during interpretation of the results and writing of the manuscript. CQ-J: microscopy analysis and interpretation of the results. RR: pulmonary data collection and interpretation of the results. CC: assisted during the exercise data collection and availability of the laboratory. AS: assisted during the project planning, writing of the manuscript, and the data collection. MT: assisted during the project planning and financial support. BR and VP: assisted during the project planning, data collection, and supervise this manuscript. All authors contributed to the article and approved the submitted version.

FUNDING

This study was supported by grants from the CNPq (Conselho Nacional de Desenvolvimento Científico e Tecnológico), CAPES (Coordenação de Aperfeiçoamento de Pessoal de Nível Superior), FAPEMIG (Fundação de Amparo à Pesquisa do Estado de Minas Gerais), Pró-Reitoria de Pesquisa da Universidade Federal de Minas Gerais, Pró-Reitoria de Pesquisa da Universidade do Estado de Minas Gerais, and INCT em dengue e interação microrganismo hospedeiro.

ACKNOWLEDGMENTS

We would like to thank Rosemeire Oliveira and Ilma Marçal for their technical assistance.

SUPPLEMENTARY MATERIAL

The Supplementary Material for this article can be found online at: https://www.frontiersin.org/articles/10.3389/fcell.2021.625680/full#supplementary-material

Supplementary Figure 1 | Effect of aerobic training on the profile of immune cells. The percentage of neutrophil $Ly6G^+$, macrophage $F480^+$, $TCD4^+$ and $TCD8^+$ cells of the sedentary (n = 7) and training (n = 8) mice were evaluated in blood (**A–D**, respectively) and bone marrow (**F–I**, respectively) by flow cytometry 72 h after fixed-speed running test until fatigue post training. Representative dot plots illustrating neutrophil $Ly6G^+$, macrophage $F480^+$, $TCD4^+$, and $TCD8^+$ cells of the sedentary (upper panel) and trained (below panel) mice in the blood **(E)** and bone marrow **(J)**. Data are expressed as mean ± SEM; $*p < 0.05$ compared to sedentary using two-tailed t-test. Cells from bone marrow and blood were plated, 1×10^6 cells/well, in a 96-well plate and stained for extracellular molecular expression patterns using mAbs against mouse CD3 (Alexa-488 conjugated), CD4 (APC conjugated), CD8 (PE conjugated), CD11b (Alexa-488 conjugated), F4/80 (PE conjugated), and Ly6G (APC conjugated) (from BD Pharmingen, Le Pont de Claix, France). The cells were incubated with 20 μl/well of antibody solution 30'/4°C, followed by fixation in 4% of paraformaldehyde. Limits for the quadrant markers were always set based on negative populations and isotype control antibodies. The frequency of positive cells was analyzed by FlowJo X v10.2 software, using a gate that included lymphocytes, neutrophils and/or macrophages. The frequency (percentage) of the analyzed population in the total acquired events was used in the construction of the graphs.

REFERENCES

Alessandri, A. L., Sousa, L. P., Lucas, C. D., Rossi, A. G., Pinho, V., and Teixeira, M. M. (2013). Resolution of inflammation: mechanisms and opportunity for drug development. *Pharmacol. Ther.* 139, 189–212. doi: 10.1016/j.pharmthera.2013.04.006

Baker, J. M., Nederveen, J. P., and Parise, G. (2017). Aerobic exercise in humans mobilizes HSCs in an intensity-dependent manner. *J. Appl. Physiol.* 122, 182–190. doi: 10.1152/japplphysiol.00696.2016

Barbieri, E., and Sestili, P. (2012). Reactive oxygen species in skeletal muscle signaling. *J. Signal. Transduct.* 2012:982794.

Bjornsen, T., Salvesen, S., Berntsen, S., Hetlelid, K. J., Stea, T. H., Lohne-Seiler, H., et al. (2016). Vitamin C and E supplementation blunts increases in total lean body mass in elderly men after strength training. *Scand. J. Med. Sci. Sports* 26, 755–763. doi: 10.1111/sms.12506

Campa, C. C., Silva, R. L., Margaria, J. P., Pirali, T., Mattos, M. S., Kraemer, L. R., et al. (2018). Inhalation of the prodrug PI3K inhibitor CL27c improves lung function in asthma and fibrosis. *Nat. Commun.* 9:5232.

Child, R., Brown, S., Day, S., Donnelly, A., Roper, H., and Saxton, J. (1999). Changes in indices of antioxidant status, lipid peroxidation and inflammation in human skeletal muscle after eccentric muscle actions. *Clin. Sci.* 96, 105–115. doi: 10.1042/cs0960105

Deyhle, M. R., Gier, A. M., Evans, K. C., Eggett, D. L., Nelson, W. B., Parcell, A. C., et al. (2015). Skeletal muscle inflammation following repeated bouts of lengthening contractions in humans. *Front. Physiol.* 6:424. doi: 10.3389/fphys.2015.00424

Febbraio, M. A., and Pedersen, B. K. (2002). Muscle-derived interleukin-6: mechanisms for activation and possible biological roles. *FASEB J.* 16, 1335–1347. doi: 10.1096/fj.01-0876rev

Ferreira, J. C., Rolim, N. P., Bartholomeu, J. B., Gobatto, C. A., Kokubun, E., and Brum, P. C. (2007). Maximal lactate steady state in running mice: effect of exercise training. *Clin. Exper. Pharmacol. Physiol.* 34, 760–765. doi: 10.1111/j.1440-1681.2007.04635.x

Fischer, C. P. (2006). Interleukin-6 in acute exercise and training: what is the biological relevance? *Exerc. Immunol. Rev.* 12, 6–33.

Flynn, M. G., Mcfarlin, B. K., and Markofski, M. M. (2007). The anti-inflammatory actions of exercise training. *Am. J. Lifestyle Med.* 1, 220–235.

Gomes, E. C., Silva, A. N., and De Oliveira, M. R. (2012). Oxidants, antioxidants, and the beneficial roles of exercise-induced production of reactive species. *Oxid. Med. Cell Longev.* 2012:756132.

Hortobagyi, T., Houmard, J., Fraser, D., Dudek, R., Lambert, J., and Tracy, J. (1998). Normal forces and myofibrillar disruption after repeated eccentric exercise. *J. Appl. Physiol.* 84, 492–498. doi: 10.1152/jappl.1998.84.2.492

Jackson, M. J., Pye, D., and Palomero, J. (2007). The production of reactive oxygen and nitrogen species by skeletal muscle. *J. Appl. Physiol.* 102, 1664–1670. doi: 10.1152/japplphysiol.01102.2006

Kerti, M., Balogh, Z., Kelemen, K., and Varga, J. T. (2018). The relationship between exercise capacity and different functional markers in pulmonary rehabilitation for COPD. *Int. J. Chron. Obstruct. Pulmon. Dis.* 13, 717–724. doi: 10.2147/copd.s153525

Kolaczkowska, E., and Kubes, P. (2013). Neutrophil recruitment and function in health and inflammation. *Nat. Rev. Immunol.* 13, 159–175. doi: 10.1038/nri3399

Lacerda, A. C., Marubayashi, U., and Coimbra, C. C. (2005). Nitric oxide pathway is an important modulator of heat loss in rats during exercise. *Brain Res. Bull.* 67, 110–116. doi: 10.1016/j.brainresbull.2005.06.002

Medzhitov, R. (2010). Inflammation 2010: new adventures of an old flame. *Cell* 140, 771–776. doi: 10.1016/j.cell.2010.03.006

Nieman, D. C., Nehlsen-Cannarella, S. L., Fagoaga, O. R., Henson, D. A., Utter, A., Davis, J. M., et al. (1998). Influence of mode and carbohydrate on the cytokine response to heavy exertion. *Med. Sci. Sports Exerc.* 30, 671–678. doi: 10.1097/00005768-199805000-00005

Nunes-Silva, A., Bernardes, P. T., Rezende, B. M., Lopes, F., Gomes, E. C., Marques, P. E., et al. (2014). Treadmill exercise induces neutrophil recruitment into muscle tissue in a reactive oxygen species-dependent manner: an intravital microscopy study. *PLoS One* 9:e96464. doi: 10.1371/journal.pone.0096464

Ogilvie, R. W., Armstrong, R. B., Baird, K. E., and Bottoms, C. L. (1988). Lesions in the rat soleus muscle following eccentrically biased exercise. *Am. J. Anat.* 182, 335–346. doi: 10.1002/aja.1001820405

Ostrowski, K., Rohde, T., Asp, S., Schjerling, P., and Pedersen, B. K. (2001). Chemokines are elevated in plasma after strenuous exercise in humans. *Eur. J. Appl. Physiol.* 84, 244–245. doi: 10.1007/s004210170012

Pedersen, B. K., and Saltin, B. (2015). Exercise as medicine - evidence for prescribing exercise as therapy in 26 different chronic diseases. *Scand. J. Med. Sci. Sports* 25(Suppl. 3), 1–72. doi: 10.1111/sms.12581

Petersen, A. M., and Pedersen, B. K. (2006). The role of IL-6 in mediating the anti-inflammatory effects of exercise. *J. Physiol. Pharmacol.* 57(Suppl. 10), 43–51. doi: 10.1249/00005768-200605001-00226

Primola-Gomes, T. N., Pires, W., Rodrigues, L. O., Coimbra, C. C., Marubayashi, U., and Lima, N. R. (2007). Activation of the central cholinergic pathway increases post-exercise tail heat loss in rats. *Neurosci. Lett.* 413, 1–5. doi: 10.1016/j.neulet.2006.10.042

Rezende, B. M., Athayde, R. M., Goncalves, W. A., Resende, C. B., Teles De Toledo Bernardes, P., Perez, D. A., et al. (2017). Inhibition of 5-lipoxygenase alleviates graft-versus-host disease. *J. Exp. Med.* 214, 3399–3415.

Rizo-Roca, D., Rios-Kristjansson, J. G., Nunez-Espinosa, C., Ascensao, A., Magalhaes, J., Torrella, J. R., et al. (2015). A semiquantitative scoring tool to evaluate eccentric exercise-induced muscle damage in trained rats. *Eur. J. Histochem.* 59:2544.

Rothschild, J. A., and Bishop, D. J. (2020). Effects of dietary supplements on adaptations to endurance training. *Sports Med.* 50, 25–53. doi: 10.1007/s40279-019-01185-8

Russo, R. C., Savino, B., Mirolo, M., Buracchi, C., Germano, G., Anselmo, A., et al. (2018). The atypical chemokine receptor ACKR2 drives pulmonary fibrosis by tuning influx of CCR2(+) and CCR5(+) IFNgamma-producing gammadeltaT cells in mice. *Am. J. Physiol. Lung Cell Mol. Physiol.* 314, L1010–L1025.

Saini, J., Mcphee, J. S., Al-Dabbagh, S., Stewart, C. E., and Al-Shanti, N. (2016). Regenerative function of immune system: modulation of muscle stem cells. *Age. Res. Rev.* 27, 67–76. doi: 10.1016/j.arr.2016.03.006

Serrano, A. L., Baeza-Raja, B., Perdiguero, E., Jardi, M., and Munoz-Canoves, P. (2008). Interleukin-6 is an essential regulator of satellite cell-mediated skeletal muscle hypertrophy. *Cell Metab.* 7, 33–44. doi: 10.1016/j.cmet.2007.11.011

Summers, C., Rankin, S. M., Condliffe, A. M., Singh, N., Peters, A. M., and Chilvers, E. R. (2010). Neutrophil kinetics in health and disease. *Trends Immunol.* 31, 318–324. doi: 10.1016/j.it.2010.05.006

Suzuki, K., Naganuma, S., Totsuka, M., Suzuki, K. J., Mochizuki, M., Shiraishi, M., et al. (1996). Effects of exhaustive endurance exercise and its one-week daily repetition on neutrophil count and functional status in untrained men. *Int. J. Sports Med.* 17, 205–212. doi: 10.1055/s-2007-972833

Suzuki, K., Nakaji, S., Yamada, M., Totsuka, M., Sato, K., and Sugawara, K. (2002). Systemic inflammatory response to exhaustive exercise, Cytokine kinetics. *Exerc. Immunol. Rev.* 8, 6–48.

Suzuki, K., Totsuka, M., Nakaji, S., Yamada, M., Kudoh, S., Liu, Q., et al. (1999). Endurance exercise causes interaction among stress hormones, cytokines, neutrophil dynamics, and muscle damage. *J. Appl. Physiol.* 87, 1360–1367. doi: 10.1152/jappl.1999.87.4.1360

Suzuki, K., Yamada, M., Kurakake, S., Okamura, N., Yamaya, K., Liu, Q., et al. (2000). Circulating cytokines and hormones with immunosuppressive but neutrophil-priming potentials rise after endurance exercise in humans. *Eur. J. Appl. Physiol.* 81, 281–287. doi: 10.1007/s004210050044

Taherkhani, S., Suzuki, K., and Castell, L. (2020). A short overview of changes in inflammatory cytokines and oxidative stress in response to physical activity and antioxidant supplementation. *Antioxidants* 9:886. doi: 10.3390/antiox9090886

Tavares-Murta, B. M., Zaparoli, M., Ferreira, R. B., Silva-Vergara, M. L., Oliveira, C. H., Murta, E. F., et al. (2002). Failure of neutrophil chemotactic function in septic patients. *Crit. Care Med.* 30, 1056–1061. doi: 10.1097/00003246-200205000-00017

Yamada, M., Suzuki, K., Kudo, S., Totsuka, M., Nakaji, S., and Sugawara, K. (2002). Raised plasma G-CSF and IL-6 after exercise may play a role in neutrophil mobilization into the circulation. *J. Appl. Physiol.* 92, 1789–1794. doi: 10.1152/japplphysiol.00629.2001

Conflict of Interest: The authors declare that the research was conducted in the absence of any commercial or financial relationships that could be construed as a potential conflict of interest.

frontiers in Cell and Developmental Biology

REVIEW
published: 04 February 2021
doi: 10.3389/fcell.2021.624082

Glycans and Glycan-Binding Proteins as Regulators and Potential Targets in Leukocyte Recruitment

*Franziska Krautter and Asif J. Iqbal**

Institute of Cardiovascular Sciences, University of Birmingham, Birmingham, United Kingdom

Leukocyte recruitment is a highly controlled cascade of interactions between proteins expressed by the endothelium and circulating leukocytes. The involvement of glycans and glycan-binding proteins in the leukocyte recruitment cascade has been well-characterised. However, our understanding of these interactions and their regulation has expanded substantially in recent years to include novel lectins and regulatory pathways. In this review, we discuss the role of glycans and glycan-binding proteins, mediating the interactions between endothelium and leukocytes both directly and indirectly. We also highlight recent findings of key enzymes involved in glycosylation which affect leukocyte recruitment. Finally, we investigate the potential of glycans and glycan binding proteins as therapeutic targets to modulate leukocyte recruitment and transmigration in inflammation.

Keywords: glycan, glycan-binding protein, leukocyte recruitment, transmigration, lectins, glycomimetics

OPEN ACCESS

Edited by:
Xunbin Wei,
Peking University, China

Reviewed by:
Jennifer Catherine Brazil,
University of Michigan, United States
Alex Marki,
La Jolla Institute for Immunology (LJI), United States

***Correspondence:**
Asif J. Iqbal
a.j.iqbal@bham.ac.uk

Specialty section:
This article was submitted to Cell Adhesion and Migration, a section of the journal Frontiers in Cell and Developmental Biology

Received: *30 October 2020*
Accepted: *12 January 2021*
Published: *04 February 2021*

Citation:
Krautter F and Iqbal AJ (2021) Glycans and Glycan-Binding Proteins as Regulators and Potential Targets in Leukocyte Recruitment. Front. Cell Dev. Biol. 9:624082. doi: 10.3389/fcell.2021.624082

INTRODUCTION

Glycosylation is a post-translational modification whereby carbohydrates are added to proteins or lipids to expand their functional profile. Approximately 10% of the human genome encodes for proteins which play roles in glycosylation and about 10^{12} possible glycan structures have been previously predicted, highlighting the importance and complexity of this post-translational modification (Laine, 1994; Haslam et al., 2008). The majority of glycan structures are found on the cell surface, but can also be detected intracellularly in the cytoplasm and nucleus. Glycosylation is a tightly controlled process involving glycosyltransferases and glycosidases which form the carbohydrate structures dependent upon sugar precursors, cellular environment and cell type (Reily et al., 2019). Structurally and biosynthetically, glycans can be divided into N- and O-glycans (**Figure 1**).

N-glycans all share the same core structure and are added to an asparagine (Asn) side chain via N-linked glycosylation initiated by oligosaccharyltransferase complex in the endoplasmic reticulum membrane (Schjoldager et al., 2020). N-glycans are attached to Asn located in a sequence of Asn-X-Serine/Threonine, whereby X can be any amino acid apart from proline (**Figure 1B**). The N-glycan core structure comprises of two N-Acetyl-D-glucosamine (GlcNAc) and three mannose molecules. This core structure is expanded through galactosylation, further GlcNAclyation, sialylation or fucosylation. These additions define three subclasses of N-glycans: high-mannose, hybrid and complex (**Figure 1B**).

O-glycans have eight different core structures and are attached to an -OH group of either serine or threonine via a O-glycosidic bond with an N-Acetyl-D-galactosamine (GalNAc) (**Figure 1C**) (Brockhausen et al., 2009). The glycan is attached to the amino acid residue via one of at

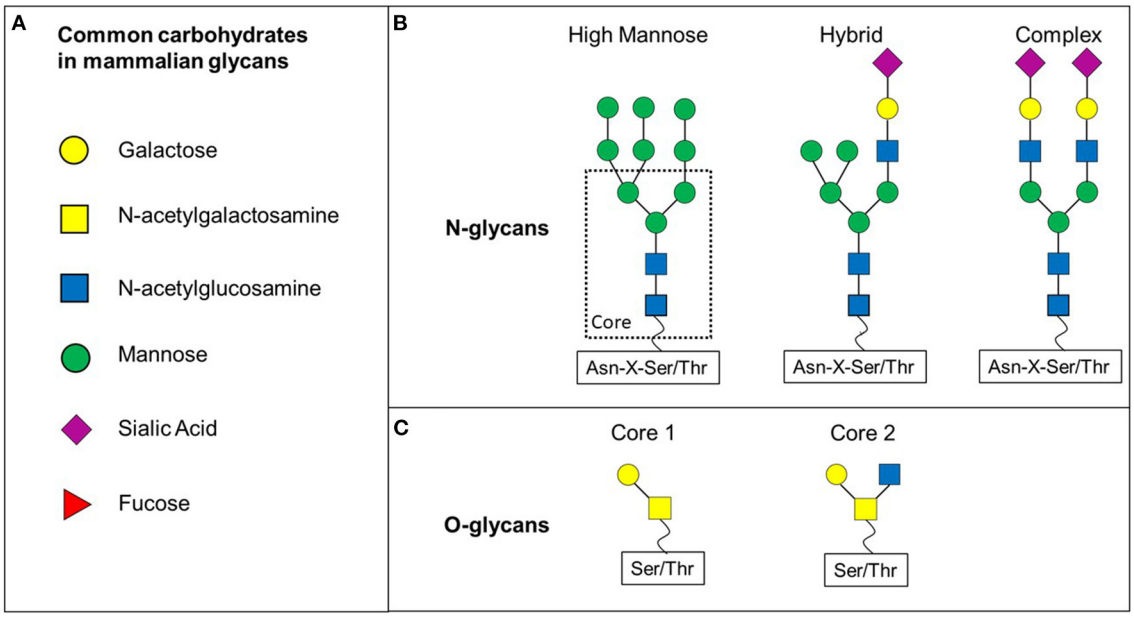

FIGURE 1 | N- and O-glycan differ in their core structure. **(A)** Various carbohydrates are making up mammalian glycans. **(B)** N-glycans share a common core structure. The carbohydrates added to the core structure define the three subtypes of N-glycans: high-mannose, hybrid and complex. **(C)** O-glycans discussed in this review are based on core 1 or core 2 O-glycans.

least 21 known polypeptide-N-acetylgalactosaminetransferases (ppGalNAcT-1 to−21) (Brockhausen et al., 2009). However, further glycosyltransferases are involved in the formation of O-glycans by adding to specific core structures (**Figure 1C**). Not only the availability of the enzyme substrate, but also the subcellular localisation affects the activity of these enzymes and therefore contributes to a wide range of (branched) O-glycans (Brockhausen et al., 2009).

Due to the great heterogeneity of structures, the functions of glycans also vary greatly. The biological roles of mammalian glycans can be broadly classified into three groups: (I) structural and modulatory functions such as in membrane organisation and epigenetic histone modifications(II) extrinsic recognition, for example of bacterial or viral adhesins (III) intrinsic recognition, for example in cell adhesion or intercellular signalling (Varki, 2017). We will focus on the role of glycans in leukocyte recruitment and migration in this review. This function, as any other, requires the glycomic code to be translated into function. Glycan-binding proteins are proteins which recognise and bind specific sequences of glycans and therefore facilitate cellular processes based on the glycomic profile. Various families of these proteins have been described: ß-galactoside binding lectins (Galectins, Gal), C-type lectins which require calcium for binding, I-type lectins which are a subset of the immunoglobulin superfamily, L-type lectins which are similar to leguminous plant lectins, P-type lectins which recognise phosphorylated mannose residues and R-type lectins which have a similar carbohydrate recognition domain (CRD) as ricin (Varki et al., 2009). However, not all of the mentioned lectin families have been shown to play a role in leukocyte migration.

The migration of leukocytes was first described in the nineteenth century (Dutrochet, 1824; Wagner, 1839) and has since been characterised extensively. Leukocyte recruitment to sites of inflammation, infection or tissue damage involves a series of tightly regulated, co-ordinated steps (**Figure 2**). Traditionally, the leukocyte recruitment cascade was described as a three-step process of rolling, activation and firm adhesion. However, this model has been expanded upon to include slow rolling, crawling and transmigration (Ley et al., 2007). Numerous proteins involved in the regulation of these steps have been identified over the years (**Figure 2**) [we refer to the excellent review by Ley et al. (2007)]. Briefly, leukocytes are captured and roll along activated endothelium through interactions between selectins (E-, L-, and P-selectin) and glycosylated proteins such as P-selectin glycoprotein ligand (PSGL)-1, CD44 and E-selectin ligand (ESL)-1 (Katayama et al., 2005; Hidalgo et al., 2007). This leads to activation of leukocytes and conformational changes to integrins, enabling integrin-mediated leukocyte rolling followed by irreversible binding between integrins, such as Macrophage (Mac)-1 antigen found on neutrophils and monocytes, lymphocyte function-associated antigen (LFA)-1, found on lymphocytes, monocytes and neutrophils or Very late antigen (VLA)-1 found on monocytes and T-lymphocytes and adhesion molecules such as intercellular adhesion molecule (ICAM)-1 and vascular cell adhesion molecule (VCAM)-1 on the endothelium (Diamond and Springer, 1993; Mitroulis et al., 2015). Which types of integrins and adhesion molecules dominate in the adhesion is cell type and tissue dependent (Rossaint and Zarbock, 2013; Maas et al., 2018; Schnoor et al., 2021). For example, integrin-mediated lymphocyte and monocyte rolling is mainly dependent on VLA-1 (Berlin et al.,

1995; Huo et al., 2000; Chan et al., 2001; Singbartl et al., 2001). ß2-integrins such as LFA-1 which interacts with ICAM-1 on the endothelial surface also support rolling, as has been shown for mouse neutrophils (Kadono et al., 2002). Integrin-mediated adhesion is also regulated by chemokines which trigger integrin activation and crawling. However, more recent studies have also highlighted tissue specific differences in leukocyte recruitment independent of selectins and integrins [reviewed in Schnoor et al. (2021)]. For example dipeptidase-1 acts as adhesion molecule for murine neutrophils in lung and liver, but not in the cremaster muscle (Choudhury et al., 2019). Various studies have identified ICAM-1, VCAM-1, platelet endothelial cell adhesion molecule (PECAM)-1, junctional adhesion molecule (JAM)-A and -C as well as ICAM-2 and Cluster of Differentiation (CD)99 as key molecules involved in transmigration, whereby leukocytes cross the endothelial layer in a trans- or paracellular manner.

The roles of glycan-binding proteins such as selectins and glycosylated proteins including ICAM-1 in leukocyte recruitment and transmigration have been well-documented. However, advances in experimental procedures, such as glycomic profiling now enable researches to investigate glycans and the glycomic profiles in cells and tissues in much more depth. Nevertheless, the research in this field is still in its infancy and requires further exploration to uncover the potential use of glycans as significant therapeutic targets. This review will provide an overview over glycans and novel glycan-binding proteins in leukocyte trafficking and how they are regulated. Finally, we will discuss how glycans and glycan-binding proteins can be targeted by therapeutics using glycan analogues, antibodies, lectins and glycomimetics to treat inflammatory diseases.

GLYCANS AND GLYCAN BINDING PROTEINS IN LEUKOCYTE CAPTURE AND ROLLING

The initial interactions between the endothelium and leukocytes is mediated by selectins, a group of C-type lectins. Three types of selectins have been identified to date in mammals: (I) E-selectin, which requires transcriptional activation and is expressed on the endothelium upon pro- inflammatory stimulation with e.g. tumour necrosis factor (TNF) a (Gedeit, 1996); (II) L-selectin, expressed on leukocytes, but shed upon activation with e.g., N-Formylmethionyl-leucyl-phenylalanine (fMLP); and (III) P-selectin, expressed by platelets and endothelial cells, where it is stored in granules and mobilised to the cell surface upon activation of the endothelium. These selectins all bind to core 2 O-glycans on glycosylated proteins such as PSGL-1 and CD44. E- and P-selectins bind to glycans on leukocytes whereas L-selectin can bind core 2 O-glycans on endothelium and leukocytes. The generation of these core 2 O-glycans is facilitated by a range of different glycosyltransferases (**Figure 3D**). Core 1 ß-1,3-galacotsyltransferase, an enzyme catalysing the transfer of galactose from UDP-alpha-D-galactose to a beta-N-acetylgalactosamine, forms the core 1 backbone which is the basis of core 2. ß-1,6-N-acetylglucosaminyltransferase-1, ß-1,4-galactosyltransferases, α-2,3-sialyltransferases and α-1,3-fucosyltransferases, enzymes catalysing the transfers of N-acetylglucosamine, galactose, sialic acid and fucose respectively, further extend core 2 O-glycans (**Figure 3D**) (Sperandio et al., 2006; Buffone et al., 2013; Mondal et al., 2013; Wright and Cooper, 2014) and have been demonstrated to affect leukocyte recruitment *in vivo* (Weninger et al., 2000; Sperandio et al., 2006). For example, it was shown that leukocytes from mice with genetic ablation for both α-1,3-fucosyltransferase (Fut) IV and VII resulted in significant inhibition of rolling as observed using intravital microscopy of the post-capillary and collecting venules of mice ears (**Table 1**). The authors also found that rolling velocities were significantly increased in single knockouts for either Fut IV or VII (Weninger et al., 2000). Studies using bone marrow derived neutrophils from α-1,3-fucosyltransferase IV, VII and IX deficient mice (*Fut4*$^{-/-}$, *Fut7*$^{-/-}$, and *Fut9*$^{-/-}$ respectively) as well as corresponding knock downs in human cell lines further confirmed the importance of fucosylation of PSGL-1 in leukocyte rolling. The knock down of *Fut7* and to a lesser extent *Fut4* and *Fut9* in human leukocytic HL-60 cells as well as in murine bone-marrow derived neutrophils decreased leukocyte interactions with recombinant selectins under hydrodynamic shear stress (Buffone et al., 2013). Polypeptide N-acetylgalactosamine transferase-1 (ppGalNAcT-1), which links the glycan molecule to the peptide (**Figure 3D**), has been also shown to play a crucial role in glycosylation of ligands for P-selectin (Tenno et al., 2007). More recently, its role in leukocyte rolling, adhesion and transmigration *in vivo* was characterised. These steps in the leukocyte trafficking cascade were significantly impeded in TNFα-treated cremaster muscles of ppGalNacT-1 knock out (*Galnt1*$^{-/-}$) mice compared to littermate controls (**Table 1**). Chimera experiments suggest that the presence of the enzyme in hematopoietic cells is crucial for recruitment since less neutrophils migrated to the peritoneum after i. p. injection of thioglycollate in the *Galnt1*$^{-/-}$ mice who received bone marrow from *Galnt1*$^{-/-}$ animals compared to *Galnt1*$^{-/-}$ mice who received bone marrow from *Galnt*$^{+/+}$ mice (Block et al., 2012). While these studies highlight the importance of various enzymes in leukocyte recruitment and their expression in certain cell types, other studies have shown that the glycosylation of cells can depend on their state. For example, naïve T-cells do not synthesise core 2 O-glycans and therefore do not bind to P-and E-selectins. Only upon stimulation T-cells increase the expression of enzymes encoded by *Gcnt1* and *Fut7*, which generate core 2 glycans and enable activated T-cells to bind selectins (Buffone et al., 2013; Chen et al., 2016; Hobbs and Nolz, 2017). Not just glycans are altered, core 2 bearing glycoprotein CD43 has been found to be upregulated on activated T-cells, providing increased binding sites for E-selectin and therefore enabling capture and migration (Matsumoto et al., 2005, 2007; Fuhlbrigge et al., 2006; Alcaide et al., 2007; Clark and Baum, 2012). Lymphocytes are not the only cells to alter their glycosylation upon stimulation. Other studies have shown that the glycosylation changes upon stimulation also occur in monocytes: for example, PSGL-1 and sialyl Lewis X (sLe^x) have both been demonstrated to be upregulated on human CD14$^+$ monocytes in a time-dependent manner upon IL-1ß stimulation (Kanabar et al., 2016). Interestingly, the same

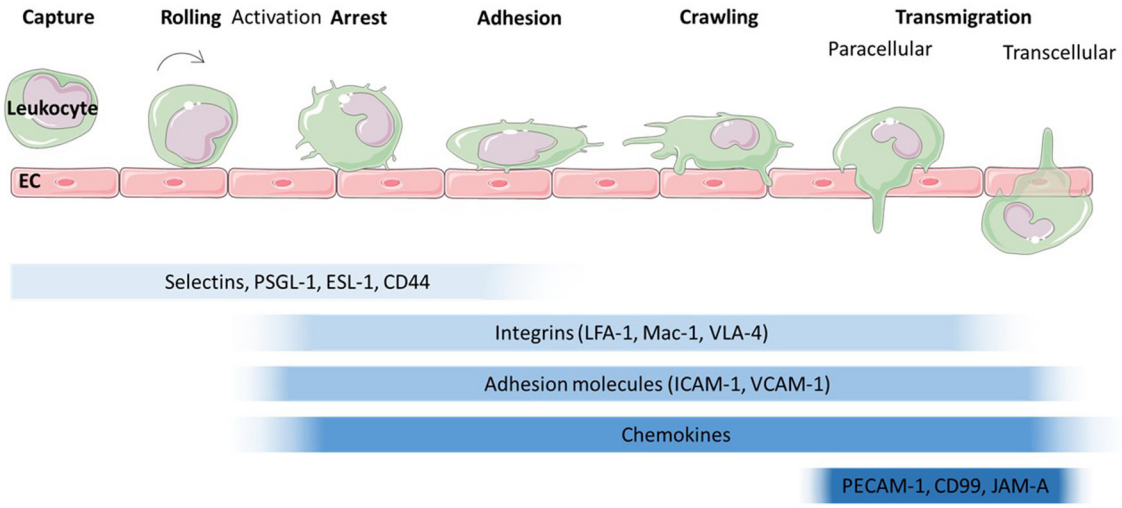

FIGURE 2 | Leukocyte migration cascade across endothelium. The leukocyte migration cascade comprises of a sequence of steps which are mediated by a range of proteins. The initial steps of capture and rolling are dominated by the interaction of selectins with proteins such as P-selectin glycoprotein ligand (PSGL)-1, E-selectin ligand (ESL)-1 and Cluster of differentiation (CD) 44. Activation leads to a conformational change in integrins such as lymphocyte function-associated antigen (LFA)-1, Macrophage (Mac)-1 antigen and Very Late Antigen (VLA)-4 which then interact with adhesion molecules such as Intercellular Cell Adhesion Molecule (ICAM-1) and Vascular Cell Adhesion Molecule (VCAM)-1. Together with chemokines presented on the endothelial surface, arrest and adhesion are triggered. The final step, transmigration through the endothelial cell layer is mediated by proteins such as platelet endothelial cell adhesion molecule (PECAM)−1, CD99 and junctional adhesion molecule (JAM) -A.

study showed that the ß-1,4-galactosyltransferase inhibitor, 5-(5-formylthien-2-yl) UDP-Gal, could prevent IL-1ß-mediated increase in PSGL-1 and sLe^x without affecting basal levels of the protein and sugar (Kanabar et al., 2016). However, the study did not address the effects of IL-1ß-mediated upregulation of PSGL-1 or the impact of treatment with the inhibitor on monocyte trafficking. Nevertheless, it highlights the therapeutic potential of targeting glycosyltransferases, especially, since the basal levels of PSGL-1 and sLe^x remained unaffected by the treatment. Other studies have also targeted glycosyltransferases acting in the generation of sLe^x or sialyl Lewis a (sLe^a), another core 2 glycan recognised by selectins (Rillahan et al., 2012). Even though inhibitors were able to interfere with the activity of the enzymes, their application *in vivo* remains limited due to off-target effects such as renal injury and difficulties in the delivery to the target site (Galeano et al., 2007; Patel et al., 2017). Interestingly, a recent study by May et al. (2020) has shown that alternative splicing of PGANTs, the *Drosophila* analogues of mammalian ppGalNTs (**Table 1**), which catalyse the addition of the glycan to serine or threonine, can alter the substrate and peptide preference of the enzyme. Even though this study investigates *Drosophila* PGANTs, a previous study has demonstrated the presence of splice variants in humans (Festari et al., 2017). Whether the splice variants of human ppGalNTs also affect the recognition of substrate in the same manner as the *Drosophila* splice variants and whether this impacts leukocyte recruitment remains unknown. Nevertheless, these findings offer a novel insight into previously unknown regulatory mechanisms of these enzymes which could be targeted by drugs. By targeting a more specific splice variant rather than all variants of one enzyme, it may offer a more precise treatment with less off-target effects.

Not only selectin-glycan interactions mediate leukocyte capture and rolling: the interaction between CD44 and the glycosaminoglycan (GAG) hyaluronic acid (HA) (**Figure 3C**) has previously been described to contribute to lymphocyte rolling *in vitro* (DeGrendele et al., 1996) and C-AM labelled leukocyte rolling *in vivo* (Xu et al., 2002). Further roles of the interaction between CD44 and HA in leukocyte trafficking have been reviewed elsewhere (McDonald and Kubes, 2015).

Although the changes in glycosylation of cells evidently contribute to the regulation of leukocyte rolling, other modes of regulation have been described. Galectins, a family of ß-galactoside binding proteins have been demonstrated to affect leukocyte rolling. Interestingly, even though from the same protein family, different galectins have been shown to affect leukocyte migration in opposing manner. Exogenous Gal-1, for example was described to inhibit rolling of polymorphonuclear cells (PMN) *in vitro* as well as *in vivo* during acute inflammation (**Figure 3A**) (La et al., 2003; Cooper et al., 2008). Conversely, endogenous chimera-type Gal-3 has been reported to promote recruitment of PMN and lymphocytes *in vivo* (Alves et al., 2013; Gittens et al., 2017). Impaired slow rolling and emigration was observed in *Gal3*$^{-/-}$ mice during acute inflammation, while the administration of recombinant Gal-3 reduced rolling velocity and increased the number of adherent neutrophils and monocytes *in vivo* (Gittens et al., 2017) (**Figure 3B**). The *in vitro* models support direct effects of Gal-1 and−3 on leukocyte migration (**Figures 3A,B**). However, *in vivo* studies using endothelial-specific knock out mice or bone marrow chimera

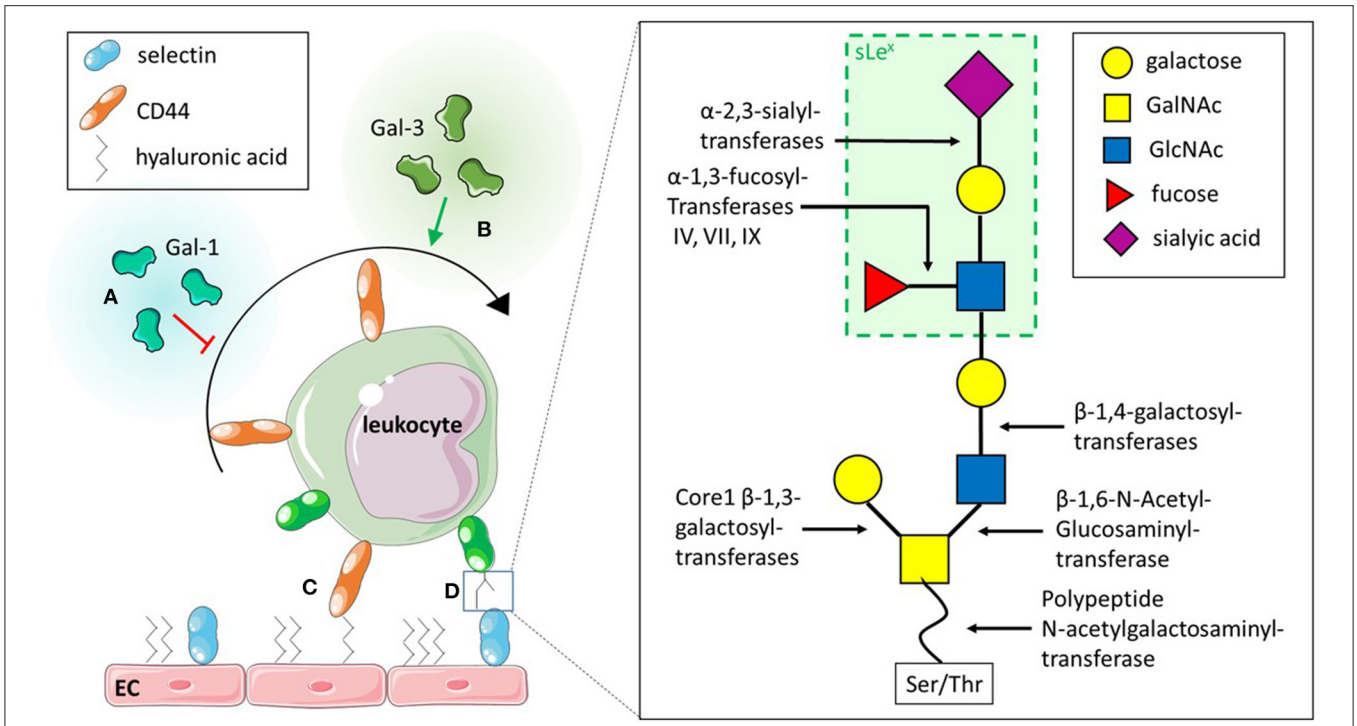

FIGURE 3 | Role of glycans and glycan binding proteins in leukocyte capture and rolling. **(A)** Exogenous Galectin (Gal)-1 inhibits capture and rolling of leukocytes. **(B)** Exogenous Gal-3 on the other hand promotes capture of leukocytes. **(C)** CD44 on leukocytes and the glycosaminoglycan hyaluronic acid on the endothelial cell (EC) surface interact to contribute to leukocyte capture. **(D)** Selectins are glycan binding proteins which bind to specific O-glycan structures such as sLe^x. These glycan structures are formed through a multitude of enzymes which catalyse the addition of different carbohydrates to the glycan precursor.

TABLE 1 | Enzymes involved in the capture of leukocytes.

Enzyme type		Enzmye function	Effect on Leukocyte Capture	References
Polypeptide N-acetylgalactosmaine transferase	ppGalNT1	Connects glycan to peptide	Crucial in glycosylation of ligands for P-selectin Knock down impedes leukocyte rolling, adhesion and transmigration	Tenno et al., 2007 Block et al., 2012
	PGANT		Drosophila analogue of mammalian ppGalNT, alternative splicing alters substrate and peptide preference	May et al., 2020
Fucosyltransferase	Fut IV Fut VII Fut IX	Addition of fucose to glycan	Necessary for fucosylation of PSGL-1 Knock downs decrease interaction with selectins *in vitro* and *in vivo* under flow Expression of Fut VII increased in activated T-cells so they can bind to selectins	Buffone et al., 2013 Chen et al., 2016 Hobbs and Nolz, 2017

models could help to distinguish between the role of endogenous galectins in hematopoietic and non-hematopoietic cells in context of recruitment (Suryawanshi et al., 2013; Robinson et al., 2019). Interestingly, various studies have demonstrated increased levels of soluble galectins in serum or plasma of patients with inflammatory diseases such systemic sclerosis, atherosclerotic stroke and systemic lupus erythematosus (He et al., 2017; Chihara et al., 2018; Matsuoka et al., 2020). Whether these increased levels of soluble protein affect the migration of leukocytes in these inflammatory diseases remains unknown, but merit further investigation.

GLYCANS AND GLYCAN BINDING PROTEINS IN LEUKOCYTE ADHESION

While the interaction between PSGL-1 and selectins is critical in the first stage of leukocyte recruitment, integrins such as Mac-1 and LFA-1, and adhesion molecules such as ICAM-1 and

VCAM-1, are known to facilitate firm adhesion. Nevertheless, these two steps in the recruitment cascade must not be seen as separate entities: the interaction between PSGL-1 and selectins is required for E-selectin-mediated direct activation of integrins (Taylor et al., 1996; Schaff et al., 2008; Chase et al., 2012; Morikis et al., 2017) or for the exposure of rolling leukocytes to chemokines on the endothelium which triggers G-protein coupled receptors (GPCR)-mediated integrin activation (Tsang et al., 1997; Stadtmann et al., 2013) on leukocytes followed by firm adhesion. The interaction between O-glycans and L-selectin has been demonstrated to be vital in regulating integrin activation and thereby mediating neutrophil adhesion *in vitro* and *in vivo* (Stadtmann et al., 2013). Recently, several studies have also highlighted the role of glycans on Mac-1, an integrin made up of an alpha subunit (αM; CD11b) and beta subunit (β2; CD18), in neutrophil adhesion and migration (Zen et al., 2007; Brazil et al., 2016; Saggu et al., 2018; Kelm et al., 2020). Saggu et al. (2018) showed that the CD18 subunit of Mac-1 interacts with FcγRIIA to reduce the affinity to IgG and therefore inhibit FcγRIIA-mediated neutrophil recruitment. They further demonstrated that this interaction was glycan dependent and mediated between the αI-domain of CD18 and sialylated glycans on FcγRIIA. The glycosylation of integrins is also important for adhesion of monocytes (Yang et al., 2012). Yang et al. (2012) demonstrated that the pro-inflammatory cytokine interferon (IFN)γ changes the glycosylation of monocytes which affects their adhesion and migration (**Figure 4D**). More specifically, they found that the treatment with IFNγ downregulated N-acetylglucosaminyltransferase V which affected the levels of ß-1,6- linked GlcNAc on integrins α5 and ß1 without affecting their protein levels (**Table 2**). The decrease in N-acetylglucosaminyltransferase V increased the phosphorylation of focal adhesion kinase, which in turn phosphorylates Extracellular Signal-regulated Kinase (ERK). Utilising an ERK inhibitor, they were able to inhibit the IFNγ-mediated monocyte adhesion and transmigration (Yang et al., 2012).

Evidently, the correct glycosylation of leukocytic proteins contributes greatly to the regulation of leukocyte migration. However, in the adhesion process, glycoproteins on the endothelium such as ICAM-1 and VCAM-1 also play a crucial role (Ley et al., 2007). They are expressed by the endothelium upon inflammatory stimuli and interact with integrins such as Mac-1 and LFA-1 (Diamond et al., 1991; Diamond and Springer, 1993). The importance of glycosylation in this interaction has been explored in a series of studies (Diamond et al., 1991; Sriramarao et al., 1993). Interestingly, contrary to O-glycan-mediated capture and rolling, N-glycans are the main type of glycans involved in adhesion. Particularly one type of N-glycan, high-mannose N-glycans (**Figure 1B**), increase monocyte adhesion (**Figure 4A**) (Scott et al., 2012). Specifically, high-mannose glycans on ICAM-1 have been demonstrated to drive the adhesion of the human monocytic cell line THP-1, independent of ICAM-1 and E-selectin expression (Chacko et al., 2011), as well as rolling and adhesion of primary monocytes (Scott et al., 2013a,b). This appears to be a mechanism occurring during acute inflammation; the pro-inflammatory cytokine TNFα, for example has been shown to downregulate mannosidases, enzymes which remove mannoses from glycans, due to hydrogen peroxidase released from endoplasmatic reticulum oxidoreductase-1-α (**Figure 4A**) (McDonald et al., 2020). This TNFα-mediated reduction in mannosidases in turn results in an increase of high-mannose N-glycans on the endothelial surface (**Table 2**) (Chacko et al., 2011; McDonald et al., 2020). Whether this is also occurring in chronic inflammation remains unknown. However, not only inflammatory cytokines appear to increase high mannose N-glycan levels on endothelium: oscillatory shear stress has been shown to increase these types of glycans too (**Table 2**) (Scott et al., 2012). Subsequent studies have shown that the increase of ICAM-1 glycosylated with mannose-rich glycans (high mannose ICAM-1) has functional consequences. High mannose ICAM-1 selectively recruits non-classical/intermediate ($CD16^+$) monocytes over classical ($CD16^-$) monocytes in a Mac-1 dependent manner (Regal-McDonald et al., 2019). Interestingly, studies using human and murine samples have shown that this high-mannose ICAM-1 glycoform is present in atherosclerotic lesions (Scott et al., 2012; Regal-McDonald et al., 2020) and positively correlates with macrophage burden in these lesions. α-2,6-sialylated ICAM-1 levels on the other hand, did not associate with increased macrophage content in lesions (Regal-McDonald et al., 2020). However, whether the selective recruitment of $CD16^+$ monocytes by high-mannose ICAM-1 contributed to increased macrophage content in high-mannose positive atherosclerotic lesions still remains to be determined. The selectivity of recruitment caused by differential glycosylation of adhesion proteins is an interesting area for drug targeting. A study by Chacko et al. (2011) showed that the PPARγ agonist rosiglitazone, an anti-diabetic drug, reduced TNFα-induced expression of high-mannose N-glycans and successfully reduced adhesion of THP-1 cells and primary human monocytes under physiological flow. Whether this PPARγ agonist can also prevent increases in high-mannose glycans caused by oscillatory shear stress have not been established. While rosiglitazone successfully reduced the adhesion of monocytes, it has also been linked to an increased risk of cardiovascular disease (Chen et al., 2012) and therefore may not be a suitable therapeutic option. Other *in vitro* studies targeting high mannose glycans with specific antibodies or lectins have successfully decreased monocyte adhesion further highlighting the therapeutic potential of targeting these glycan structures (Scott et al., 2012), however, these effects need to be validated *in vivo*.

Chemokine-mediated arrest and spreading of leukocytes has been shown to also depend on GAGs such as heparan sulphate (Middleton et al., 2002). More recently, various studies showed that chemokine presentation such as that of CXCL-8 and CCL-21 depend on GAGs (**Figure 4B**) (Proudfoot et al., 2003; Bao et al., 2010; Weber et al., 2013; Joseph et al., 2015; Goldblatt et al., 2019). Bao et al. (2010) demonstrated that mutant heparan sulphate leads to diminished chemokine presentation, resulting in decreased integrin-mediated recruitment of lymphocytes *in vivo* while specifically CCL-21 has been demonstrated to be immobilised by GAGs on the cell surface (Weber et al., 2013). Furthermore, the ablation of GAGs on neutrophils *in vitro* resulted in reduced chemotaxis towards CXCL-8 (Goldblatt

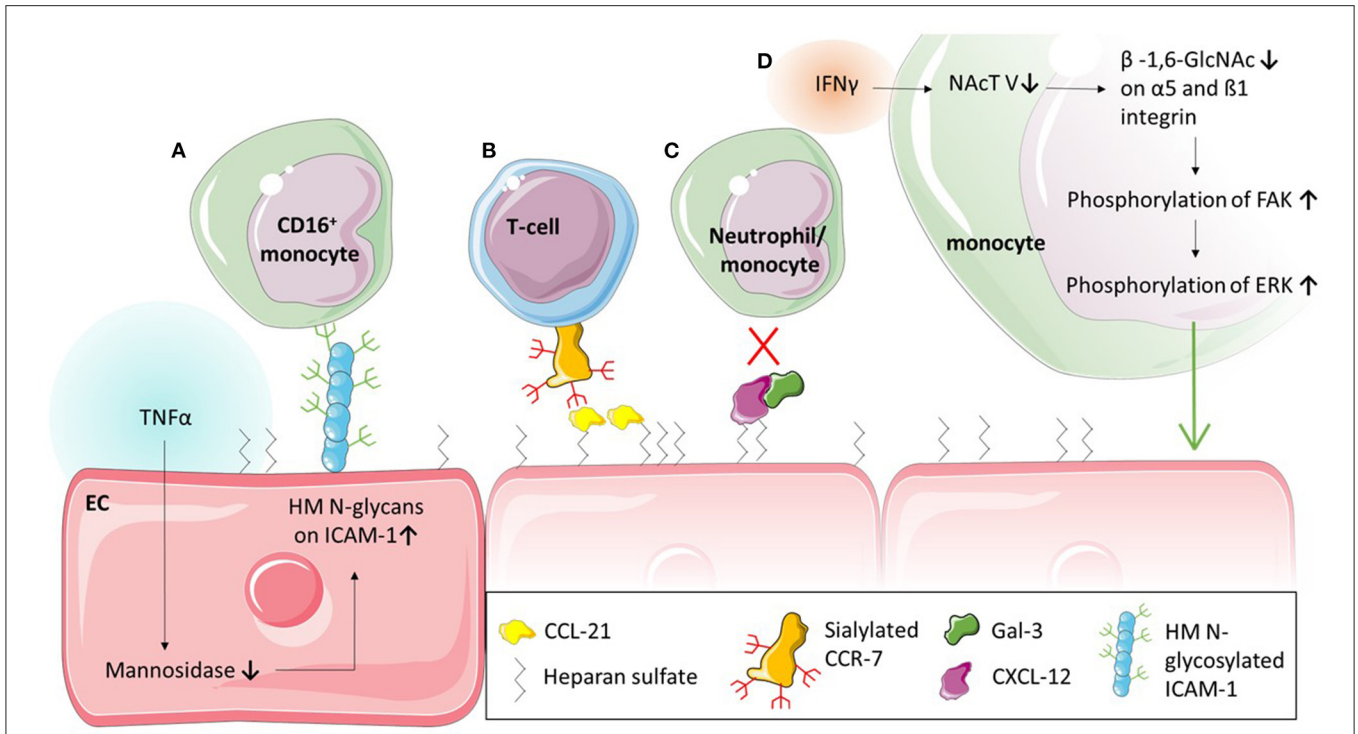

FIGURE 4 | Glycans and glycan binding proteins in leukocyte adhesion. **(A)** Tumour necrosis factor (TNF) α stimulation of endothelial cells (EC) leads to a decrease of mannosidases and in turn to an upregulation of high mannose (HM) ICAM-1 on the EC. This glycoform of ICAM-1 selectively causes the adhesion of $CD16^+$ monocytes. **(B)** Chemokines such as CCL-21 are bound to the endothelial surface via glycosaminoglycan heparan sulfate and interact with sialylated CCR-7 to mediate T-cell adhesion. **(C)** Glycan binding protein Galectin (Gal)-3 forms heterodimers with CXCL-12 which inhibit adhesion of neutrophils and monocytes *in vivo*. **(D)** Interferon (IFN) γ stimulation of monocytes reduces N-acetylglucosaminyltransferase (NAcT) V, which in turn decreases glycosylation of α5 and β1 integrin. This increases the phosphorylation of Focal adhesion kinase (FAK) and consequently Extracellular signal-regulated kinase (ERK), resulting in increased adhesion of monocytes.

TABLE 2 | Enzymes involved in Leukocyte Adhesion and Transmigration.

Enzyme type		Enzyme Function	Effect on Leukocyte adhesion and transmigration	References
N-acetylglucosaminyl-transferase	GNT-V	Addition of GlcNAc to OH-group of α-linked mannose	IFNγ-mediated decrease of GNT-V caused decrease of β-1,6-linked GalNAc on integrins, resulting in IFNγ-mediated adhesion of monocytes	Yang et al., 2012
Mannosidase		Remove mannose from glycan	TNFα treatment of EC downregulates mannosidase in turn resulting in high-mannose N-glycans on EC High-mannose ICAM-1 selectively recruits non-classical ($CD16^+$) monocytes Oscillatory shear stress increases mannose on EC	Chacko et al., 2011 McDonald et al., 2020 Scott et al., 2012
Sialyltransferase	St6Gal1	Addition of α-2,6-linked sialic acid to terminal N-glycans	Needed for PECAM-1 presentation on EC surface	Kitazume et al., 2010

et al., 2019). These studies suggest that the immobilisation of chemokines through GAGs on the cell surface contribute to a high local concentrations of chemokines, concentration gradients and chemokine-receptor binding, all potentially modulating leukocyte migration. However, more studies are required to understand the regulatory mechanisms involved in GAG-chemokine interactions and their effect on leukocyte migration. Particularly tissue-specific differences in these interactions, as suggested by Gangavarapu et al. and others (Gangavarapu et al., 2012; Rajarathnam et al., 2018), are of interest in order to understand tissue-specific differences in leukocyte trafficking. A range of studies have also highlighted the importance of glycosylation of chemokines (Ludwig et al., 2000; Frommhold et al., 2008). Glycosylation, especially sialylation, was found to contribute to chemokine binding to their cognate receptors (Frommhold et al., 2008; White et al., 2013; Doring et al., 2014; Su et al., 2014; Wright and Cooper, 2014; Hauser et al., 2016). For example, sialyation of CCR-7, a receptor of CCL-19

and−21, inhibits its signalling and therefore migration of T-cells *in vitro* (**Figure 4B**) (Hauser et al., 2016). Interestingly, dendritic cells release enzymes which can de-sialylate CCR-7 and therefore increase T-cell chemotaxis (Hauser et al., 2016). However, not only chemokine-chemokine receptor interactions are dependent on glycosylation. More recently, a study revealed how glycan-binding protein Gal-3 can mediate chemokine function. The study revealed Gal-3 forms heterodimers with CXCL12 (**Figure 4C**) (Eckardt et al., 2020), a chemokine known to interact with CXCR4. This interaction between CXCL12 and CXCR4 is known to modulate tissue infiltration of neutrophils and monocytes in myocardial infarction and atherosclerosis (Zernecke et al., 2008; Liehn et al., 2011; De Filippo and Rankin, 2018). Eckardt et al. (2020) showed that Gal-3 inhibited CXCL12 mediated migration of neutrophils and monocytes *in vitro* as well as the infiltration of the peritoneum *in vivo* (**Figure 4C**). The study also showed that the recruitment of classical monocytes *in vivo* was significantly increased to the peritoneum of Gal-$3^{-/-}$ mice after thioglycollate treatment compared to wild type mice, further indicating a role for Gal-3 in CXCL12 mediated recruitment of classical monocytes. Whether circulating Gal-3, which is upregulated in various inflammatory pathologies (He et al., 2017; Dong et al., 2018; Di Gregoli et al., 2020) is also able to interfere with CXCL12 mediated leukocyte recruitment *in situ* remains unknown. The authors of the study nevertheless suggest that, based on their data, the CRD of Gal-3 may be a promising anti-inflammatory target. Other galectins have also been shown to modulate leukocyte adhesion (La et al., 2003; Norling et al., 2008; Yamamoto et al., 2008; Gittens et al., 2017); multiple studies have found that Gal-1 inhibits leukocyte extravasation (La et al., 2003; Norling et al., 2008; Iqbal et al., 2011). Conversely, several other galectins have been shown to promote leukocyte adhesion to the endothelium (Yamamoto et al., 2008). Yamamoto et al. (2008) treated peripheral blood leukocytes with Gal-8, and found increased adhesion to HUVECs which they believed was α4-integrin-dependent. An important caveat of this study was that these assays were performed under static conditions. Due to the lack of physiological flow, the leukocytes automatically come into contact with the endothelium and the effect of these galectins on the capture of leukocytes by the endothelium cannot be assessed. The use of physiological flow would help to uncover whether galectins also affect the capture, and therefore adhesion and transmigration.

These studies demonstrate the importance of glycosylation for leukocyte adhesion and suggest possible mechanisms which could be targeted by therapeutics.

GLYCANS AND GLYCAN BINDING PROTEINS IN LEUKOCYTE TRANSMIGRATION

During the final stages of the migration cascade, leukocytes transmigrate across the endothelium. This can happen in either a transcellular or paracellular manner. Similar to the previous steps of the recruitment cascade, leukocyte transmigration is regulated by a range of different proteins: including PECAM-1, JAM-A, ICAM-2 and CD99 on the endothelium.

JAM-A is known to contribute to the barrier function of the endothelium since it is located within tight junctions. It contributes to cell migration by acting as ligand for LFA-1 on leukocytes. Whether glycans play a role in this interaction remains unknown. However, a recent study has shown that a particular N-glycan at position N185 of JAM-A contributes to barrier function. The study showed that mutating the glycosylation site of JAM-A in CHO cells resulted in a decrease of LFA-1 dependent adhesion of leukocytes compared to cells expressing wild type JAM-A (Scott et al., 2015).

PECAM-1 is another key junctional molecule involved in transmigration. It forms homophilic interactions which play a key role in vascular permeability (Ferrero et al., 1995; Privratsky et al., 2011), detecting flow (Osawa et al., 2002; Tzima et al., 2005) and leukocyte transmigration (Muller et al., 1993; Nourshargh et al., 2006). Levels of PECAM-1 are reduced in sialyltransferase knock out (*ST6Gal1*$^{-/-}$) mice (Kitazume et al., 2010). This suggests that the siaylation of PECAM-1 contributes to its presentation on the endothelial cell surface (**Table 2**). However, how this potentially contributes to the regulation of leukocyte migration remains unknown. A more recent study suggests that glycosylation plays a role in the homophilic interactions of PECAM-1 therefore potentially affecting leukocyte transmigration. It was found that glycans at the asparagine at position 25, which is located within the trans-homophilic binding interface of PECAM-1 contribute to the homophilic interactions (Lertkiatmongkol et al., 2016). The same study suggests that negatively charged 2,3-sialic acid moieties form electrostatic bridges with a positively charged lysine at position 89 (Lertkiatmongkol et al., 2016) which has previously been described to play a role in the homophilic interactions of PECAM-1 (Newton et al., 1997). Interestingly, 2,6 sialic acid moieties blocked the homophilic interactions. A N25Q mutant of PECAM-1, lacking the glycan at position 25 was shown to localise in the same manner as the native protein, however, the recovery of its barrier function was significantly damaged, highlighting an important role of the glycosylation in the permeability of the endothelium. How the lack of this glycan and therefore the homophilic interaction affects leukocyte migration remains unknown. Interestingly murine PECAM-1 lacks the asparagine at position 25 and therefore also the glycosylation. It has however two more glycosylation sites, a total of nine, compared to human PECAM-1 and highlights key differences of glycosylation between species. Also, how or if the glycosylation sites of PECAM-1 are affected in pathological conditions, especially during inflammation remains to be determined.

As previously mentioned, the various steps in the recruitment cascade are not separate mechanisms. Therefore, it is no surprise that glycans associated with selectins and therefore capture and rolling, can also act in transmigration, as demonstrated by various studies. The use of antibodies targeting sLe^x as well as the removal of sLe^x on Mac-1 disrupted the interaction between Mac-1 and E-selectin while causing degranulation of neutrophil secondary granules without stimulation with chemoattractants. Neutrophil transmigration across intestinal

epithelial cell monolayers was also significantly decreased when the neutrophils were treated with these anti-sLe^x antibodies compared to neutrophils treated with a control antibody (Zen et al., 2007). A study by Brazil et al. (2016) also showed a role of Le^x in neutrophil transmigration when targeting with antibodies. They observed that terminal glycans rather than subterminal Le^x drive an increase in degranulation and a decrease in transepithelial migration of neutrophils, important in mucosa-lined organs such as the intestine and lung. Antibodies are not the only modalities used to target glycan moieties, Kelm et al. (2020) utilised lectins specifically targeting high-mannose or bi-antennary galactosylated N-glycans on CD11b and inhibited transepithelial migration among other inflammatory functions of neutrophils. Contrary to targeting Le^x, targeting Le^a, a stereoisomer of Le^x, with antibodies or lectins increased transepithelial migration of neutrophils and therefore suggests a potential role of Le^a in the inhibition of transepithelial migration. Interestingly, the same group had previously shown that targeting the sialylated version of Le^a, sLe^a, on CD44v6 expressed by epithelial cells prevented transepithelial migration of neutrophils (Brazil et al., 2010, 2013). Whether the opposing results of antibodies and lectins targeting Le^x and Le^a are due to the presence of Le^x and Le^a on different proteins and therefore affecting the migration differently seems likely, since the expression of Le^x and Mac-1 is increased with activation of neutrophils whereas Le^a was not. Additionally, the ligation of Le^x affected multiple cellular functions including migration and apoptosis, whereas targeting Le^a only affected transepithelial migration (Brazil et al., 2017). Collectively, these studies highlight the potential of glycan specific antibodies and lectins as inhibitors of glycan-mediated functions.

INHIBITION OF GLYCAN BIOSYNTHESIS OR RECOGNITION

Several studies have highlighted the potential of glycosylation as a suitable therapeutic target to treat inflammatory diseases characterised by dysregulated leukocyte trafficking (Mertens et al., 2006; Gaber et al., 2011; Dwivedi et al., 2018; Kelm et al., 2020). This might be particularly promising since changes in the glycomic profile of cells and tissues have been previously described in various inflammatory diseases such as rheumatoid arthritis, ulcerative colitis and systemic lupus erythematosus (Axford et al., 1992; Gornik and Lauc, 2008; Larsson et al., 2011). Various approaches to target glycosylation can be taken: (i) interference with the biosynthesis of glycans using inhibitors of glycosyltransferases or (ii) interference with the recognition of glycans either by using targeted antibodies or lectins (Kelm et al., 2020) or (iii) blocking the glycan receptor with recombinant glycoproteins or glycomimetics (Dwivedi et al., 2018). The use of these different approaches as therapeutics to treat dysregulated leukocyte trafficking in inflammatory disease will be discussed in the following section (**Figure 5**).

Interfering With Biosynthesis of Glycans–Glycosyltransferase Inhibitors

The biosynthesis of glycans is a tightly controlled pathway whereby a multitude of different glycosyltransferases are involved to generate thousands of glycan structures found in cells. Studies have revealed that the glycosylation changes in diseases (Axford et al., 1992; Gornik and Lauc, 2008; Larsson et al., 2011) and therefore, the enzymes involved in these processes may provide a suitable target. Introduction of synthetic glycan building blocks offer the opportunity to interfere with glycan recognition without disrupting enzyme activity by targeted delivery to the affected cell type or tissue. Disrupting the enzyme function in other tissues could lead to off target effects. Numerous studies have investigated the potential of such analogues i*n vitro* (Barthel et al., 2011; Rillahan et al., 2012; Agarwal et al., 2013; Jiang et al., 2016; Kanabar et al., 2016; Dwivedi et al., 2018; Moons et al., 2019) and *in vivo* (Dimitroff et al., 2003; Gainers et al., 2007; Marathe et al., 2010) (**Figure 5A**). These approaches targeted various glycosyltransferases such as ß-1,4-galactosyltransferase, fucosyltransferase III, V, VI and VII as well as sialyl transferases (Burkart et al., 2000) and reported reductions in the respective O- and N-glycan structures. Particularly successful were fluorinated glycan analogues. Rillahan et al. (2012) found that the fluorinated fucose analogue GDP-2F-Fuc and sialic acid analogue 3F-Ax-NeuAc inhibited various fucosyltransferases and sialyl-transferases which resulted in reduced fucosylation and sialylation of N- and O-glycans. Particularly sLe^x was reduced, which impaired the binding of HL-60 cells to recombinant E and P -selectin under flow.

Even though these studies demonstrate the potential of glycan analogues as inhibitors of glycan biosynthesis, there is a lack of studies investigating their effects on leukocyte migration, particularly *in vivo*. Only such studies can evaluate the true potential of these inhibitors as drugs since targeting the biosynthesis of glycans may prove challenging since glycans are implicated in virtually all cell types and tissues. Currently, too little is known about their regulation, especially in pathological conditions to make reliable predictions. And while the inhibitors and analogues may provide the necessary insight into pathways of biosynthesis as well as cellular mechanisms *in vitro*, the overlapping specificities, multi-substrate specificities and structural homology of glycosyltransferases could prove too difficult to use as therapeutic targets *in vivo* (Videira et al., 2018).

Interfering With Glycan Recognition–Antibodies, Lectins and Glycomimetics

While glycan analogues target the biosynthesis of glycans, another approach to interfere with glycan function is to inhibit their recognition by glycan-binding proteins. We have previously mentioned studies targeting glycan structures with specific antibodies (Zen et al., 2007; Brazil et al., 2016, 2017) (**Figure 5B**). While these studies showed successful inhibition of glycan function through the use of specific antibodies, their potential *in vivo* remains untested. Lectins have also been previously used in *in vitro* studies to inhibit the recognition of glycans

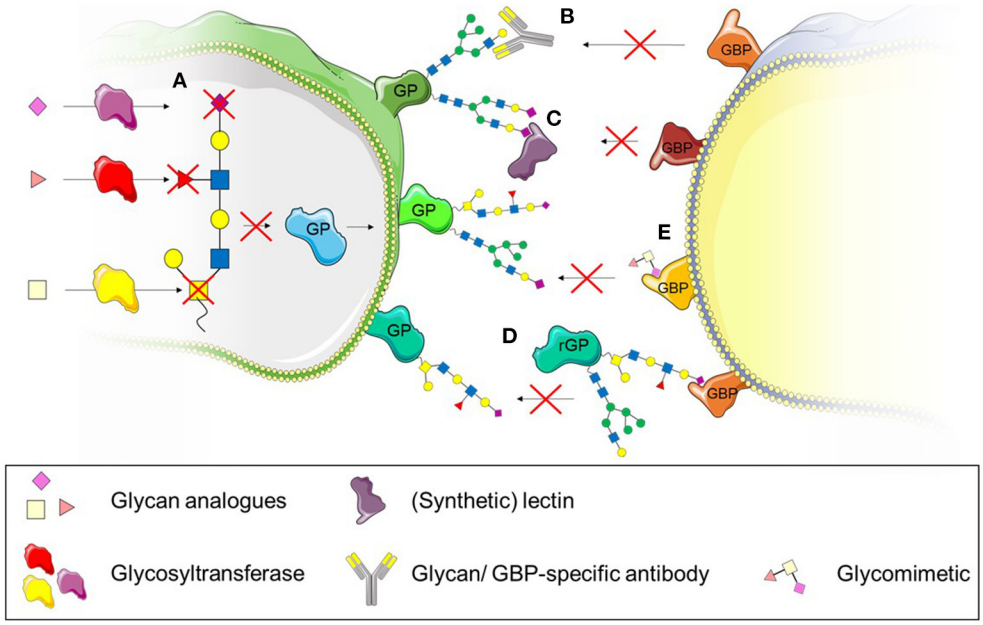

FIGURE 5 | Therapeutic strategies to interfere with leukocyte recruitment and transmigration. **(A)** The use of synthetic glycan substrates impairs enzyme-catalysed glycan formation and prevents recognition by glycan-binding proteins (GBP). **(B)** Specific antibodies targeting glycans can also be used to interfere with glycan recognition by GBPs. **(C)** (Synthetic) lectins bind to specific glycan structures and interfere with recognition by GBPs. **(D)** Recombinant glycoproteins (rGP) bind to GPBs and therefore prevent binding to native glycoproteins (GP). **(E)** Glycomimetics can also be used to bind to GBPs and prevent binding to glycoproteins.

(Brazil et al., 2017; Kelm et al., 2020) (**Figure 5C**). Similar to antibodies, they bind specific glycan structures and interfere with recognition through glycan-binding proteins. The lectins used experimentally generally stem from natural sources such as tomatoes (*Lycopersicon Esculentum* lectin, LEL), peanuts (peanut agglutinin lectin, PNA) or mussels (*Crenomytilus grayanus* lectin, CGL) and are used as tools to investigate the function and expression of glycans rather than pharmacological agents. The use of synthetic lectins may provide a more promising approach since their specificity can be higher than of naturally occurring lectins (Ferrand et al., 2009). One study has used synthetic lectins to demonstrate their specificity for glycans as cancer diagnostics tools (Bicker et al., 2012). They used an array of various synthetic lectins and various cancerous metastatic and non-metastatic cell lines and showed that the synthetic lectins differentially bind to the glycans of these cell types, distinguishing subtle differences between healthy and different pathological glycan structures (Bicker et al., 2012). This may also be helpful as diagnostic tool in inflammatory diseases but requires further investigation. Even though these synthetic lectins provide high sensitivity, no studies, to our knowledge have used them to interfere with cellular functions in a therapeutic context.

Instead of glycans, glycan binding proteins could also be targeted to interfere with the recognition of glycans. For example, recombinant glycoproteins have been used to bind to glycan binding proteins, interfering with the binding of native glycoprotein (**Figure 5D**). This has been tested in clinical trials in the case of PSGL-1. Recombinant PSGL-1-immunoglobulin was successfully used *in vivo* before clinical trials in patients with myocardial infarction and renal allografts (Mertens et al., 2006; Gaber et al., 2011). Unfortunately, neither of the clinical studies could demonstrate significant beneficial outcomes for patients. Whether the glycosylation of recombinant PSGL-1 reflected the glycosylation of naturally occurring PSGL-1 is not known, but may be crucial for the success of it as a therapeutic modality. The choice of cell type producing the recombinant protein is important to ensure correct glycosylation. While the use of *Escherichia coli* (*E. coli*) is a cheaper option of generating proteins, *E. coli* glycosylation is significantly different to mammalian glycosylation (Lee et al., 2013) and has to be taken into account when generating proteins for the interference of glycan recognition. Other approaches of targeting the interaction between selectins and PSGL-1 might therefore be more promising. For example the use a mimetic of the N-terminus of PSGL-1, GsnP-6, which has successfully inhibited P-selectin function *in vitro* and *in vivo* (Krishnamurthy et al., 2015). GsnP-6 interfered in the interaction between PSGL-1 and P-selectin which resulted in increased rolling velocity of human neutrophils and monocytes *in vitro*. This PSGL-1 mimetic was also able to interfere with the interaction of P-selectin and PSGL-1 *in vivo* while inhibiting early thromboinflammatory events such as platelet aggregation and platelet-leukocyte interactions (Krishnamurthy et al., 2015). This interference may not only affect leukocyte recruitment, but may also be beneficial in inhibiting dendritic cell driven atherogenesis mediated through the interaction of P-selectin with PSGL-1 (Ye et al., 2019).

The use of glycomimetics (**Figure 5E**), rather than recombinant glycosylated proteins might improve the

outcome of therapies targeting glycan recognition due to their high affinity to respective glycan-binding proteins and improved pharmacokinetics compared to their naturally occurring counterparts (Hevey, 2019). Synthetically generated glycomimetics can act as small molecule inhibitors by binding to glycan binding proteins with higher affinity. For example, Rivipansel (or GMI-1070), a pan-selectin targeting glycomimetic was successfully used to reduce sickle red blood cell-leukocyte interactions *in vivo* and therefore improved blood flow and survival of sickle cell mice (Chang et al., 2010). However, the Phase III, double-blind, placebo controlled clinical trial to treat vaso-occlusive events in humans with Sickle Cell Disease (clinicaltrials.gov, NCT02187003) did not meet the primary and secondary efficacy endpoints and was therefore unsuccessful[1].

Various studies have used glycomimetics to target galectins (**Figure 5D**). While some glycomimetics have specific affinities to just one carbohydrate recognition domain of tandem-repeat galectins, other glycomimetics can bind to several galectins, revealing the complexity of these compounds (Pal et al., 2018, 2019; Stegmayr et al., 2019; Mahanti et al., 2020). For example, a quinolone-derivatised galactoside bound selectively to the N-terminal domain of Gal-8 (Pal et al., 2018) while 3 N-aryl galactosides were shown to selectively bind the C-terminal domain of Gal-9 and N-aryl gulosides to the N-termainal domain of Gal-9 (Mahanti et al., 2020). Their efficacy was demonstrated for extra- and intracellular galectins and they were able to interfere with cellular functions dependent on the respective galectin (Delaine et al., 2016; Stegmayr et al., 2019). Glycomimetics targeting Gal-3 have been shown to block extracellular binding of Gal-3 to CHO cells and also successful in inhibiting intracellular accumulation of Gal-3 around the disrupted membrane of intracellular vesicles of JIMT-1 breast cancer cells while having a low basal toxicity (Stegmayr et al., 2019). The inhibitor GB0139 (formerly TD139) targeting Gal-3 has been tested as therapeutic in lung fibrosis, successfully passed Ib/IIa clinical trials, and has moved into IIb trials which are currently in progress (clinicaltrials.gov; NCT03832946). Another glycomimetic Gal-3 inhibitor (Salameh et al., 2010), Cpd47, blocked Gal-3 inhibition of insulin-stimulated glucose transport in L6 myocytes and has also been tested in Type 2 diabetes models *in vivo*. The Gal-3 inhibitor improved the glucose tolerance in obese mice after a single dose of the inhibitor as well as continuous administration over 2 weeks via a minipump, suggesting a promising treatment for Type 2 diabetes in acute and chronic settings (Li et al., 2016).

These studies clearly demonstrate the potential of glycomimetics as therapeutics. Whether they could also interfere with glycan-dependent steps of the leukocyte recruitment cascade remains to be tested.

DISCUSSION

Here, we have reviewed novel roles of glycans in leukocyte recruitment and transmigration as well as their potential as therapeutic targets in the treatment of inflammatory diseases. While the roles of glycans in leukocyte recruitment were reported decades ago, more recent research has uncovered roles in virtually all steps of the pathway. Each step in the recruitment cascade has a number of enzymes involved which can alter the glycosylation of certain proteins and therefore the capture, adhesion and transmigration of leukocytes. More specifically, this review has shown, that the enzymes can act in a tissue- or leukocyte subset-dependent manner. However, differences between acute and chronic inflammatory settings, the translatability of preclinical *in vitro* and *in vivo* studies still requires more validation. Various studies have also highlighted the potential of targeting glycan biosynthesis by interfering with enzyme activity or by targeting glycan recognition directly with specific antibodies, lectins or glycomimetics. However, to be able to target these safely, more studies are needed to limit off-target effects. Nevertheless, the inflammation-dependent changes in glycosylation provide a promising therapeutic target.

AUTHOR CONTRIBUTIONS

FK and AI wrote the manuscript. AI edited the manuscript. All authors contributed to the article and approved the submitted version.

FUNDING

AI was supported by Birmingham Fellowship and AMS Springboard Award (grant number SBF003/1156). FK studentship was supported by AMS Springboard award (grant number SBF003/1156) and the University of Birmingham. The Institute of Cardiovascular Sciences, University of Birmingham was recipient of a BHF Accelerator Award (AA/18/2/34,218).

[1]https://www.pfizer.com/news/press-release/press-release-detail/pfizer_announces_phase_3_top_line_results_for_rivipansel_in_patients_with_sickle_cell_disease_experiencing_a_vaso_occlusive_crisis

REFERENCES

Agarwal, K., Kaul, R., Garg, M., Shajahan, A., Jha, S. K., and Sampathkumar, S. G. (2013). Inhibition of mucin-type O-glycosylation through metabolic processing and incorporation of N-thioglycolyl-D-galactosamine peracetate (Ac5GalNTGc). *J. Am. Chem. Soc.* 135, 14189–14197. doi: 10.1021/ja405189k

Alcaide, P., King, S. L., Dimitroff, C. J., Lim, Y. C., Fuhlbrigge, R. C., and Luscinskas, F. W. (2007). The 130-kDa glycoform of CD43 functions as an E-selectin ligand for activated Th1 cells *in vitro* and in delayed-type hypersensitivity reactions *in vivo*. *J. Invest. Dermatol.* 127, 1964–1972. doi: 10.1038/sj.jid.5700805

Alves, C. M., Silva, D. A., Azzolini, A. E., Marzocchi-Machado, C. M., Lucisano-Valim, Y. M., Roque-Barreira, M. C., et al. (2013). Galectin-3 is essential for reactive oxygen species production by peritoneal neutrophils from mice infected with a virulent strain of *Toxoplasma gondii*. *Parasitology* 140, 210–219. doi: 10.1017/S0031182012001473

Axford, J. S., Sumar, N., Alavi, A., Isenberg, D. A., Young, A., Bodman, K. B., et al. (1992). Changes in normal glycosylation mechanisms in autoimmune rheumatic disease. *J. Clin. Invest.* 89, 1021–1031. doi: 10.1172/JCI115643

Bao, X., Moseman, E. A., Saito, H., Petryniak, B., Thiriot, A., Hatakeyama, S., et al. (2010). Endothelial heparan sulfate controls chemokine presentation in recruitment of lymphocytes and dendritic cells to lymph nodes. *Immunity* 33, 817–829. doi: 10.1016/j.immuni.2010.10.018

Barthel, S. R., Antonopoulos, A., Cedeno-Laurent, F., Schaffer, L., Hernandez, G., Patil, S. A., et al. (2011). Peracetylated 4-fluoro-glucosamine reduces the content and repertoire of N- and O-glycans without direct incorporation. *J. Biol. Chem.* 286, 21717–21731. doi: 10.1074/jbc.M110.194597

Berlin, C., Bargatze, R. F., Campbell, J. J., Von Andrian, U. H., Szabo, M. C., Hasslen, S. R., et al. (1995). Alpha 4 integrins mediate lymphocyte attachment and rolling under physiologic flow. *Cell* 80, 413–422. doi: 10.1016/0092-8674(95)90491-3

Bicker, K. L., Sun, J., Harrell, M., Zhang, Y., Pena, M. M., Thompson, P. R., et al. (2012). Synthetic lectin arrays for the detection and discrimination of cancer associated glycans and cell lines. *Chem. Sci.* 3, 1147–1156. doi: 10.1039/c2sc00790h

Block, H., Ley, K., and Zarbock, A. (2012). Severe impairment of leukocyte recruitment in ppGalNAcT-1-deficient mice. *J. Immunol.* 188, 5674–5681. doi: 10.4049/jimmunol.1200392

Brazil, J. C., Lee, W. Y., Kolegraff, K. N., Nusrat, A., Parkos, C. A., and Louis, N. A. (2010). Neutrophil migration across intestinal epithelium: evidence for a role of CD44 in regulating detachment of migrating cells from the luminal surface. *J. Immunol.* 185, 7026–7036. doi: 10.4049/jimmunol.1001293

Brazil, J. C., Liu, R., Sumagin, R., Kolegraff, K. N., Nusrat, A., Cummings, R. D., et al. (2013). alpha3/4 Fucosyltransferase 3-dependent synthesis of Sialyl Lewis A on CD44 variant containing exon 6 mediates polymorphonuclear leukocyte detachment from intestinal epithelium during transepithelial migration. *J. Immunol.* 191, 4804–4817. doi: 10.4049/jimmunol.1301307

Brazil, J. C., Sumagin, R., Cummings, R. D., Louis, N. A., and Parkos, C. A. (2016). Targeting of Neutrophil Lewis X Blocks transepithelial migration and increases phagocytosis and degranulation. *Am. J. Pathol.* 186, 297–311. doi: 10.1016/j.ajpath.2015.10.015

Brazil, J. C., Sumagin, R., Stowell, S. R., Lee, G., Louis, N. A., Cummings, R. D., et al. (2017). Expression of Lewis-a glycans on polymorphonuclear leukocytes augments function by increasing transmigration. *J. Leukoc. Biol.* 102, 753–762. doi: 10.1189/jlb.1MA0117-013R

Brockhausen, I., Schachter, H., and Stanley, P. (2009). "Chapter 9: O-GalNAc glycans," in *Essentials of Glycobiology, 2nd Edn.*, eds A. Varki, R. D. Cummings, J. D. Esko, et al. (Cold Spring Harbor, NY: Cold Spring Harbor Laboratory Press) 2009.

Buffone, A. Jr., Mondal, N., Gupta, R., Mchugh, K. P., Lau, J. T., and Neelamegham, S. (2013). Silencing alpha1,3-fucosyltransferases in human leukocytes reveals a role for FUT9 enzyme during E-selectin-mediated cell adhesion. *J. Biol. Chem.* 288, 1620–1633. doi: 10.1074/jbc.M112.400929

Burkart, M. D., Vincent, S. P., Duffels, A., Murray, B. W., Ley, S. V., and Wong, C. H. (2000). Chemo-enzymatic synthesis of fluorinated sugar nucleotide: useful mechanistic probes for glycosyltransferases. *Bioorg. Med. Chem.* 8, 1937–1946. doi: 10.1016/S0968-0896(00)00139-5

Chacko, B. K., Scott, D. W., Chandler, R. T., and Patel, R. P. (2011). Endothelial surface N-glycans mediate monocyte adhesion and are targets for anti-inflammatory effects of peroxisome proliferator-activated receptor gamma ligands. *J. Biol. Chem.* 286, 38738–38747. doi: 10.1074/jbc.M111.247981

Chan, J. R., Hyduk, S. J., and Cybulsky, M. I. (2001). Chemoattractants induce a rapid and transient upregulation of monocyte alpha4 integrin affinity for vascular cell adhesion molecule 1 which mediates arrest: an early step in the process of emigration. *J. Exp. Med.* 193, 1149–1158. doi: 10.1084/jem.193.10.1149

Chang, J., Patton, J. T., Sarkar, A., Ernst, B., Magnani, J. L., and Frenette, P. S. (2010). GMI-1070, a novel pan-selectin antagonist, reverses acute vascular occlusions in sickle cell mice. *Blood* 116, 1779–1786. doi: 10.1182/blood-2009-12-260513

Chase, S. D., Magnani, J. L., and Simon, S. I. (2012). E-selectin ligands as mechanosensitive receptors on neutrophils in health and disease. *Ann. Biomed. Eng.* 40, 849–859. doi: 10.1007/s10439-011-0507-y

Chen, J., Haller, C. A., and Chaikof, E. L. (2016). Immune checkpoint regulator: a new assignment proposed for the classic adhesion molecule P-selectin glycoprotein ligand-1. *Transl. Cancer Res.* 5, S668–S671. doi: 10.21037/tcr.2016.10.05

Chen, X., Yang, L., and Zhai, S. D. (2012). Risk of cardiovascular disease and all-cause mortality among diabetic patients prescribed rosiglitazone or pioglitazone: a meta-analysis of retrospective cohort studies. *Chin. Med. J.* 125, 4301–4306. doi: 10.3760/cma.j.issn.0366-6999.2012.23.025

Chihara, M., Kurita, M., Yoshihara, Y., Asahina, A., and Yanaba, K. (2018). Clinical significance of serum galectin-9 and soluble CD155 levels in patients with systemic sclerosis. *J. Immunol. Res.* 2018:9473243. doi: 10.1155/2018/9473243

Choudhury, S. R., Babes, L., Rahn, J. J., Ahn, B. Y., Goring, K. R., King, J. C., et al. (2019). Dipeptidase-1 Is an Adhesion Receptor for Neutrophil Recruitment in Lungs and Liver. *Cell* 178, 1205–1221.e1217. doi: 10.1016/j.cell.2019.07.017

Clark, M. C., and Baum, L. G. (2012). T cells modulate glycans on CD43 and CD45 during development and activation, signal regulation, and survival. *Ann. N. Y. Acad. Sci.* 1253, 58–67. doi: 10.1111/j.1749-6632.2011.06304.x

Cooper, D., Norling, L. V., and Perretti, M. (2008). Novel insights into the inhibitory effects of Galectin-1 on neutrophil recruitment under flow. *J. Leukoc. Biol.* 83, 1459–1466. doi: 10.1189/jlb.1207831

De Filippo, K., and Rankin, S. M. (2018). CXCR4, the master regulator of neutrophil trafficking in homeostasis and disease. *Eur. J. Clin. Invest.* 48(Suppl. 2):e12949. doi: 10.1111/eci.12949

DeGrendele, H. C., Estess, P., Picker, L. J., and Siegelman, M. H. (1996). CD44 and its ligand hyaluronate mediate rolling under physiologic flow: a novel lymphocyte-endothelial cell primary adhesion pathway. *J. Exp. Med.* 183, 1119–1130. doi: 10.1084/jem.183.3.1119

Delaine, T., Collins, P., Mackinnon, A., Sharma, G., Stegmayr, J., Rajput, V. K., et al. (2016). Galectin-3-binding glycomimetics that strongly reduce bleomycin-induced lung fibrosis and modulate intracellular glycan recognition. *Chembiochem* 17, 1759–1770. doi: 10.1002/cbic.201600285

Di Gregoli, K., Somerville, M., Bianco, R., Thomas, A. C., Frankow, A., Newby, A. C., et al. (2020). Galectin-3 identifies a subset of macrophages with a potential beneficial role in atherosclerosis. *Arterioscler. Thromb. Vasc. Biol.* 40, 1491–1509. doi: 10.1161/ATVBAHA.120.314252

Diamond, M. S., and Springer, T. A. (1993). A subpopulation of Mac-1 (CD11b/CD18) molecules mediates neutrophil adhesion to ICAM-1 and fibrinogen. *J. Cell Biol.* 120, 545–556. doi: 10.1083/jcb.120.2.545

Diamond, M. S., Staunton, D. E., Marlin, S. D., and Springer, T. A. (1991). Binding of the integrin Mac-1 (CD11b/CD18) to the third immunoglobulin-like domain of ICAM-1 (CD54) and its regulation by glycosylation. *Cell* 65, 961–971. doi: 10.1016/0092-8674(91)90548-D

Dimitroff, C. J., Kupper, T. S., and Sackstein, R. (2003). Prevention of leukocyte migration to inflamed skin with a novel fluorosugar modifier of cutaneous lymphocyte-associated antigen. *J. Clin. Invest.* 112, 1008–1018. doi: 10.1172/JCI19220

Dong, R., Zhang, M., Hu, Q., Zheng, S., Soh, A., Zheng, Y., et al. (2018). Galectin-3 as a novel biomarker for disease diagnosis and a target for therapy (Review). *Int. J. Mol. Med.* 41, 599–614. doi: 10.3892/ijmm.2017.3311

Doring, Y., Noels, H., Mandl, M., Kramp, B., Neideck, C., Lievens, D., et al. (2014). Deficiency of the sialyltransferase St3Gal4 reduces Ccl5-mediated myeloid cell recruitment and arrest: short communication. *Circ. Res.* 114, 976–981. doi: 10.1161/CIRCRESAHA.114.302426

Dutrochet, M. H. (1824). *Recherches Anatomiques et Physiologiques sur la Structure Intime des Animaux et des Végétaux et sur leur Motilité*. Paris: J. B. Baillière. doi: 10.5962/bhl.title.117365

Dwivedi, V., Saini, P., Tasneem, A., Agarwal, K., and Sampathkumar, S. G. (2018). Differential inhibition of mucin-type O-glycosylation (MTOG) induced by peracetyl N-thioglycolyl-d-galactosamine (Ac5GalNTGc) in myeloid cells. *Biochem. Biophys. Res. Commun.* 506, 60–65. doi: 10.1016/j.bbrc.2018.08.131

Eckardt, V., Miller, M. C., Blanchet, X., Duan, R., Leberzammer, J., Duchene, J., et al. (2020). Chemokines and galectins form heterodimers to modulate inflammation. *EMBO Rep.* 21:e47852. doi: 10.15252/embr.201947852

Ferrand, Y., Klein, E., Barwell, N. P., Crump, M. P., Jimenez-Barbero, J., Vicent, C., et al. (2009). A synthetic lectin for O-linked beta-N-acetylglucosamine. *Angew. Chem. Int. Ed Engl.* 48, 1775–1779. doi: 10.1002/anie.200804905

Ferrero, E., Ferrero, M. E., Pardi, R., and Zocchi, M. R. (1995). The platelet endothelial cell adhesion molecule-1 (PECAM1) contributes to endothelial barrier function. *FEBS Lett.* 374, 323–326. doi: 10.1016/0014-5793(95)01110-Z

Festari, M. F., Trajtenberg, F., Berois, N., Pantano, S., Revoredo, L., Kong, Y., et al. (2017). Revisiting the human polypeptide GalNAc-T1 and T13 paralogs. *Glycobiology* 27, 140–153. doi: 10.1093/glycob/cww111

Frommhold, D., Ludwig, A., Bixel, M. G., Zarbock, A., Babushkina, I., Weissinger, M., et al. (2008). Sialyltransferase ST3Gal-IV controls CXCR2-mediated firm leukocyte arrest during inflammation. *J. Exp. Med.* 205, 1435–1446. doi: 10.1084/jem.20070846

Fuhlbrigge, R. C., King, S. L., Sackstein, R., and Kupper, T. S. (2006). CD43 is a ligand for E-selectin on CLA+ human T cells. *Blood* 107, 1421–1426. doi: 10.1182/blood-2005-05-2112

Gaber, A. O., Mulgaonkar, S., Kahan, B. D., Woodle, E. S., Alloway, R., Bajjoka, I., et al. (2011). YSPSL (rPSGL-Ig) for improvement of early renal allograft function: a double-blind, placebo-controlled, multi-center Phase IIa study. *Clin. Transplant.* 25, 523–533. doi: 10.1111/j.1399-0012.2010.01295.x

Gainers, M. E., Descheny, L., Barthel, S. R., Liu, L., Wurbel, M. A., and Dimitroff, C. J. (2007). Skin-homing receptors on effector leukocytes are differentially sensitive to glyco-metabolic antagonism in allergic contact dermatitis. *J. Immunol.* 179, 8509–8518. doi: 10.4049/jimmunol.179.12.8509

Galeano, B., Klootwijk, R., Manoli, I., Sun, M., Ciccone, C., Darvish, D., et al. (2007). Mutation in the key enzyme of sialic acid biosynthesis causes severe glomerular proteinuria and is rescued by N-acetylmannosamine. *J. Clin. Invest.* 117, 1585–1594. doi: 10.1172/JCI30954

Gangavarapu, P., Rajagopalan, L., Kolli, D., Guerrero-Plata, A., Garofalo, R. P., and Rajarathnam, K. (2012). The monomer-dimer equilibrium and glycosaminoglycan interactions of chemokine CXCL8 regulate tissue-specific neutrophil recruitment. *J. Leukoc. Biol.* 91, 259–265. doi: 10.1189/jlb.0511239

Gedeit, R. G. (1996). Tumor necrosis factor-induced E-selectin expression on vascular endothelial cells. *Crit. Care Med.* 24, 1543–1546. doi: 10.1097/00003246-199609000-00019

Gittens, B. R., Bodkin, J. V., Nourshargh, S., Perretti, M., and Cooper, D. (2017). Galectin-3: a positive regulator of leukocyte recruitment in the inflamed microcirculation. *J. Immunol.* 198, 4458–4469. doi: 10.4049/jimmunol.1600709

Goldblatt, J., Lawrenson, R. A., Muir, L., Dattani, S., Hoffland, A., Tsuchiya, T., et al. (2019). A requirement for neutrophil glycosaminoglycans in chemokine:receptor interactions is revealed by the streptococcal protease SpyCEP. *J. Immunol.* 202, 3246–3255. doi: 10.4049/jimmunol.1801688

Gornik, O., and Lauc, G. (2008). Glycosylation of serum proteins in inflammatory diseases. *Dis. Markers* 25, 267–278. doi: 10.1155/2008/493289

Haslam, S. M., Julien, S., Burchell, J. M., Monk, C. R., Ceroni, A., Garden, O. A., et al. (2008). Characterizing the glycome of the mammalian immune system. *Immunol. Cell Biol.* 86, 564–573. doi: 10.1038/icb.2008.54

Hauser, M. A., Kindinger, I., Laufer, J. M., Spate, A. K., Bucher, D., Vanes, S. L., et al. (2016). Distinct CCR7 glycosylation pattern shapes receptor signaling and endocytosis to modulate chemotactic responses. *J. Leukoc. Biol.* 99, 993–1007. doi: 10.1189/jlb.2VMA0915-432RR

He, X. W., Li, W. L., Li, C., Liu, P., Shen, Y. G., Zhu, M., et al. (2017). Serum levels of galectin-1, galectin-3, and galectin-9 are associated with large artery atherosclerotic stroke. *Sci. Rep.* 7:40994. doi: 10.1038/srep40994

Hevey, R. (2019). Strategies for the development of glycomimetic drug candidates. *Pharmaceuticals* 12:55. doi: 10.3390/ph12020055

Hidalgo, A., Peired, A. J., Wild, M., Vestweber, D., and Frenette, P. S. (2007). Complete identification of E-selectin ligands on neutrophils reveals distinct functions of PSGL-1, ESL-1, and CD44. *Immunity* 26, 477–489. doi: 10.1016/j.immuni.2007.03.011

Hobbs, S. J., and Nolz, J. C. (2017). Regulation of T cell trafficking by enzymatic synthesis of O-glycans. *Front. Immunol.* 8:600. doi: 10.3389/fimmu.2017.00600

Huo, Y., Hafezi-Moghadam, A., and Ley, K. (2000). Role of vascular cell adhesion molecule-1 and fibronectin connecting segment-1 in monocyte rolling and adhesion on early atherosclerotic lesions. *Circ. Res.* 87, 153–159. doi: 10.1161/01.RES.87.2.153

Iqbal, A. J., Sampaio, A. L., Maione, F., Greco, K. V., Niki, T., Hirashima, M., et al. (2011). Endogenous galectin-1 and acute inflammation: emerging notion of a galectin-9 pro-resolving effect. *Am. J. Pathol.* 178, 1201–1209. doi: 10.1016/j.ajpath.2010.11.073

Jiang, J., Kanabar, V., Padilla, B., Man, F., Pitchford, S. C., Page, C. P., et al. (2016). Uncharged nucleoside inhibitors of beta-1,4-galactosyltransferase with activity in cells. *Chem. Commun.* 52, 3955–3958. doi: 10.1039/C5CC09289B

Joseph, P. R., Mosier, P. D., Desai, U. R., and Rajarathnam, K. (2015). Solution NMR characterization of chemokine CXCL8/IL-8 monomer and dimer binding to glycosaminoglycans: structural plasticity mediates differential binding interactions. *Biochem. J.* 472, 121–133. doi: 10.1042/BJ20150059

Kadono, T., Venturi, G. M., Steeber, D. A., and Tedder, T. F. (2002). Leukocyte rolling velocities and migration are optimized by cooperative L-selectin and intercellular adhesion molecule-1 functions. *J. Immunol.* 169, 4542–4550. doi: 10.4049/jimmunol.169.8.4542

Kanabar, V., Tedaldi, L., Jiang, J., Nie, X., Panina, I., Descroix, K., et al. (2016). Base-modified UDP-sugars reduce cell surface levels of P-selectin glycoprotein 1 (PSGL-1) on IL-1beta-stimulated human monocytes. *Glycobiology* 26, 1059–1071. doi: 10.1093/glycob/cww053

Katayama, Y., Hidalgo, A., Chang, J., Peired, A., and Frenette, P. S. (2005). CD44 is a physiological E-selectin ligand on neutrophils. *J. Exp. Med.* 201, 1183–1189. doi: 10.1084/jem.20042014

Kelm, M., Lehoux, S., Azcutia, V., Cummings, R. D., Nusrat, A., Parkos, C. A., et al. (2020). Regulation of neutrophil function by selective targeting of glycan epitopes expressed on the integrin CD11b/CD18. *FASEB J.* 34, 2326–2343. doi: 10.1096/fj.201902542R

Kitazume, S., Imamaki, R., Ogawa, K., Komi, Y., Futakawa, S., Kojima, S., et al. (2010). Alpha2,6-sialic acid on platelet endothelial cell adhesion molecule (PECAM) regulates its homophilic interactions and downstream antiapoptotic signaling. *J. Biol. Chem.* 285, 6515–6521. doi: 10.1074/jbc.M109.073106

Krishnamurthy, V. R., Sardar, M. Y., Ying, Y., Song, X., Haller, C., Dai, E., et al. (2015). Glycopeptide analogues of PSGL-1 inhibit P-selectin *in vitro* and *in vivo*. *Nat. Commun.* 6:6387. doi: 10.1038/ncomms7387

La, M., Cao, T. V., Cerchiaro, G., Chilton, K., Hirabayashi, J., Kasai, K.-I., et al. (2003). A novel biological activity for galectin-1: inhibition of leukocyte-endothelial cell interactions in experimental inflammation. *Am. J. Pathol.* 163, 1505–1515. doi: 10.1016/S0002-9440(10)63507-9

Laine, R. A. (1994). A calculation of all possible oligosaccharide isomers both branched and linear yields 1.05 x 10(12) structures for a reducing hexasaccharide: the Isomer Barrier to development of single-method saccharide sequencing or synthesis systems. *Glycobiology* 4, 759–767. doi: 10.1093/glycob/4.6.759

Larsson, J. M., Karlsson, H., Crespo, J. G., Johansson, M. E., Eklund, L., Sjovall, H., et al. (2011). Altered O-glycosylation profile of MUC2 mucin occurs in active ulcerative colitis and is associated with increased inflammation. *Inflamm. Bowel Dis.* 17, 2299–2307. doi: 10.1002/ibd.21625

Lee, T. H., Mitchell, A., Liu Lau, S., An, H., Rajeaskariah, P., Wasinger, V., et al. (2013). Glycosylation in a mammalian expression system is critical for the production of functionally active leukocyte immunoglobulin-like receptor A3 protein. *J. Biol. Chem.* 288, 32873–32885. doi: 10.1074/jbc.M113.478578

Lertkiatmongkol, P., Paddock, C., Newman, D. K., Zhu, J., Thomas, M. J., and Newman, P. J. (2016). The role of sialylated glycans in human platelet endothelial cell adhesion molecule 1 (PECAM-1)-mediated trans homophilic interactions and endothelial cell barrier function. *J. Biol. Chem.* 291, 26216–26225. doi: 10.1074/jbc.M116.756502

Ley, K., Laudanna, C., Cybulsky, M. I., and Nourshargh, S. (2007). Getting to the site of inflammation: the leukocyte adhesion cascade updated. *Nat. Rev. Immunol.* 7, 678–689. doi: 10.1038/nri2156

Li, P., Liu, S., Lu, M., Bandyopadhyay, G., Oh, D., Imamura, T., et al. (2016). Hematopoietic-derived galectin-3 causes cellular and systemic insulin resistance. *Cell* 167, 973–984.e912. doi: 10.1016/j.cell.2016.10.025

Liehn, E. A., Tuchscheerer, N., Kanzler, I., Drechsler, M., Fraemohs, L., Schuh, A., et al. (2011). Double-edged role of the CXCL12/CXCR4 axis in experimental myocardial infarction. *J. Am. Coll. Cardiol.* 58, 2415–2423. doi: 10.1016/j.jacc.2011.08.033

Ludwig, A., Ehlert, J. E., Flad, H. D., and Brandt, E. (2000). Identification of distinct surface-expressed and intracellular CXC-chemokine receptor 2 glycoforms in neutrophils: N-glycosylation is essential for maintenance of receptor surface expression. *J. Immunol.* 165, 1044–1052. doi: 10.4049/jimmunol.165.2.1044

Maas, S. L., Soehnlein, O., and Viola, J. R. (2018). Organ-specific mechanisms of transendothelial neutrophil migration in the lung, liver, kidney, and aorta. *Front. Immunol.* 9:2739. doi: 10.3389/fimmu.2018.02739

Mahanti, M., Pal, K. B., Sundin, A. P., Leffler, H., and Nilsson, U. J. (2020). Epimers switch galectin-9 domain selectivity: 3N-Aryl galactosides bind the C-terminal and gulosides bind the N-terminal. *ACS Med. Chem. Lett.* 11, 34–39. doi: 10.1021/acsmedchemlett.9b00396

Marathe, D. D., Buffone, A. Jr., Chandrasekaran, E. V., Xue, J., Locke, R. D., Nasirikenari, M., et al. (2010). Fluorinated per-acetylated GalNAc metabolically alters glycan structures on leukocyte PSGL-1 and reduces cell binding to selectins. *Blood* 115, 1303–1312. doi: 10.1182/blood-2009-07-231480

Matsumoto, M., Atarashi, K., Umemoto, E., Furukawa, Y., Shigeta, A., Miyasaka, M., et al. (2005). CD43 functions as a ligand for E-selectin on activated T cells. *J. Immunol.* 175, 8042–8050. doi: 10.4049/jimmunol.175.12.8042

Matsumoto, M., Shigeta, A., Furukawa, Y., Tanaka, T., Miyasaka, M., and Hirata, T. (2007). CD43 collaborates with P-selectin glycoprotein ligand-1 to mediate E-selectin-dependent T cell migration into inflamed skin. *J. Immunol.* 178, 2499–2506. doi: 10.4049/jimmunol.178.4.2499

Matsuoka, N., Fujita, Y., Temmoku, J., Furuya, M. Y., Asano, T., Sato, S., et al. (2020). Galectin-9 as a biomarker for disease activity in systemic lupus erythematosus. *PLoS ONE* 15:e0227069. doi: 10.1371/journal.pone.0227069

May, C., Ji, S., Syed, Z. A., Revoredo, L., Daniel, E. J. P., Gerken, T. A., et al. (2020). Differential splicing of the lectin domain of an O-glycosyltransferase modulates both peptide and glycopeptide preferences. *J. Biol. Chem.* 295, 12525–12536. doi: 10.1074/jbc.RA120.014700

McDonald, B., and Kubes, P. (2015). Interactions between CD44 and hyaluronan in leukocyte trafficking. *Front. Immunol.* 6:68. doi: 10.3389/fimmu.2015.00068

McDonald, K. R., Hernandez-Nichols, A. L., Barnes, J. W., and Patel, R. P. (2020). Hydrogen peroxide regulates endothelial surface N-glycoforms to control inflammatory monocyte rolling and adhesion. *Redox Biol.* 34:101498. doi: 10.1016/j.redox.2020.101498

Mertens, P., Maes, A., Nuyts, J., Belmans, A., Desmet, W., Esplugas, E., et al. (2006). Recombinant P-selectin glycoprotein ligand-immunoglobulin, a P-selectin antagonist, as an adjunct to thrombolysis in acute myocardial infarction. The P-selectin antagonist limiting myonecrosis (PSALM) trial. *Am. Heart J.* 152, 125.e121–128. doi: 10.1016/j.ahj.2006.04.020

Middleton, J., Patterson, A. M., Gardner, L., Schmutz, C., and Ashton, B. A. (2002). Leukocyte extravasation: chemokine transport and presentation by the endothelium. *Blood* 100, 3853–3860. doi: 10.1182/blood.V100.12.3853

Mitroulis, I., Alexaki, V. I., Kourtzelis, I., Ziogas, A., Hajishengallis, G., and Chavakis, T. (2015). Leukocyte integrins: role in leukocyte recruitment and as therapeutic targets in inflammatory disease. *Pharmacol. Ther.* 147, 123–135. doi: 10.1016/j.pharmthera.2014.11.008

Mondal, N., Buffone, A. Jr., and Neelamegham, S. (2013). Distinct glycosyltransferases synthesize E-selectin ligands in human vs. mouse leukocytes. *Cell Adh. Migr.* 7, 288–292. doi: 10.4161/cam.24714

Moons, S. J., Adema, G. J., Derks, M. T., Boltje, T. J., and Bull, C. (2019). Sialic acid glycoengineering using N-acetylmannosamine and sialic acid analogs. *Glycobiology* 29, 433–445. doi: 10.1093/glycob/cwz026

Morikis, V. A., Chase, S., Wun, T., Chaikof, E. L., Magnani, J. L., and Simon, S. I. (2017). Selectin catch-bonds mechanotransduce integrin activation and neutrophil arrest on inflamed endothelium under shear flow. *Blood* 130, 2101–2110. doi: 10.1182/blood-2017-05-783027

Muller, W. A., Weigl, S. A., Deng, X., and Phillips, D. M. (1993). PECAM-1 is required for transendothelial migration of leukocytes. *J. Exp. Med.* 178, 449–460. doi: 10.1084/jem.178.2.449

Newton, J. P., Buckley, C. D., Jones, E. Y., and Simmons, D. L. (1997). Residues on both faces of the first immunoglobulin fold contribute to homophilic binding sites of PECAM-1/CD31. *J. Biol. Chem.* 272, 20555–20563. doi: 10.1074/jbc.272.33.20555

Norling, L. V., Sampaio, A. L., Cooper, D., and Perretti, M. (2008). Inhibitory control of endothelial galectin-1 on *in vitro* and *in vivo* lymphocyte trafficking. *FASEB J.* 22, 682–690. doi: 10.1096/fj.07-9268com

Nourshargh, S., Krombach, F., and Dejana, E. (2006). The role of JAM-A and PECAM-1 in modulating leukocyte infiltration in inflamed and ischemic tissues. *J. Leukoc. Biol.* 80, 714–718. doi: 10.1189/jlb.1105645

Osawa, M., Masuda, M., Kusano, K., and Fujiwara, K. (2002). Evidence for a role of platelet endothelial cell adhesion molecule-1 in endothelial cell mechanosignal transduction: is it a mechanoresponsive molecule? *J. Cell Biol.* 158, 773–785. doi: 10.1083/jcb.200205049

Pal, K. B., Mahanti, M., Huang, X., Persson, S., Sundin, A. P., Zetterberg, F. R., et al. (2018). Quinoline-galactose hybrids bind selectively with high affinity to a galectin-8 N-terminal domain. *Org. Biomol. Chem.* 16, 6295–6305. doi: 10.1039/C8OB01354C

Pal, K. B., Mahanti, M., Leffler, H., and Nilsson, U. J. (2019). A galactoside-binding protein tricked into binding unnatural pyranose derivatives: 3-deoxy-3-methyl-gulosides selectively inhibit galectin-1. *Int. J. Mol. Sci.* 20:3786. doi: 10.3390/ijms20153786

Patel, M. S., Miranda-Nieves, D., Chen, J., Haller, C. A., and Chaikof, E. L. (2017). Targeting P-selectin glycoprotein ligand-1/P-selectin interactions as a novel therapy for metabolic syndrome. *Transl. Res* 183, 1–13. doi: 10.1016/j.trsl.2016.11.007

Privratsky, J. R., Paddock, C. M., Florey, O., Newman, D. K., Muller, W. A., and Newman, P. J. (2011). Relative contribution of PECAM-1 adhesion and signaling to the maintenance of vascular integrity. *J. Cell Sci.* 124, 1477–1485. doi: 10.1242/jcs.082271

Proudfoot, A. E., Handel, T. M., Johnson, Z., Lau, E. K., Liwang, P., Clark-Lewis, I., et al. (2003). Glycosaminoglycan binding and oligomerization are essential for the *in vivo* activity of certain chemokines. *Proc. Natl. Acad. Sci. U.S.A.* 100, 1885–1890. doi: 10.1073/pnas.0334864100

Rajarathnam, K., Sepuru, K. M., Joseph, P. R. B., Sawant, K. V., and Brown, A. J. (2018). Glycosaminoglycan interactions fine-tune chemokine-mediated neutrophil trafficking: structural insights and molecular mechanisms. *J. Histochem. Cytochem.* 66, 229–239. doi: 10.1369/0022155417739864

Regal-McDonald, K., Somarathna, M., Lee, T., Litovsky, S. H., Barnes, J., Peretik, J. M., et al. (2020). Assessment of ICAM-1 N-glycoforms in mouse and human models of endothelial dysfunction. *PLoS ONE* 15:e0230358. doi: 10.1371/journal.pone.0230358

Regal-McDonald, K., Xu, B., Barnes, J. W., and Patel, R. P. (2019). High-mannose intercellular adhesion molecule-1 enhances CD16(+) monocyte adhesion to the endothelium. *Am. J. Physiol. Heart Circ. Physiol.* 317, H1028–H1038. doi: 10.1152/ajpheart.00306.2019

Reily, C., Stewart, T. J., Renfrow, M. B., and Novak, J. (2019). Glycosylation in health and disease. *Nat. Rev. Nephrol.* 15, 346–366. doi: 10.1038/s41581-019-0129-4

Rillahan, C. D., Antonopoulos, A., Lefort, C. T., Sonon, R., Azadi, P., Ley, K., et al. (2012). Global metabolic inhibitors of sialyl- and fucosyltransferases remodel the glycome. *Nat. Chem. Biol.* 8, 661–668. doi: 10.1038/nchembio.999

Robinson, B. S., Arthur, C. M., Evavold, B., Roback, E., Kamili, N. A., Stowell, C. S., et al. (2019). The sweet-side of leukocytes: galectins as master regulators of neutrophil function. *Front. Immunol.* 10:1762. doi: 10.3389/fimmu.2019.01762

Rossaint, J., and Zarbock, A. (2013). Tissue-specific neutrophil recruitment into the lung, liver, and kidney. *J. Innate Immun.* 5, 348–357. doi: 10.1159/000345943

Saggu, G., Okubo, K., Chen, Y., Vattepu, R., Tsuboi, N., Rosetti, F., et al. (2018). Cis interaction between sialylated FcgammaRIIA and the alphaI-domain of Mac-1 limits antibody-mediated neutrophil recruitment. *Nat. Commun.* 9:5058. doi: 10.1038/s41467-018-07506-1

Salameh, B. A., Cumpstey, I., Sundin, A., Leffler, H., and Nilsson, U. J. (2010). 1H-1,2,3-triazol-1-yl thiodigalactoside derivatives as high affinity galectin-3 inhibitors. *Bioorg. Med. Chem.* 18, 5367–5378. doi: 10.1016/j.bmc.2010.05.040

Schaff, U., Mattila, P. E., Simon, S. I., and Walcheck, B. (2008). Neutrophil adhesion to E-selectin under shear promotes the redistribution and co-clustering of ADAM17 and its proteolytic substrate L-selectin. *J. Leukoc. Biol.* 83, 99–105. doi: 10.1189/jlb.0507304

Schjoldager, K. T., Narimatsu, Y., Joshi, H. J., and Clausen, H. (2020). Global view of human protein glycosylation pathways and functions. *Nat. Rev. Mol. Cell Biol.* 21, 729–749. doi: 10.1038/s41580-020-00294-x

Schnoor, M., Vadillo, E., and Guerrero-Fonseca, I. M. (2021). The extravasation cascade revisited from a neutrophil perspective. *Curr. Opin. Physiol.* 19, 119–128. doi: 10.1016/j.cophys.2020.09.014

Scott, D. W., Chen, J., Chacko, B. K., Traylor, J. G. Jr., Orr, A. W., and Patel, R. P. (2012). Role of endothelial N-glycan mannose residues in monocyte recruitment during atherogenesis. *Arterioscler. Thromb. Vasc. Biol.* 32, e51–e59. doi: 10.1161/ATVBAHA.112.253203

Scott, D. W., Dunn, T. S., Ballestas, M. E., Litovsky, S. H., and Patel, R. P. (2013a). Identification of a high-mannose ICAM-1 glycoform: effects of

ICAM-1 hypoglycosylation on monocyte adhesion and outside in signaling. *Am. J. Physiol. Cell Physiol.* 305, C228–237. doi: 10.1152/ajpcell.00116.2013

Scott, D. W., Tolbert, C. E., Graham, D. M., Wittchen, E., Bear, J. E., and Burridge, K. (2015). N-glycosylation controls the function of junctional adhesion molecule-A. *Mol. Biol. Cell* 26, 3205–3214. doi: 10.1091/mbc.e14-12-1604

Scott, D. W., Vallejo, M. O., and Patel, R. P. (2013b). Heterogenic endothelial responses to inflammation: role for differential N-glycosylation and vascular bed of origin. *J. Am. Heart Assoc.* 2:e000263. doi: 10.1161/JAHA.113.000263

Singbartl, K., Thatte, J., Smith, M. L., Wethmar, K., Day, K., and Ley, K. (2001). A CD2-green fluorescence protein-transgenic mouse reveals very late antigen-4-dependent CD8+ lymphocyte rolling in inflamed venules. *J. Immunol.* 166, 7520–7526. doi: 10.4049/jimmunol.166.12.7520

Sperandio, M., Frommhold, D., Babushkina, I., Ellies, L. G., Olson, T. S., Smith, M. L., et al. (2006). Alpha 2,3-sialyltransferase-IV is essential for L-selectin ligand function in inflammation. *Eur. J. Immunol.* 36, 3207–3215. doi: 10.1002/eji.200636157

Sriramarao, P., Berger, E., Chambers, J. D., Arfors, K. E., and Gehlsen, K. R. (1993). High mannose type N-linked oligosaccharides on endothelial cells may influence beta 2 integrin mediated neutrophil adherence *in vitro*. *J. Cell. Biochem.* 51, 360–368. doi: 10.1002/jcb.240510316

Stadtmann, A., Germena, G., Block, H., Boras, M., Rossaint, J., Sundd, P., et al. (2013). The PSGL-1-L-selectin signaling complex regulates neutrophil adhesion under flow. *J. Exp. Med.* 210, 2171–2180. doi: 10.1084/jem.20130664

Stegmayr, J., Zetterberg, F., Carlsson, M. C., Huang, X., Sharma, G., Kahl-Knutson, B., et al. (2019). Extracellular and intracellular small-molecule galectin-3 inhibitors. *Sci. Rep.* 9:2186. doi: 10.1038/s41598-019-38497-8

Su, M. L., Chang, T. M., Chiang, C. H., Chang, H. C., Hou, M. F., Li, W. S., et al. (2014). Inhibition of chemokine (C-C motif) receptor 7 sialylation suppresses CCL19-stimulated proliferation, invasion and anti-anoikis. *PLoS ONE* 9:e98823. doi: 10.1371/journal.pone.0098823

Suryawanshi, A., Cao, Z., Thitiprasert, T., Zaidi, T. S., and Panjwani, N. (2013). Galectin-1-mediated suppression of Pseudomonas aeruginosa-induced corneal immunopathology. *J. Immunol.* 190, 6397–6409. doi: 10.4049/jimmunol.1203501

Taylor, A. D., Neelamegham, S., Hellums, J. D., Smith, C. W., and Simon, S. I. (1996). Molecular dynamics of the transition from L-selectin- to beta 2-integrin-dependent neutrophil adhesion under defined hydrodynamic shear. *Biophys. J.* 71, 3488–3500. doi: 10.1016/S0006-3495(96)79544-9

Tenno, M., Ohtsubo, K., Hagen, F. K., Ditto, D., Zarbock, A., Schaerli, P., et al. (2007). Initiation of protein O glycosylation by the polypeptide GalNAcT-1 in vascular biology and humoral immunity. *Mol. Cell. Biol.* 27, 8783–8796. doi: 10.1128/MCB.01204-07

Tsang, Y. T., Neelamegham, S., Hu, Y., Berg, E. L., Burns, A. R., Smith, C. W., et al. (1997). Synergy between L-selectin signaling and chemotactic activation during neutrophil adhesion and transmigration. *J. Immunol.* 159, 4566–4577.

Tzima, E., Irani-Tehrani, M., Kiosses, W. B., Dejana, E., Schultz, D. A., Engelhardt, B., et al. (2005). A mechanosensory complex that mediates the endothelial cell response to fluid shear stress. *Nature* 437, 426–431. doi: 10.1038/nature 03952

Varki, A. (2017). Biological roles of glycans. *Glycobiology* 27, 3–49. doi: 10.1093/glycob/cww086

Varki, A., Etzler, M. E., Cummings, R. D., and Esko, J. D. (2009). "Chapter 26: Discovery and classification of glycan-binding proteins," in *Essentials of Glycobiology. 2nd Edn.*, eds A. Varki, R. D. Cummings, J. D. Esko, et al. (Cold Spring Harbor, NY: Cold Spring Harbor Laboratory Press).

Videira, P. A., Marcelo, F., and Grewal, R. K. (2018). "Glycosyltransferase inhibitors: a promising strategy to pave a path from laboratory to therapy," in *Carbohydrate Chemistry: Chemical and Biological Approaches, Vol. 43*, eds A. P. Rauter, T. K. Lindhorst, Y. Bleriot, and Y. Queneau (London: The Royal Society of Chemistry), 135–158. doi: 10.1039/9781788010641-00135

Wagner, R. (1839). *Erläuterungstafeln zur Phyisologie und Entwicklungsgeschichte.* Leipzig: L. Voss. doi: 10.5962/bhl.title.122892

Weber, M., Hauschild, R., Schwarz, J., Moussion, C., De Vries, I., Legler, D. F., et al. (2013). Interstitial dendritic cell guidance by haptotactic chemokine gradients. *Science* 339, 328–332. doi: 10.1126/science.1228456

Weninger, W., Ulfman, L. H., Cheng, G., Souchkova, N., Quackenbush, E. J., Lowe, J. B., et al. (2000). Specialized contributions by alpha(1,3)-fucosyltransferase-IV and FucT-VII during leukocyte rolling in dermal microvessels. *Immunity* 12, 665–676. doi: 10.1016/S1074-7613(00)80217-4

White, G. E., Iqbal, A. J., and Greaves, D. R. (2013). CC chemokine receptors and chronic inflammation–therapeutic opportunities and pharmacological challenges. *Pharmacol. Rev.* 65, 47–89. doi: 10.1124/pr.111.005074

Wright, R. D., and Cooper, D. (2014). Glycobiology of leukocyte trafficking in inflammation. *Glycobiology* 24, 1242–1251. doi: 10.1093/glycob/cwu101

Xu, H., Manivannan, A., Liversidge, J., Sharp, P. F., Forrester, J. V., and Crane, I. J. (2002). Involvement of CD44 in leukocyte trafficking at the blood-retinal barrier. *J. Leukoc. Biol.* 72, 1133–1141. doi: 10.1189/jlb.72.6.1133

Yamamoto, H., Nishi, N., Shoji, H., Itoh, A., Lu, L.-H., Hirashima, M., et al. (2008). Induction of cell adhesion by galectin-8 and its target molecules in Jurkat T-cells. *J. Biochem.* 143, 311–324. doi: 10.1093/jb/mvm223

Yang, H. M., Yu, C., and Yang, Z. (2012). N-acetylglucosaminyltransferase V negatively regulates integrin alpha5beta1-mediated monocyte adhesion and transmigration through vascular endothelium. *Int. J. Oncol.* 41, 589–598. doi: 10.3892/ijo.2012.1484

Ye, Z., Zhong, L., Zhu, S., Wang, Y., Zheng, J., Wang, S., et al. (2019). The P-selectin and PSGL-1 axis accelerates atherosclerosis via activation of dendritic cells by the TLR4 signaling pathway. *Cell Death Dis.* 10:507. doi: 10.1038/s41419-019-1736-5

Zen, K., Cui, L. B., Zhang, C. Y., and Liu, Y. (2007). Critical role of mac-1 sialyl lewis x moieties in regulating neutrophil degranulation and transmigration. *J. Mol. Biol.* 374, 54–63. doi: 10.1016/j.jmb.2007.09.014

Zernecke, A., Bot, I., Djalali-Talab, Y., Shagdarsuren, E., Bidzhekov, K., Meiler, S., et al. (2008). Protective role of CXC receptor 4/CXC ligand 12 unveils the importance of neutrophils in atherosclerosis. *Circ. Res.* 102, 209–217. doi: 10.1161/CIRCRESAHA.107.160697

Conflict of Interest: The authors declare that the research was conducted in the absence of any commercial or financial relationships that could be construed as a potential conflict of interest.

frontiers in Cell and Developmental Biology

REVIEW
published: 04 February 2021
doi: 10.3389/fcell.2021.626136

Monitoring Phosphoinositide Fluxes and Effectors During Leukocyte Chemotaxis and Phagocytosis

Fernando Montaño-Rendón [1,2], Sergio Grinstein [1,2,3,4] and Glenn F. W. Walpole [1,3]*

[1] Program in Cell Biology, Hospital for Sick Children, Toronto, ON, Canada, [2] Institute of Medical Sciences, University of Toronto, Toronto, ON, Canada, [3] Department of Biochemistry, University of Toronto, Toronto, ON, Canada, [4] Keenan Research Centre for Biomedical Science, St. Michael's Hospital, Toronto, ON, Canada

The dynamic re-organization of cellular membranes in response to extracellular stimuli is fundamental to the cell physiology of myeloid and lymphoid cells of the immune system. In addition to maintaining cellular homeostatic functions, remodeling of the plasmalemma and endomembranes endow leukocytes with the potential to relay extracellular signals across their biological membranes to promote rolling adhesion and diapedesis, migration into the tissue parenchyma, and to ingest foreign particles and effete cells. Phosphoinositides, signaling lipids that control the interface of biological membranes with the external environment, are pivotal to this wealth of functions. Here, we highlight the complex metabolic transitions that occur to phosphoinositides during several stages of the leukocyte lifecycle, namely diapedesis, migration, and phagocytosis. We describe classical and recently developed tools that have aided our understanding of these complex lipids. Finally, major downstream effectors of inositides are highlighted including the cytoskeleton, emphasizing the importance of these rare lipids in immunity and disease.

Keywords: phosphoinositides, inositol lipids, macrophage, neutrophil, chemotaxis, phagocytosis, lipid biosensors, lipid signaling

OPEN ACCESS

Edited by:
Emilio Hirsch,
University of Turin, Italy

Reviewed by:
Federico Gulluni,
University of Turin, Italy
Stephen Geoffrey Ward,
University of Bath, United Kingdom

***Correspondence:**
Sergio Grinstein
sergio.grinstein@sickkids.ca

Specialty section:
This article was submitted to Cell Adhesion and Migration, a section of the journal Frontiers in Cell and Developmental Biology

Received: *04 November 2020*
Accepted: *06 January 2021*
Published: *04 February 2021*

Citation:
Montaño-Rendón F, Grinstein S and Walpole GFW (2021) Monitoring Phosphoinositide Fluxes and Effectors During Leukocyte Chemotaxis and Phagocytosis. Front. Cell Dev. Biol. 9:626136. doi: 10.3389/fcell.2021.626136

INTRODUCTION

Chemotaxis and phagocytosis are fundamental processes employed by myeloid cells of the immune system to protect the body from harmful invading microorganisms and maintain tissue homeostasis. Neutrophils, which are prototypical of myeloid cells, are the dominant circulating leukocytes; every day billions of neutrophils enter and exit the circulation (Teng et al., 2017). Their importance is revealed in cases of neutropenia –a decrease in the number or quality of circulating neutrophils—which results in recurrent bacterial infections (Leliefeld et al., 2016).

When pathogens break through the epithelial barriers of the host, circulating neutrophils are rapidly recruited to the site of infection. Upon invasion, pathogens cause the local release of molecules such as formyl peptides, peptidoglycans or lipoproteins. Further, proximal tissues are flagged for recognition by the production of inflammatory mediators (Nathan, 2006). Neutrophils sense these pathogen-associated molecules and inflammatory signals through various receptors including Toll-like receptors (TLRs) and G protein-coupled receptors (GPCRs). Upon receptor activation, neutrophils undertake diapedesis to exit blood vessels and migrate toward the site of infection within the tissue parenchyma to deploy antimicrobial functions, including but not limited to phagocytosis (Mayadas et al., 2014). They generate reactive oxygen species, release antimicrobial

peptides and other cytotoxic granule components, and form neutrophil extracellular traps, all of which are effective in creating a microbicidal environment intended to eliminate pathogenic organisms (Segal, 2005). The multistep process of rolling adhesion, paracellular extravasation through endothelial junctions, migration, and ultimately the deployment of antimicrobial functions demands great morphological and functional diversity of leukocytes.

Importantly, the roles of neutrophils and other myeloid cells extend far beyond the clearance of pathogenic microorganisms. Excellent reviews are available that highlight their roles in cancer (Coffelt et al., 2016), auto-immunity (Thieblemont et al., 2016), and overall health and disease (Liew and Kubes, 2019).

Here, we describe the dynamic receptor-mediated processes of leukocyte chemotaxis and phagocytosis, two responses that are highly dependent on lipidic signals. We highlight the role that phosphoinositides, key signaling lipid molecules, play in regulating the complex series of events involved in the actin re-organization that underlies cell migration and phagocytosis. Furthermore, we describe the current tools used to study and manipulate phosphoinositides and, when possible, offer insights of their relevance to health and disease.

Part I: Introduction to Phosphoinositides

Cellular processes, such as signal transduction, endocytosis, exocytosis, and cell migration are dependent on cellular membranes. These membranes (plasmalemmal and endomembranes) are dynamic entities that constantly undergo remodeling events, typified by fusion, budding and fission. Understandably, regulation of membrane dynamics is critical for cellular physiology. Pivotal to this regulation is the timely recruitment of effector proteins to specific membranes and to sub-domains therein. Phosphoinositides (PPIns) contribute importantly to this recruitment.

Phosphoinositides are phosphorylated derivates of phosphatidylinositol (PtdIns). They represent a minor fraction of the cellular phospholipids, yet they regulate a plethora of biological responses. PtdIns consists of a diacylglycerol (DAG) linked to D-myo-inositol-1-phosphate ring by a phosphodiester linkage. Phosphorylation can occur in the 3-, 4-, and 5-hydroxyl groups of the inositol ring, giving rise to the seven naturally occurring PPIns species. The interconversion of PPIns into other lipid species or other secondary messengers is facilitated by numerous kinases, phosphatases, and lipases which possess refined activities toward a subset of the 1-, 3-, 4-, or 5-moieities of the inositol ring. As a result, PPIns are differentially distributed among cellular membranes and within distinct membrane sub-domains, where they selectively recruit effector proteins and act as landmarks for membrane identity (Balla, 2013).

Phosphoinositides exert their functions by interacting with membrane resident molecules such as transporters and ion channels, or by selectively recruiting signaling molecules in a reversible manner. These interactions are facilitated by stereospecific inositide-binding domains present in the signaling molecules that get recruited by PPIns. The first of these domains was identified in pleckstrin (Harlan et al., 1994) and since then, the term pleckstrin homology (PH) domain has been used to refer to these homologous modules. A vast array of regulatory modules bear PH domains (Cozier et al., 2004). However, it is worth mentioning that not all PH domains bind phosphoinositides and that many also have protein-binding properties. Other classes of PPIns-binding domains have been identified: these include FERM domains that link the actin cytoskeleton to PPIns of the plasma membrane (PM) (Chishti et al., 1998), BAR and EHD domains that can sense and induce membrane curvature, and FYVE and PX domains that target several protein families to endolysosomal membranes (Chishti et al., 1998; Frost et al., 2009).

The discovery of such domains has been instrumental for studying the function and localization of PPIns (Hammond and Balla, 2015) *in situ*. As discussed below, the use of specific PPIns-binding domains as biosensors has been crucial in gaining insight of the distribution, dynamics and function of PPIns. These probes have made it possible to establish that different PPIns mark distinct membranes. Thus, PtdIns(4)P, PtdIns(4,5)P_2, PtdIns(3,4,5)P_3, and PtdIns(3,4)P_2 are present almost exclusively at the PM, whereas PtdIns(4)P is recognized as the signature PPIns of the Golgi complex, and pools of PtdIns(3)P and PtdIns(4)P are present in early and late endosomes, respectively. Given the fact that many PPIns-binding proteins exhibit low affinity for their ligand, recruitment of these proteins often requires coincident detection of other binding determinants such as specific protein motifs (Simonsen et al., 1998; Wijdeven et al., 2015) or by sensing membrane curvature (Carlton et al., 2004).

Part II: Methods to Monitor Phosphoinositides in Leukocytes

Classical biochemical techniques provided the first insight into PPIns biology in leukocytes. The discovery of PtdIns(3,4,5)P_3 (Traynor-Kaplan et al., 1988) and PtdIns(3,4)P_2 (Traynor-Kaplan et al., 1989), two species formed *de novo* following the stimulation of neutrophils with formylated chemotactic peptides, was possible by loading large numbers of cells with radiolabeled [^{3}H]inositol or [^{32}P]phosphate. Following acid extraction, inositol headgroups were deacylated by enzymatic or chemical means allowing the water-soluble radiolabelled headgroup to be isolated and analyzed. Following nuanced separation by thin-layer chromatography or by high-performance liquid chromatography (HPLC) the relative amounts of different inositide species could be inferred. Alternatively, the deacylated headgroups can be quantitatively analyzed by radioreceptor assays (Várnai and Balla, 1998), or without radiolabeling by anion-exchange HPLC coupled to conductivity detection (Nasuhoglu et al., 2002).

More recent developments in the field of lipidomics are based on ultra-high-pressure HPLC coupled to mass spectrometry (HPLC-MS/MS) (Wenk et al., 2003; Clark et al., 2011; Bui et al., 2018). Following methylation of inositol headgroups to render them electroneutral, ionization and subsequent detection allows for sensitive quantitation of the amount of different PPIns in parallel with other phospholipids. Quite importantly, although early iterations of this technique could not resolve regio-isomers (e.g., PtdIns(3,4)P_2, PtdIns(3,5)P_2, PtdIns(4,5)P_2)

(Kielkowska et al., 2014), harnessing differences in isomer-specific methylation patterns now allows the separation of such isomers, with the exception of PtdIns(4)P and PtdIns(5)P (Wang et al., 2016). These mass spectrometry approaches have the additional benefit of reporting fatty acyl chain length and degree of saturation, and have even been extended to analyze PPIns in whole organs (Wang et al., 2016). However, all the above biochemical readouts suffer from a major limitation: as they analyze extracts of multiple whole cells, small changes occurring asynchronously in subcellular compartments cannot be resolved. Subcellular fractionation could in principle be performed to refine the detection, but the inevitable exposure of the membranes to kinases, phosphatases and phospholipases during the lengthy fractionation schemes distorts the composition of the samples.

The sub-cellular distribution and relative levels of specific PPIns species can instead be monitored by immunostaining with specific antibodies coupled to fluorescent or chemiluminescent secondary antibodies. Originally developed by immunizing mice with immunogen-cationized inositides (Chen et al., 2002) or with liposomes containing specific PPIns (Thomas et al., 1999), this antibody collection is carried today by Echelon Biosciences. It is important to note, however, that PPIns do not contain primary amines and, therefore, cannot be easily cross-linked and stabilized during traditional fixation with paraformaldehyde. A great deal of time has been invested to develop and understand which PPIns pools can be reliably detected by immunostaining and under what conditions (Hammond et al., 2006, 2009; Yip et al., 2008). For example, preserving plasma membrane integrity requires careful adjustments to standard immunostaining methods such as the addition of the fixative glutaraldehyde, careful buffering of pH, the use of reduced temperatures and saponin for permeabilization. Unfortunately, in attempting to preserve one membrane, conditions may fail to recognize the lipid of interest in another, possibly important, cellular organelle (Hammond et al., 2009, 2012). As such, these tools should be employed only with a clear experimental focus (e.g., a defined organelle of interest in mind) and great caution. Nonetheless, immunostaining aided in revealing the presence of PtdIns(3,4)P_2 in clathrin-coated pits (Posor et al., 2013), PtdIns(4)P in the plasma membrane (Hammond et al., 2009), and PtdIns(3,4,5)P_3 at the leading edge of migrating leukocytes (Wang et al., 2002).

The dynamic and localized responsiveness of living organisms to stimuli presents several challenges to biologists interested in PPIns signaling: the spatiotemporal nature of events, rapid turnover, and low abundance of PPIns cannot be properly appreciated by any one of the techniques discussed above. Indeed, many cellular processes necessitate the ability to track organelles or sub-domains of organelles on a second-to-second basis. The introduction of genetically-encoded biosensors based on high-affinity PPIns-binding domains provided a way to address many of these shortcomings, and led to an explosion of knowledge and interest in the field of PPIns biology (Hammond and Balla, 2015; Wills et al., 2018). PPIns biosensors exploit high-affinity, stereospecific interactions of protein domains with available lipids, an interaction that drives protein recruitment to biological membranes (**Figure 1A**). The PH domain of phospholipase C (PLC) δ1 was the first to demonstrate clear stereospecificity for PtdIns(4,5)P_2 and soluble Ins(1,4,5)P_3 (Ferguson et al., 1995; Lemmon et al., 1995). Soon after, the fusion of PH-PLCδ1 to a fluorescent protein created a reporter that has been widely utilized as an indicator of PtdIns(4,5)P_2. The potential of GFP-tagged PH-PLCδ1 to monitor PtdIns(4,5)P_2 in real time was demonstrated by its dynamic relocalization in response to platelet-activating factor treatment of leukocytes (Stauffer et al., 1998), and to calcium ionophore or hormone treatment of fibroblasts (Várnai and Balla, 1998). The growing knowledge of PPIns-binding domains rapidly expanded the repertoire of tools to monitor PPIns at a single-cell level (**Table 1**). Our toolbox today allows for monitoring of PtdIns(4,5)P_2 (Stauffer et al., 1998; Várnai and Balla, 1998), PtdIns(4)P (Brombacher et al., 2009; Dolinsky et al., 2014; Hammond et al., 2014; Weber and Hilbi, 2014), PtdIns(3)P (Gaullier et al., 2000; Ellson et al., 2001; Kanai et al., 2001), PtdIns(3,4,5)P_3/PtdIns(3,4)P_2 (Frech et al., 1997; Gray et al., 1999; Watton and Downward, 1999; Manna et al., 2007), PtdIns(3,4,5)P_3 (Klarlund et al., 1997, 2000; Venkateswarlu et al., 1998a,b; Várnai et al., 1999, 2005; Cronin et al., 2004; Manna et al., 2007), PtdIns(3,4)P_2 (Thomas et al., 2001; Goulden et al., 2019), and PtdIns (Pemberton et al., 2020) with great selectivity, although several cautionary notes discussed below should be considered before working with these reporters.

Many inositide-binding domains found in nature are not selective for a single PPIns species or have too low an affinity to direct protein localization. As well, some domains exhibit protein-protein or protein-lipid interactions other than their PPIns binding and impact their localization (Hammond and Balla, 2015). Therefore, the task of generating a successful lipid biosensor is not a straightforward one. It is important and obvious that a successful biosensor must demonstrate selectivity for the lipid species of interest and depend on the lipid for its localization to the membrane. However, less obvious is the fact that the sensor should demonstrate sufficiency to recognize the lipid in a membrane where the lipid is not normally found (Hammond and Balla, 2015; Wills et al., 2018). Sufficiency for biosensor recruitment has been elucidated elegantly *in vivo* by several methods, including chemical dimerization and optogenetic activation (discussed further below) that induce ectopic synthesis of the lipid of interest in its non-native organelle. Unfortunately, several first-generation PtdIns(4)P probes did not comply with the latter requisite in that their membrane targeting required both PtdIns(4)P and active Arf1 resulting in a biased localization to the Golgi (Levine and Munro, 2002; Godi et al., 2004; Balla et al., 2005). Similarly, several biosensors developed for PtdIns(3,4,5)P_3 based on domains of cytohesin-family proteins require Arf/Arl GTPase and/or adjacent polybasic regions for successful membrane targeting (Cohen et al., 2007; Hofmann et al., 2007; Li et al., 2007). Similarly, the PH domain from Bruton's Tyrosine Kinase which recognizes PtdIns(3,4,5)P_3 can be influenced by direct interaction with heterotrimeric G proteins (Tsukada et al., 1994) and protein kinase C (Yao et al., 1994). The complexities that may arise because of these compounding variables should not

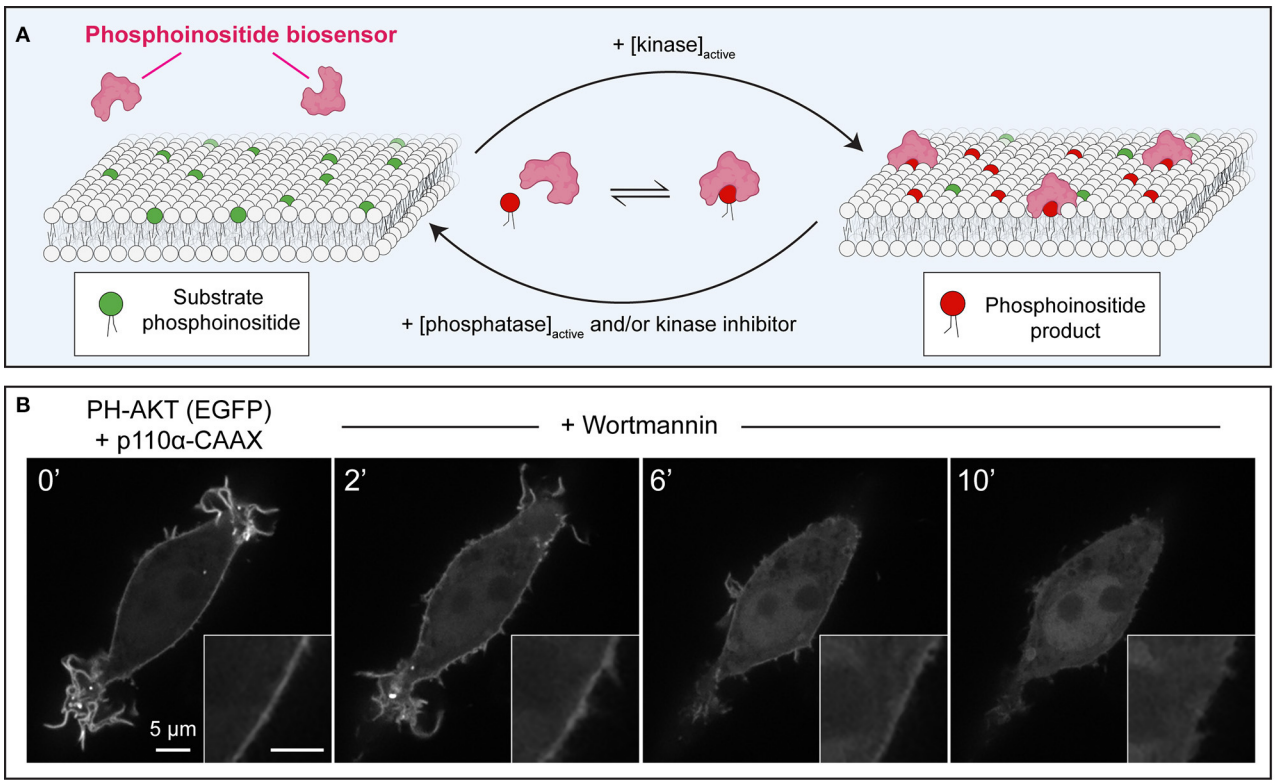

FIGURE 1 | Principles of operation of phosphoinositide biosensors in leukocytes. **(A)** Model of a generic phosphoinositide-specific biosensor in equilibrium between the cytosol and membrane following activation of the kinase that generates the target lipid, or its disappearance due to phosphatase activation, or pharmacological kinase inhibition. **(B)** Dynamic redistribution of the PH-AKT biosensor in response to changes in 3-phosphorylated species. PH-AKT was co-transfected with class I PI3K-CAAX into RAW264.7 cells, leading to constitutive production of PtdIns(3,4,5)P_3 and PtdIns(3,4)P_2 at the plasma membrane. PI3Ks were then inhibited pharmacologically with wortmannin (100 nM). Note both the decrease in plasma membrane fluorescence and the concomitant increase in cytosolic GFP intensity over time.

fully preclude researchers from utilizing these tools, however. For example, first-generation sensors for PtdIns(4)P provided useful insights to the functions of this lipid in the Golgi, despite being "blind" to other PtdIns(4)P pools (Szentpetery et al., 2010). Likewise, mutations can be introduced into binding domains to prevent protein-protein interactions while preserving PPIns-specificity (Várnai et al., 2005; Cohen et al., 2007; Hofmann et al., 2007; Goulden et al., 2019). Such considerations will be critical in the continued development of improved PPIns biosensors.

Part III: Tools to Manipulate Phosphoinositides in Leukocytes

Along with the rapid expansion of tools to monitor PPIns came developments that enabled researchers to selectively disrupt these lipids. Many of these experimental approaches can serve "double-duty" by either validating the ability to monitor a specific PPIns pool (Part II) and/or to assess the consequences on downstream effector signaling (Part III). These tools revolve around the manipulation of the kinases, phosphatases, and phospholipases that control phosphoinositide metabolism.

Pharmacological approaches to inhibit PPIns synthesis or degradation are a simple and widely accessible method. As exemplified in **Figure 1**, membrane-targeted, constitutively-active class I phosphoinositide 3-kinase α (PI3Kα) can be utilized to increase PtdIns(3,4,5)P_3 in the membrane; this is evinced by the strong membrane enrichment of the AKT PH domain sensor. The addition of the fungal metabolite wortmannin, which can potently inhibit the activity of PI3Ks (Arcaro and Wymann, 1993; Ui et al., 1995), causes the abrupt release of PH-AKT from the membrane (**Figure 1B**). This simple approach validates the notion that PPIns products of PI3K-activity are required to recruit and retain the biosensor at the plasma membrane, while also demonstrating that the toxin is active against PI3K.

Inhibitors of class I PI3Ks have been a major class of candidates for the treatment of solid and blood-borne cancers. This has resulted in the development of several pan- and isoform-specific class I PI3K inhibitors [reviewed in (Burke, 2018)]. Specific inhibitors have also been developed for several PI4K (Knight et al., 2006; Tóth et al., 2006; Bojjireddy et al., 2014; Li et al., 2017) and PIP5K isoforms (Semenas et al., 2014; Wright et al., 2014). On the other hand, useful inhibitors have also been described for several PPIns phosphatases including those of the SHIP (SH2 domain-containing inositol polyphosphate 5-phosphatase) family which dephosphorylate PtdIns(3,4,5)P_3 to PtdIns(3,4)P_2 (Brooks et al., 2010; Fuhler et al., 2012), and

TABLE 1 | Summary of phosphoinositides, effectors in leukocytes, and biosensors used for their detection.

Phosphoinositide	Effectors	Biosensors (Fixable)	Biosensor source
PtdIns(4,5)P_2	- WASP/N-WASP - PLC (*β, δ isoforms*) - Dynamin - AP2, Epsin, CALM (*clathrin-adaptor proteins*) - FCHo, FBP17, Amphiphysin (*BAR-domain proteins*) - Spectrin - ERM proteins - GRAF1 - PTEN	PH-PLCδ1 (+) PH-PLCδ4 (?)	Stauffer et al., 1998; Várnai and Balla, 1998; Lee et al., 2004b
PtdIns(4)P	- OSBP and ORPs - CERT - FAPP1/2 - GOLPH3 - SKIP/PLEKHM2	P4M (±) P4C (±)	Hammond et al., 2014; Weber and Hilbi, 2014
PtdIns(3,4,5)P_3	- WAVE1/2/3 - GRP1, ARNO, Cytohesin-1 (*Cytohesin family*) - PLC (*β, γ isoforms*) - Protein Kinase B/AKT - PDK1 - BTK - SNX9/18/33 (*PX-BAR domain proteins*) - Vav1/3, Tiam1/2, P-rex1, Dock2 (*RhoGEFs*) - ARHGAP12, ARHGAP25, and SH3BP1 (*RhoGAPS*) - ARAP3, GBF1 (*ArfGEFs*) - Sos (*RasGEF*)	PH-ARNO(2G)^{I303E} (+) PH-BTK (+) PH-AKT (+)	Gray et al., 1999; Várnai et al., 1999; Watton and Downward, 1999; Goulden et al., 2019
PtdIns(3,4)P_2	- TAPP1/2 - Protein Kinase B/AKT - SNX9/18/33 (*PX-BAR domain proteins*) - FCHSD1/2 (*F-BAR-domain proteins*) - Lamellipodin - RasGAP2* - RapGAP3*	cPH (+) PH-AKT (+)	Gray et al., 1999; Watton and Downward, 1999; Goulden et al., 2019
PtdIns(3)P	- EEA1 - Hrs (*ESCRT-0*) - WDFY2 - Rabankyrin - SNX1/2 - DFCP1, WIPI1 (*Autophagy*) - p40phox, p47phox (*NADPH Oxidase*) - PIKfyve	FYVE (+) PX (+)	Gaullier et al., 2000; Ellson et al., 2001; Kanai et al., 2001

Effectors of each phosphoinositide species are listed in ***Column 2****. To provide context where possible, the relevant isoforms, protein family, and biological pathways are italicized in parentheses. Please note that protein effectors may require additional coincident signals for their recruitment to cellular membranes and/or additional co-factors in addition to the listed interacting lipid. In some instances, proteins can be recruited to sub-domains of biological membranes independently of phosphoinositides but be activated by the lipid allosterically. Effectors reported in Dictyostelium but not yet tested in mammalian leukocytes are marked with an asterisk (*). Selective lipid-binding domains are listed in* ***Column 3*** *that form the basis of phosphoinositide-specific biosensors utilized in leukocytes and other cell types. All domains are from mammalian origin except for P4M and P4C, which are derived from the Legionella pneumophila effectors SidM and SidC, respectively. The ARNO PH domain-containing biosensor specifically encodes the diglycine (2G) splice variant which exhibits strong selectivity for PtdIns(3,4,5)P_3 over other phosphoinositide species. Additionally, interactions with host Arl GTPases are predicted to be disrupted by mutation of Isoleucine at position 303. The cPH domain-containing biosensor encodes the isolated C-terminal PH domain from TAPP1. Whether biosensor localization is retained following chemical fixation with paraformaldehyde is indicated in parentheses (+, localization retained; ±, partial disruption; ?, untested), based on the experience in our laboratory.* ***Column 4*** *provides the primary reference to the development of each biosensor, many of which have been deposited and are freely available on Addgene (https://www.addgene.org/). PH, Pleckstrin-homology domain; BTK, Bruton's Tyrosine Kinase; FYVE (Fab1, YOTB, Vac1, and EEA1); PX, Phox homology domain; PLC, phospholipase C.*

several for the INPP5 family (Pirruccello et al., 2014) that dephosphorylate both PtdIns(3,4,5)P_3 and PtdIns(4,5)P_2 in the 5-position. The mechanism by which these compounds inhibit SHIP phosphatase activity is unclear, while the INPP5-specific inhibitors bind directly to the catalytic domain. Several PPIns 3- and 4-phosphatases are members of the redox-sensitive protein tyrosine phosphatase family. Oxidizing compounds containing vanadate (e.g., bisperoxovanadate) or the addition of hydrogen peroxide acutely and potently inhibit their activity (Rosivatz et al., 2006; Ross et al., 2007). The acute and reversible nature of this inhibition has been harnessed to understand SAC1 activity in the endoplasmic reticulum (ER) (Zewe et al., 2018) and derivatives have even been applied *in vivo* (Zhang et al., 2017). Lastly, it is possible to deliver PPIns to the cytosol of intact cells by utilizing membrane-permeable acetoxymethyl esterified derivatives. In the cytosol, endogenous esterases cleave the acetoxymethyl group, releasing intact PPIns that then partition into the cytosolic leaflet of organelles.

In addition to pharmacological manipulation, PPIns-metabolizing enzymes can be genetically manipulated by over-expression, RNA interference-mediated depletion, genetic knockout or knock-in mutations, or by exploiting mutations from human samples or model systems. In contrast to pharmacological approaches, these methods are generally chronic in nature and can be susceptible to cellular compensation that may cloud the interpretation. Nonetheless, they represent a valuable way to tease out biological mechanisms when effective and specific pharmacological inhibition is not available for an enzyme of interest (Zunder et al., 2008; Huw et al., 2013). Knock-in mutations incorporated directly into the lipid-binding domains of cellular proteins or PPIns-metabolizing enzymes is a particularly clever way to understand their regulation by phospholipids. Indeed, mutations in amino acids that coordinate the inositol headgroup within biosensors are often included to control for non-lipid-mediated localization (Stauffer et al., 1998; Várnai and Balla, 1998; Várnai et al., 1999, 2005). Conversely, relatively high expression of biosensors or tandem domains of biosensors that have higher avidity can be utilized to effectively occlude downstream signaling by PPIns. Although normally avoided during routine experiments, this approach has been useful in understanding the roles of PtdIns(4,5)P_2 in controlling cortical actin networks (Raucher et al., 2000; Ueno et al., 2011) and of PtdIns(3)P during resolution of endocytic compartments (Freeman et al., 2019).

PPIns-metabolizing enzymes and their activity can be targeted to virtually any cellular organelle constitutively or acutely to manipulate local PPIns signaling. Constitutive targeting can be accomplished by including defined, well-characterized motifs in the primary sequence of kinases, phosphatases, or phospholipases that dock the enzyme onto the organelle of choice (**Figure 1B**). Targeting motifs are often transmembrane domains of integral membrane proteins or tail-anchored proteins but electrostatic interactions can also mediate targeting of domains to the plasma membrane (Won et al., 2006; Yeung et al., 2006). PPIns enzyme domains can be recruited to the cytosolic leaflets of specific organelles more acutely (within seconds) by chemically-induced dimerization. The first such system developed was based on the

domains from FK506 binding protein (FKBP) and mTOR (FRB domain) that undergo heterodimerization in the presence of rapamycin (Spencer et al., 1993; Inoue et al., 2005). The elegance of this method quickly gained traction for cell biologists as it can allow the tightly controlled depletion of phosphoinositide pools from specific organelles, while largely bypassing any adverse effects of chronic over-expression of PPIns-metabolizing enzymes (Fili et al., 2006; Suh et al., 2006; Varnai et al., 2006; Szentpetery et al., 2010; Hammond et al., 2014). As an alternative to rapamycin-based dimerization, analogous systems have since been developed utilizing the gibberellin plant hormone GA_3 (Miyamoto et al., 2012), and photoactivation-induced dimerization (Idevall-Hagren et al., 2012). The rate and magnitude of depletion of PPIns can be monitored by co-expression with biosensors and monitoring fluorescence intensity changes or changes in Förster resonance energy transfer (FRET) with fluorophore pairs in the organelle of interest (Varnai et al., 2006; Hammond et al., 2014). In these complex multi-variable experiments, several controls should be implemented for robust conclusions: visualization of the pre- and post-stimulated localization of the protein of interest, recruitment of domains lacking the active cargo (i.e., without the PPIns-metabolizing enzyme) or encoding catalytically-inactive enzymes to control for non-lipid-mediated effects.

Lastly, recent developments have enabled the optogenetic activation of enzymes by incorporating unnatural amino acids (Luo et al., 2014; Courtney and Deiters, 2018). In this case, "caged" (inactive) versions of PPIns-converting enzymes can be expressed in cells at high levels without adverse effects, that can then be activated acutely (Goulden et al., 2019).

PHOSPHOINOSITIDES IN LEUKOCYTE CHEMOTAXIS

The ability of immune cells to migrate is fundamental to embryonic development, infection control, sterile wound healing, the clearance of transformed cells, and tissue regeneration. Its aberrant activation can, however, contribute to inflammatory diseases, tissue necrosis, atherosclerosis, and hematological cancers (Ley et al., 2018; Weavers and Martin, 2020). During chemotaxis, leukocytes extend pseudopods at their leading edge that are directed toward chemoattractants like formyl-peptides, leukotrienes and complement fragments, or away from chemorepellants (Andrew and Insall, 2007; Westman et al., 2019). Through an iterative process, extremely shallow concentration differences (often $< 5\%$ from leading-to-trailing edge) of the attractants are detected across the plasmalemmal surface and amplified intracellularly. The periodic extension, bifurcation and retraction of leading-edge pseudopodia are driven by dynamic remodeling of the underlying actin cytoskeleton and supported by adherence to the underlying substratum via integrins (Kinashi, 2005; Renkawitz and Sixt, 2010; Weavers and Martin, 2020). In contrast, the trailing edge uropod –which is comprised of more stable actin networks– must simultaneously release from the substratum and retract (Hind et al., 2016). The polarized gliding movement that results can attain speeds $>10\ \mu m$/min in some leukocytes. The information directing actin polymerization and ongoing feedback for its remodeling are communicated by several parallel pathways involving PPIns that are in turn responsive to the extracellular gradient of the chemoattractants.

Broadly speaking, pseudopod formation requires activation of the Rho-family GTPases Rac and Cdc42 to drive F-actin polymerization into protrusions that drive forward motion (Kraynov et al., 2000; Itoh et al., 2002; Ridley et al., 2003; Willard and Devreotes, 2006; Yang et al., 2016). Conversely, the sides and uropod contain active RhoA, myosin light chain kinase, and ezrin-radixin-moesin (ERM) protein scaffolding to support actomyosin-based contraction of the trailing edge and stabilize adhesion to the endothelium during extravasation (Yoshinaga-Ohara et al., 2002; Xu et al., 2003; Lee et al., 2004a; Hind et al., 2016).

Pseudopod Organization by 3-Phosphorylated Inositides

The 3-phosphorylated species PtdIns(3,4,5)P_3 and PtdIns(3,4)P_2 are markedly enriched at the leading edge of migrating cells (**Figure 2A**). This hallmark of polarized migration has been recognized across numerous subsets of leukocytes, though the first identification occurred in the social amoebae *Dictyostelium* (Meili et al., 1999; Dormann et al., 2002). Robust signaling through class I PI3Ks is the principal determinant of accumulation of 3-phosphorylated species at the leading edge. Of note, PtdIns(3,4,5)P_3 and/or PtdIns(3,4)P_2 are polarized toward chemoattractants despite depolymerization of the underlying actin cytoskeleton (Servant et al., 2000; Dormann et al., 2002; Janetopoulos et al., 2004; Xu et al., 2005) demonstrating that gradient sensing and PPIns polarization are upstream of the cytoskeletal rearrangement and morphological changes. Evidence for the role of PI3Ks in chemotaxis came from pharmacological treatment with wortmannin or LY294002, which effectively block PtdIns(3,4,5)P_3 production and recruitment of PH-AKT to the inner leaflet of the PM in response to several chemoattractants (Knall et al., 1997; Niggli and Keller, 1997; Servant et al., 2000). Further, the importance of 3-phosphorylated species has been highlighted by the sufficiency of exogenously delivered PtdIns(3,4,5)P_3 (Niggli, 2000; Weiner et al., 2002) or the synthetic activation of endogenous PI3Ks (Inoue and Meyer, 2008) to polarize neutrophils, signal downstream actin polymerization, and elicit random leukocyte migration.

Class I PI3Ks are activated in response to chemokines via two major pathways: signaling through G protein $\beta\gamma$ subunits liberated from αi downstream of activated GPCRs, and by the small GTPase Ras through Ras-binding domains in several PI3Ks (**Figure 2B**, left) (Suire et al., 2006; Kurig et al., 2009; Surve et al., 2014). Of the four class I PI3K isoforms which are expressed in leukocytes, the class IB isoform PI3Kγ was identified as the chief kinase generating PtdIns(3,4,5)P_3 in response to chemotactic stimuli in leukocytes. Neutrophils and macrophages, natural killer (NK) lymphocytes, and T lymphocytes that are deficient in PI3Kγ do not migrate efficiently toward various

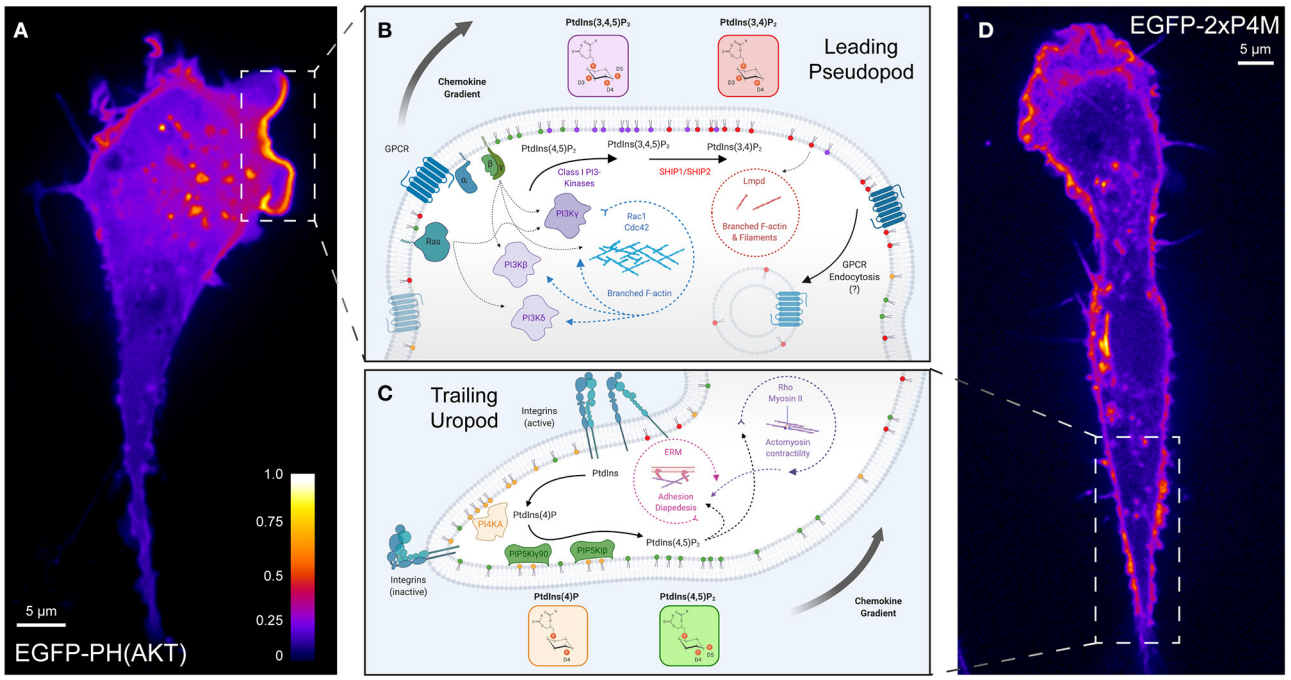

FIGURE 2 | Polarization of phosphoinositide signals during chemotaxis. **(A)** A representative confocal micrograph of PH-AKT expressed in a RAW264.7 monocytic cell undergoing chemokinesis (random motion) in the presence of growth factors from fetal-bovine serum. PH-AKT bi-specifically recognizes PtdIns(3,4,5)P_3 and PtdIns(3,4)P_2. The image has been pseudocolored to reflect the abundance of the probe. **(B)** Phosphoinositide signaling controlling "frontness" during leukocyte chemotaxis. A signal arising from the stimulation of cell surface GPCRs and associated activation of G-proteins (β, γ) by chemokines lead to the activation of class I PI3Ks to produce PtdIns(3,4,5)P_3 from PtdIns(4,5)P_2. Together with PtdIns(3,4)P_2, the product of dephosphorylation of PtdIns(3,4,5)P_3, 3-phosphoinositides in the leading-edge membrane mediate a feed-forward loop that activates Rho- and Arf-family GTPases and Lmpd to drive actin polymerization and locally amplify PI3K-signaling. **(C)** Engagement of substratum by leukocytes favors the "backness" signals PtdIns(4)P and PtdIns(4,5)P_2. PI4KA mediates the synthesis of PtdIns(4)P from PtdIns, which is necessary for the activation of PIP5KIγ90 and the generation of PtdIns(4,5)P_2. RhoA signaling networks and ERM proteins regulated by PtdIns(4,5)P_2 are critical for leukocyte rolling adhesion, diapedesis, and uropod contraction during migration. **(D)** A representative confocal micrograph of 2xP4M expressed in a RAW264.7 cell undergoing chemokinesis (random motion) in the presence of growth factors from fetal-bovine serum. The P4M domain derived from *Legionella*'s SidM specifically recognizes PtdIns(4)P. The image has been pseudocolored to reflect the abundance of the probe in the Golgi, endolysosomes, and the plasma membrane including in the region of the uropod. GPCR, G protein-coupled receptor; PI3K, phosphoinositide 3-kinase; SHIP, SH2 domain-containing inositol polyphosphate 5-phosphatase; Lmpd, Lamellipodin; ERM, Ezrin-Radixin-Moesin.

chemoattractants *in vitro* or to sites of inflammation *in vivo* (Hirsch et al., 2000; Li et al., 2000; Sasaki et al., 2000; Hannigan et al., 2002; Reif et al., 2004; Suire et al., 2006; Ferguson et al., 2007; Nishio et al., 2007; Saudemont et al., 2009). Interestingly, substantial positive crosstalk exists between PI3K, its initial PtdIns(3,4,5)P_3 synthesis, and cytoskeletal regulators. A secondary activation of PI3Ks has been posited to amplify and sustain this important signaling node during chemotaxis (Niggli, 2000; Sadhu et al., 2003; Boulven et al., 2006). One way this occurs is by initiating a feedback loop between PI3Ks and Rho-family GTPases (**Figure 2B**, center circle), which activates additional PtdIns(3,4,5)P_3 synthesis (Servant et al., 2000; Wang et al., 2002; Weiner et al., 2002; Srinivasan et al., 2003; Park et al., 2004; Inoue and Meyer, 2008; Kuiper et al., 2011). The pre-treatment of cells with *Clostridioides*-derived toxins (which inactivate several Rho-family GTPases) or interference with Rho-family activating proteins can strongly reduce the polarization of PH-AKT in response to chemokines (Weiner et al., 2002; Srinivasan et al., 2003; Kunisaki et al., 2006). How does this occur mechanistically? Both active Rac1 and Cdc42 can directly associate with PI3Kβ and stimulate its lipid kinase activity (Fritsch et al., 2013). Additionally, the activation of PI3Kβ by G-protein βγ subunits (**Figure 2B**, center) when GPCRs and receptor tyrosine kinases (RTKs) are co-stimulated (Houslay et al., 2016) could mechanistically explain the contribution of PI3Kβ to leukocyte migration (Vanhaesebroeck et al., 1999; Ferguson et al., 2007). In parallel, genetic or pharmacological inhibition of the hemopoietic-specific class IA PI3Kδ revealed a pronounced role of this isoform in PtdIns(3,4,5)P_3 synthesis, polarization, and directed migration of neutrophils, lymphocytes, and NK cells (Sadhu et al., 2003; Reif et al., 2004; Saudemont et al., 2009). The activation of PI3Kδ is likely secondary to the PI3Kγ-mediated activation of Rho-family effectors or occurs downstream of Ras activation (**Figure 2B**) (Burke, 2018). Importantly, despite similar enzymatic activity, distinct PI3K isoform-specific roles have been revealed *in vivo*: PI3Kγ mediates early extravasation and chemotaxis, while PI3Kδ sustains long-term chemotaxis into inflamed tissues (Liu et al., 2007). Lastly, effectors of Rac1 recruited by the products of PI3K (discussed further below) can in turn support the

polarization of 3-phosphorylated inositides in the pseudopod (Kunisaki et al., 2006).

Beyond the edges of the leading pseudopod, PtdIns(3,4,5)P_3 is limited in abundance and distribution by the PPIns 3-phosphatase, PTEN (phosphatase and tensin homolog) (Ferguson et al., 2007; Nishio et al., 2007), and by the action of the Type III 5-phosphatases SHIP1 (Nishio et al., 2007) and SHIP2 (Lam et al., 2012). Collectively, the 5-phosphatases convert PtdIns(3,4,5)P_3 to PtdIns(3,4)P_2, while PTEN terminates signaling by hydrolyzing both PtdIns(3,4,5)P_3 and PtdIns(3,4)P_2 to generate PtdIns(4,5)P_2 and PtdIns(4)P, respectively (Malek et al., 2017; Goulden et al., 2019). Although data on the role of PTEN in mammalian leukocytes is somewhat discrepant (Nishio et al., 2007; Wang, 2009; Balla, 2013), the phosphatase has been localized to the trailing uropod of neutrophils (Li et al., 2005), similar to its polarized localization in *Dictyostelium* (Iijima and Devreotes, 2002). The depletion of PTEN in both systems causes abnormal actin polymerization into multiple pseudopods and prolongs the duration of AKT signaling (Funamoto et al., 2002; Iijima and Devreotes, 2002; Huang et al., 2003; Subramanian et al., 2007; Li et al., 2019). Although the resulting migration is error-prone and often fails to prioritize between chemotactic signals, migration speed actually increases, augmenting the number of PTEN-null neutrophils that enter inflamed tissues *in vivo* (Subramanian et al., 2007; Heit et al., 2008b; Sarraj et al., 2009). Recruitment of PTEN to the membrane, which is critical for its lipid phosphatase activity, occurs largely through its interaction with PtdIns(4,5)P_2 (Rahdar et al., 2009), but also by front-to-back signaling networks involving PI3Kδ and RhoA (Li et al., 2005; Papakonstanti et al., 2007) (**Figure 2C**). Unlike *Dictyostelium*, mammalian cells are also regulated by SHIP1 and SHIP2. The deletion of SHIP1 in neutrophils and macrophages severely inhibits their speed and ability to polarize their actin cytoskeleton toward various chemoattractants *in vitro*, phenocopying cells lacking PI3Kγ (Ferguson et al., 2007; Nishio et al., 2007). PtdIns(3,4,5)P_3 levels are elevated at rest and during stimulation in these cells and SHIP1$^{-/-}$ cells have multiple broad, distorted lamellae marked by the AKT biosensor. This implies an important regulatory role for SHIP phosphatases and their enzymatic activity in organizing the pseudopod (Nishio et al., 2007).

It is nevertheless important to note that although PI3Ks and their downstream products are critical for many aspects of chemotaxis –such as speed and initiating morphological polarization—PI3Ks do not comprise the basis for the "biological compass" that orients cells toward or away from the chemical stimulus itself. In many settings, the deletion or inhibition of PI3Ks does not ultimately eliminate the ability of cells to bias their motility in the direction of a chemotactic signal; PI3Ks merely help to get them there (Loovers et al., 2006; Hoeller and Kay, 2007; Nishio et al., 2007; Takeda et al., 2007; Heit et al., 2008a). Studies of leukocyte recruitment *in vivo* have revealed that several other pathways operate in parallel or in conjunction with PI3K-related pathways to properly resolve the complex collective of endogenous and exogenous chemotactic signals (Heit et al., 2002, 2008a,b).

PtdIns(4)P, PtdIns(4,5)P_2, and the Control of "Backness"

In contrast to 3-phosphorylated species, PtdIns(4)P and PtdIns(4,5)P_2 are sustained in an opposing back-to-front gradient (**Figures 2C,D**) which has important consequences for extravasation and to establish the "biological compass" of migrating leukocytes. In addition to its phosphorylation by class I PI3Ks, PtdIns(4,5)P_2 is selectively hydrolyzed at the leading edge by PLC. The activation of G proteins βγ by chemokines triggers several isoforms, including PLCβ2 and PLCβ3, to be activated at the leading edge of migrating leukocytes (Tang et al., 2011; Balla, 2013). PLCβs possess N-terminal PH domains that interact with PtdIns(4,5)P_2 and Ins(1,4,5)P_3, as well as a polybasic C-terminal region (Balla, 2013) that likely favors association with negatively charged lipids [i.e., PtdIns(3,4,5)P_3] at the leading edge. Interestingly, PLCβ2 is also regulated by Rho-family GTPases, as exemplified by its binding to Rac and sequestration into subdomains of the PM (Illenberger et al., 2003; Gutman et al., 2010; Tang et al., 2011). Together, these membrane-targeting mechanisms support PLC-mediated hydrolysis of PtdIns(4,5)P_2 to diacylglycerol (DAG) and Ins(1,4,5)P_3 in the pseudopod (Keizer-Gunnink et al., 2007; Nishioka et al., 2008)—two intermediates with important consequences on the activation of integrin-based adhesiveness (Kinashi, 2005; Herter and Zarbock, 2013). In combination with PI3K activity, PLCβ2 and β3 enzymes are clearly important for establishing the back-to-front gradient of RhoA signaling and myosin contractility in leukocytes (Gao et al., 2015), which ultimately impact chemotaxis greatly (Tang et al., 2011).

Within the uropod, several type I PIP5Ks (PIP5KI) are activated to generate a modest enrichment of PtdIns(4,5)P_2, which can be visualized with the biosensor PH-PLCδ (**Figure 2C**) (Lokuta et al., 2007; Xu et al., 2010). The engagement of $\alpha_L\beta_2$ and $\alpha_M\beta_2$-integrins triggers the polarization of PIP5KIγ90 (also called PIP5K1C90) to the uropod of migrating cells (Xu et al., 2010), likely supported by the ability of the kinase to bind anionic lipids within the PM (Fairn et al., 2009). PIP5KIβ also has been localized to the uropod of migrating leukocytes, supported by its interaction with ERM proteins (Lacalle et al., 2007; Mañes et al., 2010). PtdIns(4,5)P_2 produced by PIP5KIs was initially posited to be sufficient to control "backness" by positively-regulating RhoA-signaling and ERM-mediated linkage to the plasma membrane (Xu et al., 2010) –both critical features of the uropod (**Figure 2C,** center). However, more recently it was realized that the PIP5KI-mediated synthesis of PtdIns(4,5)P_2 is accompanied by an enrichment of its substrate, PtdIns(4)P, within the uropod (Ren et al., 2019) (**Figure 2D**). An innovative study by Ren *et al.* revealed that not only is plasmalemmal PtdIns(4)P polarized toward the uropod during extravasation but depleting the inositide destroys the polarization to the uropod of several proteins including PIP5KIγ90 itself and active myosin light chain. The resulting PtdIns(4)P-depleted neutrophils are defective in their ability to bind to inflamed endothelium as a result of these polarization defects.

PtdIns(4)P is maintained in multiple sub-cellular compartments including the Golgi, late endosomes/lysosomes,

and the PM by the activity of four PI4-kinases (Balla, 2013; Hammond et al., 2014). In the uropod membrane, PtdIns(4)P is synthesized by PI4KA following its activation by srGAP, an inverted F-BAR protein that senses increased membrane curvature (Ren et al., 2019). These studies present an interesting paradigm in which the polyanionic lipids PtdIns(4)P and PtdIns(4,5)P_2 positively influence each other, orchestrate the stereospecific and electrostatic recruitment of effector proteins that scaffold the uropod, and ultimately the adhesion and initial directionality of leukocyte migration.

Phosphoinositide Effectors During Chemotaxis

The actin cytoskeleton receives multiple inputs via PPIns. One important cytoskeletal effector at the leading edge is the five-membered WAVE (SCAR/WASP family verprolin-homologous protein) regulatory complex. WAVE is one of several nucleation-promoting factors (NPFs) necessary for the full activation of the Arp2/3 complex that generates branching actin filaments (Takenawa and Suetsugu, 2007). The importance of WAVE for migration is supported by numerous studies in different cell types and organisms (Krause and Gautreau, 2014) including leukocytes, where WAVE complex members rapidly localize to the leading pseudopod (Weiner et al., 2006, 2007; Millius et al., 2009). Although the WAVE complex can be recruited and activated directly by receptors (including possibly the CXCR5 chemokine receptor) (Chen et al., 2014), this complex is generally recruited and activated at the membrane by factors such as lipids. Within the WAVE complex, WAVE1, WAVE2, and WAVE3 possess a carboxy-terminal basic region that has a higher affinity for PtdIns(3,4,5)P_3 over other inositides and can promote its membrane recruitment (Oikawa et al., 2004). Normally inhibited *in trans* by other complex members (Eden et al., 2002), the WAVE complex can be activated by GTP-bound Rac on PtdIns(3,4,5)P_3-containing liposomes (Lebensohn and Kirschner, 2009) and by Arf GTPases that synergize with Rac in the presence of this inositide (Koronakis et al., 2011).

Supporting these notions, a number of guanine nucleotide exchange factors (GEFs) and GTPase-activating proteins (GAPs) for Rho-, Arf-, and Ras-families of GTPases are recruited to membrane domains by PPIns-binding domains that recognize PtdIns(3,4,5)P_3 and/or PtdIns(3,4)P_2 (Krugmann et al., 2002; Rossman et al., 2005; Campa et al., 2015; McCormick et al., 2019). GEFs aid in the exchange of GDP for GTP, thereby promoting effector association, while GAPs enhance their intrinsically low GTPase activity. Therefore, the recruitment of Rac, Cdc42, and Arf GEFs and GAPs to the leading edge can indirectly regulate effectors of cytoskeletal remodeling. Prototypical examples have been reported for several Rac GEFs such as Vav1/3, Tiam1/2, and P-rex1, which are recruited to the pseudopod membrane in a PI3K-dependent manner to stimulate chemotaxis via Rac [see (McCormick et al., 2019) and (Campa et al., 2015)]. Leukocytes also express several atypical Rac GEFs from the Dock family that function through association with Elmo proteins (Sanui et al., 2003). These bipartite GEFs specifically associate with PtdIns(3,4,5)P_3 for activation (Côté et al., 2005) but, conversely, are also required for full PI3K activation and 3-PPIns polarization during chemotaxis (Kunisaki et al., 2006). Similarly, the recruitment to the pseudopod of several Arf GEFs, including ARAP3 (Krugmann et al., 2002; Gambardella et al., 2013) and GBF1 (Mazaki et al., 2012), occurs via 3-PPIns.

The recruitment and activation of the WAVE complex is independently promoted by PtdIns(3,4)P_2 and its binding partner, lamellipodin (Lmpd) (**Figure 2B**, right). Initially described during fibroblast migration, Lmpd recruitment to activated RTKs is dictated by its PH domain, that has affinity for PtdIns(3,4)P_2, and by its Ras-association domain which can interact with both active Ras and Rac (Krause et al., 2004; Law et al., 2013); these determinants promote the direct interaction between Lmpd and the WAVE complex at the leading edge that controls migration speed and directional persistence. Lmpd can also promote actin filament elongation at the leading edge by recruiting Ena/VASP proteins (Krause et al., 2004; Michael et al., 2010; Hansen and Mullins, 2015; Carmona et al., 2016). This molecular axis has since been extended to other settings which include leukocyte migration: the depletion of PtdIns(3,4)P_2 by overexpressing the PPIns 4-phosphatases INPP4A/B severely inhibits the migration speed and ability of lymphocytes to orient toward chemokines (Li et al., 2016). The details of how Lmpd is activated downstream of G proteins in leukocytes is unclear, but a mechanism can be gleaned by analogy with its activation by RTKs. Not only are class IA PI3Ks and SHIP2 activated by RTKs to produce PtdIns(3,4,5)P_3 and PtdIns(3,4)P_2, respectively, but so too are several GEFs for Rac and Ras GTPases. Lmpd could sense similar inputs downstream of GPCR activation.

Lastly, in addition to directly regulating the actin cytoskeleton, a tantalizing possible function of PtdIns(3,4)P_2 and Lmpd in leukocyte migration may be that they regulate the selective endocytosis of activated GPCRs via a pathway termed Fast Endophilin-Mediated Endocytosis, or FEME for short (Boucrot et al., 2015) (**Figure 2B**, right). This clathrin-independent pathway relies on the localized synthesis of PtdIns(3,4)P_2 sensed by Lmpd, to engage endophilin and pre-localize this endocytic complex at the leading edge of migrating cells (Chan Wah Hak et al., 2018). In the event of receptor activation, PtdIns(3,4)P_2 synthesis can trigger the downregulation of PI3K-signaling by endocytosis of activated cell surface receptors. Although the FEME pathway is active in lymphocytes, the role of endophilin and FEME in leukocyte chemotaxis and GPCR trafficking are yet to be explored.

Pathogens Interfere With Phosphoinositide Signaling During Chemotaxis

Considering the fundamental role that PPIns play in various cellular processes, it is not surprising that certain pathogens have developed strategies to hijack inositide signaling to create or sustain their replicative niche (Kumar and Valdivia, 2009; Pizarro-Cerdá et al., 2015; Walpole and Grinstein, 2020). The deployment of PPIns-specific metabolizing kinases and phosphatases into the host cell by several pathogens is one exemplary case.

The Gram-negative obligate anaerobe *Treponema denticola* (*T. denticola*) is a key bacterial pathogen in the development of oral periodontitis (Sela, 2001), the leading cause of tooth-loss worldwide (Darveau, 2010). In addition, periodontitis has been increasingly implicated as a driver of other systemic diseases, underscoring the importance of understanding its pathogenesis. *T. denticola* is normally a minor component of the diverse microbial community within the oral cavity, but can opportunistically take hold during dysbiosis and contribute to the inflammation-mediated breakdown of soft tissues, bone resorption, and resulting tooth loss. Following its attachment to the extracellular matrix, the spirochete expresses a major outer membrane sheath protein known as Msp that targets PI3K-signaling in neutrophils. Specifically, Msp reduces neutrophil PI3K activity (Visser et al., 2013) and hyperactivates PTEN (Jones et al., 2019), reducing cellular PtdIns(3,4,5)P_3 and PtdIns(3,4)P_2 levels. Consistent with its hyperactivation, PTEN is constitutively recruited to the plasma membrane in Msp treated-neutrophils (Jones et al., 2019). Because of the aberrant PPIns signaling, Msp potently blocks the activation of Rac1 and precludes the necessary actin rearrangements that drive effective chemotaxis (Thomas et al., 2006; Jones et al., 2019). The C-terminus of Msp is necessary for such effects (Jones et al., 2017), but how or if the effector is delivered into the host cell cytosol to manipulate PPIns-metabolizing enzymes remains an unresolved question in periodontal research.

PHOSPHOINOSITIDES DURING PHAGOCYTOSIS

Phagocytosis is the process whereby cells internalize and dispose of solid particles. Specific cell surface receptors recognize phagocytic targets and deliver them into vacuoles known as phagosomes. Phagocytosis plays essential roles throughout the body and can be carried out by multiple cell types. Phagocytosis carried out by myeloid cells such as macrophages, neutrophils and dendritic cells, constitutes the first line of defense against invading microorganisms and is also essential for the development of the adaptive immune response through antigen presentation. These myeloid cells are collectively known as professional phagocytes. Secondly, phagocytosis is fundamental for the daily clearance of billions of apoptotic cells, maintaining homeostasis within an organism. Professional, as well as non-professional phagocytes such as fibroblasts, epithelial, endothelial and mesenchymal cells, can clear apoptotic cells. Finally, phagocytosis of effete cells plays a pivotal role in wound healing, tissue development, morphogenesis and regeneration. The elimination of effete cells is carried out by both professional and non-professional phagocytes.

Given this variety of biological functions and the myriad phagocytic ligands, a sizeable number of receptors are required to recognize and discriminate the diversity of phagocytic targets (Flannagan et al., 2012). Amongst these receptors are: (1) pattern-recognition receptors (PRRs) like MARCO that bind pathogen-associated molecular patterns (PAMPs) present on microbial surfaces; (2) receptors like TIM-4 that bind phosphatidylserine and other apoptotic corpse markers; and (3) opsonic receptors such as FcγR and iC3b that recognize immunoglobulin-opsonized pathogens or complement-opsonized foreign and self-antigens, respectively. The most studied of these is by far the Fcγ receptor family, which we will use as a prototype throughout this review.

The diversity of phagocytic targets and receptors entails patently different molecular mechanisms of phagosome formation, maturation and resolution. Despite these differences, all types of phagocytosis share an inherent dependence on the rearrangement of the actin cytoskeleton and on the dynamic remodeling of the plasma membrane, as the phagosome evolves.

Phagocytosis can be divided into three main stages: phagosome formation, phagosome maturation and phagosome resolution. The formation of the phagosome involves probing for potential targets by plasma membrane ruffling, followed by target binding, pseudopod progression around the target, and scission of the phagosome from the plasma membrane (Hoppe and Swanson, 2004; Levin et al., 2016). During the maturation stage nascent phagosomes convert into early phagosomes that in turn evolve into late phagosomes and then to phagolysosomes (Vieira et al., 2002; Canton, 2017; Levin et al., 2017). The ultimate resolution of phagolysosomes entails their shrinkage and recycling of membrane and luminal components (Levin-Konigsberg et al., 2019).

Phosphoinositides in the cytosolic leaflet of the phagosomal and plasma membrane orchestrate the changes in membrane composition and actin cytoskeleton during each stage of phagocytosis. The phosphoinositides with documented essential roles during phagocytosis are PtdIns(3)P, PtdIns(4)P, PtdIns(4,5)P_2 and PtdIns(3,4,5)P_3 (Bohdanowicz and Grinstein, 2013; Swanson, 2014; Levin-Konigsberg et al., 2019); these will therefore occupy center-stage in this section of the review. The following pages describe the dynamics of phosphoinositides during phagosome formation, maturation and resolution (**Figure 3**).

PHAGOSOME FORMATION

The formation of the phagosome can be divided into three main stages: (1) Ruffling and probing for targets; (2) binding of the target particle and pseudopod progression, and (3) phagosomal scission. The following pages provide a detailed description of the role of phosphoinositides during these sub-stages.

1. Ruffling and target probing: elevated PtdIns(4,5)P_2 and PtdIns(3,4,5)P_3.

Phagocytic cells, such as macrophages and dendritic cells, constantly probe for targets by ruffling their plasma membrane and extending pseudopods (Bohdanowicz et al., 2013). As described in the chemotaxis section, these membranous protrusions are driven by actin polymerization, which is facilitated by elevated PtdIns(4,5)P_2 levels. Additionally, accumulation of PtdIns(3,4,5)P_3 and PtdIns(3,4)P_2 at the leading edge of ruffling membranes control actin assembly and

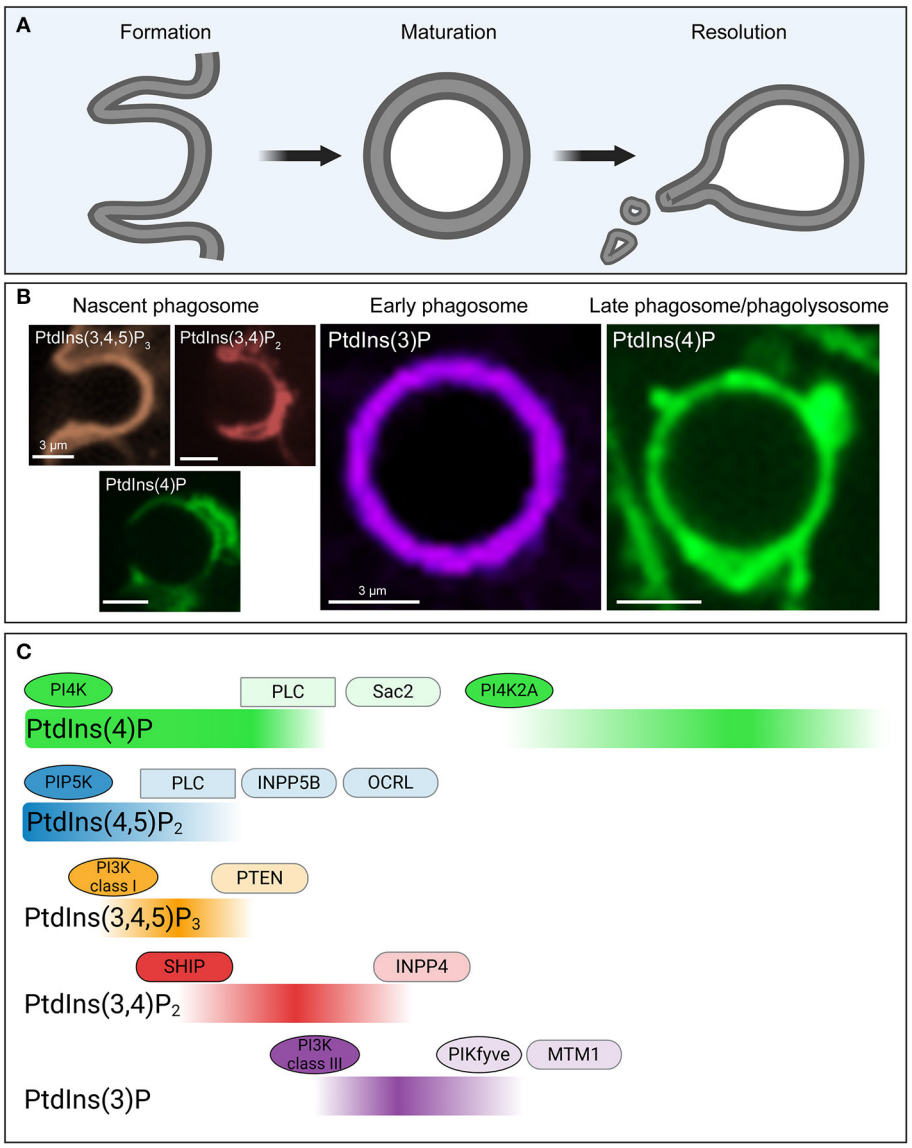

FIGURE 3 | Phosphoinositide fluxes drive phagosome formation, maturation, and resolution. **(A)** Graphic representation of the process of phagocytosis. The three main stages (phagosome formation, phagosome maturation and phagosome resolution) are depicted. **(B)** Representative confocal micrographs of some of the biosensors used to detect phosphoinositides during the three main stages of phagocytosis, color-coded to match **(C)**. **(C)** Temporal distribution of five major phosphoinositides and the enzymes involved in their metabolism during phagosome formation, maturation and resolution. During these stages the levels of PtdIns4P (green), PtdIns(4,5)P_2 (blue), PtdIns (3,4,5)P_3 (orange), PtdIns(3,4)P_2 (red), and PtdIns(3)P (purple) in the cytosolic leaflet of the phagosome undergo drastic changes, as indicated. These changes are mediated by a series of kinases (ovals), phosphatases (rounded rectangles/capsules), and phospholipases (rectangles) that accumulate and are activated at the phagosomal membrane at distinct timepoints during the process of phagocytosis. PI4K, phosphoinositide 4-kinase; PI3K, phosphoinositide 3-kinase; PLC, phospholipase C; SHIP, SH2 domain containing inositol polyphosphate 5-phosphatase; INPP, inositol polyphosphate phosphatase; OCRL, oculocerebrorenal Lowe syndrome protein; PTEN, phosphatase and tensin homolog; MTM, myotubularin.

disassembly. PtdIns(4)P is also present in the plasma membrane of resting phagocytes and during phagosome formation, however its role during this stage is undefined.

At rest, PtdIns(4,5)P_2 is localized in the cytosolic leaflet of the plasma membrane primarily, where it accounts for about 1–2% of the total phospholipid content (McLaughlin and Murray, 2005). The elevated levels of PtdIns(4,5)P_2 in ruffling membranes are generated by PIP5KI, which phosphorylate PtdIns(4)P at the D5 position of the inositol ring. Type II phosphatidylinositol phosphate kinases could conceivably phosphorylate PtdIns(5)P at the D4 position and generate PtdIns(4,5)P_2. Moreover, dephosphorylation of PtdIns(3,4,5)P_3 by PTEN would also yield PtdIns(4,5)P_2. However, the contribution of the these latter pathways to PtdIns(4,5)P_2 formation in the resting state is thought to be insignificant (Mondal et al., 2011; Bohdanowicz and Grinstein, 2013) (**Figure 3**).

The increased activity of PIP5KI observed during ruffling is triggered, at least partially, through stimulation by Rho-family (Tolias et al., 1995; Weernink et al., 2004) and Arf GTPases (Honda et al., 1999; Brown et al., 2001). PtdIns(4,5)P_2, can in turn stimulate Rho GTPases, making this positive regulation reciprocal (Tolias et al., 2000). Elevated levels of phosphatidic acid have been reported in the plasma membrane of ruffling phagocytic cells (Bohdanowicz et al., 2013), where it is thought to activate PIP5KI via Arf6 (Honda et al., 1999). Remarkably, production of phosphatidic acid from phosphatidylcholine by PLD is also dependant on PtdIns(4,5)P_2 as a cofactor (Divecha et al., 2000). Accordingly, a constitutive positive feedback loop between Rho and Arf GTPases, phosphatidic acid, and PIP5KI allows for continuous probing by resting phagocytic cells.

Actin polymerization in ruffles and pseudopods is coordinated by elevated levels of PtdIns(4,5)P_2 in multiple ways. Firstly, PtdIns(4,5)P_2 provides stability to the active state of NPFs such as WASP and N-WASP, members of the of the Wiskott-Aldrich syndrome protein (WASP) family (Rohatgi et al., 2000, 2001). NPFs activate the Arp2/3 complex, which in turn catalyzes branched actin filament nucleation (May et al., 2000). PtdIns(4,5)P_2-mediated WASP stabilization was also shown to be dependent on Rho GTPases (Caron and Hall, 1998; May et al., 2000; Park and Cox, 2009). Furthermore, PtdIns(4,5)P_2 can directly activate formins, a family of linear actin nucleators (Rousso et al., 2013). Secondly, PtdIns(4,5)P_2 inhibits actin-severing proteins, such as gelsolin (Janmey and Stossel, 1987) and cofilin (Gorbatyuk et al., 2006), thus curtailing the depolymerization of the actin cytoskeleton. Thirdly, PtdIns(4,5)P_2 allows for the growth of actin filaments by recruiting I-BAR proteins to the tip of the pseudopods, fostering actin polymerization (Hotulainen and Saarikangas, 2016). Lastly, PtdIns(4,5)P_2 facilitates the tethering of the plasma membrane to the underlying actin cytoskeleton through the ERM family of anchor proteins (Bretscher et al., 2002).

Elevated basal levels of PtdIns(3,4,5)P_3 have also been reported in the plasma membrane of probing phagocytic cells (Bohdanowicz et al., 2013; Canton et al., 2016), allowing for the rearrangement of the actin cytoskeleton necessary for pseudopod protrusion and increased phagocytic receptor mobility. As described earlier in this review, PtdIns(3,4,5)P_3 production primarily occurs through the phosphorylation of PtdIns(4,5)P_2 by class I PI3Ks. Mechanisms by which PtdIns(3,4,5)P_3 can promote actin rearrangement are described in the following section but share similarities with proposed functions in chemotaxis.

2. Target binding: high PtdIns(4,5)P_2 and appearance of PtdIns(3,4,5)P_3 in the phagocytic cup and Pseudopod progression: decline of PtdIns(4,5)P_2 with sustained PtdIns(3,4,5)P_3.

Ruffling and probing increase the probability of contacting a phagocytic target. Phagocytosis is initiated upon the binding of phagocytic target ligands to one or more receptors expressed on the surface of phagocytic cells. During the first stage of phagocytosis PtdIns(4,5)P_2 transiently rises, whereas a marked accumulation of PtdIns(3,4,5)P_3 occurs at the newly formed phagocytic cup.

Ligation of multiple vicinal ligands causes receptor clustering and activation (Jones et al., 1985). In the case of Fcɣ receptors, clustering prompts the phosphorylation of their immunoreceptor tyrosine-based activation motifs (ITAMs) by non-receptor tyrosine kinases of the Src family (Ghazizadeh et al., 1994), which include Lyn and Hck (Wang et al., 1994; Carréno et al., 2002). Phosphorylated ITAMs interact with Syk kinase which has two Src-homology two domains (Greenberg et al., 1996). Syk then recruits and phosphorylates scaffolding adaptors like Gab2, which in turn recruit p85, the catalytic domain of PI3K to the site of receptor binding (Gu et al., 2003). PI3K catalyzes the formation of PtdIns(3,4,5)P_3 from PtdIns(4,5)P_2, and important signal for the progression and completion of phagocytic cup formation (**Figure 3**).

Concomitant with the synthesis of PtdIns(3,4,5)P_3 is the formation of its precursor PtdIns(4,5)P_2. Extending pseudopods exhibit a moderate elevation of PtdIns(4,5)P_2 relative to resting plasma membrane. Increased production rather than reduced consumption explains this elevation. PIP5KI activity is stimulated by elevated phosphatidic acid levels catalyzed by the enhanced activity of PLD (Divecha et al., 2000) observed during phagocytosis (Kusner et al., 1999; Lee et al., 2002; Iyer et al., 2004). In addition, activated Rho GTPases downstream of engaged phagocytic receptor signaling sustain the activity of PIP5KI (Fairn et al., 2009). Together, these effectors elevate PtdIns(4,5)P_2 in the periphery of forming phagocytic cups (Botelho et al., 2000; Hoppe and Swanson, 2004).

Upon particle engagement and receptor clustering, the extending pseudopods wrap around the phagocytic target in a zipper-like manner. Two opposing modalities of actin dynamics favor the expansion of the contact area with the phagocytic target. Initially, branched and linear actin filament polymerization is required to drive the plasma membrane around the particle. Conversely, actin disassembly must occur at the base of the phagocytic cup; otherwise, polymerised actin would act as a mechanical obstacle to proper engulfment (O'Callaghan et al., 2011), preventing delivery of endomembranes (Bajno et al., 2000; Dewitt et al., 2006) and restricting receptor clustering at the phagocytic synapse (Treanor et al., 2011; Freeman et al., 2015). While PtdIns(4,5)P_2 is known to facilitate the growth of actin filaments in a manner analogous to the one described above for the ruffling membranes, PtdIns(3,4)P_2 can also coordinate actin assembly. PtdIns(3,4)P_2 formed by the dephosphorylation of PtdIns(3,4,5)P_3 is known to recruit Lamellipodin and thereby ENA/VASP to the leading edge of migrating cells (Krause et al., 2004) and could tentatively play an analogous role during phagosome formation. In line with this, Ena/VASP family proteins seem to be essential for the FcγR receptor-mediated remodeling of the actin cytoskeleton (Coppolino, 2001) (**Figure 3**).

PtdIns(4,5)P_2 then disappears from the base of the phagocytic cup, coinciding in time and space with the disassembly of cortical actin (Scott et al., 2005). PtdIns(4,5)P_2 disappearance from the base of the phagocytic cup can be attributed to three main factors. Firstly, PtdIns(4,5)P_2 is consumed by PI3K when producing

PtdIns(3,4,5)P_3. Secondly, PtdIns(3,4,5)P_3 recruits PLC (see **Table 1**) to the phagosome where it hydrolyzes PtdIns(4,5)P_2 (Falasca et al., 1998) and is likely to represent the main factor responsible for the disappearance of PtdIns(4,5)P_2 (Azzoni et al., 1992; Liao et al., 1992). Lastly, PtdIns(4,5)P_2 can also be dephosphorylated by the inositol 5-phosphatases INPP5B (Bohdanowicz et al., 2012) and OCRL (Mehta et al., 2014) that are recruited to sites of phagocytosis, producing a transient increase in PtdIns(4)P (Bohdanowicz et al., 2012; Levin et al., 2015).

Breakdown of PtdIns(4,5)P_2 is required for completion of phagocytosis for two main reasons. Firstly, its removal terminates actin polymerisation at the base of the cup, which is necessary to induce membrane curvature and for the focal secretion of endomembranes. Consistently, inhibition of PLC impairs phagosome formation (Botelho et al., 2000) and is accompanied by persistent actin accumulation at the base of the phagocytic cup (Scott et al., 2005). Secondly, DAG and IP_3, the two second messengers produced by the PLC-mediated hydrolysis of PtdIns(4,5)P_2 play important roles in phagocytosis (Bengtsson et al., 1993; Ueyama et al., 2004; Nunes et al., 2012; Schlam et al., 2013). DAG is not only a source of PA following its phosphorylation by DAG-kinase (Bohdanowicz and Grinstein, 2013), but it also activates conventional and novel protein kinase C (PKC) which seemingly participates in phagocytosis (Ueyama et al., 2004) and promotes the activation of the NADPH oxidase (He et al., 2004; Cheng et al., 2007). Furthermore, IP_3 induces calcium release from the ER that is thought to promote membrane fusion during phagosome formation (Jaconi et al., 1990; Bajno et al., 2000; Braun et al., 2004; Dewitt et al., 2006). Thus, the disappearance of PtdIns(4,5)P_2 from the base of the phagocytic cup is not purely a consequence of the formation of PtdIns(3,4,5)P_3, but is in effect, an important outcome of PtdIns(3,4,5)P_3 formation.

Lastly, accumulation of PtdIns(3,4,5)P_3, together with the clearance of PtdIns(4,5)P_2, play an essential role in regulating the ability of receptors to diffuse and recycle by directly removing actin from the base of the phagocytic cup. PtdIns(3,4,5)P_3 binds and recruits GAPs, such as ARHGAP12, ARHGAP25, and SH3BP1 to the phagocytic cup (Schlam et al., 2015). This, along with the elimination of PtdIns(4,5)P_2, results in the inactivation of Rho GTPases and prompts the termination of actin polymerisation that would otherwise curtail the mobility of transmembrane proteins (including receptors) via the cytoskeletal picket fence.

3. Phagosome Scission: disappearance of PtdIns(3,4,5)P_3 and production of PtdIns(3)P

Sealing of the phagosome occurs when the pseudopods fully surround the target particle and fuse at their distal ends. Effectors of PtdIns(3,4,5)P_3 appear to be crucial for the two main events necessary for proper internalization at this stage. These are (1) clearance of actin surrounding the phagosome (Cox et al., 1999; Beemiller et al., 2010) and (2) constriction of the exofacial leaflets of the plasma membrane where the pseudopods meet to promote scission of the phagosome.

The role of PtdIns(3,4,5)P_3 and its effectors in mediating actin clearance has been described above. In support of PtdIns(3,4,5)P_3 being necessary for phagocytic cup formation is the observation that inhibition of PI3K arrests phagosome formation and leads to actin accumulation at the base of frustrated phagosomes (Araki et al., 1996; Cox et al., 1999). Furthermore, expression of constitutively active mutants of Rho GTPases that antagonize actin disassembly yields a similar phenotype of abortive phagocytic cups (Beemiller et al., 2010).

Relatively little is known about the mechanisms behind membrane fusion during scission; however, myosin-driven contractility is probably involved. Myosin X (Cox et al., 2002) and myosin IC (Swanson et al., 1999) localize to sites of phagosome closure, where they are thought to play independent roles during sealing. Interestingly, myosin X harbors a PH domain that binds PtdIns(3,4,5)P_3 enabling its recruitment to the plasma membrane (Isakoff et al., 1998). Accordingly, the PI3K inhibitor wortmannin prevents myosin X accumulation and expression of a truncated mutant of myosin X reduces phagocytic efficiency (Cox et al., 2002). Surprisingly, the antagonistic effects on phagosomal scission caused by PI3K inhibition seem to be size dependent. PI3K inhibitors only arrest phagocytosis of comparatively large targets ($>1\,\mu m$) (Cox et al., 2002) while internalization of smaller particles ($<1\,\mu m$) seems to be largely unaffected (Cox et al., 1999; Vieira et al., 2001).

PtdIns(3,4,5)P_3 disappears from the phagosomal membrane shortly after scission occurs (Marshall et al., 2001) (**Figure 3**). Conversion of PtdIns(3,4,5)P_3 into PtdIns(3,4)P_2 occurs at this stage since SHIP, a 5-phosphatase (McCrea and De Camilli, 2009), accumulates at the phagosomal membrane (Marshall et al., 2001; Kamen et al., 2007). It is unclear whether PtdIns(3,4)P_2 plays a role during this stage, other than being a substrate for the formation PtdIns(3)P by INPP4B, a 4-phosphatase (Nigorikawa et al., 2015). PtdIns(3,4,5)P_3 also can be dephosphorylated by PTEN to regenerate PtdIns(4,5)P_2 (Maehama and Dixon, 1998).

Lastly, PIP5KIs detach from the membrane of the newly formed phagosome, likely preventing further formation of PtdIns(4,5)P_2 from PtdIns(4)P (**Figure 3**). This detachment is partially due to the reduced electronegativity of the early phagosomal membrane, since PIP5KI isoforms contain a polycationic region that preferentially binds negatively charged membranes (Fairn et al., 2009).

PHAGOSOME MATURATION

The maturation of the phagosome is characterized by a series of fission and fusion events that occur soon after sealing. These steps modify both luminal and membrane components of the phagosome and give rise to the ultimate stage of degradation and reabsorption of the cargo during phagosome resolution. The nascent phagosome undergoes stepwise fusion events with early endosomes, late endosomes and lysosomes, which leads to the formation of the early phagosome, late phagosome and phagolysosome, respectively. Microbicidal properties, acidic pH and degradative enzymatic machinery are gradually acquired during phagosome maturation. Nevertheless, it is worth mentioning that differences in the extent and rate of phagosome maturation have been reported

between different phagocytic cells (Nordenfelt and Tapper, 2011; Canton et al., 2014). The nature of the engulfed material also accounts for some of the heterogeneity observed during phagosome maturation. For example, phagosomes containing pathogens need to preserve selected peptides for posterior antigen presentation to lymphocytes (Savina and Amigorena, 2007). On the other hand, clearance of apoptotic cells requires rapid acidification and maturation, in addition to secretion of anti-inflammatory cytokines in order to prevent auto-immunity (Ravichandran, 2010; Uderhardt et al., 2012).

As mentioned earlier, phagosome maturation can be additionally sub-classified into three main sequential stages: the early phagosome, the late phagosome and the phagolysosome. These are discussed individually below.

PtdIns(3)P Defines the Early Phagosome

Phagosome maturation starts as soon as the nascent phagosome detaches from the plasma membrane. Nevertheless, fusion events with endomembranes occur even before phagosome sealing is completed (Bohdanowicz et al., 2012). The newly formed phagosome preferentially fuses with early endosomes (Mayorga et al., 1991; Desjardins et al., 1997), resulting in a poorly degradative, slightly acidic hybrid organelle. Rab family proteins are crucial for vesicular traffic and phagosome fusion events during this and subsequent stages of maturation (Kinchen and Ravichandran, 2008; Fairn and Grinstein, 2012). Rab5 is involved in the early steps and is the prototypical marker of early phagosomes (Bucci et al., 1992; Roberts et al., 2000; Vieira et al., 2003).

Relevant to this review is the fact that the class III phosphatidylinositol 3-kinase, Vps34, is one of the key effectors of Rab5 (Christoforidis et al., 1999; Vieira et al., 2001; Munksgaard et al., 2002). Vps34 is present in early endosomes where it generates PtdIns(3)P by phosphorylating PtdIns on the D3 position. PtdIns(3)P is also the defining phosphoinositide of the early phagosome (Vieira et al., 2001) (**Figure 3**). Depletion of PtdIns(3)P through pharmacological inhibition of Vps34 arrests phagosome maturation at the early stage (Stephens et al., 1994; Fratti et al., 2001), demonstrating the crucial role of PtdIns(3)P in the progression of phagosomes. Multiple effectors are recruited to the early phagosome by virtue of PX and FYVE domains that bind selectively to PtdIns(3)P.

EEA1 is one of the effectors of PtdIns(3)P that binds the phosphoinositide through its FYVE domain (Simonsen et al., 1998). EEA1 interacts simultaneously with the active form of Rab5 (Mishra et al., 2010) and with PtdIns(3)P in the membrane of early phagosomes and early endosomes. This dual interaction favors early endosome-early phagosome tethering. In addition, EEA1 interacts with the soluble NSF-attachment protein receptors (SNAREs) including syntaxins 6 and 13, which further promotes membrane fusion after tethering (Simonsen et al., 1999; Collins et al., 2002). Accordingly, microinjection of neutralizing EEA1 antibodies arrest phagosome maturation (Fratti et al., 2001).

The disappearance of PtdIns(3)P from the phagosomal membrane signals the termination of the early phagosomal stage. Three different mechanisms could account for PtdIns(3)P disappearance: phosphorylation, dephosphorylation, or hydrolysis. The relative contribution of these pathways is currently unknown; however, the enzymes that can catalyze these reactions are known to be present. PtdIns(3)P can be phosphorylated by PIKfyve on its D5 position, yielding PtdIns(3,5)P_2 (Burd and Emr, 1998). Additionally, MTM1, a member of the myotubularin family of 3-phosphatases capable of breaking down PtdIns(3)P into PtdIns can also displace Vps34 from endosomal membrane, favoring PtdIns(3)P depletion (Yan and Backer, 2007). Lastly, lysosomal phospholipases can break down PtdIns(3)P (Ching et al., 1999), an event likely to occur upon formation of intraluminal vesicles (ILVs).

Despite the fact that multiple fusion events take place during phagosome maturation, the surface area of the phagosome remains virtually unchanged. This suggests that membrane recycling mechanisms must occur concomitantly. Retrograde transport of phagosomal components to the *trans*-Golgi network is partially responsible for membrane recycling, a process mediated by the retromer complex (Hierro et al., 2007). The retromer is composed of a sorting nexin (SNX) dimer (SNX1/SNX2 and SNX5/SNX6) and a cargo-recognition trimer (Vps26-Vps29-Vps35). SNXs contain a PX domain that serves to recruit them to the early phagosome, where PtdIns(3)P is present. Tellingly, the last steps of retrograde traffic are completed during the late stages of phagosome maturation (Bonifacino and Hurley, 2008).

As previously mentioned, in addition to outward vesiculation, the phagosomal membrane experiences inward budding and generates ILVs destined for degradation (Lee et al., 2005). ILV formation in phagosomes and endosomes is dependent on the endosomal sorting complex required for transport (ESCRT) (Vieira et al., 2004; Babst, 2011). The ESCRT super-complex consists of four smaller complexes (ESCRT-0-III) that together recognize ubiquitinated cargo such as Fcγ receptor (Booth et al., 2002; Wollert and Hurley, 2010). Most relevant to this review, ESCRT-0 bears a FYVE domain-containing subunit, known as Hrs, through which it binds to PtdIns(3)P. Thus, ESCRT-0 gets recruited to the maturing phagosome (Vieira et al., 2004), triggering the assembly of the entire ESCRT super-complex. This results in the inward budding of PtdIns(3)P-enriched ILVs that are degraded at later stages of phagosome maturation.

Reactive oxygen species, a crucial component of the microbicidal properties of phagocytic cells (Nunes et al., 2013), are produced by the action of NOX2 in the phagosomal lumen. Most significant to this review is the fact that $p40^{phox}$, one of the six subunits that make up the oxidase, has a PX domain that binds PtdIns(3)P, making the phosphoinositide crucial for the sustained stimulation of NOX2 in early phagosomes (Ueyama et al., 2007, 2008). Inhibition of PI3K, consequently, prevents the retention of $p40^{phox}$ at the phagosomal membrane and reduces the production of reactive oxygen species (Tian et al., 2008).

PtdIns(4)P Defines the Late Phagosome

The early phagosome then transitions into a late phagosome, which is more acidic and degradative than earlier stages. A crucial step for this transition is the conversion from a Rab5-positive to a Rab7-positive organelle. As maturation continues,

the phagosome migrates toward the microtubule-organizing center (MTOC), which promotes the fusion with late endosomes and lysosomes (Harrison et al., 2003). The active form of Rab7, together with two of its effectors –the Rab7-interacting lysosomal protein (RILP) and the oxysterol-binding protein-related protein 1L (ORP1L)– link the phagosome with the dynein/dynactin motor and are therefore responsible for this centripetal movement (Johansson et al., 2007). Rab7 and RILP also induce the formation of tubular membrane protrusions that promote phagosome-lysosome biogenesis and acidification (Harrison et al., 2003; Sun-Wada et al., 2009).

As mentioned earlier, the retromer is recruited initially to the early phagosome by PtdIns(3)P. Nevertheless, completion of retrograde transport occurs during the late stages through the interaction of Rab7 with the retromer's cargo-recognition trimer (Vps26-Vps29-Vps35). Rab7 depletion affects the structure of the retromer in endosomes and consequently impairs the retrieval of the mannose 6-phosphate receptor to the *trans*-Golgi network (Rojas et al., 2008).

From a phosphoinositide perspective, a marked transition is observed when the early phagosome becomes a late phagosome. Whereas PtdIns(3)P is characteristic of the early phagosome, PtdIns(4)P is the major phosphoinositide present at the late phagosome and phagolysosome stages (Jeschke et al., 2015). Soon after PtdIns(3)P disappears, PtdIns(4)P kinase 2A (PI4K2A), an enzyme responsible for PtdIns(4)P synthesis, accumulates in endosomes (Ketel et al., 2016) and late phagosomes (Jeschke et al., 2015). PtdIns(4)P persists in the phagosomal membrane well into the resolution stage, when its concentration gradually decreases (**Figure 3**). The accumulation of PtdIns(4)P was shown to be indispensable for proper phagosomal acidification (Levin et al., 2017). A similar role for PI4K2A and PtdIns(4)P as important determinants of maturation has also been recognized in autophagosomes (Albanesi et al., 2015). Yet, the specific effectors of PtdIns(4)P mediating late maturation and resolution are still poorly understood.

The Phagolysosome

Phagolysosome biogenesis is the next stage in phagosome maturation. Fusion of the late phagosome with lysosomes gives rise to the phagolysosome, the most acidic, degradative and microbicidal organelle. The phagolysosome has an extremely low luminal pH due to the acquisition of additional copies of the proton-pumping V-ATPase. This acidic pH allows for the optimal activity of hydrolytic enzymes (Appelqvist et al., 2013) essential for the ultimate degradation of phagosomal contents.

Of particular interest is the accumulation of PtdIns(3,5)P_2 in the lysosomal system (Samie et al., 2013; Takatori et al., 2016). PtdIns(3,5)P_2 is produced via phosphorylation of PtdIns(3)P on its D5 position by PIKfyve (Burd and Emr, 1998). The phosphatase Fig4 harbors a Sac domain and is responsible for the reverse reaction, dephosphorylating PtdIns(3,5)P_2 back to PtdIns(3)P (Mccartney et al., 2014). PtdIns(3,5)P_2 breakdown can additionally be catalyzed by myotubularin 3-phosphatases, yielding PtdIns(5)P (Oppelt et al., 2012). Remarkably, PtdIns(3,5)P_2, PIKfyve and Fig4 all localize to lysosomes, together with the scaffold protein ArPIKfyve/Vac14 (Duex et al., 2006; Jin et al., 2008; Sbrissa et al., 2008). Observations that depleting PtdIns(3,5)P_2 results in enlarged lysosomes and disrupts lysosomal activity suggest that this complex plays an important functional role in endolysosomes (Ho et al., 2012; Mccartney et al., 2014). Purely in the context of phagocytosis, inhibition of PIKfyve blocks phagosome maturation, seemingly through the inactivation of the transient receptor potential cation channel of the mucolipin subfamily member 1 (TRPML1) (Kim et al., 2014). Previously, PtdIns(3,5)P_2 was shown to control the activity of TRPML1 (Dong et al., 2010), a cation channel found in lysosomes that promotes Ca^{2+} efflux from the lysosome into the cytosol (Wang et al., 2014). The role of Ca^{2+} in phagosome maturation and endomembrane fusion has been documented (Vergne et al., 2003), accounting for the observation that TRPML1 inhibition blocks fusion of phagosomes and lysosomes (Dayam et al., 2015).

PHAGOSOME RESOLUTION

The final stage of phagocytosis, phagosome resolution, entails the redirection and degradation of the phagosomal membrane and of luminal components. This stage is also the least well understood. The phagosomal membrane needs to be resorbed once the phagosomal luminal contents are cleared; this includes disposal or recycling of the phosphoinositide constituents of the phagosomal membrane. Earlier stages of phagosome maturation exhibit membrane recycling to the plasma membrane or the *trans*-Golgi network, as well as some degradation through the formation of ILVs. In contrast, relatively little is known about the degradation of the phagolysosomal membrane. In lysosomes, tubulation and fission of vesicles can occur and seems to require the activity of both mTOR and Arl8B (Zoncu et al., 2011; Saric et al., 2016). A similar process putatively promotes the transport of membranous components out of the phagolysosome, analogous to the process observed during antigen presentation (Mantegazza et al., 2014). Evidence from the last decade suggests that PtdIns(4)P and PI4K2A, present in late phagosomes and phagolysosomes, are able to recruit the exocyst, a multimeric complex involved in exocytosis, and mediate membrane recycling to the plasma membrane (Ketel et al., 2016). Further, PtdIns(4)P regulates retromer function and has been linked to actin nucleation via WASH. In the phagolysosomal membrane, WASH and actin-rich regions have also been reported to co-localize with PtdIns(4)P (Levin-Konigsberg et al., 2019) and may serve to propel the initial extension of resorption tubules. In this regard it is interesting to note that PI4K2A and late phagosomal PtdIns(4)P have recently been described to support Toll-like receptor signaling and antigen presentation in dendritic cells (López-Haber et al., 2020).

PtdIns(4)P, which is abundant in maturing phagolysosomes, becomes depleted as the phagolysosome undergoes tubulation and resorbs (**Figure 3**). PtdIns(4)P can be converted into PtdIns(3,4)P_2 or PtdIns(4,5)P_2 by class II PI3Ks (Misawa et al., 1998) and PI5 kinases (Desrivières et al., 1998), respectively. Still, these lipids have not been reliably detected in phagolysosomes and neither have PtdIns(4)P-specific phosphatases. Rather,

the main enzyme known to dephosphorylate PtdIns(4)P into PtdIns is Sac1 which resides in the ER (Moser von Filseck et al., 2015). Recently, we showed that PtdIns(4)P is extracted from the phagosomal membrane, and transferred to the ER, where it is available to Sac1 for hydrolysis (Levin-Konigsberg et al., 2019). This removal is facilitated by the lipid transfer protein and Rab7 effector ORP1L at membrane contact sites between the ER and the phagolysosome (Levin-Konigsberg et al., 2019). Furthermore, we showed that tubules emerge from the PtdIns(4)P-rich clusters in the resolving phagolysosome, where ADP-ribosylation factor-like protein 8B (ARL8B) and SifA- and kinesin-interacting protein/pleckstrin homology domain-containing family M member 2 (SKIP/PLEKHM2) accumulate. Accordingly, premature hydrolysis of PtdIns(4)P impairs SKIP recruitment and phagosome resolution (Levin-Konigsberg et al., 2019).

CONCLUDING REMARKS

The development of fluorescent biosensors of PPIns provided an unparalleled tool to investigate the role of these key lipids in leukocyte biology. By enabling their visualization in live cells, we have started to learn about their distribution, dynamics and metabolism under physiologically relevant conditions. These critical determinants of PPIns function could not previously be divined by conventional lipidomic approaches. While great strides have been made in the last two decades using biosensors, it bears emphasizing that the probes are inevitably invasive and that caution must be used limiting their expression, as they can compete for and scavenge endogenous ligands, potentially altering responsiveness. In addition, suitable probes still need to be developed to visualize species like PtdIns(3,5)P_2, that have been identified as critical determinants of endomembrane traffic and of ion transport. Developing improved probes and applying them to increasingly complex biological systems by intravital and lattice light-sheet microscopy will undoubtedly be the focus of research in the immediate future.

AUTHOR CONTRIBUTIONS

All authors listed have made a substantial, direct and intellectual contribution to the work, and approved it for publication.

FUNDING

FM-R was supported by the Mary H. Beatty Fellowship at the University of Toronto. GFWW was supported by a Vanier Canada Graduate Scholarship from the Canadian Institutes of Health Research and an MD/Ph.D. Studentship from the University of Toronto. This work was supported by Canadian Institutes of Health Research grant FDN-143202 to SG.

REFERENCES

Albanesi, J., Wang, H., Sun, H. Q., Levine, B., and Yin, H. (2015). GABARAP-mediated targeting of PI4K2A/PI4KIIα at autophagosomes regulates PtdIns4P-dependent autophagosome-lysosome fusion. *Autophagy* 11, 2127–2129. doi: 10.1080/15548627.2015.1093718

Andrew, N., and Insall, R. H. (2007). Chemotaxis in shallow gradients is mediated independently of PtdIns 3-kinase by biased choices between random protrusions. *Nat. Cell Biol.* 9, 193–200. doi: 10.1038/ncb1536

Appelqvist, H., Wäster, P., Kågedal, K., and Öllinger, K. (2013). The lysosome: from waste bag to potential therapeutic target. *J. Mol. Cell Biol.* 5, 214–226. doi: 10.1093/jmcb/mjt022

Araki, N., Johnson, M. T., and Swanson, J. A. (1996). A role for phosphoinositide 3-kinase in the completion of macropinocytosis and phagocytosis by macrophages. *J. Cell Biol.* 135, 1249–1260. doi: 10.1083/jcb.135.5.1249

Arcaro, A., and Wymann, M. P. (1993). Wortmannin is a potent phosphatidylinositol 3-kinase inhibitor: the role of phosphatidylinositol 3,4,5-trisphosphate in neutrophil responses. *Biochem. J.* 296 (Pt 2, 297–301. doi: 10.1042/bj2960297

Azzoni, L., Kamoun, M., Salcedo, T. W., Kanakaraj, P., and Perussia, B. (1992). Stimulation of FcγRIIIA results in phospholipase C-γ1 tyrosine phosphorylation and $p56^{lck}$ activation. *J. Exp. Med.* 176, 1745–1750. doi: 10.1084/jem.176.6.1745

Babst, M. (2011). MVB vesicle formation: ESCRT-dependent, ESCRT-independent and everything in between. *Curr. Opin. Cell Biol.* 23, 452–457. doi: 10.1016/j.ceb.2011.04.008

Bajno, L., Peng, X. R., Schreiber, A. D., Moore, H. P., Trimble, W. S., and Grinstein, S. (2000). Focal exocytosis of VAMP3-containing vesicles at sites of phagosome formation. *J. Cell Biol.* 149, 697–705. doi: 10.1083/jcb.149.3.697

Balla, A., Tuymetova, G., Tsiomenko, A., Várnai, P., and Balla, T. (2005). A plasma membrane pool of phosphatidylinositol 4-phosphate is generated by phosphatidylinositol 4-kinase type-III alpha: studies with the PH domains of the oxysterol binding protein and FAPP1. *Mol. Biol. Cell* 16, 1282–1295. doi: 10.1091/mbc.e04-07-0578

Balla, T. (2013). Phosphoinositides: tiny lipids with giant impact on cell regulation. *Physiol. Rev.* 93, 1019–1137. doi: 10.1152/physrev.00028.2012

Beemiller, P., Zhang, Y., Mohan, S., Levinsohn, E., Gaeta, I., Hoppe, A. D., et al. (2010). A Cdc42 activation cycle coordinated by PI 3-kinase during Fc receptor-mediated phagocytosis. *Mol. Biol. Cell* 21, 470–480. doi: 10.1091/mbc.E08-05-0494

Bengtsson, T., Jaconi, M. E., Gustafson, M., Magnusson, K. E., Theler, J. M., Lew, D. P., et al. (1993). Actin dynamics in human neutrophils during adhesion and phagocytosis is controlled by changes in intracellular free calcium. *Eur. J. Cell Biol.* 62, 49–58

Bohdanowicz, M., Balkin, D. M., De Camilli, P., and Grinstein, S. (2012). Recruitment of OCRL and Inpp5B to phagosomes by Rab5 and APPL1 depletes phosphoinositides and attenuates Akt signaling. *Mol. Biol. Cell* 23, 176–187. doi: 10.1091/mbc.E11-06-0489

Bohdanowicz, M., and Grinstein, S. (2013). Role of phospholipids in endocytosis, phagocytosis, and macropinocytosis. *Physiol. Rev.* 93, 69–106. doi: 10.1152/physrev.00002.2012

Bohdanowicz, M., Schlam, D., Hermansson, M., Rizzuti, D., Fairn, G. D., Ueyama, T., et al. (2013). Phosphatidic acid is required for the constitutive ruffling and macropinocytosis of phagocytes. *Mol. Biol. Cell* 24, 1700–1712. doi: 10.1091/mbc.E12-11-0789

Bojjireddy, N., Botyanszki, J., Hammond, G., Creech, D., Peterson, R., Kemp, D. C., et al. (2014). Pharmacological and genetic targeting of the PI4KA enzyme reveals its important role in maintaining plasma membrane phosphatidylinositol 4-phosphate and phosphatidylinositol 4,5-bisphosphate levels. *J. Biol. Chem.* 289, 6120–6132. doi: 10.1074/jbc.M113.531426

Bonifacino, J. S., and Hurley, J. H. (2008). Retromer. *Curr. Opin. Cell Biol.* 20, 427–436. doi: 10.1016/j.ceb.2008.03.009

Booth, J. W., Kim, M.-K., Jankowski, A., Schreiber, A. D., and Grinstein, S. (2002). Contrasting requirements for ubiquitylation during Fc

receptor-mediated endocytosis and phagocytosis. *EMBO J.* 21, 251–258. doi: 10.1093/emboj/21.3.251

Botelho, R. J., Teruel, M., Dierckman, R., Anderson, R., Wells, A., York, J. D., et al. (2000). Localized Biphasic Changes in Phosphatidylinositol-4,5-Bisphosphate at Sites of Phagocytosis. *J. Cell Biol.* 151, 1353 LP—1368. doi: 10.1083/jcb.151.7.1353

Boucrot, E., Ferreira, A. P. A., Almeida-Souza, L., Debard, S., Vallis, Y., Howard, G., et al. (2015). Endophilin marks and controls a clathrin-independent endocytic pathway. *Nature* 517, 460–465. doi: 10.1038/nature14067

Boulven, I., Levasseur, S., Marois, S., Par,é, G., Rollet-Labelle, E., and Naccache, P. H. (2006). Class I A phosphatidylinositide 3-kinases, rather than p110γ, regulate formyl-methionyl-leucyl-phenylalanine-stimulated chemotaxis and superoxide production in differentiated neutrophil-like PLB-985 cells. *J. Immunol.* 176, 7621–7627. doi: 10.4049/jimmunol.176.12.7621

Braun, V., Fraisier, V., Raposo, G., Hurbain, I., Sibarita, J.-B., Chavrier, P., et al. (2004). TI-VAMP/VAMP7 is required for optimal phagocytosis of opsonised particles in macrophages. *EMBO J.* 23, 4166–4176. doi: 10.1038/sj.emboj.7600427

Bretscher, A., Edwards, K., and Fehon, R. G. (2002). ERM proteins and merlin: integrators at the cell cortex. *Nat. Rev. Mol. Cell Biol.* 3, 586–599. doi: 10.1038/nrm882

Brombacher, E., Urwyler, S., Ragaz, C., Weber, S. S., Kami, K., Overduin, M., et al. (2009). Rab1 guanine nucleotide exchange factor SidM is a major phosphatidylinositol 4-phosphate-binding effector protein of Legionella pneumophila. *J. Biol. Chem.* 284, 4846–4856. doi: 10.1074/jbc.M807505200

Brooks, R., Fuhler, G. M., Iyer, S., Smith, M. J., Park, M.-Y., Paraiso, K. H. T., et al. (2010). SHIP1 inhibition increases immunoregulatory capacity and triggers apoptosis of hematopoietic cancer cells. *J. Immunol.* 184, 3582–3589. doi: 10.4049/jimmunol.0902844

Brown, F. D., Rozelle, A. L., Yin, H. L., Balla, T., and Donaldson, J. G. (2001). Phosphatidylinositol 4,5-bisphosphate and Arf6-regulated membrane traffic. *J. Cell Biol.* 154, 1007–1017. doi: 10.1083/jcb.200103107

Bucci, C., Parton, R. G., Mather, I. H., Stunnenberg, H., Simons, K., Hoflack, B., et al. (1992). The small GTPase rab5 functions as a regulatory factor in the early endocytic pathway. *Cell* 70, 715–728. doi: 10.1016/0092-8674(92)90306-W

Bui, H. H., Sanders, P. E., Bodenmiller, D., Kuo, M. S., Donoho, G. P., and Fischl, A. S. (2018). Direct analysis of PI(3,4,5)P 3 using liquid chromatography electrospray ionization tandem mass spectrometry. *Anal. Biochem.* 547, 66–76. doi: 10.1016/j.ab.2018.02.014

Burd, C. G., and Emr, S. D. (1998). Phosphatidylinositol(3)-phosphate signaling mediated by specific binding to RING FYVE domains. *Mol. Cell* 2, 157–162. doi: 10.1016/S1097-2765(00)80125-2

Burke, J. E. (2018). Structural basis for regulation of phosphoinositide kinases and their involvement in human disease. *Mol. Cell* 71, 653–673. doi: 10.1016/j.molcel.2018.08.005

Côté, J. F., Motoyama, A. B., Bush, J. A., and Vuori, K. (2005). A novel and evolutionarily conserved Ptdlns(3,4,5)P3-binding domain is necessary for DOCK180 signalling. *Nat. Cell Biol.* 7, 797–807. doi: 10.1038/ncb1280

Campa, C. C., Ciraolo, E., Ghigo, A., Germena, G., and Hirsch, E. (2015). Crossroads of PI3K and Rac pathways. *Small GTPases* 6, 71–80. doi: 10.4161/21541248.2014.989789

Canton, J. (2017). Phagosome maturation in polarized macrophages. *J. Leukoc. Biol.* 96, 729–738. doi: 10.1189/jlb.1MR0114-021R

Canton, J., Khezri, R., Glogauer, M., and Grinstein, S. (2014). Contrasting phagosome pH regulation and maturation in human M1 and M2 macrophages. *Mol. Biol. Cell* 25, 3330–3341. doi: 10.1091/mbc.E14-05-0967

Canton, J., Schlam, D., Breuer, C., Gu, M., Glogauer, M., Grinstein, S., et al. (2016). Calcium-sensing receptors signal constitutive macropinocytosis and facilitate the uptake of NOD2 ligands in macrophages. *Nat. Commun.* 7:11284. doi: 10.1038/ncomms11284

Carlton, J., Bujny, M., Peter, B. J., Oorschot, V. M. J., Rutherford, A., Mellor, H., et al. (2004). Sorting nexin-1 mediates tubular endosome-to-TGN transport through coincidence sensing of high- curvature membranes and 3-phosphoinositides. *Curr. Biol.* 14, 1791–1800. doi: 10.1016/j.cub.2004.09.077

Carmona, G., Perera, U., Gillett, C., Naba, A., Law, A. L., Sharma, V. P., et al. (2016). Lamellipodin promotes invasive 3D cancer cell migration via regulated interactions with Ena/VASP and SCAR/WAVE. *Oncogene* 35, 5155–5169. doi: 10.1038/onc.2016.47

Caron, E., and Hall, A. (1998). Identification of two distinct mechanisms of phagocytosis controlled by different Rho GTPases. *Science.* 282, 1717–1721. doi: 10.1126/science.282.5394.1717

Carréno, S., Caron, E., Cougoule, C., Emorine, L. J., and Maridonneau-Parini, I. (2002). p59Hck isoform induces F-actin reorganization to form protrusions of the plasma membrane in a Cdc42- and Rac-dependent manner. *J. Biol. Chem.* 277, 21007–21016. doi: 10.1074/jbc.M201212200

Chan Wah Hak, L., Khan, S., Di Meglio, I., Law, A. L., Häsler, S. L. A., Quintaneiro, L. M., et al. (2018). FBP17 and CIP4 recruit SHIP2 and lamellipodin to prime the plasma membrane for fast endophilin-mediated endocytosis. *Nat. Cell Biol.* 20, 1023–1031. doi: 10.1038/s41556-018-0146-8

Chen, B., Brinkmann, K., Chen, Z., Pak, C. W., Liao, Y., Shi, S., et al. (2014). The WAVE regulatory complex links diverse receptors to the actin cytoskeleton. *Cell* 156, 195–207. doi: 10.1016/j.cell.2013.11.048

Chen, R., Kang, V. H., Chen, J., Shope, J. C., Torabinejad, J., DeWald, D. B., et al. (2002). A monoclonal antibody to visualize PtdIns(3,4,5)P3 in cells. *J. Histochem. Cytochem.* 50, 697–708. doi: 10.1177/002215540205000511

Cheng, N., He, R., Tian, J., Dinauer, M. C., and Ye, R. D. (2007). A critical role of protein kinase Cδ activation loop phosphorylation in formyl-methionyl-leucyl-phenylalanine-induced phosphorylation of p47phox and rapid activation of nicotinamide adenine dinucleotide phosphate oxidase. *J. Immunol.* 179, 7720–7728. doi: 10.4049/jimmunol.179.11.7720

Ching, T. T., Wang, D. S., Hsu, A. L., Lu, P. J., and Chen, C. S. (1999). Identification of multiple phosphoinositide-specific phospholipases D as new regulatory enzymes for phosphatidylinositol 3,4,5-trisphosphate. *J. Biol. Chem.* 274, 8611–8617. doi: 10.1074/jbc.274.13.8611

Chishti, A. H., Kim, A. C., Marfatia, S. M., Lutchman, M., Hanspal, M., Jindal, H., et al. (1998). The FERM domain: a unique module involved in the linkage of cytoplasmic proteins to the membrane. *Trends Biochem. Sci.* 23, 281–282. doi: 10.1016/s0968-0004(98)01237-7

Christoforidis, S., Miaczynska, M., Ashman, K., Wilm, M., Zhao, L., Yip, S. C., et al. (1999). Phosphatidylinositol-3-OH kinases are Rab5 effectors. *Nat. Cell Biol.* 1, 249–252. doi: 10.1038/12075

Clark, J., Anderson, K. E., Juvin, V., Smith, T. S., Karpe, F., Wakelam, M. J. O., et al. (2011). Quantification of PtdInsP3 molecular species in cells and tissues by mass spectrometry. *Nat. Methods* 8, 267–272. doi: 10.1038/nmeth.1564

Coffelt, S. B., Wellenstein, M. D., and de Visser, K. E. (2016). Neutrophils in cancer: neutral no more. *Nat. Rev. Cancer* 16, 431–446. doi: 10.1038/nrc.2016.52

Cohen, L. A., Honda, A., Varnai, P., Brown, F. D., Balla, T., and Donaldson, J. G. (2007). Active Arf6 recruits ARNO/cytohesin GEFs to the PM by binding their PH domains. *Mol. Biol. Cell* 18, 2244–2253. doi: 10.1091/mbc.e06-11-0998

Collins, R. F., Schreiber, A. D., Grinstein, S., and Trimble, W. S. (2002). Syntaxins 13 and 7 function at distinct steps during phagocytosis. *J. Immunol.* 169, 3250–3256. doi: 10.4049/jimmunol.169.6.3250

Coppolino, M. G. (2001). Evidence for a molecular complex consisting of Fyb/SLAP, SLP-76, Nck, VASP and WASP that links the actin cytoskeleton to Fcgamma receptor signalling during phagocytosis. *J. Cell. Sci.* 114(Pt 23), 4307–4318. Available online at: https://jcs.biologists.org/content/114/23/4307

Courtney, T., and Deiters, A. (2018). Recent advances in the optical control of protein function through genetic code expansion. *Curr. Opin. Chem. Biol.* 46, 99–107. doi: 10.1016/j.cbpa.2018.07.011

Cox, D., Berg, J. S., Cammer, M., Chinegwundoh, J. O., Dale, B. M., Cheney, R. E., et al. (2002). Myosin X is a downstream effector of PI(3)K during phagocytosis. *Nat. Cell Biol.* 4, 469–477. doi: 10.1038/ncb805

Cox, D., Tseng, C. C., Bjekic, G., and Greenberg, S. (1999). A requirement for phosphatidylinositol 3-kinase in pseudopod extension. *J. Biol. Chem.* 274, 1240–1247. doi: 10.1074/jbc.274.3.1240

Cozier, G. E., Carlton, J., Bouyoucef, D., and Cullen, P. J. (2004). Membrane targeting by pleckstrin homology domains. *Curr. Top. Microbiol. Immunol.* 282, 49–88. doi: 10.1007/978-3-642-18805-3_3

Cronin, T. C., DiNitto, J. P., Czech, M. P., and Lambright, D. G. (2004). Structural determinants of phosphoinositide selectivity in splice variants of Grp1 family PH domains. *EMBO J.* 23, 3711–3720. doi: 10.1038/sj.emboj.7600388

Darveau, R. P. (2010). Periodontitis: a polymicrobial disruption of host homeostasis. *Nat. Rev. Microbiol.* 8, 481–490. doi: 10.1038/nrmicro2337

Dayam, R. M., Saric, A., Shilliday, R. E., and Botelho, R. J. (2015). The Phosphoinositide-Gated Lysosomal Ca^{2+} Channel, TRPML1, Is Required for Phagosome Maturation. *Traffic* 16, 1010–1026. doi: 10.1111/tra.12303

Desjardins, M., Nzala, N. N., Corsini, R., and Rondeau, C. (1997). Maturation of phagosomes is accompanied by changes in their fusion properties and size-selective acquisition of solute materials from endosomes. *J. Cell Sci.* 110, 2303–2314.

Desrivières, S., Cooke, F. T., Parker, P. J., and Hall, M. N. (1998). MSS4, a phosphatidylinositol-4-phosphate 5-kinase required for organization of the actin cytoskeleton in Saccharomyces cerevisiae. *J. Biol. Chem.* 273, 15787–15793. doi: 10.1074/jbc.273.25.15787

Dewitt, S., Tian, W., and Hallett, M. B. (2006). Localised PtdIns(3,4,5)P_3 or PtdIns(3,4)P_2 at the phagocytic cup is required for both phagosome closure and Ca^{2+} signalling in HL60 neutrophils. *J. Cell Sci.* 119, 443–451. doi: 10.1242/jcs.02756

Divecha, N., Roefs, M., Halstead, J. R., D'Andrea, S., Fernandez-Borga, M., Oomen, L., et al. (2000). Interaction of the type Iα PIPkinase with phospholipase D: a role for the local generation of phosphatidylinositol 4, 5-bisphosphate in the regulation of PLD2 activity. *EMBO J.* 19, 5440–5449. doi: 10.1093/emboj/19.20.5440

Dolinsky, S., Haneburger, I., Cichy, A., Hannemann, M., Itzen, A., and Hilbi, H. (2014). The Legionella longbeachae Icm/Dot substrate SidC selectively binds phosphatidylinositol 4-phosphate with nanomolar affinity and promotes pathogen vacuole-endoplasmic reticulum interactions. *Infect. Immun.* 82, 4021–4033. doi: 10.1128/IAI.01685-14

Dong, X., Shen, D., Wang, X., Dawson, T., Li, X., Zhang, Q., et al. (2010). PI(3,5)P_2 controls membrane trafficking by direct activation of mucolipin Ca^{2+} release channels in the endolysosome. *Nat. Commun.* 1, 1–11. doi: 10.1038/ncomms1037

Dormann, D., Weijer, G., Parent, C. A., Devreotes, P. N., and Weijer, C. J. (2002). Visualizing PI3 kinase-mediated cell-cell signaling during dictyostelium development. *Curr. Biol.* 12, 1178–1188. doi: 10.1016/S0960-9822(02)00950-8

Duex, J. E., Tang, F., and Weisman, L. S. (2006). The Vac14p-Fig4p complex acts independently of Vac7p and couples PI3,5P_2 synthesis and turnover. *J. Cell Biol.* 172, 693–704. doi: 10.1083/jcb.200512105

Eden, S., Rohatgi, R., Podtelejnikov, A. V., Mann, M., and Kirschner, M. W. (2002). Mechanism of regulation of WAVE1-induced actin nucleation by Rac1 and Nck. *Nature* 418, 790–793. doi: 10.1038/nature00859

Ellson, C. D., Gobert-Gosse, S., Anderson, K. E., Davidson, K., Erdjument-Bromage, H., Tempst, P., et al. (2001). Ptdlns(3)P regulates the neutrophil oxidase complex by binding to the PX domain of p40phox. *Nat. Cell Biol.* 3, 679–682. doi: 10.1038/35083076

Fairn, G. D., and Grinstein, S. (2012). How nascent phagosomes mature to become phagolysosomes. *Trends Immunol.* 33, 397–405. doi: 10.1016/j.it.2012.03.003

Fairn, G. D., Ogata, K., Botelho, R. J., Stahl, P. D., Anderson, R. A., De Camilli, P., et al. (2009). An electrostatic switch displaces phosphatidylinositol phosphate kinases from the membrane during phagocytosis. *J. Cell Biol.* 187, 701–714. doi: 10.1083/jcb.200909025

Falasca, M., Logan, S. K., Lehto, V. P., Baccante, G., Lemmon, M. A., and Schlessinger, J. (1998). Activation of phospholipase Cγ by PI 3-kinase-induced PH domain-mediated membrane targeting. *EMBO J.* 17, 414–422.

Ferguson, G. J., Milne, L., Kulkarni, S., Sasaki, T., Walker, S., Andrews, S., et al. (2007). PI(3)Kγ has an important context-dependent role in neutrophil chemokinesis. *Nat. Cell Biol.* 9, 86–91. doi: 10.1038/ncb1517

Ferguson, K. M., Lemmon, M. A., Schlessinger, J., and Sigler, P. B. (1995). Structure of the high affinity complex of inositol trisphosphate with a phospholipase C pleckstrin homology domain. *Cell* 83, 1037–1046. doi: 10.1016/0092-8674(95)90219-8

Fili, N., Calleja, V., Woscholski, R., Parker, P. J., and Larijani, B. (2006). Compartmental signal modulation: endosomal phosphatidylinositol 3-phospate controls endosome morphology and selective cargo sorting. *Proc. Natl. Acad. Sci. U.S.A.* 103, 15473–15478. doi: 10.1073/pnas.0607040103

Flannagan, R. S., Jaumouill,é, V., and Grinstein, S. (2012). The Cell Biology of Phagocytosis. *Annu. Rev. Pathol. Mech. Dis.* 7, 61–98. doi: 10.1146/annurev-pathol-011811-132445

Fratti, R. A., Backer, J. M., Gruenberg, J., Corvera, S., and Deretic, V. (2001). Role of phosphatidylinositol 3-kinase and Rab5 effectors in phagosomal biogenesis and mycobacterial phagosome maturation arrest. *J. Cell Biol.* 154, 631–644. doi: 10.1083/jcb.200106049

Frech, M., Andjelkovic, M., Ingley, E., Reddy, K. K., Falck, J. R., and Hemmings, B. A. (1997). High affinity binding of inositol phosphates and phosphoinositides to the pleckstrin homology domain of RAC/protein kinase B and their influence on kinase activity. *J. Biol. Chem.* 272, 8474–8481. doi: 10.1074/jbc.272.13.8474

Freeman, S. A., Jaumouillé, V., Choi, K., Hsu, B. E., Wong, H. S., Abraham, L., et al. (2015). Toll-like receptor ligands sensitize B-cell receptor signalling by reducing actin-dependent spatial confinement of the receptor. *Nat. Commun.* 6:6168. doi: 10.1038/ncomms7168

Freeman, S. A., Uderhardt, S., Saric, A., Collins, R. F., Buckley, C. M., Mylvaganam, S., et al. (2019). Lipid-gated monovalent ion fluxes regulate endocytic traffic and support immune surveillance. *Science* 9544, 1–10. doi: 10.1126/science.aaw9544

Fritsch, R., de Krijger, I., Fritsch, K., George, R., Reason, B., Kumar, M. S., et al. (2013). RAS and RHO families of GTPases directly regulate distinct phosphoinositide 3-kinase isoforms. *Cell* 153, 1050–1063. doi: 10.1016/j.cell.2013.04.031

Frost, A., Unger, V. M., and De Camilli, P. (2009). The BAR domain superfamily: membrane-molding macromolecules. *Cell* 137, 191–196. doi: 10.1016/j.cell.2009.04.010

Fuhler, G. M., Brooks, R., Toms, B., Iyer, S., Gengo, E. A., Park, M. Y., et al. (2012). Therapeutic potential of SH2 domain-containing inositol-5′-phosphatase 1 (SHIP1) and SHIP2 inhibition in cancer. *Mol. Med.* 18, 65–75. doi: 10.2119/molmed.2011.00178

Funamoto, S., Meili, R., Lee, S., Parry, L., and Firtel, R. A. (2002). Spatial and temporal regulation of 3-phosphoinositides by PI 3-kinase and PTEN mediates chemotaxis. *Cell* 109, 611–623. doi: 10.1016/S0092-8674(02)00755-9

Gambardella, L., Anderson, K. E., Jakus, Z., Kovács, M., Voigt, S., Hawkins, P. T., et al. (2013). Phosphoinositide 3-OH kinase regulates integrin-dependent processes in neutrophils by signaling through its effector ARAP3. *J. Immunol.* 190, 381–391. doi: 10.4049/jimmunol.1201330

Gao, K., Tang, W., Li, Y., Zhang, P., Wang, D., Yu, L., et al. (2015). Front-signal-dependent accumulation of the RHOA inhibitor FAM65B at leading edges polarizes neut. *J. Cell Sci.* 128, 992–1000. doi: 10.1242/jcs.161497

Gaullier, J. M., Ronning, E., Gillooly, D. J., and Stenmark, H. (2000). Interaction of the EEA1 FYVE finger with phosphatidylinositol 3-phosphate and early endosomes. Role of conserved residues. *J. Biol. Chem.* 275, 24595–24600. doi: 10.1074/jbc.M906554199

Ghazizadeh, S., Bolen, J. B., and Fleit, H. B. (1994). Physical and functional association of Src-related protein tyrosine kinases with FcγRII in monocytic THP-1 cells. *J. Biol. Chem.* 269, 8878–8884.

Godi, A., Di Campli, A., Konstantakopoulos, A., Di Tullio, G., Alessi, D. R., Kular, G. S., et al. (2004). FAPPS control Golgi-to-cell-surface membrane traffic by binding to ARF and PtdIns(4)P. *Nat. Cell Biol.* 6, 393–404. doi: 10.1038/ncb1119

Gorbatyuk, V. Y., Nosworthy, N. J., Robson, S. A., Bains, N. P. S., Maciejewski, M. W., dos Remedios, C. G., et al. (2006). Mapping the phosphoinositide-binding site on chick cofilin explains how PIP_2 regulates the cofilin-actin interaction. *Mol. Cell* 24, 511–522. doi: 10.1016/j.molcel.2006.10.007

Goulden, B. D., Pacheco, J., Dull, A., Zewe, J. P., Deiters, A., and Hammond, G. R. V. (2019). A high-avidity biosensor reveals plasma membrane PI(3,4)P2 is predominantly a class I PI3K signaling product. *J. Cell Biol.* 218, 1066–1079. doi: 10.1083/jcb.201809026

Gray, A., Van Der Kaay, J., and Downes, C. P. (1999). The pleckstrin homology domains of protein kinase B and GRP1 (general receptor for phosphoinositides-1) are sensitive and selective probes for the cellular detection of phosphatidylinositol 3,4-bisphosphate and/or phosphatidylinositol 3,4,5-trisphosphate. *Biochem. J.* 344 (Pt 3), 929–36. doi: 10.1042/0264-6021:3440929

Greenberg, S., Chang, P., Wang, D. C., Xavier, R., and Seed, B. (1996). Clustered syk tyrosine kinase domains trigger phagocytosis. *Proc. Natl. Acad. Sci. U.S.A.* 93, 1103–1107. doi: 10.1073/pnas.93.3.1103

Gu, H., Botelho, R. J., Yu, M., Grinstein, S., and Neel, B. G. (2003). Critical role for scaffolding adapter Gab2 in Fc gamma R-mediated phagocytosis. *J. Cell Biol.* 161, 1151–1161. doi: 10.1083/jcb.200212158

Gutman, O., Walliser, C., Piechulek, T., Gierschik, P., and Henis, Y. I. (2010). Differential regulation of phospholipase C-β2 activity and membrane interaction by Gαq, Gβ1γ 2, and Rac2. *J. Biol. Chem.* 285, 3905–3915. doi: 10.1074/jbc.M109.085100

Hammond, G. R. V., and Balla, T. (2015). Polyphosphoinositide binding domains: key to inositol lipid biology. *Biochim. Biophys. Acta - Mol. Cell Biol. Lipids*. 1851, 746–758. doi: 10.1016/j.bbalip.2015.02.013

Hammond, G. R. V., Dove, S. K., Nicol, A., Pinxteren, J. A., Zicha, D., and Schiavo, G. (2006). Elimination of plasma membrane phosphatidylinositol (4,5)-bisphosphate is required for exocytosis from mast cells. *J. Cell Sci.* 119, 2084–2094. doi: 10.1242/jcs.02912

Hammond, G. R. V., Fischer, M. J., Anderson, K. E., Holdich, J., Koteci, A., Balla, T., et al. (2012). PI4P and PI(4,5)P2 are essential but independent lipid determinants of membrane identity. *Science* 337, 727–730. doi: 10.1126/science.1222483

Hammond, G. R. V., Machner, M. P., and Balla, T. (2014). A novel probe for phosphatidylinositol 4-phosphate reveals multiple pools beyond the Golgi. *J. Cell Biol.* 205, 113–126. doi: 10.1083/jcb.201312072

Hammond, G. R. V., Schiavo, G., and Irvine, R. F. (2009). Immunocytochemical techniques reveal multiple, distinct cellular pools of PtdIns4P and PtdIns(4,5)P(2). *Biochem. J.* 422, 23–35. doi: 10.1042/BJ20090428

Hannigan, M., Zhan, L., Li, Z., Ai, Y., Wu, D., and Huang, C. K. (2002). Neutrophils lacking phosphoinositide 3-kinase γ show loss of directionality during N-formyl-Met-Leu-Phe-induced chemotaxis. *Proc. Natl. Acad. Sci. U.S.A.* 99, 3603–3608. doi: 10.1073/pnas.052010699

Hansen, S. D., and Mullins, R. D. (2015). Lamellipodin promotes actin assembly by clustering Ena/VASP proteins and tethering them to actin filaments. *Elife* 4, 1–29. doi: 10.7554/eLife.06585

Harlan, J. E., Hajduk, P. J., Yoon, H. S., and Fesik, S. W. (1994). Pleckstrin homology domains bind to phosphatidylinositol-4,5-bisphosphate. *Nature* 371, 168–170. doi: 10.1038/371168a0

Harrison, R. E., Bucci, C., Vieira, O. V., Schroer, T. A., and Grinstein, S. (2003). Phagosomes fuse with late endosomes and/or lysosomes by extension of membrane protrusions along microtubules: role of Rab7 and RILP. *Mol. Cell. Biol.* 23, 6494–6506. doi: 10.1128/MCB.23.18.6494

He, R., Nanamori, M., Sang, H., Yin, H., Dinauer, M. C., and Ye, R. D. (2004). Reconstitution of chemotactic peptide-induced nicotinamide adenine dinucleotide phosphate (reduced) oxidase activation in transgenic COS-phox cells. *J. Immunol.* 173, 7462–7470. doi: 10.4049/jimmunol.173.12.7462

Heit, B., Liu, L., Colarusso, P., Puri, K. D., and Kubes, P. (2008a). PI3K accelerates, but is not required for, neutrophil chemotaxis to fMLP. *J. Cell Sci.* 121, 205–214. doi: 10.1242/jcs.020412

Heit, B., Robbins, S. M., Downey, C. M., Guan, Z., Colarusso, P., Miller, B. J., et al. (2008b). PTEN functions to "prioritize" chemotactic cues and prevent "distraction" in migrating neutrophils. *Nat. Immunol.* 9, 743–752. doi: 10.1038/ni.1623

Heit, B., Tavener, S., Raharjo, E., and Kubes, P. (2002). An intracellular signaling hierarchy determines direction of migration in opposing chemotactic gradients. *J. Cell Biol.* 159, 91–102. doi: 10.1083/jcb.200202114

Herter, J., and Zarbock, A. (2013). Integrin Regulation during Leukocyte Recruitment. *J. Immunol.* 190, 4451–4457. doi: 10.4049/jimmunol.1203179

Hierro, A., Rojas, A. L., Rojas, R., Murthy, N., Effantin, G., Kajava, A. V., et al. (2007). Functional architecture of the retromer cargo-recognition complex. *Nature* 449, 1063–1067. doi: 10.1038/nature06216

Hind, L. E., Vincent, W. J. B., and Huttenlocher, A. (2016). Leading from the back: the role of the uropod in neutrophil polarization and migration. *Dev. Cell* 38, 161–169. doi: 10.1016/j.devcel.2016.06.031

Hirsch, E., Katanaev, V. L., Garlanda, C., Azzolino, O., Pirola, L., Silengo, L., et al. (2000). Central role for G protein-coupled phosphoinositide 3-kinase γ in inflammation. *Science* 287, 1049–1052. doi: 10.1126/science.287.5455.1049

Ho, C. Y., Alghamdi, T. A., and Botelho, R. J. (2012). Phosphatidylinositol-3,5-bisphosphate: no longer the poor PIP_2. *Traffic* 13, 1–8. doi: 10.1111/j.1600-0854.2011.01246.x

Hoeller, O., and Kay, R. R. (2007). Chemotaxis in the Absence of PIP3 Gradients. *Curr. Biol.* 17, 813–817. doi: 10.1016/j.cub.2007.04.004

Hofmann, I., Thompson, A., Sanderson, C. M. M., and Munro, S. (2007). The Arl4 family of small G proteins can recruit the cytohesin Arf6 exchange factors to the plasma membrane. *Curr. Biol.* 17, 711–716. doi: 10.1016/j.cub.2007.03.007

Honda, A., Nogami, M., Yokozeki, T., Yamazaki, M., Nakamura, H., Watanabe, H., et al. (1999). Phosphatidylinositol 4-phosphate 5-kinase alpha is a downstream effector of the small G protein ARF6 in membrane ruffle formation. *Cell* 99, 521–532. doi: 10.1016/S0092-8674(00)81540-8

Hoppe, A. D., and Swanson, J. A. (2004). Cdc42, Rac1, and Rac2 display distinct patterns of activation during phagocytosis. *Mol. Biol. Cell* 15, 3509–3519. doi: 10.1091/mbc.E03

Hotulainen, P., and Saarikangas, J. (2016). The initiation of post-synaptic protrusions. *Commun. Integr. Biol.* 9:e1125053. doi: 10.1080/19420889.2015.1125053

Houslay, D. M., Anderson, K. E., Chessa, T., Kulkarni, S., Fritsch, R., Downward, J., et al. (2016). Coincident signals from GPCRs and receptor tyrosine kinases are uniquely transduced by PI3Kβ in myeloid cells. *Sci. Signal.* 9, 1–13. doi: 10.1126/scisignal.aae0453

Huang, Y. E., Iijima, M., Parent, C. A., Funamoto, S., Firtel, R. A., and Devreotes, P. (2003). Receptor-mediated regulation of PI3Ks Confines PI(3,4,5)P 3 to the leading edge of chemotaxing cells. *Mol. Biol. Cell* 14, 1913–1922. doi: 10.1091/mbc.e02-10-0703

Huw, L.-Y., O'Brien, C., Pandita, A., Mohan, S., Spoerke, J. M., Lu, S., et al. (2013). Acquired PIK3CA amplification causes resistance to selective phosphoinositide 3-kinase inhibitors in breast cancer. *Oncogenesis* 2, e83–e83. doi: 10.1038/oncsis.2013.46

Idevall-Hagren, O., Dickson, E. J., Hille, B., Toomre, D. K., and De Camilli, P. (2012). Optogenetic control of phosphoinositide metabolism. *Proc. Natl. Acad. Sci. U.S.A.* 109:E2316-23. doi: 10.1073/pnas.1211305109

Iijima, M., and Devreotes, P. (2002). Tumor suppressor PTEN mediates sensing of chemoattractant gradients. *Cell* 109, 599–610. doi: 10.1016/S0092-8674(02)00745-6

Illenberger, D., Walliser, C., Strobel, J., Gutman, O., Niv, H., Gaidzik, V., et al. (2003). Rac2 regulation of phospholipase C-β2 activity and mode of membrane interactions in intact cells. *J. Biol. Chem.* 278, 8645–8652. doi: 10.1074/jbc.M211971200

Inoue, T., Heo, W., Do, G.rimley, J. S., Wandless, T. J., and Meyer, T. (2005). An inducible translocation strategy to rapidly activate and inhibit small GTPase signaling pathways. *Nat. Methods* 2, 415–418. doi: 10.1038/nmeth763

Inoue, T., and Meyer, T. (2008). Synthetic activation of endogenous PI3K and Rac identifies an AND-gate switch for cell polarization and migration. *PLoS* ONE 3:e3068. doi: 10.1371/journal.pone.0003068

Isakoff, S. J., Cardozo, T., Andreev, J., Li, Z., Ferguson, K. M., Abagyan, R., et al. (1998). Identification and analysis of PH domain-containing targets of phosphatidylinositol 3-kinase using a novel in vivo assay in yeast. *EMBO J.* 17, 5374–5387. doi: 10.1093/emboj/17.18.5374

Itoh, R. E., Kurokawa, K., Ohba, Y., Yoshizaki, H., Mochizuki, N., and Matsuda, M. (2002). Activation of rac and cdc42 video imaged by fluorescent resonance energy transfer-based single-molecule probes in the membrane of living cells. *Mol. Cell. Biol.* 22, 6582–6591. doi: 10.1128/mcb.22.18.6582-6591.2002

Iyer, S. S., Barton, J. A., Bourgoin, S., and Kusner, D. J. (2004). Phospholipases D1 and D2 coordinately regulate macrophage phagocytosis. *J. Immunol.* 173, 2615–2623. doi: 10.4049/jimmunol.173.4.2615

Jaconi, M. E. E., Lew, D. P., Carpentier, J. L., Magnusson, K. E., Sjögren, M., and Stendahl, O. (1990). Cytosolic free calcium elevation mediates the phagosome-lysosome fusion during phagocytosis in human neutrophils. *J. Cell Biol.* 110, 1555–1564. doi: 10.1083/jcb.110.5.1555

Janetopoulos, C., Ma, L., Devreotes, P. N., and Iglesias, P. A. (2004). Chemoattractant-induced phosphatidylinositol 3,4,5-trisphosphate accumulation is spatially amplified and adapts, independent of the actin cytoskeleton. *Proc. Natl. Acad. Sci. U.S.A.* 101, 8951–8956. doi: 10.1073/pnas.0402152101

Janmey, P. A., and Stossel, T. P. (1987). Modulation of gelsolin function by phosphatidylinositol 4,5-bisphosphate. *Nature* 325, 362–364. doi: 10.1038/325362a0

Jeschke, A., Zehethofer, N., Lindner, B., Krupp, J., Schwudke, D., Haneburger, I., et al. (2015). Phosphatidylinositol 4-phosphate and phosphatidylinositol 3-phosphate regulate phagolysosome biogenesis. *Proc. Natl. Acad. Sci. U.S.A.* 112, 4636–4641. doi: 10.1073/pnas.1423456112

Jin, N., Chow, C. Y., Liu, L., Zolov, S. N., Bronson, R., Davisson, M., et al. (2008). VAC14 nucleates a protein complex essential for the acute interconversion of PI3P and $PI(3,5)P_2$ in yeast and mouse. *EMBO J.* 27, 3221–3234. doi: 10.1038/emboj.2008.248

Johansson, M., Rocha, N., Zwart, W., Jordens, I., Janssen, L., Kuijl, C., et al. (2007). Activation of endosomal dynein motors by stepwise assembly of Rab7-RILP-$p150^{Glued}$, ORP1L, and the receptor βIII spectrin. *J. Cell Biol.* 176, 459–471. doi: 10.1083/jcb.200606077

Jones, D. H., Nusbacher, J., and Anderson, C. L. (1985). Fc receptor-mediated binding and endocytosis by human mononuclear phagocytes: monomeric IgG

is not endocytosed by U937 cells and monocytes. *J. Cell Biol.* 100, 558–564. doi: 10.1083/jcb.100.2.558

Jones, M. M., Vanyo, S. T., and Visser, M. B. (2017). The C-terminal region of the major outer sheath protein of Treponema denticola inhibits neutrophil chemotaxis. *Mol. Oral Microbiol.* 32, 375–389. doi: 10.1111/omi.12180

Jones, M. M., Vanyo, S. T., and Visser, M. B. (2019). The Msp protein of treponema denticola interrupts activity of phosphoinositide processing in neutrophils. *Infect. Immun.* 87, 1–20. doi: 10.1128/IAI.00553-19

Kamen, L. A., Levinsohn, J., and Swanson, J. A. (2007). Differential association of phosphatidylinositol 3-kinase, SHIP-1, and PTEN with forming phagosomes. *Mol. Biol. Cell* 18, 2463–2472. doi: 10.1091/mbc.E07-01-0061

Kanai, F., Liu, H., Field, S. J., Akbary, H., Matsuo, T., Brown, G. E., et al. (2001). The PX domains of p47phox and p40phox bind to lipid products of PI(3)K. *Nat. Cell Biol.* 3, 675–678. doi: 10.1038/35083070

Keizer-Gunnink, I., Kortholt, A., and Van Haastert, P. J. M. (2007). Chemoattractants and chemorepellents act by inducing opposite polarity in phospholipase C and PI3-kinase signaling. *J. Cell Biol.* 177, 579–585. doi: 10.1083/jcb.200611046

Ketel, K., Krauss, M., Nicot, A.-S., Puchkov, D., Wieffer, M., Müller, R., et al. (2016). A phosphoinositide conversion mechanism for exit from endosomes. *Nature* 529, 408–412. doi: 10.1038/nature16516

Kielkowska, A., Niewczas, I., Anderson, K. E., Durrant, T. N., Clark, J., Stephens, L. R., et al. (2014). A new approach to measuring phosphoinositides in cells by mass spectrometry. *Adv. Biol. Regul.* 54, 131–141. doi: 10.1016/j.jbior.2013.09.001

Kim, G. H. E., Dayam, R. M., Prashar, A., Terebiznik, M., and Botelho, R. J. (2014). PIKfyve inhibition interferes with phagosome and endosome maturation in macrophages. *Traffic* 15, 1143–1163. doi: 10.1111/tra.12199

Kinashi, T. (2005). Intracellular signalling controlling integrin activation in lymphocytes. *Nat. Rev. Immunol.* 5, 546–559. doi: 10.1038/nri1646

Kinchen, J. M., and Ravichandran, K. S. (2008). Phagosome maturation: going through the acid test. *Nat. Rev. Mol. Cell Biol.* 9, 781–795. doi: 10.1038/nrm2515

Klarlund, J. K., Guilherme, A., Holik, J. J., Virbasius, J. V., Chawla, A., and Czech, M. P. (1997). Signaling by phosphoinositide-3,4,5-trisphosphate through proteins containing pleckstrin and Sec7 homology domains. *Science* 275, 1927–1930. doi: 10.1126/science.275.5308.1927

Klarlund, J. K., Tsiaras, W., Holik, J. J., Chawla, A., and Czech, M. P. (2000). Distinct polyphosphoinositide binding selectivities for pleckstrin homology domains of GRP1-like proteins based on diglycine versus triglycine motifs. *J. Biol. Chem.* 275, 32816–32821. doi: 10.1074/jbc.M002435200

Knall, C., Worthen, G. S., and Johnson, G. L. (1997). Interleukin 8-stimulated phosphatidylinositol-3-kinase activity regulates the migration of human neutrophils independent of extracellular signal-regulated kinase and p38 mitogen-activated protein kinases. *Proc. Natl. Acad. Sci. U.S.A.* 94, 3052–3057. doi: 10.1073/pnas.94.7.3052

Knight, Z. A., Gonzalez, B., Feldman, M. E., Zunder, E. R., Goldenberg, D. D., Williams, O., et al. (2006). A pharmacological map of the PI3-K family defines a role for p110α in insulin signaling. *Cell* 125, 733–747. doi: 10.1016/j.cell.2006.03.035

Koronakis, V., Hume, P. J., Humphreys, D., Liu, T., Hørning, O., Jensen, O. N., et al. (2011). WAVE regulatory complex activation by cooperating GTPases Arf and Rac1. *Proc. Natl. Acad. Sci. U. S.A.* 108, 14449–14454. doi: 10.1073/pnas.1107666108

Krause, M., and Gautreau, A. (2014). Steering cell migration: lamellipodium dynamics and the regulation of directional persistence. *Nat. Rev. Mol. Cell Biol.* 15, 577–590. doi: 10.1038/nrm3861

Krause, M., Leslie, J. D., Stewart, M., Lafuente, E. M., Valderrama, F., Jagannathan, R., et al. (2004). Lamellipodin, an Ena/VASP ligand, is implicated in the regulation of lamellipodial dynamics. *Dev. Cell* 7, 571–583. doi: 10.1016/j.devcel.2004.07.024

Kraynov, V. S., Chamberlain, C., Bokoch, G. M., Schwartz, M. A., Slabaugh, S., and Hahn, K. M. (2000). Localized Rac activation dynamics visualized in living cells. *Science* 290, 333–337. doi: 10.1126/science.290.5490.333

Krugmann, S., Anderson, K. E., Ridley, S. H., Risso, N., McGregor, A., Coadwell, J., et al. (2002). Identification of ARAP3, a novel PI3K effector regulating both Arf and Rho GTPases, by selective capture on phosphoinositide affinity matrices. *Mol. Cell* 9, 95–108. doi: 10.1016/s1097-2765(02)00434-3

Kuiper, J. W. P., Sun, C., Magalhães, M. A. O., and Glogauer, M. (2011). Rac regulates PtdInsP3 signaling and the chemotactic compass through a redox-mediated feedback loop. *Blood* 118, 6164–6171. doi: 10.1182/blood-2010-09-310383

Kumar, Y., and Valdivia, R. H. (2009). Leading a Sheltered Life: Intracellular Pathogens and Maintenance of Vacuolar Compartments. *Cell Host Microbe* 5, 593–601. doi: 10.1016/j.chom.2009.05.014

Kunisaki, Y., Nishikimi, A., Tanaka, Y., Takii, R., Noda, M., Inayoshi, A., et al. (2006). DOCK2 is a Rac activator that regulates motility and polarity during neutrophil chemotaxis. *J. Cell Biol.* 174, 647–652. doi: 10.1083/jcb.200602142

Kurig, B., Shymanets, A., Bohnacker, T., Prajwal, B. C., Ahmadian, M. R., Schaefer, M., et al. (2009). Ras is an indispensable coregulator of the class IB phosphoinositide 3-kinase p87/p110gamma. *Proc. Natl. Acad. Sci. U.S.A.* 106, 20312–20317. doi: 10.1073/pnas.0905506106

Kusner, D. J., Hall, C. F., and Jackson, S. (1999). Fcγ receptor-mediated activation of phospholipase D regulates macrophage phagocytosis of IgG-opsonized particles. *J. Immunol.* 162, 2266–2274.

Lacalle, R. A., Peregil, R. M., Albar, J. P., Merino, E., Martínez,-A., C., et al. (2007). Type I phosphatidylinositol 4-phosphate 5-kinase controls neutrophil polarity and directional movement. *J. Cell Biol.* 179, 1539–1553. doi: 10.1083/jcb.200705044

Lam, P., ying, Yoo, S. K., Green, J. M., and Huttenlocher, A. (2012). The SH2-domain-containing inositol 5-phosphatase (SHIP) limits the motility of neutrophils and their recruitment to wounds in zebrafish. *J. Cell Sci.* 125, 4973–4978. doi: 10.1242/jcs.106625

Law, A. L., Vehlow, A., Kotini, M., Dodgson, L., Soong, D., Theveneau, E., et al. (2013). Lamellipodin and the Scar/WAVE complex cooperate to promote cell migration in vivo. *J. Cell Biol.* 203, 673–689. doi: 10.1083/jcb.201304051

Lebensohn, A. M., and Kirschner, M. W. (2009). Activation of the WAVE complex by coincident signals controls actin assembly. *Mol. Cell* 36, 512–524. doi: 10.1016/j.molcel.2009.10.024

Lee, J.-H., Katakai, T., Hara, T., Gonda, H., Sugai, M., and Shimizu, A. (2004a). Roles of p-ERM and Rho–ROCK signaling in lymphocyte polarity and uropod formation. *J. Cell Biol.* 167, 327–337. doi: 10.1083/jcb.200403091

Lee, S. B., Várnai, P., Balla, A., Jalink, K., Rhee, S. G., and Balla, T. (2004b). The pleckstrin homology domain of phosphoinositide-specific phospholipase Cδ4 is not a critical determinant of the membrane localization of the enzyme. *J. Biol. Chem.* 279, 24362–24371. doi: 10.1074/jbc.M312772200

Lee, W. L., Kim, M.-K., Schreiber, A. D., and Grinstein, S. (2005). Role of ubiquitin and proteasomes in phagosome maturation. *Mol. Biol. Cell* 16, 2077–2090. doi: 10.1091/mbc.E04-06-0464

Lee, Y., Song, S., Park, S., Kim, S., Koh, E., and Lee, Y. (2002). Elevation of oleate-activated phospholipase D activity during thymic atrophy. *Immunology* 107, 435–443. doi: 10.1046/j.1365-2567.2002.01532.x

Leliefeld, P. H. C., Wessels, C. M., Leenen, L. P. H., Koenderman, L., and Pillay, J. (2016). The role of neutrophils in immune dysfunction during severe inflammation. *Crit. Care* 20, 73. doi: 10.1186/s13054-016-1250-4

Lemmon, M. A., Ferguson, K. M., O'Brien, R., Sigler, P. B., and Schlessinger, J. (1995). Specific and high-affinity binding of inositol phosphates to an isolated pleckstrin homology domain. *Proc. Natl. Acad. Sci. U.S.A.* 92, 10472–10476. doi: 10.1073/pnas.92.23.10472

Levin, R., Grinstein, S., and Canton, J. (2016). The life cycle of phagosomes: formation, maturation, and resolution. *Immunol. Rev.* 273, 156–179. doi: 10.1111/imr.12439

Levin, R., Grinstein, S., and Schlam, D. (2015). Phosphoinositides in phagocytosis and macropinocytosis. *Biochim. Biophys. Acta - Mol. Cell Biol. Lipids* 1851, 805–823. doi: 10.1016/j.bbalip.2014.09.005

Levin, R., Hammond, G. R. V., Balla, T., Camilli, P., De, F.airn, G. D., and Grinstein, S. (2017). Multiphasic dynamics of phosphatidylinositol 4-phosphate during phagocytosis. *Mol. Biol. Cell* 28, 128–140. doi: 10.1091/mbc.E16-06-0451

Levine, T. P., and Munro, S. (2002). Targeting of Golgi-specific pleckstrin homology domains involves both PtdIns 4-kinase-dependent and -independent components. *Curr. Biol.* 12, 695–704. doi: 10.1016/S0960-9822(02)00779-0

Levin-Konigsberg, R., Montaño-Rendón, F., Keren-Kaplan, T., Li, R., Ego, B., Mylvaganam, S., et al. (2019). Phagolysosome resolution requires contacts with the endoplasmic reticulum and phosphatidylinositol-4-phosphate signalling. *Nat. Cell Biol.* 21, 1234–1247. doi: 10.1038/s41556-019-0394-2

Ley, K., Hoffman, H. M., Kubes, P., Cassatella, M. A., Zychlinsky, A., Hedrick, C. C., et al. (2018). Neutrophils: New insights and open questions. *Sci. Immunol.* 3:eaat4579. doi: 10.1126/sciimmunol.aat4579

Li, C.-C., Chiang, T.-C., Wu, T.-S., Pacheco-Rodriguez, G., Moss, J., and Lee, F.-J. S. (2007). ARL4D recruits cytohesin-2/ARNO to modulate actin remodeling. *Mol. Biol. Cell* 18, 4420–4437. doi: 10.1091/mbc.e07-02-0149

Li, H., Wu, X., Hou, S., Malek, M., Kielkowska, A., Noh, E., et al. (2016). Phosphatidylinositol-3,4-bisphosphate and its binding protein lamellipodin regulate chemotaxis of malignant B lymphocytes. *J. Immunol.* 196, 586–595. doi: 10.4049/jimmunol.1500630

Li, J., Gao, Z., Zhao, D., Zhang, L., Qiao, X., Zhao, Y., et al. (2017). PI-273, a substrate-competitive, specific small-molecule inhibitor of PI4KIIα, inhibits the growth of breast cancer cells. *Cancer Res.* 77, 6253–6266. doi: 10.1158/0008-5472.CAN-17-0484

Li, Y., Jin, Y., Liu, B., Lu, D., Zhu, M., Jin, Y., et al. (2019). PTENα promotes neutrophil chemotaxis through regulation of cell deformability. *Blood* 133, 2079–2089. doi: 10.1182/blood-2019-01-899864

Li, Z., Dong, X., Wang, Z., Liu, W., Deng, N., Ding, Y., et al. (2005). Regulation of PTEN by Rho small GTPases. *Nat. Cell Biol.* 7, 399–404. doi: 10.1038/ncb1236

Li, Z., Jiang, H., Xie, W., Zhang, Z., Smrcka, A. V., and Wu, D. (2000). Roles of PLC-β2 and -β3 and PI3kγ in chemoattractant-mediated signal transduction. *Science* 287, 1046–1049. doi: 10.1126/science.287.5455.1046

Liao, F., Shin, H. S., and Rhee, S. G. (1992). Tyrosine phosphorylation of phospholipase C-γ 1 induced by cross-linking of the high-affinity or low-affinity Fc receptor for IgG in U937 cells. *Proc. Natl. Acad. Sci. U.S.A.* 89, 3659–3663. doi: 10.1073/pnas.89.8.3659

Liew, P. X., and Kubes, P. (2019). The Neutrophil's Role During Health and Disease. *Physiol. Rev.* 99, 1223–1248. doi: 10.1152/physrev.00012.2018

Liu, L., Puri, K. D., Penninger, J. M., and Kubes, P. (2007). Leukocyte PI3Kγ and PI3Kδ have temporally distinct roles for leukocyte recruitment in vivo. *Blood* 110, 1191–1198. doi: 10.1182/blood-2006-11-060103

Lokuta, M. A., Senetar, M. A., Bennin, D. A., Nuzzi, P. A., Chan, K. T., Ott, V. L., et al. (2007). Type Iγ PIP kinase is a novel uropod component that regulates rear retraction during neutrophil chemotaxis. *Mol. Biol. Cell* 18, 5069–5080. doi: 10.1091/mbc.e07-05-0428

Loovers, H. M., Postma, M., Keizer-Gunnink, I., Huang, Y. E., Devreotes, P. N., and van Haastert, P. J. M. (2006). Distinct roles of PI(3,4,5)P3 during chemoattractant signaling in Dictyostelium: a quantitative in vivo analysis by inhibition of PI3-kinase. *Mol. Biol. Cell* 17, 1503–1513. doi: 10.1091/mbc.e05-09-0825

López-Haber, C., Levin-Konigsberg, R., Zhu, Y., Bi-Karchin, J., Balla, T., Grinstein, S., et al. (2020). Phosphatidylinositol-4-kinase IIα licenses phagosomes for TLR4 signaling and MHC-II presentation in dendritic cells. *Proc. Natl. Acad. Sci. U.S.A.* 117, 28251–28262. doi: 10.1073/pnas.2001948117

Luo, J., Uprety, R., Naro, Y., Chou, C., Nguyen, D. P., Chin, J. W., et al. (2014). Genetically encoded optochemical probes for simultaneous fluorescence reporting and light activation of protein function with two-photon excitation. *J. Am. Chem. Soc.* 136, 15551–15558. doi: 10.1021/ja5055862

Maehama, T., and Dixon, J. E. (1998). The tumor suppressor, PTEN/ MMAC1, dephosphorylates the lipid second messenger, phosphatidylinositol 3,4,5-trisphosphate. *J. Biol. Chem.* 273, 13375–13378.

Malek, M., Kielkowska, A., Chessa, T., Anderson, K. E., Barneda, D., Pir, P., et al. (2017). PTEN regulates PI(3,4)P2 signaling downstream of class I PI3K. *Mol. Cell* 68, 566–580.e10. doi: 10.1016/j.molcel.2017.09.024

Mañes, S., Fuentes, G., Peregil, R. M., Rojas, A. M., and Lacalle, R. A. (2010). An isoform-specific PDZ-binding motif targets type I PIP5 kinase beta to the uropod and controls polarization of neutrophil-like HL60 cells. *FASEB J.* 24, 3381–3392. doi: 10.1096/fj.09-153106

Manna, D., Albanese, A., Park, W. S., and Cho, W. (2007). Mechanistic basis of differential cellular responses of phosphatidylinositol 3,4-bisphosphate- and phosphatidylinositol 3,4,5-trisphosphate-binding pleckstrin homology domains. *J. Biol. Chem.* 282, 32093–32105. doi: 10.1074/jbc.M703517200

Mantegazza, A. R., Zajac, A. L., Twelvetrees, A., Holzbaur, E. L. F., Amigorena, S., and Marks, M. S. (2014). TLR-dependent phagosome tubulation in dendritic cells promotes phagosome cross-talk to optimize MHC-II antigen presentation. *Proc. Natl. Acad. Sci. U.S.A.* 111, 15508–15513. doi: 10.1073/pnas.1412998111

Marshall, J. G., Booth, J. W., Stambolic, V., Mak, T., Balla, T., Schreiber, A. D., et al. (2001). Restricted accumulation of phosphatidylinositol 3-kinase products in a plasmalemmal subdomain during Fcγ receptor-mediated phagocytosis. *J. Cell Biol.* 153, 1369–1380. doi: 10.1083/jcb.153.7.1369

May, R. C., Caron, E., Hall, A., and Machesky, L. M. (2000). Involvement of the Arp2/3 complex in phagocytosis mediated by FcγR or CR3. *Nat. Cell Biol.* 2, 246–248. doi: 10.1038/35008673

Mayadas, T. N., Cullere, X., and Lowell, C. A. (2014). The multifaceted functions of neutrophils. *Annu. Rev. Pathol.* 9, 181–218. doi: 10.1146/annurev-pathol-020712-164023

Mayorga, L. S., Bertini, F., and Stahl, P. D. (1991). Fusion of newly formed phagosomes with endosomes in intact cells and in a cell-free system. *J. Biol. Chem.* 266, 6511–6517

Mazaki, Y., Nishimura, Y., and Sabe, H. (2012). GBF1 bears a novel phosphatidylinositol-phosphate binding module, BP3K, to link PI3Kγ activity with Arf1 activation involved in GPCR-mediated neutrophil chemotaxis and superoxide production. *Mol. Biol. Cell* 23, 2457–2467. doi: 10.1091/mbc.E12-01-0062

Mccartney, A. J., Zhang, Y., and Weisman, L. S. (2014). Phosphatidylinositol 3,5-bisphosphate: Low abundance, high significance. *BioEssays* 36, 52–64. doi: 10.1002/bies.201300012

McCormick, B., Chu, J. Y., and Vermeren, S. (2019). Cross-talk between Rho GTPases and PI3K in the neutrophil. *Small GTPases* 10, 187–195. doi: 10.1080/21541248.2017.1304855

McCrea, H. J., and De Camilli, P. (2009). Mutations in phosphoinositide metabolizing enzymes and human disease. *Physiology* 24, 8–16. doi: 10.1152/physiol.00035.2008

McLaughlin, S., and Murray, D. (2005). Plasma membrane phosphoinositide organization by protein electrostatics. *Nature* 438, 605–611. doi: 10.1038/nature04398

Mehta, Z. B., Pietka, G., and Lowe, M. (2014). The cellular and physiological functions of the lowe syndrome protein OCRL1. *Traffic* 15, 471–487. doi: 10.1111/tra.12160

Meili, R., Ellsworth, C., Lee, S., Reddy, T. B., Ma, H., and Firtel, R. A. (1999). Chemoattractant-mediated transient activation and membrane localization of Akt/PKB is required for efficient chemotaxis to cAMP in Dictyostelium. *EMBO J.* 18, 2092–2105. doi: 10.1093/emboj/18.8.2092

Michael, M., Vehlow, A., Navarro, C., and Krause, M. (2010). c-Abl, Lamellipodin, and Ena/VASP proteins cooperate in dorsal ruffling of fibroblasts and axonal morphogenesis. *Curr. Biol.* 20, 783–791. doi: 10.1016/j.cub.2010.03.048

Millius, A., Dandekar, S. N., Houk, A. R., and Weiner, O. D. (2009). Neutrophils establish rapid and robust WAVE complex polarity in an actin-dependent fashion. *Curr. Biol.* 19, 253–259. doi: 10.1016/j.cub.2008.12.044

Misawa, H., Ohtsubo, M., Copeland, N. G., Gilbert, D. J., Jenkins, N. A., and Yoshimura, A. (1998). Cloning and characterization of a novel class II phosphoinositide 3-kinase containing C2 domain. *Biochem. Biophys. Res. Commun.* 244, 531–539. doi: 10.1006/bbrc.1998.8294

Mishra, A., Eathiraj, S., Corvera, S., and Lambright, D. G. (2010). Structural basis for Rab GTPase recognition and endosome tethering by the C2H2 zinc finger of Early Endosomal Autoantigen 1 (EEA1). *Proc. Natl. Acad. Sci. U.S.A.* 107, 10866–10871. doi: 10.1073/pnas.1000843107

Miyamoto, T., DeRose, R., Suarez, A., Ueno, T., Chen, M., Sun, T., et al. (2012). Rapid and orthogonal logic gating with a gibberellin-induced dimerization system. *Nat. Chem. Biol.* 8, 465–470. doi: 10.1038/nchembio.922

Mondal, S., Ghosh-Roy, S., Loison, F., Li, Y., Jia, Y., Harris, C., et al. (2011). PTEN negatively regulates engulfment of apoptotic cells by modulating activation of Rac GTPase. *J. Immunol.* 187, 5783–5794. doi: 10.4049/jimmunol.1100484

Moser von Filseck, J., Copi,č, A., Delfosse, V., Vanni, S., and Jackson, C. L., Bourguet, W., et al. (2015). Phosphatidylserine transport by ORP/Osh proteins is driven by phosphatidylinositol 4-phosphate. *Science* 349, 432–436. doi: 10.1126/science.aab1346

Munksgaard, B., Murray, J. T., Panaretou, C., Stenmark, H., Miaczynska, M., and Backer, J. M. (2002). Role of Rab5 in the Recruitment of hVps34/p150 to the Early Endosome. *Traffic* 3, 416–427. doi: 10.1034/j.1600-0854.2002.30605.x

Nasuhoglu, C., Feng, S., Mao, J., Yamamoto, M., Yin, H. L., Earnest, S., et al. (2002). Nonradioactive analysis of phosphatidylinositides and other anionic phospholipids by anion-exchange high-performance liquid chromatography with suppressed conductivity detection. *Anal. Biochem.* 301, 243–254. doi: 10.1006/abio.2001.5489

Nathan, C. (2006). Neutrophils and immunity: challenges and opportunities. *Nat. Rev. Immunol.* 6, 173–182. doi: 10.1038/nri1785

Niggli, V. (2000). A membrane-permeant ester of phosphatidylinositol 3,4, 5-trisphosphate (PIP_3) is an activator of human neutrophil migration. *FEBS Lett.* 473, 217–221. doi: 10.1016/s0014-5793(00)01534-9

Niggli, V., and Keller, H. (1997). The phosphatidylinositol 3-kinase inhibitor wortmannin markedly reduces chemotactic peptide-induced locomotion and increases in cytoskeletal actin in human neutrophils. *Eur. J. Pharmacol.* 335, 43–52. doi: 10.1016/s0014-2999(97)01169-2

Nigorikawa, K., Hazeki, K., Sasaki, J., Omori, Y., Miyake, M., Morioka, S., et al. (2015). Inositol Polyphosphate-4-Phosphatase Type I Negatively Regulates Phagocytosis via Dephosphorylation of Phagosomal PtdIns(3,4)P2. *PLoS ONE* 10:e0142091. doi: 10.1371/journal.pone.0142091

Nishio, M., Watanabe, K., Sasaki, J., Taya, C., Takasuga, S., Iizuka, R., et al. (2007). Control of cell polarity and motility by the PtdIns(3,4,5)P3 phosphatase SHIP1. *Nat. Cell Biol.* 9, 36–44. doi: 10.1038/ncb1515

Nishioka, T., Aoki, K., Hikake, K., Yoshizaki, H., Kiyokawa, E., and Matsuda, M. (2008). Rapid turnover rate of phosphoinositides at the front of migrating MDCK cells. *Mol. Biol. Cell* 19, 4213–4223. doi: 10.1091/mbc.e08-03-0315

Nordenfelt, P., and Tapper, H. (2011). Phagosome dynamics during phagocytosis by neutrophils. *J. Leukoc. Biol.* 90, 271–284. doi: 10.1189/jlb.0810457

Nunes, P., Cornut, D., Bochet, V., Hasler, U., Oh-Hora, M., Waldburger, J. M., et al. (2012). STIM1 juxtaposes ER to phagosomes, generating Ca2+ hotspots that boost phagocytosis. *Curr. Biol.* 22, 1990–1997. doi: 10.1016/j.cub.2012.08.049

Nunes, P., Demaurex, N., and Dinauer, M. C. (2013). Regulation of the NADPH oxidase and associated ion fluxes during phagocytosis. *Traffic* 14, 1118–1131. doi: 10.1111/tra.12115

O'Callaghan, R., Job, K. M., Dull, R. O., and Hlady, V. (2011). Stiffness and heterogeneity of the pulmonary endothelial glycocalyx measured by atomic force microscopy. *Am. J. Physiol. Lung Cell. Mol. Physiol.* 301, L353–L360. doi: 10.1152/ajplung.00342.2010

Oikawa, T., Yamaguchi, H., Itoh, T., Kato, M., Ijuin, T., Yamazaki, D., et al. (2004). PtdIns(3,4,5)P3 binding is necessary for WAVE2-induced formation of lamellipodia. *Nat. Cell Biol.* 6, 420–426. doi: 10.1038/ncb1125

Oppelt, A., Lobert, V. H., Haglund, K., Mackey, A. M., Rameh, L. E., Liestøl, K., et al. (2012). Production of phosphatidylinositol 5-phosphate via PIKfyve and MTMR3 regulates cell migration. *EMBO Rep.* 14, 57–64. doi: 10.1038/embor.2012.183

Papakonstanti, E. A., Ridley, A. J., and Vanhaesebroeck, B. (2007). The p110delta isoform of PI 3-kinase negatively controls RhoA and PTEN. *EMBO J.* 26, 3050–3061. doi: 10.1038/sj.emboj.7601763

Park, H., and Cox, D. (2009). Cdc42 regulates Fcγ receptor-mediated phagocytosis through the activation and phosphorylation of Wiskott-Aldrich Syndrome Protein (WASP) and neural-WASP. *Mol. Biol. Cell* 20, 4500–4508. doi: 10.1091/mbc.E09-03-0230

Park, K. C., Rivero, F., Meili, R., Lee, S., Apone, F., and Firtel, R. A. (2004). Rac regulation of chemotaxis and morphogenesis in Dictyostelium. *EMBO J.* 23, 4177–4189. doi: 10.1038/sj.emboj.7600368

Pemberton, J. G., Kim, Y. J., Humpolickova, J., Eisenreichova, A., Sengupta, N., Toth, D. J., et al. (2020). Defining the subcellular distribution and metabolic channeling of phosphatidylinositol. *J. Cell Biol.* 219, 1689–1699. doi: 10.1083/jcb.201906130

Pirruccello, M., Nandez, R., Idevall-Hagren, O., Alcazar-Roman, A., Abriola, L., Berwick, S. A., et al. (2014). Identification of inhibitors of inositol 5-phosphatases through multiple screening strategies. *ACS Chem. Biol.* 9, 1359–1368. doi: 10.1021/cb500161z

Pizarro-Cerdá, J., Kühbacher, A., and Cossart, P. (2015). Phosphoinositides and host-pathogen interactions. *Biochim. Biophys. Acta* 1851, 911–918. doi: 10.1016/j.bbalip.2014.09.011

Posor, Y., Eichhorn-Gruenig, M., Puchkov, D., Schöneberg, J., Ullrich, A., Lampe, A., et al. (2013). Spatiotemporal control of endocytosis by phosphatidylinositol-3,4- bisphosphate. *Nature* 499, 233–237. doi: 10.1038/nature12360

Rahdar, M., Inoue, T., Meyer, T., Zhang, J., Vazquez, F., and Devreotes, P. N. (2009). A phosphorylation-dependent intramolecular interaction regulates the membrane association and activity of the tumor suppressor PTEN. *Proc. Natl. Acad. Sci. U.S.A.* 106, 480–485. doi: 10.1073/pnas.0811212106

Raucher, D., Stauffer, T., Chen, W., Shen, K., Guo, S., York, J. D., et al. (2000). Phosphatidylinositol 4,5-bisphosphate functions as a second messenger that regulates cytoskeleton-plasma membrane adhesion. *Cell* 100, 221–228. doi: 10.1016/s0092-8674(00)81560-3

Ravichandran, K. S. (2010). Find-me and eat-me signals in apoptotic cell clearance: progress and conundrums. *J. Exp. Med.* 207, 1807–1817. doi: 10.1084/jem.20101157

Reif, K., Okkenhaug, K., Sasaki, T., Penninger, J. M., Vanhaesebroeck, B., and Cyster, J. G. (2004). Cutting edge: differential roles for phosphoinositide 3-kinases, p110γ and p110δ, in lymphocyte chemotaxis and homing. *J. Immunol.* 173, 2236–2240. doi: 10.4049/jimmunol.173.4.2236

Ren, C., Yuan, Q., Braun, M., Zhang, X., Petri, B., Zhang, J., et al. (2019). Leukocyte Cytoskeleton Polarization Is Initiated by Plasma Membrane Curvature from Cell Attachment. *Dev. Cell* 49, 206–219.e7. doi: 10.1016/j.devcel.2019.02.023

Renkawitz, J., and Sixt, M. (2010). Mechanisms of force generation and force transmission during interstitial leukocyte migration. *EMBO Rep.* 11, 744–750. doi: 10.1038/embor.2010.147

Ridley, A. J., Schwartz, M. A., Burridge, K., Firtel, R. A., Ginsberg, M. H., Borisy, G., et al. (2003). Cell migration: integrating signals from front to Back. *Science* 302, 1704–1709. doi: 10.1126/science.1092053

Roberts, R. L., Barbieri, M. A., Ullrich, J., and Stahl, P. D. (2000). Dynamics of Rab5 activation in endocytosis and phagocytosis. *J. Leukoc. Biol.* 68, 627–632. doi: 10.1189/jlb.68.5.627

Rohatgi, R., Ho, H. H., and Kirschner, M. W. (2000). Mechanism of N-Wasp Activation by Cdc42 and Phosphatidylinositol 4,5-Bisphosphate. *J. Cell Biol.* 150, 1299 LP – 1310. doi: 10.1083/jcb.150.6.1299

Rohatgi, R., Nollau, P., Henry Ho, H. Y., Kirschner, M. W., and Mayer, B. J. (2001). Nck and phosphatidylinositol 4,5-bisphosphate synergistically activate actin polymerization through the N-WASP-Arp2/3 pathway. *J. Biol. Chem.* 276, 26448–26452. doi: 10.1074/jbc.M103856200

Rojas, R., Van Vlijmen, T., Mardones, G. A., Prabhu, Y., Rojas, A. L., Mohammed, S., et al. (2008). Regulation of retromer recruitment to endosomes by sequential action of Rab5 and Rab7. *J. Cell Biol.* 183, 513–526. doi: 10.1083/jcb.200804048

Rosivatz, E., Matthews, J. G., McDonald, N. Q., Mulet, X., Ho, K. K., Lossi, N., et al. (2006). A small molecule inhibitor for phosphatase and tensin homologue deleted on chromosome 10 (PTEN). *ACS Chem. Biol.* 1, 780–790. doi: 10.1021/cb600352f

Ross, S. H., Lindsay, Y., Safrany, S. T., Lorenzo, O., Villa, F., Toth, R., et al. (2007). Differential redox regulation within the PTP superfamily. *Cell. Signal.* 19, 1521–1530. doi: 10.1016/j.cellsig.2007.01.026

Rossman, K. L., Der, C. J., and Sondek, J. (2005). GEF means go: turning on Rho GTPases with guanine nucleotide-exchange factors. *Nat. Rev. Mol. Cell Biol.* 6, 167–180. doi: 10.1038/nrm1587

Rousso, T., Shewan, A. M., Mostov, K. E., Schejter, E. D., and Shilo, B. Z. (2013). Apical targeting of the formin diaphanous in Drosophila tubular epithelia. *Elife* 2013, 1–19. doi: 10.7554/eLife.00666

Sadhu, C., Masinovsky, B., Dick, K., Sowell, C. G., and Staunton, D. E. (2003). Essential role of phosphoinositide 3-Kinase δ in neutrophil directional movement. *J. Immunol.* 170, 2647–2654. doi: 10.4049/jimmunol.170.5.2647

Samie, M., Wang, X., Zhang, X., Goschka, A., Li, X., Cheng, X., et al. (2013). A TRP channel in the lysosome regulates large particle phagocytosis via focal exocytosis. *Dev. Cell* 26, 511–524. doi: 10.1016/j.devcel.2013.08.003

Sanui, T., Inayoshi, A., Noda, M., Iwata, E., Stein, J. V., Sasazuki, T., et al. (2003). DOCK2 regulates Rac activation and cytoskeletal reorganization through interaction with ELMO1. *Blood* 102, 2948–2950. doi: 10.1182/blood-2003-01-0173

Saric, A., Hipolito, V. E. B., Kay, J. G., Canton, J., Antonescu, C. N., and Botelho, R. J. (2016). mTOR controls lysosome tubulation and antigen presentation in macrophages and dendritic cells. *Mol. Biol. Cell* 27, 321–333. doi: 10.1091/mbc.E15-05-0272

Sarraj, B., Massberg, S., Li, Y., Kasorn, A., Subramanian, K., Loison, F., et al. (2009). Myeloid-specific deletion of tumor suppressor PTEN augments neutrophil transendothelial migration during inflammation. *J. Immunol.* 182, 7190–7200. doi: 10.4049/jimmunol.0802562

Sasaki, T., Irie-Sasaki, J., Jones, R. G., Oliveira-Dos-Santos, A. J., Stanford, W. L., Bolon, B., et al. (2000). Function of PI3Kγ in thymocyte development, T cell activation, and neutrophil migration. *Science* 287, 1040–4046. doi: 10.1126/science.287.5455.1040

Saudemont, A., Garçon, F., Yadi, H., Roche-Molina, M., Kim, N., Segonds-Pichon, A., et al. (2009). p110gamma and p110delta isoforms of phosphoinositide 3-kinase differentially regulate natural killer cell migration in health and disease. *Proc. Natl. Acad. Sci. U.S.A.* 106, 5795–5800. doi: 10.1073/pnas.0808594106

Savina, A., and Amigorena, S. (2007). Phagocytosis and antigen presentation in dendritic cells. *Immunol. Rev.* 219, 143–156. doi: 10.1111/j.1600-065X.2007.00552.x

Sbrissa, D., Ikonomov, O. C., Fenner, H., and Shisheva, A. (2008). ArPIKfyve homomeric and heteromeric interactions scaffold PIKfyve and Sac3 in a complex to promote PIKfyve activity and functionality. *J. Mol. Biol.* 384, 766–779. doi: 10.1016/j.jmb.2008.10.009

Schlam, D., Bagshaw, R. D., Freeman, S. A., Collins, R. F., Pawson, T., Fairn, G. D., et al. (2015). Phosphoinositide 3-kinase enables phagocytosis of large particles by terminating actin assembly through Rac/Cdc42 GTPase-activating proteins. *Nat. Commun.* 6:8623. doi: 10.1038/ncomms9623

Schlam, D., Bohdanowicz, M., Chatilialoglu, A., Steinberg, B. E., Ueyama, T., Du, G., et al. (2013). Diacylglycerol kinases terminate diacylglycerol signaling during the respiratory burst leading to heterogeneous phagosomal NADPH oxidase activation. *J. Biol. Chem.* 288, 23090–23104. doi: 10.1074/jbc.M113.457606

Scott, C. C., Dobson, W., Botelho, R. J., Coady-Osberg, N., Chavrier, P., Knecht, D. A., et al. (2005). Phosphatidylinositol-4, 5-bisphosphate hydrolysis directs actin remodeling during phagocytosis. *J. Cell Biol.* 169, 139–149. doi: 10.1083/jcb.200412162

Segal, A. W. (2005). How neutrophils kill microbes. *Annu. Rev. Immunol.* 23, 197–223. doi: 10.1146/annurev.immunol.23.021704.115653

Sela, M. N. (2001). Role of Treponema denticola in periodontal diseases. *Crit. Rev. Oral Biol. Med.* 12, 399–413. doi: 10.1177/10454411010120050301

Semenas, J., Hedblom, A., Miftakhova, R. R., Sarwar, M., Larsson, R., Shcherbina, L., et al. (2014). The role of PI3K/AKT-related PIP5K1α and the discovery of its selective inhibitor for treatment of advanced prostate cancer. *Proc. Natl. Acad. Sci. U.S.A.* 111. doi: 10.1073/pnas.1405801111

Servant, G., Weiner, O. D., Herzmark, P., Balla, T., Sedat, J. W., and Bourne, H. R. (2000). Polarization of chemoattractant receptor signaling during neutrophil chemotaxis. *Science* 287, 1037–1040. doi: 10.1126/science.287.5455.1037

Simonsen, A., Gaullier, J. M., D'Arrigo, A., and Stenmark, H. (1999). The Rab5 effector EEA1 interacts directly with syntaxin-6. *J. Biol. Chem.* 274, 28857–28860. doi: 10.1074/jbc.274.41.28857

Simonsen, A., Lipp,é, R., Christoforidis, S., Gaullier, J. M., Brech, A., Callaghan, J., et al. (1998). EEA1 links PI(3)K function to Rab5 regulation of endosome fusion. *Nature* 394, 494–498. doi: 10.1038/28879

Spencer, D. M., Wandless, T. J., Schreiber, S. L., and Crabtree, G. R. (1993). Controlling signal transduction with synthetic ligands. *Science* 262, 1019–1024. doi: 10.1126/science.7694365

Srinivasan, S., Wang, F., Glavas, S., Ott, A., Hofmann, F., Aktories, K., et al. (2003). Rac and Cdc42 play distinct roles in regulating PI(3,4,5)P3 and polarity during neutrophil chemotaxis. *J. Cell Biol.* 160, 375–385. doi: 10.1083/jcb.200208179

Stauffer, T. P., Ahn, S., and Meyer, T. (1998). Receptor-induced transient reduction in plasma membrane PtdIns(4,5)P2 concentration monitored in living cells. *Curr. Biol.* 8, 343–346. doi: 10.1016/s0960-9822(98)70135-6

Stephens, L., Cooke, F. T., Walters, R., Jackson, T., Volinia, S., Gout, I., et al. (1994). Characterization of a phosphatidylinositol-specific phosphoinositide 3-kinase from mammalian cells. *Curr. Biol.* 4, 203–214. doi: 10.1016/S0960-9822(00)00049-X

Subramanian, K. K., Jia, Y., Zhu, D., Simms, B. T., Jo, H., Hattori, H., et al. (2007). Tumor suppressor PTEN is a physiologic suppressor of chemoattractant- mediated neutrophil functions. *Blood* 109, 4028–4037. doi: 10.1182/blood-2006-10-055319

Suh, B.-C., Inoue, T., Meyer, T., and Hille, B. (2006). Rapid chemically induced changes of PtdIns(4,5)P2 gate KCNQ ion channels. *Science* 314, 1454–1457. doi: 10.1126/science.1131163

Suire, S., Condliffe, A. M., Ferguson, G. J., Ellson, C. D., Guillou, H., Davidson, K., et al. (2006). Gbetagammas and the Ras binding domain of p110gamma are both important regulators of PI(3)Kgamma signalling in neutrophils. *Nat. Cell Biol.* 8, 1303–1309. doi: 10.1038/ncb1494

Sun-Wada, G.-H., Tabata, H., Kawamura, N., Aoyama, M., and Wada, Y. (2009). Direct recruitment of H^+-ATPase from lysosomes for phagosomal acidification. *J. Cell Sci.* 122, 2504–2513. doi: 10.1242/jcs.050443

Surve, C. R., Lehmann, D., and Smrcka, A. V. (2014). A chemical biology approach demonstrates G protein βγ subunits are sufficient to mediate directional neutrophil chemotaxis. *J. Biol. Chem.* 289, 17791–17801. doi: 10.1074/jbc.M114.576827

Swanson, J. A. (2014). Microreview. Phosphoinositides and engulfment. *Cell. Microbiol.* 16, 1473–1483. doi: 10.1111/cmi.12334

Swanson, J. A., Johnson, M. T., Beningo, K., Post, P., Mooseker, M., and Araki, N. (1999). A contractile activity that closes phagosomes in macrophages. *J. Cell Sci.* 112, 307–316.

Szentpetery, Z., Várnai, P., and Balla, T. (2010). Acute manipulation of Golgi phosphoinositides to assess their importance in cellular trafficking and signaling. *Proc. Natl. Acad. Sci. U.S.A.* 107, 8225–8230. doi: 10.1073/pnas.1000157107

Takatori, S., Tatematsu, T., Cheng, J., Matsumoto, J., Akano, T., and Fujimoto, T. (2016). Phosphatidylinositol 3,5-bisphosphate-rich membrane domains in endosomes and lysosomes. *Traffic* 17, 154–167. doi: 10.1111/tra.12346

Takeda, K., Sasaki, A. T., Ha, H., Seung, H. A., and Firtel, R. A. (2007). Role of phosphatidylinositol 3-kinases in chemotaxis in Dictyostelium. *J. Biol. Chem.* 282, 11874–11884. doi: 10.1074/jbc.M610984200

Takenawa, T., and Suetsugu, S. (2007). The WASP-WAVE protein network: connecting the membrane to the cytoskeleton. *Nat. Rev. Mol. Cell Biol.* 8, 37–48. doi: 10.1038/nrm2069

Tang, W., Zhang, Y., Xu, W., Harden, T. K., Sondek, J., Sun, L., et al. (2011). A PLCβ/PI3Kγ-GSK3 signaling pathway regulates cofilin phosphatase slingshot2 and neutrophil polarization and chemotaxis. *Dev. Cell* 21, 1038–1050. doi: 10.1016/j.devcel.2011.10.023

Teng, T. S., Ji, A. L., Ji, X. Y., and Li, Y. Z. (2017). Neutrophils and immunity: from bactericidal action to being conquered. *J. Immunol. Res.* 2017:9671604. doi: 10.1155/2017/9671604

Thieblemont, N., Wright, H. L., Edwards, S. W., and Witko-Sarsat, V. (2016). Human neutrophils in auto-immunity. *Semin. Immunol.* 28, 159–173. doi: 10.1016/j.smim.2016.03.004

Thomas, B. P., Sun, C. X., Bajenova, E., Ellen, R. P., and Glogauer, M. (2006). Modulation of human neutrophil functions in vitro by Treponema denticola major outer sheath protein. *Infect. Immun.* 74, 1954–1957. doi: 10.1128/IAI.74.3.1954-1957.2006

Thomas, C. C., Dowler, S., Deak, M., Alessi, D. R., and van Aalten, D. M. (2001). Crystal structure of the phosphatidylinositol 3,4-bisphosphate-binding pleckstrin homology (PH) domain of tandem PH-domain-containing protein 1 (TAPP1): molecular basis of lipid specificity. *Biochem. J.* 358, 287–294. doi: 10.1042/0264-6021:3580287

Thomas, C. L., Steel, J., Prestwich, G. D., and Schiavo, G. (1999). Generation of phosphatidylinositol-specific antibodies and their characterization. *Biochem. Soc. Trans.* 27, 648–652. doi: 10.1042/bst0270648

Tian, W., Li, X. J., Stull, N. D., Ming, W., Suh, C.-I., Bissonnette, S. A., et al. (2008). FcγR-stimulated activation of the NADPH oxidase: phosphoinositide-binding protein $p40^{phox}$ regulates NADPH oxidase activity after enzyme assembly on the phagosome. *Blood* 112, 3867–3877. doi: 10.1182/blood-2007-11-126029

Tolias, K. F., Cantley, L. C., and Carpenter, C. L. (1995). Rho family GTPases bind to phosphoinositide kinases. *J. Biol. Chem.* 270, 17656–17659. doi: 10.1074/jbc.270.30.17656

Tolias, K. F., Hartwig, J. H., Ishihara, H., Shibasaki, Y., Cantley, L. C., and Carpenter, C. L. (2000). Type Iα phosphatidylinositol-4-phosphate 5-kinase mediates Rac-dependent actin assembly. *Curr. Biol.* 10, 153–156. doi: 10.1016/S0960-9822(00)00315-8

Tóth, B., Balla, A., Ma, H., Knight, Z. A., Shokat, K. M., and Balla, T. (2006). Phosphatidylinositol 4-kinase IIIβ regulates the transport of ceramide between the endoplasmic reticulum and Golgi. *J. Biol. Chem.* 281, 36369–36377. doi: 10.1074/jbc.M604935200

Traynor-Kaplan, A. E., Harris, A. L., Thompson, B. L., Taylor, P., and Sklar, L. A. (1988). An inositol tetrakisphosphate-containing phospholipid in activated neutrophils. *Nature* 334, 353–356. doi: 10.1038/334353a0

Traynor-Kaplan, A. E., Thompson, B. L., Harris, A. L., Taylor, P., Omann, G. M., and Sklar, L. A. (1989). Transient increase in phosphatidylinositol 3,4-bisphosphate and phosphatidylinositol trisphosphate during activation of human neutrophils. *J. Biol. Chem.* 264, 15668–15673

Treanor, B., Depoil, D., Bruckbauer, A., and Batista, F. D. (2011). Dynamic cortical actin remodeling by ERM proteins controls BCR microcluster organization and integrity. *J. Exp. Med.* 208, 1055–1068. doi: 10.1084/jem.20101125

Tsukada, S., Simon, M. I., Witte, O. N., and Katz, A. (1994). Binding of βγ subunits of heterotrimeric G proteins to the PH domain of Bruton tyrosine kinase. *Proc. Natl. Acad. Sci. U.S.A.* 91, 11256–11260. doi: 10.1073/pnas.91.23.11256

Uderhardt, S., Herrmann, M., Oskolkova, O. V., Aschermann, S., Bicker, W., Ipseiz, N., et al. (2012). 12/15-lipoxygenase orchestrates the clearance of apoptotic cells and maintains immunologic tolerance. *Immunity* 36, 834–846. doi: 10.1016/j.immuni.2012.03.010

Ueno, T., Falkenburger, B. H., Pohlmeyer, C., and Inoue, T. (2011). Triggering actin comets versus membrane ruffles: distinctive effects of phosphoinositides on actin reorganization. *Sci. Signal.* 4:ra87. doi: 10.1126/scisignal.2002033

Ueyama, T., Kusakabe, T., Karasawa, S., Kawasaki, T., Shimizu, A., Son, J., et al. (2008). Sequential binding of cytosolic Phox complex to phagosomes through regulated adaptor proteins: evaluation using the novel monomeric Kusabira-Green system and live imaging of phagocytosis. *J. Immunol.* 181, 629–640. doi: 10.4049/jimmunol.181.1.629

Ueyama, T., Lennartz, M. E., Noda, Y., Kobayashi, T., Shirai, Y., Rikitake, K., et al. (2004). Superoxide production at phagosomal cup/phagosome through βI protein kinase C during FcγR-mediated phagocytosis in microglia. *J. Immunol.* 173, 4582–4589. doi: 10.4049/jimmunol.173.7.4582

Ueyama, T., Tatsuno, T., Kawasaki, T., Tsujibe, S., Shirai, Y., Sumimoto, H., et al. (2007). A regulated adaptor function of $p40^{phox}$: distinct $p67^{phox}$ membrane targeting by $p40^{phox}$ and by $p47^{phox}$. *Mol. Biol. Cell* 18, 441–454. doi: 10.1091/mbc.E06-08-0731

Ui, M., Okada, T., Hazeki, K., and Hazeki, O. (1995). Wortmannin as a unique probe for an intracellular signalling protein, phosphoinositide 3-kinase. *Trends Biochem. Sci.* 20, 303–307. doi: 10.1016/s0968-0004(00)89056-8

Vanhaesebroeck, B., Jones, G. E., Allen, W. E., Zicha, D., Hooshmand-Rad, R., Sawyer, C., et al. (1999). Distinct PI(3)Ks mediate mitogenic signalling and cell migration in macrophages. *Nat. Cell Biol.* 1, 69–71. doi: 10.1038/9045

Várnai, P., and Balla, T. (1998). Visualization of phosphoinositides that bind pleckstrin homology domains: calcium- and agonist-induced dynamic changes and relationship to myo-[3H]inositol-labeled phosphoinositide pools. *J. Cell Biol.* 143, 501–510. doi: 10.1083/jcb.143.2.501

Várnai, P., Bondeva, T., Tamás, P., Tóth, B., Buday, L., Hunyady, L., et al. (2005). Selective cellular effects of overexpressed pleckstrin-homology domains that recognize PtdIns(3,4,5)P3 suggest their interaction with protein binding partners. *J. Cell Sci.* 118, 4879–4888. doi: 10.1242/jcs.02606

Várnai, P., Rother, K. I., and Balla, T. (1999). Phosphatidylinositol 3-kinase-dependent membrane association of the bruton's tyrosine kinase pleckstrin homology domain visualized in single living cells. *J. Biol. Chem.* 274, 10983–10989. doi: 10.1074/jbc.274.16.10983

Varnai, P., Thyagarajan, B., Rohacs, T., and Balla, T. (2006). Rapidly inducible changes in phosphatidylinositol 4,5-bisphosphate levels influence multiple regulatory functions of the lipid in intact living cells. *J. Cell Biol.* 175, 377–382. doi: 10.1083/jcb.200607116

Venkateswarlu, K., Gunn-Moore, F., Oatey, P. B., Tavar,é, J. M., and Cullen, P. J. (1998a). Nerve growth factor- and epidermal growth factor-stimulated translocation of the ADP-ribosylation factor-exchange factor GRP1 to the plasma membrane of PC12 cells requires activation of phosphatidylinositol 3-kinase and the GRP1 pleckstrin homology domain. *Biochem. J.* 335 (Pt 1), 139–46. doi: 10.1042/bj3350139

Venkateswarlu, K., Oatey, P. B., Tavar,é, J. M., and Cullen, P. J. (1998b). Insulin-dependent translocation of ARNO to the plasma membrane of adipocytes requires phosphatidylinositol 3-kinase. *Curr. Biol.* 8, 463–466. doi: 10.1016/s0960-9822(98)70181-2

Vergne, I., Chua, J., and Deretic, V. (2003). Tuberculosis toxin blocking phagosome maturation inhibits a novel Ca^{2+}/calmodulin-PI3K hVPS34 cascade. *J. Exp. Med.* 198, 653–659. doi: 10.1084/jem.20030527

Vieira, O. V., Botelho, R. J., and Grinstein, S. (2002). Phagosome maturation: aging gracefully. *Biochem. J.* 366, 689–704. doi: 10.1042/BJ20020691

Vieira, O. V., Botelho, R. J., Rameh, L., Brachmann, S. M., Matsuo, T., Davidson, H. W., et al. (2001). Distinct roles of class I and class III phosphatidylinositol 3-kinases in phagosome formation and maturation. *J. Cell Biol.* 155, 19–26. doi: 10.1083/jcb.200107069

Vieira, O. V., Bucci, C., Harrison, R. E., Trimble, W. S., Lanzetti, L., Gruenberg, J., et al. (2003). Modulation of Rab5 and Rab7 recruitment to phagosomes by phosphatidylinositol 3-kinase. *Mol. Cell. Biol.* 23, 2501–2514. doi: 10.1128/MCB.23.7.2501-2514.2003

Vieira, O. V., Harrison, R. E., Scott, C. C., Stenmark, H., Alexander, D., Liu, J., et al. (2004). Acquisition of Hrs, an essential component of phagosomal maturation, is impaired by mycobacteria. *Mol. Cell. Biol.* 24, 4593–4604. doi: 10.1128/MCB.24.10.4593-4604.2004

Visser, M. B., Sun, C.-X., Koh, A., Ellen, R. P., and Glogauer, M. (2013). Treponema denticola major outer sheath protein impairs the cellular phosphoinositide balance that regulates neutrophil chemotaxis. *PLoS ONE* 8:e66209. doi: 10.1371/journal.pone.0066209

Walpole, G. F. W., and Grinstein, S. (2020). Endocytosis and the internalization of pathogenic organisms: focus on phosphoinositides. *F1000Research* 9:368. doi: 10.12688/f1000research.22393.1

Wang, A. V., Scholl, P. R., and Geha, R. S. (1994). Physical and functional association of the high affinity immunoglobulin G receptor (FcγRI) with the kinases Hck and Lyn. *J. Exp. Med.* 180, 1165–1170. doi: 10.1084/jem.180.3.1165

Wang, C., Palavicini, J. P., Wang, M., Chen, L., Yang, K., Crawford, P. A., et al. (2016). Comprehensive and quantitative analysis of polyphosphoinositide species by shotgun lipidomics revealed their alterations in db/db mouse brain. *Anal. Chem.* 88, 12137–12144. doi: 10.1021/acs.analchem.6b02947

Wang, F. (2009). The signaling mechanisms underlying cell polarity and chemotaxis. *Cold Spring Harb. Perspect. Biol.* 1:a002980. doi: 10.1101/cshperspect.a002980

Wang, F., Herzmark, P., Weiner, O. D., Srinivasan, S., Servant, G., and Bourne, H. R. (2002). Lipid products of PI(3)Ks maintain persistent cell polarity and directed motility in neutrophils. *Nat. Cell Biol.* 4, 513–518. doi: 10.1038/ncb810

Wang, W., Zhang, X., Gao, Q., and Xu, H. (2014). TRPML1: An ion channel in the lysosome. *Handb. Exp. Pharmacol.* 222, 631–645. doi: 10.1007/978-3-642-54215-2_24

Watton, S. J., and Downward, J. (1999). Akt/PKB localisation and 3' phosphoinositide generation at sites of epithelial cell-matrix and cell-cell interaction. *Curr. Biol.* 9, 433–436. doi: 10.1016/s0960-9822(99)80192-4

Weavers, H., and Martin, P. (2020). The cell biology of inflammation: From common traits to remarkable immunological adaptations. *J. Cell Biol.* 219, 1–14. doi: 10.1083/jcb.202004003

Weber, S., and Hilbi, H. (2014). Live cell imaging of phosphoinositide dynamics during Legionella infection. *Methods Mol. Biol.* 1197, 153–167. doi: 10.1007/978-1-4939-1261-2_9

Weernink, P. A. O., Meletiadis, K., Hommeltenberg, S., Hinz, M., Ishihara, H., Schmidt, M., et al. (2004). Activation of type I phosphatidylinositol 4-phosphate 5-kinase isoforms by the Rho GTPases, RhoA, Rac1, and Cdc42. *J. Biol. Chem.* 279, 7840–7849. doi: 10.1074/jbc.M312737200

Weiner, O. D., Marganski, W. A., Wu, L. F., Altschuler, S. J., and Kirschner, M. W. (2007). An actin-based wave generator organizes cell motility. *PLoS Biol.* 5, 2053–2063. doi: 10.1371/journal.pbio.0050221

Weiner, O. D., Neilsen, P. O., Prestwich, G. D., Kirschner, M. W., Cantley, L. C., and Bourne, H. R. (2002). A PtdInsP3- and Rho GTPase-mediated positive feedback loop regulates neutrophil polarity. *Nat. Cell Biol.* 4, 509–512. doi: 10.1038/ncb811

Weiner, O. D., Rentel, M. C., Ott, A., Brown, G. E., Jedrychowski, M., Yaffe, M. B., et al. (2006). Hem-1 complexes are essential for Rac activation, actin polymerization, and myosin regulation during neutrophil chemotaxis. *PLoS Biol.* 4, 186–199. doi: 10.1371/journal.pbio.0040038

Wenk, M. R., Lucast, L., Di Paolo, G., Romanelli, A. J., Suchy, S. F., Nussbaum, R. L., et al. (2003). Phosphoinositide profiling in complex lipid mixtures using electrospray ionization mass spectrometry. *Nat. Biotechnol.* 21, 813–817. doi: 10.1038/nbt837

Westman, J., Grinstein, S., and Marques, P. E. (2019). Phagocytosis of Necrotic Debris at Sites of Injury and Inflammation. *Front. Immunol.* 10:3030. doi: 10.3389/fimmu.2019.03030

Wijdeven, R. H., Jongsma, M. L. M., Neefjes, J., and Berlin, I. (2015). ER contact sites direct late endosome transport. *BioEssays* 37, 1298–1302. doi: 10.1002/bies.201500095

Willard, S. S., and Devreotes, P. N. (2006). Signaling pathways mediating chemotaxis in the social amoeba, Dictyostelium discoideum. *Eur. J. Cell Biol.* 85, 897–904. doi: 10.1016/j.ejcb.2006.06.003

Wills, R. C., Goulden, B. D., and Hammond, G. R. V. (2018). Genetically encoded lipid biosensors. *Mol. Biol. Cell* 29, 1526–1532. doi: 10.1091/mbc.E17-12-0738

Wollert, T., and Hurley, J. H. (2010). Molecular mechanism of multivesicular body biogenesis by ESCRT complexes. *Nature* 464, 864–869. doi: 10.1038/nature08849

Won, D. H., Inoue, T., Wei, S. P., Man, L. K., Byung, O. P., Wandless, T. J., et al. (2006). PI(3,4,5)P3 and PI(4,5)P2 lipids target proteins with polybasic clusters to the plasma membrane. *Science* 314, 1458–1461. doi: 10.1126/science.1134389

Wright, B. D., Loo, L., Street, S. E., Ma, A., Taylor-Blake, B., Stashko, M. A., et al. (2014). The lipid kinase PIP5K1C regulates pain signaling and sensitization. *Neuron* 82, 836–847. doi: 10.1016/j.neuron.2014.04.006

Xu, J., Wang, F., Van Keymeulen, A., Herzmark, P., Straight, A., Kelly, K., et al. (2003). Divergent signals and cytoskeletal assemblies regulate self-organizing polarity in neutrophils. *Cell* 114, 201–214. doi: 10.1016/S0092-8674(03)00555-5

Xu, W., Wang, P., Petri, B., Zhang, Y., Tang, W., Sun, L., et al. (2010). Integrin-induced PIP5K1C kinase polarization regulates neutrophil polarization, directionality, and in vivo infiltration. *Immunity* 33, 340–350. doi: 10.1016/j.immuni.2010.08.015

Xu, X., Meier-Schellersheim, M., Jiao, X., Nelson, L. E., and Jin, T. (2005). Quantitative imaging of single live cells reveals spatiotemporal dynamics of multistep signaling events of chemoattractant gradient sensing in Dictyostelium. *Mol. Biol. Cell* 16, 676–688. doi: 10.1091/mbc.E04-07-0544

Yan, Y., and Backer, J. M. (2007). Regulation of class III (Vps34) PI3Ks. *Biochem. Soc. Trans.* 35, 239–241. doi: 10.1042/BST0350239

Yang, H. W., Collins, S. R., and Meyer, T. (2016). Locally excitable Cdc42 signals steer cells during chemotaxis. *Nat. Cell Biol.* 18, 191–201. doi: 10.1038/ncb3292

Yao, L., Kawakami, Y., and Kawakami, T. (1994). The pleckstrin homology domain of Bruton tyrosine kinase interacts with protein kinase C. *Proc. Natl. Acad. Sci. U.S.A.* 91, 9175–9179. doi: 10.1073/pnas.91.19.9175

Yeung, T., Terebiznik, M., Yu, L., Silvius, J., Abidi, W. M., Philips, M., et al. (2006). Receptor activation alters inner surface potential during phagocytosis. *Science* 313, 347–351. doi: 10.1126/science.1129551

Yip, S. C., Eddy, R. J., Branch, A. M., Pang, H., Wu, H., Yan, Y., et al. (2008). Quantification of PtdIns(3,4,5)P3 dynamics in EGF-stimulated carcinoma cells: A comparison of PH-domain-mediated methods with immunological methods. *Biochem. J.* 411, 441–448. doi: 10.1042/BJ20071179

Yoshinaga-Ohara, N., Takahashi, A., Uchiyama, T., and Sasada, M. (2002). Spatiotemporal Regulation of Moesin Phosphorylation and Rear Release by Rho and Serine/Threonine Phosphatase during Neutrophil Migration. *Exp. Cell Res.* 278, 112–122. doi: 10.1006/excr.2002.5571

Zewe, J. P., Wills, R. C., Sangappa, S., Goulden, B. D., and Hammond, G. R. (2018). SAC1 degrades its lipid substrate PtdIns4P in the endoplasmic reticulum to maintain a steep chemical gradient with donor membranes. *Elife* 7, 49–52. doi: 10.7554/eLife.35588

Zhang, Z. F., Chen, J., Han, X., Zhang, Y., Liao, H. B., Lei, R. X., et al. (2017). Bisperoxovandium (pyridin-2-squaramide) targets both PTEN and ERK1/2 to confer neuroprotection. *Br. J. Pharmacol.* 174, 641–656. doi: 10.1111/bph.13727

Zoncu, R., Efeyan, A., and Sabatini, D. M. (2011). mTOR: from growth signal integration to cancer, diabetes and ageing. *Nat. Rev. Mol. Cell Biol.* 12, 21–35. doi: 10.1038/nrm3025

Zunder, E. R., Knight, Z. A., Houseman, B. T., Apsel, B., and Shokat, K. M. (2008). Discovery of drug-resistant and drug-sensitizing mutations in the oncogenic PI3K Isoform p110α. *Cancer Cell* 14, 180–192. doi: 10.1016/j.ccr.2008.06.014

Conflict of Interest: The authors declare that the research was conducted in the absence of any commercial or financial relationships that could be construed as a potential conflict of interest.

frontiers in Cell and Developmental Biology

REVIEW
published: 11 February 2021
doi: 10.3389/fcell.2021.624025

Complement Receptors and Their Role in Leukocyte Recruitment and Phagocytosis

Sofie Vandendriessche†, *Seppe Cambier*†, *Paul Proost and Pedro E. Marques**

Laboratory of Molecular Immunology, Department of Microbiology, Immunology and Transplantation, Rega Institute for Medical Research, Katholieke Universiteit Leuven (KU Leuven), Leuven, Belgium

The complement system is deeply embedded in our physiology and immunity. Complement activation generates a multitude of molecules that converge simultaneously on the opsonization of a target for phagocytosis and activation of the immune system via soluble anaphylatoxins. This response is used to control microorganisms and to remove dead cells, but also plays a major role in stimulating the adaptive immune response and the regeneration of injured tissues. Many of these effects inherently depend on complement receptors expressed on leukocytes and parenchymal cells, which, by recognizing complement-derived molecules, promote leukocyte recruitment, phagocytosis of microorganisms and clearance of immune complexes. Here, the plethora of information on the role of complement receptors will be reviewed, including an analysis of how this functionally and structurally diverse group of molecules acts jointly to exert the full extent of complement regulation of homeostasis.

Keywords: complement, complement receptors, leukocyte, inflammation, cell migration, phagocytosis

OPEN ACCESS

Edited by:
Hao Sun,
University of California, San Diego, United States

Reviewed by:
James L. Stafford,
University of Alberta, Canada
Maurice Bartlett Hallett,
Cardiff University, United Kingdom
Michael Hickey,
Monash University, Australia

***Correspondence:**
Pedro E. Marques
pedro.marques@kuleuven.be

†*These authors have contributed equally to this work*

Specialty section:
This article was submitted to Cell Adhesion and Migration, a section of the journal Frontiers in Cell and Developmental Biology

Received: *30 October 2020*
Accepted: *15 January 2021*
Published: *11 February 2021*

Citation:
Vandendriessche S, Cambier S, Proost P and Marques PE (2021) Complement Receptors and Their Role in Leukocyte Recruitment and Phagocytosis. Front. Cell Dev. Biol. 9:624025. doi: 10.3389/fcell.2021.624025

INTRODUCTION TO THE COMPLEMENT SYSTEM

Evolution of Complement

The mammalian complement system comprises more than 50 fluid and membrane-associated proteins that control multiple aspects of physiology and immunity (Hajishengallis et al., 2017). The complement system is classically associated to a rapid response to invading microorganisms, which are either opsonized or directly lysed by the proteolytic cascade of complement proteins, as result of the generation of a lytic membrane attack complex (MAC). Complement is a core component of the immune system and is found (in less complex forms) in invertebrates as ancient as corals, jellyfish and sea anemones (phylum Cnidaria), a suggestion that complement may have originated near the appearance of multicellular organisms (Dishaw et al., 2005; Zhang and Cui, 2014). Complement is also found in invertebrates such as snails and clams (phylum Mollusca), insects and arachnids (phylum Arthropoda) and in the amphioxus (phylum Chordata) (Dodds and Matsushita, 2007; Prado-Alvarez et al., 2009; Sekiguchi and Nonaka, 2015). In vertebrates, complement versions resembling the mammalian system are found in jawed fish, such as zebrafish, in which research on complement function and evolution can be performed (Zhang and Cui, 2014). Although discovered first, the classical pathway (see section The Complement Cascade) is the latest in evolutionary terms, since it is closely associated to the function of IgM and IgG antibodies. Instead, the ancestral complement system likely relied on the combined action of prototypic versions of the complement protein C3, Factor B, and a protease (Nakao and Somamoto, 2016). Interestingly, complement in

invertebrates and ancestral vertebrates lacks cytolytic activity, which suggests that opsonization was the central role of complement in these animals and that complement-mediated cytolysis appeared later on (Dodds and Matsushita, 2007; Nonaka, 2014).

The Complement Cascade

The complement system in mammals possesses three main pathways: the classical, the lectin and the alternative pathway (**Figure 1**) (Densen and Ram, 2015). The classical pathway is initiated by complement protein C1q, which can bind to Fc regions of IgM and IgG immune complexes, but also to a variety of antigens directly through its pattern-recognition capabilities (Kouser et al., 2015). Binding of C1q leads to the activation of the C1q-associated proteases C1r and C1s, which will in turn cleave C4 and C2 available in the extracellular fluids. Cleavage of C4 generates C4b, which binds covalently to molecules in the vicinity of the active C1 proteases, associating stably to nearby antigens and to the antibodies. The C2 cleavage fragment C2a associates with C4b to form the C3 convertase, the central step of complement activation. The C3 convertase will cleave thousands of C3 molecules, present abundantly in the blood, into the highly-reactive C3b fragment that associates covalently to neighboring molecules and effectively opsonizes the target (Cooper, 1985). In addition, at this step occurs the release of the other fragment produced during C3 cleavage, the soluble anaphylatoxin C3a, that has pro-inflammatory properties through interaction with its G protein-coupled receptor (GPCR).

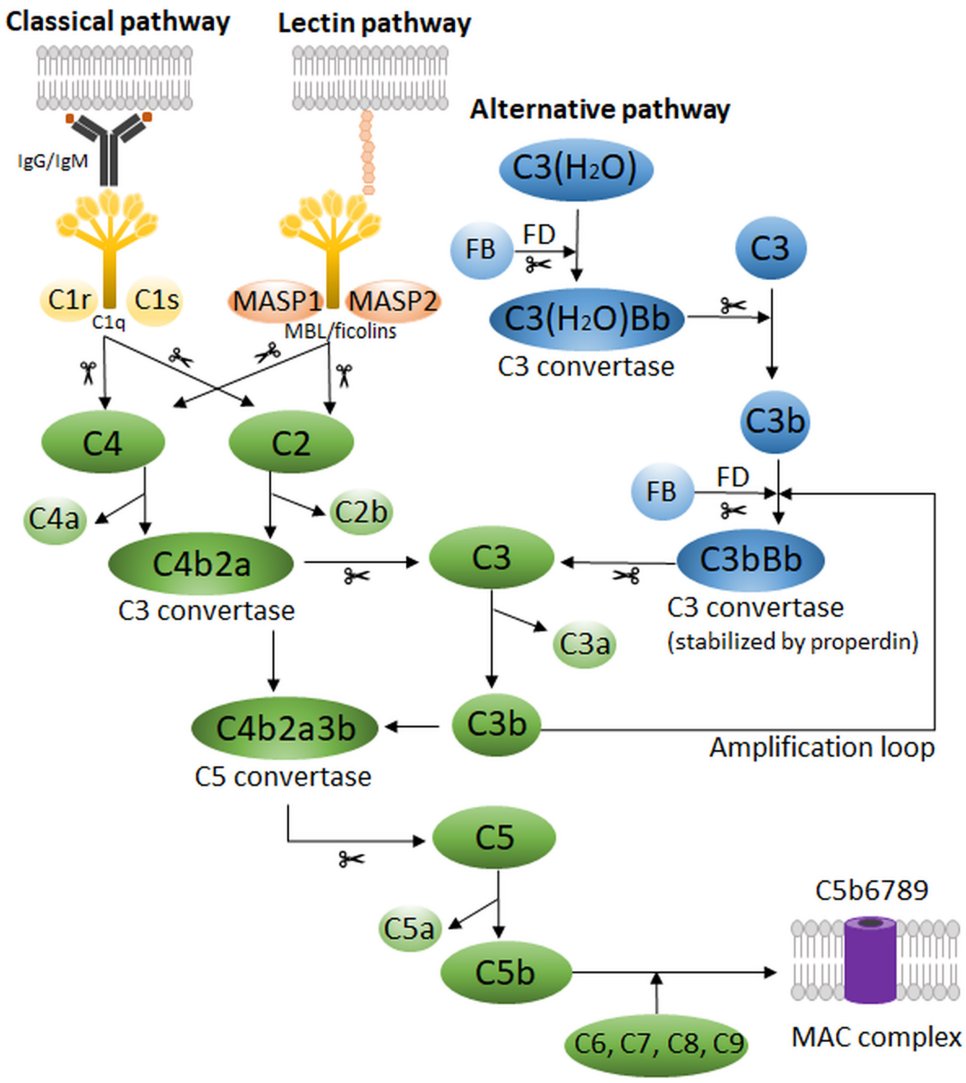

FIGURE 1 | Schematic representation of the human complement system, which possesses three main pathways: the classical, the lectin and the alternative pathway. Scissors indicate proteolytic cleavage. FB, Factor B; FD, Factor D; MAC, membrane attack complex; MASP, MBL-associated serum protease; MBL, mannose-binding lectin.

Subsequently, C3b binding to C3 convertases *in situ* leads to the formation of the C5 convertases, which are responsible for cleavage of C5 into C5b and C5a. As before, C5b associates to the target, although non-covalently, whereas C5a acts as an anaphylatoxin. The remaining components of the complement cascade; C6, C7, C8, and C9 will associate sequentially to the target-bound C5b to form the MAC, which is a pore with cytolytic properties. At its final configuration, the MAC is composed of one copy of C5b, C6, C7, and C8 and up to 18 copies of C9, which constitute the bulk of the MAC pore (Müller-Eberhard, 1986; Merle et al., 2015). The lectin pathway differs from the classical mainly because it is driven by mannose-binding lectin (MBL) and ficolins (**Figure 1**). Analogously to C1q, they bind to antigens to initiate the complement cascade, but in this case, the antigens are carbohydrates such as mannose, glucose and N-acetyl-glucosamine (Holers, 2014; Merle et al., 2015). Binding of MBL to sugars on microbial membranes leads to activation of MBL-associated serum proteases (MASPs) 1 and 2, which structurally and functionally similar to C1r and C1s, will initiate the cleavage of C4 and C2 to form the C3 convertase and unleash the complement cascade.

The complement cascade can also be initiated spontaneously by C3, the so-called alternative pathway (**Figure 1**). In the fluid phase, C3 can undergo spontaneous low-rate hydrolysis, or "tick-over," to yield C3(H_2O) (Holers, 2014; Hajishengallis et al., 2017). This form can bind Factor B, which when cleaved by the protease Factor D, produces a fluid-phase C3 convertase [C3(H_2O)Bb]. This enzyme produces C3b in solution, which may deposit on nearby surfaces and complex with more Factor B, forming the C3 convertase of the alternative pathway (C3bBb). It is important to mention that this cascade is short-lived and insufficient to promote full complement activation. For that, the alternative pathway requires properdin, a phagocyte-derived protein that stabilizes C3bBb and allows it to cleave C3 for long enough to enter the amplification phase of complement activation. Interestingly, the alternative pathway does not require antibodies for initiation, however, the presence of antibodies, polysaccharides, lipopolysaccharides (LPS), gas bubbles, heme, and properdin are all known to facilitate its activation. Moreover, the alternative pathway contributes to the full activation of complement via all pathways (e.g. classical and lectin) by providing an "amplification loop," in which deposited C3b continuously forms new C3 convertases by binding to Factor B. This dramatically increases the cascade activity and is associated to its effects *in vivo*, including complement-mediated injury (Holers, 2014; Hajishengallis et al., 2017).

Complement Regulation

Considering the high concentration of complement components in the serum and the ability of the cascade to self-amplify, a number of inhibitory mechanisms and molecules were developed throughout evolution in order to regulate the effects of complement on host cells (Ricklin et al., 2010; Holers, 2014; Densen and Ram, 2015; Merle et al., 2015). The initiation of the cascade is regulated by the C1 inhibitor (C1-INH/SERPIN 1), which inactivates the C1 proteases and dissociates them from C1q. Also, C1-INH inhibits several other proteases, including MASPs, thus regulating the lectin pathway. It is worth noting that the C3 convertases are unstable and undergo decay spontaneously, stopping the cascade unless stimuli are present. There are multiple soluble molecules that accelerate the deactivation of convertases, namely: Factor I, a protease that cleaves C3b into the enzymatically inactive form iC3b; Factor H, which accelerates the dissociation of Bb from C3 convertases and facilitates Factor I cleavage of C3b; C4 binding protein (C4BP), which stimulates the dissociation of C2a from C4b (classical C3 convertase) and also acts as co-factor for Factor I-mediated cleavage of C4b into iC4b. Additionally, the soluble proteins clusterin (SP-40) and vitronectin (S protein) bind to nascent C5b-C9 complexes and inhibit MAC assembly. Importantly, the activity of anaphylatoxins C3a and C5a is regulated via cleavage by carboxypeptidase-N, a plasma zinc metalloprotease, which cleaves a C-terminal arginine residue that severely reduces the anaphylatoxins' inflammatory effects. There are also a number of membrane-associated complement inhibitors. They serve to restrain the deleterious effects of excessive complement activation, but also offers a means to separate healthy host cells from other complement targets, such as microorganisms, dead cells and crystals, which most often do not express complement inhibitors. These include: Membrane cofactor protein (MCP, CD46), which binds to C3b and C4b fragments and stimulate Factor I-mediated cleavage; Decay-accelerating factor (DAF, CD55), which dissociates C3 convertases by binding to C3b and C4b; CR1 (CD35), that shares both dissociation and cofactor activities of MCP and DAF; and CD59, which binds C8 and C9 to prevent MAC assembly.

Complement-Associated Diseases and Therapies

Taking into account its ancient origin and broad reach, it is not surprising that complement regulates central aspects of physiology and immunity. Deficiencies in the complement system predispose individuals to severe recurrent infections and higher incidence of autoimmune disorders as systemic lupus erythematosus (SLE) (Ricklin et al., 2010; Holers, 2014). Conversely, deficiencies in the complement regulatory proteins DAF, MCP, and factor H lead to paroxysmal nocturnal hemoglobinuria and atypical hemolytic uremic syndrome, conditions in which complement attacks and destroys red blood cells and endothelial cells, respectively. Moreover, complement activation has been implicated in the progression of rheumatoid arthritis and Alzheimer's disease, driven by, respectively, recognition of immune complexes in the joints and amyloid deposits in the brain. Interestingly, it was demonstrated recently that complement gene variants also control the incidence of disorders between males and females (Kamitaki et al., 2020). It was shown that higher levels of C4 and C3 in men are correlated to their higher risk of developing schizophrenia, whereas the lower levels of these proteins in women are correlated to their substantial predisposition to develop SLE. Likewise, a number of treatments targeting complement-mediated diseases have been developed and are currently undergoing clinical trials (Ricklin et al., 2019). Complement inhibitors are being

evaluated in a variety of kidney diseases (Zipfel et al., 2019), brain injury and neurodegenerative disorders (Brennan et al., 2016), rheumatic diseases (SLE and rheumatoid arthritis) (Trouw et al., 2017), and transplantation (Biglarnia et al., 2018; Thorgersen et al., 2019). Notably, Eculizumab and Ravulizumab (anti-C5 monoclonal antibodies), CCX168 (C5aR receptor antagonist), purified/recombinant C1-INH, and AMY-101 (C3 cleavage inhibitor) have undergone successful phase II/III trials for several diseases. For an extensive review on complement inhibitors in clinical trials see (Mastellos et al., 2019).

Although complement is a self-sustaining cascade with effector functions, the biological effects of complement depend largely on complement receptors. Complement receptors are functionally and structurally diverse, which goes along with their varied roles in leukocyte activation, recruitment, adhesion and phagocytosis. This article aims to review the plethora of information on the role of complement receptors in these functions, with focus on receptor expression, structure and ligand recognition, and connections to effector functions in leukocytes and human disease.

ROLE OF COMPLEMENT RECEPTORS IN LEUKOCYTE RECRUITMENT

Acute inflammation is a reaction of the host to tissue damage or infection by microorganisms. The inflammatory response is usually beneficial, as it will try to resolve this pathological condition by neutralizing damaging agents so that homeostasis can be restored. Due to recognition of pathogen-associated molecular patterns (PAMPs) or damage-associated molecular patterns (DAMPs), pro-inflammatory chemical mediators will be produced and released by tissue-resident cells at the inflammatory site. These mediators including cytokines, chemokines, histamine, prostaglandins and leukotrienes will not only provoke the classical inflammatory symptoms of erythema, heat, pain, and edema but also leukocyte chemotaxis and extravasation into the surrounding inflamed tissue. Once the leukocytes have arrived at the inflammatory site, they can neutralize the inflammatory trigger [by phagocytosis, production of reactive oxygen species (ROS), degranulation, etc.], hence stressing the importance of the leukocyte recruitment process (Medzhitov, 2008). In this section of the review, we will specifically focus on the role of complement receptors in this recruitment process. First, we will focus on the complement anaphylatoxins and their receptors, followed by the role of integrins in leukocyte adhesion and extravasation into the inflamed tissue.

Complement Anaphylatoxins

Complement fragments C3a and C5a are small anaphylatoxins, mediating pro-inflammatory effects by binding to their respective G protein-coupled complement receptors C3aR and C5aR. Both human C3a (1–77 amino acids) and C5a (1–74 amino acids) are structurally composed of a core of four α-helices stabilized by three disulfide bonds and connected by loop segments (**Figure 2**) (Huber et al., 1980; Zuiderweg et al., 1989; Zhang et al., 1997). C-terminally in C3a, there is a flexible, cationic, irregular structure (Hugli, 1975; Huber et al., 1980) from which the five final C-terminal amino acids, LGLAR, form the active site of C3a. More specifically, the hydrophobic side chains of leucine-73 and leucine-75 and the guanidinium group of arginine-77 are key in the active site (Caporale et al., 1980). In C5a, the α-helical bundle core is connected with a small loop to the five final C-terminal amino acids, that adopt an α-helical conformation (Zhang et al., 1997). Interestingly, and in contrast to C3a, C5a contains a complex carbohydrate chain N-linked to asparagine-64 (Fernandez and Hugli, 1978). The activity of C3a and C5a is tightly controlled; Carboxypeptidase-N cleaves the carboxy-terminal arginine from both C3a and C5a in the bloodstream, reducing their biological activity 10-100 fold [reviewed in (Matthews et al., 2004)]. It is noteworthy that complement fragment C4a is also considered an anaphylatoxin. Although structurally similar to C3a and C5a (Moon et al., 1981), it lacks an identified complement receptor and its functional capacities are poorly characterized (Barnum, 2015). Recently, it was shown that C4a can act as a ligand for protease-activated receptor (PAR)1 and PAR4, affecting endothelial permeability. However, no role for C4a in direct leukocyte chemotaxis has been described (Wang et al., 2017).

C3aR

Receptor characterization

C3aR is a cell surface complement receptor part of the GPCR family, first cloned by Ames et al. (1996) and Crass et al. (1996). Its gene *C3AR*, only comprising one exon located on chromosome 12p13 (Paral et al., 1998), shares 37% nucleotide identity throughout the coding regions with C5aR. C3aR is not a classical GPCR as it has an unusually large second extracellular loop (∼172 amino acids) between transmembrane domains 4 and 5 (**Figure 2**) (Ames et al., 1996). Deletion mutagenesis studies showed that multiple aspartate residues in the loop, adjacent to the transmembrane domains, are essential for C3a binding and the following downstream mobilization of intracellular Ca^{2+} (Ames et al., 1996; Chao et al., 1999). Indeed, they provide a secondary interaction site through electrostatic interaction with cationic residues in the C-terminal helical region of C3a (Hugli, 1975; Chao et al., 1999). The primary ligand effector binding site in C3aR, identified to be mainly formed by charged residues in a cluster of transmembrane helices (Sun et al., 1999), is engaged by the active site of C3a being the C-terminal sequence LGLAR (Caporale et al., 1980; Chao et al., 1999). Interestingly, the natural C3a catabolite C3a(desArg) has no binding affinity and cannot activate C3aR (Wilken et al., 1999).

Expression and function in leukocyte recruitment

The transcript of C3aR is widely expressed in peripheral tissues such as the lung, spleen, ovary, placenta, small intestine, heart, peripheral blood leukocytes and in the central nervous system (Ames et al., 1996). C3aR expression could be identified on neutrophils, basophils, eosinophils, monocytes and mast cells through flow cytometry, northern blotting, calcium release and binding assays (**Table 1**) (Hartmann et al., 1997; Martin et al., 1997; Zwirner et al., 1999). It was shown however that C3aR

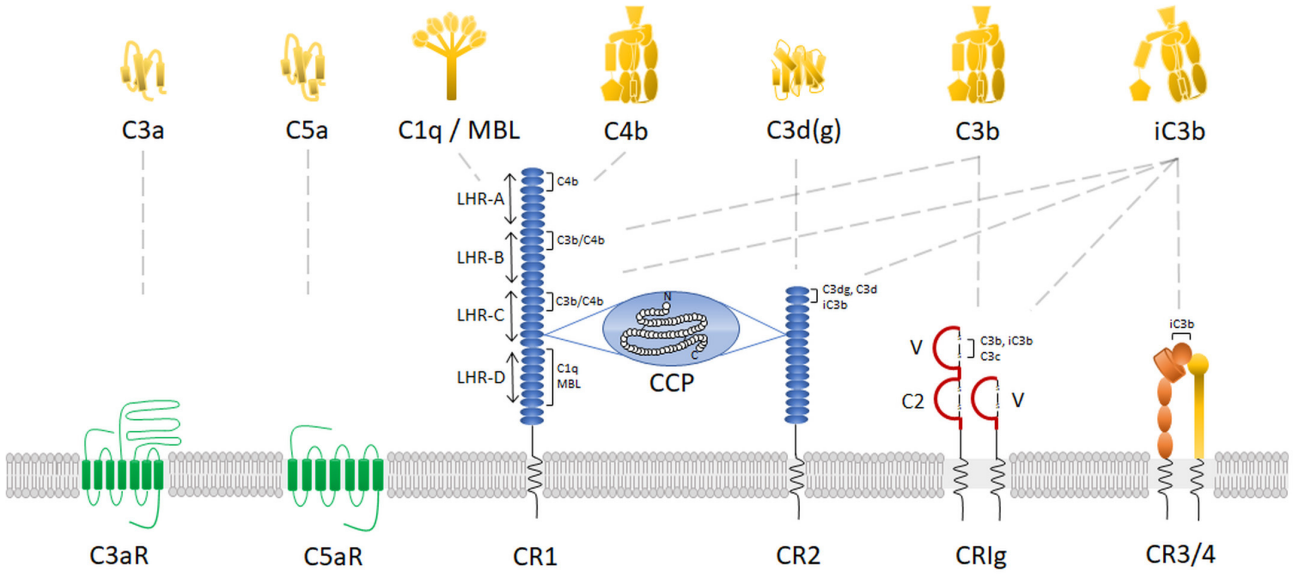

FIGURE 2 | Complement receptors and their main ligands. Schematic representation of human complement receptors on the plasma membrane with their corresponding complement protein ligands. For CR1, CR2, CRIg, and CR3/4, the binding areas for each specific ligand are indicated. In addition, for CR1, the receptor domains are identified at the left side of the receptor. CCP, complement control protein repeats; LHR, long homologous repeats; MBL, mannose-binding lectin.

expression on monocytes and neutrophils is about 6 to 20 times lower than C5aR expression, respectively (Zwirner et al., 1999). Receptor expression has not been demonstrated on unchallenged B-lymphocytes and T-lymphocytes (Martin et al., 1997; Zwirner et al., 1999) but expression has been shown on activated T-lymphocytes (Werfel et al., 2000) and on tonsil-derived B-lymphocytes (Fischer and Hugli, 1997). Besides leukocytes, expression of C3aR on bronchial epithelial and smooth muscle cells of the lung has been shown (Drouin et al., 2001). In the central nervous system, C3aR is expressed in astrocytes and microglia during inflammation (Gasque et al., 1998). Moreover, constitutive expression has also been shown on neurons, which suggests a role in physiological conditions (Davoust et al., 1999). In the rat, it was already shown that C3aR plays a role in the development of the cerebellum (Bénard et al., 2008).

C3aR activation is associated with G protein-coupled downstream signaling and an increase in intracellular Ca^{2+}, which is blocked by pertussis toxin (Norgauer et al., 1993; Elsner et al., 1994). Activation of the receptor induces dissociation of the Gα (primarily $G\alpha_i$) subunit and the $G_{\beta\gamma}$ subunit. $G\alpha_i$ inhibits adenylyl cyclase, resulting in a reduced intracellular cyclic adenosine monophosphate (cAMP) concentration. $G_{\beta\gamma}$ activates phospholipase Cβ (PLCβ), leading to increased intracellular Ca^{2+} and protein kinase C (PKC) activation. In addition, it activates phosphoinositide 3-kinase γ (PI3Kγ) resulting in activation of extracellular signal–regulated kinases (ERKs) and phosphokinase B (Akt) (Futosi et al., 2013). This signaling cascade, has been shown to induce chemotaxis of mast cells (Hartmann et al., 1997) and eosinophils (Daffern et al., 1995). Induction of macrophage chemotaxis by C3a was first shown in the mouse macrophage cell line J774 (Zwirner et al., 1998). Activation of C3aR does not induce direct neutrophil chemotaxis (Fernandez et al., 1978; Elsner et al., 1994; Daffern et al., 1995). However, C3a was able to induce ROS production in neutrophils (Elsner et al., 1994) and C3aR activation also induced formation of neutrophil extracellular traps (NETosis), leading to hypercoagulation and tumor-promoting effects *in vivo* (Guglietta et al., 2016). Wu et al. reported a role for C3aR as inhibitor of neutrophil mobilization and protection from intestinal ischemia-reperfusion injury. Indeed, $C3aR^{-/-}$ mice had an augmented number of tissue-infiltrating and circulating neutrophils, which were associated to worsening of intestinal damage, whereas stimulation of C3aR in WT mice reduced neutrophil mobilization and consequent intestinal injury (Wu et al., 2013). An interesting study showed a role for C3a in the retention of hematopoietic stem cells in the bone marrow. C3a-C3aR interaction can counteract mobilization of hematopoietic stem cells by increasing their response to stromal-derived factor 1 (SDF-1/CXCL12), of which the expression decreases in the bone marrow during mobilization (Reca et al., 2003; Ratajczak et al., 2004). In the central nervous system, it was shown using $C3^{-/-}$ and $C3aR^{-/-}$ mice that C3a plays a role in cerebral endothelial activation (by upregulation of adhesion molecules) and leukocyte recruitment to the LPS-inflamed brain (Wu et al., 2016). Also, a specific link between C3a and depression was found. In mice, it was shown that C3a induces monocyte infiltration into the prefrontal cortex after exposure to chronic stress, which is specifically associated with depressive-like behavior (Crider et al., 2018). Interestingly, C3a-C3aR interaction promotes monocyte recruitment into inflamed skeletal muscle. There, it plays an essential role during regeneration of skeletal muscle, as this regeneration can be impaired by C3a inactivation or C3aR deletion (Zhang et al.,

TABLE 1 | Expression, function and main ligands of complement receptors.

Receptor	Alternative name	Main ligands	Main leukocyte expression	Main functions
C3aR	/	C3a	Neutrophils Basophils Eosinophils Monocytes Mast cells Activated T-lymphocytes Tonsil-derived B-lymphocytes	Chemotaxis of mast cells, eosinophils and monocytes/macrophages (Daffern et al., 1995; Hartmann et al., 1997; Zwirner et al., 1998) Induction of ROS production in neutrophils (Elsner et al., 1994) No (or inhibition of) chemotaxis of neutrophils (Daffern et al., 1995; Wu et al., 2013) Retention of hematopoietic stem cells in the bone marrow (Reca et al., 2003; Ratajczak et al., 2004) Leukocyte recruitment to the brain (Wu et al., 2016; Crider et al., 2018) Regeneration of skeletal muscle and hepatic tissue (Strey et al., 2003; Markiewski et al., 2004; Zhang et al., 2017)
C5aR	C5aR1	C5a	Neutrophils Monocytes/macrophages Dendritic cells T-lymphocytes B-lymphocytes Mast cells	Chemotaxis of neutrophils, monocytes, dendritic cells, T- and B-lymphocytes (Morgan et al., 1993; Sozzani et al., 1995; Nataf et al., 1999; Ottonello et al., 1999) Degranulation of neutrophils (Morgan et al., 1993) Induction of ROS production in neutrophils (Sacks et al., 1978) Cytokine production in monocytes (Morgan et al., 1993) Mast cell histamine release (Johnson et al., 1975; Füreder et al., 1995) Liver regeneration (Mastellos et al., 2001; Daveau et al., 2004; Marshall et al., 2014)
C5L2	C5aR2	C5a	Immature dendritic cells Granulocytes (Myeloid immune cells) T cell subsets	Immune suppressing and immune activating functions due to regulation of C5aR activation and signaling (Li et al., 2019)
CR1	CD35 C3b/C4b receptor	C1q C3b C4b iC3b MBL	Erythrocytes Monocytes/macrophages Granulocytes B-lymphocytes CD4+ T-lymphocytes FDCs Glomerular podocytes	Immune regulatory role (Iida and Nussenzweig, 1981; Masaki et al., 1992) Immune-complex clearance (Cornacoff et al., 1983) Phagocytosis (Fällman et al., 1993)
CRIg	VSIG4/B7 family-related protein Z39Ig	C3b C3c iC3b	Tissue-resident macrophages MDDCs	Complement-mediated phagocytosis (Wiesmann et al., 2006) Immune regulatory role (Vogt et al., 2006; Munawara et al., 2019)
CR2	CD21	iC3b C3dg C3d gp350/220 (EBV) CD23 Interferon-alpha	B-lymphocytes FDCs T-lymphocytes Epithelial cells	Lowering B-lymphocyte activation threshold (Carter and Fearon, 1992) Retention of C3-opsonized antigens (Reynes et al., 1985) Promotion of B-lymphocyte class switching and IgE production (Aubry et al., 1992) EBV cell entry (Tanner et al., 1987)
CR3	Mac-1 CD11b/CD18 Integrin $\alpha_M\beta_2$	ICAM-1 ICAM-2 Fibrinogen iC3b Collagen Factor X NIF	Neutrophils Monocytes/macrophages Dendritic cells NK cells Activated lymphocytes	Leukocyte extravasation (Dustin and Springer, 1988; Meerschaert and Furie, 1995; Ding et al., 1999; Phillipson et al., 2006) Phagocytosis (Beller et al., 1982)
CR4	p150,95 CD11c/CD18 Integrin $\alpha_X\beta_2$	ICAM-1 ICAM-2 Fibrinogen iC3b Collagen Factor X NIF	Neutrophils Monocytes/macrophages Dendritic cells NK cells Activated lymphocytes	Adhesion to fibrinogen (Sándor et al., 2016) Phagocytosis (Keizer et al., 1987)

EBV, Epstein-Barr virus; FDCs, follicular dendritic cells; ICAM, intercellular adhesion molecule; Mac-1, macrophage-1 antigen; MBL, mannose-binding lectin; MDDCs, monocyte-derived dendritic cells; NIF, neutrophil inhibitory factor; NK, natural killer; ROS, reactive oxygen species; VSIG4, V-set and Ig domain 4.

2017). C3a is also involved in the regeneration of hepatic tissue after injury. After partial hepatectomy in $C3^{-/-}$ mice, normal liver regeneration was impaired, which was associated with clinical deterioration and higher mortality compared to WT mice (Strey et al., 2003). Moreover, liver regeneration was impaired after a toxic challenge in $C3^{-/-}$ mice. This could however be reversed by administration of C3a and activation of C3aR (Markiewski et al., 2004).

C5aR

Receptor characterization

C5aR (C5aR1 or CD88) is a cell surface GPCR first discovered in 1991 (**Figure 2**) (Gerard and Gerard, 1991). The gene *C5AR1* comprises two exons and is located on chromosome 19, band position q13.3 (Gerard et al., 1993). C5aR is bound by its ligand complement fragment C5a according to a two-site binding model (Siciliano et al., 1994). The extracellular N-terminal portion of C5aR [with required aspartic acids (DeMartino et al., 1994) and sulfations of N-terminal tyrosines (Farzan et al., 2001)] is essential in the formation of the docking site for the core of C5a via electrostatic interactions (Mery and Boulay, 1994; Siciliano et al., 1994). Interaction of C5a with the N-terminal part of the receptor is required for high affinity binding and full activation of the receptor (DeMartino et al., 1994). However, just as in the C3a-C3aR interaction, the primary ligand binding site is located between the transmembrane helices at the base of the C5aR extracellular loops. This binding site interacts with the C-terminal part of C5a (Siciliano et al., 1994). In line with this, C-terminal peptide fragments of C5a are sufficient to activate C5aR, even if the receptor is N-terminally truncated. It is believed that the interaction between C5a and the N-terminal part of C5aR is essential to induce a conformational change in C5a, which allows its C-terminal part to interact with and to activate the receptor (DeMartino et al., 1994). Interestingly, the highest residue homology with C3aR is found in the transmembrane domains and in the second intracellular loop (Ames et al., 1996). Later on, it was shown via receptor mutagenesis that arginine-206 located in the 5th transmembrane helix of C5aR is essential for high-affinity binding to C5a (Raffetseder et al., 1996).

Expression and function in leukocyte recruitment

The C5aR transcript is co-expressed with C3aR in several peripheral tissues such as the lung, spleen, placenta and the central nervous system. C5aR is expressed to a higher extent than C3aR in peripheral blood leukocytes and the heart (**Table 1**) (Ames et al., 1996). More specifically, its expression was described on human polymorphonuclear leukocytes in Chenoweth and Hugli (1978) and on murine macrophages in Chenoweth et al. (1982). Nevertheless, induction of directed chemotaxis of polymorphonuclear leukocytes by C5a had already been shown *in vitro* and in simulated *in vivo* conditions before the receptor was known (Shin et al., 1968; Fernandez et al., 1978). Later on, with the use of polyclonal antibodies directed against the extracellular N-terminal part of C5aR, inhibition of C5a-mediated neutrophil chemotaxis and -degranulation, and inhibition of cytokine production by monocytes was demonstrated (Morgan et al., 1993). Furthermore, C5a can induce production of ROS in granulocytes, which resulted in endothelial cell cytotoxicity *in vitro* (Sacks et al., 1978). Moreover, C5a-C5aR interaction plays a specific role in neutrophil and monocyte migration to the synovium of rheumatoid and psoriatic arthritis patients (Hornum et al., 2017). In a mouse model of autoantibody-induced inflammatory arthritis, activation of C5aR on neutrophils in the joint vasculature perpetuates their own recruitment. Indeed, C5a production due to complement opsonization on immune complexes in the joints, results in release of the chemotactic lipid leukotriene B4 (LTB4) from arrested neutrophils which promote further neutrophil migration to the interstitium (Sadik et al., 2018). Functional expression of C5aR has also been shown on dendritic cells (Sozzani et al., 1995) and skin mast cells. Expression of C5aR was specifically associated with histamine release after C5a stimulation (Johnson et al., 1975; Füreder et al., 1995). Conversely, expression of C5aR on human T-lymphocytes was relatively low, but T-lymphocytes are responsive to a C5a gradient when receptor expression is increased by phytohemagglutinin stimulation (Nataf et al., 1999). Ottonello et al. also showed low expression of C5aR on naive and memory B-lymphocytes, which was sufficient to promote a response to recombinant C5a *in vitro* (Ottonello et al., 1999). However, on murine (un)stimulated T- or B-lymphocytes no expression of C5aR was observed, in contrast to granulocytes and macrophages (Soruri et al., 2003).

Besides leukocytes, C5aR is expressed in several cell types of the lung (lung vascular smooth muscle, endothelium, bronchial and alveolar epithelium) and in liver parenchymal cells (Haviland et al., 1995; Drouin et al., 2001). Together with C3a, C5a-C5aR interaction is required in liver regeneration. Indeed, $C5^{-/-}$ mice display abnormal liver regeneration after partial hepatectomy or toxic injury (Mastellos et al., 2001; Strey et al., 2003). Moreover, mice deficient in both C3 and C5 have an even more severe defect in regeneration, which can be partially reversed by reconstitution with C3a or C5a. Administration of both anaphylatoxins together led to a better recovery, suggesting that C3a and C5a act cooperatively in the early priming stages of hepatocyte regeneration. Furthermore, in a rat model of partial hepatectomy, C5aR was upregulated on hepatocytes promoting their regrowth after injury (Daveau et al., 2004). Blockade of C5aR reduces the intrahepatic release of interleukin-6 (IL-6) and tumor necrosis factor alpha (TNF-α). However, in contrast to their inflammatory roles in most tissues, these cytokines are essential for hepatocytes to reenter the cell cycle and initiate liver regeneration via activation of the transcription factors nuclear factor kappa-light-chain-enhancer of activated B cells (NF-κB) and signal transducer and activator of transcription 3 (STAT-3) (Strey et al., 2003). Interestingly, the site-targeted murine complement inhibitor CR2-CD59 (which specifically inhibits the assembly of the MAC) is able to promote hepatocyte proliferation, and so, liver regeneration after hepatectomy. CR2-CD59 can increase the intrahepatic IL-6 and TNF-α levels, resulting in STAT-3 and Akt activation required for liver regeneration (Marshall et al., 2014).

C5L2

Human C5a receptor-like 2 (C5L2 or C5aR2) is a seven-transmembrane spanning receptor related to the C5a and C3a receptor, first discovered in 2000 in immature dendritic cells and granulocytes (Ohno et al., 2000). Expression was also described in the bone marrow, spleen, lung, in most myeloid immune cells and T cell subsets, and it is present both intracellularly and on the cell surface (Li et al., 2019). C5L2 is able to bind C5a and hence functions as a second C5a receptor (Okinaga et al., 2003). However, it lacks the ability to induce downstream signaling due to an amino acid (R→L) replacement in the DRY motif. This highly conserved motif, located at the end of the third transmembrane segment, is necessary for GPCR interaction with G proteins. As a consequence, C5L2 is unable to induce downstream signaling and calcium increase, and it may function as a decoy receptor (Okinaga et al., 2003). Several studies however reported C5L2 as an important regulator of C5aR activation and downstream signaling. Bamberg et al. indicated that C5L2 might function as a negative modulator of ERK1/2 signal transduction through modulation of β-arrestin after C5aR activation by C5a. Inhibition of C5L2 resulted in increased C5a-mediated chemotaxis, but no alterations in C5a-induced Ca^{2+}-responses (Bamberg et al., 2010). It was also shown that C5L2 can physically interact with C5aR, forming heterodimers (Croker et al., 2013). Thus, C5a stimulation may trigger C5aR–C5L2 heterodimerization and β-arrestin recruitment, facilitating C5aR internalization and downregulating C5aR-mediated ERK signaling (Croker et al., 2014; Li et al., 2019). In contrast, it has been shown that C5L2 also exerts stimulatory functions: On the endothelium, it promotes C5a translocation into the blood vessel lumen, mediating neutrophil arrest through C5aR activation in a murine arthritis model (Miyabe et al., 2019). More elaborated information about the current knowledge of this controversial receptor and its role in pathophysiology was recently reviewed by Li et al. (2019).

β_2-Integrin Family Complement Receptors CR3 and CR4

Receptor Characterization

In contrast to the chemotactic receptors C3aR and C5aR, β2-integrins are heterodimeric cell surface adhesion receptors that play a crucial role in cell adhesion, migration and communication. They are involved in cell-cell and cell-extracellular matrix interactions and have the unique capacity to mediate bidirectional transmission of mechanical and biochemical signals across the membrane. Structurally, integrins are characterized by a non-covalent association of two type I membrane glycoproteins, the α and β subunit, consisting of a small cytoplasmic tail (<75 amino acids, except for the β4 subunit), a transmembrane region and a large extracellular domain containing ligand-binding sites (>100 kDa for α subunits and >75 kDa for β subunits) (Hynes, 1992). The subunits form together an extracellular domain composed of a N-terminal globular ligand-binding head and a C-terminal tailpiece, formed by two long "legs" or "stalks," connecting with the transmembrane and short cytoplasmic domains of each subunit (Nermut et al., 1988) (**Figure 2**). The N-terminal region of the α-domain contains seven segments of about 60 amino acids, which fold into a seven-bladed β-propeller domain that forms the globular head region of the receptor. About half of the integrins, more specifically the leukocyte β_2-integrins and the integrin collagen receptors, have an approximately 200 amino acid insertion in between the second and third beta sheet that is known as the inserted (I) domain. This domain contains a metal ion-dependent adhesion site (MIDAS) for binding of divalent cations required for ligand binding (Diamond et al., 1993; Michishita et al., 1993; Lee et al., 1995; Tuckwell et al., 1995). The leukocyte β_2-integrin family includes four members that share a common β_2-subunit (CD18) linked to one of four α-chains: $\alpha L\beta_2$-integrin [also referred to as lymphocyte function-associated antigen 1 (LFA-1) or CD11a/CD18], $\alpha M\beta_2$-integrin [macrophage-1 antigen (Mac-1), CR3 or CD11b/CD18], $\alpha X\beta_2$-integrin [p150,95; CR4 or CD11c/CD18] and $\alpha D\beta_2$-integrin [CD11d/CD18] (Springer et al., 1979; Kürzinger et al., 1981; Sanchez-Madrid et al., 1983; Van der Vieren et al., 1995). Within the β2-integrin family, there are two complement receptors: CR3 and CR4 (**Table 1**).

Expression and Function in Leukocyte Recruitment

Leukocyte recruitment to tissues is an essential step in the inflammatory response that requires the binding and extravasation of leukocytes in the vasculature. In the muscle and intestines, it starts with rolling of the leukocyte over the activated endothelium, followed by leukocyte activation and firm adhesion, diapedesis through the endothelial layer and further migration into the tissue matrix (**Figure 3**) (Muller, 2013). Integrins play a crucial role in this complex and tightly controlled process. In steady state, passively moving blood leukocytes express bent, non-activated "resting" integrins. In this conformation, the ligand-binding head domain of the integrin is folded over the tailpiece, moving the ligand binding site close to the C-terminal, membrane-proximal end of the tailpiece ("legs" of the integrin). This is an unfavorable orientation for ligand binding and consequently bent integrins have only low affinity for their endothelial ligands, including the immunoglobulin superfamily members intercellular adhesion molecule 1 and 2 (ICAM-1 and -2) and vascular cell adhesion molecule 1 (VCAM-1) (Xiong et al., 2001, 2002; Takagi et al., 2002; Chen et al., 2010a). In response to microbial infection or tissue damage, release of pro-inflammatory mediators increases the blood flow and the expression of endothelial adhesion molecules. This allows leukocytes to increase rolling along the luminal side of the activated endothelium, mediated by weak and transient selectin-glycoprotein interactions (McEver, 2002). These interactions can already change the integrin conformation to a more extended one which supports slower leukocyte rolling, as shown for the integrin LFA-1 in neutrophils (Kuwano et al., 2010; Stadtmann et al., 2013). Indeed, binding of P-selectin glycoprotein ligand-1 (PSGL-1) to endothelial selectins leads to activation of Src kinases and Ras-related protein 1 (Rap-1) [see below], supporting slow rolling (Yago et al., 2018). In monocytes, interaction between the β1-integrin very late antigen-4 (VLA-4; integrin α4β1) and

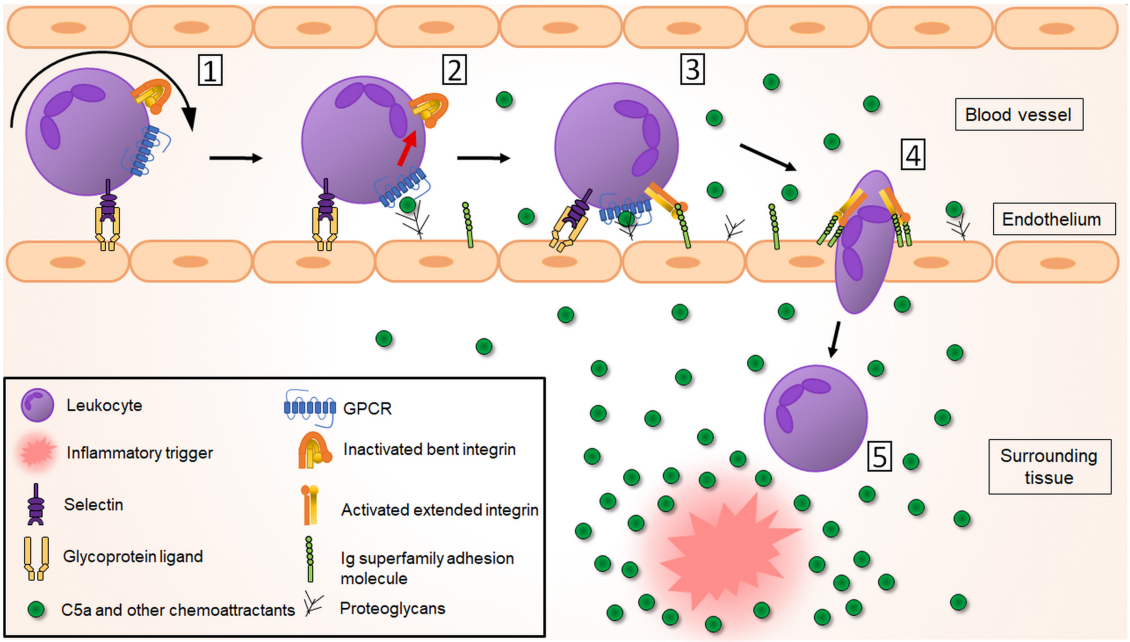

FIGURE 3 | Complement receptors play a crucial role in leukocyte recruitment to the inflammatory site. [1] In response to an inflammatory trigger (infection/tissue damage), leukocytes first roll over the activated endothelium through weak selectin-glycoprotein interactions (for clarity only leukocyte selectins and endothelial glycoproteins are shown here). [2] This allows interaction of leukocyte GPCRs (including C5aR but also other chemoattractant receptors) with chemoattractant molecules, produced by tissue-resident cells in response to and forming a chemotactic gradient toward the inflammatory trigger. This results in inside-out activation of integrins, changing their global conformation from a bent non-activated conformation to an extended, activated conformation with higher affinity for the integrin ligands ICAM-1, ICAM-2 and VCAM-1, which belong to the immunoglobulin (Ig) superfamily adhesion molecules [3]. This leads to a tight adhesion and arrest of the leukocytes to the endothelium. After integrin-mediated crawling to an optimal emigration spot directed by the chemotactic gradient, a transmigratory cup is formed and leukocytes transmigrate [4] through the endothelial barrier and the basement membrane into the surrounding tissue, where their migration will be guided further to the inflammatory site directed by the chemoattractant gradient [5].

VCAM-1 supports transition to slow rolling followed by firm adhesion (Huo et al., 2000).

Due to slow rolling, leukocytes can be activated through interaction with chemokines, C5a, platelet-activating factor (PAF) or LTB4, which are present in the endothelial vicinity or found bound to proteoglycans on the endothelial surface (Middleton et al., 1997; Lefort and Ley, 2012; Miyabe et al., 2017). Leukocyte activation then induces integrin activation via inside-out signaling (also called priming), in which intracellular signals initiated by the GPCR activation are transduced to the cytoplasmic domain and further to the extracellular part of the integrin. A global conformational change in the integrin structure (via a switchblade-like opening) will result in less than a second in an extended, activated, higher affinity state of the integrin. The inside-out signaling process was recently reviewed by Bednarczyk et al. (2020). In short, GPCR-mediated activation of the small GTPase Rap-1 causes it to colocalize with the effector Rap1-GTP-interaction adapter molecule (RIAM). RIAM recruits the cytoskeletal protein talin, which is required for the unbending of the two integrin subunits. The N-terminal globular head of talin contains a four-point-one, ezrin, radixin, moesin (FERM) domain that interacts with the conserved NPXY motifs in the β cytoplasmic integrin domain, thereby disrupting the α and β tail salt bridge to generate the high affinity conformation which enables ligand binding (Calderwood et al., 2002; Campbell and Ginsberg, 2004). Also, the adapter protein Kindlin-3 is able to bind to NPXY motifs and contributes to the full integrin activation (Moser et al., 2008). Eventually, the extended, higher affinity state of the integrin results in a firm adhesion and arrest of the leukocytes to the endothelium (Takagi et al., 2002; Xiao et al., 2004; Nishida et al., 2006). More details on structural rearrangements of integrins is provided by Luo et al. (2007). Due to binding of ligands to the integrins and consequent outside-in signaling, the conformation of the integrin can again slightly change resulting in even higher affinity, further strengthening and stabilizing leukocyte adhesion (Takagi et al., 2002) which has been shown for the interaction between LFA-1 and ICAM-1 (CD54) (Chen et al., 2010b). Moreover, Src kinases are involved in sustaining the adhesion of neutrophils through outside-in signaling. Indeed, lack of this outside-in signaling leads to rapid detachment of adherent neutrophils from the endothelium (Giagulli et al., 2006).

Once leukocytes arrest, intraluminal crawling is performed toward optimal emigration sites nearby endothelial cell borders (Massena et al., 2010). In neutrophils, it was shown using intravital microscopy that this crawling mechanism is dependent

on interaction between CR3 and endothelial ICAM-1 (Diamond et al., 1991; Phillipson et al., 2006) and ICAM-2 (Halai et al., 2014). Of note, binding of LFA-1 to ICAM-1 and VLA-4 to VCAM-1 has also been shown to contribute to neutrophil adhesion (Staunton et al., 1990; Reinhardt et al., 1997; Ding et al., 1999; Phillipson et al., 2006). In monocytes, however, the primary integrin involved in monocyte adhesion and arrest is VLA-4, due to its interaction with VCAM-1 (Hyduk et al., 2007), with a secondary role for LFA-1 and CR3 (Meerschaert and Furie, 1995). In addition, in monocytes both LFA-1 (Auffray et al., 2007) and CR3 are involved in crawling via interactions with ICAM-1 and ICAM-2 (Schenkel et al., 2004; Sumagin et al., 2010). In lymphocytes, LFA-1 binding to ICAM-1 on endothelial cells is required for lymphocyte adhesion (Dustin and Springer, 1988), but on stimulated endothelium, also interaction between VLA-4 and VCAM-1 was observed (Elices et al., 1990; Vennegoor et al., 1992). The actual crossing of leukocytes through the endothelial layer (diapedesis) into the tissue happens via a transcellular or a paracellular route (Carman and Springer, 2004). Integrins are also involved in this process. To initiate diapedesis, a "transmigratory cup" on the endothelial surface is formed by redistribution of leukocyte integrins LFA-1, CR3 and VLA-4. They colocalize with clusters of ICAM-1 and VCAM-1 on endothelial microvilli-like projections at the junctional interface between the adherent leukocyte and the endothelium (Carman and Springer, 2004; Shaw et al., 2004). In neutrophils, also ICAM-2 seems to play a role as genetic deletion or blockade of ICAM-2 partially inhibits the neutrophil transmigration process (Huang et al., 2006). ICAM-2 mediates neutrophil transmigration in a stimulus-dependent manner, alongside other adhesion molecules (Woodfin et al., 2009). For more details on transendothelial migration see (Filippi, 2019) and (Gerhardt and Ley, 2015).

Once beyond the endothelial layer, leukocytes still have to cross a discontinuous layer of pericytes, which are long cells surrounding the endothelium and embedded within the basement membrane. The interaction of CR3 and LFA-1 with ICAM-1 on the pericytes is necessary for abluminal crawling of neutrophils, guiding them to gaps (exit points) into the interstitium (Proebstl et al., 2012). This seems to happen specifically at regions poor in extracellular matrix proteins, such as sites low on laminins and collagen IV (Wang et al., 2006). A slightly different process is performed by monocytes. Monocytes were shown to be more deformable, so they do not need to remodel the basement membrane to enlarge these low expression regions, as neutrophils do (Voisin et al., 2009). Using intravital imaging, it has been shown that individual neutrophils, once inside the locally inflamed tissue, can show highly coordinated chemotaxis forming neutrophil clusters ("swarms"). This migration process in extravascular spaces was shown in several mouse models and tissues. "Neutrophil swarming" occurs during infection with bacteria, fungi or parasites, as well as during sterile inflammation (Kienle and Lämmermann, 2016; Lämmermann, 2016). Neutrophil swarming can be of a transient or persistent nature (Chtanova et al., 2008) and its phenotype is influenced by the size of the initial tissue damage, the presence of pathogens, the number of recruited neutrophils and induction of secondary cell death (Kienle and Lämmermann, 2016). Long-distance migration in the neutrophil "swarms" is integrin independent (Lämmermann et al., 2008), but integrin adhesive forces are required to maintain the dense neutrophil clusters. These allow neutrophils to accumulate in the wound center, excluding collagen fibers and making a collagen-free zone. Based on knock out of neutrophil integrins, it was identified that both LFA-1 and CR3 are important to maintain the cell adhesion in the neutrophil "swarm" (Lämmermann et al., 2013).

The role of CR4 (CD11c/CD18) in cellular adhesion is less well characterized. CR4 is closely related to CR3: the entire CR4 α-chain (CD11c) shares 63% sequence homology to the CR3 α-chain (CD11b) (Corbi et al., 1988). Both receptors recognize similar ligands such as iC3b, fibrinogen and ICAMs and so it was believed they also mediate similar functions. However, expression of CD11c is dominating in monocyte-derived macrophages (MDMs) and monocyte-derived dendritic cells (MDDCs) where the ratio with CD11b expression is close to 1:1. In circulating monocytes, in contrast, CD11c expression is about 7 times lower than CD11b. Functionally, it was shown that CR4 is the main receptor for strong adhesion to the extracellular matrix component fibrinogen. Although CD11b can also bind to fibrinogen, it was shown that blockade of CD11c strongly reduces adhesion strength whereas blockade of CD11b enhances the attachment of MDDCs and MDMs to fibrinogen. Thus, CD11b can have a competitive, negative role in adhesion of MDDCs and MDMs to fibrinogen (Sándor et al., 2016).

Defects in the synthesis of the common β-chain (CD18) of integrins LFA-1, CR3 or CR4 lead to the rare autosomal-recessive disease leukocyte adhesion deficiency (LAD)-I, characterized by absence or reduced expression of these integrins on leukocytes. As a result, patients have deficiencies in leukocyte adhesion and abnormalities in several adherence-dependent functions like chemotaxis and aggregation. LAD patients are susceptible to recurrent bacterial infections and impaired wound healing, amongst other symptoms, and often die during childhood (Anderson and Springer, 1987; Hogg et al., 1999). A LAD-I-like phenotype is also seen in LAD-III, another autosomal-recessive disease characterized by mutations in Kindlin-3, which is required in the inside-out signaling and activation of β2-integrins (Stepensky et al., 2015). However, LAD-II which yields similar immunodeficiency, is not directly related to integrin functions. Instead, in LAD-II, mutations in a specific GDP-fucose transporter result in impaired synthesis of selectin glycoprotein ligands, impairing the leukocyte rolling and eventually resulting in impaired leukocyte extravasation (Sturla et al., 2001).

ROLE OF COMPLEMENT RECEPTORS IN PHAGOCYTOSIS

Introduction to Phagocytosis

Phagocytosis is a cellular process characterized by the recognition and ingestion of particles larger than 0.5 μm into a membrane-encased vesicle, the phagosome (Nordenfelt and Tapper, 2011; Flannagan et al., 2012). This process contributes to tissue homeostasis and remodeling, and participates in the host defense as it eliminates microorganisms and foreign substances

(**Figure 4**). Classical phagocytosis is initiated by the interaction of a particle with specific receptors on the surface of professional phagocytes, more specifically, macrophages and neutrophils. Those receptors include non-opsonic phagocytic receptors, such as Dectin-1 and Mincle that directly recognize conserved PAMPs. Moreover, other receptors recognize host-derived opsonins attached to pathogens, such as complement (e.g., CR3) and Fc gamma receptors (FcγRs), which are extensively studied phagocytic receptors for opsonized particles. FcγRs bind the conserved Fc domain of immunoglobulins (Ig), which causes receptor clustering and phosphorylation of immunoreceptor tyrosine-based activation motifs (ITAMs) in the cytoplasmatic tail of the receptor, leading to the recruitment of Syk kinases. This activates various downstream signaling pathways (e.g., ERK, phospholipase D, PKC) mediating cell effector functions such as actin-dependent pseudopod extensions of the plasma membrane around the particle to draw it into the cell (May and Machesky, 2001). In contrast, studies using electron microscopy showed that little to no membrane protrusions were formed during complement-mediated internalization of an opsonized particle, as the particle appeared to "sink" into the cell (Griffin et al., 1975; Kaplan, 1977). The more recent idea, validated by live-cell imaging of the entire phagocytic process, is that actin-based membrane protrusions (pseudopods) are formed that surround iC3b-opsonized beads, a mechanism that could have been previously missed during electron microscopy processing (Hall et al., 2006; Patel and Harrison, 2008; Rotty et al., 2017; Jaumouille et al., 2019). This active, phagocytic cup-mediated internalization of the complement-coated particle has become a consensus in the field, replacing the older particle "sinking" model.

Activation of complement receptors leads to signaling pathways and actin cytoskeleton reorganization in such a way that the membrane completely surrounds the target particle, thereby forming the phagosome. The phagocytic cup formation is primed by integrin inside-out signaling induced by Toll-like receptor (TLR) or GPCR stimulation (Freeman and Grinstein, 2014). Talin recruitment induces the high-affinity, extended integrin conformation that enables ligand binding (Calderwood et al., 2002; Campbell and Ginsberg, 2004). Talin also mediates the mechanical coupling of integrins to actin filaments, as forces arising during phagocytosis expose vinculin binding sites on talin (del Rio et al., 2009). This will promote focal adhesion kinase (FAK)-mediated tyrosine phosphorylation of paxillin together with vinculin binding to talin and actin, which serves as a "molecular clutch" that drives phagocytosis (Jaumouille et al., 2019). In turn, integrin "outside-in" signaling will promote actin reorganization to form plasma membrane protrusions. This formation is driven by the Arp2/3 complex, nucleating actin filaments branches from the sides of pre-existing filaments. The activity of the Arp2/3 complex is indispensable during complement-mediated phagocytosis, since Arp2/3 inhibition

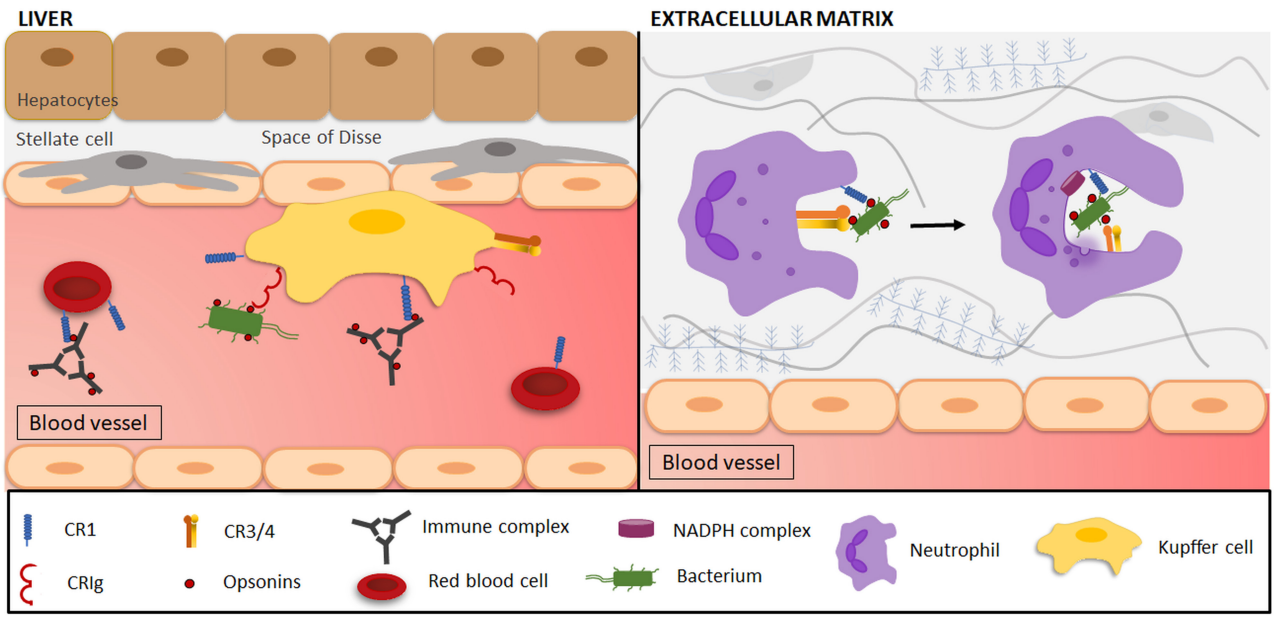

FIGURE 4 | Complement-mediated phagocytosis in the clearance of microorganisms and immune complexes. (Left side) Resident liver macrophages (Kupffer cells/KCs) engulf pathogens, immune complexes and various other particles through interactions with complement receptors. Opsonized (red dots) immune complexes (ICs) are transported to the liver via CR1 on the plasma membrane of circulating red blood cells (RBCs). In the liver, ICs interact with CR1 and scavenger receptors (not shown) on KCs, leading to IC phagocytosis, where after RBCs return to the circulation. Opsonized and free pathogens are recognized by CRIg on KCs and are subsequently engulfed. (Right side) Phagocytes (e.g., neutrophils) are attracted to a site of infection and reach the extracellular matrix by transmigrating across the endothelium. Once there, CR1 on neutrophils will be involved in the attachment of C3-opsonized particles to the cell, after which interaction with CR3 mediates phagocytosis. As the plasma membrane surrounds the target, forming a phagosome, the activation of the nicotinamide adenine dinucleotide phosphate (NADPH) complex and degranulation of neutrophilic granules initiate target degradation.

with CK-666 inhibits phagocytosis (May et al., 2000; Rotty et al., 2017; Jaumouille et al., 2019). This activity depends on the activation of the GTPase Rho in complement phagocytosis, while GTPases Cdc42 and Rac are required in Fc-mediated phagocytosis (Caron and Hall, 1998). Rho recruits and stimulates the formin mDia, which drives actin protrusions to the particle surface and connects the actin cytoskeleton to microtubules (Palazzo et al., 2001). Active Rho also enables actomyosin contractions by activating the Rho kinase (ROCK), responsible for the increased myosin light chain phosphorylation (Olazabal et al., 2002). Syk kinase activity is required for vinculin recruitment and strengthening of force transmission for optimal particle uptake. Once the target particle is internalized, it combines with early endosomes coming from the endoplasmic reticulum and Golgi apparatus to form the early phagosome. The early phagosome is characterized by the presence of Rab5 and EEA1 proteins at the phagosomal membrane, and does not increase in size, as recycling endosomes are removed from the phagosome and trafficked back to the plasma membrane. Upon phagosome maturation, the fusion with late endosomes modifies the now called late phagosome, which is characterized by the presence of Rab7 and the incorporation of additional copies of the vacuolar-type H+-ATPase (V-ATPase). Finally, lysosomes fuse with the late phagosome to become phagolysosomes which have an acidic pH, and contain hydrolytic enzymes and nicotinamide adenine dinucleotide phosphate (NADPH) oxidase to produce ROS that jointly degrade the ingested particle (Allen and Aderem, 1996).

The importance of complement opsonization in phagocytosis has been demonstrated by a number of studies. C3-deficient mice are immunocompromised and susceptible to lethal bacterial infections. Moreover, clearance of bacteria in the bloodstream by Kupffer cells (KCs) (Helmy et al., 2006) and in the lungs by alveolar macrophages (Neupane et al., 2020) is impaired in C3-deficient mice. Other examples include the reduced phagocytic clearance of microorganisms in the presence of serum that has been depleted of complement by heat-inactivation (Scribner and Fahrney, 1976) or treatment with cobra venom factor (Shin et al., 1969). Cobra venom factor has been extensively used *in vitro* and *in vivo*: It binds to complement Factor B of the alternative pathway to form a venom factor-Bb complex that functions as a C3/C5 convertase (Cooper, 1973; von Zabern et al., 1980). This results in the cleavage of C3 and C5, consequently consuming complement components and ultimately leading to the depletion of serum complement activity. The key role of complement opsonization in phagocytosis was also demonstrated by the interference of complement activation by pathogenic virulence factors. In the case of gram-positive *S. pneumoniae*, the viral capsule inhibits IgG binding and decreases bacterial opsonization with iC3b, preventing phagocytosis by FcR and complement receptors (Hyams et al., 2010). Also, the *E. coli* capsule may block complement opsonization by masking surface components (such as LPS) capable of activating the complement pathway (Horwitz and Silverstein, 1980). Impairing complement opsonization of bacteria is not only a defense mechanism that impairs phagocytosis, but also NETosis. In general, complement opsonization has been proven to promote NETosis, as shown by the enhanced NET release by neutrophils in the presence of the serum-opsonized bacteria *A. actinomycetemcomitans* (Palmer et al., 2016). Yet, this effect was not observed with serum-treated *S. Aureus,* suggesting again that complement-inactivating properties of bacteria might impair effector functions such as phagocytosis and NETosis.

Inherited deficiencies of early classical complement proteins are closely associated with the development of SLE. This systemic autoimmune disease is characterized by antinuclear antibodies, disturbed complement activation and the occurrence of large immunocomplexes (ICs). Homozygous deficiency of C1q is associated with a 93% risk of developing SLE. In addition, 75% of patients with homozygous C4 deficiency develop lupus-like illness (Lewis and Botto, 2006). SLE was observed in 10–30% of C2-deficient patients, indicating a higher risk of SLE when deficiencies occur in complement proteins of earlier stages of the cascade. How complement deficiency exactly contributes to the development of SLE is not known. One possible mechanism is impairment of complement-mediated immune complex clearance (**Figure 4**), which leads to the deposition of large non-soluble complexes in tissues. These ICs drive proinflammatory cytokine release and local tissue injury (Davies et al., 1992, 1994). This mechanism is supported by the lower expression of CR1 found on erythrocytes of SLE patients, which is the main receptor involved in IC clearance (Ross et al., 1985). Also, the impaired clearance of apoptotic cells due to complement deficiency might serve as a source of self-antigens to initiate autoimmunity. This is evidenced by the impaired phagocytosis of dead/necrotic cells by macrophages in the absence of C1q (Böttcher et al., 2006; Gullstrand et al., 2009).

Complement Receptor 1 (CR1)

Receptor Characterization

Complement receptor 1 (CR1, CD35, C3b/C4b receptor) is a type 1 membrane bound glycoprotein that specifically interacts with MBL and complement proteins C1q, C3b, C4b, and with a lower affinity with iC3b (**Figure 2** and **Table 1**) (Nelson, 1953; Gigli and Nelson, 1968; Ghiran et al., 2000). Four polymorphic variants of the receptor exist, the most common one having a molecular mass of approximately 220 kDa and an extracellular domain of 30 tandemly repeating complement control proteins (CCPs), also known as short consensus repeats or sushi domains. The CCP repeats are 59–72 amino acids long, each having four conserved cysteines that form a pattern of disulfide bridges connecting Cys1-Cys3 and Cys2-Cys4 (Reid et al., 1986; Ahearn and Fearon, 1989; Hannan et al., 2005). The CCPs are further grouped into 4 longer homologous repeats (LHR) containing each 7-9 CCPs. There are several binding sites for C3b and C4b: CCPs 1-3 (LHR-A) contains a C4b binding site, whereas CCPs 8–10 (LHR-B) and CCPs 15–17 (LHR-C) contain both C4b and C3b binding sites, although C3b will bind with a higher affinity (Klickstein et al., 1988; Krych et al., 1991). LHR-D is responsible for the binding of two other CR1 ligands, C1q and MBL. CR1 is expressed on erythrocytes, monocytes/macrophages, polymorphonuclear leukocytes, B-lymphocytes, subpopulations of T-lymphocytes, follicular dendritic cells (FDCs) and glomerular podocytes (Fearon, 1980; Reynes et al., 1985; Appay et al., 1990; Rødgaard

et al., 1991). The soluble form of CR1 (sCR1) is released in the plasma by cell surface proteolytic cleavage of CR1 on leukocytes, and acts together with membrane-bound CR1 as an inhibitor of the classical and alternative complement pathway (Danielsson et al., 1994).

CR1-Mediated Functions

Protection of host cells against complement activation is mediated by a group of cell surface anchored regulatory proteins, to which CR1 belongs to. CR1 prevents unintended complement-mediated injury by decay-accelerating activity of both C3 and C5 convertases and by serving as a co-factor of the serine protease factor I. This promotes factor I-mediated degradation of C3b and C4b, and the cleavage of iC3b to C3c and C3dg (Iida and Nussenzweig, 1981; Masaki et al., 1992). Besides its regulatory function, CR1 also plays a critical role in the clearance of complement-coated ICs (**Figure 4**). Formation of ICs by binding of multiple antibodies to antigens leads to C3b deposition, causing the opsonized IC to bind to CR1 on erythrocytes. The ICs are subsequently transported to the liver and spleen on the plasma membrane of circulating erythrocytes, where they interact with Fc-receptors and CR1 on macrophages, leading to IC phagocytosis (Cornacoff et al., 1983; Yoshida et al., 1986). After IC delivery, erythrocytes return to the circulation partially lacking CR1 due to proteolytic cleavage during phagocytosis by macrophages, however, CR1 loss on erythrocytes might also be a consequence of erythrocyte maturation (Pascual et al., 1994; Imrie and Jones, 1997; Miot et al., 2002). Ninety-five percent of the CR1 receptors in the peripheral blood circulation are located on erythrocytes, even though the absolute amount of CR1 on erythrocytes is remarkably lower than on neutrophils (950 vs. 57,000 receptors per cell, respectively). However, the high number of circulating erythrocytes makes the clearance of C3b-opsonized ICs by erythrocytes 500–1,000 times more likely than by leukocytes (Siegel et al., 1981).

CR1 activity also modulates humoral immunity since it facilitates the retention of antigens to FDCs in the germinal center within secondary lymphoid organs. CR1 on FDCs will capture complement-opsonized immune complexes that carry antigens, which stimulate follicular B-lymphocytes via the B-cell receptor (BCR) (Fang et al., 1998). Deficiency in C3 or depletion of circulating C3 with cobra venom factor inhibited memory B-lymphocyte formation and showed the indispensable role of C3 opsonization of ICs for appropriate B-lymphocyte function (Klaus and Humphrey, 1977). In addition, a CR1 knock-out mouse model showed a reduced amount of activated B-lymphocytes in the germinal center and a decreased antibody response (Donius et al., 2013).

In mice, CR1 and CR2 are derived from alternative splicing of the *Cr2* gene, while in humans they are a product of two distinct but closely linked genes on chromosome 1: *CR1* and *CR2* [extensively reviewed by (Jacobson and Weis, 2008)]. In addition, CR1 and CR2 expression in mice is limited to B-lymphocytes and FDCs, complicating the use of a mouse model to investigate CR1 functions on myeloid cells. In mice, CR1 still possesses binding sites for C3b and C4b and serves as a cofactor for C3b cleavage by murine factor I, however, its prominent role in phagocytosis and immune adherence is absent (Kinoshita et al., 1985; Molina et al., 1994). Instead, CR1 on FDCs enhances the retention of antigens on their surface to generate an appropriate antibody response by activated B-lymphocytes of the germinal center, as discussed above (Donius et al., 2013). Interestingly, rodents carry the Cr1-related protein Y (*Crry*) gene, from which the human *CR1* gene has evolved, encoding a membrane-bound complement regulatory protein that is expressed in almost every cell type. Thus, it explains the high degree of protein sequence similarity with human CR1, which is translated to a similar effector function, since it also accelerates the decay of C3/C5 convertases and acts as a cofactor for factor I-mediated cleavage of C3b and C4b (Kim et al., 1995). However, the involvement in phagocytosis and adhesion has not been demonstrated yet for *Crry*, indicating that the mouse homolog for CR1's immune adherence and phagocytosis roles is still unidentified.

The limited research into the phagocytic role of human CR1 has mostly been conducted in the 1980s. The adhesive and phagocytic function of CR1 were mainly assessed through rosette or cluster formation of immunoglobulin and complement-coated sheep erythrocytes to polymorphonuclear leukocytes, monocytes and macrophages, and their subsequent ingestion. The phagocytosis of C3b/C4b-opsonized particles occurs in synergy with CR1 and Fc-receptors on both human and murine neutrophils and macrophages (Mantovani, 1975; Ehlenberger and Nussenzweig, 1977). CR1 is primarily involved in the attachment of C3b-opsonized particles to the cell as shown by the impaired attachment of C3b-coated erythrocytes after anti-CR1 treatment (Newman et al., 1985), whereafter interaction with the Fc-receptors or CR3 mediates phagocytosis (**Figure 4**) (Fällman et al., 1993). C3 opsonization by itself is not able to trigger CR1-mediated phagocytosis, therefore the presence of IgG complexes is essential to stimulate particle ingestion through its Fc fragments (Newman et al., 1984). CR1 phagocytosis is only mediated after receptor transition from a resting state, in which it binds ligand-coated particles, to an activated state. Even though the biochemical events that account for the shift in activity are unknown, an important role for CR1 phosphorylation has been suggested as PKC stimulation with phorbol myristate acetate (PMA) and PAF enabled phagocytic function by CR1 (Changelian and Fearon, 1986; Bussolino et al., 1989). Likewise, the signaling pathway used by activated CR1 to mediate its effector functions has not yet been characterized.

Complement Receptor of the Immunoglobulin Family (CRIg)

Receptor Characterization

In 2000, a novel human *Z39Ig* gene on chromosome X was reported, encoding a new member of the immunoglobulin superfamily (Langnaese et al., 2000). A few years later, the complement receptor of the immunoglobulin family (CRIg), also referred to as V-set and Ig domain (VSIG4)/B7 family-related protein or Z39Ig, was identified as a receptor expressed on tissue resident and sinusoidal macrophages, especially hepatic KCs, and more recently also on human monocyte derived dendritic cells (**Table 1**) (Helmy et al., 2006; Munawara et al., 2019).

CRIg is a type 1 transmembrane receptor with two alternatively spliced variants in humans: long huCRIg(L) and short huCRIg(S) (**Figure 2**). The latter consists only of an extracellular variable (V-type) Ig domain, while huCRIg(L) also contains a constant (C2-type) Ig domain. Mice express only one form of muCRIg with a single Ig V-type domain and therefore resembles the shorter human splice variant.

CRIg-Mediated Functions

CRIg binds to the beta chain of C3b, to iC3b and C3c, and this receptor is required for the binding and phagocytosis of opsonized pathogens from the circulation, thereby limiting systemic bacteremia or parasitemia (Wiesmann et al., 2006). This has been shown by the reduced capture and elimination of *S. aureus* and *L. monocytogenes* by the liver KCs in CRIg knock-out mice compared to wild-type mice (Helmy et al., 2006). Also, complement opsonization of parasites has been shown to be indispensable for capture and clearance via CRIg by KCs (Liu et al., 2016). However, other investigators observed that complement depletion did not affect the capture of gram-positive bacteria, suggesting that CRIg may bind microorganisms directly in a complement-independent manner (Zeng et al., 2016). This led to the discovery that CRIg functions as a pattern recognition receptor that recognizes gram-positive bacteria via lipoteichoic acid binding *in vitro*. Nevertheless, whether this occurs under high shear forces *in vivo* was questionable (Zeng et al., 2016). Moreover, un-opsonized gram-negative bacteria also displayed an efficient clearance, which cannot be explained by the direct recognition of lipoteichoic acid (Broadley et al., 2016). Therefore, a "dual track clearance" mechanism consisting of parallel "fast" and "slow" clearance of circulating bacteria has been described (Broadley et al., 2016). Circulating bacteria (opsonized or not) are rapidly cleared by the liver KCs via CRIg and scavenger receptors, whereas the slower process of complement opsonization enables a second clearance step via platelet binding and phagocytosis by KCs, also using CRIg. Even though the liver captures and kills >90% of all circulating pathogens, a shift toward spleen clearance has been observed with growing particle size. This mechanism adds another layer to the efficient and fast clearance of circulating bacteria by the liver and spleen. Interestingly, CRIg has also been found to be a negative regulator of T-lymphocyte responses in tissues. CRIg can function as a coinhibitory molecule of the B7/CD28 superfamily, suppressing T-lymphocyte proliferation and cytokine production, thereby maintaining peripheral T-lymphocyte tolerance in healthy tissues (Vogt et al., 2006; Yuan et al., 2017; Munawara et al., 2019). Interestingly, this inhibitory function is regulated by CRIg internalization when bound to C3b or iC3b (e.g., opsonized target), allowing an adequate T-lymphocyte response to progress during tissue inflammation (Fearon et al., 1981; Sengeløv et al., 1994).

Murine KCs express CRIg and CR3 on the plasma membrane, while human KCs additionally express CR1 and CR4. However, none of these receptors on KCs are more involved in pathogen clearance than CRIg. The relationship between CRIg and CR3 was investigated in mice. Even though both receptors are expressed on KCs and share a common ligand, distinct modes of pathogen clearance have been observed. CRIg binds and internalizes opsonized pathogens independently of receptor crosslinking, additional activation stimuli or the presence of divalent cations, which are all indispensable requirements for CR3-mediated phagocytosis (Gorgani et al., 2008). Thus, CR3 contributes rather indirectly to pathogen clearance by the recruitment of neutrophils through their interaction with ICAM-1 (Gregory et al., 2002). The subcellular localization and intracellular trafficking of CRIg also differs from CR3: CRIg is mostly expressed on recycling endosomes where they aid in delivering membrane to the forming phagosome and ensure a sufficient supply of CRIg to the plasma membrane to mediate CRIg-dependent internalization (Helmy et al., 2006). In contrast, CR3 is located in secretory vesicles that fuse with the plasma membrane upon cytokine stimulation. CRIg is not degraded after particle internalization, instead, CRIg is recycled to the endosome pool prior or during phagosome-lysosome fusion. The signaling mechanism induced by CRIg activation is not known. CR3 and CRIg potentially share some intracellular mediators of the CR3 signaling pathway, as they are co-expressed on macrophages and share a common ligand, however, more studies are needed to clarify this.

The ability of CRIg to bind to the beta chain subunit of C3b abrogates the interaction of C3 and C5 convertases of the alternative pathway (Wiesmann et al., 2006). The potential immune regulatory role of CRIg has further been investigated and led to the development of a soluble CRIg-Fc fusion protein with enhanced complement inhibitory efficacy. Because CRIg only blocks complement activation of the alternative pathway, and not the classical or lectin pathway, the novel CRIg-Fc complement inhibitor was thought to have an effect on the progression of diseases in which the alternative pathway contributes greatly. Its benefits were confirmed in mouse models of arthritis, where CRIg-Fc injection caused a reduction of inflammation and bone loss compared to control mice, even when the disease was already established (Katschke et al., 2007). Also, lupus-prone MRL lymphoproliferation (MRL/lpr) mice showed significantly less skin lesions, proteinuria and kidney pathology when treated with CRIg-Fc (Lieberman et al., 2015), and it prevented local and remote tissue injury induced by ischemia-reperfusion (Chen et al., 2011). A novel CRIg/FH fusion protein, combining the extracellular domain of CRIg and the functional domain of factor H, was designed to inhibit both the classical and alternative complement pathway and displayed similar effects in ischemia-reperfusion injury and lupus nephritis (Qiao et al., 2018; Hu et al., 2019; Shi et al., 2019). All together, these results indicate the potential effective role of soluble CRIg proteins in clinical settings of intestinal and renal ischemia-reperfusion injury, SLE, inflammatory arthritis, autoimmune liver disease (Jung et al., 2012) and potentially other diseases in which the alternative pathway is involved.

Complement Receptor 2 (CR2)

Receptor Characterization

CR2 (CD21) is a 145 kDa type 1 membrane bound glycoprotein that comprises 15–16 CCPs (depending on the alternative splicing of one exon), a transmembrane domain and a short 34 amino acid cytoplasmic tail (**Figure 2**) (Hannan et al., 2002).

The receptor structure closely resembles CR1, but lacks a few N-terminal CCP repeats that are known to bind C3b/C4b. Instead, CR2 binds the ligands iC3b, C3dg, and C3d (Molina et al., 1994). In humans, CR2 binds the gp350/220 viral envelope protein of the Epstein-Barr virus (EBV) (Fingeroth et al., 1984), the immunoregulatory protein CD23 (Aubry et al., 1992) and interferon-alpha (Asokan et al., 2006). Szakonyi et al. provided substantial information on the structure of CR2 by determining the crystal structure of CCP1 and CCP2 in complex with C3d at 2.0 Å (Szakonyi et al., 2001). Human CR2 is expressed primarily on mature B-lymphocytes and FDCs, although a subset of peripheral and thymic T-lymphocytes and epithelial cells also express the receptor (**Table 1**).

CR2-Mediated Functions

CR2 exerts distinct functions depending on ligand binding: (1) On B-lymphocytes, CR2 promotes antigen receptor-mediated signal transduction by the formation of a B-lymphocyte co-receptor complex with the signaling protein CD19 and the tetraspanin CD81. Co-ligation of the B-cell receptor with CR2-CD19-CD81 complexes by C3d-coated antigens/immune complexes can significantly amplify signaling in B-lymphocytes and lower the threshold for B-lymphocyte activation by at least two orders of magnitude (Carter and Fearon, 1992). (2) On FDCs, CR2 mediates the retention of C3-coated antigens, presumably to enhance interactions with B-lymphocytes of the germinal center (Reynes et al., 1985). (3) As a receptor for CD23, one of the main functions of CR2 is the promotion of B-lymphocyte class switching and the increased production of IgE (Aubry et al., 1992). (4) EBV hijacks CR2 for B-cell infection; binding to CR2 initiates the entry of the virus in B-lymphocytes (Tanner et al., 1987).

CR2 is not directly implicated in adhesion or phagocytosis. However, there are indications that CR2 contributes to the pathogenesis of SLE. In patients with SLE, the expression of CR1 and CR2 on B-lymphocytes is decreased by 50% and a CR2 variant with three single nucleotide polymorphisms (SNPs) was associated with a 1.54 increased risk of SLE (Wilson et al., 1986; Wu et al., 2007). However, whether CR2 defects are the consequence or the drivers of the disease is not completely clear. In the mouse model of SLE (MRL/lpr), reduced expression of CR1 and CR2 occurred on B-lymphocytes before the clinical signs of SLE appear (Takahashi et al., 1997). Also, SNPs in the *Cr2* gene are sufficient for mice to develop an SLE-like disease (Boackle et al., 2001). Moreover, increased serum levels of antinuclear Abs and anti-DNA Abs have been found in $Cr2^{null}$ mice (Wu et al., 2002). These results indicate a role for CR2 in SLE pathogenesis, however, one must keep in mind that these were obtained in mice, in which a single gene encodes for both CR1 and CR2. Human CR2 has been shown to bind DNA and chromatin in the absence of C3 opsonization, therefore, CR2 deficiency in SLE might also influence the development of autoimmunity in SLE through altered receptor interactions with DNA (Asokan et al., 2013).

Complement Receptors CR3 and CR4

CR3 and CR4-Mediated Functions

Out of all complement receptors, CR3 (CD11b/CD18) is the most widely expressed and a highly versatile receptor. It is expressed by macrophages, monocytes, neutrophils, dendritic cells, NK cells and activated lymphocytes (**Table 1**) (Ho and Springer, 1982; Ross and Vetvicka, 1993). The importance of CR3 is highlighted by its contribution to both the recruitment of leukocytes (via adhesion) and phagocytosis of targets. CR4, which contains the CD11c α-chain instead, is highly expressed in monocytes, macrophages and DCs, where it mediates similar functions to CR3 (Torres-Gomez et al., 2020a). For a detailed description of CR3 and CR4 structure and motifs, see section β2-Integrin Family Complement Receptors CR3 and CR4.

CR3 and CR4 interact predominantly with iC3b to promote phagocytosis, a fragment that is generated from factor I-dependent cleavage of C3b (Beller et al., 1982; Keizer et al., 1987). In general, presence of iC3b-opsonized particles is not sufficient to induce CR3-mediated phagocytosis. CR3 requires inside-out activation which includes a receptor conformational change into the high-affinity "extended" and "open" state (E^+H^+) and receptor clustering in the membrane, together resulting in efficiently binding and internalizing iC3b-opsonized particles. Integrin clustering has been found to be indispensable for ligand binding and receptor signaling, with FcγR stimulation promoting CR3 aggregation in phagocytic cups by enhancing the receptor's lateral mobility (Jongstra-Bilen et al., 2003). Also, ligand binding to CR3 was enhanced in neutrophils with increased receptor clustering after PMA stimulation, with loss of clustering correlating with a loss in receptor activity (Detmers et al., 1987). The stimuli for inside-out signaling include inflammatory cytokines (TNF-α), chemokines, N-formylmethionine-leucyl-phenylalanine (fMLP), TLR agonists and adhesion to extracellular matrix (laminin, fibronectin) (Sampson et al., 1991). These lead to inside-out activation via the Rap1-RIAM-Talin pathway. Genetic ablation of these proteins leads to defects in complement-mediated phagocytosis, as illustrated by impaired adhesion, phagocytosis and ROS production by RIAM-deficient phagocytes *in vitro*, and signs of LAD in RIAM knockout mice *in vivo* (Klapproth et al., 2015; Torres-Gomez et al., 2020b). Inside-out signaling drives the phosphorylation of CD18 on serine residues, but not of the alpha chains (CD11b or CD11c), which are constitutively phosphorylated (Chatila et al., 1989; Fagerholm et al., 2006). These phosphorylations, although originating differently, are both required for CR3- and CR4-mediated leukocyte adhesion and phagocytosis.

Ligand binding initiates a phagocytic signal that promotes particle internalization via a signaling pathway that relies on well-defined molecular players, described in detail in section Introduction to Phagocytosis. It requires Arp2/3 and mDia-mediated actin polymerization, and Rho activity. Actin polymerization that drives the phagosomal cup expansion is coupled to integrins via the activity of tyrosine kinases (e.g., Src and Syk) and binding to talin and vinculin which create anchoring points for the force transmission from actin

polymerization (Jaumouille et al., 2019). Besides iC3b, a wide range of unrelated ligands are also capable of interacting with CR3, including but not limited to fibrinogen, factor X, neutrophil inhibitory factor (NIF), collagen, denatured proteins and plastics (Yakubenko et al., 2002). Studies with inhibitory mAbs directed to multiple regions of this receptor showed that the I domain of CR3 contains multiple overlapping ligand binding sites which are responsible for the receptor's broad ligand specificity (Diamond et al., 1993). Within this domain, three amino acids (Phe^{246}, Asp^{254}, Pro^{257}) were identified as critical for CR3-dependent ligand binding (Yakubenko et al., 2002). Although CR3 and CR4 interact with a number of unrelated ligands with no clear receptor consensus motif, the MIDAS of the I domain is apparently a common ligand recognition site for both receptors (Vorup-Jensen and Jensen, 2018). In addition to the I domain, a unique lectin domain, located C-terminally to the I domain, participates in the binding of microbial carbohydrates (e.g., beta-glucan) (Ross et al., 1987). The binding of cell wall carbohydrates to the lectin domain serves as an additional signal to mediate phagocytosis of iC3b-opsonized fungi (Cain et al., 1987). In addition, the lectin domain has been shown to be responsible for the non-opsonized phagocytosis properties of CR3, as demonstrated by the phagocytosis of non-opsonized zymosan (Le Cabec et al., 2002).

Although CR3 and CR4 share a high degree of homology, functional differences between these receptors are becoming progressively clearer. For instance, CR3 and CR4 bind iC3b differently (Xu et al., 2017). CR3 binds iC3b at two separate sites, which are distinct from the two iC3b-binding sites found in CR4. Moreover, CR3 has generally more affinity toward positively-charged ligands, such as major basic protein in the brain and the antimicrobial peptide LL-37. On the other hand, CR4 binds well to heparin and osteopontin, both highly negative molecules (Vorup-Jensen and Jensen, 2018). CR3 and CR4 may also differ in which function they perform preferentially in cells. Studies *in vitro* suggested CR3 as the main phagocytic receptor for iC3b-opsonized bacteria, whereas CR4 predominated as an adhesion molecule for monocytic cells (Erdei et al., 2019). In alveolar macrophages, CR3 mediated the majority of the attachment to C3-opsonized sheep erythrocytes, whereas CR4, although more abundant, had a minor role. That disparity was correlated to differences in plasma membrane motility of CR3 and CR4, with CR4 being less mobile (Ross et al., 1992). Also, there is only 56% homology between the cytoplasmic tail of CR3 α and CR4 α, indicating cytoplasmatic structural differences that might affect the binding of signaling molecules, possibly contributing to some distinct receptor functional properties (Ross et al., 1992).

Deficiencies in CR3 and CR4 recapitulate in many ways the deficiency of complement components, such as in the susceptibility to recurrent infections (Rosetti and Mayadas, 2016). These are of particular importance in CR3 and CR4 since the receptors not only control phagocytosis of opsonized material, but of unrelated ligands and also mediate the recruitment of leukocytes. CD11b deficiency leads to more severe sepsis and larger bacterial load in a model of murine cecal-ligation and puncture (Liu et al., 2014). Similarly, mice infected with *S. aureus* (Flick et al., 2004) or *S. pneumoniae* (Prince et al., 2001) have increased bacteremia and mortality when lacking a functional CR3. Deficiency in CD18 causes LAD-I, characterized by frequent life-threatening infections, elevated neutrophil numbers in the bloodstream, and impaired wound healing. Patients with LAD-I-related mutations in CD18 present reduced expression of CR3 and functional defects, such as low binding to iC3b, bovine serum albumin and fibrinogen (Hogg et al., 1999; Mathew et al., 2000). Some unexpected aspects of infection are also revealed in the absence of CR3 and CR4. Phagocytosis of the pathogen *C. neoformans* requires complement receptors, although it does not require complement opsonization (Taborda and Casadevall, 2002). Antibody mediated blockade of CR3 and CR4, or deficiency in CD18 impaired macrophage phagocytosis of the yeast significantly, which was triggered by glucuronoxylomannan molecules exposed at the yeast capsule. Moreover, the gram-negative bacteria *F. tularensis* subvert the complement system to foster bacterial survival. *F. tularensis* is phagocytosed by DCs in a C3-, CR3-, and CR4-dependent manner, however, this internalization mechanism stimulates proinflammatory cytokine production, intracellular bacterial growth and DC death instead (Ben Nasr et al., 2006).

Complement is also involved in the clearance of dead cells. C3 opsonization and CR3 are required for the clearance of apoptotic Jurkat cells by macrophages *in vitro*. Antibody blockade of C3 or CR3 was able to inhibit apoptotic cell clearance significantly, whereas CR4 blockade had a partial effect (Takizawa et al., 1996). An interesting observation by Mevorach et al. was that addition of serum to assays of apoptotic cell phagocytosis increased the uptake efficiency several fold (Mevorach et al., 1998). In this study, complement deposition was induced, among other factors, by exposed phosphatidylserine in apoptotic cells. Interestingly, it was shown that transfection of CHO cells with CR3 alone is sufficient to promote phagocytosis of apoptotic bodies by CHO cells. More recently, numerous studies implicated CR3 and CR4 also in the clearance of necrotic cells (Gaipl et al., 2001; Gullstrand et al., 2009). It was shown that complement factors C1q and C3 bound preferentially to necrotic cells over apoptotic cells *in vitro*, which drove their phagocytosis by macrophages. In addition, CR3 and CR4 present a variety of scavenging functions that are independent of opsonization, such as its binding to nucleic acids, glycosaminoglycans and denatured proteins (Vorup-Jensen and Jensen, 2018). Both receptors, but especially CR3, are hypothesized to assist in the prevention of autoimmunity and inflammation by promoting debris clearance. In line with this, genome-wide association studies have identified 3 SNPs that are strongly associated with the development of SLE (Nath et al., 2008; Faridi et al., 2017). These SNPs are located in the *ITGAM* gene and result in a variety of dysfunctions of CD11b, including reduced integrin activation, leukocyte adhesion, ligand binding and phagocytosis. Moreover, the defective CD11b variants cause an excessive production of type I interferon, which drives SLE development and severity (Faridi et al., 2017).

CONCLUSION

In this review, the role of complement and complement receptors in the regulation of immunity and inflammation was discussed, with a focus on their function in leukocyte recruitment and phagocytosis in several tissues. Activation of complement anaphylatoxin receptors C3aR and C5aR mainly mediates chemotaxis of leukocytes to inflammatory sites for pathogen clearance or tissue regeneration. C5L2 is additionally involved in regulation of C5aR signaling, by exerting both immune suppressive as immune activating functions. Activation of anaphylatoxin- and other GPCRs during rolling is essential for further leukocyte transmigration into inflamed tissues, which is mediated by activation of CR3, CR4 and other integrins. After extension by inside-out and outside-in signaling, they participate in firm endothelial adhesion, diapedesis and leukocyte chemotaxis toward the inflammatory trigger. Within tissues, activated CR3 and CR4 are involved in phagocytosis by mainly interacting with iC3b-opsonized pathogens. Moreover, complement receptors CR1, CRIg and CR2 are interacting with several components of the complement cascade, as such contributing to complement-mediated phagocytosis and cell-type specific immune regulatory roles. The importance of a correctly functioning complement system is highlighted by diseases such as LAD and SLE, which are characterized by deficiencies in leukocyte extravasation and phagocytosis due to impaired complement molecules. Differences in complement proteins between mice and men and the differences in cells that express specific complement receptors in both species do not facilitate research on molecular pathways and partially explain remaining knowledge gaps. Examples are our lack of understanding on the mechanisms that allow CR3 to either stimulate phagocytosis or cell migration depending on the type of ligand bound. Novel therapies targeting the complement system have great beneficial potential in a number of kidney, brain and articular diseases, highlighting the significance of further research on complement receptor function and regulation.

AUTHOR CONTRIBUTIONS

SV, SC, and PM wrote the manuscript and prepared the figures. PP and PM provided critical input and corrected the manuscript. All authors contributed to the article and approved the submitted version.

FUNDING

This work was supported by the Research Foundation Flanders (FWO-Vlaanderen projects G080818N and G058421N), a C1 grant (C16/17/010) from KU Leuven and the Rega Foundation. SV and SC obtained FWO-SB (1S56521N) and FWO-FR Ph.D. (11A4220N) fellowships, respectively. PM is a beneficiary of the Marie Skłodowska-Curie fellowship (MSCA-IF-2018-839632).

REFERENCES

Ahearn, J. M., and Fearon, D. T. (1989). Structure and function of the complement receptors, CR1 (CD35) and CR2 (CD21). *Adv. Immunol.* 46, 183–219. doi: 10.1016/S0065-2776(08)60654-9

Allen, L. A., and Aderem, A. (1996). Mechanisms of phagocytosis. *Curr. Opin. Immunol.* 8, 36–40. doi: 10.1016/S0952-7915(96)80102-6

Ames, R. S., Li, Y., Sarau, H. M., Nuthulaganti, P., Foley, J. J., Ellis, C., et al. (1996). Molecular cloning and characterization of the human anaphylatoxin C3a receptor. *J. Biol. Chem.* 271, 20231–20234. doi: 10.1074/jbc.271.34.20231

Anderson, D. C., and Springer, T. A. (1987). Leukocyte adhesion deficiency: an inherited defect in the Mac-1, LFA-1, and p150,95 glycoproteins. *Annu. Rev. Med.* 38, 175–194. doi: 10.1146/annurev.me.38.020187.001135

Appay, M. D., Kazatchkine, M. D., Levi-Strauss, M., Hinglais, N., and Bariety, J. (1990). Expression of CR1 (CD35) mRNA in podocytes from adult and fetal human kidneys. *Kidney Int.* 38, 289–293. doi: 10.1038/ki.1990.198

Asokan, R., Banda, N. K., Szakonyi, G., Chen, X. S., and Holers, V. M. (2013). Human complement receptor 2 (CR2/CD21) as a receptor for DNA: implications for its roles in the immune response and the pathogenesis of systemic lupus erythematosus (SLE). *Mol. Immunol.* 53, 99–110. doi: 10.1016/j.molimm.2012.07.002

Asokan, R., Hua, J., Young, K. A., Gould, H. J., Hannan, J. P., Kraus, D. M., et al. (2006). Characterization of human complement receptor type 2 (CR2/CD21) as a receptor for IFN-alpha: a potential role in systemic lupus erythematosus. *J. Immunol.* 177, 383–394. doi: 10.4049/jimmunol.177.1.383

Aubry, J. P., Pochon, S., Graber, P., Jansen, K. U., and Bonnefoy, J. Y. (1992). CD21 is a ligand for CD23 and regulates IgE production. *Nature* 358, 505–507. doi: 10.1038/358505a0

Auffray, C., Fogg, D., Garfa, M., Elain, G., Join-Lambert, O., Kayal, S., et al. (2007). Monitoring of blood vessels and tissues by a population of monocytes with patrolling behavior. *Science* 317, 666–670. doi: 10.1126/science.1142883

Bamberg, C. E., Mackay, C. R., Lee, H., Zahra, D., Jackson, J., Lim, Y. S., et al. (2010). The C5a receptor (C5aR) C5L2 is a modulator of C5aR-mediated signal transduction. *J. Biol. Chem.* 285, 7633–7644. doi: 10.1074/jbc.M109.092106

Barnum, S. R. (2015). C4a: an anaphylatoxin in name only. *J. Innate Immun.* 7, 333–339. doi: 10.1159/000371423

Bednarczyk, M., Stege, H., Grabbe, S., and Bros, M. (2020). β2 integrins-multi-functional leukocyte receptors in health and disease. *Int. J. Mol. Sci.* 21:1402. doi: 10.3390/ijms21041402

Beller, D. I., Springer, T. A., and Schreiber, R. D. (1982). Anti-Mac-1 selectively inhibits the mouse and human type three complement receptor. *J. Exp. Med.* 156, 1000–1009. doi: 10.1084/jem.156.4.1000

Ben Nasr, A., Haithcoat, J., Masterson, J. E., Gunn, J. S., Eaves-Pyles, T., and Klimpel, G. R. (2006). Critical role for serum opsonins and complement receptors CR3 (CD11b/CD18) and CR4 (CD11c/CD18) in phagocytosis of Francisella tularensis by human dendritic cells (DC): uptake of Francisella leads to activation of immature DC and intracellular survival of the bacteria. *J. Leukoc. Biol.* 80, 774–786. doi: 10.1189/jlb.1205755

Bénard, M., Raoult, E., Vaudry, D., Leprince, J., Falluel-Morel, A., Gonzalez, B. J., et al. (2008). Role of complement anaphylatoxin receptors (C3aR, C5aR) in the development of the rat cerebellum. *Mol. Immunol.* 45, 3767–3774. doi: 10.1016/j.molimm.2008.05.027

Biglarnia, A. R., Huber-Lang, M., Mohlin, C., Ekdahl, K. N., and Nilsson, B. (2018). The multifaceted role of complement in kidney transplantation. *Nat. Rev. Nephrol.* 14, 767–781. doi: 10.1038/s41581-018-0071-x

Boackle, S. A., Holers, V. M., Chen, X., Szakonyi, G., Karp, D. R., Wakeland, E. K., et al. (2001). Cr2, a candidate gene in the murine Sle1c lupus susceptibility locus, encodes a dysfunctional protein. *Immunity* 15, 775–785. doi: 10.1016/S1074-7613(01)00228-X

Böttcher, A., Gaipl, U. S., Fürnrohr, B. G., Herrmann, M., Girkontaite, I., Kalden, J. R., et al. (2006). Involvement of phosphatidylserine, alphavbeta3, CD14, CD36, and complement C1q in the phagocytosis of primary necrotic lymphocytes by macrophages. *Arthritis Rheum.* 54, 927–938. doi: 10.1002/art.21660

Brennan, F. H., Lee, J. D., Ruitenberg, M. J., and Woodruff, T. M. (2016). Therapeutic targeting of complement to modify disease course and improve outcomes in neurological conditions. *Semin. Immunol.* 28, 292–308. doi: 10.1016/j.smim.2016.03.015

Broadley, S. P., Plaumann, A., Coletti, R., Lehmann, C., Wanisch, A., Seidlmeier, A., et al. (2016). Dual-track clearance of circulating bacteria balances rapid restoration of blood sterility with induction of adaptive immunity. *Cell Host Microbe* 20, 36–48. doi: 10.1016/j.chom.2016.05.023

Bussolino, F., Fischer, E., Turrini, F., Kazatchkine, M. D., and Arese, P. (1989). Platelet-activating factor enhances complement-dependent phagocytosis of diamide-treated erythrocytes by human monocytes through activation of protein kinase C and phosphorylation of complement receptor type one (CR1). *J. Biol. Chem.* 264, 21711–21719. doi: 10.1016/S0021-9258(20)88244-1

Cain, J. A., Newman, S. L., and Ross, G. D. (1987). Role of complement receptor type three and serum opsonins in the neutrophil response to yeast. *Complement* 4, 75–86. doi: 10.1159/000463011

Calderwood, D. A., Yan, B., de Pereda, J. M., Alvarez, B. G., Fujioka, Y., Liddington, R. C., et al. (2002). The phosphotyrosine binding-like domain of talin activates integrins. *J. Biol. Chem.* 277, 21749–21758. doi: 10.1074/jbc.M111996200

Campbell, I. D., and Ginsberg, M. H. (2004). The talin-tail interaction places integrin activation on FERM ground. *Trends Biochem. Sci.* 29, 429–435. doi: 10.1016/j.tibs.2004.06.005

Caporale, L. H., Tippett, P. S., Erickson, B. W., and Hugli, T. E. (1980). The active site of C3a anaphylatoxin. *J. Biol. Chem.* 255, 10758–10763. doi: 10.1016/S0021-9258(19)70372-X

Carman, C. V., and Springer, T. A. (2004). A transmigratory cup in leukocyte diapedesis both through individual vascular endothelial cells and between them. *J. Cell Biol.* 167, 377–388. doi: 10.1083/jcb.200404129

Caron, E., and Hall, A. (1998). Identification of two distinct mechanisms of phagocytosis controlled by different Rho GTPases. *Science* 282, 1717–1721. doi: 10.1126/science.282.5394.1717

Carter, R. H., and Fearon, D. T. (1992). CD19: lowering the threshold for antigen receptor stimulation of B lymphocytes. *Science* 256, 105–107. doi: 10.1126/science.1373518

Changelian, P. S., and Fearon, D. T. (1986). Tissue-specific phosphorylation of complement receptors CR1 and CR2. *J. Exp. Med.* 163, 101–115. doi: 10.1084/jem.163.1.101

Chao, T. H., Ember, J. A., Wang, M., Bayon, Y., Hugli, T. E., and Ye, R. D. (1999). Role of the second extracellular loop of human C3a receptor in agonist binding and receptor function. *J. Biol. Chem.* 274, 9721–9728. doi: 10.1074/jbc.274.14.9721

Chatila, T. A., Geha, R. S., and Arnaout, M. A. (1989). Constitutive and stimulus-induced phosphorylation of CD11/CD18 leukocyte adhesion molecules. *J. Cell Biol.* 109(6 Pt 2), 3435–3444. doi: 10.1083/jcb.109.6.3435

Chen, J., Crispín, J. C., Dalle Lucca, J., and Tsokos, G. C. (2011). A novel inhibitor of the alternative pathway of complement attenuates intestinal ischemia/reperfusion-induced injury. *J. Surg. Res.* 167:e131–e136. doi: 10.1016/j.jss.2009.05.041

Chen, W., Lou, J., and Zhu, C. (2010b). Forcing switch from short- to intermediate- and long-lived states of the alphaA domain generates LFA-1/ICAM-1 catch bonds. *J. Biol. Chem.* 285, 35967–35978. doi: 10.1074/jbc.M110.155770

Chen, X., Xie, C., Nishida, N., Li, Z., Walz, T., and Springer, T. A. (2010a). Requirement of open headpiece conformation for activation of leukocyte integrin alphaXbeta2. *Proc. Natl. Acad. Sci. U.S.A.* 107, 14727–14732. doi: 10.1073/pnas.1008663107

Chenoweth, D. E., Goodman, M. G., and Weigle, W. O. (1982). Demonstration of a specific receptor for human C5a anaphylatoxin on murine macrophages. *J. Exp. Med.* 156, 68–78. doi: 10.1084/jem.156.1.68

Chenoweth, D. E., and Hugli, T. E. (1978). Demonstration of specific C5a receptor on intact human polymorphonuclear leukocytes. *Proc. Natl. Acad. Sci. U.S.A.* 75, 3943–3947. doi: 10.1073/pnas.75.8.3943

Chtanova, T., Schaeffer, M., Han, S. J., van Dooren, G. G., Nollmann, M., Herzmark, P., et al. (2008). Dynamics of neutrophil migration in lymph nodes during infection. *Immunity* 29, 487–496. doi: 10.1016/j.immuni.2008.07.012

Cooper, N. R. (1973). Formation and function of a complex of the C3 proactivator with a protein from cobra venom. *J. Exp. Med.* 137, 451–460. doi: 10.1084/jem.137.2.451

Cooper, N. R. (1985). The classical complement pathway: activation and regulation of the first complement component. *Adv. Immunol.* 37, 151–216. doi: 10.1016/S0065-2776(08)60340-5

Corbi, A. L., Kishimoto, T. K., Miller, L. J., and Springer, T. A. (1988). The human leukocyte adhesion glycoprotein Mac-1 (complement receptor type 3, CD11b) alpha subunit. Cloning, primary structure, and relation to the integrins, von Willebrand factor and factor B. *J. Biol. Chem.* 263, 12403–12411. doi: 10.1016/S0021-9258(18)37770-6

Cornacoff, J. B., Hebert, L. A., Smead, W. L., VanAman, M. E., Birmingham, D. J., and Waxman, F. J. (1983). Primate erythrocyte-immune complex-clearing mechanism. *J. Clin. Invest.* 71, 236–247. doi: 10.1172/JCI110764

Crass, T., Raffetseder, U., Martin, U., Grove, M., Klos, A., Köhl, J., et al. (1996). Expression cloning of the human C3a anaphylatoxin receptor (C3aR) from differentiated U-937 cells. *Eur. J. Immunol.* 26, 1944–1950. doi: 10.1002/eji.1830260840

Crider, A., Feng, T., Pandya, C. D., Davis, T., Nair, A., Ahmed, A. O., et al. (2018). Complement component 3a receptor deficiency attenuates chronic stress-induced monocyte infiltration and depressive-like behavior. *Brain Behav. Immun.* 70, 246–256. doi: 10.1016/j.bbi.2018.03.004

Croker, D. E., Halai, R., Fairlie, D. P., and Cooper, M. A. (2013). C5a, but not C5a-des Arg, induces upregulation of heteromer formation between complement C5a receptors C5aR and C5L2. *Immunol Cell Biol.* 91, 625–633. doi: 10.1038/icb.2013.48

Croker, D. E., Halai, R., Kaeslin, G., Wende, E., Fehlhaber, B., Klos, A., et al. (2014). C5a2 can modulate ERK1/2 signaling in macrophages via heteromer formation with C5a1 and β-arrestin recruitment. *Immunol Cell Biol.* 92, 631–639. doi: 10.1038/icb.2014.32

Daffern, P. J., Pfeifer, P. H., Ember, J. A., and Hugli, T. E. (1995). C3a is a chemotaxin for human eosinophils but not for neutrophils. I. C3a stimulation of neutrophils is secondary to eosinophil activation. *J. Exp. Med.* 181, 2119–2127. doi: 10.1084/jem.181.6.2119

Danielsson, C., Pascual, M., French, L., Steiger, G., and Schifferli, J. A. (1994). Soluble complement receptor type 1 (CD35) is released from leukocytes by surface cleavage. *Eur. J. Immunol.* 24, 2725–2731. doi: 10.1002/eji.1830241123

Daveau, M., Benard, M., Scotte, M., Schouft, M. T., Hiron, M., Francois, A., et al. (2004). Expression of a functional C5a receptor in regenerating hepatocytes and its involvement in a proliferative signaling pathway in rat. *J. Immunol.* 173, 3418–3424. doi: 10.4049/jimmunol.173.5.3418

Davies, K. A., Peters, A. M., Beynon, H. L., and Walport, M. J. (1992). Immune complex processing in patients with systemic lupus erythematosus. *In vivo* imaging and clearance studies. *J. Clin. Invest.* 90, 2075–2083. doi: 10.1172/JCI116090

Davies, K. A., Schifferli, J. A., and Walport, M. J. (1994). Complement deficiency and immune complex disease. *Immunopathol.* 15, 397–416. doi: 10.1007/BF01837367

Davoust, N., Jones, J., Stahel, P. F., Ames, R. S., and Barnum, S. R. (1999). Receptor for the C3a anaphylatoxin is expressed by neurons and glial cells. *Glia* 26, 201–211. doi: 10.1002/(SICI)1098-1136(199905)26:3<201::AID-GLIA2>3.0.CO;2-M

del Rio, A., Perez-Jimenez, R., Liu, R., Roca-Cusachs, P., Fernandez, J. M., and Sheetz, M. P. (2009). Stretching single talin rod molecules activates vinculin binding. *Science* 323, 638–641. doi: 10.1126/science.1162912

DeMartino, J. A., Van Riper, G., Siciliano, S. J., Molineaux, C. J., Konteatis, Z. D., Rosen, H., et al. (1994). The amino terminus of the human C5a receptor is required for high affinity C5a binding and for receptor activation by C5a but not C5a analogs. *J. Biol. Chem.* 269, 14446–14450.

Densen, P., and Ram, S. (2015). "Chapter 9 - complement and deficiencies," in *Mandell, Douglas, and Bennett's Principles and Practice of Infectious Diseases,* eds J. E. Bennett, R. Dolin, M. J. Blaser (Amsterdam: Elsevier), 93–115. doi: 10.1016/B978-1-4557-4801-3.00009-6

Detmers, P. A., Wright, S. D., Olsen, E., Kimball, B., and Cohn, Z. A. (1987). Aggregation of complement receptors on human neutrophils in the absence of ligand. *J. Cell Biol.* 105, 1137–1145. doi: 10.1083/jcb.105.3.1137

Diamond, M. S., Garcia-Aguilar, J., Bickford, J. K., Corbi, A. L., and Springer, T. A. (1993). The I domain is a major recognition site on the leukocyte integrin Mac-1 (CD11b/CD18) for four distinct adhesion ligands. *J. Cell Biol.* 120, 1031–1043. doi: 10.1083/jcb.120.4.1031

Diamond, M. S., Staunton, D. E., Marlin, S. D., and Springer, T. A. (1991). Binding of the integrin Mac-1 (CD11b/CD18) to the third immunoglobulin-like domain of ICAM-1 (CD54) and its regulation by glycosylation. *Cell* 65, 961–971. doi: 10.1016/0092-8674(91)90548-D

Ding, Z. M., Babensee, J. E., Simon, S. I., Lu, H., Perrard, J. L., Bullard, D. C., et al. (1999). Relative contribution of LFA-1 and Mac-1 to neutrophil adhesion and migration. *J. Immunol.* 163, 5029–5038.

Dishaw, L. J., Smith, S. L., and Bigger, C. H. (2005). Characterization of a C3-like cDNA in a coral: phylogenetic implications. *Immunogenetics* 57, 535–548. doi: 10.1007/s00251-005-0005-1

Dodds, A. W., and Matsushita, M. (2007). The phylogeny of the complement system and the origins of the classical pathway. *Immunobiology* 212, 233–243. doi: 10.1016/j.imbio.2006.11.009

Donius, L. R., Handy, J. M., Weis, J. J., and Weis, J. H. (2013). Optimal germinal center B cell activation and T-dependent antibody responses require expression of the mouse complement receptor Cr1. *J. Immunol.* 191, 434–447. doi: 10.4049/jimmunol.1203176

Drouin, S. M., Kildsgaard, J., Haviland, J., Zabner, J., Jia, H. P., McCray, P. B., et al. (2001). Expression of the complement anaphylatoxin C3a and C5a receptors on bronchial epithelial and smooth muscle cells in models of sepsis and asthma. *J. Immunol.* 166, 2025–2032. doi: 10.4049/jimmunol.166.3.2025

Dustin, M. L., and Springer, T. A. (1988). Lymphocyte function-associated antigen-1 (LFA-1) interaction with intercellular adhesion molecule-1 (ICAM-1) is one of at least three mechanisms for lymphocyte adhesion to cultured endothelial cells. *J. Cell Biol.* 107, 321–331. doi: 10.1083/jcb.107.1.321

Ehlenberger, A. G., and Nussenzweig, V. (1977). The role of membrane receptors for C3b and C3d in phagocytosis. *J. Exp. Med.* 145, 357–371. doi: 10.1084/jem.145.2.357

Elices, M. J., Osborn, L., Takada, Y., Crouse, C., Luhowskyj, S., Hemler, M. E., et al. (1990). VCAM-1 on activated endothelium interacts with the leukocyte integrin VLA-4 at a site distinct from the VLA-4/fibronectin binding site. *Cell* 60, 577–584. doi: 10.1016/0092-8674(90)90661-W

Elsner, J., Oppermann, M., Czech, W., and Kapp, A. (1994). C3a activates the respiratory burst in human polymorphonuclear neutrophilic leukocytes via pertussis toxin-sensitive G-proteins. *Blood* 83, 3324–3331. doi: 10.1182/blood.V83.11.3324.3324

Erdei, A., Lukacsi, S., Macsik-Valent, B., Nagy-Balo, Z., Kurucz, I., and Bajtay, Z. (2019). Non-identical twins: different faces of CR3 and CR4 in myeloid and lymphoid cells of mice and men. *Semin Cell Dev. Biol.* 85, 110–121. doi: 10.1016/j.semcdb.2017.11.025

Fagerholm, S. C., Varis, M., Stefanidakis, M., Hilden, T. J., and Gahmberg, C. G. (2006). alpha-Chain phosphorylation of the human leukocyte CD11b/CD18 (Mac-1) integrin is pivotal for integrin activation to bind ICAMs and leukocyte extravasation. *Blood* 108, 3379–3386. doi: 10.1182/blood-2006-03-013557

Fällman, M., Andersson, R., and Andersson, T. (1993). Signaling properties of CR3 (CD11b/CD18) and CR1 (CD35) in relation to phagocytosis of complement-opsonized particles. *J. Immunol.* 151, 330–338.

Fang, Y., Xu, C., Fu, Y. X., Holers, V. M., and Molina, H. (1998). Expression of complement receptors 1 and 2 on follicular dendritic cells is necessary for the generation of a strong antigen-specific IgG response. *J. Immunol.* 160, 5273–5279.

Faridi, M. H., Khan, S. Q., Zhao, W., Lee, H. W., Altintas, M. M., Zhang, K., et al. (2017). CD11b activation suppresses TLR-dependent inflammation and autoimmunity in systemic lupus erythematosus. *J. Clin. Invest.* 127, 1271–1283. doi: 10.1172/JCI88442

Farzan, M., Schnitzler, C. E., Vasilieva, N., Leung, D., Kuhn, J., Gerard, C., et al. (2001). Sulfated tyrosines contribute to the formation of the C5a docking site of the human C5a anaphylatoxin receptor. *J. Exp. Med.* 193, 1059–1066. doi: 10.1084/jem.193.9.1059

Fearon, D. T. (1980). Identification of the membrane glycoprotein that is the C3b receptor of the human erythrocyte, polymorphonuclear leukocyte, B lymphocyte, and monocyte. *J. Exp. Med.* 152, 20–30. doi: 10.1084/jem.152.1.20

Fearon, D. T., Kaneko, I., and Thomson, G. G. (1981). Membrane distribution and adsorptive endocytosis by C3b receptors on human polymorphonuclear leukocytes. *J. Exp. Med.* 153, 1615–1628. doi: 10.1084/jem.153.6.1615

Fernandez, H. N., Henson, P. M., Otani, A., and Hugli, T. E. (1978). Chemotactic response to human C3a and C5a anaphylatoxins. I. Evaluation of C3a and C5a leukotaxis in vitro and under stimulated *in vivo* conditions. *J. Immunol.* 120, 109–115.

Fernandez, H. N., and Hugli, T. E. (1978). Primary structural analysis of the polypeptide portion of human C5a anaphylatoxin. Polypeptide sequence determination and assignment of the oligosaccharide attachment site in C5a. *J. Biol. Chem.* 253, 6955–6964. doi: 10.1016/S0021-9258(17)38013-4

Filippi, M. D. (2019). Neutrophil transendothelial migration: updates and new perspectives. *Blood* 133, 2149–2158. doi: 10.1182/blood-2018-12-844605

Fingeroth, J. D., Weis, J. J., Tedder, T. F., Strominger, J. L., Biro, P. A., and Fearon, D. T. (1984). Epstein-Barr virus receptor of human B lymphocytes is the C3d receptor CR2. *Proc. Natl. Acad. Sci. U.S.A.* 81, 4510–4514. doi: 10.1073/pnas.81.14.4510

Fischer, W. H., and Hugli, T. E. (1997). Regulation of B cell functions by C3a and C3a(desArg): suppression of TNF-alpha, IL-6, and the polyclonal immune response. *J. Immunol.* 159, 4279–4286.

Flannagan, R. S., Jaumouille, V., and Grinstein, S. (2012). The cell biology of phagocytosis. *Annu. Rev. Pathol.* 7, 61–98. doi: 10.1146/annurev-pathol-011811-132445

Flick, M. J., Du, X., Witte, D. P., Jirouskova, M., Soloviev, D. A., Busuttil, S. J., et al. (2004). Leukocyte engagement of fibrin(ogen) via the integrin receptor alphaMbeta2/Mac-1 is critical for host inflammatory response *in vivo*. *J. Clin. Invest.* 113, 1596–1606. doi: 10.1172/JCI20741

Freeman, S. A., and Grinstein, S. (2014). Phagocytosis: receptors, signal integration, and the cytoskeleton. *Immunol Rev.* 262, 193–215. doi: 10.1111/imr.12212

Füreder, W., Agis, H., Willheim, M., Bankl, H. C., Maier, U., Kishi, K., et al. (1995). Differential expression of complement receptors on human basophils and mast cells. Evidence for mast cell heterogeneity and CD88/C5aR expression on skin mast cells. *J. Immunol.* 155, 3152–3160.

Futosi, K., Fodor, S., and Mócsai, A. (2013). Reprint of Neutrophil cell surface receptors and their intracellular signal transduction pathways. *Int. Immunopharmacol.* 17, 1185–1197. doi: 10.1016/j.intimp.2013.11.010

Gaipl, U. S., Kuenkele, S., Voll, R. E., Beyer, T. D., Kolowos, W., Heyder, P., et al. (2001). Complement binding is an early feature of necrotic and a rather late event during apoptotic cell death. *Cell Death Differ.* 8, 327–334. doi: 10.1038/sj.cdd.4400826

Gasque, P., Singhrao, S. K., Neal, J. W., Wang, P., Sayah, S., Fontaine, M., et al. (1998). The receptor for complement anaphylatoxin C3a is expressed by myeloid cells and nonmyeloid cells in inflamed human central nervous system: analysis in multiple sclerosis and bacterial meningitis. *J. Immunol.* 160, 3543–3554.

Gerard, N. P., Bao, L., Xiao-Ping, H., Eddy, R. L., Shows, T. B., and Gerard, C. (1993). Human chemotaxis receptor genes cluster at 19q13.3-13.4. Characterization of the human C5a receptor gene. *Biochemistry* 32, 1243–1250. doi: 10.1021/bi00056a007

Gerard, N. P., and Gerard, C. (1991). The chemotactic receptor for human C5a anaphylatoxin. *Nature* 349, 614–617. doi: 10.1038/349614a0

Gerhardt, T., and Ley, K. (2015). Monocyte trafficking across the vessel wall. *Cardiovasc Res.* 107, 321–330. doi: 10.1093/cvr/cvv147

Ghiran, I., Barbashov, S. F., Klickstein, L. B., Tas, S. W., Jensenius, J. C., and Nicholson-Weller, A. (2000). Complement receptor 1/CD35 is a receptor for mannan-binding lectin. *J. Exp. Med.* 192, 1797–1808. doi: 10.1084/jem.192.12.1797

Giagulli, C., Ottoboni, L., Caveggion, E., Rossi, B., Lowell, C., Constantin, G., et al. (2006). The Src family kinases Hck and Fgr are dispensable for inside-out, chemoattractant-induced signaling regulating beta 2 integrin affinity and valency in neutrophils, but are required for beta 2 integrin-mediated outside-in signaling involved in sustained adhesion. *J. Immunol.* 177, 604–611. doi: 10.4049/jimmunol.177.1.604

Gigli, I., and Nelson, R. A. (1968). Complement dependent immune phagocytosis. I. Requirements for C'1, C'4, C'2, C'3. *Exp. Cell Res.* 51, 45–67. doi: 10.1016/0014-4827(68)90158-4

Gorgani, N. N., He, J. Q., Katschke, K. J., Helmy, K. Y., Xi, H., Steffek, M., et al. (2008). Complement receptor of the Ig superfamily enhances complement-mediated phagocytosis in a subpopulation of tissue resident macrophages. *J. Immunol.* 181, 7902–7908. doi: 10.4049/jimmunol.181.11.7902

Gregory, S. H., Cousens, L. P., van Rooijen, N., Döpp, E. A., Carlos, T. M., and Wing, E. J. (2002). Complementary adhesion molecules promote neutrophil-Kupffer cell interaction and the elimination of bacteria taken up by the liver. *J. Immunol.* 168, 308–315. doi: 10.4049/jimmunol.168.1.308

Griffin, F. M., Griffin, J. A., Leider, J. E., and Silverstein, S. C. (1975). Studies on the mechanism of phagocytosis. I. Requirements for circumferential attachment of particle-bound ligands to specific receptors on the macrophage plasma membrane. *J. Exp. Med.* 142, 1263–1282. doi: 10.1084/jem.142.5.1263

Guglietta, S., Chiavelli, A., Zagato, E., Krieg, C., Gandini, S., Ravenda, P. S., et al. (2016). Coagulation induced by C3aR-dependent NETosis drives protumorigenic neutrophils during small intestinal tumorigenesis. *Nat. Commun.* 7:11037. doi: 10.1038/ncomms11037

Gullstrand, B., Martensson, U., Sturfelt, G., Bengtsson, A. A., and Truedsson, L. (2009). Complement classical pathway components are all important in clearance of apoptotic and secondary necrotic cells. *Clin. Exp. Immunol.* 156, 303–311. doi: 10.1111/j.1365-2249.2009.03896.x

Hajishengallis, G., Reis, E. S., Mastellos, D. C., Ricklin, D., and Lambris, J. D. (2017). Novel mechanisms and functions of complement. *Nat. Immunol.* 18, 1288–1298. doi: 10.1038/ni.3858

Halai, K., Whiteford, J., Ma, B., Nourshargh, S., and Woodfin, A. (2014). ICAM-2 facilitates luminal interactions between neutrophils and endothelial cells *in vivo*. *J. Cell Sci.* 127(Pt 3), 620–629. doi: 10.1242/jcs.137463

Hall, A. B., Gakidis, M. A., Glogauer, M., Wilsbacher, J. L., Gao, S., Swat, W., et al. (2006). Requirements for Vav guanine nucleotide exchange factors and Rho GTPases in FcgammaR- and complement-mediated phagocytosis. *Immunity* 24, 305–316. doi: 10.1016/j.immuni.2006.02.005

Hannan, J., Young, K., Szakonyi, G., Overduin, M. J., Perkins, S. J., Chen, X., et al. (2002). Structure of complement receptor (CR) 2 and CR2-C3d complexes. *Biochem. Soc. Trans.* 30(Pt 6), 983–989. doi: 10.1042/bst0300983

Hannan, J. P., Young, K. A., Guthridge, J. M., Asokan, R., Szakonyi, G., Chen, X. S., et al. (2005). Mutational analysis of the complement receptor type 2 (CR2/CD21)-C3d interaction reveals a putative charged SCR1 binding site for C3d. *J. Mol. Biol.* 346, 845–858. doi: 10.1016/j.jmb.2004.12.007

Hartmann, K., Henz, B. M., Krüger-Krasagakes, S., Köhl, J., Burger, R., Guhl, S., et al. (1997). C3a and C5a stimulate chemotaxis of human mast cells. *Blood* 89, 2863–2870. doi: 10.1182/blood.V89.8.2863

Haviland, D. L., McCoy, R. L., Whitehead, W. T., Akama, H., Molmenti, E. P., Brown, A., et al. (1995). Cellular expression of the C5a anaphylatoxin receptor (C5aR): demonstration of C5aR on nonmyeloid cells of the liver and lung. *J. Immunol.* 154, 1861–1869.

Helmy, K. Y., Katschke, K. J., Gorgani, N. N., Kljavin, N. M., Elliott, J. M., Diehl, L., et al. (2006). CRIg: a macrophage complement receptor required for phagocytosis of circulating pathogens. *Cell* 124, 915–927. doi: 10.1016/j.cell.2005.12.039

Ho, M. K., and Springer, T. A. (1982). Mac-1 antigen: quantitative expression in macrophage populations and tissues, and immunofluorescent localization in spleen. *J. Immunol.* 128, 2281–2286.

Hogg, N., Stewart, M. P., Scarth, S. L., Newton, R., Shaw, J. M., Law, S. K., et al. (1999). A novel leukocyte adhesion deficiency caused by expressed but nonfunctional beta2 integrins Mac-1 and LFA-1. *J. Clin. Invest.* 103, 97–106. doi: 10.1172/JCI3312

Holers, V. M. (2014). Complement and its receptors: new insights into human disease. *Annu. Rev. Immunol.* 32, 433–459. doi: 10.1146/annurev-immunol-032713-120154

Hornum, L., Hansen, A. J., Tornehave, D., Fjording, M. S., Colmenero, P., Wätjen, I. F., et al. (2017). C5a and C5aR are elevated in joints of rheumatoid and psoriatic arthritis patients, and C5aR blockade attenuates leukocyte migration to synovial fluid. *PLoS ONE* 12:e0189017. doi: 10.1371/journal.pone.0189017

Horwitz, M. A., and Silverstein, S. C. (1980). Influence of the Escherichia coli capsule on complement fixation and on phagocytosis and killing by human phagocytes. *J. Clin. Invest.* 65, 82–94. doi: 10.1172/JCI109663

Hu, C., Li, L., Ding, P., Ge, X., Zheng, L., Wang, X., et al. (2019). Complement Inhibitor CRIg/FH Ameliorates Renal Ischemia Reperfusion Injury via Activation of PI3K/AKT Signaling. *J. Immunol.* 201, 3717–3730. doi: 10.4049/jimmunol.1800987

Huang, M. T., Larbi, K. Y., Scheiermann, C., Woodfin, A., Gerwin, N., Haskard, D. O., et al. (2006). ICAM-2 mediates neutrophil transmigration *in vivo*: evidence for stimulus specificity and a role in PECAM-1-independent transmigration. *Blood* 107, 4721–4727. doi: 10.1182/blood-2005-11-4683

Huber, R., Scholze, H., Påques, E. P., and Deisenhofer, J. (1980). Crystal structure analysis and molecular model of human C3a anaphylatoxin. *Hoppe Seylers Z Physiol Chem* 361, 1389–1399. doi: 10.1515/bchm2.1980.361.2.1389

Hugli, T. E. (1975). Human anaphylatoxin (C3a) from the third component of complement. Primary structure. *J. Biol. Chem.* 250, 8293–8301. doi: 10.1016/S0021-9258(19)40758-8

Huo, Y., Hafezi-Moghadam, A., and Ley, K. (2000). Role of vascular cell adhesion molecule-1 and fibronectin connecting segment-1 in monocyte rolling and adhesion on early atherosclerotic lesions. *Circ. Res.* 87, 153–159. doi: 10.1161/01.RES.87.2.153

Hyams, C., Camberlein, E., Cohen, J. M., Bax, K., and Brown, J. S. (2010). The Streptococcus pneumoniae capsule inhibits complement activity and neutrophil phagocytosis by multiple mechanisms. *Infect. Immun.* 78, 704–715. doi: 10.1128/IAI.00881-09

Hyduk, S. J., Chan, J. R., Duffy, S. T., Chen, M., Peterson, M. D., Waddell, T. K., et al. (2007). Phospholipase C, calcium, and calmodulin are critical for alpha4beta1 integrin affinity up-regulation and monocyte arrest triggered by chemoattractants. *Blood* 109, 176–184. doi: 10.1182/blood-2006-01-029199

Hynes, R. O. (1992). Integrins: versatility, modulation, and signaling in cell adhesion. *Cell* 69, 11–25. doi: 10.1016/0092-8674(92)90115-S

Iida, K., and Nussenzweig, V. (1981). Complement receptor is an inhibitor of the complement cascade. *J. Exp. Med.* 153, 1138–1150. doi: 10.1084/jem.153.5.1138

Imrie, H. J., and Jones, D. R. (1997). Complement coating of erythrocytes is reduced following their interaction with neutrophils in vitro without loss of complement receptor 1 (CR1). *Clin. Exp. Immunol.* 109, 217–222. doi: 10.1046/j.1365-2249.1997.4151312.x

Jacobson, A. C., and Weis, J. H. (2008). Comparative functional evolution of human and mouse CR1 and CR2. *J. Immunol.* 181, 2953–2959. doi: 10.4049/jimmunol.181.5.2953

Jaumouille, V., Cartagena-Rivera, A. X., and Waterman, C. M. (2019). Coupling of beta2 integrins to actin by a mechanosensitive molecular clutch drives complement receptor-mediated phagocytosis. *Nat. Cell Biol.* 21, 1357–1369. doi: 10.1038/s41556-019-0414-2

Johnson, A. R., Hugli, T. E., and Müller-Eberhard, H. J. (1975). Release of histamine from rat mast cells by the complement peptides C3a and C5a. *Immunology* 28, 1067–1080.

Jongstra-Bilen, J., Harrison, R., and Grinstein, S. (2003). Fcgamma-receptors induce Mac-1 (CD11b/CD18) mobilization and accumulation in the phagocytic cup for optimal phagocytosis. *J. Biol. Chem.* 278, 45720–45729. doi: 10.1074/jbc.M303704200

Jung, K., Kang, M., Park, C., Hyun Choi, Y., Jeon, Y., Park, S. H., et al. (2012). Protective role of V-set and immunoglobulin domain-containing 4 expressed on kupffer cells during immune-mediated liver injury by inducing tolerance of liver T- and natural killer T-cells. *Hepatology* 56, 1838–1848. doi: 10.1002/hep.25906

Kamitaki, N., Sekar, A., Handsaker, R. E., de Rivera, H., Tooley, K., Morris, D. L., et al. (2020). Complement genes contribute sex-biased vulnerability in diverse disorders. *Nature* 582, 577–581. doi: 10.1038/s41586-020-2277-x

Kaplan, G. (1977). Differences in the mode of phagocytosis with Fc and C3 receptors in macrophages. *Scand J. Immunol.* 6, 797–807. doi: 10.1111/j.1365-3083.1977.tb02153.x

Katschke, K. J., Helmy, K. Y., Steffek, M., Xi, H., Yin, J., Lee, W. P., et al. (2007). A novel inhibitor of the alternative pathway of complement reverses inflammation and bone destruction in experimental arthritis. *J. Exp. Med.* 204, 1319–1325. doi: 10.1084/jem.20070432

Keizer, G. D., Te Velde, A. A., Schwarting, R., Figdor, C. G., and De Vries, J. E. (1987). Role of p150,95 in adhesion, migration, chemotaxis and phagocytosis of human monocytes. *Eur. J. Immunol.* 17, 1317–1322. doi: 10.1002/eji.1830170915

Kienle, K., and Lämmermann, T. (2016). Neutrophil swarming: an essential process of the neutrophil tissue response. *Immunol. Rev.* 273, 76–93. doi: 10.1111/imr.12458

Kim, Y. U., Kinoshita, T., Molina, H., Hourcade, D., Seya, T., Wagner, L. M., et al. (1995). Mouse complement regulatory protein Crry/p65 uses the specific mechanisms of both human decay-accelerating factor and membrane cofactor protein. *J. Exp. Med.* 181, 151–159. doi: 10.1084/jem.181.1.151

Kinoshita, T., Lavoie, S., and Nussenzweig, V. (1985). Regulatory proteins for the activated third and fourth components of complement (C3b and C4b) in mice. II. Identification and properties of complement receptor type 1 (CR1). *J. Immunol.* 134, 2564–2570.

Klapproth, S., Sperandio, M., Pinheiro, E. M., Prunster, M., Soehnlein, O., Gertler, F. B., et al. (2015). Loss of the Rap1 effector RIAM results in leukocyte adhesion deficiency due to impaired beta2 integrin function in mice. *Blood* 126, 2704–2712. doi: 10.1182/blood-2015-05-647453

Klaus, G. G., and Humphrey, J. H. (1977). The generation of memory cells. I. The role of C3 in the generation of B memory cells. *Immunology* 33, 31–40.

Klickstein, L. B., Bartow, T. J., Miletic, V., Rabson, L. D., Smith, J. A., and Fearon, D. T. (1988). Identification of distinct C3b and C4b recognition sites in the human C3b/C4b receptor (CR1, CD35) by deletion mutagenesis. *J. Exp. Med.* 168, 1699–1717. doi: 10.1084/jem.168.5.1699

Kouser, L., Madhukaran, S. P., Shastri, A., Saraon, A., Ferluga, J., Al-Mozaini, M., et al. (2015). Emerging and Novel Functions of Complement Protein C1q. *Front. Immunol.* 6:317. doi: 10.3389/fimmu.2015.00317

Krych, M., Hourcade, D., and Atkinson, J. P. (1991). Sites within the complement C3b/C4b receptor important for the specificity of ligand binding. *Proc. Natl. Acad. Sci. U.S.A.* 88, 4353–4357. doi: 10.1073/pnas.88.10.4353

Kürzinger, K., Reynolds, T., Germain, R. N., Davignon, D., Martz, E., and Springer, T. A. (1981). A novel lymphocyte function-associated antigen (LFA-1): cellular distribution, quantitative expression, and structure. *J. Immunol.* 127, 596–602.

Kuwano, Y., Spelten, O., Zhang, H., Ley, K., and Zarbock, A. (2010). Rolling on E- or P-selectin induces the extended but not high-affinity conformation of LFA-1 in neutrophils. *Blood* 116, 617–624. doi: 10.1182/blood-2010-01-266122

Lämmermann, T. (2016). In the eye of the neutrophil swarm-navigation signals that bring neutrophils together in inflamed and infected tissues. *J. Leukoc. Biol.* 100, 55–63. doi: 10.1189/jlb.1MR0915-403

Lämmermann, T., Afonso, P. V., Angermann, B. R., Wang, J. M., Kastenmüller, W., Parent, C. A., et al. (2013). Neutrophil swarms require LTB4 and integrins at sites of cell death *in vivo*. *Nature* 498, 371–375. doi: 10.1038/nature12175

Lämmermann, T., Bader, B. L., Monkley, S. J., Worbs, T., Wedlich-Söldner, R., Hirsch, K., et al. (2008). Rapid leukocyte migration by integrin-independent flowing and squeezing. *Nature* 453, 51–55. doi: 10.1038/nature06887

Langnaese, K., Colleaux, L., Kloos, D. U., Fontes, M., and Wieacker, P. (2000). Cloning of Z39Ig, a novel gene with immunoglobulin-like domains located on human chromosome X. *Biochim Biophys Acta* 1492, 522–525. doi: 10.1016/S0167-4781(00)00131-7

Le Cabec, V., Carreno, S., Moisand, A., Bordier, C., and Maridonneau-Parini, I. (2002). Complement receptor 3 (CD11b/CD18) mediates type I and type II phagocytosis during nonopsonic and opsonic phagocytosis, respectively. *J. Immunol.* 169, 2003–2009. doi: 10.4049/jimmunol.169.4.2003

Lee, J. O., Rieu, P., Arnaout, M. A., and Liddington, R. (1995). Crystal structure of the A domain from the alpha subunit of integrin CR3 (CD11b/CD18). *Cell* 80, 631–638. doi: 10.1016/0092-8674(95)90517-0

Lefort, C. T., and Ley, K. (2012). Neutrophil arrest by LFA-1 activation. *Front. Immunol.* 3:157. doi: 10.3389/fimmu.2012.00157

Lewis, M. J., and Botto, M. (2006). Complement deficiencies in humans and animals: links to autoimmunity. *Autoimmunity* 39, 367–378. doi: 10.1080/08916930600739233

Li, X. X., Lee, J. D., Kemper, C., and Woodruff, T. M. (2019). The complement receptor C5aR2: a powerful modulator of innate and adaptive immunity. *J. Immunol.* 202, 3339–3348. doi: 10.4049/jimmunol.1900371

Lieberman, L. A., Mizui, M., Nalbandian, A., Bossé R., Crispín, J. C., and Tsokos, G. C. (2015). Complement receptor of the immunoglobulin superfamily reduces murine lupus nephritis and cutaneous disease. *Clin. Immunol.* 160, 286–291. doi: 10.1016/j.clim.2015.05.006

Liu, G., Fu, Y., Yosri, M., Chen, Y., Sun, P., Xu, J., et al. (2016). CRIg plays an essential role in intravascular clearance of bloodborne parasites by interacting with complement. *Proc. Natl. Acad. Sci. U.S.A.* 116, 24214–20. doi: 10.1073/pnas.1913443116

Liu, J. R., Han, X., Soriano, S. G., and Yuki, K. (2014). The role of macrophage 1 antigen in polymicrobial sepsis. *Shock* 42, 532–539. doi: 10.1097/SHK.0000000000000250

Luo, B. H., Carman, C. V., and Springer, T. A. (2007). Structural basis of integrin regulation and signaling. *Annu. Rev. Immunol.* 25, 619–647. doi: 10.1146/annurev.immunol.25.022106.141618

Mantovani, B. (1975). Different roles of IgG and complement receptors in phagocytosis by polymorphonuclear leukocytes. *J. Immunol.* 115, 15–17.

Markiewski, M. M., Mastellos, D., Tudoran, R., DeAngelis, R. A., Strey, C. W., Franchini, S., et al. (2004). C3a and C3b activation products of the third component of complement (C3) are critical for normal liver recovery after toxic injury. *J. Immunol.* 173, 747–754. doi: 10.4049/jimmunol.173.2.747

Marshall, K. M., He, S., Zhong, Z., Atkinson, C., and Tomlinson, S. (2014). Dissecting the complement pathway in hepatic injury and regeneration with a novel protective strategy. *J. Exp. Med.* 211, 1793–1805. doi: 10.1084/jem.20131902

Martin, U., Bock, D., Arseniev, L., Tornetta, M. A., Ames, R. S., Bautsch, W., et al. (1997). The human C3a receptor is expressed on neutrophils and monocytes, but not on B or T lymphocytes. *J. Exp. Med.* 186, 199–207. doi: 10.1084/jem.186.2.199

Masaki, T., Matsumoto, M., Nakanishi, I., Yasuda, R., and Seya, T. (1992). Factor I-dependent inactivation of human complement C4b of the classical pathway by C3b/C4b receptor (CR1, CD35) and membrane cofactor protein (MCP, CD46). *J. Biochem.* 111, 573–578. doi: 10.1093/oxfordjournals.jbchem.a123799

Massena, S., Christoffersson, G., Hjertström, E., Zcharia, E., Vlodavsky, I., Ausmees, N., et al. (2010). A chemotactic gradient sequestered on endothelial heparan sulfate induces directional intraluminal crawling of neutrophils. *Blood* 116, 1924–1931. doi: 10.1182/blood-2010-01-266072

Mastellos, D., Papadimitriou, J. C., Franchini, S., Tsonis, P. A., and Lambris, J. D. (2001). A novel role of complement: mice deficient in the fifth component of complement (C5) exhibit impaired liver regeneration. *J. Immunol.* 166, 2479–2486. doi: 10.4049/jimmunol.166.4.2479

Mastellos, D. C., Ricklin, D., and Lambris, J. D. (2019). Clinical promise of next-generation complement therapeutics. *Nat. Rev. Drug Discov.* 18, 707–729. doi: 10.1038/s41573-019-0031-6

Mathew, E. C., Shaw, J. M., Bonilla, F. A., Law, S. K., and Wright, D. A. (2000). A novel point mutation in CD18 causing the expression of dysfunctional CD11/CD18 leucocyte integrins in a patient with leucocyte adhesion deficiency (LAD). *Clin. Exp. Immunol.* 121, 133–138. doi: 10.1046/j.1365-2249.2000.01277.x

Matthews, K. W., Mueller-Ortiz, S. L., and Wetsel, R. A. (2004). Carboxypeptidase N: a pleiotropic regulator of inflammation. *Mol. Immunol.* 40, 785–793. doi: 10.1016/j.molimm.2003.10.002

May, R. C., Caron, E., Hall, A., and Machesky, L. M. (2000). Involvement of the Arp2/3 complex in phagocytosis mediated by FcgammaR or CR3. *Nat. Cell Biol.* 2, 246–248. doi: 10.1038/35008673

May, R. C., and Machesky, L. M. (2001). Phagocytosis and the actin cytoskeleton. *J. Cell Sci.* 114(Pt 6), 1061–1077.

McEver, R. P. (2002). Selectins: lectins that initiate cell adhesion under flow. *Curr. Opin. Cell Biol.* 14, 581–586. doi: 10.1016/S0955-0674(02)00367-8

Medzhitov, R. (2008). Origin and physiological roles of inflammation. *Nature* 454, 428–435. doi: 10.1038/nature07201

Meerschaert, J., and Furie, M. B. (1995). The adhesion molecules used by monocytes for migration across endothelium include CD11a/CD18, CD11b/CD18, and VLA-4 on monocytes and ICAM-1, VCAM-1, and other ligands on endothelium. *J. Immunol.* 154, 4099–4112.

Merle, N. S., Church, S. E., Fremeaux-Bacchi, V., and Roumenina, L. T. (2015). Complement System Part I - Molecular Mechanisms of Activation and Regulation. *Front. Immunol.* 6:262. doi: 10.3389/fimmu.2015.00262

Mery, L., and Boulay, F. (1994). The NH2-terminal region of C5aR but not that of FPR is critical for both protein transport and ligand binding. *J. Biol. Chem.* 269, 3457–3463. doi: 10.1016/S0021-9258(17)41884-9

Mevorach, D., Mascarenhas, J. O., Gershov, D., and Elkon, K. B. (1998). Complement-dependent clearance of apoptotic cells by human macrophages. *J. Exp. Med.* 188, 2313–2320. doi: 10.1084/jem.188.12.2313

Michishita, M., Videm, V., and Arnaout, M. A. (1993). A novel divalent cation-binding site in the A domain of the beta 2 integrin CR3 (CD11b/CD18) is essential for ligand binding. *Cell* 72, 857–867. doi: 10.1016/0092-8674(93)90575-B

Middleton, J., Neil, S., Wintle, J., Clark-Lewis, I., Moore, H., Lam, C., et al. (1997). Transcytosis and surface presentation of IL-8 by venular endothelial cells. *Cell* 91, 385–395. doi: 10.1016/S0092-8674(00)80422-5

Miot, S., Marfurt, J., Lach-Trifilieff, E., González-Rubio, C., López-Trascasa, M., Sadallah, S., et al. (2002). The mechanism of loss of CR1 during maturation of

erythrocytes is different between factor I deficient patients and healthy donors. *Blood Cells Mol. Dis.* 29, 200–212. doi: 10.1006/bcmd.2002.0559

Miyabe, Y., Miyabe, C., Mani, V., Mempel, T. R., and Luster, A. D. (2019). Atypical complement receptor C5aR2 transports C5a to initiate neutrophil adhesion and inflammation. *Sci. Immunol.* 4:eaav5951. doi: 10.1126/sciimmunol.aav5951

Miyabe, Y., Miyabe, C., Murooka, T. T., Kim, E. Y., Newton, G. A., Kim, N. D., et al. (2017). Complement C5a Receptor is the key initiator of neutrophil adhesion igniting immune complex-induced arthritis. *Sci. Immunol.* 2:eaaj2195. doi: 10.1126/sciimmunol.aaj2195

Molina, H., Kinoshita, T., Webster, C. B., and Holers, V. M. (1994). Analysis of C3b/C3d binding sites and factor I cofactor regions within mouse complement receptors 1 and 2. *J. Immunol.* 153, 789–795.

Moon, K. E., Gorski, J. P., and Hugli, T. E. (1981). Complete primary structure of human C4a anaphylatoxin. *J. Biol. Chem.* 256, 8685–8692. doi: 10.1016/S0021-9258(19)68898-8

Morgan, E. L., Ember, J. A., Sanderson, S. D., Scholz, W., Buchner, R., Ye, R. D., et al. (1993). Anti-C5a receptor antibodies. Characterization of neutralizing antibodies specific for a peptide, C5aR, derived from the predicted amino-terminal sequence of the human C5a receptor. *J. Immunol.* 151, 377–388.

Moser, M., Nieswandt, B., Ussar, S., Pozgajova, M., and Fässler, R. (2008). Kindlin-3 is essential for integrin activation and platelet aggregation. *Nat. Med.* 14, 325–330. doi: 10.1038/nm1722

Muller, W. A. (2013). Getting leukocytes to the site of inflammation. *Vet. Pathol.* 50, 7–22. doi: 10.1177/0300985812469883

Müller-Eberhard, H. J. (1986). The membrane attack complex of complement. *Annu. Rev. Immunol.* 4, 503–528. doi: 10.1146/annurev.iy.04.040186.002443

Munawara, U., Perveen, K., Small, A. G., Putty, T., Quach, A., Gorgani, N. N., et al. (2019). Human dendritic cells express the complement receptor immunoglobulin which regulates T cell responses. *Front. Immunol.* 10:2892. doi: 10.3389/fimmu.2019.02892

Nakao, M., and Somamoto, T. (2016). "Chapter 6 - the evolution of complement system functions and pathways in vertebrates, in *The Evolution of the Immune System*, ed M. Davide (Academic Press), 151–171. doi: 10.1016/B978-0-12-801975-7.00006-2

Nataf, S., Davoust, N., Ames, R. S., and Barnum, S. R. (1999). Human T cells express the C5a receptor and are chemoattracted to C5a. *J. Immunol.* 162, 4018–4023.

Nath, S. K., Han, S., Kim-Howard, X., Kelly, J. A., Viswanathan, P., Gilkeson, G. S., et al. (2008). A nonsynonymous functional variant in integrin-alpha(M) (encoded by ITGAM) is associated with systemic lupus erythematosus. *Nat. Genet.* 40, 152–154. doi: 10.1038/ng.71

Nelson, R. A. (1953). The immune-adherence phenomenon; an immunologically specific reaction between microorganisms and erythrocytes leading to enhanced phagocytosis. *Science* 118, 733–737. doi: 10.1126/science.118.3077.733

Nermut, M. V., Green, N. M., Eason, P., Yamada, S. S., and Yamada, K. M. (1988). Electron microscopy and structural model of human fibronectin receptor. *EMBO J.* 7, 4093–4099. doi: 10.1002/j.1460-2075.1988.tb03303.x

Neupane, A. S., Willson, M., Chojnacki, A. K., Vargas, E. S. C. F., Morehouse, C., Carestia, A., et al. (2020). Patrolling alveolar macrophages conceal bacteria from the immune system to maintain homeostasis. *Cell* 183, 110–125.e11. doi: 10.1016/j.cell.2020.08.020

Newman, S. L., Becker, S., and Halme, J. (1985). Phagocytosis by receptors for C3b (CR1), iC3b (CR3), and IgG (Fc) on human peritoneal macrophages. *J. Leukoc. Biol.* 38, 267–278. doi: 10.1002/jlb.38.2.267

Newman, S. L., Devery-Pocius, J. E., Ross, G. D., and Henson, P. M. (1984). Phagocytosis by human monocyte-derived macrophages. Independent function of receptors for C3b (CR1) and iC3b (CR3). *Complement* 1, 213–227. doi: 10.1159/000467840

Nishida, N., Xie, C., Shimaoka, M., Cheng, Y., Walz, T., and Springer, T. A. (2006). Activation of leukocyte beta2 integrins by conversion from bent to extended conformations. *Immunity* 25, 583–594. doi: 10.1016/j.immuni.2006.07.016

Nonaka, M. (2014). Evolution of the complement system. *Subcell Biochem.* 80, 31–43. doi: 10.1007/978-94-017-8881-6_3

Nordenfelt, P., and Tapper, H. (2011). Phagosome dynamics during phagocytosis by neutrophils. *J. Leukoc. Biol.* 90, 271–284. doi: 10.1189/jlb.0810457

Norgauer, J., Dobos, G., Kownatzki, E., Dahinden, C., Burger, R., Kupper, R., et al. (1993). Complement fragment C3a stimulates Ca2+ influx in neutrophils via a pertussis-toxin-sensitive G protein. *Eur. J. Biochem.* 217, 289–294. doi: 10.1111/j.1432-1033.1993.tb18245.x

Ohno, M., Hirata, T., Enomoto, M., Araki, T., Ishimaru, H., and Takahashi, T. A. (2000). A putative chemoattractant receptor, C5L2, is expressed in granulocyte and immature dendritic cells, but not in mature dendritic cells. *Mol. Immunol.* 37, 407–412. doi: 10.1016/S0161-5890(00)00067-5

Okinaga, S., Slattery, D., Humbles, A., Zsengeller, Z., Morteau, O., Kinrade, M. B., et al. (2003). C5L2, a nonsignaling C5A binding protein. *Biochemistry* 42, 9406–9415. doi: 10.1021/bi034489v

Olazabal, I. M., Caron, E., May, R. C., Schilling, K., Knecht, D. A., and Machesky, L. M. (2002). Rho-kinase and myosin-II control phagocytic cup formation during CR, but not FcgammaR, phagocytosis. *Curr. Biol.* 12, 1413–1418. doi: 10.1016/S0960-9822(02)01069-2

Ottonello, L., Corcione, A., Tortolina, G., Airoldi, I., Albesiano, E., Favre, A., et al. (1999). rC5a directs the in vitro migration of human memory and naive tonsillar B lymphocytes: implications for B cell trafficking in secondary lymphoid tissues. *J. Immunol.* 162, 6510–6517.

Palazzo, A. F., Cook, T. A., Alberts, A. S., and Gundersen, G. G. (2001). mDia mediates Rho-regulated formation and orientation of stable microtubules. *Nat. Cell Biol.* 3, 723–729. doi: 10.1038/35087035

Palmer, L. J., Damgaard, C., Holmstrup, P., and Nielsen, C. H. (2016). Influence of complement on neutrophil extracellular trap release induced by bacteria. *J. Periodontal. Res.* 51, 70–76. doi: 10.1111/jre.12284

Paral, D., Sohns, B., Crass, T., Grove, M., Köhl, J., Klos, A., et al. (1998). Genomic organization of the human C3a receptor. *Eur. J. Immunol.* 28, 2417–2423.

Pascual, M., Danielsson, C., Steiger, G., and Schifferli, J. A. (1994). Proteolytic cleavage of CR1 on human erythrocytes *in vivo*: evidence for enhanced cleavage in AIDS. *Eur. J. Immunol.* 24, 702–708. doi: 10.1002/eji.1830240332

Patel, P. C., and Harrison, R. E. (2008). Membrane ruffles capture C3bi-opsonized particles in activated macrophages. *Mol. Biol. Cell* 19, 4628–4639. doi: 10.1091/mbc.e08-02-0223

Phillipson, M., Heit, B., Colarusso, P., Liu, L., Ballantyne, C. M., and Kubes, P. (2006). Intraluminal crawling of neutrophils to emigration sites: a molecularly distinct process from adhesion in the recruitment cascade. *J. Exp. Med.* 203, 2569–2575. doi: 10.1084/jem.20060925

Prado-Alvarez, M., Rotllant, J., Gestal, C., Novoa, B., and Figueras, A. (2009). Characterization of a C3 and a factor B-like in the carpet-shell clam, Ruditapes decussatus. *Fish Shellfish Immunol.* 26, 305–315. doi: 10.1016/j.fsi.2008.11.015

Prince, J. E., Brayton, C. F., Fossett, M. C., Durand, J. A., Kaplan, S. L., Smith, C. W., et al. (2001). The differential roles of LFA-1 and Mac-1 in host defense against systemic infection with Streptococcus pneumoniae. *J. Immunol.* 166, 7362–7369. doi: 10.4049/jimmunol.166.12.7362

Proebstl, D., Voisin, M. B., Woodfin, A., Whiteford, J., D'Acquisto, F., Jones, G. E., et al. (2012). Pericytes support neutrophil subendothelial cell crawling and breaching of venular walls *in vivo*. *J. Exp. Med.* 209, 1219–1234. doi: 10.1084/jem.20111622

Qiao, Q., Teng, X., Wang, N., Lu, R., Guo, L., Zhang, X., et al. (2018). A novel CRIg-targeted complement inhibitor protects cells from complement damage. *FASEB J.* 28, 4986–99. doi: 10.1096/fj.14-258046

Raffetseder, U., Röper, D., Mery, L., Gietz, C., Klos, A., Grötzinger, J., et al. (1996). Site-directed mutagenesis of conserved charged residues in the helical region of the human C5a receptor. Arg2O6 determines high-affinity binding sites of C5a receptor. *Eur. J. Biochem.* 235, 82–90. doi: 10.1111/j.1432-1033.1996.00082.x

Ratajczak, J., Reca, R., Kucia, M., Majka, M., Allendorf, D. J., Baran, J. T., et al. (2004). Mobilization studies in mice deficient in either C3 or C3a receptor (C3aR) reveal a novel role for complement in retention of hematopoietic stem/progenitor cells in bone marrow. *Blood* 103, 2071–2078. doi: 10.1182/blood-2003-06-2099

Reca, R., Mastellos, D., Majka, M., Marquez, L., Ratajczak, J., Franchini, S., et al. (2003). Functional receptor for C3a anaphylatoxin is expressed by normal hematopoietic stem/progenitor cells, and C3a enhances their homing-related responses to SDF-1. *Blood* 101, 3784–3793. doi: 10.1182/blood-2002-10-3233

Reid, K. B., Bentley, D. R., Campbell, R. D., Chung, L. P., Sim, R. B., Kristensen, T., et al. (1986). Complement system proteins which interact with C3b or C4b A superfamily of structurally related proteins. *Immunol. Today* 7, 230–234. doi: 10.1016/0167-5699(86)90110-6

Reinhardt, P. H., Elliott, J. F., and Kubes, P. (1997). Neutrophils can adhere via alpha4beta1-integrin under flow conditions. *Blood* 89, 3837–3846. doi: 10.1182/blood.V89.10.3837

Reynes, M., Aubert, J. P., Cohen, J. H., Audouin, J., Tricottet, V., Diebold, J., et al. (1985). Human follicular dendritic cells express CR1, CR2, and CR3 complement receptor antigens. *J. Immunol.* 135, 2687–2694.

Ricklin, D., Hajishengallis, G., Yang, K., and Lambris, J. D. (2010). Complement: a key system for immune surveillance and homeostasis. *Nat. Immunol.* 11, 785–797. doi: 10.1038/ni.1923

Ricklin, D., Mastellos, D. C., and Lambris, J. D. (2019). Therapeutic targeting of the complement system. *Nat. Rev. Drug Discov.* doi: 10.1038/s41573-019-0055-y

Rødgaard, A., Christensen, L. D., Thomsen, B. S., Wiik, A., and Bendixen, G. (1991). Complement receptor type 1 (CR1, CD35) expression on peripheral T lymphocytes: both CD4- and CD8-positive cells express CR1. *Complement Inflamm.* 8, 303–309. doi: 10.1159/000463200

Rosetti, F., and Mayadas, T. N. (2016). The many faces of Mac-1 in autoimmune disease. *Immunol Rev* 269, 175–193. doi: 10.1111/imr.12373

Ross, G. D., Cain, J. A., Myones, B. L., Newman, S. L., and Lachmann, P. J. (1987). Specificity of membrane complement receptor type three (CR3) for beta-glucans. *Complement* 4, 61–74. doi: 10.1159/000463010

Ross, G. D., Reed, W., Dalzell, J. G., Becker, S. E., and Hogg, N. (1992). Macrophage cytoskeleton association with CR3 and CR4 regulates receptor mobility and phagocytosis of iC3b-opsonized erythrocytes. *J. Leukoc. Biol.* 51, 109–117. doi: 10.1002/jlb.51.2.109

Ross, G. D., and Vetvicka, V. (1993). CR3 (CD11b, CD18): a phagocyte and NK cell membrane receptor with multiple ligand specificities and functions. *Clin. Exp. Immunol.* 92, 181–184. doi: 10.1111/j.1365-2249.1993.tb03377.x

Ross, G. D., Yount, W. J., Walport, M. J., Winfield, J. B., Parker, C. J., Fuller, C. R., et al. (1985). Disease-associated loss of erythrocyte complement receptors (CR1, C3b receptors) in patients with systemic lupus erythematosus and other diseases involving autoantibodies and/or complement activation. *J. Immunol.* 135, 2005–2014.

Rotty, J. D., Brighton, H. E., Craig, S. L., Asokan, S. B., Cheng, N., Ting, J. P., et al. (2017). Arp2/3 complex is required for macrophage integrin functions but Is dispensable for FcR phagocytosis and *in vivo* motility. *Dev. Cell* 42, 498–513.e6. doi: 10.1016/j.devcel.2017.08.003

Sacks, T., Moldow, C. F., Craddock, P. R., Bowers, T. K., and Jacob, H. S. (1978). Oxygen radicals mediate endothelial cell damage by complement-stimulated granulocytes. An in vitro model of immune vascular damage. *J. Clin. Invest.* 61, 1161–1167. doi: 10.1172/JCI109031

Sadik, C. D., Miyabe, Y., Sezin, T., and Luster, A. D. (2018). The critical role of C5a as an initiator of neutrophil-mediated autoimmune inflammation of the joint and skin. *Semin Immunol.* 37, 21–29. doi: 10.1016/j.smim.2018.03.002

Sampson, L. L., Heuser, J., and Brown, E. J. (1991). Cytokine regulation of complement receptor-mediated ingestion by mouse peritoneal macrophages. M-CSF and IL-4 activate phagocytosis by a common mechanism requiring autostimulation by IFN-beta. *J. Immunol.* 146, 1005–1013.

Sanchez-Madrid, F., Nagy, J. A., Robbins, E., Simon, P., and Springer, T. A. (1983). A human leukocyte differentiation antigen family with distinct alpha-subunits and a common beta-subunit: the lymphocyte function-associated antigen (LFA-1), the C3bi complement receptor (OKM1/Mac-1), and the p150,95 molecule. *J. Exp. Med.* 158, 1785–1803. doi: 10.1084/jem.158.6.1785

Sándor, N., Lukácsi, S., Ungai-Salánki, R., Orgován, N., Szabó B., Horváth, R., et al. (2016). CD11c/CD18 dominates adhesion of human monocytes, macrophages and dendritic cells over CD11b/CD18. *PLoS ONE* 11:e0163120. doi: 10.1371/journal.pone.0163120

Schenkel, A. R., Mamdouh, Z., and Muller, W. A. (2004). Locomotion of monocytes on endothelium is a critical step during extravasation. *Nat. Immunol.* 5, 393–400. doi: 10.1038/ni1051

Scribner, D. J., and Fahrney, D. (1976). Neutrophil receptors for IgG and complement: their roles in the attachment and ingestion phases of phagocytosis. *J. Immunol.* 116, 892–897.

Sekiguchi, R., and Nonaka, M. (2015). Evolution of the complement system in protostomes revealed by de novo transcriptome analysis of six species of Arthropoda. *Dev. Comp. Immunol.* 50, 58–67. doi: 10.1016/j.dci.2014.12.008

Sengeløv, H., Kjeldsen, L., Kroeze, W., Berger, M., and Borregaard, N. (1994). Secretory vesicles are the intracellular reservoir of complement receptor 1 in human neutrophils. *J. Immunol.* 153, 804–810.

Shaw, S. K., Ma, S., Kim, M. B., Rao, R. M., Hartman, C. U., Froio, R. M., et al. (2004). Coordinated redistribution of leukocyte LFA-1 and endothelial cell ICAM-1 accompany neutrophil transmigration. *J. Exp. Med.* 200, 1571–1580. doi: 10.1084/jem.20040965

Shi, Y., Yao, W., Sun, L., Li, G., Liu, H., Ding, P., et al. (2019). The new complement inhibitor CRIg/FH ameliorates lupus nephritis in lupus-prone MRL/lpr mice. *BMC Nephrol.* 20:424. doi: 10.1186/s12882-019-1599-0

Shin, H. S., Smith, M. R., and Wood, W. B. (1969). Heat labile opsonins to pneumococcus. II. Involvement of C3 and C5. *J. Exp. Med.* 130, 1229–1241. doi: 10.1084/jem.130.6.1229

Shin, H. S., Snyderman, R., Friedman, E., Mellors, A., and Mayer, M. M. (1968). Chemotactic and anaphylatoxic fragment cleaved from the fifth component of guinea pig complement. *Science* 162, 361–363. doi: 10.1126/science.162.3851.361

Siciliano, S. J., Rollins, T. E., DeMartino, J., Konteatis, Z., Malkowitz, L., Van Riper, G., et al. (1994). Two-site binding of C5a by its receptor: an alternative binding paradigm for G protein-coupled receptors. *Proc. Natl. Acad. Sci. U.S.A.* 91, 1214–1218. doi: 10.1073/pnas.91.4.1214

Siegel, I., Liu, T. L., and Gleicher, N. (1981). The red-cell immune system. *Lancet* 2, 556–559. doi: 10.1016/S0140-6736(81)90941-7

Soruri, A., Kim, S., Kiafard, Z., and Zwirner, J. (2003). Characterization of C5aR expression on murine myeloid and lymphoid cells by the use of a novel monoclonal antibody. *Immunol. Lett.* 88, 47–52. doi: 10.1016/S0165-2478(03)00052-X

Sozzani, S., Sallusto, F., Luini, W., Zhou, D., Piemonti, L., Allavena, P., et al. (1995). Migration of dendritic cells in response to formyl peptides, C5a, and a distinct set of chemokines. *J. Immunol.* 155, 3292–3295.

Springer, T., Galfré G., Secher, D. S., and Milstein, C. (1979). Mac-1: a macrophage differentiation antigen identified by monoclonal antibody. *Eur. J. Immunol.* 9, 301–306. doi: 10.1002/eji.1830090410

Stadtmann, A., Germena, G., Block, H., Boras, M., Rossaint, J., Sundd, P., et al. (2013). The PSGL-1-L-selectin signaling complex regulates neutrophil adhesion under flow. *J. Exp. Med.* 210, 2171–2180. doi: 10.1084/jem.20130664

Staunton, D. E., Dustin, M. L., Erickson, H. P., and Springer, T. A. (1990). The arrangement of the immunoglobulin-like domains of ICAM-1 and the binding sites for LFA-1 and rhinovirus. *Cell* 61, 243–254. doi: 10.1016/0092-8674(90)90805-O

Stepensky, P. Y., Wolach, B., Gavrieli, R., Rousso, S., Ben Ami, T., Goldman, V., et al. (2015). Leukocyte adhesion deficiency type III: clinical features and treatment with stem cell transplantation. *J. Pediatr. Hematol. Oncol.* 37, 264–268. doi: 10.1097/MPH.0000000000000228

Strey, C. W., Markiewski, M., Mastellos, D., Tudoran, R., Spruce, L. A., Greenbaum, L. E., et al. (2003). The proinflammatory mediators C3a and C5a are essential for liver regeneration. *J. Exp. Med.* 198, 913–923. doi: 10.1084/jem.20030374

Sturla, L., Puglielli, L., Tonetti, M., Berninsone, P., Hirschberg, C. B., De Flora, A., et al. (2001). Impairment of the Golgi GDP-L-fucose transport and unresponsiveness to fucose replacement therapy in LAD II patients. *Pediatr. Res.* 49, 537–542. doi: 10.1203/00006450-200104000-00016

Sumagin, R., Prizant, H., Lomakina, E., Waugh, R. E., and Sarelius, I. H. (2010). LFA-1 and Mac-1 define characteristically different intralumenal crawling and emigration patterns for monocytes and neutrophils *in situ*. *J. Immunol.* 185, 7057–7066. doi: 10.4049/jimmunol.1001638

Sun, J., Ember, J. A., Chao, T. H., Fukuoka, Y., Ye, R. D., and Hugli, T. E. (1999). Identification of ligand effector binding sites in transmembrane regions of the human G protein-coupled C3a receptor. *Protein Sci.* 8, 2304–2311. doi: 10.1110/ps.8.11.2304

Szakonyi, G., Guthridge, J. M., Li, D., Young, K., Holers, V. M., and Chen, X. S. (2001). Structure of complement receptor 2 in complex with its C3d ligand. *Science* 292, 1725–1728. doi: 10.1126/science.1059118

Taborda, C. P., and Casadevall, A. (2002). CR3 (CD11b/CD18) and CR4 (CD11c/CD18) are involved in complement-independent antibody-mediated phagocytosis of Cryptococcus neoformans. *Immunity* 16, 791–802. doi: 10.1016/S1074-7613(02)00328-X

Takagi, J., Petre, B. M., Walz, T., and Springer, T. A. (2002). Global conformational rearrangements in integrin extracellular domains in outside-in and inside-out signaling. *Cell* 110, 599–511. doi: 10.1016/S0092-8674(02)00935-2

Takahashi, K., Kozono, Y., Waldschmidt, T. J., Berthiaume, D., Quigg, R. J., Baron, A., et al. (1997). Mouse complement receptors type 1 (CR1;CD35) and type 2 (CR2;CD21): expression on normal B cell subpopulations and decreased levels during the development of autoimmunity in MRL/lpr mice. *J. Immunol.* 159, 1557–1569.

Takizawa, F., Tsuji, S., and Nagasawa, S. (1996). Enhancement of macrophage phagocytosis upon iC3b deposition on apoptotic cells. *FEBS Lett.* 397, 269–272. doi: 10.1016/S0014-5793(96)01197-0

Tanner, J., Weis, J., Fearon, D., Whang, Y., and Kieff, E. (1987). Epstein-Barr virus gp350/220 binding to the B lymphocyte C3d receptor mediates adsorption, capping, and endocytosis. *Cell* 50, 203–213. doi: 10.1016/0092-8674(87)90216-9

Thorgersen, E. B., Barratt-Due, A., Haugaa, H., Harboe, M., Pischke, S. E., Nilsson, P. H., et al. (2019). The role of complement in liver injury, regeneration, and transplantation. *Hepatology* 70, 725–736. doi: 10.1002/hep.30508

Torres-Gomez, A., Cabanas, C., and Lafuente, E. M. (2020a). Phagocytic integrins: activation and signaling. *Front. Immunol.* 11:738. doi: 10.3389/fimmu.2020.00738

Torres-Gomez, A., Sanchez-Trincado, J. L., Toribio, V., Torres-Ruiz, R., Rodriguez-Perales, S., Yanez-Mo, M., et al. (2020b). RIAM-VASP module relays integrin complement receptors in outside-in signaling driving particle engulfment. *Cells* 9:1166. doi: 10.3390/cells9051166

Trouw, L. A., Pickering, M. C., and Blom, A. M. (2017). The complement system as a potential therapeutic target in rheumatic disease. *Nat. Rev. Rheumatol.* 13, 538–547. doi: 10.1038/nrrheum.2017.125

Tuckwell, D., Calderwood, D. A., Green, L. J., and Humphries, M. J. (1995). Integrin alpha 2 I-domain is a binding site for collagens. *J. Cell Sci.* 108 (Pt 4), 1629–1637.

Van der Vieren, M., Le Trong, H., Wood, C. L., Moore, P. F., St John, T., Staunton, D. E., et al. (1995). A novel leukointegrin, alpha d beta 2, binds preferentially to ICAM-3. *Immunity* 3, 683–690. doi: 10.1016/1074-7613(95)90058-6

Vennegoor, C. J., van de Wiel-van Kemenade, E., Huijbens, R. J., Sanchez-Madrid, F., Melief, C. J., and Figdor, C. G. (1992). Role of LFA-1 and VLA-4 in the adhesion of cloned normal and LFA-1 (CD11/CD18)-deficient T cells to cultured endothelial cells. Indication for a new adhesion pathway. *J. Immunol.* 148, 1093–1101.

Vogt, L., Schmitz, N., Kurrer, M. O., Bauer, M., Hinton, H. I., Behnke, S., et al. (2006). VSIG4, a B7 family-related protein, is a negative regulator of T cell activation. *J. Clin. Invest.* 116, 2817–2826. doi: 10.1172/JCI25673

Voisin, M. B., Woodfin, A., and Nourshargh, S. (2009). Monocytes and neutrophils exhibit both distinct and common mechanisms in penetrating the vascular basement membrane *in vivo*. *Arterioscler. Thromb. Vasc. Biol.* 29, 1193–1199. doi: 10.1161/ATVBAHA.109.187450

von Zabern, I., Hinsch, B., Przyklenk, H., Schmidt, G., and Vogt, W. (1980). Comparison of Naja n. naja and Naja h. haje cobra-venom factors: correlation between binding affinity for the fifth component of complement and mediation of its cleavage. *Immunobiology* 157, 499–514. doi: 10.1016/S0171-2985(80)80018-0

Vorup-Jensen, T., and Jensen, R. K. (2018). Structural Immunology of Complement Receptors 3 and 4. *Front. Immunol.* 9:2716. doi: 10.3389/fimmu.2018.02716

Wang, H., Ricklin, D., and Lambris, J. D. (2017). Complement-activation fragment C4a mediates effector functions by binding as untethered agonist to protease-activated receptors 1 and 4. *Proc. Natl. Acad. Sci. U.S.A.* 114, 10948–10953. doi: 10.1073/pnas.1707364114

Wang, S., Voisin, M. B., Larbi, K. Y., Dangerfield, J., Scheiermann, C., Tran, M., et al. (2006). Venular basement membranes contain specific matrix protein low expression regions that act as exit points for emigrating neutrophils. *J. Exp. Med.* 203, 1519–1532. doi: 10.1084/jem.20051210

Werfel, T., Kirchhoff, K., Wittmann, M., Begemann, G., Kapp, A., Heidenreich, F., et al. (2000). Activated human T lymphocytes express a functional C3a receptor. *J. Immunol.* 165, 6599–6605. doi: 10.4049/jimmunol.165.11.6599

Wiesmann, C., Katschke, K. J., Yin, J., Helmy, K. Y., Steffek, M., Fairbrother, W. J., et al. (2006). Structure of C3b in complex with CRIg gives insights into regulation of complement activation. *Nature* 444, 217–220. doi: 10.1038/nature05263

Wilken, H. C., Götze, O., Werfel, T., and Zwirner, J. (1999). C3a(desArg) does not bind to and signal through the human C3a receptor. *Immunol. Lett.* 67, 141–145. doi: 10.1016/S0165-2478(99)00002-4

Wilson, J. G., Ratnoff, W. D., Schur, P. H., and Fearon, D. T. (1986). Decreased expression of the C3b/C4b receptor (CR1) and the C3d receptor (CR2) on B lymphocytes and of CR1 on neutrophils of patients with systemic lupus erythematosus. *Arthritis Rheum.* 29, 739–747. doi: 10.1002/art.1780290606

Woodfin, A., Voisin, M. B., Imhof, B. A., Dejana, E., Engelhardt, B., and Nourshargh, S. (2009). Endothelial cell activation leads to neutrophil transmigration as supported by the sequential roles of ICAM-2, JAM-A, and PECAM-1. *Blood* 113, 6246–6257. doi: 10.1182/blood-2008-11-188375

Wu, F., Zou, Q., Ding, X., Shi, D., Zhu, X., Hu, W., et al. (2016). Complement component C3a plays a critical role in endothelial activation and leukocyte recruitment into the brain. *J. Neuroinflamm.* 13:23. doi: 10.1186/s12974-016-0485-y

Wu, H., Boackle, S. A., Hanvivadhanakul, P., Ulgiati, D., Grossman, J. M., Lee, Y., et al. (2007). Association of a common complement receptor 2 haplotype with increased risk of systemic lupus erythematosus. *Proc. Natl. Acad. Sci. U.S.A.* 104, 3961–3966. doi: 10.1073/pnas.0609101104

Wu, M. C., Brennan, F. H., Lynch, J. P., Mantovani, S., Phipps, S., Wetsel, R. A., et al. (2013). The receptor for complement component C3a mediates protection from intestinal ischemia-reperfusion injuries by inhibiting neutrophil mobilization. *Proc. Natl. Acad. Sci. U.S.A.* 110, 9439–9444. doi: 10.1073/pnas.1218815110

Wu, X., Jiang, N., Deppong, C., Singh, J., Dolecki, G., Mao, D., et al. (2002). A role for the Cr2 gene in modifying autoantibody production in systemic lupus erythematosus. *J. Immunol.* 169, 1587–1592. doi: 10.4049/jimmunol.169.3.1587

Xiao, T., Takagi, J., Coller, B. S., Wang, J. H., and Springer, T. A. (2004). Structural basis for allostery in integrins and binding to fibrinogen-mimetic therapeutics. *Nature* 432, 59–67. doi: 10.1038/nature02976

Xiong, J. P., Stehle, T., Diefenbach, B., Zhang, R., Dunker, R., Scott, D. L., et al. (2001). Crystal structure of the extracellular segment of integrin alpha Vbeta3. *Science* 294, 339–345. doi: 10.1126/science.1064535

Xiong, J. P., Stehle, T., Zhang, R., Joachimiak, A., Frech, M., Goodman, S. L., et al. (2002). Crystal structure of the extracellular segment of integrin alpha Vbeta3 in complex with an Arg-Gly-Asp ligand. *Science* 296, 151–155. doi: 10.1126/science.1069040

Xu, S., Wang, J., Wang, J. H., and Springer, T. A. (2017). Distinct recognition of complement iC3b by integrins alphaXbeta2 and alphaMbeta2. *Proc. Natl. Acad. Sci. U.S.A.* 114, 3403–3408. doi: 10.1073/pnas.1620881114

Yago, T., Zhang, N., Zhao, L., Abrams, C. S., and McEver, R. P. (2018). Selectins and chemokines use shared and distinct signals to activate β2 integrins in neutrophils. *Blood Adv.* 2, 731–744. doi: 10.1182/bloodadvances.2017015602

Yakubenko, V. P., Lishko, V. K., Lam, S. C., and Ugarova, T. P. (2002). A molecular basis for integrin alphaMbeta 2 ligand binding promiscuity. *J. Biol. Chem.* 277, 48635–48642. doi: 10.1074/jbc.M208877200

Yoshida, K., Yukiyama, Y., and Miyamoto, T. (1986). Interaction between immune complexes and C3b receptors on erythrocytes. *Clin. Immunol. Immunopathol.* 39, 213–221. doi: 10.1016/0090-1229(86)90085-1

Yuan, X., Yang, B. H., Dong, Y., Yamamura, A., and Fu, W. (2017). CRIg, a tissue-resident macrophage specific immune checkpoint molecule, promotes immunological tolerance in NOD mice, via a dual role in effector and regulatory T cells. *Elife* 6:e28083. doi: 10.7554/eLife.29540.028

Zeng, Z., Surewaard, B. G., Wong, C. H., Geoghegan, J. A., Jenne, C. N., and Kubes, P. (2016). CRIg functions as a macrophage pattern recognition receptor to directly bind and capture blood-borne gram-positive bacteria. *Cell Host Microbe* 20, 99–106. doi: 10.1016/j.chom.2016.06.002

Zhang, C., Wang, C., Li, Y., Miwa, T., Liu, C., Cui, W., et al. (2017). Complement C3a signaling facilitates skeletal muscle regeneration by regulating monocyte function and trafficking. *Nat. Commun.* 8:2078. doi: 10.1038/s41467-017-01526-z

Zhang, S., and Cui, P. (2014). Complement system in zebrafish. *Dev. Comp. Immunol.* 46, 3–10. doi: 10.1016/j.dci.2014.01.010

Zhang, X., Boyar, W., Toth, M. J., Wennogle, L., and Gonnella, N. C. (1997). Structural definition of the C5a C terminus by two-dimensional nuclear magnetic resonance spectroscopy. *Proteins* 28, 261–267.

Zipfel, P. F., Wiech, T., Rudnick, R., Afonso, S., Person, F., and Skerka, C. (2019). Complement inhibitors in clinical trials for glomerular diseases. *Front. Immunol.* 10:2166. doi: 10.3389/fimmu.2019.02166

Zuiderweg, E. R., Nettesheim, D. G., Mollison, K. W., and Carter, G. W. (1989). Tertiary structure of human complement component C5a in solution from nuclear magnetic resonance data. *Biochemistry* 28, 172–185. doi: 10.1021/bi00427a025

Zwirner, J., Götze, O., Begemann, G., Kapp, A., Kirchhoff, K., and Werfel, T. (1999). Evaluation of C3a receptor expression on human leucocytes by the use of novel monoclonal antibodies. *Immunology* 97, 166–172. doi: 10.1046/j.1365-2567.1999.00764.x

Zwirner, J., Werfel, T., Wilken, H. C., Theile, E., and Götze, O. (1998). Anaphylatoxin C3a but not C3a(desArg) is a chemotaxin for the mouse macrophage cell line J774. *Eur. J. Immunol.* 28, 1570–1577.

Conflict of Interest: The authors declare that the research was conducted in the absence of any commercial or financial relationships that could be construed as a potential conflict of interest.

frontiers in Cell and Developmental Biology

MINI REVIEW
published: 11 February 2021
doi: 10.3389/fcell.2021.623906

Intravital Imaging Allows Organ-Specific Insights Into Immune Functions

Selina K. Jorch[1] *and Carsten Deppermann*[2]*

[1] Institute of Experimental Immunology, University Hospital of Bonn, Rheinische Friedrich-Wilhelms Universität, Bonn, Germany, [2] Institute of Clinical Chemistry and Laboratory Medicine, University Medical Center Hamburg-Eppendorf, Hamburg, Germany

Leukocytes are among the most mobile and versatile cells that have many essential functions in homeostasis and survival. Especially cells from the innate immune system, i.e., neutrophils and macrophages, play an important role as rapid first responders against invading microorganisms. With the advent of novel imaging techniques, new ways of visualizing innate immune cells have become available in recent years, thereby enabling more and more detailed discoveries about their nature, function and interaction partners. Besides intravital spinning-disc and 2-photon microscopy, clearing and 3D-imaging techniques provide new insights into the mechanism of innate immune cell behavior in their natural environment. This mini review focuses on the contributions of novel-imaging techniques to provide insight into the functions of neutrophils and macrophages under homeostasis and in infections. Imaging setups for different organs like the liver, kidney, heart, lung, and the peritoneal cavity are discussed as well as the current limitations of these imaging techniques.

Keywords: Intravital microscopy, liver, peritoneal cavity, lung, kidney, macrophage, neutrophil

OPEN ACCESS

Edited by:
Xunbin Wei,
Peking University, China

Reviewed by:
Daniele Vergara,
University of Salento, Italy
Dan Zhu,
Huazhong University of Science and Technology, China

***Correspondence:**
Carsten Deppermann
c.deppermann@uke.de

Specialty section:
This article was submitted to Cell Adhesion and Migration, a section of the journal Frontiers in Cell and Developmental Biology

Received: *30 October 2020*
Accepted: *12 January 2021*
Published: *11 February 2021*

Citation:
Jorch SK and Deppermann C (2021) Intravital Imaging Allows Organ-Specific Insights Into Immune Functions. Front. Cell Dev. Biol. 9:623906. doi: 10.3389/fcell.2021.623906

INTRODUCTION

The immune system is composed of many different cell types distributed throughout the body. While some immune cells are sessile, most are very motile, and able to migrate in tissues. Intravital microscopy had a huge impact on our understanding of the immune system as it is the only technique that allows to simultaneously study structure and function at a cellular to subcellular level with high spatial and temporal resolution *in vivo*.

The first attempt of looking into vessels to observe moving cells dates back more than a century ago (Pittet and Weissleder, 2011). Since then, imaging techniques have developed a lot and nowadays it is possible to visualize the immune processes taking place in almost every organ—brain, eye, lung, heart, lymph node, joints, spleen, liver, gut, kidney, bladder, peritoneal cavity, mammary ducts and more using experimental mouse, or rat models. The development of better and faster microscopy techniques had a tremendous impact. We moved from simple light microscopy to more complex techniques. From confocal microscopy including laser scanning (LSM) and spinning-disc (SDM), to multiphoton microscopy (MP). In confocal microscopes the light is focused on a single point and the emitted fluorescence goes thru a pinhole before reaching the detector, which results in less out-of-focus fluorescence. However, scanning the specimen point by point slows the process down significantly. A spinning-disc setup consists of multiple pinholes on a rotating disc which speeds up the scanning process significantly thereby allowing to capture fast events like bacteria or platelets moving in the blood

TABLE 1 | Overview of microscopy techniques.

Technique	Speed	Versatility	Intravital capability	Imaging depth
Laser scanning	+	++	+	+
Confocal	+	++	+	+**
Spinning disk	+++	++	+++	+
Lightsheet	O	+	(+)*	+++
2-photon	++	+	++	++

Only in animals that are transparent, e.g., zebrafish embryos or pigment-deficient zebrafish.
***Higher penetration-depth of point scanners vs. spinning disk, e.g., observed in kidney.*

stream in real time. However, the penetration depth of LSM and SDM are limited and in dense organs like the kidney, much better results are obtained with MP excitation. In 2-photon imaging, a pulsed-laser directs two exciting photons of about half the energy to the specimen. When these two low energy photons hit a fluorophore, they cause excitation to the same level as one high-energy photon, which contributes to a very specific focal point. Compared to single-photon imaging, no pinhole is necessary for a single focus point and in combination with the use of longer wavelengths this results in less out-of-focus excitation and reduced photodamage (Ntziachristos, 2010). The choice between using LSM/SDM or MP depends largely on the tissue and phenomenon of interest. In **Table 1** we give an overview about the microscopy techniques mostly used for intravital imaging and their properties regarding speed, versatility, and imaging depth.

Although intravital imaging is indispensable to gain insights into dynamic processes, it is important to know its limitations. The biggest is the imaging depth. Even with MP it is usually not possible to penetrate the whole tissue. The kidney is a very good example for this limitation. LSM/SDM is able to give beautiful details about the tubules in the outer layer of the cortex and new MP techniques allow to easily observe glomeruli which are located at the beginning of nephrons deep inside the kidney cortex, but until today it is almost impossible to image the medulla region with intravital techniques since it is located even further inside the dense kidney tissue. That is the point where clearing techniques can add valuable knowledge at least about the 3D spatial location of cells (**Figure 1**). Cleared organs can be analyzed with lightsheet microscopes to get an overview or with confocal techniques to image smaller structures at high resolution. Regardless of the microscopy techniques, another important point to always keep in mind is that the dark matter matters and can make up a big portion of the organs and cells we look at, as we can only see what is labeled or what is auto-fluorescent. In the following sections we summarize recent findings regarding neutrophils and macrophage behavior that could not have been achieved without intravital imaging or lightsheet microscopy.

Visualizing the Rapid Capture of Bacteria Through Kupffer Cells in the Liver

Cellular interactions under dynamic conditions outside of solid tissues, e.g., in the bloodstream can be transient or permanent. Investigating this type of interactions using standard tissue histology can only provide a snapshot with no insight into the true nature of the interaction observed. Since the formation and dissolution of such interactions can be very fast, visualization requires high-imaging speed that can be provided by state-of-the-art spinning-disk intravital microscopy (SD-IVM) or microscopes using very fast (resonant) scanners.

One example of such an interaction which is rapidly formed and permanent is the removal of bacteria from the bloodstream. Using SD-IVM it was shown that sequestration of blood-borne staphylococci occurs by Kupffer cells, the tissue resident macrophages of the liver residing in the sinusoids (Surewaard et al., 2016). Importantly, no sequestration takes place by sinusoidal endothelial cells, hepatocytes or other liver cells. One explanation might be that hepatocytes have no direct access to the bloodstream and endothelial cells lack CRIg, the complement receptor required to trap *Staphylococcus aureus* under shear conditions (Helmy et al., 2006). SD-IVM was essential in identifying that CRIg directly binds to lipoteichoic acid—a cell wall component of gram-positive bacteria—independent of complement proteins or antibodies (Zeng et al., 2016).

Modern SDMs are not only able to image a large field of view e.g., to follow the fate of dozens of Kupffer cells; Using high magnification objectives allows to zoom into single cells and observe the processes unfold once bacteria have been phagocytosed. While the vast majority is destroyed by means of reactive oxygen species, a small fraction of staphylococci is able to survive and proliferate inside Kupffer cells after they have been phagocytosed (Surewaard et al., 2016)—hidden from the surveillance program of the innate immune system.

SD-IVM further helped to demonstrate that during staphylococcal infection, when bacteria are caught, platelets start to adhere to Kupffer cells, and help clearing bacteria through their von Willebrand factor (vWF) and fibrinogen receptors GPIb and integrin αIIbβ3, respectively (Wong et al., 2013). During sepsis, platelet aggregates can block blood vessels (van der Poll et al., 2017). Severity of *S. aureus* sepsis correlates with expression levels of its virulence factor α-toxin (Jenkins et al., 2015). A recent study using SD-IVM of the mouse liver and 2-photon IVM of the mouse kidney visualized the events following intravascular α-toxin injection and observed rapid platelet aggregation formation in the liver sinusoids and kidney glomeruli causing organ damage (Surewaard et al., 2018). Intravital microscopy therefore helped to unravel the Janus face of platelets in *S. aureus* bacteremia: On the one hand they assist Kupffer cells in clearing bacteria, on the other hand *S. aureus* α-toxin causes excessive platelet aggregation leading to organ dysfunction.

Solid organ transplantation offers a new lease on life to thousands of patients worldwide every year. To prevent graft rejection, patients have to be on lifelong immunosuppression after transplantation, which increases their risk of infection. In fact, infections are a leading cause of morbidity and mortality in the first year post-transplantation (Fishman and Issa, 2010). *S. aureus*, especially methicillin-resistant *S. aureus* (MRSA) is a serious threat to liver transplant recipients. Studies show that over 20% of patients develop MRSA infections with

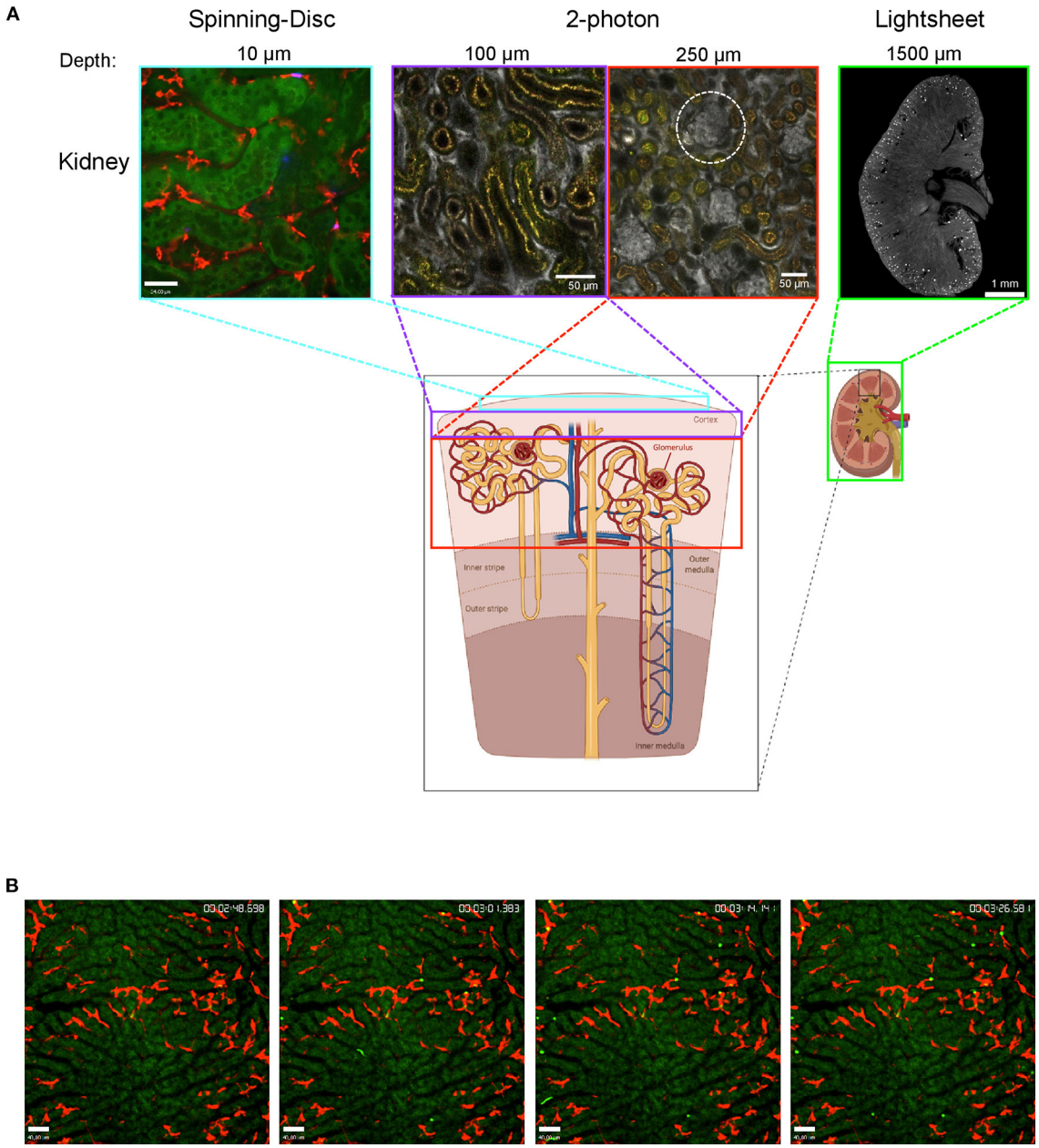

FIGURE 1 | Imaging the mouse kidney and liver using different microscopy techniques. **(A)** Outer kidney cortex imaged using spinning-disc microscopy (left) showing autofluorescent tubules (green) and F4/80^{+} macrophages (red). Images obtained using 2-photon microscopy (center) at 100 and 250 µm tissue penetration showing vasculature (albumin, gray) with glomeruli (white-dotted circle) and autofluorescent tubulues (yellow). Lightsheet microscopy image showing a cross-section of the whole kidney (right) with vasculature stained (CD31, gray) and glomeruli (bright spots). The areas that can be visualized with each technique are indicated with colored boxes. Lightsheet image was provided by Dr. Alexander Böhner, Bonn. Sub-figure was created with BioRender.com. **(B)** Mouse liver was imaged using spinning-disc microscopy showing capture of bacteria (bright green) by Kupffer cells (F4/80, red) over time (timestamp top right); hepatocytes are autofluorescent (dark green).

a mortality rate of 86% from MRSA pneumonia and 6% from catheter-related bacteremia (Singh et al., 2000). This was confirmed in a recent retrospective analysis of 2,700 transplant recipients that observed significantly increased likelihood of *S. aureus* infection in patients taking tacrolimus, a calcineurin inhibitor that is used to prevent graft rejection. In a mouse model of MRSA-induced sepsis using SD-IVM the authors observed that bacteria were more likely to disseminate and kill the host in tacrolimus-treated mice. Intravital imaging helped to uncover the underlying mechanism: reduced capacity of Kupffer cells to

capture, phagocyte and destroy the bacteria (Deppermann et al., 2020).

Women show significantly lower disease severity and mortality from sepsis caused by Gram-negative bacteria such as *Escherichia coli* (Klein and Flanagan, 2016) suggesting they might be better at clearing bacteria from the bloodstream. Indeed, a sex difference in the capture of blood-borne bacteria by Kupffer cells could be shown using SD-IVM (Zeng et al., 2018). The female advantage was based on pre-existing antibodies against certain oligosaccharides in the bacterial lipopolysaccharide which were transferrable to pubs to provide protection during infancy. The fact that this antibody could also be found in humans demonstrates how useful intravital microscopy can be for preclinical studies which then also translate into the clinic.

Visualizing Fast Platelet-Kupffer Cell Interactions Using SD-IVM

Platelets are small, anucleated cell fragments derived from bone marrow megakaryocytes that patrol the vasculature to maintain hemostasis. The human body produces 100 billion platelets every single day that circulate in the bloodstream for several days (Quach et al., 2018). At the end of their lifespan, platelets are cleared in the liver by a process that is incompletely understood (Aster, 1969). Previously, it had been suggested that platelets become desialylated as they circulate, that old platelets are phagocytosed by hepatocytes through their Ashwell-Morell receptor causing thrombopoietin production which then drives platelet production (Grozovsky et al., 2015). A recent study applied intravital microscopy to investigate the specific contributions of endothelial cells, hepatocytes and Kupffer cells in the clearing of aged, desialylated platelets. Using SD-IVM they found frequent interactions of platelets with Kupffer cells under steady-state conditions. The vast majority of interactions was short-lived, however, there was a small population that formed long-term interactions, which is in-line with previous studies describing continuous "touch-and-go" activity of platelets in the sinusoids of the liver (Wong et al., 2013). Using 3D reconstructions of z-stacks recorded of the liver, they found that indeed a small percentage of platelets is constantly being taken up by Kupffer cells. Upon desialylation, the vast majority of platelets rapidly bound to and was phagocytosed by Kupffer cells, with only a few binding to endothelial cells and basically none to hepatocytes. This unambiguously showed for the first time that Kupffer cells play an important role in the clearance of aged, desialylated platelets (Deppermann et al., accepted).

Visualizing Neutrophil Extracellular Trap Formation

Neutrophil extracellular traps (NETs) are DNA filaments released from activated neutrophils coated with histones, proteases, and other granular proteins that entangle bacteria to support pathogen elimination. NET formation also takes place during sterile inflammation, e.g., in autoimmunity, coagulation and cancer (Jorch and Kubes, 2017) an can lead to organ damage (Jimenez-Alcazar et al., 2017). SD-IVM and resonance-scanning confocal intravital microscopy were used in combination with a mouse model of sepsis to show significant platelet aggregation, thrombin activation and fibrin clot formation downstream or within NETs *in vivo*. Thrombin generation was visualized using an internally quenched Förster resonance energy transfer (FRET) substrate. Active thrombin cleaves the FRET substrate resulting in the release of a fluorescent green dye. NET degradation *via* DNase infusion significantly reduced thrombin generation and platelet aggregation (McDonald et al., 2017).

Neutrophils are an essential part of the innate immunity and provide a first line of dense against invading bacteria and other pathogens. However, they are also recruited to sterile injury through tissue damage signals and this has been elegantly demonstrated in a study using a mouse model of focal hepatic necrosis and SD-IVM. Mice expressing enhanced green fluorescent protein under the control of the lysozyme M promoter (LysM-eGFP) were used to visualize the rapid "sprint" of neutrophils toward the injury site (McDonald et al., 2010). Besides ATP released from the injury, platelets surrounding the site were necessary for neutrophil recruitment and subsequent repair (Slaba et al., 2015).

Immune Cells and Bacteria in the Peritoneal Cavity

The peritoneum harbors a large number of immune cells including B cells, mast cells, and different types of macrophages but under steady-state conditions no neutrophils. These peritoneal macrophages have been often used for *in vitro* experiments as they are easy to isolate. The number of studies that actually investigate the role of these cells in their natural environment *in vivo*, however, is limited. A phenomenon known since a long time is the "macrophage disappearance reaction" (Nelson, 1963). After injection of inflammatory stimuli like lipopolysaccharide or zymosan the macrophages become irretrievable through peritoneal lavage. Recently, two studies used different microscopy approaches that helped to understand the disappearance reaction. One study investigated the dissemination of *S. aureus* after it escaped from the liver Kupffer cells. Surprisingly, they discovered that the mesothelium of the liver ruptures and bacteria disseminate into the peritoneal cavity. There, *S. aureus* was first phagocytosed by large peritoneal macrophages (LPMs) thereby "hiding" the bacteria from detection by neutrophils. The LPMs were not able to kill *S. aureus* and in fact got overgrown and killed themselves from the bacteria within. At that point, neutrophils arrived in the peritoneal cavity. LPMs, which have been infected *in vivo* by bacteria that previously escaped KCs, were harvested to image them in culture *ex vivo* with common fluorescence microscopy. This rather straightforward-imaging technique nicely demonstrated that almost all LPMs got overgrown and killed by *S. aureus* while the neutrophils that infiltrated the peritoneal cavity at later time points were able to kill the bacteria (Jorch et al., 2019). The second recent paper, which directly investigated the macrophage disappearance reaction, used for the first time 2-photon IVM to visualize the inside of the closed peritoneal cavity. This imaging revealed that the macrophages are free floating and non-adherent under homeostasis but became

adherent after i.p. injection of zymosan or *E. coli*. Coagulation factor V expression on the peritoneal macrophages was needed to form clots of macrophages and bacteria, which in turn was necessary to control bacterial expansion (Zhang et al., 2019). While imaging the closed peritoneal cavity could benefit other studies than peritonitis e.g., to investigate the immune- and cancer cell interactions in peritoneal metastatic disease which often arise from primary colorectal and ovarian carcinoma, it still has its limitations regarding depth and areas that can be observed. The macrophage-bacteria clots were isolated from the cavity and imaged *ex vivo* (Zhang et al., 2019). This gives two possible explanations for the macrophage disappearance reaction: Either the macrophages die during systemic infections or they become adherent and cannot be isolated anymore in the peritonitis model. It would be interesting to use intravital imaging to find out if in the systemic model clots are also formed and the macrophages become adherent, as maybe both mechanisms go hand in hand and the macrophages die after they formed clots.

Imaging Macrophages in Organs With Natural Motions

Cavity macrophages do not only exist in the peritoneum, they also appear in other body cavities like the lung or the heart. Both organs are not trivial to use for intravital imaging because of their inherent motion. After myocardial infarction, macrophages play a central role in functional recovery of the heart. Until recently it was believed that recruited macrophages are exclusively monocyte-derived and induce a proinflammatory response (Heidt et al., 2014) while resident macrophages could proliferate locally and contribute to healing and non-healing responses (Epelman et al., 2014; Dick et al., 2019). Imaging the cleared infarcted heart in combination with reporter mice has revealed a new population of pericardial cavity macrophages that relocate from the pericardial cavity to the ischemic heart and help to prevent post-injury cardiac fibrosis (Deniset et al., 2019). Recently, using cleared heart tissue and lightsheet microscopy, cardiac-resident macrophages were found to contribute to mitochondrial homeostasis in the heart and prevent ventricular dysfunction (Nicolas-Avila et al., 2020). Regarding intravital imaging of the heart, there have been a few different approaches including high frame rate imaging, micro-endoscopy or mechanical stabilization but all of these studies have been limited to the epicardial layer because of limitations of imaging depth. However, micro-endoscopy provided evidence that following acute myocardial infarction, monocytes are first recruited from the vascular reservoir and later from the spleen (Jung et al., 2013). More details about the current standard of intravital imaging of the heart are reviewed and summarized in Allan-Rahill et al. (2020).

For the lung the most widely used imaging technique involves placing an imaging window its surface while applying gentle suction (Looney et al., 2011). Using this technique in combination with SD-IVM, Neupane and colleagues could now demonstrate that, contrary to previous assumptions, alveolar macrophages are not sessile and are able to crawl from one alveolus to another through pores. Inhaled bacteria causes chemotaxis and phagocytosis of the intruders and blocking this process resulted in inflammation including neutrophil recruitment (Neupane et al., 2020). While of disadvantage in the peritoneal cavity, in the lung, where the alveoli are in contact with non-sterile air under homeostasis, it makes sense that inhaled bacteria are phagocytosed by macrophages without the recruitment of neutrophils that could cause further tissue damage.

Imaging the Kidney

Examining the kidney with intravital microscopy is challenging because of the high tissue density and therefore limited penetration depth. As demonstrated in **Figure 1**, imaging the cortex region is possible using SD-IVM. Using this approach, Sedin and colleagues could recently demonstrate, that after light-induced sterile tissue injury and after microinfusion of uropathogenic *E. coli* into a single nephron, neutrophils rapidly accumulated at the injury or infection site while the number of renal mononuclear phagocytes was not increased (Sedin et al., 2019). However, this study does not reflect the usual transition of bacteria from the bladder to the kidneys *via* the ureter. To detect ascending bacteria with intravital approaches at least 2-photon IVM is necessary. An even more elegant approach would be the usage of an abdominal imaging window on the kidney. This approach allows to observe the same kidney over time and was used to study renal epithelial cells and podocytes (Schiessl et al., 2020) but not yet to investigate immune cells in pyelonephritis or other pathophysiologic conditions like acute kidney injury or glomerulonephritis that progress over time. Nevertheless, the limited tissue penetration will most likely not allow to study the medulla region of the kidneys. Here, clearing techniques become relevant to at least be able to investigate the specimen in a spatial manner, as the organs can first be screened with lightsheet microscopy and afterwards, for better resolution, the region of interest of the cleared organ can be analyzed with 2-photon microscopy. As cleared organs can be imaged from all sides and penetration of light is much deeper, it is usually possible to visualize the region of interest. Lightsheet microscopy helped to determine the total number of glomeruli and their capillary tufts size in mice, which allowed to quantify the average creatinine clearance rate per glomerulus under steady-state and experimental nephrotoxic nephritis, where first the average creatinine clearance rate per glomerulus decreases followed by the total number of glomeruli (Klingberg et al., 2016).

CONCLUSION AND PERSPECTIVE

Intravital imaging has provided new insights into immunologic processes in a large number of organs and diseases. Combining mouse models with IVM has helped us understand (patho)physiologic processes and to unravel the underlying mechanisms. With IVM and relevant mouse models becoming more widely available, we expect that it will help to solve research questions in many different fields.

AUTHOR CONTRIBUTIONS

SJ and CD conceptualization. SJ and CD writing—original draft. SJ and CD writing—review and editing. Both authors contributed to the article and approved the submitted version.

FUNDING

SJ is funded by the Deutsche Forschungsgemeinschaft (DFG, German Research Foundation) under Germany's Excellence Strategy—EXC2151—390873048.

REFERENCES

Allan-Rahill, N. H., Lamont, M. R. E., Chilian, W. M., Nishimura, N., and Small, D. M. (2020). Intravital microscopy of the beating murine heart to understand cardiac leukocyte dynamics. *Front. Immunol.* 11:92. doi: 10.3389/fimmu.2020.00092

Aster, R. H. (1969). Studies of the fate of platelets in rats and man. *Blood* 34, 117–128. doi: 10.1182/blood.V34.2.117.117

Deniset, J. F., Belke, D., Lee, W. Y., Jorch, S. K., Deppermann, C., Hassanabad, A. F., et al. (2019). Gata6(+) pericardial cavity macrophages relocate to the injured heart and prevent cardiac fibrosis. *Immunity* 51, 131–40 e5. doi: 10.1016/j.immuni.2019.06.010

Deppermann, C., Kratofil, R. M., Peiseler, M., David, B. A., Zindel, J., Castanheira, F., et al. (2020). Macrophage galactose lectin is critical for Kupffer cells to clear aged platelets. *J. Exp. Med.* 217:20190723. doi: 10.1084/jem.20190723

Deppermann, C., Peiseler, M., Zindel, J., Zbytnuik, L., Lee, W. Y., Pasini, E., et al. (accepted). Tacrolimus impairs Kupffer cell capacity to control bacteremia: why transplant recipients are susceptible to infection. *Hepatology*. doi: 10.1002/hep.31499

Dick, S. A., Macklin, J. A., Nejat, S., Momen, A., Clemente-Casares, X., Althagafi, M. G., et al. (2019). Self-renewing resident cardiac macrophages limit adverse remodeling following myocardial infarction. *Nat. Immunol.* 20, 29–39. doi: 10.1038/s41590-018-0272-2

Epelman, S., Lavine, K. J., Beaudin, A. E., Sojka, D. K., Carrero, J. A., Calderon, B., et al. (2014). Embryonic and adult-derived resident cardiac macrophages are maintained through distinct mechanisms at steady state and during inflammation. *Immunity* 40, 91–104. doi: 10.1016/j.immuni.2013.11.019

Fishman, J. A., and Issa, N. C. (2010). Infection in organ transplantation: risk factors and evolving patterns of infection. *Infect. Dis. Clin. North Am.* 24, 273–283. doi: 10.1016/j.idc.2010.01.005

Grozovsky, R., Begonja, A. J., Liu, K., Visner, G., Hartwig, J. H., Falet, H., et al. (2015). The Ashwell-Morell receptor regulates hepatic thrombopoietin production via JAK2-STAT3 signaling. *Nat. Med.* 21, 47–54. doi: 10.1038/nm.3770

Heidt, T., Courties, G., Dutta, P., Sager, H. B., Sebas, M., Iwamoto, Y., et al. (2014). Differential contribution of monocytes to heart macrophages in steady-state and after myocardial infarction. *Circ. Res.* 115, 284–295. doi: 10.1161/CIRCRESAHA.115.303567

Helmy, K. Y., Katschke, K. J. Jr., Gorgani, N. N., Kljavin, N. M., Elliott, J. M., et al. (2006). CRIg: a macrophage complement receptor required for phagocytosis of circulating pathogens. *Cell* 124, 915–927. doi: 10.1016/j.cell.2005.12.039

Jenkins, A., Diep, B. A., Mai, T. T., Vo, N. H., Warrener, P., Suzich, J., et al. (2015). Differential expression and roles of *Staphylococcus aureus* virulence determinants during colonization and disease. *mBio* 6, e02272–e02214. doi: 10.1128/mBio.02272-14

Jimenez-Alcazar, M., Rangaswamy, C., Panda, R., Bitterling, J., Simsek, Y. J., Long, A. T., et al. (2017). Host DNases prevent vascular occlusion by neutrophil extracellular traps. *Science* 358, 1202–1206. doi: 10.1126/science.aam8897

Jorch, S. K., and Kubes, P. (2017). An emerging role for neutrophil extracellular traps in noninfectious disease. *Nat. Med.* 23, 279–287. doi: 10.1038/nm.4294

Jorch, S. K., Surewaard, B. G., Hossain, M., Peiseler, M., Deppermann, C., Deng, J., et al. (2019). Peritoneal GATA6+ macrophages function as a portal for *Staphylococcus aureus* dissemination. *J. Clin. Investig.* 129, 4643–4656. doi: 10.1172/JCI127286

Jung, K., Kim, P., Leuschner, F., Gorbatov, R., Kim, J. K., Ueno, T., et al. (2013). Endoscopic time-lapse imaging of immune cells in infarcted mouse hearts. *Circ. Res.* 112, 891–899. doi: 10.1161/CIRCRESAHA.111.300484

Klein, S. L., and Flanagan, K. L. (2016). Sex differences in immune responses. *Nat. Rev. Immunol.* 16, 626–638. doi: 10.1038/nri.2016.90

Klingberg, A., Hasenberg, A., Ludwig-Portugall, I., Medyukhina, A., Mann, L., Brenzel, A., et al. (2016). Fully automated evaluation of total glomerular number and capillary tuft size in nephritic kidneys using lightsheet microscopy. *J. Am. Soc. Nephrol.* 28, 452–459. doi: 10.1681/ASN.2016020232

Looney, M. R., Thornton, E. E., Sen, D., Lamm, W. J., Glenny, R. W., and Krummel, M. F. (2011). Stabilized imaging of immune surveillance in the mouse lung. *Nat. Methods* 8, 91–96. doi: 10.1038/nmeth.1543

McDonald, B., Davis, R. P., Kim, S. J., Tse, M., Esmon, C. T., Kolaczkowska, E., et al. (2017). Platelets and neutrophil extracellular traps collaborate to promote intravascular coagulation during sepsis in mice. *Blood* 129, 1357–1367. doi: 10.1182/blood-2016-09-741298

McDonald, B., Pittman, K., Menezes, G. B., Hirota, S. A., Slaba, I., Waterhouse, C. C., et al. (2010). Intravascular danger signals guide neutrophils to sites of sterile inflammation. *Science* 330, 362–366. doi: 10.1126/science.1195491

Nelson, D. S. (1963). Reaction to antigens *in vivo* of the peritoneal macrophages of guinea-pigs with delayed type hypersensitivity. Effects of anticoagulants and other drugs. *Lancet* 2, 175–176. doi: 10.1016/S0140-6736(63)92808-3

Neupane, A. S., Willson, M., Chojnacki, A. K., Vargas, E. S. C. F., Morehouse, C., Carestia, A., et al. (2020). Patrolling alveolar macrophages conceal bacteria from the immune system to maintain homeostasis. *Cell.* 183, 110–125.e11. doi: 10.1016/j.cell.2020.08.020

Nicolas-Avila, J. A., Lechuga-Vieco, A. V., Esteban-Martinez, L., Sanchez-Diaz, M., Diaz-Garcia, E., Santiago, D. J., et al. (2020). A network of macrophages supports mitochondrial homeostasis in the heart. *Cell* 183, 94–109 e23. doi: 10.1016/j.cell.2020.08.031

Ntziachristos, V. (2010). Going deeper than microscopy: the optical imaging frontier in biology. *Nat. Methods* 7, 603–614. doi: 10.1038/nmeth.1483

Pittet, M. J., and Weissleder, R. (2011). Intravital imaging. *Cell* 147, 983–991. doi: 10.1016/j.cell.2011.11.004

Quach, M. E., Chen, W., and Li, R. (2018). Mechanisms of platelet clearance and translation to improve platelet storage. *Blood* 131, 1512–1521. doi: 10.1182/blood-2017-08-743229

Schiessl, I. M., Fremter, K., Burford, J. L., Castrop, H., and Peti-Peterdi, J. (2020). Long-term cell fate tracking of individual renal cells using serial intravital microscopy. *Methods Mol. Biol.* 2150, 25–44. doi: 10.1007/7651_2019_232

Sedin, J., Giraud, A., Steiner, S. E., Ahl, D., Persson, A. E. G., Melican, K., et al. (2019). High resolution intravital imaging of the renal immune response to injury and infection in mice. *Front. Immunol.* 10:2744. doi: 10.3389/fimmu.2019.02744

Singh, N., Paterson, D. L., Chang, F. Y., Gayowski, T., Squier, C., Wagener, M. M., et al. (2000). Methicillin-resistant *Staphylococcus aureus*: the other emerging resistant gram-positive coccus among liver transplant recipients. *Clin. Infect. Dis.* 30, 322–327. doi: 10.1086/313658

Slaba, I., Wang, J., Kolaczkowska, E., McDonald, B., Lee, W. Y., and Kubes, P. (2015). Imaging the dynamic platelet-neutrophil response in sterile liver injury and repair in mice. *Hepatology* 62, 1593–1605. doi: 10.1002/hep.28003

Surewaard, B. G., Deniset, J. F., Zemp, F. J., Amrein, M., Otto, M., Conly, J., et al. (2016). Identification and treatment of the *Staphylococcus aureus* reservoir *in vivo*. *J. Exp. Med.* 213, 1141–1151. doi: 10.1084/jem.20160334

Surewaard, B. G. J., Thanabalasuriar, A., Zeng, Z., Tkaczyk, C., Cohen, T. S., Bardoel, B. W., et al. (2018). Alpha-toxin induces platelet aggregation and liver injury during *Staphylococcus aureus* sepsis. *Cell Host Microbe.* 24, 271–84 e3. doi: 10.1016/j.chom.2018.06.017

van der Poll, T., van de Veerdonk, F. L., Scicluna, B. P., and Netea, M. G. (2017). The immunopathology of sepsis and potential therapeutic targets. *Nat. Rev. Immunol.* 17, 407–420. doi: 10.1038/nri.2017.36

Wong, C. H., Jenne, C. N., Petri, B., Chrobok, N. L., and Kubes, P. (2013). Nucleation of platelets with blood-borne pathogens on Kupffer cells precedes

other innate immunity and contributes to bacterial clearance. *Nat. Immunol.* 14, 785–792. doi: 10.1038/ni.2631

Zeng, Z., Surewaard, B. G., Wong, C. H., Geoghegan, J. A., Jenne, C. N., and Kubes, P. (2016). CRIg functions as a macrophage pattern recognition receptor to directly bind and capture blood-borne gram-positive bacteria. *Cell Host Microbe.* 20, 99–106. doi: 10.1016/j.chom.2016.06.002

Zeng, Z., Surewaard, B. G. J., Wong, C. H. Y., Guettler, C., Petri, B., Burkhard, R., et al. (2018). Sex-hormone-driven innate antibodies protect females and infants against EPEC infection. *Nat. Immunol.* 19, 1100–1111. doi: 10.1038/s41590-018-0211-2

Zhang, N., Czepielewski, R. S., Jarjour, N. N., Erlich, E. C., Esaulova, E., Saunders, B. T., et al. (2019). Expression of factor V by resident macrophages boosts host defense in the peritoneal cavity. *J. Exp. Med.* 216, 1291–1300. doi: 10.1084/jem.20182024

Conflict of Interest: The authors declare that the research was conducted in the absence of any commercial or financial relationships that could be construed as a potential conflict of interest.

frontiers in Cell and Developmental Biology

MINI REVIEW
published: 18 February 2021
doi: 10.3389/fcell.2021.635527

Inflammatory Cell Recruitment in Cardiovascular Disease

*Timoteo Marchini[1,2,3], Lucía Sol Mitre[1,2] and Dennis Wolf[1,2]**

[1] Department of Cardiology and Angiology I, University Heart Center Freiburg, Freiburg, Germany, [2] Faculty of Medicine, University of Freiburg, Freiburg, Germany, [3] Facultad de Farmacia y Bioquímica, Instituto de Bioquímica y Medicina Molecular (IBIMOL), Universidad de Buenos Aires, CONICET, Buenos Aires, Argentina

Atherosclerosis, the main underlying pathology for myocardial infarction and stroke, is a chronic inflammatory disease of middle-sized to large arteries that is initiated and maintained by leukocytes infiltrating into the subendothelial space. It is now clear that the accumulation of pro-inflammatory leukocytes drives progression of atherosclerosis, its clinical complications, and directly modulates tissue-healing in the infarcted heart after myocardial infarction. This inflammatory response is orchestrated by multiple soluble mediators that enhance inflammation systemically and locally, as well as by a multitude of partially tissue-specific molecules that regulate homing, adhesion, and transmigration of leukocytes. While numerous experimental studies in the mouse have refined our understanding of leukocyte accumulation from a conceptual perspective, only a few anti-leukocyte therapies have been directly validated in humans. Lack of tissue-tropism of targeted factors required for leukocyte accumulation and unspecific inhibition strategies remain the major challenges to ultimately translate therapies that modulate leukocytes accumulation into clinical practice. Here, we carefully describe receptor and ligand pairs that guide leukocyte accumulation into the atherosclerotic plaque and the infarcted myocardium, and comment on potential future medical therapies.

Keywords: atherosclerosis, myocardial infarction, recruitment, leukocyte, selectin, integrin, cytokine, chemokine

OPEN ACCESS

Edited by:
Zhichao Fan,
UCONN Health, United States

Reviewed by:
Gabriel Courties,
Médecine Régénératrice Et Immunothérapies, France
Yvonne Döring,
Ludwig Maximilian University of Munich, Germany

***Correspondence:**
Dennis Wolf
dennis.wolf@universitaets-herzzentrum.de

Specialty section:
This article was submitted to Cell Adhesion and Migration, a section of the journal Frontiers in Cell and Developmental Biology

Received: *30 November 2020*
Accepted: *21 January 2021*
Published: *18 February 2021*

Citation:
Marchini T, Mitre LS and Wolf D (2021) Inflammatory Cell Recruitment in Cardiovascular Disease. Front. Cell Dev. Biol. 9:635527. doi: 10.3389/fcell.2021.635527

INFLAMMATORY LEUKOCYTE RECRUITMENT PROMOTES CARDIOVASCULAR DISEASE

Cardiovascular disease (CVD) represents the leading cause of mortality worldwide (Braunwald, 2012) and is mostly caused by atherosclerosis, a chronic inflammatory disease of middle- to large-sized arteries that is characterized by vessel-obstructing atherosclerotic plaques in the subendothelial space (Ross, 1999). The spontaneous rupture of atherosclerotic plaques, the subsequent formation of occlusive arterial thrombi, and the restriction of blood flow precipitates myocardial infarction (MI) and stroke (Minicucci et al., 2011). Initial atherosclerotic lesions develop in arteries with enhanced shear stress, turbulent blood flow, and endothelial dysfunction (Davignon and Ganz, 2004). This process is stimulated by traditional cardiovascular risk factors, such as smoking, hypertension, obesity, diabetes, and environmental stressors (Marchini et al., 2020). In atherosclerotic arteries, plasma low-density lipoproteins (LDL) are deposited in the subendothelial space and modified by oxidative processes. While oxidized LDL (oxLDL) exerts an inflammatory response of stromal cells itself, its uptake by tissue-resident macrophages initiates a myeloid-cell dominated pro-inflammatory cellular immune response (Swirski et al., 2007). It is now clear that inflammation is one of the key drivers of atherosclerosis, adverse cardiac remodeling, and myocardial scar formation after MI (Epelman et al., 2015). This response is characterized by the continuous accumulation of myeloid cells and lymphocytes in the atherosclerotic plaque, the

myocardium, and draining lymph nodes of the heart (Epelman et al., 2015; Winkels et al., 2018; Farbehi et al., 2019; Wolf and Ley, 2019; Zernecke et al., 2020). Infiltrated leukocytes interact with stromal cells, secrete pro- or anti-inflammatory cytokines, and curb or promote inflammation and adverse tissue remodeling (Koltsova et al., 2012; Wolf et al., 2015; Sharma et al., 2020). While heart and vascular tissue contains small fractions of tissue-resident leukocytes that partially stem from embryonic origin (Wolf et al., 2015; Ensan et al., 2016), the recruitment and accumulation of blood-derived leukocytes represents a central and ongoing process that correlates with disease severity and clinical outcomes (Galkina et al., 2006; Swirski et al., 2006; Leistner et al., 2020). In addition, tissue inflammation promotes the local proliferation of macrophages and other leukocytes, although the relative contribution of *in situ* proliferation to the overall content of tissue leukocytes remains a matter of debate. While anti-leukocyte therapies are already in clinical use against Inflammatory Bowel Disease (IBD) and Multiple Sclerosis (Ley et al., 2016), it remains unknown whether similar strategies would be effective in cardiovascular pathologies. Here, we evaluate factors that promote leukocyte accumulation into the atherosclerotic plaque and cardiac tissue in mice and discuss their potential as targets for future medical therapies in CVD.

CURRENT CONCEPT OF VASCULAR LEUKOCYTE TRAFFICKING

The stepwise cascade of leukocyte recruitment comprises leukocyte rolling, chemokine-driven cell activation, integrin-dependent cellular arrest, and transmigration. This sequence of events has lately been refined by additional (and intermediate) states, such as slow rolling, adhesion strengthening, intraluminal crawling, paracellular and transcellular migration, and migration through the endothelial basement membrane (Ley et al., 2007). These processes in the leukocyte can be attributed to distinct classes and pairs of adhesion receptors and ligands: Initial rolling is mediated by the interaction of C-type lectins with glycoprotein ligands: E-Selectin on endothelial cells with leukocyte E-Selectin Ligand 1 (ESL-1) (Levinovitz et al., 1993) and endothelial P-Selectin and leukocyte L-Selectin with P-Selectin Glycoprotein Ligand 1 (PSGL-1) (McEver and Cummings, 1997). PSGL-1 is expressed on both, leukocytes (An et al., 2008) and endothelial cells (da Costa Martins et al., 2007). Integrins, α/β-heterodimers of a heterogeneous groups of 18 α- and 8 β-subunits (Takada et al., 2007), participate in (slow) rolling and mediate cell firm adhesion (Dunne et al., 2003). Of the 24 integrins, $\alpha_L\beta_2$, $\alpha_M\beta_2$, $\alpha_x\beta_2$, $\alpha_d\beta_2$, $\alpha_4\beta_7$ and $\alpha_E\beta_7$ are selectively expressed on leukocytes while $\alpha_2\beta_1$, $\alpha_3\beta_1$, $\alpha_5\beta_1$, $\alpha_6\beta_1$, $\alpha_6\beta_4$, $\alpha_{10}\beta_1$, $\alpha_v\beta_3$ and $\alpha_v\beta_5$ are expressed on ECs (Finney et al., 2017). Integrin-dependent leukocyte arrest is best established for the interaction of Very Late Antigen 4 (VLA-4, $\alpha_4\beta_1$) with Vascular Cell Adhesion Protein 1 (VCAM-1) (Berlin et al., 1995; Ley and Huo, 2001), of Lymphocyte Function-associated Antigen 1 (LFA-1, CD11a/CD18, $\alpha_L\beta_2$) with Intercellular Adhesion Molecule 1 (ICAM-1) (Meerschaert and Furie, 1995), and of Macrophage Receptor 1 (Mac-1, CD11b/CD18, $\alpha_M\beta_2$) with EC-expressed ICAM-1 (Dunne et al., 2003) and CD40 ligand (CD40L) (Wolf et al., 2011, 2018; Michel et al., 2017). Firm adhesion is topically guided by the C-C motif chemokines CCL2 (Monocyte Chemoattractant Protein 1, MCP-1) and CCL5, and by the C-X-C motif chemokines CXCL1, CXCL4, and CXCL5 (Noels et al., 2019), which are secreted by cells in the atherosclerotic lesion or deposited by activated platelets (Drechsler et al., 2010) and subsequently presented on the glycocalyx (Graham et al., 2019). Binding of chemokines to their corresponding chemokine receptors on leukocytes, such as CCR2 (binding CCL2) or CCR5 (binding CCL3, −4, and −5), is critical for adhesion strengthening (Zernecke and Weber, 2014) and partially requires sialylation of CCRs by leukocyte-expressed α2,3-sialyltransferase IV (St3Gal4) as exemplified by CCR5 (Doring et al., 2014). Chemokine binding results in activation-dependent conformational changes in integrins (inside-out signaling) that induces an extended intermediate- and high-affinity structure of integrins (Arnaout et al., 2005; Fan and Ley, 2015; Fan et al., 2016) with a ∼10,000-fold increased affinity for their ligands (Shimaoka et al., 2003). Leukocyte migration is further supported by proinflammatory cytokines, such as IL-1β, that induce an upregulation of ICAMs, Platelet/Endothelial Cell Adhesion Molecule 1 (PECAM-1) (Mamdouh et al., 2003), and Junctional Adhesion Molecule A (JAM-A) (Martin-Padura et al., 1998). Transendothelial cell migration requires leukocyte integrins, in particular Mac-1 (Ley et al., 2007). While this cascade ultimately results in the accumulation of most leukocytes, a sub-population of $Ly6C^{low}$ monocytes remains crawling on the endothelium for surveillance of endothelial integrity engaging LFA-1, C-X_3-C Chemokine Receptor 1 (CX_3CR1) (Auffray et al., 2007), and ICAM-1 and ICAM-2 (Ancuta et al., 2009). Whether these patrolling monocytes eventually transmigrate and contribute to the pool of tissue leukocytes remains a matter of debate (Auffray et al., 2007; Nahrendorf et al., 2007; Heidt et al., 2014a; Hilgendorf et al., 2014; Quintar et al., 2017).

The (numeric) regulation of leukocyte recruitment occurs via several mechanisms: First, leukocytes are activated by cytokines such as Tumor Necrosis Factor (TNF)-α or by oxLDL that promote expression of selectins (Stocker et al., 2000) and integrins (Couffinhal et al., 1994; Kita et al., 2001). Second, leukocyte activation may occur via an interaction with other cells, such as platelets that secrete leukocyte-activating factors as serotonin (Mauler et al., 2019). Third, the endothelium upregulates expression of adhesion receptors during systemic and local inflammation. Fourth, the pool of available leukocytes in the circulation is regulated by an enhanced production in the bone marrow or at sites of extramedullary hematopoiesis (EMH), such as the spleen (Swirski et al., 2009; Dutta et al., 2012; Heidt et al., 2014b). Under steady-state conditions, haematopoietic stem cell (HSC) homeostasis is regulated by bone marrow endothelial cell expressed CXCL12 (Stromal Cell-Derived Factor 1, SDF-1) that serves as retention and quiescence factor for HSCs and progenitor cells in the bone marrow niche that express its receptor CXCR4 (Mendez-Ferrer et al., 2008, 2010; Wolf and Ley, 2015; Krohn-Grimberghe et al., 2020). In the setting of inflammation, an enhanced sympathetic tone reduces CXCL12 expression in the bone marrow and increases CCL2 in bone

marrow sinusoids that guides newly generated monocytes into the circulation (Krohn-Grimberghe et al., 2020). The migration factors required for seeding HSCs and progenitor cells to the sites of EMH are currently unknown. Fifth, tissue and cell tropism is regulated by a site-specific expression of adhesion factors: For instance, lymphocyte trafficking in the gut is predominantly facilitated by leukocyte $\alpha_4\beta_7$ and $\alpha_E\beta_7$ and endothelial Mucosal Addressin Cell Adhesion Molecule 1 (MAdCAM-1) (Briskin et al., 1993) and E-Cadherin (Higgins et al., 1998). In a secondary analysis of vascular adhesion receptors from the endothelial database EndoDB (Khan et al., 2019), we found a predominant expression of P- (*SELP*) and E-Selectin (*SELE*), integrin subunits α_3 (*ITGA3*), α_5 (*ITGA5*), α_9 (*ITGA9*), α_{10} (*ITGA10*), β_1 (*ITGB1*) and β_3 (*ITGB3*), and VCAM-1 (*VCAM1*) and ICAM-1 (*ICAM1*) in endothelial cells from human coronary arteries and the aorta compared to other vascular beds, suggesting these may figure as potent mediators of cardiac leukocyte accumulation during inflammation (**Figure 1**).

INFLAMMATORY LEUKOCYTE RECRUITMENT IN ATHEROSCLEROSIS

A multitude of established receptor-ligand pairs has been validated mostly in experimental atherosclerosis in mice deficient for LDL-receptor ($Ldlr^{-/-}$) and Apolipoprotein E ($Apoe^{-/-}$), which exhibit diet-induced hypercholesterolemia (Wolf et al., 2015). Important recruitment factors include selectins, integrins, and other classes of adhesion factors (Galkina and Ley, 2007b) that can act in different cell types (Galkina and Ley, 2007a; Soehnlein, 2012; Gerhardt and Ley, 2015; Saigusa et al., 2020; **Figure 2A**):

Cardiac Endothelial Cells

Endothelial cell expressed selectins (CD62) interact with glycoprotein ligands to mediate the capture and slow-down of circulating leukocytes. In humans, P-Selectin is not detectable in the healthy arterial endothelium but it is upregulated by oxLDL (Gebuhrer et al., 1995) and highly expressed in atherosclerotic lesions (Johnson-Tidey et al., 1994). Likewise, E-Selectin is detectable on the endothelium of human atherosclerotic plaques (Davies et al., 1993). While P-Selectin deficiency ($Psel^{-/-}$) in $Apoe^{-/-}$ and $Ldlr^{-/-}$ mice (Johnson et al., 1997; Dong et al., 2000) neutralizes leukocyte trafficking and delays disease progression (Mayadas et al., 1993), $Apoe^{-/-}Esel^{-/-}$ mice are less affected (Collins et al., 2000). A combined deficiency of P- and E-Selectin in $Ldlr^{-/-}$ mice abolishes atherosclerosis (Dong et al., 1998). P-Selectin, but not E-Selectin, expression correlates with human plaque stability (Tenaglia et al., 1997). Deficiency of VCAM-1 (Cybulsky et al., 2001) and ICAM-1 (Nageh et al., 1997) diminishes plaque size in mice. VCAM-1 is upregulated by proinflammatory cytokines at atherosclerosis-prone sites of arteries in $Apoe^{-/-}$ and WT mice and mediates leukocyte arrest by binding to VLA-4 (Nakashima et al., 1998; Ley and Huo, 2001; Jongstra-Bilen et al., 2006). Leukocyte adhesion on the endothelium is also supported by binding of ICAMs to LFA-1 (Meerschaert and Furie, 1995) and of CD40L to Mac-1 (Zirlik et al., 2007). Small interfering RNAs (siRNAs) targeting multiple endothelial adhesion molecules reduced atherosclerosis in $Apoe^{-/-}$ mice markedly (Sager et al., 2016a), while specific targeting of Mac-1 binding to CD40L by a peptide inhibitor (Wolf et al., 2011), or a blocking antibody (Wolf et al., 2018) prevented inflammatory leukocyte recruitment (Michel et al., 2017) in mice.

Monocytes

In $Apoe^{-/-}$ and $Ldlr^{-/-}$ mice, hypercholesterolemia results in an expansion of monocyte progenitors and systemic monocytosis (Soehnlein et al., 2013; Rahman et al., 2017), likely by a modulation of reverse cholesterol transport in Hematopoietic Stem Progenitor Cells (HSPCs) (Yvan-Charvet et al., 2010; Murphy et al., 2011) and accelerated extramedullary hematopoiesis (Robbins et al., 2012). Several reports have identified increased adrenergic signaling, impaired quiescence and retention of HSPCs as hallmarks of this response (Dutta et al., 2012; Courties et al., 2015; Sager et al., 2016b). In the plaque, classical/inflammatory Ly-6C^{high} monocytes represent the main monocyte subset and give rise to vascular macrophages (Swirski et al., 2007). In mice, migration of Ly-6C^{high} monocytes is regulated by an interaction of P-Selectin/PSGL-1 (An et al., 2008), VLA-4/VCAM-1 (Huo et al., 2001), Mac-1/CD40L (Wolf et al., 2011), and of CCR1 and −5 with their corresponding ligands (Tacke et al., 2007; Combadiere et al., 2008; Soehnlein et al., 2013). Notably, CCR1- but not CCR5-deficiency seems to protect only from early atherosclerosis in $Apoe^{-/-}$ mice on a WD for 4 weeks, suggesting temporal differences in CCR-dependent leukocyte

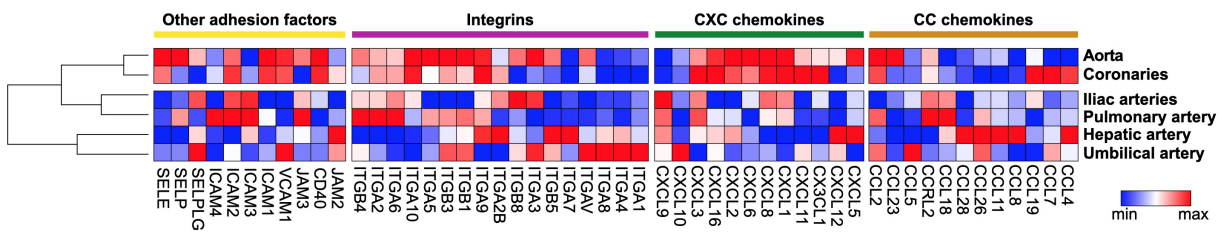

FIGURE 1 | Gene expression pattern of adhesion factors expressed in human endothelial cells. Baseline gene expression of human endothelial cells from different locations was extracted from the curated gene set collection of the EndoDB database (Khan et al., 2019). Extracted expression values were plotted as heatmap by Morpheus with column minimum and maximum normalization. Within classes of adhesion receptors, rows and columns were sorted by hierarchical clustering.

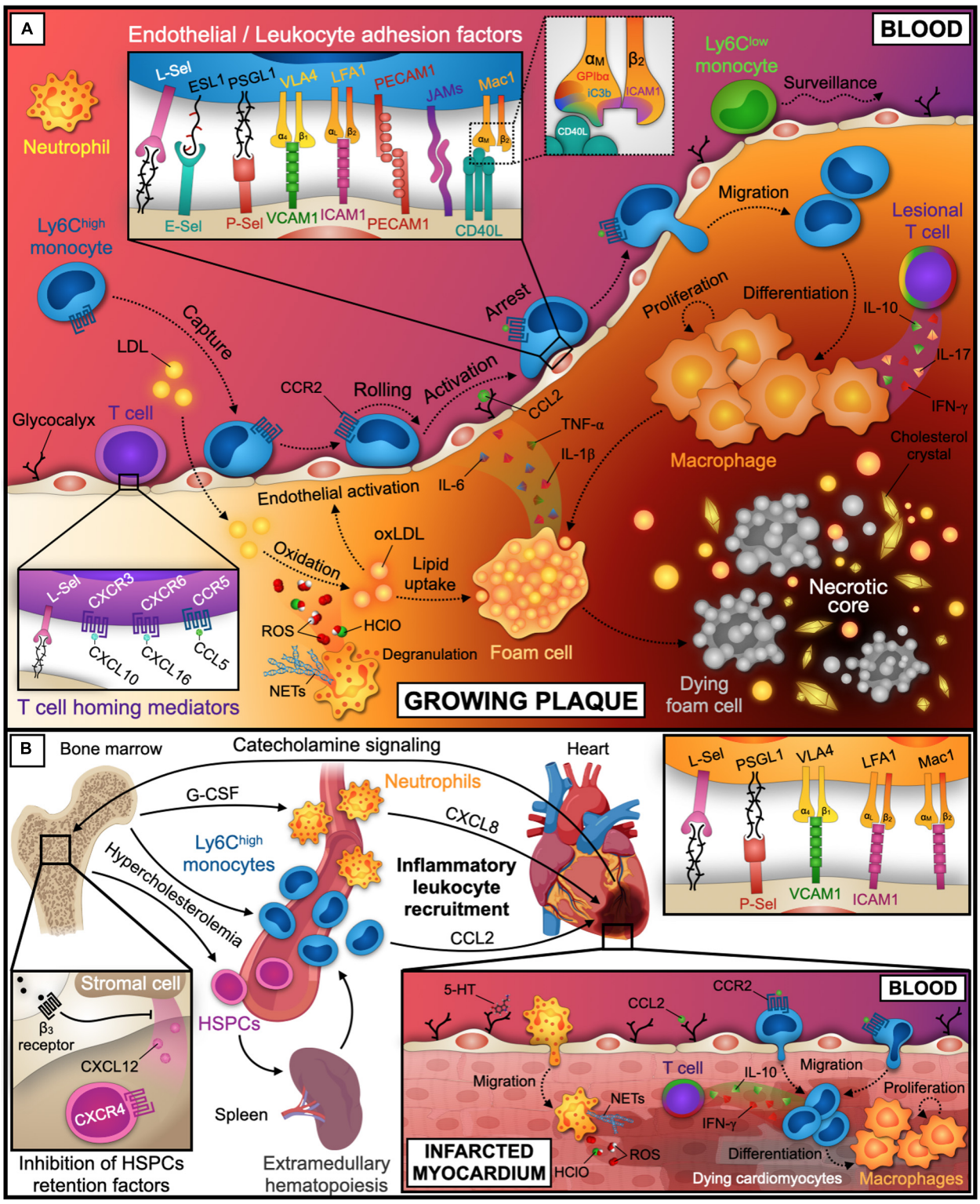

FIGURE 2 | Leukocyte recruitment into the atherosclerotic plaque and infarcted tissue. **(A)** Initial endothelial dysfunction and activation is promoted by shear stress at sites of turbulent blood flow and lipid accumulation. While Ly6C^{low} monocytes patrol the endothelial surface for tissue surveillance, neutrophils and Ly6C^{high} monocytes are recruited into the subendothelial space. Within the plaque, Ly6C^{high} monocytes differentiate into macrophages. These proliferate, became foam cells, and orchestrate the inflammatory response, eventually die and build the necrotic core together with lipids and cholesterol crystals. These processes are further instructed by plaque-infiltrating T cells. Relevant inflammatory cytokines, chemokines, and receptor-ligand pairs for monocytes and T cells are indicated in the inlays. A third inlay shows CD40L binding to a distinct site within the I-domain of α_M chain of Mac-1 that does not interfere with other Mac-1 ligands. **(B)** Coronary artery

(Continued)

FIGURE 2 | Continued
occlusion precipitates MI and triggers progenitor and inflammatory leukocyte release from the bone marrow by adrenergic signaling and decreased expression of the retention factors CXCL12 and CXCR4 in the bone marrow niche. CXCL8 and CCL2 guide neutrophils and Ly6C^{high} monocytes to infarcted tissue. Neutrophils accumulate in the lesion by the adhesion factors depicted in the inlay and promote myocardial injury by reactive oxygen species (ROS), Hypochlorous acid (HClO), and NETs release. Ly6C^{high} monocytes are recruited and differentiate to macrophages. Tissue healing after MI is further modulated by infiltrated T cells that may secrete pro- or anti-inflammatory cytokines. LDL, low-density lipoprotein; oxLDL, oxidized LDL; Sel, Selectin; ESL1, E-Selectin Ligand 1; PSGL1, P-Selectin Glycoprotein Ligand 1; VCAM1, Vascular Cell Adhesion Molecule 1; VLA4, Very Late Antigen 4 ($\alpha_4\beta_1$); ICAM1, Intercellular Adhesion Molecule 1; LFA1, Lymphocyte Function-associated Antigen 1 (CD11a/CD18, $\alpha_L\beta_2$); Mac1, Macrophage Receptor 1 (CD11b/CD18, $\alpha_M\beta_2$); PECAM1, Platelet/Endothelial Cell Adhesion Molecule 1; JAMs, Junctional Adhesion Molecules; CD40L, CD40 ligand; GPIbα, Platelet Glycoprotein Ibα; iC3b, inactive Complement component 3b; CCL, C-C Motif Chemokine Ligand; CXCL, C-X-C Motif Chemokine Ligand; CCR, C-C Motif Chemokine Receptor; CXCR, C-X-C Motif Chemokine Receptor; ROS, Reactive Oxygen Species; HClO, Hypochlorous acid; NETs, Neutrophil Extracellular Traps; IL, Interleukin; TNF, Tumor Necrosis Factor; INF, Interferon; G-CSF, Granulocyte Colony-Stimulating Factor; HSPCs, Hematopoietic Stem and Progenitor Cells. The figure was generated with schematics from BioRender.com.

recruitment. While one report has excluded a role for CCR2 in classical monocyte recruitment (Soehnlein et al., 2013), other studies have highlighted that monocyte migration into the plaque and circadian rhythms of monocyte counts in the circulation are largely regulated by the CCR2-CCL2 axis (Boring et al., 1998; Tacke et al., 2007; Combadiere et al., 2008; Winter et al., 2018). Consistently, siRNA targeting CCR2 reduced the accumulation of Ly-6C^{high} monocytes in the plaque and retards lesion progression in *Apoe*$^{-/-}$ mice (Leuschner et al., 2011). Intraluminal crawling is regulated by the interaction of LFA-1 and Mac-1 with endothelial ICAMs (Schenkel et al., 2004). PECAM-1 and JAMs mediate transendothelial migration (Gerhardt and Ley, 2015).

T Cells

T cells represent the most abundant leukocyte lineage in atherosclerotic lesions (Winkels et al., 2018; Fernandez et al., 2019) and orchestrate inflammation by a variety of T cell cytokines with pro- (TNF-α, IFN-γ, and IL-17) or anti- (IL-10) atherogenic functions (Tedgui and Mallat, 2006). A part of lesional T cells recognizes self-antigens in LDL and its core protein, Apolipoprotein B (Wolf and Ley, 2019; Wolf et al., 2020) and exhibits mixed phenotypes of proatherogenic IFN-γ secreting T_H1 and IL-10 secreting regulatory T (T_{reg}) cells. The contribution of other T_H cell subsets, $CD8^+$, and γ/δ T cells is less clear (Saigusa et al., 2020). Naïve and central memory, but not activated, T cells express L-Selectin for rolling on high endothelial venules (HEVs) and homing to lymph nodes (Weninger et al., 2001; Ley and Kansas, 2004). CCR7 acts as an homing guidance for lymph node entry of T cells (Worbs and Forster, 2007). T cell homing to mouse atherosclerotic lesions involves L-Selectin (Galkina et al., 2006) and CCL5/CCR5 (Li et al., 2016), CXCL10/CXCR3 (Mach et al., 1999), and CXCL16/CXCR6 (Wuttge et al., 2004): Decreased plaque size has been observed in *Ccr5*$^{-/-}$ (Braunersreuther et al., 2007), *Cxcr3*$^{-/-}$ (Veillard et al., 2005), *Cxcl10*$^{-/-}$ (Heller et al., 2006), and *Cxcr6*$^{-/-}$ (Galkina et al., 2007) *Apoe*$^{-/-}$ mice, which seems to be caused by reduced numbers of T_H1 cells and increased T_{reg} numbers. Consistently, CCL5 (Braunersreuther et al., 2008), CCR5, and CXCR3 (van Wanrooij et al., 2005, 2008) antagonists are atheroprotective in mice. *Apoe*$^{-/-}$ mice deficient for CCR1, an alternative receptor for CCL5 (Braunersreuther et al., 2007), and *Cxcl16*$^{-/-}$ *Ldlr*$^{-/-}$ mice (Aslanian and Charo, 2006) develop enhanced atherosclerosis. The role of CCR7 and its ligands CCL19 and CCL21, which are detectable in atherosclerotic lesions from *Apoe*$^{-/-}$ mice and humans (Damas et al., 2007), has been controversial with contradictory findings (Luchtefeld et al., 2010; Wan et al., 2013). Many adhesion factors and chemokine receptors are expressed on myeloid cells and lymphocytes, which renders results from mice with whole-body genetic deficiencies difficult to interpret.

Neutrophils

Hypercholesterolemia and inflammation promote the expression of Granulocyte Colony-Stimulating Factor (G-CSF) in the bone marrow, which triggers a release of neutrophils (Drechsler et al., 2010). Neutrophils adhere to the endothelium in a P- and E-Selectin (Eriksson et al., 2001), and β_2/ICAM dependent manner (Soehnlein, 2012). Neutrophil adhesion also involves platelet-derived CCL5 and CCR1 as well as CCR5 and CXCR2 (Drechsler et al., 2010), and leukotriene B4 binding to its high-affinity receptor BLT1 (Houard et al., 2009). Neutrophils can be detected in early and rupture-prone atherosclerotic plaques in *Apoe*$^{-/-}$ mice (Rotzius et al., 2010). Their depletion reduces atherosclerotic lesion size in *Apoe*$^{-/-}$ mice (Drechsler et al., 2010). Lesional neutrophils correlate with disease progression (Drechsler et al., 2010), the release of reactive oxygen species (ROS) (Hosokawa et al., 2011), and the formation of neutrophil extracellular traps (NETs) in mice (Warnatsch et al., 2015; Folco et al., 2018). Neutrophils promote LDL oxidation (Podrez et al., 1999), favor monocyte recruitment (Zernecke et al., 2008), macrophage activation, and foam cell formation (Gombart et al., 2005). They may contribute to endothelial erosion and plaque destabilization by hypochlorous acid production from myeloperoxidase (MPO) (Naruko et al., 2002) and matrix-degrading proteases (MMPs) activity, such as MMP-9 (Leclercq et al., 2007; Soehnlein, 2012).

INFLAMMATORY CELL RECRUITMENT AFTER MYOCARDIAL INFARCTION (MI)

MI precipitates ischemic injury, cardiomyocyte death, and cardiac tissue remodeling and accelerates atherosclerosis by an activation of hematopoietic stem cells in the bone marrow niche and increased leukocyte production (Dutta et al., 2012; **Figure 2B**). In humans, neutrophils peak within the first 24 h

after MI, likely by a G-CSF dependent response (Lieschke et al., 1994; Cannon et al., 2001; Zhang et al., 2015). Mouse neutrophils accumulate in the infarcted myocardium during the first 2 days after MI (Vafadarnejad et al., 2020) and contribute to ischemia/reperfusion injury by ROS release (Duilio et al., 2001), MPO activity (Askari et al., 2003), and NETs formation (Ge et al., 2015). Neutrophils are recruited by a process that involves CXCL8 (Sekido et al., 1993; Kukielka et al., 1995), platelet-derived serotonin (Mauler et al., 2019), L- (Ma et al., 1993) and P-Selectins (Weyrich et al., 1993), PSGL-1 (Hayward et al., 1999), β_2 (CD18) integrins (Lu et al., 1997; Kempf et al., 2011), and ICAM-1 (Palazzo et al., 1998) in mice. While preclinical studies suggested that preventing neutrophil recruitment improves the clinical outcome after MI, anti-neutrophil therapy by blocking CD11b/CD18 has failed in clinical trials (Baran et al., 2001; Faxon et al., 2002). VLA4/VCAM-1 dependent migration (Bowden et al., 2002), a narrow therapeutic time window (Williams et al., 1994), and a potential interference with protective cell types mediating tissue reparation (Horckmans et al., 2017) may explain these negative results. Monocytes and macrophages represent the dominating hematopoietic cell types in the healthy and infarcted heart (Farbehi et al., 2019) and participate in tissue healing and inflammation. Peripheral monocytosis has been associated with impaired myocardial healing in humans (Maekawa et al., 2002; van der Laan et al., 2014). While monocyte depletion abolishes tissue regeneration (van Amerongen et al., 2007), hypercholesterolemia-induced Ly-6C^{high} monocytosis accelerates cardiac remodeling and the development of heart failure in *Apoe*$^{-/-}$ mice (Panizzi et al., 2010). Ly-6C^{high} monocytes are recruited into the heart via CCR2 and CCL2, CCL7 (Kaikita et al., 2004; Dewald et al., 2005) as well as by VCAM1-depedent mechanisms (Nahrendorf et al., 2009). B cells in the infracted heart may serve as source of CCL7 (Zouggari et al., 2013). siRNA targeting CCR2 (Majmudar et al., 2013), bone marrow endothelial cell-expressed CCL2 (Krohn-Grimberghe et al., 2020), or endothelial adhesion molecules (Sager et al., 2016a) reduces Ly-6C^{high} monocyte accumulation in infarcted tissue in mice. Together with neutrophils, Ly-6C^{high} monocytes contribute to the phagocytosis of dead and dying cardiomyocytes and secrete extracellular matrix proteases and pro-inflammatory cytokines (Nahrendorf et al., 2007). While neutrophils do not persist in infarcted tissue (Dewald et al., 2004; Yan et al., 2013), monocytes continue to accumulate and give rise to early inflammatory macrophages (Nahrendorf, 2018). 5–10 days after MI, a second set of monocytes expressing Ly6C^{low} accumulate in a CX3CR1-dependent manner (Nahrendorf et al., 2007) but can also stem from Ly-6C^{high} in later tissue healing (Hilgendorf et al., 2014). Ly6C^{low} monocytes primarily involve in tissue healing and may be instructed by protective regulatory T (T_{reg}) cell-derived IL-10 (Weirather et al., 2014) or pro-inflammatory T cell expressing IFN-γ (Yang et al., 2006). The role of other chemokine ligands highly expressed in the infarcted heart, such as CCL3 and CCL4, remains unclear (Frangogiannis and Entman, 2005). In addition to traditional cardiovascular risk factors, environmental stressors (e.g., air pollutants) enhance inflammatory leukocyte recruitment to the infarcted myocardium by an upregulation of endothelial ICAM-1 and VCAM-1, Mac-1 activation, and the release of pro-inflammatory cytokines from macrophages (Marchini et al., 2016).

CLINICAL TRANSLATION AND CONCLUDING REMARKS

The inflammatory nature of atherosclerosis and MI has been established by many clinical and pre-clinical studies (Libby, 2002). Several novel therapeutic concepts targeting inflammation and immunity have arisen from this work (Libby and Everett, 2019). Consequently, the inhibition of receptors and ligands involved in the generation, adhesion, and transmigration of leukocytes has revealed a great potential for anti-leukocyte therapies at the preclinical stage. In contrast, clinical evidence has remained on a premature stage. Clinical studies indicate that leukocyte counts (Madjid et al., 2004; Adamstein et al., 2021) correlate with the appearance of MI and clinical atherosclerosis. In addition, atherosclerotic plaque size (Stone et al., 2011) and the accumulation of some, specialized leukocyte subsets predict complicated disease (Fernandez et al., 2019). However, only a few clinical studies have directly tested anti-leukocyte therapies: Administration of the P-Selectin blocking antibody Inclacumab prevented myocardial damage after MI and a percutaneous coronary intervention (PCI) (Tardif et al., 2013; Stahli et al., 2016). A neutralization of MCP-1 (CCL2) with antibodies and gene therapy showed effective in the prevention of leukocyte recruitment in atherosclerotic vessels after PCI in primates (Horvath et al., 2002; Ohtani et al., 2004). Likewise, a depletion of monocytes by liposomal alendronate partially reduced stent restenosis (Banai et al., 2013). On the other hand, inhibition of the chemokine MCP-1 (CCL2) with the compound Bindarit failed to reduce coronary restenosis following PCI and had no effect on major cardiovascular events (Colombo et al., 2016). Administration of the CCR2 blocking antibody MLN1202 proved safety in individuals at a high atherosclerotic risk. A single nucleotide polymorphism at the MCP-1 promoter region was associated with reduced high-sensitivity C-reactive protein levels (Gilbert et al., 2011), but effects on atherosclerotic lesions or cardiovascular outcomes have not been evaluated in this study. Recently, the CCR5 antagonist Maraviroc was shown to reduce atherosclerosis progression in HIV patients (Francisci et al., 2019).

Several conceptual challenges render the direct translation into cardiovascular medical therapies difficult. A lack of tissue-tropism remains the leading limitation. In contrast to an inhibition of the integrins $\alpha_4\beta_7$ and $\alpha_E\beta_7$ during IBD (Ley et al., 2016), it is unclear which adhesion receptors specifically mediate leukocyte recruitment to atherosclerotic plaques or the heart. An unspecific inhibition of homing factors involved in host-defense, tissue healing, and regeneration is at the risk to induce severe side effects. This is best documented by β_2-integrins such as Mac-1 and LFA-1 that mediates a variety of beneficial and pathogenic effects. A genetic mutation of the β_2-subunit in humans causes the severe immunodeficiency Leukocyte-Adhesion Deficiency (LAD). In addition, small molecule β_2-integrin inhibitors

and antibodies have caused the potentially fatal complication, Progressive Multifocal Leukoencephalopathy (PML) that is likely caused by a reactivation of John Cunningham Virus (JCV) in the central nervous system (Berger and Houff, 2010). Recent preclinical studies suggest that this problem could be overcome by a ligand-specific inhibition, as demonstrated for the α-subunit of Mac-1 to specifically interfere with the binding of some ligands involved in the interaction with platelets or the endothelium, but not others (Ehlers et al., 2003; Wang et al., 2005; Wolf et al., 2011, 2018). In contrast, inhibition of platelet integrins has successfully been used in cardiovascular medicine for anti-thrombotic therapy (Ley et al., 2016). The widespread clinical application of tolerable and highly effective anti-chemokine (Mollica Poeta et al., 2019) and anti-integrin therapies (Raab-Westphal et al., 2017) in inflammatory disease and cancer, however, holds the potential of future clinical trials to combat cardiovascular pathologies.

AUTHOR CONTRIBUTIONS

All authors listed made a substantial, direct and intellectual contribution to this work, and approved it for publication.

FUNDING

TM was supported by a fellowship from the German Academic Exchange Service (DAAD) and a research grant from the Agencia Nacional de Promoción Científica y Tecnológica (PICT 2016-3062) of Argentina. This study was funded by the Deutsche Forschungsgemeinschaft (DFG, German Research Foundation), SFB1425, project #422681845. This project has received funding from the European Research Council (ERC) under the European Union's Horizon 2020 Research and Innovation Program (grant agreement No. 853425).

REFERENCES

Adamstein, N. H., MacFadyen, J. G., Rose, L. M., Glynn, R. J., Dey, A. K., Libby, P., et al. (2021). The neutrophil-lymphocyte ratio and incident atherosclerotic events: analyses from five contemporary randomized trials. *Eur. Heart J.* ehaa1034. [Epub ahead of print].

An, G., Wang, H., Tang, R., Yago, T., McDaniel, J. M., McGee, S., et al. (2008). P-selectin glycoprotein ligand-1 is highly expressed on Ly-6Chi monocytes and a major determinant for Ly-6Chi monocyte recruitment to sites of atherosclerosis in mice. *Circulation* 117, 3227–3237. doi: 10.1161/circulationaha.108.771048

Ancuta, P., Liu, K. Y., Misra, V., Wacleche, V. S., Gosselin, A., Zhou, X., et al. (2009). Transcriptional profiling reveals developmental relationship and distinct biological functions of CD16+ and CD16- monocyte subsets. *BMC Genomics* 10:403. doi: 10.1186/1471-2164-10-403

Arnaout, M. A., Mahalingam, B., and Xiong, J. P. (2005). Integrin structure, allostery, and bidirectional signaling. *Annu. Rev. Cell Dev. Biol.* 21, 381–410. doi: 10.1146/annurev.cellbio.21.090704.151217

Askari, A. T., Brennan, M. L., Zhou, X., Drinko, J., Morehead, A., Thomas, J. D., et al. (2003). Myeloperoxidase and plasminogen activator inhibitor 1 play a central role in ventricular remodeling after myocardial infarction. *J. Exp. Med.* 197, 615–624. doi: 10.1084/jem.20021426

Aslanian, A. M., and Charo, I. F. (2006). Targeted disruption of the scavenger receptor and chemokine CXCL16 accelerates atherosclerosis. *Circulation* 114, 583–590. doi: 10.1161/circulationaha.105.540583

Auffray, C., Fogg, D., Garfa, M., Elain, G., Join-Lambert, O., Kayal, S., et al. (2007). Monitoring of blood vessels and tissues by a population of monocytes with patrolling behavior. *Science* 317, 666–670. doi: 10.1126/science.1142883

Banai, S., Finkelstein, A., Almagor, Y., Assali, A., Hasin, Y., Rosenschein, U., et al. (2013). Targeted anti-inflammatory systemic therapy for restenosis: the Biorest Liposomal Alendronate with Stenting sTudy (BLAST)-a double blind, randomized clinical trial. *Am. Heart J.* 165, 234–240.e1.

Baran, K. W., Nguyen, M., McKendall, G. R., Lambrew, C. T., Dykstra, G., Palmeri, S. T., et al. (2001). Double-blind, randomized trial of an anti-CD18 antibody in conjunction with recombinant tissue plasminogen activator for acute myocardial infarction: limitation of myocardial infarction following thrombolysis in acute myocardial infarction (LIMIT AMI) study. *Circulation* 104, 2778–2783. doi: 10.1161/hc4801.100236

Berger, J. R., and Houff, S. A. (2010). Neurological infections: the year of PML and influenza. *Lancet Neurol.* 9, 14–17. doi: 10.1016/s1474-4422(09)70337-0

Berlin, C., Bargatze, R. F., Campbell, J. J., von Andrian, U. H., Szabo, M. C., Hasslen, S. R., et al. (1995). alpha 4 integrins mediate lymphocyte attachment and rolling under physiologic flow. *Cell* 80, 413–422. doi: 10.1016/0092-8674(95)90491-3

Boring, L., Gosling, J., Cleary, M., and Charo, I. F. (1998). Decreased lesion formation in CCR2-/- mice reveals a role for chemokines in the initiation of atherosclerosis. *Nature* 394, 894–897. doi: 10.1038/29788

Bowden, R. A., Ding, Z. M., Donnachie, E. M., Petersen, T. K., Michael, L. H., Ballantyne, C. M., et al. (2002). Role of alpha4 integrin and VCAM-1 in CD18-independent neutrophil migration across mouse cardiac endothelium. *Circ. Res.* 90, 562–569. doi: 10.1161/01.res.0000013835.53611.97

Braunersreuther, V., Steffens, S., Arnaud, C., Pelli, G., Burger, F., Proudfoot, A., et al. (2008). A novel RANTES antagonist prevents progression of established atherosclerotic lesions in mice. *Arterioscler. Thromb. Vasc. Biol.* 28, 1090–1096. doi: 10.1161/atvbaha.108.165423

Braunersreuther, V., Zernecke, A., Arnaud, C., Liehn, E. A., Steffens, S., Shagdarsuren, E., et al. (2007). Ccr5 but not Ccr1 deficiency reduces development of diet-induced atherosclerosis in mice. *Arterioscler. Thromb. Vasc. Biol.* 27, 373–379. doi: 10.1161/01.atv.0000253886.44609.ae

Braunwald, E. (2012). The treatment of acute myocardial infarction: the past, the present, and the future. *Eur. Heart J. Acute Cardiovasc. Care* 1, 9–12. doi: 10.1177/2048872612438026

Briskin, M. J., McEvoy, L. M., and Butcher, E. C. (1993). MAdCAM-1 has homology to immunoglobulin and mucin-like adhesion receptors and to IgA1. *Nature* 363, 461–464. doi: 10.1038/363461a0

Cannon, C. P., McCabe, C. H., Wilcox, R. G., Bentley, J. H., and Braunwald, E. (2001). Association of white blood cell count with increased mortality in acute myocardial infarction and unstable angina pectoris. OPUS-TIMI 16 Investigators. *Am. J. Cardiol.* 87, 636–639, A10.

Collins, R. G., Velji, R., Guevara, N. V., Hicks, M. J., Chan, L., and Beaudet, A. L. P. - (2000). Selectin or intercellular adhesion molecule (ICAM)-1 deficiency substantially protects against atherosclerosis in apolipoprotein E-deficient mice. *J. Exp. Med.* 191, 189–194. doi: 10.1084/jem.191.1.189

Colombo, A., Basavarajaiah, S., Limbruno, U., Picchi, A., Lettieri, C., Valgimigli, M., et al. (2016). A double-blind randomised study to evaluate the efficacy and safety of bindarit in preventing coronary stent restenosis. *EuroIntervention* 12, e1385–e1394.

Combadiere, C., Potteaux, S., Rodero, M., Simon, T., Pezard, A., Esposito, B., et al. (2008). Combined inhibition of CCL2, CX3CR1, and CCR5 abrogates Ly6C(hi) and Ly6C(lo) monocytosis and almost abolishes atherosclerosis in hypercholesterolemic mice. *Circulation* 117, 1649–1657. doi: 10.1161/circulationaha.107.745091

Couffinhal, T., Duplaa, C., Moreau, C., Lamaziere, J. M., and Bonnet, J. (1994). Regulation of vascular cell adhesion molecule-1 and intercellular adhesion molecule-1 in human vascular smooth muscle cells. *Circ. Res.* 74, 225–234. doi: 10.1161/01.res.74.2.225

Courties, G., Herisson, F., Sager, H. B., Heidt, T., Ye, Y., Wei, Y., et al. (2015). Ischemic stroke activates hematopoietic bone marrow stem cells. *Circ. Res.* 116, 407–417. doi: 10.1161/circresaha.116.305207

Cybulsky, M. I., Iiyama, K., Li, H., Zhu, S., Chen, M., Iiyama, M., et al. (2001). A major role for VCAM-1, but not ICAM-1, in early atherosclerosis. *J. Clin. Invest.* 107, 1255–1262. doi: 10.1172/jci11871

da Costa Martins, P., Garcia-Vallejo, J. J., van Thienen, J. V., Fernandez-Borja, M., van, Gils JM, Beckers, C., et al. (2007). P-selectin glycoprotein ligand-1 is expressed on endothelial cells and mediates monocyte adhesion to activated endothelium. *Arterioscler. Thromb. Vasc. Biol.* 27, 1023–1029. doi: 10.1161/atvbaha.107.140442

Damas, J. K., Smith, C., Oie, E., Fevang, B., Halvorsen, B., Waehre, T., et al. (2007). Enhanced expression of the homeostatic chemokines CCL19 and CCL21 in clinical and experimental atherosclerosis: possible pathogenic role in plaque destabilization. *Arterioscler. Thromb. Vasc. Biol.* 27, 614–620. doi: 10.1161/01.atv.0000255581.38523.7c

Davies, M. J., Gordon, J. L., Gearing, A. J., Pigott, R., Woolf, N., Katz, D., et al. (1993). The expression of the adhesion molecules ICAM-1, VCAM-1, PECAM, and E-selectin in human atherosclerosis. *J. Pathol.* 171, 223–229. doi: 10.1002/path.1711710311

Davignon, J., and Ganz, P. (2004). Role of endothelial dysfunction in atherosclerosis. *Circulation* 109(23 Suppl. 1), III27–III32.

Dewald, O., Ren, G., Duerr, G. D., Zoerlein, M., Klemm, C., Gersch, C., et al. (2004). Of mice and dogs: species-specific differences in the inflammatory response following myocardial infarction. *Am. J. Pathol.* 164, 665–677.

Dewald, O., Zymek, P., Winkelmann, K., Koerting, A., Ren, G., Abou-Khamis, T., et al. (2005). CCL2/Monocyte Chemoattractant Protein-1 regulates inflammatory responses critical to healing myocardial infarcts. *Circ. Res.* 96, 881–889. doi: 10.1161/01.res.0000163017.13772.3a

Dong, Z. M., Brown, A. A., and Wagner, D. D. (2000). Prominent role of P-selectin in the development of advanced atherosclerosis in ApoE-deficient mice. *Circulation* 101, 2290–2295. doi: 10.1161/01.cir.101.19.2290

Dong, Z. M., Chapman, S. M., Brown, A. A., Frenette, P. S., Hynes, R. O., and Wagner, D. D. (1998). The combined role of P- and E-selectins in atherosclerosis. *J. Clin. Invest.* 102, 145–152. doi: 10.1172/jci3001

Doring, Y., Noels, H., Mandl, M., Kramp, B., Neideck, C., Lievens, D., et al. (2014). Deficiency of the sialyltransferase St3Gal4 reduces Ccl5-mediated myeloid cell recruitment and arrest: short communication. *Circ. Res.* 114, 976–981. doi: 10.1161/circresaha.114.302426

Drechsler, M., Megens, R. T., van Zandvoort, M., Weber, C., and Soehnlein, O. (2010). Hyperlipidemia-triggered neutrophilia promotes early atherosclerosis. *Circulation* 122, 1837–1845. doi: 10.1161/circulationaha.110.961714

Duilio, C., Ambrosio, G., Kuppusamy, P., DiPaula, A., Becker, L. C., and Zweier, J. L. (2001). Neutrophils are primary source of O2 radicals during reperfusion after prolonged myocardial ischemia. *Am. J. Physiol. Heart Circ. Physiol.* 280, H2649–H2657.

Dunne, J. L., Collins, R. G., Beaudet, A. L., Ballantyne, C. M., and Ley, K. (2003). Mac-1, but not LFA-1, uses intercellular adhesion molecule-1 to mediate slow leukocyte rolling in TNF-alpha-induced inflammation. *J. Immunol.* 171, 6105–6111. doi: 10.4049/jimmunol.171.11.6105

Dutta, P., Courties, G., Wei, Y., Leuschner, F., Gorbatov, R., Robbins, C. S., et al. (2012). Myocardial infarction accelerates atherosclerosis. *Nature* 487, 325–329.

Ehlers, R., Ustinov, V., Chen, Z., Zhang, X., Rao, R., Luscinskas, F. W., et al. (2003). Targeting platelet-leukocyte interactions: identification of the integrin Mac-1 binding site for the platelet counter receptor glycoprotein Ibalpha. *J. Exp. Med.* 198, 1077–1088.

Ensan, S., Li, A., Besla, R., Degousee, N., Cosme, J., Roufaiel, M., et al. (2016). Self-renewing resident arterial macrophages arise from embryonic CX3CR1(+) precursors and circulating monocytes immediately after birth. *Nat. Immunol.* 17, 159–168. doi: 10.1038/ni.3343

Epelman, S., Liu, P. P., and Mann, D. L. (2015). Role of innate and adaptive immune mechanisms in cardiac injury and repair. *Nat. Rev. Immunol.* 15, 117–129. doi: 10.1038/nri3800

Eriksson, E. E., Xie, X., Werr, J., Thoren, P., and Lindbom, L. (2001). Direct viewing of atherosclerosis in vivo: plaque invasion by leukocytes is initiated by the endothelial selectins. *FASEB J.* 15, 1149–1157. doi: 10.1096/fj.00-0537com

Fan, Z., and Ley, K. (2015). Leukocyte arrest: biomechanics and molecular mechanisms of beta2 integrin activation. *Biorheology* 52, 353–377. doi: 10.3233/bir-15085

Fan, Z., McArdle, S., Marki, A., Mikulski, Z., Gutierrez, E., Engelhardt, B., et al. (2016). Neutrophil recruitment limited by high-affinity bent beta2 integrin binding ligand in cis. *Nat. Commun.* 7:12658.

Farbehi, N., Patrick, R., Dorison, A., Xaymardan, M., Janbandhu, V., Wystub-Lis, K., et al. (2019). Single-cell expression profiling reveals dynamic flux of cardiac stromal, vascular and immune cells in health and injury. *Elife* 8:e43882.

Faxon, D. P., Gibbons, R. J., Chronos, N. A., Gurbel, P. A., Sheehan, F., and Investigators, H.-M. (2002). The effect of blockade of the CD11/CD18 integrin receptor on infarct size in patients with acute myocardial infarction treated with direct angioplasty: the results of the HALT-MI study. *J. Am. Coll. Cardiol.* 40, 1199–1204. doi: 10.1016/s0735-1097(02)02136-8

Fernandez, D. M., Rahman, A. H., Fernandez, N. F., Chudnovskiy, A., Amir, E. D., Amadori, L., et al. (2019). Single-cell immune landscape of human atherosclerotic plaques. *Nat. Med.* 25, 1576–1588.

Finney, A. C., Stokes, K. Y., Pattillo, C. B., and Orr, A. W. (2017). Integrin signaling in atherosclerosis. *Cell. Mol. Life Sci.* 74, 2263–2282. doi: 10.1007/s00018-017-2490-4

Folco, E. J., Mawson, T. L., Vromman, A., Bernardes-Souza, B., Franck, G., Persson, O., et al. (2018). Neutrophil extracellular traps induce endothelial cell activation and tissue factor production through interleukin-1alpha and cathepsin G. *Arterioscler. Thromb. Vasc. Biol.* 38, 1901–1912. doi: 10.1161/atvbaha.118.311150

Francisci, D., Pirro, M., Schiaroli, E., Mannarino, M. R., Cipriani, S., Bianconi, V., et al. (2019). Maraviroc intensification modulates atherosclerotic progression in HIV-suppressed patients at high cardiovascular risk. A randomized, crossover pilot study. *Open Forum Infect. Dis.* 6:ofz112.

Frangogiannis, N. G., and Entman, M. L. (2005). Chemokines in myocardial ischemia. *Trends Cardiovasc. Med.* 15, 163–169. doi: 10.2174/1570161043476375

Galkina, E., Harry, B. L., Ludwig, A., Liehn, E. A., Sanders, J. M., Bruce, A., et al. (2007). CXCR6 promotes atherosclerosis by supporting T-cell homing, interferon-gamma production, and macrophage accumulation in the aortic wall. *Circulation* 116, 1801–1811. doi: 10.1161/circulationaha.106.678474

Galkina, E., Kadl, A., Sanders, J., Varughese, D., Sarembock, I. J., and Ley, K. (2006). Lymphocyte recruitment into the aortic wall before and during development of atherosclerosis is partially L-selectin dependent. *J. Exp. Med.* 203, 1273–1282. doi: 10.1084/jem.20052205

Galkina, E., and Ley, K. (2007a). Leukocyte influx in atherosclerosis. *Curr. Drug Targets* 8, 1239–1248. doi: 10.2174/138945007783220650

Galkina, E., and Ley, K. (2007b). Vascular adhesion molecules in atherosclerosis. *Arterioscler. Thromb. Vasc. Biol.* 27, 2292–2301. doi: 10.1161/atvbaha.107.149179

Ge, L., Zhou, X., Ji, W. J., Lu, R. Y., Zhang, Y., Zhang, Y. D., et al. (2015). Neutrophil extracellular traps in ischemia-reperfusion injury-induced myocardial no-reflow: therapeutic potential of DNase-based reperfusion strategy. *Am. J. Physiol. Heart Circ. Physiol.* 308, H500–H509.

Gebuhrer, V., Murphy, J. F., Bordet, J. C., Reck, M. P., and McGregor, J. L. (1995). Oxidized low-density lipoprotein induces the expression of P-selectin (GMP140/PADGEM/CD62) on human endothelial cells. *Biochem. J.* 306(Pt 1), 293–298. doi: 10.1042/bj3060293

Gerhardt, T., and Ley, K. (2015). Monocyte trafficking across the vessel wall. *Cardiovasc. Res.* 107, 321–330. doi: 10.1093/cvr/cvv147

Gilbert, J., Lekstrom-Himes, J., Donaldson, D., Lee, Y., Hu, M., Xu, J., et al. (2011). Effect of CC chemokine receptor 2 CCR2 blockade on serum C-reactive protein in individuals at atherosclerotic risk and with a single nucleotide polymorphism of the monocyte chemoattractant protein-1 promoter region. *Am. J. Cardiol.* 107, 906–911. doi: 10.1016/j.amjcard.2010.11.005

Gombart, A. F., Krug, U., O'Kelly, J., An, E., Vegesna, V., and Koeffler, H. P. (2005). Aberrant expression of neutrophil and macrophage-related genes in a murine model for human neutrophil-specific granule deficiency. *J. Leukoc. Biol.* 78, 1153–1165. doi: 10.1189/jlb.0504286

Graham, G. J., Handel, T. M., and Proudfoot, A. E. I. (2019). Leukocyte adhesion: reconceptualizing chemokine presentation by glycosaminoglycans. *Trends Immunol.* 40, 472–481. doi: 10.1016/j.it.2019.03.009

Hayward, R., Campbell, B., Shin, Y. K., Scalia, R., and Lefer, A. M. (1999). Recombinant soluble P-selectin glycoprotein ligand-1 protects against myocardial ischemic reperfusion injury in cats. *Cardiovasc. Res.* 41, 65–76. doi: 10.1016/s0008-6363(98)00266-1

Heidt, T., Courties, G., Dutta, P., Sager, H. B., Sebas, M., Iwamoto, Y., et al. (2014a). Differential contribution of monocytes to heart macrophages in steady-state and after myocardial infarction. *Circ. Res.* 115, 284–295. doi: 10.1161/circresaha.115.303567

Heidt, T., Sager, H. B., Courties, G., Dutta, P., Iwamoto, Y., Zaltsman, A., et al. (2014b). Chronic variable stress activates hematopoietic stem cells. *Nat. Med.* 20, 754–758. doi: 10.1038/nm.3589

Heller, E. A., Liu, E., Tager, A. M., Yuan, Q., Lin, A. Y., Ahluwalia, N., et al. (2006). Chemokine CXCL10 promotes atherogenesis by modulating the local balance of effector and regulatory T cells. *Circulation* 113, 2301–2312. doi: 10.1161/circulationaha.105.605121

Higgins, J. M., Mandlebrot, D. A., Shaw, S. K., Russell, G. J., Murphy, E. A., Chen, Y. T., et al. (1998). Direct and regulated interaction of integrin alphaEbeta7 with E-cadherin. *J. Cell Biol.* 140, 197–210. doi: 10.1083/jcb.140.1.197

Hilgendorf, I., Gerhardt, L. M., Tan, T. C., Winter, C., Holderried, T. A., Chousterman, B. G., et al. (2014). Ly-6Chigh monocytes depend on Nr4a1 to balance both inflammatory and reparative phases in the infarcted myocardium. *Circ. Res.* 114, 1611–1622. doi: 10.1161/circresaha.114.303204

Horckmans, M., Ring, L., Duchene, J., Santovito, D., Schloss, M. J., Drechsler, M., et al. (2017). Neutrophils orchestrate post-myocardial infarction healing by polarizing macrophages towards a reparative phenotype. *Eur. Heart J.* 38, 187–197.

Horvath, C., Welt, F. G., Nedelman, M., Rao, P., and Rogers, C. (2002). Targeting CCR2 or CD18 inhibits experimental in-stent restenosis in primates: inhibitory potential depends on type of injury and leukocytes targeted. *Circ. Res.* 90, 488–494. doi: 10.1161/hh0402.105956

Hosokawa, T., Kumon, Y., Kobayashi, T., Enzan, H., Nishioka, Y., Yuri, K., et al. (2011). Neutrophil infiltration and oxidant-production in human atherosclerotic carotid plaques. *Histol. Histopathol.* 26, 1–11. doi: 10.1111/j.1552-6569.2012.00705.x

Houard, X., Touat, Z., Ollivier, V., Louedec, L., Philippe, M., Sebbag, U., et al. (2009). Mediators of neutrophil recruitment in human abdominal aortic aneurysms. *Cardiovasc. Res.* 82, 532–541. doi: 10.1093/cvr/cvp048

Huo, Y., Weber, C., Forlow, S. B., Sperandio, M., Thatte, J., Mack, M., et al. (2001). The chemokine KC, but not monocyte chemoattractant protein-1, triggers monocyte arrest on early atherosclerotic endothelium. *J. Clin. Invest.* 108, 1307–1314. doi: 10.1172/jci12877

Johnson, R. C., Chapman, S. M., Dong, Z. M., Ordovas, J. M., Mayadas, T. N., Herz, J., et al. (1997). Absence of P-selectin delays fatty streak formation in mice. *J. Clin. Invest.* 99, 1037–1043. doi: 10.1172/jci119231

Johnson-Tidey, R. R., McGregor, J. L., Taylor, P. R., and Poston, R. N. (1994). Increase in the adhesion molecule P-selectin in endothelium overlying atherosclerotic plaques. Coexpression with intercellular adhesion molecule-1. *Am. J. Pathol.* 144, 952–961.

Jongstra-Bilen, J., Haidari, M., Zhu, S. N., Chen, M., Guha, D., and Cybulsky, M. I. (2006). Low-grade chronic inflammation in regions of the normal mouse arterial intima predisposed to atherosclerosis. *J. Exp. Med.* 203, 2073–2083. doi: 10.1084/jem.20060245

Kaikita, K., Hayasaki, T., Okuma, T., Kuziel, W. A., Ogawa, H., and Takeya, M. (2004). Targeted deletion of CC chemokine receptor 2 attenuates left ventricular remodeling after experimental myocardial infarction. *Am. J. Pathol.* 165, 439–447. doi: 10.1016/s0002-9440(10)63309-3

Kempf, T., Zarbock, A., Widera, C., Butz, S., Stadtmann, A., Rossaint, J., et al. (2011). GDF-15 is an inhibitor of leukocyte integrin activation required for survival after myocardial infarction in mice. *Nat. Med.* 17, 581–588. doi: 10.1038/nm.2354

Khan, S., Taverna, F., Rohlenova, K., Treps, L., Geldhof, V., de Rooij, L., et al. (2019). EndoDB: a database of endothelial cell transcriptomics data. *Nucleic Acids Res.* 47, D736–D744.

Kita, T., Kume, N., Minami, M., Hayashida, K., Murayama, T., Sano, H., et al. (2001). Role of oxidized LDL in atherosclerosis. *Ann. N. Y. Acad. Sci.* 947, 199–205; discussion -6.

Koltsova, E. K., Garcia, Z., Chodaczek, G., Landau, M., McArdle, S., Scott, S. R., et al. (2012). Dynamic T cell-APC interactions sustain chronic inflammation in atherosclerosis. *J. Clin. Invest.* 122, 3114–3126. doi: 10.1172/jci61758

Krohn-Grimberghe, M., Mitchell, M. J., Schloss, M. J., Khan, O. F., Courties, G., Guimaraes, P. P. G., et al. (2020). Nanoparticle-encapsulated siRNAs for gene silencing in the haematopoietic stem-cell niche. *Nat. Biomed. Eng.* 4, 1076–1089. doi: 10.1038/s41551-020-00623-7

Kukielka, G. L., Smith, C. W., LaRosa, G. J., Manning, A. M., Mendoza, L. H., Daly, T. J., et al. (1995). Interleukin-8 gene induction in the myocardium after ischemia and reperfusion in vivo. *J. Clin. Invest.* 95, 89–103. doi: 10.1172/jci117680

Leclercq, A., Houard, X., Philippe, M., Ollivier, V., Sebbag, U., Meilhac, O., et al. (2007). Involvement of intraplaque hemorrhage in atherothrombosis evolution via neutrophil protease enrichment. *J. Leukoc. Biol.* 82, 1420–1429. doi: 10.1189/jlb.1106671

Leistner, D. M., Krankel, N., Meteva, D., Abdelwahed, Y. S., Seppelt, C., Stahli, B. E., et al. (2020). Differential immunological signature at the culprit site distinguishes acute coronary syndrome with intact from acute coronary syndrome with ruptured fibrous cap: results from the prospective translational OPTICO-ACS study. *Eur. Heart J.* 41, 3549–3560. doi: 10.1093/eurheartj/ehaa703

Leuschner, F., Dutta, P., Gorbatov, R., Novobrantseva, T. I., Donahoe, J. S., Courties, G., et al. (2011). Therapeutic siRNA silencing in inflammatory monocytes in mice. *Nat. Biotechnol.* 29, 1005–1010.

Levinovitz, A., Muhlhoff, J., Isenmann, S., and Vestweber, D. (1993). Identification of a glycoprotein ligand for E-selectin on mouse myeloid cells. *J. Cell Biol.* 121, 449–459. doi: 10.1083/jcb.121.2.449

Ley, K., and Huo, Y. (2001). VCAM-1 is critical in atherosclerosis. *J. Clin. Invest.* 107, 1209–1210. doi: 10.1172/jci13005

Ley, K., and Kansas, G. S. (2004). Selectins in T-cell recruitment to non-lymphoid tissues and sites of inflammation. *Nat. Rev. Immunol.* 4, 325–335. doi: 10.1038/nri1351

Ley, K., Laudanna, C., Cybulsky, M. I., and Nourshargh, S. (2007). Getting to the site of inflammation: the leukocyte adhesion cascade updated. *Nat. Rev. Immunol.* 7, 678–689. doi: 10.1038/nri2156

Ley, K., Rivera-Nieves, J., Sandborn, W. J., and Shattil, S. (2016). Integrin-based therapeutics: biological basis, clinical use and new drugs. *Nat. Rev. Drug Discov.* 15, 173–183. doi: 10.1038/nrd.2015.10

Li, J., McArdle, S., Gholami, A., Kimura, T., Wolf, D., Gerhardt, T., et al. (2016). CCR5+T-bet+FoxP3+ effector CD4 T cells drive atherosclerosis. *Circ. Res.* 118, 1540–1552. doi: 10.1161/circresaha.116.308648

Libby, P. (2002). Inflammation in atherosclerosis. *Nature* 420, 868–874.

Libby, P., and Everett, B. M. (2019). Novel antiatherosclerotic therapies. *Arterioscler. Thromb. Vasc. Biol.* 39, 538–545. doi: 10.1161/atvbaha.118.310958

Lieschke, G. J., Grail, D., Hodgson, G., Metcalf, D., Stanley, E., Cheers, C., et al. (1994). Mice lacking granulocyte colony-stimulating factor have chronic neutropenia, granulocyte and macrophage progenitor cell deficiency, and impaired neutrophil mobilization. *Blood* 84, 1737–1746. doi: 10.1182/blood.v84.6.1737.1737

Lu, H., Smith, C. W., Perrard, J., Bullard, D., Tang, L., Shappell, S. B., et al. (1997). LFA-1 is sufficient in mediating neutrophil emigration in Mac-1-deficient mice. *J. Clin. Invest.* 99, 1340–1350. doi: 10.1172/jci119293

Luchtefeld, M., Grothusen, C., Gagalick, A., Jagavelu, K., Schuett, H., Tietge, U. J., et al. (2010). Chemokine receptor 7 knockout attenuates atherosclerotic plaque development. *Circulation* 122, 1621–1628. doi: 10.1161/circulationaha.110.956730

Ma, X. L., Weyrich, A. S., Lefer, D. J., Buerke, M., Albertine, K. H., Kishimoto, T. K., et al. (1993). Monoclonal antibody to L-selectin attenuates neutrophil accumulation and protects ischemic reperfused cat myocardium. *Circulation* 88, 649–658. doi: 10.1161/01.cir.88.2.649

Mach, F., Sauty, A., Iarossi, A. S., Sukhova, G. K., Neote, K., Libby, P., et al. (1999). Differential expression of three T lymphocyte-activating CXC chemokines by human atheroma-associated cells. *J. Clin. Invest.* 104, 1041–1050. doi: 10.1172/jci6993

Madjid, M., Awan, I., Willerson, J. T., and Casscells, S. W. (2004). Leukocyte count and coronary heart disease: implications for risk assessment. *J. Am. Coll. Cardiol.* 44, 1945–1956.

Maekawa, Y., Anzai, T., Yoshikawa, T., Asakura, Y., Takahashi, T., Ishikawa, S., et al. (2002). Prognostic significance of peripheral monocytosis after reperfused acute myocardial infarction:a possible role for left ventricular remodeling. *J. Am. Coll. Cardiol.* 39, 241–246. doi: 10.1016/s0735-1097(01)01721-1

Majmudar, M. D., Keliher, E. J., Heidt, T., Leuschner, F., Truelove, J., Sena, B. F., et al. (2013). Monocyte-directed RNAi targeting CCR2 improves infarct healing in atherosclerosis-prone mice. *Circulation* 127, 2038–2046. doi: 10.1161/circulationaha.112.000116

Mamdouh, Z., Chen, X., Pierini, L. M., Maxfield, F. R., and Muller, W. A. (2003). Targeted recycling of PECAM from endothelial surface-connected compartments during diapedesis. *Nature* 421, 748–753. doi: 10.1038/nature01300

Marchini, T., Wolf, D., Michel, N. A., Mauler, M., Dufner, B., Hoppe, N., et al. (2016). Acute exposure to air pollution particulate matter aggravates

experimental myocardial infarction in mice by potentiating cytokine secretion from lung macrophages. *Basic Res. Cardiol.* 111:44.

Marchini, T., Zirlik, A., and Wolf, D. (2020). Pathogenic role of air pollution particulate matter in cardiometabolic disease: evidence from mice and humans. *Antioxid. Redox Signal.* 33, 263–279. doi: 10.1089/ars.2020.8096

Martin-Padura, I., Lostaglio, S., Schneemann, M., Williams, L., Romano, M., Fruscella, P., et al. (1998). Junctional adhesion molecule, a novel member of the immunoglobulin superfamily that distributes at intercellular junctions and modulates monocyte transmigration. *J. Cell Biol.* 142, 117–127. doi: 10.1083/jcb.142.1.117

Mauler, M., Herr, N., Schoenichen, C., Witsch, T., Marchini, T., Hardtner, C., et al. (2019). Platelet serotonin aggravates myocardial ischemia/reperfusion injury via neutrophil degranulation. *Circulation* 139, 918–931. doi: 10.1161/circulationaha.118.033942

Mayadas, T. N., Johnson, R. C., Rayburn, H., Hynes, R. O., and Wagner, D. D. (1993). Leukocyte rolling and extravasation are severely compromised in P selectin-deficient mice. *Cell* 74, 541–554. doi: 10.1016/0092-8674(93)80055-j

McEver, R. P., and Cummings, R. D. (1997). Perspectives series: cell adhesion in vascular biology. Role of PSGL-1 binding to selectins in leukocyte recruitment. *J. Clin. Invest.* 100, 485–491. doi: 10.1172/jci119556

Meerschaert, J., and Furie, M. B. (1995). The adhesion molecules used by monocytes for migration across endothelium include CD11a/CD18, CD11b/CD18, and VLA-4 on monocytes and ICAM-1, VCAM-1, and other ligands on endothelium. *J. Immunol.* 154, 4099–4112.

Mendez-Ferrer, S., Battista, M., and Frenette, P. S. (2010). Cooperation of beta(2)- and beta(3)-adrenergic receptors in hematopoietic progenitor cell mobilization. *Ann. N. Y. Acad. Sci.* 1192, 139–144.

Mendez-Ferrer, S., Lucas, D., Battista, M., and Frenette, P. S. (2008). Haematopoietic stem cell release is regulated by circadian oscillations. *Nature* 452, 442–447. doi: 10.1038/nature06685

Michel, N. A., Zirlik, A., and Wolf, D. (2017). CD40L and its receptors in atherothrombosis-an update. *Front. Cardiovasc. Med.* 4:40. doi: 10.3389/fcvm.2017.00040

Minicucci, M. F., Azevedo, P. S., Polegato, B. F., Paiva, S. A., and Zornoff, L. A. (2011). Heart failure after myocardial infarction: clinical implications and treatment. *Clin. Cardiol.* 34, 410–414. doi: 10.1002/clc.20922

Mollica Poeta, V., Massara, M., Capucetti, A., and Bonecchi, R. (2019). Chemokines and chemokine receptors: new targets for cancer immunotherapy. *Front. Immunol.* 10:379. doi: 10.3389/fimmu.2019.00379

Murphy, A. J., Akhtari, M., Tolani, S., Pagler, T., Bijl, N., Kuo, C. L., et al. (2011). ApoE regulates hematopoietic stem cell proliferation, monocytosis, and monocyte accumulation in atherosclerotic lesions in mice. *J. Clin. Invest.* 121, 4138–4149. doi: 10.1172/jci57559

Nageh, M. F., Sandberg, E. T., Marotti, K. R., Lin, A. H., Melchior, E. P., Bullard, D. C., et al. (1997). Deficiency of inflammatory cell adhesion molecules protects against atherosclerosis in mice. *Arterioscler. Thromb. Vasc. Biol.* 17, 1517–1520. doi: 10.1161/01.atv.17.8.1517

Nahrendorf, M. (2018). Myeloid cell contributions to cardiovascular health and disease. *Nat. Med.* 24, 711–720. doi: 10.1038/s41591-018-0064-0

Nahrendorf, M., Keliher, E., Panizzi, P., Zhang, H., Hembrador, S., Figueiredo, J. L., et al. (2009). 18F-4V for PET-CT imaging of VCAM-1 expression in atherosclerosis. *JACC Cardiovasc. Imaging* 2, 1213–1222. doi: 10.1016/j.jcmg.2009.04.016

Nahrendorf, M., Swirski, F. K., Aikawa, E., Stangenberg, L., Wurdinger, T., Figueiredo, J. L., et al. (2007). The healing myocardium sequentially mobilizes two monocyte subsets with divergent and complementary functions. *J. Exp. Med.* 204, 3037–3047. doi: 10.1084/jem.20070885

Nakashima, Y., Raines, E. W., Plump, A. S., Breslow, J. L., and Ross, R. (1998). Upregulation of VCAM-1 and ICAM-1 at atherosclerosis-prone sites on the endothelium in the ApoE-deficient mouse. *Arterioscler. Thromb. Vasc. Biol.* 18, 842–851. doi: 10.1161/01.atv.18.5.842

Naruko, T., Ueda, M., Haze, K., van der Wal, A. C., van der Loos, C. M., Itoh, A., et al. (2002). Neutrophil infiltration of culprit lesions in acute coronary syndromes. *Circulation* 106, 2894–2900. doi: 10.1161/01.cir.0000042674.89762.20

Noels, H., Weber, C., and Koenen, R. R. (2019). Chemokines as therapeutic targets in cardiovascular disease. *Arterioscler. Thromb. Vasc. Biol.* 39, 583–592. doi: 10.1161/atvbaha.118.312037

Ohtani, K., Usui, M., Nakano, K., Kohjimoto, Y., Kitajima, S., Hirouchi, Y., et al. (2004). Antimonocyte chemoattractant protein-1 gene therapy reduces experimental in-stent restenosis in hypercholesterolemic rabbits and monkeys. *Gene Ther.* 11, 1273–1282. doi: 10.1038/sj.gt.3302288

Palazzo, A. J., Jones, S. P., Girod, W. G., Anderson, D. C., Granger, D. N., and Lefer, D. J. (1998). Myocardial ischemia-reperfusion injury in CD18- and ICAM-1-deficient mice. *Am. J. Physiol.* 275, H2300–H2307.

Panizzi, P., Swirski, F. K., Figueiredo, J. L., Waterman, P., Sosnovik, D. E., Aikawa, E., et al. (2010). Impaired infarct healing in atherosclerotic mice with Ly-6C(hi) monocytosis. *J. Am. Coll. Cardiol.* 55, 1629–1638. doi: 10.1016/j.jacc.2009.08.089

Podrez, E. A., Schmitt, D., Hoff, H. F., and Hazen, S. L. (1999). Myeloperoxidase-generated reactive nitrogen species convert LDL into an atherogenic form in vitro. *J. Clin. Invest.* 103, 1547–1560. doi: 10.1172/jci5549

Quintar, A., McArdle, S., Wolf, D., Marki, A., Ehinger, E., Vassallo, M., et al. (2017). Endothelial protective monocyte patrolling in large arteries intensified by western diet and atherosclerosis. *Circ. Res.* 120, 1789–1799. doi: 10.1161/circresaha.117.310739

Raab-Westphal, S., Marshall, J. F., and Goodman, S. L. (2017). Integrins as therapeutic targets: successes and cancers. *Cancers (Basel)* 9:110. doi: 10.3390/cancers9090110

Rahman, M. S., Murphy, A. J., and Woollard, K. J. (2017). Effects of dyslipidaemia on monocyte production and function in cardiovascular disease. *Nat. Rev. Cardiol.* 14, 387–400. doi: 10.1038/nrcardio.2017.34

Robbins, C. S., Chudnovskiy, A., Rauch, P. J., Figueiredo, J. L., Iwamoto, Y., Gorbatov, R., et al. (2012). Extramedullary hematopoiesis generates Ly-6C(high) monocytes that infiltrate atherosclerotic lesions. *Circulation* 125, 364–374. doi: 10.1161/circulationaha.111.061986

Ross, R. (1999). Atherosclerosis–an inflammatory disease. *N. Engl. J. Med.* 340, 115–126.

Rotzius, P., Thams, S., Soehnlein, O., Kenne, E., Tseng, C. N., Bjorkstrom, N. K., et al. (2010). Distinct infiltration of neutrophils in lesion shoulders in ApoE-/- mice. *Am. J. Pathol.* 177, 493–500. doi: 10.2353/ajpath.2010.090480

Sager, H. B., Dutta, P., Dahlman, J. E., Hulsmans, M., Courties, G., Sun, Y., et al. (2016a). RNAi targeting multiple cell adhesion molecules reduces immune cell recruitment and vascular inflammation after myocardial infarction. *Sci. Transl. Med.* 8:342ra80. doi: 10.1126/scitranslmed.aaf1435

Sager, H. B., Hulsmans, M., Lavine, K. J., Moreira, M. B., Heidt, T., Courties, G., et al. (2016b). Proliferation and recruitment contribute to myocardial macrophage expansion in chronic heart failure. *Circ. Res.* 119, 853–864. doi: 10.1161/circresaha.116.309001

Saigusa, R., Winkels, H., and Ley, K. (2020). T cell subsets and functions in atherosclerosis. *Nat. Rev. Cardiol.* 17, 387–401. doi: 10.1038/s41569-020-0352-5

Schenkel, A. R., Mamdouh, Z., and Muller, W. A. (2004). Locomotion of monocytes on endothelium is a critical step during extravasation. *Nat. Immunol.* 5, 393–400. doi: 10.1038/ni1051

Sekido, N., Mukaida, N., Harada, A., Nakanishi, I., Watanabe, Y., and Matsushima, K. (1993). Prevention of lung reperfusion injury in rabbits by a monoclonal antibody against interleukin-8. *Nature* 365, 654–657. doi: 10.1038/365654a0

Sharma, M., Schlegel, M. P., Afonso, M. S., Brown, E. J., Rahman, K., Weinstock, A., et al. (2020). Regulatory T cells license macrophage pro-resolving functions during atherosclerosis regression. *Circ. Res.* 127, 335–353. doi: 10.1161/circresaha.119.316461

Shimaoka, M., Xiao, T., Liu, J. H., Yang, Y., Dong, Y., Jun, C. D., et al. (2003). Structures of the alpha L I domain and its complex with ICAM-1 reveal a shape-shifting pathway for integrin regulation. *Cell* 112, 99–111. doi: 10.1016/s0092-8674(02)01257-6

Soehnlein, O. (2012). Multiple roles for neutrophils in atherosclerosis. *Circ. Res.* 110, 875–888. doi: 10.1161/circresaha.111.257535

Soehnlein, O., Drechsler, M., Doring, Y., Lievens, D., Hartwig, H., Kemmerich, K., et al. (2013). Distinct functions of chemokine receptor axes in the atherogenic mobilization and recruitment of classical monocytes. *EMBO Mol. Med.* 5, 471–481. doi: 10.1002/emmm.201201717

Stahli, B. E., Gebhard, C., Duchatelle, V., Cournoyer, D., Petroni, T., Tanguay, J. F., et al. (2016). Effects of the P-selectin antagonist inclacumab on myocardial damage after percutaneous coronary intervention according to timing of infusion: insights from the SELECT-ACS trial. *J. Am. Heart Assoc.* 5:e004255.

Stocker, C. J., Sugars, K. L., Harari, O. A., Landis, R. C., Morley, B. J., and Haskard, D. O. (2000). TNF-alpha, IL-4, and IFN-gamma regulate differential expression of P- and E-selectin expression by porcine aortic endothelial cells. *J. Immunol.* 164, 3309–3315. doi: 10.4049/jimmunol.164.6.3309

Stone, G. W., Maehara, A., Lansky, A. J., de Bruyne, B., Cristea, E., Mintz, G. S., et al. (2011). A prospective natural-history study of coronary atherosclerosis. *N. Engl. J. Med.* 364, 226–235.

Swirski, F. K., Libby, P., Aikawa, E., Alcaide, P., Luscinskas, F. W., Weissleder, R., et al. (2007). Ly-6Chi monocytes dominate hypercholesterolemia-associated monocytosis and give rise to macrophages in atheromata. *J. Clin. Invest.* 117, 195–205. doi: 10.1172/jci29950

Swirski, F. K., Nahrendorf, M., Etzrodt, M., Wildgruber, M., Cortez-Retamozo, V., Panizzi, P., et al. (2009). Identification of splenic reservoir monocytes and their deployment to inflammatory sites. *Science* 325, 612–616. doi: 10.1126/science.1175202

Swirski, F. K., Pittet, M. J., Kircher, M. F., Aikawa, E., Jaffer, F. A., Libby, P., et al. (2006). Monocyte accumulation in mouse atherogenesis is progressive and proportional to extent of disease. *Proc. Natl. Acad. Sci. U.S.A.* 103, 10340–10345. doi: 10.1073/pnas.0604260103

Tacke, F., Alvarez, D., Kaplan, T. J., Jakubzick, C., Spanbroek, R., Llodra, J., et al. (2007). Monocyte subsets differentially employ CCR2, CCR5, and CX3CR1 to accumulate within atherosclerotic plaques. *J. Clin. Invest.* 117, 185–194. doi: 10.1172/jci28549

Takada, Y., Ye, X., and Simon, S. (2007). The integrins. *Genome Biol.* 8:215.

Tardif, J. C., Tanguay, J. F., Wright, S. R., Duchatelle, V., Petroni, T., Gregoire, J. C., et al. (2013). Effects of the P-selectin antagonist inclacumab on myocardial damage after percutaneous coronary intervention for non-ST-segment elevation myocardial infarction: results of the SELECT-ACS trial. *J. Am. Coll. Cardiol.* 61, 2048–2055. doi: 10.1016/j.jacc.2013.03.003

Tedgui, A., and Mallat, Z. (2006). Cytokines in atherosclerosis: pathogenic and regulatory pathways. *Physiol. Rev.* 86, 515–581. doi: 10.1152/physrev.00024.2005

Tenaglia, A. N., Buda, A. J., Wilkins, R. G., Barron, M. K., Jeffords, P. R., Vo, K., et al. (1997). Levels of expression of P-selectin, E-selectin, and intercellular adhesion molecule-1 in coronary atherectomy specimens from patients with stable and unstable angina pectoris. *Am. J. Cardiol.* 79, 742–747. doi: 10.1016/s0002-9149(96)00861-2

Vafadarnejad, E., Rizzo, G., Krampert, L., Arampatzi, P., Arias-Loza, A. P., Nazzal, Y., et al. (2020). Dynamics of cardiac neutrophil diversity in murine myocardial infarction. *Circ. Res.* 127, e232–e249.

van Amerongen, M. J., Harmsen, M. C., van Rooijen, N., Petersen, A. H., and van Luyn, M. J. (2007). Macrophage depletion impairs wound healing and increases left ventricular remodeling after myocardial injury in mice. *Am. J. Pathol.* 170, 818–829. doi: 10.2353/ajpath.2007.060547

van der Laan, A. M., Ter Horst, E. N., Delewi, R., Begieneman, M. P., Krijnen, P. A., Hirsch, A., et al. (2014). Monocyte subset accumulation in the human heart following acute myocardial infarction and the role of the spleen as monocyte reservoir. *Eur. Heart J.* 35, 376–385. doi: 10.1093/eurheartj/eht331

van Wanrooij, E. J., de Jager, S. C., van Es, T., de Vos, P., Birch, H. L., Owen, D. A., et al. (2008). CXCR3 antagonist NBI-74330 attenuates atherosclerotic plaque formation in LDL receptor-deficient mice. *Arterioscler. Thromb. Vasc. Biol.* 28, 251–257. doi: 10.1161/atvbaha.107.147827

van Wanrooij, E. J., Happe, H., Hauer, A. D., de Vos, P., Imanishi, T., Fujiwara, H., et al. (2005). HIV entry inhibitor TAK-779 attenuates atherogenesis in low-density lipoprotein receptor-deficient mice. *Arterioscler. Thromb. Vasc. Biol.* 25, 2642–2647. doi: 10.1161/01.atv.0000192018.90021.c0

Veillard, N. R., Steffens, S., Pelli, G., Lu, B., Kwak, B. R., Gerard, C., et al. (2005). Differential influence of chemokine receptors CCR2 and CXCR3 in development of atherosclerosis in vivo. *Circulation* 112, 870–878. doi: 10.1161/circulationaha.104.520718

Wan, W., Lionakis, M. S., Liu, Q., Roffe, E., and Murphy, P. M. (2013). Genetic deletion of chemokine receptor Ccr7 exacerbates atherogenesis in ApoE-deficient mice. *Cardiovasc. Res.* 97, 580–588. doi: 10.1093/cvr/cvs349

Wang, Y., Sakuma, M., Chen, Z., Ustinov, V., Shi, C., Croce, K., et al. (2005). Leukocyte engagement of platelet glycoprotein Ibalpha via the integrin Mac-1 is critical for the biological response to vascular injury. *Circulation* 112, 2993–3000. doi: 10.1161/circulationaha.105.571315

Warnatsch, A., Ioannou, M., Wang, Q., and Papayannopoulos, V. (2015). Inflammation. Neutrophil extracellular traps license macrophages for cytokine production in atherosclerosis. *Science* 349, 316–320. doi: 10.1126/science.aaa8064

Weirather, J., Hofmann, U. D., Beyersdorf, N., Ramos, G. C., Vogel, B., Frey, A., et al. (2014). Foxp3+ CD4+ T cells improve healing after myocardial infarction by modulating monocyte/macrophage differentiation. *Circ. Res.* 115, 55–67. doi: 10.1161/circresaha.115.303895

Weninger, W., Crowley, M. A., Manjunath, N., and von Andrian, U. H. (2001). Migratory properties of naive, effector, and memory CD8(+) T cells. *J. Exp. Med.* 194, 953–966. doi: 10.1084/jem.194.7.953

Weyrich, A. S., Ma, X. Y., Lefer, D. J., Albertine, K. H., and Lefer, A. M. (1993). In vivo neutralization of P-selectin protects feline heart and endothelium in myocardial ischemia and reperfusion injury. *J. Clin. Invest.* 91, 2620–2629. doi: 10.1172/jci116501

Williams, F. M., Kus, M., Tanda, K., and Williams, T. J. (1994). Effect of duration of ischaemia on reduction of myocardial infarct size by inhibition of neutrophil accumulation using an anti-CD18 monoclonal antibody. *Br. J. Pharmacol.* 111, 1123–1128. doi: 10.1111/j.1476-5381.1994.tb14861.x

Winkels, H., Ehinger, E., Vassallo, M., Buscher, K., Dinh, H., Kobiyama, K., et al. (2018). Atlas of the immune cell repertoire in mouse atherosclerosis defined by single-cell RNA-sequencing and mass cytometry. *Circ. Res.* 122, 1675–1688. doi: 10.1161/circresaha.117.312513

Winter, C., Silvestre-Roig, C., Ortega-Gomez, A., Lemnitzer, P., Poelman, H., Schumski, A., et al. (2018). Chrono-pharmacological targeting of the CCL2-CCR2 axis ameliorates atherosclerosis. *Cell Metab.* 28, 175–182.e5.

Wolf, D., Anto-Michel, N., Blankenbach, H., Wiedemann, A., Buscher, K., Hohmann, J. D., et al. (2018). A ligand-specific blockade of the integrin Mac-1 selectively targets pathologic inflammation while maintaining protective host-defense. *Nat. Commun.* 9:525.

Wolf, D., Gerhardt, T., Winkels, H., Michel, N. A., Pramod, A. B., Ghosheh, Y., et al. (2020). Pathogenic autoimmunity in atherosclerosis evolves from initially protective apolipoprotein B100-reactive CD4(+) T-regulatory cells. *Circulation* 142, 1279–1293. doi: 10.1161/circulationaha.119.042863

Wolf, D., Hohmann, J. D., Wiedemann, A., Bledzka, K., Blankenbach, H., Marchini, T., et al. (2011). Binding of CD40L to Mac-1's I-domain involves the EQLKKSKTL motif and mediates leukocyte recruitment and atherosclerosis–but does not affect immunity and thrombosis in mice. *Circ. Res.* 109, 1269–1279. doi: 10.1161/circresaha.111.247684

Wolf, D., and Ley, K. (2015). Waking up the stem cell niche: how hematopoietic stem cells generate inflammatory monocytes after stroke. *Circ. Res.* 116, 389–392. doi: 10.1161/circresaha.114.305678

Wolf, D., and Ley, K. (2019). Immunity and inflammation in atherosclerosis. *Circ. Res.* 124, 315–327. doi: 10.1161/circresaha.118.313591

Wolf, D., Zirlik, A., and Ley, K. (2015). Beyond vascular inflammation–recent advances in understanding atherosclerosis. *Cell. Mol. Life Sci.* 72, 3853–3869. doi: 10.1007/s00018-015-1971-6

Worbs, T., and Forster, R. (2007). A key role for CCR7 in establishing central and peripheral tolerance. *Trends Immunol.* 28, 274–280. doi: 10.1016/j.it.2007.04.002

Wuttge, D. M., Zhou, X., Sheikine, Y., Wagsater, D., Stemme, V., Hedin, U., et al. (2004). CXCL16/SR-PSOX is an interferon-gamma-regulated chemokine and scavenger receptor expressed in atherosclerotic lesions. *Arterioscler. Thromb. Vasc. Biol.* 24, 750–755. doi: 10.1161/01.atv.0000124102.11472.36

Yan, X., Anzai, A., Katsumata, Y., Matsuhashi, T., Ito, K., Endo, J., et al. (2013). Temporal dynamics of cardiac immune cell accumulation following acute myocardial infarction. *J. Mol. Cell. Cardiol.* 62, 24–35. doi: 10.1016/j.yjmcc.2013.04.023

Yang, Z., Day, Y. J., Toufektsian, M. C., Xu, Y., Ramos, S. I., Marshall, M. A., et al. (2006). Myocardial infarct-sparing effect of adenosine A2A receptor activation is due to its action on CD4+ T lymphocytes. *Circulation* 114, 2056–2064. doi: 10.1161/circulationaha.106.649244

Yvan-Charvet, L., Pagler, T., Gautier, E. L., Avagyan, S., Siry, R. L., Han, S., et al. (2010). ATP-binding cassette transporters and HDL suppress hematopoietic stem cell proliferation. *Science* 328, 1689–1693. doi: 10.1126/science.1189731

Zernecke, A., Bot, I., Djalali-Talab, Y., Shagdarsuren, E., Bidzhekov, K., Meiler, S., et al. (2008). Protective role of CXC receptor 4/CXC ligand 12 unveils the importance of neutrophils in atherosclerosis. *Circ. Res.* 102, 209–217. doi: 10.1161/circresaha.107.160697

Zernecke, A., and Weber, C. (2014). Chemokines in atherosclerosis: proceedings resumed. *Arterioscler. Thromb. Vasc. Biol.* 34, 742–750. doi: 10.1161/atvbaha.113.301655

Zernecke, A., Winkels, H., Cochain, C., Williams, J. W., Wolf, D., Soehnlein, O., et al. (2020). Meta-Analysis of leukocyte diversity in atherosclerotic mouse aortas. *Circ. Res.* 127, 402–426. doi: 10.1161/circresaha.120.316903

Zhang, S., Wan, Z., Zhang, Y., Fan, Y., Gu, W., Li, F., et al. (2015). Neutrophil count improves the GRACE risk score prediction of clinical outcomes in patients with ST-elevation myocardial infarction. *Atherosclerosis* 241, 723–728. doi: 10.1016/j.atherosclerosis.2015.06.035

Zirlik, A., Maier, C., Gerdes, N., MacFarlane, L., Soosairajah, J., Bavendiek, U., et al. (2007). CD40 ligand mediates inflammation independently of CD40 by interaction with Mac-1. *Circulation* 115, 1571–1580. doi: 10.1161/circulationaha.106.683201

Zouggari, Y., Ait-Oufella, H., Bonnin, P., Simon, T., Sage, A. P., Guerin, C., et al. (2013). B lymphocytes trigger monocyte mobilization and impair heart function after acute myocardial infarction. *Nat. Med.* 19, 1273–1280. doi: 10.1038/nm.3284

Conflict of Interest: DW holds patents on the inhibition of the leukocyte integrin Mac-1 by peptide mimetics and antibodies (EP 2444101 A1/EP 3 260 133 A1).

The remaining authors declare that the research was conducted in the absence of any commercial or financial relationships that could be construed as a potential conflict of interest.

frontiers in Cell and Developmental Biology

BRIEF RESEARCH REPORT
published: 18 February 2021
doi: 10.3389/fcell.2021.624201

Use of Integrated Optical Clearing and 2-Photon Imaging to Investigate Sex Differences in Neuroimmune Interactions After Peripheral Nerve Injury

*Thomas A. Szabo-Pardi†, Umar M. Syed†, Zachary W. Castillo and Michael D. Burton**

Neuroimmunology and Behavior Laboratory, Department of Neuroscience, Center for Advanced Pain Studies (CAPS), School of Behavioral and Brain Sciences, University of Texas at Dallas, Richardson, TX, United States

Peripheral nerve injury induces a myriad of immune-derived symptoms that negatively impacts pain, depression, and overall quality of life. Neuroimmune differences underlie sexual dimorphisms in various pain states. The innate immune system is a source of these sex differences, which promotes inflammation and pro-nociception through bidirectional signaling with the nervous system. Spatiotemporal interactions between leukocytes and sensory neurons could hold the key to explain ascribed differences between sexes. To date, studies have found it difficult to display these interactions. We are poised to answer important questions regarding the recruitment of peripheral leukocytes to key tissues of the pain system, the dorsal root ganglia (DRG) and sciatic nerve after nerve injury. We optically clear whole DRGs and sciatic nerves and concomitantly use multi-photon microscopy and transgenic reporter lines, to visualize leukocyte dynamics involved in neuropathic pain development following nerve injury. We observed robust sexual dimorphisms in leukocyte recruitment to the lumbar DRGs after nerve injury. We also assessed immune cell size and morphology to understand activation states in the context of nervous tissue inflammation. The altered mechanisms by which the male and female immune systems respond to nerve injury are still topics of further research, however; the continued use of next-generation imaging with advanced whole tissue image analysis remains an important tool in understanding the reciprocal interactions between neuronal and non-neuronal cells.

Keywords: optical clearing, nerve injury, sex differences, neuroimmune interactions, 2-photon, macrophage, DRG

OPEN ACCESS

Edited by:
Xunbin Wei,
Peking University, China

Reviewed by:
Irmgard Tegeder,
Goethe University Frankfurt, Germany
Veronica Shubayev,
University of California, San Diego, United States

***Correspondence:**
Michael D. Burton
michael.burton@utdallas.edu

†These authors have contributed equally to this work

Specialty section:
This article was submitted to Cell Adhesion and Migration, a section of the journal Frontiers in Cell and Developmental Biology

Received: *30 October 2020*
Accepted: *12 January 2021*
Published: *18 February 2021*

Citation:
Szabo-Pardi TA, Syed UM, Castillo ZW and Burton MD (2021) Use of Integrated Optical Clearing and 2-Photon Imaging to Investigate Sex Differences in Neuroimmune Interactions After Peripheral Nerve Injury. Front. Cell Dev. Biol. 9:624201. doi: 10.3389/fcell.2021.624201

INTRODUCTION

Peripheral nerve injury often results in neuropathic pain, which is defined by trauma or lesions that disrupt the somatosensory systems. Injury-induced neuropathic pain is estimated to occur in over 30% of patients following routine operations (Kehlet et al., 2006). Patients often report higher levels of comorbidities, such as depression and sleep disorders which further contribute to increased pathological clinical outcomes and significantly reduce quality of life (McDermott et al., 2006; Cohen et al., 2015). Although the prevalence of chronic pain continues to rise, the number and effectiveness

of existing therapeutics remains limited (Finnerup, 2015). The increasing incidence of neuropathic pain has piqued interest in understanding the key immunologic processes involved. Previous studies have found a clinically observed difference in the prevalence and perception of pain in males vs. females (Fillingim et al., 2009; Mogil, 2012). However, there is still a dearth of knowledge on the sexual dimorphisms observed in leukocyte trafficking, morphology, and neuroimmune interaction.

Macrophages, key myeloid-derived leukocytes have been shown to play a key role in facilitating maladaptive nociception following nerve injury (Zhuo et al., 2011). Moreover, the peripheral immune system, specifically macrophages, play a pivotal role in sensitization of sensory neurons (Lindborg et al., 2018). Macrophages in the dorsal root ganglia (DRG) and sciatic nerve (ScN) play a critical role in both the initiation and maintenance of neuropathic pain by enhancing sensory neuron transduction and excitability (Basbaum et al., 2009). We hypothesize that using intact tissue for 3D rendering and morphologic analysis; we will be able to differentiate spatial resolution of macrophage infiltration and their interactions with sensory neurons in a sex-specific fashion. Recent studies have shown that these macrophages demonstrate robust molecular crosstalk with sensory neurons (Yu et al., 2020). This remains an integral process of not only pain induction as a protective mechanism, but also a transition to maladaptive chronic pain in some instances (Renthal et al., 2020). Discovering the sex-dependent roles of macrophages in tissue injury is paramount as the incidence macrophage-dependent chronic pain in females is lower than in males (Wiesenfeld-Hallin, 2005; Agalave et al., 2020; Rudjito et al., 2020). As such, identifying sex differences in macrophage biology will serve as a foundation for future studies aimed at exploiting immunological regulation in pain and will serve to create a more tailored approach to therapeutics.

Our group has recently developed a technique for intravital imaging using transgenic reporter mice and multiphoton microscopy (Szabo-Pardi et al., 2019). We wanted to adapt these methods to conceptualize the immune response to injury. Changes in cellular morphology has been associated with changes in functionality of cells (McWhorter et al., 2013). We used transgenic reporter animals, fluorescently labeled ($ROSA26^{tdTomatoLSL}$) × LysozymeM:cre ($LysM^{+}$)-expressing leukocytes ($LysM^{tdT+}$). LysM is an antimicrobial enzyme (encoded by the *Lyz2* gene) that breaks down gram-positive bacterial cell walls and is predominately expressed by circulating neutrophils and tissue macrophages (Goren et al., 2009). Tissue macrophages have been shown to be upregulated within days after peripheral injury and are known to play a role in injury-induced sensitization of sensory neurons (Clausen et al., 1999; Rittner, 2005; Kiguchi et al., 2018). Prior studies have used techniques, such as flow cytometric analysis to quantify recruitment or infiltration of macrophages into peripheral nervous tissue, however, there are inherent limitations using this method (Ghasemlou et al., 2015; Lopes et al., 2017). Notably, a lack of clarity regarding pathogenesis and spatiotemporal visualization of macrophages in the extracellular space. Moreover, studies that investigate recruitment of any immune cell to peripheral nervous tissues rarely use both sexes, making it difficult to draw apt comparisons (Kwon et al., 2013; Schmid et al., 2013).

To provide a more robust understanding of interactions in nervous tissue after injury, we cleared tissue (Sca*l*eS1) to enable visualization of tdTomato-tagged macrophages via multiphoton microscopy. Not only does this technique preserve the integrity of extracted tissues, but it also provides an accurate representation of cell dynamics in a diseased state (Gómez-Gaviro et al., 2020). The ability to use whole, unsectioned tissue provides a clear advantage over conventional methods, which is made possible by visualizing the spatial relation of neuronal and non-neuronal immune cells in a three-dimensional (3-D) model. In this study, we find that male mice exhibit more robust infiltration of $LysM^{tdT+}$ macrophages after injury as compared to females. Additionally, we took advantage of advanced image analysis in concert with our experimental approach to group and classify the morphology of these macrophages. Recent literature has shown that macrophages exemplify distinct morphological changes differentiating into M1 and M2 phenotypes, pro-inflammatory or anti-inflammatory functions, respectively (McWhorter et al., 2013). In response to physiological changes and cytokine signaling, M2 macrophages are associated with an elongated, prolate morphology while M1 macrophages are associated with an oblate, flattened morphology (Bertani et al., 2017). This serves as an indispensable tool in our approach to elucidate sex differences after nerve injury and can be adapted to address the gap in understanding the intimate interactions between leukocytes and neurons in other aspects in neuroimmunology research.

MATERIALS AND METHODS

Laboratory Animals

All animal experiments were carried out in accordance with protocols approved by the Institutional Animal Care and Use Committee of the University of Texas at Dallas. Mice were housed (4–5 per cage) in a temperature-controlled facility (20–25°C) and maintained on a 12-h light/dark cycle (lights on: 6 a.m./lights off: 6 p.m.). Mice had *ad-libitum* access to food and water and were 8–12-weeks-old during the experiments (male, 25–30 g; female, 20–25 g). Transgenic mice expressing NLS-Cre recombinase under control of the endogenous *Lyz2* promoter/enhancer elements (LysM) were obtained commercially from Jackson (Stock no: 004781). Characterization of these mice showed that heterozygous cre animals have no pain phenotype and normal electrophysiological properties (Clausen et al., 1999). Furthermore, transgenic mice expressing a loxP-flanked *STOP* cassette preventing expressing of tdTomato (red fluorescent protein) were purchased from Jackson (Stock no: 007909) and bred with $LysM^{cre+}$ animals in-house ($LysM^{cre+}$ × $ROSA26^{LSLtdTomato}$ = $LysM^{tdT}$) and used for all behavioral and biochemical assays. All animals used were heterozygous for $LysM^{cre}$ and had at least one copy of

Abbreviations: SNI, spared-nerve injury; DRG, dorsal root ganglia; ScN, sciatic nerve; IL, interleukin; LysM, LysozymeM; PFA, paraformaldehyde; PBS, phosphate-buffered saline; IP, ipsilateral; CO, contralateral.

tdTomato. All strains were backcrossed to maintain C57BL/6J genetic background with animals from Jackson Lab (stock no. 000664).

Surgical Procedures

The spared nerve injury (SNI) model of neuropathic pain was used. Baseline values for behavioral experiments were established 24-h prior to surgery. Mice were anesthetized under isoflurane anesthesia (1.0–2.5%). The ipsilateral thigh was shaved and cleaned with betadine (Dynarex, NY, USA; cat no. 1425) and 70% ethanol (Decon Labs, PA, USA; cat no. 2701). The skin and muscle of the ipsilateral thigh were incised with a #11 scalpel (Thermo Fisher, MA, USA; cat no. 22-079-691) and the sciatic nerve along its three branches (common peroneal, tibial, and sural) were exposed. A tight ligature using a 5-0 silk suture (VWR, PA, USA; cat no. MV-682) was placed around the proximal tibial and common peroneal branches, after which the nerves distal to the ligature were transected, taking care to not stretch or damage the sural nerve. The skin was closed using an auto clip (Fine Science Tools, CA, USA; cat no. 12022-09) and mice were returned to their home cages to recover (Decosterd and Woolf, 2000). Sham surgeries were done identically to the SNI surgery; however, no portion of the sciatic nerve was ligated or transected. Following surgery, mice are subcutaneously administered a single dose of Gentamicin (5 mg/mL) (Sigma-Aldrich, CA, USA; cat no. G1272) as a prophylactic antibiotic. All mice were then returned to their home cages for recovery and monitored daily.

Behavioral Testing

To measure mechanical hypersensitivity, mice were individually placed on an elevated wire grid inside acrylic behavior racks and allowed to habituate for ∼2-h. Behavior racks were cleaned with a 1:3 ratio of a natural all-purpose and deodorant-free cleaner (Seventh Generation™, VT, USA; cat no. 22719BK-5) and DI water and wiped dry to eliminate odor cues between each reading, baseline, and experiment. The ipsilateral hind paw was then stimulated with von Frey filaments (Stoelting Co., IL, USA; cat no. 58011) using the up-down experimental paradigm (Chaplan et al., 1994). To assess cold allodynia (cold response) in our SNI model, mice were individually placed on the same elevated wire grid and behavior racks and allowed to habituate for ∼2-h before testing. Approximately 100 μL of biological grade acetone (Fisher Scientific, MA, USA; cat no. AI6P-4) was then applied to the lateral aspect of the ipsilateral hind paw using a 1 mL syringe (VWR, PA, USA; cat no. 309659) attached to a blunted 25 G needle (VWR, PA, USA; cat no. 305125). Cold response was assessed by paw licking, shaking, grooming behaviors and were measured over a 60-s period (Yoon et al., 1994). Baseline values were taken 24-h prior to performing surgery. Mechanical hypersensitivity and cold allodynia were then measured on post-operative days 1, 3, and 5. Mechanical measures were always taken before cold response. All behavioral testing was done between 10 a.m. and 2:00 p.m. Experimenters were blinded to genotype, surgery, or both.

Optical Clearing

Five days post-SNI, mice were deeply anesthetized using a mixture of ketamine (80 mg/kg) and xylazine (12 mg/kg), injected intraperitoneally, and were transcardially perfused with 10 mL of ice cold 1× PBS (Thermofisher, MA, USA; cat no. BP3994) and then 10 mL of ice cold 4% paraformaldehyde (Sigma-Aldrich, CA, USA; cat no. F8775) using a 25G winged infusion set (Thermofisher, MA, USA; cat no. 14-840-37). Lumbar dorsal root ganglia (DRGs) (L4-5) and sciatic nerves (ScNs) were collected in 2 mL microcentrifuge tubes (Eppendorf, CT, USA; cat no. 022-43-104-8) and post-fixed in 1.5 mL of 4% paraformaldehyde (Sigma-Aldrich, CA, USA; cat no. F8775) (made in 1× PBS) for 4-h. Fixed tissues were then transferred to a 2 mL microcentrifuge tube containing 1.5 mL of 20% sucrose solution (VWR, PA, USA; cat no. 0335-1KG) (made in 1× PBS) for 48 h. Following cryoprotection, tissues were then transferred to a 5 mL microcentrifuge tube (Eppendorf, CT, USA; cat no. 0030-119-401), immersed in 1.5–4 mL of Sca*l*eS1 solution and placed on a tissue nutator for ∼10–14 days to achieve optimal tissue clarity (Hama et al., 2015). This was to enhance perfusion of the extracted tissues. Sca*l*eS1 solution was aspirated and replaced every 48-h with fresh solution. The following reagents were used to prepare Sca*l*eS1 solution: 4 M urea crystals (Thermofischer, MA, USA; cat no. 29700), 0.1% (wt/vol) Triton X-100 (Sigma-Aldrich, CA, USA; cat no. X100), and 10% (wt/wt) glycerol (Fischer Scientific, MA, USA; cat no. BP229-1). In brief, urea crystals were dissolved in water using a stir bar Thermofisher, MA, USA; cat no. F37180). Next, the triton x-100 was added along with glycerol and was left to mix for an hour. The solution was made and allowed a minimum of 48-h to equilibrate before use and stored at room temperature.

Multiphoton Microscopy

Optically cleared DRGs and ScNs were embedded in single 13 mm glass-bottomed cell culture plates (Thermofisher, MA, USA; cat no. 150680) using 0.5% (w/v) agarose (VWR, PA, USA; cat no. MPN605) (dissolved in ultra-pure ddH_2O) as an immobilization medium. Upon polymerization of the agarose, ∼1 mL of Sca*l*eS1 solution was pipetted into the culture plates to ensure coverage and adequate hydration of immobilized samples. Samples were individually imaged using an Olympus MPE-RS TWIN multiphoton microscope outfitted with dual excitation lasers (Spectra Physics INSIGHT DS+ -OL pulsed IR LASER, tunable from 680 to 1,300 nm, 120 fs pulse width at specimen plane and SPECTRA PHYSICS MAI TAI HP DEEP SEE-OL pulsed IR LASER, tunable from 690 to 1,040 nm, 100 fs pulse width at specimen plane). We have established optimal parameters for multiphoton microscopy in a previous study (Szabo-Pardi et al., 2019). In brief, using these excitation lasers in combination with a XLPLN25XWMP2 Olympus ultra 25× MPE water-immersion objective (1.05 NA, 2 mm WD) we were able to image tdTomato-positive $LysM^+$ cells ($LysM^{tdT+}$) (1,100 nm). Tissues were scanned using a galvanometer scanning unit at 10 us/pixel; 1:1 aspect ratio; 0.5 step size; 512 × 512 area and images were acquired with 2-channel multi-alkali photomultiplier tubes (PMTs). Z-stack images were acquired of the entire sample (Y-plane) of the DRG and distal/proximal portions of the ScN. A step

size of 1 um per slice was used and images were between 300 and 400 slices. FVMPE-RS system software (FluoView) was used to acquire images. Raw Z-stack images were then exported to Imaris imaging software for appropriate processing and analysis. Images were acquired by a blinded experimenter.

Image Analysis

Analysis of ScN and DRG tissues LysM^{tdT+} labeled macrophages was done with Imaris Software (Oxford Instruments, version 9.0.1). Previously acquired z-stacks are put into Imaris where each pixel from the 2D section was converted into a 3D voxel. This information was then used to reconstruct the original 3D object that spanned across the z-stacks. Images were imported into Imaris's Arena and viewed within the 3-D view of the Surpass. The Surfaces visualization is a computer-generated representation of the specified gray value range in the data set. In order to visualize the range of interest of an object's volume, an artificial solid object is created from which measurements can be derived. Surfaces were created using background subtraction for td-Tomato positive cells in the Z-stack images. A filter based on number of voxels was used to remove both artifacts and large neuronal cells within the image. Using the most representative image for DRGs and ScNs, creation parameters were made using the corresponding creation wizard in Imaris's Surfaces feature. Surfaces of the LysM^{tdT+} macrophages were then measured for cell count, ellipticity, volume, and sphericity. In order to normalize cell count via volume of tissue, surfaces were created for the whole DRG and sections of ScN using absolute intensity thresholding. Both proximal and distal sections of ScN were analyzed and data points were labeled accordingly to determine spatial differences in macrophage infiltration and activation along the ScN. All analyses were performed by an experimenter blinded to sex, genotype, treatment, and tissue type.

1. Sphericity—Given as a value from 0.01 to 1.00 with 1.00 being a perfect sphere in which the x, y, and z axes are all equal length. The sphericity of a particle is the ratio of the surface area of an equal-volume sphere to the actual surface area of the particle. The closer to 0 this value is the less spherical and more ellipsoid the shape is.

$$\psi = \frac{\pi^{1/3}\left(6V_p\right)^{2/3}}{A_p}$$

v_p = volume of the particle
A_p = surface area of the particle

2. Prolate ellipticity—Given as a value from 0.01 to 1.00 with 1.00 representing an ellipsoid with one axis significantly longer than the others. A prolate ellipticity value moving toward 0 represents the lengths of the x, y, and z axes becoming more even. Values closer to 0 represent a more spherical shape while values closer to 1 represent a more elongated shape. A more elongated shape is typically associated with an M2 phenotype.

$$e_{prolate} = \frac{2a^2}{a^2+b^2} \cdot \left(1 - \frac{a^2+b^2}{2c^2}\right)$$

3. Oblate ellipticity—Given as a value from 0.01 to 1.00 with 1.00 representing an ellipsoid with two axes equal in length but longer than the third. An oblate ellipticity value moving toward 0 represents the lengths of the x, y, and z axes becoming more even. Values closer to 0 represent a more spherical shape while values closer to 1 represent a more flattened shape. A more flattened shape is typically associated with an M1 phenotype.

$$e_{oblate} = \frac{2b^2}{b^2+c^2} \cdot \left(1 - \frac{2a^2}{b^2+c^2}\right)$$

Statistical Analysis

Prism 8.01 software (GraphPad, San Diego, CA, USA) was utilized to generate all graphs and statistical analysis. Single comparisons were performed using Student's *t*-test, and multiple comparisons were performed using a one-way or two-way ANOVA with Bonferroni *post-hoc* tests for across-group comparisons. All data are represented as the standard error of the mean (SEM). A p-value of <0.05 was used to determine statistical significance. Blinded experimenters performed all experiments and analysis.

RESULTS

Use of Interdisciplinary Techniques to Investigate the Macrophage Response During Peripheral Nerve Injury

Macrophages are implicated in the development of pain following nerve injury and have complex immunologic, neurologic, and physical facets (Raoof et al., 2018). To improve our understanding of the dynamic immune response after peripheral nerve injury, we designed an interdisciplinary approach combining advanced multiphoton microscopy, Sca*l*eS1 tissue clearing and a well-established nerve injury model (SNI) Using these techniques, we were able to address some of the limitations of previous studies investigating the macrophage response to nerve injury. Primarily, these limitations include: a lack of appropriate male and female representation in data sets, an inability to assess morphological changes in macrophages while preserving the integrity of the microenvironment, and skewed information resulting from single-slice imaging analysis as opposed to whole tissue. While these studies greatly improve our understanding on the dynamic nature of macrophage recruitment and activation, they highlight a need to develop integrative techniques to improve our approach.

Male and Female Mice Exhibit Robust Pain Behaviors Following SNI

To adequately assess the macrophage response to nerve injury, spared nerve injury (SNI) was performed to induce a pain state in both sexes. We chose this specific model of neuropathic pain because it has been shown to cause prolonged changes in behavioral phenotypes as well as immune cell activation (Raoof et al., 2018). Moreover, the etiology of neuropathic pain that develops after SNI closely mimics the cardinal symptoms of clinically described neuropathic pain (Chen et al., 2015).

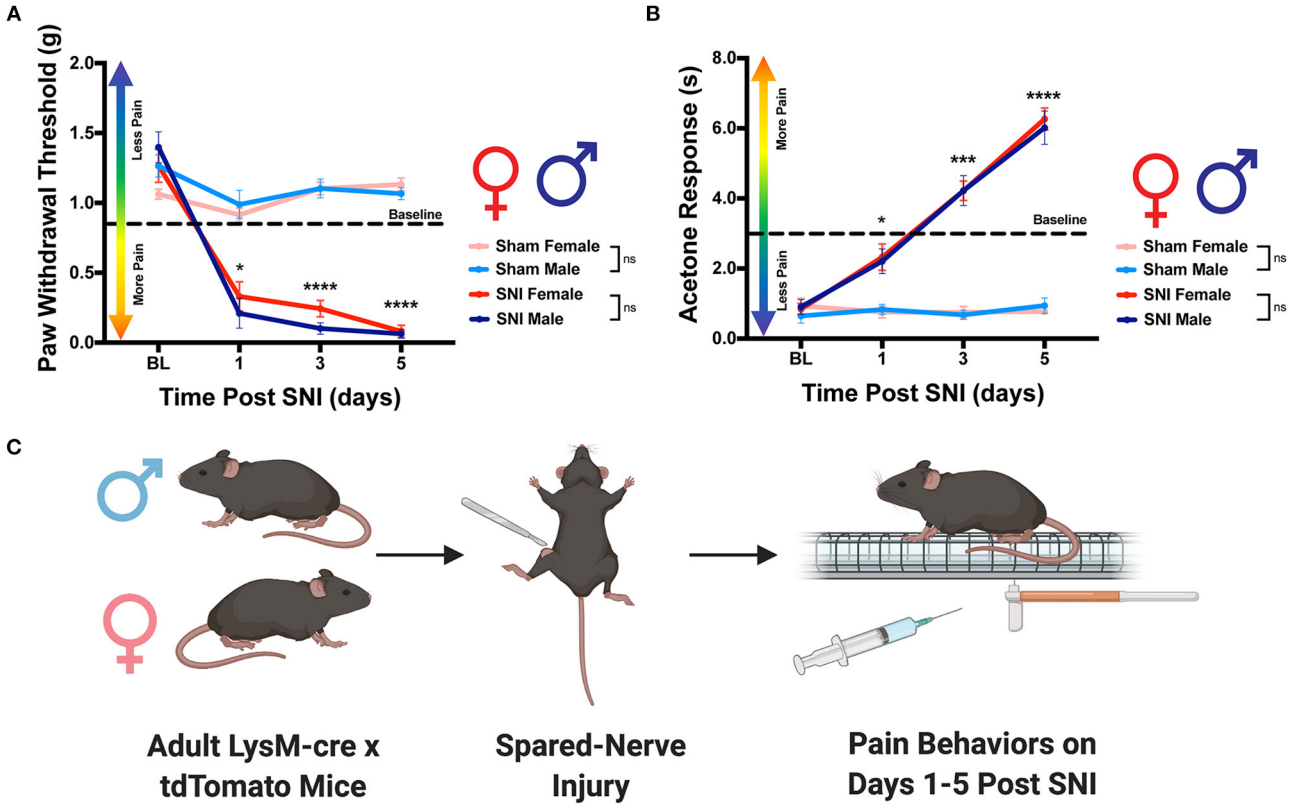

FIGURE 1 | Development of neuropathic pain behaviors following SNI. Male and female LysM^{tdT+} mice were tested for mechanical hypersensitivity and cold allodynia on days 1, 3, and 5 post-SNI. **(A)** Male ($n = 7$) and Female ($n = 7$) LysM^{tdT+} mice exhibit significantly reduced mechanical withdrawal thresholds post-SNI as compared to their respective sham controls ($n = 7$). **(B)** Male ($n = 7$) and Female ($n = 7$) LysM^{tdT+} mice exhibit significantly elevated response latency to acetone application as compared to their respective sham controls ($n = 7$). **(C)** Graphical representation of the experimental timeline where male ($n = 7$) and Female ($n = 7$) LysM^{tdT+} mice were given SNI and were assessed for mechanical hypersensitivity and cold allodynia on days 1, 3, and 5 post-SNI. *$p < 0.05$; ***$p < 0.001$; ****$p < 0.0001$. BL, Baseline. Made using BioRender.com.

In order to confirm that our procedure induced a pain state, we assessed mechanical hypersensitivity and cold allodynia in mice that received either SNI or sham. As expected, we found that males that received SNI exhibited significantly reduced paw withdrawal thresholds on days 1, 3 and 5 as compared to their sham counterparts. We report similar results in females where mice that received SNI had significantly reduced paw withdrawal thresholds on day 1, 3, and 5 as compared to sham controls (**Figures 1A,C**). Moreover, male mice that received SNI exhibited an elevated behavioral response to application of acetone to the ipsilateral hind paw on days 3 and 5 as compared to their sham counterparts. Similarly, female mice that received SNI exhibited an elevated behavioral response to application of acetone to the ipsilateral hind paw on days 1, 3, and 5 as compared to sham controls (**Figures 1B,C**). Lastly, we find no significant sex differences in the onset of mechanical hypersensitivity or cold allodynia after SNI. Taken together, these data indicate SNI induced robust pain behaviors before, and up to the day mice were euthanized and tissues were collected for analysis.

SNI Induces Macrophage Recruitment, Activation, and Morphological Changes in the DRG

To explore our initial hypothesis regarding sex differences in macrophage infiltration, lumbar DRGs (L4-5) were harvested from male and female LysM^{tdT+} reporter mice 5 days post-SNI. We integrated Sca*l*eS1 whole tissue clearing with multiphoton imaging in both male and female DRGs to visualize macrophage recruitment, activation, and changes in morphology (**Figure 2A**). Imaris image analyses revealed significant differences in macrophage recruitment to the DRG following SNI. We found that injured (SNI) male ipsilateral DRGs displayed significantly increased amounts of LysM^{tdT+} macrophages compared to the contralateral (uninjured) DRGs. Moreover, SNI induced significantly elevated LysM^{tdT+} macrophage recruitment to the ipsilateral DRG as compared to the sham surgery. Surprisingly, we do not report a significant increase in LysM^{tdT+} macrophage recruitment to the ipsilateral DRG in female mice after SNI. This remains true in the sham groups as well (**Figure 2C**). To account for differences

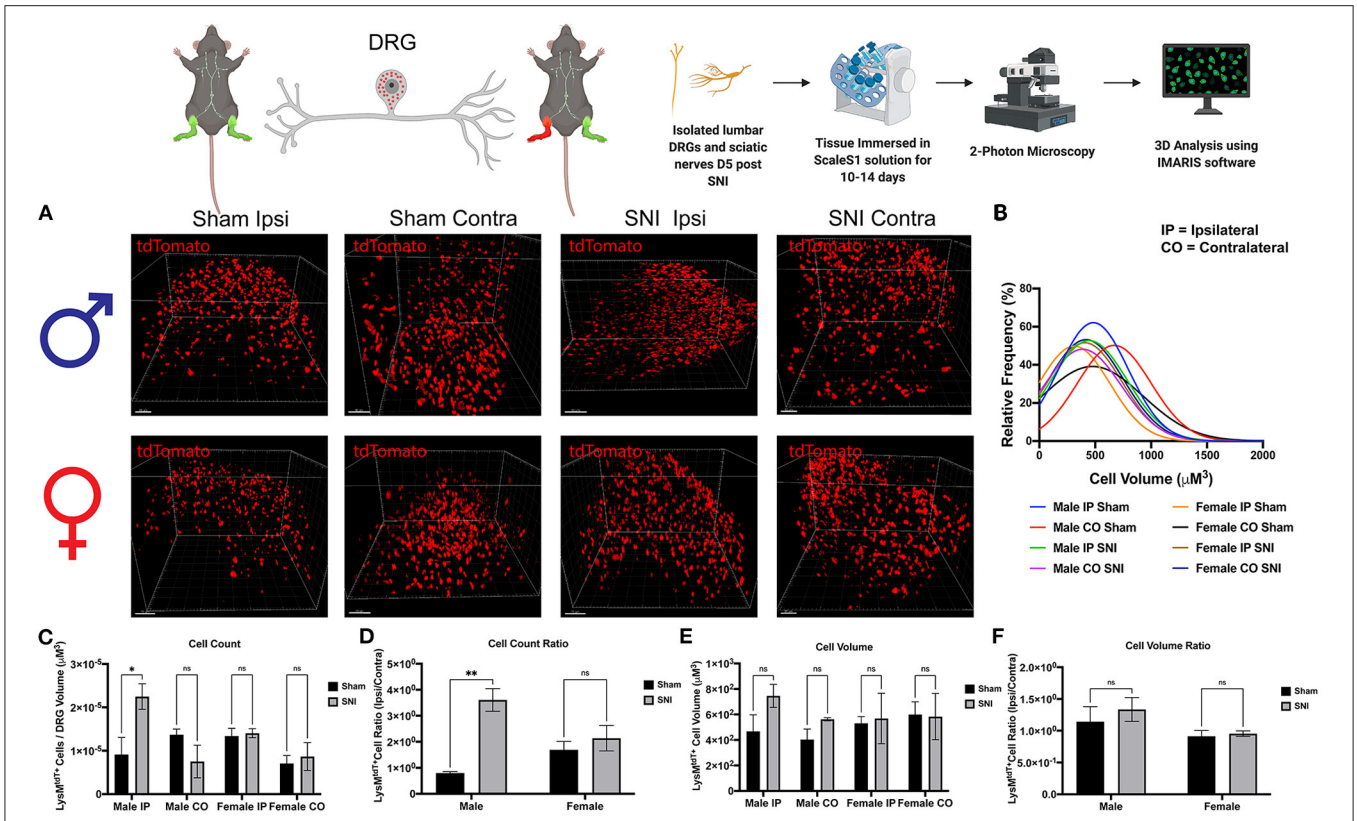

FIGURE 2 | Infiltration of LysM^{tdT+} macrophages in the lumbar DRGs 5 days post-SNI. Male and female LysM^{tdT+} mice had DRGs harvested 5 days post-SNI. Tissues were processed and cleared using ScaleS1 solution for 10–14 days and imaged using 2-photon microscopy. **(A)** Representative images from male and female LysM^{tdT+} (red; 1,100 nm) DRGs ($n = 3$). **(B)** Frequency distribution histogram comparing the frequencies of LysM^{tdT+} cell volumes in control and injured male and female lumbar DRGs. **(C)** Quantification of LysM^{tdT+} macrophage infiltration in the lumbar DRGs 5 days post-SNI ($n = 3$) in males and females. **(D)** Quantification of LysM^{tdT+} macrophage infiltration in the lumbar DRGs 5 days post-SNI as a ratio of ipsilateral over contralateral DRG ($n = 3$) in males and females. **(E)** Quantification of LysM^{tdT+} macrophage volume in the lumbar DRGs 5 days post-SNI ($n = 3$) in males and females. **(F)** Quantification of LysM^{tdT+} macrophage cell volumes in the lumbar DRGs 5 days post-SNI as a ratio of ipsilateral over contralateral DRG ($n = 3$) in males and females. *$p < 0.05$; **$p < 0.01$. Scale Bar: 100 μm. IP, Ipsilateral; CO, Contralateral. Made using BioRender.com.

in resident and infiltrating macrophages, we assessed the ratio of LysM^{tdT+} macrophages in the ipsilateral (injured) DRG with the contralateral (uninjured) DRG. Again, we found that males display significantly upregulated LysM^{tdT+} macrophages to the ipsilateral DRG. This is indicative of an upregulation of infiltrating macrophages (**Figure 2D**). To better understand the activation states of these infiltration macrophages, we analyzed the distribution and relative frequencies of LysM^{tdT+} macrophage volumes after SNI. We report no significant findings; however, male mice exhibit a trend of larger cell volumes in the injured ipsilateral DRG (**Figures 2B,E,F**). While these findings are not statistically significant, considered with the robust recruitment of LysM^{tdT+} macrophages, we can conclude that there is a biologically relevant upregulation and activation of macrophages in the DRG following SNI in male mice.

Next, we wanted to identify changes in macrophage morphology after SNI as these changes can be correlated with shifts in pro-(M1) and anti-(M2) inflammatory polarization. Macrophages have been shown to play a key role in regulating homeostasis and tissue repair after nerve injury, and polarization plays an integral role in this process (Chernykh et al., 2016). We may map changes in geometric profiles of macrophages using measures of oblate (flattened) ellipticity, prolate (elongated) ellipticity, and sphericity (Iwata et al., 2017). In response to physiologic input and cytokine signaling, M2 polarized macrophages are associated with an elongated, prolate morphology while M1 macrophages are associated with an oblate, flattened morphology (Bertani et al., 2017). Drawing upon these recent discoveries and classifications, we assessed the geometrics of these recruited LysM^{tdT+} macrophages in the DRG using Imaris analysis (**Figure 3A**). We found differences in the clustering of LysM^{tdT+} macrophages in mice that received SNI, which take on a more oblate (flattened) morphology after nerve injury. This is indicative of an M1 polarized phenotype. Moreover, we found that LysM^{tdT+} macrophages in animals that received a sham surgery take on a more prolate (elongated) morphology. This is indicative of an M2 polarized phenotype (**Figure 3C**). Lastly, we assessed sphericity of LysM^{tdT+} macrophages after nerve injury (**Figure 3B**). Although we find no significant differences, cells that take on a more prolate

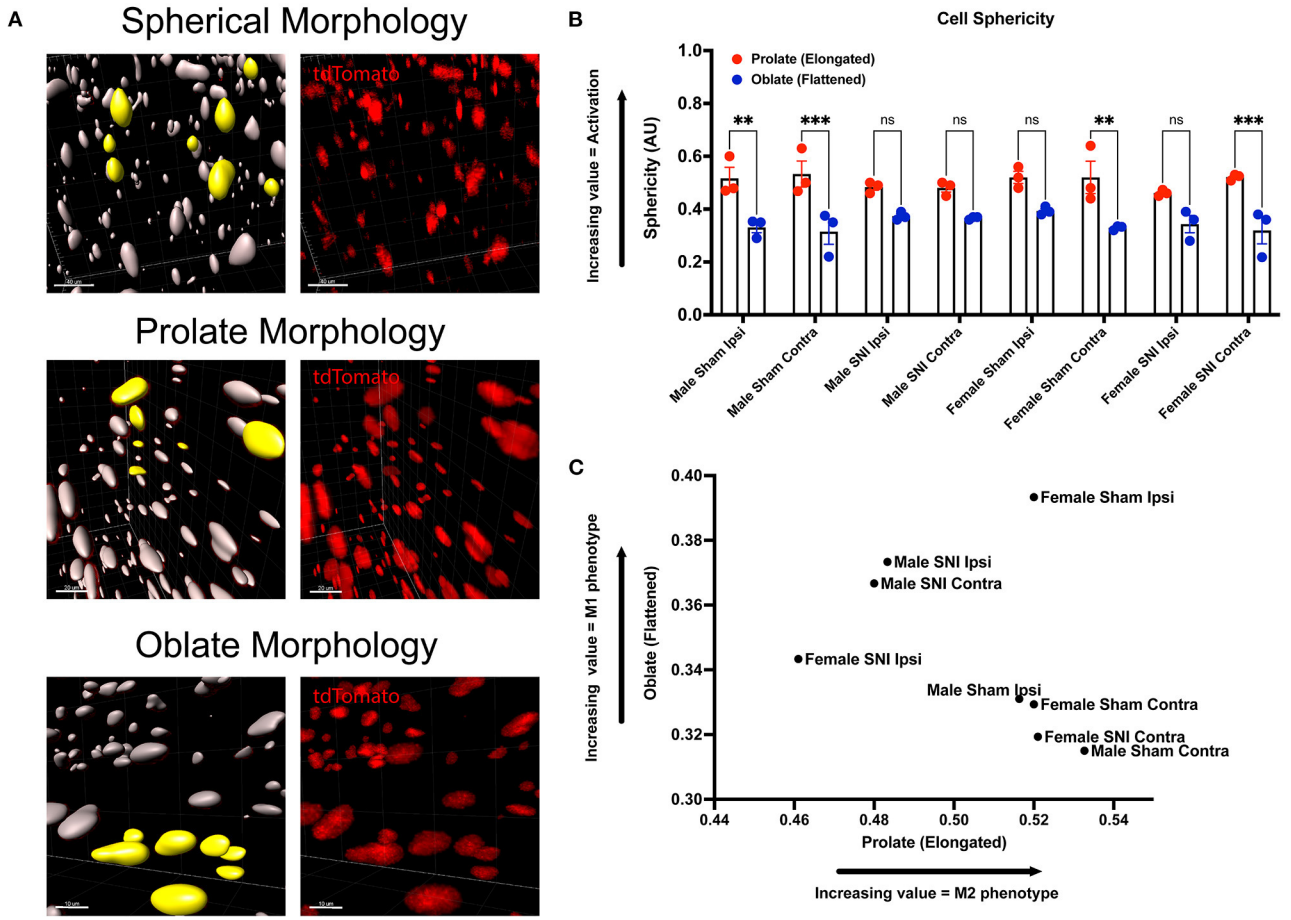

FIGURE 3 | Morphology of LysM^{tdT+} macrophages in the lumbar DRGs 5 days post-SNI. Male and female LysM^{tdT+} mice had DRGs harvested 5 days post-SNI. Tissues were processed and cleared using ScaleS1 solution for 10–14 days and imaged using 2-photon microscopy. **(A)** Representative morphology from male and female LysM^{tdT+} (red; 1,100 nm) DRGs ($n = 3$). **(B)** Imaris analysis of LysM^{tdT+} cell morphology in male and female DRGs. Cells were analyzed for three morphologic parameters (sphericity, prolate, and oblate) and are displayed comparing oblateness and prolateness with respect to sphericity. **(C)** Scatter plot of DRG LysM^{+} cell oblateness with respect to prolateness in both male and female injury and control groups. $^{**}p < 0.01$; $^{***}p < 0.001$. Scale Bar: 100 μm. IP, Ipsilateral; CO, Contralateral.

(flattened) shape after injury are also more spherical, indicating a more active phenotype (Sen et al., 2016). Taken together, we conclude that macrophages have a dynamic morphological response to injury and may be characterized based on their geometric shape.

SNI Induces Dynamic Changes in Macrophage Morphology in the ScN

To further identify the dynamic role of macrophages in response to nerve injury, we looked closer to the site of injury in the ScN. Here, we sought to distinguish the LysM^{tdT+} macrophage response between the DRG and ScN. Using the same principles, whole ScNs were harvested from male and female LysM^{tdT+} mice 5 days after SNI and were cleared using Sca*e*S1. Tissues were cleared and imaged using multiphoton imaging and tissues were analyzed using Imaris (**Figure 4A**). Analyses revealed no significant differences in LysM^{tdT+} macrophage recruitment to the distal or proximal ScN. Although, both male female mice exhibit elevated LysM^{tdT+} macrophages in the ipsilateral ScN as compared to the contralateral control. While not significant, this does indicate a surgery-induced upregulation in macrophage recruitment to the ScN in males and females (**Figures 4C,D**). We report no differences in the volumes of these recruited LysM^{tdT+} macrophages (**Figure 4D**). Moreover, we do not report any differences in the distribution or relative frequencies of LysM^{tdT+} macrophage volumes after SNI in the ScN. However, female mice exhibit a larger distribution of LysM^{tdT+} cell volumes after SNI in the ipsilateral ScN as compared to other groups, indicating increased classical activation of macrophages (**Figure 4B**). Lastly, we report no differences in the cell volumes of LysM^{tdT+} macrophages in the ScN after SNI in both males and females (**Figures 4E,F**). Taken together, we can conclude there

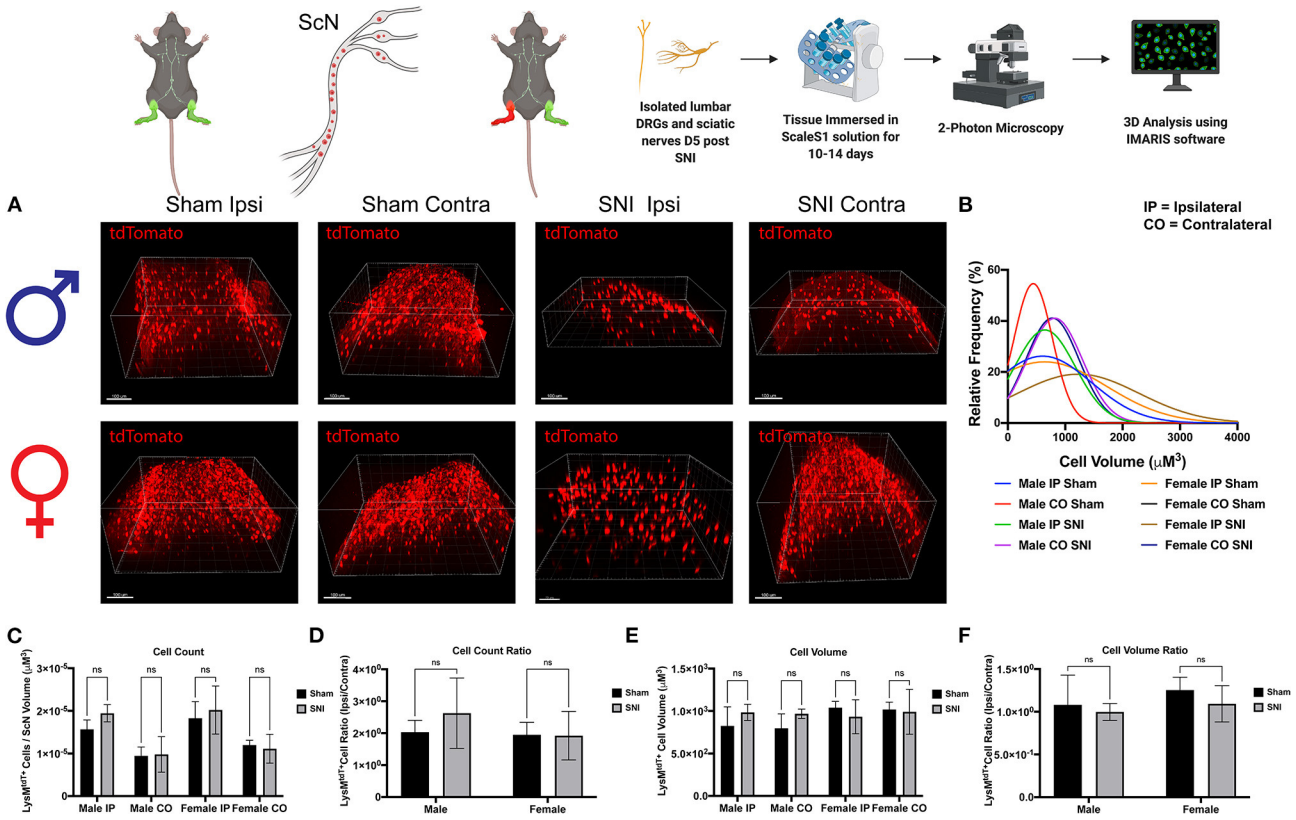

FIGURE 4 | Infiltration of LysM^{tdT+} immune cells in the ScNs 5 days post-SNI. Male and female LysM-cre × tdTomato mice had ScNs harvested 5 days post-SNI. Tissues were processed and cleared using ScaleS1 solution for 10–14 days and imaged using 2-photon microscopy. **(A)** Representative images from male and female LysM^{tdT+} (red; 1,100 nm) ScNs ($n = 3$). **(B)** Frequency distribution histogram comparing the frequencies of LysM^{tdT+} cell volumes in control and injured male and female lumbar ScNs. **(C)** Quantification of LysM^{+} immune cell infiltration in the lumbar ScNs 5 days post-SNI ($n = 3$) in males and females. **(D)** Quantification of LysM^{tdT+} macrophage infiltration in the lumbar ScNs 5 days post-SNI as a ratio of ipsilateral over contralateral ScN ($n = 3$) in males and females. **(E)** Quantification of LysM^{tdT+} macrophage volume in the lumbar ScNs 5 days post-SNI ($n = 3$) in males and females. **(F)** Quantification of LysM^{tdT+} macrophage cell volumes in the ScN 5 days post-SNI as a ratio of ipsilateral over contralateral ScN ($n = 3$) in males and females. Scale Bar: 100 μm. IP, Ipsilateral; CO, Contralateral. Made using BioRender.com.

are dynamic biological changes that occur in the ScN following SNI in males and females.

We incorporated our geometric analyses to better understand the morphological changes that may occur in macrophages in the ScN (**Figure 5A**). While we report no differences in recruitment, there may be morphological changes that are biologically relevant (Cobos et al., 2018). We investigated the sphericity of LysM^{tdT+} macrophages in the ScN and found that there were no differences between sexes or injury. Typically, a more spherical, or round, macrophage is classically activated, however, this does not mean that these macrophages have not altered their contractile state in response to injury. We report that there is a sexual dimorphism in the morphology of LysM^{tdT+} macrophages in the sciatic nerve 5 days after SNI. Male LysM^{tdT+} macrophages on the injured side exhibit more oblate, or flattened, cell morphology as opposed to females that exhibit a more prolate, or elongated, cell morphology (**Figure 5C**). This is indicative of an M1 polarization state in males as opposed to an M2 state in females. This idea has been a dogma in the field of neuroimmunology for decades (Li et al., 2009). Lastly, we find no differences in the sphericity of LysM^{tdT+} macrophages in the ScN (**Figure 5B**). This data indicates a distinction in macrophages in the DRG vs. ScN, where DRG macrophages are more M1 polarized in both sexes after surgery, and ScN macrophages are M1 polarized in males vs. M2 polarized in females.

DISCUSSION

Whole tissue *in-situ* visualization can reveal neuroimmune interactions that have been overlooked in the past. The goal of the present study was to analyze the sex-dependent dynamics of macrophage recruitment and changes in morphology after injury utilizing next generation tissue clearing and imaging techniques. We performed SNI on male and female transgenic reporter mice constitutively expressing tdTomato, a red fluorescent protein, in macrophages under the LysM promoter. We then harvested lumbar DRGs and ScNs from these animals 5

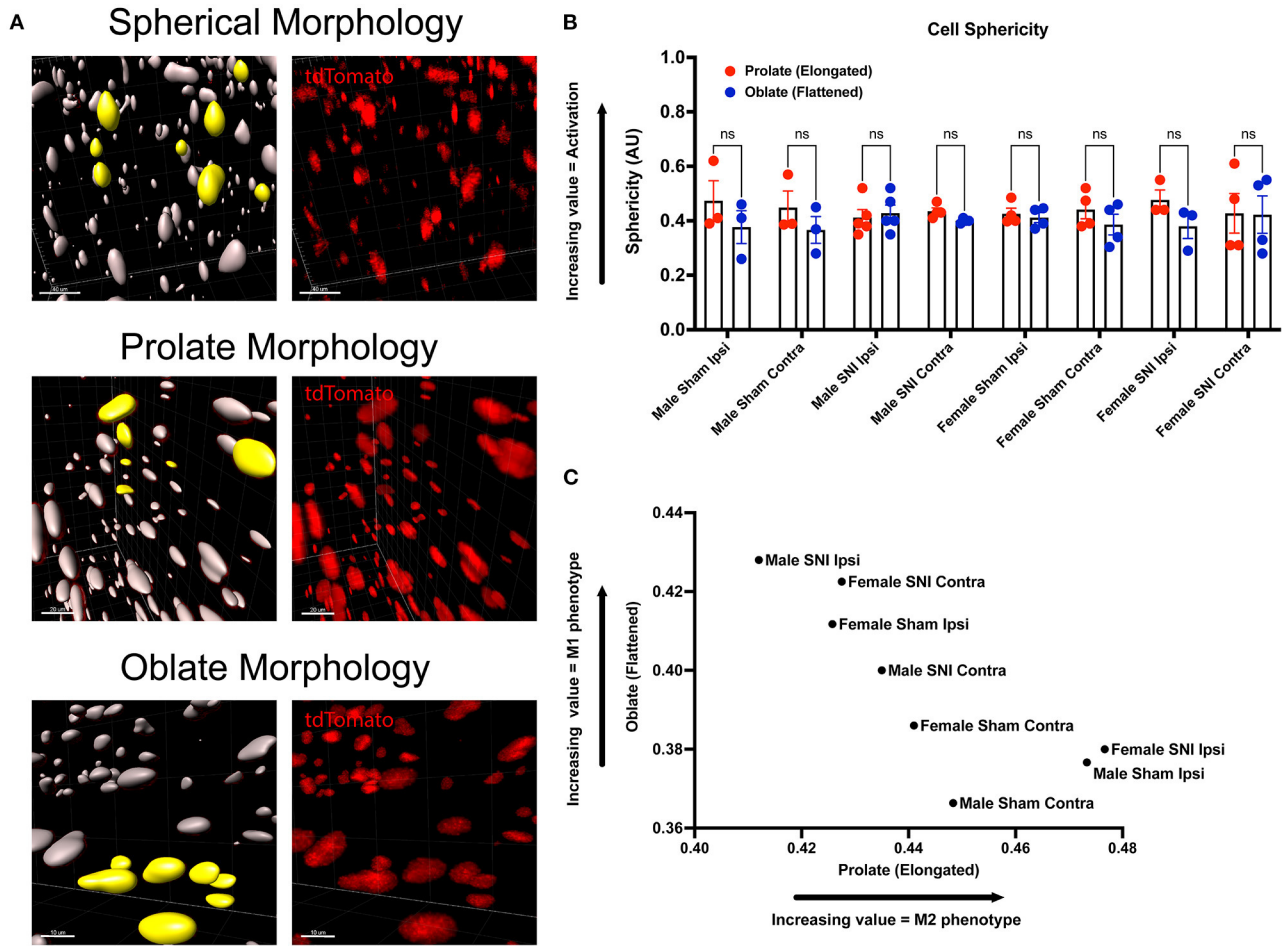

FIGURE 5 | Morphology of LysM^{tdT+} macrophages in the ScN 5 days post-SNI. Male and female LysM^{tdT+} mice had ScNs harvested 5 days post-SNI. Tissues were processed and cleared using ScaleS1 solution for 10–14 days and imaged using 2-photon microscopy. **(A)** Representative morphology from male and female LysM^{tdT+} (red; 1,100 nm) ScNs ($n = 3$). **(B)** Imaris analysis of LysM^{tdT+} cell morphology in male and female ScNs. Cells were analyzed for three morphologic parameters (sphericity, prolate, and oblate) and are displayed comparing oblateness and prolateness with respect to sphericity. **(C)** Scatter plot of ScN LysM^{+} cell oblateness with respect to prolateness in both male and female injury and control groups. Scale Bar: 100 μm. IP, Ipsilateral; CO, Contralateral.

days after the surgery and optically cleared the tissues using Sca*l*eS1. Macrophage recruitment and subsequent expansion peaks between days 3 and 7 after injury, therefore we chose day 5 to assess their physical characteristics (Chen et al., 2015). We then acquired high resolution Z-stack images of the cleared tissues using multiphoton microscopy and performed extensive analyses using Imaris Imaging Software to understand the dynamics of macrophage recruitment, activation, and morphology after injury. In this study, we found that males have higher LysM^{tdT+} macrophage counts in the lumbar DRGs (L4/5), expanding upon current literature that suggests females have alternative neuroimmune mechanisms that contribute to pain states. Moreover, we find dynamic changes in LysM^{tdT+} macrophage morphology, with SNI inducing a more pro-inflammatory, or M1, phenotype measured by cell shape (**Figure 6**). This highlights the need to improve our understanding of the sex-dependent distribution and role of other immune cells in pain. From a therapeutic perspective, there is a potential to harness the abilities of macrophages to induce anti-nociception and tissue repair after injury (Yu et al., 2020). The vast majority of our current understanding in macrophage functionality is reliant on soluble factors, such as cytokine production and cell surface protein expression. While this information is useful in providing the necessary framework to investigate the molecular underpinnings of macrophage activation in response to injury, bridging the gap between functionality and physical characteristics will discern the full spectrum of their involvement in tissue injury.

Bi-directional communication between neuronal and non-neuronal cells in the DRG is a core mechanism in mediating the mammalian response to injury (Lopes et al., 2017). Current literature highlights the complex role that macrophages play in regulating inflammation and pro-nociception following injury, but the relevant sites of action remains unclear (Echeverry et al., 2013). Moreover, the current dogma in the field dictates

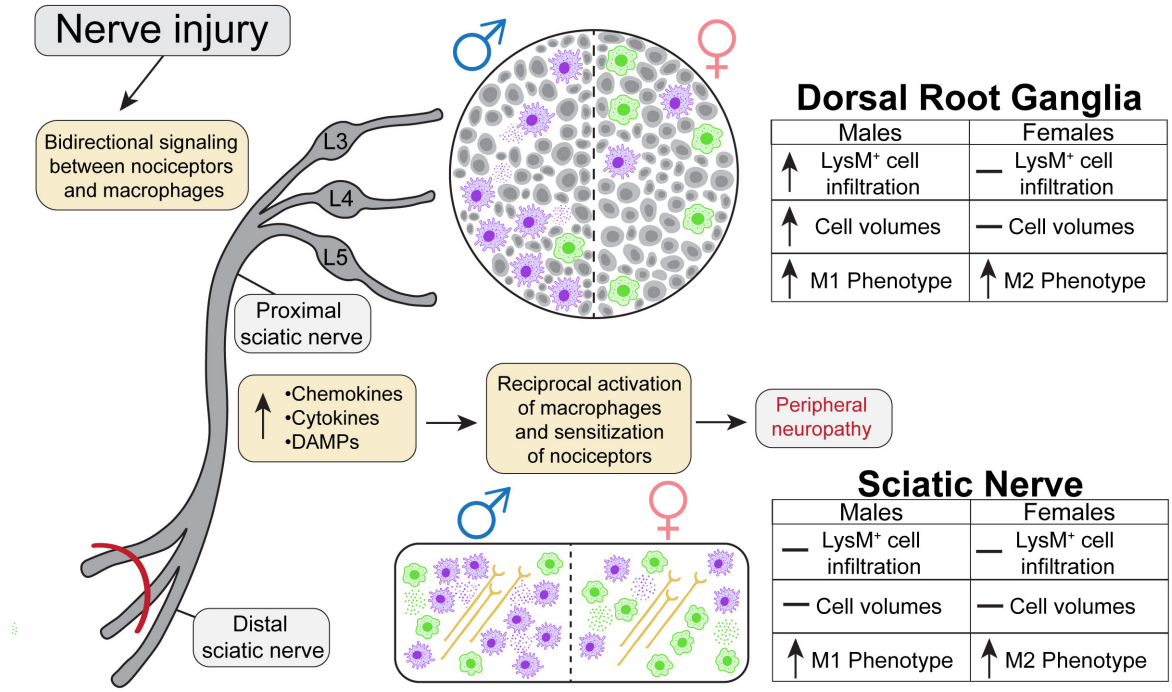

FIGURE 6 | Graphical abstract representing the dynamic nature of macrophage recruitment and morphological changes following SNI in males and females.

males utilize a myeloid cell driven mechanism of neuronal sensitization to drive neuroinflammation (McWhorter et al., 2013). Although the reported behavioral contribution of these DRG macrophages is not dimorphic in nature, there exists a key cellular difference in their recruitment a morphology, lending to the idea that etiology differences can influence pain perception over time. Our data shows the magnitude of injury-induced macrophage expansion in the lumbar DRGs is significantly higher in males than in females. These findings are also supported by a recent paper that characterizes sex differences in immune cell recruitment to both central and peripheral nervous tissues through flow cytometric analyses (Mosser and Edwards, 2008). They demonstrate an upregulation of macrophages in both males and females after peripheral nerve injury in the lumbar DRGs, with key sex differences in the adaptive immune response. However, the adaptive immune response to injury was not the focus of our study. Collectively, these studies support the idea that macrophage recruitment to the DRG plays a critical role in neuroinflammation. Furthermore, we utilized sham and contralateral data to determine that no conclusive sex differences exist in baseline cell size and volumes further strengthening our premise that immune response to injury is sex dependent.

Conflicting reports about the role of macrophages in the ScN after nerve injury has groups reporting that macrophages do not play an important role in the pathogenesis of nerve injury-induced pain (Yu et al., 2020), while other reports found that inhibiting local macrophages in the ScN impairs development of neuropathic pain following nerve injury (Paul et al., 2013). An important distinction here is that we assessed the recruitment and morphological changes in macrophages at both distal ScN and proximal ScN. Here we assessed differences in macrophage activity with more granularity than previous studies. We find no significant recruitment of LysM^{tdT+} macrophages in the ScN 5 days after SNI, however, this does not equate to a lack of biological significance. It is a potential that the differences in macrophage morphology after SNI may alter cytokine signaling. Certain M2 macrophages phenotypes, or cells that have an elongated shape, retain the ability to produce pro-inflammatory cytokines and may be a differentiating factor in the immune response to injury in males vs. females (de Paoli et al., 2014). Despite our collective efforts, a rift exits in our understanding of the role of macrophages in the ScN, but with every advance we are able to better understand the nuances of macrophages recruitment, activation and subsequent biological implications.

While the aforementioned studies have significantly improved our understanding of the dynamic nature of macrophage recruitment to peripheral nervous tissues, they have inherent limitations that we have addressed using our model. Geometric alteration of macrophages in response to injury has the ability regulate their functional phenotype (Tauer, 2002). However, it is impossible to discern this type of information by using typical immunohistochemical or flow cytometric analyses. Macrophages exhibit an elongated shape when polarized to an M2 phenotype, as opposed to a flattened shape when polarized to an M1 phenotype (Bronte and Murray, 2015). These polarization states are involved in a myriad of biological processes related to inflammation and tissue repair and are often indicative of a macrophages change in contractility as they interact with the

extracellular matrix and cell adhesion molecules (Jensen and Berg, 2017). *In vivo* these polarization states are not dichotomous, but targeted therapeutics may be better tailored to treat each sex individually. Moreover, traditional imaging acquisition and analysis techniques are not well-suited to investigate changes in cellular shape as there are significant limitations in the resolution and depth of acquired images. This severely dampens the ability of researchers to utilize common image analysis software for this purpose. Therefore, we sought to address this lack of granularity by improving our understanding of the physical characteristics of macrophages in response to nerve injury utilizing Imaris image analysis (Belle et al., 2017).

Optical clearing techniques provide additional clarity in resolving cell to cell interactions by circumventing the limitations of traditional 2-dimensional (2-D) imaging. Typically, 2-D image reconstruction of limited z-frames provides biased information as cellular density is not uniform throughout select regions of interest. By using Sca*l*eS1 optical tissue clearing in combination with deep tissue multiphoton microscopy, we were able to create a 3-D model of whole DRGs and ScNs. This allowed us to accurately assess the infiltration of immune cells to these tissues following peripheral nerve injury. Multiphoton microscopy may be used to image thicker tissue slices, but image quality quickly deteriorates when focusing deeper into a sample (Renier et al., 2014). To circumvent this limitation, we chose to utilize Sca*l*eS1 as our method of optical tissue clearing. Sca*l*eS1 was our preferred method of optical tissue clearing as it has been shown to avoid tissue expansion, preserve lipids and provide a safe immersion-medium for objectives (Hama et al., 2015). We also took into consideration other clearing methods, such as DBE or CLARITY. These alternate clearing methods offered a shorter clearing time and work better on larger tissue sizes, however they had considerable limitations with regard to preservation of fluorescence and tissue integrity (Jensen and Berg, 2017). Another clearing method we considered was DISCO which utilizes a de-lipidating agent to enhance the refractory index of the tissue (Belle et al., 2017). Similar to previously discussed alternatives, this method allows for faster clearing times, however it is accompanied with significant amounts of tissue distortion making it suboptimal for our study. Current use of this method is better suited for larger tissues, such as brain or embryos (Renier et al., 2014). Furthermore, Sca*l*eS1 utilizes materials that are inexpensive and commonly found in research labs making it easy to use and more accessible to a wider audience. Moreover, Sca*l*eS1 is well-suited for imaging fluorescent proteins, which was the primary focus of our study.

In conclusion, the combined use of our genetic model, tissue clearing, and multiphoton microscopy serves as a powerful tool for investigating neuroimmune spatiotemporal relationships, and provides a versatile framework to further our understanding of the role macrophages play in pain development. Moreover, we further delineate the sexual dimorphisms that exist in the physical phenotype of macrophages in response to nerve injury.

DATA AVAILABILITY STATEMENT

The raw data supporting the conclusions of this article will be made available by the authors, without undue reservation.

ETHICS STATEMENT

The animal study was reviewed and approved by The University of Texas at Dallas; Institutional Animal Care and Use Committee.

AUTHOR CONTRIBUTIONS

TAS-P and UMS performed experiments and updated protocol equally. TAS-P, UMS, and ZWC analyzed data and wrote the manuscript. MDB oversaw all aspects of the project, conceived and originally designed the project and acquired funding. All authors contributed to the manuscript and have approved the submitted version.

FUNDING

This work was supported by NIH grant K22NS096030 (MDB), American Pain Society Future Leaders Grant (MDB), Rita Allen Foundation Award in Pain (MDB), and the University of Texas Systems STARS program research support grant (MDB).

ACKNOWLEDGMENTS

We would like to thank the University of Texas at Dallas Imaging core, specifically Ved Prakash, for allowing us to use the extensive imaging equipment and resources that were integral to the generation of this research manuscript. Moreover, we would like to thank the imaging core for their descriptions regarding the multiphoton microscopy setup used to acquire images for analysis. We would also like to thank all current and former members of the Burton Lab for their support and assistance on this manuscript. **Figures 1**, **2**, **4** were made using BioRender.com. **Figure 6** was made by a designer we paid for rights.

SUPPLEMENTARY MATERIAL

The Supplementary Material for this article can be found online at: https://www.frontiersin.org/articles/10.3389/fcell.2021.624201/full#supplementary-material

Supplementary Figure 1 | 3-Dimensional video render of a cleared Male Sham Ipsilateral DRG. Visualized cells are LysM^{tdT+} macrophages infiltrating into the tissue.

Supplementary Figure 2 | 3-Dimensional video render of a cleared Male Sham Contralateral DRG. Visualized cells are LysM^{tdT+} macrophages infiltrating into the tissue.

Supplementary Figure 3 | 3-Dimensional video render of a cleared Male SNI Ipsilateral DRG. Visualized cells are LysM^{tdT+} macrophages infiltrating into the tissue.

Supplementary Figure 4 | 3-Dimensional video render of a cleared Male SNI Contralateral DRG. Visualized cells are LysM^{tdT+} macrophages infiltrating into the tissue.

Supplementary Figure 5 | 3-Dimensional video render of a cleared Female Sham Ipsilateral DRG. Visualized cells are LysM^{tdT+} macrophages infiltrating into the tissue.

Supplementary Figure 6 | 3-Dimensional video render of a cleared Female Sham Contralateral DRG. Visualized cells are LysM^{tdT+} macrophages infiltrating into the tissue.

Supplementary Figure 7 | 3-Dimensional video render of a cleared Female SNI Ipsilateral DRG. Visualized cells are LysM^{tdT+} macrophages infiltrating into the tissue.

Supplementary Figure 8 | 3-Dimensional video render of a cleared Female SNI Contralateral DRG. Visualized cells are LysM^{tdT+} macrophages infiltrating into the tissue.

REFERENCES

Agalave, N. M., Rudjito, R., Farinotti, A. B., Khoonsari, P. E., Sandor, K., Nomura, Y., et al. (2020). Sex-dependent role of microglia in disulfide HMGB1-mediated mechanical hypersensitivity. *Pain* 162, 446–458. doi: 10.1097/j.pain.0000000000002033

Basbaum, A. I., Bautista, D. M., Scherrer, G., and Julius, D. (2009). Cellular and molecular mechanisms of pain. *Cell* 139, 267–284. doi: 10.1016/j.cell.2009.09.028

Belle, M., Godefroy, D., Couly, G., Malone, S. A., Collier, F., Giacobini, P., et al. (2017). Tridimensional visualization and analysis of early human development. *Cell* 169, 161–173.e12. doi: 10.1016/j.cell.2017.03.008

Bertani, F. R., Mozetic, P., Fioramonti, M., Iuliani, M., Ribelli, G., Pantano, F., et al. (2017). Classification of M1/M2-polarized human macrophages by label-free hyperspectral reflectance confocal microscopy and multivariate analysis. *Sci. Rep.* 7:8965. doi: 10.1038/s41598-017-08121-8

Bronte, V., and Murray, P. J. (2015). Understanding local macrophage phenotypes in disease: modulating macrophage function to treat cancer. *Nat. Med.* 21, 117–119. doi: 10.1038/nm.3794

Chaplan, S. R., Bach, F. W., Pogrel, J. W., Chung, J. M., and Yaksh, T. L. (1994). Quantitative assessment of tactile allodynia in the rat paw. *J. Neurosci. Methods* 53, 55–63. doi: 10.1016/0165-0270(94)90144-9

Chen, P., Piao, X., and Bonaldo, P. (2015). Role of macrophages in Wallerian degeneration and axonal regeneration after peripheral nerve injury. *Acta Neuropathol.* 130, 605–618. doi: 10.1007/s00401-015-1482-4

Chernykh, E. R., Shevela, E. Y., Starostina, N. M., Morozov, S. A., Davydova, M. N., Menyaeva, E. V., et al. (2016). Safety and therapeutic potential of M2 macrophages in stroke treatment. *Cell Transplant.* 25, 146–1471. doi: 10.3727/096368915X690279

Clausen, B. E., Burkhardt, C., Reith, W., Renkawitz, R., and Förster, I. (1999). Conditional gene targeting in macrophages and granulocytes using LysMcre mice. *Transgenic Res.* 8, 265–277. doi: 10.1023/A:1008942828960

Cobos, E. J., Nickerson, C. A., Gao, F., Chandran, V., Bravo-Caparrós, I., González-Cano, R., et al. (2018). Mechanistic differences in neuropathic pain modalities revealed by correlating behavior with global expression profiling. *Cell Rep.* 22, 1301–1312. doi: 10.1016/j.celrep.2018.01.006

Cohen, C. J., Gartner, J. J., Horovitz-Fried, M., Shamalov, K., Trebska-McGowan, K., Bliskovsky, V. v., et al. (2015). Isolation of neoantigen-specific T cells from tumor and peripheral lymphocytes. *J. Clin. Invest.* 125, 3981–3991. doi: 10.1172/JCI82416

de Paoli, F., Staels, B., and Chinetti-Gbaguidi, G. (2014). Macrophage phenotypes and their modulation in atherosclerosis. *Circ. J.* 78, 1775–1781. doi: 10.1253/circj.CJ-14-0621

Decosterd, I., and Woolf, C. J. (2000). Spared nerve injury: an animal model of persistent peripheral neuropathic pain. *Pain* 87, 149–158. doi: 10.1016/S0304-3959(00)00276-1

Echeverry, S., Wu, Y., and Zhang, J. (2013). Selectively reducing cytokine/chemokine expressing macrophages in injured nerves impairs the development of neuropathic pain. *Exp. Neurol.* 240, 205–218. doi: 10.1016/j.expneurol.2012.11.013

Fillingim, R. B., King, C. D., Ribeiro-Dasilva, M. C., Rahim-Williams, B., and Riley, J. L. (2009). Sex, gender, and pain: a review of recent clinical and experimental findings. *J. Pain* 10, 447–485. doi: 10.1016/j.jpain.2008.12.001

Finnerup, N. B. (2015). Advances in pain management and research presented at the 2015 Scientific Meeting of the Scandinavian Association for the Study of Pain (SASP). *Scand. J. Pain* 8:27. doi: 10.1016/j.sjpain.2015.04.002

Ghasemlou, N., Chiu, I. M., Julien, J. P., and Woolf, C. J. (2015). CD11b+Ly6G- myeloid cells mediate mechanical inflammatory pain hypersensitivity. *Proc. Natl. Acad. Sci. U.S.A.* 112, E6808–E6817. doi: 10.1073/pnas.1501372112

Gómez-Gaviro, M. V., Sanderson, D., Ripoll, J., and Desco, M. (2020). Biomedical applications of tissue clearing and three-dimensional imaging in health and disease. *iScience* 23:101432. doi: 10.1016/j.isci.2020.101432

Goren, I., Allmann, N., Yogev, N., Schürmann, C., Linke, A., Holdener, M., et al. (2009). A transgenic mouse model of inducible macrophage depletion: effects of diphtheria toxin-driven lysozyme m-specific cell lineage ablation on wound inflammatory, angiogenic, and contractive processes. *Am. J. Pathol.* 175, 132–147. doi: 10.2353/ajpath.2009.081002

Hama, H., Hioki, H., Namiki, K., Hoshida, T., Kurokawa, H., Ishidate, F., et al. (2015). ScaleS: an optical clearing palette for biological imaging. *Nat. Neurosci.* 18, 1518–1529. doi: 10.1038/nn.4107

Iwata, K., Katagiri, A., and Shinoda, M. (2017). Neuron-glia interaction is a key mechanism underlying persistent orofacial pain. *J. Oral Sci.* 59, 173–175. doi: 10.2334/josnusd.16-0858

Jensen, K. H. R., and Berg, R. W. (2017). Advances and perspectives in tissue clearing using CLARITY. *J. Chem. Neuroanat.* 86, 19–34. doi: 10.1016/j.jchemneu.2017.07.005

Kehlet, H., Jensen, T. S., and Woolf, C. J. (2006). Persistent postsurgical pain: risk factors and prevention. *Lancet* 367, 1618–1625. doi: 10.1016/S0140-6736(06)68700-X

Kiguchi, N., Kobayashi, D., Saika, F., Matsuzaki, S., and Kishioka, S. (2018). Inhibition of peripheral macrophages by nicotinic acetylcholine receptor agonists suppresses spinal microglial activation and neuropathic pain in mice with peripheral nerve injury. *J. Neuroinflamm.* 15:96. doi: 10.1186/s12974-018-1133-5

Kwon, M. J., Kim, J., Shin, H., Jeong, S. R., Kang, Y. M., Choi, J. Y., et al. (2013). Contribution of macrophages to enhanced regenerative capacity of dorsal root ganglia sensory neurons by conditioning injury. *J. Neurosci.* 33, 15095–15108. doi: 10.1523/JNEUROSCI.0278-13.2013

Li, K., Xu, W., Guo, Q., Jiang, Z., Wang, P., Yue, Y., et al. (2009). Differential macrophage polarization in male and female BALB/c mice infected with coxsackievirus B3 defines susceptibility to viral myocarditis. *Circ. Res.* 105, 353–364. doi: 10.1161/CIRCRESAHA.109.195230

Lindborg, J. A., Niemi, J. P., Howarth, M. A., Liu, K. W., Moore, C. Z., Mahajan, D., et al. (2018). Molecular and cellular identification of the immune response in peripheral ganglia following nerve injury. *J. Neuroinflamm.* 15:192. doi: 10.1186/s12974-018-1222-5

Lopes, D. M., Malek, N., Edye, M., Jager, S. B., McMurray, S., McMahon, S. B., et al. (2017). Sex differences in peripheral not central immune responses to pain-inducing injury. *Sci. Rep.* 7:16460. doi: 10.1038/s41598-017-16664-z

McDermott, A. M., Toelle, T. R., Rowbotham, D. J., Schaefer, C. P., and Dukes, E. M. (2006). The burden of neuropathic pain: results from a cross-sectional survey. *Eur. J Pain.* 10, 127–135. doi: 10.1016/j.ejpain.2005.01.014

McWhorter, F. Y., Wang, T., Nguyen, P., Chung, T., and Liu, W. F. (2013). Modulation of macrophage phenotype by cell shape. *Proc. Natl. Acad. Sci. U.S.A.* 110, 17253–17258. doi: 10.1073/pnas.1308887110

Mogil, J. S. (2012). Sex differences in pain and pain inhibition: multiple explanations of a controversial phenomenon. *Nat. Rev. Neurosci.* 13, 859–866. doi: 10.1038/nrn3360

Mosser, D. M., and Edwards, J. P. (2008). Exploring the full spectrum of macrophage activation. *Nat. Rev. Immunol.* 8, 958–969. doi: 10.1038/nri2448

Paul, D., Cowan, A. E., Ge, S., and Pachter, J. S. (2013). Novel 3D analysis of Claudin-5 reveals significant endothelial heterogeneity among CNS microvessels. *Microvasc. Res.* 86, 1–10. doi: 10.1016/j.mvr.2012.12.001

Raoof, R., Willemen, H. L. D. M., and Eijkelkamp, N. (2018). Divergent roles of immune cells and their mediators in pain. *Rheumatology* 57, 429–440. doi: 10.1093/rheumatology/kex308

Renier, N., Wu, Z., Simon, D. J., Yang, J., Ariel, P., and Tessier-Lavigne, M. (2014). IDISCO: a simple, rapid method to immunolabel large tissue samples for volume imaging. *Cell* 159, 896–910. doi: 10.1016/j.cell.2014.10.010

Renthal, W., Tochitsky, I., Yang, L., Cheng, Y. C., Li, E., Kawaguchi, R., et al. (2020). Transcriptional reprogramming of distinct peripheral sensory neuron subtypes after axonal injury. *Neuron* 108, 128–144.e9. doi: 10.1016/j.neuron.2020.07.026

Rittner, H. L. (2005). Leukocytes in the regulation of pain and analgesia. *J. Leuk. Biol.* 78, 1215–1222. doi: 10.1189/jlb.0405223

Rudjito, R., Agalave, N. M., Farinotti, A. B., Lundbäck, P., Szabo-Pardi, T. A., Price, T. J., et al. (2020). Sex- and cell-dependent contribution of peripheral high mobility group box 1 and TLR4 in arthritis-induced pain. *Pain* 162, 459–470. doi: 10.1097/j.pain.0000000000002034

Schmid, A. B., Coppieters, M. W., Ruitenberg, M. J., and McLachlan, E. M. (2013). Local and remote immune-mediated inflammation after mild peripheral nerve compression in rats. *J. Neuropathol. Exp. Neurol.* 72, 662–680. doi: 10.1097/NEN.0b013e318298de5b

Sen, D., Jones, S. M., Oswald, E. M., Pinkard, H., Corbin, K., and Krummel, M. F. (2016). Tracking the spatial and functional gradient of monocyte-to-macrophage differentiation in inflamed lung. *PLoS ONE* 11:e0165064. doi: 10.1371/journal.pone.0165064

Szabo-Pardi, T. A., Agalave, N. M., Andrew, A. T., and Burton, M. D. (2019). *In vivo* two-color 2-photon imaging of genetically-tagged reporter cells in the skin. *J. Vis. Exp.* doi: 10.3791/59647. [Epub ahead of print].

Tauer, U. (2002). Advantages and risks of multiphoton microscopy in physiology. *Exp. Physiol.* 87, 709–714. doi: 10.1113/eph8702464

Wiesenfeld-Hallin, Z. (2005). Sex differences in pain perception. *Gender Med.* 2, 137–145. doi: 10.1016/S1550-8579(05)80042-7

Yoon, C., Young Wook, Y., Heung Sik, N., Sun Ho, K., and Jin Mo, C. (1994). Behavioral signs of ongoing pain and cold allodynia in a rat model of neuropathic pain. *Pain* 59, 369–376. doi: 10.1016/0304-3959(94)90023-X

Yu, X., Liu, H., Hamel, K. A., Morvan, M. G., Yu, S., Leff, J., et al. (2020). Dorsal root ganglion macrophages contribute to both the initiation and persistence of neuropathic pain. *Nat. Commun.* 11:264. doi: 10.1038/s41467-019-13839-2

Zhuo, M., Wu, G., and Wu, L. J. (2011). Neuronal and microglial mechanisms of neuropathic pain. *Mol. Brain* 141, 486–498. doi: 10.1186/1756-6606-4-31

Conflict of Interest: The authors declare that the research was conducted in the absence of any commercial or financial relationships that could be construed as a potential conflict of interest.

frontiers in Cell and Developmental Biology

REVIEW
published: 19 February 2021
doi: 10.3389/fcell.2021.635221

Regulation of the Migration of Distinct Dendritic Cell Subsets

*Meng Feng, Shuping Zhou, Yong Yu, Qinghong Su, Xiaofan Li and Wei Lin**

Institute of Basic Medicine, Shandong First Medical University & Shandong Academy of Medical Science, Shandong Provincial Hospital Affiliated to Shandong First Medical University, Jinan, China

Dendritic cells (DCs), a class of antigen-presenting cells, are widely present in tissues and apparatuses of the body, and their ability to migrate is key for the initiation of immune activation and tolerogenic immune responses. The importance of DCs migration for their differentiation, phenotypic states, and immunologic functions has attracted widespread attention. In this review, we discussed and compared the chemokines, membrane molecules, and migration patterns of conventional DCs, plasmocytoid DCs, and recently proposed DC subgroups. We also review the promoters and inhibitors that affect DCs migration, including the hypoxia microenvironment, tumor microenvironment, inflammatory factors, and pathogenic microorganisms. Further understanding of the migration mechanisms and regulatory factors of DC subgroups provides new insights for the treatment of diseases, such as infection, tumors, and vaccine preparation.

Keywords: dendritic cells, migration, conventional dendritic cells, plasmacytoid dendritic cells, chemokines, adhesion molecules

OPEN ACCESS

Edited by:
Zhichao Fan,
UCONN Health, United States

Reviewed by:
Damya Laoui,
Vrije University Brussel, Belgium
Chu Yi Wei,
Fudan University, China

***Correspondence:**
Wei Lin
linw1978@163.com;
weilin11@fudan.edu.cn

Specialty section:
This article was submitted to Cell Adhesion and Migration, a section of the journal Frontiers in Cell and Developmental Biology

Received: *30 November 2020*
Accepted: *01 February 2021*
Published: *19 February 2021*

Citation:
Feng M, Zhou S, Yu Y, Su Q, Li X and Lin W (2021) Regulation of the Migration of Distinct Dendritic Cell Subsets. Front. Cell Dev. Biol. 9:635221. doi: 10.3389/fcell.2021.635221

INTRODUCTION

Dendritic cells (DCs) are professional antigen-presenting cells that link innate and adaptive immune responses. In 1973, scientists isolated cells with unique dendritic processes from the peripheral lymphoid organs of mice and named them "dendritic cells" (Steinman and Cohn, 1973). Subsequently, Idoyaga and Steinman (2011) found that DCs participated in adaptive immune response after continuous migration and activation. The function of DCs, whether in maintaining immune tolerance or promoting immunity, require migration to a certain target destination. Recent studying has brought new ideas into the development of different DC subsets in immune responses. Herein, we reviewed the DC subsets that have been reported in recent years and discussed the regulatory factors and molecular mechanisms involved in DC migration. Elucidating the mechanisms underlying the migratory DCs would contribute to the development and function of different DC subsets and their role in diseases.

DC SUBSETS

Dendritic cells are highly heterogeneous cells that have historically been categorized by phenotype, function, or location. DCs are unique hematopoietic cells that originate from precursor cells, such as monocytes and pre-DCs, in bone marrow (Naik et al., 2006; Liu et al., 2009; Liu and Nussenzweig, 2010). Precursor cells migrate to peripheral tissues and secondary lymphoid organs via blood circulation and/or lymphatic vessels where they differentiate into myeloid DCs and lymphoid DCs (Naik et al., 2007) (**Figure 1**). According to specific transcription factors and chemokines, these DCs are further differentiated into three classic subsets: conventional DC1s (cDC1s), conventional DC2s

(cDC2s), and plasmacytoid DCs (pDCs). According to their states of maturity, DCs are divided into immature DCs (imDCs), mature DC (mDCs), semi-mature DCs (smDCs), and tolerogenic DCs (tol-DCs). Semi-mature DCs (smDCs), which are an activation state between immature and mature DC cells, are difficult to define (Lutz and Schuler, 2002). These classic DC subsets play a critical role in regulating immune response and immune tolerance.

cDC1s

Conventional DC1s widely exist in the blood and peripheral tissues of human and mouse, but their expression is very low in mouse blood. Mouse cDC1s have strong homogeneity in expressing CD8 and/or CD103 (Edelson et al., 2010). Mouse $CD8^+$ cDC1s are identified as $CD11c^{hi}CD45R^-MHCII^+CD8\alpha^+DEC205^+CD11b^{lo}Sirp\alpha^{lo}$ and express C-type lectin Clec9A (DNGR1), Nectin-like protein 2 (Necl2; also called CADM1). Migratory $CD103^+$ DCs in most non-lymphoid tissues are defined as $CD11c^+MHCII^+CD103^+CD11b^{lo}CX3CR1^-F4/80^-Sirp\alpha^-$ (McLellan et al., 2002; Bursch et al., 2007; Huysamen et al., 2008; Ginhoux et al., 2009). Both resident $CD8a^+$ and migrating $CD103^+$ cDCs express CD36, CD24, and XCR1 and play a critical role in immunity against intracellular pathogens, viruses, and cancer. In mouse blood, activated cDC1s secrete interleukin (IL)-12p70 and induce the T helper type 1 (Th1) response (Maldonado-Lopez et al., 1999; Farrand et al., 2009). Human $CD141^+$/BDCA-3^+ Conventional DC1s are primarily distributed in lymphoid tissues, express C-type lectin receptor 9 (Clec9) and X-C motif chemokine receptor 1 (XCR1), and contribute to antiviral immunity (Silvin et al., 2017), whereas human thymus $CD141^+$cDC1 produces high levels of IL-12 and induces the Th17 response (Vandenabeele et al., 2001). A group of specific DC subgroup $Langerin^+(CD207^+)CD103^+CD8^+$cDC1 was found in the human spleen, and it was a key regulator of immune responses toward blood-borne antigens in the steady-state and during inflammation (Backer et al., 2019). In bacteria-infected human or mouse skin, a subset of $CD59^+EpCAM^+Ly6D^+$ cDC1 promotes the infiltration of numerous neutrophils by producing the vascular endothelial growth factor (VEGF)-α (Janela et al., 2019). cDC1 contributes to antigen presentation, induces angiogenesis, and promotes inflammation.

The migration of cDC1 is primarily correlated with CXCR3 and CCR7 expression. CXCR3 expression is restricted to mice pre-cDC1 and pDC lineages and is specifically expressed in pre-cDC1 ($Siglec\text{-}H^-Ly6C^-$) but not pre-cDC2 ($Siglec\text{-}H^-Ly6C^+$). Trafficking to periphery CCR7-$CCL21\alpha^{-/-}$ interactions guides the migration of pre-cDCs ($Lin^-CD11c^+MHCII^-Flt3^+Sirp\alpha^{lo}$), which accumulate in the thymus, where they may be important for T-cell tolerance (Cosway et al., 2018).

cDC2s

Conventional DC2s have high heterogeneity and play dual roles of immune activation and regulation in the immune response. In the blood, activated cDC2s secrete IL-1β, IL-6, and IL-23 and induce the Th17 response (Persson et al., 2013). In the mouse intestine and thymus, cDC2s can induce the production of regulatory T cells (Treg) (Proietto et al., 2008; Balan et al., 2019). Recently, human cDC2s have been divided into two subsets: (1) $CD1c^{lo}CLEC10A^-CLEC4^{hi}$ cDC2A expresses a high level of amphiregulin (Areg) and matrix metalloproteinase-9 (MMP-9) but low levels of IL-23, IL-6, and tumor necrosis factor-α (TNF-α). This subset exhibits anti-inflammatory effects. (2) $CD1c^+CLEC10A^+CLEC4^{lo}$ cDC2B has pro-inflammatory effects with high expression levels of IL-6 and TNF-α (Brown et al., 2019). The corresponding two subgroups of cDC2s in mice are $T\text{-}bet^+$ cDC2A and $T\text{-}bet^-$ cDC2B (Brown et al., 2019), which are different from the previously described cDC2 subsets. Notch2 targeting of $CD11c^+CD11b^+$ $CD103^+$ $IRF4^+$ cDC2s was associated with the induction of the Th17 cell response (Lewis et al., 2011), whereas Kruppel-like factor 4 (Klf4)-dependent $CD11c^+$ $IRF4^+$ cDC2s promote Th2, but not Th17 (Tussiwand et al., 2015). In addition, CD9 divided $CD11b^+$cDC2s into two subgroups in B16-F10 tumor-bearing mice, namely $CD9^-(CD301^-)$/$CD9^+(CD301^+)CD11b^+$cDC2s, which are required for activating antitumor $CD4^+$ T_{conv} (Binnewies et al., 2019). Although cDC2s are divided into many subsets, migratory cDC2s subsets typically require CCR7, whereas extrathymic $Sirp\alpha^+$cDC2s enter the thymus primarily via CCR2 (Tomohisa et al., 2009).

pDCs

Plasmacytoid DCs were first discovered in human lymph nodes (LNs). Human $CD11c^-CD123^+CD303^+$ pDCs are equivalent to mice PDCA-1^+ pDCs. pDC differentiation depends on E2.2 and IRF7, and expresses the CD123/IL-3α chain, CD303 (BDCA-2), CD304 (BDCA-4), and immunosuppressive molecule ILT2, etc. (Dzionek et al., 2000; Swiecki et al., 2010; Mathan et al., 2013). A new subgroup, AXL^+AS DCs ($SIGLEC1^+$, $SIGLEC6^+$), exists in human blood and expresses a similar marker as that of pDCs (Villani et al., 2017). Although these subgroups are incapable of proliferation, they can activate T cells and play an antiviral role. Furthermore, pDCs can be converted into cDCs. When transcription factor E2-2 is downregulated or ID2, PU.1, and BATF3 are significantly upregulated, CC-chemokine receptor 9 $(CCR9)^-$ pDCs in intestinal epithelial cells (IECs) migrate to peripheral tissues (Chen et al., 2015). Subsequently, they are transformed into $CD11b^+CD8^+MHCII^+$ cDC-like cells under the stimulation of granulocyte-macrophage colony-stimulating factors (GM-CSF) or soluble factors produced by IEC (Schlitzer et al., 2011). This transformation leads to an imbalance or abnormal distribution of pDC and cDC subpopulations in the body, which induce autoimmune diseases (Chen et al., 2015; Qian and Cao, 2018). CCR4, CCR6, CCR7, CCR9, CCR10, and chemokine-like receptor 1/chemerin receptor 23 (CKLR1/ChemR23) are correlated with pDC migration (Penna et al., 2001; Vermi et al., 2005; Wendland et al., 2007; Sisirak et al., 2011).

tol-DCs

Tolerogenic DCs (tol-DCs) can be derived from monocytes or pre-DCs. GM-CSF and TGF-β1 stimulated mouse liver-derived pre-DCs into tol-DCs, which prolong the survival

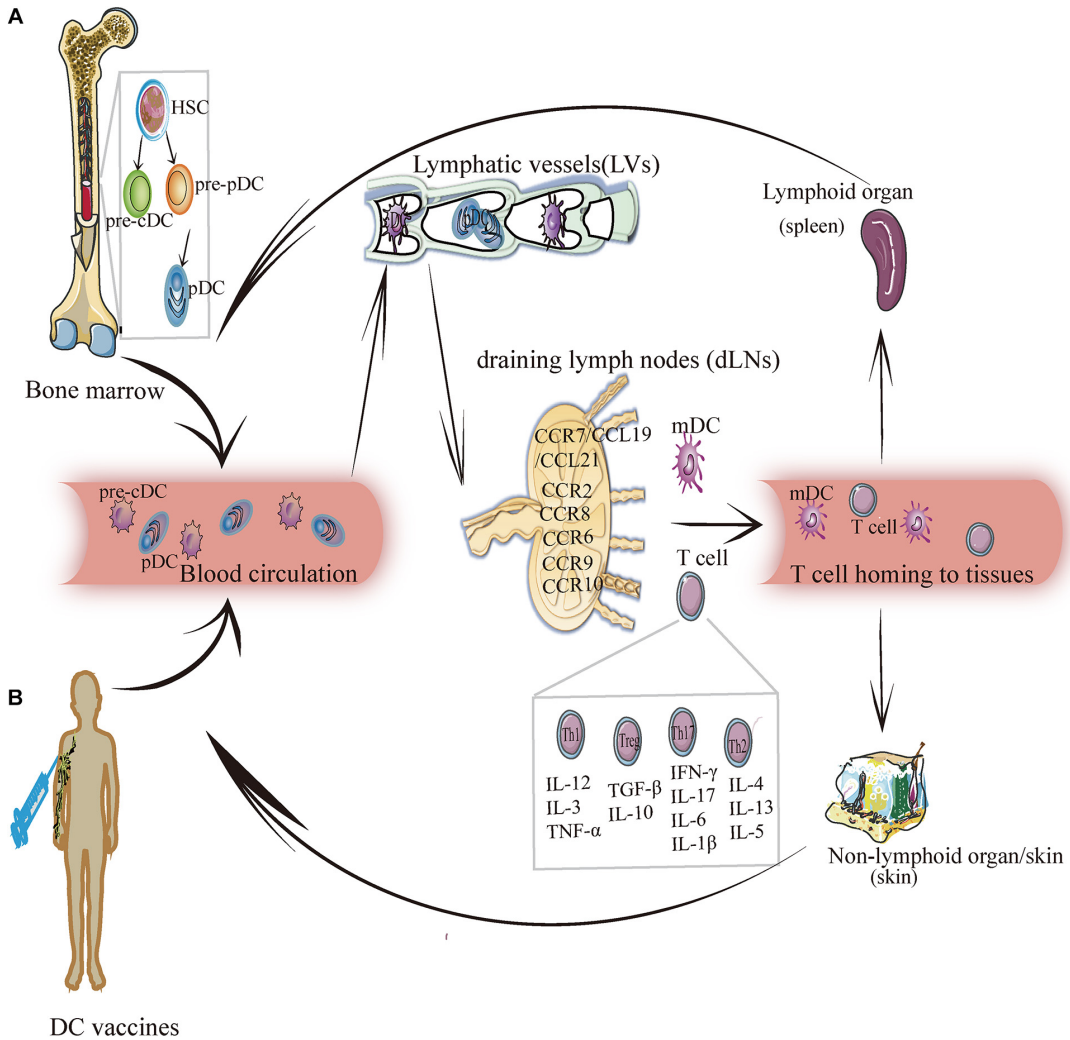

FIGURE 1 | The migration of DC subsets. **(A)** DC endogenous migration: The precursor DC (pre-DC) develops from hematopoietic stem cells and gradually differentiates into pre-cDC and pDC. Then pDC and pre-cDC migrates from the bone marrow and enters blood circulation (in this case, DC is imDC and pre-cDC differentiates into cDC). Under the mediation of chemokines and cytokines, imDC enters lymphatic vessels, and then reaches draining lymph nodes. In this process, imDC relies upon chemokines (for example: CCR7/CCL19/CCL21, CCR8, CCR6, CCR9, CCR10, etc.) to migrate and transform into mDCs and induce T cells (Th1, Th2, Th17, and Treg) to migrate into lymphoid tissues (such as: the spleen) or non-lymphoid tissues (such as: skin) to exert an immunity effect. **(B)** DC exogenous migration: After the human body is injected with the DC vaccine, DCs loaded with specific antigens enter the blood circulation, and crawls along the blood vessel wall to reach the lymphatic vessels, and then enters the draining lymph nodes to activate the adaptive immune response, by which it exerts anti-tumorigenic or antiviral effect.

time of donors in organ transplantation (Bonham et al., 1996; Khanna et al., 2000). These tol-DCs induce Treg cells to exert immune tolerance by secreting large amounts of IL-10. In addition, skin-settled $CD141^{+}CD14^{+}$ DC are derived from colonized monocytes (Chu et al., 2012; Han et al., 2014), and inhibit the $CD4^{+}$ T-cell response by secreting IL-10 and IDO. $IDO^{+}CD11b^{+}$ DC is a subset of tol-DCs (Park et al., 2012) and induces immune tolerance. Tol-DCs are classified as induced tolerogenic DCs (itDCs) and natural tolerogenic DCs (ntDCs). ItDCs contribute to the maintenance of homeostasis under potentially proinflammatory conditions. While under steady-state conditions, ntDCs facilitate the establishment of tolerance. These findings provide insights on a new framework for the use of DC-mediated mechanisms of tolerance to treat diseases (Iberg and Hawiger, 2020).

MECHANISM UNDERLYING DC MIGRATION

Migration is the key process through which DCs exercise their uptake, processing, and presentation, and it runs throughout the entire process of DC differentiation and development. DC migration affects its phenotype and maturity, thus resulting in the different localization of different DC subgroups. DCs can directly pass through the blood vessel wall and migrate from peripheral

tissues to a specific location or can enter lymph vessels from the bloodstream, from which they are passively transported to the subcapsular sinus (SCS) of the LNs through lymph flow and enter LNs to complete migration (**Figure 1A**).

Migration Kinetics of DCs

Differentiation and development of DCs occurs in four stages: (1) DC precursors, (2) imDCs, (3) migration DCs, and (4) mDCs. Previous studies have shown that only $CD34^+$ DC precursor cells express E-cadherin, which promotes DC migration and maturity (Mackensen et al., 2000). During acute inflammation, DC precursors quickly mobilize to non-lymphoid tissues. Most DCs in the peripheral organs are imDCs, as immune response sentinel, which can take up antigens more efficiently. With exogenous antigens and inflammatory factor stimulation, imDCs migrate from peripheral tissues to secondary lymphoid areas. During this process, imDCs develop into mDCs, which present antigens and induce the T-cell response in LNs (Caux et al., 2000). Differentiation from imDCs to mDCs depends on migratory DCs. This type of DC exists mainly in lymphatic tissues, input lymphatic vessels, and peripheral blood. Through blood and lymphatic circulation, migratory DCs enter the secondary lymphatic organs from the input lymphatic vessels and drive the DCs to mature.

The dynamic migration process of DCs has an important guiding role in elucidating their homeostasis and pathology in tissues. However, different DC subsets display distinct migration kinetics during migration from skin to the draining LN (dLN). After photoconversion, self-antigens that are present on $CD103^-$ dermal DCs are rapidly transported from the skin to the dLN and are responsible for the transport of invading pathogens to the dLN. In contrast, $CD103^+$ DCs reached a plateau on day 3 after photoconversion and participated in antigen cross-presentation (Tomura et al., 2014). Moreover, different DC subsets survey different regions of the spleen to induce specific T cell responses. For example, $33D1^+$ DC migrates to the periphery of the T cell zone of the spleen to induce $CD4^+$ T cell responses, whereas $XCR1^+$ DC migrates to the center of the T cell zone in the white pulp of spleen to induce $CD8^+$ T cell responses (Calabro et al., 2016). In addition, the migration of localized skin $CD1c^+/CD14^+/CD141^+$ DC subgroups to the inflammation site depends on CCR7/CXCL10 (Chu et al., 2012; Haniffa et al., 2012, 2015). However, research on the migration of a certain DC subgroup to a specific site in the tissues under steady-state and inflammatory conditions remain insufficient. Furthermore, whether independent DC subsets can selectively induce the T cell response in other immune organs warrants further research.

Essence and Mechanism of Migration

The migration of DCs is a complex and dynamic cyclical process. Cell migration occurs due to interaction between chemokines and chemokine receptors. Under the guidance of chemokines, DCs move to specific sites and exert corresponding biological functions. In addition, adhesion factors, integrins, semaphores, and cytoskeletal proteins play various roles in cell migration. Furthermore, the migration of DCs is essential for T cell responses.

Chemokines

Chemokines and chemokine receptors guide the positioning and chemotaxis effects of DCs at different developmental stages. Chemokines are a class of highly conserved small, secreted proteins that regulate DC migration by identifying chemokine receptors that bind to the DC surface. CCR7 plays an important role in DC migration from peripheral tissues to draining LNs and is a key factor that affects DC migration and function (Yanagihara et al., 1998; Hirao et al., 2000; Randolph et al., 2004). CCR7 ligands CCL19 and CCL21, which are expressed in lymphoid organs mainly, drive DC migration (Elke et al., 2004; Tiberio et al., 2018). CCL21 forms the "CCL21 gradient" by binding to heparan sulfates in the interstitium, thereby providing adhesion for DC migration and guiding DC migration into LNs (Weber et al., 2013). The discovery of chemokines and the chemokine–chemokine receptor axes facilitates research to elucidate the migration mechanism of DCs.

(1) The CCR7-CCL21/CCL19 axis: The CCR7-CCL19/CCL21 chemokine axis is vital for the regulation of adaptive immunity and tolerance by affecting mDC migration from the peripheral tissue to lymphatic vessels and LNs (Forster et al., 2008). Depending on this axis, human skin $CD141^+CD1c^-XCR1^+$ cDC1 (Igyártó et al., 2011)/$CD1a^+CD1c^+$cDC2 (Kitajima and Ziegler, 2013) migrates from the dermis to skin-draining LNs (Tamoutounour et al., 2013) or intestinal $CD103^+$ $CD11b^-XCR1^+$ $SIRP\alpha^-CD141^+DNGR1^+$cDC1 (Olga et al., 2009)/ $CD103^+$ $CD11b^+$ $XCR1^-$ $SIRP\alpha^+$ $CD141^-DNGR^-$cDC2 (Persson et al., 2013) migrate from the lamina propria to mesenteric LNs (Farache et al., 2013). CCR7-CCL19/CCL21 promote the migration of corneal mDCs to intraocular lymphatic vessels and mediate the $CD4^+$ T cell immune response (Wang et al., 2019). Migrations of Newcastle disease virus-like particles (NDV-VLP)-treated DCs to draining LNs or the spleen rely upon the CCR7-CCL19/CCL21 axis, thus leading to $CD4^+$ T cell activation (Qu et al., 2005). CCR7-CCL19/CCL21-dependent DC migration is involved in the coordination of the activation of specific Tregs, which is beneficial for maintaining peripheral tolerance (Leventhal et al., 2016). This provides new insights for further understanding the role of the CCR7-CCL19/CCL21 axis in maintaining a balance between the adaptive immune response and immune tolerance. Inflammatory factors CCRL1 (called ACKR4) (Ulvmar et al., 2014), transcription factor PU.1 (Yashiro et al., 2019), and IL-18-driven human helper NK cells (Wong et al., 2014) participated in the regulation of DC migration, which may contribute to adaptive immune responses that are associated with infection, cancer, or vaccination.

(2) The leukotriene B4 (LTB4)-BLT1 axis: This axis is critical for regulating DC transport and inducing an adaptive immune response (Del Prete et al., 2006). DCs can be stimulated by LTB4 *in vitro* and upregulate the expression of CCR7 and CCL19 while promoting chemokines CCL19 and CCL21 to induce DC migration to LNs

(Del Prete et al., 2006). This indicates that LTB4 plays an important role in regulating DC migration and inducing adaptive immune responses.

(3) The CXCR4-CXCL12 axis: This axis relies on CCR7 to promote the migration of DCs from peripheral organs to LNs and participate in the migration of DCs across lymphatic endothelial cells and lymphatic vessels, as well as the migration of epidermal DCs to the dermis (Kabashima et al., 2007; Villablanca and Mora, 2008). Thus, CXCR4-CXCL12 is a key axis for DC migration during skin inflammation.

(4) The CCR8-CCL21/CCL8 axis: CCR8 and its ligand CCL21/CCL8 promote DC homing toward LNs (Sokol et al., 2018). In addition, CCR8 and CCL21 coordinate the promotion of CCR7-mediated CD301b$^+$ DC migration from the SCS to LNs and induce Th2 effects. Th2 immunization specifically induces CCL8 expression by CD169$^+$SIGN-R1$^+$ macrophages. CCL8, and CCL21 synergistically promote CD301b$^+$ DC migration (Sokol et al., 2018). These factors may contribute to adaptive immune deviation and cancer cell metastasis associated with DC migration.

Some chemotactic signals can directly activate DC migration or promote the production of chemokines (CXCL12, CXCL14, CCL19, CCL3, etc.), thereby causing secondary recruitment of cells (Majumdar et al., 2014; Tiberio et al., 2018). New paradigms have emerged in the establishment and maintenance of gradients during directed cell migration. Such chemotactic signals include bacterial components, lipid mediators, signaling proteins, and proinflammatory cytokines. For example, cathelin-related antimicrobial peptide (CRAMP), platelet-activating factor (PAF), Activin A, serum amyloid A (SAA), and leukotriene B4 (LTB4). The formylpeptide receptor (Fpr2) expressed on the surface of DCs and CRAMP is jointly involved in the activation and aggregation of DCs involved in allergic airway inflammation (Chen et al., 2014). SAA can directly induce the migration of imDCs via the secondary release of CXCL12 and CXCL14 (Gouwy et al., 2015). Furthermore, the chemokine signals induce faster migration of DCs.

Adhesion Molecules and Proteins

The acquisition of DC migration capacity also depends on the change of its adhesion state. During inflammation, ICAM-1, ICAM-2, Mac-1 (αMβ2), and LFA-1 (αLβ2) play crucial roles in regulating DC migration. The expression of intracellular chemokine CXCR3 promote Mac-1 and LFA-1 binding to their ligand ICAM-1/2, thereby targeting cell adhesion (Springer, 1994). L/E/P-selectin on activated endothelial cells is required for the DC migration process and is involved in the DC homing of lymphoid and peripheral tissues (Tedder et al., 1995; Pendl et al., 2002; Lekakis et al., 2010).

Tetraspanins are expressed on the surface of DCs and control DC migration by coordinating the expression and aggregation of cytokines, selectins, integrins, or other cell–cell proteins on the DC surface (Charrin et al., 2009). P-selectin-independent rolling decreases in the absence of tetraspanin CD63 (Doyle et al., 2011). Tetraspanin CD53 stabilizes L-selectin surface expression and promotes lymphocyte recirculation (Demaria et al., 2020), which indicates that tetraspanin pairs with its partner protein of selectin in co-participation in DC migration.

Rho-associated protein kinases (ROCKs) affect the migration of DCs to draining LNs by mediating the activation of actin nuclear contraction (Nitschké et al., 2012), rapid reconstruction of F-actin throughout DC migration, cell polarity formation, and interaction between cell proteins (Tang and Gerlach, 2017). The actin-related protein 2/3 (Arp2/3) complex mediated F-actin formation of pseudopodia at the front end of this movement and boosted the CCR7-CCL19/CCL21 response axis to induce chemotactic migration of mDCs (Leithner et al., 2016). Under the regulation of the Rho-GTPase signaling pathway, Arp2/3-mediated actin nucleation weakened at the front end of the migration movement (Suraneni et al., 2015), whereas morphogenetic formin-protein-mediated actin nucleation increased at the end of the migration movement (Vargas et al., 2016), which resulted in the rapid migration of mDCs. Calcium ions maintain cell polarity and stabilize the actin cytoskeleton. DC migration requires the participation of a variety of adhesion factors or proteins, which provides a more comprehensive explanation of the mechanism underlying DC migration.

Migration Patterns of Different Cell Subsets

Migrating cDCs and pDCs recruited from the blood to LNs can promote peripheral Treg cells to induce immune tolerance, thereby linking migrating DCs as potential markers for the treatment of autoimmune diseases (Bonasio et al., 2006; Hadeiba et al., 2012). The development of cDCs and pDCs depends on the expression of CCR6/7 but relies upon CCR1/4/8 or CCR2/9/10, respectively (**Figure 2**).

Although cDCs usually upregulate the expression of CCR7 to induce migration, during inflammation, IRF4$^{-/-}$CD11b$^+$ cDCs could not upregulate CCR7 expression to induce migration to inflamed skin (Bajana et al., 2012; Plantinga et al., 2013). When *Staphylococcus epidermidis* infects skin tissue, dermal CD103$^+$ cDC1s carry bacterial antigens that migrate to skin LNs, promote IL-17 secretion, and induce the recruitment of CD8$^+$ T cells to the skin to resist pathogen infection (Farache et al., 2013). The chemotactic receptor Epstein–Barr virus-induced 2 (EBI2) can guide the migration of CD11b$^+$ cDC2 to the LNs and spleen by up-regulating CCR7, CXCR5, and CXCL13 and inducing CD4$^+$ T-cell effects (Gatto et al., 2011; Leon et al., 2012; Gatto et al., 2013). pDCs usually enter LNs through high endothelial veins and assist other DC subsets in performing antigen presentation functions. Upon viral infection, pDCs were directed toward two different sites in the LN, they either migrated to infected macrophages residing in the SCS area in a CXCR3-dependent manner or to CD8$^+$ T cell priming sites in a CCR5-dependent manner. This may be essential to induce antiviral immunity (Brewitz et al., 2017). Moreover, CCR9 mediates pDC migration to the intestine (Wendland et al., 2007). CKLR1/ChemR23 mediates pDC migration to LNs or inflamed

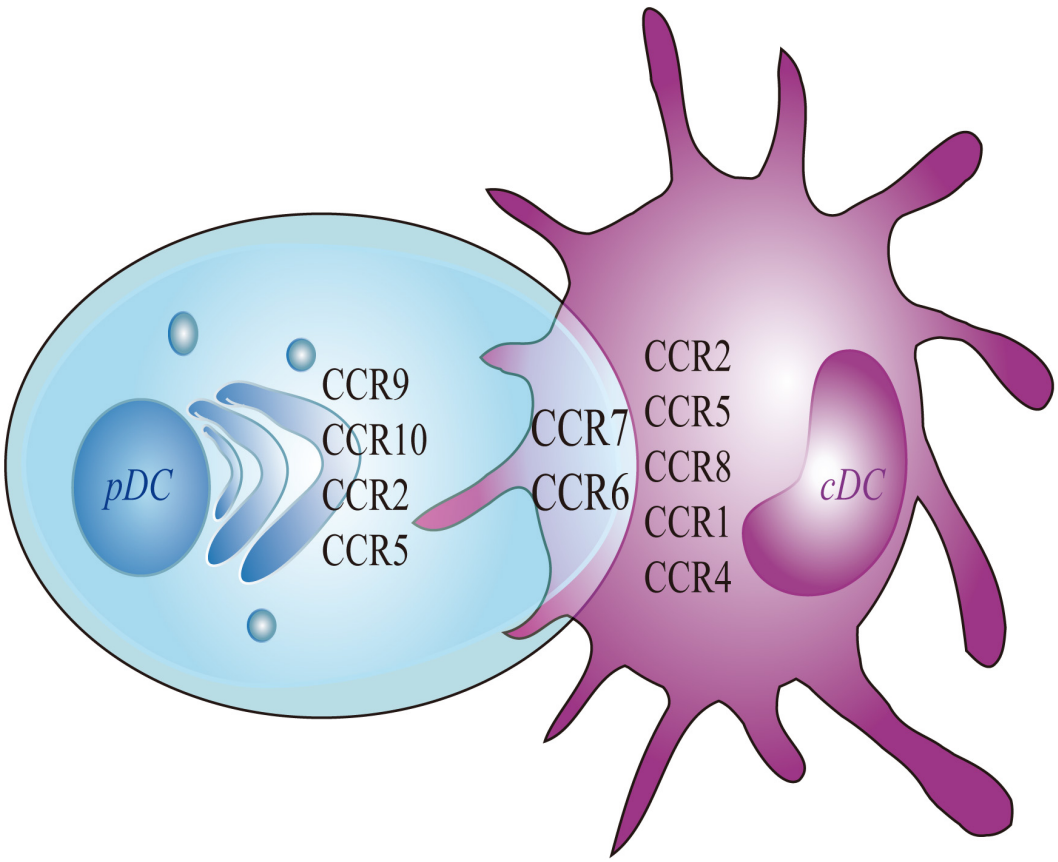

FIGURE 2 | Chemokines of pDC and cDC. Migratory pDC and cDC depends on the expression of CCR7 and CCR6. More specifically, the migration of cDC depends on the expression of CCR8, whereas the migration of pDC depends on the expressions of CCR9 and CCR10. The current study found that the migration of mouse cDC depends on CCR1 and CCR4. The migration of human cDC is dependent on CCR2 and CCR5. At the same time, the expressions of CCR2 and CCR5 are also involved in mediating the migration of mouse pDC.

skin (Zabel et al., 2005; Albanesi et al., 2009). pDCs also depend on CCR6, CCR7, and CCR10 to complete homing from the blood to inflamed skin (Sisirak et al., 2011). pDCs and cDCs express different chemokine and chemokine receptors which lead them to have different migrate route and functions (**Table 1**). However, the specific mechanism needs to be further studied.

During inflammation, the migration of imDCs mainly depends on the mediation of E/P-selectin (Pendl et al., 2002). Endothelial selectins are involved in the rolling, extravasation, and migration of imDC in the vascular endothelium. The ChemR23 ligand chemerin can increase the migration of imDCs to endothelial cells with the participation of CCL7 (Gouwy et al., 2013). imDCs and mDCs may have the opposite reactivity to the same chemokine. For example, imDCs have weak reactivity to CC-chemokine-MIP-1b and CXC-chemokine-SDF-1a, but the reverse occurs when imDCs are mature (Lore et al., 1998). In addition, the Rho-mDia1-dependent actin pool is involved in the forward movement of imDCs and the migration of mDCs to lymphatic vessels (Vargas et al., 2016). The migration patterns of different subgroups affect the progress of immune regulation, but the migration mechanism of each subgroup is unclear.

REGULATORY FACTORS AFFECTING DC MIGRATION

The Hypoxic Microenvironment

A sufficient oxygen environment is required to maintain the normal development and metabolism of cells. Hypoxia can downregulate the expression of CCR7 and DC surface adenosine receptor A2b, whereas the cyclic AMP/protein kinase A signaling pathway reduces the inhibition of *MMP-9/TIMP* gene secretion during hypoxia by acting on the A2b receptor (Qu et al., 2005). The downregulation of CCR7 and the change in *MMP-9/TIMP* gene expression are the main factors that inhibit DC migration, which cause an imbalance in the Th1/Th2 immune response.

Tumor Microenvironment

Elucidating the migration processes of DCs in the tumor microenvironment (TME) can explain how DC-derived cancer vaccines will effectively work in the human body, thus leading to the development of effective vaccines. However, knowledge of the exogenous migration pathway of DC is limited. When tumors

TABLE 1 | Migration routes, chemokines/chemokines receptor, and functions of cDC and pDC subsets.

	DC subsets	Migration routes	Chemokines/ chemokines receptor	Immunological functions	References
cDC1s	Dermis: human $CD14^+CD1a^-HLA\text{-}DR^+$cDC1 (mouse $CD11b^+CD64^+$)	Spontaneously migrate from skin explants cultured *ex vivo*.	CXCL13	Antigen presentation and activation of naive T cells; production of IL-10, IL-6, MCP-1.	Klechevsky et al. (2008); Chu et al. (2012)
	Dermis: human $CD141^+CD1c^-XCR1^+$cDC1 (mouse $CD103^+CD207^+/CD8^+XCR1^+$)	From the dermis to the skin draining lymph nodes via afferent lymphatics.	CCR7	Cross-presentation self-antigen; induction of $CD8^+$ effector T cells or Th1 cells; production of TNF-α.	den Haan and Bevan (2002); Crozat et al. (2010), Igyártó et al. (2011); Tamoutounour et al. (2013)
	Intestine: human/mouse $CD103^+CD11b^-$ $CD8\alpha^+$ $XCR1^+SIRP\alpha^-$cDC1	From Lamina propria to mesenteric lymph nodes via afferent lymphatics.	CCR7	Cross-presentation self-antigen; induction of $CD8^+$ effector T/Th1/Treg cell responses.	Laffont et al. (2010); Cerovic et al. (2015), Esterházy et al. (2016)
	Lung: human/mouse $CD103^+CD11b^-CD207^+$ $XCR1^+$ cDC1	From lung interstitium to mediastinal lymph nodes via afferent lymphatics.	CCR7, CCR2	Cross-presentation self-antigen; induction of $CD8^+$ effector T cells; airway tolerance.	del Rio et al. (2007); GeurtsvanKessel et al. (2008), Rose et al. (2010); Fossum et al. (2015), Sharma et al. (2020)
cDC2s	$CD11b^+$cDC2	Migrate to the lymph nodes and spleen dependent on EBI2.	CCR7; CXCR5, CXCL13	Cross-presentation self-antigen; induction of $CD4^+$ T/Th2 cell responses.	Rose et al. (2010); Gatto et al. (2011), Leon et al. (2012); Gatto et al. (2013)
	Skin: human $CD1a^+CD14^-$ $HLA\text{-}DR^+$cDC2 (mouse $CD11b^+CD207^-XCR1^-$)	From the dermis to the skin draining lymph nodes via afferent lymphatics.	CCR7	Antigen presentation and activation of naive T cells or Th2 cell; production of IL-15, IL-8.	Klechevsky et al. (2008); Kitajima and Ziegler (2013), Tamoutounour et al. (2013)
	Intestine: human/mouse $CD103^+CD11b^+XCR1^-$ $SIRP\alpha^+$cDC2	From lamina propria to mesenteric lymph nodes via afferent lymphatics.	CCR7; CCR9/CCL25	Induction of Th1/Th17 cells; induction of Treg cells; production of pro-inflammatory cytokines IL-6, IL-23 and so on.	Farache et al. (2013); Gao et al. (2021)
	Lung: human/mouse $CD103^-CD11b^+$ cDC2	From lung interstitium to mediastinal lymph nodes via afferent lymphatics.	CCR7; CCR1, CCR5	Induction of inflammatory response; induction of protective mucosal immune responses; expression of IL-18, IL-1, or IL-1R.	Lukens et al. (2009); Pang et al. (2013), Sharma et al. (2020)
pDCs	Skin: human $CD11c^-CD123^+BDCA\text{-}2^+$ $BDCA\text{-}4^+$pDCs (mouse $B220^+$ $PDCA1^+$ $LY6C^+$)	Migrate into inflamed epithelia of mucosae or skin.	CCR6, CCR10	Cross-presentation self-antigen, induction of $CD4^+$ effector T cells; production of IFN-γ.	Sisirak et al. (2011)
	Intestine: human $CD11c^-$ $CD123^+BDCA\text{-}2^+BDCA\text{-}4^+$pDCs (mouse $CD11c^{mid}$ $B220^+PDCA1^+$ $LY6C^+$)	Homing to the small intestine via high endothelial venules.	CCR9, CCR7	Imbalance of Th1/Th2 effects; production of TNF-α.	Wendland et al. (2007)
	Viral infection sites: pDCs	Migrate into the subcapsular sinus area or $CD8^+$ T cell priming site.	CXCR3; CCR5	Induction of $CD8^+$ effector T cells; antiviral immunity.	Brewitz et al. (2017)

occur, increased secretion of TGF-β, VEGF, and LXR ligands and anti-inflammatory factors may recruit DC precursors and convert them into tol-DCs, thereby inhibiting DC maturation and migration to LNs (Soudja et al., 2011). Likely, TGF-β may be involved in DC migration under phosphatidylinositol 3-kinase/Akt activation (Bakin et al., 2000) and increase cell tolerance (Lee et al., 1998). This confirms that the TME can inhibit DC migration. The occurrence of ectopic LNs in tumors can also induce DC migration via CCL21 (Chen et al., 2002; Di Caro et al., 2014). NK cells promote cDC1 accumulation in incipient tumors by producing CCL5 and XCL1/2 (Bottcher et al., 2018). Immunoregulatory factor PEG2 can downregulate the expression of chemokines CCL5, XCL1, XCR1, and CCR5 on cDC1 to inhibit DC accumulation and $CD8^+$ T cell action in the TME (Bottcher et al., 2018). Regulating the expression of chemokines and/or chemokine receptors may interfere with the accumulation of DC in tumors or tumor-draining LNs.

A nano-vaccine containing M-COSA/OVA/pDNA can promote the expression of MHC-I and cytokines (such as IFN-γ) after injection into the human body, enhance antigen presentation as an immune adjuvant, induce DC migration to LNs, and activate $CD8^+$ T-cell effects to inhibit tumor growth (Xiqin et al., 2018). The key to effective DC vaccines involves the migration of DC-carrying antigens to T-cell-rich LN regions. The use of magnetic resonance imaging, fluorescent labeling, and other technical methods to track the migration route of DC in the body enables DC vaccines to target their effects on cancer (de Chickera et al., 2011). In-depth understanding of DC migration routes are conducive to the preparation of targeted DC vaccines.

Inflammation Cytokines

Inflammatory cytokines promote DC migration through paracrine or autocrine signaling and induce the expression of CCR7 and its ligand CCL19/CCL21 in DCs, thereby promoting DC migration (MartIn-Fontecha et al., 2003; Del Prete et al., 2006). The TNF-α, IL-6, and IL-1β families are involved in DC migration to inflammation sites that are under mediation by CCR7, and this process may be related to the Toll-like receptor/transcription factor nuclear factor-κB (TLR/NF-κB) pathway, which can modulate the Th1/Th17 polarization effect (Cumberbatch et al., 2002; Gianello et al., 2019). In addition, CX3CL1 and CXCL12 may participate in DC migration in the inflammatory environment and promote DC migration through the vascular endothelium to lymphatic vessels (Johnson and Jackson, 2013). In the non-inflammatory environment, the atypical Iκβ-dependent pathway activated by NF-κB appears to regulate CCR7 and co-stimulatory molecule expression (Baratin et al., 2015). At the same time, TLR ligands can enhance DCs to express CCR7 and CCL19 and promote DC migration from peripheral tissues to draining LNs (González et al., 2014). Thus, the inflammatory environment or inflammatory signals (TGF-α, IL-1β, IL-6, and IL-12) promote DC maturation and migration depending on CCR7 expression.

Pathogenic Microbes

Invasion by pathogenic microbes affects the migration and location of DC subgroups. In the gut, $CD103^+CD11b^+$ cDC2 in the intestinal lamina propria of *Salmonella* infection upregulate CCR7 and migrate to the IEC layer, which helps epithelial DCs acquire bacterial infections (Farache et al., 2013). A substantial number of CCR2-dependent $LY6C^{hi}$ monocytes that secrete proinflammatory factors and accumulate in the intestine may transform into inf-DCs and then migrate to mesenteric LNs and induce T-cell effects (Zigmond et al., 2012). However, acute intestinal bacterial infection may cause a substantial number of migrating DCs to converge in the adipose tissue area of mesenteric LNs, thereby preventing transfer to mesenteric LNs (Fonseca et al., 2015).

Respiratory syncytial virus (RSA) infection promoted $CD11b^+$ DCs to carry allergens to mediastinal LNs by CCR2/CCL2 and CCR7, which induced Th2 cell immunity and caused allergic asthma (Plantinga et al., 2013). During RSV infection, the G protein receptor EOS1 caused the lung

TABLE 2 | Factors affecting DCs migration.

Influence factors			Chemokines/ chemokines receptor	Migration route	Immunological functions	References
Inhibition	Tumor microenvironment	TGF-β, VEGF, LXR ligands, anti-inflammatory factors or PGE2	CCR7-CCL19/CCL21; CCR5 and XCR1/XCL1	Inhibiting DCs to migrate from the tumor environment to the T cell cortex in tumor-draining lymph nodes.	Inhibition of $CD8^+$ T-cell response.	Soudja et al. (2011); Bottcher et al. (2018)
	Hypoxia		CCR7-CCL19/CCL21 and adenosine receptor A2b	Inhibiting DCs to migrate toward draining lymph nodes (dLNs).	Imbalance of Th1/Th2 immune response.	Qu et al. (2005), Liu et al. (2019)
	Others	lnc-Dpf3 gene	CCR7	Inhibiting late-stage of DCs migration toward dLNs.	Inhibition of inflammation responses.	Liu et al. (2019)
Promotion	Inflammatory cytokines	TNF-α, IL-6, and IL-1β family	CCR7-CCL19/CCL21; CX3CL1 and CXCL12	Promoting DCs to migrate from peripheral tissues to dLNs.	Regulation the Th1/Th17 response.	Cumberbatch et al. (2002); Johnson and Jackson (2013), Gianello et al. (2019)
	Laser or Radiation	By up-regulate IL-12 or MHC-I, CD80	CCR7	Promoting DCs to migrate toward dLNs.	Damage the collagen fibers and cell matrix.	Chen et al. (2012), Yu et al. (2018)
	Vaccines (M-COSA/OVA/pDNA vaccine/NDV-VLPs vaccine)	By up-regulateTNF-α, IFN-γ, IL-6, IL-12p70 or MHC-I, IFN-γ	CCR7-CCL19/CCL21	Promoting DCs to migrate toward dLNs or spleen.	Activation of $CD4^+/8^+$ T response.	Qu et al. (2005); Xiqin et al. (2018)

$CD103^+CD11b^+$ DC subgroup to migrate to mediastinal LNs (Lukens et al., 2009), thereby up-regulating the expressions of IL-18, IL-1, and IL-1R, which promoted respiratory DC migration and increased the inflammatory response (Pang et al., 2013). NDV-VLPs, an emerging virus vaccine (Qu et al., 2005), up-regulates MHC-II, co-stimulatory molecules, and proinflammatory cytokines TNF-α, IFN-γ, IL-6, and IL-12p70 through the TLR4/NF-κB pathway, thereby effectively activating DC maturity. In addition, NDV-VLPs induce the expression of CCR7 on DCs and cooperate with CCL19/CCL21 to mediate the migration of DCs to draining LNs or the spleen to activate $CD4^+$ T-cell response. These discoveries provides new insight toward the development of similar VLP vaccines.

Notably, the coronavirus disease 2019 (COVID-19) infection also produces a large number of chemokines (CCL2, CCL3, CCL5, CXCL8, CXCL9, CXCL10, etc.), that might promote DCs and/or T cell infiltration into infected sites, thereby causing cytokine storms that destroy lung function and cause a systemic inflammatory response that leads to organ failure (Huang et al., 2020; Rivellese and Prediletto, 2020; Xu et al., 2020). Recently, it was found that inflammatory disease-inflammatory type 2 cDCs (inf-cDC2s) (Bosteels et al., 2020), which are structurally similar to DCs but have the combined functional advantages of monocytes, macrophages, and cDC functionality, exert an anti-inflammatory effect in COVID-19 patients.

Others

Proteomic and transcriptome analyses confirmed that the *lnc-Dpf3* gene can negatively inhibit CCR7-mediated HIF-1α activation and glycolysis gene *LDHA* expression, ultimately negatively regulating CCR7-mediated DC migration and inflammation (Liu et al., 2019). This study shows that deletion of *lnc-Dpf3* gene can enhance CCR7-mediated activation of HIF-1α and DC migration and provides direction for research on the expression or role of non-coding long-chain RNAs in DC migration and inflammatory diseases.

In addition, laser irradiation or radiation may damage collagen fibers and the cell matrix of cells, thus causing collagen fibers to become disordered or broken, which affects the local recruitment of DC and promotes the migration of DCs to LNs (Chen et al., 2012; Yu et al., 2018). Laser-irradiated DCs may be accompanied by an increase in MHC-I and CD80 (Chen et al., 2012). It was established that, depending on the ATM/NF-κB signaling pathway, low-dose radiation may increase CCR7-mediated DC migration and is accompanied by an increased secretion of IL-12. Whether external infection factors or internal genetic factors affect DC migration by regulating the expression of chemotactic or adhesion factors in DCs (**Table 2**), further study of the mechanisms regulating the migration of DCs will elucidate important factors underlying the pathogenesis and immune status of disease.

CONCLUSION AND OUTLOOK

The essence of DC migration involves chemokines, adhesion factors, integrins, and contributing biological activities. Different migration modes eventually lead to differences in the DC phenotype, location, and function. DC migration has a guiding role in the development and functions of DC-tumor or DC-virus vaccines, which are injected and migrated through blood vessels or lymphatic vessels, and eventually to the site of infection or tumor to play a role in antiviral or anti-tumorigenic effects (**Figure 1B**). Further studies are needed to determine whether the DC-tumor vaccine can effectively reach the local tumor to induce an anti-tumorigenic effect and whether DC-virus vaccine can effectively reach the infected site and elicit antiviral response. The development of transcriptomes, proteomics, and other technologies will provide technical support for more precise expression and regulation of DC migration to achieve a more effective treatment.

Migration from non-lymphoid to lymphoid tissue is a key feature of DCs that regulates immune response. Chemokine/chemokine receptors, integrins, protein receptors, and transcription factors, promote DC migration and specific intra-organ localization. In tumor tissues, removing inhibitory factors on DC migration may activate immunity and anti-tumorgenicity. However, inhibiting DC migration may be related to the inhibition of excessive activation in autoimmune diseases. Targeting CCR7 or other key mediators of DC trafficking may represent more suitable approaches for targeting DCs in diseases. Research on the migration and function of specific DC subgroups in diseases requires further study.

At present, research on genomes that affect DC migration and the migration modes of pDC, cDC, and other DC subgroups are unclear, and there is still a question about how to precisely target the direction of DC migration to make DC vaccines effective in antitumor and antiviral therapies. For the development and clinical application of an effective DC antiviral vaccine for COVID-19, which has rapidly spread around the world since December 2019, an in-depth exploration of changes in DC migration during the immune response to infection by pathogenic microorganisms is key, but greater elucidation is urgently needed.

AUTHOR CONTRIBUTIONS

WL and MF contributed toward the concept and manuscript writing. SZ, YY, QS, and XL participated in the literature search and discussion. All authors contributed to the article and approved the submitted version.

FUNDING

This work was supported by grants from the Natural Science Foundation of China (81500710), Shandong Key Research and Development Project (2019GSF108189), projects of medical and health technology development program in Shandong province (2019WS186), the science and technology program from Shandong Academy of Medical Sciences (2015–2025), and the Innovation Project of Shandong Academy of Medical Sciences.

REFERENCES

Albanesi, C., Scarponi, C., Pallotta, S., Daniele, R., Bosisio, D., Madonna, S., et al. (2009). Chemerin expression marks early psoriatic skin lesions and correlates with plasmacytoid dendritic cell recruitment. *J. Exp. Med.* 206, 249–258. doi: 10.1084/jem.20080129

Backer, R. A., Diener, N., and Clausen, B. E. (2019). Langerin(+)CD8(+) dendritic cells in the splenic marginal zone: not so marginal after all. *Front. Immunol.* 10:741. doi: 10.3389/fimmu.2019.00741

Bajana, S., Roach, K., Turner, S., Paul, J., and Kovats, S. (2012). IRF4 promotes cutaneous dendritic cell migration to lymph nodes during homeostasis and inflammation. *J. Immunol.* 189, 3368–3377. doi: 10.4049/jimmunol.1102613

Bakin, A. V., Tomlinson, A. K., Bhowmick, N. A., Moses, H. L., and Arteaga, C. L. (2000). Phosphatidylinositol 3-kinase function is required for transforming growth factor beta-mediated epithelial to mesenchymal transition and cell migration. *J. Biol. Chem.* 275, 36803–36810. doi: 10.1074/jbc.M005912200

Balan, S., Saxena, M., and Bhardwaj, N. (2019). Dendritic cell subsets and locations. *Int. Rev. Cell Mol. Biol.* 348, 1–68. doi: 10.1016/bs.ircmb.2019.07.004

Baratin, M., Foray, C., Demaria, O., Habbeddine, M., Pollet, E., Maurizio, J., et al. (2015). Homeostatic NF-κB signaling in steady-state migratory dendritic cells regulates immune homeostasis and tolerance. *Immunity* 42, 627–639. doi: 10.1016/j.immuni.2015.03.003

Binnewies, M., Mujal, A. M., Pollack, J. L., Combes, A. J., Hardison, E. A., Barry, K. C., et al. (2019). Unleashing type-2 dendritic cells to drive protective antitumor CD4(+) T cell. *Immunity Cell* 177, 556–571. doi: 10.1016/j.cell.2019.02.005

Bonasio, R., Scimone, M. L., Schaerli, P., Grabie, N., Lichtman, A. H., and von Andrian, U. H. (2006). Clonal deletion of thymocytes by circulating dendritic cells homing to the thymus. *Nat. Immunol.* 7, 1092–1100. doi: 10.1038/ni1385

Bonham, C. A., Lu, L., Banas, R. A., Fontes, P., Rao, A. S., Starzl, T. E., et al. (1996). TGF-beta 1 pretreatment impairs the allostimulatory function of human bone marrow-derived antigen-presenting cells for both naive and primed T cells. *Transpl. Immuno.* 4, 186–191. doi: 10.1016/s0966-3274(96)80015-3

Bosteels, C., Neyt, K., Vanheerswynghels, M., van Helden, M. J., Sichien, D., Debeuf, N., et al. (2020). Inflammatory Type 2 cDCs Acquire Features of cDC1s and macrophages to orchestrate immunity to respiratory virus infection. *Immunity* 52, 1039.e9–1056.e9. doi: 10.1016/j.immuni.2020.04.005

Bottcher, J. P., Bonavita, E., Chakravarty, P., Blees, H., Cabeza-Cabrerizo, M., Sammicheli, S., et al. (2018). NK cells stimulate recruitment of cdc1 into the tumor microenvironment promoting cancer immune control. *Cell* 172, 1022–1037. doi: 10.1016/j.cell.2018.01.004

Brewitz, A., Eickhoff, S., Dähling, S., Quast, T., Bedoui, S., Kroczek, R. A., et al. (2017). CD8+ T cells orchestrate pDC-XCR1+ dendritic cell spatial and functional cooperativity to optimize priming. *Immunity* 46, 205–219. doi: 10.1016/j.immuni.2017.01.003

Brown, C. C., Gudjonson, H., Pritykin, Y., Deep, D., Lavallée, V., Mendoza, A., et al. (2019). Transcriptional basis of mouse and human dendritic cell heterogeneity. *Cell* 179, 846.e24–863.e24. doi: 10.1016/j.cell.2019.09.035

Bursch, L. S., Wang, L., Igyarto, B., Kissenpfennig, A., Malissen, B., Kaplan, D. H., et al. (2007). Identification of a novel population of Langerin^{+} dendritic cells. *J. Exp. Med.* 204, 3147–3156. doi: 10.1084/jem.20071966

Calabro, S., Liu, D., Gallman, A., Nascimento, M. S., Yu, Z., Zhang, T. T., et al. (2016). Differential intrasplenic migration of dendritic cell subsets tailors adaptive immunity. *Cell Rep.* 16, 2472–2485. doi: 10.1016/j.celrep.2016.07.076

Caux, C., Ait-Yahia, S., Chemin, K., de Bouteiller, O., Dieu-Nosjean, M. C., Homey, B., et al. (2000). Dendritic cell biology and regulation of dendritic cell trafficking by chemokines. *Springer Semin. Immunopathol.* 22, 345–369. doi: 10.1007/s002810000053

Cerovic, V., Houston, S. A., Westlund, J., Utriainen, L., Davison, E. S., Scott, C. L., et al. (2015). Lymph-borne CD8α^{+} dendritic cells are uniquely able to cross-prime CD8^{+} T cells with antigen acquired from intestinal epithelial cells. *Mucosal. Immunol.* 8, 38–48. doi: 10.1038/mi.2014.40

Charrin, S., Le Naour, F., Silvie, O., Milhiet, P. E., Boucheix, C., and Rubinstein, E. (2009). Lateral organization of membrane proteins: tetraspanins spin their web. *Biochem. J.* 420, 133–154. doi: 10.1042/BJ20082422

Chen, K., Xiang, Y., Huang, J., Gong, W., Yoshimura, T., Jiang, Q., et al. (2014). The formylpeptide receptor 2 (Fpr2) and its endogenous ligand cathelin-related antimicrobial peptide (CRAMP) promote dendritic cell maturation. *J. Biol. Chem.* 289, 17553–17563. doi: 10.1074/jbc.M113.535674

Chen, P., Denniston, A. K., Hirani, S., Hannes, S., and Nussenblatt, R. B. (2015). Role of dendritic cell subsets in immunity and their contribution to noninfectious uveitis. *Surv. Ophthalmol.* 60, 242–249. doi: 10.1016/j.survophthal.2015.01.003

Chen, S. C., Vassileva, G., Kinsley, D., Holzmann, S., Manfra, D., Wiekowski, M. T., et al. (2002). Ectopic expression of the murine chemokines CCL21a and CCL21b induces the formation of lymph node-like structures in pancreas, but not skin, of transgenic mice. *J. Immunol.* 168, 1001–1008. doi: 10.4049/jimmunol.168.3.1001

Chen, X., Zeng, Q., and Wu, M. X. (2012). Improved efficacy of dendritic cell-based immunotherapy by cutaneous laser illumination. *Clin. Cancer Res.* 18, 2240–2249. doi: 10.1158/1078-0432.CCR-11-2654

Chu, C. C., Ali, N., Karagiannis, P., Di Meglio, P., Skowera, A., Napolitano, L., et al. (2012). Resident CD141 (BDCA3)$^{+}$ dendritic cells in human skin produce IL-10 and induce regulatory T cells that suppress skin inflammation. *J. Exp. Med.* 209, 935–945. doi: 10.1084/jem.20112583

Cosway, E. J., Ohigashi, I., Schauble, K., Parnell, S. M., Jenkinson, W. E., Luther, S., et al. (2018). Formation of the intrathymic dendritic cell pool requires ccl21-mediated recruitment of ccr7(+) progenitors to the thymus. *J. Immunol.* 201, 516–523. doi: 10.4049/jimmunol.1800348

Crozat, K., Guiton, R., Contreras, V., Feuillet, V., Dutertre, C. A., Ventre, E., et al. (2010). The XC chemokine receptor 1 is a conserved selective marker of mammalian cells homologous to mouse CD8alpha^{+} dendritic cells. *J. Exp. Med.* 207, 1283–1292. doi: 10.1084/jem.20100223

Cumberbatch, M., Dearman, R. J., Groves, R. W., Antonopoulos, C., and Kimber, I. (2002). Differential regulation of epidermal langerhans cell migration by interleukins (IL)-1alpha and IL-1beta during irritant- and allergen-induced cutaneous immune responses. *Toxicol. Appl. Pharmacol.* 182, 126–135. doi: 10.1006/taap.2002.9442

de Chickera, S., Christy, W., Christiane, M., Ronan, F., Paula, F., and Dekaban, G. A. (2011). Cellular MRI as a suitable, sensitive non-invasive modality for correlating in vivo migratory efficiencies of different dendritic cell populations with subsequent immunological outcomes. *Int. Immunol.* 24, 29–41. doi: 10.1093/intimm/dxr095

Del Prete, A., Shao, W. H., Mitola, S., Santoro, G., Sozzani, S., and Haribabu, B. (2006). Regulation of dendritic cell migration and adaptive immune response by leukotriene B4 receptors: a role for LTB4 in up-regulation of CCR7 expression and function. *Blood* 109, 626–631. doi: 10.1182/blood-2006-02-003665

del Rio, M. L., Rodriguez-Barbosa, J. I., Kremmer, E., and Förster, R. (2007). CD103^{-} and CD103^{+} bronchial lymph node dendritic cells are specialized in presenting and cross-presenting innocuous antigen to CD4^{+} and CD8^{+} T cells. *J. Immunol.* 178, 6861–6866. doi: 10.4049/jimmunol.178.11.6861

Demaria, M. C., Yeung, L., Peeters, R., Wee, J. L., Mihaljcic, M., Jones, E. L., et al. (2020). Tetraspanin CD53 promotes lymphocyte recirculation by stabilizing L-Selectin surface expression. *iScience* 23:101104. doi: 10.1016/j.isci.2020.101104

den Haan, J. M., and Bevan, M. J. (2002). Constitutive versus activation-dependent cross-presentation of immune complexes by CD8(+) and CD8(-) dendritic cells in vivo. *J. Exp. Med.* 196, 817–827. doi: 10.1084/jem.20020295

Di Caro, G., Bergomas, F., Grizzi, F., Doni, A., Bianchi, P., Malesci, A., et al. (2014). Occurrence of tertiary lymphoid tissue is associated with T-Cell infiltration and predicts better prognosis in early-stage colorectal cancers. *Clin. Cancer Res.* 20, 2147–2158. doi: 10.1158/1078-0432.CCR-13-2590

Doyle, E. L., Ridger, V., Ferraro, F., Turmaine, M., Saftig, P., and Cutler, D. F. (2011). CD63 is an essential cofactor to leukocyte recruitment by endothelial P-selectin. *Blood* 118, 4265–4273. doi: 10.1182/blood-2010-11-321489

Dzionek, A., Fuchs, A., Schmidt, P., Cremer, S., Zysk, M., Miltenyi, S., et al. (2000). BDCA-2, BDCA-3, and BDCA-4: three markers for distinct subsets of dendritic cells in human peripheral blood. *J. Immunol.* 165, 6037–6046. doi: 10.4049/jimmunol.165.11.6037

Edelson, B. T., Kc, W., Juang, R., Kohyama, M., Benoit, L. A., Klekotka, P. A., et al. (2010). Peripheral CD103^{+} dendritic cells form a unified subset developmentally related to CD8alpha^{+} conventional dendritic cells. *J. Exp. Med.* 207, 823–836. doi: 10.1084/jem.20091627

Elke, S., Ying, M., Legler, D. F., Silke, G., Ladislav, P., Burkhard, L., et al. (2004). CCL19/CCL21-triggered signal transduction and migration of dendritic cells requires prostaglandin E2. *Blood* 103, 1595–1601. doi: 10.1182/blood-2003-05-1643

Esterházy, D., Loschko, J., London, M., Jove, V., Oliveira, T. Y., Mucida, D., et al. (2016). Classical dendritic cells are required for dietary antigen-mediated induction of peripheral T(reg) cells and tolerance. *Nat. Immunol.* 17, 545–555. doi: 10.1038/ni.3408

Farache, J., Koren, I., Milo, I., Gurevich, I., Kim, K. W., Zigmond, E., et al. (2013). Luminal bacteria recruit CD103$^+$ dendritic cells into the intestinal epithelium to sample bacterial antigens for presentation. *Immunity* 38, 581–595. doi: 10.1016/j.immuni.2013.01.009

Farrand, K. J., Dickgreber, N., Stoitzner, P., Ronchese, F., Petersen, T. R., and Hermans, I. F. (2009). Langerin$^+$ CD8alpha$^+$ dendritic cells are critical for cross-priming and IL-12 production in response to systemic antigens. *J. Immunol.* 183, 7732–7742. doi: 10.4049/jimmunol.0902707

Fonseca, D. M. D., Hand, T. W., Han, S., Gerner, M. Y., Zaretsky, A. G., Byrd, A. L., et al. (2015). Microbiota-Dependent sequelae of acute infection compromise tissue-specific immunity. *Cell* 163, 354–366. doi: 10.1016/j.cell.2015.08.030

Forster, R., Davalos-Misslitz, A. C., and Rot, A. (2008). CCR7 and its ligands: balancing immunity and tolerance. *Nat. Rev. Immunol.* 8, 362–371. doi: 10.1038/nri2297

Fossum, E., Grødeland, G., Terhorst, D., Tveita, A. A., Vikse, E., Mjaaland, S., et al. (2015). Vaccine molecules targeting Xcr1 on cross-presenting DCs induce protective CD8$^+$ T-cell responses against influenza virus. *Eur. J. Immunol.* 45, 624–635. doi: 10.1002/eji.201445080

Gao, W., Wang, Y., Bi, J., Chen, X., Li, N., Wang, Y., et al. (2021). Impaired CCR9/CCL25 signalling induced by inefficient dendritic cells contributes to intestinal immune imbalance in nonalcoholic steatohepatitis. *Biochem. Biophys. Res. Commun.* 534, 34–40. doi: 10.1016/j.bbrc.2020.12.007

Gatto, D., Wood, K., and Brink, R. (2011). EBI2 operates independently of but in cooperation with CXCR5 and CCR7 to direct B cell migration and organization in follicles and the germinal center. *J. Immunol.* 187, 4621–4628. doi: 10.4049/jimmunol.1101542

Gatto, D., Wood, K., Caminschi, I., Murphy-Durland, D., Schofield, P., Christ, D., et al. (2013). The chemotactic receptor EBI2 regulates the homeostasis, localization and immunological function of splenic dendritic cells. *Nat. Immunol.* 14, 446–453. doi: 10.1038/ni.2555

GeurtsvanKessel, C. H., Willart, M. A., van Rijt, L. S., Muskens, F., Kool, M., Baas, C., et al. (2008). Clearance of influenza virus from the lung depends on migratory langerin$^+$CD11b$^-$ but not plasmacytoid dendritic cells. *J. Exp. Med.* 205, 1621–1634. doi: 10.1084/jem.20071365

Gianello, V., Salvi, V., Parola, C., Moretto, N., Facchinetti, F., Civelli, M., et al. (2019). The PDE4 inhibitor CHF6001 modulates pro-inflammatory cytokines, chemokines and Th1- and Th17-polarizing cytokines in human dendritic cells. *Biochem. Pharmacol.* 163, 371–380. doi: 10.1016/j.bcp.2019.03.006

Ginhoux, F., Liu, K., Helft, J., Bogunovic, M., Greter, M., Hashimoto, D., et al. (2009). The origin and development of nonlymphoid tissue CD103$^+$ DCs. *J. Exp. Med.* 206, 3115–3130. doi: 10.1084/jem.20091756

González, F. E., Ortiz, C., Reyes, M., Dutzan, N., Patel, V., Pereda, C., et al. (2014). Melanoma cell lysate induces CCR7 expression andin vivo migration to draining lymph nodes of therapeutic human dendritic cells. *Immunology* 142, 396–405. doi: 10.1111/imm.12264

Gouwy, M., De Buck, M., P Rtner, N. M., Opdenakker, G., Proost, P., Struyf, S., et al. (2015). Serum amyloid a chemoattracts immature dendritic cells and indirectly provokes monocyte chemotaxis by induction of cooperating CC and CXC chemokines. *Eur. J. Immunol.* 45, 101–112. doi: 10.1002/eji.201444818

Gouwy, M., Struyf, S., Leutenez, L., Pörtner, N., Sozzani, S., and Van Damme, J. (2013). Chemokines and other GPCR ligands synergize in receptor-mediated migration of monocyte-derived immature and mature dendritic cells. *Immunobiology* 219, 218–229. doi: 10.1016/j.imbio.2013.10.004

Hadeiba, H., Lahl, K., Edalati, A., Oderup, C., Habtezion, A., Pachynski, R., et al. (2012). Plasmacytoid dendritic cells transport peripheral antigens to the thymus to promote central tolerance. *Immunity* 36, 438–450. doi: 10.1016/j.immuni.2012.01.017

Han, Y., Chen, Z., Yang, Y., Jiang, Z., Gu, Y., Liu, Y., et al. (2014). Human CD14$^+$ CTLA-4$^+$ regulatory dendritic cells suppress T-cell response by cytotoxic T-lymphocyte antigen-4-dependent IL-10 and indoleamine-2,3-dioxygenase production in hepatocellular carcinoma. *Hepatology* 59, 567–579. doi: 10.1002/hep.26694

Haniffa, M., Gunawan, M., and Jardine, L. (2015). Human skin dendritic cells in health and disease. *J. Dermatol. Sci.* 77, 85–92. doi: 10.1016/j.jdermsci.2014.08.012

Haniffa, M., Shin, A., Bigley, V., McGovern, N., Teo, P., See, P., et al. (2012). Human tissues contain CD141hi cross-presenting dendritic cells with functional homology to mouse CD103$^+$ nonlymphoid dendritic cells. *Immunity* 37, 60–73. doi: 10.1016/j.immuni.2012.04.012

Hirao, M., Onai, N., Hiroishi, K., Watkins, S. C., Matsushima, K., Robbins, P. D., et al. (2000). CC chemokine receptor-7 on dendritic cells is induced after interaction with apoptotic tumor cells: critical role in migration from the tumor site to draining lymph nodes. *Cancer Res.* 60, 2209–2217. doi: 10.1109/TPAS.1984.318706

Huang, C., Wang, Y., Li, X., Ren, L., Zhao, J., Hu, Y., et al. (2020). Clinical features of patients infected with 2019 novel coronavirus in Wuhan. *China Lancet* 395, 497–506. doi: 10.1016/S0140-6736(20)30183-5

Huysamen, C., Willment, J. A., Dennehy, K. M., and Brown, G. D. (2008). CLEC9A is a novel activation C-type lectin-like receptor expressed on BDCA3$^+$ dendritic cells and a subset of monocytes. *J. Biol. Chem.* 283, 16693–16701. doi: 10.1074/jbc.M709923200

Iberg, C. A., and Hawiger, D. (2020). Natural and induced tolerogenic dendritic cells. *J. Immunol.* 204, 733–744. doi: 10.4049/jimmunol.1901121

Idoyaga, J., and Steinman, R. M. (2011). SnapShot: dendritic cells. *Cell* 146:660. doi: 10.1016/j.cell.2011.08.010

Igyártó, B. Z., Haley, K., Ortner, D., Bobr, A., Gerami-Nejad, M., Edelson, B. T., et al. (2011). Skin-resident murine dendritic cell subsets promote distinct and opposing antigen-specific T helper cell responses. *Immunity* 35, 260–272. doi: 10.1016/j.immuni.2011.06.005

Janela, B., Patel, A. A., Lau, M. C., Goh, C. C., Msallam, R., Kong, W. T., et al. (2019). A subset of Type I conventional dendritic cells controls cutaneous bacterial infections through vegfalpha-mediated recruitment of neutrophils. *Immunity* 50, 1069–1083. doi: 10.1016/j.immuni.2019.03.001

Johnson, L. A., and Jackson, D. G. (2013). The chemokine CX3CL1 promotes trafficking of dendritic cells through inflamed lymphatics. *J. Cell Sci.* 126, 5259–5270. doi: 10.1242/jcs.135343

Rose, C. E. Jr., Lannigan, J. A., Kim, P., Lee, J. J., Fu, S. M., Sung, S. S., et al. (2010). Murine lung eosinophil activation and chemokine production in allergic airway inflammation. *Cell Mol. Immunol.* 7, 361–374. doi: 10.1038/cmi.2010.31

Kabashima, K., Shiraishi, N., Sugita, K., Mori, T., Onoue, A., Kobayashi, M., et al. (2007). CXCL12-CXCR4 engagement is required for migration of cutaneous dendritic cells. *Am. J. Pathol.* 171, 1249–1257. doi: 10.2353/ajpath.2007.070225

Khanna, A., Morelli, A. E., Zhong, C., Takayama, T., Lu, L., and Thomson, A. W. (2000). Effects of liver-derived dendritic cell progenitors on Th1- and Th2-like cytokine responses in vitro and in vivo. *J. Immunol.* 164, 1346–1354. doi: 10.4049/jimmunol.164.3.1346

Kitajima, M., and Ziegler, S. F. (2013). Cutting edge: identification of the thymic stromal lymphopoietin-responsive dendritic cell subset critical for initiation of type 2 contact hypersensitivity. *J. Immunol.* 191, 4903–4907. doi: 10.4049/jimmunol.1302175

Klechevsky, E., Morita, R., Liu, M., Cao, Y., Coquery, S., Thompson-Snipes, L., et al. (2008). Functional specializations of human epidermal Langerhans cells and CD14$^+$ dermal dendritic cells. *Immunity* 29, 497–510. doi: 10.1016/j.immuni.2008.07.013

Laffont, S., Siddiqui, K. R., and Powrie, F. (2010). Intestinal inflammation abrogates the tolerogenic properties of MLN CD103$^+$ dendritic cells. *Eur. J. Immunol.* 40, 1877–1883. doi: 10.1002/eji.200939957

Lee, W. C., Zhong, C., Qian, S., Wan, Y., Gauldie, J., Mi, Z., et al. (1998). Phenotype, function, and in vivo migration and survival of allogeneic dendritic cell progenitors genetically engineered to express TGF-beta. *Transplantation* 66, 1810–1817. doi: 10.1097/00007890-199812270-00040

Leithner, A., Eichner, A., Muller, J., Reversat, A., Brown, M., Schwarz, J., et al. (2016). Diversified actin protrusions promote environmental exploration but are dispensable for locomotion of leukocytes. *Nat. Cell. Biol.* 18, 1253–1259. doi: 10.1038/ncb3426

Lekakis, J., Ikonomidis, I., Papoutsi, Z., Moutsatsou, P., Nikolaou, M., Parissis, J., et al. (2010). Selective serotonin re-uptake inhibitors decrease

the cytokine-induced endothelial adhesion molecule expression, the endothelial adhesiveness to monocytes and the circulating levels of vascular adhesion molecules. *Int. J. Cardiol.* 139, 150–158. doi: 10.1016/j.ijcard.2008.10.010

Leon, B., Ballesteros-Tato, A., Browning, J. L., Dunn, R., Randall, T. D., and Lund, F. E. (2012). Regulation of T(H)2 development by CXCR5$^+$ dendritic cells and lymphotoxin-expressing B cells. *Nat. Immunol.* 13, 681–690. doi: 10.1038/ni.2309

Leventhal, D. S., Gilmore, D. C., Berger, J. M., Nishi, S., Lee, V., Malchow, S., et al. (2016). Dendritic cells coordinate the development and homeostasis of organ-specific regulatory T cells. *Immunity* 44, 847–859. doi: 10.1016/j.immuni.2016.01.025

Lewis, K. L., Caton, M. L., Bogunovic, M., Greter, M., Grajkowska, L. T., Ng, D., et al. (2011). Notch2 receptor signaling controls functional differentiation of dendritic cells in the spleen and intestine. *Immunity* 35, 780–791. doi: 10.1016/j.immuni.2011.08.013

Liu, J., Zhang, X., Chen, K., Cheng, Y., Liu, S., Xia, M., et al. (2019). CCR7 chemokine receptor-inducible lnc-Dpf3 restrains dendritic cell migration by inhibiting HIF-1α-mediated glycolysis. *Immunity* 50, 600–615. doi: 10.1016/j.immuni.2019.01.021

Liu, K., and Nussenzweig, M. C. (2010). Origin and development of dendritic cells. *Immunol. Rev.* 234, 45–54. doi: 10.1111/j.0105-2896.2009.00879.x

Liu, K., Victora, G. D., Schwickert, T. A., Guermonprez, P., Meredith, M. M., Yao, K., et al. (2009). In vivo analysis of dendritic cell development and homeostasis. *Science* 324, 392–397. doi: 10.1126/science.1170540

Lore, K., Sonnerborg, A., Spetz, A. L., Andersson, U., and Andersson, J. (1998). Immunocytochemical detection of cytokines and chemokines in Langerhans cells and in vitro derived dendritic cells. *J. Immunol. Methods* 214, 97–111. doi: 10.1016/s0022-1759(98)00040-4

Lukens, M. V., Kruijsen, D., Coenjaerts, F. E. J., Kimpen, J. L. L., and van Bleek, G. M. (2009). Respiratory syncytial virus-induced activation and migration of respiratory dendritic cells and subsequent antigen presentation in the lung-draining lymph node. *J. Virol.* 83, 7235–7243. doi: 10.1128/JVI.00452-09

Lutz, M. B., and Schuler, G. (2002). Immature, semi-mature and fully mature dendritic cells: which signals induce tolerance or immunity? *Trends Immunol.* 23, 445–449. doi: 10.1016/s1471-4906(02)02281-0

Mackensen, A., Herbst, B., Chen, J. L., Kohler, G., Noppen, C., Herr, W., et al. (2000). Phase I study in melanoma patients of a vaccine with peptide-pulsed dendritic cells generated in vitro from CD34(+) hematopoietic progenitor cells. *Int. J. Cancer* 86, 385–392. doi: 10.1002/(sici)1097-0215(20000501)86:3<385::aid-ijc13<3.0.co;2-t

Majumdar, R., Sixt, M., and Parent, C. A. (2014). New paradigms in the establishment and maintenance of gradients during directed cell migration. *Curr. Opin Cell Biol.* 30, 33–40. doi: 10.1016/j.ceb.2014.05.010

Maldonado-Lopez, R., De Smedt, T., Michel, P., Godfroid, J., Pajak, B., Heirman, C., et al. (1999). CD8alpha$^+$ and CD8alpha$^-$ subclasses of dendritic cells direct the development of distinct T helper cells in vivo. *J. Exp. Med.* 189, 587–592. doi: 10.1084/jem.189.3.587

MartIn-Fontecha, A., Sebastiani, S., Hopken, U. E., Uguccioni, M., Lipp, M., Lanzavecchia, A., et al. (2003). Regulation of dendritic cell migration to the draining lymph node: impact on T lymphocyte traffic and priming. *J. Exp. Med.* 198, 615–621. doi: 10.1084/jem.20030448

Mathan, T. S., Figdor, C. G., and Buschow, S. I. (2013). Human plasmacytoid dendritic cells: from molecules to intercellular communication network. *Front. Immunol.* 4:372. doi: 10.3389/fimmu.2013.00372

McLellan, A. D., Kapp, M., Eggert, A., Linden, C., Bommhardt, U., Brocker, E. B., et al. (2002). Anatomic location and T-cell stimulatory functions of mouse dendritic cell subsets defined by CD4 and CD8 expression. *Blood* 99, 2084–2093. doi: 10.1182/blood.v99.6.2084

Naik, S. H., Metcalf, D., van Nieuwenhuijze, A., Wicks, I., Wu, L., O'Keeffe, M., et al. (2006). Intrasplenic steady-state dendritic cell precursors that are distinct from monocytes. *Nat. Immunol.* 7, 663–671. doi: 10.1038/ni1340

Naik, S. H., Sathe, P., Park, H., Metcalf, D., Proietto, A. I., Dakic, A., et al. (2007). Development of plasmacytoid and conventional dendritic cell subtypes from single precursor cells derived in vitro and in vivo. *Nat. Immunol.* 8, 1217–1226. doi: 10.1038/ni1522

Nitschké, M., Aebischer, D., Abadier, M., Haener, S., Lucic, M., Vigl, B., et al. (2012). Differential requirement for ROCK in dendritic cell migration within lymphatic capillaries in steady-state and inflammation. *Blood* 120, 2249–2258. doi: 10.1182/blood-2012-03-417923

Olga, S., Elin, J., Emma, K. P., Xiaosun, L., Tim, W., William, A. W., et al. (2009). Intestinal CD103$^+$, but not CX3CR1$^+$, antigen sampling cells migrate in lymph and serve classical dendritic cell functions. *J. Exp. Med.* 206, 3101–3114. doi: 10.1084/jem.20091925

Pang, I. K., Ichinohe, T., and Iwasaki, A. (2013). IL-1R signaling in dendritic cells replaces pattern recognition receptors to promote CD8$^+$ T cell responses to influenza A virus. *Nat. Immunol.* 14, 246–253. doi: 10.1038/ni.2514

Park, M. J., Park, K. S., Park, H. S., Cho, M. L., Hwang, S. Y., Min, S. Y., et al. (2012). A distinct tolerogenic subset of splenic IDO(+)CD11b(+) dendritic cells from orally tolerized mice is responsible for induction of systemic immune tolerance and suppression of collagen-induced arthritis. *Cell Immunol.* 278, 45–54. doi: 10.1016/j.cellimm.2012.06.009

Pendl, G. G., Robert, C., Steinert, M., Thanos, R., Eytner, R., Borges, E., et al. (2002). Immature mouse dendritic cells enter inflamed tissue, a process that requires E- and P-selectin, but not P-selectin glycoprotein ligand 1. *Blood* 99:946. doi: 10.1182/blood.v99.3.946

Penna, G., Sozzani, S., and Adorini, L. (2001). Cutting edge: selective usage of chemokine receptors by plasmacytoid dendritic cells. *J. Immunol.* 167, 1862–1866. doi: 10.4049/jimmunol.167.4.1862

Persson, E. K., Uronen-Hansson, H., Semmrich, M., Rivollier, A., Hagerbrand, K., Marsal, J., et al. (2013). IRF4 transcription-factor-dependent CD103(+)CD11b(+) dendritic cells drive mucosal T helper 17 cell differentiation. *Immunity* 38, 958–969. doi: 10.1016/j.immuni.2013.03.009

Plantinga, M., Guilliams, M., Vanheerswynghels, M., Deswarte, K., Branco-Madeira, F., Toussaint, W., et al. (2013). Conventional and monocyte-derived CD11b(+) dendritic cells initiate and maintain T helper 2 cell-mediated immunity to house dust mite allergen. *Immunity* 38, 322–335. doi: 10.1016/j.immuni.2012.10.016

Proietto, A. I., van Dommelen, S., Zhou, P., Rizzitelli, A., D'Amico, A., Steptoe, R. J., et al. (2008). Dendritic cells in the thymus contribute to T-Regulatory cell induction. *Proc. Natl. Acad. Sci. U.S.A.* 105, 19869–19874. doi: 10.1073/pnas.0810268105

Qian, C., and Cao, X. (2018). Dendritic cells in the regulation of immunity and inflammation. *Semin. Immunol.* 35, 3–11. doi: 10.1016/j.smim.2017.12.002

Qu, X., Mei-Xiang, Y., Bei-Hua, K., Lan, Q., Queenie Lai, K. L., Shi, Y., et al. (2005). Hypoxia inhibits the migratory capacity of human monocyte-derived dendritic cells. *Immunol. Cell Bio.* 83, 668–673. doi: 10.1111/j.1440-1711.2005.01383.x

Randolph, G. J., Sanchez-Schmitz, G., and Angeli, V. (2004). Factors and signals that govern the migration of dendritic cells via lymphatics: recent advances. *Springer Semin. Immunopathol.* 26, 273–287. doi: 10.1007/s00281-004-0168-0

Rivellese, F., and Prediletto, E. (2020). ACE2 at the centre of COVID-19 from paucisymptomatic infections to severe pneumonia. *Autoimmun. Rev.* 19:102536. doi: 10.1016/j.autrev.2020.102536

Schlitzer, A., Loschko, J., Mair, K., Vogelmann, R., and Krug, A. (2011). Identification of CCR9- murine plasmacytoid DC precursors with plasticity to differentiate into conventional DCs. *Blood* 117, 6562–6570. doi: 10.1182/blood-2010-12-326678

Sharma, P., Levy, O., and Dowling, D. J. (2020). The TLR5 agonist flagellin shapes phenotypical and functional activation of lung mucosal antigen presenting cells in neonatal mice. *Front. Immunol.* 11:171. doi: 10.3389/fimmu.2020.00171

Silvin, A., Yu, C. I., Lahaye, X., Imperatore, F., and Manel, N. (2017). Constitutive resistance to viral infection in human CD141$^+$ dendritic cells. *Sci. Immunol.* 2:aai8071. doi: 10.1126/sciimmunol.aai8071

Sisirak, V., Vey, N., Vanbervliet, B., Duhen, T., Puisieux, I., Homey, B., et al. (2011). CCR6/CCR10-mediated plasmacytoid dendritic cell recruitment to inflamed epithelia after instruction in lymphoid tissues. *Blood* 118, 5130–5140. doi: 10.1182/blood-2010-07-295626

Sokol, C. L., Camire, R. B., Jones, M. C., and Luster, A. D. (2018). The chemokine receptor CCR8 promotes the migration of Dendritic Cells into the Lymph Node Parenchyma to initiate the allergic immune response. *Immunity* 49, 449–463. doi: 10.1016/j.immuni.2018.07.012

Soudja, S. M., Henri, S., Mello, M., Chasson, L., Mas, A., Wehbe, M., et al. (2011). Disrupted lymph node and splenic stroma in mice with induced inflammatory melanomas is associated with impaired recruitment of T and dendritic cells. *PLoS One* 6:e22639. doi: 10.1371/journal.pone.0022639

Springer, T. A. (1994). Traffic signals for lymphocyte recirculation and leukocyte emigration: the multistep paradigm. *Cell* 76, 301–314. doi: 10.1016/0092-8674(94)90337-9

Steinman, R. M., and Cohn, Z. A. (1973). Identification of a novel cell type in peripheral lymphoid organs of mice. I. morphology, quantitation, tissue distribution. *J. Exp. Med.* 137, 1142–1162. doi: 10.1084/jem.137.5.1142

Suraneni, P., Fogelson, B., Rubinstein, B., Noguera, P., Volkmann, N., Hanein, D., et al. (2015). A mechanism of leading-edge protrusion in the absence of Arp2/3 complex. *Mol. Biol. Cell* 26, 901–912. doi: 10.1091/mbc.E14-07-1250

Swiecki, M., Gilfillan, S., Vermi, W., Wang, Y., and Colonna, M. (2010). Plasmacytoid dendritic cell ablation impacts early interferon responses and antiviral NK and CD8(+) T cell accrual. *Immunity* 33, 955–966. doi: 10.1016/j.immuni.2010.11.020

Tamoutounour, S., Guilliams, M., Montanana, S. F., Liu, H., Terhorst, D., Malosse, C., et al. (2013). Origins and functional specialization of macrophages and of conventional and monocyte-derived dendritic cells in mouse skin. *Immunity* 39, 925–938. doi: 10.1016/j.immuni.2013.10.004

Tang, D. D., and Gerlach, B. D. (2017). The roles and regulation of the actin cytoskeleton, intermediate filaments and microtubules in smooth muscle cell migration. *Respir Res.* 18, 54. doi: 10.1186/s12931-017-0544-7

Tedder, T. F., Steeber, D. A., Chen, A., and Engel, P. (1995). The selectins: vascular adhesion molecules. *FASEB J.* 9, 866–873. doi: 10.1006/excr.1995.1233

Tiberio, L., Del Prete, A., Schioppa, T., Sozio, F., Bosisio, D., and Sozzani, S. (2018). Chemokine and chemotactic signals in dendritic cell migration. *Cell Mol. Immunol.* 15, 346–352. doi: 10.1038/s41423-018-0005-3

Tomohisa, B., Yasunari, N., and Naofumi, M. (2009). Crucial contribution of thymic Sirp alpha^{+} conventional dendritic cells to central tolerance against blood-borne antigens in a CCR2-dependent manner. *J. Immunol.* 183, 3053–3063. doi: 10.4049/jimmunol.0900438

Tomura, M., Hata, A., Matsuoka, S., Shand, F. H., Nakanishi, Y., Ikebuchi, R., et al. (2014). Tracking and quantification of dendritic cell migration and antigen trafficking between the skin and lymph nodes. *Sci. Rep.* 4:6030. doi: 10.1038/srep06030

Tussiwand, R., Everts, B., Grajales-Reyes, G. E., Kretzer, N. M., Iwata, A., Bagaitkar, J., et al. (2015). Klf4 expression in conventional dendritic cells is required for T helper 2 cell responses. *Immunity* 42, 916–928. doi: 10.1016/j.immuni.2015.04.017

Ulvmar, M. H., Werth, K., Braun, A., Kelay, P., Hub, E., Eller, K., et al. (2014). The atypical chemokine receptor CCRL1 shapes functional CCL21 gradients in lymph nodes. *Nat. Immunol.* 15, 623–630. doi: 10.1038/ni.2889

Vandenabeele, S., Hochrein, H., Mavaddat, N., Winkel, K., and Shortman, K. (2001). Human thymus contains 2 distinct dendritic cell populations. *Blood* 97, 1733–1741. doi: 10.1182/blood.v97.6.1733

Vargas, P., Maiuri, P., Bretou, M., Saez, P. J., Pierobon, P., Maurin, M., et al. (2016). Innate control of actin nucleation determines two distinct migration behaviours in dendritic cells. *Nat. Cell Biol.* 18, 43–53. doi: 10.1038/ncb3284

Vermi, W., Riboldi, E., Wittamer, V., Gentili, F., Luini, W., Marrelli, S., et al. (2005). Role of ChemR23 in directing the migration of myeloid and plasmacytoid dendritic cells to lymphoid organs and inflamed skin. *J. Exp. Med.* 201, 509–515. doi: 10.1084/jem.20041310

Villablanca, E. J., and Mora, J. R. (2008). A two-step model for Langerhans cell migration to skin-draining LN. *Eur. J. Immunol.* 38, 2975–2980. doi: 10.1002/eji.200838919

Villani, A. C., Satija, R., Reynolds, G., Sarkizova, S., Shekhar, K., Fletcher, J., et al. (2017). Single-cell RNA-seq reveals new types of human blood dendritic cells, monocytes, and progenitors. *Science* 356:eaah4573. doi: 10.1126/science.aah4573

Wang, T., Li, W., Cheng, H., Zhong, L., Deng, J., and Ling, S. (2019). The important role of the chemokine axis CCR7-CCL19 and CCR7-CCL21 in the Pathophysiology of the Immuno-inflammatory response in Dry Eye Disease. *Ocul. Immunol. Inflamm. [Online ahead of print]* 1–12. doi: 10.1080/09273948.2019.1674891

Weber, M., Hauschild, R., Schwarz, J., Moussion, C., de Vries, I., Legler, D., et al. (2013). Interstitial dendritic cell guidance by haptotactic chemokine gradients. *Science* 339, 328–332.

Wendland, M., Czeloth, N., Mach, N., Malissen, B., Kremmer, E., Pabst, O., et al. (2007). CCR9 is a homing receptor for plasmacytoid dendritic cells to the small intestine. *Proc. Natl. Acad. Sci. U.S.A.* 104, 6347–6352. doi: 10.1073/pnas.0609180104

Wong, J. L., Muthuswamy, R., Bartlett, D. L., and Kalinski, P. (2014). IL-18-based combinatorial adjuvants promote the intranodal production of CCL19 by NK cells and dendritic cells of cancer patients. *OncoImmunology* 2:e26245. doi: 10.4161/onci.26245

Xiqin, Y., Keke, L., Tingting, M., Xuan, L., Jing, M., Yanan, T., et al. (2018). Immune adjuvant targeting micelles allow efficient dendritic cell migration to lymph nodes for enhanced cellular immunity. *ACS Appl. Mater. Interfaces* 10, 33532–33544. doi: 10.1021/acsami.8b10081

Xu, H., Zhong, L., Deng, J., Peng, J., Dan, H., Zeng, X., et al. (2020). High expression of ACE2 receptor of 2019-nCoV on the epithelial cells of oral mucosa. *Int. J. Oral Sci.* 12, 77–81. doi: 10.1038/s41368-020-0074-x

Yanagihara, S., Komura, E., Nagafune, J., Watarai, H., and Yamaguchi, Y. (1998). EBI1/CCR7 is a new member of dendritic cell chemokine receptor that is up-regulated upon maturation. *J. Immunol.* 161, 3096–3102.

Yashiro, T., Takeuchi, H., Nakamura, S., Tanabe, A., Hara, M., Uchida, K., et al. (2019). PU.1 plays a pivotal role in dendritic cell migration from the periphery to secondary lymphoid organs *via* regulating CCR7 expression. *FASEB J.* 33:11481. doi: 10.1096/fj.201900379RR

Yu, N., Wang, S., Song, X., Gao, L., Li, W., Yu, H., et al. (2018). Low-Dose radiation promotes Dendritic Cell Migration and IL-12 Production via the ATM/NF-KappaB Pathway. *Radiat. Res.* 189:409. doi: 10.1667/RR14840.1

Zabel, B. A., Silverio, A. M., and Butcher, E. C. (2005). Chemokine-like receptor 1 expression and chemerin-directed chemotaxis distinguish plasmacytoid from myeloid dendritic cells in human blood. *J. Immunol.* 174, 244–251. doi: 10.4049/jimmunol.174.1.244

Zigmond, E., Varol, C., Farache, J., Elmaliah, E., Satpathy, A. T., Friedlander, G., et al. (2012). Ly6Chi monocytes in the inflamed colon give rise to proinflammatory effector cells and migratory antigen-presenting cells. *Immunity* 37, 1076–1090. doi: 10.1016/j.immuni.2012.08.026

Conflict of Interest: The authors declare that the research was conducted in the absence of any commercial or financial relationships that could be construed as a potential conflict of interest.

frontiers in Cell and Developmental Biology

REVIEW
published: 22 February 2021
doi: 10.3389/fcell.2021.624184

Dysregulation of Leukocyte Trafficking in Type 2 Diabetes: Mechanisms and Potential Therapeutic Avenues

*Laleh Pezhman[1], Abd Tahrani[2,3,4] and Myriam Chimen[1]**

[1] Institute of Inflammation and Ageing, College of Medical and Dental Sciences, University of Birmingham, Birmingham, United Kingdom, [2] Institute of Metabolism and Systems Research, University of Birmingham, Birmingham, United Kingdom, [3] Centre for Endocrinology, Diabetes and Metabolism, Birmingham Health Partners, Birmingham, United Kingdom, [4] University Hospitals Birmingham NHS Foundation Trust, Birmingham, United Kingdom

OPEN ACCESS

Edited by:
Hao Sun, University of California, San Diego, United States

Reviewed by:
ChangDong Lin, Center for Excellence in Molecular Cell Science, Shanghai Institute of Biochemistry and Cell Biology, Chinese Academy of Sciences, China
Sirpa Jalkanen, University of Turku, Finland
Eroboghene Ubogu, University of Alabama at Birmingham, United States

***Correspondence:**
Myriam Chimen
m.chimen@bham.ac.uk; chimenm@bham.ac.uk

Specialty section:
This article was submitted to Cell Adhesion and Migration, a section of the journal Frontiers in Cell and Developmental Biology

Received: *30 October 2020*
Accepted: *04 February 2021*
Published: *22 February 2021*

Citation:
Pezhman L, Tahrani A and Chimen M (2021) Dysregulation of Leukocyte Trafficking in Type 2 Diabetes: Mechanisms and Potential Therapeutic Avenues. Front. Cell Dev. Biol. 9:624184. doi: 10.3389/fcell.2021.624184

Type 2 Diabetes Mellitus (T2DM) is a chronic inflammatory disorder that is characterized by chronic hyperglycemia and impaired insulin signaling which in addition to be caused by common metabolic dysregulations, have also been associated to changes in various immune cell number, function and activation phenotype. Obesity plays a central role in the development of T2DM. The inflammation originating from obese adipose tissue develops systemically and contributes to insulin resistance, beta cell dysfunction and hyperglycemia. Hyperglycemia can also contribute to chronic, low-grade inflammation resulting in compromised immune function. In this review, we explore how the trafficking of innate and adaptive immune cells under inflammatory condition is dysregulated in T2DM. We particularly highlight the obesity-related accumulation of leukocytes in the adipose tissue leading to insulin resistance and beta-cell dysfunction and resulting in hyperglycemia and consequent changes of adhesion and migratory behavior of leukocytes in different vascular beds. Thus, here we discuss how potential therapeutic targeting of leukocyte trafficking could be an efficient way to control inflammation as well as diabetes and its vascular complications.

Keywords: therapies, inflammation, type 2 diabetes, obesity, trafficking, leukocyte

INTRODUCTION

Inflammation is a protective response against harmful stimuli such as injuries, infections and toxins, which requires the trafficking of leukocytes from the blood stream to the site of inflammation within damaged tissues. This process is critical for elimination of harmful stimuli and for tissue repair and is tightly regulated by a variety of mediators such as cell adhesion molecules, cytokines and chemokines (Wright and Cooper, 2014). Leukocyte behavior and their recruitment to tissues is modified under inflammatory conditions such as in Type 2 diabetes (T2DM) (Wu et al., 2011). T2DM is a chronic inflammatory disorder characterized by hyperglycemia and impaired insulin signaling and production (Calle and Fernandez, 2012). Components of the immune system are altered in T2DM, with the most apparent changes occurring in the adipose tissue, the pancreatic islets, the vasculature and in circulating leukocytes (Donath and Shoelson, 2011; Mraz and Haluzik, 2014; Eguchi and Nagai, 2017). Indeed, cellular stresses, such as oxidative stress and

lipotoxicity cause insulin resistance and pancreatic islets dysfunction, can induce an inflammatory response and also be exacerbated by local inflammation. Patients with T2D have elevated levels of inflammatory cytokines (such as IL-1β and IL-6) and chemokines (such as CCL2, CXCL8) (Donath and Shoelson, 2011). This rise in inflammatory mediators completely modifies leukocyte behavior and recruitment into tissues, which in turn contributes to maintenance of insulin resistance, loss of insulin secretion and accelerates development of micro and macro-vascular complications (Wu et al., 2011). Clinical studies show that targeting inflammation using small molecules or biological agents to turn off pro-inflammatory cytokines, deplete immune cells or block regulatory surface receptors, results in improved blood glucose levels and insulin sensitivity (Larsen et al., 2007; Donath and Shoelson, 2011). Obesity, particularly visceral adiposity, is a major risk factor for T2DM (Donath and Shoelson, 2011) and the adipose tissue of patients with T2DM and/or obese patients appears to be a major site of inflammation (Lontchi-Yimagou et al., 2013). Both innate and adaptive immune cells present in the adipose tissue have critical roles in the regulation of metabolic homeostasis. Dysregulated trafficking of leukocytes is observed in the adipose tissue and is associated with a shift in cell populations from an anti-inflammatory to a pro-inflammatory profile in obesity (Esser et al., 2014). This switch to a production of pro-inflammatory cytokines leads to the development of systemic low-grade inflammation, which results in impaired insulin signaling, beta-cell dysfunction and subsequent insulin resistance (Esser et al., 2014). Hyperglycemia rises as the pancreas fails to compensate insulin resistance (Donath and Shoelson, 2011). Hyperglycemia then leads to oxidative stress and induces systemic inflammation by stimulating the production of inflammatory cytokines (Noshita et al., 2002; Dimayuga et al., 2007) and chemokines, resulting in endothelial dysfunction (Nguyen et al., 2012). This review will summarize how T2DM-related changes in the expression of adhesion molecules and chemokine receptors/ligands drive endothelial dysfunction and dysregulates leukocyte trafficking under inflammatory conditions which ultimately leads to diabetic complications (**Figure 1**).

THE MOLECULAR PROCESSES OF LEUKOCYTE RECRUITMENT IN INFLAMMATION

Recruitment of leukocytes is triggered by the local release of inflammatory mediators such as histamine, tumor necrosis factor-alpha (TNFα) and interferon-gamma (IFNγ) in inflamed tissue (Liu et al., 2004; Zhang et al., 2011; Muller, 2013). These mediators induce the expression of specific adhesion receptors such as selectins, adhesion molecules and chemokines, which are expressed or presented at the surface of endothelial cells (ECs) and bind to integrins or chemokine receptors located at the surface of leukocytes (Zhang et al., 2011). Selectins interaction with their ligands results in leukocyte tethering and rolling from rapidly flowing blood (Kansas, 1996; Harjunpää et al., 2019). Selectins are transmembrane calcium-dependent lectins that consist of three functionally different adhesion molecules expressed by ECs (E-selectin), platelets and ECs (P-selectin) and leukocytes (L-selectin) (McEver, 2015). L-selectin and P-selectin mediate fast rolling of leukocyte through sequential interactions with their ligands. However, slow rolling events are mediated by E-selectin on ECs binding to E-selectin ligand-1 (ESL-1) or P-selectin glycoprotein ligand 1 (PSGL-1) on leukocytes (Yago et al., 2010). Leukocyte arrest and migration on the endothelium depends on chemokines (Luu et al., 2000). The shift from fast rolling to slow rolling allows G-protein-coupled receptors (GPCRs) on leukocytes to bind to the chemokines expressed on the surface of ECs, which induces leukocyte integrin activation and enables leukocyte firm adhesion to the vessel wall (Giagulli et al., 2004; Rutledge and Muller, 2020). Integrins are a family of transmembrane receptors expressed by leukocytes. Both $\alpha_4\beta_1$ integrin or very late antigen-4 (VLA-4) and $\alpha_M\beta_2$ integrin or lymphocyte function-associated antigen-1 (LFA-1) have been found to play a role in leukocyte arrest (Uotila et al., 2014). $\alpha_M\beta_2$ is expressed on leukocytes as a resting low affinity state. Conformational changes are required for integrins to switch from a low affinity state to an active high affinity state enabling them to bind to their ligands expressed on the endothelium (Kim et al., 2003; Ley et al., 2007; Fan and Ley, 2015). The activation of integrins is mediated by chemokines and results in integrin extension and changes in the cytoskeleton of leukocytes, enabling tight adhesion on the vessel wall (Rutledge and Muller, 2020). LFA-1 and VLA-4 on leukocytes, bind to their respective ligand ICAM-1 and VCAM-1 on ECs, mediate leukocyte adhesion (Hyduk et al., 2007; Kuwano et al., 2010) and induce intracellular signals to allow leukocyte arrest (Giagulli et al., 2006; Kummer and Ebnet, 2018). Leukocytes then extend lamellipodia and prepare for transendothelial migration (Rutledge and Muller, 2020). Additional downstream signals such as prostaglandin-D2 (PGD2) signals are required for shape change and dynamic transmigration of activated leukocytes (Ahmed et al., 2011). Macrophage integrin-1 (Mac-1) or CD11b/CD18, also known as $\alpha_M\beta_2$, interaction with ICAM-1 expressed by the inflamed endothelium is required for the transition of leukocytes from tight adhesion to crawling along the vessel wall (leukocyte locomotion) to then find a suitable site for transendothelial migration (Schenkel et al., 2004). Leukocytes either transmigrate (diapedesis) through the endothelial junctions (paracellular route), or through the body of the ECs (transcellular route) (Ley et al., 2007). In the paracellular route, the distribution of junctional molecules is modified in inflamed ECs in a way that facilitates transendothelial cell migration (Shaw et al., 2001). Junctional molecules such as platelet/endothelial-cell adhesion molecule 1 (PECAM-1) and junctional adhesion molecule A (JAM-A) may support leukocyte migration through mobilizing to the luminal surface where they can bind to their ligands expressed on leukocytes and guide them to the junctions (Muller, 2003). JAM-A interaction with $\alpha_L\beta_2$ allows strong adhesion of activated leukocyte to the endothelium (Kummer and Ebnet, 2018). PECAM-1 is expressed at EC junctions and leukocytes (Newman et al., 1990). When leukocytes reach the site of transmigration, the homophilic interactions between PECAM-1 on leukocytes with PECAM-1 on the endothelium causes a transient increase in cytosolic calcium in ECs which guide

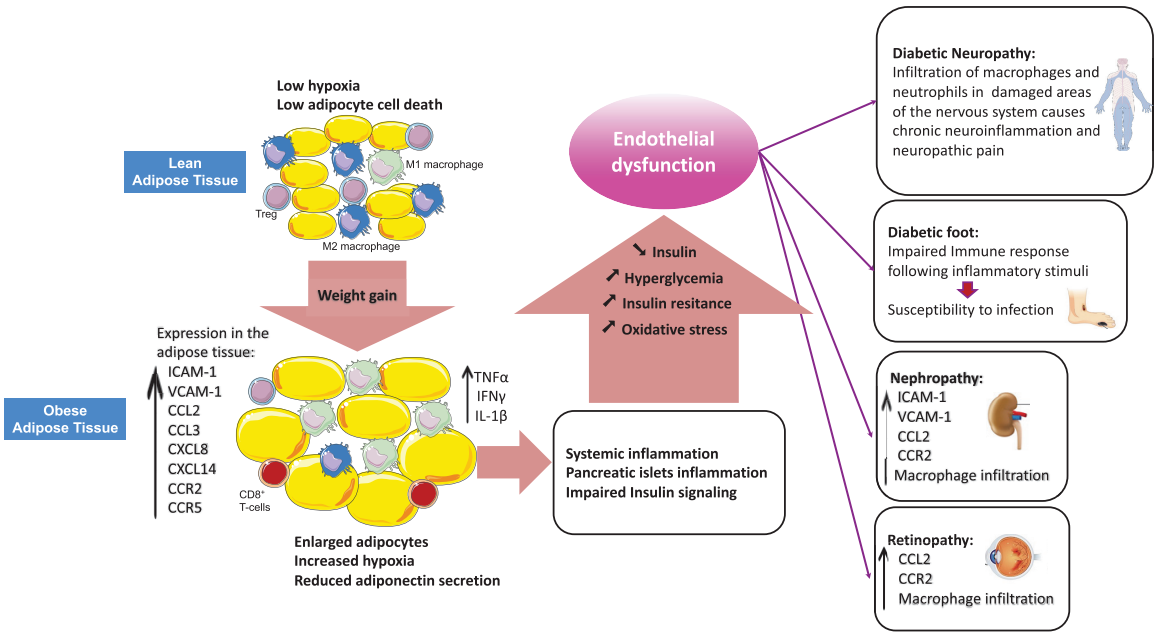

FIGURE 1 | Obesity-related dysregulation of leukocyte trafficking in T2DM. Adipose tissue from lean individuals is characterized by increased numbers of anti-inflammatory M2 macrophages and higher presence of regulatory T-cells (Tregs). Obesity induces adipose tissue enrichment of cytotoxic $CD8^+$ T-cells and pro-inflammatory M1 macrophages with a shift from an anti-inflammatory to a pro-inflammatory state. In obesity, the imbalance among leukocytes results in production of inflammatory cytokines (TNFα, IFNγ, IL-1β) and chemokines which promote systemic inflammation and peripheral insulin resistance as well as beta-cell dysfunction. Hyperglycemia occurs as a result of beta-cells failure to compensate for insulin resistance. Hyperglycemia exacerbates systemic inflammation by inducing pro-inflammatory cytokines production and modulating leukocyte trafficking through alteration of the expression of adhesion molecules, chemokines and chemokine receptors in different vascular beds, which ultimately results in vascular complications.

the leukocytes to the junctions (Ley, 2007; Muller, 2011). Like PECAM-1, CD99 (Schenkel et al., 2002) and CD99L2, expressed at EC junctions and on leukocytes, rely on a homophilic interactions to promote leukocyte extravasation (Schenkel et al., 2002; Seelige et al., 2013; Rutledge et al., 2015). In ECs, the major functional component of the adherent junction is VE-cadherin. During transendothelial migration, there is a transient gap in VE-cadherin at the site of the transmigrating leukocytes, which facilitates transmigration (Dejana and Giampietro, 2012). This gap has been shown to be triggered by constitutive shedding of VE-cadherin by ADAM-10, which is promoted by Tspan5 and Tspan17 and therefore allows T-cell diapedesis (Reyat et al., 2017).

Transcellular leukocyte migration only occurs for a minority of emigrating cells and mostly takes place in thin parts of the endothelium (Carman and Springer, 2004). In this route, leukocyte migration occurs through membrane-associated channels, which act as a gateway for leukocytes through the body of ECs. In fact, the preferred route of leukocyte transmigration depends on the leukocyte type and also the type of vascular bed (Dvorak and Feng, 2001). The endothelium is heterogeneous in different vascular beds, depending on the size and the organ considered (Aird, 2007). ECs in the arterioles of the vascular system have lower permeability to leukocytes, whereas those in the venules are thinner and permissive allowing leukocytes to easily transmigrate particularly in postcapillary venules (Dejana et al., 2009). In addition, the endothelial barrier can be even more permissive such as in lymphoid organs (Miyasaka and Tanaka, 2004), or very tight such as in the central nervous system (Wolburg and Lippoldt, 2002).

To reach inflamed tissues, leukocytes need to migrate through the basement membrane. The basement membrane is made up of laminin and collagen type IV (Mutgan et al., 2020). In murine models, leukocytes cross the basement membrane at areas with low expression of laminin (Song et al., 2017). PECAM-1, CD99, and CD99L2 are required for homophilic interactions between leukocyte and ECs to initiate the migration through the basement membrane (Thompson et al., 2001; Bixel et al., 2010; Sullivan et al., 2016). Leukocytes express several membrane-type matrix metalloproteinases (MMP) including the secreted- and membrane-anchored MT-MMPs, which develop an appropriate proteolytic reaction (Marco et al., 2013) and enable cells to cross this structural barrier. However, the exact mechanisms still remain to be fully characterized. Finally, following a successful diapedesis, leukocytes utilize a chemokine gradient to migrate toward the site of infection upon their entry into inflamed tissues (Ley et al., 2007).

EXPRESSION OF ADHESION MOLECULES IN T2DM

Cell adhesion molecules (CAMs) are glycoproteins expressed on the surface of various cell types such as ECs and leukocytes

(Galkina and Ley, 2007). Upon inflammation, vascular ECs express or up-regulate the expression of CAMs that increase the attachment of leukocytes to the endothelium (Cook-Mills et al., 2011). Selectins, ICAM-1 and VCAM-1 are the major CAMs responsible for leukocyte adhesion (Huo and Ley, 2001). Soluble form of CAMs (sCAMs) in the circulation indirectly reflect the rate of endothelial expression and activation of CAMs since they are shed from the surface of ECs and lymphocytes after being activated (Abe et al., 1998). Elevated expression and activity of CAMs are therefore indicative of inflammation and endothelial dysfunction (Cook-Mills et al., 2011).

Soluble CAMs and Selectins

The baseline levels of circulating E-selectin, ICAM-1, and VCAM-1 were found higher in patients with T2DM compared to healthy controls (Meigs et al., 2004). A study on 150 Japanese patients with T2DM showed that higher serum concentrations of sVCAM-1 and sE-selectin were positively correlated with fasting plasma glucose levels, and negatively correlated with insulin sensitivity (Matsumoto et al., 2002). Higher levels of circulating CAMs in T2DM is linked to an increased production of advanced glycosylation end products (AGEs) and oxidative stress occurring under hyperglycemic conditions (Hadi and Al Suwaidi, 2007). The interaction of AGEs with the vessel wall components increases the generation of reactive oxygen species, which results in an increase in the surface expression of CAMs on activated ECs (Wen et al., 2002; Basta et al., 2004; Farhangkhoee et al., 2006).

Hyperinsulinemia can also directly affect the surface expression of adhesion molecules on ECs from healthy volunteers and from patients with non-insulin-dependent diabetes *in vitro* (Okouchi et al., 2002). Culture of ECs in insulin-rich medium (over 50 microUnit/ml) for 24 h increased the surface expression of PECAM-1 but not of ICAM-1, P-selectin or E-selectin (Okouchi et al., 2002). This was clearly associated with an increase in neutrophil adhesion therefore suggesting that high insulin conditions promote vascular injury and therefore T2DM-associated macro- and micro-vascular complications.

However, a recent study on 58 patients with T2DM on insulin therapy and displaying microvascular complications found lower levels of serum sICAM-1 in these patients irrespective of the type of diabetic complication when compared to age-matched healthy controls (Hocaoglu-Emre et al., 2017). Since the participants with T2DM were also receiving angiotensin-converting enzyme (ACE)-inhibitor agents, decreased levels of sICAM-1 might have resulted from the combination of insulin and ACE-inhibitor therapies. Indeed, both insulin and ACE inhibitors can individually inhibit CAMs surface expression on ECs as well as their circulating levels (Drexler et al., 1995; Aljada et al., 2000). However much remain to be clarified in this area as the effect of both insulin and ACE inhibitors seems to vary in different patient cohorts. Some studies have hypothesized that these discrepancies between cohorts are linked to the degree of complications and the bigger impact seems to occur in late-stage diabetic complications when other treatments such as ACE-inhibitors are used. The conflicting evidence about the levels of sCAMs in the circulation suggests that different CAMs may play different roles in the different stages of vascular complications in T2DM (Hocaoglu-Emre et al., 2017).

Surface Expression of CAMs on the Endothelium

Variations in the expression of adhesion molecules on the vasculature play a role in microangiopathy in patients with T2DM by enhancing leukocyte adhesion in the vasculature and causing capillary obstruction (McLeod et al., 1995). This has been observed in different vascular beds and is linked to a majority of complications such as diabetic nephropathy (Gu et al., 2013) and retinopathy (McLeod et al., 1995). A study on 40 patients with T2DM showed a significant increase in the expression of ICAM-1 and VCAM-1 on vascular ECs from the conjunctiva in comparison with conjunctiva from healthy controls (Khalfaoui et al., 2008). Confocal microscopy imaging of retina vessels in streptozotocin (STZ)-induced hyperglycemic mice reported increased VCAM-1 protein levels after 8 weeks, and this was synchronized with the expression of the inflammatory cytokines TNFα, IL-6 and interleukin 1 beta (IL-1β) in the retina (Gustavsson et al., 2010). However, not many studies have performed in depth study of leukocyte recruitment in patients and in mice models to show that defects in leukocyte recruitment could mean leukocyte trafficking is impaired despite upregulation of endothelial CAMs.

Vascular adhesion protein-1 (VAP-1) is an enzyme and an adhesion molecule mainly expressed by ECs, smooth muscle, and the adipose tissue (Kuo et al., 2019). Endothelial VAP-1 supports leukocyte rolling, firm adhesion, and transmigration (Salmi and Jalkanen, 2019). The catalytic activity of VAP-1 can be damaging and cytotoxic to ECs via the generation of AGEs, which are involved in the pathogenesis of diabetic complications such as retinopathy, nephropathy, neuropathy, and atherosclerosis (Stolen et al., 2004).

Vascular adhesion protein-1 expressed on the vessels in the pancreatic islet of Non-Obese Diabetic (NOD) mice (model of T1DM) was associated with high degree of lymphocyte infiltration into the islets (Bono et al., 1999). Invalidation of the gene encoding VAP-1, using a null mutation in the amine oxidase copper-containing-3 (AOC3), decreased infiltration of T-cells, macrophages and NK cells in both epididymal and inguinal white adipose tissue of AOC3-KO mice compared to age-matched wild-type controls. This reduction in leukocyte infiltration was associated to a reduced capacity of leukocyte extravasation normally enabled via VAP-1 (Jargaud et al., 2020). Serum VAP-1 levels are higher in patients with T2DM and in patients with chronic kidney disease, which makes serum VAP-1, a good predictor of end-stage renal disease in diabetic patients and a useful biomarker to improve risk stratification of patients with T2DM (Li et al., 2016). Many *in vivo* studies further validate the role of VAP-1 as an anti-inflammatory target (Xu et al., 2006; Foot et al., 2013; Carpéné et al., 2019). Indeed, administration of a long-lasting VAP-1 and 2 inhibitor, PXS-4681A, in a mouse model of LPS-induced lung inflammation attenuated neutrophil migration into the lungs (Foot et al., 2013). PXS-4681A is a promising drug candidate as it ensures

complete and long-lasting inhibition of the enzymes after a single low dose *in vivo* and could also be tested in other models of chronic inflammation.

Surface Expression of CAMs on Leukocytes

Leukocyte adhesion to the endothelium is mediated by surface integrins expressed on leukocytes such as macrophage integrin-1 (Mac-1) or CD11b/CD18, also known as $\alpha_M\beta_2$ (Carlos and Harlan, 1994). In a study comparing patients with T2DM to age-matched healthy controls, basal expression of CD11b on monocytes and neutrophils did not differ between the groups (Sampson et al., 2002). However, higher expression of CD11b was observed on monocytes after a glucose load in both T2DM and control groups. This suggests, an association between hyperglycemia and monocyte-endothelial interactions through increased expression of monocytic CD11b (Sampson et al., 2002). Higher expression of CD11b in both diabetic and control groups after a glucose load could be due to the translocation of stored CD11b to the cell surface in response to any acute or sudden change in glucose levels regardless of basal plasma glucose (Sampson et al., 2002). However, another group later found higher monocyte expression of CD11b at baseline in patients with obesity, which may suggest higher degree of leukocyte activation with increased adhesive properties in this group compared to lean participants (Van Oostrom et al., 2004). This was not limited to monocytes as later de Vries et al. (2015) also found up-regulation of CD66b (glycosylated antigen implicated in adhesion to E-selectin) on neutrophils from patients with T2DM. Change in CD66 can be implicated in aberrant neutrophil recruitment to the vasculature but also indicates neutrophil activation and degranulation (Weber, 2003), which confirms how hyperglycemia can lead to exacerbated inflammatory responses.

Dipeptidyl peptidase-4 (DPP-4) or CD26 is an amino-peptidase expressed in numerous tissues including the vasculature and in immune cells (Mentlein, 1999; Lambeir et al., 2003). DPP-4 cleaves dipeptides from the N-terminus of many chemokines and cytokines, usually after a penultimate proline or an alanine (Broxmeyer et al., 2016). DPP-4 controls glucose homeostasis through regulating bioactivity of the incretin hormone and glucagon-like peptide 1 (Augustyns et al., 2010). Involvement of DPP-4 in metabolic control raises the possibility that it may play a role in metabolic diseases such as diabetes and obesity (Mulvihill and Drucker, 2014; Omar and Ahrén, 2014). Given its various roles and its altered expression and activity, DPP-4 has been implicated in several pathological processes, including inflammation, viral entry and immune-mediated diseases (Lambeir et al., 2003; Yu et al., 2010).

Plasma levels of DPP-4 and circulating DPP-4 activity both increase with obesity and this correlates with insulin resistance (Mulvihill and Drucker, 2014; Ahmed et al., 2017). Numerous studies have detailed the effects of DPP-4 inhibitors on insulin and/or glucagon secretion, but little evidence indicates that DPP-4 inhibitors directly improve chronic inflammation. The effects of DPP-4 inhibition was investigated in diet-induced adipose tissue inflammation using ($Gck^{+/2}$) diabetic mice, an animal model of non-obese T2DM (Shirakawa et al., 2011). DPP-4 inhibition in this model led to a significant reduction in adipose tissue infiltration of $CD8^+$ T-cells and M1 macrophages which was associated to decreased mRNA expression levels of TNF-α and MCP-1 in the adipose tissue (Shirakawa et al., 2011). Because DPP-4 mediates the cleavage of many chemokines and adipokines, inhibition of DPP-4 may cause off-target side effects and further research is needed to clarify this (Shirakawa et al., 2011).

In addition, Zhuge et al. (2016) found that the expression of DPP-4 was mainly detected and up-regulated on $F4/80^+$ macrophages in the white adipose tissue of HFD-induced obese mice). Oral administration of the DPP-4 inhibitor, linagliptin, caused an anti-inflammatory macrophage polarization with a dynamic M2 shift of macrophages within the adipose tissue of HFD-induced obese mice compared to non-treated obese mice, and this contributed to the attenuation of whole-body insulin resistance (Zhuge et al., 2016). In this study, the anti-inflammatory effects of DPP-4 inhibition were due to a decreased in ROS generation and an attenuation of oxidative stress in the white adipose tissue (Zhuge et al., 2016). Loss of macrophage inflammatory protein-1α (MIP-1α), a chemokine and potential DPP-4 substrate, abrogated the M2 macrophage-polarizing and insulin-sensitizing effects of linagliptin in MIP-$1\alpha^{-/-}$ mice on HFD. This suggests that MIP-1α may be a substrate for DPP-4 and contributes to the regulation of macrophage polarization in obesity models (Zhuge et al., 2016).

Altogether the *in vivo* studies highlight a potential role of DPP-4 in the modulation of leukocyte migration by affecting chemokines. However, this has not been extensively investigated in the studies presented here as not all studies seem to have linked this to migration despite the important role of DPP-4 at inhibiting chemokines. The approved DPP4 inhibitors being used in clinic, such as sitagliptin and vildagliptin are based on the ability of DPP4 to lower glucose rather than its regulatory effects on inflammation (Deacon, 2018).

Similar to studies investigating endothelial expression of adhesion molecules in T2DM, data showing changes in adhesion molecules/integrins on leukocytes have not performed analysis of leukocyte recruitment in targeted tissues, instead this has been extrapolated from knowledge on adhesion molecule profiles and function in "normal" inflammatory responses, in other models and/or diseases.

EXPRESSION OF CHEMOKINES AND CHEMOKINE RECEPTORS IN T2DM

Chemokines and their receptors play a central role in leukocyte trafficking and are involved in the pathophysiology of T2DM (Buraczynska et al., 2012). Production and release of cytokines and chemokines including CC-chemokine ligand 2 (CCL2), CCL3 and CXC-chemokine ligand 8 (CXCL8) is increased in the adipose tissue and pancreatic islets of patients with T2DM (Donath and Shoelson, 2011; Xu et al., 2015). This is associated with an increased recruitment of macrophages in these tissues, and thus contributes to tissue inflammation

(Donath and Shoelson, 2011; Xu et al., 2015). CCL2 (also known as MCP-1) is known to regulate monocyte recruitment by directing monocytes migration from the bone marrow to inflamed tissues (Crane et al., 2009; Boels et al., 2017). The CCL2-CCR2 axis has a key role in diabetes-related complications such as retinopathy, nephropathy and neuropathy (White et al., 2009; Zhu et al., 2014; Moreno et al., 2018; Monickaraj et al., 2020). Indeed, contribution of CCL2-CCR2 axis to leukocytes recruitment into the injured nerve was shown using a preclinical model of peripheral neuropathic pain induced by chronic nerve constriction (CCI) in Sprague–Dawley rats (Van Steenwinckel et al., 2015). This study shows that CCl-induced mechanical hypersensitivity in rats upregulated the expression of CCL2 and increased local macrophage infiltration in the sciatic nerve compared to the sham group (Van Steenwinckel et al., 2015). In contrast, in the same study, CCL2-deficient mice presented attenuated CCI-induced mechanical hypersensitivity as well as decreased number of macrophages infiltrating the injured sciatic nerve. Altogether, these findings suggest that CCL2 could play an important role in mediating neuropathic pain by increasing leukocyte infiltration in nerves but also by mediating neuro-immune interactions during inflammation-induced pain (reviewed in White et al., 2009).

In addition, upregulation of the CCL2 gene was also demonstrated in retinas of STZ-induced diabetic rats, and this was coincident with the trafficking and infiltration of numerous monocytes into the retina (Rangasamy et al., 2014). Furthermore, using CCL2 knockout ($Ccl2^{-/-}$) mice, the same authors found significantly decreased monocyte/macrophage trafficking into diabetic $Ccl2^{-/-}$ retinas, indicating that this chemokine may be essential for the alteration of the blood-retinal barrier (Rangasamy et al., 2014). The role of CCL2-CCR2 axis is also widely investigated in diabetic renal injuries. Indeed, accumulation of macrophages in the kidney was reduced in *Ccl2* $^{-/-}$ *db*/*db* double knock-out diabetic mice compared to *Ccl2* $^{+/+}$ *db*/*db* animals (Chow et al., 2007). Immunohistochemistry results from kidney biopsies of patients with T2DM showed overexpression of CCL2 and CCR2 in the glomeruli of these patients compare to healthy kidneys (Tarabra et al., 2009). This was accompanied with reduced nephrin expression in cultured podocytes from T2DM patients (Tarabra et al., 2009). Moreover, in the STZ- model of diabetes, induction of diabetes increased albuminuria in $CCL2^{+/+}$ mice, which was significantly reduced in CCL2-deficient mice. Together these studies suggest a pathogenic role of the CCL2/CCR2 axis in the development of diabetic nephropathy (Tarabra et al., 2009) and targeting this pathway could be a potential therapeutic avenue to reduce common diabetic complications associated with aberrant infiltration of leukocytes.

Other chemokines and their receptors are also changed in T2DM. CX3CL1 was found at higher levels in the subcutaneous adipose tissue of patients with T2DM and in obese people when compared to patients with normal weight and also was shown to modulate monocyte adhesion to adipocytes (Shah et al., 2011). CCL5 (RANTES) was also found at higher levels in the circulation of 236 patients with T2DM, 242 individuals with impaired glucose tolerance (IGT) but not in 244 individuals with normal glycemic control (Herder et al., 2005). However, higher circulating levels of CCL5 were not significantly associated with other inflammatory variables and metabolic parameters, suggesting more studies are required to evaluate the novel hypothesis that CCL5 is a risk factor for T2DM.

Infiltration of inflammatory leukocytes in adipose tissue plays an important role in the development of insulin resistance. The inflammatory cytokines secreted by these cells interfere with insulin signaling and decrease glucose uptake in peripheral tissues (Asghar and Sheikh, 2017). Studies looking at ways to down-regulate aberrant recruitment of leukocytes as a mean to control inflammation and therefore restore insulin sensitivity have targeted chemokine receptors such as CCR5 and CCR2. CCR5 a chemokine receptor expressed by T-cells and macrophages, plays a critical role in recruitment and polarization of macrophage in inflammation. Kitade et al. (2012) showed that a higher gene expression of CCR5 in the white adipose tissue of High Fat Diet (HFD)-induced obese mice was concomitant to an accumulation of macrophages in this tissue. Importantly, mice deficient for CCR5 in their myeloid lineage did not develop insulin resistance and diabetes normally induced by HFD. Loss of CCR5 was associated with a reduction in total adipose tissue macrophage content and polarization of macrophages toward and an anti-inflammatory M2-dominant phenotype in the adipose tissue (Kitade et al., 2012).

The administration of a dual CCR2/CCR5 antagonist has shown to improve obesity-associated insulin resistance and glucose intolerance via reducing macrophages and $CD8^+$ T-cell numbers in the white adipose tissue of HFD-fed mice, indicating that blocking both CCR2 and CCR5 has potential to maintain both metabolic and immune homeostasis in obesity-induced inflammation (Huh et al., 2018).

Overall, these studies clearly demonstrate how up-regulation of chemokine pathways, which in turn leads to aberrant recruitment of leukocytes in different tissues is contributing to some of the common diabetic complications and targeting this pathophysiological process could be a promising therapeutic advance. However, further research is required to fully characterize the interactions and redundancy of chemokine with chemokine receptors in T2DM.

INNATE AND ADAPTIVE IMMUNE CELL IN T2DM

In this section, we will explore how the recruitment of innate and adaptive immune cells changes in obesity and T2DM as summarized in **Table 1**. Obesity-induced inflammatory events originating from the adipose tissue such as production of local inflammatory molecules are responsible for the activation of immune responses and progression of systemic inflammation in patients with T2DM (Richardson et al., 2013).

Innate Immune Cells

Monocytes and Macrophages

Innate immune cells play a critical role in the early stage of adipose tissue inflammation in T2DM (Weisberg et al., 2003).

TABLE 1 | A summary of studies discussed in this review assessing obesity/T2DM-related changes to the trafficking of innate and adaptive immune cells.

	Effect of obesity/T2DM on cell recruitment	Potential mechanisms	References
Monocyte/ macrophage	↑ recruitment of macrophages in retinas of STZ-induced diabetic rats	CCL2-CCR2 axis	Rangasamy et al., 2014
	↑ recruitment of macrophages in kidney of STZ-induced diabetic mice	CCL2-CCR2 axis	Tarabra et al., 2009
	↑ adhesion of monocyte to adipocytes in the subcutaneous adipose tissue of patients with T2DM and obesity **(Human study)**	↑ CX3CL1 expression in adipose tissue	Shah et al., 2011
	↑ recruitment of macrophages in white adipose tissue of HFD-induced obese mice	↑ CCR5 expression in white adipose tissue	Kitade et al., 2012
	↑ levels of F4/80 and CD11c mRNA expression in adipose tissue of HFD fed mice	↑ Adipose tissue expression of ICAM-1, VCAM-1, CCL2, CXCL14	Kawanishi et al., 2010
	↑ expression of F4/80 in adipose tissue of HFD fed mice	↑ Adipose tissue expression of mRNA for ICAM-1	Brake et al., 2006
	↓ RPMs in db/db mice ↑ Increased M2 polarization	Ongoing chronic inflammation in the peritoneal cavity in db/db mice	Liu et al., 2012
	In vitro ↓ adhesion and phagocytosis capacity of RPMs from in *db/db* mice	abnormal microenvironment in db/db mouse	Liu et al., 2012)
	↓ monocyte/macrophages in lung tissue of diabetic $DPP4^{H/M}$ mice following infection by *MERS-CoV*	↓ lung tissue expression of *Ccl2* and *Cxcl10*	Kulcsar et al., 2019
DCs	↑ $CD11c^{high}F4/80^{low}$ DCs in mice visceral adipose tissue in HFD-induced obese mice	Not described	Bertola et al., 2012.
	↑ $CD11c^{+}CD1c^{+}$ cDCs in obese human subcutaneous adipose tissue **(Human study)**	Not described	Bertola et al., 2012.
	↑ $CD11c^{+}$ cDCs numbers in the adipose tissue of HFD-fed mice	Not described	Chen et al., 2014
Neutrophils	↑ trafficking of neutrophil into mice visceral adipose tissue after 3 days on HFD	↑ CD11b surface expression on neutrophils	Elgazar-Carmon et al., 2008
	↑ recruitment of neutrophils into the adipose tissue of HFD-fed mice after 3 days on HFD (sustained infiltration for up to 90 days on HFD)	↑ expression and activity of neutrophil-secreted elastase in the adipose tissue of HFD-fed mice	Talukdar et al., 2012
$CD8^{+}$ T-cells	↑ infiltrated $CD8^{+}$ effector T-cells in visceral adipose tissue in HFD-fed mice	Activation of $CD8^{+}$T cells by endogenous stimuli localized in the adipose tissue	Nishimura et al., 2009.
	↓ lower numbers of $CD8^{+}$ T-cells in their brains in *db/db* mice following infection with *West Nile virus*	↓ expression of E-selectin and ICAM-1 in *db/db* brains	Kumar et al., 2014
$CD4^{+}$ T-cells	↓ CD4 + T-cells in lung tissue of diabetic $DPP4^{H/M}$ mice following infection by *MERS-CoV*	↓ lung tissue expression of *Ccl2* and *Cxcl10*	Kulcsar et al., 2019
Tregs	↓ regulatory T-cells in visceral adipose tissue of HFD-fed mice	Not described	Nishimura et al., 2009.
	↓ $CD4^{+}$ Tregs HFD-fed mice	↓ levels of adiponectin in obese fat	Feuerer et al., 2009; Ilan et al., 2010.
B-cells	↑ number of B-cells in the bone marrow of HFD-fed mice	Not described	Trottier et al., 2012
	↓ number of B-cells in the bone marrow of HFD-fed mice	lower expression of Pax5 in the bone marrow of HFD-fed mice	Chan et al., 2012
Granulocytes	↓ granulocytes in the alveolar airspace of stz-induced diabetic mice following infection by *Klebsiella pneumoniae*	↓ levels of (CXCL1, CXCL2) and (IL-1β, TNFα) in lung tissue	Martinez et al., 2016

Monocytes derived from the bone marrow remain in the circulatory system for 1–2 days before they migrate into peripheral tissues, where they turn into fully mature resident macrophages (Martinez-Pomares et al., 2003) either with a M1 pro-inflammatory or M2 anti-inflammatory phenotype in response to local factors (Mosser, 2003). In a recent *in vivo* study, an acute decrease in number of circulating monocytes was synchronized with a concomitant infiltration of macrophages into visceral adipose tissue, therefore demonstrating dynamic changes in blood monocyte trafficking at the early stages of HFD-induced diabetes (Liu et al., 2020). Higher levels of F4/80 and CD11c mRNA expression in adipose tissue of HFD fed mice, representative of a M1 polarization, were attributed to an elevated gene expression of ICAM-1, VCAM-1, CCL2 and CXCL14 in this tissue, which facilitates macrophage trafficking (Kawanishi et al., 2010). Similarly, Brake et al., found higher levels of mRNA for ICAM-1 in mice on a 3-week HFD, as well as an increased expression of F4/80 in their adipose tissue

(Brake et al., 2006). The activation of M1 macrophages is associated with release of pro-inflammatory mediators, such as TNFα and IL-6 (Biswas and Mantovani, 2010). Using an HFD-induced rat model of T2DM, Shanaki et al. reported increased serum and adipose tissue levels of IL-6 and TNFα in T2DM rats compared to control animals. This pro-inflammatory shift was linked to higher fasting plasma glucose levels and insulin resistance in the diabetic animals (Shanaki et al., 2020). The impact of long-term diabetes on the functions of macrophages was investigated using a 5-month old *db/db* mice model of T2DM (Liu et al., 2012). In this study, the authors focused on resident peritoneal macrophages (RPMs) to investigate potential changes of their function, phenotype and migratory capacity. RPMs numbers were reduced in *db/db* mice compared to C57BL/6 control mice and most were preferentially polarized toward a M2 phenotype. Since M2 macrophages exhibit immunosuppressive functions and therefore contribute to the resolution of harmful inflammation, their increased proportion in the *db/db* mice may be caused by an effort to control the chronic low-grade inflammation observed in the peritoneal cavity of these mice (Liu et al., 2012). Furthermore, in this study, *in vitro* assessment of *db/db* RPMs highlighted their decreased adhesion capacity along with a decreased phagocytosis ability compared to wild-type RPMs. These observations validate that diabetes and obesity are associated with immune dysfunction which predispose these patients to an increased susceptibility to infections (Liu et al., 2012).

Human studies also indicate a role of macrophages in mediating insulin resistance. Indeed, higher numbers of circulating leukocytes are found in patients with T2DM along with higher Free Fatty Acid (FFA) and IL-6 circulating levels (van Beek et al., 2014). Elevated number of total leukocytes counts in patients with T2DM was also characterized in other studies (Kizilgul et al., 2018; Palella et al., 2020) and were often indicative of macro- and micro-vascular complications and diabetes duration (Papazafiropoulou et al., 2010; Moradi et al., 2012). In particular, Wouters et al. demonstrated higher numbers of circulating classical monocytes and this was associated with higher presence of M1 macrophages in the white adipose tissue of individuals with obesity compared to individuals with normal weight (Wouters et al., 2017). In addition, impaired glucose tolerance was associated with the presence of crown-like structures (marker of adipose inflammation) in the adipose tissue of patients with obesity and T2DM compare to patients with obesity and normal glucose tolerance (van Beek et al., 2014).

Most of the current observations seem to indicate a crucial role of macrophage infiltration in the adipose tissue of patients with obesity and T2DM. However, it is not entirely clear what mechanisms mediate recruitment of macrophages in these tissues and more research is needed to understand whether macrophage infiltration could be limited to improve insulin sensitivity and glucose tolerance and therefore prevent diabetic complications.

Neutrophils

Neutrophils are the most abundant subsets of leukocytes of the innate immune system in humans and are the first to infiltrate inflamed tissue and promote subsequent recruitment of other leukocytes such as monocytes (Soehnlein et al., 2008). The number of circulating neutrophils in patients with T2DM increases in comparison to age- and gender-matched healthy controls (Huang et al., 2019). However, neutrophils isolated from patients with T2DM displayed normal migratory capacity and phagocytic rate (Huang et al., 2019). Neutrophil trafficking into murine visceral adipose tissue was reported after 3 days on HFD. The same study reported an absence of neutrophils in the adipose tissue after 7 days on HFD and that neutrophil adhesion to mouse adipocytes depends on their activation state (Elgazar-Carmon et al., 2008). Here, the degree of CD11b surface expression on neutrophils correlated with their capacity to adhere. However, the mechanisms responsible for the absence of neutrophils in the adipose tissue after 7 days on HFD was not explained in this study (Elgazar-Carmon et al., 2008). Similarly, Talukdar et al. (2012) found an early recruitment of neutrophils into the adipose tissue of HFD-fed mice after 3 days. Here, the time course of neutrophil infiltration into the adipose tissue showed a sustained infiltration in the adipose tissue for up to 90 days on HFD (Talukdar et al., 2012). According to this study, the trafficking of neutrophils was associated with an elevated expression and activity of neutrophil-secreted elastase in the adipose tissue of HFD-fed mice which increased after only 3 days of HFD and remained high after 12 weeks. Elastase is a neutrophil-specific protease which can promote inflammatory responses (Pham, 2006) and inhibition of neutrophil elastase in HFD-induced obese mice improved glucose tolerance and reduced trafficking of neutrophils into the adipose tissue (Talukdar et al., 2012).

Dendritic Cells

Dendritic cells (DCs) are antigen-presenting immune cells that mediate lymphocytes polarization into effector cells (Yu and Martin-Gayo, 2019). In humans, two major subtypes of DCs are identified according to their markers expression: conventional or myeloid DCs (cDCs) ($CD11c^+$ $CD1c^+$ $CD141^+$) and plasmacytoid DCs (pDCs) ($CD11c^-$ $CD123^+$) (Tamura et al., 2005; Gilliet et al., 2008; Sundara Rajan and Longhi, 2016). In mice, two major DC subsets have also been described: $CD11c^{low}B220^+$ (pDCs) and $CD11c^{high}B220^-$ cells that include cDCs (O'Keeffe et al., 2002). The number of circulating cDCs increases in obese post-menopausal women with T2DM compared to age-matched healthy women and a smaller increase was observed for pDCs (Musilli et al., 2011). This change in DCs numbers in the circulation suggests that DCs might contribute to pathological vascular remodeling (Musilli et al., 2011). Mráz et al. reported a decrease in the number of total DCs in the subcutaneous adipose tissue from patients with T2DM compared to non-diabetic individuals. In contrast, the number of pDCs was increased in the subcutaneous adipose tissue of the T2DM group. These differences suggest a potential role of pDCs in the development of T2DM-associated adipose tissue low-grade inflammation (Mráz et al., 2019). Bertola et al. investigated the role of DCs in the regulation of adipose tissue inflammation in a murine HFD-induced obesity model and in two cohorts of obese subjects (Bertola et al., 2012). The authors in this study only found $CD11c^{high}B220^-$ DCs in the visceral adipose tissue of lean mice. In contrast, obesity

was associated with the presence of $CD11c^{high}F4/80^{low}$ DCs in murine visceral adipose tissue, and $CD11c^{+}CD1c^{+}$ cDCs in human subcutaneous adipose tissue (Bertola et al., 2012). $CD11c^{high}B220^{-}$ DCs resident in the adipose tissue of lean mice participate in the differentiation of naive $CD4^{+}$ T-cells into effector T-cells with a predominance of Th1 cells over Th17 cells. In contrast, the adipose tissue of HFD-induced insulin resistant mice displayed a switch from Th1 towards a Th17 phenotype (Bertola et al., 2012). In addition, the presence of $CD11c^{+}CD1c^{+}$ cDCs in the subcutaneous adipose tissue of obese subjects correlated with CD1c expression and a concomitant skew towards a Th17 T-cell phenotype. Finally, CD1c expression strongly correlated with insulin resistance in patients with a high Body Mass Index (BMI) (Bertola et al., 2012). Altogether, these observations suggests an important role of inflammatory DCs in obese and diabetic adipose tissue inflammation by switching T-cell responses toward Th17 responses, which is associated with insulin resistance (Bertola et al., 2012). These observations were confirmed by another group who showed that $CD11c^{+}$ cDCs infiltrated the adipose tissue of HFD-fed mice and also secrete high levels of IL-6 and IL-23, which promoted a Th17 T-cell phenotype (Chen et al., 2014). The presence of DCs in the visceral adipose tissue of HFD-mice can also induce the formation of crown-like structures which enclose macrophages and were linked to adipose tissue inflammation and insulin resistance (Stefanovic-Racic et al., 2012). Depletion of DCs results in loss of adipose tissue macrophage infiltration, and this could be restored by DC replacement in DC-null mice (Stefanovic-Racic et al., 2012). All together, these studies show the importance of DCs in determining the immune phenotype of lean versus obese or diabetic adipose tissue.

Adaptive Immune Cells

The mucosal immune system is a compartment of the adaptive immune system which is located near the surface, where most pathogens invade, providing the first line of defense (Janeway et al., 2001). The gut microbiota is key to the development and modulation of mucosal immune responses and maintains perfect balance between commensal flora and pathogens, as well as the microbiota and the immune system (Wang and Li, 2015). The alteration of such balance is called dysbiosis (Pagliari et al., 2018). Given that the pancreas does not have its own microbial collection, the gut microbiota may be involved in the pathogenesis of pancreatic disorders such as pancreatitis (Signoretti et al., 2017). Recently, Guo et al. (2017) demonstrated that HFD was able to alter gut microbial communities and increase circulating pro-inflammatory cytokines, such as TNFα, IL-6 and IL-1β. In addition, recent evidence demonstrated that intestinal dysbiosis may also cause alterations in the Th17 cells/Tregs balance which are responsible for the development inflammatory disease including obesity-related T2DM (Luo et al., 2017).Thus, understanding the mechanisms responsible for this alteration will allow to develop novel translational therapeutic targets to potentially treat these inflammatory diseases (Pagliari et al., 2018). In this section, we mostly focus on T- and B-cells as very little is known on mucosa-associated homing mechanisms in the context of T2DM.

T-Cells

Although, earlier studies focused on the role of innate immunity (macrophages) as the major cause of chronic low-grade inflammation in T2DM, the adaptive immune system also plays a role in progression of T2DM (Zhou et al., 2018). Evidence shows that B-cells are the first to infiltrate the adipose tissue of mice on HFD, quickly followed by T-cells and finally an accumulation of macrophages leading to insulin resistance, but no changes in resident macrophages populations (Duffaut et al., 2009). Nishimura et al. (2009) found larger number of infiltrated $CD8^{+}$ effector T-cells along with reduced numbers of $CD4^{+}$ helper and regulatory T-cells in visceral adipose tissue of HFD fed mice). In these conditions, a majority of $CD8^{+}$ T-cells infiltrate the adipose tissue thereby promoting recruitment and activation of macrophages. This sequential accumulation of leukocytes is clearly linked with glucose intolerance and a decrease in insulin sensitivity in wild-type animals (Duffaut et al., 2009). Studies in the lymphocyte-deficient $RAG2^{-/-}$ knockout mouse provide strong evidence for the role of lymphocytes in HFD-mediated adipose tissue inflammation. Unexpectedly, lymphocyte-deficient animals displayed striking accumulation of macrophages and NK cells in the adipose tissue compared to wild-type mice (Duffaut et al., 2009). This accumulation of NK cells highlights an overreaction of the innate immunity in absence of the adaptive immune system. Indeed, NK cells have potent cytotoxic effector functions and produce chemokines and cytokines that can recruit macrophages (Duffaut et al., 2009). The exaggerated recruitment of macrophages in lymphocyte-deficient mice demonstrates that early lymphocyte infiltration could be considered a protective process to decrease adipose tissue inflammation and suggests adipose tissue as a site of dynamic innate and adaptive immune system during diet-induced obesity and insulin resistance (Duffaut et al., 2009).

According to recent reports, the changes in quantity and polarization of adipose tissue T-cells during weight gain is a key regulator of systemic insulin sensitivity (Deng et al., 2017). HFD is associated with increased numbers of Th1 $CD4^{+}$ T-cells and decreased numbers of $CD4^{+}$ Tregs in the adipose tissue (Feuerer et al., 2009; Ilan et al., 2010). The depletion of Tregs using diphtheria toxin in mice leads to an induction of genes encoding inflammatory cytokines such as TNFα and IL-6 in visceral adipose tissue and enhance levels of fasting insulin (Feuerer et al., 2009). On the other hand, in the same study, increasing the quantity Tregs in the adipose tissue using a Tregs–enriched HFD-fed mice model, improved insulin resistance and glucose tolerance (Feuerer et al., 2009). Since, the gene expression of IL-10 was increased in the adipose tissue of Tregs–enriched animals, the metabolic changes observed can be attributed to IL-10 synthesis by Tregs in the adipose tissue of these mice (Feuerer et al., 2009). These findings suggest a strong therapeutic potential for Tregs to suppress inflammation and improve insulin action in obesity and T2DM. It is therefore key to understand how Tregs migratory capacity and infiltration in the adipose tissue

could be manipulated in patients. In addition, further studies are required to fully characterize the involvement of different T-cell subsets and characterize the intricate balance between innate and adaptive immune regulations.

B-Cells

B-cells have been shown to play important roles in many chronic inflammatory and autoimmune conditions (Yanaba et al., 2008; Mariño and Grey, 2012) but only recently has their role been revealed in obesity-associated insulin resistance. B-cells infiltrate the white adipose tissue in diet-induced obesity models and contribute to insulin resistance (Winer et al., 2011). The data on the development of B-cells in the bone marrow of obese models is controversial. Indeed, B-cells numbers in the bone marrow of mice on HFD were significantly increased after 90 days (Trottier et al., 2012). However, number of B-cells in the bone marrow were reduced in C57BL/6 mice on HFD for 210 days in another study (Chan et al., 2012). This reduction was associated to a lower expression of Pax5 in the bone marrow of HFD-fed mice (Chan et al., 2012). Differences between these studies may be due the type and duration of HFD. B-cell infiltration in the white adipose tissue of C57BL/6 mice peaks at around 3–4 weeks of HFD (Duffaut et al., 2009). The importance of B-cells in adipose tissue inflammation has been studied *in vivo* using B-cell null mice (μMT mice). Attenuated inflammation in visceral adipose tissue of μMT mice was shown by a reduced infiltration of macrophages. In this study, following 15 weeks of HFD, serum glucose levels were unchanged in obese μMT mice while fasting glucose levels increased in the control wild-type group (DeFuria et al., 2013). These data support the conclusion that B-cells regulate macrophage infiltration into the adipose tissue during inflammation and this contributes to insulin resistance.

IMMUNE RESPONSE FOLLOWING INFLAMMATORY STIMULUS IN T2DM

Hyperglycemia in diabetes can impair immune response to pathogens such as, fungi, bacterial and viral infections (Hostetter, 1990; Javid et al., 2016; Kulcsar et al., 2019). As a result, patients with diabetes are more susceptible to infections (Berbudi et al., 2020). Although the plasma concentration of sCAMs tends to be generally higher in patients with T2DM compared to healthy controls, their expression is differently affected in response to inflammatory pathogens in patients with T2DM. Indeed, plasma levels of sE-selectin, sVCAM-1 and sICAM-1 after intravenous injection of *E.coli* lipopolysaccharide (LPS) were lower in patients with T2DM compared to healthy volunteers. This study revealed that patients responded with an attenuated up-regulation of sCAMs even though the basal plasma concentration of these adhesion molecules were generally higher in diabetic individuals compared to healthy controls (Andreasen et al., 2010). Also, in this study, T2DM was associated with less pronounced LPS-induced cytokine responses. This weaker cytokine response following inflammatory stimuli in T2DM is also shown *in vitro* with cultures of peripheral blood mononuclear cells (PBMCs). Stimulation of PBMC from patients with diabetes with LPS and *Burkholderia pseudomallei* lead to a lower production of IL-1β and IFNγ respectively, compared to PBMCs from healthy donors (Mooradian et al., 1991; Tan et al., 2012). All together these findings may explain the immune dysfunction and increased risk of infections associated with T2DM (Andreasen et al., 2010). However, the evidence demonstrating changes in leukocyte recruitment following pathogen invasion in T2DM is rare and mostly limited to animal experimental studies. Accordingly, *db/db* mice infected with West Nile virus, had lower numbers of $CD45^+$ leukocytes and $CD8^+$ T-cells in their brains compared to wild-type mice (Kumar et al., 2014). Effector $CD8^+$ T-cells are necessary to limit viral load and therefore a lack of $CD8^+$ T-cells infiltration, which may be caused by a decreased migratory capacity or changes in the brain vasculature, lead to an increased viral burden in the brain of infected mice (Shrestha and Diamond, 2004; Kumar et al., 2014). This defect in leukocyte recruitment was in fact due to a reduced expression of E-selectin and ICAM-1 in *db/db* brains which failed to properly support the $CD8^+$ T-cells adhesion and migration (Kumar et al., 2014). Furthermore, impaired recruitment of leukocytes is not only due to changes on leukocytes themselves and in the local environment but can also be attributed to attenuated cytokine and chemokine production in diabetic mice. In STZ-diabetic mice infected by *Klebsiella pneumoniae*, which causes pneumonia (Bengoechea and Sa Pessoa, 2019) lower numbers of granulocytes were found in the alveolar airspace along with attenuated chemokines (CXCL1, CXCL2) and cytokines (IL-1β, TNFα) levels in lung tissue when compared to control mice (Martinez et al., 2016). Moreover, a recent study investigated the impact of T2DM on respiratory infection caused by Middle East respiratory syndrome coronavirus (MERS-CoV) (Kulcsar et al., 2019). In this study, humanized DDP4 mice were susceptible to MERS-CoV and T2DM was induced by HFD (Kulcsar et al., 2019). Following infection with MERS-CoV, diabetic $DPP4^{H/M}$ mice displayed weight loss and had a longer phase of severe disease with delayed recovery. Importantly, lung tissue analysis in the diabetic mice showed a decreased number of macrophages, $CD4^+$ T-cells, and lower expression of TNFα and IL-6 in the HFD group, compared to control $DPP4^{H/M}$ mice following infection (Kulcsar et al., 2019). These results suggest that MERS-CoV infection in patients with T2DM diabetes may develop more severe disease as a result of a dysregulated immune response targeting not only migratory capacities of leukocytes but the local environment by modulating secreted factors and expression of adhesion molecules. Maximal endothelial cell adhesion molecule expression or chemokine/cytokine receptor downregulation/internalization in chronic inflammatory conditions could theoretically cause an impaired immune response to an infection. In addition to alternative mechanisms, it is also plausible that insulin could have agonist and antagonist effects on the same signaling pathway based on its concentration and receptor expression state (i.e., the "U-shaped" biologic dose-response curve) (Calabrese and Baldwin, 2001). In general, it seems that high glucose levels are associated with impaired expression of adhesion molecules, cytokines and the chemokines supporting efficient leukocyte migration during an inflammatory response to infections in T2DM conditions. This is in contrast

with studies mentioned above which show how basal expression of adhesion molecules and chemokines/chemokine receptors is increased in different vascular beds and leukocytes in T2DM conditions. The defect in cytokine response to pathogen in T2DM is partially related to insulin deficiency and recently has been discussed by Tessaro and Martins (Tessaro et al., 2017). In their study, insulin increased TNFα and IL-6 release by bone marrow-derived macrophages from diabetic C57BL/6 mice following LPS stimulation. This finding supports the idea that insulin is crucial to induce a proper immune reaction in response to inflammatory stimuli. However, in the same study insulin inhibited LPS-induced pro-inflammatory cytokine secretion by peritoneal macrophages from diabetic mice (Tessaro et al., 2017). Together findings suggest that beyond its glucose modulatory effects, insulin also has distinctly immunomodulatory effects in macrophages and these urgently require to be fully understood.

THERAPEUTIC TARGETING OF LEUKOCYTE TRAFFICKING IN T2DM

Given that T2DM is a chronic inflammatory disorder, characterizing and targeting possible inflammatory pathways could be efficient to prevent and control diabetes and its vascular complications.

Chemokine and Cytokine Inhibition

Chemokine and cytokine pathways are known to govern the trafficking of leukocytes into peripheral tissues (Yao et al., 2014). Potential antagonists targeting chemokine receptors and drugs blocking inflammatory cytokines have been developed and tested in many inflammatory conditions, but little is known about their efficacy in obesity or T2DM and associated complications. In this section, we will discuss some of these targets.

CC-chemokine ligand 2 and CCL5 are key mediators of monocyte recruitment induced by high glucose levels via their receptor CCR2 and CCR5 (Nunemaker et al., 2014). Oral administration of RO5234444, a CCR2 antagonist, to *db/db* mice, reduced infiltration of monocytes in the glomerulus, resulted in preservation of glomeruli podocytes numbers and reduced albuminuria (Sayyed et al., 2011). Similarly, intraperitoneal administration of TAK-779, a dual inhibitor of chemokine receptors CCR2 and CCR5, reduced macrophage infiltration and expression of ICAM-1 in the retinas of STZ-diabetic mice (Monickaraj et al., 2020). These studies clearly indicate that blocking key recruitment chemokine receptors such as CCR2 and/or CCR5 is a promising therapeutic avenue to ameliorate common diabetic complications such as nephropathy and retinopathy. Those compounds are currently pursued in human clinical trials as well as others such as INCB8761/PF-413630, which are a new series of CCR2 antagonists that are orally bioavailable (Xue et al., 2011).

Due to their pro-inflammatory nature, IL-1β and TNFα actions have been widely studied in many inflammatory conditions and their blockade resulted in improvements in T2DM-related conditions such as chronic kidney disease (Lei et al., 2019) and pancreatic islet inflammation (Zha et al., 2016). However, it remains unsure whether targeting these cytokines affects leukocyte infiltration in peripheral tissues in T2DM. Circulating levels of IL-1β are higher in T2DM (Reinehr et al., 2016) and macrophages are the primary source of IL-1β in obesity-induced inflammation (Gao et al., 2014). Administration of LY2189102, a neutralizing IL-1β antibody, in patients with T2DM, improved glycemic control and demonstrated significant anti-inflammatory effects by lowering circulating IL-6 levels when compared with placebo treatment (Sloan-Lancaster et al., 2013). Moreover, islets from IL-1β-deficient mice exposed to high glucose *in vitro*, produced lower IL-6 and chemokines compared to wild-type islets (Ehses et al., 2009). Thus, efficacy of IL-1β blocking on inflammatory biomarkers and glycemic control raises the possibility of its use as a treatment in T2DM and other inflammatory conditions.

Although, anti-TNFα is an approved medication for some patients with rheumatoid arthritis (Katsumata et al., 2019), the evidence showing the efficacy of this drug in T2DM is conflicting. Indeed, anti-TNFα treatment using recombinant soluble TNFα receptor-immuno-globulin G increased insulin sensitivity in obese rodents (Hotamisligil et al., 1993). However, treatment with Ro 45-2081, a TNFα antagonist (recombinant fusion protein that consists of the soluble TNF-receptor linked to the Fc portion of human IgG1), had no effect on blood glucose levels and insulin-mediated glucose uptake in patients with T2DM (Paquot et al., 2000). The inefficiency of Ro 45-2081 to control blood glucose in patients with T2DM suggest that in addition its endocrine action, TNFα may also act through an autocrine or paracrine route. Consequently, sole neutralization of circulating TNFα might not be enough to observe improvements on insulin action (Paquot et al., 2000).

Anti-integrins

The importance of integrins in leukocyte adhesion and arresting clearly offer potential therapeutical avenues in relapsing inflammatory conditions such as rheumatoid arthritis (von Andrian and Engelhardt, 2003) and multiple sclerosis (Chaudhuri and Behan, 2003). Neutralization of integrins has been tested in murine experimental models of diabetes, particularly for the treatment and/or prevention of diabetic complications (Barouch et al., 2000; Iliaki et al., 2009; Miyachi et al., 2017). However, data showing efficacy in human clinical trials is not available in the context of T2DM.

The expression of CD11a, CD11b, and CD18 integrins is increased on the surface of neutrophils from STZ-induced diabetic rats (Barouch et al., 2000). This increase was associated with an enhanced adhesion of diabetic neutrophils to rat EC monolayers *in vitro*. Pre-treatment of leukocytes with either anti-CD11b or anti-CD18 antibodies significantly lowered the proportion of adherent diabetic neutrophils (Barouch et al., 2000). In the same study, systemic administration of anti-CD18 $F(ab')_2$ fragments to STZ-induced diabetic rats significantly decreased diabetic retinal leukostasis (Barouch et al., 2000). Furthermore, intraperitoneal administration of anti-α_4 integrin neutralizing antibody to a STZ-induced rat model of diabetes retinopathy attenuated leukocyte adhesion to the retina and suppressed TNFα expression and NF-κB activity in the retina

of treated rats (Iliaki et al., 2009). Notably, blockage of VLA-4 using a neutralizing antibody in HFD-fed mice attenuated myeloid cell accumulation in the liver and improved systemic glucose tolerance in treated mice compared to control HFD-fed mice (Miyachi et al., 2017). Overall, all these animal data identify the integrins as functional adhesive molecule in diabetic complications and provides a potential target for the prevention and/or treatment of the disease.

A humanized anti–VLA-4 monoclonal antibody (Natalizumab) was clinically beneficial in the treatment of Crohn's disease (Lew and Stoffel, 2003), and rheumatoid arthritis (von Andrian and Engelhardt, 2003). However, VLA-4 also has key regulatory roles in immune response, including the formation of the immune synapse (Mittelbrunn et al., 2004) and the differentiation of Th1 T-cells (Isobe et al., 1997). Obviously, the long-term administration of anti-integrins drugs to patients with inflammatory conditions may have undesirable or unexpected effects and more studies are required to fully understand their action.

Fatty Acids

Long-chain *n*–3 polyunsaturated fatty acid (*n*–3 PUFA) such as eicosatetraenoic acid (EPA) and docosahexaenoic acid (DHA), found in marine fish oils, are able to down-regulate the activity of NF-kB directly and therefore reduce the production of inflammatory cytokines (Xu et al., 2001). *n*–3 PUFA can also control leukocyte recruitment during inflammation and display immunomodulatory properties (Yates et al., 2011). Inclusion of *n*–3 PUFA in HFD prevented macrophage infiltration into the adipose tissue of *db/db* mice (Todoric et al., 2006). Interestingly, *n*–3 PUFA efficiently prevented the HFD-induced downregulation of adiponectin circulating levels normally observed in *db/db* (Todoric et al., 2006). These data therefore suggest that the beneficial effects of *n*–3 PUFA on diabetes could be mediated by their effect on adipose tissue inflammation, which could in turn contribute to improving insulin sensitivity (Oliver et al., 2010). However, much of the human evidence examining the beneficial effects of n–3 PUFA in patients with T2DM have limited follow-up periods (Vessby et al., 2001). As a result, it is unclear whether *n*–3 PUFA supplementation has long lasting beneficial effects and the exact mechanisms of *n*–3 PUFA action and how they modulate the adipose tissue, macrophages and even T-cells remain unknown.

Insulin

Several studies suggest a direct anti-inflammatory action of insulin irrespectively of its glucose modulating capacity as mentioned here in previous sections (Hyun et al., 2011). Insulin was found to attenuates the activity of NF-κB and MCP-1 on human aortic ECs *in vitro* (Aljada et al., 2001). Insulin infusion in individuals with obesity reduced plasma sICAM-1 and CCL2 levels (Dandona et al., 2001). In addition, treatment of human monocytes with insulin *in vitro* promoted the secretion of IL-8 (CXCL8), a potent chemoattractant for neutrophils (Dandona et al., 2001). All together, these findings suggest a possible regulatory effect of insulin on leukocyte trafficking via regulating chemokine and cytokine secretion as well as modulating adhesion molecules shedding. However, more studies are required to clarify the effect of insulin on leukocyte migration by including *in vitro* models taking into account the high glucose levels observed in some patients with T2DM, their associated complications and BMI to accurately determine the mechanism of insulin action and lift the controversy in this field.

Adiponectin and PEPITEM

Since obesity is a key feature in T2DM, studies demonstrate that changes in adipose tissue induce dysregulation in adipokines such as adiponectin and receptors involved in lipid metabolism such as Proliferator–activated receptor γ (PPAR-γ) (Bermudez et al., 2010). Adiponectin is well characterized as an insulin-sensitizing hormone as well as an anti-inflammatory adipokine (Ruan and Dong, 2016). Circulating levels of adiponectin are decreased in patients with obesity and T2DM (Hotta et al., 2000; Engeli et al., 2003), suggesting that dysregulation of adiponectin may be relevant to obesity-linked endothelial dysfunction in these individuals (Cho et al., 2002; Katsiki et al., 2017). In addition, adiponectin is also a regulator of adhesion molecules on ECs (Ouchi et al., 1999). Treating ECs with adiponectin inhibited the expression of adhesion molecules such as VCAM-1, E-selectin, and ICAM-1 *in vitro* (Ouchi et al., 1999) and *in vivo* (Ouedraogo et al., 2007). We also know that adiponectin is able to regulate T-cell trafficking during inflammation in a novel pathway characterized in our laboratory a few years ago (Chimen et al., 2015). In this novel pathway, adiponectin induces the release of the novel PEPtide Inhibitor of Trans-endothelial Migration (PEPITEM) by B-cells via signaling through the adiponectin receptors (AdipoR1/2). PEPITEM induces the release of sphingosine-1-phosphate (S1P) by ECs via binding with endothelial cadherin-15 (CDH15). In turn, S1P inhibits T-cell transmigration by preventing integrin activation (Chimen et al., 2015). The PEPITEM/Adiponectin pathway is dysregulated in inflammatory conditions such as Type 1 Diabetes Melitus, Rheumatoid Arthritis and in older adults. Dysregulation of this pathway is caused by a lack of AdipoR1/2 expression on B-cells in these patient groups leading to insufficient secretion of PEPITEM and consequently allowing aberrant T-cell trafficking. PEPITEM shows great therapeutic potential since it is an endogenous peptide and developing strategies to restore this pathway could help regain control on chronic inflammation. However, more work is needed to understand the full profile of T-cell subsets recruitment in adipose and pancreatic tissues in T2DM as this would allow to characterize whether PEPITEM could be used as a therapeutic avenue in T2DM.

PPAR Agonists

Proliferator–activated receptor-γ is a member of the PPAR family of nuclear receptors (Braissant et al., 1996) and its activation is associated with the induction of glucoregulatory molecules and enhanced insulin sensitivity (Olefsky, 2000). Pioglitazone is a PPARγ agonist that enhances the action of insulin mainly by promoting glucose utilization in peripheral tissues (Yki-Järvinen, 2004). Treatment of patients with T2DM with pioglitazone rapidly reduced systemic inflammation in those patients who were also receiving angiotensin II receptor blockers. This trial

also showed decreased CRP levels accompanied by a reduction in sICAM-1 and sVCAM. These observations uncovered anti-atherogenic effects of the PPAR-γ agonist which may also contribute to a reduction of cardiovascular events in patients at risk such as those with T2DM (Takase et al., 2007).

Current drugs such as IL-1β blockers and thiazolidinediones targeting the metabolic side of T2DM and aiming to restore glucose tolerance have shown to also have anti-inflammatory effects (Yki-Järvinen, 2004; Sloan-Lancaster et al., 2013). However, the evidence showing a potential effect of these drugs on leukocyte recruitment as a way to control inflammation are limited and this area needs further investigations. Blocking cytokines such as TNF- α may reduce inflammation but also renders the host susceptible to infection by silencing the danger signals, which are necessary for adequate immune cell activation (Rider et al., 2016) and maybe even to cancer (reviewed in Dinarello, 2005). On the other hand, anti-cytokine therapy has little or no organ toxicity or gastrointestinal disturbances and so is well tolerated. Therefore, new site-restricted biologics which block inflammatory cytokines only at sites of inflammation are needed (Rider et al., 2016). In addition, it seems that targeting inflammation in T2DM and obesity is promising but still only show partial reduction of disease. This could be explained by the fact that diabetes and obesity-mediated inflammation involve multiple mechanisms and are not necessarily always linked to hyperglycemia. This clearly highlights the need to identify how anti-inflammatory treatments modulate glucose tolerance and the complications associated with T2DM, but also an urgent necessity to understand how inflammation is dysregulated in T2DM and in obesity. More work is clearly required to fully characterize the mechanisms behind the changes in leukocyte phenotype and in local environments which directly influence leukocyte migration. Finally, more specialistic studies from leukocyte trafficking groups are needed to entirely determine the changes in leukocyte migratory capacity and behaviors *in vitro* and *in vivo* to complete the findings showing changes in expression profiles such as those of adhesion molecules.

AUTHOR CONTRIBUTIONS

LP wrote the first draft of the manuscript. MC and AT contributed to the manuscript revision, read and approved the submitted version. All authors contributed to the article and approved the submitted version.

FUNDING

LP was supported by a Rosetrees Trust award (M814) and MC was supported by a Royal Society Dorothy Hodgkin Research fellowship (DH160044).

REFERENCES

Abe, Y., El-Masri, B., Kimball, K. T., Pownall, H., Reilly, C. F., Osmundsen, K., et al. (1998). Soluble cell adhesion molecules in hypertriglyceridemia and potential significance on monocyte adhesion. *Arterioscler. Thromb. Vasc. Biol.* 18, 723–731. doi: 10.1161/01.atv.18.5.723

Ahmed, R. H., Huri, H. Z., Muniandy, S., Al-Hamodi, Z., Al-absi, B., Alsalahi, A., et al. (2017). Altered circulating concentrations of active glucagon-like peptide (GLP-1) and dipeptidyl peptidase 4 (DPP4) in obese subjects and their association with insulin resistance. *Clin. Biochem.* 50, 746–749. doi: 10.1016/j.clinbiochem.2017.03.008

Ahmed, S. R., McGettrick, H. M., Yates, C. M., Buckley, C. D., Ratcliffe, M. J., Nash, G. B., et al. (2011). Prostaglandin D2 regulates CD4+ memory T cell trafficking across blood vascular endothelium and primes these cells for clearance across lymphatic endothelium. *J. Immunol.* 187, 1432–1439. doi: 10.4049/jimmunol.1100299

Aird, W. C. (2007). Phenotypic heterogeneity of the endothelium: I. Structure function, and mechanisms. *Circul. Res.* 100, 158–173. doi: 10.1161/01.res.0000255691.76142.4a

Aljada, A., Ghanim, H., Saadeh, R., and Dandona, P. (2001). Insulin inhibits NFκB and MCP-1 expression in human aortic endothelial cells. *J. Clin. Endocrinol. Metab.* 86, 450–453. doi: 10.1210/jc.86.1.450

Aljada, A., Saadeh, R., Assian, E., Ghanim, H., and Dandona, P. (2000). Insulin inhibits the expression of intercellular adhesion molecule-1 by human aortic endothelial cells through stimulation of nitric oxide. *J. Clin. Endocrinol. Metab.* 85, 2572–2575. doi: 10.1210/jc.85.7.2572

Andreasen, A. S., Pedersen-Skovsgaard, T., Berg, R. M., Svendsen, K. D., Feldt-Rasmussen, B., and Pedersen, B. K. (2010). Type 2 diabetes mellitus is associated with impaired cytokine response and adhesion molecule expression in human endotoxemia. *Intensive Care Med.* 36, 1548–1555. doi: 10.1007/s00134-010-1845-1

Asghar, A., and Sheikh, N. (2017). Role of immune cells in obesity induced low grade inflammation and insulin resistance. *Cell Immunol.* 315, 18–26. doi: 10.1016/j.cellimm.2017.03.001

Augustyns, K., Bal, G., Thonus, G., Belyaev, A., Zhang, X., Bollaert, W., et al. (2010). ChemInform abstract: the unique properties of dipeptidyl-peptidase IV (DPP IV/CD26) and the therapeutic potential of DPP IV inhibitors*. *ChemInform* 30,

Barouch, F. C., Miyamoto, K., Allport, J. R., Fujita, K., Bursell, S. E., Aiello, L. P., et al. (2000). Integrin-mediated neutrophil adhesion and retinal leukostasis in diabetes. *Invest. Ophthalmol. Vis. Sci.* 41, 1153–1158.

Basta, G., Del, S. T., and De, R. C. (2004). Advanced glycation endproducts: implications for accelerated atherosclerosis in diabetes. *Recenti Prog. Med.* 95, 67–80.

Bengoechea, J. A., and Sa Pessoa, J. (2019). *Klebsiella pneumoniae* infection biology: living to counteract host defences. *FEMS Microbiol. Rev.* 43, 123–144. doi: 10.1093/femsre/fuy043

Berbudi, A., Rahmadika, N., Tjahjadi, A. I., and Ruslami, R. (2020). Type 2 diabetes and its impact on the immune system. *Curr. Diabetes Rev.* 16:442. doi: 10.2174/1573399815666191024085838

Bermudez, V., Finol, F., Parra, N., Parra, M., Pérez, A., Penaranda, L., et al. (2010). PPAR-γ agonists and their role in type 2 diabetes mellitus management. *Am. J. Ther.* 17, 274–283. doi: 10.1097/mjt.0b013e3181c08081

Bertola, A., Ciucci, T., Rousseau, D., Bourlier, V., Duffaut, C., Bonnafous, S., et al. (2012). Identification of adipose tissue dendritic cells correlated with obesity-associated insulin-resistance and inducing Th17 responses in mice and patients. *Diabetes* 61, 2238–2247. doi: 10.2337/db11-1274

Biswas, S. K., and Mantovani, A. (2010). Macrophage plasticity and interaction with lymphocyte subsets: cancer as a paradigm. *Nat. Immunol.* 11, 889–896. doi: 10.1038/ni.1937

Bixel, M. G., Li, H., Petri, B., Khandoga, A. G., Khandoga, A., Zarbock, A., et al. (2010). CD99 and CD99L2 act at the same site as, but independently of, PECAM-1 during leukocyte diapedesis. *Blood* 116, 1172–1184. doi: 10.1182/blood-2009-12-256388

Boels, M. G., Koudijs, A., Avramut, M. C., Sol, W. M., Wang, G., van Oeveren-Rietdijk, A. M., et al. (2017). Systemic monocyte chemotactic protein-1 inhibition modifies renal macrophages and restores glomerular endothelial

glycocalyx and barrier function in diabetic nephropathy. *Am. J. Pathol.* 187, 2430–2440. doi: 10.1016/j.ajpath.2017.07.020

Bono, P., Jalkanen, S., and Salmi, M. (1999). Mouse vascular adhesion protein 1 is a sialoglycoprotein with enzymatic activity and is induced in diabetic insulitis. *Am. J. Pathol.* 155, 1613–1624. doi: 10.1016/s0002-9440(10)65477-6

Braissant, O., Foufelle, F., Scotto, C., Dauça, M., and Wahli, W. (1996). Differential expression of peroxisome proliferator-activated receptors (PPARs): tissue distribution of PPAR-alpha,-beta, and-gamma in the adult rat. *Endocrinology* 137, 354–366. doi: 10.1210/endo.137.1.8536636

Brake, D. K., Smith, E. O. B., Mersmann, H., Smith, C. W., and Robker, R. L. (2006). ICAM-1 expression in adipose tissue: effects of diet-induced obesity in mice. *Am. J. Physiol. Cell Physiol.* 291, C1232–C1239.

Broxmeyer, H. E., Capitano, M., Campbell, T. B., Hangoc, G., and Cooper, S. (2016). Modulation of hematopoietic chemokine effects in vitro and in vivo by DPP-4/CD26. *Stem Cells Dev.* 25, 575–585. doi: 10.1089/scd.2016.0026

Buraczynska, M., Zukowski, P., Wacinski, P., Berger-Smyka, B., Dragan, M., and Mozul, S. (2012). Chemotactic cytokine receptor 5 gene polymorphism: relevance to microvascular complications in type 2 diabetes. *Cytokine* 58, 213–217. doi: 10.1016/j.cyto.2012.01.007

Calabrese, E. J., and Baldwin, L. A. (2001). U-shaped dose-responses in biology, toxicology, and public health. *Annu. Rev. Public Health* 22, 15–33. doi: 10.1146/annurev.publhealth.22.1.15

Calle, M., and Fernandez, M. (2012). Inflammation and type 2 diabetes. *Diabetes Metab.* 38, 183–191. doi: 10.1016/j.diabet.2011.11.006

Carlos, T. M., and Harlan, J. M. (1994). Leukocyte-endothelial adhesion molecules. *Blood* 84, 2068–2101. doi: 10.1182/blood.v84.7.2068.bloodjournal8472068

Carman, C. V., and Springer, T. A. (2004). A transmigratory cup in leukocyte diapedesis both through individual vascular endothelial cells and between them. *J. Cell Biol.* 167, 377–388. doi: 10.1083/jcb.200404129

Carpéné, C., Boulet, N., Chaplin, A., and Mercader, J. (2019). Past, present and future anti-obesity effects of flavin-containing and/or copper-containing amine oxidase inhibitors. *Medicines* 6:9. doi: 10.3390/medicines6010009

Chan, M. E., Adler, B. J., Green, D. E., and Rubin, C. T. (2012). Bone structure and B-cell populations, crippled by obesity, are partially rescued by brief daily exposure to low-magnitude mechanical signals. *FASEB J.* 26, 4855–4863. doi: 10.1096/fj.12-209841

Chaudhuri, A., and Behan, P. O. (2003). Natalizumab for relapsing multiple sclerosis. *N. Engl. J. Med.* 348:1598. doi: 10.1056/nejm200304173481614

Chen, Y., Tian, J., Tian, X., Tang, X., Rui, K., Tong, J., et al. (2014). Adipose tissue dendritic cells enhances inflammation by prompting the generation of Th17 cells. *PLoS One* 9:e92450. doi: 10.1371/journal.pone.0092450

Chimen, M., McGettrick, H. M., Apta, B., Kuravi, S. J., Yates, C. M., Kennedy, A., et al. (2015). Homeostatic regulation of T cell trafficking by a B cell–derived peptide is impaired in autoimmune and chronic inflammatory disease. *Nat. Med.* 21:467. doi: 10.1038/nm.3842

Cho, E., Rimm, E. B., Stampfer, M. J., Willett, W. C., and Hu, F. B. (2002). The impact of diabetes mellitus and prior myocardial infarction on mortality from all causes and from coronary heart disease in men. *J. Am. Coll. Cardiol.* 40, 954–960. doi: 10.1016/s0735-1097(02)02044-2

Chow, F., Nikolic-Paterson, D. J., Ma, F., Ozols, E., Rollins, B., and Tesch, G. H. (2007). Monocyte chemoattractant protein-1-induced tissue inflammation is critical for the development of renal injury but not type 2 diabetes in obese db/db mice. *Diabetologia* 50, 471–480. doi: 10.1007/s00125-006-0497-8

Cook-Mills, J. M., Marchese, M. E., and Abdala-Valencia, H. (2011). Vascular cell adhesion molecule-1 expression and signaling during disease: regulation by reactive oxygen species and antioxidants. *Antioxid. Redox Signal.* 15, 1607–1638. doi: 10.1089/ars.2010.3522

Crane, M. J., Hokeness-Antonelli, K. L., and Salazar-Mather, T. P. (2009). Regulation of inflammatory monocyte/macrophage recruitment from the bone marrow during murine cytomegalovirus infection: role for type I interferons in localized induction of CCR2 ligands. *J. Immunol.* 183, 2810–2817. doi: 10.4049/jimmunol.0900205

Dandona, P., Aljada, A., Mohanty, P., Ghanim, H., Hamouda, W., Assian, E., et al. (2001). Insulin inhibits intranuclear nuclear factor κB and stimulates IκB in mononuclear cells in obese subjects: evidence for an anti-inflammatory effect?". *J. Clin. Endocrinol. Metab.* 86, 3257–3265. doi: 10.1210/jc.86.7.3257

de Vries, M. A., Alipour, A., Klop, B., van de Geijn, G. J. M., Janssen, H. W., Njo, T. L., et al. (2015). Glucose-dependent leukocyte activation in patients with type 2 diabetes mellitus, familial combined hyperlipidemia and healthy controls. *Metabolism* 64, 213–217. doi: 10.1016/j.metabol.2014.10.011

Deacon, C. F. (2018). Peptide degradation and the role of DPP-4 inhibitors in the treatment of type 2 diabetes. *Peptides* 100, 150–157. doi: 10.1016/j.peptides.2017.10.011

DeFuria, J., Belkina, A. C., Jagannathan-Bogdan, M., Snyder-Cappione, J., Carr, J. D., Nersesova, Y. R., et al. (2013). B cells promote inflammation in obesity and type 2 diabetes through regulation of T-cell function and an inflammatory cytokine profile. *Proc. Natl. Acad. Sci. U.S.A.* 110, 5133–5138. doi: 10.1073/pnas.1215840110

Dejana, E., and Giampietro, C. (2012). Vascular endothelial-cadherin and vascular stability. *Curr. Opin. Hematol.* 19, 218–223. doi: 10.1097/moh.0b013e3283523e1c

Dejana, E., Orsenigo, F., Molendini, C., Baluk, P., and McDonald, D. M. (2009). Organization and signaling of endothelial cell-to-cell junctions in various regions of the blood and lymphatic vascular trees. *Cell Tissue Res.* 335, 17–25. doi: 10.1007/s00441-008-0694-5

Deng, T., Liu, J., Deng, Y., Minze, L., Xiao, X., Wright, V., et al. (2017). Adipocyte adaptive immunity mediates diet-induced adipose inflammation and insulin resistance by decreasing adipose Treg cells. *Nat. Communi.* 8:15725.

Dimayuga, F. O., Wang, C., Clark, J. M., Dimayuga, E. R., Dimayuga, V. M., and Bruce-Keller, A. J. (2007). SOD1 overexpression alters ROS production and reduces neurotoxic inflammatory signaling in microglial cells. *J. Neuroimmunol.* 182, 89–99. doi: 10.1016/j.jneuroim.2006.10.003

Dinarello, C. A. (2005). Differences between anti-tumor necrosis factor-alpha monoclonal antibodies and soluble TNF receptors in host defense impairment. *J. Rheumatol. Suppl.* 74, 40–47.

Donath, M. Y., and Shoelson, S. E. (2011). Type 2 diabetes as an inflammatory disease. *Nat. Rev. Immunol.* 11, 98–107.

Drexler, H., Kurz, S., Jeserich, M., Münzel, T., and Hornig, B. (1995). Effect of chronic angiotensin-converting enzyme inhibition on endothelial function in patients with chronic heart failure. *Am. J. Cardiol.* 76, 13E–18E.

Duffaut, C., Galitzky, J., Lafontan, M., and Bouloumié, A. (2009). Unexpected trafficking of immune cells within the adipose tissue during the onset of obesity. *Biochem. Biophys. Res. Commun.* 384, 482–485. doi: 10.1016/j.bbrc.2009.05.002

Dvorak, A. M., and Feng, D. (2001). The vesiculo–vacuolar organelle (VVO): a new endothelial cell permeability organelle. *J. Histochem. Cytochem.* 49, 419–431. doi: 10.1177/002215540104900401

Eguchi, K., and Nagai, R. (2017). Islet inflammation in type 2 diabetes and physiology. *J. Clin. Invest.* 127, 14–23. doi: 10.1172/jci88877

Ehses, J., Lacraz, G., Giroix, M.-H., Schmidlin, F., Coulaud, J., Kassis, N., et al. (2009). IL-1 antagonism reduces hyperglycemia and tissue inflammation in the type 2 diabetic GK rat. *Proc. Natl. Acad. Sci. U.S.A.* 106, 13998–14003. doi: 10.1073/pnas.0810087106

Elgazar-Carmon, V., Rudich, A., Hadad, N., and Levy, R. (2008). Neutrophils transiently infiltrate intra-abdominal fat early in the course of high-fat feeding. *J. Lipid Res.* 49, 1894–1903. doi: 10.1194/jlr.m800132-jlr200

Engeli, S., Feldpausch, M., Gorzelniak, K., Hartwig, F., Heintze, U., Janke, J., et al. (2003). Association between adiponectin and mediators of inflammation in obese women. *Diabetes* 52, 942–947. doi: 10.2337/diabetes.52.4.942

Esser, N., Legrand-Poels, S., Piette, J., Scheen, A. J., and Paquot, N. (2014). Inflammation as a link between obesity, metabolic syndrome and type 2 diabetes. *Diabetes. Res. Clin. Pract.* 105, 141–150. doi: 10.1016/j.diabres.2014.04.006

Fan, Z., and Ley, K. (2015). Leukocyte arrest: biomechanics and molecular mechanisms of β2 integrin activation. *Biorheology* 52, 353–377. doi: 10.3233/bir-15085

Farhangkhoee, H., Khan, Z. A., Kaur, H., Xin, X., Chen, S., and Chakrabarti, S. (2006). Vascular endothelial dysfunction in diabetic cardiomyopathy: pathogenesis and potential treatment targets. *Pharmacol. Ther.* 111, 384–399. doi: 10.1016/j.pharmthera.2005.10.008

Feuerer, M., Herrero, L., Cipolletta, D., Naaz, A., Wong, J., Nayer, A., et al. (2009). Lean, but not obese, fat is enriched for a unique population of regulatory T cells that affect metabolic parameters. *Nat. Med.* 15, 930–939. doi: 10.1038/nm.2002

Foot, J. S., Yow, T. T., Schilter, H., Buson, A., Deodhar, M., Findlay, A. D., et al. (2013). PXS-4681A, a potent and selective mechanism-based inhibitor of SSAO/VAP-1 with anti-inflammatory effects in vivo. *J. Pharmacol. Exp. Ther.* 347, 365–374. doi: 10.1124/jpet.113.207613

Galkina, E., and Ley, K. (2007). Vascular adhesion molecules in atherosclerosis. *Arterioscler. Thromb. Vasc. Biol.* 27, 2292–2301. doi: 10.1161/atvbaha.107.149179

Gao, D., Madi, M., Ding, C., Fok, M., Steele, T., Ford, C., et al. (2014). Interleukin-1β mediates macrophage-induced impairment of insulin signaling in human primary adipocytes. *Am. J. Physiol. Endocrinol. Metab.* 307, E289–E304.

Giagulli, C., Ottoboni, L., Caveggion, E., Rossi, B., Lowell, C., Constantin, G., et al. (2006). The Src family kinases Hck and Fgr are dispensable for inside-out, chemoattractant-induced signaling regulating β2 integrin affinity and valency in neutrophils, but are required for β2 integrin-mediated outside-in signaling involved in sustained adhesion. *J. Immunol.* 177, 604–611. doi: 10.4049/jimmunol.177.1.604

Giagulli, C., Scarpini, E., Ottoboni, L., Narumiya, S., Butcher, E. C., Constantin, G., et al. (2004). RhoA and ζ PKC control distinct modalities of LFA-1 activation by chemokines: critical role of LFA-1 affinity triggering in lymphocyte in vivo homing. *Immunity* 20, 25–35. doi: 10.1016/s1074-7613(03)00350-9

Gilliet, M., Cao, W., and Liu, Y. J. (2008). Plasmacytoid dendritic cells: sensing nucleic acids in viral infection and autoimmune diseases. *Nat. Rev. Immunol.* 8, 594–606. doi: 10.1038/nri2358

Gu, H. F., Ma, J., Gu, K. T., and Brismar, K. (2013). Association of intercellular adhesion molecule 1 (ICAM1) with diabetes and diabetic nephropathy. *Front. Endocrinol.* 3:179. doi: 10.3389/fendo.2012.00179

Guo, X., Li, J., Tang, R., Zhang, G., Zeng, H., Wood, R. J., et al. (2017). High fat diet alters gut microbiota and the expression of paneth cell-antimicrobial peptides preceding changes of circulating inflammatory cytokines. *Mediators Inflamm.* 2017:9474896.

Gustavsson, C., Agardh, C.-D., Zetterqvist, A. V., Nilsson, J., Agardh, E., and Gomez, M. F. (2010). Vascular cellular adhesion molecule-1 (VCAM-1) expression in mice retinal vessels is affected by both hyperglycemia and hyperlipidemia. *PLoS One* 5:e12699. doi: 10.1371/journal.pone.0012699

Hadi, H. A., and Al Suwaidi, J. (2007). Endothelial dysfunction in diabetes mellitus. *Vasc. Health Risk Manag.* 3, 853–876.

Harjunpää, H., Llort Asens, M., Guenther, C., and Fagerholm, S. C. (2019). Cell adhesion molecules and their roles and regulation in the immune and tumor microenvironment. *Front. Immunol.* 10:1078. doi: 10.3389/fimmu.2019.01078

Herder, C., Haastert, B., Müller-Scholze, S., Koenig, W., Thorand, B., Holle, R., et al. (2005). Association of systemic chemokine concentrations with impaired glucose tolerance and type 2 diabetes: results from the cooperative health research in the region of augsburg survey S4 (KORA S4). *Diabetes* 54(Suppl. 2), S11–S17.

Hocaoglu-Emre, F. S., Saribal, D., Yenmis, G., and Guvenen, G. (2017). Vascular cell adhesion molecule 1, intercellular adhesion molecule 1, and cluster of differentiation 146 levels in patients with Type 2 diabetes with complications. *Endocrinol. Metab.* 32, 99–105. doi: 10.3803/enm.2017.32.1.99

Hostetter, M. K. (1990). Handicaps to host defense: effects of hyperglycemia on C3 and *Candida albicans*. *Diabetes* 39, 271–275. doi: 10.2337/diabetes.39.3.271

Hotamisligil, G. S., Shargill, N. S., and Spiegelman, B. M. (1993). Adipose expression of tumor necrosis factor-alpha: direct role in obesity-linked insulin resistance. *Science* 259, 87–91. doi: 10.1126/science.7678183

Hotta, K., Funahashi, T., Arita, Y., Takahashi, M., Matsuda, M., Okamoto, Y., et al. (2000). Plasma concentrations of a novel, adipose-specific protein, adiponectin, in type 2 diabetic patients. *Arterioscler. Thromb. Vasc. Biol.* 20, 1595–1599. doi: 10.1161/01.atv.20.6.1595

Huang, J., Xiao, Y., Zheng, P., Zhou, W., Wang, Y., Huang, G., et al. (2019). Distinct neutrophil counts and functions in newly diagnosed type 1 diabetes, latent autoimmune diabetes in adults, and type 2 diabetes. *Diabetes Metab. Res. Rev.* 35:e3064. doi: 10.1002/dmrr.3064

Huh, J. H., Kim, H. M., Lee, E. S., Kwon, M. H., Lee, B. R., Ko, H. J., et al. (2018). Dual CCR2/5 antagonist attenuates obesity-induced insulin resistance by regulating macrophage recruitment and M1/M2 status. *Obesity* 26, 378–386. doi: 10.1002/oby.22103

Huo, Y., and Ley, K. (2001). Adhesion molecules and atherogenesis. *Acta Physiol. Scand.* 173, 35–43. doi: 10.1046/j.1365-201x.2001.00882.x

Hyduk, S. J., Chan, J. R., Duffy, S. T., Chen, M., Peterson, M. D., Waddell, T. K., et al. (2007). Phospholipase C, calcium, and calmodulin are critical for α4β1 integrin affinity up-regulation and monocyte arrest triggered by chemoattractants. *Blood* 109, 176–184. doi: 10.1182/blood-2006-01-029199

Hyun, E., Ramachandran, R., Hollenberg, M. D., and Vergnolle, N. (2011). Mechanisms behind the anti-inflammatory actions of insulin. *Crit. Rev. Immunol.* 31, 307–340. doi: 10.1615/critrevimmunol.v31.i4.30

Ilan, Y., Maron, R., Tukpah, A.-M., Maioli, T. U., Murugaiyan, G., Yang, K., et al. (2010). Induction of regulatory T cells decreases adipose inflammation and alleviates insulin resistance in ob/ob mice. *Proc. Natl. Acad. Sci. U.S.A.* 107, 9765–9770. doi: 10.1073/pnas.0908771107

Iliaki, E., Poulaki, V., Mitsiades, N., Mitsiades, C. S., Miller, J. W., and Gragoudas, E. S. (2009). Role of α4 integrin (CD49d) in the pathogenesis of diabetic retinopathy. *Invest. Ophthalmol. Vis. Sci.* 50, 4898–4904. doi: 10.1167/iovs.08-2013

Isobe, M., Suzuki, J.-I., Yamazaki, S., Yazaki, Y., Horie, S., Okubo, Y., et al. (1997). Regulation by differential development of Th1 and Th2 cells in peripheral tolerance to cardiac allograft induced by blocking ICAM-1/LFA-1 adhesion. *Circulation* 96, 2247–2253. doi: 10.1161/01.cir.96.7.2247

Janeway, C. A. Jr., Travers, P., Walport, M., and Shlomchik, M. J. (2001). *The Mucosal Immune System. Immunobiology: The Immune System in Health and Disease*, 5th Edn. New York, NY: Garland Science.

Jargaud, V., Bour, S., Tercé, F., Collet, X., Valet, P., Bouloumié, A., et al. (2020). Obesity of mice lacking VAP-1/SSAO by Aoc3 gene deletion is reproduced in mice expressing a mutated vascular adhesion protein-1 (VAP-1) devoid of amine oxidase activity. *J. Physiol. Biochem.* doi: 10.1007/s13105-020-00756-y Online ahead of print

Javid, A., Zlotnikov, N., Pětrošová, H., Tang, T. T., Zhang, Y., Bansal, A. K., et al. (2016). Hyperglycemia impairs neutrophil-mediated bacterial clearance in mice infected with the Lyme disease pathogen. *PLoS One* 11:e0158019. doi: 10.1371/journal.pone.0158019

Kansas, G. S. (1996). Selectins and their ligands: current concepts and controversies. *Blood* 88, 3259–3287. doi: 10.1182/blood.v88.9.3259.bloodjournal8893259

Katsiki, N., Mantzoros, C., and Mikhailidis, D. P. (2017). Adiponectin, lipids and atherosclerosis. *Curr. Opin. Lipidol.* 28, 347–354. doi: 10.1097/mol.0000000000000431

Katsumata, K., Ishihara, J., Fukunaga, K., Ishihara, A., Yuba, E., Budina, E., et al. (2019). Conferring extracellular matrix affinity enhances local therapeutic efficacy of anti-TNF-α antibody in a murine model of rheumatoid arthritis. *Arthritis Res. Ther.* 21:298.

Kawanishi, N., Yano, H., Yokogawa, Y., and Suzuki, K. (2010). Exercise training inhibits inflammation in adipose tissue via both suppression of macrophage infiltration and acceleration of phenotypic switching from M1 to M2 macrophages in high-fat-diet-induced obese mice. *Exerc. Immunol. Rev.* 16, 105–118.

Khalfaoui, T., Lizard, G., and Ouertani-Meddeb, A. (2008). Adhesion molecules (ICAM-1 and VCAM-1) and diabetic retinopathy in type 2 diabetes. *J. Mol. Histol.* 39, 243–249. doi: 10.1007/s10735-007-9159-5

Kim, M., Carman, C. V., and Springer, T. A. (2003). Bidirectional transmembrane signaling by cytoplasmic domain separation in integrins. *Science* 301, 1720–1725. doi: 10.1126/science.1084174

Kitade, H., Sawamoto, K., Nagashimada, M., Inoue, H., Yamamoto, Y., Sai, Y., et al. (2012). CCR5 plays a critical role in obesity-induced adipose tissue inflammation and insulin resistance by regulating both macrophage recruitment and M1/M2 status. *Diabetes* 61, 1680–1690. doi: 10.2337/db11-1506

Kizilgul, M., Sencar, E., Bekir, U., Beysel, S., Ozcelik, O., Ozbek, M., et al. (2018). Components of the complete blood count in type 2 diabetes mellitus with inadequate glycemic control. *Dicle Tıp Dergisi* 45, 113–120.

Kulcsar, K. A., Coleman, C. M., Beck, S. E., and Frieman, M. B. (2019). Comorbid diabetes results in immune dysregulation and enhanced disease severity following MERS-CoV infection. *JCI Insight* 4:e131774.

Kumar, M., Roe, K., Nerurkar, P. V., Orillo, B., Thompson, K. S., Verma, S., et al. (2014). Reduced immune cell infiltration and increased pro-inflammatory mediators in the brain of Type 2 diabetic mouse model infected with West Nile virus. *J. Neuroinflammation* 11:80. doi: 10.1186/1742-2094-11-80

Kummer, D., and Ebnet, K. (2018). Junctional adhesion molecules (JAMs): the JAM-integrin connection. *Cells* 7:25. doi: 10.3390/cells7040025

Kuo, C.-H., Wei, J.-N., Yang, C.-Y., Ou, H.-Y., Wu, H.-T., Fan, K.-C., et al. (2019). Serum vascular adhesion protein-1 is up-regulated in hyperglycemia

and is associated with incident diabetes negatively. *Int. J. Obes.* 43, 512–522. doi: 10.1038/s41366-018-0172-4

Kuwano, Y., Spelten, O., Zhang, H., Ley, K., and Zarbock, A. (2010). Rolling on E-or P-selectin induces the extended but not high-affinity conformation of LFA-1 in neutrophils. *Blood* 116, 617–624. doi: 10.1182/blood-2010-01-266122

Lambeir, A.-M., Durinx, C., Scharpé, S., and De Meester, I. (2003). Dipeptidyl-peptidase IV from bench to bedside: an update on structural properties, functions, and clinical aspects of the enzyme DPP IV. *Crit. Rev. Clin. Lab. Sci.* 40, 209–294. doi: 10.1080/713609354

Larsen, C. M., Faulenbach, M., Vaag, A., Vølund, A., Ehses, J. A., Seifert, B., et al. (2007). Interleukin-1–receptor antagonist in type 2 diabetes mellitus. *N. Engl. J. Med.* 356, 1517–1526.

Lei, Y., Devarapu, S. K., Motrapu, M., Cohen, C., Lindenmeyer, M. T., Moll, S., et al. (2019). Interleukin-1β inhibition for chronic kidney disease in obese mice with type 2 diabetes. *Front. Immunol.* 10:1223. doi: 10.3389/fimmu.2019.01223

Lew, E. A., and Stoffel, E. M. (2003). Natalizumab for active Crohn's disease. *N. Engl. J. Med.* 348:1599.

Ley, K. (2007). *Adhesion Molecules: Function and Inhibition*. Berlin: Springer Science & Business Media.

Ley, K., Laudanna, C., Cybulsky, M. I., and Nourshargh, S. (2007). Getting to the site of inflammation: the leukocyte adhesion cascade updated. *Nat. Rev. Immunol.* 7, 678–689. doi: 10.1038/nri2156

Li, H.-Y., Lin, H.-A., Nien, F.-J., Wu, V.-C., Jiang, Y.-D., Chang, T.-J., et al. (2016). Serum vascular adhesion protein-1 predicts end-stage renal disease in patients with type 2 diabetes. *PLoS One* 11:e0147981. doi: 10.1371/journal.pone.0147981

Liu, H.-F., Zhang, H.-J., Hu, Q.-X., Liu, X.-Y., Wang, Z.-Q., Fan, J.-Y., et al. (2012). Altered polarization, morphology, and impaired innate immunity germane to resident peritoneal macrophages in mice with long-term type 2 diabetes. *J. Biomed. Biotechnol.* 2012:867023.

Liu, Y., Lu, X., Li, X., Du, P., and Qin, G. (2020). High-fat diet triggers obesity-related early infiltration of macrophages into adipose tissue and transient reduction of blood monocyte count. *Mol. Immunol.* 117, 139–146.

Liu, Y., Shaw, S. K., Ma, S., Yang, L., Luscinskas, F. W., and Parkos, C. A. (2004). Regulation of leukocyte transmigration: cell surface interactions and signaling events. *J. Immunol.* 172, 7–13.

Lontchi-Yimagou, E., Sobngwi, E., Matsha, T. E., and Kengne, A. P. (2013). Diabetes mellitus and inflammation. *Curr. Diab. Rep.* 13, 435–444.

Luo, A., Leach, S. T., Barres, R., Hesson, L. B., Grimm, M. C., and Simar, D. (2017). The microbiota and epigenetic regulation of T helper 17/regulatory T cells: in search of a balanced immune system. *Front. Immunol.* 8:417. doi: 10.3389/fimmu.2017.00417

Luu, N. T., Rainger, G. E., and Nash, G. B. (2000). Differential ability of exogenous chemotactic agents to disrupt transendothelial migration of flowing neutrophils. *J. Immunol.* 164, 5961–5969.

Marco, M., Fortin, C., and Fulop, T. (2013). Membrane-type matrix metalloproteinases: key mediators of leukocyte function. *J. Leukoc. Biol.* 94, 237–246.

Mariño, E., and Grey, S. T. (2012). B cells as effectors and regulators of autoimmunity. *Autoimmunity* 45, 377–387.

Martinez, N., Ketheesan, N., Martens, G. W., West, K., Lien, E., and Kornfeld, H. (2016). Defects in early cell recruitment contribute to the increased susceptibility to respiratory *Klebsiella pneumoniae* infection in diabetic mice. *Microbes Infect.* 18, 649–655.

Martinez-Pomares, L., Reid, D. M., Brown, G. D., Taylor, P. R., Stillion, R. J., Linehan, S. A., et al. (2003). Analysis of mannose receptor regulation by IL-4, IL-10, and proteolytic processing using novel monoclonal antibodies. *J. Leukoc. Biol.* 73, 604–613.

Matsumoto, K., Sera, Y., Nakamura, H., Ueki, Y., and Miyake, S. (2002). Serum concentrations of soluble adhesion molecules are related to degree of hyperglycemia and insulin resistance in patients with type 2 diabetes mellitus. *Diabetes. Res. Clin. Pract.* 55, 131–138.

McEver, R. P. (2015). Selectins: initiators of leucocyte adhesion and signalling at the vascular wall. *Cardiovasc. Res.* 107, 331–339.

McLeod, D. S., Lefer, D. J., Merges, C., and Lutty, G. A. (1995). Enhanced expression of intracellular adhesion molecule-1 and P-selectin in the diabetic human retina and choroid. *Am. J. Pathol.* 147:642.

Meigs, J. B., Hu, F. B., Rifai, N., and Manson, J. E. (2004). Biomarkers of endothelial dysfunction and risk of type 2 diabetes mellitus. *JAMA* 291, 1978–1986.

Mentlein, R. (1999). Dipeptidyl-peptidase IV (CD26)-role in the inactivation of regulatory peptides. *Regul. Pept.* 85, 9–24.

Mittelbrunn, M., Molina, A., Escribese, M. M., Yáñez-Mó, M., Escudero, E., Ursa, Á, et al. (2004). VLA-4 integrin concentrates at the peripheral supramolecular activation complex of the immune synapse and drives T helper 1 responses. *Proc. Natl. Acad. Sci. U.S.A.* 101, 11058–11063.

Miyachi, Y., Tsuchiya, K., Komiya, C., Shiba, K., Shimazu, N., Yamaguchi, S., et al. (2017). Roles for cell-cell adhesion and contact in obesity-induced hepatic myeloid cell accumulation and glucose intolerance. *Cell Rep.* 18, 2766–2779.

Miyasaka, M., and Tanaka, T. (2004). Lymphocyte trafficking across high endothelial venules: dogmas and enigmas. *Nat. Rev. Immunol.* 4, 360–370.

Monickaraj, F., Oruganti, S. R., McGuire, P., and Das, A. (2020). A potential novel therapeutic target in diabetic retinopathy: a chemokine receptor (CCR2/CCR5) inhibitor reduces retinal vascular leakage in an animal model. *Graefes Arch. Clin. Exp. Ophthalmol.* 259, 93–100.

Mooradian, A. D., Reed, R. L., Meredith, K. E., and Scuderi, P. (1991). Serum levels of tumor necrosis factor and IL-1α and IL-1β in diabetic patients. *Diabetes Care* 14, 63–65.

Moradi, S., Kerman, S. R. J., Rohani, F., and Salari, F. (2012). Association between diabetes complications and leukocyte counts in Iranian patients. *J. Inflamm. Res.* 5, 7–11.

Moreno, J. A., Gomez-Guerrero, C., Mas, S., Sanz, A. B., Lorenzo, O., Ruiz-Ortega, M., et al. (2018). Targeting inflammation in diabetic nephropathy: a tale of hope. *Expert Opin. Investig. Drugs* 27, 917–930.

Mosser, D. M. (2003). The many faces of macrophage activation. *J. Leukoc. Biol.* 73, 209–212.

Mráz, M., Cinkajzlová, A., Kloučková, J., Lacinová, Z., Kratochvílová, H., Lipš, M., et al. (2019). Dendritic cells in subcutaneous and epicardial adipose tissue of subjects with type 2 diabetes, obesity, and coronary artery disease. *Mediators Inflamm.* 2019:5481725.

Mraz, M., and Haluzik, M. (2014). The role of adipose tissue immune cells in obesity and low-grade inflammation. *J. Endocrinol.* 222, R113–R127.

Muller, W. A. (2003). Leukocyte–endothelial-cell interactions in leukocyte transmigration and the inflammatory response. *Trends Immunol.* 24, 326–333.

Muller, W. A. (2011). Mechanisms of leukocyte transendothelial migration. *Annu. Rev. Pathol.* 6, 323–344.

Muller, W. A. (2013). Getting leukocytes to the site of inflammation. *Vet. Pathol.* 50, 7–22.

Mulvihill, E. E., and Drucker, D. J. (2014). Pharmacology, physiology, and mechanisms of action of dipeptidyl peptidase-4 inhibitors. *Endocr. Rev.* 35, 992–1019.

Musilli, C., Paccosi, S., Pala, L., Gerlini, G., Ledda, F., Mugelli, A., et al. (2011). Characterization of circulating and monocyte-derived dendritic cells in obese and diabetic patients. *Mol. Immunol.* 49, 234–238.

Mutgan, A. C., Jandl, K., and Kwapiszewska, G. (2020). Endothelial basement membrane components and their products, matrikines: active drivers of pulmonary hypertension?". *Cells* 9:2029.

Newman, P. J., Berndt, M. C., Gorski, J., White, G. C., Lyman, S., Paddock, C., et al. (1990). PECAM-1 (CD31) cloning and relation to adhesion molecules of the immunoglobulin gene superfamily. *Science* 247, 1219–1222.

Nguyen, D. V., Shaw, L., and Grant, M. (2012). Inflammation in the pathogenesis of microvascular complications in diabetes. *Front. Endocrinol.* 3:170. doi: 10.3389/fendo.2012.00170

Nishimura, S., Manabe, I., Nagasaki, M., Eto, K., Yamashita, H., Ohsugi, M., et al. (2009). CD8+ effector T cells contribute to macrophage recruitment and adipose tissue inflammation in obesity. *Nat. Med.* 15, 914–920.

Noshita, N., Sugawara, T., Hayashi, T., Lewén, A., Omar, G., and Chan, P. H. (2002). Copper/zinc superoxide dismutase attenuates neuronal cell death by preventing extracellular signal-regulated kinase activation after transient focal cerebral ischemia in mice. *J. Neurosci.* 22, 7923–7930.

Nunemaker, C. S., Chung, H. G., Verrilli, G. M., Corbin, K. L., Upadhye, A., and Sharma, P. R. (2014). Increased serum CXCL1 and CXCL5 are linked to obesity, hyperglycemia, and impaired islet function. *J. Endocrinol.* 222, 267–276.

O'Keeffe, M., Hochrein, H., Vremec, D., Caminschi, I., Miller, J. L., Anders, E. M., et al. (2002). Mouse plasmacytoid cells: long-lived cells, heterogeneous

in surface phenotype and function, that differentiate into CD8+ dendritic cells only after microbial stimulus. *J. Exp. Med.* 196, 1307–1319.

Okouchi, M., Okayama, N., Imai, S., Omi, H., Shimizu, M., Fukutomi, T., et al. (2002). High insulin enhances neutrophil transendothelial migration through increasing surface expression of platelet endothelial cell adhesion molecule-1 via activation of mitogen activated protein kinase. *Diabetologia* 45, 1449–1456.

Olefsky, J. M. (2000). Treatment of insulin resistance with peroxisome proliferator–activated receptor γ agonists. *J. Clin. Invest.* 106, 467–472.

Oliver, E., McGillicuddy, F., Phillips, C., Toomey, S., and Roche, H. M. (2010). Postgraduate Symposium. The role of inflammation and macrophage accumulation in the development of obesity-induced type 2 diabetes mellitus and the possible therapeutic effects of long-chain n-3 PUFA. *Proc. Nutr. Soc.* 69, 232–243.

Omar, B., and Ahrén, B. (2014). Pleiotropic mechanisms for the glucose-lowering action of DPP-4 inhibitors. *Diabetes* 63, 2196–2202.

Ouchi, N., Kihara, S., Arita, Y., Maeda, K., Kuriyama, H., Okamoto, Y., et al. (1999). Novel modulator for endothelial adhesion molecules: adipocyte-derived plasma protein adiponectin. *Circulation* 100, 2473–2476.

Ouedraogo, R., Gong, Y., Berzins, B., Wu, X., Mahadev, K., Hough, K., et al. (2007). Adiponectin deficiency increases leukocyte-endothelium interactions via upregulation of endothelial cell adhesion molecules in vivo. *J. Clin. Invest.* 117, 1718–1726.

Pagliari, D., Saviano, A., Newton, E., Serricchio, M., Dal Lago, A., Gasbarrini, A., et al. (2018). Gut microbiota-immune system crosstalk and pancreatic disorders. *Mediators Inflamm.* 2018:7946431.

Palella, E., Cimino, R., Pullano, S. A., Fiorillo, A. S., Gulletta, E., Brunetti, A., et al. (2020). Laboratory parameters of hemostasis, adhesion molecules, and inflammation in type 2 diabetes mellitus: correlation with glycemic control. *Int. J. Environ. Res. Public Health* 17:300.

Papazafiropoulou, A., Kardara, M., Sotiropoulos, A., Bousboulas, S., Stamataki, P., and Pappas, S. (2010). Plasma glucose levels and white blood cell count are related with ankle brachial index in type 2 diabetic subjects. *Hellenic J. Cardiol.* 51, 402–406.

Paquot, N., Castillo, M. J., Lefeȉbvre, P. J., and Scheen, A. J. (2000). No increased insulin sensitivity after a single intravenous administration of a recombinant human tumor necrosis factor receptor: Fc fusion protein in obese insulin-resistant patients. *J. Clin. Endocrinol. Metab.* 85, 1316–1319.

Pham, C. T. (2006). Neutrophil serine proteases: specific regulators of inflammation. *Nat. Rev. Immunol.* 6, 541–550.

Rangasamy, S., McGuire, P. G., Nitta, C. F., Monickaraj, F., Oruganti, S. R., and Das, A. (2014). Chemokine mediated monocyte trafficking into the retina: role of inflammation in alteration of the blood-retinal barrier in diabetic retinopathy. *PLoS One* 9:e108508. doi: 10.1371/journal.pone.0108508

Reinehr, T., Karges, B., Meissner, T., Wiegand, S., Stoffel-Wagner, B., Holl, R. W., et al. (2016). Inflammatory markers in obese adolescents with type 2 diabetes and their relationship to hepatokines and adipokines. *J. Pediatr.* 173, 131–135. doi: 10.1016/j.jpeds.2016.02.055

Reyat, J. S., Chimen, M., Noy, P. J., Szyroka, J., Rainger, G. E., and Tomlinson, M. G. (2017). ADAM10-interacting tetraspanins Tspan5 and Tspan17 regulate VE-cadherin expression and promote T lymphocyte transmigration. *J. Immunol.* 199, 666–676. doi: 10.4049/jimmunol.1600713

Richardson, V. R., Smith, K. A., and Carter, A. M. (2013). Adipose tissue inflammation: feeding the development of type 2 diabetes mellitus. *Immunobiology* 218, 1497–1504. doi: 10.1016/j.imbio.2013.05.002

Rider, P., Carmi, Y., and Cohen, I. (2016). Biologics for targeting inflammatory cytokines, clinical uses, and limitations. *Int. J. Cell Biol.* 2016:9259646. doi: 10.1155/2016/9259646

Ruan, H., and Dong, L. Q. (2016). Adiponectin signaling and function in insulin target tissues. *J. Mol. Cell Biol.* 8, 101–109. doi: 10.1093/jmcb/mjw014

Rutledge, N. S., and Muller, W. A. (2020). Understanding molecules that mediate leukocyte extravasation. *Curr. Pathobiol. Rep.* 8, 25–35. doi: 10.1007/s40139-020-00207-9

Rutledge, N. S., Weber, E. W., Winger, R., Tourtellotte, W. G., Park, S. H., and Muller, W. A. (2015). CD99-like 2 (CD99L2)-deficient mice are defective in the acute inflammatory response. *Exp. Mol. Pathol.* 99, 455–459. doi: 10.1016/j.yexmp.2015.08.011

Salmi, M., and Jalkanen, S. (2019). Vascular adhesion protein-1: a cell surface amine oxidase in translation. *Antioxid. Redox Signal.* 30, 314–332. doi: 10.1089/ars.2017.7418

Sampson, M., Davies, I., Brown, J., Ivory, K., and Hughes, D. (2002). Monocyte and neutrophil adhesion molecule expression during acute hyperglycemia and after antioxidant treatment in type 2 diabetes and control patients. *Arterioscler. Thromb. Vasc. Biol.* 22, 1187–1193. doi: 10.1161/01.ATV.0000021759.08060.63

Sayyed, S. G., Ryu, M., Kulkarni, O. P., Schmid, H., Lichtnekert, J., Grüner, S., et al. (2011). An orally active chemokine receptor CCR2 antagonist prevents glomerulosclerosis and renal failure in type 2 diabetes. *Kidney Int.* 80, 68–78. doi: 10.1038/ki.2011.102

Schenkel, A. R., Mamdouh, Z., Chen, X., Liebman, R. M., and Muller, W. A. (2002). CD99 plays a major role in the migration of monocytes through endothelial junctions. *Nat. Immunol.* 3, 143–150. doi: 10.1038/ni749

Schenkel, A. R., Mamdouh, Z., and Muller, W. A. (2004). Locomotion of monocytes on endothelium is a critical step during extravasation. *Nat. Immunol.* 5, 393–400. doi: 10.1038/ni1051

Seelige, R., Natsch, C., März, S., Jing, D., Frye, M., Butz, S., et al. (2013). Cutting edge: endothelial-specific gene ablation of CD99L2 impairs leukocyte extravasation in vivo. *J. Immunol.* 190, 892–896. doi: 10.4049/jimmunol.1202721

Shah, R., Hinkle, C. C., Ferguson, J. F., Mehta, N. N., Li, M., Qu, L., et al. (2011). Fractalkine is a novel human adipochemokine associated with type 2 diabetes. *Diabetes* 60, 1512–1518. doi: 10.2337/db10-0956

Shanaki, M., Khosravi, M., Khoshdooni-Farahani, A., Dadashi, A., Heydari, M. F., Delfan, M., et al. (2020). High-intensity interval training reversed high-fat diet–induced M1-macrophage polarization in rat adipose tissue via inhibition of NOTCH signaling. *J. Inflamm. Res.* 13, 165–174. doi: 10.2147/JIR.S237049

Shaw, S. K., Bamba, P. S., Perkins, B. N., and Luscinskas, F. W. (2001). Real-time imaging of vascular endothelial-cadherin during leukocyte transmigration across endothelium. *J. Immunol.* 167, 2323–2330. doi: 10.4049/jimmunol.167.4.2323

Shirakawa, J., Fujii, H., Ohnuma, K., Sato, K., Ito, Y., Kaji, M., et al. (2011). Diet-induced adipose tissue inflammation and liver steatosis are prevented by DPP-4 inhibition in diabetic mice. *Diabetes* 60, 1246–1257. doi: 10.2337/db10-1338

Shrestha, B., and Diamond, M. S. (2004). Role of CD8+ T cells in control of West Nile virus infection. *J. Virol.* 78, 8312–8321. doi: 10.1128/JVI.78.15.8312-8321.2004

Signoretti, M., Roggiolani, R., Stornello, C., Fave Delle, G., and Capurso, G. (2017). Gut microbiota and pancreatic diseases. *Minerva Gastroenterol. Dietol.* 63, 399–410.

Sloan-Lancaster, J., Abu-Raddad, E., Polzer, J., Miller, J. W., Scherer, J. C., De Gaetano, A., et al. (2013). Double-blind, randomized study evaluating the glycemic and anti-inflammatory effects of subcutaneous LY2189102, a neutralizing IL-1β antibody, in patients with type 2 diabetes. *Diabetes Care* 36, 2239–2246. doi: 10.2337/dc12-1835

Soehnlein, O., Zernecke, A., Eriksson, E. E., Rothfuchs, A. G., Pham, C. T., Herwald, H., et al. (2008). Neutrophil secretion products pave the way for inflammatory monocytes. *Blood* 112, 1461–1471. doi: 10.1182/blood-2008-02-139634

Song, J., Zhang, X., Buscher, K., Wang, Y., Wang, H., Di, J., et al. (2017). Endothelial basement membrane laminin 511 contributes to endothelial junctional tightness and thereby inhibits leukocyte transmigration. *Cell Rep.* 18, 1256–1269. doi: 10.1016/j.celrep.2016.12.092

Stefanovic-Racic, M., Yang, X., Turner, M. S., Mantell, B. S., Stolz, D. B., Sumpter, T. L., et al. (2012). Dendritic cells promote macrophage infiltration and comprise a substantial proportion of obesity-associated increases in CD11c+ cells in adipose tissue and liver. *Diabetes* 61, 2330–2339. doi: 10.2337/db11-1523

Stolen, M. C., Madanat, R., Marti, L., Kari, S., Yegutkin, G. G., Sariola, H., et al. (2004). Semicarbazide-sensitive amine oxidase overexpression has dual consequences: insulin mimicry and diabetes-like complications. *FASEB J.* 18, 702–704. doi: 10.1096/fj.03-0562fje

Sullivan, D. P., Watson, R. L., and Muller, W. A. (2016). 4D intravital microscopy uncovers critical strain differences for the roles of PECAM and CD99 in

leukocyte diapedesis. *Am. J. Physiol. Heart Circul. Physiol.* 311, H621–H632. doi: 10.1152/ajpheart.00289.2016

Sundara Rajan, S., and Longhi, M. P. (2016). Dendritic cells and adipose tissue. *Immunology* 149, 353–361. doi: 10.1111/imm.12653

Takase, H., Nakazawa, A., Yamashita, S., Toriyama, T., Sato, K., Ueda, R., et al. (2007). Pioglitazone produces rapid and persistent reduction of vascular inflammation in patients with hypertension and type 2 diabetes mellitus who are receiving angiotensin II receptor blockers. *Metabolism* 56, 559–564. doi: 10.1016/j.metabol.2007.01.002

Talukdar, S., Bandyopadhyay, G., Li, D., Xu, J., McNelis, J., Lu, M., et al. (2012). Neutrophils mediate insulin resistance in mice fed a high-fat diet through secreted elastase. *Nat. Med.* 18, 1407–1412. doi: 10.1038/nm.2885

Tamura, T., Tailor, P., Yamaoka, K., Kong, H. J., Tsujimura, H., O'Shea, J. J., et al. (2005). IFN regulatory factor-4 and-8 govern dendritic cell subset development and their functional diversity. *J. Immunol.* 174, 2573–2581. doi: 10.4049/jimmunol.174.5.2573

Tan, K. S., Lee, K. O., Low, K. C., Gamage, A. M., Liu, Y., Tan, G.-Y. G., et al. (2012). Glutathione deficiency in type 2 diabetes impairs cytokine responses and control of intracellular bacteria. *J. Clin. Invest.* 122, 2289–2300. doi: 10.1172/JCI57817

Tarabra, E., Giunti, S., Barutta, F., Salvidio, G., Burt, D., Deferrari, G., et al. (2009). Effect of the monocyte chemoattractant protein-1/CC chemokine receptor 2 system on nephrin expression in streptozotocin-treated mice and human cultured podocytes. *Diabetes* 58, 2109–2118. doi: 10.2337/db08-0895

Tessaro, F. H., Ayala, T. S., Nolasco, E. L., Bella, L. M., and Martins, J. O. (2017). Insulin influences LPS-Induced TNF-α and IL-6 release through distinct pathways in mouse macrophages from different compartments. *Cell Physiol. Biochem.* 42, 2093–2104. doi: 10.1159/000479904

Thompson, R. D., Noble, K. E., Larbi, K. Y., Dewar, A., Duncan, G. S., Mak, T. W., et al. (2001). Platelet-endothelial cell adhesion molecule-1 (PECAM-1)–deficient mice demonstrate a transient and cytokine-specific role for PECAM-1 in leukocyte migration through the perivascular basement membrane. *Blood* 97, 1854–1860. doi: 10.1182/blood.V97.6.1854

Todoric, J., Löffler, M., Huber, J., Bilban, M., Reimers, M., Kadl, A., et al. (2006). Adipose tissue inflammation induced by high-fat diet in obese diabetic mice is prevented by n- 3 polyunsaturated fatty acids. *Diabetologia* 49, 2109–2119. doi: 10.1007/s00125-006-0300-x

Trottier, M. D., Naaz, A., Li, Y., and Fraker, P. J. (2012). Enhancement of hematopoiesis and lymphopoiesis in diet-induced obese mice. *Proc. Natl. Acad. Sci. U.S.A.* 109, 7622–7629.

Uotila, L. M., Jahan, F., Hinojosa, L. S., Melandri, E., Grönholm, M., and Gahmberg, C. G. (2014). Specific phosphorylations transmit signals from leukocyte β2 to β1 integrins and regulate adhesion. *J. Biol. Chem.* 289, 32230–32242. doi: 10.1074/jbc.M114.588111

van Beek, L., Lips, M. A., Visser, A., Pijl, H., Ioan-Facsinay, A., Toes, R., et al. (2014). Increased systemic and adipose tissue inflammation differentiates obese women with T2DM from obese women with normal glucose tolerance. *Metabolism* 63, 492–501. doi: 10.1016/j.metabol.2013.12.002

Van Oostrom, A., Van Wijk, J., Sijmonsma, T., Rabelink, T., and Castro Cabezas, M. (2004). Increased expression of activation markers on monocytes and neutrophils in type 2 diabetes. *Neth. J. Med.* 62, 320–325.

Van Steenwinckel, J., Auvynet, C., Sapienza, A., Reaux-Le Goazigo, A., Combadière, C., and Parsadaniantz, S. M. (2015). Stromal cell-derived CCL2 drives neuropathic pain states through myeloid cell infiltration in injured nerve. *Brain Behav. Immun.* 45, 198–210. doi: 10.1016/j.bbi.2014.10.016

Vessby, B., Uusitupa, M., Hermansen, K., Riccardi, G., Rivellese, A. A., Tapsell, L. C., et al. (2001). Substituting dietary saturated for monounsaturated fat impairs insulin sensitivity in healthy men and women: the Kanwu study. *Diabetologia* 44, 312–319. doi: 10.1007/s001250051620

von Andrian, U. H., and Engelhardt, B. (2003). α4 integrins as therapeutic targets in autoimmune disease*. *Mass Med. Soc.* doi: 10.1056/NEJMe020157

Wang, C., and Li, J. (2015). Pathogenic microorganisms and pancreatic cancer. *Gastrointest. Tumors* 2, 41–47. doi: 10.1159/000380896

Weber, C. (2003). Novel mechanistic concepts for the control of leukocyte transmigration: specialization of integrins, chemokines, and junctional molecules. *J. Mol. Med.* 81, 4–19. doi: 10.1007/s00109-002-0391-x

Weisberg, S. P., McCann, D., Desai, M., Rosenbaum, M., Leibel, R. L., and Ferrante, A. W. (2003). Obesity is associated with macrophage accumulation in adipose tissue. *J. Clin. Invest.* 112, 1796–1808. doi: 10.1172/JCI200319246

Wen, Y., Skidmore, J., Porter-Turner, M., Rea, C., Khokher, M., and Singh, B. (2002). Relationship of glycation, antioxidant status and oxidativestress to vascular endothelial damage in diabetes. *Diabetes. Obes. Metab.* 4, 305–308. doi: 10.1046/j.1463-1326.2002.00212.x

White, F. A., Feldman, P., and Miller, R. J. (2009). Chemokine signaling and the management of neuropathic pain. *Mol. Interv.* 9:188. doi: 10.1124/mi.9.4.7

Winer, D. A., Winer, S., Shen, L., Wadia, P. P., Yantha, J., Paltser, G., et al. (2011). B cells promote insulin resistance through modulation of T cells and production of pathogenic IgG antibodies. *Nat. Med.* 17, 610–617. doi: 10.1038/nm.2353

Wolburg, H., and Lippoldt, A. (2002). Tight junctions of the blood–brain barrier: development, composition and regulation. *Vascul. Pharmacol.* 38, 323–337. doi: 10.1016/S1537-1891(02)00200-8

Wouters, K., Gaens, K., Bijnen, M., Verboven, K., Jocken, J., Wetzels, S., et al. (2017). Circulating classical monocytes are associated with CD11c+ macrophages in human visceral adipose tissue. *Sci. Rep.* 7:42665. doi: 10.1038/srep42665

Wright, R. D., and Cooper, D. (2014). Glycobiology of leukocyte trafficking in inflammation. *Glycobiology* 24, 1242–1251. doi: 10.1093/glycob/cwu101

Wu, C.-C., Sytwu, H.-K., Lu, K.-C., and Lin, Y.-F. (2011). Role of T cells in type 2 diabetic nephropathy. *Exp. Diabetes Res.* 2011:514738. doi: 10.1155/2011/514738

Xu, H. E., Lambert, M. H., Montana, V. G., Plunket, K. D., Moore, L. B., Collins, J. L., et al. (2001). Structural determinants of ligand binding selectivity between the peroxisome proliferator-activated receptors. *Proc. Natl. Acad. Sci. U.S.A.* 98, 13919–13924. doi: 10.1073/pnas.241410198

Xu, H.-L., Salter-Cid, L., Linnik, M. D., Wang, E. Y., Paisansathan, C., and Pelligrino, D. A. (2006). Vascular adhesion protein-1 plays an important role in postischemic inflammation and neuropathology in diabetic, estrogen-treated ovariectomized female rats subjected to transient forebrain ischemia. *J. Pharmacol. Exp. Ther.* 317, 19–29. doi: 10.1124/jpet.105.096958

Xu, L., Kitade, H., Ni, Y., and Ota, T. (2015). Roles of chemokines and chemokine receptors in obesity-associated insulin resistance and nonalcoholic fatty liver disease. *Biomolecules* 5, 1563–1579. doi: 10.3390/biom5031563

Xue, C.-B., Wang, A., Han, Q., Zhang, Y., Cao, G., Feng, H., et al. (2011). Discovery of INCB8761/PF-4136309, a potent, selective, and orally bioavailable CCR2 antagonist. *ACS Med. Chem. Lett.* 2, 913–918. doi: 10.1021/ml200199c

Yago, T., Shao, B., Miner, J. J., Yao, L., Klopocki, A. G., Maeda, K., et al. (2010). E-selectin engages PSGL-1 and CD44 through a common signaling pathway to induce integrin αLβ2-mediated slow leukocyte rolling. *Blood* 116, 485–494. doi: 10.1182/blood-2009-12-259556

Yanaba, K., Bouaziz, J. D., Matsushita, T., Magro, C. M., St. Clair, E. W., and Tedder, T. F. (2008). B-lymphocyte contributions to human autoimmune disease. *Immunol. Rev.* 223, 284–299. doi: 10.1111/j.1600-065X.2008.00646.x

Yao, L., Herlea-Pana, O., Heuser-Baker, J., Chen, Y., and Barlic-Dicen, J. (2014). Roles of the chemokine system in development of obesity, insulin resistance, and cardiovascular disease. *J. Immunol. Res.* 2014:81450. doi: 10.1155/2014/181450

Yates, C. M., Tull, S. P., Madden, J., Calder, P. C., Grimble, R. F., Nash, G. B., et al. (2011). Docosahexaenoic acid inhibits the adhesion of flowing neutrophils to cytokine stimulated human umbilical vein endothelial cells. *J. Nutr.* 141, 1331–1334. doi: 10.3945/jn.111.139287

Yki-Järvinen, H. (2004). Thiazolidinediones. *N. Engl. J. Med.* 351, 1106–1118. doi: 10.1056/NEJMra041001

Yu, D. M., Yao, T. W., Chowdhury, S., Nadvi, N. A., Osborne, B., Church, W. B., et al. (2010). The dipeptidyl peptidase IV family in cancer and cell biology. *FEBS J.* 277, 1126–1144. doi: 10.1111/j.1742-4658.2009.07526.x

Yu, X., and Martin-Gayo, E. (2019). Role of dendritic cells in natural immune control of HIV-1 infection. *Front. Immunol.* 10:1306. doi: 10.3389/fimmu.2019.01306

Zha, J., Chi, X.-W., Yu, X.-L., Liu, X.-M., Liu, D.-Q., Zhu, J., et al. (2016). Interleukin-1β-targeted vaccine improves glucose control and β-cell function in a diabetic KK-Ay mouse model. *PLoS One* 11:e0154298. doi: 10.1371/journal.pone.0154298

Zhang, J., Alcaide, P., Liu, L., Sun, J., He, A., Luscinskas, F. W., et al. (2011). Regulation of endothelial cell adhesion molecule expression by mast cells, macrophages, and neutrophils. *PLoS One* 6:e14525. doi: 10.1371/journal.pone.0014525

Zhou, T., Hu, Z., Yang, S., Sun, L., Yu, Z., and Wang, G. (2018). Role of adaptive and innate immunity in type 2 diabetes mellitus. *J. Diabetes Res.* 2018:7457269. doi: 10.1155/2018/7457269

Zhu, X., Cao, S., Zhu, M.-D., Liu, J.-Q., Chen, J.-J., and Gao, Y. J. (2014). Contribution of chemokine CCL2/CCR2 signaling in the dorsal root ganglion and spinal cord to the maintenance of neuropathic pain in a rat model of lumbar disc herniation. *J. Pain* 15, 516–526. doi: 10.1016/j.jpain.2014.01.492

Zhuge, F., Ni, Y., Nagashimada, M., Nagata, N., Xu, L., Mukaida, N., et al. (2016). DPP-4 inhibition by linagliptin attenuates obesity-related inflammation and insulin resistance by regulating M1/M2 macrophage polarization. *Diabetes* 65, 2966–2979. doi: 10.2337/db16-0317

Conflict of Interest: The authors declare that the research was conducted in the absence of any commercial or financial relationships that could be construed as a potential conflict of interest.

frontiers in Cell and Developmental Biology

REVIEW
published: 09 March 2021
doi: 10.3389/fcell.2021.635102

Insights Into Leukocyte Trafficking in Inflammatory Arthritis – Imaging the Joint

*Julia E. Manning†, Jonathan W. Lewis†, Lucy-Jayne Marsh and Helen M. McGettrick**

Rheumatology Research Group, Institute of Inflammation and Ageing, University of Birmingham, Birmingham, United Kingdom

The inappropriate accumulation and activation of leukocytes is a shared pathological feature of immune-mediated inflammatory diseases (IMIDs), such as rheumatoid arthritis (RA) and psoriatic arthritis (PsA). Cellular accumulation is therefore an attractive target for therapeutic intervention. However, attempts to modulate leukocyte entry and exit from the joint have proven unsuccessful to date, indicating that gaps in our knowledge remain. Technological advancements are now allowing real-time tracking of leukocyte movement through arthritic joints or *in vitro* joint constructs. Coupling this technology with improvements in analyzing the cellular composition, location and interactions of leukocytes with neighboring cells has increased our understanding of the temporal dynamics and molecular mechanisms underpinning pathological accumulation of leukocytes in arthritic joints. In this review, we explore our current understanding of the mechanisms leading to inappropriate leukocyte trafficking in inflammatory arthritis, and how these evolve with disease progression. Moreover, we highlight the advances in imaging of human and murine joints, along with multi-cellular *ex vivo* joint constructs that have led to our current knowledge base.

Keywords: imaging, leukocyte, adhesion, migration, arthritis

OPEN ACCESS

Edited by:
Hao Sun,
University of California, San Diego, United States

Reviewed by:
Juan D. Cañete,
Hospital Clínic de Barcelona, Spain
Gerard M. Moloney,
University College Cork, Ireland
Elena Zenaro,
University of Verona, Italy
John MacSharry,
University College Cork, Ireland

***Correspondence:**
Helen M. McGettrick
h.m.mcgettrick@bham.ac.uk

†These authors have contributed equally to this work

Specialty section:
This article was submitted to Cell Adhesion and Migration, a section of the journal Frontiers in Cell and Developmental Biology

Received: *29 November 2020*
Accepted: *11 February 2021*
Published: *09 March 2021*

Citation:
Manning JE, Lewis JW, Marsh L-J and McGettrick HM (2021) Insights Into Leukocyte Trafficking in Inflammatory Arthritis – Imaging the Joint. Front. Cell Dev. Biol. 9:635102. doi: 10.3389/fcell.2021.635102

OVERVIEW OF THE LEUKOCYTE RECRUITMENT CASCADE

Over the last 30 years, the general understanding of how leukocytes migrate out of the blood, across the endothelium and through inflamed tissues has been extensively researched providing us with a step by step cascade of events (**Figure 1**) (Ley et al., 2007; Vestweber, 2015). In line with this, imaging techniques for analyzing the individual steps of the cascade, from leukocyte capture through to migration into the tissue, have improved exponentially giving us much more granularity on the temporal and dynamic kinetics of these events and the key molecules involved. Chronic inflammatory arthritis is characterized by the aberrant accumulation and activation of such leukocytes within the synovial tissue, along with tissue-resident stromal cells (fibroblasts) becoming epigenetically reprogrammed, both of which drive tissue and bone damage leading to pain and immobility in patients with, for example, rheumatoid arthritis (RA) or psoriatic arthritis (PsA). The clinical urgency to identify new drug targets that limit the trafficking of pathogenic leukocytes and promote the entry of regulatory cells into chronically inflamed tissues, such as the joint, are partly responsible for driving forward the imaging techniques necessary to visualize these processes in real-time. Here, we explore our current understanding of the mechanisms leading to inappropriate leukocyte trafficking in inflammatory arthritis, and how these evolve with disease progression.

We provide a historic overview of the imaging techniques that have led to our current knowledge base – considering our progression from 2-D imaging of tissue sections; through to *in vitro* adhesion and migration assays on sections, purified proteins or single-cell layers; into the realm of real-time imaging of 3-D multicellular *ex vivo* joint constructs or whole joints, and beyond. For each technique we will highlight the key kinetics, leukocyte subpopulations and molecules discovered and how these advanced our understanding of process-driven pathology of inflammatory arthritis.

IMAGING SYNOVIAL TISSUE – EARLY INSIGHTS INTO PATHOLOGY

As early as the 1960's researchers used haematoxylin and eosin (H&E) to stain tissue sections to visualize tissue architecture (Campbell-Thompson et al., 2012) (**Figure 2A**) and cellular accumulation in the joints from patients with RA or PsA (Muirden and Senator, 1968; Muirden and Mills, 1971). Time-course experiments in murine models of inflammatory arthritis revealed the accumulation of leukocytes peaked 1–2 days after onset of adjuvant-induced arthritis (AIA) model (Szántó et al., 2004; Gonçalves et al., 2020), day 10 in the KRN serum transfer induced arthritis (STIA) model (LaBranche et al., 2010); and 21 days after immunization in the collagen-induced arthritis (CIA) model (Knoerzer et al., 1997). Similarly, H&E revealed a substantial number of leukocytes accumulating in the synovium of patients with early (disease duration less than 1 year) and established RA (1.5–20 years), with the degree of infiltration correlating with disease activity rather than symptom duration (Baeten et al., 2000). For both human and murine studies, H&E analysis of synovium has highlighted the significant role of tumor necrosis factor-α (TNFα) in driving leukocyte infiltration into the inflamed joint: with TNFα inhibitors (TNFi) reducing leukocyte numbers in the joint leading to reduced clinical scores, which were not seen in non-responders (Williams et al., 1992; Baeten et al., 2000; Barrera et al., 2001), as well as reducing the expression of chemokines within the synovium (Taylor et al., 2000). Similarly, H&E revealed a potential therapeutic benefit of inhibiting chemokine interactions in AIA, where short-chain peptides modeled on the chemokine glycosaminoglycan binding domain of CXCL8 (interleukin-8) decreased leukocyte accumulation and the overall inflammatory score in treated joints (McNaughton et al., 2018). Whilst H&E analysis of tissue sections is an integral outcome measure in almost all studies, it is unable to provide any insight into the specific subsets of leukocytes infiltrating the joint, how these evolve with disease or the mechanisms underpinning their accumulation.

Advances in immunohistochemistry (IHC) and subsequently fluorescence microscopy and *in situ* hybridization (ISH) have expanded our ability to identify individual leukocyte subsets in synovial tissue sections (Menon et al., 2017; Traylor-Knowles, 2018) (**Figures 2B,C**), furthering our understanding of the composition of leukocytes within the inflamed joint in the various murine models of inflammatory arthritis and human arthritides. For example, monocytes and CD4 T-cell infiltration peaked 2–3 days following onset of AIA, followed by an influx of CD8 T-cells and B-cells which peaked at day 7 (Verschure et al., 1989). Moreover, monocytes and macrophages were observed in the sublining layer of the AIA joint, whilst T and B-cells were located in perivascular clusters and some in small isolated groups (Dijkstra et al., 1987). Indeed, elevated numbers of $CD3^+$ T-cells, $CD20^+$ B-cells, and $CD68^+$ macrophages, along with a concomitant decrease in the numbers of regulatory T-cells (Tregs) were also observed using IHC in synovial biopsies from RA patients with high disease activity scores compared to patients with lower disease activity or in remission (Zhang et al., 2005; Behrens et al., 2007; Alivernini et al., 2017). Moreover, anti-TNFα therapy reduced the numbers of $CD3^+$ T-cells, $CD22^+$ B-cells, and $CD68^+$ macrophages in the joints of patients with RA over a 2 weeks period (Taylor et al., 2000). Indeed, the combination of CD20, CD138 (marking plasma cells), CD3, and CD68 revealed 3 distinct leukocyte profiles (pathotypes) in the synovium of patients with early and established RA based on the absence of leukocytes (pauci-immune), diffuse myeloid infiltrate or the formation of lympho-myeloid aggregates (Humby et al., 2019; Nerviani et al., 2020). Agreeing with earlier studies that described pauci-immune; diffuse and follicular infiltrates (Wagner et al., 1998; Pitzalis et al., 2013). Crucially these different leukocyte synovial pathotypes impact on a patient's response to therapy – where over 80% of patients with a lympho-myeloid or diffuse myeloid pathotype showed a decrease in their disease activity (DAS28 score) following treatment with the anti-TNFα drug, certolizumab-pegol, whilst less than 30% of patients with the pauci-immune pathotype responded (Nerviani et al., 2020). Such studies reveal two important insights – firstly leukocyte pathotypes highlight the existence of different leukocyte recruitment and retention signatures in subgroups of RA patients. Secondly, although the exact molecular mechanisms for these signatures remain undetermined, TNFα clearly plays a major role in the two pathotypes where elevated levels of leukocytes are observed.

Early IHC and ISH studies revealed for the first time the expression pattern of adhesion molecules and chemokines within arthritic joints (Johnson et al., 1993; Salmi et al., 1997; Matsui et al., 2001; Wang et al., 2004). Macroscopically, expression of certain adhesion molecules (selectins and VCAM-1) have been reported to be restricted to a subpopulation of synovial vessels in patients with chronic arthritis; whilst others [intracellular adhesion molecules 1 and 2 (ICAM-1 and ICAM-2)] were ubiquitously expressed (Salmi et al., 1997). In contrast, little E-selectin was detected on vessels in PsA (Veale et al., 1993). Synovial blood endothelial cells located near or within tertiary lymphoid structures appear to acquire a high endothelial vessel (HEV)-like phenotype with the expression of peripheral node addressin (PNAd), an adhesion molecule normally restricted to HEV's, observed on synovial endothelial cells in some, but not all, RA and PsA sections analyzed (Salmi et al., 1997; Cañete et al., 2007) – and which may account for the lympho-myeloid/follicular pathotype described (Wagner et al., 1998; Pitzalis et al., 2013). Similarly, rheumatoid synovial endothelium abnormally expresses high levels of the mucosal specific vascular adhesion protein-1 (VAP-1) (Salmi et al., 1997) – indicating that

the synovial endothelium acquires the capacity to support the trafficking of gut-homing T-cells during RA pathology. Crucially, the activation status of synovial endothelial cells is sensitive to anti-TNFα therapy, with reduced expression of E-selectin (Paleolog et al., 1996; Tak et al., 1996) and vascular cell adhesion protein 1 (VCAM-1) (Tak et al., 1996) reported in the rheumatoid synovium following treatment – almost certainly accounting for the improvement in disease activity seen in patients with leukocyte rich pathotypes (Nerviani et al., 2020).

In 1976 Stamper and Woodruff transformed tissue analysis from spatial 2-D phenotypic studies to 3-D functional assays (Hirata et al., 2004) (**Figure 2D**), by allowing lymphocytes to adhere to fixed murine lymph node tissue sections before visualizing their interactions using methyl-green-thionin and light microscopy (Stamper and Woodruff, 1976). Subsequently, groups adapted the Stamper–Woodruff (S–W) assay and began assessing the molecular mechanisms supporting leukocyte adhesion to arthritic synovial tissue. For example, significantly more monocytes adhered to RA synovium compared to other tissues analyzed (foreskin, placenta, and inflamed tonsils), and blocking the capture receptors P-selectin and E-selectin reduced this by >90% and 20–50%, respectively (Grober et al., 1993). Similarly, HL-60 cell (a neutrophil-like leukaemic cell line) adhesion to frozen sections of RA synovium was significantly reduced following treatment with an anti-E-selectin function-blocking antibody or the TNFα inhibitor certolizumab pegol (Shu et al., 2012). Thus demonstrating a pivotal role TNFα, P- and E-selectin in supporting neutrophil and monocyte recruitment to the RA synovium. Furthermore, Salmi et al. (1997) revealed for the first time mucosal lymphocytes bind to VAP-1 expressed by RA synovial vessels, further supporting the concept that gut-specific trafficking address-codes for lymphocytes are hijacked by the rheumatoid joint. Indeed, the mucosal microbiome is now believed to play a crucial role in lymphocyte trafficking outside the inflamed joint, and is highly likely to influence the phenotype of the cells recruited to the joint (reviewed by Buckley and McGettrick, 2018; Manasson et al., 2020; Xu et al., 2020). This functional analysis of tissue sections allowed for the first time mechanistic studies on the proportion of leukocytes binding with or without interventions to be analyzed. Further studies using tissues from other inflammatory arthritides and at different phases of disease are now required to distinct shared and unique features across arthritides, and how these evolve with disease progression.

DISSECTING THE MOLECULAR MECHANISMS SUPPORTING ABERRANT LEUKOCYTE TRAFFICKING – THE CREATION OF *IN VITRO* JOINT CONSTRUCTS

The vast majority of our understanding on the dynamics of leukocyte recruitment has been discovered by visualizing cell–cell interactions *in vitro* using assays that incorporate purified proteins or different tissue-resident cells (e.g., blood vascular endothelial cells or fibroblasts) in either 2-D or 3-D formats, and in some cases that also mimic blood flow (Butler et al., 2009; Mcgettrick et al., 2017). These *in vitro* static or flow-based adhesion/migration assays enable the real-time imaging of leukocyte behavior as they interact with the substrate, including their motility (**Figures 2E,F**). As such they have been a vital tool in aiding our understanding of the molecular processes governing disease onset and perpetuation in many arthritides, especially when patient cells or pharmacological agents have been assessed.

2-Dimensional Models

Surprisingly few studies have visualized each step of the adhesion cascade using leukocytes isolated from patients with inflammatory arthritis and models mimicking the joint that incorporate endothelial cells alone or with relevant stromal components (**Figures 2E,F**). For example, more T-cells adhered and migrated through inflamed endothelium *in vitro* when they were isolated from RA (Taylor et al., 2000) or PsA (Dunky et al., 1997) patients compared cells from the control group – this was thought to be mediated by $\alpha_L\beta_2$-integrin. Interestingly, the adhesive capability of T-cells appeared to be unaffected by whether a patient exhibits active or inactive RA, with similar numbers of fluorescently labeled T-cells observed binding to either resting or IL-1β stimulated endothelial cells over a 6-h timeframe (Mertens et al., 1994). Similarly, greater numbers of effector memory $CD4^+$ T-cells from RA patients migrated further into collagen gels over 48 h following *in vitro* anti-$CD3^+$ CD28-induced activation compared to cells isolated from healthy controls (Shen et al., 2017). Combining these data with IHC and metabolite quantification revealed that T-cells from these clinically active RA patients had reduced glycolytic flux that resulted in the overexpression of TSK5, a podosome scaffolding protein found at the leading edge of the cells causing enhanced migratory capacity *in vitro* (Shen et al., 2017). This was one of the first studies to highlight the importance of disease-induced metabolic changes in leukocytes on their adhesive and migratory potential. Similar observations have been linked to genes associated with increased risk of developing RA – for example, super-resolution studies revealed that the expression of the PTPN22 variant (PTPN22W) increased $\alpha_L\beta_2$-integrin clustering in T-cells resulting in them being more sticky (Burn et al., 2016). Genetic risk factors and abnormal cellular metabolism promote the adhesive and migratory properties of T-cells in patients with RA (Weyand et al., 2020), and potentially other inflammatory arthritides by altering the expression levels or cellular localization of $\alpha_L\beta_2$-integrin. Whilst directly targeting $\alpha_L\beta_2$-integrin is not a viable treatment option [see review on leukocyte adhesion deficiency (Harlan, 1993; Kuijpers et al., 1997)], targeting the processes regulating its expression and distribution may provide alternative treatment options for arthritides.

TNFα signaling, itself, can induce leukocytes to shed β_2-integrins (Gjelstrup et al., 2010), resulting in increased plasma soluble β_2-integrin (sCD18) concentrations that bind to ICAM-1 on the endothelium to reduce the availability of this molecule to leukocytes, thus reducing adhesive interactions (Kragstrup et al., 2014). However, this homeostatic regulatory pathway is

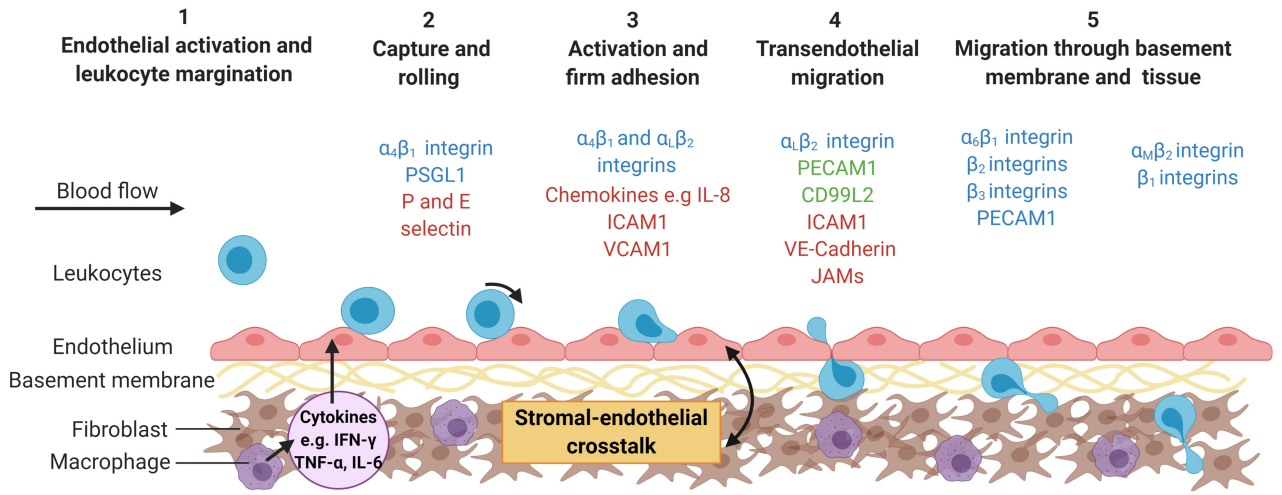

FIGURE 1 | The multi-step leukocyte adhesion cascade. Infection or tissue damage causes the localized release of danger signals, including cytokines, which (1) activate the endothelium causing the expression of capture receptors (P- or E-selectins), adhesion molecules (IgSF members – ICAM-1; VCAM-1) and presentation of chemokines or lipids on their surface (2) (Zhang et al., 2011). Marginated leukocytes are captured, roll along the endothelial surface until (3) they receive an activation signal (typically chemokine mediated) resulting in inside-out signaling and integrin activation ($\alpha_L\beta_2$-integrin; $\alpha_4\beta_1$-integrin) (Ley et al., 2007). This allows for stabilization of the adhesive interactions ($\alpha_L\beta_2$-ICAM-1 and $\alpha_4\beta_1$-VCAM-1 interactions) and cytoskeletal rearrangement in the leukocyte allowing (4) them to crawl over the endothelium, migrate across the endothelium (ICAM-1; JAM-1; CD31; VE-cadherin) and into the subendothelial space (Ley et al., 2007), (5) where they encounter the basement membrane and stromal compartment. This process is tightly regulated by the haemodynamic forces of the flowing blood and the stromal derived signals experienced by the endothelium (McGettrick et al., 2012). Some of the major molecules involved in this process are represented in the schematic, with molecules colored according to cell type expressing them; leukocytes = blue; endothelial cells (ECs) = red and expressed by both leukocytes and ECs = green. ICAM-1, Intracellular adhesion protein 1; IL-8, interleukin-8; JAM, junctional adhesion molecule; PECAM-1, platelet endothelial cell adhesion molecule 1; PSGL1, P-selectin glycoprotein ligand-1; VE-cadherin, vascular endothelial cadherin; VCAM-1, vascular adhesion protein 1. Created with BioRender.com.

lost in patients with RA and spondyloarthritis (SpA) (Kragstrup et al., 2014), where patients with high disease activity scores have lower plasma sCD18 compared to OA, and thus the potential for elevated levels of leukocyte trafficking (Gjelstrup et al., 2010). Furthermore, B-cells from patients with RA have lost their ability to respond to the adipokine, adiponectin, and therefore their ability to release the peptide hormone, PEPITEM, which acts to limit T-cell migration into inflamed tissues (Chimen et al., 2015). So in addition to lymphocytes acquiring pro-migratory traits, there is also a loss of tonic regulators that normally act to limit tissue infiltration in patients with RA and SpA.

Considering other leukocyte subtypes, patients with RA have higher levels of "reverse migrated" neutrophils in their circulation, suggesting that these cells have sampled the tissue microenvironment and re-entered the circulation across the blood vascular endothelial cells rather than through the lymphatics (Buckley et al., 2006). Moreover, expression of RA susceptibility gene, PTPN22W, enhanced neutrophil migration across TNFα-activated endothelium *in vitro* (Bayley et al., 2015) and may account for the rapid transit of neutrophils through the rheumatoid joint into the synovial fluid. RA neutrophil chemotaxis toward the synovial fluid rich CXCL8 (IL-8) was blocked with the Janus kinase inhibitors (JAKi) (Mitchell et al., 2017), along with reduced neutrophil and T-cell numbers observed in the joints of RA patients treated with baricitinib (Tanaka et al., 2018) – suggesting JAKi have potential therapeutic benefit by limiting leukocyte migration in arthritic patients. The higher expression the α_M subunit of the $\alpha_M\beta_2$-integrin on monocytes from RA patients contributed to their enhanced adhesion to resting (uninflamed) and IL-1β stimulated endothelium *in vitro* when compared to the levels observed for monocytes from normal controls (Lioté et al., 1996). By contrast, fewer fluorescently labeled monocytes migrated through TNFα activated human dermal microvascular endothelial cells when they were isolated from PsA patients, compared to monocytes from patients with osteoarthritis, fibromyalgia or type-2-diabetes (as controls) – most likely due to a reduction in surface expression of the $\alpha_M\beta_2$-integrin required for stable/firm adhesion, explaining the reduced number of monocytes in the psoriatic joint, compared to RA (Neumüller et al., 2001). Akin to lymphocytes, pathological alterations in the expression of the β_2-integrins by neutrophils and monocytes contribute to the synovial leukocyte composition in these inflammatory arthritides.

Synovial blood vascular endothelial cells (sEC) act as the gatekeepers to the joint. Crucially, Abbot et al. (1999) demonstrated that sEC from RA patients are imprinted with a disease-specific tissue memory and are in a pre-primed state that is maintained in culture. This pathogenic phenotype enables TNFα-stimulated rheumatoid sEC to support greater levels of neutrophil and T-cell capture from flow and induced stable adhesion (Abbot et al., 1999). Further research examining the phenotype of sEC through the evolution of inflammatory arthritides, across diseases and its impact on the inflammatory infiltrate is urgently required. Similarly, synovial fibroblasts from inflammatory arthritides are epigenetically imprinted with a

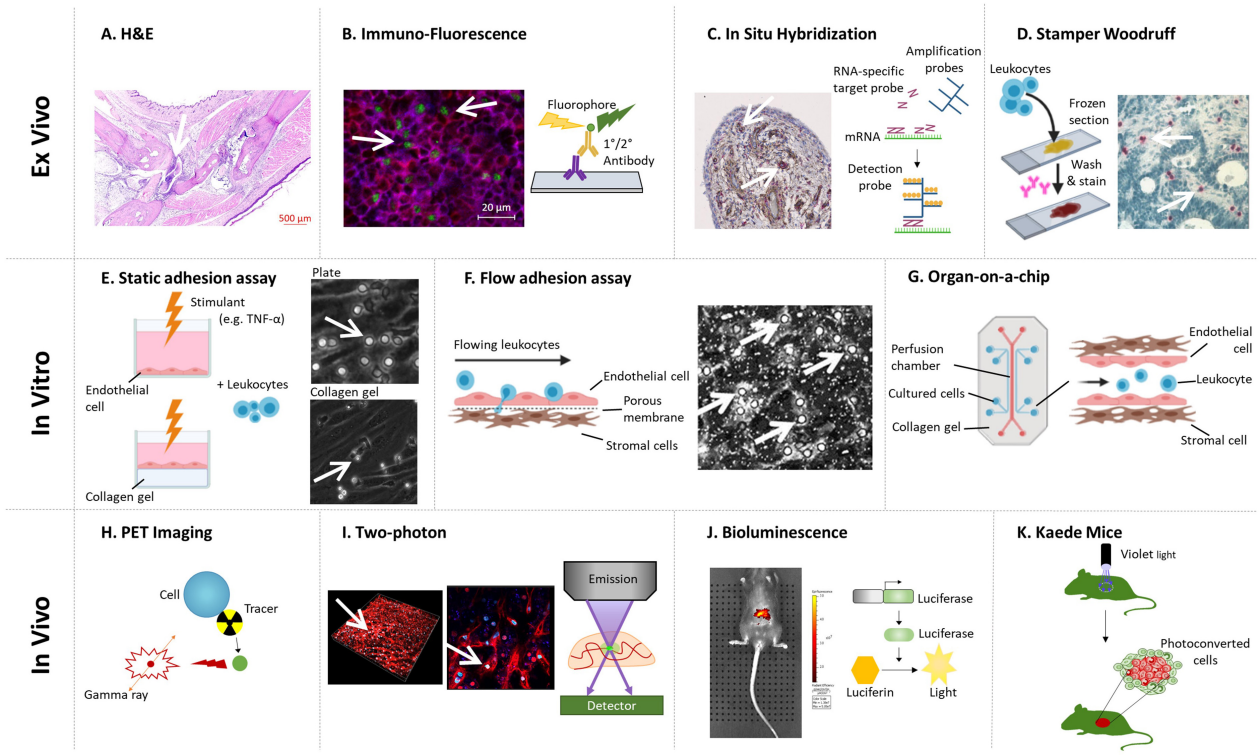

FIGURE 2 | Methodologies for imaging leukocyte infiltration. **(A)** H&E staining (Tucker et al., 2016): decalcified joints are paraffin embedded, sectioned, and stained with H&E to identify leukocyte infiltration. **(B)** Immuno-fluorescence (Honvo-Houéto and Truchet, 2015; JoVE, 2021): tissue sections are stained with fluorescently tagged antibodies against specific proteins to visualize cellular localization using a fluorescent microscope. Representative image shows a lymph node stained for $CD3^+$ (Red), $CD4^+$ (Blue), and $FoxP3^+$ (Green) T-cells. In **(A,B)**, images courtesy of Miss Jenefa Begum (University of Birmingham). **(C)** *In Situ* Hybridization (Menon et al., 2017): an RNA-specific target probe is added to tissue sections, where it hybridizes to its corresponding gene. Amplification probes are added to enhance the detection, which are bound by detection probes. Detection probes can either be fluorescent-, antibody- or radio- labeled. Image of arthritic joint replacement tissue section stained for PDGFRβ (Red), nuclei (Pale Blue), and CD90 (Brown), courtesy of Dr. Triin Major (University of Birmingham). **(D)** Stamper–Woodruff assay (Hirata et al., 2004): leukocytes are added to frozen tissue sections on slides and rotated for 30 min. Non-adherent cells are washed off and the section stained with nuclear dye and/or antibodies of choice. Image courtesy of Dr. Patricia Lalor and Dr. Sarah Edwards (University of Birmingham, Edwards et al., 2006). **(E,F)** Static and flow based adhesion assays (Butler et al., 2009): Endothelial cells or the ligand of interest are seeded onto the well, a filter or onto a collagen gel and treated with stimulant(s) of choice (e.g., TNF-α) for the desired amount of time. Stromal cells can be cultured beneath the endothelium to assess how they regulate endothelial recruitment of leukocytes (Munir et al., 2015; Mcgettrick et al., 2017). **(E)** Leukocytes are added to the well and left to adhere under static conditions, before non-adherent cells washed off and remaining adherent cells imaged via phase contrast microscopy. Image courtesy of Miss Sophie Hopkin (University of Birmingham). **(F)** Leukocytes are perfused across the surface (e.g., endothelial cells or purified protein/carbohydrate) at a wall shear rate determined by the flow rate of a syringe pump. In **(E,F)**, adherent cells appear circular and phase bright, as they become activated and migrate they change morphology and appear phase dark once underneath the endothelial monolayer. **(G)** Organ-on-a-chip (Rothbauer et al., 2020): a micro-scale system to mimic the environment within the human body, combining cultured cells and microfluidic systems – where leukocytes are perfused through a channel coated with endothelial cells, with pericytes and stromal cells cultured on the opposite (basal) side to the endothelial cell. **(H)** PET imaging (White et al., 2017; Momcilovic et al., 2018): cells are tagged using a radioactive tracer that emits a small quantity of Gamma rays. Tagged cells are injected into participants and the location of cells can be tracked and imaged. **(I)** Two photon microscopy (Chen et al., 2017; Cai et al., 2019): fluorescently labeled cells are visualized and their movement tracked in real-time with two-photon microscope either *in vivo* and *ex vivo*. Image of human liver tissue perfused with wheat germ agglutinin and Hoechst and imaged *ex vivo*, courtesy of Dr. Scott P. Davies (University of Birmingham). **(J)** Bioluminescence (Lim et al., 2009): cell specific luciferase knock-in lines are visualized using the whole animal *in vivo* imaging system (IVIS), allowing the tracking of endogenous or injected cells. Image shows 1,1′-dioctadecyltetramethyl indotricarbocyanine Iodide tagged bone marrow mesenchymal stem cells accumulation following injection into wildtype mice; courtesy of Dr. Lozan Sheriff (University of Birmingham). **(K)** Kaede mice (Porter et al., 2018; Steele et al., 2019): UV light illumination of tissues (e.g., draining lymph nodes) *in situ* photoconverts cells from green to red fluorescence. The movement of red fluorescent cells to, and their interaction with cells at, distant tissues can be tracked. In **(A–F,I)**, arrows denote leukocytes on the representative images. Created with BioRender.com.

pathogenic phenotype (Parsonage et al., 2005). For example, RA synovial fibroblasts support elevated levels of B-cell (Shimaoka et al., 1998; Burger et al., 2001) and T-cell (Bradfield et al., 2003) pseudoemperipolesis (sub-fibroblast migration) in a CXCL12 dependent manner compared to dermal fibroblasts. Further to this, peripheral blood $CD4^+$ T-cells from RA patients exhibit higher expression of the α6 integrin subunit and were more efficiently captured from flow to the extracellular matrix components, laminin and fibronectin, than control cells (Haworth et al., 2008). These interactions are likely to be responsible for localizing $CD4^+$ T-cells in the laminin bordered perivascular cuff in the rheumatoid joint (Haworth et al., 2008) – as observed by confocal microscopy on tissue sections. Whilst neutrophils from healthy controls and clinically active RA bind

at similar levels to fibronectin *in vitro*, significantly fewer cells adhered when they were isolated from patients in clinical remission – these observations were linked to reductions in the expression of L-selectin and α_L-integrin on neutrophils following anti-TNFα therapy (Dominical et al., 2011). These studies start to elucidate the molecular mechanisms responsible for leukocyte interactions in the subendothelial space, and how these are altered by drug-induced clinical remission.

The combination of altered adhesive and migratory properties of leukocytes and endothelial cells in patients with RA further amplifies the aberrant trafficking of inflammatory cells during disease – the critical question of which cell type becomes dysregulated first remains to be answered.

3-Dimensional Models

Over the last 20 years, considerable effort has been made to address the limitations of 2-D culture systems in an attempt to generate a more representative 3-D model of the tissue (McGettrick et al., 2012; Buckley and McGettrick, 2018), in which leukocyte trafficking under static and physiological flow conditions can be observed (Munir et al., 2015; Mcgettrick et al., 2017) (**Figure 2F**). As a result, it is clear that tissue-resident stromal cells communicate with the neighboring endothelial cells to generate "stromal address codes" for tissue-specific and disease-specific regulation of leukocyte trafficking (Parsonage et al., 2005). Crucially the absence of these signals results in lymphocyte migration being frustrated, such that they shuttle back and forth across the inflamed endothelial barrier, with few cells penetrating a 400 μm deep collagen gel (McGettrick et al., 2008; Jeffery et al., 2013). A series of studies using phase-contrast microscopy has revealed that primary synovial fibroblasts from patients with acutely resolving synovitis or primary dermal fibroblasts from patients with RA undergoing joint replacement surgery limit the ability of endothelial cells to recruit lymphocytes from flow - in effect acting in an anti-inflammatory manner (McGettrick et al., 2009; Filer et al., 2017). By contrast, synovial fibroblasts from patients with RA undergoing joint replacement surgery were able to stimulate the endothelium, such that they were able to recruit neutrophils and lymphocytes in the absence of any other exogenous cytokines - thus exerting a pro-inflammatory action (Rainger et al., 2001; Lally et al., 2005; Smith et al., 2008; McGettrick et al., 2009; Filer et al., 2017). In particular, this response was due to the trafficking and presentation of fibroblast-derived chemokines (CXCL5 and CXCL12) on the endothelial surface, and enhanced leukocyte capture mediated through P-selectin (neutrophils) and $\alpha_4\beta_1$-integrin-VCAM-1 interactions (lymphocytes) (Lally et al., 2005; McGettrick et al., 2009). Interestingly the synovial fibroblasts from patients at the earliest phase of RA communicate with the endothelium in a manner that is distinct from fibroblasts isolated from resolving synovitis (i.e., they do not suppress cytokine-induced lymphocyte recruitment), and also from fibroblasts from patients with RA undergoing joint replacement surgery [i.e., they are unable to activate the endothelium to recruit leukocytes in the absence of cytokines (Filer et al., 2017)] – this crucially reveals that the cross-talk, and therefore the patterns of leukocyte trafficking in RA, evolve as the disease progresses and suggest that therapies targeting these processes should also change as the disease evolves. Furthermore, blocking either hydrocortisone or IL-6 was able to reverse the pro-inflammatory effects of fibroblasts from patients with RA who had to undergo joint replacement surgery (Lally et al., 2005; Smith et al., 2008; McGettrick et al., 2009), adding further evidence to the mode of action of glucocorticoid or tocilizumab therapy in these patients. Of note, all these studies focused on the interaction of fibroblasts from patients with inflammatory arthritis with endothelial cells isolated from healthy donors. Additional studies are now required to expand this further by incorporating patient-derived sEC's that exhibit disease-specific phenotypes (as highlighted above) and to elucidate the impact this has on the ability of fibroblasts to regulate leukocyte trafficking. Furthermore, there is also a need to broaden the inflammatory arthritides from which cells are isolated to reveal those features of arthritis that are shared across a range of arthritides and those that are unique.

IMAGING LEUKOCYTE TRAFFICKING *IN VIVO* – OBSERVATIONAL STUDIES

The regulation of leukocyte trafficking is multifactorial – involving blood flow; endothelial and stromal responses. Similarly, inflammatory arthritides can be systemic diseases, affecting multiple joints and other organ systems. The only way to truly understand how arthritic pathology influences the kinetics, spatial location and molecular mechanisms of leukocyte migration into, through and away from the joint is through *in vivo* analysis – either preclinical murine models of disease or imaging of patients joints. However, these approaches are significantly more complicated than those we have discussed above, due to the intricate nature of joints (Gompels et al., 2010). As a result, most studies to date have focused on mapping cellular movement, with few conducting mechanistic investigations.

Initial efforts to observe infiltration of human leukocytes movement in real-time began by metal-tagging purified leukocytes subsets and re-injecting them back into the subject, allowing the small gamma particles released by the tagged cells to be detected and tracked (Uno et al., 1986; Dudhia et al., 2015). Tagging human leukocytes with indium-111 (^{111}In) revealed the accumulation of tagged cells in the joints of human patients with swelling and active RA, which were not observed in patients where swelling and pain were not present (Uno et al., 1986) or those with inactive disease (Uno et al., 1992). Moreover, anti-TNFα therapy reduced ^{111}In-labeled granulocyte trafficking into patient joints over 22 h (Taylor et al., 2000). Techniques subsequently progressed to enable tagging of specific cell types, such as anti-T-cell (CD3) technetium-99m (^{99m}Tc) tagged antibodies, which were observed accumulating in the moderately or severely painful joints in RA and PsA patients, but not in those joints where pain levels were low or absent (Marcus et al., 1994). Indeed, clinically active and inactive joints have also been identified using radiolabeled E-selectin in patients with RA (Chapman et al., 1994; Chapman et al., 1996; Jamar et al., 2002). Once again, anti-TNF-α therapy (adalimumab) decreased ^{99m}Tc-labeled leukocyte accumulation

into the joints of RA patients 2 weeks after the treatment onset, which subsequent studies suggested that this was due to increased ^{99m}Tc monocyte/macrophage egress from the joint as numbers of monocytes entering remained unaffected by adalimumab treatment (Thurlings et al., 2009; Herenius et al., 2011). Similarly, metal tagged antibodies against E-selectin have also revealed its up-regulation in porcine arthritic joints but not control joints (Chapman et al., 1994). Thus linking the active movement of T-cells into the joint and changes in capture receptor expression with swelling, pain and disease activity experienced by the patients. Similarly, blood neutrophils tagged with technetium-99m hexametazime were observed ingressing into the rheumatoid joint over 22 h by gamma camera imaging, a response that was blocked by glucocorticoid therapy (methylprednisolone) (Youssef et al., 1996). By contrast, when synovial fluid neutrophils tagged with ^{111}In were injected intra-articularly their egress from the synovial space into the periphery was unaffected by methylprednisolone treatment (Youssef et al., 1996). Further supporting the involvement of migrating neutrophils in the RA pathology, and the beneficial action of glucocorticoid therapy on limiting their movement/effector functions.

Positron emission tomography (PET) tracers allow a non-invasive means to measure cellular accumulation (White et al., 2017; Momcilovic et al., 2018) (**Figure 2H**). For instance, higher levels of the PET tracer [18F]F-AraG were detected in the arthritic paws of AIA mice, whilst no tracer was observed in control paws (Franc et al., 2017). Similarly, in RA and PsA patients, the [18F]-FDG PET tracer was shown to accumulate at sites of synovitis, but not in unaffected joints (Chaudhari et al., 2016). Thus, indicating an accumulation of activated immune cells in the arthritic joint, which could result from either increased leukocyte migration or enhanced proliferation of the cells within the tissue or a combination of both. Protein specific PET tracers, such as ^{68}Ga-Aquibeprin or ^{68}Ga-Avebetrin that bind specifically to $\alpha_5\beta_1$-integrin or $\alpha_V\beta_3$-integrin, respectively, can also be used to track the expression pattern of molecules involved in leukocyte trafficking (Notni et al., 2019). Such tracers showed increased expression of $\alpha_5\beta_1$- and $\alpha_V\beta_3$-integrins in arthritic joints compared to non-arthritic joints in mice with CIA (Notni et al., 2019), suggesting arthritis increases the expression of these integrins to facilitate leukocyte accumulation. Tracer studies are currently limited to detecting global cellular activity (accumulation/proliferation) but are unable to identify individual cells or subsets or their movement.

The greatest advancement in imaging the dynamics of leukocyte trafficking *in vivo* has come from the development of two-photon microscopy, which allows tissues, including the joints and blood vessels, of living organisms to be imaged in real-time enabling the observer to visualize specific parts of the adhesion cascade including velocities (Chen et al., 2017; Cai et al., 2019) (**Figure 2I**). For example, leukocyte rolling and adhesion to arthritic joints (Veihelmann et al., 1999), or neighboring tendons [achilles and patella (Gál et al., 2005)], increased in a time-dependent manner in the initial phases of the disease, after which the number (Veihelmann et al., 1999) and velocity (Gál et al., 2005) of rolling cells steadily declined, whilst the absolute numbers of adherent cells remained elevated in both AIA and proteoglycan induced arthritis (PGIA) models relative to the control animals. Moreover, rolling velocities increased at early time points (4 h) and absolute numbers of adherent leukocytes were reduced over the first 24 h in L-selectin knockout mice with AIA - observed using intravital microscopy of the synovial post-capillary venules (Szántó et al., 2004). Similarly, more LysM-eGFP granulocytic myeloid cells were observed moving at a much slower mean migration velocity through metatarsal tissue of AIA mice using intravital microscopy compared to controls (Byrne et al., 2012). Moreover, adoptively transferred fluorescently labeled antigen-presenting cells (APC) isolated from the spleen and draining lymph nodes of PGIA mice were detected inside the ankles of severe combined immunodeficient (SCID) mice by multiphoton imaging (Angyal et al., 2010). However, when splenic T-cells were transferred they were only detected in the lymph nodes, revealing low levels of T-cell migration directly into the joint following induction of PGIA (Angyal et al., 2010). Near-infrared whole animal imaging tracked the increased infiltration of F4/80$^+$ monocyte/macrophages into arthritic joints over the first 6 h of AIA (Hansch et al., 2004). Taking this further, biofluorescence whole animal imaging studies revealed the more effective localization of anti-TNFα drugs (certolizumab pegol, adalimumab, and infliximab) to arthritic joints than non-arthritic joints in mice with CIA (Palframan et al., 2009).

Alternative strategies employing the use of bioluminescence, commonly involving luciferase, avoid the need for excitation of the label of interest (**Figure 2J**). For instance, Nakajima et al. (2001) tracked the localization of type-II collagen specific GFP-luciferase CD4 T-cell hybridomas following their injection into mice with CIA using whole animal real-time live bioluminescence imaging with the *in vivo* imaging system (IVIS) over a 7 days period (Nakajima et al., 2001). Initially GFP-luciferase CD4 T-cells were observed accumulating in the lungs after 24 h, but subsequently moved to the arthritic joints where the intensity of GFP-luciferase signal, and therefore the accumulation of cells, increased between 3 and 5 days and was still detectable at the same level 7 days post-injection (Nakajima et al., 2001). Using this technology, the locations of specific cell types can be observed throughout an experiment, however, it does not provide detailed data outlining specific cell numbers.

Advances in photoconvertible reporter mice (e.g., Kaede) are now allowing us to gain some insights into the migratory journey of leukocytes to and from tissues. For example, in Kaede mice, cells are converted from green to red fluorescence with a UV light, allowing researchers to track the movement of cells from the tissue of photoconversion into distance sites (Porter et al., 2018; Steele et al., 2019) (**Figure 2K**). On a technical note, it is crucial that tissues neighboring the photoconversion site are appropriately shielded from the light source to avoid converting these cells also. Whilst there are currently no publications reporting photoconversion of an inflamed joint or the neighboring draining lymph nodes we are aware of several groups working in this area and await the outcome of these studies. That said, groups have photoconverted areas of the small intestine and colon in arthritic mice (CIA and KRN, respectively) and detected converted cells, mainly CD4$^+$ T-cells, in the joint

and the draining lymph node between 1 (Morton et al., 2014) and 4 days (Tajik et al., 2020) later by flow cytometry. Combining these data with the earlier IHC studies from the late 1990s further confirms the importance of the ability of gut-derived leukocytes to migrate into arthritic joints in the pathogenesis of the disease.

Whilst advancements in imaging technologies allow the dynamics of leukocyte trafficking patterns or the expression profile of adhesion molecules and cytokines to be observed *in vivo*, we are not yet in the position to fully track these processes in patients over their disease and treatment journey. Improving imaging of molecular mechanistic changes, such as alterations in receptors and ligands, that occur as leukocytes enter and exit the joint is essential to fully understanding these processes and to identify targets to limit trafficking of pathogenic leukocytes whilst promoting the movement of regulatory leukocytes necessary to resolve the inflammatory response and repair the damaged joint.

SUMMARIZING OUR CURRENT UNDERSTANDING OF THE MECHANISMS DRIVING INFLAMMATORY ARTHRITIS

It is clear that patients with inflammatory arthritides, such as RA or PsA, have defects in one or more of the security checkpoints that normally regulate leukocyte trafficking (Buckley and McGettrick, 2018) (**Figure 3**). Firstly synovial endothelial cells (Abbot et al., 1999) and fibroblasts (Parsonage et al., 2005) are imprinted with a pathogenic pro-inflammatory phenotype that is maintained in culture, and which causes these cells to express elevated levels of proinflammatory and pro-recruitment mediators, such as adhesion molecules, chemokines, lipids and cytokines (Parsonage et al., 2005). Moreover, synovial endothelial cells acquire tissue-specific traits associated with mucosal endothelium (VAP-1) (Salmi et al., 1997) and high endothelial venules (PNAd) (Salmi et al., 1997; Cañete et al., 2007) allowing the aberrant trafficking of gut-homing and lymph node homing leukocytes to the joints, and in some cases the formation of tertiary lymphoid structures (Morton et al., 2014; Tajik et al., 2020). Synovial fibroblasts also display positional memory for their location within a joint (Croft et al., 2019; Wei et al., 2020), and differ across joints (Frank-Bertoncelj et al., 2017) – this adds further complexity to the regulation of leukocyte migration within the synovium itself, and for which newer imaging modalities are just starting to reveal insights. Finally, the bi-directional cross-talk between endothelial cells and fibroblasts evolves as the disease progresses (Filer et al., 2017), altering the composition of leukocytes in the joint over the disease history. Thus pathogenic changes in the joint tissue microenvironment actively support the aberrant leukocyte trafficking and accumulation, and so one strategy would be to reset the tissue microenvironment to reverse pathology. Yet, leukocytes from these patients can also display pro-adhesive, pro-migratory phenotypes, linked to genetics [e.g., PTPN22W (Bayley et al., 2015; Burn et al., 2016)], altered metabolism (Pucino et al., 2019, 2020) or protein expression [adiponectin receptors (Chimen et al., 2015); TSK5 (Shen et al., 2017)], which tend to lead to enhanced or prolonged $\alpha_L\beta_2$-integrin expression (Yokota et al., 1995; Burn et al., 2016) facilitating their entry and retention within the inflamed joint. However, this raises the "chicken and egg" question of whether changes in the tissue or changes in leukocytes are the first to happen. Of note, we know much more about the molecular mechanism governing these processes in the context of RA, than other inflammatory arthritides.

Many imaging studies using a wide range of technologies have demonstrated the significant role TNFα plays in the initiation and propagation of inflammation in the joints of humans with RA (Barrera et al., 2001) and mice (Williams et al., 1992; Sudoł-Szopińska et al., 2013). Of relevance here is the reduction in leukocyte accumulation in arthritic joints, as well as changes in the expression of adhesion molecules [e.g., E-selectin and VCAM-1 (Tak et al., 1996)] and chemokines (e.g., IL-8) (Butler et al., 1995) in response to TNFα inhibitors. Despite this, not all RA patients respond to the various on the market, which might be explained, at least in part, by the distinct synovium leukocyte pathotypes observed in tissue sections from patients (Nerviani et al., 2020). Few, if any studies have examined leukocyte numbers or expression of key molecules involved in the recruitment cascade for other chemical or biological disease-modifying anti-rheumatic drugs (DMARDs). Understanding how DMARDs impact the key components and cells of the cascade will allow the mechanism of initiation, development and resolution of inflammatory arthritides to be identified, possibly leading to personalized medicine depending on disease stage.

THE FUTURE OF THE *IN VITRO* JOINT

Technologies to make more *in vivo-like* constructs are continuing to vastly improve: ranging from 3-D self-organizing tissue culture organoids; through to microfluidic channels and building up to 3-D cell cultures incorporating microfluidic technology to create organs-on-chips, and finally the fabrication of tissue-like structures. All of these techniques have improved tremendously over the past 10 years, but their use in studies of leukocyte trafficking in the context of inflammatory arthritides remains limited (reviewed by Damerau and Gaber, 2020).

Given inflammatory arthritides are driven by multiple cell–cell interactions, 3-D organoids offer an excellent way of interrogating these communication pathways in more detail. Unfortunately, the 3-D nature of these constructs currently restricts the possibility of real-time live imaging, so these models are commonly analyzed upon sectioning as seen for whole tissue. For example, TNFα induced the self-organization and proliferation of a 3-D micromass of fibroblast-like synoviocytes from RA patients into the two distinct layers found in the joint (a lining and sublining layer), implying fibroblasts maintain positional memory in culture enabling them to organize themselves as seen in the joint (Calvo et al., 2017). Building upon this, organoids consisting of fibroblasts and endothelial cells suspended in a matrigel droplet revealed that up-regulation of NOTCH3 ligands on the vasculature help to drive the spatial organization of fibroblasts into lining and sublining layers, where

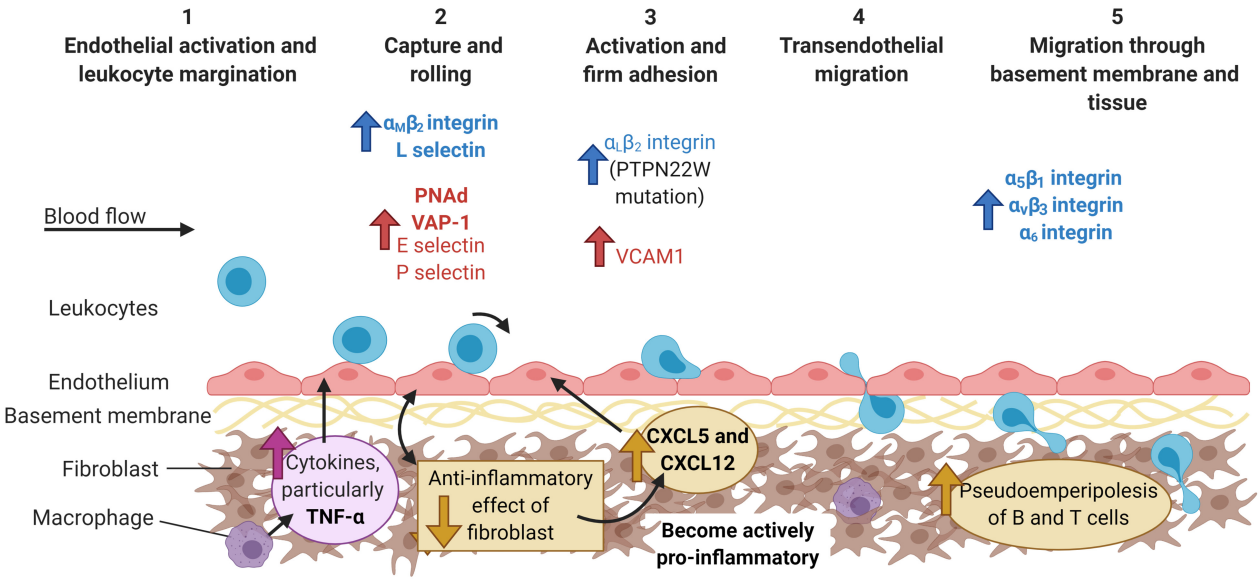

FIGURE 3 | The multi-step adhesion cascade in chronically inflamed joints. The etiology of most inflammatory arthritides remains unknown. At some point during the initial phases of disease, the endothelial cells up-regulate the expression of the typical adhesion molecules (E and P selectin, VCAM), as well as other molecules usually found in HEV venules (PNAd) or the gut (VAP-1). Furthermore, fibroblasts switch from homeostatically anti-inflammatory, to actively pro-inflammatory with the production of chemokines (CXCL5 and CXCL12) that are shuttled to the endothelium. Leukocytes from arthritic patients exhibit higher expression of integrins, such as $\alpha_L\beta_2$-, $\alpha_M\beta_2$-, and α_6-, and are recruited to the endothelium via P-selectin (neutrophils) and $\alpha_4\beta_1$-integrin-VCAM-1 interactions (lymphocytes). Increased expression of α5β1, αvβ3, and α6 integrins on leukocytes aids their migration through the basement membrane and tissue, whilst fibroblast interactions with T and B cells increases pseudoemperipolesis. Molecules are colored according to cell type: leukocytes = blue and endothelial cells = red, and highlighted bold to denote major contributors to infiltration during inflammatory arthritis, but not in response to infection or damage. PNAd, peripheral node addressin; VAP-1, vascular adhesion protein 1; VCAM-1, vascular adhesion protein 1. Created with BioRender.com.

deletion of NOTCH3 reduced the clinical score and inflammatory infiltrated observed by H&E in mice with STIA (Wei et al., 2020). Crucially a subpopulation of synovial fibroblast (fibroblast activation protein α+; FAPα+) is responsible for driving leukocyte infiltration in STIA mice, where deleting FAPα+ fibroblasts reduced leukocyte numbers in the arthritic joint (Croft et al., 2019). Collectively these studies highlight the importance of fibroblast subtypes in regulating leukocyte trafficking and the ability of endothelial cells to influence the phenotype of the neighboring stroma, but crucially they demonstrate the possibility of modeling the human diseased joint using fibroblast-endothelial cell 3-D organoids *in vitro*. Of note, tumor and mural organoid models incorporating mesodermal progenitor cells were able to form a hierarchical structure of blood vessels (Wörsdörfer et al., 2019), suggesting the same could be done and used to model the vasculature in inflammatory arthritides.

Advances in 3-D printing are driving forward the field of microfluidic modeling of leukocyte recruitment in a disease context (Sackmann et al., 2012; Venugopal Menon et al., 2018), where incorporating precious, but limited, patient material into high-throughput mechanistic screening studies is becoming a reality. Such systems have effectively mimicked the disturbed flow patterns seen in vessel bifurcations, highlighting these as areas where endothelial cells can support the recruitment of the monocyte cell line, THP-1 – as seen in atherosclerosis (Khan and Sefton, 2011). Hence microfluidic channels may help to elucidate the disparities seen in the vascular patterns in patients with PsA and RA (Kennedy et al., 2010). Addition of collagen scaffolds; tuneable chemical gradients (Wu et al., 2017) and stromal cells, to the microfluidic channels are paving the way for the development of personalized "organs-on-a-chip" which present the possibility of precision medicine (Van Den Berg et al., 2019). In the context of inflammatory arthritis, microfluidic systems have been used to track the migration of the cadherin-11 expressing synovial cell line (SW982) toward an activated osteoclast cell line (RAW264.7), where the co-culture construct enhanced SW982 migration and osteoclast activity compared to the monocultures (Ma et al., 2018). Moreover, 3-D "synovium-on-a-chip" with an integrated time-resolved light scatter biosensor has been generated that allows the visualization of TNFα induced fibroblast organization into lining and sublining layers over 2 days (Rothbauer et al., 2020) (e.g., **Figure 2G**). Incorporating endothelial cells and leukocytes into such models would enable *in vivo* like analysis of recruitment and it is most likely only a matter of time before these are generated. Furthermore, other *in vivo* like constructs are being formed, such as the living vascular tissue fabricated by direct culture of collagen, smooth muscle cells and endothelial cells, presenting another way to move away from *in vivo* models, whilst accessing leukocyte infiltration (Meghezi et al., 2015). These studies highlight how rapidly microfluidic and *in vivo* models are improving, providing the opportunity to access multiple cell:cell interactions, whilst also mimicking physiological aspects such as blood flow. This is crucial in understanding inflammatory

diseases such as RA, PsA and IA, which are known to be driven by uncontrolled leukocyte recruitment, but exactly how and why this occurs is yet to be elucidated.

The era of precision medicine for inflammatory arthritis is fast approaching (reviewed by Aletaha, 2020; Miyagawa and Tanaka, 2020) with "big data" providing insights into different patient populations and further subgrouping patients according to their underlying process driven pathology – yet imaging remains crucial for initial discoveries and confirming outputs of omics analysis (e.g., Lewis et al., 2019). Indeed, the use of synovial tissue signatures improves the prediction that a patient will require biological therapy 12 months after diagnosis (Lliso-Ribera et al., 2019). Furthermore, advances in spatial transcriptomics now enables mapping of gene expression profiles onto images of tissues, providing for the first-time spatial context to gene expression data (Burgess, 2019). Such technology has revealed that central memory T-cells were dominant in RA synovial tissue sections, whilst in SpA tissues effector memory T-cells were most prominent (Carlberg et al., 2019), and thus will enable more targeted therapies to be delivered to these patients in the future. Advances in imaging technologies, in particular the "synovium-on-a-chip" described above, incorporating patient synovial material provides the opportunity to pre-screen possible treatment options based on identified "patient specific signatures," ultimately offering the realistic hope of achieving precision medicine for all patients based on their cellular and molecular processes driving their disease pathology.

CONCLUSION

Significant advances in imaging modalities over the last 60 years have vastly improved our understanding of leukocyte infiltrates in the inflamed joints in numerous inflammatory arthritides in patients as well as *in vitro/in vivo* models. It is evidently clear that the local microenvironment of an inflamed joint dictates the spatiotemporal dynamics of leukocyte entry and egress, and it is highly likely this differs in different regions of a given joint, between patients, as the disease evolves and in response to treatments. Despite our advances, there is still much we do not fully understand particularly in the context of human disease, and for that further advances are needed to image these processes directly in patients but more realistically to enable the imaging of complex *in vitro* constructs of a patient's joint microenvironment. Only then will we be able to truly map the spatiotemporal dynamics and molecular mechanisms for a patient at a given time point in their disease history. Ultimately the aim would be to develop drug combinations that can limit the trafficking of pathogenic effector leukocytes whilst promoting the function and presence of regulatory leukocytes to switch off the inflammatory response and induce clinical remission/cure the disease.

AUTHOR CONTRIBUTIONS

All authors listed have made a substantial, direct and intellectual contribution to the work, and approved it for publication.

FUNDING

JM, JL, and L-JM were supported by Ph.D. studentships funded by MRC iCase (MR/P016154/1); MRC-Versus Arthritis Centre for Musculoskeletal Ageing Research Ph.D. studentship (MR/R502364/1); and Kennedy Trust for Rheumatology Research, respectively. This work was also supported by MRC project grant MR/T028025/1.

ACKNOWLEDGMENTS

We would like to extend our thanks to our colleagues at the University of Birmingham, United Kingdom whom kindly provided representative images obtained from the techniques detailed in **Figure 2**: Miss Jenefa Begum, Dr. Scott P. Davies (NC3Rs – NC/R002061/1), Dr. Sarah Edwards, Dr. Triin Major, Dr. Patricia Lalor, Miss Sophie Hopkin, and Dr. Lozan Sheriff.

REFERENCES

Abbot, S. E., Whish, W. J. D., Jennison, C., Blake, D. R., and Stevens, C. R. (1999). Tumour necrosis factor α stimulated rheumatoid synovial microvascular endothelial cells exhibit increased shear rate dependent leucocyte adhesion in vitro. *Ann. Rheum. Dis.* 58, 573–581. doi: 10.1136/ard.58.9.573

Aletaha, D. (2020). Precision medicine and management of rheumatoid arthritis. *J. Autoimmun.* 110:102405. doi: 10.1016/j.jaut.2020.102405

Alivernini, S., Tolusso, B., Petricca, L., Bui, L., Di Sante, G., Peluso, G., et al. (2017). Synovial features of patients with rheumatoid arthritis and psoriatic arthritis in clinical and ultrasound remission differ under anti-TNF therapy: a clue to interpret different chances of relapse after clinical remission? *Ann. Rheum. Dis.* 76, 1228–12396. doi: 10.1136/annrheumdis-2016-210424

Angyal, A., Egelston, C., Kobezda, T., Olasz, K., László, A., Glant, T. T., et al. (2010). Development of proteoglycan-induced arthritis depends on T cell-supported autoantibody production, but does not involve significant influx of T cells into the joints. *Arthritis Res. Ther.* 12:R44.

Baeten, D., De Keyser, F., Demetter, P., Cuvelier, C., Van den Bosch, F., Kruithof, E., et al. (2000). Comparative study of the synovial histology in rheumatoid arthritis, spondyloarthropathy, and osteoarthritis: influence of disease duration and activity. *Ann. Rheum. Dis.* 59, 945–953. doi: 10.1136/ard.59.12.945

Barrera, P., Joosten, L. A. B., Den Broeder, A. A., Van de Putte, L. B. A., Van Riel, P. L. C. M., and Van den Berg, W. B. (2001). Effects of treatment with a fully human anti-tumour necrosis factor α monoclonal antibody on the local and systemic homeostasis of interleukin 1 and TNFα in patients with rheumatoid arthritis. *Ann. Rheum. Dis.* 60, 660–669. doi: 10.1136/ard.60.7.660

Bayley, R., Kite, K. A., McGettrick, H. M., Smith, J. P., Kitas, G. D., Buckley, C. D., et al. (2015). The autoimmune-associated genetic variant PTPN22 R620W enhances neutrophil activation and function in patients with rheumatoid arthritis and healthy individuals. *Ann. Rheum. Dis.* 74, 1588–1595. doi: 10.1136/annrheumdis-2013-204796

Behrens, F., Himsel, A., Rehart, S., Stanczyk, J., Beutel, B., Zimmermann, S. Y., et al. (2007). Imbalance in distribution of functional autologous regulatory T cells in rheumatoid arthritis. *Ann. Rheum. Dis.* 66, 1151–1156. doi: 10.1136/ard.2006.068320

Bradfield, P. F., Amft, N., Vernon-Wilson, E., Exley, A. E., Parsonage, G., Rainger, G. E., et al. (2003). Rheumatoid fibroblast-like synoviocytes

overexpress the chemokine stromal cell-derived factor 1 (CXCL12), which supports distinct patterns and rates of CD4+ and CD8+ T cell migration within synovial tissue. *Arthritis Rheum.* 48, 2472–2482. doi: 10.1002/art.11219

Buckley, C. D., and McGettrick, H. M. (2018). Leukocyte trafficking between stromal compartments: lessons from rheumatoid arthritis. *Nat. Rev. Rheumatol.* 14, 476–487. doi: 10.1038/s41584-018-0042-4

Buckley, C. D., Ross, E. A., McGettrick, H. M., Osborne, C. E., Haworth, O., Schmutz, C., et al. (2006). Identification of a phenotypically and functionally distinct population of long-lived neutrophils in a model of reverse endothelial migration. *J. Leukoc. Biol.* 79, 303–311. doi: 10.1189/jlb.0905496

Burger, J. A., Zvaifler, N. J., Tsukada, N., Firestein, G. S., and Kipps, T. J. (2001). Fibroblast-like synoviocytes support B-cell pseudoemperipolesis via a stromal cell-derived factor-1- and CD106 (VCAM-1)-dependent mechanism. *J. Clin. Invest.* 107, 305–315. doi: 10.1172/jci11092

Burgess, D. J. (2019). Spatial transcriptomics coming of age. *Nat. Rev. Genet.* 20:317. doi: 10.1038/s41576-019-0129-z

Burn, G. L., Cornish, G. H., Potrzebowska, K., Samuelsson, M., Griffié, J., Minoughan, S., et al. (2016). Superresolution imaging of the cytoplasmic phosphatase PTPN22 links integrin-mediated T cell adhesion with autoimmunity. *Sci. Signal.* 9:ra99, doi: 10.1126/scisignal.aaf2195

Butler, D. M., Maini, R. N., Feldmann, M., and Brennan, F. M. (1995). Modulation of proinflammatory cytokine release in rheumatoid synovial membrane cell cultures. Comparison of monoclonal anti TNF-α antibody with the interleukin-1 receptor antagonist. *Eur. Cytokine Netw.* 6, 225–230.

Butler, L. M., McGettrick, H. M., and Nash, G. B. (2009). Static and dynamic assays of cell adhesion relevant to the vasculature. *Methods Mol. Biol.* 467, 211–228. doi: 10.1007/978-1-59745-241-0_12

Byrne, R., Rath, E., Hladik, A., Niederreiter, B., Bonelli, M., Frantal, S., et al. (2012). A dynamic real time in vivo and static ex vivo analysis of granulomonocytic cell migration in the collagen- induced arthritis model. *PLoS One* 7:e35194. doi: 10.1371/journal.pone.0035194

Cai, C., Zambach, S. A., Fordsmann, J. C., Lønstrup, M., Thomsen, K. J., Jensen, A. G. K., et al. (2019). In vivo three-dimensional two-photon microscopy to study conducted vascular responses by local ATP ejection using a glass micro-pipette. *J. Vis. Exp.* 148:e59286.

Calvo, I. O., Byrne, R. A., Karonitsch, T., Niederreiter, B., Kartnig, F., Alasti, F., et al. (2017). 04.19 3D synovial organoid culture reveals cellular mechanisms of tissue formation and inflammatory remodelling. *Ann. Rheum. Dis.* 76(Suppl 1), A49.3–A50.

Campbell-Thompson, M. L., Heiple, T., Montgomery, E., Zhang, L., and Schneider, L. (2012). Staining protocols for human pancreatic islets. *J. Vis. Exp.* 63:4068.

Cañete, J. D., Santiago, B., Cantaert, T., Sanmartí, R., Palacin, A., Celis, R., et al. (2007). Ectopic lymphoid neogenesis in psoriatic arthritis. *Ann. Rheum. Dis.* 66, 720–726. doi: 10.1136/ard.2006.062042

Carlberg, K., Korotkova, M., Larsson, L., Catrina, A. I., Ståhl, P. L., and Malmström, V. (2019). Exploring inflammatory signatures in arthritic joint biopsies with spatial transcriptomics. *Sci. Rep.* 9:18975.

Chapman, P. T., Jamar, F., Harrison, A. A., Binns, R. M., Peters, A. M., and Haskard, D. O. (1994). Noninvasive imaging of e-selectin expression by activated endothelium in urate crystal–induced arthritis. *Arthritis Rheum.* 37, 1752–1756. doi: 10.1002/art.1780371207

Chapman, P. T., Jamar, F., Keelan, E. T. M., Peters, A. M., and Haskard, D. O. (1996). Use of a radiolabeled monoclonal antibody against e-selectin for imaging of endothelial activation in rheumatoid arthritis. *Arthritis Rheum.* 39, 1371–1375. doi: 10.1002/art.1780390815

Chaudhari, A. J., Ferrero, A., Godinez, F., Yang, K., Shelton, D. K., Hunter, J. C., et al. (2016). High-resolution 18F-FDG PET/CT for assessing disease activity in rheumatoid and psoriatic arthritis: findings of a prospective pilot study. *Br. J. Radiol.* 89:20160138. doi: 10.1259/bjr.20160138

Chen, C., Zhang, Y. P., Sun, Y., Xiong, W., Shields, L. B. E., Shields, C. B., et al. (2017). An in vivo duo-color method for imaging vascular dynamics following contusive spinal cord injury. *J. Vis. Exp.* 130:56565.

Chimen, M., McGettrick, H. M., Apta, B., Kuravi, S. J., Yates, C. M., Kennedy, A., et al. (2015). Homeostatic regulation of T cell trafficking by a B cell-derived peptide is impaired in autoimmune and chronic inflammatory disease. *Nat. Med.* 21, 467–475. doi: 10.1038/nm.3842

Croft, A. P., Campos, J., Jansen, K., Turner, J. D., Marshall, J., Attar, M., et al. (2019). Distinct fibroblast subsets drive inflammation and damage in arthritis. *Nature.* 570, 246–251. doi: 10.1038/s41586-019-1263-7

Damerau, A., and Gaber, T. (2020). Modeling rheumatoid arthritis in vitro: from experimental feasibility to physiological proximity. *Int. J. Mol. Sci.* 21:7916. doi: 10.3390/ijms21217916

Dijkstra, C. D., Döpp, E. A., Vogels, I. M. C., and Van Noorden, C. J. (1987). Macrophages and dendritic cells in antigen-induced arthritis: an immunohistochemical study using cryostat sections of the whole knee joint of rat. *Scand. J. Immunol.* 26, 513–523. doi: 10.1111/j.1365-3083.1987.tb02285.x

Dominical, V. M., Bértolo, M. B., Almeida, C. B., Garrido, V. T., Miguel, L. I., Costa, F. F., et al. (2011). Neutrophils of rheumatoid arthritis patients on anti-TNF-α therapy and in disease remission present reduced adhesive functions in association with decreased circulating neutrophil-attractant chemokine levels. *Scand. J. Immunol.* 73, 309–318. doi: 10.1111/j.1365-3083.2011.02503.x

Dudhia, J., Becerra, P., Valdés, M. A., Neves, F., Hartman, N. G., and Smith, R. K. W. (2015). In vivo imaging and tracking of technetium-99m labeled bone marrow mesenchymal stem cells in equine tendinopathy. *J. Vis. Exp.* 106:e52748.

Dunky, A., Neumüller, J., and Menzel, J. (1997). Interactions of lymphocytes from patients with psoriatic arthritis or healthy controls and cultured endothelial cells. *Clin. Immunol. Immunopathol.* 85, 297–314. doi: 10.1006/clin.1997.4440

Edwards, S., Lalor, P. F., Tuncer, C., and Adams, D. H. (2006). Vitronectin in human hepatic tumours contributes to the recruitment of lymphocytes in an αvβ3-independent manner. *Br. J. Cancer.* 95, 1545–1554. doi: 10.1038/sj.bjc.6603467

Filer, A., Ward, L. S. C., Kemble, S., Davies, C. S., Munir, H., Rogers, R., et al. (2017). Identification of a transitional fibroblast function in very early rheumatoid arthritis. *Ann. Rheum. Dis.* 76, 2105–2112. doi: 10.1136/annrheumdis-2017-211286

Franc, B. L., Goth, S., MacKenzie, J., Li, X., Blecha, J., Lam, T., et al. (2017). In vivo PET imaging of the activated immune environment in a small animal model of inflammatory arthritis. *Mol. Imaging* 16:1536012117712638.

Frank-Bertoncelj, M., Trenkmann, M., Klein, K., Karouzakis, E., Rehrauer, H., Bratus, A., et al. (2017). Epigenetically-driven anatomical diversity of synovial fibroblasts guides joint-specific fibroblast functions. *Nat. Commun.* 8:14852.

Gál, I., Bajnok, É, Szántó, S., Sarraj, B., Glant, T. T., and Mikecz, K. (2005). Visualization and in situ analysis of leukocyte trafficking into the ankle joint in a systemic murine model of rheumatoid arthritis. *Arthritis Rheum.* 52, 3269–3278. doi: 10.1002/art.21532

Gjelstrup, L. C., Boesen, T., Kragstrup, T. W., Jørgensen, A., Klein, N. J., Thiel, S., et al. (2010). Shedding of large functionally active CD11/CD18 integrin complexes from leukocyte membranes during synovial inflammation distinguishes three types of arthritis through differential epitope exposure. *J. Immunol.* 185, 4154–4168. doi: 10.4049/jimmunol.1000952

Gompels, L. L., Lim, N. H., Vincent, T., and Paleolog, E. M. (2010). In vivo optical imaging in arthritis-an enlightening future? *Rheumatology (Oxford)* 49, 1436–1446. doi: 10.1093/rheumatology/keq012

Gonçalves, W. A., Rezende, B. M., de Oliveira, M. P. E., Ribeiro, L. S., Fattori, V., da, Silva WN, et al. (2020). Sensory ganglia-specific TNF expression is associated with persistent nociception after resolution of inflammation. *Front. Immunol.* 10:3120. doi: 10.3389/fimmu.2019.03120

Grober, J. S., Bowen, B. L., Ebling, H., Athey, B., Thompson, C. B., Fox, D. A., et al. (1993). Monocyte-endothelial adhesion in chronic rheumatoid arthritis: In situ detection of selectin and integrin-dependent interactions. *J. Clin. Invest.* 91, 2609–2619. doi: 10.1172/jci116500

Hansch, A., Frey, O., Sauner, D., Hilger, I., Haas, M., Malich, A., et al. (2004). In vivo imaging of experimental arthritis with near-infrared fluorescence. *Arthritis Rheum.* 50, 961–967. doi: 10.1002/art.20112

Harlan, J. M. (1993). Leukocyte adhesion deficiency syndrome: insights into the molecular basis of leukocyte emigration. *Clin. Immunol. Immunopathol.* 67, S16–S24.

Haworth, O., Hardie, D. L., Burman, A., Rainger, G. E., Eksteen, B., Adams, D. H., et al. (2008). A role for the integrin α6β1 in the differential distribution of CD4

and CD8 T-cell subsets within the rheumatoid synovium. *Rheumatology* 47, 1329–1334. doi: 10.1093/rheumatology/ken263

Herenius, M. M. J., Thurlings, R. M., Wijbrandts, C. A., Bennink, R. J., Dohmen, S. E., Voermans, C., et al. (2011). Monocyte migration to the synovium in rheumatoid arthritis patients treated with adalimumab. *Ann. Rheum. Dis.* 70, 1160–1162. doi: 10.1136/ard.2010.141549

Hirata, T., Furie, B. B. C., and Furie, B. B. C. (2004). "Lymphocyte homing to the skin," in *Lymphocyte Homing to the Skin: Immunology, Immunopathology, and Therapeutic Perspectives*, ed. W.-H. Boehncke (Boca Raton, FL: CRC Press), 53–88. doi: 10.1201/b15729-4

Honvo-Houéto, E., and Truchet, S. (2015). Indirect immunofluorescence on frozen sections of mouse mammary gland. *J. Vis. Exp.* 16:53179.

Humby, F., Lewis, M., Ramamoorthi, N., Hackney, J. A., Barnes, M. R., Bombardieri, M., et al. (2019). Synovial cellular and molecular signatures stratify clinical response to csDMARD therapy and predict radiographic progression in early rheumatoid arthritis patients. *Ann. Rheum. Dis.* 78, 761–772. doi: 10.1136/annrheumdis-2018-214539

Jamar, F., Houssiau, F. A., Devogelaer, J. P., Chapman, P. T., Haskard, D. O., Beaujean, V., et al. (2002). Scintigraphy using a technetium 99m-labelled anti-E-selectin Fab fragment in rheumatoid arthritis. *Rheumatology* 41, 53–61. doi: 10.1093/rheumatology/41.1.53

Jeffery, H. C., Buckley, C. D., Moss, P., Rainger, G. E., Nash, G. B., and McGettrick, H. M. (2013). Analysis of the effects of stromal cells on the migration of lymphocytes into and through inflamed tissue using 3-D culture models. *J. Immunol. Methods* 400–401, 45–57. doi: 10.1016/j.jim.2013.10.004

Johnson, B. A., Haines, G. K., Harlow, L. A., and Koch, A. E. (1993). Adhesion molecule expression in human synovial tissue. *Arthritis Rheum.* 36, 137–146. doi: 10.1002/art.1780360203

JoVE (2021). *Protocol for Immunofluorescence Staining of Paraffin Tissue Sections [Internet]*. Available online at: https://www.jove.com/v/10500/immunofluorescence-microscopy-immunofluorescence-staining-paraffin (accessed January 29, 2021).

Kennedy, A., Ng, C. T., Biniecka, M., Saber, T., Taylor, C., O'Sullivan, J., et al. (2010). Angiogenesis and blood vessel stability in inflammatory arthritis. *Arthritis Rheum.* 62, 711–721. doi: 10.1002/art.27287

Khan, O. F., and Sefton, M. V. (2011). Endothelial cell behaviour within a microfluidic mimic of the flow channels of a modular tissue engineered construct. *Biomed. Microdevices* 13, 69–87. doi: 10.1007/s10544-010-9472-8

Knoerzer, D. B., Donovan, M. G., Schwartz, B. D., and Mengle-Gaw, L. J. (1997). Clinical and histological assessment of collagen-induced arthritis progression in the diabetes-resistant BB/Wor rat. *Toxicol Pathol.* 25, 13–19. doi: 10.1177/019262339702500103

Kragstrup, T. W., Jalilian, B., Hvid, M., Kjærgaard, A., Østgård, R., Schiøttz-Christensen, B., et al. (2014). Decreased plasma levels of soluble CD18 link leukocyte infiltration with disease activity in spondyloarthritis. *Arthritis Res. Ther.* 16:R42.

Kuijpers, T. W., Van Lier, R. A. W., Hamann, D., De Boer, M., Thung, L. Y., Weening, R. S., et al. (1997). Leukocyte adhesion deficiency type 1 (LAD-1)/variant. A novel immunodeficiency syndrome characterized by dysfunctional β2 integrins. *J. Clin. Invest.* 100, 1725–1733. doi: 10.1172/jci119697

LaBranche, T. P., Hickman-Brecks, C. L., Meyer, D. M., Storer, C. E., Jesson, M. I., Shevlin, K. M., et al. (2010). Characterization of the KRN cell transfer model of rheumatoid arthritis (KRN-CTM), a chronic yet synchronized version of the K/BxN mouse. *Am. J. Pathol.* 177, 1388–1396. doi: 10.2353/ajpath.2010.100195

Lally, F., Smith, E., Filer, A., Stone, M. A., Shaw, J. S., Nash, G. B., et al. (2005). A novel mechanism of neutrophil recruitment in a coculture model of the rheumatoid synovium. *Arthritis Rheum.* 52, 3460–3469. doi: 10.1002/art.21394

Lewis, M. J., Barnes, M. R., Blighe, K., Goldmann, K., Rana, S., Hackney, J. A., et al. (2019). Molecular portraits of early rheumatoid arthritis identify clinical and treatment response phenotypes. *Cell Rep.* 28, 2455.e–2470.e5.

Ley, K., Laudanna, C., Cybulsky, M. I., and Nourshargh, S. (2007). Getting to the site of inflammation: the leukocyte adhesion cascade updated. *Nat. Rev. Immunol.* 7, 678–689. doi: 10.1038/nri2156

Lim, E., Modi, K. D., and Kim, J. B. (2009). In vivo bioluminescent imaging of mammary tumors using IVIS spectrum. *J. Vis. Exp.* 26:1210.

Lioté, F., Boval-Boizardy, B., Weillz, D., Kuntz, D., and Wautieryz, J.-L. (1996). Blood monocyte activation in rheumatoid arthritis: increased monocyte adhesiveness, integrin expression, and cytokine release. *Clin. Exp. Immunol.* 106, 13–19. doi: 10.1046/j.1365-2249.1996.d01-820.x

Lliso-Ribera, G., Humby, F., Lewis, M., Nerviani, A., Mauro, D., Rivellese, F., et al. (2019). Synovial tissue signatures enhance clinical classification and prognostic/treatment response algorithms in early inflammatory arthritis and predict requirement for subsequent biological therapy: results from the pathobiology of early arthritis cohort (PEAC). *Ann. Rheum. Dis.* 78, 1642–1652. doi: 10.1136/annrheumdis-2019-215751

Ma, H. P., Deng, X., Chen, D. Y., Zhu, D., Tong, J. L., Zhao, T., et al. (2018). A microfluidic chip-based co-culture of fibroblast-like synoviocytes with osteoblasts and osteoclasts to test bone erosion and drug evaluation. *R. Soc. Open Sci.* 5:180528. doi: 10.1098/rsos.180528

Manasson, J., Blank, R. B., and Scher, J. U. (2020). The microbiome in rheumatology: where are we and where should we go? *Ann. Rheum. Dis.* 79, S727–S733.

Marcus, C., Thakur, M. L., Huynh, T. V., Louie, J. S., Leibling, M., Minami, C., et al. (1994). Imaging rheumatic joint diseases with anti-T lymphocyte antibody OKT-3. *Nucl. Med. Commun.* 15, 824–830. doi: 10.1097/00006231-199410000-00008

Matsui, T., Akahoshi, T., Namai, R., Hashimoto, A., Kurihara, Y., Rana, M., et al. (2001). Selective recruitment of CCR6-expressing cells by increased production of MIP-3α in rheumatoid arthritis. *Clin. Exp. Immunol.* 125, 155–161. doi: 10.1046/j.1365-2249.2001.01542.x

McGettrick, H. M., Butler, L. M., Buckley, C. D., Rainger, G., and Nash, G. B. (eds) (2012). Tissue stroma as a regulator of leukocyte recruitment in inflammation. *J. Leukoc. Biol.* 91, 385–400. doi: 10.1189/jlb.0911458

McGettrick, H. M., Hunter, K., Moss, P. A., Buckley, C. D., Rainger, G. E., and Nash, G. B. (2008). Direct observations of the kinetics of migrating T cells suggest active retention by endothelial cells with continual bidirectional migration. *J. Leukoc. Biol.* 85, 98–107. doi: 10.1189/jlb.0508301

McGettrick, H. M., Smith, E., Filer, A., Kissane, S., Salmon, M., Buckley, C. D., et al. (2009). Fibroblasts from different sites may promote or inhibit recruitment of flowing lymphocytes by endothelial cells. *Eur. J. Immunol.* 39, 113–125. doi: 10.1002/eji.200838232

Mcgettrick, H. M., Ward, L. S. C., Rainger, G. E., and Nash, G. B. (2017). Mesenchymal stromal cells as active regulators of lymphocyte recruitment to blood vascular endothelial cells. *Methods Mol. Biol.* 1591, 121–142. doi: 10.1007/978-1-4939-6931-9_9

McNaughton, E. F., Eustace, A. D., King, S., Sessions, R. B., Kay, A., Farris, M., et al. (2018). Novel anti-inflammatory peptides based on chemokine–glycosaminoglycan interactions reduce leukocyte migration and disease severity in a model of rheumatoid arthritis. *J. Immunol.* 200, 3201–3217. doi: 10.4049/jimmunol.1701187

Meghezi, S., Seifu, D. G., Bono, N., Unsworth, L., Mequanint, K., and Mantovani, D. (2015). Engineering 3D cellularized collagen gels for vascular tissue regeneration. *J. Vis. Exp.* 100:e52812,

Menon, M., Benechet, A. P., and Khanna, K. M. (2017). Visualizing endogenous effector T cell egress from the lymph nodes. *Methods Mol. Biol.* 1591, 59–71. doi: 10.1007/978-1-4939-6931-9_5

Mertens, A. V., de Clerck, L. S., Moens, M. M., Bridts, C. H., and Stevens, W. J. (1994). Lymphocyte activation status, expression of adhesion molecules and adhesion to human endothelium in rheumatoid arthritis – relationship to disease activity. *Res. Immunol.* 145, 101–108. doi: 10.1016/s0923-2494(94)80020-0

Mitchell, T. S., Moots, R. J., and Wright, H. L. (2017). Janus kinase inhibitors prevent migration of rheumatoid arthritis neutrophils towards interleukin-8, but do not inhibit priming of the respiratory burst or reactive oxygen species production. *Clin. Exp. Immunol.* 189, 250–258. doi: 10.1111/cei.12970

Miyagawa, I., and Tanaka, Y. (2020). The approach to precision medicine for the treatment of psoriatic arthritis. *Immunol. Med.* 43, 98–102. doi: 10.1080/25785826.2020.1753430

Momcilovic, M., Bailey, S. T., Lee, J. T., Zamilpa, C., Jones, A., Abdelhady, G., et al. (2018). Utilizing18F-FDG PET/CT imaging and quantitative histology to measure dynamic changes in the glucose metabolism in mouse models of lung cancer. *J. Vis. Exp.* 137:57167.

Morton, A. M., Sefik, E., Upadhyay, R., Weissleder, R., Benoist, C., and Mathis, D. (2014). Endoscopic photoconversion reveals unexpectedly broad leukocyte trafficking to and from the gut. *Proc. Natl. Acad. Sci. U. S. A.* 111, 6696–6701. doi: 10.1073/pnas.1405634111

Muirden, K. D., and Mills, K. W. (1971). Do lymphocytes protect the rheumatoid joint? *Br. Med. J.* 4, 219–221. doi: 10.1136/bmj.4.5781.219

Muirden, K. D., and Senator, G. B. (1968). Iron in the synovial membrane in rheumatoid arthritis and other joint diseases. *Ann. Rheum. Dis.* 27, 38–48. doi: 10.1136/ard.27.1.38

Munir, H., Rainger, G., Nash, G. B., and McGettrick, H. (eds) (2015). Analyzing the effects of stromal cells on the recruitment of leukocytes from flow. *J. Vis. Exp.* 95:e52480.

Nakajima, A., Seroogy, C. M., Sandora, M. R., Tarner, I. H., Costa, G. L., Taylor-Edwards, C., et al. (2001). Antigen-specific T cell-mediated gene therapy in collagen-induced arthritis. *J. Clin. Invest.* 107, 1293–1301. doi: 10.1172/jci12037

Nerviani, A., Di Cicco, M., Mahto, A., Lliso-Ribera, G., Rivellese, F., Thorborn, G., et al. (2020). A pauci-immune synovial pathotype predicts inadequate response to TNFα-Blockade in rheumatoid arthritis patients. *Front. Immunol.* 11:845. doi: 10.3389/fimmu.2020.00845

Neumüller, J., Dunky, A., Burtscher, H., Jilch, R., and Menzel, J. E. (2001). Interaction of monocytes from patients with psoriatic arthritis with cultured microvascular endothelial cells. *Clin. Immunol.* 98, 143–152. doi: 10.1006/clim.2000.4953

Notni, J., Gassert, F. T., Steiger, K., Sommer, P., Weichert, W., Rummeny, E. J., et al. (2019). In vivo imaging of early stages of rheumatoid arthritis by α5β1-integrin-targeted positron emission tomography. *EJNMMI Res.* 9:87,

Paleolog, E. M., Hunt, M., Elliott, M. J., Feldmann, M., Maini, R. N., and Woody, J. N. (1996). Deactivation of vascular endothelium by monoclonal anti-tumor necrosis factor α antibody in rheumatoid arthritis. *Arthritis Rheum.* 39, 1082–1091. doi: 10.1002/art.1780390703

Palframan, R., Airey, M., Moore, A., Vugler, A., and Nesbitt, A. (2009). Use of biofluorescence imaging to compare the distribution of certolizumab pegol, adalimumab, and infliximab in the inflamed paws of mice with collagen-induced arthritis. *J. Immunol. Methods* 348, 36–41. doi: 10.1016/j.jim.2009.06.009

Parsonage, G., Filer, A. D., Haworth, O., Nash, G. B., Rainger, G. E., Salmon, M., et al. (2005). A stromal address code defined by fibroblasts. *Trends in Immunol.* 26, 150–156. doi: 10.1016/j.it.2004.11.014

Pitzalis, C., Kelly, S., and Humby, F. (2013). New learnings on the pathophysiology of RA from synovial biopsies. *Curr. Opin. Rheumatol.* 25, 334–344. doi: 10.1097/bor.0b013e32835fd8eb

Porter, C., Ennamorati, M., and Jain, N. (2018). In vivo photolabeling of cells in the colon to assess migratory potential of hematopoietic cells in neonatal mice. *J. Vis. Exp.* 138:57929.

Pucino, V., Certo, M., Bombardieri, M., Pitzalis, C., and Correspondence, C. M. (2019). Lactate buildup at the site of chronic inflammation promotes disease by inducing CD4+ T cell metabolic rewiring. *Cell. Metab.* 30, 1055–1074.e8.

Pucino, V., Certo, M., Varricchi, G., Marone, G., Ursini, F., Rossi, F. W., et al. (2020). Metabolic checkpoints in rheumatoid arthritis. *Front. Physiol.* 11:347. doi: 10.3389/fphys.2020.00347

Rainger, G. E., Stone, P., Morland, C. M., and Nash, G. B. (2001). A novel system for investigating the ability of smooth muscle cells and fibroblasts to regulate adhesion of flowing leukocytes to endothelial cells. *J. Immunol. Methods.* 255, 73–82. doi: 10.1016/s0022-1759(01)00427-6

Rothbauer, M., Höll, G., Eilenberger, C., Kratz, S. R. A., Farooq, B., Schuller, P., et al. (2020). Monitoring tissue-level remodelling during inflammatory arthritis using a three-dimensional synovium-on-a-chip with non-invasive light scattering biosensing. *Lab Chip* 20, 1461–1471. doi: 10.1039/c9lc01097a

Sackmann, E. K., Berthier, E., Young, E. W. K., Shelef, M. A., Wernimont, S. A., Huttenlocher, A., et al. (2012). Microfluidic kit-on-a-lid: a versatile platform for neutrophil chemotaxis assays. *Blood* 120:e45–e53,

Salmi, M., Rajala, P., and Jalkanen, S. (1997). Homing of mucosal leukocytes to joints: distinct endothelial ligands in synovium mediate leukocyte-subtype specific adhesion. *J. Clin. Invest.* 99, 2165–2172. doi: 10.1172/jci119389

Shen, Y., Wen, Z., Li, Y., Matteson, E. L., Hong, J., Goronzy, J. J., et al. (2017). Metabolic control of the scaffold protein TKS5 in tissue-invasive, proinflammatory T cells. *Nat. Immunol.* 18, 1025–1034. doi: 10.1038/ni.3808

Shimaoka, Y., Attrep, J. F., Hirano, T., Ishihara, K., Suzuki, R., Toyosaki, T., et al. (1998). Nurse-like cells from bone marrow and synovium of patients with rheumatoid arthritis promote survival and enhance function of human B cells. *J. Clin. Invest.* 102, 606–618. doi: 10.1172/jci3162

Shu, Q., Amin, M. A., Ruth, J. H., Campbell, P. L., and Koch, A. E. (2012). Suppression of endothelial cell activity by inhibition of TNFα. *Arthritis Res. Ther.* 14:R88.

Smith, E., McGettrick, H. M., Stone, M. A., Shaw, J. S., Middleton, J., Nash, G. B., et al. (2008). Duffy antigen receptor for chemokines and CXCL5 are essential for the recruitment of neutrophils in a multicellular model of rheumatoid arthritis synovium. *Arthritis Rheum.* 58, 1968–1973. doi: 10.1002/art.23545

Stamper, H. B., and Woodruff, J. J. (1976). Lymphocyte homing into lymph nodes: In vitro demonstration of the selective affinity of recirculating lymphocytes for high-endothelial venules*. *J. Exp. Med.* 144, 828–833. doi: 10.1084/jem.144.3.828

Steele, M. M., Churchill, M. J., Breazeale, A. P., Lane, R. S., Nelson, N. A., and Lund, A. W. (2019). Quantifying leukocyte egress via lymphatic vessels from murine skin and tumors. *J. Vis. Exp.* 143:e58704.

Sudoł-Szopińska, I., Kontny, E., Maśliński, W., Prochorec-Sobieszek, M., Warczyńska, A., and Kwiatkowska, B. (2013). Significance of bone marrow edema in pathogenesis of rheumatoid arthritis. *Pol. J. Radiol.* 78, 57–63. doi: 10.12659/pjr.883768

Szántó, S., Gál, I., Gonda, A., Glant, T. T., and Mikecz, K. (2004). Expression of L-selectin, but not CD44, is required for early neutrophil extravasation in antigen-induced arthritis. *J. Immunol.* 172, 6723–6734. doi: 10.4049/jimmunol.172.11.6723

Tajik, N., Frech, M., Schulz, O., Schälter, F., Lucas, S., Azizov, V., et al. (2020). Targeting zonulin and intestinal epithelial barrier function to prevent onset of arthritis. *Nat. Commun.* 11:1995.

Tak, P. P., Taylor, P. C., Breedveld, F. C., Smeets, T. J. M., Daha, M. R., Kluin, P. M., et al. (1996). Decrease in cellularity and expression of adhesion molecules by anti- tumor necrosis factor α monoclonal antibody treatment in patients with rheumatoid arthritis. *Arthritis Rheum.* 39, 1077–1081. doi: 10.1002/art.1780390702

Tanaka, Y., McInnes, I. B., Taylor, P. C., Byers, N. L., Chen, L., de Bono, S., et al. (2018). Characterization and changes of lymphocyte subsets in baricitinib-treated patients with rheumatoid arthritis: an integrated analysis. *Arthritis Rheumatol.* 70, 1923–1932. doi: 10.1002/art.40680

Taylor, P. C., Michael Peters, A., Paleolog, E., Chapman, P. T., Elliott, M. J., McCloskey, R., et al. (2000). Reduction of chemokine levels and leukocyte traffic to joints by tumor necrosis factor α blockade in patients with rheumatoid arthritis. *Arthritis Rheum.* 43, 38–47. doi: 10.1002/1529-0131(200001)43:1<38::aid-anr6>3.0.co;2-l

Thurlings, R. M., Wijbrandts, C. A., Bennink, R. J., Dohmen, S. E., Voermans, C., Wouters, D., et al. (2009). Monocyte scintigraphy in rheumatoid arthritis: the dynamics of monocyte migration in immune-mediated inflammatory disease. *PLoS One* 4:e7865. doi: 10.1371/journal.pone.0007865

Traylor-Knowles, N. (2018). In situ hybridization techniques for paraffin-embedded adult coral samples. *J. Vis. Exp.* 138:57853.

Tucker, D. K., Foley, J. F., Hayes-Bouknight, S. A., and Fenton, S. E. (2016). Preparation of high-quality hematoxylin and eosin-stained sections from rodent mammary gland whole mounts for histopathologic review. *Toxicol. Pathol.* 44, 1059–1064. doi: 10.1177/0192623316660769

Uno, K., Matsui, N., Nohira, K., Suguro, T., Kitakata, Y., Uchiyama, G., et al. (1986). Indium-111 leukocyte imaging in patients with rheumatoid arthritis. *J. Nucl. Med.* 27, 339–344.

Uno, K., Suguro, T., Nohira, K., Moriya, H., Saegusa, K., Anzai, Y., et al. (1992). Comparison of Indium-111-labeled leukocyte scintigraphy and Technetium-99m joint scintigraphy in rheumatoid arthritis and osteoarthritis. *Ann. Nucl. Med.* 6, 247–251. doi: 10.1007/bf03164662

Van Den Berg, A., Mummery, C. L., Passier, R., and Van der Meer, A. D. (2019). Personalised organs-on-chips: functional testing for precision medicine. *Lab Chip* 19, 198–205. doi: 10.1039/c8lc00827b

Veale, D., Yanni, G., Rogers, S., Barnes, L., Bresnihan, B., and Fitzgerald, O. (1993). Reduced synovial membrane macrophage numbers, elam-1 expression, and

lining layer hyperplasia in psoriatic arthritis as compared with rheumatoid arthritis. *Arthritis Rheum.* 36, 893–900. doi: 10.1002/art.1780360705

Veihelmann, A., Harris, A. G., Krombach, F., Schütze, E., Refior, H. J., and Messmer, K. (1999). In vivo assessment of synovial microcirculation and leukocyte-endothelial cell interaction in mouse antigen-induced arthritis. *Microcirculation* 6, 281–290. doi: 10.1080/713773963

Venugopal Menon, N., Tay, H. M., Pang, K. T., Dalan, R., Wong, S. C., Wang, X., et al. (2018). A tunable microfluidic 3D stenosis model to study leukocyte-endothelial interactions in atherosclerosis. *APL Bioeng* 2:016103. doi: 10.1063/1.4993762

Verschure, P. J., Noorden, C. J. F., and Dijkstra, C. D. (1989). Macrophages and dendritic cells during the early stages of antigen-induced arthritis in rats: immunohistochemical analysis of cryostat sections of the whole knee joint. *Scand. J. Immunol.* 29, 371–381. doi: 10.1111/j.1365-3083.1989.tb01136.x

Vestweber, D. (2015). How leukocytes cross the vascular endothelium. *Nat. Rev. Immunol.* 15, 692–704. doi: 10.1038/nri3908

Wagner, U. G., Kurtin, P. J., Wahner, A., Brackertz, M., Berry, D. J., Goronzy, J. J., et al. (1998). The role of CD8+ CD40L+ T cells in the formation of germinal centers in rheumatoid synovitis. *J. Immunol.* 161, 6390–6397.

Wang, C. R., Liu, M. F., Huang, Y. H., and Chen, H. C. (2004). Up-regulation of XCR1 expression in rheumatoid joints. *Rheumatology* 43, 569–573. doi: 10.1093/rheumatology/keh147

Wei, K., Korsunsky, I., Marshall, J. L., Gao, A., Watts, G. F. M., Major, T., et al. (2020). Notch signalling drives synovial fibroblast identity and arthritis pathology. *Nature* 582, 259–264. doi: 10.1038/s41586-020-2222-z

Weyand, C. M., Wu, B., and Goronzy, J. J. (2020). The metabolic signature of T cells in rheumatoid arthritis. *Curr. Opin. Rheumatol.* 32, 159–167. doi: 10.1097/bor.0000000000000683

White, A. G., Maiello, P., Coleman, M. T., Tomko, J. A., Frye, L. J., Scanga, C. A., et al. (2017). Analysis of 18FDG PET/CT imaging as a tool for studying *Mycobacterium tuberculosis* infection and treatment in non-human primates. *J. Vis. Exp.* 127:56375.

Williams, R. O., Feldmann, M., and Maini, R. N. (1992). Anti-tumor necrosis factor ameliorates joint disease in murine collagen-induced arthritis. *Proc. Natl. Acad. Sci. U. S. A.* 89, 9784–9788. doi: 10.1073/pnas.89.20.9784

Wörsdörfer, P., Dalda, N., Kern, A., Krüger, S., Wagner, N., Kwok, C. K., et al. (2019). Generation of complex human organoid models including vascular networks by incorporation of mesodermal progenitor cells. *Sci. Rep.* 9:15663,

Wu, X., Newbold, M. A., Gao, Z., and Haynes, C. L. (2017). A versatile microfluidic platform for the study of cellular interactions between endothelial cells and neutrophils. *Biochim. Biophys. Acta Gen. Subj.* 1861, 1122–1130. doi: 10.1016/j.bbagen.2017.02.012

Xu, H., Zhao, H., Fan, D., Liu, M., Cao, J., Xia, Y., et al. (2020). Interactions between gut microbiota and immunomodulatory cells in rheumatoid arthritis. *Mediators Inflamm.* 2020:1430605.

Yokota, A., Murata, N., Saiki, O., Shimizu, M., Springer, T. A., and Kishimoto, T. (1995). High avidity state of leukocyte function-associated antigen-1 on rheumatoid synovial fluid T lymphocytes. *J. Immunol.* 155, 4118–4124.

Youssef, P. P., Cormack, J., Evill, C. A., Peter, D. T., Roberts-Thomson, P. J., Ahern, M. J., et al. (1996). Neutrophil trafficking into inflamed joints in patients with rheumatoid arthritis, and the effects of methylprednisolone. *Arthritis Rheum.* 39, 216–225. doi: 10.1002/art.1780390207

Zhang, J., Alcaide, P., Liu, L., Sun, J., He, A., Luscinskas, F. W., et al. (2011). Regulation of endothelial cell adhesion molecule expression by mast cells, macrophages, and neutrophils. *PLoS One* 6:e14525. doi: 10.1371/journal.pone.0014525

Zhang, X., Nakajima, T., Goronzy, J. J., and Weyand, C. M. (2005). Tissue trafficking patterns of effector memory CD4+ T cells in rheumatoid arthritis. *Arthritis Rheum.* 52, 3839–3849. doi: 10.1002/art.21482

Conflict of Interest: JM's Ph.D. studentship was partially funded by Novartis.

The remaining authors declare that the research was conducted in the absence of any commercial or financial relationships that could be construed as a potential conflict of interest.

frontiers in Cell and Developmental Biology

REVIEW
published: 29 March 2021
doi: 10.3389/fcell.2021.635263

Elucidating the Biomechanics of Leukocyte Transendothelial Migration by Quantitative Imaging

Amy B. Schwartz[1], Obed A. Campos[1], Ernesto Criado-Hidalgo[1], Shu Chien[2,3], Juan C. del Álamo[1,3,4,5], Juan C. Lasheras[1,2,3]* and Yi-Ting Yeh[1,2,3]**

[1] Department of Mechanical and Aerospace Engineering, University of California, San Diego, La Jolla, CA, United States, [2] Department of Bioengineering, University of California, San Diego, La Jolla, CA, United States, [3] Institute of Engineering in Medicine, University of California, San Diego, La Jolla, CA, United States, [4] Department of Mechanical Engineering, University of Washington, Seattle, WA, United States, [5] Center for Cardiovascular Biology, University of Washington, Seattle, WA, United States

OPEN ACCESS

Edited by:
Hao Sun,
University of California, San Diego,
United States

Reviewed by:
Francis Luscinskas,
Harvard University, United States
Dietmar Vestweber,
Max Planck Institute for Molecular Biomedicine, Germany

***Correspondence:**
Yi-Ting Yeh
yiyeh@ucsd.edu
Juan C. del Álamo
juancar@uw.edu
Juan C. Lasheras
jlasheras@eng.ucsd.edu

Specialty section:
This article was submitted to Cell Adhesion and Migration, a section of the journal Frontiers in Cell and Developmental Biology

Received: 30 November 2020
Accepted: 09 March 2021
Published: 29 March 2021

Citation:
Schwartz AB, Campos OA, Criado-Hidalgo E, Chien S, del Álamo JC, Lasheras JC and Yeh Y-T (2021) Elucidating the Biomechanics of Leukocyte Transendothelial Migration by Quantitative Imaging. Front. Cell Dev. Biol. 9:635263. doi: 10.3389/fcell.2021.635263

Leukocyte transendothelial migration is crucial for innate immunity and inflammation. Upon tissue damage or infection, leukocytes exit blood vessels by adhering to and probing vascular endothelial cells (VECs), breaching endothelial cell-cell junctions, and transmigrating across the endothelium. Transendothelial migration is a critical rate-limiting step in this process. Thus, leukocytes must quickly identify the most efficient route through VEC monolayers to facilitate a prompt innate immune response. Biomechanics play a decisive role in transendothelial migration, which involves intimate physical contact and force transmission between the leukocytes and the VECs. While quantifying these forces is still challenging, recent advances in imaging, microfabrication, and computation now make it possible to study how cellular forces regulate VEC monolayer integrity, enable efficient pathfinding, and drive leukocyte transmigration. Here we review these recent advances, paying particular attention to leukocyte adhesion to the VEC monolayer, leukocyte probing of endothelial barrier gaps, and transmigration itself. To offer a practical perspective, we will discuss the current views on how biomechanics govern these processes and the force microscopy technologies that have enabled their quantitative analysis, thus contributing to an improved understanding of leukocyte migration in inflammatory diseases.

Keywords: leukocyte, vascular endothelial cell, transednothelial migration, biomechanics, force microscopy

INTRODUCTION

Leukocytes encompass a diverse group of white blood cells in the immune system, including lymphocytes, monocytes, dendritic cells, and neutrophils, which exhibit a versatile and broad range of migratory abilities. Leukocyte migration from the bloodstream to sites of injury or infection is a primary component of the innate immune and inflammatory responses. Functioning as first responders, leukocytes can efficiently overcome biophysical barriers in their response to pro-inflammatory stimuli, including the vascular wall and dense three-dimensional (3-D) extravascular spaces. This efficient pathfinding is essential for leukocyte trafficking and provides potential therapeutic targets for immune-related and inflammatory diseases.

The scope and speed of the innate immune response are primarily dictated by transendothelial migration (TEM). The endothelium is formed by a monolayer of vascular endothelial cells (VECs) lining the vessel walls and functions as a physical barrier between the circulation and the underlying interstitial tissue. During TEM, leukocytes adhere to the VECs, transmigrate across the endothelium, and cross the vascular basement membrane to the extravascular space (Ley et al., 2007; Muller, 2014; Nourshargh and Alon, 2014; Vestweber, 2015; **Figure 1**). Pro-inflammatory stimuli such as TNF-α and IL-8 can activate both leukocytes and VECs to initiate TEM at the affected site (Middleton et al., 1997; Chandrasekharan et al., 2007). Circulating leukocytes bind to selectin molecules on the VECs via counter glycoprotein ligands, beginning a rolling and adhesion process (Kansas, 1996). Immobilized IL-8 chemokines on inflamed endothelial surfaces switch the leukocytes' integrins LFA-1 and VLA-4 to high-affinity states, triggering the transition from rolling to firm adhesion and lateral migration, followed by direct TEM. The concomitance of high-affinity states in leukocyte integrins and increased expressions of ICAM-1 and VCAM-1 on inflamed VECs promotes cellular contractile forces, which regulate junctional integrity, endothelial permeability, and ultimately leukocyte trafficking (Cook-Mills and Deem, 2005; Stroka and Aranda-Espinoza, 2010). TEM occurs via one of two routes: at endothelial adherens junctions (paracellular migration) or through the VEC itself (transcellular migration). Although the factors governing route selection are not fully understood, both *in-vitro* and *in-vivo* experiments have demonstrated that the paracellular route is preferred, accounting for 90% of TEM events (Muller, 2003; Schulte et al., 2011; Woodfin et al., 2011). It remains unclear whether and how leukocytes probe the endothelium to find permissive sites for TEM and how leukocytes coordinate the force generation with VECs to facilitate their passage across the monolayer.

TEM involves several physical interaction cascades between leukocytes and VECs, characterized by the sequences of motions happening at the interfaces between the two cell types. Receptor-ligand interactions govern leukocyte TEM by modulating cellular functions, as mentioned above. For example, the activation of cell surface proteins triggers cytoskeletal rearrangements leading to increased cellular contractility and force transmission between the leukocytes, VECs, and the substrate. In this regard, TEM can be viewed as a biomechanically regulated process with contributions from both leukocytes and VECs. Recent advances in microfabrication, microscopy, and quantitative analysis allowed researchers to measure the mechanical forces involved in leukocyte-VEC interactions, contributing to delineating their roles in deciding the TEM route and driving cell motion. This review primarily focuses on two phases that play a determinant role in leukocyte trafficking: (1) adhesion and probing, and (2) direct TEM. Furthermore, we discuss current advances in force microscopy techniques for each phase and applications of force measurements in elucidating biomechanical mechanisms of leukocyte TEM. For additional background information on the biology of leukocyte TEM, we recommend previous reviews on this topic (Ley et al., 2007; Muller, 2014; Nourshargh and Alon, 2014; Vestweber, 2015).

BIOMECHANICS OF LEUKOCYTE ENDOTHELIAL ADHESION AND PROBING

Almost immediately in response to pro-inflammatory signals, circulating leukocytes roll on the endothelial monolayer and then attach firmly to it (**Figure 1A**). Subsequently, they crawl over the endothelium using integrin-dependent adhesions. These interactions allow leukocytes and VECs to communicate by well-regulated surface receptors and their counter ligands on the opposing cell membrane. For example, the rolling step is mediated by rapid interaction between leukocyte selectin and P-selectin glycoprotein ligand-1 and endothelial P- and E-selectins (Alon et al., 1995; Lawrence et al., 1997; da Costa Martins et al., 2007; Hidalgo et al., 2007). Chemokine-induced integrin activation facilitates firm adhesion, spreading, crawling, and TEM by strengthening the leukocyte-VEC bond via leukocyte integrins (CD11/CD18, VLA-4) and their counter ligands, i.e., the adhesion molecules on VECs (e.g., ICAM-1, VCAM-1). This cascade of interactions has been characterized using specific blocking antibodies, pharmacological manipulations, and genetic perturbations to demonstrate each molecule's role and downstream signaling effects *in vitro* and *in vivo* (Berlin et al., 1995; Huo et al., 2000; Singbartl et al., 2001; Chesnutt et al., 2006). This interaction cascade is also highly mechanically regulated. For example, during leukocyte rolling, the tensile forces on selectin catch-bonds have been shown to activate leukocyte integrins and facilitate leukocyte firm adhesion under shear stresses (Morikis et al., 2017).

In addition to regulating biochemical receptor-ligand interactions, leukocytes rely on mechanical forces to identify endothelial sites with decreased barrier function and to burrow through the endothelium. TEM does not occur with equal probability at all locations within the endothelium. Rather, it happens more often across the junctions between adjacent VECs than across the cytoplasm of single VECs. Moreover, it is observed more frequently at the confluence of three VECs (tricellular junctions) (Lampi et al., 2017) and between junctions loosened by inflammatory mediators (Schaefer and Hordijk, 2015). Following rolling and firm attachment to the endothelium, leukocytes spread out and initiate the protrusion and retraction of podosome-like structures that indent on endothelial membranes (**Figure 1B**). These structures are speculated to continually probe the underlying monolayer and play a decisive role in determining the leukocyte TEM route (Burns et al., 1997; Martinelli et al., 2014; Schaefer and Hordijk, 2015).

Podosomes are integrin-mediated adhesion structures observed in cells originating from myeloid tissue such as leukocytes and osteoclasts (Calle et al., 2006). These cells, especially leukocytes, migrate on comparatively soft substrates like endothelial or epithelial cells and their underlying interstitial

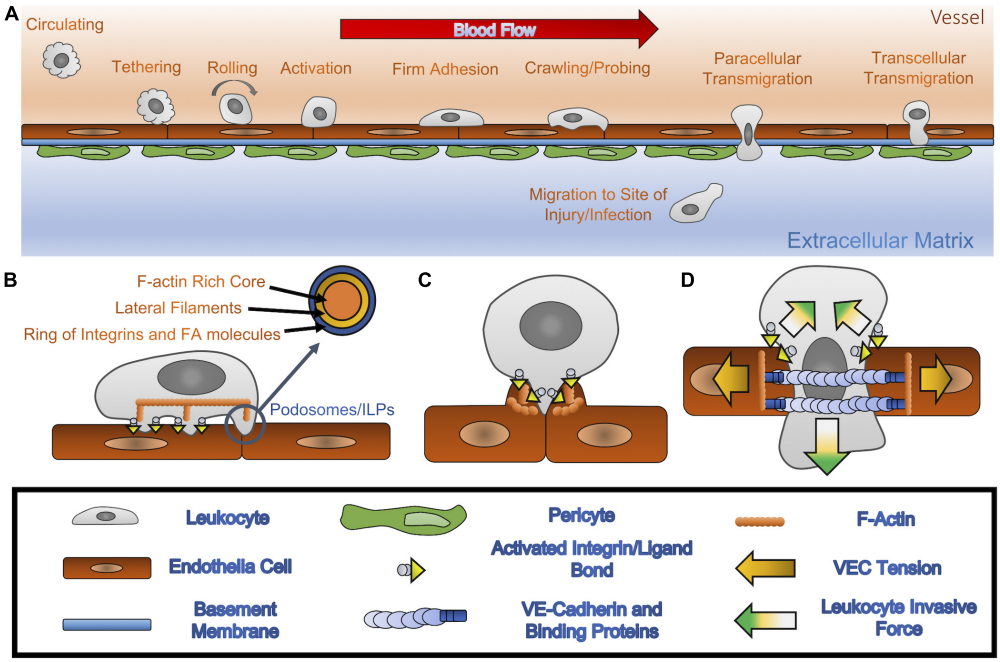

FIGURE 1 | (A) Leukocyte extravasation: through the presence of inflamed VECs, circulating leukocytes localize themselves in the proximity of affected tissues. Once in range, leukocytes use carbohydrate ligands to tether themselves to VECs that express specific selectins. Once tethered, the leukocyte is then able to roll along the endothelium by creating and breaking bonds between the selectins and carbohydrate ligands. Upon the activation of integrins into a high affinity state, triggered by chemokines binding to leukocyte's chemokine receptors, the leukocyte can transition into a firm adhesion state that stops the rolling and allows the leukocyte to spread out. The leukocyte then crawls and probes the vessel wall in search of VEC hotspots through which it is then able to transmigrate. This maneuver allows for leukocytes to breach the endothelium and basement membrane, thus permitting them to reach the affected tissue area. **(B)** Crawling/probing: leukocyte-VEC interactions, through high affinity integrins coupled with their respective CAMs, allow the leukocyte to migrate laterally, with the CAMs dictating the migration pattern of the leukocyte along the vascular wall. Furthermore, the leukocyte can convert focal adhesions to invadosome/podosomes like protrusive (ILP) structures, which are sensory organelles that they then utilize to search for TEM hotspots. **(C)** The transmigratory docking structure: once a hotspot is identified, a cluster of ICAM-1 creates a cup formation to hold on to the transmigrating leukocyte. This docking structure allows the leukocyte to transition from lateral migration to TEM. **(D)** TEM (paracellular): once in position at the sides of the VEC junction, leukocytes can increase VEC contractility, disrupting the local monolayer tension and creating strong downward pushing forces, which allow for a junctional gap to form and increase in size, and for invasion of the basement membrane. This widened gap allows for the leucocyte to push through the junction and break cellular bonds between VECs.

tissues (Zen and Parkos, 2003; Sabri et al., 2006; Carman et al., 2007; Hidalgo and Frenette, 2007; Cougoule et al., 2010; Dehring et al., 2011). They develop their focal adhesions into specialized podosomes and invadosome/podosome-like protrusions (ILPs), all similar and highly specialized subcellular structures, when interacting with extracellular matrices and endothelial membranes, respectively (Martinelli et al., 2014). High-resolution microscopy revealed that the podosome supramolecular organization consists of a central F-actin core surrounded by a ring of integrins and focal adhesion molecules, including talin, vinculin, and paxillin (Pfaff and Jurdic, 2001; Vijayakumar et al., 2015; Foxall et al., 2019). The core and ring structures are interconnected by F-actin networks containing non-muscle myosin IIA (Pfaff and Jurdic, 2001; van den Dries et al., 2013, 2014). F-actin polymerization in the podosome core creates pushing forces, which are counterbalanced by the lateral pulling forces generated through actomyosin contractility in the cable-like structures connecting the core to adhesion sites (Labernadie et al., 2014). This actomyosin apparatus confers upon podosomes a highly dynamic behavior, including fast turnover times of a few minutes (Destaing et al., 2003; Evans et al., 2003) and the control over podosome growth, stiffness, and protrusive force generation (Labernadie et al., 2010, 2014; Bouissou et al., 2017).

These results have raised the fundamental question of how leukocytes utilize podosomes and ILPs to mechanosense their microenvironment. Podosomes generate forces via their actomyosin apparatus and sense their extracellular environments via the integrin-based ring substructures in association with mechanosensitive proteins, which activate downstream mechanotransduction pathways to control various cell functions. This process can be utilized to probe substrate topographies, trigger extracellular matrix degradation, and sense the stiffness of the surrounding matrix or underlying endothelium.

Studies on leukocyte adhesion to microfabricated substrates have found that leukocyte podosomes align themselves along substrate microgrooves (van den Dries et al., 2012). Because conforming to 3-D microgroove topographies alters leukocyte membrane curvature, this finding suggests that membrane curvature could play a critical role in regulating both the dynamics and spatial organization of podosomes. Given that the microtopographic features of tricellular VEC junctions can

promote membrane curvature, specific subsets of protein and lipids associating with membrane curvatures (e.g., the BAR domain) might be involved in the podosome response to substrate topographies during the leukocyte TEM process.

Super-resolution microscopy has revealed that the F-actin podosome core is connected to a ventral F-actin module bound by vinculin and a dorsal module, crosslinked by myosin IIA and linked to other podosomes. Substrate stiffness influences the balance between these two modules allowing mesoscale podosome connections to collectively switch between the explorative, degradative behavior and the protrusive, non-degradative behavior (van den Dries et al., 2019). This stiffness sensing behavior is crucial for podosomes to explore spots compliant to protrusion. Moreover, clustered podosome force oscillations have been associated with expansion and retraction of the cell's leading edge, demonstrating the exploratory role of podosomes during leukocyte migration (Kronenberg et al., 2017). The generation of vertical protrusive forces from cancer cell invadopodia has also been linked to cancer cell protease activity to degrade extracellular matrices (Aung et al., 2014; Dalaka et al., 2020). However, local disruption of integrin tensions in fibroblast podosomes had no effect on distal podosomes (Glazier et al., 2019), implying that collective podosome mechanosensing may be cell-type dependent and/or more complex than currently understood.

Given that integrins are a primary structural component of the podosome ring, chemokines play an essential role in podosome formation by promoting the high-affinity state of leukocyte integrins (Carman et al., 2007; Shulman et al., 2009). Immobilized or soluble chemokines bind to their receptors on leukocyte surfaces to regulate both actin polymerization at the core and integrin activation at the ring and promote the initiation of specific podosome architectures (Hoshino et al., 2013). However, there is no clear evidence showing any chemokine receptors exist on the podosome structures, and the detailed interplay between chemokine receptors and integrins will be needed for further investigations.

Vascular endothelial cells can modulate ILP activities by providing different ICAM-1 dependent ligand patterns (Andersen et al., 2016), which could influence how leukocytes select and migrate toward TEM hotspots. Conversely, ILPs have also been implicated in sensing VEC junctional integrity and cytoskeletal stiffness, and modulation of these factors has been shown to affect the TEM route (Martinelli et al., 2014). However, the precise nature of these biomechanical interactions is far from understood (Vestweber, 2015). Leukocyte ILPs are not just a sensory organelle and may, in fact, have additional functions. VECs regulate endogenous tension to maintain monolayer integrity and it is highly suspected that adhering leukocytes can alter this tensional balance (Yeh et al., 2018). For example, transcellular electron microscopy imaging suggests that ILPs may distort and bend underlying actin filaments inside of VECs by pushing directly on them (Martinelli et al., 2014).

In addition, ILPs display different characteristics from podosomes. In particular, ILPs on VECs have shorter lifetime than podosomes on extracellular matrices (seconds to mins vs. seconds to ten of mins) (Carman, 2009). Furthermore, leukocytes employ ILPs to probe the underlying VEC cytoskeleton and preferentially migrate toward compliant areas with low F-actin densities or loose junctions (Martinelli et al., 2014; Schaefer and Hordijk, 2015). Also, while leukocyte migration has been shown to vary with substrate compliance in substrates of uniform stiffness (Stroka and Aranda-Espinoza, 2009), there is a lack of data regarding leukocyte migration on substrates with stiffness gradients. Existing data on other cell types, however, suggest that integrin-mediated mechanosensing promotes durotaxis (i.e., migration toward stiffness gradient) rather than tenertaxis (Choquet et al., 1997; Lo et al., 2000; Vincent et al., 2013). Thus, there are still crucial outstanding questions regarding mechanosensing by trafficking leukocytes and the role of ILPs in this important cell function.

BIOMECHANICS OF DIRECT TEM

After locating a hotspot on the endothelium, leukocytes shift from 2-D crawling to 3-D transmigration. Paracellular TEM is the most common route through the monolayer, mediated by the rapid disassembly of endothelial adherens junctions in response to an adherent leukocyte. The biomechanical interactions between leukocytes and VECs govern three crucial steps in this process. Specifically, mechanical forces contribute to opening endothelial gaps by destabilizing the junctions, help pull the leukocyte across the monolayer, and mediate the closure of the junctional gaps after TEM. This section discusses the currently recognized mechanisms and outlines open questions related to these three TEM steps.

The Initiation of TEM: The Transmigratory Docking Structure

It has long been believed that VECs may play an active role in facilitating leukocyte TEM. VECs protrude microvilli-like projections perpendicular to the endothelium to form a specific "transmigratory docking structure" shaped like a cup, which can surround and hold an adherent leukocyte (Carman et al., 2003; Carman and Springer, 2004; Yang et al., 2005; Gerard et al., 2009; Teijeira et al., 2013). These structures are ICAM-1 or VCAM-1 enriched after actively binding to leukocyte integrin LFA-1 and VLA-4 (Barreiro et al., 2002; Carman and Springer, 2004; van Buul et al., 2007). Initially speculated to inhibit TEM (Carman et al., 2003), the docking structure is now understood to play an essential role in guiding leukocytes through the initial stages of transmigration (Carman and Springer, 2004). High-resolution time-lapse 3-D imaging has shown that ICAM-1 clusters appearing at docking structures during early TEM remain detectable surrounding the transmigrating leukocyte through the late stages of TEM (Carman and Springer, 2004). Disruption of these structures correlates with a reduction in TEM events (Carman and Springer, 2004). Of note, this imaging data revealed that ICAM-1 protrusions and docking structures align perpendicular to the endothelium (i.e., parallel to the direction of TEM). This spatial organization could help orient leukocyte

integrins so that leukocytes can shift from 2-D lateral crawling and probing to an invasive 3-D migratory behavior.

The anchoring and embracing functions of VEC docking structures are regulated by mechanosensitive ICAM-1-triggered signaling, including recruitment of actin-binding proteins, an increase in F-actin assemblies, and activation of Rho-ROCK pathways, all of which result in increased actomyosin contractility (Yang et al., 2006; Heemskerk et al., 2014; **Figure 1C**). F-actin forms two types of assemblies with distinct functions in docking structures: (1) F-actin filaments extending ventrally from the apical side of endothelial membranes control VEC membrane protrusions while (2) F-actin rich cable-like structures confine transmigrating leukocytes at the basolateral side of VECs. In the early stages of TEM, vertically protruding F-actin filaments and VEC membrane fingers mediated by Myosin X activity secure adherent leukocytes (Franz et al., 2016; Kroon et al., 2018). The formation of these protrusions in inflamed VECs is regulated by the ICAM-1 cluster-mediated Cdc42-myosin-PAK4-F-actin signaling pathway, which generates mechanical forces to hold the leukocyte in place and subsequently pull it toward the VECs (Kroon et al., 2018). As TEM progresses, endothelial pores form to accommodate transmigrating leukocytes. Pore generation is regulated by the F-actin-rich cable-like structures (Heemskerk et al., 2016), which exert contractile forces against transmigrating leukocytes in order to maintain endothelial barrier functions throughout the entire TEM process and assist gap closure after it is complete (Mooren et al., 2014). Investigators employed inert beads coated with ICAM-1 antibodies to mimic adherent leukocytes, engage endothelial ICAM-1 clustering, and demonstrate the active role of VECs in TEM. These beads triggered a VEC process reminiscent of phagocytosis, in which VEC membrane extensions protruded to dock and embrace the beads (Carman et al., 2003; van Buul et al., 2010; Kroon et al., 2018). In addition, the functionalized beads were sufficient to induce strong localized VEC cellular traction forces (Liu et al., 2010; Yeh et al., 2018). The mechanical stresses created during docking structure formation and those observed during phagocytosis share common features, suggesting similarities between phagocytosis and leukocyte TEM (Vorselen et al., 2020a).

The Crux of TEM: Junctional Gap Formation

Because leukocyte sizes can be more than 20 times greater than the size of endothelial cell-cell junctions (∼10 μm vs. ∼0.5 μm), transmigration must involve precise biomechanical coordination between leukocytes and VECs. VECs actively respond to the leukocyte's presence by forming gaps to accommodate paracellular TEM. The activation of endothelial ICAM-1 through leukocyte binding can trigger a downstream signaling pathway that promotes cytosolic calcium-mediated myosin activity, resulting in increased endothelial contractility. The resulting increase in the tensile force supported by the F-actin cytoskeleton (i.e., endothelial tension, **Figure 1D**) is transmitted to VE-Cadherin, which connects F-actin to the VEC adherens junctional complex (Arif et al., 2021). This process causes the endothelial gap to enlarge for accommodating the transmigrating leukocyte (Shaw et al., 2001; Alcaide et al., 2008; Wee et al., 2009; Heemskerk et al., 2014). There is ample evidence that endothelial tension regulates paracellular TEM. Manipulating endothelial contractility by soluble inflammatory or anti-inflammatory agents such as thrombin and angiotensin I, biophysical cues such as stiff or soft subendothelial substrates, or by activating or inhibiting the RhoA GTPase all respectively increased or decreased the rates of leukocyte TEM (Hixenbaugh et al., 1997; Saito et al., 1998, 2002; Adamson et al., 1999; Carman et al., 2003; Yeh et al., 2018).

Apart from this VE-Cadherin-mediated junctional gap formation mechanism, the homophilic interaction between leukocyte PECAM-1 and VEC junctional PECAM-1 also plays a crucial role in leukocyte TEM by recruiting the lateral border recycling compartment (LBRC) to the site of TEM (Muller, 2003). LBRCs are networks of dynamic VEC vesicle-like membrane invaginations at cell-cell borders transported to TEM sites by kinesin motors along microtubules (Mamdouh et al., 2008). The primary molecule of LBRCs is endothelial PECAM-1, although they also contain other junctional molecules such as JAM-A and CD99 (Mamdouh et al., 2009). The LBRC surrounds the leukocyte, clears junctional VEC-Cadherin to open junctional gaps, and enlarges these gaps by contributing additional membrane material, all of which facilitates the transmigration process (Muller, 2014). Pharmacological perturbations inhibiting the formation or recruitment of LBRCs prevent TEM.

To complete the picture provided by the above studies, one must consider that leukocytes are mechanosensitive cells that exert forces during migration and invasion (Huse, 2017; **Figure 1D**). Recent 3-D traction force microscopy (TFM) studies have shown that leukocytes exert large burrowing stresses (∼1 KPa) to invade Matrigel substrates (Yeh et al., 2018). Simultaneous quantification of cell shape changes, position, and 3-D force exertion during leukocyte TEM revealed that burrowing vertical forces increase significantly during TEM events (Yeh et al., 2018). The tangential forces also become stronger and display a vector pattern directed inward toward VEC junctions, which lowers VEC monolayer tension (Yeh et al., 2018). In contrast, VEC monolayer tension raises when endothelial gaps form in response to mechanically inert anti-ICAM-1-coated beads. Moreover, gap formation mediated by these beads is significantly slower (∼120 min) than leukocyte TEM (∼10 min) (Yeh et al., 2018). Consistent with these findings, high-resolution correlative microscopy imaging of VEC cytoskeletal remodeling during TEM suggests that junctional gaps can be actively generated by leukocytes squeezing between adjacent VECs (Barzilai et al., 2017). In particular, the stiff leukocyte nucleus has been suggested to act as battering ram that displaces nearby VEC F-actin stress fibers to initiate and sustain junctional gaps (Barzilai et al., 2017).

Altogether, these studies show that junctional gap generation for TEM requires highly orchestrated biomechanical contributions from both leukocytes and VECs. Future studies are required to provide additional insight on exactly how these forces work together to promote leukocyte TEM.

The Resolution of TEM: Junctional Gap

Preservation of endothelial barrier function requires that VEC junctional gaps be sealed once TEM concludes. The highly dynamic VEC F-actin cytoskeleton plays a crucial role in this process by continually polymerizing to form lamellipodial protrusions that make contact with neighboring VECs to signal gap closure (Mooren et al., 2014). Intact VECs exist under isometric tensions with contractile forces balanced by the cell-matrix and cell-cell adhesions (Charras and Yap, 2018). Gap formation during TEM is thought to disturb monolayer tension, triggering the formation of the F-actin lamellipodial structures that mediate gap closure (Phillipson et al., 2008; Martinelli et al., 2013). Concomitantly, Rho GEF Ect2- and LARG-activated RhoA signaling promotes actomyosin contractility in the F-actin-rich cable-like structures surrounding the leukocyte, similar to a purse string closure (Heemskerk et al., 2016). Inhibition of RhoA activity *in vitro* and *in vivo* did not affect the rate of leukocyte TEM events but caused leukocyte-induced vascular leaks. Moreover, a recent *in vivo* study found another Tie-2 receptor/Cdc42 GEF FGD5-stimulated mechanism responsible for preventing plasma leakage during leukocyte TEM. This study identified that platelets recruited to endothelial VWF activate the Tie-2 receptor by releasing Angiopoietin-1, reinforcing cable-like F-actin to close the endothelial pore (Braun et al., 2020). Further supporting the contribution of a purse string mechanism to maintaining barrier integrity during late TEM, the tangential traction stress patterns during gap closure are consistent with the presence of increased hoop tension (Yeh et al., 2018). Overall, these results indicate that F-actin-mediated signaling is essential for regulating gap closure, although there are not yet any direct measurements of endothelial monolayer tension during this process.

QUANTIFYING THE MECHANICS OF LEUKOCYTE ENDOTHELIAL CRAWLING AND TRANSMIGRATION

The trans-well assay has been widely used to quantify leukocyte TEM for over two decades, unveiling several mechanisms crucial to this process. For example, leukocytes can actively respond to the exogeneous chemotactic gradient applied across the VEC monolayers such C5a or fMLP (Cooper et al., 1995). Without the application of exogeneous chemokines, the activation of VECs by TNF-α or IL-8 can induce expression and secretion of chemokines resulting in leukocyte integrin activation and the subsequent firm adhesion, crawling and transmigration (Adams and Lloyd, 1997). The trans-well device can easily create a chemotactic gradient via a micropore-based membrane separating the device's upper and the lower chambers. However, this assay is not ideally suited to quantify the mechanics of TEM because it is not compatible with high magnification microscope objectives, customized substrates, and real-time imaging of most force microscopy methods.

The most common current method to quantify cell-generated forces is TFM (Tan et al., 2003; Wang and Lin, 2007; Fu et al., 2010; Hall et al., 2013; Style et al., 2014; Polacheck and Chen, 2016; **Figures 2A–C**). This technique relies on measuring the cell-induced deformations in a continuous elastic substrate (e.g., a hydrogel) or an array of discrete elastic elements (e.g., microposts) of known mechanical properties. Using these data as inputs, a mathematical inverse problem is solved to recover traction forces (Style et al., 2014; Polacheck and Chen, 2016). TFM experiments have revealed that, similar to other cell types (Hur et al., 2009; Legant et al., 2013; Alvarez-Gonzalez et al., 2015), neutrophils and macrophages in an adherent state exert pulling forces around the cell edge and an unstructured bulk pushing force under the main cell body (Kronenberg et al., 2017; Yeh et al., 2018). The observation of subtle variations in the bulk pushing force has been attributed to the force from podosomes (Kronenberg et al., 2017). The joint requirements of fine spatial resolution and high temporal sensitivity to measure such minute forces make it challenging to quantify podosome exerted forces by TFM. Thus, specialized methods based on atomic force microscopy (AFM) and molecular sensors have been developed for this application. Finally, VEC contractility contributes to building tissue-level mechanical tension in monolayers, which is modulated in response to external stimuli such as flow shear stresses or the presence of an adhering leukocyte (Hur et al., 2012; Yeh et al., 2018). Motivated by reports showing that monolayer tension is known to regulate junctional integrity and endothelial barrier function (Tornavaca et al., 2015; Andresen Eguiluz et al., 2017), monolayer stress microscopy (MSM) techniques have been developed to measure this tension. Below, we discuss techniques developed to quantify the mechanics of leukocyte TEM. These techniques are illustrated in **Figure 2** and their specific applications, strengths, and limitations are summarized in **Table 1**.

Quantifying Subcellular Forces

Early efforts to assess the dynamics and physical properties of podosomes combined the application of AFM, micropatterned substrates, and correlative fluorescent microscopy (Labernadie et al., 2010; **Figure 2D**). Macrophages were plated on a glass coverslip patterned with arrays of fibrinogen squares, encouraging podosome formation in the protein spots in order to restrict the size of the analysis field. AFM, in which a cantilever applies a known force to the substrate in order to determine its stiffness, was then used to identify the location of membrane bumps corresponding to fluorescently labeled F-actin rich structures (Henderson et al., 1992; Lu et al., 2008). Time series of AFM topological images enabled accurate measurement of podosome height (mean 578 $\pm$ 209 nm) while force-distance mapping provided a wealth of information on podosome stiffness. Not only was the mean Young's modulus of podosomes found to be approximately five times higher than surrounding regions, but rapidly acquired force-distance curves reproducibly demonstrated periodic oscillations in podosome stiffness (Labernadie et al., 2010). This targeted application of AFM permitted a refined analysis of podosome structure and function. However, it also highlighted several key limitations of standard AFM to quantify the biomechanics of podosomes. Specifically, the impossibility of probing the basal tip of the

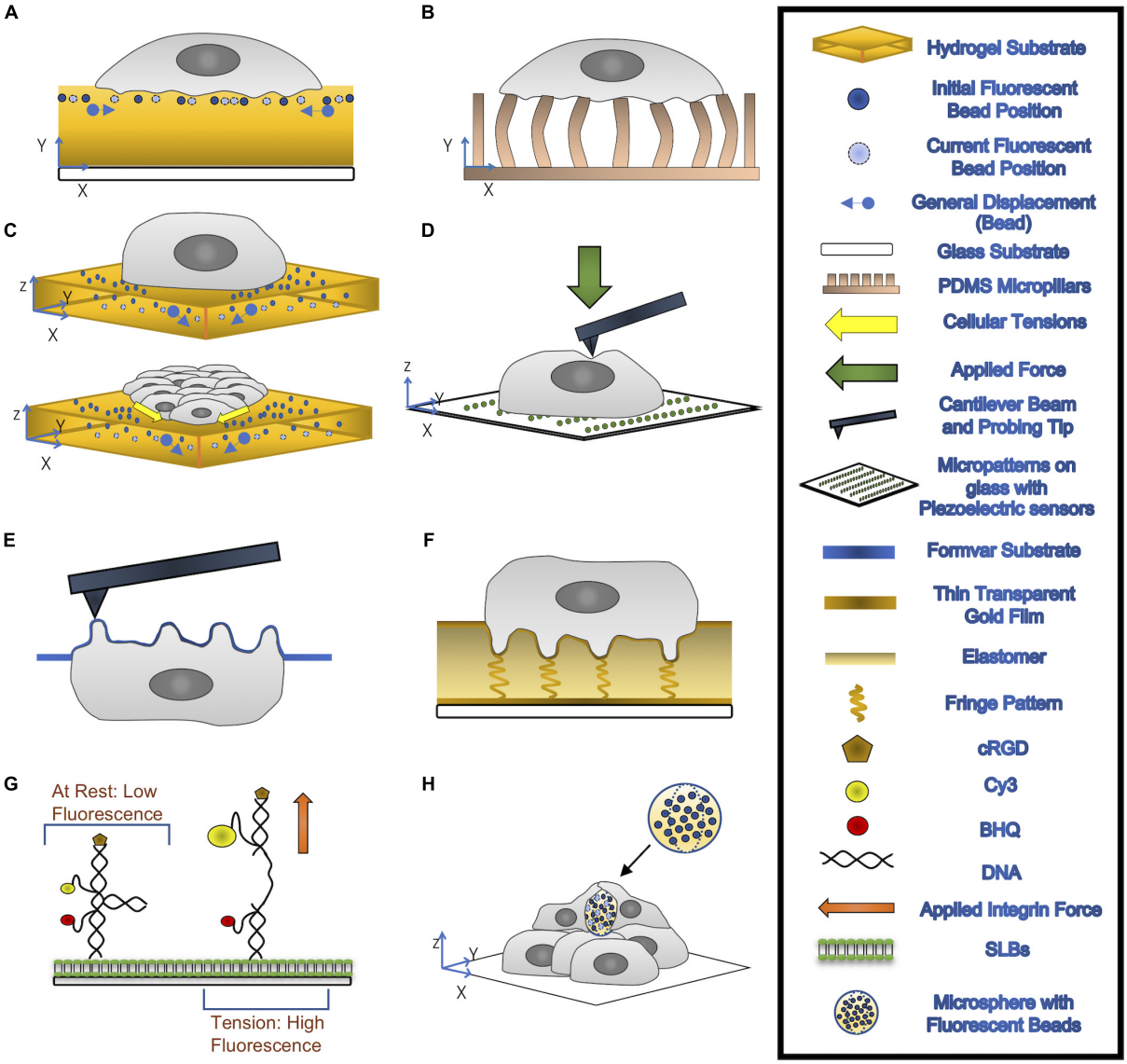

FIGURE 2 | (A,B) 2-D TFM: cells are seeded on top of a hydrogel substrate containing fluorescent beads (**A**) or elastic micropillars **(B)**. Traction Forces can be measured through the imaging of the beads' displacements or deflections of micropillars. **(C)** 3-D TFM (top) and 3-D MSM (bottom): 3-D TFM takes vertical direction displacement into account by comparing 3-D interrogate boxes between the deformed and undeformed state of substrates. 3-D MSM is derived from 3-D TFM and takes bending effects on cellular tensions into account. **(D)** AFM: A cantilever beam with a probing tip at one end applies a force onto the cell. **(E)** PFM: cells are seeded onto a formvar substrate, which is then stretched over a mesh grid. This formvar membrane is place upside, allowing for accurate topological information about the podosomes to be recorded through AFM. With the use of mathematical modeling, forces exerted by the podosomes can be calculated. **(F)** ERISM: thin transparent gold films are placed on top of and below an ultra-soft siloxane-based elastomer. The top gold film is protein coated to allow for cell adhesion. Local deformation caused by the cell to the elastomer form resonance fringes that are captured using established imaging modalities. **(G)** MT-FILM: surface functionalization of SLB with FRET-based DNA tension probe. When the integrin force applied is greater than $F_{1/2}$, the rated force the probe can handle, the linker arms come together and open, causing the florescence of the probe increases. **(H)** microsphere-based TFM: Microspheres with fluorescent beads embedded are placed within multilayer of cells. After a few days, the cells exert compressive forces that deform the microspheres.

podosome which is in contact with the substrate, the difficulty of localizing podosomes from profiles of apical cell height, and, most notably, the impossibility of measuring podosome protrusive forces.

In order to address these limitations, protrusion force microscopy (PFM) was developed as an extension of standard AFM to measure indentations made by cells seeded on a specially fabricated, compliant formvar substrate (Labernadie et al., 2014; **Figure 2E**). The formvar membrane, stretched over a square mesh grid, was seeded with cells before being mounted upside down in the microscope so that AFM could be performed directly on the membrane bumps caused by podosomes. The force generated by each podosome was calculated by fitting the height and radius of each protrusion to a mathematical model of

TABLE 1 | Summary of cellular force measurement techniques.

	Resolution (x/y/z/F/t)	Cell substrate	System requirements	Post-processing	Advantages	Disadvantages	References
Traction force microscopy (TFM) **Figures 2A–C**	Depends mostly on substrate properties and microscopy setup	Hydrogel, PDMS, elastomers, fibrillar matrices (e.g., collagen); Arrays of elastic micropillars	Standard fluorescent microscope; Confocal microscopy for out of plane bead tracking and 3-D tractions	Single particle tracking, correlation tracking, and/or particle image velocimetry; Theoretical/ computational solid mechanics analysis	Cell substrate can be physiologically realistic (except micropillar arrays); Image based – highly versatile; Simple experimental setup and high throughput; Can be extended to provide collective cellular force measurements (e.g., monolayer stress microscopy)	Requires zero force state (except micropillar arrays) and calibrating substrate elastic properties; Limited sensitivity to vertical forces; Fluorescence microscopy over long periods can cause phototoxic effects	Tan et al., 2003; Wang and Lin, 2007; Fu et al., 2010; del Alamo et al., 2013; Hall et al., 2013; Style et al., 2014; Polacheck and Chen, 2016; Serrano et al., 2019
Atomic force microscopy (AFM) **Figure 2D**	Resolution depends on the imaging force and probe geometries; Lateral resolution 1–1.5 nm; Vertical resolution 0.1 nm; Force resolution 100 pN	Mica, glass, or glass slides modified with Silane to enhance cell adhesions	Piezoelectric scanner for mounting samples; Proper probes attached to pliable silicon or silicon nitride cantilever; Laser beam/photodiode setup for measuring cantilever deflection	Cantilever deflection as a function of vertical displacements; Conversion a force-versus-separation distance curve	Probes for molecular interactions, physiochemical properties, surface stiffnesses, and macromolecular elasticities	Requires careful sample preparation and data collection; Requires physical contact between the AFM probe and the sample – cannot probe basal structures (e.g., podosomes tips) Localizing specific cell structures (e.g., podosomes) by AFM alone is challenging	Labernadie et al., 2010
Protrusion force microscopy (PFM) **Figure 2E**	The same as AFM; Vertical resolution 10 nm; Line rate on order of 1 Hz; Force resolution to the order of nN	Compliant formvar membranes	AFM system and fluorescence microscopy	The same as AFM, plus mathematical model to infer podosomes forces from formvar membrane deformation	Measures protrusive forces applied perpendicularly to the substrate at a single podosome level; High spatiotemporal resolution	The same as AFM, except for localizing podosomes; Narrow range of applications.	Labernadie et al., 2014; Bouissou et al., 2017
Elastic resonator interference stress microscopy (ERISM)**Figure 2F**	Displacement resolution 2nm (limited by surface); Temporal resolution <0.5 s; Lateral resolution $\sim 1.6\ \mu m$;	Elastic optical micro-cavity comprized of a layer of ultra-soft siloxane-based elastomer sandwiched between semi-transparent gold layers	Conventional wide-field phase contrast or fluorescent microscopy with a tunable light source capable of providing monochromatic illumination	Each light fringe $\sim$ 200 nm = $\geq$ count fringes to determine size of deformations; Conversion of forces by utilizing substrate mechanical properties	Unlike many TFM methods, no zero-force state required; No phototoxic effects; Versatile, and compatible with other microscopy methods; Excellent vertical and lateral force sensitivities	Experimental setup and fabrication of ERISM cavities are relatively involved; 2D soft substrate may not be physiologically realistic for some applications	Kronenberg et al., 2017; Liehm et al., 2018

(Continued)

TABLE 1 | Continued

	Resolution (x/y/z/F/t)	Cell substrate	System requirements	Post-processing	Advantages	Disadvantages	References
Molecular tension-fluorescence lifetime imaging microscopy (MT-FLIM) **Figure 2G**	Force threshold $F_{1/2}$ is a measure of the applied force at which 50% of probes are open, estimating applied force ranges; Force resolution to the order of pN exerted by individual integrins	Supported lipid bilayer (SLB) – phospholipid membranes; Confined in the Z-direction but are laterally fluid	Inverted microscopes with perfect focus capabilities and appropriate lasers for excitation; Specific software required;	Matlab Bioformats Toolbox and semiautomated custom scripts; FIJI plugins, including MultiKymograph and TrackMate	Highly specific observations of integrin behavior and force generation as it relates to podosome formation and mechanosensing	Highly technical in the development and implementation of molecular tension probes, and in microscopy set-up Misses forces transmitted via non-specific interactions	Wang and Ha, 2013; Blakely et al., 2014; Zhang et al., 2014; Brockman et al., 2018; Glazier et al., 2019
Microsphere-based traction force microscopy **Figure 2H**	Force resolution to the order of nN	Hydrogel-based microspheres; Fabricated by water-oil emulsions	Standard fluorescent microscope; Confocal microscopy for tracking 3-D shape deformations	Comparison between deformed and undeformed states from 3-D shape reconstructions	Suitable for studying forces in environments with complex mechanical properties, where TFM and ESRIM would be challenging	Intensive image processing requirements Resolution is limited by spatial distribution of microspheres in sample	Girardo et al., 2018; Mohagheghian et al., 2018; Kaytanli et al., 2020; Vorselen et al., 2020b

a clamped membrane subject to a point force (Labernadie et al., 2014). By increasing the thickness of the formvar sheet and thus the substrate stiffness sensed by cells, PFM results demonstrated that leukocyte podosomes increase their protrusive forces in response to stiffer substrates, suggesting that podosomes have a mechanosensing function (Labernadie et al., 2014). Periodic oscillations in podosome protrusive forces concomitant with the aforementioned periodic stiffness oscillations were uncovered using time-lapse PFM, which functions by keeping the AFM cantilever tip at a constant force in contact with the top of a protrusion as it moves in real-time (Labernadie et al., 2014). The similarities between periods of podosome protrusive forces (40 ± 14s), core stiffness (37 ± 20s) as measured by PFM, and F-actin intensities at the podosome core (44 ± 11s) as measured by total internal reflection fluorescent imaging indicate a correlation between the generation of oscillating protrusion forces and the stiffness and F-actin content of the podosome core. This correlation was validated by pharmacological perturbations, demonstrating that both F-actin polymerization and actomyosin contractility regulate periodic protrusion forces.

While PFM provides invaluable information about the biomechanics of podosomes, it is a highly specialized technique. For instance, it is not straightforward to integrate PFM measurements of protrusive forces with long-term, whole-cell measurements of tangential traction stresses and motility. The emergence of elastic resonator interference stress microscopy (ERISM, **Figure 2F**) now allows for quantifying whole-scale lateral and protrusive cell-substrate forces, with enough resolution to detect the minute forces exerted by podosomes and over extended periods of time. ERISM implements interferometric detection of cell-induced deformations in an elastic microcavity, allowing for high sensitivity to weak forces in a non-destructive manner such that cells can be retained on the substrate after imaging for subsequent measurements and assays (Kronenberg et al., 2017; Liehm et al., 2018). ERISM measurements could in principle be analyzed to recover collective cellular stresses such as endothelial monolayer tension. Thus, although it cannot currently be applied to 3-D physiologically relevant environments like, (e.g., Matrigel or collagen matrices), ERISM constitutes a promising technique to quantify the biomechanics of leukocyte TEM.

Pursuant to these developments, specialized microscopic methods were developed to investigate the contributions of specific proteins to podosome force generation. Specifically, DNA-based subcellular tools were developed to explore the role of integrin tensile forces in podosome formation and illustrate the mechanical link between integrin tension at the podosome ring and actin protrusion at the podosome core (Glazier et al., 2019; **Figure 2G**). Molecular Tension-Fluorescence Lifetime Imaging Microscopy (MT-FLIM) allows for precise, piconewton (pN) resolution measurement of integrin tensile forces. MT-FLIM relies on the surface functionalization of a laterally fluid, self-assembling phospholipid membrane on glass (supported lipid bilayer, or SLB) with FRET-based DNA tension probes (Wang and Ha, 2013; Blakely et al., 2014; Zhang et al., 2014; Brockman et al., 2018; Glazier et al., 2019). The probes consist of a binary DNA hairpin with an internal loop structure and two

linker arms hybridized to include (1) a Cy3/BHQ FRET pair, which is brought into proximity when a force greater than the tunable $F_{1/2}$ threshold is applied to the probe, opening the hairpin and (2) cyclic Arg-Gly-Asp-*D*-Phe-Lys (cRGD), which is localized on the upper arm and whose depletion is a proxy for podosome protrusive forces as measured by percentage decrease in fluorescence. Application of a force greater than or equal to $F_{1/2}$ will open the probe, increasing both fluorescence intensity and lifetime (Glazier et al., 2019). Using tunable $F_{1/2}$ DNA probes, MT-FLIM enabled the identification of a narrow range of integrin mediated forces and used time-course imaging to establish a picture of the spatiotemporal evolution of podosome force generations at a subcellular level.

Quantifying Single Cell Forces

Two-dimensional (2-D) TFM, which measures the lateral traction forces parallel to the surface of cell attachment, was first applied by Dembo and Wang to fibroblasts migrating on flat substrates (Dembo and Wang, 1999). This technique has been widely used to quantify the biomechanics of leukocyte adhesion and crawling on substrates of varying stiffness of 0.05–8 kPa, providing traction stress maps with a lateral resolution of 1–5 μm (Rabodzey et al., 2008; Liu et al., 2010; Yeh et al., 2018). The experimental assay used in this type of experiments has been refined over the years and consists of a protein-coated gel (e.g., polyacrylamide) containing fluorescent microspheres near its surface (**Figure 2A**). Substrate deformations are quantified from the movement of the fluorescent beads by image correlation techniques, using reference images obtained after treating the cells (e.g., by trypsin) to detach from the substrate or after the cells move away from the region of interest. The partial differential equation of elastic equilibrium for the substrate (i.e., the elastostatic equation) can be solved to determine the traction stresses from the measured deformations using a variety of inversion and regularization procedures (Schwarz et al., 2002; Sabass et al., 2008). Notably, the computationally efficient Fourier analysis of the elastostatic equation proposed by Butler et al. (2002) makes it possible to calculate traction stresses from raw microscopy images virtually in real time.

In micropost-based TFM, protein-coated arrays of microscopic pillars made from the deformable elastomer polydimethylsiloxane (PDMS) serve as a substrate (**Figure 2B**). Cells attached to these arrays induce pillar deflections that can be converted into force vectors using the known height, width, and material properties of the pillars (Tan et al., 2003; Fu et al., 2010; Polacheck and Chen, 2016). In principle, micropost-based TFM does not require a reference image since the undeflected positions of the pillars are known theoretically (Lemmon et al., 2009), which is advantageous. On the other hand, microfabrication and imaging constraints limit the spatial resolution of this technique (Amato et al., 2012). Furthermore, the highly particular substrate topography created by the micropost arrays differs from physiologically relevant scenarios and can affect cell adhesion. Pioneering micropost-TFM studies of leukocyte endothelial crawling showed that VECs exert increased tangential forces in response to a firmly adherent leukocyte, uncovering that biomechanical interactions between VECs and adherent leukocytes and play a role in TEM (Rabodzey et al., 2008; Liu et al., 2010).

The 2-D TFM is relatively straightforward on standard fluorescent microscopes, has excellent resolution, and can be adapted to a wide variety of applications (Style et al., 2014; Polacheck and Chen, 2016). However, leukocyte TEM is an inherently 3-D process involving significant forces in the vertical direction of invasion. TFM measurement of these vertical forces requires more involved imaging setups and careful postprocessing to balance resolution with phototoxic effects. Motivated by the fact that cells generate both lateral and vertical traction forces while adhering to and migrating over planar substrates (Hur et al., 2009; Maskarinec et al., 2009), TFM methods to measure these 3-D forces have been developed (Hur et al., 2009; Maskarinec et al., 2009). These techniques are loosely referred to as 2.5-D TFM because they provide 3-D traction forces in the 2-D plane of cell attachment, differentiating them from volumetric TFM experiments where cells are fully embedded inside 3-D matrices (Legant et al., 2010). In 2.5-D TFM experiments the substrate is the same as in 2-D TFM, but confocal imaging is required to record 3-D substrate deformations. To minimize the phototoxicity generated by laser radiation when acquiring a z-stack of confocal images, del Alamo et al. developed a methodology that inputs the 3-D deformation at the top plane of the substrate into the solution of the 3-D elastostatic equation (del Alamo et al., 2013), thus requiring only ∼10-slice z-stacks (or approximately 10 μm in depth). By adding deformation data from additional planes, this methodology can be extended to substrates of unknown mechanical properties or used to detect substrate degradation (Aung et al., 2014; Alvarez-Gonzalez et al., 2017). Overall, 2.5-D TFM constitutes a powerful tool to study the biomechanics of TEM and delineate the distinct roles of VEC and leukocyte forces in coordinating this process.

Quantifying Tissue-Level Cell Forces

In order to maintain homeostatic barrier function, VECs must regulate their monolayer tension to balance the biomechanical stability of cell-cell junctions and cell-substrate adhesions. This balance prevents cell adhesion forces from tearing the endothelium apart or detaching it from the substrate (Charras and Yap, 2018). During inflammatory responses, both the magnitude and fluctuations of VEC monolayer tension tend to increase, leading to inherently unstable junctions (Yeh et al., 2018). Measurements of endothelial monolayer tensions over time suggest that the rate of leukocyte TEM correlates with tension fluctuations, which can be actively induced by leukocytes at TEM sites (Yeh et al., 2018). Recent mathematical models also support the idea that monolayer tension fluctuations play a crucial role in monolayer integrity and leukocyte TEM (Escribano et al., 2019). However, joint quantitative measurements of endothelial traction forces, monolayer tensions, and the forces exerted by leukocytes on the endothelium are still scarce.

In comparison to AFM or TFM, the development of experimental, image analysis, and computational tools to quantify collective cellular forces has been recent. A salient technique is MSM, an extension of TFM that quantifies the

collective distribution of intracellular stresses in thin confluent cell layers (Trepat et al., 2009). Of note, MSM can measure monolayer tension, which is the tensile intracellular stress. Most MSM methods calculate intracellular stresses in the monolayer from 2-D measurements of in-plane traction stresses by applying Newton's third law in differential (Trepat et al., 2009) or integral (Hur et al., 2012) form after averaging across monolayer thickness. The differential formulation provides significantly better lateral spatial resolution than the integral one, although it relies on a number of simplifying assumptions such as linearly elastic material behavior, constant elastic moduli, and known Poisson ratio. For the most part, these assumptions do not seem to severely affect the recovered intracellular stresses (Trepat et al., 2009; Tambe et al., 2013). Furthermore, they can be relaxed using particle dynamics simulations (Zimmermann et al., 2014) or Bayesian inference analyses (Nier et al., 2016). However, these 2-D approaches do not consider that cell monolayers respond to not only in-plane tangential stresses, but also out-of-plane stresses that induce monolayer bending. Confluent VECs adhering to soft substrates can generate strong out-of-plane traction stresses that bend the monolayer, particularly near the monolayer edges (Serrano et al., 2019). The invasive forces exerted by leukocytes during TEM also cause monolayer bending, leading to significant perturbations in intracellular tension (Yeh et al., 2018). To overcome the limitations of 2-D MSM, Serrano et al. recently developed a new MSM method (Serrano et al., 2019) that uses 2.5-D TFM measurements to calculate the contributions of lateral and bending deformations to monolayer tension (**Figure 2C**).

An inherent difficulty in quantifying the biomechanics of TEM is to tease out the forces exerted by the leukocytes from those exerted by the VECs. To this end, ICAM-1 antibody-coated polystyrene beads mimicking firmly adherent leukocytes have been used in combination with TFM and MSM methods (Liu et al., 2010; Yeh et al., 2018; Serrano et al., 2019). Given that the microbeads are mechanically inert, these experiments provide useful information about how VECs regulate monolayer tension during TEM. However, polystyrene beads are rigid, which makes it impossible to quantify the forces that VECs exert on the beads, and the recent development of methods to quantify mechanical forces *in vivo* via deformable hydrogel microspheres could overcome this limitation. Inspired by the seminal use of functionalized oil droplets to measure anisotropic stresses within 3-D cell aggregates (Campas et al., 2014), emerging microfabrication methods can now produce deformable hydrogel-based spherical force sensors, with sizes ranging from a few μm up to hundreds of microns (Girardo et al., 2018; Mohagheghian et al., 2018; Kaytanli et al., 2020; Vorselen et al., 2020b; **Figure 2H**). These elastic microspheres can be employed to study cellular forces induced by specific ligand-receptor interactions, known as microsphere-based TFM. Comparisons between the deformed and the stress-free state of microspheres allows force measurements to be performed using analysis methods similar to those employed in TFM. These techniques are anticipated to generate novel quantitative insights about the mechanical progression of VEC docking structure formation during the initial TEM process.

Finally, it is important to note that, although shear stress is an important regulator in inducing leukocyte TEM (Cinamon et al., 2001), most existing force microscopy studies of leukocyte TEM have not considered shear flow conditions so far. While it requires a more complicated experimental setting, it is not unfeasible to consider shear flow in force microscopy assays and, in fact, there are established TFM and FRET imaging assays that include shear flow (Hur et al., 2012; Perrault et al., 2015; Heemskerk et al., 2016). Future efforts shall exploit these tools to study how shear affects the mechanics of leukocyte TEM by directly measure the forces involved in the process.

CONCLUDING REMARKS

Leukocyte recruitment is a hallmark of all acute and chronic inflammatory disorders. Understanding leukocyte TEM to inflammation sites could help identify therapeutic targets to boost immune defense and minimize inflammatory tissue damage. Currently, medical treatments of chronic inflammation employ general immune suppressors, which have numerous adverse side effects. This lack of success is attributed to the complexity of and the multitude of redundancies and interdependencies in the molecular pathways involved. Although many molecules, some of which are discussed above, have been implicated in TEM, their specific roles remain elusive. In particular, we still know little about how VECs and leukocytes orchestrate pathfinding and localized endothelial barrier modulation. These processes can depend on direct receptor-ligand biomechanical interactions and more intricate, collective mechanosensitive pathways. Their understanding requires advanced experimental techniques to detect subcellular, single-cell, and tissue-level deformations during leukocyte TEM, along with the corresponding development of computational models to analyze data streams of increasing complexity and size.

During the past ten years, the progress in the development of soft materials have brought *in vitro* assays close to reproducing physiological microenvironments under controlled conditions. In parallel, advances in 3-D imaging and force quantification have opened a window to data of unprecedented richness and quality. Indeed, these methodologies have significantly extended our current understanding of leukocyte trafficking. The current technological frontier is methods to allow investigation of these biomechanical events *in vivo*. Of note, emerging microscopy techniques such as two-photon, light sheet, and super-resolution microscopy will most likely play a transformative role in bridging the gap going from *in vitro* conditions to more realistic animal models. Heavy interdisciplinary efforts involving engineers, physicists, and mathematicians will certainly be required to overcome these formidable challenges.

AUTHOR CONTRIBUTIONS

AS, EC-H, SC, JÁ, JL, and Y-TY wrote the manuscript. AS and OC composed the figures and table. All authors contributed to the article and approved the submitted version.

FUNDING

This work was supported by National Institutes of Health Grants GM084227 (to JL and JÁ), American Heart Association Grant 18CDA34110462 (to Y-TY), Fundación Bancaria 'la Caixa' (ID 100010434), and the partial financial support through a 'la Caixa' Fellowship LCF/BQ/US12/10110011 (to EC-H).

REFERENCES

Adams, D. H., and Lloyd, A. R. (1997). Chemokines: leucocyte recruitment and activation cytokines. *Lancet* 349, 490–495. doi: 10.1016/s0140-6736(96)07524-1

Adamson, P., Etienne, S., Couraud, P. O., Calder, V., and Greenwood, J. (1999). Lymphocyte migration through brain endothelial cell monolayers involves signaling through endothelial ICAM-1 via a rho-dependent pathway. *J. Immunol.* 162, 2964–2973.

Alcaide, P., Newton, G., Auerbach, S., Sehrawat, S., Mayadas, T. N., Golan, D. E., et al. (2008). p120-Catenin regulates leukocyte transmigration through an effect on VE-cadherin phosphorylation. *Blood* 112, 2770–2779. doi: 10.1182/blood-2008-03-147181

Alon, R., Hammer, D. A., and Springer, T. A. (1995). Lifetime of the P-selectin-carbohydrate bond and its response to tensile force in hydrodynamic flow. *Nature* 374, 539–542. doi: 10.1038/374539a0

Alvarez-Gonzalez, B., Meili, R., Bastounis, E., Firtel, R. A., Lasheras, J. C., and Del Alamo, J. C. (2015). Three-dimensional balance of cortical tension and axial contractility enables fast amoeboid migration. *Biophys. J.* 108, 821–832. doi: 10.1016/j.bpj.2014.11.3478

Alvarez-Gonzalez, B., Zhang, S., Gomez-Gonzalez, M., Meili, R., Firtel, R. A., Lasheras, J. C., et al. (2017). Two-Layer Elastographic 3-D Traction Force Microscopy. *Sci. Rep.* 7:39315. doi: 10.1038/srep39315

Amato, L., Keller, S. S., Heiskanen, A., Dimaki, M., Emneius, J., Boisen, A., et al. (2012). Fabrication of high-aspect ratio SU-8 micropillar arrays. *Microelectron. Eng.* 98, 5.

Andersen, A. S., Aslan, H., Dong, M., Jiang, X., and Sutherland, D. S. (2016). Podosome formation and development in monocytes restricted by the nanoscale spatial distribution of ICAM1. *Nano Lett.* 16, 2114–2121. doi: 10.1021/acs.nanolett.6b00519

Andresen Eguiluz, R. C., Kaylan, K. B., Underhill, G. H., and Leckband, D. E. (2017). Substrate stiffness and VE-cadherin mechano-transduction coordinate to regulate endothelial monolayer integrity. *Biomaterials* 140, 45–57. doi: 10.1016/j.biomaterials.2017.06.010

Arif, N., Zinnhardt, M., Nyamay'Antu, A., Teber, D., Bruckner, R., Schaefer, K., et al. (2021). PECAM-1 supports leukocyte diapedesis by tension-dependent dephosphorylation of VE-cadherin . *EMBO J.* e106113. doi: 10.15252/embj.2020106113<pmid>. [Epub ahead of print].

Aung, A., Seo, Y. N., Lu, S., Wang, Y., Jamora, C., del Alamo, J. C., et al. (2014). 3D traction stresses activate protease-dependent invasion of cancer cells. *Biophys. J.* 107, 2528–2537. doi: 10.1016/j.bpj.2014.07.078

Barreiro, O., Yanez-Mo, M., Serrador, J. M., Montoya, M. C., Vicente-Manzanares, M., Tejedor, R., et al. (2002). Dynamic interaction of VCAM-1 and ICAM-1 with moesin and ezrin in a novel endothelial docking structure for adherent leukocytes. *J. Cell Biol.* 157, 1233–1245. doi: 10.1083/jcb.200112126

Barzilai, S., Yadav, S. K., Morrell, S., Roncato, F., Klein, E., Stoler-Barak, L., et al. (2017). Leukocytes breach endothelial barriers by insertion of nuclear lobes and disassembly of endothelial actin filaments. *Cell Rep.* 18, 685–699. doi: 10.1016/j.celrep.2016.12.076

Berlin, C., Bargatze, R. F., Campbell, J. J., von Andrian, U. H., Szabo, M. C., Hasslen, S. R., et al. (1995). alpha 4 integrins mediate lymphocyte attachment and rolling under physiologic flow. *Cell* 80, 413–422. doi: 10.1016/0092-8674(95)90491-3

Blakely, B. L., Dumelin, C. E., Trappmann, B., McGregor, L. M., Choi, C. K., Anthony, P. C., et al. (2014). A DNA-based molecular probe for optically reporting cellular traction forces. *Nat. Methods* 11, 1229–1232. doi: 10.1038/nmeth.3145

Bouissou, A., Proag, A., Bourg, N., Pingris, K., Cabriel, C., Balor, S., et al. (2017). Podosome force generation machinery: a local balance between protrusion at the core and traction at the ring. *ACS Nano* 11, 4028–4040. doi: 10.1021/acsnano.7b00622

Braun, L. J., Stegmeyer, R. I., Schafer, K., Volkery, S., Currie, S. M., Kempe, B., et al. (2020). Platelets docking to VWF prevent leaks during leukocyte extravasation by stimulating Tie-2. *Blood* 136, 627–639. doi: 10.1182/blood.2019003442

Brockman, J. M., Blanchard, A. T., Pui-Yan, V. M., Derricotte, W. D., Zhang, Y., Fay, M. E., et al. (2018). Mapping the 3D orientation of piconewton integrin traction forces. *Nat. Methods* 15, 115–118. doi: 10.1038/nmeth.4536

Burns, A. R., Walker, D. C., Brown, E. S., Thurmon, L. T., Bowden, R. A., Keese, C. R., et al. (1997). Neutrophil transendothelial migration is independent of tight junctions and occurs preferentially at tricellular corners. *J. Immunol.* 159, 2893–2903.

Butler, J. P., Tolic-Norrelykke, I. M., Fabry, B., and Fredberg, J. J. (2002). Traction fields, moments, and strain energy that cells exert on their surroundings. *Am. J. Physiol. Cell Physiol.* 282, C595–C605. doi: 10.1152/ajpcell.00270.2001

Calle, Y., Burns, S., Thrasher, A. J., and Jones, G. E. (2006). The leukocyte podosome. *Eur. J. Cell Biol.* 85, 151–157. doi: 10.1016/j.ejcb.2005.09.003

Campas, O., Mammoto, T., Hasso, S., Sperling, R. A., O'Connell, D., Bischof, A. G., et al. (2014). Quantifying cell-generated mechanical forces within living embryonic tissues. *Nat. Methods* 11, 183–189. doi: 10.1038/nmeth.2761

Carman, C. V. (2009). Mechanisms for transcellular diapedesis: probing and pathfinding by 'invadosome-like protrusions'. *J. Cell Sci.* 122(Pt 17), 3025–3035. doi: 10.1242/jcs.047522

Carman, C. V., Jun, C. D., Salas, A., and Springer, T. A. (2003). Endothelial cells proactively form microvilli-like membrane projections upon intercellular adhesion molecule 1 engagement of leukocyte LFA-1. *J. Immunol.* 171, 6135–6144. doi: 10.4049/jimmunol.171.11.6135

Carman, C. V., Sage, P. T., Sciuto, T. E., de la Fuente, M. A., Geha, R. S., Ochs, H. D., et al. (2007). Transcellular diapedesis is initiated by invasive podosomes. *Immunity* 26, 784–797. doi: 10.1016/j.immuni.2007.04.015

Carman, C. V., and Springer, T. A. (2004). A transmigratory cup in leukocyte diapedesis both through individual vascular endothelial cells and between them. *J. Cell Biol.* 167, 377–388. doi: 10.1083/jcb.200404129

Chandrasekharan, U. M., Siemionow, M., Unsal, M., Yang, L., Poptic, E., Bohn, J., et al. (2007). Tumor necrosis factor alpha (TNF-alpha) receptor-II is required for TNF-alpha-induced leukocyte-endothelial interaction in vivo. *Blood* 109, 1938–1944. doi: 10.1182/blood-2006-05-020875

Charras, G., and Yap, A. S. (2018). Tensile forces and mechanotransduction at cell-cell junctions. *Curr. Biol.* 28, R445–R457. doi: 10.1016/j.cub.2018.02.003

Chesnutt, B. C., Smith, D. F., Raffler, N. A., Smith, M. L., White, E. J., and Ley, K. (2006). Induction of LFA-1-dependent neutrophil rolling on ICAM-1 by engagement of E-selectin. *Microcirculation* 13, 99–109. doi: 10.1080/10739680500466376

Choquet, D., Felsenfeld, D. P., and Sheetz, M. P. (1997). Extracellular matrix rigidity causes strengthening of integrin-cytoskeleton linkages. *Cell* 88, 39–48. doi: 10.1016/s0092-8674(00)81856-5

Cinamon, G., Shinder, V., and Alon, R. (2001). Shear forces promote lymphocyte migration across vascular endothelium bearing apical chemokines. *Nat. Immunol.* 2, 515–522. doi: 10.1038/88710

Cook-Mills, J. M., and Deem, T. L. (2005). Active participation of endothelial cells in inflammation. *J. Leukoc. Biol.* 77, 487–495. doi: 10.1189/jlb.0904554

Cooper, D., Lindberg, F. P., Gamble, J. R., Brown, E. J., and Vadas, M. A. (1995). Transendothelial migration of neutrophils involves integrin-associated protein (CD47). *Proc. Natl. Acad. Sci. U.S.A.* 92, 3978–3982. doi: 10.1073/pnas.92.9.3978

Cougoule, C., Le Cabec, V., Poincloux, R., Al Saati, T., Mege, J. L., Tabouret, G., et al. (2010). Three-dimensional migration of macrophages requires Hck for podosome organization and extracellular matrix proteolysis. *Blood* 115, 1444–1452. doi: 10.1182/blood-2009-04-218735

da Costa Martins, P., Garcia-Vallejo, J. J., van Thienen, J. V., Fernandez-Borja, M., van Gils, J. M., Beckers, C., et al. (2007). P-selectin glycoprotein ligand-1 is expressed on endothelial cells and mediates monocyte adhesion to activated

endothelium. *Arterioscler. Thromb. Vasc. Biol.* 27, 1023–1029. doi: 10.1161/ATVBAHA.107.140442

Dalaka, E., Kronenberg, N. M., Liehm, P., Segall, J. E., Prystowsky, M. B., and Gather, M. C. (2020). Direct measurement of vertical forces shows correlation between mechanical activity and proteolytic ability of invadopodia. *Sci. Adv.* 6:eaax6912. doi: 10.1126/sciadv.aax6912

Dehring, D. A., Clarke, F., Ricart, B. G., Huang, Y., Gomez, T. S., Williamson, E. K., et al. (2011). Hematopoietic lineage cell-specific protein 1 functions in concert with the Wiskott-Aldrich syndrome protein to promote podosome array organization and chemotaxis in dendritic cells. *J. Immunol.* 186, 4805–4818. doi: 10.4049/jimmunol.1003102

del Alamo, J. C., Meili, R., Alvarez-Gonzalez, B., Alonso-Latorre, B., Bastounis, E., Firtel, R., et al. (2013). Three-dimensional quantification of cellular traction forces and mechanosensing of thin substrata by fourier traction force microscopy. *PLoS One* 8:e69850. doi: 10.1371/journal.pone.0069850

Dembo, M., and Wang, Y. L. (1999). Stresses at the cell-to-substrate interface during locomotion of fibroblasts. *Biophys. J.* 76, 2307–2316. doi: 10.1016/S0006-3495(99)77386-8

Destaing, O., Saltel, F., Geminard, J. C., Jurdic, P., and Bard, F. (2003). Podosomes display actin turnover and dynamic self-organization in osteoclasts expressing actin-green fluorescent protein. *Mol. Biol. Cell* 14, 407–416. doi: 10.1091/mbc.e02-07-0389

Escribano, J., Chen, M. B., Moeendarbary, E., Cao, X., Shenoy, V., Garcia-Aznar, J. M., et al. (2019). Balance of mechanical forces drives endothelial gap formation and may facilitate cancer and immune-cell extravasation. *PLoS Comput. Biol.* 15:e1006395. doi: 10.1371/journal.pcbi.1006395

Evans, J. G., Correia, I., Krasavina, O., Watson, N., and Matsudaira, P. (2003). Macrophage podosomes assemble at the leading lamella by growth and fragmentation. *J. Cell Biol.* 161, 697–705. doi: 10.1083/jcb.200212037

Foxall, E., Staszowska, A., Hirvonen, L. M., Georgouli, M., Ciccioli, M., Rimmer, A., et al. (2019). PAK4 kinase activity plays a crucial role in the podosome ring of myeloid cells. *Cell Rep.* 29, 3385–3393.e6. doi: 10.1016/j.celrep.2019.11.016

Franz, J., Brinkmann, B. F., Konig, M., Huve, J., Stock, C., Ebnet, K., et al. (2016). Nanoscale imaging reveals a tetraspanin-CD9 coordinated elevation of endothelial ICAM-1 clusters. *PLoS One* 11:e0146598. doi: 10.1371/journal.pone.0146598

Fu, J., Wang, Y. K., Yang, M. T., Desai, R. A., Yu, X., Liu, Z., et al. (2010). Mechanical regulation of cell function with geometrically modulated elastomeric substrates. *Nat. Methods* 7, 733–736. doi: 10.1038/nmeth.1487

Gerard, A., van der Kammen, R. A., Janssen, H., Ellenbroek, S. I., and Collard, J. G. (2009). The Rac activator Tiam1 controls efficient T-cell trafficking and route of transendothelial migration. *Blood* 113, 6138–6147. doi: 10.1182/blood-2008-07-167668

Girardo, S., Traber, N., Wagner, K., Cojoc, G., Herold, C., Goswami, R., et al. (2018). Standardized microgel beads as elastic cell mechanical probes. *J. Mater. Chem. B* 6, 6245–6261. doi: 10.1039/c8tb01421c

Glazier, R., Brockman, J. M., Bartle, E., Mattheyses, A. L., Destaing, O., and Salaita, K. (2019). DNA mechanotechnology reveals that integrin receptors apply pN forces in podosomes on fluid substrates. *Nat. Commun.* 10:4507. doi: 10.1038/s41467-019-12304-4

Hall, M. S., Long, R., Feng, X., Huang, Y., Hui, C. Y., and Wu, M. (2013). Toward single cell traction microscopy within 3D collagen matrices. *Exp Cell Res* 319, 2396–2408. doi: 10.1016/j.yexcr.2013.06.009

Heemskerk, N., Schimmel, L., Oort, C., van Rijssel, J., Yin, T., Ma, B., et al. (2016). F-actin-rich contractile endothelial pores prevent vascular leakage during leukocyte diapedesis through local RhoA signalling. *Nat. Commun.* 7:10493. doi: 10.1038/ncomms10493

Heemskerk, N., van Rijssel, J., and van Buul, J. D. (2014). Rho-GTPase signaling in leukocyte extravasation: an endothelial point of view. *Cell Adh. Migr.* 8, 67–75. doi: 10.4161/cam.28244

Henderson, E., Haydon, P. G., and Sakaguchi, D. S. (1992). Actin filament dynamics in living glial cells imaged by atomic force microscopy. *Science* 257, 1944–1946. doi: 10.1126/science.1411511

Hidalgo, A., and Frenette, P. S. (2007). Leukocyte podosomes sense their way through the endothelium. *Immunity* 26, 753–755. doi: 10.1016/j.immuni.2007.06.002

Hidalgo, A., Peired, A. J., Wild, M., Vestweber, D., and Frenette, P. S. (2007). Complete identification of E-selectin ligands on neutrophils reveals distinct functions of PSGL-1, ESL-1, and CD44. *Immunity* 26, 477–489. doi: 10.1016/j.immuni.2007.03.011

Hixenbaugh, E. A., Goeckeler, Z. M., Papaiya, N. N., Wysolmerski, R. B., Silverstein, S. C., and Huang, A. J. (1997). Stimulated neutrophils induce myosin light chain phosphorylation and isometric tension in endothelial cells. *Am. J. Physiol.* 273(2 Pt 2), H981–H988. doi: 10.1152/ajpheart.1997.273.2.H981

Hoshino, D., Branch, K. M., and Weaver, A. M. (2013). Signaling inputs to invadopodia and podosomes. *J. Cell Sci.* 126(Pt 14), 2979–2989. doi: 10.1242/jcs.079475

Huo, Y., Hafezi-Moghadam, A., and Ley, K. (2000). Role of vascular cell adhesion molecule-1 and fibronectin connecting segment-1 in monocyte rolling and adhesion on early atherosclerotic lesions. *Circ. Res.* 87, 153–159. doi: 10.1161/01.res.87.2.153

Hur, S. S., del Alamo, J. C., Park, J. S., Li, Y. S., Nguyen, H. A., Teng, D., et al. (2012). Roles of cell confluency and fluid shear in 3-dimensional intracellular forces in endothelial cells. *Proc. Natl. Acad. Sci. U.S.A.* 109, 11110–11115. doi: 10.1073/pnas.1207326109

Hur, S. S., Zhao, Y., Li, Y. S., Botvinick, E., and Chien, S. (2009). Live cells exert 3-dimensional traction forces on their substrata. *Cell Mol. Bioeng.* 2, 425–436. doi: 10.1007/s12195-009-0082-6

Huse, M. (2017). Mechanical forces in the immune system. *Nat. Rev. Immunol.* 17, 679–690. doi: 10.1038/nri.2017.74

Kansas, G. S. (1996). Selectins and their ligands: current concepts and controversies. *Blood* 88, 3259–3287. doi: 10.1182/blood.v88.9.3259.bloodjournal8893259

Kaytanli, B., Khankhel, A. H., Cohen, N., and Valentine, M. T. (2020). Rapid analysis of cell-generated forces within a multicellular aggregate using microsphere-based traction force microscopy. *Soft Matter* 16, 4192–4199. doi: 10.1039/c9sm02377a

Kronenberg, N. M., Liehm, P., Steude, A., Knipper, J. A., Borger, J. G., Scarcelli, G., et al. (2017). Long-term imaging of cellular forces with high precision by elastic resonator interference stress microscopy. *Nat. Cell Biol.* 19, 864–872. doi: 10.1038/ncb3561

Kroon, J., Schaefer, A., van Rijssel, J., Hoogenboezem, M., van Alphen, F., Hordijk, P., et al. (2018). Inflammation-sensitive myosin-X functionally supports leukocyte extravasation by Cdc42-mediated ICAM-1-rich endothelial filopodia formation. *J. Immunol.* 200, 1790–1801. doi: 10.4049/jimmunol.1700702

Labernadie, A., Bouissou, A., Delobelle, P., Balor, S., Voituriez, R., Proag, A., et al. (2014). Protrusion force microscopy reveals oscillatory force generation and mechanosensing activity of human macrophage podosomes. *Nat. Commun.* 5:5343. doi: 10.1038/ncomms6343

Labernadie, A., Thibault, C., Vieu, C., Maridonneau-Parini, I., and Charriere, G. M. (2010). Dynamics of podosome stiffness revealed by atomic force microscopy. *Proc. Natl. Acad. Sci. U.S.A.* 107, 21016–21021. doi: 10.1073/pnas.1007835107

Lampi, M. C., Guvendiren, M., Burdick, J. A., and Reinhart-King, C. A. (2017). Photopatterned hydrogels to investigate the endothelial cell response to matrix stiffness heterogeneity. *ACS Biomater. Sci. Eng.* 3:10.

Lawrence, M. B., Kansas, G. S., Kunkel, E. J., and Ley, K. (1997). Threshold levels of fluid shear promote leukocyte adhesion through selectins (CD62L,P,E). *J. Cell Biol.* 136, 717–727. doi: 10.1083/jcb.136.3.717

Legant, W. R., Choi, C. K., Miller, J. S., Shao, L., Gao, L., Betzig, E., et al. (2013). Multidimensional traction force microscopy reveals out-of-plane rotational moments about focal adhesions. *Proc. Natl. Acad. Sci. U.S.A.* 110, 881–886. doi: 10.1073/pnas.1207997110

Legant, W. R., Miller, J. S., Blakely, B. L., Cohen, D. M., Genin, G. M., and Chen, C. S. (2010). Measurement of mechanical tractions exerted by cells in three-dimensional matrices. *Nat. Methods* 7, 969–971. doi: 10.1038/nmeth.1531

Lemmon, C. A., Chen, C. S., and Romer, L. H. (2009). Cell traction forces direct fibronectin matrix assembly. *Biophys. J.* 96, 729–738. doi: 10.1016/j.bpj.2008.10.009

Ley, K., Laudanna, C., Cybulsky, M. I., and Nourshargh, S. (2007). Getting to the site of inflammation: the leukocyte adhesion cascade updated. *Nat. Rev. Immunol.* 7, 678–689. doi: 10.1038/nri2156

Liehm, P., Kronenberg, N. M., and Gather, M. C. (2018). Analysis of the precision, robustness, and speed of elastic resonator interference stress microscopy. *Biophys. J.* 114, 2180–2193. doi: 10.1016/j.bpj.2018.03.034

Liu, Z., Sniadecki, N. J., and Chen, C. S. (2010). Mechanical forces in endothelial cells during firm adhesion and early transmigration of human monocytes. *Cell Mol. Bioeng.* 3, 50–59. doi: 10.1007/s12195-010-0105-3

Lo, C. M., Wang, H. B., Dembo, M., and Wang, Y. L. (2000). Cell movement is guided by the rigidity of the substrate. *Biophys. J.* 79, 144–152. doi: 10.1016/S0006-3495(00)76279-5

Lu, L., Oswald, S. J., Ngu, H., and Yin, F. C. (2008). Mechanical properties of actin stress fibers in living cells. *Biophys. J.* 95, 6060–6071. doi: 10.1529/biophysj.108.133462

Mamdouh, Z., Kreitzer, G. E., and Muller, W. A. (2008). Leukocyte transmigration requires kinesin-mediated microtubule-dependent membrane trafficking from the lateral border recycling compartment. *J. Exp. Med.* 205, 951–966. doi: 10.1084/jem.20072328

Mamdouh, Z., Mikhailov, A., and Muller, W. A. (2009). Transcellular migration of leukocytes is mediated by the endothelial lateral border recycling compartment. *J. Exp. Med.* 206, 2795–2808. doi: 10.1084/jem.20082745

Martinelli, R., Kamei, M., Sage, P. T., Massol, R., Varghese, L., Sciuto, T., et al. (2013). Release of cellular tension signals self-restorative ventral lamellipodia to heal barrier micro-wounds. *J. Cell Biol.* 201, 449–465. doi: 10.1083/jcb.201209077

Martinelli, R., Zeiger, A. S., Whitfield, M., Sciuto, T. E., Dvorak, A., Van Vliet, K. J., et al. (2014). Probing the biomechanical contribution of the endothelium to lymphocyte migration: diapedesis by the path of least resistance. *J. Cell Sci.* 127(Pt 17), 3720–3734. doi: 10.1242/jcs.148619

Maskarinec, S. A., Franck, C., Tirrell, D. A., and Ravichandran, G. (2009). Quantifying cellular traction forces in three dimensions. *Proc. Natl. Acad. Sci. U.S.A.* 106, 22108–22113. doi: 10.1073/pnas.0904565106

Middleton, J., Neil, S., Wintle, J., Clark-Lewis, I., Moore, H., Lam, C., et al. (1997). Transcytosis and surface presentation of IL-8 by venular endothelial cells. *Cell* 91, 385–395. doi: 10.1016/s0092-8674(00)80422-5

Mohagheghian, E., Luo, J., Chen, J., Chaudhary, G., Chen, J., Sun, J., et al. (2018). Quantifying compressive forces between living cell layers and within tissues using elastic round microgels. *Nat. Commun.* 9:1878. doi: 10.1038/s41467-018-04245-1

Mooren, O. L., Li, J., Nawas, J., and Cooper, J. A. (2014). Endothelial cells use dynamic actin to facilitate lymphocyte transendothelial migration and maintain the monolayer barrier. *Mol. Biol. Cell* 25, 4115–4129. doi: 10.1091/mbc.E14-05-0976

Morikis, V. A., Chase, S., Wun, T., Chaikof, E. L., Magnani, J. L., and Simon, S. I. (2017). Selectin catch-bonds mechanotransduce integrin activation and neutrophil arrest on inflamed endothelium under shear flow. *Blood* 130, 2101–2110. doi: 10.1182/blood-2017-05-783027

Muller, W. A. (2003). Leukocyte-endothelial-cell interactions in leukocyte transmigration and the inflammatory response. *Trends Immunol.* 24, 327–334. doi: 10.1016/s1471-4906(03)00117-0

Muller, W. A. (2014). How endothelial cells regulate transmigration of leukocytes in the inflammatory response. *Am. J. Pathol.* 184, 886–896. doi: 10.1016/j.ajpath.2013.12.033

Nier, V., Jain, S., Lim, C. T., Ishihara, S., Ladoux, B., and Marcq, P. (2016). Inference of internal stress in a cell monolayer. *Biophys. J.* 110, 1625–1635. doi: 10.1016/j.bpj.2016.03.002

Nourshargh, S., and Alon, R. (2014). Leukocyte migration into inflamed tissues. *Immunity* 41, 694–707. doi: 10.1016/j.immuni.2014.10.008

Perrault, C. M., Brugues, A., Bazellieres, E., Ricco, P., Lacroix, D., and Trepat, X. (2015). Traction forces of endothelial cells under slow shear flow. *Biophys. J.* 109, 1533–1536. doi: 10.1016/j.bpj.2015.08.036

Pfaff, M., and Jurdic, P. (2001). Podosomes in osteoclast-like cells: structural analysis and cooperative roles of paxillin, proline-rich tyrosine kinase 2 (Pyk2) and integrin alphaVbeta3. *J. Cell Sci.* 114(Pt 15), 2775–2786.

Phillipson, M., Kaur, J., Colarusso, P., Ballantyne, C. M., and Kubes, P. (2008). Endothelial domes encapsulate adherent neutrophils and minimize increases in vascular permeability in paracellular and transcellular emigration. *PLoS One* 3:e1649. doi: 10.1371/journal.pone.0001649

Polacheck, W. J., and Chen, C. S. (2016). Measuring cell-generated forces: a guide to the available tools. *Nat. Methods* 13, 415–423. doi: 10.1038/nmeth.3834

Rabodzey, A., Alcaide, P., Luscinskas, F. W., and Ladoux, B. (2008). Mechanical forces induced by the transendothelial migration of human neutrophils. *Biophys. J.* 95, 1428–1438. doi: 10.1529/biophysj.107.119156

Sabass, B., Gardel, M. L., Waterman, C. M., and Schwarz, U. S. (2008). High resolution traction force microscopy based on experimental and computational advances. *Biophys. J.* 94, 207–220. doi: 10.1529/biophysj.107.113670

Sabri, S., Foudi, A., Boukour, S., Franc, B., Charrier, S., Jandrot-Perrus, M., et al. (2006). Deficiency in the Wiskott-Aldrich protein induces premature proplatelet formation and platelet production in the bone marrow compartment. *Blood* 108, 134–140. doi: 10.1182/blood-2005-03-1219

Saito, H., Minamiya, Y., Kitamura, M., Saito, S., Enomoto, K., Terada, K., et al. (1998). Endothelial myosin light chain kinase regulates neutrophil migration across human umbilical vein endothelial cell monolayer. *J. Immunol.* 161, 1533–1540.

Saito, H., Minamiya, Y., Saito, S., and Ogawa, J. (2002). Endothelial Rho and Rho kinase regulate neutrophil migration via endothelial myosin light chain phosphorylation. *J. Leukoc. Biol.* 72, 829–836.

Schaefer, A., and Hordijk, P. L. (2015). Cell-stiffness-induced mechanosignaling – a key driver of leukocyte transendothelial migration. *J. Cell Sci.* 128, 2221–2230. doi: 10.1242/jcs.163055

Schulte, D., Kuppers, V., Dartsch, N., Broermann, A., Li, H., Zarbock, A., et al. (2011). Stabilizing the VE-cadherin-catenin complex blocks leukocyte extravasation and vascular permeability. *EMBO J.* 30, 4157–4170. doi: 10.1038/emboj.2011.304

Schwarz, U. S., Balaban, N. Q., Riveline, D., Bershadsky, A., Geiger, B., and Safran, S. A. (2002). Calculation of forces at focal adhesions from elastic substrate data: the effect of localized force and the need for regularization. *Biophys. J.* 83, 1380–1394. doi: 10.1016/S0006-3495(02)73909-X

Serrano, R., Aung, A., Yeh, Y. T., Varghese, S., Lasheras, J. C., and Del Alamo, J. C. (2019). Three-dimensional monolayer stress microscopy. *Biophys. J.* 117, 111–128. doi: 10.1016/j.bpj.2019.03.041

Shaw, S. K., Bamba, P. S., Perkins, B. N., and Luscinskas, F. W. (2001). Real-time imaging of vascular endothelial-cadherin during leukocyte transmigration across endothelium. *J. Immunol.* 167, 2323–2330. doi: 10.4049/jimmunol.167.4.2323

Shulman, Z., Shinder, V., Klein, E., Grabovsky, V., Yeger, O., Geron, E., et al. (2009). Lymphocyte crawling and transendothelial migration require chemokine triggering of high-affinity LFA-1 integrin. *Immunity* 30, 384–396. doi: 10.1016/j.immuni.2008.12.020

Singbartl, K., Thatte, J., Smith, M. L., Wethmar, K., Day, K., and Ley, K. (2001). A CD2-green fluorescence protein-transgenic mouse reveals very late antigen-4-dependent CD8+ lymphocyte rolling in inflamed venules. *J. Immunol.* 166, 7520–7526. doi: 10.4049/jimmunol.166.12.7520

Stroka, K. M., and Aranda-Espinoza, H. (2009). Neutrophils display biphasic relationship between migration and substrate stiffness. *Cell Motil. Cytoskeleton* 66, 328–341. doi: 10.1002/cm.20363

Stroka, K. M., and Aranda-Espinoza, H. (2010). A biophysical view of the interplay between mechanical forces and signaling pathways during transendothelial cell migration. *FEBS J.* 277, 1145–1158. doi: 10.1111/j.1742-4658.2009.07545.x

Style, R. W., Boltyanskiy, R., German, G. K., Hyland, C., MacMinn, C. W., Mertz, A. F., et al. (2014). Traction force microscopy in physics and biology. *Soft Matter* 10, 4047–4055. doi: 10.1039/c4sm00264d

Tambe, D. T., Croutelle, U., Trepat, X., Park, C. Y., Kim, J. H., Millet, E., et al. (2013). Monolayer stress microscopy: limitations, artifacts, and accuracy of recovered intercellular stresses. *PLoS One* 8:e55172. doi: 10.1371/journal.pone.0055172

Tan, J. L., Tien, J., Pirone, D. M., Gray, D. S., Bhadriraju, K., and Chen, C. S. (2003). Cells lying on a bed of microneedles: an approach to isolate mechanical force. *Proc. Natl. Acad. Sci. U.S.A.* 100, 1484–1489. doi: 10.1073/pnas.0235407100

Teijeira, A., Garasa, S., Pelaez, R., Azpilikueta, A., Ochoa, C., Marre, D., et al. (2013). Lymphatic endothelium forms integrin-engaging 3D structures during DC transit across inflamed lymphatic vessels. *J. Invest. Dermatol.* 133, 2276–2285. doi: 10.1038/jid.2013.152

Tornavaca, O., Chia, M., Dufton, N., Almagro, L. O., Conway, D. E., Randi, A. M., et al. (2015). ZO-1 controls endothelial adherens junctions, cell-cell tension, angiogenesis, and barrier formation. *J. Cell Biol.* 208, 821–838. doi: 10.1083/jcb.201404140

Trepat, X., Wasserman, M. R., Angelini, T. E., Millet, E., Weitz, D. A., Butler, J. P., et al. (2009). Physical forces during collective cell migration. *Nat. Phys.* 5:4.

van Buul, J. D., Allingham, M. J., Samson, T., Meller, J., Boulter, E., Garcia-Mata, R., et al. (2007). RhoG regulates endothelial apical cup assembly downstream from

ICAM1 engagement and is involved in leukocyte trans-endothelial migration. *J. Cell Biol.* 178, 1279–1293. doi: 10.1083/jcb.200612053

van Buul, J. D., van Rijssel, J., van Alphen, F. P., van Stalborch, A. M., Mul, E. P., and Hordijk, P. L. (2010). ICAM-1 clustering on endothelial cells recruits VCAM-1. *J. Biomed. Biotechnol.* 2010:120328. doi: 10.1155/2010/120328

van den Dries, K., Bolomini-Vittori, M., and Cambi, A. (2014). Spatiotemporal organization and mechanosensory function of podosomes. *Cell Adh. Migr.* 8, 268–272. doi: 10.4161/cam.28182

van den Dries, K., Nahidiazar, L., Slotman, J. A., Meddens, M. B. M., Pandzic, E., Joosten, B., et al. (2019). Modular actin nano-architecture enables podosome protrusion and mechanosensing. *Nat. Commun.* 10:5171. doi: 10.1038/s41467-019-13123-3

van den Dries, K., Schwartz, S. L., Byars, J., Meddens, M. B., Bolomini-Vittori, M., Lidke, D. S., et al. (2013). Dual-color superresolution microscopy reveals nanoscale organization of mechanosensory podosomes. *Mol. Biol. Cell* 24, 2112–2123. doi: 10.1091/mbc.E12-12-0856

van den Dries, K., van Helden, S. F., te Riet, J., Diez-Ahedo, R., Manzo, C., Oud, M. M., et al. (2012). Geometry sensing by dendritic cells dictates spatial organization and PGE(2)-induced dissolution of podosomes. *Cell Mol. Life Sci.* 69, 1889–1901. doi: 10.1007/s00018-011-0908-y

Vestweber, D. (2015). How leukocytes cross the vascular endothelium. *Nat. Rev. Immunol.* 15, 692–704. doi: 10.1038/nri3908

Vijayakumar, V., Monypenny, J., Chen, X. J., Machesky, L. M., Lilla, S., Thrasher, A. J., et al. (2015). Tyrosine phosphorylation of WIP releases bound WASP and impairs podosome assembly in macrophages. *J. Cell Sci.* 128, 251–265. doi: 10.1242/jcs.154880

Vincent, L. G., Choi, Y. S., Alonso-Latorre, B., del Alamo, J. C., and Engler, A. J. (2013). Mesenchymal stem cell durotaxis depends on substrate stiffness gradient strength. *Biotechnol. J.* 8, 472–484. doi: 10.1002/biot.201200205

Vorselen, D., Labitigan, R. L. D., and Theriot, J. A. (2020a). A mechanical perspective on phagocytic cup formation. *Curr. Opin. Cell Biol.* 66, 112–122. doi: 10.1016/j.ceb.2020.05.011

Vorselen, D., Wang, Y., de Jesus, M. M., Shah, P. K., Footer, M. J., Huse, M., et al. (2020b). Microparticle traction force microscopy reveals subcellular force exertion patterns in immune cell-target interactions. *Nat. Commun.* 11:20. doi: 10.1038/s41467-019-13804-z

Wang, J. H., and Lin, J. S. (2007). Cell traction force and measurement methods. *Biomech. Model. Mechanobiol.* 6, 361–371. doi: 10.1007/s10237-006-0068-4

Wang, X., and Ha, T. (2013). Defining single molecular forces required to activate integrin and notch signaling. *Science* 340, 991–994. doi: 10.1126/science.1231041

Wee, H., Oh, H. M., Jo, J. H., and Jun, C. D. (2009). ICAM-1/LFA-1 interaction contributes to the induction of endothelial cell-cell separation: implication for enhanced leukocyte diapedesis. *Exp. Mol. Med.* 41, 341–348. doi: 10.3858/emm.2009.41.5.038

Woodfin, A., Voisin, M. B., Beyrau, M., Colom, B., Caille, D., Diapouli, F. M., et al. (2011). The junctional adhesion molecule JAM-C regulates polarized transendothelial migration of neutrophils in vivo. *Nat. Immunol.* 12, 761–769. doi: 10.1038/ni.2062

Yang, L., Froio, R. M., Sciuto, T. E., Dvorak, A. M., Alon, R., and Luscinskas, F. W. (2005). ICAM-1 regulates neutrophil adhesion and transcellular migration of TNF-alpha-activated vascular endothelium under flow. *Blood* 106, 584–592. doi: 10.1182/blood-2004-12-4942

Yang, L., Kowalski, J. R., Yacono, P., Bajmoczi, M., Shaw, S. K., Froio, R. M., et al. (2006). Endothelial cell cortactin coordinates intercellular adhesion molecule-1 clustering and actin cytoskeleton remodeling during polymorphonuclear leukocyte adhesion and transmigration. *J. Immunol.* 177, 6440–6449. doi: 10.4049/jimmunol.177.9.6440

Yeh, Y. T., Serrano, R., Francois, J., Chiu, J. J., Li, Y. J., Del Alamo, J. C., et al. (2018). Three-dimensional forces exerted by leukocytes and vascular endothelial cells dynamically facilitate diapedesis. *Proc. Natl. Acad. Sci. U.S.A.* 115, 133–138. doi: 10.1073/pnas.1717489115

Zen, K., and Parkos, C. A. (2003). Leukocyte-epithelial interactions. *Curr. Opin. Cell Biol.* 15, 557–564. doi: 10.1016/s0955-0674(03)00103-0

Zhang, Y., Ge, C., Zhu, C., and Salaita, K. (2014). DNA-based digital tension probes reveal integrin forces during early cell adhesion. *Nat. Commun.* 5:5167. doi: 10.1038/ncomms6167

Zimmermann, J., Hayes, R. L., Basan, M., Onuchic, J. N., Rappel, W. J., and Levine, H. (2014). Intercellular stress reconstitution from traction force data. *Biophys. J.* 107, 548–554. doi: 10.1016/j.bpj.2014.06.036

Conflict of Interest: The authors declare that the research was conducted in the absence of any commercial or financial relationships that could be construed as a potential conflict of interest.

frontiers in Cell and Developmental Biology

REVIEW
published: 16 April 2021
doi: 10.3389/fcell.2021.636778

The Role of PDE8 in T Cell Recruitment and Function in Inflammation

*Paul M. Epstein[1], Chaitali Basole[2] and Stefan Brocke[2]**

[1] Department of Cell Biology, UConn Health, Farmington, CT, United States, [2] Department of Immunology, UConn Health, Farmington, CT, United States

Inhibitors targeting cyclic nucleotide phosphodiesterases (PDEs) expressed in leukocytes have entered clinical practice to treat inflammatory disorders, with three PDE4 inhibitors currently in clinical use as therapeutics for psoriasis, psoriatic arthritis, atopic dermatitis and chronic obstructive pulmonary disease. In contrast, the PDE8 family that is upregulated in pro-inflammatory T cells is a largely unexplored therapeutic target. It was shown that PDE8A plays a major role in controlling T cell and breast cancer cell motility, including adhesion to endothelial cells under physiological shear stress and chemotaxis. This is a unique function of PDE8 not shared by PDE4, another cAMP specific PDE, employed, as noted, as an anti-inflammatory therapeutic. Additionally, a regulatory role was shown for the PDE8A-rapidly accelerated fibrosarcoma (Raf)-1 kinase signaling complex in myelin antigen reactive $CD4^+$ effector T cell adhesion and locomotion by a mechanism differing from that of PDE4. The PDE8A-Raf-1 kinase signaling complex affects T cell motility, at least in part, via regulating the LFA-1 integrin mediated adhesion to ICAM-1. The findings that PDE8A and its isoforms are expressed at higher levels in naive and myelin oligodendrocyte glycoprotein $(MOG)_{35-55}$ activated effector T (Teff) cells compared to regulatory T (Treg) cells and that PDE8 inhibition specifically affects MOG_{35-55} activated Teff cell adhesion, indicates that PDE8A could represent a new beneficial target expressed in pathogenic Teff cells in CNS inflammation. The implications of this work for targeting PDE8 in inflammation will be discussed in this review.

Keywords: cAMP, phosphodiesterase, PDE8, Raf-1 kinase, T cell motility, leukocyte recruitment, inflammation, integrin adhesion

OPEN ACCESS

Edited by:
Xunbin Wei,
Peking University, China

Reviewed by:
Lai Wen,
La Jolla Institute for Immunology (LJI), United States
Clive P. Page,
King's College London, United Kingdom
Donald H. Maurice,
Queen's University, Canada
Martina Schmidt,
University of Groningen, Netherlands

****Correspondence:***
Stefan Brocke
sbrocke@uchc.edu

Specialty section:
This article was submitted to Cell Adhesion and Migration, a section of the journal Frontiers in Cell and Developmental Biology

Received: *02 December 2020*
Accepted: *29 March 2021*
Published: *16 April 2021*

Citation:
Epstein PM, Basole C and Brocke S (2021) The Role of PDE8 in T Cell Recruitment and Function in Inflammation. Front. Cell Dev. Biol. 9:636778. doi: 10.3389/fcell.2021.636778

INTRODUCTION

With over 800 members identified in humans, G protein coupled receptors (GPCRs) constitute a large group of signaling molecules expressed on many cells. Together with their other associated signaling molecules, they are the targets for nearly 35% of approved therapeutics (Sriram and Insel, 2018). The majority of therapeutically targeted GPCRs affect the cAMP signaling pathway which is also a major target of potent anti-inflammatory drugs (Schett et al., 2010; Rabe, 2011; Tenor et al., 2011; De Souza et al., 2012; Milara et al., 2012; Schafer, 2012; Wittmann and Helliwell, 2013; Victoni et al., 2014; Dong et al., 2016; Jarnagin et al., 2016; Tom et al., 2016; Zane et al., 2016a,b; Sriram and Insel, 2018; Blokland et al., 2019). cAMP is involved in many physiological

functions and a well-established key regulator of chemotaxis and inflammation (Bourne et al., 1974; Amarandi et al., 2016). Binding of extracellular ligands such as chemokines to Gs-coupled GPCRs leads to cAMP synthesis via activation of adenylyl cyclase and conversion of ATP to cAMP (Weis and Kobilka, 2018). Additionally, T cell activation leads to a temporary upregulation of cAMP which is then degraded by cyclic nucleotide phosphodiesterase (PDE) enzymes (Wang et al., 1978). PDEs constitute the sole group of molecules known to hydrolyze cAMP and hence maintain spatial and temporal control over cAMP gradients within a cell (Baillie, 2009). PDEs are grouped into 11 different gene families considering their action on cAMP or cGMP, structural similarity and mode of regulation (Lerner and Epstein, 2006). While PDEs had been considered early as good targets for anti-inflammatory drugs, bringing specific PDE inhibitors into clinical use has faced decades of challenges (Francis et al., 2011), mostly because of off target effects including emesis (Giembycz, 2000; Beavo et al., 2007). The approval of small molecule inhibitors of PDE4 to treat major immunologic conditions demonstrates a tremendous progress over the last 7 years with indications expanding at an almost yearly pace (Maurice et al., 2014; Baillie et al., 2019). Current clinical practice includes several small molecule compounds that target PDE4 for the therapy of lung disease (COPD) (Hatzelmann et al., 2010; Weis and Kobilka, 2018), psoriatic arthritis and plaque psoriasis (Schett et al., 2012) and topically for atopic dermatitis (Callender et al., 2019). Hence PDE inhibitors are proving to be of great clinical benefit in inflammatory disorders (Ahmad et al., 2015). This review will focus on the selective and shared roles of PDE isoforms during the regulation of T cell motility with emphasis on novel insights of PDE8 functions.

PDE EXPRESSION IN IMMUNE CELLS

As shown in **Table 1** [adapted from Lerner and Epstein (2006)], PDEs are encoded by twenty one genes and are by convention organized into 11 gene families based on their key properties. These include overlap in sequence, specificity for cAMP or cGMP as substrate and their mode of regulation. With alternative splicing as well as the existence of multiple transcription initiation sites, at least 100 different forms of PDE have been cloned and many are expressed in a cell and tissue selective manner. Among the 11 PDE gene families, PDE4, PDE7, and PDE8 selectively hydrolyze cAMP as substrate and degrade it into 5′-AMP, PDE5, PDE6, and PDE9 selectively hydrolyze cGMP as substrate, and PDE1, PDE2, PDE3, PDE10, and PDE11 hydrolyze both cAMP and cGMP as substrate. Of note, the affinity of PDE8 for cAMP is greater than that of any of the other PDE gene families (Fisher et al., 1998a; Hayashi et al., 1998; Soderling et al., 1998a; Gamanuma et al., 2003; Bender and Beavo, 2006).

PDE4

Early studies showed PDE4 to be the predominant form of PDE expressed in the cytosolic fraction of human lymphocytes (Epstein and Hachisu, 1984), with PDE4A, 4B, and 4D, but not 4C being expressed (Jiang et al., 1998). PDE4 has long been known to play a key role in regulating T cell activation and functions (Michie et al., 1996; Ekholm et al., 1997; Erdogan and Houslay, 1997; Gantner et al., 1997a,b; Sommer et al., 1997; Barnette et al., 1998; Jin et al., 1998, 2010; Bielekova et al., 2000; Hatzelmann and Schudt, 2001; Kanda and Watanabe, 2001; Arp et al., 2003; Abrahamsen et al., 2004; Asirvatham et al., 2004; Claveau et al., 2004; Jimenez et al., 2004; Bjorgo and Tasken, 2006; Peter et al., 2007; Bjorgo et al., 2010, 2011; Vang et al., 2016). A key mechanism appears to be the modulation of signal transduction through the T cell receptor (TCR). Activation of the TCR leads to cAMP production localized in lipid rafts, activation of cAMP dependent protein kinase A (PKA) and subsequent inhibition of the TCR signal (Abrahamsen et al., 2004; Bjorgo and Tasken, 2006; Wehbi and Tasken, 2016; **Figure 1**). However, engagement of the co-stimulatory receptor CD28 leads to the recruitment of beta-arrestin and PDE4 to lipid rafts and the decrease of the local cAMP pool and PKA activity. PDE4 inhibitors downregulate the TCR signal by increasing local cAMP concentrations and PKA activity and counteract the CD28-induced recruitment of PDE4. Thus, localized activities of cAMP, PKA, and PDE4 regulate the upstream TCR signal necessary for T cell activation and the subsequent initiation of effector functions.

PDE3

PDE3 was found to be the predominant form expressed in particulate fractions of human lymphocytes, solely as PDE3B (Tenor et al., 1995; Ekholm et al., 1997; Sheth et al., 1997). In contrast, PDE3B expression is low in regulatory T(reg) cells, and it appears that the low catalytic activity of PDE3B is critical for the regulation of Treg cell-specific gene expression (Gavin et al., 2007). When PDE expression profiles of human T and B lymphocytes were compared, it is of note that in contrast to T cells, which expressed high amounts of PDE3, B cells expressed little or no PDE3 (Gantner et al., 1998).

PDE7

PDE7, primarily PDE7A, was also found to be expressed in human lymphocytes, to a lesser extent than PDE3 and PDE4, with PDE7A1 primarily cytosolic and PDE7A2 mainly associated with a particulate fraction (Bloom and Beavo, 1996; Giembycz et al., 1996; Bender and Beavo, 2006). Subsequent studies also showed that PDE1B, PDE7A, and PDE8A were all induced following activation of human lymphocytes (Epstein et al., 1980, 1987; Jiang et al., 1998; Glavas et al., 2001; Kanda and Watanabe, 2001). A critical role of the induction of PDE7 for a full T cell activation has been reported (Li et al., 1999; Guo et al., 2009; Szczypka, 2020). Inhibition studies using PDE7 selective inhibitors have yielded divergent results and seem to point to a context and other PDE isoform dependent role of PDE7 in T cell functions and T cell mediated inflammation (Li et al., 1999; Nakata et al., 2002; Yang et al., 2003; Nueda et al., 2006; Goto et al., 2009; Guo et al., 2009; Kadoshima-Yamaoka et al., 2009; Redondo et al., 2012; Gonzalez-Garcia et al., 2013; Xu et al., 2016; Martin-Alvarez et al., 2017; Szczypka, 2020).

TABLE 1 | Pde gene families.

Family[1]	Type	Genes	Km cAMP (μM)	Km cGMP (μM)	Commonly Used Inhibitors[2]	References
PDE1	CaM-Dependent	1A 1B 1C	50–100 7–24 1	5 3 1	Vinpocetine (5–25) 8-MM-IBMX (4)	Wang et al., 1990; Yan et al., 1995; Loughney et al., 1996; Sharma and Hickie, 1996; Yu et al., 1997; Zhao et al., 1997; Kakkar et al., 1999; Goraya and Cooper, 2005
PDE2	cGMP-Stimulated	2A	30	10	EHNA (1)	Martins et al., 1982; Manganiello et al., 1990b; Mery et al., 1995; Podzuweit et al., 1995
PDE3	cGMP-Inhibited	3A/B	0.2–0.5	0.02–0.2	Cilostamide (0.005) Milrinone (0.3)	Manganiello et al., 1990a; Komas et al., 1996; Kambayashi et al., 2003
PDE4	cAMP-Specific	4A–D	1–4	–	Rolipram (1) RO 20-1724 (2) Piclamilast (0.001) Roflumilast (0.0002–0.0043) Apremilast (0.07) Crisaborole (0.5)	Epstein et al., 1982; Conti and Swinnen, 1990; Conti et al., 1995; Houslay et al., 1998; Wallace et al., 2005; Akama et al., 2009; Man et al., 2009; Hatzelmann et al., 2010; Schafer et al., 2010
PDE5	cGMP-Specific	5A	–	1–5	Sildenafil (0.003) Zaprinast (0.3) Dipyridamole (0.9)	Francis et al., 1990; Kotera et al., 1998; Loughney et al., 1998; Lin et al., 2000; Wang et al., 2001; Bischoff, 2004
PDE6	Photoreceptor	6A–C	–	20	Zaprinast (0.15) Dipyridamole (0.4)	Gillespie and Beavo, 1989; Gillespie, 1990
PDE7	cAMP-Specific	7A/B	0.03–0.2	–	Dipyridamole (42, 7A; 0.5–9, 7B)	Michaeli et al., 1993; Han et al., 1997; Gardner et al., 2000; Hetman et al., 2000b; Sasaki et al., 2000; Wang et al., 2000
PDE8	cAMP-Specific	8A/B	0.04–0.15	–	Dipyridamole (4–9, 8A; 23–40, 8B) PF-4957325 (0.0007, 8A; <0.0003, 8B, >1.5 all other PDEs)	Fisher et al., 1998a; Hayashi et al., 1998; Soderling et al., 1998a; Gamanuma et al., 2003; Bender and Beavo, 2006; Vang et al., 2010; DeNinno et al., 2011; DeNinno, 2012
PDE9	cGMP-Specific	9A	–	0.07–0.39	Zaprinast (30) SCH 51866 (2)	Fisher et al., 1998b; Soderling et al., 1998b; Wang et al., 2003
PDE10	Dual Substrate	10A	0.05–0.26	3–9	Papaverine (0.03)	Fujishige et al., 1999a,b; Loughney et al., 1999; Soderling et al., 1999
PDE11	Dual Substrate	11A	1–6	0.5–4	Tadalafil (0.07) Zaprinast (11–33) Dipyridamole (0.3–1.8)	Fawcett et al., 2000; Hetman et al., 2000a; Yuasa et al., 2000; Loughney et al., 2005; Weeks et al., 2005

[1]Shown in this table [adapted from Lerner and Epstein (2006)] are the eleven PDE gene families, the known genes within them, their affinity constants for cAMP and cGMP, and commonly used pharmacological inhibitors for each of the families. The substrate affinity constants listed are approximate and where ranges are given, they represent the range of different Kms reported for these family members in the references cited.

[2]The numbers in parentheses are the approximate reported Kis or IC_{50}s for inhibition of that PDE gene family, given in μM. Note: the non-specific methylxanthine inhibitor IBMX inhibits all of the PDE families with the notable exception of the PDE8 and PDE9 gene families, which appear to be resistant to IBMX inhibition.

PDE8

The expression of PDE8 in immune cells is listed in **Table 2**. The function of PDE8 in T cells and cancer cells is discussed in detail below.

Additionally, very low levels of PDE1, PDE2, and PDE5 activity were also detected in $CD4^+$ and $CD8^+$ human T cells (Tenor et al., 1995).

Regulatory T(reg) Cells

As mentioned, PDE3 expression was found to be diminished in Treg cells as compared to $CD4^+$ T cells (Gavin et al., 2007). Subsequently it was found that gene expression of *Pde1B*, *Pde2A*, *Pde3B*, *Pde4B*, *Pde5A*, *Pde7A*, and *Pde8A* and protein expression of PDE3B, PDE4B2, and PDE8Awere all reduced in Treg cells as compared to $CD4^+$ Teff cells (Bopp et al., 2007, 2009; Vang et al., 2010, 2013; Vaeth et al., 2011; Basole et al., 2017). The low expression levels of PDEs in Treg cells and high level of cAMP have been linked to the mechanism by which Treg cells suppress the function of effector T(eff) cells through the direct cell-to-cell transfer of cAMP (Bopp et al., 2007).

PDE8A BUT NOT PDE4 IS CONTROLLING ACTIVATED T CELL MOTILITY

Inhibition of PDEs regulates T cell proliferation, cytokine production and motility (Sommer et al., 1997; Pette et al., 1999; Bielekova et al., 2000; Vang et al., 2010, 2016; Bjorgo et al., 2011; Mosenden and Tasken, 2011; Wehbi and Tasken, 2016; Basole et al., 2017; **Figure 1**). Only a small number

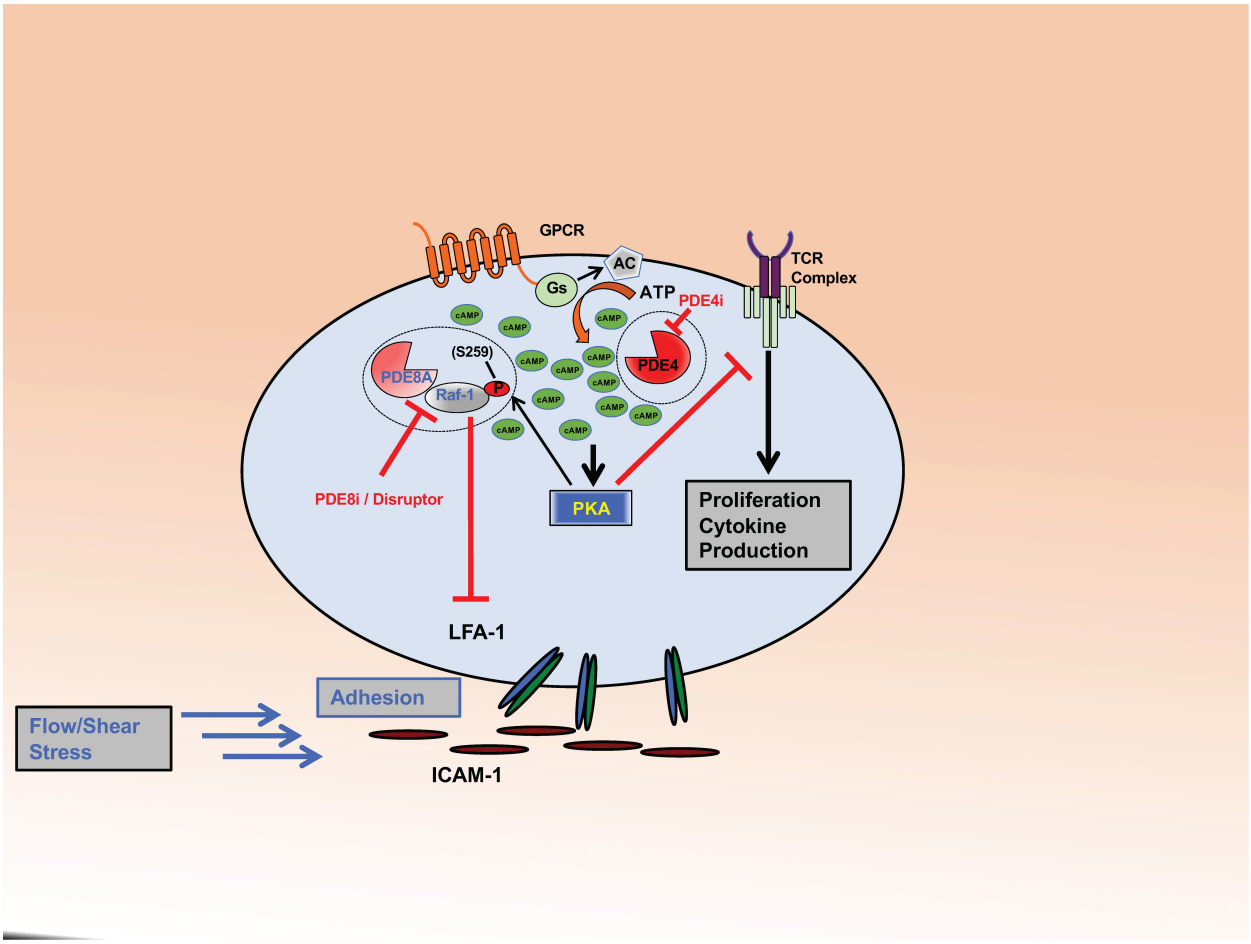

FIGURE 1 | PDE8 regulates Teff cell adhesion. The complex formed between PDE8A and Raf-1 controls adhesion of activated Teff cells through the establishment of tethers between integrin LFA-1 and ICAM-1. PKA becomes activated through the cAMP signaling pathway in response to ligand binding to GPCRs or the Tell receptor. PKA phosphorylates Raf-1 at S259 (P) which inhibits its function to promote adhesion. PDE8A in complex with Raf-1 protects Raf-1 from inhibitory PKA phosphorylation by locally degrading cAMP. PDE8 inhibition or complex disruption leads to an increase of cAMP-dependent PKA activation and Raf-1 phosphorylation at the inhibitory site S259 (P). Action of the PDE8 selective inhibitor PF-04957325 (PDE8i) or disruption of the PDE8A-Raf-1 complex by a signaling disruptor promotes Raf-1 phosphorylation and subsequently inhibits T cell adhesion. This significantly changes Raf-1 activity in T cells. Inhibiting PDE8 targets the tethers formed between LFA-1 and ICAM-1, thereby altering adhesion, spreading and migration of T cells when tested under shear stress conditions. In contrast, PDE4 inhibition (PDE4i) leads to an increase of a pool of cAMP and the activation of PKA signaling localized in signaling complexes that inhibit T cell receptor (TCR) signaling and subsequent T cell activation, cytokine production and proliferation.

of PDEs are currently targeted by approved therapeutics, and there is a significant knowledge gap about the specific and potentially therapeutic role of other PDE isoforms. This led to the development of novel PDE inhibitors, including those for therapy of inflammatory conditions. Recently, there have been numerous studies on PDE8A and PDE8B, a family of cAMP specific PDEs (Fisher et al., 1998a; Hayashi et al., 1998; Soderling et al., 1998a; Glavas et al., 2001; Kobayashi et al., 2003; Dong et al., 2006, 2010, 2015; Chen et al., 2009; Vang et al., 2010, 2016; DeNinno et al., 2011; Tsai and Beavo, 2012; Brown et al., 2013; Demirbas et al., 2013; Maurice, 2013; Shimizu-Albergine et al., 2016; Basole et al., 2017; Johnstone et al., 2017; Kelly, 2018). PDE8A and B are expressed widely in human tissue (Wang et al., 2008) with functions identified in testosterone and corticosteroid production (Tsai et al., 2010; Demirbas et al., 2013), myocyte contraction (Patrucco et al., 2010), lymphocyte adhesion and chemotaxis (Dong et al., 2006, 2015; Vang et al., 2010, 2013; Basole et al., 2017), memory and coordination (Tsai et al., 2012), human airway smooth muscle regulation (Johnstone et al., 2017), strong association with immune protection against intracellular pathogens (Blanco et al., 2017), brain disorders associated with inflammation (Chimienti et al., 2019) and T cells in systemic lupus erythematosus (SLE) (Orlowski et al., 2008). In a recent study, single nucleotide polymorphisms in the *PDE8* region were found to be associated with Sjögren's Syndrome (Taylor et al., 2017). T cell activation induces PDE8A1 (Glavas et al., 2001), a PDE isoform with a cAMP affinity up to 100 times higher than PDE4 isoforms (Fisher et al., 1998a; Hayashi et al., 1998; Soderling et al., 1998a; Gamanuma et al., 2003; Bender and Beavo, 2006). This property of the PDE8 family suggests that

TABLE 2 | PDE8A expression and function in immune cells.

Immune cell subpopulation	PDE gene expression	PDE protein expression	Results	References
$CD4^+$ T cells	PDE8A1	PDE8A1	Upregulation of PDE8A1 after polyclonal T cell activation	Glavas et al., 2001
Mitogen-activated splenocytes, anti-CD3 activated $CD4^+$ T cells	PDE8A		Induction of PDE8A expression in response to stimulus	Dong et al., 2006; Vang et al., 2010
Antigen exposed naïve and memory $CD4^+$ T cells	PDE8A		Changes in temporal expression patterns in response to antigen challenge	Vang et al., 2010
$CD4^+$ T cells	PDE8A	PDE8A	Association of PDE8A expression and accumulation of sensitized T cells in draining lymph node of in an animal model of allergic airway disease (AAD)	Vang et al., 2016
$CD4^-$ T cells	Low PDE8A	Low PDE8A	Control cell population in AAD	Vang et al., 2016
$CD4^+$ T cells	High PDE8A	High PDE8A	Hilar lymph node in AAD	Vang et al., 2016
$CD4^+$ effector T(eff) cells	Increased PDE8A expression after polyclonal activation	Increased PDE8A expression after polyclonal activation	PDE8A inhibition by enzymatic inhibitor or a PDE8A-Raf-1 kinase complex disruptor decreases Teff cell adhesion and migration under shear stress conditions	Basole et al., 2017
$CD4^+$ regulatory T(reg) cells	Low PDE8A (and all other PDEs expressed in T cells)	Low PDE8A (and all other PDEs expressed in T cells)	High cAMP levels in Treg cells	Bopp et al., 2009; Vang et al., 2010; Vang et al., 2013; Basole et al., 2017
T cells in systemic lupus erythematosus (SLE)	PDE8A1		Upregulation of PDE8A1 transcripts in SLE T cells vs. normal controls	Orlowski et al., 2008
Macrophages	PDE8A		Promotes susceptibility to HIV-1 infection	Booiman et al., 2014

they may regulate changes of baseline cAMP gradients around cell signaling complexes. The availability of PDE8 inhibitors and disruptors (**Table 3**) greatly enhanced the ability to conduct studies on the function of PDE8 *in vitro* and *in vivo*.

It was shown that PDE8A regulates motility of lymphocytes and breast cancer cells, including adhesion to endothelial cells under physiological shear stress and chemotaxis (Dong et al., 2006, 2015; Vang et al., 2010, 2013; Basole et al., 2017). This seems to be a unique feature of PDE8 that is distinct from PDE4 activity (Vang et al., 2016). The therapeutic potency of biologics and compounds interacting with molecular targets on pathogenic T cells has been shown *in vitro* and *in vivo* (Yednock et al., 1992; Brocke et al., 1999; Steinman, 2005; Healy and Antel, 2016). Current observations demonstrate PDE8 to be one of those targets for blocking Teff cell motility and potentially inflammation (Dong et al., 2006, 2015; Vang et al., 2010, 2013, 2016; Basole et al., 2017). The potential role of PDE8 in models of inflammation and cancer is summarized in **Table 4**.

TABLE 3 | Broad and selective PDE8 inhibitors.

Inhibitor, selectivity	References
PF-4957325, PDE8A/B	Vang et al., 2010; DeNinno et al., 2011; DeNinno, 2012
BC8–15, Dual PDE4/8	Demirbas et al., 2013
Dual PDE7/8	Jankowska et al., 2017
Multiple PDE8 inhibiting compounds	Vang et al., 2010; DeNinno et al., 2011; DeNinno, 2012
Dipyridamole, PDE 4–8, 10, and 11	Lerner and Epstein, 2006
Multiple 2-chloroadenine derivatives, PDE8A	Huang et al., 2020
Cell-penetrating peptide agent (PPL-008) inhibiting the PDE8A–C-Raf complex	Blair et al., 2019
Stearylated cell-permeable peptide disrupting the Raf-1–PDE8A Complex based on the Raf-1–docking sequence from PDE8A, encompassing residues R454–T465	Brown et al., 2013

DIFFERENTIAL ROLES OF PDES IN T CELL ADHESION

Previous studies on the role of PDE8 were done using the prototypic chemokine CXCL12 which is known to induce migration of leukocytes, including murine splenocytes (Cinamon et al., 2001). As measured in a transwell assay system CXCL12 stimulates equally the migration of mouse splenocytes, both unstimulated and stimulated with the mitogen concanavalin A (Con A). Interestingly, when probing the cAMP signaling pathway in CXCL12-induced chemotaxis, differential effects were observed on directed leukocyte migration between exposure of cells to a cell permeable cAMP analog vs. stimulation of adenylyl cyclase or inhibition of PDE. While CXCL12 dependent chemotaxis of both naïve and mitogen activated splenocytes was inhibited by direct exposure to dibutyryl cAMP, activated cells were resistant to indirect cAMP regulation through stimulation of adenylyl cyclase or PDE inhibition (Dong et al., 2006). Activation of adenylyl cyclase through Forskolin (Fsk) or PDE inhibition through the broad PDE enzymatic inhibitor IBMX, significantly reduced CXCL12-induced migration of naive but not activated splenocytes. Additionally, chemotaxis of mitogen-activated splenocytes was not inhibited by PDE3-, PDE4-, and PDE7-selective inhibitors. It is important to note that IBMX is a pan-cAMP specific PDE inhibitor that inhibits all known cAMP PDEs with the exception of PDE8 (Soderling et al., 1998a; Soderling and Beavo, 2000). In contrast, dipyridamole (DP), a broad PDE inhibitor that also targets

TABLE 4 | PDE8 in models of inflammation and cancer.

PDE8 isoform/assay	Model and Function	References
PDE8A/Expression study	Temporal changes of PDE8A expression in $CD4^+$ T cell specific for a cytochrome C peptide/I-E^k antigen complex transferred into wildtype (non-transgenic) mice, activated with antigen *in vivo*.	Vang et al., 2010
PDE8A/Expression study	$CD4^+$ and $CD4^-$ T cell populations in a model of ovalbumin-induced allergic airway disease in mice	Vang et al., 2016
PDE8 inhibition study *ex vivo* and *in vitro*	T cells responding to myelin oligodendrocyte glycoprotein (MOG)peptide MOG_{35-55}[1]	Vang et al., 2016
PDE8A1/PDE8A2 Expression study	*In vivo* MOG_{35-55} activated $CD4^+CD25^-$ effector and $CD4^+CD25^+$ regulatory cells[1]	Basole et al., 2017
PDE8A and B/ Regulating T cell adhesion through inhibitor and peptide disruptor study	*In vivo* MOG_{35-55} activated $CD4^+CD25^-$ effector and $CD4^+CD25^+$ regulatory T cells[1]	Basole et al., 2017
PDE 4–8, 10, and 11/Use of broad PDE inhibitor dipyridamole *in vivo* treatment	Treatment of experimental autoimmune encephalomyelitis[2]	Sloka et al., 2013
PDE8A-C-Raf complex/PDE8A-C-Raf complex disruptor PPL-008	Treatment of human malignant MM415 melanoma cell line *in vitro* and a MM415 melanoma xenograft mouse model *in vivo* with cell-penetrating PDE8A-C-Raf complex disruptor peptide agent (PPL-008) leads to reduced phospho-ERK signaling and growth inhibition	Blair and Baillie, 2019; Blair et al., 2019
PDE8A and B/Expression study	Human breast adenocarcinoma estrogen receptor-positive MCF-7 and T-47D cell lines Human breast adenocarcinoma estrogen receptor-negative MDA-MB-123 MB-231 and MDA-MB-435 cell lines	Dong et al., 2015
PDE8A and B, Expression study	Human breast cancer patient biopsies and tissue arrays	Dong et al., 2015
PDE8A and B, Inhibitor study	Inhibition of MDA-MB-231 breast cancer cell migration and wound healing	Dong et al., 2015
PDE 4–8, 10, and 11/Use of the broad PDE inhibitor dipyridamole *in vivo* treatment	Prevention of triple-negative breast-cancer progression in a mouse model	Virgilio et al., 2012; Spano et al., 2013
PDE 4–8, 10, and 11/Use of the broad PDE inhibitor dipyridamole *in vivo* treatment	Delay of breast cancer lesion onset, tumor progression and suppression of lung metastasis in a mouse model	Wang et al., 2013b

[1] *Myelin oligodendrocyte glycoprotein (MOG) peptide MOG_{35-55} is a myelin autoantigen used to induce experimental autoimmune encephalomyelitis (EAE) in vivo and is recognized by T and B cells in multiple sclerosis (MS).*
[2] *Experimental autoimmune encephalomyelitis (EAE) is an autoimmune disease model for multiple sclerosis (MS).*

PDE8 (Soderling et al., 1998a), was found to inhibit migration of naïve and activated splenocytes in response to CXCL12 (Dong et al., 2006). Addition of Fsk in combination with DP increased inhibition of chemotaxis of both naïve and activated splenocytes.

Of note, Rp-cAMPS, an inhibitor of PKA, reversed the DP mediated inhibition of splenocyte migration when exposed to CXCL12. DP is also known to inhibit nucleoside transporters, thereby increasing extracellular adenosine which causes increased levels of cAMP in T cells (Wang et al., 2013a). However, in these assays the action of DP on motility was unaffected by extracellular adenosine deaminase, suggesting that the effect of DP is independent of a possible increase in extracellular adenosine. Expression studies of splenocyte and T cell mRNA demonstrated upregulation of PDE4B2, PDE7A1 and A3, and PDE8A1 in response to T cell activation (Glavas et al., 2001; Dong et al., 2006; Vang et al., 2010). The results indicate that PDE8A1 may have a critical function in regulating cAMP pools that control T cell motility (Dong et al., 2006).

PDE8A EXPRESSION IN EFFECTOR T (Teff) CELLS *IN VIVO*

PDE8 expression was not only seen in unactivated and polyclonally stimulated splenocytes and $CD4^+$ T cells *in vitro*, but also in highly purified $CD4^+$ T cell populations *in vivo*. In a widely used TCR transgenic mouse model to investigate highly purified T cell populations *in vivo* in the absence of other leukocytes (Ben-Sasson et al., 2009, 2013), it was shown that antigenic activation resulted in PDE3, 4, and 8 expression in the transgenic T cell subset. Expression levels of the PDE8A gene in activated $CD4^+$ T cells were up to fifty percent of those of the PDE3B and PDE4B genes (Vang et al., 2010).

SELECTIVE INHIBITION OF PDE8 BLOCKS SPLENOCYTE ADHESION

Integrins including αL or α4 chains have been shown to promote firm adhesion to endothelial cell ligands. cAMP is known to regulate expression and activation of integrin molecules on lymphocytes and other leukocyte populations.

As mentioned, DP was found to inhibit PDE8 and leukocyte migration. Incubation with DP led to a significant reduction of the proportion of αL^{hi} and $\alpha 4^{hi}$ Teff cells.

In contrast, IBMX did not significantly reduce integrin surface expression. Similarly, DP reduced the proportion of activated splenocytes to endothelial cells while IBMX did not have the same effect (Vang et al., 2010). Of note, the potent PDE4 inhibitor piclamilast (PICL) and the PDE3 inhibitor motapizone also did not suppress adhesion. Further, no significant effect of the canonical PDE4 inhibitor rolipram was reported when the interactions between activated T cells and immobilized VCAM-1 or endothelial cells were tested. The specific role of PDE8 action in T cell adhesion could be confirmed using PF-4957325, a selective PDE inhibitor with IC_{50} for PDE8A = 0.0007 μM

and IC_{50} for PDE8B < 0.0003 μM, and with IC_{50} for all other PDEs > 1.5 μM (Vang et al., 2010; DeNinno et al., 2011; DeNinno, 2012; **Tables 1**, **3**). As with DP, PF-4957325 significantly suppressed T cell blast adhesion to endothelial cells. Interestingly, when tested in T cell proliferation in response to anti-CD3 stimulation, PICL was significantly more potent at inhibiting T cell proliferation in comparison to PF-4957325 at identical concentrations. These data suggest a specific role for PDE8 in regulating Teff cell adhesion to endothelial cells. Subsequently, it was shown that cAMP signaling controls adhesion in these assays which could account for the effect of PDE8 inhibition.

One of the mechanisms by which cAMP regulates T cell adhesion is through the action of PKA which regulates cell surface expression and affinity of integrin molecules and phosphorylates α4 integrin involved in cellular adhesion (Goldfinger et al., 2003; Lim et al., 2007; Chilcoat et al., 2008). Thus, dibutyryl-cAMP, acting through PKA, inhibits T cell adhesion to endothelial cell ligands. The effect of increased cAMP levels on cell adhesion was not reversed by CXCL12 (Vang et al., 2010).

ENDOTHELIAL CELLS ALSO EXPRESS PDE8A

Cells of the murine brain endothelium-derived cell line bEnd.3, a polyoma virus middle T oncogene expressing endothelioma cell line (Montesano et al., 1990; Takeuchi and Baichwal, 1995) used for *in vitro* adhesion studies (Vang et al., 2010, 2016; Basole et al., 2017), have been shown to express PDE1, 2, 3, 4, 5, and 7 (Ashikaga et al., 1997; Netherton and Maurice, 2005). Additionally, bEnd.3 cells express PDE8A at levels that are about 25 percent of PDE4B, which is comparable to expression of PDE2A, a functionally critical isoform in endothelial cells (Vang et al., 2010). DP did not induce PDE8A in bEnd.3 or T cells. These results are in contrast to PDE4B which was significantly upregulated in both of these cell populations in response to the increase in intracellular cAMP. These differential responses of PDEs to cAMP signaling further point to different and non-overlapping roles of PDE8 and other PDE isoforms within the same cell populations (Vang et al., 2010).

PDE8A GENE EXPRESSION IN $CD4^+$ $CD25^+$ REGULATORY T (Treg) CELLS

It is well established that Teff cells and Treg cells express significantly different levels of PDEs. The transcription factor forkhead box P3 (Foxp3) expressed in Treg cells has been shown to selectively repress genes, including *PDE* genes, leading to elevated levels of intracellular cAMP (Bopp et al., 2007, 2009; Vaeth et al., 2011).

Remarkably, the Treg cell subsets show significantly lower expression for *Pde1a*, *Pde1b*, *Pde2a*, *Pde 3b*, *Pde 4b*, *Pde5a*, *Pde7a*, and *Pde8a* genes compared to naive Teff cell subsets. In addition to lower expression of PDE3B and PDE4B2, T reg cells express significantly lower levels of PDE8A in comparison to Teff cells (Vang et al., 2013). Consistent with these findings, it was shown that Foxp3 represses PDE3B, while reduced PDE3B expression through genetic means permits normal Treg cell homeostasis and Treg cell-specific gene expression (Gavin et al., 2007). In contrast, Treg and Teff cells express comparable levels of PDE4B3, PDE4D, and PDE7A (Vang et al., 2013). While the regulation of select PDE isoforms including PDE8 through Foxp3 in Treg cells is well established, the exact role of PDE isoforms regulating Treg cell function remains to be elucidated.

$CD4^+$ T CELLS SELECTIVELY EXPRESS PDE8A IN INFLAMMATORY DISEASE

PDE8A but not PDE8B has been shown to be expressed in T cells (Hayashi et al., 1998, 2002; Dong et al., 2006, 2010).

To test the potential of PDE8 as a target to treat inflammation *in vivo*, the expression of PDE8 was determined in draining lymph nodes of mice that were immunized with ovalbumin (OVA) in an allergic airway disease (AAD) model (Vang et al., 2016).

In this mouse model of AAD, clinical and pathologic resolution occurs with long-term exposure to OVA aerosol. T cells accumulate in hilar and inguinal lymph nodes that drain the exposed lung tissue. The expression of PDE8A protein was determined by Western immunoblot in the $CD4^+$ T cell population that was isolated from the lymph nodes at various time points after the induction of AAD. It was found that PDE8A was significantly higher in the $CD4^+$ population as compared to the $CD4^-$ lymph node populations. Importantly, the increased PDE8A expression was only seen in *in vivo* activated $CD4^+$ T cell populations, i.e., after antigen exposure, but not in $CD4^+$ T cells from naïve lymph nodes.

Taken together, these results demonstrate that PDE8A expression is higher in the hilar $CD4^+$ lymph node cell population than in the hilar $CD4^-$ lymph node cell population at various stages of AAD. Additionally, expression levels of the *Pde8a* gene were higher during the acute AAD phase than at the late stage tolerance stage of the disease model (Vang et al., 2016).

PDE8 AND PDE4 INHIBITION SHOW DIFFERENTIAL EFFECTS ON THE *IN VITRO* ADHESION OF T CELLS TO ENDOTHELIAL CELLS

Studies including a combination of selective and broad PDE inhibitors established overlapping and distinct effects of PDEs in T cell adhesion. Specifically, only the use of PDE inhibitors that target PDE8, including the broad PDE8 inhibitor DP and the highly PDE8-selective inhibitor PF-04957325 (Vang et al., 2010), demonstrated significant inhibition of splenocyte and T cell adhesion. Of note, the PDE inhibitor IBMX, which inhibits all known PDEs that hydrolyze cAMP with the exception of PDE8, shows little inhibitory effect when tested in assays measuring T cell adhesion to endothelial cells. Surprisingly, the potent PDE4 inhibitor PICL showed opposite effects both when used

alone or in combination with a PDE8 inhibitor by enhancing adhesion of T cells to endothelial cells. Taken together, these studies show that PDE4 and PDE8 inhibitors exert opposite effects on T cell–endothelial cell interactions in adhesion assays (Vang et al., 2016).

OPPOSING EFFECTS OF PDE8 AND PDE4 INHIBITORS ON PROLIFERATION OF ANTIGEN OR ANTI-CD3 STIMULATED T CELLS

In contrast to the observations in adhesion assays, T cell proliferation could be significantly inhibited by the PDE4 inhibitor PICL while the PDE8 inhibitor PF-04957325 showed little effect on proliferation in these studies (Vang et al., 2016). This indicates an action of PDE8 inhibitors on T cell adhesion that is independent of the well-documented inhibition of mitogen-activated protein kinase (MAP) kinase signaling by PDE inhibitors (Giembycz et al., 1996; Essayan et al., 1997; Bjorgo et al., 2011). T cells that were stimulated by specific antigen or anti-CD3 *in vitro* responded significantly lower in proliferation assays when exposed to PICL in comparison to exposure of equal doses of PF-04957325. Importantly, the opposing effects that were seen in adhesion assays were not seen in proliferation assays since combining PICL and PF-04957325 led to a small increase in suppression of proliferation (Vang et al., 2016). These results clearly demonstrate differential actions of PDE4 and PDE8 in regulating key T cell functions.

REGULATION OF VASCULAR ADHESION OF Teff CELLS VS. Treg CELLS THROUGH INHIBITION OF PDE8 UNDER PHYSIOLOGIC SHEAR STRESS

It was found that Treg cells form significantly stronger tethers to endothelial cells compared to Teff cells (Maganto-Garcia et al., 2011). It was also established that PDE8A expression in Teff cells differed significantly from that in Treg cells (Vang et al., 2013). Based on these observations adhesion and migration of Teff and Treg cells were investigated for the effects of PDE8 inhibition on these processes (Basole et al., 2017). This question was addressed in a mouse model of autoimmune disease using encephalitogenic Teff cell populations mediating experimental autoimmune encephalomyelitis (EAE). T cells were isolated from draining lymph nodes of mice immunized with a myelin derived peptide, myelin oligodendrocyte glycoprotein $(MOG)_{35-55}$, an antigen that is used to induce EAE in susceptible strains of mice (Brocke et al., 1996; Biton et al., 2011). PDE8A1 and PDE8A2 expression at the protein level was compared in the fraction of $CD4^+CD25^-$ Teff cells and $CD4^+CD25^+$ Treg cells, and it was shown that there was significantly higher expression of these PDE8 isoforms in Teff cells than in Treg cells (Vang et al., 2013). However, expression of rapidly accelerated fibrosarcoma (Raf)-1 in Teff cells was not significantly different from that in Treg cells (Basole et al., 2017).

Previous studies demonstrated that Raf-1 profoundly regulates cell motility (Juliano et al., 2004). A study addressing the role of PDE8 in this process used T cells that were derived from *Foxp3gfp.KI* mice (Basole et al., 2017). In these mice, expression of FoxP3, a known regulator of the development of functional Treg cell populations, is tagged with green fluorescent protein (GFP). Using Teff and Treg cell populations from these mice immunized with the myelin derived peptide facilitated separate measurements of inhibitor effects on each cell population under identical conditions. A flow chamber model using physiologic shear stress to measure various categories of tethers of T cell populations to bEnd.3 cells was employed. PDE8 inhibition using PF-04957325 significantly reduced firm tethers of $CD4^+Foxp^+GFP^-$ Teff cells. In contrast, no significant effect of PDE8 inhibition was observed in adhesion assays of $CD4^+Foxp^+GFP^+$ Treg cells. It is conceivable that the different sensitivity of Teff and Treg cells to PDE8 inhibition when forming firm adhesive tethers is related to the different expression levels of PDE8A in both cell populations (Basole et al., 2017).

ADHESION OF Teff CELLS TO ENDOTHELIAL CELLS IS REGULATED BY A PDE8A-RAF-1 KINASE SIGNALING COMPLEX

The studies on PDE8 inhibition were followed by mechanistic investigations testing the role of the signaling complex formed by PDE8A and Raf-1 kinase in regulating adhesion of Teff and Treg cells to endothelial cells (Basole et al., 2017). Both molecules assemble in the cytoplasm whereby PDE8A protects RAF-1 kinase from PKA mediated inhibitory phosphorylation (Brown et al., 2013; Maurice, 2013). Vascular adhesion of T cells has been shown to be regulated by members of the Ras family of signaling molecules (Brown et al., 2014). Disruption of the PDE8A-Raf-1 complex by a cell permeable peptide specifically engineered to disrupt this complex (Brown et al., 2013) was tested for its effect on $CD4^+$ T cell adhesion and migration under shear stress conditions. Adhesion of $CD4^+GFP^-Foxp3^-$ Teff cells to vascular endothelial cells was significantly decreased by the disruptor peptide in experiments employing $CD4^+$ T cells isolated from the draining lymph nodes of *Foxp3gfp.KI* mice immunized with MOG_{35-55}, whereas a scrambled control peptide was without effect. Disruption of the PDE8A-Raf-1 complex by the peptide similarly decreased adhesion, spreading and locomotion of Teff cells to isolated ICAM-1 molecules. In contrast, the use of PF-04957325 which targets the enzymatic site of PDE8, did not show comparable effects (Basole et al., 2017). In further comparing the disruptor peptide with the PDE8 enzymatic inhibitor, PF-04957325, it was found that adhesion of $CD4^+$ Teff or Treg cells via LFA-1 integrin to ICAM-1 was not markedly altered through the exposure to PF-04957325. In contrast the PDE8A-Raf-1 disruptor peptide significantly reduced cell adherence,

spreading and locomotion of $CD4^+GFP^-Foxp3^-$ Teff cells. The disruptor peptide also reduced transient Treg cell adhesion to ICAM-1, while having no effect on firm tether formation and detachment of these cells. Taken together, this indicates the tether formation between LFA-1 and ICAM-1 on T cells and vascular targets is in part regulated by a signaling complex that is formed between PDE8A and Raf-1. The regulation appears to be LFA-1 integrin specific in that no significant effects were observed when the VLA-4–VCAM-1 interactions were examined using the comparable assay systems and cells (Basole et al., 2017).

INHIBITION OF PDE8 CATALYTIC ACTIVITY SIGNIFICANTLY SUPPRESSES EXTRACELLULAR SIGNAL-REGULATED KINASE (ERK) PHOSPHORYLATION IN ACTIVATED $CD4^+$ T CELLS

Inhibition of PDE8 catalytic activity and disruption of the complex of PDE8A-Raf-1 were both investigated for their potential to affect Raf-1 or ERK signaling by analyzing Raf-1 phosphorylation at residue S259 that inhibits its activity (Brown et al., 2013; Maurice, 2013) by PKA and the phosphorylation sites known to activate ERK1/2 in $CD4^+$ T cells that were treated with PF-04957325 or disruptor peptide and polyclonally activated (Basole et al., 2017). Inhibitory Raf-1 phosphorylation at S259 and activating ERK1/2 phosphorylation at residues Thr202/Tyr204 were determined by Western immunoblot. Inhibitor treatment did not affect phosphorylation of Raf-1, but a significant decrease of the phosphorylation of ERK1/2 was seen after inhibitor treatment of Teff cells. These observations demonstrate an effect of PDE8 on the ERK1/2 signaling pathway as has been seen with PDE4 in T cells (Baillie and Houslay, 2005). Of note, the abundance of PDE8A increased in response to PDE8 inhibition. Similar results were reported for PDE7A, PDE3B, PDE4B, and PDE4D which were increased when cAMP was elevated in cells (Jiang et al., 1998; Lee et al., 2002; Moon et al., 2002), and this upregulation apparently occurs with PDE8A as well.

PDE8A-RAF-1 COMPLEX DISRUPTION WITHIN ACTIVATED Teff CELLS LEADS TO RAF-1 AND ERK1/2 PHOSPHORYLATION WITH OPPOSING EFFECTS

Treatment of $CD4^+$ T cells with the complex disruptor peptide increases phosphorylation of Raf-1 at the inhibitory site at S259 while phosphorylation of ERK1/2 increases at activating sites at Thr202/Tyr204 (Basole et al., 2017). Based on these observations, it is conceivable that the PDE8A-Raf-1 complex regulates motility of T cells through Raf-1 and not through the canonical ERK-MAPK pathway. The exact mechanism underlying these experimental results needs to be elucidated since the reported increase in the phosphorylation of ERK within activated Teff cells can be the result of actions of many effectors interacting in this process (Kortum et al., 2013).

PDE8A AND BREAST CANCER CELL MOTILITY

It has been observed that stimulation of cAMP signaling, in many cases through inhibition of PDEs, inhibits migration and motility of some types of cells, including fibroblasts (Fleming et al., 2004), epithelial cells (Lyle et al., 2008), endothelial cells (Netherton and Maurice, 2005), melanoma cells (Dua and Gude, 2008), colon cancer cells (Murata et al., 2000), pancreatic cancer cells (Burdyga et al., 2013; Zimmerman et al., 2015), bladder cancer cells (Ou et al., 2014), cervical cancer cells (Lee et al., 2014), and breast cancer cells (Dong et al., 2015). In the breast cancer study a complete analysis of the expression of PDE genes at the mRNA and protein level in established estrogen receptor positive and negative breast cancer cell lines and in patients' primary breast cancer biopsies by microarray analysis, qPCR, Western blot analysis, immunofluorescence and immunohistochemistry was performed (Dong et al., 2015). Although a wide range of PDE genes were seen to be expressed in some of these breast cancers by these methods, the PDE8A gene was prominently expressed at the mRNA level in all the breast cancer cells as well as all the breast cancer tissues examined. In addition to its prominent expression in breast cancer cells, expression of PDE8A in the form of an AKAP13-PDE8A fusion transcript has been reported to be highly recurrent in colon cancer cells as well (Nome et al., 2013). Breast cancer cell migration was analyzed both by transwell migration and wound healing assays, and was found to be inhibited by several agonistic cAMP analogs, Fsk, and several PDE inhibitors, in particular DP and the PDE8 selective inhibitor, PF-04957325. Therefore, consistent with our observation of PDE8A being important in the regulation of lymphocyte chemotaxis, it may also be an important regulator, and thus an important target for control of breast cancer cell migration as well.

CONCLUSION

Numerous studies demonstrate that T cell adhesion and migration under shear stress conditions are regulated by the enzymatic activity of PDE8 proteins. Additionally, the PDE8A-Raf-1 kinase signaling complex has been identified as a functional site for PDE8A controlling T cell motility (**Figure 1**). Inasmuch as treatment with the peptide designed to disrupt the PDE8A-Raf-1 complex led to phosphorylation of Raf-1 at an inhibitory site but phosphorylation of ERK1/2 at activating sites, it suggests that PDE8 displacement from the complex exerts a Raf-1 dependent but ERK independent effect on T cell motility. Thus, it is conceivable that the effect of PDE8 inhibition on the formation of tethers and directed migration by T cells is mediated by Raf-1 but not ERK. This model is supported by reports demonstrating regulation of cell motility by Raf-1 and B-Raf through Rho GTPases regulating the actin cytoskeleton and focal adhesions

(Ehrenreiter et al., 2005; Klein et al., 2008). The studies on PDE8 identify a novel signaling complex of PDE8-RAF regulating $CD4^+$ T cell motility. Upon T cell activation through the TCR, Raf-1 links Ras activation to MAPK signaling (Kortum et al., 2013). Of note, B-Raf most strongly interacts with Ras (Marais et al., 1997; Weber et al., 2000) and activates ERK (Pritchard et al., 1995, 2004; Wojnowski et al., 2000) while cell proliferation and ERK activation are independent of Raf-1. In contrast, Raf-1 is capable of activating Rho and inducing subsequent downstream events in migrating cells without MAPK activity (Ehrenreiter et al., 2005). Thus, MAPKs have been known to act independently in specific signaling pathways. Activation of ERK independent of Ras/Raf-1 can also occur through activation of T cells through the TCR (Kortum et al., 2013). An effect on T cell function that is independent of ERK is also suggested by the finding that PDE8 inhibition does not affect T cell proliferation (Vang et al., 2010, 2016). PDE4 inhibition has been shown to suppress T cell proliferation and ERK1 signaling (Norambuena et al., 2009), but T cell motility is little affected (Lerner and Epstein, 2006; Vang et al., 2016). Collectively, reports over the last few years suggest that PDE8 and the PDE8A-Raf-1 signaling complex selectively regulate the motility of T cells but not T cell proliferation and support the notion that PDE8A exerts its action primarily on Raf-1 kinase and not on MAPK signaling.

AUTHOR CONTRIBUTIONS

All authors researched the literature, wrote the manuscript, and reviewed and approved the final version. SB prepared the figure. CB and PE reviewed and approved the final figure.

FUNDING

We received support from the NMSS (grant no. RG 4544A1/1) on the Role of PDE8 in EAE, from the Smart Family Foundation on Targeting PDE8 for Treatment of Autoimmune Diseases and the Lea's Foundation for Leukemia Research Inc. on phosphodiesterase as a Target for Leukemia Treatment. The funders had no influence on the research design and experiments.

REFERENCES

Abrahamsen, H., Baillie, G., Ngai, J., Vang, T., Nika, K., Ruppelt, A., et al. (2004). TCR- and CD28-mediated recruitment of phosphodiesterase 4 to lipid rafts potentiates TCR signaling. *J. Immunol.* 173, 4847–4858. doi: 10.4049/jimmunol.173.8.4847

Ahmad, F., Murata, T., Shimizu, K., Degerman, E., Maurice, D., and Manganiello, V. (2015). Cyclic nucleotide phosphodiesterases: important signaling modulators and therapeutic targets. *Oral Dis.* 21, e25–e50.

Akama, T., Baker, S. J., Zhang, Y. K., Hernandez, V., Zhou, H., Sanders, V., et al. (2009). Discovery and structure-activity study of a novel benzoxaborole anti-inflammatory agent (AN2728) for the potential topical treatment of psoriasis and atopic dermatitis. *Bioorg. Med. Chem. Lett.* 19, 2129–2132. doi: 10.1016/j.bmcl.2009.03.007

Amarandi, R. M., Hjorto, G. M., Rosenkilde, M. M., and Karlshoj, S. (2016). Probing biased signaling in chemokine receptors. *Methods Enzymol.* 570, 155–186. doi: 10.1016/bs.mie.2015.09.001

Arp, J., Kirchhof, M. G., Baroja, M. L., Nazarian, S. H., Chau, T. A., Strathdee, C. A., et al. (2003). Regulation of T-cell activation by phosphodiesterase 4B2 requires its dynamic redistribution during immunological synapse formation. *Mol. Cell. Biol.* 23, 8042–8057. doi: 10.1128/mcb.23.22.8042-8057.2003

Ashikaga, T., Strada, S. J., and Thompson, W. J. (1997). Altered expression of cyclic nucleotide phosphodiesterase isozymes during culture of aortic endothelial cells. *Biochem. Pharmacol.* 54, 1071–1079. doi: 10.1016/s0006-2952(97)00287-6

Asirvatham, A. L., Galligan, S. G., Schillace, R. V., Davey, M. P., Vasta, V., Beavo, J. A., et al. (2004). A-kinase anchoring proteins interact with phosphodiesterases in T lymphocyte cell lines. *J. Immunol.* 173, 4806–4814. doi: 10.4049/jimmunol.173.8.4806

Baillie, G. S. (2009). Compartmentalized signalling: spatial regulation of cAMP by the action of compartmentalized phosphodiesterases. *FEBS J.* 276, 1790–1799. doi: 10.1111/j.1742-4658.2009.06926.x

Baillie, G. S., and Houslay, M. D. (2005). Arrestin times for compartmentalised cAMP signalling and phosphodiesterase-4 enzymes. *Curr. Opin. Cell Biol.* 17, 129–134. doi: 10.1016/j.ceb.2005.01.003

Baillie, G. S., Tejeda, G. S., and Kelly, M. P. (2019). Therapeutic targeting of 3',5'-cyclic nucleotide phosphodiesterases: inhibition and beyond. *Nat. Rev. Drug Discov.* 18, 770–796. doi: 10.1038/s41573-019-0033-4

Barnette, M. S., Christensen, S. B., Essayan, D. M., Grous, M., Prabhakar, U., Rush, J. A., et al. (1998). SB 207499 (Ariflo), a potent and selective second-generation phosphodiesterase 4 inhibitor: in vitro anti-inflammatory actions. *J. Pharmacol. Exp. Ther.* 284, 420–426.

Basole, C. P., Nguyen, R. K., Lamothe, K., Vang, A., Clark, R., Baillie, G. S., et al. (2017). PDE8 controls CD4(+) T cell motility through the PDE8A-Raf-1 kinase signaling complex. *Cell Signal.* 40, 62–72. doi: 10.1016/j.cellsig.2017.08.007

Beavo, J., Houslay, M., and Francis, S. (2007). "Cyclic nucleotide phosphodiesterase superfamily," in *Cyclic Nucleotide Phosphodiesterases in Health and Disease*, eds J. A. Beavo, S. H. Francis, and M. D. Houslay (New York, NY: CRC Press), 3–18. doi: 10.1201/9781420020847-1

Bender, A. T., and Beavo, J. A. (2006). Cyclic nucleotide phosphodiesterases: molecular regulation to clinical use. *Pharmacol. Rev.* 58, 488–520. doi: 10.1124/pr.58.3.5

Ben-Sasson, S. Z., Hu-Li, J., Quiel, J., Cauchetaux, S., Ratner, M., Shapira, I., et al. (2009). IL-1 acts directly on CD4 T cells to enhance their antigen-driven expansion and differentiation. *Proc. Natl. Acad. Sci. U.S.A.* 106, 7119–7124. doi: 10.1073/pnas.0902745106

Ben-Sasson, S. Z., Wang, K., Cohen, J., and Paul, W. E. (2013). IL-1beta strikingly enhances antigen-driven CD4 and CD8 T-cell responses. *Cold Spring Harb. Symp. Quant. Biol.* 78, 117–124. doi: 10.1101/sqb.2013.78.021246

Bielekova, B., Lincoln, A., Mcfarland, H., and Martin, R. (2000). Therapeutic potential of phosphodiesterase-4 and -3 inhibitors in Th1-mediated autoimmune diseases. *J. Immunol.* 164, 1117–1124. doi: 10.4049/jimmunol.164.2.1117

Bischoff, E. (2004). Potency, selectivity, and consequences of nonselectivity of PDE inhibition. *Int. J. Impot. Res.* 16(Suppl. 1), S11–S14.

Biton, A., Ansorge, S., Bank, U., Tager, M., Reinhold, D., and Brocke, S. (2011). Divergent actions by inhibitors of DP IV and APN family enzymes on CD4+ Teff cell motility and functions. *Immunobiology* 216, 1295–1301. doi: 10.1016/j.imbio.2011.07.001

Bjorgo, E., Moltu, K., and Tasken, K. (2011). Phosphodiesterases as targets for modulating T-cell responses. *Handb. Exp. Pharmacol.* 204, 345–363. doi: 10.1007/978-3-642-17969-3_15

Bjorgo, E., Solheim, S. A., Abrahamsen, H., Baillie, G. S., Brown, K. M., Berge, T., et al. (2010). Cross talk between phosphatidylinositol 3-kinase and cyclic AMP (cAMP)-protein kinase a signaling pathways at the level of a protein kinase B/beta-arrestin/cAMP phosphodiesterase 4 complex. *Mol. Cell. Biol.* 30, 1660–1672. doi: 10.1128/mcb.00696-09

Bjorgo, E., and Tasken, K. (2006). Role of cAMP phosphodiesterase 4 in regulation of T-cell function. *Crit. Rev. Immunol.* 26, 443–451. doi: 10.1615/critrevimmunol.v26.i5.40

Blair, C. M., and Baillie, G. S. (2019). Reshaping cAMP nanodomains through targeted disruption of compartmentalised phosphodiesterase signalosomes. *Biochem. Soc. Trans.* 47, 1405–1414. doi: 10.1042/bst20190252

Blair, C. M., Walsh, N. M., Littman, B. H., Marcoux, F. W., and Baillie, G. S. (2019). Targeting B-Raf inhibitor resistant melanoma with novel cell penetrating peptide disrupters of PDE8A - C-Raf. *BMC Cancer* 19:266.

Blanco, F. C., Soria, M. A., Klepp, L. I., and Bigi, F. (2017). ERAP1 and PDE8A are downregulated in cattle protected against bovine tuberculosis. *J. Mol. Microbiol. Biotechnol.* 27, 237–245. doi: 10.1159/000479183

Blokland, A., Heckman, P., Vanmierlo, T., Schreiber, R., Paes, D., and Prickaerts, J. (2019). Phosphodiesterase type 4 inhibition in CNS diseases. *Trends Pharmacol. Sci.* 40, 971–985. doi: 10.1016/j.tips.2019.10.006

Bloom, T. J., and Beavo, J. A. (1996). Identification and tissue-specific expression of PDE7 phosphodiesterase splice variants. *Proc. Natl. Acad. Sci. U.S.A.* 93, 14188–14192. doi: 10.1073/pnas.93.24.14188

Booiman, T., Cobos Jimenez, V., Van Dort, K. A., Van 'T Wout, A. B., and Kootstra, N. A. (2014). Phosphodiesterase 8a supports HIV-1 replication in macrophages at the level of reverse transcription. *PLoS One* 9:e109673. doi: 10.1371/journal.pone.0109673

Bopp, T., Becker, C., Klein, M., Klein-Hessling, S., Palmetshofer, A., Serfling, E., et al. (2007). Cyclic adenosine monophosphate is a key component of regulatory T cell-mediated suppression. *J. Exp. Med.* 204, 1303–1310. doi: 10.1084/jem.20062129

Bopp, T., Dehzad, N., Reuter, S., Klein, M., Ullrich, N., Stassen, M., et al. (2009). Inhibition of cAMP degradation improves regulatory T cell-mediated suppression. *J. Immunol.* 182, 4017–4024. doi: 10.4049/jimmunol.0803310

Bourne, H. R., Lichtenstein, L. M., Melmon, K. L., Henney, C. S., Weinstein, Y., and Shearer, G. M. (1974). Modulation of inflammation and immunity by cyclic AMP. *Science* 184, 19–28. doi: 10.1126/science.184.4132.19

Brocke, S., Piercy, C., Steinman, L., Weissman, I. L., and Veromaa, T. (1999). Antibodies to CD44 and integrin alpha4, but not L-selectin, prevent central nervous system inflammation and experimental encephalomyelitis by blocking secondary leukocyte recruitment. *Proc. Natl. Acad. Sci. U.S.A.* 96, 6896–6901. doi: 10.1073/pnas.96.12.6896

Brocke, S., Quigley, L., Mcfarland, H. F., and Steinman, L. (1996). Isolation and characterization of autoreactive T cells in experimental autoimmune encephalomyelitis of the mouse. *Methods* 9, 458–462. doi: 10.1006/meth.1996.0053

Brown, K. M., Day, J. P., Huston, E., Zimmermann, B., Hampel, K., Christian, F., et al. (2013). Phosphodiesterase-8A binds to and regulates Raf-1 kinase. *Proc. Natl. Acad. Sci. U.S.A.* 110, E1533–E1542.

Brown, W. S., Khalili, J. S., Rodriguez-Cruz, T. G., Lizee, G., and Mcintyre, B. W. (2014). B-Raf regulation of integrin alpha4beta1-mediated resistance to shear stress through changes in cell spreading and cytoskeletal association in T cells. *J. Biol. Chem.* 289, 23141–23153. doi: 10.1074/jbc.m114.562918

Burdyga, A., Conant, A., Haynes, L., Zhang, J., Jalink, K., Sutton, R., et al. (2013). cAMP inhibits migration, ruffling and paxillin accumulation in focal adhesions of pancreatic ductal adenocarcinoma cells: effects of PKA and EPAC. *Biochim. Biophys. Acta* 1833, 2664–2672. doi: 10.1016/j.bbamcr.2013.06.011

Callender, V. D., Alexis, A. F., Stein Gold, L. F., Lebwohl, M. G., Paller, A. S., Desai, S. R., et al. (2019). Efficacy and safety of crisaborole ointment, 2%, for the treatment of mild-to-moderate atopic dermatitis across racial and ethnic groups. *Am. J. Clin. Dermatol.* 20, 711–723. doi: 10.1007/s40257-019-00450-w

Chen, C., Wickenheisser, J., Ewens, K. G., Ankener, W., Legro, R. S., Dunaif, A., et al. (2009). PDE8A genetic variation, polycystic ovary syndrome and androgen levels in women. *Mol. Hum. Reprod.* 15, 459–469. doi: 10.1093/molehr/gap035

Chilcoat, C. D., Sharief, Y., and Jones, S. L. (2008). Tonic protein kinase A activity maintains inactive beta2 integrins in unstimulated neutrophils by reducing myosin light-chain phosphorylation: role of myosin light-chain kinase and Rho kinase. *J. Leukoc Biol.* 83, 964–971. doi: 10.1189/jlb.0405192

Chimienti, F., Cavarec, L., Vincent, L., Salvetat, N., Arango, V., Underwood, M. D., et al. (2019). Brain region-specific alterations of RNA editing in PDE8A mRNA in suicide decedents. *Transl. Psychiatry* 9:91.

Cinamon, G., Grabovsky, V., Winter, E., Franitza, S., Feigelson, S., Shamri, R., et al. (2001). Novel chemokine functions in lymphocyte migration through vascular endothelium under shear flow. *J. Leukoc Biol.* 69, 860–866.

Claveau, D., Chen, S. L., O'keefe, S., Zaller, D. M., Styhler, A., Liu, S., et al. (2004). Preferential inhibition of T helper 1, but not T helper 2, cytokines in vitro by L-826,141 [4-[2-(3,4-Bisdifluromethoxyphenyl)-2-[4-(1,1,1,3,3,3-hexafluoro-2-hydroxy propan-2-yl)-phenyl]-ethyl]3-methylpyridine-1-oxide], a potent and selective phosphodiesterase 4 inhibitor. *J. Pharmacol. Exp. Ther.* 310, 752–760. doi: 10.1124/jpet.103.064691

Conti, M., Nemoz, G., Sette, C., and Vicini, E. (1995). Recent progress in understanding the hormonal regulation of phosphodiesterases. *Endocr. Rev.* 16, 370–389. doi: 10.1210/edrv-16-3-370

Conti, M., and Swinnen, J. V. (1990). "Structure and function of the rolipram-sensitive low-Km cyclic AMP phosphodiesterases: a family of highly related enzymes," in *Cyclic Nucleotide Phosphodiesterases: Structure, Regulation and Drug Action*, eds J. Beavo and M. D. Houslay (West Sussex: John Wiley & Sons Ltd.), 243–265.

De Souza, A., Strober, B. E., Merola, J. F., Oliver, S., and Franks, A. G. Jr. (2012). Apremilast for discoid lupus erythematosus: results of a phase 2, open-label, single-arm, pilot study. *J. Drugs Dermatol.* 11, 1224–1226.

Demirbas, D., Wyman, A. R., Shimizu-Albergine, M., Cakici, O., Beavo, J. A., and Hoffman, C. S. (2013). A yeast-based chemical screen identifies a PDE inhibitor that elevates steroidogenesis in mouse Leydig cells via PDE8 and PDE4 inhibition. *PLoS One* 8:e71279. doi: 10.1371/journal.pone.0071279

DeNinno, M. P. (2012). Future directions in phosphodiesterase drug discovery. *Bioorg. Med. Chem. Lett.* 22, 6794–6800. doi: 10.1016/j.bmcl.2012.09.028

DeNinno, M. P., Wright, S. W., Visser, M. S., Etienne, J. B., Moore, D. E., Olson, T. V., et al. (2011). 1,5-Substituted nipecotic amides: selective PDE8 inhibitors displaying diastereomer-dependent microsomal stability. *Bioorg. Med. Chem. Lett.* 21, 3095–3098. doi: 10.1016/j.bmcl.2011.03.022

Dong, C., Virtucio, C., Zemska, O., Baltazar, G., Zhou, Y., Baia, D., et al. (2016). Treatment of skin inflammation with benzoxaborole phosphodiesterase inhibitors: selectivity, cellular activity, and effect on cytokines associated with skin inflammation and skin architecture changes. *J. Pharmacol. Exp. Ther.* 358, 413–422. doi: 10.1124/jpet.116.232819

Dong, H., Claffey, K. P., Brocke, S., and Epstein, P. M. (2015). Inhibition of breast cancer cell migration by activation of cAMP signaling. *Breast Cancer Res. Treat.* 152, 17–28. doi: 10.1007/s10549-015-3445-9

Dong, H., Osmanova, V., Epstein, P. M., and Brocke, S. (2006). Phosphodiesterase 8 (PDE8) regulates chemotaxis of activated lymphocytes. *Biochem. Biophys. Res. Commun.* 345, 713–719. doi: 10.1016/j.bbrc.2006.04.143

Dong, H., Zitt, C., Auriga, C., Hatzelmann, A., and Epstein, P. M. (2010). Inhibition of PDE3, PDE4 and PDE7 potentiates glucocorticoid-induced apoptosis and overcomes glucocorticoid resistance in CEM T leukemic cells. *Biochem. Pharmacol.* 79, 321–329. doi: 10.1016/j.bcp.2009.09.001

Dua, P., and Gude, R. P. (2008). Pentoxifylline impedes migration in B16F10 melanoma by modulating Rho GTPase activity and actin organisation. *Eur. J. Cancer* 44, 1587–1595. doi: 10.1016/j.ejca.2008.04.009

Ehrenreiter, K., Piazzolla, D., Velamoor, V., Sobczak, I., Small, J. V., Takeda, J., et al. (2005). Raf-1 regulates Rho signaling and cell migration. *J. Cell. Biol.* 168, 955–964. doi: 10.1083/jcb.200409162

Ekholm, D., Hemmer, B., Gao, G., Vergelli, M., Martin, R., and Manganiello, V. (1997). Differential expression of cyclic nucleotide phosphodiesterase 3 and 4 activities in human T cell clones specific for myelin basic protein. *J. Immunol.* 159, 1520–1529.

Epstein, P. M., and Hachisu, R. (1984). Cyclic nucleotide phosphodiesterase in normal and leukemic human lymphocytes and lymphoblasts. *Adv. Cyclic Nucleotide Protein Phosphorylation Res.* 16, 303–324.

Epstein, P. M., Mills, J. S., Hersh, E. M., Strada, S. J., and Thompson, W. J. (1980). Activation of cyclic nucleotide phosphodiesterase from isolated human peripheral blood lymphocytes by mitogenic agents. *Cancer Res.* 40, 379–386.

Epstein, P. M., Moraski, S. Jr., and Hachisu, R. (1987). Identification and characterization of a Ca2+-calmodulin-sensitive cyclic nucleotide phosphodiesterase in a human lymphoblastoid cell line. *Biochem. J.* 243, 533–539. doi: 10.1042/bj2430533

Epstein, P. M., Strada, S. J., Sarada, K., and Thompson, W. J. (1982). Catalytic and kinetic properties of purified high-affinity cyclic AMP phosphodiesterase from dog kidney. *Arch. Biochem. Biophys.* 218, 119–133. doi: 10.1016/0003-9861(82)90327-7

Erdogan, S., and Houslay, M. D. (1997). Challenge of human Jurkat T-cells with the adenylate cyclase activator forskolin elicits major changes in cAMP

phosphodiesterase (PDE) expression by up-regulating PDE3 and inducing PDE4D1 and PDE4D2 splice variants as well as down-regulating a novel PDE4A splice variant. *Biochem. J.* 321(Pt 1), 165–175. doi: 10.1042/bj3210165

Essayan, D. M., Huang, S. K., Kagey-Sobotka, A., and Lichtenstein, L. M. (1997). Differential efficacy of lymphocyte- and monocyte-selective pretreatment with a type 4 phosphodiesterase inhibitor on antigen-driven proliferation and cytokine gene expression. *J. Allergy Clin. Immunol.* 99, 28–37. doi: 10.1016/s0091-6749(97)81041-x

Fawcett, L., Baxendale, R., Stacey, P., Mcgrouther, C., Harrow, I., Soderling, S., et al. (2000). Molecular cloning and characterization of a distinct human phosphodiesterase gene family: PDE11A. *Proc. Natl. Acad. Sci. U.S.A.* 97, 3702–3707. doi: 10.1073/pnas.97.7.3702

Fisher, D. A., Smith, J. F., Pillar, J. S., St Denis, S. H., and Cheng, J. B. (1998a). Isolation and characterization of PDE8A, a novel human cAMP-specific phosphodiesterase. *Biochem. Biophys. Res. Commun.* 246, 570–577. doi: 10.1006/bbrc.1998.8684

Fisher, D. A., Smith, J. F., Pillar, J. S., St Denis, S. H., and Cheng, J. B. (1998b). Isolation and characterization of PDE9A, a novel human cGMP-specific phosphodiesterase. *J. Biol. Chem.* 273, 15559–15564. doi: 10.1074/jbc.273.25.15559

Fleming, Y. M., Frame, M. C., and Houslay, M. D. (2004). PDE4-regulated cAMP degradation controls the assembly of integrin-dependent actin adhesion structures and REF52 cell migration. *J. Cell Sci.* 117, 2377–2388. doi: 10.1242/jcs.01096

Francis, S. H., Houslay, M. D., and Conti, M. (2011). Phosphodiesterase inhibitors: factors that influence potency, selectivity, and action. *Handb. Exp. Pharmacol.* 204, 47–84. doi: 10.1007/978-3-642-17969-3_2

Francis, S. H., Thomas, M. K., and Corbin, J. D. (1990). "Cyclic GMP-binding cyclic GMP-specific phosphodiesterase from lung," in *Cyclic Nucleotide Phosphodiesterases: Structure, Regulation and Drug Action*, eds J. Beavo and M. D. Houslay (West Sussex: John Wiley & Sons Ltd.), 117–139.

Fujishige, K., Kotera, J., Michibata, H., Yuasa, K., Takebayashi, S., Okumura, K., et al. (1999a). Cloning and characterization of a novel human phosphodiesterase that hydrolyzes both cAMP and cGMP (PDE10A). *J. Biol. Chem.* 274, 18438–18445. doi: 10.1074/jbc.274.26.18438

Fujishige, K., Kotera, J., and Omori, K. (1999b). Striatum- and testis-specific phosphodiesterase PDE10A isolation and characterization of a rat PDE10A. *Eur. J. Biochem.* 266, 1118–1127. doi: 10.1046/j.1432-1327.1999.00963.x

Gamanuma, M., Yuasa, K., Sasaki, T., Sakurai, N., Kotera, J., and Omori, K. (2003). Comparison of enzymatic characterization and gene organization of cyclic nucleotide phosphodiesterase 8 family in humans. *Cell Signal.* 15, 565–574. doi: 10.1016/s0898-6568(02)00146-8

Gantner, F., Gotz, C., Gekeler, V., Schudt, C., Wendel, A., and Hatzelmann, A. (1998). Phosphodiesterase profile of human B lymphocytes from normal and atopic donors and the effects of PDE inhibition on B cell proliferation. *Br. J. Pharmacol.* 123, 1031–1038. doi: 10.1038/sj.bjp.0701688

Gantner, F., Kusters, S., Wendel, A., Hatzelmann, A., Schudt, C., and Tiegs, G. (1997a). Protection from T cell-mediated murine liver failure by phosphodiesterase inhibitors. *J. Pharmacol. Exp. Ther.* 280, 53–60.

Gantner, F., Tenor, H., Gekeler, V., Schudt, C., Wendel, A., and Hatzelmann, A. (1997b). Phosphodiesterase profiles of highly purified human peripheral blood leukocyte populations from normal and atopic individuals: a comparative study. *J. Allergy Clin. Immunol.* 100, 527–535. doi: 10.1016/s0091-6749(97)70146-5

Gardner, C., Robas, N., Cawkill, D., and Fidock, M. (2000). Cloning and characterization of the human and mouse PDE7B, a novel cAMP-specific cyclic nucleotide phosphodiesterase. *Biochem. Biophys. Res. Commun.* 272, 186–192. doi: 10.1006/bbrc.2000.2743

Gavin, M. A., Rasmussen, J. P., Fontenot, J. D., Vasta, V., Manganiello, V. C., Beavo, J. A., et al. (2007). Foxp3-dependent programme of regulatory T-cell differentiation. *Nature* 445, 771–775. doi: 10.1038/nature05543

Giembycz, M. A. (2000). Phosphodiesterase 4 inhibitors and the treatment of asthma: where are we now and where do we go from here? *Drugs* 59, 193–212. doi: 10.2165/00003495-200059020-00004

Giembycz, M. A., Corrigan, C. J., Seybold, J., Newton, R., and Barnes, P. J. (1996). Identification of cyclic AMP phosphodiesterases 3, 4 and 7 in human CD4+ and CD8+ T-lymphocytes: role in regulating proliferation and the biosynthesis of interleukin-2. *Br. J. Pharmacol.* 118, 1945–1958. doi: 10.1111/j.1476-5381.1996.tb15629.x

Gillespie, P. G. (1990). "Phosphodiesterases in visual transduction by rods and cones," in *Cyclic Nucleotide Phosphodiesterases: Structure, Regulation and Drug Action*, eds J. Beavo and M. D. Houslay (West Sussex: John Wiley & Sons Ltd.), 163–183.

Gillespie, P. G., and Beavo, J. A. (1989). Inhibition and stimulation of photoreceptor phosphodiesterases by dipyridamole and M&B 22,948. *Mol. Pharmacol.* 36, 773–781.

Glavas, N. A., Ostenson, C., Schaefer, J. B., Vasta, V., and Beavo, J. A. (2001). T cell activation up-regulates cyclic nucleotide phosphodiesterases 8A1 and 7A3. *Proc. Natl. Acad. Sci. U.S.A.* 98, 6319–6324. doi: 10.1073/pnas.101131098

Goldfinger, L. E., Han, J., Kiosses, W. B., Howe, A. K., and Ginsberg, M. H. (2003). Spatial restriction of alpha4 integrin phosphorylation regulates lamellipodial stability and alpha4beta1-dependent cell migration. *J. Cell Biol.* 162, 731–741. doi: 10.1083/jcb.200304031

Gonzalez-Garcia, C., Bravo, B., Ballester, A., Gomez-Perez, R., Eguiluz, C., Redondo, M., et al. (2013). Comparative assessment of PDE 4 and 7 inhibitors as therapeutic agents in experimental autoimmune encephalomyelitis. *Br. J. Pharmacol.* 170, 602–613. doi: 10.1111/bph.12308

Goraya, T. A., and Cooper, D. M. (2005). Ca2+-calmodulin-dependent phosphodiesterase (PDE1): current perspectives. *Cell Signal.* 17, 789–797. doi: 10.1016/j.cellsig.2004.12.017

Goto, M., Murakawa, M., Kadoshima-Yamaoka, K., Tanaka, Y., Inoue, H., Murafuji, H., et al. (2009). Phosphodiesterase 7A inhibitor ASB16165 suppresses proliferation and cytokine production of NKT cells. *Cell Immunol.* 258, 147–151. doi: 10.1016/j.cellimm.2009.04.005

Guo, J., Watson, A., Kempson, J., Carlsen, M., Barbosa, J., Stebbins, K., et al. (2009). Identification of potent pyrimidine inhibitors of phosphodiesterase 7 (PDE7) and their ability to inhibit T cell proliferation. *Bioorg. Med. Chem. Lett.* 19, 1935–1938. doi: 10.1016/j.bmcl.2009.02.060

Han, P., Zhu, X., and Michaeli, T. (1997). Alternative splicing of the high affinity cAMP-specific phosphodiesterase (PDE7A) mRNA in human skeletal muscle and heart. *J. Biol. Chem.* 272, 16152–16157. doi: 10.1074/jbc.272.26.16152

Hatzelmann, A., Morcillo, E. J., Lungarella, G., Adnot, S., Sanjar, S., Beume, R., et al. (2010). The preclinical pharmacology of roflumilast–a selective, oral phosphodiesterase 4 inhibitor in development for chronic obstructive pulmonary disease. *Pulm. Pharmacol. Ther.* 23, 235–256. doi: 10.1016/j.pupt.2010.03.011

Hatzelmann, A., and Schudt, C. (2001). Anti-inflammatory and immunomodulatory potential of the novel PDE4 inhibitor roflumilast in vitro. *J. Pharmacol. Exp. Ther.* 297, 267–279.

Hayashi, M., Matsushima, K., Ohashi, H., Tsunoda, H., Murase, S., Kawarada, Y., et al. (1998). Molecular cloning and characterization of human PDE8B, a novel thyroid-specific isozyme of 3′,5′-cyclic nucleotide phosphodiesterase. *Biochem. Biophys. Res. Commun.* 250, 751–756. doi: 10.1006/bbrc.1998.9379

Hayashi, M., Shimada, Y., Nishimura, Y., Hama, T., and Tanaka, T. (2002). Genomic organization, chromosomal localization, and alternative splicing of the human phosphodiesterase 8B gene. *Biochem. Biophys. Res. Commun.* 297, 1253–1258. doi: 10.1016/s0006-291x(02)02371-9

Healy, L. M., and Antel, J. P. (2016). Sphingosine-1-phosphate receptors in the central nervous and immune systems. *Curr. Drug Targets* 17, 1841–1850. doi: 10.2174/1389450116666151001112710

Hetman, J. M., Robas, N., Baxendale, R., Fidock, M., Phillips, S. C., Soderling, S. H., et al. (2000a). Cloning and characterization of two splice variants of human phosphodiesterase 11A. *Proc. Natl. Acad. Sci. U.S.A.* 97, 12891–12895. doi: 10.1073/pnas.200355397

Hetman, J. M., Soderling, S. H., Glavas, N. A., and Beavo, J. A. (2000b). Cloning and characterization of PDE7B, a cAMP-specific phosphodiesterase. *Proc. Natl. Acad. Sci. U.S.A.* 97, 472–476. doi: 10.1073/pnas.97.1.472

Houslay, M. D., Sullivan, M., and Bolger, G. B. (1998). The multienzyme PDE4 cyclic adenosine monophosphate-specific phosphodiesterase family: intracellular targeting, regulation, and selective inhibition by compounds exerting anti-inflammatory and antidepressant actions. *Adv. Pharmacol.* 44, 225–342. doi: 10.1016/s1054-3589(08)60128-3

Huang, Y., Wu, X. N., Zhou, Q., Wu, Y., Zheng, D., Li, Z., et al. (2020). Rational design of 2-chloroadenine derivatives as highly selective phosphodiesterase

8A inhibitors. *J. Med. Chem.* 63, 15852–15863. doi: 10.1021/acs.jmedchem.0c01573

Jankowska, A., Swierczek, A., Chlon-Rzepa, G., Pawlowski, M., and Wyska, E. (2017). PDE7-selective and dual inhibitors: advances in chemical and biological research. *Curr. Med. Chem.* 24, 673–700. doi: 10.2174/0929867324666170116125159

Jarnagin, K., Chanda, S., Coronado, D., Ciaravino, V., Zane, L. T., Guttman-Yassky, E., et al. (2016). Crisaborole topical ointment, 2%: a nonsteroidal, topical, anti-inflammatory phosphodiesterase 4 inhibitor in clinical development for the treatment of atopic dermatitis. *J. Drugs Dermatol.* 15, 390–396.

Jiang, X., Paskind, M., Weltzien, R., and Epstein, P. M. (1998). Expression and regulation of mRNA for distinct isoforms of cAMP-specific PDE-4 in mitogen-stimulated and leukemic human lymphocytes. *Cell Biochem. Biophys.* 28, 135–160. doi: 10.1007/bf02737809

Jimenez, J. L., Iniguez, M. A., Munoz-Fernandez, M. A., and Fresno, M. (2004). Effect of phosphodiesterase 4 inhibitors on NFAT-dependent cyclooxygenase-2 expression in human T lymphocytes. *Cell Signal.* 16, 1363–1373. doi: 10.1016/j.cellsig.2004.04.002

Jin, S. L., Bushnik, T., Lan, L., and Conti, M. (1998). Subcellular localization of rolipram-sensitive, cAMP-specific phosphodiesterases. Differential targeting and activation of the splicing variants derived from the PDE4D gene. *J. Biol. Chem.* 273, 19672–19678. doi: 10.1074/jbc.273.31.19672

Jin, S. L., Goya, S., Nakae, S., Wang, D., Bruss, M., Hou, C., et al. (2010). Phosphodiesterase 4B is essential for T(H)2-cell function and development of airway hyperresponsiveness in allergic asthma. *J. Allergy Clin. Immunol.* 126, 1252–1259.e1212.

Johnstone, T. B., Smith, K. H., Koziol-White, C. J., Li, F., Kazarian, A. G., Corpuz, M. L., et al. (2017). PDE8 is expressed in human airway smooth muscle and selectively regulates cAMP signaling by beta2AR-AC6. *Am. J. Respir Cell Mol. Biol.* 58, 530–541. doi: 10.1165/rcmb.2017-0294oc

Juliano, R. L., Reddig, P., Alahari, S., Edin, M., Howe, A., and Aplin, A. (2004). Integrin regulation of cell signalling and motility. *Biochem. Soc. Trans.* 32, 443–446. doi: 10.1042/bst0320443

Kadoshima-Yamaoka, K., Murakawa, M., Goto, M., Tanaka, Y., Inoue, H., Murafuji, H., et al. (2009). Effect of phosphodiesterase 7 inhibitor ASB16165 on development and function of cytotoxic T lymphocyte. *Int. Immunopharmacol.* 9, 97–102. doi: 10.1016/j.intimp.2008.10.005

Kakkar, R., Raju, R. V., and Sharma, R. K. (1999). Calmodulin-dependent cyclic nucleotide phosphodiesterase (PDE1). *Cell Mol. Life Sci.* 55, 1164–1186. doi: 10.1007/s000180050364

Kambayashi, J., Liu, Y., Sun, B., Shakur, Y., Yoshitake, M., and Czerwiec, F. (2003). Cilostazol as a unique antithrombotic agent. *Curr. Pharm. Des.* 9, 2289–2302. doi: 10.2174/1381612033453910

Kanda, N., and Watanabe, S. (2001). Regulatory roles of adenylate cyclase and cyclic nucleotide phosphodiesterases 1 and 4 in interleukin-13 production by activated human T cells. *Biochem. Pharmacol.* 62, 495–507. doi: 10.1016/s0006-2952(01)00688-8

Kelly, M. P. (2018). Cyclic nucleotide signaling changes associated with normal aging and age-related diseases of the brain. *Cell Signal.* 42, 281–291. doi: 10.1016/j.cellsig.2017.11.004

Klein, R. M., Spofford, L. S., Abel, E. V., Ortiz, A., and Aplin, A. E. (2008). B-RAF regulation of Rnd3 participates in actin cytoskeletal and focal adhesion organization. *Mol. Biol. Cell* 19, 498–508. doi: 10.1091/mbc.e07-09-0895

Kobayashi, T., Gamanuma, M., Sasaki, T., Yamashita, Y., Yuasa, K., Kotera, J., et al. (2003). Molecular comparison of rat cyclic nucleotide phosphodiesterase 8 family: unique expression of PDE8B in rat brain. *Gene* 319, 21–31. doi: 10.1016/s0378-1119(03)00809-6

Komas, N., Movsesian, M., Kedov, S., Degerman, E., Belfrage, P., and Manganiello, V. (1996). "cGMP-inhibited phosphodiesterases (PDE3)," in *Phosphodiesterase Inhibitors*, eds C. Schudt, G. Dent, and K. F. Rabe (London: Academic Press), 89–110. doi: 10.1016/b978-012210720-7/50008-3

Kortum, R. L., Rouquette-Jazdanian, A. K., and Samelson, L. E. (2013). Ras and extracellular signal-regulated kinase signaling in thymocytes and T cells. *Trends Immunol.* 34, 259–268. doi: 10.1016/j.it.2013.02.004

Kotera, J., Fujishige, K., Akatsuka, H., Imai, Y., Yanaka, N., and Omori, K. (1998). Novel alternative splice variants of cGMP-binding cGMP-specific phosphodiesterase. *J. Biol. Chem.* 273, 26982–26990. doi: 10.1074/jbc.273.41.26982

Lee, J. W., Lee, J., and Moon, E. Y. (2014). HeLa human cervical cancer cell migration is inhibited by treatment with dibutyryl-cAMP. *Anticancer Res.* 34, 3447–3455.

Lee, R., Wolda, S., Moon, E., Esselstyn, J., Hertel, C., and Lerner, A. (2002). PDE7A is expressed in human B-lymphocytes and is up-regulated by elevation of intracellular cAMP. *Cell Signal.* 14, 277–284. doi: 10.1016/s0898-6568(01)00250-9

Lerner, A., and Epstein, P. M. (2006). Cyclic nucleotide phosphodiesterases as targets for treatment of haematological malignancies. *Biochem. J.* 393, 21–41. doi: 10.1042/bj20051368

Li, L., Yee, C., and Beavo, J. A. (1999). CD3- and CD28-dependent induction of PDE7 required for T cell activation. *Science* 283, 848–851. doi: 10.1126/science.283.5403.848

Lim, C. J., Han, J., Yousefi, N., Ma, Y., Amieux, P. S., Mcknight, G. S., et al. (2007). Alpha4 integrins are type I cAMP-dependent protein kinase-anchoring proteins. *Nat. Cell Biol.* 9, 415–421. doi: 10.1038/ncb1561

Lin, C. S., Lau, A., Tu, R., and Lue, T. F. (2000). Expression of three isoforms of cGMP-binding cGMP-specific phosphodiesterase (PDE5) in human penile cavernosum. *Biochem. Biophys. Res. Commun.* 268, 628–635. doi: 10.1006/bbrc.2000.2187

Loughney, K., Hill, T. R., Florio, V. A., Uher, L., Rosman, G. J., Wolda, S. L., et al. (1998). Isolation and characterization of cDNAs encoding PDE5A, a human cGMP-binding, cGMP-specific 3′,5′-cyclic nucleotide phosphodiesterase. *Gene* 216, 139–147. doi: 10.1016/s0378-1119(98)00303-5

Loughney, K., Martins, T. J., Harris, E. A., Sadhu, K., Hicks, J. B., Sonnenburg, W. K., et al. (1996). Isolation and characterization of cDNAs corresponding to two human calcium, calmodulin-regulated, 3′,5′-cyclic nucleotide phosphodiesterases. *J. Biol. Chem.* 271, 796–806. doi: 10.1074/jbc.271.2.796

Loughney, K., Snyder, P. B., Uher, L., Rosman, G. J., Ferguson, K., and Florio, V. A. (1999). Isolation and characterization of PDE10A, a novel human 3', 5'-cyclic nucleotide phosphodiesterase. *Gene* 234, 109–117. doi: 10.1016/s0378-1119(99)00171-7

Loughney, K., Taylor, J., and Florio, V. A. (2005). 3',5'-Cyclic nucleotide phosphodiesterase 11A: localization in human tissues. *Int. J. Impot. Res.* 17, 320–325.

Lyle, K. S., Raaijmakers, J. H., Bruinsma, W., Bos, J. L., and De Rooij, J. (2008). cAMP-induced Epac-Rap activation inhibits epithelial cell migration by modulating focal adhesion and leading edge dynamics. *Cell. Signal.* 20, 1104–1116.

Maganto-Garcia, E., Bu, D. X., Tarrio, M. L., Alcaide, P., Newton, G., Griffin, G. K., et al. (2011). Foxp3+-inducible regulatory T cells suppress endothelial activation and leukocyte recruitment. *J. Immunol.* 187, 3521–3529.

Man, H. W., Schafer, P., Wong, L. M., Patterson, R. T., Corral, L. G., Raymon, H., et al. (2009). Discovery of (S)-N-[2-[1-(3-ethoxy-4-methoxyphenyl)-2-methanesulfonylethyl]-1,3-dioxo-2,3-dihy dro-1H-isoindol-4-yl] acetamide (apremilast), a potent and orally active phosphodiesterase 4 and tumor necrosis factor-alpha inhibitor. *J. Med. Chem.* 52, 1522–1524.

Manganiello, V. C., Smith, C. J., Degerman, E., and Belfrage, P. (1990a). "Cyclic GMP-inhibited cyclic nucleotide phosphodiesterases," in *Cyclic Nucleotide Phosphodiesterases: Structure, Regulation and Drug Action*, eds J. Beavo and M. D. Houslay (West Sussex: John Wiley & Sons Ltd.), 87–115.

Manganiello, V. C., Tanaka, T., and Murashima, S. (1990b). "Cyclic GMP-stimulated cyclic nucleotide phosphodiesterases," in *Cyclic Nucleotide Phosphodiesterases: Structure, Regulation and Drug Action*, eds J. Beavo and M. D. Houslay (West Sussex: John Wiley & Sons Ltd.), 61–85.

Marais, R., Light, Y., Paterson, H. F., Mason, C. S., and Marshall, C. J. (1997). Differential regulation of Raf-1, A-Raf, and B-Raf by oncogenic ras and tyrosine kinases. *J. Biol. Chem.* 272, 4378–4383.

Martin-Alvarez, R., Paul-Fernandez, N., Palomo, V., Gil, C., Martinez, A., and Mengod, G. (2017). A preliminary investigation of phoshodiesterase 7 inhibitor VP3.15 as therapeutic agent for the treatment of experimental autoimmune encephalomyelitis mice. *J. Chem. Neuroanat.* 80, 27–36.

Martins, T. J., Mumby, M. C., and Beavo, J. A. (1982). Purification and characterization of a cyclic GMP-stimulated cyclic nucleotide phosphodiesterase from bovine tissues. *J. Biol. Chem.* 257, 1973–1979.

Maurice, D. H. (2013). PDE8A runs interference to limit PKA inhibition of Raf-1. *Proc. Natl. Acad. Sci. U.S.A.* 110, 6248–6249.

Maurice, D. H., Ke, H., Ahmad, F., Wang, Y., Chung, J., and Manganiello, V. C. (2014). Advances in targeting cyclic nucleotide phosphodiesterases. *Nat. Rev. Drug Discov.* 13, 290–314.

Mery, P. F., Pavoine, C., Pecker, F., and Fischmeister, R. (1995). Erythro-9-(2-hydroxy-3-nonyl)adenine inhibits cyclic GMP-stimulated phosphodiesterase in isolated cardiac myocytes. *Mol. Pharmacol.* 48, 121–130.

Michaeli, T., Bloom, T. J., Martins, T., Loughney, K., Ferguson, K., Riggs, M., et al. (1993). Isolation and characterization of a previously undetected human cAMP phosphodiesterase by complementation of cAMP phosphodiesterase-deficient Saccharomyces cerevisiae. *J. Biol. Chem.* 268, 12925–12932.

Michie, A. M., Lobban, M., Muller, T., Harnett, M. M., and Houslay, M. D. (1996). Rapid regulation of PDE-2 and PDE-4 cyclic AMP phosphodiesterase activity following ligation of the T cell antigen receptor on thymocytes: analysis using the selective inhibitors erythro-9-(2-hydroxy-3-nonyl)-adenine (EHNA) and rolipram. *Cell Signal.* 8, 97–110.

Milara, J., Armengot, M., Banuls, P., Tenor, H., Beume, R., Artigues, E., et al. (2012). Roflumilast N-oxide, a PDE4 inhibitor, improves cilia motility and ciliated human bronchial epithelial cells compromised by cigarette smoke in vitro. *Br. J. Pharmacol.* 166, 2243–2262.

Montesano, R., Pepper, M. S., Mohle-Steinlein, U., Risau, W., Wagner, E. F., and Orci, L. (1990). Increased proteolytic activity is responsible for the aberrant morphogenetic behavior of endothelial cells expressing the middle T oncogene. *Cell* 62, 435–445.

Moon, E., Lee, R., Near, R., Weintraub, L., Wolda, S., and Lerner, A. (2002). Inhibition of PDE3B augments PDE4 inhibitor-induced apoptosis in a subset of patients with chronic lymphocytic leukemia. *Clin. Cancer Res.* 8, 589–595.

Mosenden, R., and Tasken, K. (2011). Cyclic AMP-mediated immune regulation–overview of mechanisms of action in T cells. *Cell Signal.* 23, 1009–1016.

Murata, K., Sudo, T., Kameyama, M., Fukuoka, H., Muka, M., Doki, Y., et al. (2000). Cyclic AMP specific phosphodiesterase activity and colon cancer cell motility. *Clin. Exp. Metastasis* 18, 599–604.

Nakata, A., Ogawa, K., Sasaki, T., Koyama, N., Wada, K., Kotera, J., et al. (2002). Potential role of phosphodiesterase 7 in human T cell function: comparative effects of two phosphodiesterase inhibitors. *Clin. Exp. Immunol.* 128, 460–466.

Netherton, S. J., and Maurice, D. H. (2005). Vascular endothelial cell cyclic nucleotide phosphodiesterases and regulated cell migration: implications in angiogenesis. *Mol. Pharmacol.* 67, 263–272.

Nome, T., Thomassen, G. O., Bruun, J., Ahlquist, T., Bakken, A. C., Hoff, A. M., et al. (2013). Common fusion transcripts identified in colorectal cancer cell lines by high-throughput RNA sequencing. *Transl. Oncol.* 6, 546–553. doi: 10.1593/tlo.13457

Norambuena, A., Metz, C., Vicuna, L., Silva, A., Pardo, E., Oyanadel, C., et al. (2009). Galectin-8 induces apoptosis in Jurkat T cells by phosphatidic acid-mediated ERK1/2 activation supported by protein kinase A down-regulation. *J. Biol. Chem.* 284, 12670–12679. doi: 10.1074/jbc.m808949200

Nueda, A., Garcia-Roger, N., Domenech, T., Godessart, N., Cardenas, A., Santamaria-Babi, L. F., et al. (2006). Phosphodiesterase 7A1 is expressed in human CD4+ naive T cells at higher levels than in CD4+ memory cells and is not required during their CD3/CD28-dependent activation. *Cell Immunol.* 242, 31–38. doi: 10.1016/j.cellimm.2006.09.001

Orlowski, R. J., O'rourke, K. S., Olorenshaw, I., Hawkins, G. A., Maas, S., and Laxminarayana, D. (2008). Altered editing in cyclic nucleotide phosphodiesterase 8A1 gene transcripts of systemic lupus erythematosus T lymphocytes. *Immunology* 125, 408–419. doi: 10.1111/j.1365-2567.2008.02850.x

Ou, Y., Zheng, X., Gao, Y., Shu, M., Leng, T., Li, Y., et al. (2014). Activation of cyclic AMP/PKA pathway inhibits bladder cancer cell invasion by targeting MAP4-dependent microtubule dynamics. *Urol. Oncol.* 32, 47.e21–e48.

Patrucco, E., Albergine, M. S., Santana, L. F., and Beavo, J. A. (2010). Phosphodiesterase 8A (PDE8A) regulates excitation-contraction coupling in ventricular myocytes. *J. Mol. Cell Cardiol.* 49, 330–333. doi: 10.1016/j.yjmcc.2010.03.016

Peter, D., Jin, S. L., Conti, M., Hatzelmann, A., and Zitt, C. (2007). Differential expression and function of phosphodiesterase 4 (PDE4) subtypes in human primary CD4+ T cells: predominant role of PDE4D. *J. Immunol.* 178, 4820–4831. doi: 10.4049/jimmunol.178.8.4820

Pette, M., Muraro, P. A., Pette, D. F., Dinter, H., Mcfarland, H. F., and Martin, R. (1999). Differential effects of phosphodiesterase type 4-specific inhibition on human autoreactive myelin-specific T cell clones. *J. Neuroimmunol.* 98, 147–156.

Podzuweit, T., Nennstiel, P., and Muller, A. (1995). Isozyme selective inhibition of cGMP-stimulated cyclic nucleotide phosphodiesterases by erythro-9-(2-hydroxy-3-nonyl) adenine. *Cell Signal.* 7, 733–738. doi: 10.1016/0898-6568(95)00042-n

Pritchard, C. A., Hayes, L., Wojnowski, L., Zimmer, A., Marais, R. M., and Norman, J. C. (2004). B-Raf acts via the ROCKII/LIMK/cofilin pathway to maintain actin stress fibers in fibroblasts. *Mol. Cell. Biol.* 24, 5937–5952. doi: 10.1128/mcb.24.13.5937-5952.2004

Pritchard, C. A., Samuels, M. L., Bosch, E., and Mcmahon, M. (1995). Conditionally oncogenic forms of the A-Raf and B-Raf protein kinases display different biological and biochemical properties in NIH 3T3 cells. *Mol. Cell. Biol.* 15, 6430–6442. doi: 10.1128/mcb.15.11.6430

Rabe, K. F. (2011). Update on roflumilast, a phosphodiesterase 4 inhibitor for the treatment of chronic obstructive pulmonary disease. *Br. J. Pharmacol.* 163, 53–67. doi: 10.1111/j.1476-5381.2011.01218.x

Redondo, M., Brea, J., Perez, D. I., Soteras, I., Val, C., Perez, C., et al. (2012). Effect of phosphodiesterase 7 (PDE7) inhibitors in experimental autoimmune encephalomyelitis mice. Discovery of a new chemically diverse family of compounds. *J. Med. Chem.* 55, 3274–3284. doi: 10.1021/jm201720d

Sasaki, T., Kotera, J., Yuasa, K., and Omori, K. (2000). Identification of human PDE7B, a cAMP-specific phosphodiesterase. *Biochem. Biophys. Res. Commun.* 271, 575–583. doi: 10.1006/bbrc.2000.2661

Schafer, P. (2012). Apremilast mechanism of action and application to psoriasis and psoriatic arthritis. *Biochem. Pharmacol.* 83, 1583–1590. doi: 10.1016/j.bcp.2012.01.001

Schafer, P. H., Parton, A., Gandhi, A. K., Capone, L., Adams, M., Wu, L., et al. (2010). Apremilast, a cAMP phosphodiesterase-4 inhibitor, demonstrates anti-inflammatory activity in vitro and in a model of psoriasis. *Br. J. Pharmacol.* 159, 842–855. doi: 10.1111/j.1476-5381.2009.00559.x

Schett, G., Sloan, V. S., Stevens, R. M., and Schafer, P. (2010). Apremilast: a novel PDE4 inhibitor in the treatment of autoimmune and inflammatory diseases. *Ther. Adv. Musculoskelet Dis.* 2, 271–278. doi: 10.1177/1759720x10381432

Schett, G., Wollenhaupt, J., Papp, K., Joos, R., Rodrigues, J. F., Vessey, A. R., et al. (2012). Oral apremilast in the treatment of active psoriatic arthritis: results of a multicenter, randomized, double-blind, placebo-controlled study. *Arthritis Rheum.* 64, 3156–3167. doi: 10.1002/art.34627

Sharma, R. K., and Hickie, R. A. (1996). "Ca2+/calmodulin-dependent cyclic nucleotide phosphodiesterase (PDE1)," in *Phosphodiesterase Inhibitors*, eds C. Schudt, G. Dent, and K. F. Rabe (London: Academic Press), 65–80. doi: 10.1016/b978-012210720-7/50006-x

Sheth, S. B., Chaganti, K., Bastepe, M., Ajuria, J., Brennan, K., Biradavolu, R., et al. (1997). Cyclic AMP phosphodiesterases in human lymphocytes. *Br. J. Haematol.* 99, 784–789. doi: 10.1046/j.1365-2141.1997.4803282.x

Shimizu-Albergine, M., Van Yserloo, B., Golkowski, M. G., Ong, S. E., Beavo, J. A., and Bornfeldt, K. E. (2016). SCAP/SREBP pathway is required for the full steroidogenic response to cyclic AMP. *Proc. Natl. Acad. Sci. U.S.A.* 113, E5685–E5693.

Sloka, S., Metz, L. M., Hader, W., Starreveld, Y., and Yong, V. W. (2013). Reduction of microglial activity in a model of multiple sclerosis by dipyridamole. *J. Neuroinflammation* 10:89.

Soderling, S. H., Bayuga, S. J., and Beavo, J. A. (1998a). Cloning and characterization of a cAMP-specific cyclic nucleotide phosphodiesterase. *Proc. Natl. Acad. Sci. U.S.A.* 95, 8991–8996. doi: 10.1073/pnas.95.15.8991

Soderling, S. H., Bayuga, S. J., and Beavo, J. A. (1998b). Identification and characterization of a novel family of cyclic nucleotide phosphodiesterases. *J. Biol. Chem.* 273, 15553–15558. doi: 10.1074/jbc.273.25.15553

Soderling, S. H., Bayuga, S. J., and Beavo, J. A. (1999). Isolation and characterization of a dual-substrate phosphodiesterase gene family: PDE10A. *Proc. Natl. Acad. Sci. U.S.A.* 96, 7071–7076. doi: 10.1073/pnas.96.12.7071

Soderling, S. H., and Beavo, J. A. (2000). Regulation of cAMP and cGMP signaling: new phosphodiesterases and new functions. *Curr. Opin. Cell. Biol.* 12, 174–179. doi: 10.1016/s0955-0674(99)00073-3

Sommer, N., Martin, R., Mcfarland, H. F., Quigley, L., Cannella, B., Raine, C. S., et al. (1997). Therapeutic potential of phosphodiesterase type 4 inhibition in chronic autoimmune demyelinating disease. *J. Neuroimmunol.* 79, 54–61. doi: 10.1016/s0165-5728(97)00111-2

Spano, D., Marshall, J. C., Marino, N., De Martino, D., Romano, A., Scoppettuolo, M. N., et al. (2013). Dipyridamole prevents triple-negative breast-cancer progression. *Clin. Exp. Metastasis* 30, 47–68. doi: 10.1007/s10585-012-9506-0

Sriram, K., and Insel, P. A. (2018). G protein-coupled receptors as targets for approved drugs: how many targets and how many drugs? *Mol. Pharmacol.* 93, 251–258. doi: 10.1124/mol.117.111062

Steinman, L. (2005). Blocking adhesion molecules as therapy for multiple sclerosis: natalizumab. *Nat. Rev. Drug Discov.* 4, 510–518. doi: 10.1038/nrd1752

Szczypka, M. (2020). Role of phosphodiesterase 7 (PDE7) in T cell activity. effects of selective PDE7 inhibitors and dual PDE4/7 inhibitors on T cell functions. *Int. J. Mol. Sci.* 21:6118. doi: 10.3390/ijms21176118

Takeuchi, M., and Baichwal, V. R. (1995). Induction of the gene encoding mucosal vascular addressin cell adhesion molecule 1 by tumor necrosis factor alpha is mediated by NF-kappa B proteins. *Proc. Natl. Acad. Sci. U.S.A.* 92, 3561–3565. doi: 10.1073/pnas.92.8.3561

Taylor, K. E., Wong, Q., Levine, D. M., Mchugh, C., Laurie, C., Doheny, K., et al. (2017). Genome-wide association analysis reveals genetic heterogeneity of sjogren's syndrome according to ancestry. *Arthritis Rheumatol.* 69, 1294–1305. doi: 10.1002/art.40040

Tenor, H., Hatzelmann, A., Beume, R., Lahu, G., Zech, K., and Bethke, T. D. (2011). Pharmacology, clinical efficacy, and tolerability of phosphodiesterase-4 inhibitors: impact of human pharmacokinetics. *Handb. Exp. Pharmacol.* 204, 85–119. doi: 10.1007/978-3-642-17969-3_3

Tenor, H., Staniciu, L., Schudt, C., Hatzelmann, A., Wendel, A., Djukanovic, R., et al. (1995). Cyclic nucleotide phosphodiesterases from purified human CD4+ and CD8+ T lymphocytes. *Clin. Exp. Allergy* 25, 616–624. doi: 10.1111/j.1365-2222.1995.tb01109.x

Tom, W. L., Van Syoc, M., Chanda, S., and Zane, L. T. (2016). Pharmacokinetic profile, safety, and tolerability of crisaborole topical ointment, 2% in adolescents with atopic dermatitis: an open-label phase 2a study. *Pediatr. Dermatol.* 33, 150–159. doi: 10.1111/pde.12780

Tsai, L. C., and Beavo, J. A. (2012). Regulation of adrenal steroidogenesis by the high-affinity phosphodiesterase 8 family. *Horm. Metab. Res.* 44, 790–794. doi: 10.1055/s-0032-1321861

Tsai, L. C., Chan, G. C., Nangle, S. N., Shimizu-Albergine, M., Jones, G. L., Storm, D. R., et al. (2012). Inactivation of Pde8b enhances memory, motor performance, and protects against age-induced motor coordination decay. *Genes Brain Behav.* 11, 837–847. doi: 10.1111/j.1601-183x.2012.00836.x

Tsai, L. C., Shimizu-Albergine, M., and Beavo, J. A. (2010). The high affinity cAMP-specific phosphodiesterase 8B (PDE8B) controls steroidogenesis in the mouse adrenal gland. *Mol. Pharmacol.* 79, 639–648. doi: 10.1124/mol.110.069104

Vaeth, M., Gogishvili, T., Bopp, T., Klein, M., Berberich-Siebelt, F., Gattenloehner, S., et al. (2011). Regulatory T cells facilitate the nuclear accumulation of inducible cAMP early repressor (ICER) and suppress nuclear factor of activated T cell c1 (NFATc1). *Proc. Natl. Acad. Sci. U.S.A.* 108, 2480–2485. doi: 10.1073/pnas.1009463108

Vang, A. G., Basole, C., Dong, H., Nguyen, R. K., Housley, W., Guernsey, L., et al. (2016). Differential expression and function of PDE8 and PDE4 in effector T cells: implications for PDE8 as a drug target in inflammation. *Front. Pharmacol.* 7:259.

Vang, A. G., Ben-Sasson, S. Z., Dong, H., Kream, B., Deninno, M. P., Claffey, M. M., et al. (2010). PDE8 regulates rapid Teff cell adhesion and proliferation independent of ICER. *PLoS One* 5:e12011. doi: 10.1371/journal.pone.0012011

Vang, A. G., Housley, W., Dong, H., Basole, C., Ben-Sasson, S. Z., Kream, B. E., et al. (2013). Regulatory T-cells and cAMP suppress effector T-cells independently of PKA-CREM/ICER: a potential role for Epac. *Biochem. J.* 456, 463–473. doi: 10.1042/bj20130064

Victoni, T., Gleonnec, F., Lanzetti, M., Tenor, H., Valenca, S., Porto, L. C., et al. (2014). Roflumilast N-oxide prevents cytokine secretion induced by cigarette smoke combined with LPS through JAK/STAT and ERK1/2 inhibition in airway epithelial cells. *PLoS One* 9:e85243. doi: 10.1371/journal.pone.0085243

Virgilio, A., Spano, D., Esposito, V., Di Dato, V., Citarella, G., Marino, N., et al. (2012). Novel pyrimidopyrimidine derivatives for inhibition of cellular proliferation and motility induced by h-prune in breast cancer. *Eur. J. Med. Chem.* 57, 41–50. doi: 10.1016/j.ejmech.2012.08.020

Wallace, D. A., Johnston, L. A., Huston, E., Macmaster, D., Houslay, T. M., Cheung, Y. F., et al. (2005). Identification and characterization of PDE4A11, a novel, widely expressed long isoform encoded by the human PDE4A cAMP phosphodiesterase gene. *Mol. Pharmacol.* 67, 1920–1934.

Wang, C., Lin, W., Playa, H., Sun, S., Cameron, K., and Buolamwini, J. K. (2013a). Dipyridamole analogs as pharmacological inhibitors of equilibrative nucleoside transporters. Identification of novel potent and selective inhibitors of the adenosine transporter function of human equilibrative nucleoside transporter 4 (hENT4). *Biochem. Pharmacol.* 86, 1531–1540.

Wang, C., Schwab, L. P., Fan, M., Seagroves, T. N., and Buolamwini, J. K. (2013b). Chemoprevention activity of dipyridamole in the MMTV-PyMT transgenic mouse model of breast cancer. *Cancer Prev. Res. (Phila)* 6, 437–447.

Wang, H., Yan, Z., Yang, S., Cai, J., Robinson, H., and Ke, H. (2008). Kinetic and structural studies of phosphodiesterase-8A and implication on the inhibitor selectivity. *Biochemistry* 47, 12760–12768.

Wang, J. H., Sharma, R. K., and Mooibroek, M. J. (1990). "Calmodulin-stimulated cyclic nucleotide phosphodiesterases," in *Cyclic Nucleotide Phosphodiesterases: Structure, Regulation and Drug Action*, eds J. Beavo and M. D. Houslay (West Sussex: John Wiley & Sons Ltd), 19–59.

Wang, P., Wu, P., Egan, R. W., and Billah, M. M. (2000). Cloning, characterization, and tissue distribution of mouse phosphodiesterase 7A1. *Biochem. Biophys. Res. Commun.* 276, 1271–1277.

Wang, P., Wu, P., Egan, R. W., and Billah, M. M. (2003). Identification and characterization of a new human type 9 cGMP-specific phosphodiesterase splice variant (PDE9A5). Differential tissue distribution and subcellular localization of PDE9A variants. *Gene* 314, 15–27.

Wang, P., Wu, P., Myers, J. G., Stamford, A., Egan, R. W., and Billah, M. M. (2001). Characterization of human, dog and rabbit corpus cavernosum type 5 phosphodiesterases. *Life Sci.* 68, 1977–1987.

Wang, T., Sheppard, J. R., and Foker, J. E. (1978). Rise and fall of cyclic AMP required for onset of lymphocyte DNA synthesis. *Science* 201, 155–157.

Weber, C. K., Slupsky, J. R., Herrmann, C., Schuler, M., Rapp, U. R., and Block, C. (2000). Mitogenic signaling of Ras is regulated by differential interaction with Raf isozymes. *Oncogene* 19, 169–176.

Weeks, J. L., Zoraghi, R., Beasley, A., Sekhar, K. R., Francis, S. H., and Corbin, J. D. (2005). High biochemical selectivity of tadalafil, sildenafil and vardenafil for human phosphodiesterase 5A1 (PDE5) over PDE11A4 suggests the absence of PDE11A4 cross-reaction in patients. *Int. J. Impot. Res.* 17, 5–9.

Wehbi, V. L., and Tasken, K. (2016). Molecular mechanisms for cAMP-mediated immunoregulation in T cells–role of anchored protein kinase A signaling units. *Front. Immunol.* 7:222.

Weis, W. I., and Kobilka, B. K. (2018). The molecular basis of G protein-coupled receptor activation. *Annu. Rev. Biochem.* 87, 897–919.

Wittmann, M., and Helliwell, P. S. (2013). Phosphodiesterase 4 inhibition in the treatment of psoriasis, psoriatic arthritis and other chronic inflammatory diseases. *Dermatol. Ther. (Heidelb)* 3, 1–15.

Wojnowski, L., Stancato, L. F., Larner, A. C., Rapp, U. R., and Zimmer, A. (2000). Overlapping and specific functions of Braf and Craf-1 proto-oncogenes during mouse embryogenesis. *Mech. Dev.* 91, 97–104.

Xu, C., Wyman, A. R., Alaamery, M. A., Argueta, S. A., Ivey, F. D., Meyers, J. A., et al. (2016). Anti-inflammatory effects of novel barbituric acid derivatives in T lymphocytes. *Int. Immunopharmacol.* 38, 223–232.

Yan, C., Zhao, A. Z., Bentley, J. K., Loughney, K., Ferguson, K., and Beavo, J. A. (1995). Molecular cloning and characterization of a calmodulin-dependent phosphodiesterase enriched in olfactory sensory neurons. *Proc. Natl. Acad. Sci. U.S.A.* 92, 9677–9681.

Yang, G., Mcintyre, K. W., Townsend, R. M., Shen, H. H., Pitts, W. J., Dodd, J. H., et al. (2003). Phosphodiesterase 7A-deficient mice have functional T cells. *J. Immunol.* 171, 6414–6420.

Yednock, T. A., Cannon, C., Fritz, L. C., Sanchez-Madrid, F., Steinman, L., and Karin, N. (1992). Prevention of experimental autoimmune encephalomyelitis by antibodies against alpha 4 beta 1 integrin. *Nature* 356, 63–66.

Yu, J., Wolda, S. L., Frazier, A. L., Florio, V. A., Martins, T. J., Snyder, P. B., et al. (1997). Identification and characterisation of a human calmodulin-stimulated phosphodiesterase PDE1B1. *Cell Signal.* 9, 519–529.

Yuasa, K., Kotera, J., Fujishige, K., Michibata, H., Sasaki, T., and Omori, K. (2000). Isolation and characterization of two novel phosphodiesterase PDE11A variants showing unique structure and tissue-specific expression. *J. Biol. Chem.* 275, 31469–31479.

Zane, L. T., Chanda, S., Jarnagin, K., Nelson, D. B., Spelman, L., and Gold, L. S. (2016a). Crisaborole and its potential role in treating atopic dermatitis: overview of early clinical studies. *Immunotherapy* 8, 853–866.

Zane, L. T., Kircik, L., Call, R., Tschen, E., Draelos, Z. D., Chanda, S., et al. (2016b). Crisaborole topical ointment, 2% in patients ages 2 to 17 years with atopic dermatitis: A phase 1b, Open-Label, maximal-use systemic exposure study. *Pediatr. Dermatol.* 33, 380–387.

Zhao, A. Z., Yan, C., Sonnenburg, W. K., and Beavo, J. A. (1997). Recent advances in the study of Ca2+/CaM-activated phosphodiesterases: expression and physiological functions. *Adv. Second Messenger Phosphoprotein Res.* 31, 237–251.

Zimmerman, N. P., Roy, I., Hauser, A. D., Wilson, J. M., Williams, C. L., and Dwinell, M. B. (2015). Cyclic AMP regulates the migration and invasion potential of human pancreatic cancer cells. *Mol. Carcinog.* 54, 203–215.

Conflict of Interest: The authors declare that the research was conducted in the absence of any commercial or financial relationships that could be construed as a potential conflict of interest.

Advantages of publishing in Frontiers

OPEN ACCESS
Articles are free to read for greatest visibility and readership

FAST PUBLICATION
Around 90 days from submission to decision

HIGH QUALITY PEER-REVIEW
Rigorous, collaborative, and constructive peer-review

TRANSPARENT PEER-REVIEW
Editors and reviewers acknowledged by name on published articles

Frontiers
Avenue du Tribunal-Fédéral 34
1005 Lausanne | Switzerland

Visit us: www.frontiersin.org
Contact us: frontiersin.org/about/contact

REPRODUCIBILITY OF RESEARCH
Support open data and methods to enhance research reproducibility

DIGITAL PUBLISHING
Articles designed for optimal readership across devices

FOLLOW US
@frontiersin

IMPACT METRICS
Advanced article metrics track visibility across digital media

EXTENSIVE PROMOTION
Marketing and promotion of impactful research

LOOP RESEARCH NETWORK
Our network increases your article's readership